THE PHOTOCHEMISTRY OF CAROTENOIDS

Edited by

Harry A. Frank

KLUWER ACADEMIC PUBLISHERS

The Photochemistry of Carotenoids

Advances in Photosynthesis

VOLUME 8

Advances in Photosynthesis is an ambitious book series seeking to provide a comprehensive and state-of-the-art account of photosynthesis research. Photosynthesis is the process by which higher plants, algae and certain species of bacteria transform and store solar energy in the form of energy-rich organic molecules. These compounds are in turn used as the energy source for all growth and reproduction in these organisms. As such, virtually all life on the planet ultimately depends on photosynthetic energy conversion. This series of books spans topics from physics to agronomy, from femtosecond reactions to season long production, from the photophysics of reaction centers to the physiology of whole organisms, and from X-ray crystallography of proteins to the morphology of intact plants. The intent of this series of publications is to offer beginning researchers, advanced undergraduate students, graduate students, and even research specialists a comprehensive current picture of the remarkable advances across the full scope of photosynthesis research.

The titles published in this series are listed at the end of this volume and those of forthcoming volumes on the back cover.

The Photochemistry of Carotenoids

Edited by

Harry A. Frank
University of Connecticut,
Storrs, CT, U.S.A.

Andrew J. Young
Liverpool John Moores University,
Liverpool, U.K.

George Britton
University of Liverpool,
Liverpool, U.K.

and

Richard J. Cogdell
University of Glasgow,
Glasgow, U.K.

KLUWER ACADEMIC PUBLISHERS
NEW YORK, BOSTON, DORDRECHT, LONDON, MOSCOW

eBook ISBN: 0-306-48209-6
Print ISBN: 0-7923-5942-9

Visit Kluwer Online at: http://kluweronline.com
and Kluwer's eBookstore at: http://ebooks.kluweronline.com

Contents

Part II: Structure of Carotenoid-Chlorophyll Protein Complexes

Part III: Electronic Structure, Stereochemistry, Spectroscopy, Dynamics and Radicals

Preface

The Photochemistry of Carotenoids is the eighth volume to be published in the series *Advances in Photosynthesis* by Kluwer Academic Publishers (Series Editor: Govindjee). Volume 1 dealt with *The Molecular Biology of Cyanobacteria*; Volume 2 with *Anoxygenic Photosynthetic Bacteria*; Volume 3 with *Biophysical Techniques in Photosynthesis*; Volume 4 with *Oxygenic Photosynthesis: The Light Reactions*; Volume 5 with *Photosynthesis and the Environment*; Volume 6 with Lipids in *Photosynthesis: Structure, Function and Genetics*; volume 7 with *The Molecular Biology of Chloroplasts and Mitochondria in Chlamydomonas.* The next volume in the Series, Volume 9, will focus on the so-called dark reactions of photosynthesis entitled *Photosynthesis: Physiology and Metabolism.*

The present book, *The Photochemistry of Carotenoids,* has emerged out of the enormous growth in research on carotenoids that has taken place within the past few years. During this time, the structures of several carotenoid-containing pigment-protein complexes from photosynthetic organisms have been solved to atomic resolution by X-ray and electron diffraction methods; pioneering developments in technology have allowed ultrafast laser spectroscopic techniques to reveal photochemical events at the earliest stages of light absorption and energy transfer by carotenoids; and significant advances in genetic engineering and biochemical methodologies have elucidated the roles carotenoids play in protecting the photosynthetic apparatus from oxidative damage. Novel investigations have been brought to bear on carotenoids in vitro and in vivo which challenge the existing models of how carotenoids function and confront the theoretical frameworks which describe π-electron conjugated molecules. All of these issues, and more, are dealt with in this book.

The book covers a wide range of topics about the photochemistry of carotenoids in substantial detail. These chapters are contributed by authors who are leading experts in the field and provide a detailed picture of current thinking in the areas. It has been subdivided into five parts:

(1) Biosynthetic Pathways and the Distribution of Carotenoids in Photosynthetic Organisms, with chapters on Carotenoids in Photosynthesis by Govindjee, Carotenoid Synthesis and Function in Plants by Dean DellaPenna, and Carotenoids and Carotenogenesis in Anoxygenic Photosynthetic Bacteria by Shinichi Takaichi;

(2) Structure of Carotenoid-Chlorophyll Protein Complexes, with chapters on The Structure and Function of the LH2 complex by Richard J. Cogdell et al., Carotenoids as Components of the Light-harvesting Proteins of Eukaryotic Algae by Roger G. Hiller, The Structure of Reaction Centers from Purple Bacteria by Günter Fritzsch and Andreas Kuglstatter, and Carotenoids and the Assembly of Light-harvesting Complexes by Harald Paulsen;

(3) Electronic Structure, Stereochemistry, Spectroscopy, Dynamics and Radicals, with chapters on The Electronic States of Carotenoids by Ronald L. Christensen, Configurations, Excited State Properties, and Physiological Functions by Yasushi Koyama and Ritsuko Fujii, Electronic Structure, Stereochemistry and Resonance Raman Spectroscopy by Bruno Robert, Electron Magnetic Resonance of Carotenoids by Alexander Angerhofer, Carotenoid Radicals and the Interactions of Carotenoids with Active Oxygen Species by Ruth Edge and T. George Truscott, and The Incorporation of Carotenoids into Pigment-protein complexes by Harry A. Frank;

(4) Eco-physiology and the Xanthophyll Cycle, with chapters on this topic by Barbara Demmig-Adams et al., The Regulation of the Structure and Function of the Light-harvesting Complexes of Photosystem II by the Xanthophyll Cycle by Peter Horton et al., Biochemistry and Molecular Biology of the Xanthophyll Cycle, by Harry Y. Yamamoto et al., and the Relationships between Antioxidant Metabolism and Carotenoids in the Regulation of Photosynthesis by Christine H. Foyer and Jeremy Harbinson; and

(5) Model Systems with chapters on Novel and Biomimetic Functions of Carotenoids in Artificial Photosynthesis by Thomas A. Moore et al., Physical

Properties of Carotenoids in Solid States by Hideki Hashimoto, and Carotenoids in Membranes by Wieslaw I. Gruszecki. These chapters are contributed by authors who are leading experts in the field and provide a detailed picture of current thinking in the areas.

Organizing the expansive findings of the authors into a coherent structure for this book was facilitated by the complementary expertise of the four editors, who in addition to working together on this book, have also shared many productive and enjoyable collaborative investigations in each other's laboratories. The general topics of protein structure were dealt with by Cogdell, spectroscopy and electronic structure by Frank, biosynthesis and reactions by Britton, and biochemistry by Young. We hope that the organizational structure of the book will provide not only a valuable reference for researchers in the field, but also a useful introductory text for students seeking to embark on projects aimed at understanding the photochemistry of carotenoids. To this end, an historical perspective of research into carotenoids, contributed by the series editor, Govindjee, has been included in this volume. Carotenoids, with their ability to play a significant number of diverse and important photochemical roles, should be recognized as one of the truly exceptional creations in all of Nature. We hope that this point-of-view, shared by the editors, authors, and investigators in the carotenoid field, is conveyed through this book.

This book is dedicated to Professors Norman Krinsky and Trevor Goodwin for their kindness and continued support of our endeavors, and for the enormous impact their work has had on developments in the field of carotenoid research.

A note of special thanks goes to Larry Orr, who with great facility with numerous software packages on several different computer platforms, converted the word-processed documents submitted by the authors into the attractive chapter format that has now become a standard in the industry. His organizational skills and sense of humor were much appreciated in the course of producing this book.

We also want to thank Meena Stout for her extraordinary talent and skill in producing an attractive and thoughtful cover art graphic image for this book on very short notice.

HAF and RJC acknowledge a NATO grant for International Collaboration that provided travel support that helped foster this project.

Finally, we thank our families for their love and understanding, and for willingly giving us the time to pursue our goals, which the present work is but one small part.

Harry A. Frank
Richard J. Cogdell
George Britton
Andrew J. Young

Color Plates

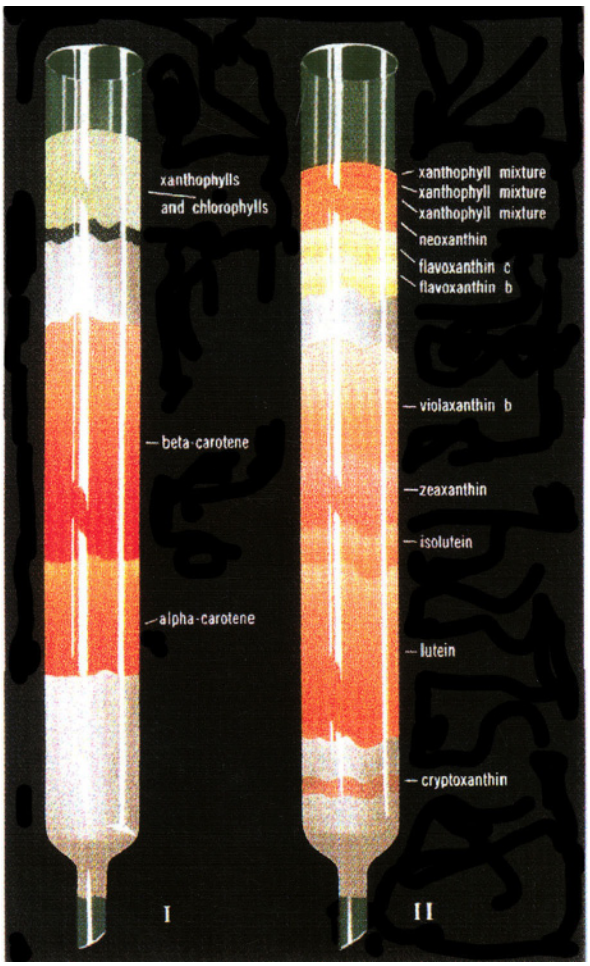

Color *Plate 1.* Separation of leaf carotenes and leaf xanthophylls by chromatographic adsorption, obtained in 1938 by Harold Strain. I. Separation of **α-carotene** from **β-carotene** by adsorption of petroleum ether extracts of leaves on a magnesia column. II. Separation of leaf xanthophylls by adsorption of a dichloroethane solution of these pigments on a magnesium column; note the separation of violaxanthin, zeaxanthin and lutein, mentioned in the text. The figure is taken from Strain (1938, p. ii, frontispiece). (See Chapter 1, p. 3, Fig. 1.)

H. A. Frank. A. J. Young, G. Britton and R. J. Cogdell (eds): The Photochemistry of Carotenoids, pp. CP1–CP6.

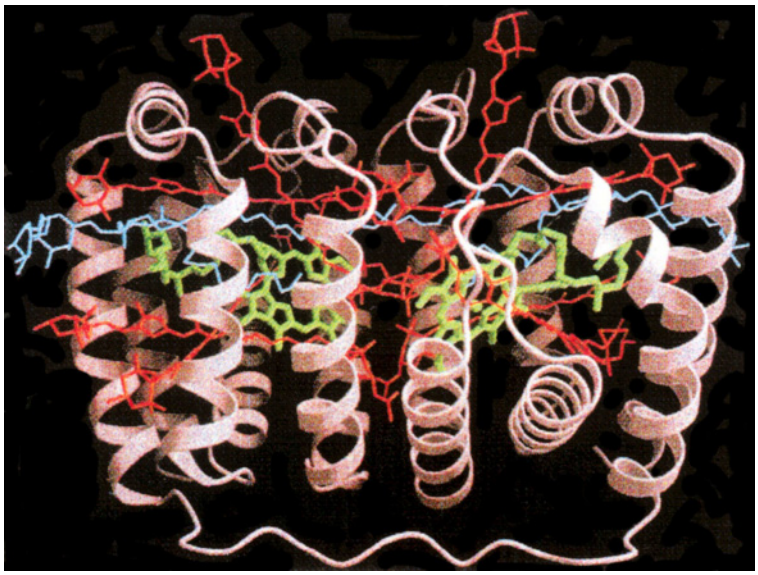

Color Plate 2. A 2 A resolution structure of a peridinin Chl *a* complex of a dinoflagellate. The eight peridinin molecules are shown in red, whereas the two Chls are in green. A lipid molecule is shown in blue, and two proteins are shown in gray The proximity of peridinin molecules to each other and to Chl *a* molecules explains the efficient excitation energy transfer from peridinin to Chl *a.* observed by Haxo et al. (1976). The diagram is reproduced from Hoffman et al. (1996). (See Chapter 1, p. 14, Fig. 11.)

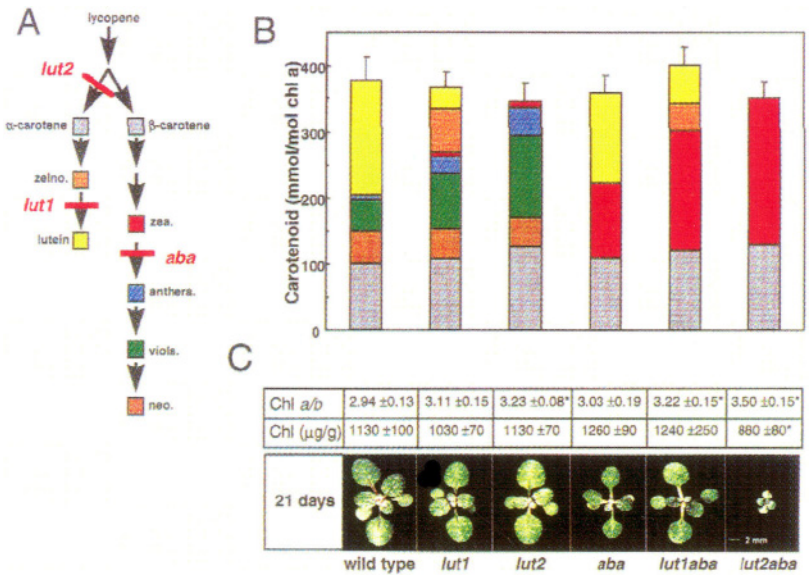

Color Plate 3. Carotenoid pathway, mutant locations, pigment profiles and seedlings. Panel A shows the carotenoid biosynthetic pathway in higher plant chloroplasts commencing with lycopene and the location of the *lut1, lut2* and *aba1* mutations in the pathway. Panel B shows the carotenoid content of mature green leaves of 21 day-old wild type and the five indicated xanthophyll mutant lines. Each section of the bars corresponds to a specific carotenoid of the pathway (refer to color code of Panel A). The standard deviations of the total pool of carotenoids per mole chl *a* are shown on each bar. Panel C shows photographs of 21d old seedlings of wild type and the five indicated xanthophyll mutant lines and their corresponding chlorophyll content and Chl a/*b* ratios. Photographs are of soil-grown wild type and xanthophyll mutant seedlings grown 21 days on a 12 h light cycle. Chlorophyll ratios and content of mature green leaves (C). The chl *a/b* ratio (mol/mol) and total chlorophyll content of green leaves (µg/g fresh weight) with standard deviations are shown. Values that are significantly different ($p < 0.05$) from wild-type are marked with an asterisk (*). (See Chapter 2, p. 30. Fig. 4.).

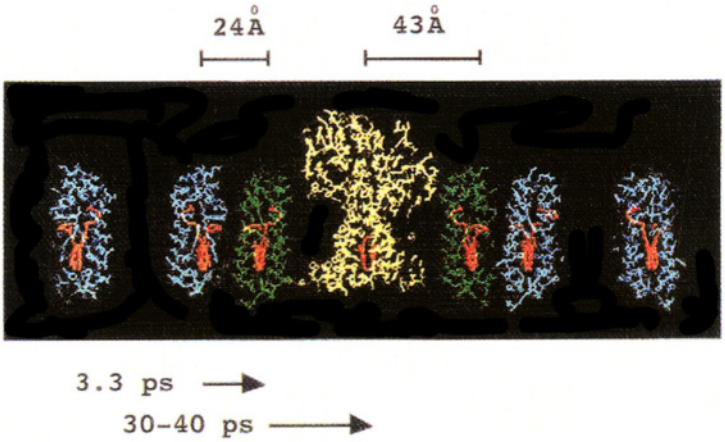

Color Plate 4. A pictorial representation of a section through the purple bacterial photosynthetic unit normal to the presumed membrane plane. The representation is: LH2 - blue; LH1 - green; RC - yellow. The tightly coupled rings of BChl *a* in LH2 and LH1 and the primary dimer BChl *a*/s in the RC are shown in red. The times shown represent the rate constants for energy transfer from LH2 to LH1 and from LH1 to the RC respectively. This figure was adapted from Papiz et al., (1996). (See Chapter 4, p. 72, Fig. 1.)

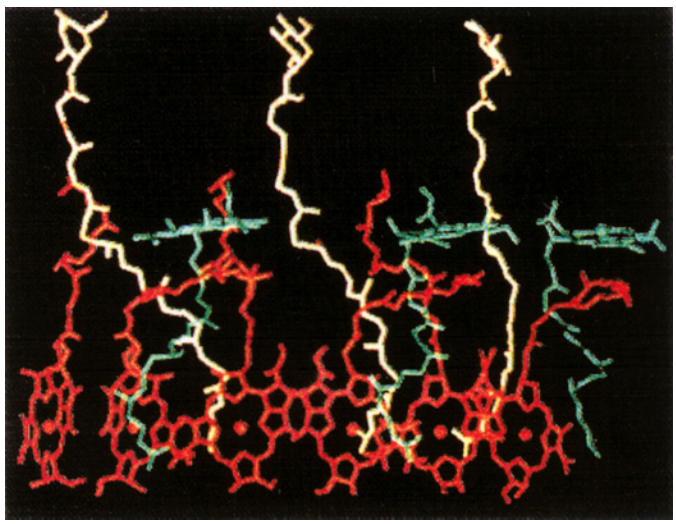

Color Plate 5. A section of the structure of the LH2 complex from *Rhodopseudomonas acidophila* strain 10050 only showing the pigment. The representation is: B850 BChl *a*/s – red; B800 BChl *a*/s – green; rhodopin glucoside – yellow. This figure was redrawn from McDermott et al. (1995). (See Chapter 4, p. 74, Fig. 4.).

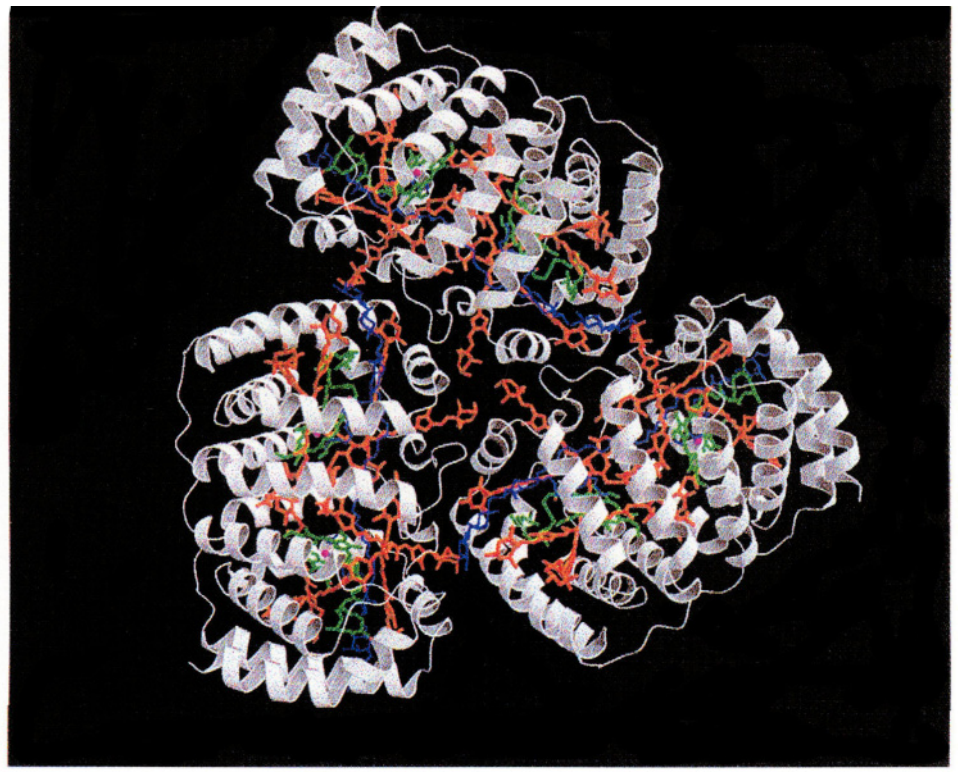

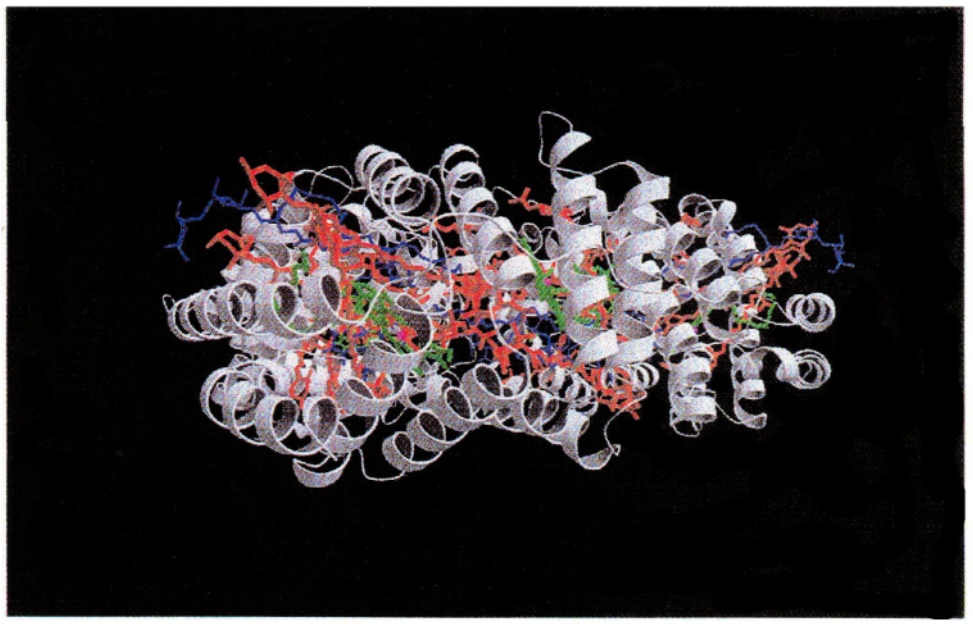

Color Plate 6. a) Top and b) side views of trimeric PCP. (See Chapter 5, p. 86, Fig. 4.)

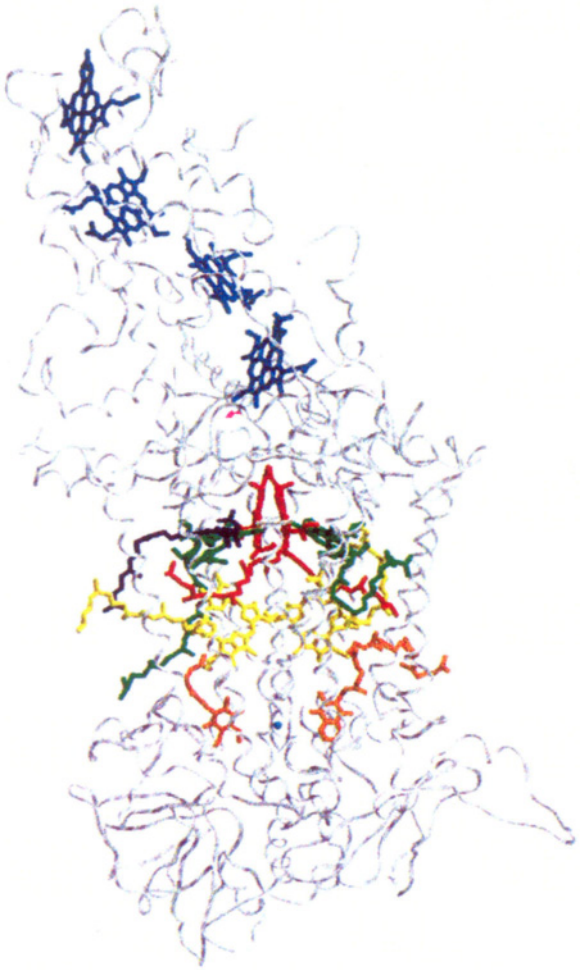

Color Plate 7. Overall view of the RC structure. The C_α chains of the protein are shown as grey ribbons. The cofactors are represented as: blue (heme groups), red (special pair), green (accessory bacteriochlorophylls), lilac (carotenoid), yellow (bacteriopheophytins), orange (quinones) and cyan (non-heme iron). (See Chapter 6, p. 104, Fig. 4.)

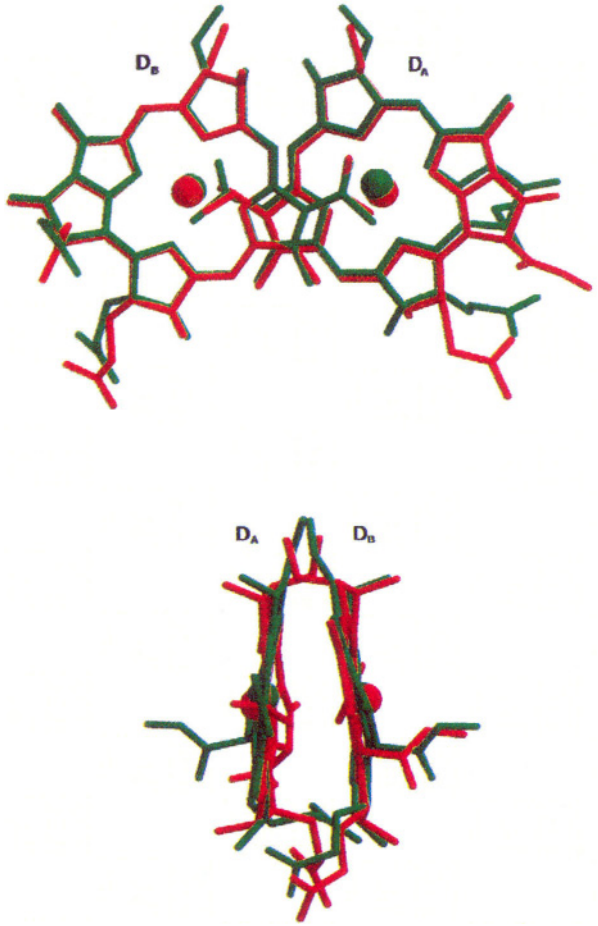

Color Plate 8. Superposition of the special pairs of the RCs from *Rb. sphaeroides* (red) and *Rp. viridis* (green) represented without their phytyl chains. top: View perpendicular to the planes of the macrocycles. bottom: View rotated by 90°. The superposition shows the high degree of structural identity of both RCs. As shown in bottom view, the ester methyl groups of ring V have different orientations in both RCs. (See Chapter 6, p. 109, Fig. 8.)

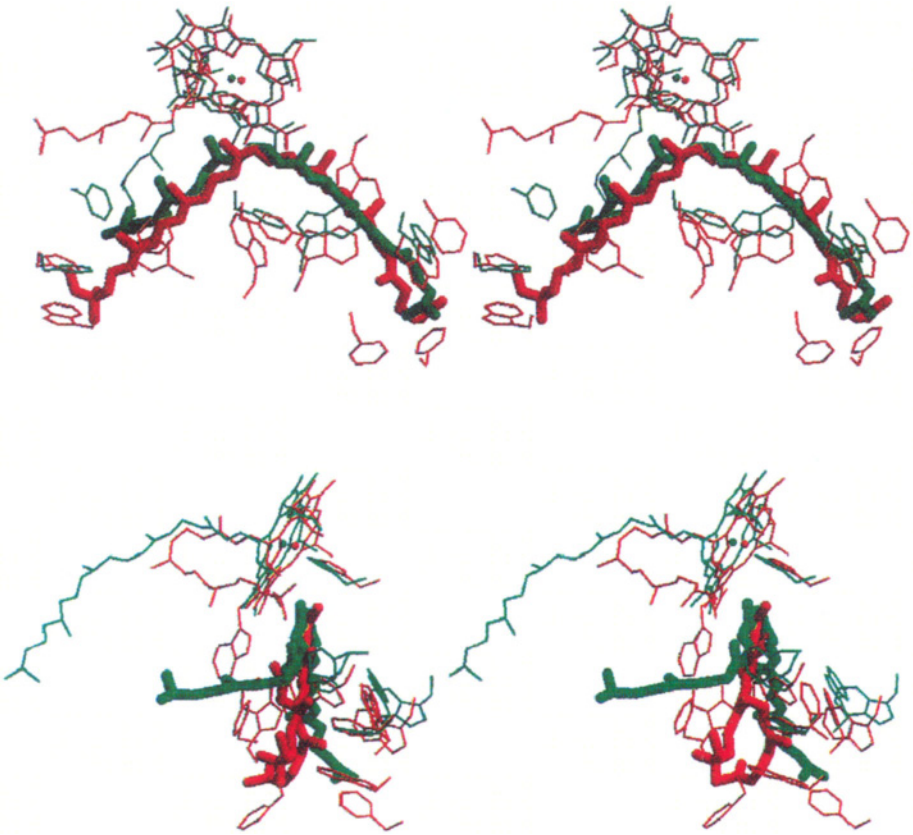

Color Plate 9. The carotenoids. Superposition of the spheroidene and 1,2-dihydroneurosporene molecules from *Rb. sphaeroides* (red) and *Rp. viridis* (green) RC. The binding pocket is formed by six (three) phenylalanines and five (two) tryptophans in the *Rb. sphaeroides* (*Rp. viridis*) RC. Upper: View perpendicular to the planes of the carotenoids. Lower: View rotated by 90°. (See Chapter 6, p. 111, Fig. 9.)

Chapter 1

Carotenoids in Photosynthesis: An Historical Perspective

Govindjee
Departments of Biochemistry and Plant Biology, and Center of Biophysics and Computational Biology, University of Illinois, Urbana, IL 61801–3707, U.S.A.

Summary

This chapter presents a personal historical perspective of the role of carotenoids in photosynthesis. It leads the reader into the early literature on the carotenoids and photosynthesis that are related to the discoveries on the excitation energy transfer and, to a lesser extent, on photoprotection. Excitation energy transfer from the carotenoid fucoxanthin to chlorophyll (Chl) *a* was shown first in the diatoms by H. Dutton, W. M. Manning and B. M. Duggar, in 1943, at the University of Wisconsin at Madison. After the extensive researches of E. C. Wassink (in the Netherlands) on this topic, the classical doctoral thesis of L. N. M. Duysens became available in 1952, at the State University in Utrecht. This thesis dealt with the evidence of excitation energy transfer in many photosynthetic systems, including anoxygenic photosynthetic bacteria. The experiments of R. Emerson and C. M. Lewis, done at the Carnegie Institute of Washington, Stanford, California, in the 1940s, dealt with the quantum yield action spectra of photosynthesis. In these experiments, the famous *red drop* phenomenon was discovered; further, the authors showed here the low efficiency of carotenoids in the photosynthesis of both green algae and blue-green algae (cyanobacteria). In 1956, R. Stanier and his coworkers discovered, at the University of California at Berkeley, a special role of carotenoids in protection against death in phototrophic bacteria. Finally, in 1962, H. Yamamoto (of Hawaii) pioneered the role of xanthophyll cycle pigments in photoprotection. This was followed by key experiments and concepts from B. Demmig-Adams (1987, now in Colorado), and O. Björkman (at Stanford, California), among others mentioned in the text. In 1954, a 515 nm absorbance change was discovered by Duysens (1954) and has now become a quantitative measure of the membrane potential changes in photosynthesis. Historical aspects of some of the basic principles of light absorption and excitation energy transfer, and references to selected current literature are also included in this chapter to allow the reader to link the past with the present.

H. A. Frank, A. J. Young, G. Britton and R. J. Cogdell (eds): The Photochemistry of Carotenoids, pp. 1–19.

I. Introduction

The intent in this chapter is to present a historical perspective of the two major functions of carotenoids in photosynthesis, namely, light harvesting and photoprotection, with emphasis on the former. As a novice in both the history of photosynthesis and in the study of the role of carotenoids, I am unencumbered by any bias except that of personal and close associations with (1) Robert Emerson, who, with Charleton M. Lewis, measured the first most precise action spectra of photosynthesis (that included the carotenoid region) in the cyanobacterium *Chroococcus* (Emerson and Lewis, 1942) and the green alga *Chlorella* (Emerson and Lewis, 1943), and discovered the enhancing effect of light absorbed by the carotenoid fucoxanthin on the quantum yield of photosynthesis sensitized by Chl *a* of what we now call Photosystem I (PS I) in the diatom *Navicula minima* (Emerson and Rabinowitch, 1960; Govindjee and Rabinowitch, 1960; Rabinowitch, 1961); and (2) with Eugene Rabinowitch, who wrote the most detailed single-authored treatise, more than 2000 pages long, on all aspects of photosynthesis including carotenoids, published in 1945 (Vol. I), 1951 (Vol. II, part 1), and 1956 (Vol. II, part 2) (Bannister, 1972; Brody, 1995). The personal perspective of Duysens (1989) provides an account of the discovery of the two light reactions of photosynthesis, necessary for understanding the context of the present day view of photosynthesis.

A. Why History?

Retracing historical developments and comprehending the overview of the history of the ideas are essential in grasping the nature of scientific enquiry in any field. From another perspective, I also believe in what Pliny, the Younger (see a translation by Firth, 1909) implied in Book V, Letter V to Nonius Maximus (pp. 224–225) that it is a noble employment to rescue from oblivion those who deserve to be remembered. In writing this chapter, I do not even know if this would be achieved here. I shall attempt to present a view that I consider worthy of thought by the readers of a book that deals with the Photochemistry of Carotenoids. I know that a great many scientists are filled with a glow when they see others citing and recognizing their work; they feel that what they did was indeed useful to society.

Abbreviations: BChl – bacteriochlorophyll; Chl – chlorophyll; PS I – Photosystem I; PS II – Photosystem II

B. Carotenoids: Carotenes and Xanthophylls

Everything connected with color has always held, and will continue to hold, a captivating interest for me. The brilliant yellow pigments known as carotenes and xanthophylls are no exception. Carotene was first isolated in 1831 by Heinrich Wilhelm Ferdinand Wackenroder (1798–1854). Berzelius (1837a,b) named the yellow pigments obtained from the autumn leaves xanthophylls (xanthos being Greek for yellow, and phyll for leaf) as a counterpart to chlorophyll, Chl (leaf green). Fremy (1860) reviewed the knowledge on carotenoids at that time. By 1902, however, there were 800 publications in this field (Kohl, 1902). One of the two major yellow pigments present in leaves was found to be identical with the carotene from the carrot root. Xanthophylls were discovered in algae, and one leaf xanthophyll, lutein, was found in egg yolk (for these and other early accounts on the carotenoids, see Lubimenko, 1927 and Smith, 1930). Strain (1938) used the name carotenes for the hydrocarbons, and xanthophylls for oxygenated derivatives of carotenes, but Bogert (1938) suggested that xanthophylls be called carotenols because of their chemical structure and because they were not restricted to leaves. In his famous treatise on photosynthesis, Rabinowitch (1945, 1951, 1956) adopted the term carotenols; thus, lutein was luteol, violaxanthin was violaxanthol, zeaxanthin was zeaxanthol, etc. We no longer use the 'ol' ending, which is too restrictive, and we are back to the terminology used by Harold Strain.

The first separation and purification of the carotenes and xanthophylls must be credited to the Russian botanist Tswett (1906, 1911) who invented chromatography for the separation of the leaf pigments i.e. green Chls, and yellow-to-orange carotenes and xanthophylls (also see discussion of paper chromatography by Jensen and Liaaen-Jensen, 1959). Tswett already provided the concept of a family of many pigments, the carotenoids (carotenes and xanthophylls). (Figure 1 is taken from Strain (1938) and shows the separation of some of the carotenoids on two systems.) This was followed by the extensive work on the separation and chemistry of the carotenoids by R. Wilstätter (Nobel Prize in Chemistry in 1915, mostly for work on Chl chemistry) (see Wilstätter and Stoll, 1913) although his ideas on

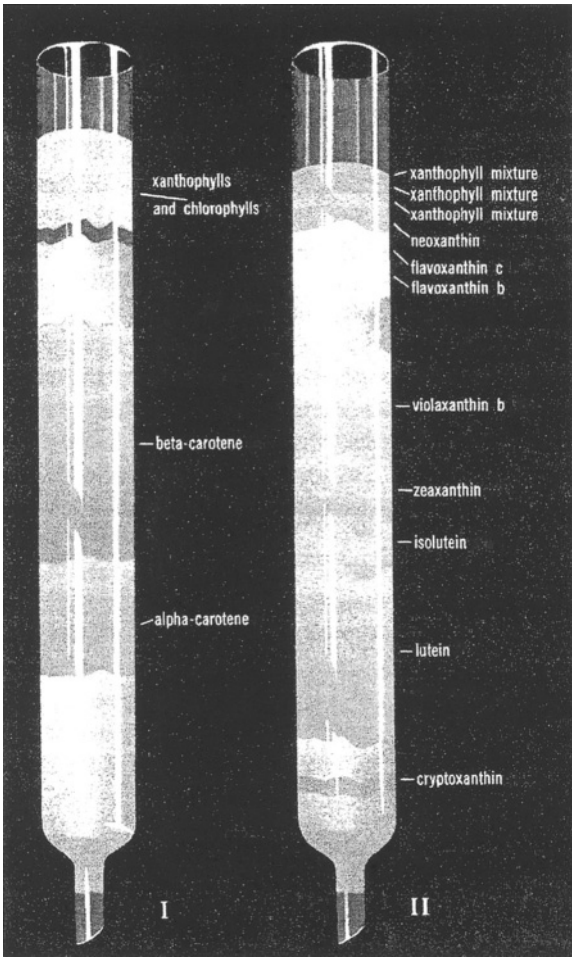

Fig. 1. Separation of leaf carotenes and leaf xanthophylls by chromatographic adsorption, obtained in 1938 by Harold Strain. I. Separation of α carotene from β-carotene by adsorption of petroleum ether extracts of leaves on a magnesia column. II. Separation of leaf xanthophylls by adsorption of a dichloroethane solution of these pigments on a magnesium column; note the separation of violaxanthin, zeaxanthin and lutein, mentioned in the text. The figure is taken from Strain (1938, p. ii, frontispiece). See also Color Plate 1.

the functions of these pigments were not substantiated. Following these early days, research on the carotenoids was reviewed by Palmer (1922), Zechmeister (1934, 1962), Lederer (1934), Karrer and Jucker (1948, English translation, 1950), Goodwin (1952, 1976), Cogdell (1978; 1985: for interactions with Chls), Britton and Goodwin (1982), Cogdell and Frank (1987), Mimuro and Katoh (1991), Britton et al. (1995) and Bartley and Scolnik (1995). Nobel prizes in Chemistry were successively awarded to Paul Karrer (in 1937) and Richard Kühn (in 1938) for their work on the structure and chemistry of the carotenoids. A book edited by Isler (1971) was dedicated to the memory of Paul Karrer. Kühn (1935) showed that the carotenoids absorb in the visible (at about 480 nm) due to the alternation of single and double bonds, which produces a so-called Brillouin gap when one resonance structure is dominant. It was Karrer, however, who had recognized the symmetrical nature of the various carotenoids (β-carotene; lycopene; zeaxanthin) and that vitamin A was related to half of the β-carotene molecule (Karrer, 1934; Karrer and Helfenstein, 1933). The nomenclature at that time was summarized by Palmer (1934). By 1948 about 80 carotenoids were known, and structures of about half of those were established; by 1950 total synthesis of β carotene was achieved by Karrer and others. For chemistry of carotenes, see McKinney (1935), Liaaen-Jensen (1978), and Packer's two volumes (1992a,b); for antheraxanthin, see Karrer and Oswald (1935), for spirilloxanthin, see van Niel and Smith (1935), for xanthophylls of algae, see Strain et al. (1944), and for carotenoids in cyanobacteria, see Hirschberg and Chamowitz (1994). For rules on the nomenclature of carotenoids, see IUPAC and IUB (1971, 1975).

C. Function: Light Harvesting and Photoprotection

Karrer and Jucker (1948), when dealing with the function of carotenoids, wrote, 'All these investigations are still at a preliminary stage and further researches will be required in order to elucidate the importance of carotenoids in plants.' Similarly, Goodwin (1952) stated, 'With regard to formation and function (of carotenoids), knowledge is rudimentary.' However, by this time, Dutton and Manning (1941) in Wisconsin had already shown that light energy absorbed by fucoxanthin was used efficiently for photosynthesis in the diatom *Nitzschia closterium,* and Dutton et al. (1943) had clearly established that this process took place by transfer of energy absorbed by fucoxanthin to Chl *a*, because excitation of fucoxanthin led to Chl *a* fluorescence (i.e., the phenomenon of sensitized fluorescence was observed). This was a clear case of the light-harvesting function of one of the carotenoids in vivo (Dutton, 1997). Further coverage of the history on this topic will be presented in Section II.

Carotenoids are known to have another major function, i.e. that of photoprotection of reaction centers, pigment-protein antennae, and cells and

tissues (Krinsky, 1968, 1979). The work of Roger Stanier and his coworkers provided the most compelling evidence for the belief that carotenoids perform a photoprotective function. In 1955 Griffiths et al. discovered that a blue-green (BG) mutant of the non-sulfur purple bacterium *Rhodopseudomonas* (now *Rhodobacter*) *sphaeroides*, which is deficient in colored carotenoids, is photosensitive in the presence of air. The mutation was lethal. It was suggested that carotenoids are universally associated with photosynthetic systems because they protect these systems against photodynamic damage catalyzed by BChl (in photosynthetic bacteria) or by Chl (in plants and algae). More recently, a third function was discovered in higher plants exposed to strong light. Zeaxanthin and antheraxanthin, formed from violaxanthin by the xanthophyll cycle (Yamamoto et al., 1962) increase non-radiative dissipation of energy as heat in the pigment bed of the antenna of Photosystem II (PS II) (Demmig et al., 1987; Gilmore et al., 1995). Further discussion on this topic will be presented in Section IV (Horton et al., 1994, Demmig-Adams et al., 1996; Yamamoto and Bassi, 1996; Gilmore, 1997).

The reader is referred to Siefermann-Harms (1987a, b) for earlier discussions on the light harvesting and photoprotective functions of carotenoids.

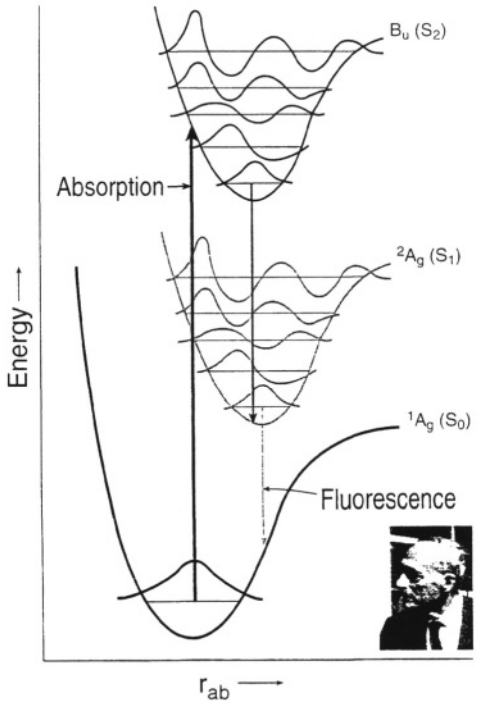

Fig. 2. **Franck Condon principle as applied to carotenoids. The photograph of James Franck, the co-discoverer of the principle is shown as an inset, and was taken by the author in 1963 when Franck attended the Airlie House Conference on 'Photosynthetic Mechanisms of Green Plants,' organized by Bessel Kok and André Jagendorf.**

D. Franck-Condon Principle

Pigment excitation occurs after the absorption of light. This promotes the molecule from the ground state (S_o) to an excited state (S_o). All further reactions occur after de-excitation of this higher excited state. This upward transition occurs in 1–2 fs in visible light. A historical suggestion was that of James Franck (1925; who had shared, with Hertz, the 1925 Nobel Prize in Physics for the experimental verification of the quantum theory). He argued simply that because of the large masses of the nuclei in a molecule, their relative momentum cannot be directly affected by an electronic transition, so that those transitions will be most likely that conform most closely to a Principle: The nuclei do not move during an electronic transition. Thus, on a diagram of energy (ordinate) versus distance between the nuclei of a diatomic molecule (abscissa), this transition is vertical promoting the electron from the lowest vibrational state of a molecule in the ground state to a higher vibrational state of the excited state (e.g. S_1 or S_2) of the molecule (Fig. 2). The molecule in the excited state then dissipates immediately (within 10 to 100 fs) some energy as heat and the electron reaches the lowest vibrational level of the excited state. When the molecule relaxes to the ground state giving off light (fluorescence), it generally occurs at longer wavelength than the absorbing wavelength (*Rotverschiebung*, the red shift, Franck, 1927). The Franck-Condon principle, then, explains the observed red shift (Stokes, 1852) of the fluorescence spectrum from the absorption spectrum. The history of how the principle became known as the Franck-Condon principle was beautifully presented by Condon (1947). The original idea is in a paper at a Faraday Society meeting in London by Franck (1925); the proofs of this paper were sent to his student Hertha Sponer, who was then at the University of California at Berkeley on an International Education Board Fellowship. She generously shared the proofs with Condon; he was able to generalize Franck's ideas (Condon, 1926). Condon (1947) states, 'This work was all done in a few days. Doctor Sponer showed

me Franck's paper one afternoon, and a week later all the quantitative work for my 1926 paper was done.' With carotenoids, one does not usually observe by conventional absorption spectroscopy, transitions involving the first singlet excited state, (S_1) but mainly the second singlet state (B_u or S_2), The transition from the S_0 state to S_1 is optically forbidden (for a fuller discussion, see Chapter 8, Christensen; also see a review by Koyama, 1991). Fluorescence of carotenoids in general is very weak (S_1 to S_0 transition).

II. Excitation Energy Transfer: Sensitized Fluorescence and Photosynthesis

The first major function of carotenoids is to act as an accessory pigment, i.e., to capture light and transfer the energy to Chl *a* to drive photochemistry. The methods used to obtain evidence for this are basically two: (1) measurement of action spectrum of photosynthesis in the region carotenoids and Chls absorb and evaluation of the quantum efficiency of light absorbed by carotenoids in photosynthesis; and (2) measurement of action spectrum of Chl *a* fluorescence in the region where carotenoids and Chls absorb and evaluation of the quantum efficiency of excitation energy transfer from the carotenoids to Chl *a.* The latter technique is called the sensitized fluorescence method. If the energy donor is fluorescent, one would observe decreases (quenching) in donor fluorescence and increases in acceptor fluorescence when the donor is excited, whereas excitation of the acceptor would lead to acceptor fluorescence only; this method was first applied by Cario and Franck (1923) in gases. Since then it has been successfully used in liquids, solids, proteins and photosynthetic systems (Knox, 1975; Stryer, 1978; Pearlstein, 1982; van Grondelle and Amesz, 1986; Frank et al., 1991; van Grondelle et al., 1994).

A. Photosynthetic Yields in Different Wavelength Regions

Engelmann (1883, 1884) was an ingenious scientist (Kamen, 1986). He projected the visible spectrum on to green, red and brown algae, mounted on the stage of a microscope, and used the number of aerotactic motile bacteria accumulating in the different wavelengths of the light as an indication of the rate of oxygen evolution. He concluded that light absorbed by various accessory pigments (including carotenoids, particularly fucoxanthin) was used for photosynthesis. Warburg and Negelein (1923), using precise manometric methods, measured absolute quantum yields of oxygen evolution by the green alga *Chlorella* in different colors of light. Although the absolute quantum yield of oxygen evolution in blue light, where both carotenoids and Chls absorb light, was later questioned by others, it was slightly lower than in the red where only Chls absorb light. Thus, this experiment indicated that, although carotenoids contribute to photosynthesis, their efficiency is somewhat lower than that of Chls. It was Montfort (1936, 1940) who compared, although rather crudely and from unreliable experiments, absorption by various extracted photosynthetic pigments and oxygen evolution in various colors of light, and concluded that light absorbed by fucoxanthin of marine brown algae is fully utilized in photosynthesis. The first extensive and reliable measurements on the quantum yield of oxygen evolution as a function of wavelength of light (i.e., of the action spectrum of photosynthesis) were, however, carried out by Emerson and Lewis (1942, 1943) on the cyanobacterium *Chroococcus* and the green alga *Chlorella* (Fig. 3). These experiments were done with a large home-built monochromator with the grating obtained from Mt. Wilson observatory and the use of the most precise manometry, where 0.01 mm pressure changes, due to oxygen evolution, could be measured! Independent of Emerson's work, Dutton and Manning (1941) carried out similar experiments with the diatom *Nitzschia closterium* (now *Phaeodactylum tricornutum),* using a dropping mercury electrode. Their conclusions were that fucoxanthin in the diatom is almost 90% efficient, whereas the carotenoids are about 40–50% efficient in *Chlorella,* and much less efficient (perhaps, only 10%) in *Chroococcus.* Although Wassink and Kersten (1945,1946) came to the same conclusion as Dutton and Manning (1941), it was Tanada (1951), a student of Emerson, who provided the most thorough and precise data. He used the Emerson-Lewis monochromator, and showed a very high quantum yield of oxygen evolution at 500 nm, where fucoxanthin absorbs most of the light (Fig. 4). On the other hand, Haxo and Blinks (1950) made a large number of action spectra of photosynthesis plotted per incident photons in many marine algae, but were able to make only qualitative statements regarding energy transfer from carotenoids to Chl *a.* They concluded that carotenoids were

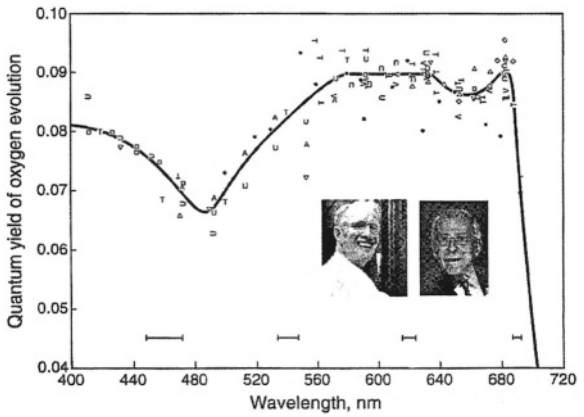

Fig. 3. The first detailed quantum yield action spectra of oxygen evolution in the green alga *Chlorella pyrenoidosa*, obtained by Emerson and Lewis (1943) using Warburg manometry. Nineteen sets of experiments were made and the phenomenon of the *red drop* (drop in the quantum yield of oxygen evolution, beyond 680 nm) was discovered; this later led to the discovery of the two pigment system and two light reaction scheme when Emerson and co-workers discovered the Enhancement effect in 1957 (Emerson et al., 1957). The dip in the blue (minima at 490 nm) was due to only 40–50% efficiency of excitation energy transfer from the carotenoids to Chl *a*. The experiments were done at the Carnegie Institution of Washington at 290 Panama Street, Stanford, California, using a grating monochromator assembled by Emerson and Lewis themselves. The minimum quanta of light needed to evolve one molecule of oxygen approached 10 in these experiments. Also shown as inserts are the photographs of late Robert Emerson (in 1958) and the late Charleton M. Lewis (in 1996) taken by the author.

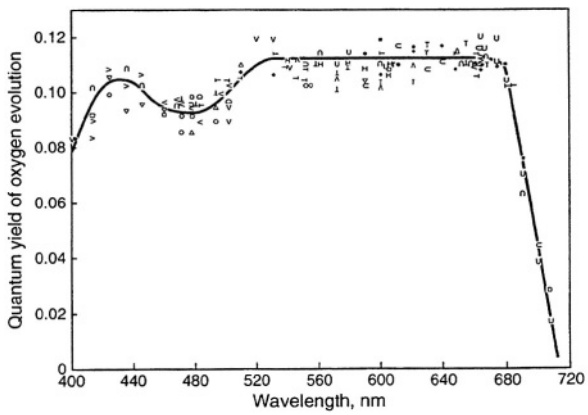

Fig. 4. The quantum yield action spectra of oxygen evolution in the diatom *Navicula minima* obtained by Tanada (1951), then a doctoral student of Robert Emerson at the University of Illinois, Urbana, Illinois, using the Emerson-Lewis monochromator and Emerson's perfected Warburg manometry. Here, the existence of the 'red drop' (beyond 680 nm) was confirmed, but more importantly, the almost 80–90% efficiency of fucoxanthin absorbing in the blue to green region was established. Further, the minimum quantum requirement of oxygen evolution (inverse of the maximum quantum yield of oxygen evolution) was found to be 8. It was the same instrument, located in the 155 Natural History Building at Urbana, that was used later for the finding that fucoxanthin was a major sensitizer in the then-called 'short wave' system (now PS II), whereas the Chl *a* absorbing beyond 680 nm was in the then-called 'long wave' system (now PS I) (Emerson and Rabinowitch, 1960; Govindjee and Rabinowitch, 1960).

relatively inactive in the green alga *Ulva*, but considered that some carotenoids must be active in photosynthesis in some systems. For a review on the action spectra of photosynthesis, see Fork and Amesz (1969).

Measurements on the action spectra of photosynthesis do not distinguish between the direct photochemistry by the carotenoids versus that by Chl *a* after excitation energy transfer from them to the Chls. This distinction is possible only from measurements on excitation energy transfer.

B. Excitation of Chl a Fluorescence by Different Wavelengths of Light: Sensitized Fluorescence

Vermeulen et al. (1937), in the laboratories of L. S. Ornstein of Utecht and A. J. Kluyver of Delft, published their results on the intensity of fluorescence per quantum absorbed as a function of wavelength of light for the green alga *Chlorella*. Although the measured quantum yields of Chl *a* fluorescence were too low to be true, the yield of Chl *a* fluorescence after excitation by 496 nm light was about 20% lower than after excitation at 607 nm. The authors stated that both the quantum yield of the Chl *a* fluorescence and that of photosynthesis (Warburg and Negelein, 1923) were independent of wavelength in the region where only Chl *a* absorbs. Since the data show 10–30% decreases in the blue (see Table III in Vermeulen et al., 1937), we can conclude that carotenoids did not transfer 100% of their excitation energy to Chl *a* although the authors did not make any comment on this problem.

The first and clear evidence for excitation energy transfer from fucoxanthin leading to Chl *a* fluorescence was obtained by Dutton et al. (1943). It was demonstrated that light absorbed by fucoxanthin was almost 90% as efficient in producing Chl *a* fluorescence as was light absorbed by Chl *a* itself. This was the clearest pioneering paper dealing with sensitized fluorescence evidence for excitation energy transfer in photosynthesis (see Dutton, 1997, for the experimental background prior to the actual

experiment). Excitation energy transfer, in general, in photosynthesis was implied already in the paper of Gaffron and Wohl (1936) when they were explaining the photosynthetic unit experiments of Emerson and Arnold (1932a,b). Further, Oppenheimer (1941) had called it *internal conversion* while thinking about the still earlier unpublished experiments of William Arnold (see Knox, 1996, for the history of this work, as well as Arnold and Oppenheimer, 1950). Wassink and Kersten (1946) confirmed the conclusion of Dutton et al. (1943) on excitation energy transfer from fucoxanthin to Chl *a.*

Although Van Norman et al. (1948) did not really discuss excitation energy transfer from phycoerythrin (a phycobilin, not a carotenoid) to Chl *a* in the red algae they had examined, it was clear that the higher yield of red fluorescence by excitation with green light, absorbed by phycoerythrin, than by red light, absorbed by Chl *a,* suggested efficient excitation energy transfer from phycoerythrin to Chl *a.* Excellent evidence for this transfer was published by French and Young (1952), and was known to and fully recognized by L. N. M. Duysens (1951, 1952). No discussion of energy transfer from carotenoids to Chl *a* is available in the papers of French and coworkers. The classical work of Duysens (1951, 1952) established that: (1) carotenoids transfer 35–40% of their absorbed energy to bacteriochlorophyll *a* (BChl *a*) in the B890 complex of *Chromatium* strain D, and about 50% to BChl *a* in the B890 complex of *Rhodospirillum molischianum;* (2) about 40% of energy absorbed by carotenoids is transferred to Chl *a* in green algae; and (3) about 70% of energy absorbed by fucoxanthin is transferred to Chl *a* in diatoms and brown algae. In none of the early experiments, except for the work on fucoxanthin, was any distinction made between carotenes and xanthophylls. In 1956, Arnold and Meek presented their work on the depolarization of Chl *a* fluorescence (see Perrin, 1926, 1929), thus supporting clearly the concept of excitation energy migration in photosynthesis. To me, this was an important experiment of its time.

When I joined the research group of Robert Emerson in 1956, Emerson was very keen that I work on the problem of the separate roles of carotenes and xanthophylls in photosynthesis. I grew several types of algae (*Tribonema, Muriella, Tolypothrix*) in different colors and intensities of light and extracted carotenes and xanthophylls and monitored the variations in the ratios of the two groups of carotenoids under various experimental conditions. Unfortunately, for me, Emerson was not interested in measuring action spectra of Chl *a* fluorescence, but was only interested in measuring quantum yield action spectra of photosynthesis, an art he had perfected. The progress on my research was extremely slow due to my impatience, the tedious nature of manometry and difficulties in measuring absolute quantum yield of photosynthesis in low intensities of different wavelengths of light. My work was never finished in spite of piles and piles of data I had collected. (I moved on to other research after Emerson's death on February 4,1959.) However, Goedheer (1969a, b; see his review, 1972), also from the same laboratory as Duysens, published a paper on chloroplasts treated with petroleum ether (this treatment selectively removes carotenes, not xanthophylls) and concluded that, in red algae and in cyanobacteria whose phycobilins he had also removed, β carotene transfers energy to Chl *a* (of PS I with 100% efficiency, whereas the β carotene of green algae and greening leaves transfers energy to Chl *a* of both PS I and II. Surprisingly, Goedheer concluded that xanthophylls in these organisms do not transfer any energy to Chl *a.* The observed peaks for the carotenoids were at 471 nm and 504 (or 506) nm, at 77K, in the action spectra of Chl *a* fluorescence. I believe there is a need for further research on this topic in intact systems without such solvent treatments, as used by Goedheer. There is, however, evidence that lutein, a xanthophyll, transfers energy to Chl *a* with 100% efficiency in the isolated light harvesting complex (LHC) of *Lactuca sativa* (see Siefermann-Harms and Ninnemann, 1982). Although many authors state that violaxanthin transfers excitation energy to Chl *a,* Barrett and Anderson (1980) could not detect any significant excitation energy transfer in the green Chl *a/c*-violaxanthin protein from the brown alga *Acrocarpia paniculata.*

After I finished my PhD under Eugene Rabinowitch and had established that Chl *a* was in both the photosystems (Govindjee and Rabinowitch, 1960) and that Chl *a* fluorescence measurements can be used to support the existence of two light reactions and two photosystems (Govindjee et al., 1960; Duysens, 1989), I went back to measure the action spectra of Chl *a* fluorescence, but not so much from the point of deciding the role of carotenoids in photosynthesis, but of simply using Chl *a* fluorescence as an intrinsic, sensitive, and non-invasive probe of photosynthesis (Govindjee, 1995). A major interest

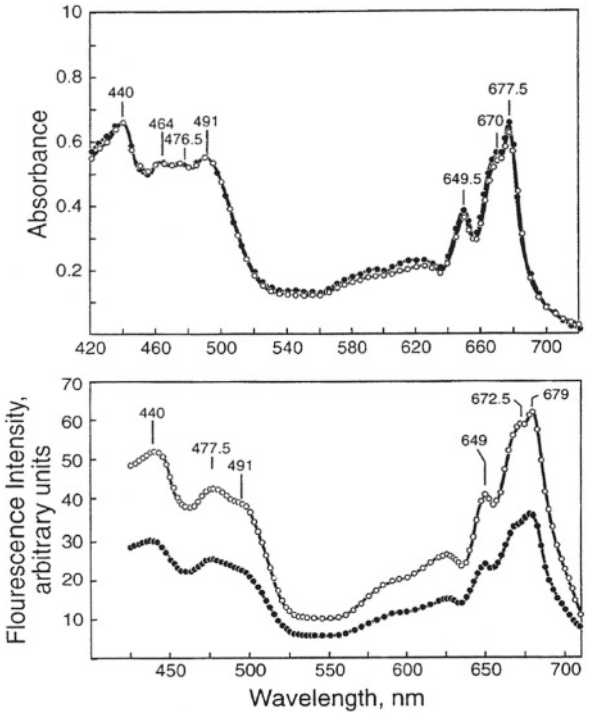

Fig. 5. Absorption spectra (top panel) and action (or excitation) spectra of Chl *a* fluorescence measured at 725 nm (bottom panel) at cryogenic temperatures (open circles, 4K; closed circles, 77K) in *Chlorella pyrenoidosa*. In addition to Chl *a* bands (440 nm, 670–672 nm, and 678–679 nm) and Chl b bands (477 nm and 649 nm), a carotenoid band at 491 nm in both absorption spectra and action spectra of fluorescence was observed. This experiment was done at the University of Illinois at Urbana, Illinois, by my PhD student Frederick Yi-Tung Cho (Cho and Govindjee, 1970a).

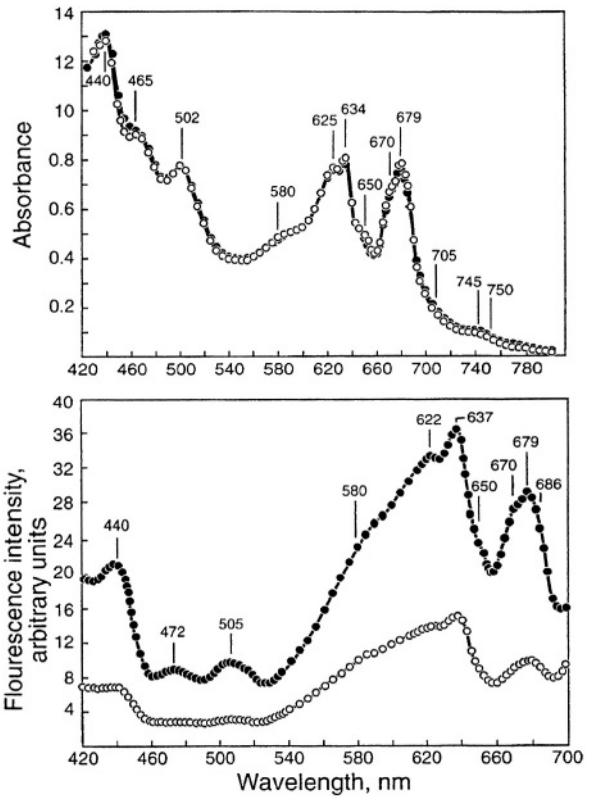

Fig. 6. Absorption spectra (top panel) and action (or excitation) spectra of Chl *a* fluorescence measured at 715 nm (bottom panel) at cryogenic temperatures (open circles, 77 K; closed circles, 4 K) in the blue oxygenic bacterium *Anacystis nidulans*. In addition to Chl *a* bands (440 nm, 670 nm, and 679 nm) and phycobilin bands (580 nm, 622–625 nm, 634–637 nm, and 650 nm), carotenoid bands at around 470 nm and 502–505 nm were observed in both absorption and action spectra of fluorescence. However, the calculated efficiency of excitation energy transfer from the carotenoids to Chl *a* was much lower than in the green algae (Cho and Govindjee, 1970b). [Unknown to the author at that time, Goedheer (1969a,b), in Utrecht, the Netherlands, had observed similar bands at 471 nm and 504 nm (at 77 K) in the action spectra of several algae that were specially treated; Goedheer concluded that these bands were from β-carotene, and that they transferred energy with 100% efficiency to Chl *a*, whereas there was no energy transfer from the xanthophylls to Chl *a*.]

was in using temperature dependence of fluorescence down to liquid nitrogen and helium (4 K) temperatures. Figure 5 (Cho and Govindjee, 1970a) shows the absorption spectra and action spectra of Chl *a* fluorescence in the green alga *Chlorella pyrenoidosa* at 77 and 4K. Several bands can be observed including the one at 491 nm from carotenoids. Excitation energy transfer from carotenoids to Chl *a* is clearly indicated, but no further information is available. With the blue-green alga (cyanobacterium) *Anacystis nidulans,* bands at 472 nm and 505 nm, due to carotenoids, are observed (Fig. 6, Cho and Govindjee, 1970b; also see Kramer et al., 1981, for similar data on spinach and barley) in the action spectra of Chl *a* fluorescence, again showing energy transfer from carotenoids to Chl *a.* In grana and stroma lamellae fractions from thylakoids, Gasanov et al. (1979) calculated the efficiency of excitation energy transfer from the carotenoids (without distinction between carotenes and xanthophylls) to Chl *a* (Fig. 7). It appears that there are two pools of carotenoids, one absorbing at shorter wavelengths and transferring energy to Chl *a* with an efficiency of about 40–50% and another at slightly longer wavelengths transferring energy, with an efficiency of about 20–25%. This conclusion has never been confirmed or pursued, and the question of the precise roles of carotenes and xanthophylls in light harvesting remains still an open question worthy of research.

It was already known in the nineteenth century

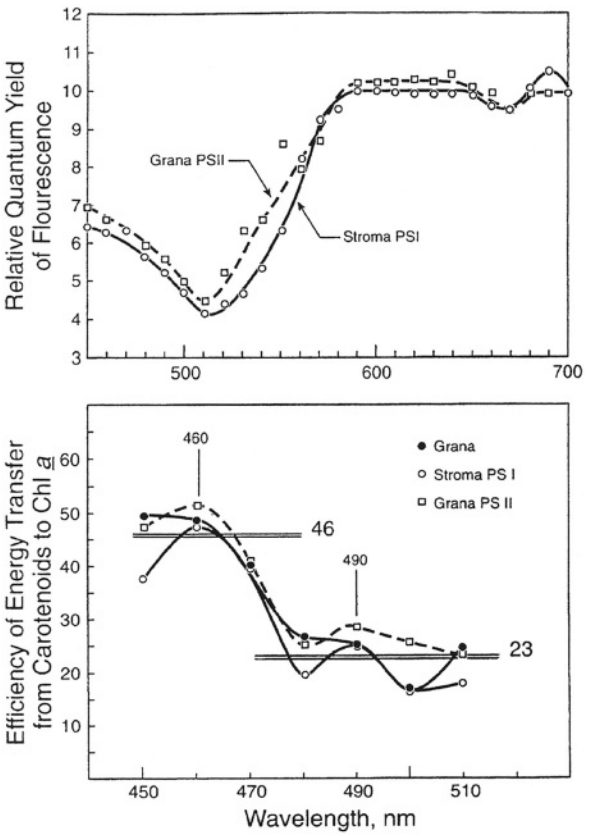

Fig. 7. Action spectra of (relative) quantum yield of Chl *a* fluorescence measured at 740 nm, at 77 K, in grana and stroma lamellae (top panel) showing the relative inefficiency of excitation energy transfer from the carotenoids (the blue region) to Chl *a* in both the systems. Using the methods and assumptions of Emerson and Lewis (1943) and of Duysens (1952), the efficiency of energy transfer to Chl *a* was calculated (bottom panel). The data were suggestive of two pools of carotenoids, one absorbing in the short wave region and transferring energy with 40–45 % efficiency, and the other in the longwave region and transferring energy with only 20% efficiency (after Gasanov et al., 1979). No firm conclusions are available. Further research is necessary to investigate the light harvesting and energy transfer capabilities of not only carotenoids as a group, but of individual carotenoids in PS I and II.

that a part of another carotenoid (peridinin) is bound to a protein in vivo in dinoflagellates (Schuett, 1890). The excitation spectrum of Chl *a* fluorescence in the chromoprotein from *Amphidinium carterae*, obtained by Haxo et al. (1976), showed that light absorbed by peridinin is transferred efficiently to Chl *a*. Song et al. (1976) showed 100% efficiency of energy transfer from peridinin to Chl *a* in Chl *a*-proteins of two dinoflagellates, a *Glenodinium* sp. and *Gonyaulax polyedra*. Further, efficient energy transfer has been reported from siphonaxanthin (absorbing in the green region) to Chl *a* in the thalli of the green algae *Ulva japonica* and *Ulva pertusa* (Kageyama et al., 1977) and in the isolated green protein, containing siphonaxanthin, from *Codium* (Anderson, 1983; also see a review by Govindjee and Satoh, 1986).

C. Resonance Excitation Transfer Model Compared to Electron Exchange

As already mentioned, evidence for excitation energy transfer to Chl *a* was established, first from fucoxanthin and then from peridinin, as well as from β-carotene. This raises the question of how excitation energy moves from one molecule to another. In 1940, William Arnold had observed excitation energy transfer from phycocyanin to Chl *a* and had discussed it with JR Oppenheimer (see Arnold, 1991, p. 77). Knox (1996) has traced the history of Arnold's contribution; he states that the R^{-6} dependence of excitation energy transfer (to be evolved later by Förster) must have been evident to Oppenheimer in whose 1941 paper the conclusion of Arnold and Oppenheimer (1950) was already stated. There are two major theories for exciton transfer: (A) *Förster's resonance energy transfer mechanism* (Förster, 1946, 1948, 1965) (called the Heller-Marcus mechanism in the crystal field) that depends upon the transfer of excitons where the decay of the excited state in the donor molecule is coupled with the upward transition promoting the ground state of the acceptor to the excited state. Energy (i.e., hole and electron together) is transferred from one molecule to the other. This mechanism is based upon a dipole -(induced) dipole interaction and includes the following: (1) an R^{-6} dependence of energy transfer, where R is the distance between the donor and the acceptor; (2) an appropriate orientation of the dipoles for a efficient transfer; and (3) a good proximity of the energy levels, as measured usually by the overlap integral of the absorption spectrum of the acceptor molecule and the fluorescence spectrum of the donor molecule (Knox, 1975; van Grondelle and Amesz, 1986). [The R^{-6} dependence was clearly proven in in vitro by studying excitation energy transfer from an α-naphthyl group at the carboxyl end of a polypeptide to the energy acceptor dansyl group at the amino end, when the distance was changed by spacers of oligomers of poly-L-proline (Stryer and Haugland, 1967).] (B) *Dexter's electron exchange mechanism* (Dexter, 1953); here, there is electron exchange, i.e., the simultaneous movement of two electrons between the molecular orbitals of the donor and acceptor molecules. This mechanism requires extremely close

proximity of the donor and acceptor molecules. The energy level diagram (the Jablonski diagram, Jablonski, 1935) shows that the energy level of the optically allowed B_u (S_2) state of the carotenoid molecule is higher than the S_2 level of Chl or BChl. In general, however, the lifetime of the S_2 state of the molecules is too short and most of the de-excitation occurs by loss of heat and the attainment of the S_1 state. There are, however, reports that excitation energy transfer may be possible originating from S_2 (see Chapter 8, Christensen). The consensus is that the lower level of carotenoids is expected to be involved in excitation energy transfer. Now, since the ^2Ag (S_1) to Ag (S_0) is optically forbidden, it has been suggested that the singlet energy transfer reaction, involving the S_1 states, must take place through the electron exchange mechanism. For a review see Frank and Cogdell (1993).

I consider it interesting to mention an old idea of Platt (1959) who predicted that energy can be transferred from carotenoids to Chls, but entertained the possibility of energy transfer from Chl to a charge-separated state involving carotene. He had predicted large red shifts from an absorption at 480 nm, to the orange-red region, and then to 1100 nm for various states of carotenes. No one since then has provided any specific experimental support for Platt's ideas.

III. The 515 nm Effect: Carotenoids as a Microvoltmeter

An outline of the history of the role of carotenoids in photosynthesis would certainly be incomplete without a discussion of the so-called 515 nm effect (ΔA 518 as some call it). When a pigment is placed in an electric field, its absorption spectrum is shifted because the field changes the energy levels of the pigment. This is so-called Stark effect. During photosynthesis, electrons are transferred from one side of the thylakoid membrane to the other side since the primary electron donors (P680, P700, P870, etc) are located on one side and the stable electron acceptors on the other side (Fig. 8). This produces a membrane potential (electric field). Thus, the light-absorbing properties of the pigments present in the membrane are then affected as a result of the Stark effect; this produces what we call *electrochromism.* Carotenoids are affected in this way and are responsible for a major portion of the absorption change (ΔA 515 or $\Delta A518$).

A positive absorbance change around 515 nm was discovered in the green alga *Chlorella,* in a leaf, in the thallus of a marine alga, and in the blades of *Valisneria* (Fig. 9) by Duysens (1954) when he was a visiting fellow at the Carnegie Institute of Washington at Stanford, after his brief stint as a fellow at the UIUC, Urbana, Illinois, with Eugene Rabinowitch. This positive change was accompanied by negative changes at 480 nm and 420 nm; the latter was assigned to cytochrome *f.* It was Strehler (1957) who suggested its relationship to carotenoids (Govindjee and Govindjee, 1965). Wolff et al. (1969), in the laboratory of H. T. Witt, pioneered the relationship of the 515 nm change to the fast charge separation processes at the reaction centers because they observed that the change occurred within nano-seconds after a flash of light. It was later shown by H. T. Witt and coworkers that about 50% of the fast change arises from PS I and the other 50% from PS II (see e.g., a review by Witt, 1975). According to the chemiosmotic hypothesis of Peter Mitchell (1961), proton motive force (i.e., ΔpH and $\Delta\Psi$) is used to produce free ATP. The 515 nm change was found to decay faster in the presence of gramicidin D, an uncoupler of photophosphorylation, as expected if the change is a monitor of membrane potential (Junge and Witt, 1968). I note that in this paper, the authors assumed that they were monitoring changes *only* in Chl *b* at 515 nm. Jackson and Crofts (1969) made another important observation in bacteria. They found a shift in the carotenoid spectrum (523 minus 509 nm absorbance change) in darkness when a potential is generated that is positive with respect to the inside of the chromatophores; the shift mimicked that observed as a response to light. De Grooth et al. (1979) observed a flash number dependency of the biphasic decay of the electrochromic shift of the carotenoids, related to the changes in the membrane potential, in the chromatophores of *Rhodobacter sphaeroides.* The carotenoid absorbance change is accepted now to be a monitor of the membrane potential.

IV. Photoprotection

The hypotheses to explain how carotenoids play a role in protecting plants against damage by excess light have been discussed very extensively. Crucial work on the topic of photoprotection was done in the summer of 1954 in C. B. van Niel's Lab at the Hopkins Marine Station by Roger Stanier and his

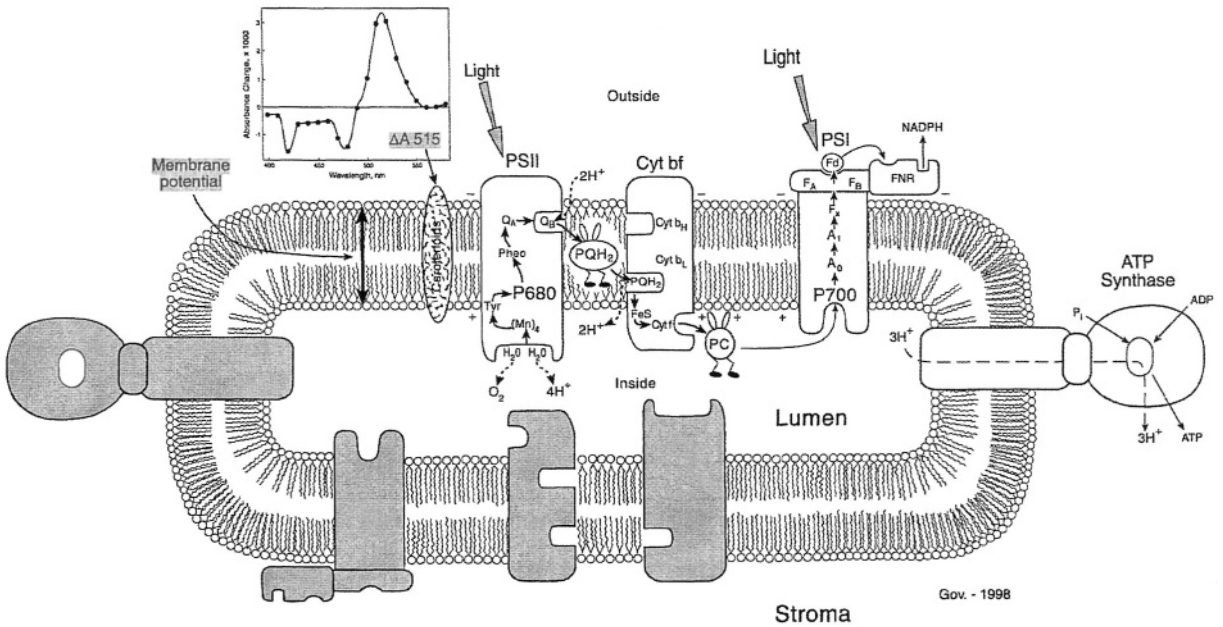

Fig. 8. A cartoon for the arrangement of four protein complexes in the thylakoid membrane. Shaded boxes (protein complexes) are equivalent to unshaded boxes in details. Also shown, in cartoon form, is the creation of membrane potential as the electrons are transferred from the inner side of the membrane to the outerside of the membrane during primary charge separation in both Photosystems I and II. It has been suggested that carotenoids, along with other pigments, sense this membrane potential through electrochromism leading to a 515 nm absorbance change (ΔA 515) (see inset). The four major protein complexes, embedded in the thylakoid membrane, are used for the production of the reducing power NADPH and ATP, both needed for the fixation of CO_2 and the production of glucose. These complexes are: *Photosystem II* (PS II, that oxidizes water to oxygen, reduces a plastoquinone molecule, and releases protons in the interior of the thylakoid membrane, and is also called water-plastoquinone oxido-reductase); *Cytochrome b/f* (Cyt *bf*) complex (that oxidizes reduced plastoquinone, reduces a copper protein plastocyanin (PC), and releases protons in the interior of the thylakoid membrane, and is called plastoquinol-plastocyanin oxido-reductase); *Photosystem I* (PS I, that oxidizes reduced plastocyanin and reduces $NADP^+$, to NADPH, and is called plastocyanin-ferredoxin oxido-reductase); and *ATP Synthase* (that uses the membrane potential and the proton gradient to produce ATP from ADP and inorganic phosphate). The membrane potential is formed and electron transport takes place when photosynthesis is simultaneously powered by light absorbed in both PS I and II leading to electron transfer from the inner side of the thylakoid membrane to the outer side of the membrane; this makes one side of the membrane more negative than the other. The reaction center Chls P680 (in PS II) and P700 (in PS I) are located on the inner side of the membrane. Photosynthesis starts by simultaneous excitation of P680 and P700. Excited P680 (P680*) and P700 (P700*) have energy resulting from light absorption. An electron is transferred from P700* to A_0 (another special Chl *a* molecule) producing oxidized P700 ($P700^+$) and reduced A_0 (A_0^-). At about the same time, an electron is transferred from P680* to a pheophytin (Pheo) molecule producing oxidized P680 ($P680^+$) and reduced Pheo ($Pheo^-$). These are the only steps where light energy is used to produce oxidation-reduction energy. The rest of the reactions are energetically downhill. $P700^+$ is reduced to P700 by receiving an electron that originates in $Pheo^-$, and is passed on to $P700^+$ via the following intermediates: from $Pheo^-$ to Q_A (a bound plastoquinone), to Q_B (another bound plastoquinone) to PQ (freely *mobile* plastoquinone) to an iron sulfur protein (FeS), to a cytochrome (Cyt *f*), to a freely mobile plastocyanin (PC), and finally to $P700^+$. On the other hand, an electron on A_0^- is passed on, ultimately, to the $NADP^+$ via several other intermediates (A_1, a phylloquinone, Fx, F_A and F_B, three iron-sulfur proteins, and Fd, ferredoxin). The missing electron on $P680^+$ is recovered, ultimately, from water molecules via an amino acid tyrosine (D1-Y-161, Y_z) and a manganese complex (Mn). Four such reactions (utilizing a total of 8 photons, 4 in PS II and 4 in PS I) are required to oxidize H_2O to $1O_2$ and reduce 2 $NADP^+$ to 2NADPH. Carotenoids are not known to play any role in the electron transport pathway of photosynthesis.

colleagues (Griffiths et al., 1955; Sistrom et al., 1956; Stanier, 1960; the participation of Germaine Cohen-Bazire in this work was acknowledged). Based on experiments with a blue-green mutant of *Rhodopseudomonas* (now *Rhodobacter) sphaeroides* that contained no colored carotenoids, it was suggested that 'the primary function of carotenoid pigments in phototrophs is to act as chemical buffers against photooxidation of other cell constituents by (B)Chl, thus conferring a high degree of immunity to endogenous photosensitization.' The mutant was unable to live normally. The mechanism of action was shown later to involve removal of singlet oxygen by carotenoids, and the formation of triplet states of carotenes (see reviews by Krinsky, 1968, 1971). We shall not discuss this function further. However, we note that Mimuro et al. (1995) have detected two β-carotene molecules in the reaction center of PS II

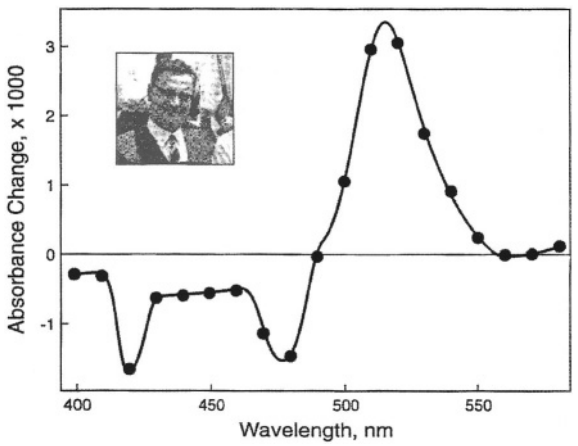

Fig. 9. Change in absorption spectrum of a *Chlorella* suspension upon irradiation with red light. This experiment, published by Duysens (1954), was done at the Carnegie Institute of Washington at Stanford, California. The 515 nm change was later associated with a shift of absorbance of some carotenoids, among other pigments, to longer wavelengths. Further, this change, on a nanosecond time scale, was shown to monitor the membrane potential component of the proton motive force created in the thylakoid membrane (also see Fig. 8). Inset shows a 1963 photograph of L. N. M. Duysens.

by fluorescence and linear dichroism spectroscopy. It was shown that the two β-carotene molecules in the reaction center of PS II are spectrally different and transfer excitation energy to Chl *a* at 77 K; one has an absorption band at 489 nm, and the other has bands at 506 and 467 nm. It is assumed that these β-carotene molecules must function to protect the reaction center Chls from damage. (Telfer et al., 1994). Further, Trebst and Depka (1997) have shown that β-carotene is essential for the assembly of the D1 protein into functional PS II.

One of the several mechanisms by which plants protect themselves against excess light is by dissipating excess energy as heat through the participation of the xanthophyll cycle and the pH gradient (see reviews by Horton et al., 1994, 1996; Demmig-Adams et al., 1996; Demmig-Adams and Adams, 1996; Gilmore, 1997; Gilmore and Govindjee, 1999, and Chapters 14, Demmig-Adams et al. and 15, Horton et al.). De-excitation of a molecule, excited by light, occurs by fluorescence, heat, excitation energy transfer, or photochemistry. At high light intensities, when photosynthesis is saturated, unusual photochemistry can take place that can lead to damage of the photosynthetic apparatus. This could be avoided if there were a mechanism to increase energy loss as heat or fluorescence. However, during exposure of plants to high light, Chl *a* fluorescence intensity has been shown to decrease (fluorescence quenching). One of the current suggestions is that excess light somehow promotes the formation of zeaxanthin from violaxanthin, with antheraxanthin as an intermediate. It is now generally believed that it is mostly zeaxanthin (or antheraxanthin) that removes the excess energy from the excited Chls and loses this energy as heat. The history of the xanthophyll cycle goes back to Sapozhnikov et al. (1957), who first observed that violaxanthin levels changed in light/dark or high light/low light treatments in Sakhlin buckwheat (*Polygonum sacchalinense* F. Schmidt), in cyclamen (*Cyclamen persicum* L), broad bean (*Vicia faba* L.) and medicinal dandelion (*Taraxacum officinale* L s.l). They thought that violaxanthin was converted into lutein and speculated on the possibility that this may have significance for oxygen evolution in photosynthesis. Yamamoto got involved at this stage and it was he who discovered the currently accepted stepwise and cyclical pathway, now known as the xanthophyll cycle (Yamamoto et al., 1962; Yamamoto, 1979). The stepwise pathway excluded the possibility of involvement in photosynthetic oxygen evolution. Further, the kinetics was too slow and Yamamoto showed soon thereafter that the effect of light was indirect. There have been many other researchers in this field that are also currently active. It was Barbara Demmig, Olle Björkman and their coworkers (Björkman, 1987: in this paper the author mentions two unpublished manuscripts of Demmig and Björkman; Demmig et al., 1987: work done in the pharmaceutical laboratory of Professor Czygan; Björkman and Demmig-Adams, 1994) who suggested that the excess energy is lost as heat in the antenna complexes, and related the phenomenon to the xanthophyll cycle. The concept that there is an increase in heat loss assumes that the observed decrease in fluorescence intensity is indeed a decrease in the fluorescence yield. A decrease in fluorescence intensity could also be due to a decrease in the absorption cross-section of the fluorescing component. While he was in my laboratory Adam Gilmore, who had earlier worked with Harry Yamamoto and Olle Björkman, made the measurements on the lifetime of Chl *a* fluorescence that directly measures the quantum yield of fluorescence (Gilmore et al., 1995, 1996, 1998). We established that in thylakoid samples there is a dimmer switch in

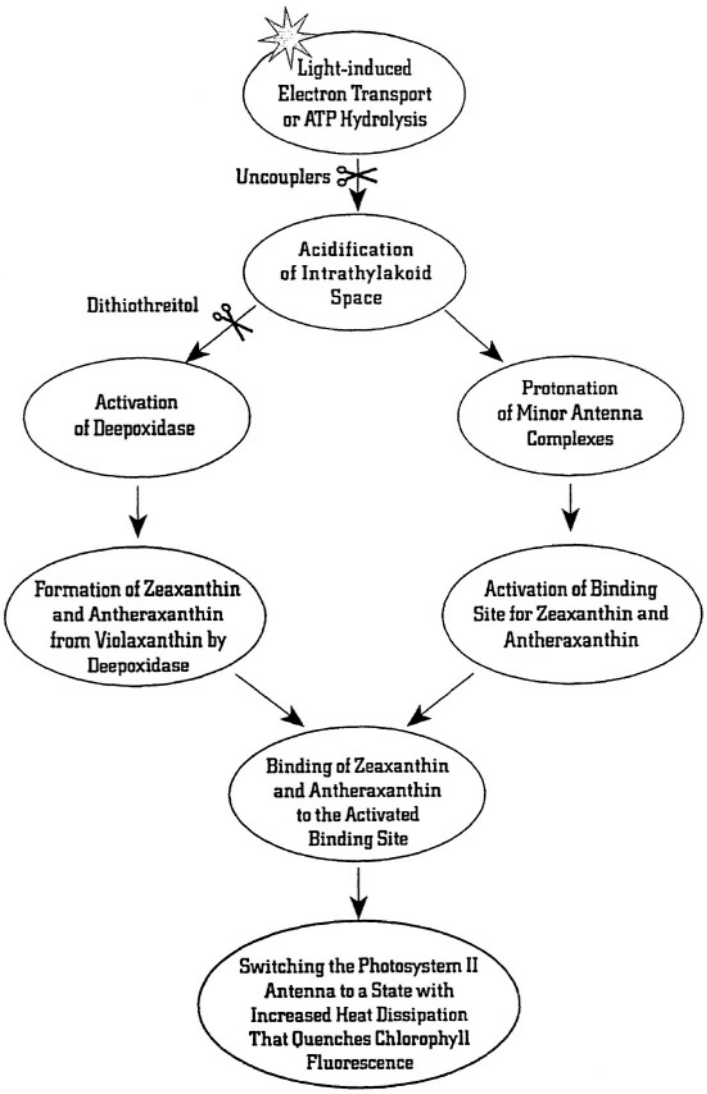

Fig. 10. One of the several schemes used to explain the mechanism of photoprotection by xanthophyll cycle pigments. It is suggested that, at high light intensities, when photosynthesis is saturated, there are excess protons in the lumen of the thylakoid (see Fig. 8) and these have a double function: (1) they protonate minor antenna complexes of PS II leading to the activation of a binding site for xanthophylls (right side of the diagram); and (2) they activate de-epoxidase allowing the conversion of violaxanthin into antheraxanthin and then into zeaxanthin (left side of the diagram). The two events together then lead to the quenching of Chl a fluorescence through dissipation of energy as heat. The scheme shown here was modified from Gilmore and Govindjee (1999).

which the fraction of a long-lifetime component (a 2 ns component) of fluorescence decreases with a concomitant increase in the fraction of a short-lifetime fluorescence component (a 0.4 ns component). The latter component was suggested to have increased dissipation of energy as heat because, in these experiments, photochemistry was blocked by the use of a herbicide, diuron. It is also now clear that both a proton gradient (or a low internal pH) and the presence of zeaxanthin (or antheraxanthin) are required for this process. The protons are suggested to have a dual role: (i) activation of de-epoxidase that leads to increased conversion of violaxanthin into zeaxanthin, and (ii) conformational changes that lead to efficient binding of zeaxanthin or (antheraxanthin) on antenna complexes where dissipation of energy as heat takes place (Fig. 10). Whether the heat loss occurs via zeaxanthin directly, as stated above, or is induced in Chl by association with zeaxanthin remains an open question. The possibility that S_1 state of zeaxanthin (that has not yet been directly observed) lies below the S_1 state of Chl *a* (Frank et al. 1994; Owens, 1996)

is a grand and a reasonable hypothesis. It makes it easy to accept that Chl *a* can transfer excitation energy to zeaxanthin. Several investigators have now established that the photoprotection mechanism need not require light-harvesting complex IIb (Gilmore et al., 1996; Briantais et al., 1996). Thus, it was suggested that the inner antenna complexes are involved. Bassi et al. (1993) have shown that the xanthophyll-cycle pigments are preferentially associated with the inner antenna Chl *a* complexes (CP) 26 and 28. This idea was elegantly supported by Crofts and Yerkes (1994) when they compared the amino acid sequences of the various light harvesting complexes (LHCIIb, CP26, CP28, etc). Current research on the mutants of *Chlamydomonas reinhardtii* and *Arabidopsis thaliana*, that are blocked in the interconversions of the xanthophyll-cycle pigments, are providing information on the molecular mechanism of the photoprotection process (Niyogi et al., 1997a,b, 1998; Pogson et al., 1996, 1998). A possibility has been raised that lutein may also be important in the mechanism of photoprotection in *Chlamydomonas,* but not in *Arabidopsis.*

Polivka et al. (1999) have recently reported a direct observation of the energy gap between the S_1 and S_2 states of violaxanthin and zeaxanthin and from that deduced the energy of their S_1 states. The implication to the mechanism of photoprotection will soon be investigated by several research groups.

V. Conclusions

What is certain is that both β-carotene and the xanthophyll fucoxanthin transfer excitation energy to Chl *a*; β-carotene, in addition, protects against photochemical damage of the reaction centers, and the xanthophyll zeaxanthin protects plants against excess light by initiating reactions, in combination with those initiated by pH gradient, that lead to loss of excess energy as heat. Much research is needed to prove the roles of other carotenoids (e.g., lutein, violaxanthin, and others). It is however currently assumed that violaxanthin acts as a light harvester, i.e., transfers energy to Chl *a,* and that lutein may indeed substitute for zeaxanthin in some systems. Research on both the mechanism of excitation energy transfer from Chls to carotenoids and vice versa is ongoing. The availability of structures at atomic levels is certainly important for this purpose. For example, the atomic level structure of the reaction center of photosynthetic bacteria shows a carotenoid (1,2-dihydroneurosporene, Deisenhofer and Michel, 1989). In addition, the peridinin-Chl *a* complex from

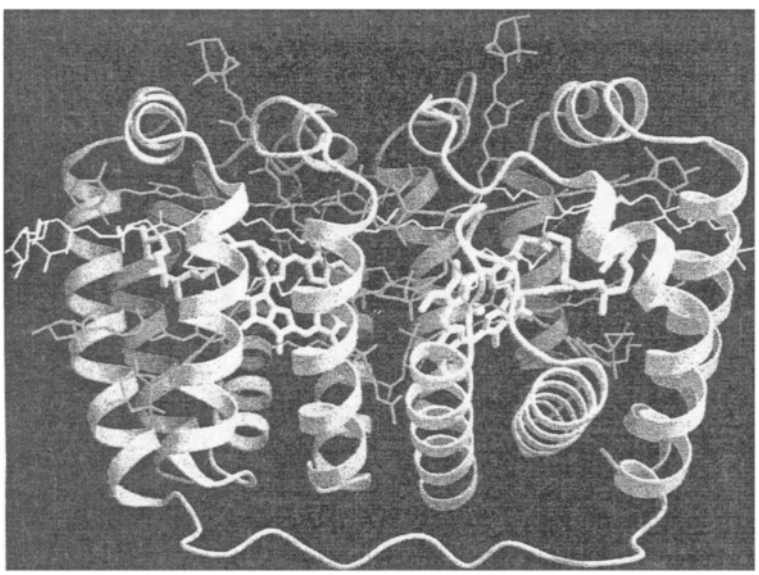

Fig. 11. A 2 Å resolution structure of a peridinin Chl *a* complex of a dinoflagellate. In the color version, the eight peridinin molecules are shown in red, whereas the two Chls are in green. A lipid molecule is shown in blue, and two proteins are shown in gray The proximity of peridinin molecules to each other and to Chl *a* molecules explains the efficient excitation energy transfer from peridinin to Chl *a,* observed by Haxo et al. (1976). The diagram is reproduced from Hoffman et al. (1996). See also Color Plate 2.

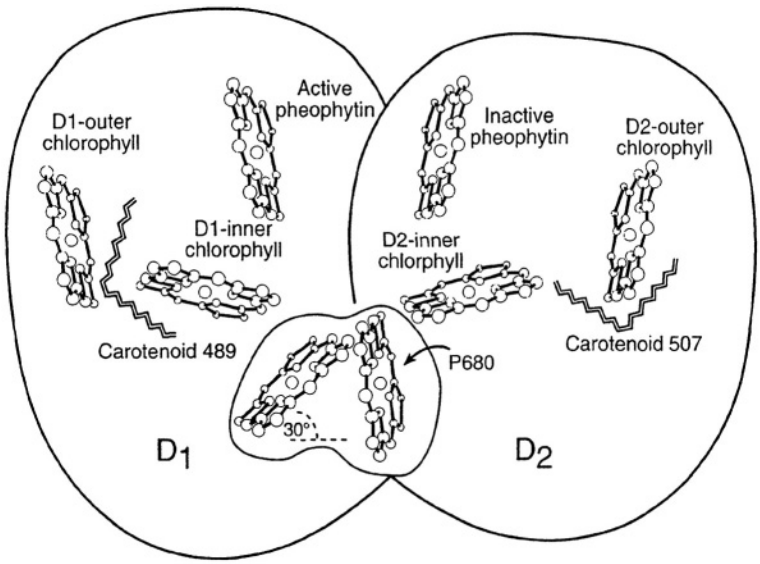

Fig. 12. A diagrammatic model of the arrangement of two carotenes (labeled as carotenoid 489 and carotenoid 507) in the reaction center molecule of PS II. P680 is the reaction center Chl *a* dimer, whereas D1 and D2 are the two proteins where the chromophores are housed. The scheme shown here was modified and adapted from Mimuro et al. (1995). For a more complete model of Photosystem II reaction center and a different view of the arrangement of carotenoids, see Xiong et al. (1998).

Amphidinium carterae also shows precisely where the carotenoid peridinin is located in this antenna complex (Hofmann et al., 1996; Fig. 11). Kühlbrandt et al. (1994) have provided the atomic level structure of LHCIIb, the major light harvesting Chl *a*/Chl *b* complex of plants and green algae; this has allowed the rationalization of the proposed mechanisms of excitation energy transfer among the Chls.

In my laboratory, Xiong et al. (1996, 1998) have produced a hypothetical structural model of PS II reaction center where the two β-carotenes molecules are parallel to each other, although there is reason to believe that they may be perpendicular to each other (see e.g., Mimuro et al., 1995; Fig. 12). The entire field seems to be still in its infancy and the present book should help encourage further research to unfold the relationship between the molecular structure and the molecular function of all the carotenoids.

Acknowledgments

Drs. Harry Yamamoto and Barbara Demmig-Adams have provided important information on Section IV of this chapter; however, all omissions and errors are mine. I am thankful to all of my current photosynthesis colleagues at the University of Illinois at Urbana for social and intellectual support. In particular, I owe deep gratitude to Drs. John Whitmarsh, Colin Wraight, Don Ort and Tony Crofts for being there for intellectual interactions. Photosynthesis training of graduate students and post-doctoral associates at Urbana was recently supported by NSF DBI 96-02240.

References

Anderson JM (1983) Chl-protein complexes of a *Codium* species, including a light- harvesting siphonaxanthin-Chl *a*/b-protein complex, an evolutionary relic of some chlorophyta. Biochim Biophys Acta 724: 370–380

Arnold WA (1991) Experiments. Photosynth Res 27: 73–82

Arnold W and Meek ES (1956) The polarization of fluorescence and energy transfer in grana. Arch Biochem Biophys 60: 82–90

Arnold W and Oppenheimer JR (1950) Internal conversion in the photosynthetic mechanism of blue-green algae. J Gen Physiol 33: 423–435

Bannister TT (1972) The careers and contributions of Eugene Rabinowitch. Biophys J 12: 707–718

Barrett J and Anderson JM (1980) The P–700-Chl *a*-protein complex and two major light-harvesting complexes of *Acrocarpia paniculata* and other brown algae. Biochim Biophys Acta 590: 309–323

Bartley GE and Scolnik PA (1995) Plant carotenoids: Pigments for photoprotection, visual attraction and human health. The Plant Cell 7: 1027–1038

Bassi R, Pineau B, Dainese P and Marquardt J (1993) Carotenoid-

binding proteins of Photosystem II. Eur J Biochem 212: 297–303

Berzelius J (1837a) Über de gelbe Farbe der Blaetter im Herbste. Ann der Pharm 21: 257–262

Berzelius J (1837b) Einige Untersuchungen ueber die Farbe, welche das Laub verschiedener Baumgattungen im Herbste vor dem Abfallen annimmt. (Poggendorf's) Annalen der Physik und Chemie (Liebig) 42: 422–433

Björkman O (1987) High irradiance stress in higher plants and interaction with other stress factors. In: Biggins J (ed) Progress in Photosynthesis Research, Volume 4, pp 11–18. Martinus Nijhoff, Dordrecht

Björkman O and Demmig-Adams B (1994) Regulation of photosynthetic light energy capture, conversion and dissipation in leaves of higher plants. In: Schulze E-D and Caldwell M (eds) Ecological Studies, Vol 100, pp 17–47. Springer Verlag, Berlin

Bogert MT (1938) Carotenoids. In: Gilman A (ed) Organic Chemistry, Vol II, p 1138. Wiley, New York

Briantais J-M, Dacosta J, Goulas Y, Ducruet JM, Moya I (1996) Heat stress induces in leaves an increase of the minimum level of chlorophyll fluorescence, F_0—a time resolved analysis. Photosynth Res 48: 189–196

Britton G and Goodwin TW (eds) (1982) Carotenoid Chemistry and Biochemistry. Pergamon Press, Oxford

Britton G, Liaaen-Jensen S and Pfander HP (eds) (1995) Carotenoids, Vol I and II, Birkhäuser Verlag, Basel

Brody SS (1995) We remember Eugene (Rabinowitch and his laboratory, during the fifties). Photosynth Res 43: 67–74

Cario G and Franck J (1923) Über sensibilisierte Fluoreszenz von Gasen. Z Phys 17: 202– 212

Cho F and Govindjee (1970a) Low-temperature (4–77 K) spectroscopy of *Chlorella*: Temperature dependence of energy transfer efficiency. Biochim Biophys Acta 216: 139–150

Cho, F and Govindjee (1970b) Low temperature (4–77 K) spectroscopy of *Anacystis*: Temperature dependence of energy transfer efficiency. Biochim Biophys Acta 216: 151–161

Cogdell RJ (1978) Carotenoids in photosynthesis. Phil Trans Roy Soc London Series B 284: 569–579

Cogdell RJ (1985) Carotenoid-bacteriochlorophyll interactions. Springer Ser Chem Phys 42: 62–66

Cogdell RJ and Frank HA (1987) How Carotenoids function in photosynthetic bacteria. Biochim Biophys Acta 895: 63–79

Condon EU (1926) A theory of intensity distribution in band systems. Phys Rev 28: 1182–1201

Condon EU (1947) The Franck-Condon Principle and Related Topics. Am J Phys 15: 365–374

Crofts A R and Yerkes CT (1994) A molecular mechanism for q_E quenching. FEBS Lett 352: 265–270

de Grooth BG, van Grondelle R, Romijn JC and Pulles MPJ (1979) The mechanism of reduction of the ubiquinone pool in photosynthetic bacteria at different redox potential. Biochim Biophys Acta 503: 480–490

Deisenhofer J and Michel H (1989) The photosynthesis reaction center from the bacterium *Rhodopseudomonas viridis.* EMBO J8: 2149–2170

Demmig B, Winter K, Krueger A and Czygan FC (1987) Photoinhibition and zeaxanthin formation in intact leaves. Plant Physiol 84: 218–224

Demmig-Adams B and Adams WW III (1996) The role of xanthophyll cycle carotenoids in the protection of photosynthesis. Trends Plant Sci 1: 21–26

Demmig-Adams B, Gilmore A and Adams WW III (1996) In vivo functions of carotenoids in plants. FASEB J 10: 403–412

Dexter DL (1953) A theory of sensitized luminescence in solids. J Chem Phys 21: 836–850

Dutton HJ (1997) Carotenoid-sensitized photosynthesis: Quantum efficiency, fluorescence and energy transfer. Photosynth Res 52: 175–185

Dutton HJ and Manning (1941) Evidence for carotenoid-sensitized photosynthesis in the diatom *Nitzschia closterium.* Am J Bot 28: 516–526

Dutton HJ, Manning WM and Duggar BM (1943) Chl fluorescence and energy transfer in the diatom *Nitzscia closterium.* J Phys Chem 47: 308–317

Duysens LNM (1951) Transfer of light energy within the pigment systems present in photosynthesizing cells. Nature 168: 548–550

Duysens LNM (1952) Transfer of excitation energy in photosynthesis. Doctoral thesis. State University at Utrecht, Drukkerij en uitgevers-maatschappij v/h Kemink en zoon NV, Domplein 2, Utrecht

Duysens LNM (1954) Reversible changes in the absorption spectrum of *Chlorella* upon irradiation. Science 120: 353–354

Duysens LNM (1989) The discovery of the two photosynthetic systems: A personal account. Photosynth Res 21; 61–79

Emerson R and Arnold WA (1932a). A separation of the reactions in photosynthesis by means of intermittent light. J Gen Physiol 15: 391–420.

Emerson R and Arnold WA (1932b)The photochemical reaction in photosynthesis. J Gen Physiol 16: 191–205.

Emerson R and Lewis CM (1942) The photosynthetic efficiency of phycocyanin in *Chrococcus* and the problem of carotenoid participation in photosynthesis. J Gen Physiol 25: 579–595

Emerson R and Lewis CM (1943) The dependence of quantum yield of *Chlorella* photosynthesis on wavelength of light. Am J Bot 30: 165–178

Emerson R and Rabinowitch E (1960). Red drop and role of auxiliary pigments in photosynthesis. Plant Physiol 35: 477–485.

Emerson R, Chalmers RV and Cederstrand CN (1957) Some factors influencing the long-wave limit of photosynthesis. Proc Natl Acad Sci USA 43: 133–143

Engelmann TW (1883) Farbe und Assimilation. Botan Zeitung 41: 1–16

Engelmann TW (1884) Untersuchungen ueber die quantitativen bezieschungen zwischen Absorption des Lichts und Assimilation in Pflanzenzellen. Bot Zeit 42: 81–96

Firth JB (transl) (1909) The Letters of the Younger Pliny. Walter Scott, Ltd., London

Förster Th (1946) Energiewanderung und Fluoreszenz. Naturwissenschaften 33: 166–175

Förster Th (1948) Zwischenmolekulare Energiewanderung und Fluoreszenz. Ann Physik [6] 2: 55–75 (English translation 'Intermolecular energy migration and fluorescence' is available from Professor RS Knox, Department of Physics and Astronomy, University of Rochester, Rochester, New York)

Förster Th (1965) Delocalized excitation and excitation transfer. In: Sinanoglu O (ed) Part II.B. 1 of Modern Quantum Chemistry: Istanbul lectures. Part III. Action of Light and Organic Crystals, pp. 93–137. Academic Press, New York

Fork DC and Amesz J (1969) Action spectra and energy transfer

in photosynthesis. Ann Rev Plant Physiol 20: 305–328
Franck J (1925) Elementary processes of photochemical reactions. Trans Faraday Soc 21: 536–542
Franck J (1927) Über eine Rotverschiebung der Resonanzfluoreszenz durch vielfach wiederholte Streuung. Naturwiss 15: 236–238
Frank HA and Cogdell RJ (1993) Photochemistry and functions of carotenoids. In: Young A and Britton G (eds) Carotenoids in Photosynthesis, pp. 252–326. Springer Verlag, London
Frank HA, Violette CA, Trautman JK, Shreve AP, Owens TG and Albrecht AC (1991) Carotenoids in photosynthesis: Structure and photochemistry. Pure Appl Chem 63: 109–114
Frank HA, Cua A, Chynwat V, Young A, Gosztola D and Wasielewski M R (1994) Photophysics of carotenoids associated with the xanthophyll cycle in photosynthesis. Photosynth Res 41:389–395
Fremy E (1860) Recherches sur la matière colorante verte des feuilles. Compt Rend 50: 405–412
French CS and Young VMK (1952) The fluorescence spectra of red algae and the transfer of energy from phycoerythrin to phycocyanin and Chl. J Gen Physiol 35: 873–890
Gaffron H and Wohl K (1936) Zur Theorie der Assimilation. Naturwissenschaften 24: 81–90; 103–107
Gasanov R. Abilov ZK, Gazanchyan, RM, KurbonovaUM, Khanna, R and Govindjee (1979) Excitation energy transfer in Photosystems I and II from grana and in Photosystem I from stroma lamellae, and identification of emission bands with pigment-protein complexes at 77K. Z Pflanzenophysiol 95: 149–169
Gilmore A (1997) Mechanistic aspects of xanthophyll cycle-dependent photoprotection in higher plant chloroplasts and leaves. Physiol Plant 99: 197–205
Gilmore A and Govindjee (1999) How higher plants respond to excess light: Energy dissipation in Photosystem II. In: Singhal GS, Renger G, Sopory S, Irrgang K-D and Govindjee (eds) Concepts in Photobiology: Photosynthesis and Photomorphogenesis. Narosa Publishers, New Delhi/ Kluwer Academic Publishers, Dordrecht, in press
Gilmore AM, Hazlett TL and Govindjee (1995) Xanthophyll cycle dependent quenching of Photosystem II Chl *a* fluorescence: Formation of a quenching complex with a short fluorescence lifetime. Proc Nat Acad Sci USA 92: 2273–2277
Gilmore AM, Hazlett TL, Debrunner PG and Govindjee (1996) Photosystem II chlorophyll a fluorescence lifetimes are independent of the antenna size differences between barley wild-type and chlorina mutants: Comparison of xanthophyll dependent quenching and photochemical quenching. Photosynth Res 48: 171–187
Gilmore AM, Shinkarev V, Hazlett TL and Govindjee (1998) Quantitative analysis of the effects of intrathylakoid pH and xanthophyll cycle pigments on chlorophyll *a* fluorescence lifetime distributions and intensity in thylakoids. Biochemistry 37: 13582- 13593
Goedheer JHC (1969a) Carotenoids in blue-green and red algae. In: Metzner H (ed) Progress in Photosynthesis Research, Vol II. Plastid Pigments, Electron Transfer, pp 811–817. H. Laupp Jr., Tübingen
Goedheer JHC (1969b) Energy transfer from carotenoids to chlorophyll in blue-green, red and green algae and greening bean leaves. Biochim Biophys Acta 172: 252–265
Goedheer JC (1972) Fluorescence in relation to photosynthesis. Ann Rev Plant Physiol 23: 87–112
Goodwin TW (1952) The Comparative Biochemistry of Carotenoids. Chapman and Hall, London
Goodwin TW (ed) (1976) Chemistry and Biochemistry of Plant Pigments. Academic Press, New York
Govindjee (1995) Sixty-three years since Kautsky: Chl a fluorescence. Aust J Plant Physiol 22: 131–160
Govindjee and Govindjee R (1965) Action spectra for the appearance of difference absorption bands at 480 and 520 nm in illuminated *Chlorella* cells and their possible significance to a two-step mechanism of photosynthesis. Photochem Photobiol 4: 675- 683
Govindjee and Rabinowitch E (1960) Two forms of Chl *a* in vivo with distinct photochemical function. Science 132: 355–356
Govindjee and Satoh K (1986) Fluorescence properties of Chl *b*- and Chl *c*-containing algae. In: Govindjee, Amesz J and Fork DC (eds) Light emission by plants and bacteria, pp. 497–537. Academic Press, Orlando
Govindjee, Ichimura S, Cederstrand C and Rabinowitch E (1960) Effect of combining far-red light with shorter wave light on the excitation of fluorescence in *Chlorella.* Arch Biochem Biophys 89: 322–323
Griffiths M, Sistrom WR, Cohen-Bazire G and Stanier RY (1955) Function of carotenoids in photosynthesis. Nature 176: 1211–1214
Haxo F and Blinks LR (1950) Photosynthetic action spectra of marine algae. J Gen Physiol 33: 389–422
Haxo FT, Kychia JH, Somers GH, Bennett A and Siegelman HS (1976) Peridinin-Chl *a* proteins of the dinoflagellate *Amphidinium carterae* (Plymouth 450). Plant Physiol 57: 297–303
Hirschberg J and Chamovitz D (1994) Carotenoids in cyanobacteria. In Bryant D (ed) The Molecular Biology of Cyanobacteria, pp. 559–579. Kluwer Academic Publishers, Dordrecht
Hofmann E, Wrench PM, Sharples FP, Hiller RG, Welte W and Dietrichs K (1996) Structural basis of light harvesting by carotenoids-peridinin–chlorophyll protein from *Amphidinium carterae.* Science 272: 1788–1791
Horton P, Ruban AV and Walters RG (1994) Regulation of light harvesting in green plants: Indication by nonphotochemical quenching of Chl fluorescence. Plant Physiol 106: 415–420
Horton P, Ruban AV and Walters RG (1996) Regulation of light harvesting in green plants. Ann Rev Plant Physiol Plant Mol Biol 47: 655–684
Isler O (1971) Carotenoids. Birkhäuser Verlag, Basel and Stuttgart
IUPAC and IUB (1971) IUPAC commission on the nomenclature of organic chemistry and IUPAC-IUB commission on biochemical nomenclature: Tentative rules for the nomenclature of carotenoids. Biochemistry 10: 4827–4837
IUPAC and IUB (1975) Nomenclature of carotenoids (Recommendations 1974). Biochemistry 14: 1803–1804
Jablonski A Z (1935) Über den Mechanismus des Photolumineszenz von Farbstoffphosphoren. Zs Phys 94: 38–46
Jackson JB and Crofts AR (1969) The high energy state in chromatophores from *Rhodopseudomonas sphaeroides.* FEBS Lett 4: 185–189
Jensen A and Liaaen-Jensen S (1959) Quantitative paper chromatography of carotenoids. Acta Chem Scand 13: 1863–1868
Junge W and Witt HT (1968) On the ion transport system of

photosynthesis—Investigations on a molecular level. Z Naturforsch 23b: 244–254

Kageyama A, Yokohama Y, Shimura S and Ikawa T (1977) An efficient excitation energy transfer from a carotenoid, siphonaxanthin to Chl *a* observed in a deep-water species of chlorophycean seaweed. Plant Cell Physiol 18: 477–480

Kamen MD (1986) On creativity of eye and ear: A commentary on the career of TW Engelmann. Proc Amer Philos Sci 130: 232–246

Karrer P (1934) Über Carotinoidfarbstoffe. Z Angew Chem 42: 918–924

Karrer P and Helfenstein A (1933) Plant Pigments. Ann Rev Biochem2:397–418

Karrer P and Jucker E (1948) Carotinoide. Birkhäuser, Basle (English translation, 1950, by Braude EA, Elsevier, Amsterdam)

Karrer P and Oswald A (1935) Carotinoide aus den Staubbeuteln von Lilium trignirum. Ein neues carotinoid Antheraxanthin. Helv Chim Acta 18: 1303–1305

Knox RS (1975) Excitation energy transfer and migration: theoretical considerations. In : Govindjee (ed) Bioenergetics of Photosynthesis, pp. 183–221. Academic Press, New York

Knox RS (1996) Electronic excitation transfer in the photosynthetic unit: Reflections on work of William Arnold. Photosynth Res 48: 35–39

Kramer HJM, Amesz J and Rijgersberg CP (1981) Excitation spectra of chlorophyll fluorescence in spinach and barley chloroplasts at 4 K. Biochim Biophys Acta 637: 272–277

Kohl FG (1902) Untersuchungen ueber das Carotin und seine physiologische Bedeutung in der Pflanze. Borntraeger, Leipzig

Koyama FY (1991) Structures and functions of carotenoids in photosynthetic systems. J Photochem Photobiol B9: 265–280

Krinsky NI (1968) The protective function of carotenoid pigments. In: Giese AC (ed) Photophysiology, Vol 3, pp 123–195. Academic Press, New York

Krinsky N (1971) Function (of carotenoids) In: Isler O (ed) Carotenoids, pp. 670–716. Birkhauser Verlag, Basel and Stuttgart

Krinsky NI (1979) Carotenoid protection against photooxidation. Pure Appl Chem 51 : 649–660

Kühlbrandt W, Wang DN and Fujiyoshi Y (1994) Atomic model of plant light harvesting complex by electron crystallography. Nature 367: 614–621

Kühn R (1935) Plant Pigments. Ann Rev Biochem 4: 479–496

Lederer E (1934) Les carotinoides des plantes. Hermann et Cie, Paris

Liaaen–Jensen S (1978) Chemistry of carotenoid pigments. In: Clayton R and Sistrom WR (eds) The Photosynthetic Bacteria, pp 233–247. Plenum Press, New York

Lubimenko V (1927) Recherches sur les pigments des plastes et sur la photosynthese. Rev Gen Botan 39: 547–559

MacKinney G (1935) Leaf carotenes. J Biol Chem 111: 75–84

Mimuro M and Katoh T (1991) Carotenoids in photosynthesis—absorption, transfer and dissipation of light energy. Pure Appl Chem 63: 123–130

Mimuro M, Tomo T, Nishimura Y, Yamazaki I and Satoh K (1995) Identification of a photochemically inactive pheophytin molecule in the spinach D1-D2-cyt *b*559 complex. Biochim Biophys Acta 1232: 81–88

Mitchell P (1961) Coupling of phosphorylation to electron and proton transfer by a chemiosmotic type of mechanism. Nature 191: 144–148

Montfort C (1936) Carotinoide, Photosynthese und Quantentheorie. Jahrb Wiss Botan 83: 725–772

Montfort C (1940) Die Photosynthese brauner Zellen im Zusammenwirken von Chlorophyll und Carotinoiden. Zeit Physik Chem A 186: 57–93

Niyogi KK, Björkman O and Grossman AR (1997a) *Chlamydomonas* xanthophyll cycle mutants identified by video imaging of Chl fluorescence quenching. Plant Cell 9: 1369- 1380

Niyogi KK, Björkman O and Grossman AR (1997b) The roles of specific xanthophylls in photoprotection. Proc Natl Acad Sci USA 94: 14162–14167

Niyogi KK, Grossman and Björkman O (1998) *Arabidopsis* mutants define a central role for the xanthophyll cycle in the regulation of photosynthetic energy conversion. Plant Cell 10: 1121–1134

Oppenheimer JR (1941) Internal conversion in photosynthesis. Phys Rev 60: 158

Owens TG (1996) Processing of excitation energy by antenna pigments. In: Baker NR (ed) Photosynthesis and the Environment, pp 1–23. Kluwer Academic, Dordrecht

Packer L (ed) (1992a) Carotenoids, part A. Methods Enzymol 213: 1–538

Packer L (ed) (1992b) Carotenoids, part B. Methods Enzymol 214: 1–468

Palmer LS (1922) Carotenoids and Related Pigments. American Chemical Society Monographs Ser, Chemical Catalog, New York

Palmer LS (1934) The biological and chemical nomenclature of the carotenoids. Science 79: 488–490

Pearlstein RM (1982) Chlorophyll singlet excitons. In: Govindjee (ed) Photosynthesis. Vol I, Energy Conversion by Plants and Bacteria, pp 293–330. Academic Press, New York

Perrin F (1926) Polarisation de la lumiere de fluorescence. Vie moyenne des molecules dans l'etat excité. J Physique 7: 390–401

Perrin F (1929) La fluorescence des solutions: Induction moleculaire, polarisation et duree d'emission, photochemie. Annales de Physique 12: 169- 275

Platt JR (1959) Carotene-donor-acceptor complexes in photosynthesis. Science 129: 372–374

Pogson B, McDonald KA, Truong M, Britton G and DellaPenna D (1996) Arabidopsis carotenoid mutants demonstrate that lutein is not essential for photosynthesis in higher plants. Plant Cell 8: 1627–1639

Pogson B, Niyogi KK, Björkman O and Dellapenna D (1998) Altered xanthophyll compositions adversely affect chlorophyll accumulation and nonphotochemical quenching in Arabidopsis mutants. Proc Natl Acad Sci USA 95: 13324–13329

Polivka T, Herek JL, Zigmantas D, Åkerlund H-E and Sundström V (1999) Direct observation of the (forbidden) S_1 state in carotenoids. Proc Natl Acad Sci USA 96: 4914–4917

Rabinowitch E (1945) Photosynthesis and Related Processes. Vol. I. Chemistry of Photosynthesis, Chemosynthesis and Related Processes in Vitro and in Vivo. (See scheme 7.V on p. 162.) Interscience Publishers Inc., New York

Rabinowitch E (1951) Photosynthesis and Related Topics, Vol. II, Part 1, Spectroscopy and fluorescence; Kinetics of Photosynthesis. Interscience Publishers Inc., New York

Rabinowitch E (1956)Photosynthesis and Related Processes. Vol. II. Part 2. Kinetics of Photosynthesis (continued); Addenda to Vol. I and Vol. II, Part I. (See p. 1862, paragraph 2.)

Interscience Publishers Inc., New York
Rabinowitch E (1961) Robert Emerson. Nat Acad Sci USA Biographical Memoirs. 35: 112–131
Sapozhnikov DI, Krasovskaya TA and Maevskaya AN (1957) Change in the interrelationship of the basic carotenoids of the plastids of green leaves under the action of light. Dokl Akad Nauk SSSR (English Translation) 113: 465–167
Schuett F (1890) Über Peridineen farbstoffe. Ber Deutsch Bot Ges 8: 9–32
Siefermann-Harms D (1987a) The light-harvesting and protective functions of carotenoids in photosynthetic membranes. Physiol Plant 69: 561–568
Siefermann-Harms D (1987b) Carotenoids in photosynthesis I. Location in photosynthetic membranes and light-harvesting function. Biochim Biophys Acta 811: 325–355
Siefermann-Harms, D and Ninnemann, H (1982) Pigment organization in the light- harvesting Chl-*a/b* protein complex of lettuce chloroplasts. Evidence obtained from protection of the Chls against proton attack and from excitation energy transfer. Photochem Photobiol 35: 719–731.
Sistrom WR, Griffiths M and Stanier RY (1956) The biology of a photosynthetic bacterium which lacks colored carotenoids. J Cell Comp Physiol 48: 473–515
Smith JHC (1930) The yellow pigments of green leaves: Their chemical constitution and possible function in photosynthesis. Contributions to Marine Biology, pp. 145–160. Stanford University, Stanford
Song PS, Koka P, Prezelin B and Haxo F (1976) Molecular topology of the photosynthetic light-harvesting pigment complex, peridinin-Chl *a*-protein, from marine dinoflagellates. Biochemistry 15: 4422–4427
Stanier RY (1960) Carotenoid pigments: Problems of synthesis and function. The Harvey Lectures 54: 219- 255
Strehler BL (1957) Some energy transduction problems in photosynthesis. In: Rudnick D (ed) Rhythmic and Synthetic Processes in Growth, pp 171–199. Princeton University Press, Princeton
Stokes GG (1852) On the change of refrangibility of light. Phil Trans Roy Soc London 142: 463–562
Strain HH (1938) Leaf Xanthophylls. Carnegie Institute of Washington Publication No. 490, Stanford
Strain HH, Manning WM and Hardin G (1944) Xanthophylls and carotenes of diatoms, brown algae, dinoflagellates and sea anemones. Biol Bull 86: 169–191
Stryer L (1978) Fluorescence energy transfer as a spectroscopic ruler. Ann Rev Biochem 467: 819–846
Stryer L and Haugland RP (1967) Energy transfer: A spectroscopic ruler. Proc Nat Acad Sci USA 58: 719–726
Tanada T (1951) The photosynthetic efficiency of carotenoid pigments in *Navicula minima.* Am J Bot 38: 276–283
Telfer A, Dhami S, Bishop SM, Phillips D and Barber J (1994) Beta-carotene quenches singlet oxygen formed by isolated Photosystem II reaction centers. Biochemistry 33: 14469–14474
Trebst A and Depka B (1997) Role of carotene in the rapid turnover and assembly of Photosystem II in *Chlamydomonas reinhardtii.* FEBS Lett 400: 359–362
Tswett M (1906) Adsorptionsanalyse und Chromatographische Methode. Anwendung auf die Chemie des Chlorophylls. Ber Deutsch Botan Ges 24: 384- 393
Tswett M (1911) Über den makro-und microchemischen Nachweis des Carotins. Ber Deut Botan Ges 29: 630–636
Van Grondelle R and Amesz J (1986) Excitation energy transfer in photosynthetic systems. In: Govindjee, Amesz J and Fork DC (eds) Light Emission by Plants and Bacteria, pp 191–223. Academic Press, Orlando
Van Grondelle R, Dekker JP, Gilbro T and Sundström V (1994) Energy transfer and trapping in photosynthesis. Biochim Biophys Acta 1187: 1–65
Van Niel CB and Smith JHC (1935) Studies on the pigments of the purple bacteria. I: On spirilloxanthin, a component of the pigment complex of *Spirillum rubrum.* Arch Mikrobiol 6: 219–229
Van Norman RW, French CS and MacDowall FDH (1948) The absorption and fluorescence spectra of two red marine algae. Plant Physiol 23: 455–466
Vermeulen D, Wassink EC and Reman GH (1937) On the fluorescence of photosynthesizing cells. Enzymologia 4: 254–268
Wackenroder H W F (1831) Über das oleum rad. Danci aethereum, das Carotin, den Carotlenzucher und den officinellum succus Danci. Mag Pharm 33: 144 et seq
Warburg O and Negelein E (1923) Über den Einfluss der Wellenlänge auf den Energie Umsatz bei der Kohlensaeureassimilation. Z Phys Chem 106: 191–216
Wassink EC and Kersten JAH (1945) Photosynthesis and fluorescence of the chlorophylls of diatoms. Enzymologia 11: 282–312
Wassink EC and Kersten JAH (1946) Observations sur le spectre d'absorption et sur le role des carotenoides dans la photosynthèse des diatomes. Enzymologia 12: 3–32
Willstädt H (1934) Carotinoide, Bakterien- und Pilzfarbstoffe. Stuttgart
Wilstätter R and Stoll A (1913) Unterssuchungen über chlorophyll. Springer, Berlin (American edition, 1928)
Witt HT (1975) Energy conservation in the functional membrane. In: Govindjee (ed) Bioenergetics of Photosynthesis, pp 493–554. Academic Press, New York
Wolff C, Buchwald H-E, Rüppel, Witt K and Witt HT (1969) Rise time of the light-induced electrical field across the function membrane of photosynthesis. Z Naturforsch B 24: 1038–1041
Xiong J, Subramaniam S and Govindjee (1996) Modeling of the D1/D2 proteins and cofactors of the Photosystem II reaction center. Protein Sci 5: 513–532
Xiong J, Subramaniam S and Govindjee (1998) A knowledge-based three dimensional model of the Photosystem II reaction center of *Chlamydomonas reinhardtii.* Photosynth Res 56: 229–254
Yamamoto HY (1979) Biochemistry of the violaxanthin cycle in higher plants. Pure Appl Chem 51: 639–648
Yamamoto HY and Bassi R (1996) Carotenoids: Localization and function. In: Ort DO and Yocum CF (eds) Oxygenic Photosynthesis: The Light Reactions, pp 539–563. Kluwer Academic, Dordrecht
Yamamoto HY, Nakayama TOM and Chichester CO (1962) Studies on the light and dark interconversion of leaf Xanthophylls. Arch Biochem Biophys 97: 168–173
Zechmeister L (1934) Carotinoide, ein biochemischer Berichte über pflanzliche und tierische Polyenfarbstoffe. Springer Verlag, Berlin
Zechmeister L (1962) Cis-trans Isomeric Carotenoids, Vitamins A and Arylpolyenes. Springer Verlag, Vienna and Berlin

This page intentionally left blank

Chapter 2

Carotenoid Synthesis and Function in Plants: Insights from Mutant Studies in *Arabidopsis thaliana*

Dean DellaPenna
Department of Biochemistry/200, University of Nevada-Reno, Reno, NV 89557, U.S.A.

Summary

Carotenoids are integral components of higher plant photosystems and their composition in photosynthetic plant tissues (lutein, β-carotene, violaxanthin and neoxanthin) is remarkably conserved throughout evolution. Carotenoids perform a variety of critical functions including acting as structural components of LHCs, accessory pigments for light harvesting, substrates for abscisic acid synthesis and components of photoprotection involved in dissipating excess energy and scavenging singlet oxygen. In order to increase understanding of carotenoid synthesis and function(s) in plants, several laboratories have recently taken a molecular genetic approach in *Arabidopsis thaliana* to define and disrupt the carotenoid biosynthetic pathway and thereby modify carotenoid production and accumulation in vivo. This chapter reviews recent work which has resulted in the identification and characterization of several novel mutations in *Arabidopsis* defining genes essential for

H. A. Frank, A. J. Young, G. Britton and R. J. Cogdell (eds): The Photochemistry of Carotenoids, pp. 21–37.

xanthophyll synthesis in photosynthetic plant tissues. The use of these mutations, both singly and in combination, allows one to dramatically manipulate the carotenoid composition of *Arabidopsis* photosystems in vivo, in the most extreme cases eliminating synthesis of all wild-type xanthophylls (lutein, violaxanthin and neoxanthin). This analysis has demonstrated a surprising plasticity in the carotenoid compositions plant photosystems will accept in vivo. Ongoing physiological, biochemical and photochemical analyses of these carotenoid biosynthetic mutants will provide insight into the regulation and integration of carotenoid synthesis with other chloroplast components and the functional role(s) of individual carotenoids in the photosystems.

I. Scope of This Chapter

The decade of the 1990s has seen remarkable advancements in our fundamental understanding of carotenoid synthesis and function in all organisms. From a molecular and genetic perspective, the decade has been truly unparalleled in the study of carotenoids. New technologies and approaches have combined to allow our understanding in these areas to proceed at such an accelerated rate. Some of these advances include the isolation of carotenoid biosynthetic genes from non-photosynthetic and photosynthetic bacteria, the use of these genes in *E. coli* to allow functional identification of higher plant homologues based on color complementation, ongoing genome sequencing efforts in several carotenoid containing organisms (both plants and bacteria) and transgenic and mutant studies of the pathway in various organisms. The primary focus of this chapter is to review recent progress and insights obtained from molecular genetic studies of carotenoid synthesis and function in the model plant system *Arabidopsis thaliana.* However, it is important to stress that the numerous aforementioned advances in the carotenoid field, particularly in the molecular biology of plant carotenoid synthesis, have synergistically impacted the molecular genetic studies in *Arabidopsis* described in this chapter. While the author feels somewhat remiss in not providing a detailed discussion of the full scope of advances in the area of plant carotenoid molecular biology, this is an unfortunate necessity as such a discussion could easily fill two additional chapters in this book. Fortuitously, an excellent, comprehensive review of plant carotenoid molecular biology has recently been published (Cunningham and Gantt, 1998) and readers are directed there for in depth information on the molecular biology of carotenoid synthesis in plants. For the purposes of this chapter brief discussions of selected aspects of plant carotenoid molecular biology are included below only where relevant to the specific biosynthetic genes that have been identified by mutational analysis in *Arabidopsis.*

Abbreviations: *aba1* – abscisic acid-deficient locus 1; cM – centiMorgan; EMS – ethylmethanesulfonic acid; GGDP – geranylgeranyl diphosphate; LHC – light harvesting chlorophyll protein complex; *lut1* – lutein deficient locus 1; *lut2* – lutein deficient locus 2; Mb – megabase; NPQ – non-photochemical quenching; PCR–polymerase chain reaction; PQ–plastoquinone; RFLP – restriction fragment length polymorphism

II. Introduction: An Overview of Carotenoid Synthesis

Carotenoids are a diverse group of naturally occurring, lipophilic pigment molecules that are widely distributed in nature and present in all photosynthetic and many non-photosynthetic plant tissues. Carotenoids are the pigments most often responsible for the red, orange or yellow color of fruits, vegetables, flowers and autumn leaves. Plant carotenoids are synthesized and accumulated exclusively in plastids and most are composed of a C_{40} hydrocarbon backbone, constructed from eight C_5 isoprenoid units and contain a series of conjugated double bonds (Britton, 1988; Bartley and Scolnik, 1994). Two major groups of carotenoids are synthesized by higher plants: *carotenes,* which are cyclized or uncyclized hydrocarbons, and *xanthophylls,* which are oxygenated derivatives of carotenes.

The biosynthesis of carotenoids in plants has been reviewed extensively in recent years and is only briefly described here (Britton, 1988; Bartley and Scolnik, 1994; Sandmann, 1994). The committed step to carotenoid synthesis is the formation of the first C_{40} compound phytoene by the head-to-head condensation of two molecules of GGDP by phytoene synthase. Phytoene is subjected to a series of four sequential desaturation reactions, by two separate enzymes to yield lycopene, which has eleven conjugated double bonds. Lycopene is then cyclized to β-carotene by two β-cyclizations or to α-carotene

by one β- and one ε-cyclization (Fig. 1). The two types of rings (ε and β) are produced by distinct enzymatic mechanisms (Britton, 1985, 1988) now known to be carried out by two structurally related enzymes, the lycopene β-cyclase and the lycopene ε-cyclase (Cunningham et al., 1996). The formation of ε-rings and production of β, ε-carotenoids (α-carotene derivatives) is one of the key differences distinguishing carotenoid biosynthesis in plants from cyanobacteria, fungi, and bacteria (Britton, 1988). α-Carotene serves as the precursor for hydroxylation (twice) to lutein, the most abundant carotenoid in green plant tissues. β-Carotene is subjected to a series of hydroxylation and epoxidation reactions to yield the other common leaf xanthophyll1s: zeaxanthin, antheraxanthin, violaxanthin and neoxanthin (Fig. 1). The reversible epoxidation/deepoxidation of zeaxanthin into violaxanthin (the xanthophyll cycle) is a light-dependent reaction thought to play an important role in adaptation to high light stress (see Chapters 14 (Demmig-Adams et al.), 15 (Horton et al.) and 16 (Yamamoto)).

Carotenoid synthesis is a highly regulated, integral part of chloroplast biogenesis and is intimately associated with the synthesis of other chloroplast components (i.e. lipids, proteins and chlorophylls). The major stimulus for carotenoid synthesis in greening leaf tissue is light (Oelmuller and Mohr, 1985), however, some xanthophylls are also present in substantial amounts in etiolated tissues (Grumbach and Lichtenthaler, 1982), indicating a large portion of the pathway is operational in the absence of light. The synthesis of various leaf carotenoids does not appear to be coordinately regulated and there is good kinetic evidence for differential synthesis of xanthophylls and β-carotene during photomorpho-

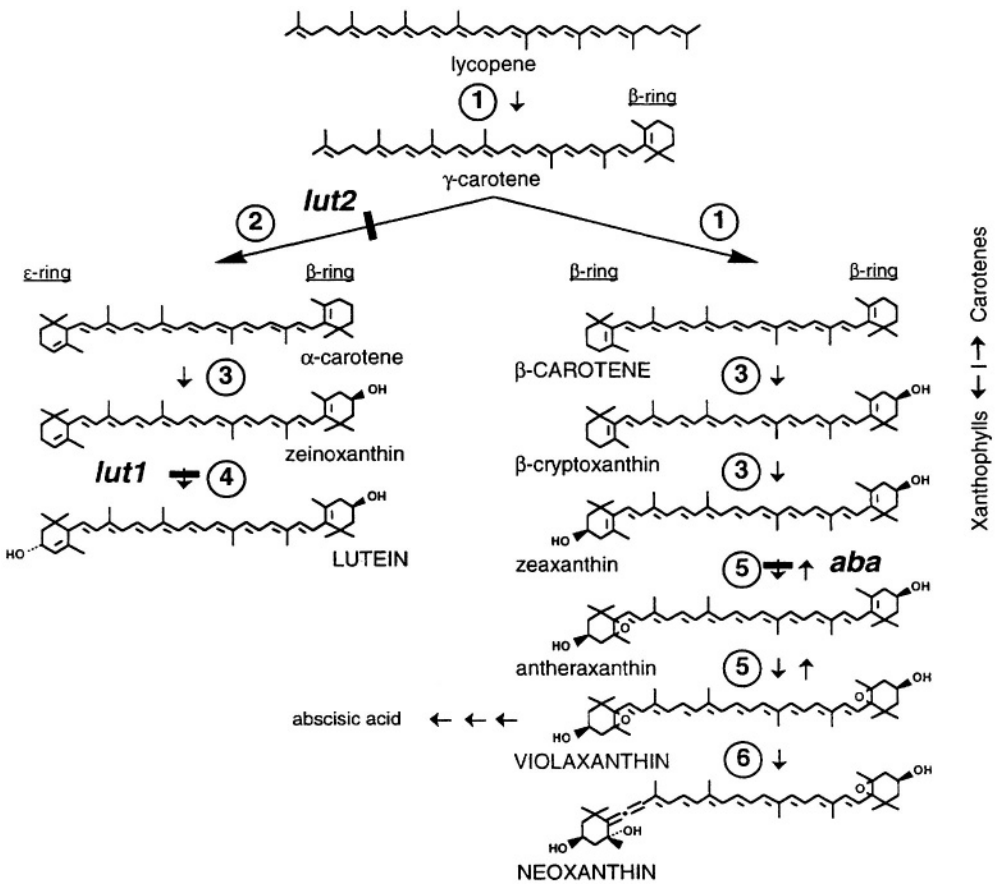

Fig. 1. Carotenoid biosynthetic pathway in plants. For clarity, only the portion of the biosynthetic pathway starting with lycopene is shown. Enzymes are indicated by numbers as follows: 1, β-cyclase; 2, ε-cyclase; 3, β-ring hydroxylase; 4, ε-ring hydroxylase; 5, zeaxanthin epoxidase and violaxanthin de-epoxidase enzymes; 6, neoxanthin forming enzyme. The location of the *lut1*, *lut2*, and *aba* mutations are indicated. Carotenoids that typically accumulate in photosynthetic tissues are given in capital letters.

genesis (Britton, 1988). Tissue-specific and developmental cues also regulate the pathway as ripening fruit and flowers often synthesize massive quantities of carotenoids, many of which are normally not accumulated in leaf tissues. Finally, environmental conditions can alter leaf carotenoid profiles, most notably by elevating the levels of xanthophyll cycle carotenoids in response to high light stress.

A. Molecular and Biochemical Analysis of the Carotenoid Pathway

While the carotenoid biochemical pathway has been known for several decades, the biosynthetic enzymes have until relatively recently proven largely recalcitrant to isolation and study. This is primarily due to the fact that most enzymes of the pathway are labile, membrane-associated proteins that are present at low specific activities and rapidly lose activity upon solubilization (Bramley, 1985; Beyer, 1987). It is only recently that purification of the two earliest enzymes in the pathway, phytoene synthase and phytoene desaturase, has been achieved from pepper fruit (Dogbo et al., 1988; Hugueney et al., 1992). The breakthrough in our understanding of the pathway and enzymes in recent years can be attributed largely to molecular and genetic approaches which have together allowed the majority of plant carotenoid biosynthetic enzymes to be cloned (Chamovitz et al., 1989, 1992; Hugueney et al., 1992, 1995; Pecker et al., 1992, 1996; Cunningham et al., 1993, 1994, 1996; Sun et al., 1996). These accomplishments have provided a wealth of information about the encoded proteins and the tools necessary to begin addressing many fundamental biochemical and molecular questions of the pathway (Cunningham and Gantt, 1998). To this end, several studies have demonstrated that mRNA levels for early steps of the pathway are strongly upregulated in tissues such as flowers and fruits and to a much lesser extent during leaf development (Kuntz et al., 1989, 1992; Romer et al., 1993; Giuliano et al., 1993; Kajiwara et al., 1995). The availability of cDNAs has also greatly aided biochemical studies which can now utilize large quantities of highly purified protein over-expressed in *E. coli* and other heterologous systems, rather than relying on partially purified, low specific activity natural sources (Sandmann et al., 1993; Misawa et al., 1994). While this allows individual enzyme activities to be studied in some detail it provides little information about integration and regulation of the pathway in vivo and the function of individual carotenoids in photosystems.

B. Carotenoid Functions

In leaf chloroplasts carotenoids are generally non-covalently bound to pigment-protein complexes where they are involved in and affect a large number of fundamental processes in the chloroplast (Gabellini et al., 1982; Siefermann Harms, 1985, 1987; Demmig Adams and Adams, 1992; Dreyfuss and Thornber, 1994a,b; Frank et al., 1994; Grossman et al., 1995; Frank and Cogdell, 1996). These include acting (i) as essential structural components for LHC assembly and stability, (ii) as accessory pigments in light harvesting, (iii) as components of excess energy dissipation in high light situations, and (iv) as scavengers of singlet oxygen. Most of the proposed carotenoid functions and localizations are covered in considerable detail in other chapters of this volume and the reader is referred to Chapters 3 (Takaichi), 4 (Cogdell et al.), 8 (Christensen), 9 (Koyama and Fujii), 13 (Frank), 14 (Demmig-Adams et al.), 15 (Horton et al.) and 16 (Yamamoto) for detailed discussions of these topics.

C. Carotenoid Distribution in Pigment Protein Complexes

Carotenoids are non-covalently bound to complexes in the thylakoid membrane and are fundamentally important functional and structural components of the photosynthetic apparatus (Siefermann Harms, 1985, 1987; Peter and Thornber, 1991; Demmig Adams and Adams, 1992; Dreyfuss and Thornber, 1994a, 1994b; Horton et al., 1994; Grossman et al., 1995). Higher plant chloroplasts typically accumulate lutein, β-carotene, violaxanthin, and neoxanthin (in order of abundance) as their major carotenoids. In general, carotenoid levels are directly proportional to the amount of chlorophyll in photosynthetic tissues, with lutein and neoxanthin being correlated with Chl *b* levels and β-carotene with Chl *a* (Juhler et al., 1993). Photosystems I and II (PSI and PSII) are large pigment-protein complexes consisting of a reaction center (CCI or CCII) surrounded by antennae complexes that harvest and transfer light energy to the reaction centers. Reaction centers contain Chl *a* and β-carotene while the adjacent core complex proteins (CP43 and CP47 for PSII) additionally contain minor amounts of lutein as their major

pigments (Peter and Thornber, 1991; Bassi et al., 1993). The antennae complexes (light harvesting complex proteins or LHCs) are a large family of related proteins that bind xanthophylls (typically lutein, violaxanthin and neoxanthin), Chl *a* and Chl *b* and collectively are the most abundant pigment: protein complexes in the plastid (Peter and Thornber, 1991; Bassi et al., 1993).

The LHCs of higher plants are the primary harvesters of light energy and their pigment: protein compositions and assembly during photomorphogenesis have been the subject of intensive analysis (Peter and Thornber, 1991; Anandan et al., 1993; Dreyfuss and Thornber, 1994a). LHC polypeptides assemble and associate with their respective core complexes to form functional photosynthetic units (LHCII with PSII and LHCI with PSI). The LHCII is the most abundant complex and is actually composed of four different pigment: protein complexes, LHCIIa, LHCIIb, LHCIIc and LHCIId. LHCIIa, c and d are also called CP29, CP26 and CP24, respectively, and are collectively referred to as the minor LHCII components. LHCIIb binds 60% of the Chl in PSII, while the minor LHCII components collectively contain between 5 and 10% of the total chlorophyll (Ruban et al., 1994). A fifth complex highly enriched in xanthophylls, LHCIIe, has also been identified but its functional role is unclear (Peter and Thornber, 1991).

The pigment compositions of the four LHCII complexes vary significantly and have been characterized in considerable detail in maize (Bassi et al., 1993), spinach (Ruban et al., 1994) and barley. While there are some minor differences in these data, in general the results are in agreement. The Chl *a/b* ratio of LHCIIb is generally 1.3–1.4 while that of the minor complexes are much higher, in the range of 2–3. Lutein is the predominant xanthophyll in all LHCs and ranges between a low of <40% of total carotenoids in LHCIIa to >65% in LHCIIb. Other carotenoids, particularly the β-carotene derived xanthophylls, violaxanthin and neoxanthin, vary much more widely in concentration. Neoxanthin is present at similar proportions in LHCIIa, b and c but is virtually absent from LHCIId (Bassi et al., 1993). Interestingly, LHCIIb is nearly devoid of β-carotene but the minor complexes contain 5–10% of their total carotenoids as β-carotene (Bassi et al., 1993; Ruban et al., 1994). Violaxanthin is also proportionally enriched in the minor LHCs accounting for 30–40% of the total minor LHC carotenoids and in aggregate up to 80% of the total violaxanthin in thylakoids (Peter and Thornber, 1991; Bassi et al., 1993; Ruban et al., 1994).

One of the most significant advancements in LHCII structural analysis has been the recent solving of its atomic structure at 3.4 Å which has provided important insight into the structure of all higher plant LHCs (Kuhlbrandt et al., 1994). Each LHC contains 12–13 chlorophyll molecules as well as what are thought to be two lutein molecules in the central portion of the complex as the sole carotenoid present. The position of these lutein molecules suggests they form an internal crossbrace in the center of the complex. Furthermore, their close contact with several chlorophylls of the complex suggest they are important in quenching excited triplets during high light stress. Their central position in this complex may explain why lutein is essential for the highest efficiency in vitro LHC reconstitution, and why lutein synthesis and abundance is so highly conserved in all higher plants and green algae.

D. In Vivo and In Vitro Studies of LHC Assembly: Critical Roles for Carotenoids

The biogenesis of LHCs during photomorphogenesis has been studied in considerable detail. In general the synthesis of LHC mRNAs and proteins are induced by the quantity and quality of light, as well as developmental cues (Grossman et al., 1995). It is thought that the minor LHCs first associate with the core complexes, then monomers of LHCIIb associate with the growing complex as trimers (Dreyfuss and Thornber, 1994b). There is a growing consensus that LHCIIb exists as a trimer in mature photosystems (reviewed in Jansson, 1994). Pigments play a central role in LHC biogenesis and are required for proper folding, assembly and stability of LHC apoproteins and mature proteins (Humbeck et al., 1989; Paulsen et al., 1993). Genetically or chemically disrupting chlorophyll or carotenoid synthesis causes decreased levels of LHC proteins to accumulate, often without drastically affecting expression of the corresponding mRNAs (Humbeck et al., 1989; Paulsen et al., 1993). The most convincing evidence of the importance of posttranslational processes for LHC assembly come from antisense inhibition studies that reduced LHC mRNAs levels to the limits of detection with virtually no effect on LHC protein levels, assembly or photosynthesis (Flachman and Kuhnbrant, 1995).

Elegant in vitro reconstitution studies of heat

denatured native LHCII polypeptides or those expressed in and purified from *E. coli* have allowed dissection of the optimal and minimal pigment and lipid requirements for LHC assembly in vitro (Plumley and Schmidt, 1987; Paulsen et al., 1990, 1993; Cammarata et al., 1992; Cammarata and Schmidt, 1992). These studies also point to a critical role for carotenoids in proper folding and integrity of LHC complexes. Chl *a*, Chl *b* and the three native leaf xanthophylls (lutein, violaxanthin, neoxanthin) were required for maximal in vitro reconstitution efficiency and lipids were required for trimer formation. With regard to the minimal xanthophyll requirements, any two of these three were found to support assembly, but to varying degrees (Plumley and Schmidt, 1987), such that omitting violaxanthin had little effect on LHC assembly, omitting lutein greatly reduced efficiency while omitting neoxanthin nearly eliminated assembly. When single xanthophylls were tested, only lutein supported assembly, albeit at low levels. Analysis by CD, fluorescence and absorption spectroscopy indicated that complexes assembled with all three xanthophylls were similar in all regards to native complexes isolated from leaves. Reconstituted complexes without the normal xanthophyll complement were initially similar to native complexes but rapidly deteriorated, suggesting decreased stability as a result of their modified xanthophyll composition. Fluorescence excitation spectra of such complexes showed decreased efficiency of energy transfer from Chl *b* to Chl *a*, suggesting inefficient pigment organization in these complexes. These in vitro studies suggest complexes assembled in vivo without a full xanthophyll complement may not be as stable or efficient in energy transfer as those with a native carotenoid complement.

III. Rationale for Identifying and Studying Carotenoid Biosynthetic Mutants in Higher Plants

The biochemical and photochemical approaches described thus far have allowed significant advances in our understanding of the structural and functional roles of carotenoids in photosynthesis and photosystem assembly and have laid the groundwork for many of the most widely accepted theories in the field. The continued development and use of these approaches will be of central importance to research progress in the field, however, as most of these approaches are in vitro based and rely on isolated or reconstituted chloroplasts and complexes, in vivo testing of the hypotheses developed has been limited. A complementary approach that has not been fully utilized and integrated in the study of carotenoid synthesis and function in plants is that of molecular genetics, which allows one to genetically disrupt key components of pathways in vivo and assess the consequences on the pathway or process under study. The use of molecular genetic approaches has been a critical additional dimension to the study of carotenoid synthesis and function in other systems, especially with regard to various bacterial systems, and provides an attractive means for critically testing the in vivo validity of current theories. The identification, characterization and utilization of *Arabidopsis* mutant lines in which the carotenoid composition of photosystems can be predictably manipulated at the genetic level should allow analogous insights into the in vivo role of carotenoids in plant photosystem structure, assembly and function.

The studies described in this chapter represent ongoing programs in several laboratories taking a molecular genetic approach to study the biosynthesis and function of carotenoids in *Arabidopsis thaliana.* To date, this work has helped define the enzymes responsible for the suite of native carotenoids produced in plants (Cunningham et al., 1996; Pogson et al., 1996), critically test the role of individual enzymes and xanthophylls in photosynthetic processes and provide insight into the integration of carotenoid synthesis with other components of the photosynthetic apparatus, namely the PQ pool and electron transport chain (Norris et al., 1995). Through this work, various single and double mutant lines have been generated that are blocked at one or more steps in the carotenoid biosynthetic pathway and as a result show dramatically altered carotenoid profiles relative to wild type *Arabidopsis.* These carotenoid biosynthetic mutants are currently being used to investigate the physiological, structural and biochemical effects of altered carotenoid compositions on photosynthesis and photosystem structure and function in vivo. Because our understanding of the role of carotenoids in photosynthesis has been derived primarily from in vitro biochemical and biophysical studies and in vitro correlations, it is anticipated these mutants will be useful for critically testing current ideas regarding the structural and functional role of specific carotenoids in vivo.

IV. *Arabidopsis* as a Model System for Studying Carotenoid Synthesis and Functions in Plants

A molecular genetic approach to study biochemical pathway and processes in plants, such as the carotenoid biosynthetic pathway is basically sound, but, to be fully utilized requires a plant system that is tractable from biochemical, genetic and molecular perspectives to the isolation and characterization of phenotypically-identified genes. In order to be fully utilized such a system should: 1) enable easy screening of large numbers of mutant individuals, 2) allow the rapid identification, characterization, mapping and crossing of novel mutations, 3) be technically amenable to the physical isolation of phenotypically-identified genes by a variety of methods, and, 4) be technically amenable to detailed characterization of the resulting mutant phenotypes using existing, well established tools in the research field. *Arabidopsis* is a small, cruciferous, model plant system that fulfills these criteria and has proven to be an excellent tool in the identification and isolation of genes from other plant biochemical pathways. The small genome size (approx. 120 Mb), rapid life cycle, large seed production, self-fertilization and amenability to *Agrobacterium*-mediated transformation make *Arabidopsis* an ideal molecular and genetic plant system for studies of carotenoid synthesis and function. Several RFLP maps have been constructed and recent techniques using PCR based markers and recombinant inbred lines greatly facilitates the process of mapping genes identified from mutational studies (Chang et al., 1988; Konieczny and Ausubel, 1993; Bell and Ecker, 1994).

Arabidopsis also continues to be the focus of technological developments to facilitate the identification and cloning of plant genes (Konieczny and Ausubel, 1993; Bell and Ecker, 1994; McKinney et al., 1995). These include gene disruption/tagging procedures based on T-DNA and transposons, functional complementation of mutations in other organisms (principally yeast and bacteria) with *Arabidopsis* cDNA libraries as well as map based cloning of phenotypically identified genes. These combined approaches have allowed numerous novel biosynthetic and regulatory genes to be isolated from *Arabidopsis* based solely on their biochemical or developmental mutant phenotype (Feldmann et al., 1989; Yanofsky et al., 1990; Young and Phillips, 1994; McKinney et al., 1995). Finally, a large scale project to partially sequence 50,000 random *Arabidopsis* cDNAs (Expressed Sequence Tags; (Newman et al., 1994) as well as a separate program to sequence the entire *Arabidopsis* genome (estimated completion date 2001) are well underway. These genomic based systems provide an incredible resource for computer based identification of cDNAs and genes based on genetic, structural, biochemical and functional parameters (http: //genome-www.stanford.edu/Arabidopsis/). Importantly, standard methods for analyzing photosystem structure, composition and function have also been applied to *Arabidopsis* in recent years (Walters and Horton, 1994, 1995a, 1995b; Hurry, 1995; Russell et al., 1995; Meurer et al., 1996; Tardy and Havaux, 1996; Hurry et al., 1997). The combination of molecular genetics, biochemistry and photobiology can be an extremely powerful approach for in vivo studies and is particularly useful when biochemical knowledge, but not necessarily gene identity is known. These and other attributes of *Arabidopsis* combined with mutant screening procedures targeting specific aspects of photosystem structure or function make *Arabidopsis* an attractive system for furthering our understanding of carotenoid synthesis and function in higher plants in vivo.

A. The Xanthophyll Biosynthetic Mutants of Arabidopsis thaliana*: An Overview*

Prior to 1995, only one locus affecting Xanthophyll biosynthesis in photosynthetic tissues of *Arabidopsis* had been identified, the *ABA 1* locus, the mutation of which disrupts zeaxanthin deepoxidase, one of two xanthophyll cycle enzymes (Koornneef et al., 1982; Rock and Zeevaart, 1991; Rock et al., 1992). As a step toward advancing understanding of xanthophyll biosynthesis, incorporation, and function in plants, the author's laboratory has screened for and identified mutations defining two additional loci required for xanthophyll biosynthesis in *Arabidopsis, LUT1* and *LUT2* (*LUT*= *LUT*ein deficient). Mutations at either locus result in defects in the synthesis of lutein, the most predominant xanthophyll in plants. Singly and in combination with the *aba* mutation, these *lut* mutations have allowed the genetic construction of five distinct mutant lines which differ dramatically in their carotenoid composition relative to wild-type *Arabidopsis.* In the remainder of this chapter I will first briefly discuss the *aba* mutation followed by a

detailed description of the *lut2* and *lut1* single mutants. Finally, I will end with a discussion from recent experiments in which we have introduced the *aba* mutation into each *lut* mutant background and characterized the effect of the combined mutations on growth, pigment profiles and NPQ.

B. The Arabidopsis aba 1 *Mutation and its Effect on LHC Structure and Function*

The *aba 1* mutation was fortuitously discovered over 15 years ago in a mutant screen designed to identify *Arabidopsis* mutants whose seed were desiccation intolerant and could be germinated in the absence of gibberellic acid synthesis (Koornneef et al., 1982). The *abal* mutation is now know to be the result of a lesion in the structural gene encoding the carotenoid biosynthetic enzyme zeaxanthin epoxidase whose mutation virtually eliminates production of antheraxanthin, violaxanthin and neoxanthin in mutant tissues and results in their equimolar replacement with constitutively high levels of zeaxanthin (Rock and Zeevaart, 1991). As violaxanthin is the precursor for abscisic acid synthesis in plants, the *aba1* mutant does not synthesize abscisic acid, is desiccation intolerant and as a result germinates in the absence of gibberellic acid. The *aba1* mutant has recently been used to study the effect of replacing violaxanthin and neoxanthin with zeaxanthin on LHC structure, chlorophyll fluorescence, photosynthesis and photoinhibition in vivo (Rock et al., 1992; Tardy and Havaux, 1996; Hurry et al., 1997). These studies have reported no significant differences in *aba1* with respect to photosynthetic performance or amplitude of NPQ relative to wild-type, though NPQ developed faster and reverted slower in the dark in the mutant. LHC protein levels were also not affected in the mutant though non-denaturing Deriphat-PAGE did indicate a decrease in trimeric LHC in favor of monomers, an increase in free pigments and a reduction in supramolecular complexes of PSII and LHCs, all of which are consistent with decreased stability of the *aba1* LHC complexes (Tardy and Havaux, 1996; Hurry et al., 1997). The mutant also exhibited a slight decrease in PSII thermostability and a biphasic photoinhibition response to long-term high light stress in which the first phase paralleled wild-type while a second phase deteriorated more rapidly.

C. Isolation/Characterization of Arabidopsis *Mutants Defective in Lutein Synthesis*

To further our understanding of xanthophyll biosynthesis and function in higher plants, my laboratory has have taken a molecular genetic approach to isolate and characterize novel mutations in *A. thaliana* that result in defects in specific aspects of xanthophyll synthesis (Pogson et al., 1996). During an 18 month period more than 4,500 individual soil-grown EMS-generated M2 mutant lines were screened individually for abnormal pigment profiles by HPLC. The vast majority showed a wild-type pigment profile, but several lines impaired in their ability to accumulate xanthophylls were also identified (Fig. 2). These mutants could be divided into two groups: one group accumulated zeaxanthin, lacked violaxanthin and neoxanthin and was allelic with the previously identified *aba1* locus; while a second group was impaired in lutein accumulation. This later group, named *lut* for *lut*ein deficient, was further divided into two classes on the basis of biochemical phenotypes and allelism tests: the *lut2* class had no detectable lutein and increased amounts of β-carotene and xanthophyll cycle pigments; the *lut1* class also had severely reduced lutein, increased amounts of the xanthophyll cycle pigments but, in addition, accumulated a carotenoid that was not present in wild type. These two *lut* loci represent the first mutations in higher plants specifically disrupting the synthesis of the α-carotene derived xanthophyll lutein and have genetically defined the α-carotene branch of the carotenoid pathway in plants (Pogson et al., 1996).

1. lut1 *Mutants Accumulate Zeinoxanthin and are Defective in ε-ring Hydroxylation*

All *lut1* alleles are recessive mutations (Fig. 3 A) that accumulate an additional carotenoid with an HPLC retention time and UV/visible absorption spectrum characteristic of a monohydroxy β, ε-carotenoid (an α-carotene derived xanthophyll). The identification of the accumulating compound as zeinoxanthin (β,ε-caroten-3-ol) was confirmed by mass spectrometry (Pogson et al., 1996). The only difference between lutein and zeinoxanthin is the presence of an hydroxyl group on carbon 3 of the ε-ring in lutein. The decrease in lutein and its partial replacement by its immediate precursor, zeinoxanthin, defines *lut1* as a mutation

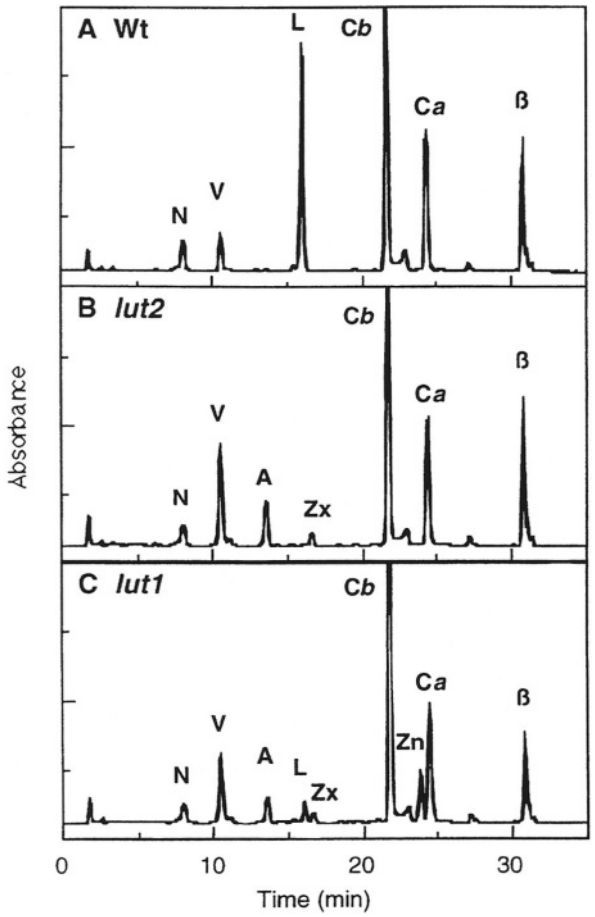

Fig. 2. Pigment analysis of wild type, *lut2* and *lut1* leaves. All panels are C18 HPLC separation of lipid-soluble pigments from leaves of 4-week-old plants. (A) show the pigment profile of wild type; (B) show the pigment profile of *lut2-1*; (C) show the pigment profile of *lut1-1*. N, neoxanthin; V, violaxanthin; A, antheraxanthin; L, lutein; Zx, zeaxanthin; C*b*, Chl *b*; C*a*, Chl *a*; Zn, zeinoxanthin; *β*, *β*-carotene; wt, wild type. Carotenoids were separated by reversed-phase HPLC on a Spherisorb ODS2, 5 micron C_{18} column using a 45-minute gradient of ethyl acetate (0–100%) in acetonitrile-water-triethylamine (9: 1: 0.01 [v/v]), at a flow rate of 1 mL per min. Carotenoids were identified by retention time relative to known standards with detection at 440 nm. Each profile represents absorbance at 440 nm of pigments extracted from 5 mg fresh weight of tissue.

disrupting ε-ring hydroxylation (Fig. 1). *lut1* mutations are specific for ε-ring hydroxylation, and do not impede other reactions including, most significantly, β-ring hydroxylation. Thus, *lut1* genetically defines a minimum of two hydroxylation enzymes in the pathway, one specific for ε-rings and a second, unaffected by *lut1*, specific for β-rings.

2. The lut2 *Mutations are Semidominant and Disrupt ε-ring Cyclization*

In contrast to *lut1*, *lut2* mutants do not accumulate any lutein precursors. The synthesis of β, β-carotenoids is unimpeded in *lut2*, so *lut2* is not a β-cyclase or β-ring hydroxylase mutation. Also, as *lut2 is* not allelic with *lut1*, the mutation does not affect ε-ring hydroxylation. Thus, based solely on biochemical data, *lut2* most likely affects ε-cyclization, the committed step in the synthesis of lutein (Fig. 1). Mapping data are consistent with this hypothesis as the *lut2* mutation cosegregates (±2 cM) with the recently isolated *Arabidopsis* ε-cyclase cDNA (Cunningham et al., 1996; Pogson et al, 1996). Most recently, the *lut2* mutant has been transformed with a wild type *Arabidopsis* ε-cyclase cDNA driven by a constitutive promoter and shown to be complemented by the transgene (results not shown). Thus, genetic, biochemical and molecular complementation data support *lut2* being a disruption of the ε-cyclase gene. The *lut2* mutations genetically define a minimum of two cyclization enzymes in the pathway, an ε-cyclase and a β-cyclase. Interestingly, both *lut2* alleles are semidominant as when crossed to wild type plants, F_1 progeny show a partial decrease in lutein with a comparable increase in violaxanthin, which also segregates in the expected 1: 2: 1 ratio in F_2 progeny (Figs. 3 A and B). The semidominance of *lut2* mutations suggest the ε-cyclase is a rate limiting enzymatic step for lutein synthesis and a key regulatory step in the production of α-and β-carotene derivatives (Cunningham et al., 1996; Pogson et al., 1996).

3. Carotenoid but not Chlorophyll Composition is Altered in lut1 *and* lut2

The loss of lutein (80 to 100 %) in *lut1* and *lut2* is compensated for by increases in the abundance of other carotenoids, most notably specific β, β-carotenoids (Fig. 4). *lut1* mutants accumulate the biosynthetic intermediate, zeinoxanthin to approximately 50% of the wild-type lutein level and in addition have elevated levels of the xanthophyll cycle carotenoids violaxanthin, antheraxanthin and zeaxanthin. *lut2* mutants have an even larger increase in xanthophyll cycle pigments, plus a smaller increase in β-carotene. Antheraxanthin and zeaxanthin normally accumulate transiently in response to high

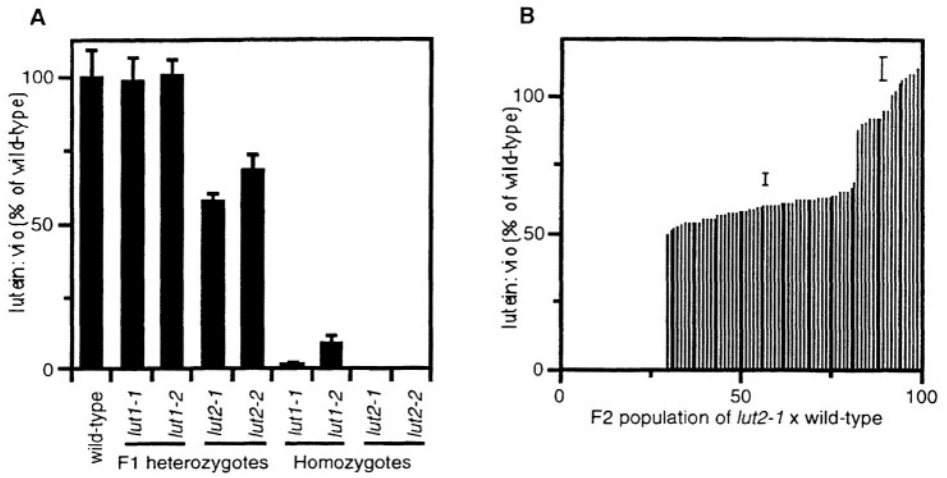

Fig. 3. lut1 alleles are recessive and *lut2* alleles are semidominant. The peak area ratio at 440 nm of lutein to violaxanthin (lutein: vio) as a proportion of wild type was determined. Panel A shows the ratio for wild type, heterozygous and homozygous *lut1* and *lut2* alleles. Panel B shows a segregating population of F_2 plants of a *lut2-1* x *LUT2* cross. Standard deviations are shown in Panel A only. vio, violaxanthin.

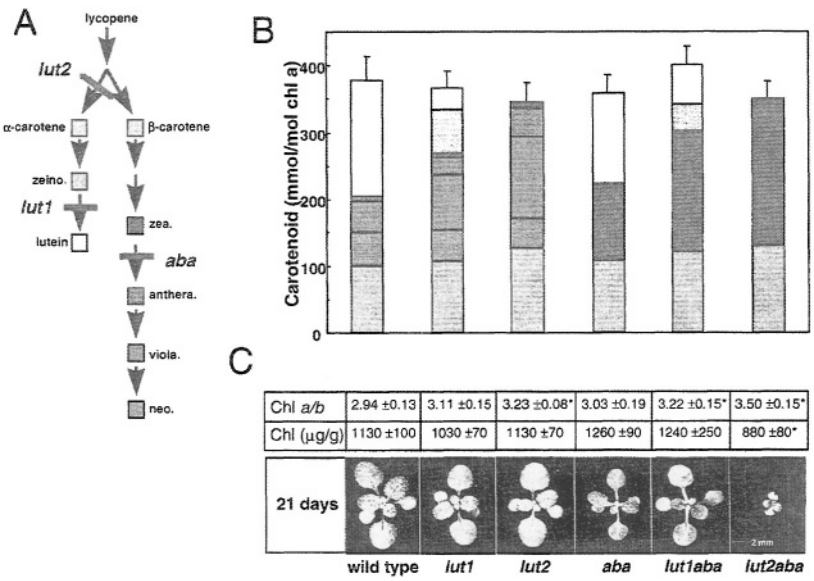

Fig. 4. Carotenoid pathway, mutant locations, pigment profiles and seedlings. Panel A shows the carotenoid biosynthetic pathway in higher plant chloroplasts commencing with lycopene and the location of the *lut1*, *lut2* and *aba1* mutations in the pathway. Panel B shows the carotenoid content of mature green leaves of 21 day-old wild type and the five indicated xanthophyll mutant lines. Each section of the bars corresponds to a specific carotenoid of the pathway (refer to color code of Panel A). The standard deviations of the total pool of carotenoids per mole chl *a* are shown on each bar. Panel C shows photographs of 21d old seedlings of wild type and the five indicated xanthophyll mutant lines and their corresponding chlorophyll content and Chl *a/b* ratios. Photographs are of soil-grown wild type and xanthophyll mutant seedlings grown 21 days on a 12 h light cycle. Chlorophyll ratios and content of mature green leaves (C). The chl *a/b* ratio (mol/mol) and total chlorophyll content of green leaves (µg/g fresh weight) with standard deviations are shown. Values that are significantly different ($p < 0.05$) from wild-type are marked with an asterisk (*). See also Color Plate 3.

light stress due to deepoxidation of violaxanthin and in darkness are epoxidated back into violaxanthin. However, their accumulation in *lut1* and *lut2* is clearly not stress related as all plants were grown at a light intensity that did not induce the xanthophyll cycle in wild type and, more importantly, after a 24 h dark treatment, over 80% of the antheraxanthin and zeaxanthin was still present in *lut1* and *lut2*. Apparently, the bulk of these xanthophyll cycle pigments in the *lut* mutants are no longer in a location accessible to the epoxidase, most likely as a result of their preferential incorporation into sites normally occupied by lutein.

Because lutein is generally proportional to Chl *b* content and β-carotene to Chl *a,* one would expect that a decrease in lutein and an increase in β-carotene (as observed in *lut2*) would be reflected by dramatic alterations in Chl *a/b* ratios and hence, reaction center/LHC ratios (Peter and Thornber, 1991; Bassi et al., 1993; Juhler et al., 1993). Surprisingly there is no significant difference between the *lut2* and *lut1* mutants and wild type plants for Chl *a,* Chl *b,* or the Chl a-to-Chl *b* ratio in fully grown (six-week old) plants, though, in 21-day old plants the chl *a/b* ratio of *lut2* was slightly, but significantly higher than wild type (3.23 versus 2.94). Therefore, an 80 to 100% reduction in the most abundant carotenoid, lutein, and its replacement with equimolar amounts of other carotenoids has not markedly affected the amount and ratio of Chl *a/b* synthesized and incorporated into the photosynthetic apparatus.

Analogous mutations affecting lutein production also exist in green algae and there seems to be significant differences in the effects of xanthophyll deficiency in these organisms relative to *Arabidopsis.* In a putative *lut2* orthologous mutant of the alga *Scenedesmus obliquus,* a decrease in the levels of lutein was accompanied by an increase in β-carotene, a reduction in total chlorophyll, a decrease in chl *b* (the chl *a/b* ratio was 6.54 versus 3.06 for wild type) (Bishop et al., 1995; Bishop, 1996) and the near complete absence of the major LHCII proteins, although minor LHCII proteins were largely unaffected. Another putative orthologous mutant to *lut2* is the *lor1* mutation in the green alga *Chlamydomonas* (Chunaev et al., 1991; Niyogi et al., 1997). The pleiotropic effects of this mutation appear to be intermediate between that of *Scenedesmus* and *Arabidopsis* with a chl *a/b* ratio of 4.02 verse 2.64 in wild type. These algal mutants are in contrast to the *Arabidopsis lut2* mutant in which the change in lutein and β-carotene content did not significantly alter the Chl *a/b* ratio or affect neoxanthin levels, which, in turn, implies no or little change in reaction center to LHC ratio. These data suggest that although lutein synthesis is evolutionarily conserved in green algae and plants, there are marked differences in the effects of lutein deficiency on LHC pigment content, assembly and function in these organisms. This suggests either the functional roles of lutein or the degree of functional plasticity of different xanthophylls differ somewhat between plants and algae.

4. Function of Lutein and the Carotenoids That Accumulate in Its Absence

Lutein is the most abundant carotenoid in all photosynthetic plant tissues and its synthesis and presence are evolutionarily conserved both in land plants and green algae. The apparent localization of lutein in the atomic structure of LHCII (Kuhlbrandt et al., 1994) and its requirement for optimal in vitro assembly of LHCs (Plumley and Schmidt, 1987; Paulsen et al., 1990, 1993) had led to the assumption that lutein is critical for higher plant photosystem assembly and function. Yet, paradoxically, the complete elimination of lutein in a higher plant via the *Arabidopsis lut* mutants has no obvious deleterious effect on growth and development, chlorophyll content or the Chl *a/b* ratio in moderate light. The most reasonable explanation for the viability of the *lut1* and *lut2* plants is that some, or all, of the carotenoids that accumulate in its absence can functionally complement lutein, at least to some degree. In vitro studies indicate that, while less than optimal, various xanthophyll combinations enable LHC assembly in the absence of lutein. Interestingly, violaxanthin was the one xanthophyll tested that could be omitted without severely inhibiting assembly. Why then should it be that violaxanthin and antheraxanthin are preferentially accumulated in *lut* mutants and not the closest structural homologue to lutein, zeaxanthin? We can only speculate that a combination of structural, energy transfer and binding site considerations dictates the preferential accumulation of specific xanthophylls in *lut* mutants. Violaxanthin has an S_1 energy higher than chlorophyll and along with lutein, is presumed to augment light harvesting. Antheraxanthin does not normally accumulate, but has an S_1 energy nearly identical to lutein and based solely on energetic considerations would be its closest homologue (Frank et al., 1994).

Zeaxanthin, on the other hand, while chemically most similar to lutein, has an S_1 energy below chlorophyll and binding sites for this xanthophyll may be both weaker and more limited in the photosystems. These combined characteristics may explain why violaxanthin and antheraxanthin accumulate preferentially in the absence of lutein.

D. Xanthophyll 'Plasticity' and Xanthophyll Double Mutants

The individual *lut1, lut2* and *aba1* mutants have provided insight into the regulation of carotenoid biosynthesis and have demonstrated a surprising in vivo flexibility of LHCs for carotenoids. In all three mutant lines the total quantity of carotenoids did not change but instead deletions were replaced by compensating molar increases in specific carotenoids (Fig. 4B). This is significant as it suggests there is no net alteration in carbon flow to the pathway in mutations disrupting either branch of xanthophyll synthesis. Additionally, the single mutant lines appeared to grow and develop as well as plants with wild-type carotenoid profiles.

During the course of studies with single xanthophyll mutants we began to consider the limitations to plasticity in xanthophyll substitutions which would still enable viable assembly, light harvesting and photoprotection of higher plant photosystems in vivo. In all three single mutants, there was at least one 'native' xanthophyll still present: lutein in *aba1* and neoxanthin and violaxanthin in *lut1* and *lut2*. In order to further test the plasticity and minimum xanthophyll requirements of plant LHCs in vivo, we attempted to generate *lut1/aba1* and *lut2/aba1* double mutant lines, the net effect of which would be to eliminate the synthesis of all 'native' leaf xanthophylls in both double mutant lines. Based on in vitro LCH assembly studies with various xanthophylls, one would predict detrimental effects on photosystem assembly/function in these double mutants, however, both were viable and photoauxotrophic at moderate light levels, *lut1/aba1* accumulates β-carotene, zeinoxanthin and zeaxanthin and is indistinguishable in growth from wild type and either single parental mutant line. *lut2/aba1* only accumulates β-carotene and zeaxanthin, is approximately 50% smaller than wild type or either single parental mutant *but is still viable. lut2/aba1* is also unique among the various mutant lines as it exhibits some seedling lethality in soil which appears to be a function of germination light intensity.

Greening of etiolated plants in tissue culture and soil indicated *lut2/aba1, lut1 aba1* and *aba1* are severely delayed in chlorophyll accumulation (Fig. 5, only wild type, *lut2aba1, lut2* and *aba1* are shown). Exogenous application of abscisic acid did not have an effect on greening suggesting that delayed greening is predominantly due to alterations in xanthophyll content rather than to a deficiency in abscisic acid levels. Eventually, *aba1* and *lut1aba1* seedlings accumulated substantial quantities of chlorophyll, reaching wild-type levels on a fresh weight basis (See Fig. 4C). In contrast, the amount of chlorophyll per gram fresh weight of tissue of *lut2aba1* was marginally but significantly lower than wild type (Fig. 4C), and *lut2aba1* plants were much smaller than wild type or either single parent mutant lines at all points of development (Fig. 4C). The *lut1aba1* and *lut2aba1* also had slightly, but significantly higher chlorophyll *a/b* ratios. All of these results suggest some difficulty in LHC assembly in these mutant lines, however, the plant photosystems are quite remarkably able to compensate and allow photoauxotrophic growth, at least under moderate light conditions.

E. Analysis of NPQ in lut *and* aba *Single and Double Mutants*

We have also used the five different mutant lines shown in Fig. 4 to investigate the effects of altered xanthophyll compositions on the magnitude and timing of nonphotochemical quenching (NPQ) of chlorophyll fluorescence during exposure to high light. In wild-type plants, the NPQ response was rapid, reaching a plateau after 80 sec of illumination with high light (Fig. 6). However, in the *lut2* and *lut1* mutants, which are defective in lutein synthesis, the induction of NPQ was significantly inhibited. After 10 s of illumination, the level of NPQ in *lut2* was only one-third that of wild-type, and 120 sec were required before NPQ plateaued, albeit at a significantly lower maximum level than wild type. The patterns of NPQ induction and maximal NPQ levels were similar for *lut1* and *lut2* (compare Fig. 6A and 6B). In contrast, the *aba1* mutant, which has lutein and zeaxanthin as its xanthophylls, had a greater rate of NPQ induction, being 3-fold and 10-fold higher at 10 sec than wild type and *lut2,* respectively. The maximum level of NPQ in *aba1* appeared lower than in wild type, because *aba1* had a 30% lower F_m,

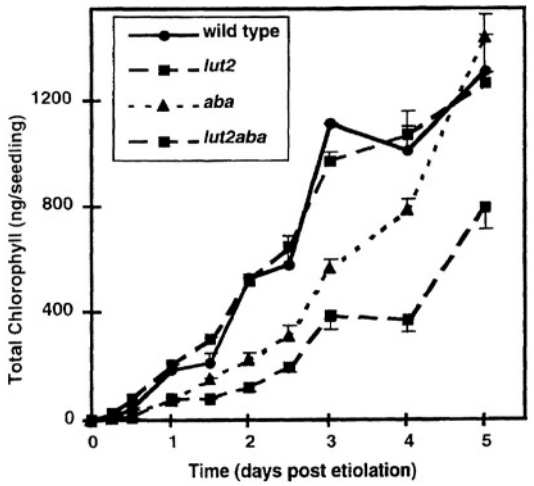

Fig. 5. The rate of chlorophyll accumulation in etiolated seedlings exposed to continuous light for 5 d. Wild type, *lut2*, *aba1* and *lut2aba1* etiolated tissue culture-grown seedlings were vernalized, germinated in the dark for 3 d and then transferred to continuous light. At each time point, 2 replicate extracts of 10 pooled seedlings were analyzed and the chlorophyll content expressed on a per plant basis (μg/seedling). Standard deviations greater than the size of the symbol are shown.

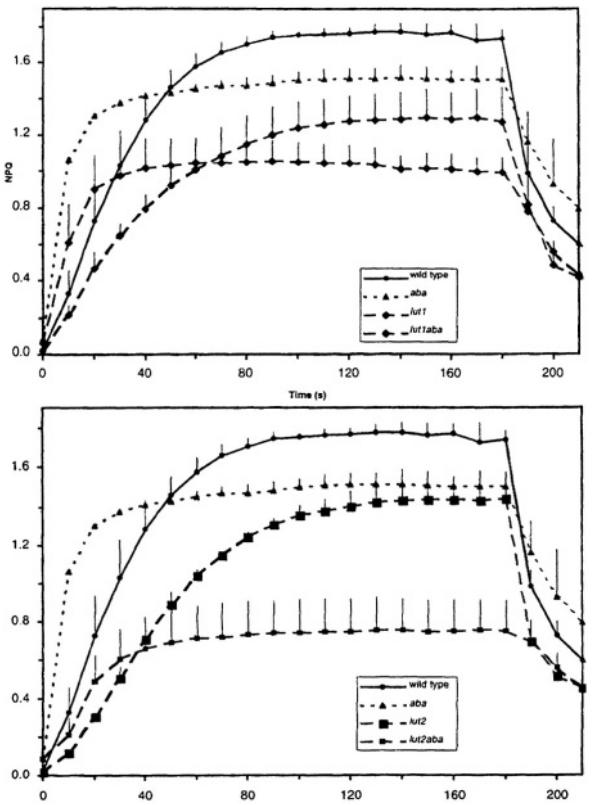

Fig. 6. Induction of nonphotochemical quenching (NPQ) in wild type and xanthophyll mutant lines in *lut2*, *aba1* and *lut2aba1* backgrounds (A) and the *lut1*, *aba1* and *lut1aba1* backgrounds (B). Plants were grown at 140 μmol m^{-2} sec^{-1} for 12 h cycles and dark adapted overnight. Fluorescence was measured before (zero time), during (0–180 sec), and after (180–210 sec, weak far red background light only) exposure to actinic light (PAR of 1083 μmol m^{-2} sec^{-1}). Three replicate plants were analyzed for each line and averaged. Standard deviations greater than the size of the symbol are shown.

resulting in a lower calculated NPQ. In the *lut1aba1* and *lut2aba1* double mutants, high constitutive levels of zeaxanthin restored the rapid phase of NPQ that was defective in the lutein-deficient single mutants. However, the maximal level of NPQ in these double mutants was much lower than wild type or any of the single mutants.

The widely held view of the xanthophyll cycle is that zeaxanthin (and possibly antheraxanthin) are the only carotenoid(s) that contribute to NPQ (Pfundel and Bilger, 1994; Demmig Adams and Adams, 1996a; 1996b; Gilmore, 1996). In complete contrast, we have shown that the *Arabidopsis* lutein mutants have both delayed and reduced levels of NPQ (Fig. 6). Likewise, a reduction in the level of NPQ was also obtained in the *lor1* mutant of *Chlamydomonas* which lacks lutein (Niyogi et al., 1997). Therefore, the genetic analysis in both *Chlamydomonas* and *Arabidopsis* suggests that lutein, in addition to zeaxanthin and antheraxanthin, contributes to NPQ either directly or indirectly. Specifically, lutein appears to be involved in the rapid induction of NPQ, which was markedly delayed in the *lut* mutants upon illumination with high light. The reduction in NPQ in the *lor1* and *lut* mutants was seen despite increased levels of violaxanthin and antheraxanthin. Violaxanthin would not be expected to quench, however, antheraxanthin is a photophysical homologue of lutein in vitro and thus might be expected to contribute to the rapid phase of NPQ. It is possible that the accumulated antheraxanthin in *lut2* and *lut1* is unavailable to the site of NPQ, or perhaps the role of antheraxanthin in NPQ needs to be re-evaluated. The conservation of lutein's augmentation of NPQ in *Arabidopsis* and *Chlamydomonas* implies that not only is lutein ubiquitous in green algae and higher plants, so may be its contribution to NPQ. Although these results are far from conclusive, the hypothesis that zeaxanthin and antheraxanthin are the only xanthophylls contributing to NPQ in plants appears to need critical reexamination in light of the results observed with the lutein deficient mutants.

While it is clear that the genetic removal of lutein from photosystems in vivo affects the rapid phase of

NPQ the question remains open as to whether lutein directly or indirectly impacts NPQ. A valid argument for an indirect contribution would be that the absence of lutein alters LHC antenna structure in such a way as to impede quenching. The LHC is protonated during light stress which is hypothesized to result in conformation change promoting NPQ (Walters et al., 1996). It may be that the loss of lutein from the antenna deleteriously affects this protonation-induced conformation change and thereby reduces quenching. The alternative thesis is that lutein directly contributes to fluorescence quenching. This would necessitates that lutein have both the appropriate energy state and location to quench singlet chlorophyll. Both requirements can be met theoretically as the predicted excited S_1 energy state of lutein has a spectral overlap with the excited states of chlorophyll which would enable it to act as a quencher (Frank et al., 1994) and the proposed location of lutein in the atomic structure of the LHCII would be spatially appropriate (Kuhlbrandt et al., 1994). When considering the potential mechanism of lutein-induced quenching it should be noted that the constitutive presence of zeaxanthin in the *lut2aba1* double mutant complemented the role of lutein in the rapid phase of NPQ (Fig. 6). While much work is required to define whether lutein directly or indirectly contributes to quenching, the genetic and photophysical results to date are consistent with the idea that lutein can act directly as an integral component of NPQ.

V. Conclusions and Prospectus

The studies described in this chapter have provided novel insights into carotenoid synthesis and function and demonstrated a surprising plasticity of plant photosystems in their xanthophyll composition. From in vitro and in vivo studies of photosystem assembly and function, evolutionary and energetic considerations of the highly conserved carotenoid composition in photosynthetic plant tissues, more detrimental effects would be anticipated when entire classes, and in some cases all, wild type xanthophylls are eliminated in *Arabidopsis*. Nonetheless, most xanthophyll deficient mutant lines are not visibly affected at moderate light conditions, indicating various carotenoid combinations are capable of allowing the assembly of functional pigment: protein complexes under these conditions, although some combinations (e.g. *lut2/aba1*) are clearly less efficient at assembly than others. As such, our results present a seeming paradox: Why would the 'native' carotenoid composition of higher plants be so highly conserved evolutionarily (lutein, β-carotene, violaxanthin, neoxanthin) when our mutants make it clear that plant photosystems are tremendously flexible in the carotenoids they will tolerate?

One possible explanation, and a hypothesis to be tested in the near future, is that the 'native' carotenoid composition represents, as a group, those best suited to provide the full range of structural and functional flexibility required for photosynthesis in a natural environment where light levels often change dramatically in a time frame of seconds (sun flecks), minutes (clouds) or days (germination and growth through soil). It follows that at moderate light and temperature conditions where many carotenoids functions are likely to be needed sparingly if at all, differences between wild type and mutant xanthophyll compositions would not be readily evident. However, at high light extremes and/or low temperature situations where excitation pressure is high within the photosystems, and the full range of carotenoid functions are of necessity more fully utilized, mutant xanthophyll compositions may prove inferior both structurally and functionally to wild-type. These and other hypotheses are directly testable by analyzing, comparing and correlating the biochemical, structural and photochemical responses of the five mutant lines with each other and wild-type in response to a range of conditions. In the process we expect to greatly increase our understanding about the role of specific carotenoids in various aspects of photosystem structure and function in vivo.

Acknowledgments

The author would like to thank all the undergraduates, graduate students, postdocs and colleagues whose hard work, dedication and scientific curiosity over the past several years made the work presented in this chapter possible. I would especially like to thank Drs. Kris Niyogi and Olle Bjorkmann for their assistance with NPQ studies, Dr. Francis X. Cunningham for an enjoyable collaboration in cloning genes of the carotenoid biosynthetic pathway, Ms. Kelly MacDonald and Maria Troung for their heroic efforts during HPLC screening for mutants and Dr. Barry Pogson, who was a key participant in all phases of the described work. A special note of

thanks goes out to Dr. George Britton for his unfailing guidance, encouragement and good humor during the course of this research.

References

Anandan S, Morishige DT and Thornber JP (1993) Light-induced biogenesis of light-harvesting complex I (LHC I) during chloroplast development in barley (*Hordeum vulgare*). Plant Physiol 101: 227–236

Bartley GE and Scolnik PA (1994) Molecular biology of carotenoid biosynthesis in plants. Ann Rev Plant Physiol Plant Mol Biol 45: 287–301

Bassi R, Pineau B, Dainese P and Marquardt J (l993) Carotenoid-binding proteins of photosystem II. Eur J Biochem 212: 297–303

Bell CJ and Ecker JR (1994) Assignment of 30 microsatellite loci to the linkage map of *Arabidopsis*. Genomics 19: 137–144

Beyer P (1987) Solubilization and reconstitution of carotenogenic enzymes from daffodil chromoplast membranes using 3-[(3-Cholamidopropyl)dimethylammonio]–l-propane Sulfonate. In Methods Enzymol 148: 392–400

Bishop NI (1996) The beta, epsilon-carotenoid, lutein, is specifically required for the formation of the oligomeric forms of the light harvesting complex in the green alga, *Scenedesmus obliquus*. J Photochem and Photobiol 36: 279–283

Bishop N I, Urbig T and Senger H (1995) Complete separation of the beta, epsilon- and beta, beta-carotenoid biosynthetic pathways by a unique mutation of the lycopene cyclase in the green alga, *Scenedesmus obliquus*. FEBS Letters 367: 158–162

Bramley PM (1985) The in vitro biosynthesis of carotenoids. Adv Lipid Res 21: 243–279

Britton G (1985) General carotenoid methods. Methods Enzymol 3: 113–149

Britton G (1988) Biosynthesis of Carotenoids. In: Goodwin T (ed) Plant Pigments, pp 133–182. Academic Press Limited, San Diego

Cammarata KV, Plumley FG and Schmidt GW (1992) Pigment and protein composition of reconstituted light-harvesting complexes and effects of some protein modifications. Photosynth Res 33: 235–250

Cammarata KV and Schmidt GW (1992) In vitro reconstitution of a light-harvesting gene product: Deletion mutagenesis and analyses of pigment binding. Biochemistry 31: 2779–2789

Chamovitz D, Pecker I, Sandmann G, Boger P and Hirschberg J (1989) Cloning a gene coding for norflurazon resistance in cyanobacteria. Z. Naturforsch 45: 482–486

Chamovitz D, Misawa N, Sandmann G and Hirschberg J (1992) Molecular cloning and expression in *Escherichia coli* of a cyanobacterial gene coding for phytoene synthase, a carotenoid biosynthesis enzyme. FEBS 296: 305–310

Chang C, Bowman JL, DeJohn AW, Lander ES and Meyerowitz EM (1988) Restriction fragment length polymorphism linkage map for *Arabidopsis thaliana*. Proc Natl Acad Sci USA 85: 6856–6860

Chunaev AS, Mirnaya ON, Maslov VG and Boschetti A (1991) Chlorophyll *b*- and loroxanthin-deficent mutants of *Chlamydomonas reinharti*. Photosynthetica 25: 291–301

Cunningham FX and Gantt E (1998) Genes and enzymes of carotenoid biosynthesis in plants. Ann Rev Plant Physiol Plant Mol Biol 49: 557–583

Cunningham FX Jr, Chamovitz D, Misawa N, Gantt E and Hirschberg J (1993) Cloning and functional expression in *Escherichia coli* of a cyanobacterial gene for lycopene cyclase, the enzyme that catalyzes the biosynthesis of beta-carotene. FEES Let 328: 130–138

Cunningham FX Jr, Sun Z, Chamovitz D, Hirschberg J and Gantt E. (1994) Molecular structure and enzymatic function of lycopene cyclase from the cyanobacterium *Synechococcus* sp strain PCC7942. Plant Cell 6: 1107–1121.

Cunningham FX Jr., Pogson B, Sun Z, McDonald KA, DellaPenna D and Gantt E (1996) Functional analysis of the b and e lycopene cyclase enzymes of *Arabidopsis* reveals a mechanism for control of cyclic carotenoid formation. Plant Cell 8: 1613–1626

Demmig-Adams B and Adams WW III (1992) Photoprotection and other responses of plants to high light stress. Ann Rev Plant Physiol Plant Mol Biol 43: 599–626

Demmig-Adams B and Adams WW III (1996a) Xanthophyll cycle and light stress in nature: Uniform response to excess direct sunlight among higher plant species. Planta 198: 460–470

Demmig-Adams B and Adams, WW III (1996b) The role of xanthophyll cycle carotenoids in the protection of photosynthesis. Trends Plant Sci 1: 21–26

Dogbo O, Laferriere A, D'Harlingue A and Camara B (1988) Carotenoid biosynthesis: isolation and characterization of a bifunctional enzyme catalyzing the synthesis of phytoene. Proc Natl Acad Sci USA 85: 7054–7058

Dreyfuss BW and Thornber JP (I994a) Assembly of the light-harvesting complexes (LHCs) of photosystem II. Monomeric LHC 11b complexes are intermediates in the formation of oligomeric LHC 11b complexes. Plant Physiol 106: 829–839

Dreyfuss BW and Thornber JP (1994b) Organization of the light-harvesting complex of photosystem I and its assembly during plastid development. Plant Physiol 106: 841–848

Feldmann KA, Marks MD, Christianson ML and Quatrano RS (1989) A dwarf mutant of *Arabidopsis* generated by T-DNA insertion mutagenesis. Science 243: 1351–1354

Flachmann R and Kuhlbrandt W (1995) Accumulation of plant antenna complexes is regulated by post-transcriptional mechanisms in tobacco. Plant Cell 7: 149–162

Frank HA and Cogdell RJ (1996) Carotenoids in Photosynthesis. Photochem Photobiol 63: 257–264

Frank HA, Cua A, Chynwat V, Young A, Gosztola D and Wasielewski MR (1994) Photophysics of the carotenoids associated with the xanthophyll cycle in photosynthesis. Photosynth Res 41: 389–395

Gabellini N, Bowyer JR, Hurt E, Melandri A and Hauska G (1982) A cytochrome b/c_1 complex with ubiquinol-cytochrome c_2 oxidoreductase activity from *Rhodopseudomonas sphaeroides*. Eur J Biochem 126: 105–111

Gilmore AM (1996) Mechanistic aspects of xanthophyll cycle-dependent photoprotection in higher plant chloroplasts and leaves. Physiol Plantarum 98: 1–13

Giuliano G, Bartley GE and Scolnik PA (1993) Regulation of carotenoid biosynthesis during tomato development. Plant Cell 5: 379–387

Grossman AR, Bhaya D, Apt K.E and Kehoe DM (1995) Light-

harvesting complexes in oxygenic photosynthesis: Diversity, control, and evolution. Ann Rev Genetics 29: 231–288

Grumbach K H and Lichtenthaler HK (1982) Chloroplast pigments and their biosynthesis in relation to light intensity Radish seedlings. Photochem Photobiol 35: 209–212

Horton P, Ruban AV and Walters RG (1994) Regulation of light harvesting in green plants. Indication by nonphotochemical quenching of chlorophyll fluorescence. Plant Physiol 106: 415–420

Hugueney P, Romer S, Kuntz M and Camara B (1992) Characterization and molecular cloning of a flavoprotein catalyzing the synthesis of phytofluene and zeta-carotene in *Capsicum* chromoplasts. Eur J Biochem 209, 399–407

Hugueney P, Badillo A, Chen HC, Klein A, Hirschberg J, Camara B and Kuntz M (1995) Metabolism of cyclic carotenoids: A model for the alteration of this biosynthetic pathway in *Capsicum annum* chromoplasts. Plant Journal 8: 417–424

Humbeck K, Romer S and Senger H (1989) Evidence for an essential role of carotenoids in the assembly of an active photosystem II. Planta 179: 242–250

Hurry VM (1995) Non-photochemical quenching in xanthophyll cycle mutants of *Arabidopsis* and tobacco deficient in cytochrome B_6/F and ATPase activity. In Mathis P (ed) Photosynthesis: From Light to Biosphere, pp 417–420. Kluwer Academic Publishers, Dordrecht

Hurry V, Anderson JM, Chow WS and Osmond CB (1997) Accumulation of Zeaxanthin in abscisic acid-deficient mutants of *Arabidopsis* does not affect chlorophyll fluorescence quenching or sensitivity to photoinhibition in vivo. Plant Physiol 113:639–648

Jansson S (1994) The light-harvesting chlorophyll *a/b*-binding proteins. Biochim Biophys Acta 1184: 1–19

Juhler RK, Andreasson E, Yu SG and Albertsson PA (1993) Composition of photosynthetic pigments in thylakoid membrane vesicles from spinach. Photosynth Res 35: 171–178

Kajiwara S, Kakizono T, Saito T, Kondo K, Ohtani T, Nishio N, Nagai S and Misawa N (1995) Isolation and functional identification of a novel cDNA for astaxanthin biosynthesis from *Haematococcus pluvialis,* and astaxanthin synthesis in *Escherichia coli.* Plant Mol Biol 29: 343–352

Konieczny A and Ausubel FM (1993) A procedure for mapping *Arabidopsis* mutations using co-dominant ecotype-specific PCR-based markers. Plant J 4: 403–410

Koornneef M, Jorna ML, Brinkhorst van der Swan DLC and Karssen CM (1982) The isolation of abscisic acid (ABA) deficient mutants by selection of induced revertants in non-germinating gibberellin sensitive lines of *Arabidopsis thaliana* (L.) Heynh. Theor Appl Genet 61: 385–393

Kühlbrandt W, Wang DN and Fujiyoshi Y (1994) Atomic model of a plant light-harvesting complex by electron crystallography. Nature 367: 614–621

Kuntz M, Evrard JL, d'Harlingue A, Weil JH and Camara B (1989) Expression of plastid and nuclear genes during chromoplast differentiation in bell pepper (*Capsicum annum*) and sunflower (*Helianthus annuus*). Mol Gen Genet 216:156–163

Kuntz M, Romer S, Suire C, Hugueney P, Weil JH, Schantz R and Camara B (1992) Identification of a cDNA for the plastid-located geranylgeranyl pyrophosphate synthase from *Capsicum annuum*: correlative increase in enzyme activity and transcript level during fruit ripening. Plant J 2: 25–34

McKinney EC, Ali N, Traut A, Feldmann KA, Belostotsky DA, McDowel JM and Meagher RB (1995) Sequence-based identification of T-DNA insertion mutations in *Arabidopsis*: actin mutants *act2-1* and *act4-1*. Plant J 8: 613–622

Meurer J, Meierghoff D and Westhoff P (1996) Isolation of high-chlorophyll-fluorescence mutants of *Arabidopsis thaliana* and their characterization by spectroscopy, immunoblotting and Northern hybridisation. Planta 198: 385–396

Misawa N, Truesdale MR, Sandmann G, Fraser PD, Bird C, Schuch W and Bramley PM (1994) Expression of a tomato cDNA coding for phytoene synthase in *Escherichia coli,* phytoene formation in vivo and in vitro, and functional analysis of the various truncated gene products. J Biochem 116: 980–985

Newman T, De Bruijn FJ, Green P, Keegstra K, Kende H, McIntosh L, Ohlrogge J, Raikhel N, Somerville S, Thomashow M, Retzel E and Somerville C (1994) Genes Galore: A summary of methods for accessing results from large-scale partial sequencing of anonymous *Arabidopsis* cDNA clones. Plant Physiol 106: 1241–1255

Niyogi KK, Bjorkman O and Grossman AR (1997) The roles of specific xanthophylls in photoprotection. Proc NatI Acad Sci USA 94: 14162–14167

Norris SR, Barrette TR and DellaPenna D (1995) Genetic dissection of carotenoid synthesis in *Arabidopsis* defines plastoquinone as an essential component of phytoene desaturation. Plant Cell 7: 2139–2149

Oelmuller R and Mohr H (1985) Carotenoid composition in milo (*Sorghum vulgare*) shoots as affected by phytochrome and chlorophyll. Planta 164: 390–395

Paulsen H, Rumler U and Rudiger W (1990) Reconstitution of pigment-containing complexes from light-harvesting chlorophyll *a/b*-binding protein overexpressed in *Escherichia coli.* Planta 181:204–211

Paulsen H, Finkenzeller B and Kuhlein N (1993) Pigments induce folding of light-harvesting chlorophyll *a/b* binding protein. Eur J Biochem 215: 809–816

Pecker I, Chamovitz D, Linden H, Sandmann G and Hirschberg J (1992) A single polypeptide catalyzing the conversion of phytoene to zeta-carotene is transcriptionally regulated during tomato fruit ripening. Proc Natl Acad Sci USA 89:4962–4966

Pecker I, Gabbay R, Cunningham FX Jr and Hirschberg J (1996) Cloning and characterization of the cDNA for lycopene beta-cyclase from tomato reveals decrease in its expression during fruit ripening. Plant Mol Biol 30: 807–819

Peter GF and Thornber JP (1991) Biochemical composition and organization of higher plant Photosystem II light-harvesting pigment-proteins. J Biol Chem 266: 16745–16754

Pfundel E and Bilger W (1994) Regulation and possible function of the violaxanthin cycle. Photosynth Res 42: 89–109

Plumley FG and Schmidt GW (1987) Reconstitution of chlorophyll *a/b* light-harvesting complexes: Xanthophyll-dependent assembly and energy transfer. Proc Natl Acad Sci USA 84: 146–150

Pogson B, McDonald K, Truong M, Britton G and DellaPenna D (1996) *Arabidopsis* carotenoid mutants demonstrate that lutein is not essential for photosynthesis in higher plants. Plant Cell 8: 1627–1639

Rock CD and Zeevaart JAD (1991) The aba mutant of *Arabidopsis*

thaliana is impaired in epoxy-carotenoid biosynthesis. Proc Natl Acad Sci USA 88: 7496–7499

Rock CD, Bowlby NR, Hoffmann Benning S and Zeevaart JAD (1992) The *aba* mutant of *Arabidopsis thaliana* (L.) Heynh. has reduced chlorophyll fluorescence yields and reduced thylakoid stacking. Plant Physiol 100: 1796–1801

Romer S, Hugueney P, Bouvier F, Camara B and Kuntz M (1993) Expression of the genes encoding the early carotenoid biosynthetic enzymes in Capsicum annuum. Biochem Biophys ResComm 196: 1414–1421

Ruban AV, Young AJ, Pascal AA and Horton P (1994) The effects of illumination on the xanthophyll composition of the photosystem II light-harvesting complexes of spinach thylakoid membranes. Plant Physiol 104: 227–234

Russell AW, Critchley C, Robinson SA, Franklin LA, Seaton GGR, Chow WS, Anderson JM and Osmond CB (1995) Photosystem II regulation and dynamics of the chloroplast D1 protein in *Arabidopsis* leaves during photosynthesis and photoinhibition. Plant Physiol 107: 943–952

Sandmann G, Kuhn M and Boger P (1993) Carotenoids in photosynthesis: Protection of D1 degradation in the light. Photosynth Res 35: 185–190

Sandmann G (1994) Carotenoid biosynthesis in microorganisms and plants. Eur J Biochem 223: 7–24

Siefermann-Harms D (1985) Carotenoids in photosynthesis. I. Location in photosynthetic membranes and light-harvesting function. Biochim Biophys Acta 811: 325–355

Siefermann-Harms D (1987) The light-harvesting and protective functions of carotenoids in photosynthetic membranes. Physiol Plantarum 69: 561–568

Sun Z, Gantt E and Cunningham FX Jr (1996) Cloning and functional analysis of the β-carotene hydroxylase of *Arabidopsis thaliana*. J Biol Chem 271: 24349–24352

Tardy F and Havaux M (1996) Photosynthesis, chlorophyll fluorescence, light-harvesting system and photoinhibition resistance of a zeaxanthin-accumulating mutant of *Arabidopsis thaliana*. J Photochem Photobio 34: 87–94

Walters RG and Horton P (1994) Acclimation of *Arabidopsis thaliana* to the light environment: Changes in composition of the photosynthetic apparatus. Planta 195: 248–256

Walters RG and Horton P (1995a) Acclimation of *Arabidopsis thaliana* to the light environment: Changes in photosynthetic function. Planta 197: 306–312

Walters RG and Horton P (1995b) Acclimation of *Arabidopsis thaliana* to the light environment: Regulation of chloroplast composition. Planta 197: 475–481

Walters RG, Ruban AV and Horton P (1996) Identification of proton-active residues in a higher plant light-harvesting complex. Proc Natl Acad Sci USA 93: 1–5

Yanofsky MF, Ma H, Bowman JL, Drews GN, Feldmann KA and Meyerowitz EM (1990) The protein encoded by the *Arabidopsis* homeotic gene *agamous* resembles transcription factors. Nature 346: 35–39

Young ND and Phillips RL (1994) Cloning plant genes known only by phenotype. Plant Cell 6: 1193–1195

This page intentionally left blank

Chapter 3

Carotenoids and Carotenogenesis in Anoxygenic Photosynthetic Bacteria

Shinichi Takaichi
Nippon Medical School, Biological Laboratory, 297, Kosugi-cho 2, Nakahara, Kawasaki 211-0063, Japan

H. A. Frank, A. J. Young, G. Britton and R. J. Cogdell (eds): The Photochemistry of Carotenoids, pp. 39–69.

Summary

More than 50 genera including about 130 species of anoxygenic photosynthetic bacteria have been described. These bacteria produce around 100 different carotenoids. In this chapter, the carotenoid compositions of all the photosynthetic bacteria so far described are summarized. All of the carotenogenesis genes from *Rhodobacter,* and some of them from other bacteria have been cloned, and the characteristics of their products have been investigated. Schmidt (1978) proposed four main pathways for carotenogenesis. In this chapter, five main pathways within anaerobic photosynthetic bacteria are now suggested based on these new findings: the spirilloxanthin pathway (normal spirilloxanthin, unusual spirilloxanthin, spheroidene, and carotenal pathways), the okenone pathway (okenone, and *R.g.*-keto carotenoid pathways), the isorenieratene pathway (isorenieratene, and chlorobactene pathways), the γ- and β-carotene pathway, and the diapocarotene pathway. In addition, carotenoid glucosides and carotenoid glucoside fatty acid esters have also been found in some species.

The Rhodospirillaceae and Chromatiaceae have the spirilloxanthin or the okenone pathway depending on the genus or species. All of the Ectothiorhodospiraceae have the spirilloxanthin pathway. The isorenieratene, the γ- and β-carotene, and the diapocarotene pathways are found specifically in the Chlorobiaceae, Chloroflexaceae, and Heliobacteriaceae, respectively. Aerobic photosynthetic bacteria mostly have the spirilloxanthin pathway, further most of these species have unusual carotenoids including 'non-photosynthetic' carotenoids, such as carotenoid sulfates and carotenoic acids, which have no photosynthetic functions.

I. Introduction

Anoxygenic photosynthetic bacteria necessarily synthesize not only BChl but also carotenoids. About two decades ago, Schmidt (1978) summarized the distribution of carotenoids in 19 genera including 38 species of photosynthetic bacteria. Now, more than 50 genera including more than 130 species have been described. Based on the results of new techniques for the classification, some genera have been reorganized and some species have been re-named. Further, two new categories of photosynthetic bacteria have been described, Heliobacteriaceae and aerobic photosynthetic bacteria (Pfennig and Trüper, 1989; International Journal of Systematic Bacteriology; Blankenship et al., 1995). The recommended three-letter abbreviations for genera of the anoxygenic photosynthetic bacteria which have been proposed by the International Committee on Systematic Bacteriology, Subcommittee on the Taxonomy of Phototrophic Bacteria, are listed in Tables 3–9 (Trüper and Imhoff, 1999).

Around 100 different carotenoids have been found in the photosynthetic bacteria, and most of their chemical structures are distinct from those found in algae, fungi, higher plants and non-photosynthetic bacteria. These carotenoids were characterized with the following ways by Schmidt (1978) and some characteristics newly found are also indicated: (1) They most often occur as acyclic compounds. (2) They often contain tertiary hydroxyl and methoxy groups at C-1. (3) There are frequently double bonds in the C-3,4 position. (4) Keto groups in conjugation with the polyene chain are found attached to C-2 and to C-4 of the ψ end group. (5) Aldehyde groups in conjugation with the polyene chain are sometimes present at the C-20 position. (6) Cyclic carotenoids commonly have aromatic rings, ϕ and χ end groups, synthesized from the β end group. (7) Heliobacteriaceae have only C_{30} carotenes, 4,4′-diapocarotenes. (8) Some Ectothiorhodospiraecae, Chlorobiaceae and Chloroflexaceae have carotenoid glucoside esters. (9) Most aerobic photosynthetic bacteria have unusual carotenoids, such as carotenoid sulfates, carotenoic acids and hydroxyl derivatives of β-carotene. (10) In most cases, there are small amounts of intermediates.

Many carotenoids have trivial names. However all carotenoids have been named semisystematically based on IUPAC-IUB nomenclature (IUPAC Commission on Nomenclature of Organic Chemistry and the IUPAC-IUB Commission on Biochemical Nomenclature, 1975; Weedon and Moss, 1995). The structure of the end groups and carbon numberings of carotenoids within photosynthetic bacteria are illustrated in Fig. 1. A list of these names and the structures of all known naturally occurring carotenoids, and references giving data for each compound

Abbreviations: BChl – bacteriochlorophyll; Erb-type – erythrobacter-type; G – glucoside; G-FA – glucoside ester; LH – light-harvesting; PS – photosystem; RC – reaction center

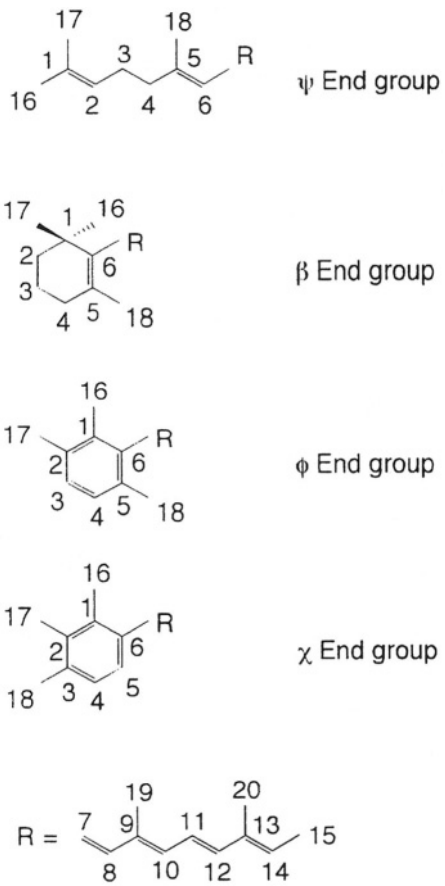

Fig. 1. Structure of the end groups and carbon numberings of carotenoids within photosynthetic bacteria based on IUPAC-IUP nomenclature (1975).

are presented by Straub (1987) and Kull and Pfander (1995).

In this chapter, five main pathways for carotenogenesis within anaerobic photosynthetic bacteria are proposed (Table 1). The carotenoid compositions in both anaerobic and aerobic photosynthetic bacteria are also summarized in Tables 3 to 9. Note that the compositions are rather variable depending on the culture conditions, such as light intensity (Gardiner, 1992; Gardiner et al., 1993), oxygen concentration (Goodwin, 1956), and growth phases (Schwerzmann and Bachofen, 1989), and also depend on the strain in some species, such as *Rps. acidophila* (Gardiner, 1992) and *Rcy. tenuis* (Schmidt, 1978). Identification of carotenoids cited in the Tables are based on the description given in each reference, although it should be noted that some are doubtful or were identified with insufficient data.

II. Carotenogenesis

A. Classification of Carotenogenesis

From the analysis of carotenoid compositions, four main pathways for Carotenogenesis were proposed by Schmidt (1978): the spirilloxanthin pathway (normal spirilloxanthin series and rhodopinal series), the spheroidene pathway (alternative spirilloxanthin series), the okenone pathway, and the isorenieratene pathway. Since then, many new species have been described, some Carotenogenesis genes have been cloned (Table 2) and the characteristics of their products have been investigated (Sandmann, 1994, 1997; Armstrong, 1995, 1997). Based on these new results and the changes in the classification of photosynthetic bacteria, five main pathways within anaerobic photosynthetic bacteria are now suggested in Table 1: The spheroidene pathway is included in the spirilloxanthin pathway, the γ- and β-carotene pathway is independent, and the diapocarotene pathway is described for the newly found Heliobacteriaceae.

1. Spirilloxanthin pathway (normal spirilloxanthin, unusual spirilloxanthin, spheroidene, and carotenal pathways).

2. Okenone pathway (okenone, and *R.g.*-keto carotenoid pathways).

3. Isorenieratene pathway (isorenieratene, and chlorobactene pathways).

4. γ- And β-carotene pathway.

5. Diapocarotene pathway.

Most of the aerobic photosynthetic bacteria so far described have the spirilloxanthin pathway, further some also have unusual carotenoids as described below.

B. Types of Reactions in Carotenogenesis

Carotenoids are usually tetraterpenoids consisting of eight isoprene units, C_5-compound. Four of the C_5 units combine to yield a C_{20}-compound, geranylgeranyl pyrophosphate. In a tail-to-tail condensation of two these C_{20}, the C_{40}, phytoene, is formed by phytoene synthase (CrtB) whose reaction needs ATP

Table 1. Carotenogenesis pathways and their distribution within anaerobic photosynthetic bacteria [a]

Carotenogenesis pathways	Abbreviations [b]	Family	Figure numbers
Spirilloxanthin			
Normal spirilloxanthin	Spirilloxanthin	Rhodospirillaceae, Chromatiaceae, Ectothiorhodospiraceae	4
Unusual spirilloxanthin	Unusual-Spirillo	Rhodospirillaceae, Chromatiaceae, Ectothiorhodospiraceae	
Spheroidene	Spheroidene	Rhodospirillaceae	5
Carotenal	Carotenal	Rhodospirillaceae, Chromatiaceae	6
Okenone			
Okenone	Okenone	Chromatiaceae	7
R.g.-Keto carotenoid	*R.g.*-keto	Rhodospirillaceae	7
Isorenieratene			
Isorenieratene	Isorenieratene	Chlorobiaceae	8
Chlorobactene	Chlorobactene	Chlorobiaceae	8, 9
γ- And β-carotene	$\gamma + \beta$	Chloroflexaceae	10
Diapocarotene	Diapocarotene	Heliobacteriaceae	11
Additional pathway			
Glucoside	G	Rhodospirillaceae, Ectothiorhodospiraceae	12
Glucoside ester	G-FA	Ectothiorhodospiraceae, Chlorobiaceae, Chloroflexaceae	9, 10, 12

[a] Since aerobic photosynthetic bacteria contain many unusual carotenoids, it is difficult to list in this Table (See Table 9 and Fig. 13).
[b] These abbreviations are used in Tables 3–9.

Table 2. Types of reactions seen in the carotenoid biosynthesis within anaerobic photosynthetic bacteria, and cloned genes from photosynthetic bacteria and other bacteria [a]

Reactions	Genes	Abbreviations [b]
Geranylgeranyl pyrophosphate synthesis	*crtE* [c,d,e,f]	
Phytoene synthesis	*crtB* [c,d,e,f]	
Desaturation of phytoene	*crtI* [c,d,e,f,g]	
C-3,4 Desaturation	*crtD* [c,f]	–2H
C-7,8 Desaturation		
C-1,2 Saturation		+2H
Lycopene cyclization	*crtY* [d,e,g]	β
γ-Carotene synthesis [i]		γ
Aromatization from β to ϕ end group	*crtT,U* [e]	ϕ
Aromatization from β to χ end group		χ
C-1,2 Hydration	*crtC* [c,f]	$+H_2O$
Methylation at C-1 hydroxyl group	*crtF* [c,f]	+Me
Ketolation at C-2 of ψ end group	*crtA* [c]	2-Keto
Ketolation at C-4 of ψ end group		4-Keto ψ
Ketolation at C-4 of β end group	*crtW* [h]	4-Keto β
Hydroxylation at C-20		20-OH
Aldehyde at C-20		20-Aldehyde
Glucosylation	*crtX* [d]	+G
Fatty acid esterification		+FA

[a] Since aerobic photosynthetic bacteria contain many unusual carotenoids, it is difficult to list in this Table (see Table 9 and Fig. 13).
[b] These abbreviations are used in Figs. 2–11.
[c] *Rba. capsulatus* (Armstrong et al., 1989) and *Rba. sphaeroides* (Lang et al., 1995).
[d] *Erwinia uredovora* (Misawa et al., 1990) and *Erwinia herbicola* (Hundle et al., 1992).
[e] *Streptomyces grisens*; methyltransferase and dehydrogenase (Schumann et al., 1996).
[f] *Rvi. gelatinosus* (Ouchane et al., 1997a,b; Igarashi et al., 1998; . V. P. Nagashima, personal communications).
[g] *Erb. longus* (Matsumura et al., 1997).
[h] *Agrobacterium aurantiacum* (Misawa et al., 1995).
[i] It is unknown whether γ-carotene synthase is the same with lycopene cyclase or not.

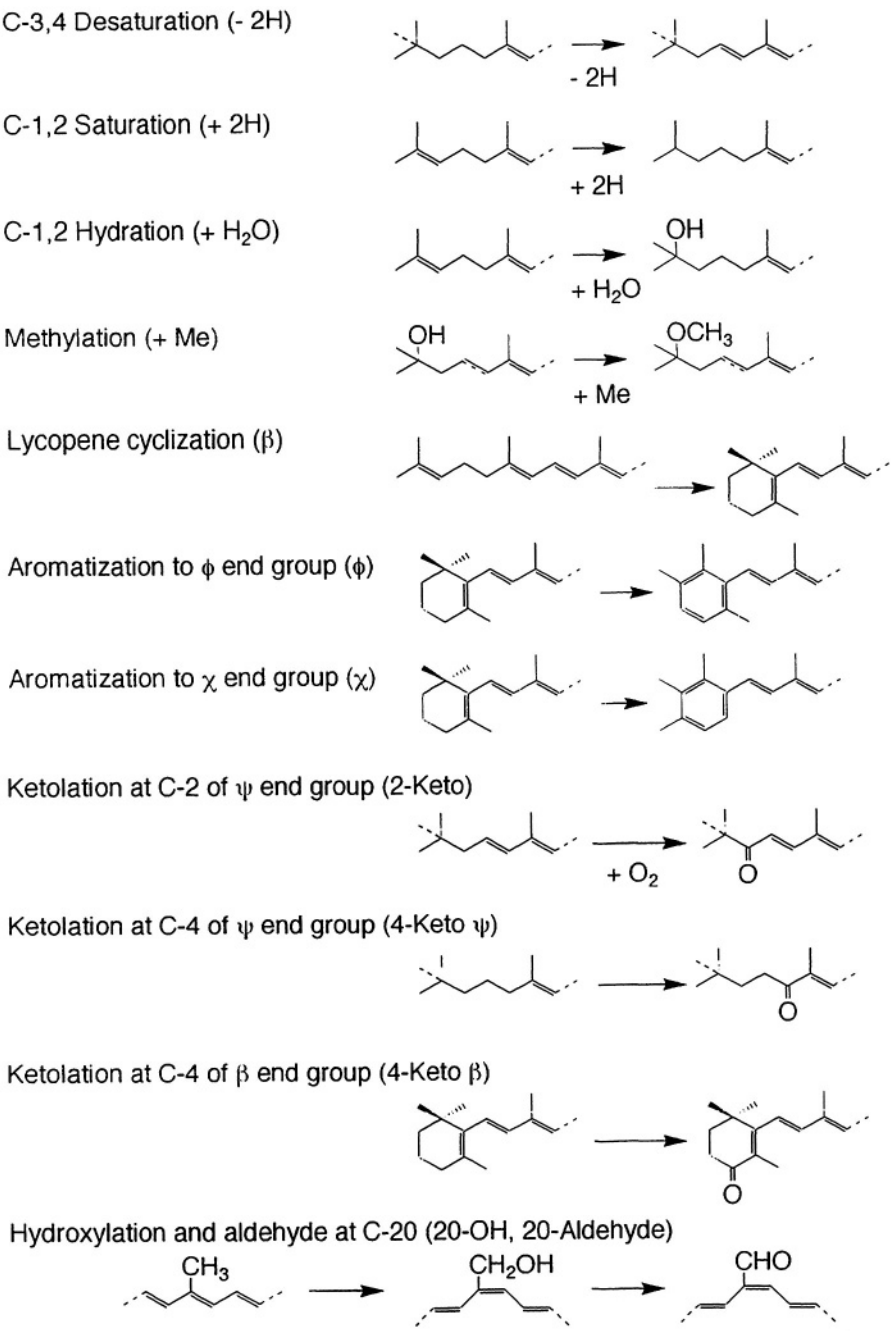

Fig. 2. Types of reactions seen in carotenoid biosynthesis within anaerobic photosynthetic bacteria. Parentheses indicate abbreviations of the reactions (see Table 2).

(Sandmann, 1997). This pathway was confirmed by the cloning of the genes from *Rhodobacter* and *Erwinia* (Sandmann, 1994, 1997; Armstrong, 1995, 1997; Lang et al., 1995).

Phytoene is desaturated to neurosporene or lycopene by the photosynthetic bacteria. These are then converted to carotenes by desaturation, saturation, cyclization and aromatization, and/or to xanthophylls by introduction of the oxy groups, such as hydroxyl, methoxy, keto and aldehyde groups. These reactions, found in the anaerobic photosynthetic bacteria, can be grouped into about 20 types (Table 2, Fig. 2). The carotenogenesis genes cloned from photosynthetic bacteria and other bacteria are also indicated in Table 2.

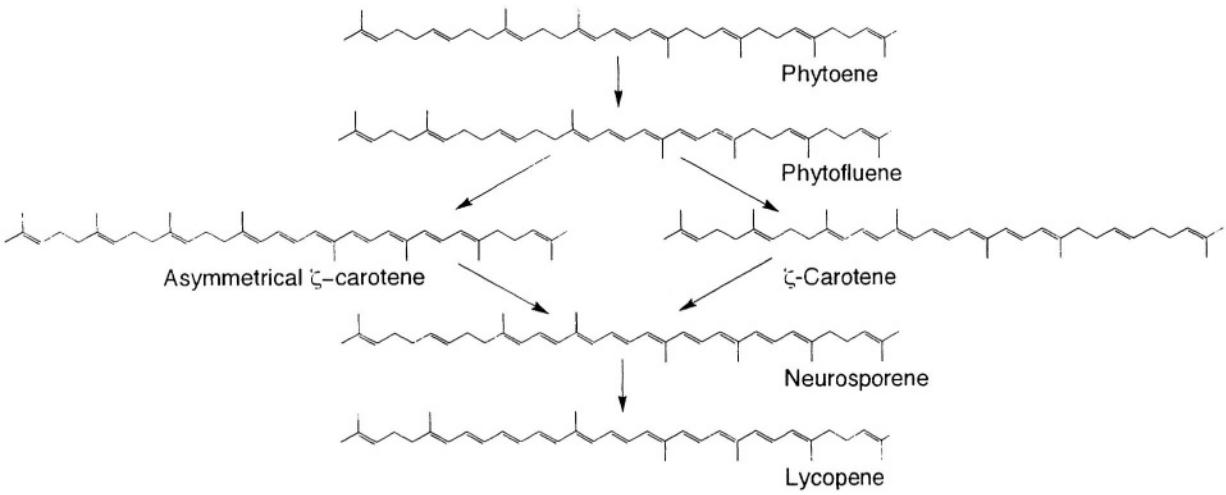

Fig. 3. Desaturation of phytoene to lycopene by phytoene desaturase.

C. Desaturation of Phytoene to Lycopene

Phytoene is the first carotenoid in carotenogenesis, and it usually in the 15-*cis* form. Four desaturation steps are performed in the conversion of phytoene to lycopene by phytoene desaturase (CrtI) in bacteria except for cyanobacteria (Fig. 3). Isomerization from the 15-*cis* form to the all-*trans* form is reported to occur non-enzymatically during the desaturation reactions, since there are no isomerase genes in the carotenoid gene clusters from *Rba. capsulatus* (Armstrong et al., 1989) and *Rba. sphaeroides* (Lang et al., 1995), and gradual conversion of 15-*cis* phytoene to all-*trans* lycopene is found when the *crtI* gene is expressed in *Escherichia coli* in a phytoene background (Misawa et al., 1990). FAD is a cofactor for the phytoene desaturase from *Rba. capsulatus* (Raisig et al., 1996).

During desaturation, two pathways are involved: via ζ-carotene and asymmetrical ζ-carotene (Fig. 3). ζ-Carotene is found in *Rba. capsulatus, Rba. sphaeroides* and *Rvi. gelatinosus* (S. Takaichi, unpublished), *Chl. limicola* and *Pld. luteolum* (Schmidt and Schiburr, 1970) and *Rsb. denitrificans* (Harashima and Nakada, 1983), while asymmetrical ζ-carotene in *Rsp. rubrum* (Davies, 1970), *Rpi. globiformis* (Schmidt and Liaaen-Jensen, 1973), *Rmi. vannielii* (Britton et al., 1975), *Bla. viridis, Chl. tepidum* and *Cfl. aurantiacus* (S. Takaichi, unpublished) and *Erb. longus* (Takaichi et al., 1990). The two pathways via ζ-carotene and asymmetrical ζ-carotene seem not to be related to the final products of the phytoene desaturase, neurosporene and lycopene, or to the classification of photosynthetic bacteria.

Usually the final product of the phytoene desaturase is lycopene, while in *Rhodobacter,* the final product is neurosporene. The deduced amino acid sequences of the *crtI* gene from *Rhodobacter* (final product, neurosporene), and *Erb. longus* and *Erwinia* (lycopene) show significant similarity, but the final products are different (Sandmann, 1994; Armstrong, 1995; Matsumura et al., 1997). The mechanism for recognition of the position on carotenoid by the phytoene desaturase is still unknown; that is, how the intermediate of ζ-carotene or asymmetrical ζ-carotene and the final product of neurosporene or lycopene are controlled.

D. Biosynthesis of Spirilloxanthin

1. Normal Spirilloxanthin Pathway

Carotenogenesis of the normal spirilloxanthin pathway is found in a large number of species of purple bacteria: Rhodospirillaceae, Chromatiaceae and Ectothiorhodospiraceae (Tables 3–5). Spirilloxanthin is a symmetrical compound containing the methoxy groups at C-1 and C-1´ and additional double bonds in the C-3,4 and C-3´,4´ positions. It has 13 conjugated double bonds (Fig. 4).

A sequence of the reactions leading from lycopene

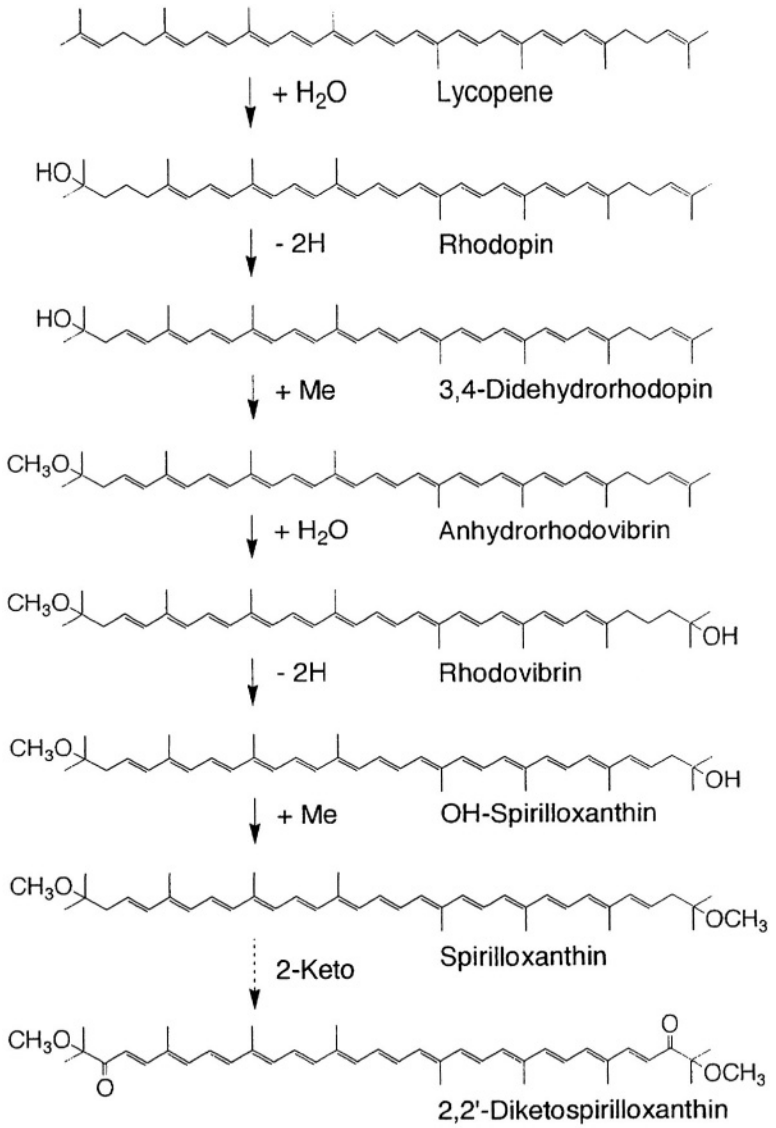

Fig. 4. The predicted pathway for the biosynthesis of spirilloxanthin. Usually, the introduction of 2-keto is not involved in this pathway.

to spirilloxanthin has been proposed (Fig. 4; Schmidt, 1978). This sequence includes the successive reactions of (1) hydration at C-1,2, (2) desaturation at C-3,4, and (3) methylation of the tertiary hydroxyl group at C-1. These reactions occur at first on the one half of the molecule and then on another half. The major component is the final product spirilloxanthin, and usually small amounts of all or a few of five intermediates are also found (Fig. 4). Other postulated intermediates were, however, rarely found as described below. These reactions may be catalyzed by three enzymes similar to CrtC, CrtD and CrtF of *Rhodobacter* (Fig. 5). At present, how the successive reactions are controlled with reactions first one end and then another of the molecule has not been elucidated.

2. Unusual Spirilloxanthin Pathway

When one enzyme of the normal spirilloxanthin pathway is lacking or is present with reduced activity, the composition will be expected to change. Some species have indeed been reported to have such unusual compositions (Tables 3–5). Lycopene is

Table 3. Carotenoids in Rhodospirillaceae

Genus (abbreviation) [a] Species strain	Carotenogenesis type [b]	Carotenoids (% of total)	Ref. No.
α1-Subclass			
Rhodospirillum (*Rsp.*) [c]			
rubrum S1=DSM467	Spirilloxanthin	rhodopin (1), anhydrorhodovibrin (2), rhodovibrin (6), spirilloxanthin (91)	1
S1 (24 h culture)	Spirilloxanthin	lycopene (<3), rhodopin (10-15), anhydrorhodovibrin + rhodovibrin (50), spirilloxanthin (34)	2
(120 h culture)	Spirilloxanthin	anhydrorhodovibrin + rhodovibrin (3), spirilloxanthin (>95)	2
photometricum DSM122	Unusual-Spirillo	lycopene (7), rhodopin (28), anhydrorhodovibrin (20), rhodovibrin (45)	1,3
E11	Unusual-Spirillo	lycopene (46), rhodopin (53)	4
molischianum DSM120	Unusual-Spirillo	lycopene (26), rhodopin (61), OH-rhodopin (11)	4
fulvum 1360=DSM113	Unusual-Spirillo & G	lycopene (15), rhodopin (77), OH-rhodopin (2), unidentified polar compounds (rhodopin glycoside) (6)	1,5
salexigens DSM2132	Spirilloxanthin	rhodopin (2), anhydrorhodovibrin (4), rhodovibrin (2), OH-spirilloxanthin (4), spirilloxanthin (87)	6
salinarum ATCC35394	Spirilloxanthin	lycopene (2), rhodopin (10), anhydrorhodovibrin (6), rhodovibrin (4), spirilloxanthin (79)	5
mediosalinum L1-66	Spirilloxanthin	spirilloxanthin, (intermediate(s) from absorption spectrum)	7
sodomense ATCC51195	Spirilloxanthin	rhodovibrin (1), spirilloxanthin (99)	5
Rhodocista (*Rcs.*)			
centenaria IAM14193=ATCC43720	Spirilloxanthin		8
Rhodospira (*Rsa.*)			
trueperi ATCC700224	Unusual-Spirillo	3,4,3′,4′-tetrahydrospirilloxanthin	9
Rhodopila (*Rpi.*)			
globiformis 7950=ATCC35887	*R.g.*-keto	asymmetrical ζ-carotene + neurosporene (3), lycopene, *R.g.*-keto IV (5), *R.g.*-keto II (80), *R.g.*-keto III (12)	1,5,10
α2-Subclass			
Rhodopseudomonas (*Rps.*)			
palustris ATH2.1.6=ATCC17001	Unusual-Spirillo	lycopene (2), anhydrorhodovibrin (3), rhodovibrin (73), OH-spirilloxanthin (15), spirilloxanthin (7)	1
Morita	Unusual-Spirillo	lycopene (19), rhodopin (61), anhydrorhodovibrin (10), rhodovibrin (6), spirilloxanthin (5)	5
acidophila 7050=ATCC25092 (low) [d]	Spirilloxanthin, carotenal & G	lycopene (9), rhodopin (10), anhydrorhodovibrin (2), spirilloxanthin (2) rhodopinal (5), rhodopin glucoside (1), rhodopinol glucoside (7), rhodopinal glucoside(61)	11
(high) [d]	Spirilloxanthin & G	lycopene (22), rhodopin (37), anhydrorhodovibrin (4), spirilloxanthin (2),rhodopin glucoside (34)	11
7750 (low) [d]	Spirilloxanthin & G	lycopene (24), rhodopin (48), anhydrorhodovibrin (3), spirilloxanthin (1), rhodopin glucoside (24)	11
(high) [d]	Spirilloxanthin & G	lycopene (27), rhodopin (15), anhydrorhodovibrin (4), spirilloxanthin (2), rhodopin glucoside (53)	11
julia KR-11-67=ATCC51105	Spirilloxanthin	rhodovibrin (2), spirilloxanthin (98)	5
cryptolactis ATCC49414	Unusual-Spirillo	lycopene (12), rhodopin (51), anhydrorhodovibrin (12), rhodovibrin (10), spirilloxanthin (16)	5
Rhodomicrobium (*Rmi.*)			
vannielii Douglas=ATCC17100	Unusual-Spirillo & γ+β	lycopene (25), rhodopin (65), OH-rhodopin (1), spirilloxanthin (8), β-carotene (2), β-cryptoxanthin	1,12,13
Rhodoplanes (*Rpl.*)			
roseus DSM5909	Spirilloxanthin	lycopene (2), rhodopin (18), anhydrorhodovibrin (19), rhodovibrin (7), spirilloxanthin (54)	5
elegans JCM9224	Spirilloxanthin		14
Rhodobium (*Rbi.*)			
orientis JCM9337	Spirilloxanthin		15
marinum DSM2698	Spirilloxanthin	lycopene (1), anhydrorhodovibrin (8), rhodovibrin (24), OH-spirilloxanthin (2), spirilloxanthin (65)	16
Blastochloris (*Bla.*)			
viridis DSM133	Unusual-Spirillo	neurosporene (3), 1,2-dihydroneurosporene (72), lycopene (1), 1,2-dihydrolycopene (17), 1,2-dihydro-3,4-dehydrolycopene (5)	17
sulfoviridis DSM729	Spirilloxanthin	neurosporene, spirilloxanthin	18

α3-Subclass			
Rhodobacter (*Rba.*)			
capsulatus NCIB8254	Spheroidene	spheroidene (83), OH-spheroidene (4), spheroidenone (11), OH-spheroidenone (2)	1,3
veldkampii ATCC35703	Spheroidene		19
sphaeroides ATH2.4.1=DSM158	Spheroidene	spheroidene (90), spheroidenone (10)	1,20
G1C [e]	Spheroidene	neurosporene (97), lycopene (3)	5
Ga [e]	Spheroidene	neurosporene (48), chloroxanthin (37), 3,4-dihydrospheroidene (14)	5
azotoformans JCM9340	Spheroidene		21
blasticus NCIB11576	Spheroidene	neurosporene (1), spheroidene (47), OH-spheroidene (47), spheroidenone (5)	5
Rhodovulum (*Rdv.*)			
sulfidophilum W4=DSM1374	Spheroidene	neurosporene (3), demethylspheroidene (43), spheroidene (49), OH-spheroidene (1), spheroidenone (4)	5
adriaticum DSM2781	Spheroidene		19
euryhalinum DSM4868	Spheroidene	ζ-carotene, neurosporene, spheroidene, OH-spheroidene, spheroidenone	22
strictum JCM9220	Spheroidene	spheroidene, spheroidenone	23
β-Subclass			
Rhodocyclus (*Rcy.*)			
purpureus 6770=DSM168	Carotenal	lycopene (2), rhodopin (22), lycopenal (7), rhodopinol (6), rhodopinal (63)	1,24
tenuis 3661=DSM112	Carotenal	lycopene (12), rhodopin (23), lycopenal (10), rhodopinol (5), rhodopinal (50)	1,24
2761=DSM109	Unusual-Spirillo	lycopene (37), rhodopin (16), anhydrorhodovibrin (32), rhodovibrin (7), spirilloxanthin (8)	1
Rhodoferax (*Rfx.*)			
fermentans JCM7819	Spirilloxanthin & spheroidene	spirilloxanthin spheroidene, OH-spheroidene	25
Rubrivivax (*Rvi.*)			
gelatinosus DSM1709 (anaerobic) [f]	Spirilloxanthin & spheroidene	spirilloxanthin (6), spheroidene (36), OH-spheroidene (52), OH-spheroidenone (6)	5
(semi-aerobic) [f]	Spirilloxanthin & spheroidene	2-ketospirilloxanthin (3), 2,2′-diketospirilloxanthin (10), spheroidene (1), OH-spheroidene (3), spheroidenone (11), OH-spheroidenone (73)	5

[a] Recommended 3-letter abbreviations for genera (Trüper and Imhoff, 1999).
[b] See Table 1.
[c] This genus has recently been reclassified (Imhoff et al., 1998a).
[d] low and high: cultured in low and high light intensity, respectively.
[e] Carotenoid mutant.
[f] anaerobic and semi-aerobic: cultured in anaerobic and semi-aerobic, respectively.
1, Schmidt, 1978; 2, Schwerzmann and Bachofen, 1989; 3, Goodwin, 1956; 4, Matuura and Shimada, 1993; 5, S. Takaichi, unpublished; 6, Drews, 1981; 7, Kompantseva and Gorlenko, 1984; 8, Kawasaki et al., 1992; 9, Pfennig et al., 1997; 10, Schmidt and Liaaen-Jensen, 1973; 11, Gardiner, 1992; 12, Ryvarden and Liaaen-Jensen, 1964; 13, Britton et al., 1975; 14, Hiraishi and Ueda, 1994; 15, Hiraishi et al., 1995b; 16, Imhoff, 1983; 17, Malhotra et al., 1970; 18, Keppen and Gorlenko, 1975; 19, Pfennig and Trüper, 1989; 20, Shneour, 1962a; 21, Hiraishi et al., 1995a; 22, Kompantseva, 1985; 23, Hiraishi and Ueda, 1995; 24, Schmidt, 1971; 25, Hiraishi et al., 1991.

Table 4. Carotenoids in Chromatiaceae

Genus (abbreviation) [a] Species strain	Carotenogenesis type [b]	Carotenoids (% of total)	Ref. No.
Thiospirillum (*Tsp.*)			
jenense 1112=DSM216	Unusual-Spirillo	lycopene (12), rhodopin (88)	1,2
Thiorhodovibrio (*Trv.*)			
winogradskii SSP1=DSM6702	Unusual-Spirillo	lycopene (6), rhodopin (47), anhydrorhodovibrin (14), rhodovibrin (4), spirilloxanthin (29)	3
Chromatium (*Chr.*) [c]			
okenii 1111=DSM169	Okenone	okenone (100)	1,2
weissei 2111=DSM171	Okenone	okenone (100)	1,2
minus 1211=DSM178	Okenone	okenone (100)	1,2
purpuratum DSM1591	Okenone	okenone (100)	4
tepidum ATCC43061	Unusual-Spirillo	lycopene (3), rhodopin (68), anhydrorhodovibrin (4), OH-spirilloxanthin (2), spirilloxanthin (22)	4
vinosum D=ATCC17899	Unusual-Spirillo	lycopene (7), rhodopin (48), 3,4-didehydrorhodopin (1), anhydrorhodovibrin (13), rhodovibrin (4), OH-spirilloxanthin (1), spirilloxanthin (27)	1,2
salexigens DSM4395	Spirilloxanthin	lycopene (8), rhodopin (12), anhydrorhodovibrin (27), rhodovibrin (7), spirilloxanthin (46-50)	5
gracile DSM203	Spirilloxanthin	lycopene, rhodopin, spirilloxanthin	6
minutissimum DSM1376	Spirilloxanthin	spirilloxanthin	7
glycolicum DSM11080	Spirilloxanthin	lycopene (11), rhodopin (13), anhydrorhodovibrin (33), rhodovibrin (9), spirilloxanthin (34)	8
violascens 6111=DSM198	Spirilloxanthin & carotenal	lycopene (5), rhodopin (37), spirilloxanthin (11) lycopenal (1), rhodopinol (17), rhodopinal (29)	1,2
warmingii 6512=DSM173	Carotenal	lycopene (13), rhodopin (17), lycopenal (1), rhodopinol (21), rhodopinal (48)	1,2
buderi DSM176	Carotenal	rhodopinal	7
Thiocystis (*Tcs.*)			
violacea 2311=DSM208	Spirilloxanthin & carotenal	lycopene (4), rhodopin (20), spirilloxanthin (1), lycopenol (4), rhodopinol (36), rhodopinal (36)	1,2
gelatinosa 2611=DSM215	Okenone & *R.g.*-keto	thiothece-474 (3), thiothece-484 (5), thiothece-OH-484 (10), okenone (82)	1,9
Lamprocystis (*Lpc.*)			
roseopersicina 3012=DSM229	Carotenal	lycopene (4), lycopenol (27), rhodopinol (3), methoxylycopenal (66)	1,9,10
Lamprobacter (*Lpb.*)			
modestohalophilus R0-1	Okenone		7
Thiodictyon (*Tdc.*)			
elegans 3011=DSM232	Carotenal	lycopene (4), rhodopin (23),lycopenal (2), rhodopinol (15), rhodopinal (54)	1,9
bacillosum 1814=DSM234	Carotenal	lycopene (4), rhodopin (8), lycopenal (3), rhodopinol (4), rhodopinal (81)	1,2

Amoebobacter (*Amb.*) [d]			
roseus 6611=DSM235	Spirilloxanthin	anhydrorhodovibrin (5), spirilloxanthin (95)	1,2
pendens 1314=DSM236	Spirilloxanthin	rhodopin (4), anhydrorhodovibrin (11), OH-spirilloxanthin (3), spirilloxanthin (82)	1,2
pedioformis DSM3802	Spirilloxanthin	rhodopin, anhydrorhodovibrin, OH-spirilloxanthin, spirilloxanthin (major)	11
purpureus DSM4197	Okenone	okenone (90)	12
Thiopedia (*Tpd.*)			
rosea 4211	Okenone	okenone	7
Thiocapsa (*Tca.*) [d]			
roseopersicina 1711=DSM217	Spirilloxanthin	spirilloxanthin (100)	1,2
pfennigii Nidelven	Carotenal	3,4,3′,4′-tetrahydrospirilloxanthin (96), 3,4,3′,4′-tetrahydrospirilloxanthinal (4)	1,13
halophila DSM6210	Spirilloxanthin, okenone & *R.g.*-keto	spirilloxanthin (minor), okenone (major), *R.g.*-keto carotenoids (minor)	14
Thiorhodococcus (*Trc.*)			
minus DSM11518	Unusual-Spirillo	neurosporene (3), lycopene (9), rhodopin (65), anhydrorhodovibrin (13), rhodovibrin (2), spirilloxanthin (5)	15

[a] Recommended 3-letter abbreviations for genera (Trüper and Imhoff, 1999).
[b] See Table 1.
[c] This genus has recently been reclassified (Imhoff et al., 1998b).
[d] These genera have recently been rearranged (Guyoneaud et al., 1998).
1, Schmidt, 1978; 2, Schmidt et al., 1965; 3, Overmann et al., 1992; 4, S. Takaichi, unpublished; 5, Caumette et al., 1988; 6, Madigan, 1986; 7, Pfennig and Trüper, 1989; 8, Caumette et al., 1997; 9, Pfennig et al., 1968; 10, Frances and Liaaen-Jensen, 1970; 11, Eichler and Pfennig, 1986; 12, Eichler and Pfennig, 1988; 13, Eimhjellen et al., 1967; 14, Caumette et al., 1991; 15, Guyoneaud et al., 1997.

Table 5. Carotenoids in Ectothiorhodospiraceae

Genus (abbreviation) [a] Species strain	Carotenogenesis type [b]	Carotenoids (% of total)	Ref. No.
Ectothiorhodospira (*Ect.*)			
mobilis 8112=DSM237	Spirilloxanthin	lycopene (6), rhodopin (19), rhodovibrin (9), OH-spirilloxanthin (5), spirilloxanthin (61)	1,2
shaposhnikovii N1=DSM243	Spirilloxanthin	lycopene (7), rhodopin (18), rhodovibrin (3), OH-spirilloxanthin (2), spirilloxanthin (70)	1,2
vacuolata DSM2111	Spirilloxanthin	lycopene (10), rhodopin (8), anhydrorhodovibrin (22), rhodovibrin (3), spirilloxanthin (57)	3
marismortui DSM4180	Unusual-Spirillo	lycopene (25), rhodopin (58), anhydrorhodovibrin (10), rhodovibrin (5), spirilloxanthin (1)	3
marina DSM241	Spirilloxanthin	spirilloxanthin	4
haloalkaliphila ATCC51935	Unusual-Spirillo	lycopene (9), rhodopin (29), anhydrorhodovibrin (15), rhodovibrin (7), spirilloxanthin (40)	3
Rhabdochromatium (*Rbc.*)			
marinum 8315=DSM5261	Unusual-Spirillo	lycopene (83), rhodopin (5), anhydrorhodovibrin (4), rhodovibrin (8)	5
Halorhodospira (*Hlr.*)			
halophila SL1=DSM244	Spirilloxanthin	rhodovibrin (1), OH-spirilloxanthin (4), spirilloxanthin (88)	1,2
halochloris BN9850=DSM1059	Unusual-Spirillo & G-FA	lycopene (1), rhodopin (1), rohodopin glycoside (20), dimethoxylycopene (1), dihydroxylycopene glycoside (6), methoxyhydroxlycopene glycoside (31), dihydroxylycopene diglycoside (19), methoxyhydroxlycopene glycoside ester (4), dihydroxlycopene diglycoside ester (10), dihydroxlycopene diglycoside diester (17)	3
abdelmalekii BN9840=DSM2110	Unusual-Spirillo & G-FA	lycopene (1), rhodopin (2), rohodopin glycoside (20), dimethoxylycopene (1), dihydroxylycopene glycoside (5), methoxyhydroxlycopene glycoside (30), dihydroxylycopene diglycoside (11), methoxyhydroxlycopene glycoside ester (4), dihydroxlycopene diglycoside ester (10), dihydroxlycopene diglycoside diester (17)	3

[a] Recommended 3-letter abbreviations for genera (Trüper and Imhoff, 1999).

[b] See Table 1.

1, Schmidt, 1978; 2, Schmidt and Trüper, 1971; 3, S. Takaichi, unpublished; 4, Imhoff and Süling, 1996; 5, Dilling et al., 1995.

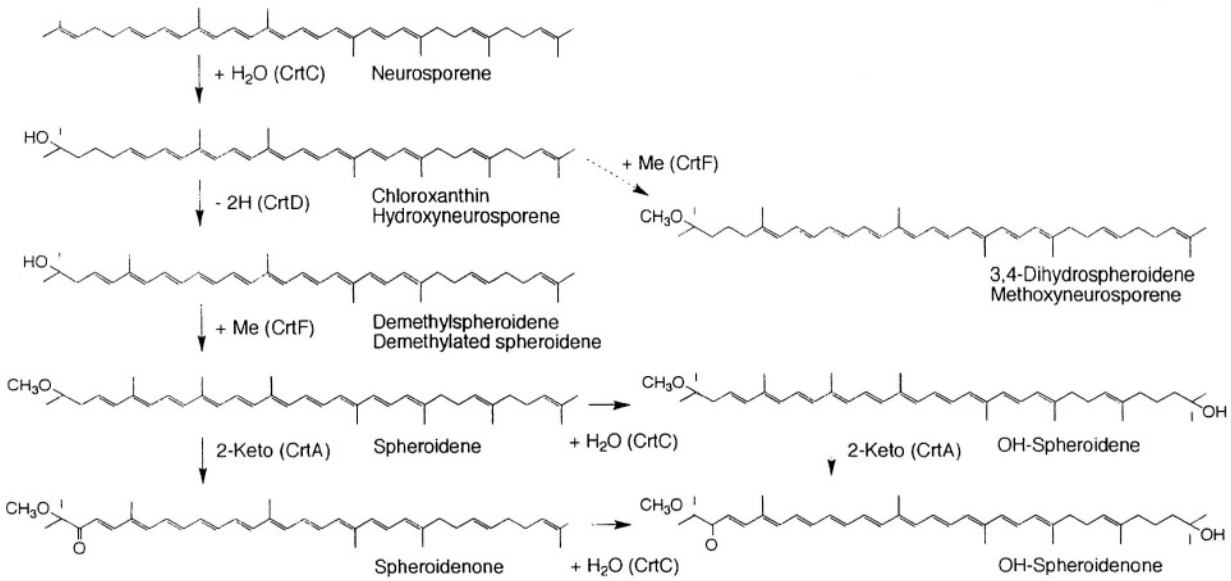

Fig. 5. The pathway for the biosynthesis of spheroidene including enzymes (see Table 2). The pathway from chloroxanthin to 3,4-dihydrospheroidene may not be involved in in vivo, and 3,4-dihydrospheroidene may not be changed to spheroidene.

accumulated in *Rbc. marinum* (Dilling et al., 1995), and this may be due to low activity of C-1,2 hydration (CrtC). Rhodopin is the major carotenoid in some species: *Rsp.photometricum* and *Rsp. molischianum* (Matsuura and Shimada, 1993), *Rsp. fulvum, Rmi. vannielii, Tsp. jenense* and *Chr. vinosum* (Schmidt, 1978), *Trv. winogradskii* (Overmann et al., 1992), *Trc. minus* (Guyoneand et al., 1997), and *Rps. palustris, Rps. cryptolactis, Chr. tepidum* and *Ect. marismortui* (S. Takaichi, unpublished). This may be due to low activity of C-3,4 desaturation (CrtD), and the 1-hydroxy-ψ end group may not be a suitable substrate for the methylation enzyme (CrtF). Rhodovibrin has been reported to be the major component in the type strains of *Rsp. photometricum* and *Rps. palustris* (Schmidt, 1978). Further, 3,4,3′,4′-tetrahydrospirilloxanthin (Fig. 12) is the major component in *Rsa. trueperi* (Pfennig et al., 1997) and *Tca. pfennigii* (Eimhjellen et el., 1967) probably due to lack of the C-3,4 desaturase (CrtD), but the 1-hydroxy-ψ end group can be methylated by CrtF. The same carotenoid is also found in a carotenegenesis mutant of *Rsp. rubrum* (Komori et al., 1998).

3. Spheroidene Pathway

The spheroidene pathway is found only from four genera, *Rhodobacter, Rhodoferax, Rubrivivax* and *Rhodovulum,* this includes 13 species of the Rhodospirillaceae, and from some species of aerobic photosynthetic bacteria (Tables 3 and 9). Spheroidene is an asymmetrical compound containing the same end group as spirilloxanthin on one side and the 7,8-dihydro-ψ end group on the other side (Fig. 5).

All of the carotenogenesis genes in *Rba. capsulatus* (Armstrong et al., 1989) and *Rba. sphaeroides* (Lang et al., 1995) have been reported to form a gene cluster of seven *crt* genes. The characteristics of their products have been investigated (Fig. 5; Sandmann, 1994, 1997). Phytoene desaturase (CrtI) produces neurosporene from phytoene in three desaturation steps. The next sequence includes the successive reactions of (1) hydration at C-1,2 by hydroxyneurosporene synthase (CrtC) to yield chloroxanthin (hydroxyneurosporene), (2) desaturation at C-3,4 by methoxyneurosporene dehydrogenase (CrtD) to yield demethylspheroidene, and (3) methylation at the C-1 hydroxyl group by hydroxyneurosporene-*O*-methyltransferase (CrtF) to yield spheroidene. Further, CrtC can also hydrate at the 1′,2′-dihydro-π end group to yield OH-spheroidene. In semi-aerobic conditions, spheroidene monooxygenase (CrtA) introduces the keto group at C-2 to yield spheroidenone. The 1′-hydroxy-7′,8′-dihydro-ψ end group can not be modified further due to the single bond at C-7′,8′. The keto group of spheroidenone from *Rsb. denitrificans* is in the single bond *cis*-conformation around the conjugated double bond (Fig. 5; Takaichi et al., 1991b). Water is the source of hydration in *Rba. sphaeroides* (Yeliseev and Kaplan, 1997). The

hydrogen acceptor in C-3,4 desaturation of *Rba. sphaeroides* is molecular oxygen (Albrecht et al., 1997). The methyl residue in the methoxy groups arises from *S*-adenosylmethionine in *Rba. sphaeroides* (Singh et al., 1973) and *Rba. capsulatus* (Scolnik et al., 1980). The oxygen of the keto group at C-2 is derived directly from the atmosphere in *Rba. sphaeroides* (Shneour, 1962b).

3,4-Dihydrospheroidene (methoxyneurosporene) can rarely be found from the wild type strains (Fig. 5). Two strains of the carotenoid mutants, *Rba. capsulatus* MT1131 (Frank et al., 1986) and *Rba. sphaeroides* Ga (Table 3; S. Takaichi, unpublished), accumulate this carotenoid accompanied by neurosporene and chloroxanthin. These strains may be *crtD* gene mutants. When the *crtD* gene of *Rba. sphaeroides* is disrupted, the same three carotenoids described above are accumulated (Lang et al., 1995). Further, in in vitro experiments, 3,4-dihydrospheroidene is not able to be the substrate for CrtD from *Rba. sphaeroides* (Albrecht et al., 1997). These results indicate that CrtC, CrtD and CrtF sequentially operate in this order, and a part of chloroxanthin can be the substrate of CrtF but only when chloroxanthin is significantly accumulated. Consequently, 3,4-dihydrospheroidene may not be involved in carotenogenesis in the spheroidene pathway (Fig. 5). Similarly, in the normal spirilloxanthin pathway, 3,4-dihydroanhydrorhodovibrin and 3,4-dihydrospirilloxanthin, which are produced by methylation prior to desaturation, can be rarely found in the wild type strains. This may be also due to similar properties of CrtD and CrtF.

Rvi. gelatinosus produces carotenoids of both spheroidene and spirilloxanthin (Table 3; Goodwin, 1956). Trace amounts (Goodwin, 1956) or a few percent (S. Takaichi, unpublished) of lycopene are also found, and the *crtC* mutant is reported to accumulate both neurosporene and lycopene (Ouchane et al., 1997a). These results indicate that phytoene desaturase (CrtI) of *Rvi. gelatinosus* can produce both neurosporene and lycopene. When the *crtD* gene is disrupted, neurosporene, chloroxanthin, 3,4-dihydrospheroidene, lycopene and rhodopin are accumulated (Ouchane et al., 1997a). Therefore, *Rvi. gelatinosus* produces spheroidene and spirilloxanthin from neurosporene and lycopene, respectively. Although the reaction of ketolation at C-2 of the ψ end group (CrtA) is involved in the spheroidene pathway and not in the normal spirilloxanthin one (Figs. 4 and 5), this bacterium can oxidize spheroidene to spheroidenone by CrtA and moreover spirilloxanthin to 2,2´-diketospirilloxanthin. Schmidt (1978) proposed an alternative pathway of spirilloxanthin synthesis with the conversion of spheroidene to spirilloxanthin by 7´,8´-desaturation. However, there is no evidence for this enzyme. This reaction seems, therefore, not to be involved in the carotenogenesis of either the spheroidene and the normal spirilloxanthin pathways.

This spheroidene pathway is a variant of the unusual spirilloxanthin pathway as a result of the different properties of the phytoene desaturases (CrtI).

4. Carotenal Pathway

Four kinds of cross-conjugated carotenals are found in the Rhodospirillaceae and the Chromatiaceae (seven genera including 11 species) (Tables 3 and 4). Most species contain rhodopinal as a major component, which has an aldehyde group at C-20 of rhodopin with the 13-*cis* form (Fig. 6). Usually, small amounts of rhodopinol, lycopenol and lycopenal can also be detected. Methoxylycopenal is found as a major component in *Lpc. roseopersicina* (Pfennig et al., 1968; Francis and Liaaen-Jensen, 1970), and tetrahydrospirilloxanthinal is in *Tca. phennigii* (Eimhjellen et al., 1967). *Rps. acidophila* strain *7050* contains rhodopinal glucoside as a major component (Gardiner, 1992) and small amount of methoxylycopenal (Schmidt, 1971). Often, spirilloxanthin and its precursors are also found in *Rps. acidophila* (Schmidt, 1971; Gardiner, 1992), *Chr. violascens* and *Tcs. violacea* (Schmidt et al., 1965), while in other species, spirilloxanthin intermediates occurring later than rhodopin are not found (Table 3 and 4).

From the structure of these carotenals, Francis and Liaaen-Jensen (1970) have postulated a branched path for each of the derivatives of cross-conjugated carotenals. Up to now, further support for this has not been forthcoming, and a partially modified carotenogenesis pathway is shown in Fig. 6. Rhodopin and lycopene are hydroxylated at C-20 to yield rhodopinol and lycopenol, then the hydroxyl groups are oxidized to the aldehyde groups to yield rhodopinal and lycopenal, respectively. Whether lycopenol and lycopenal are precursors of rhodopinol and rhodopinal, respectively, has not been confirmed. Since all of these carotenals have a C-3,4 single bond, the C-3,4 desaturase (CrtD) may be inactive for these. Further, the activity of methylation to the hydroxyl

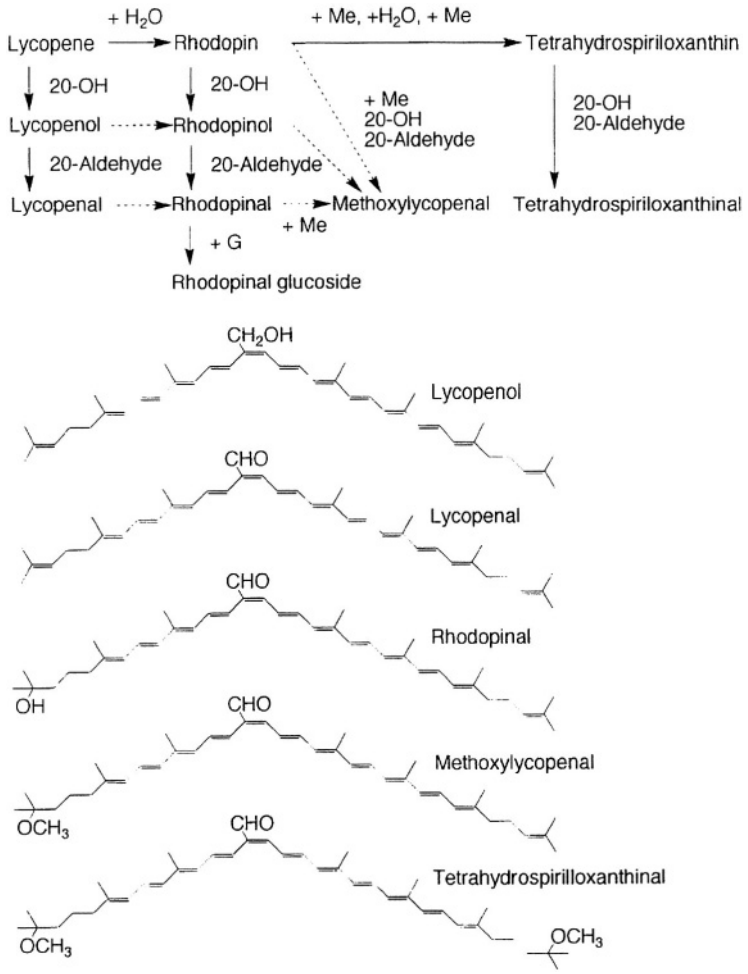

Fig. 6. The predicted pathway for the biosynthesis of cross-conjugated carotenals and their structures.

group at C-1 (CrtF) is either absent or low. Additional enzymes for hydroxylation at C-20 and for oxidation to the aldehyde group may be involved in this pathway, whereas nothing is known about how the aldehyde group is introduced under the anaerobic conditions. It has been reported that, under aerobic conditions, the methyl group of chlorophyll *a* is oxidized to the aldehyde group of chlorophyll *b* using molecular oxygen, catalyzed by chlorophyll *a* monooxygenase which contains methyl-monooxygenase and alcohol dehydrogenase activity (Tanaka et al., 1998; A. Tanaka, personal communication). The position is necessarily at C-20, not C-20´ or C-19. They take necessarily the 13-*cis* form, since this form is more stable than the all-*trans* form due to the hydroxyl or the aldehyde groups at C-20.

Erb. longus, an aerobic photosynthetic bacterium, has very unique cross-conjugated carotenal, bacteriorubixanthinal (Fig. 13; Takaichi et al., 1988), as described below.

E. Biosynthesis of Okenone

1. Okenone and R .g.*-Keto Carotenoid Pathways*

R.g.-Keto carotenoids are found from *Rpi. globiformis,* a member of the Rhodospirillaceae, and okenone is found from nine species of the Chromatiaceae, such as *Chr. okenii* and *Tcs. gelatinosa,* together with small amounts of *R.g.*-keto carotenoids. Okenone has one aromatic χ end group (Fig. 1), and one aliphatic ψ end group substituted with the methoxy group at C-1 and the keto group at C-4. The keto group of okenone from *Chr. purpuratum*

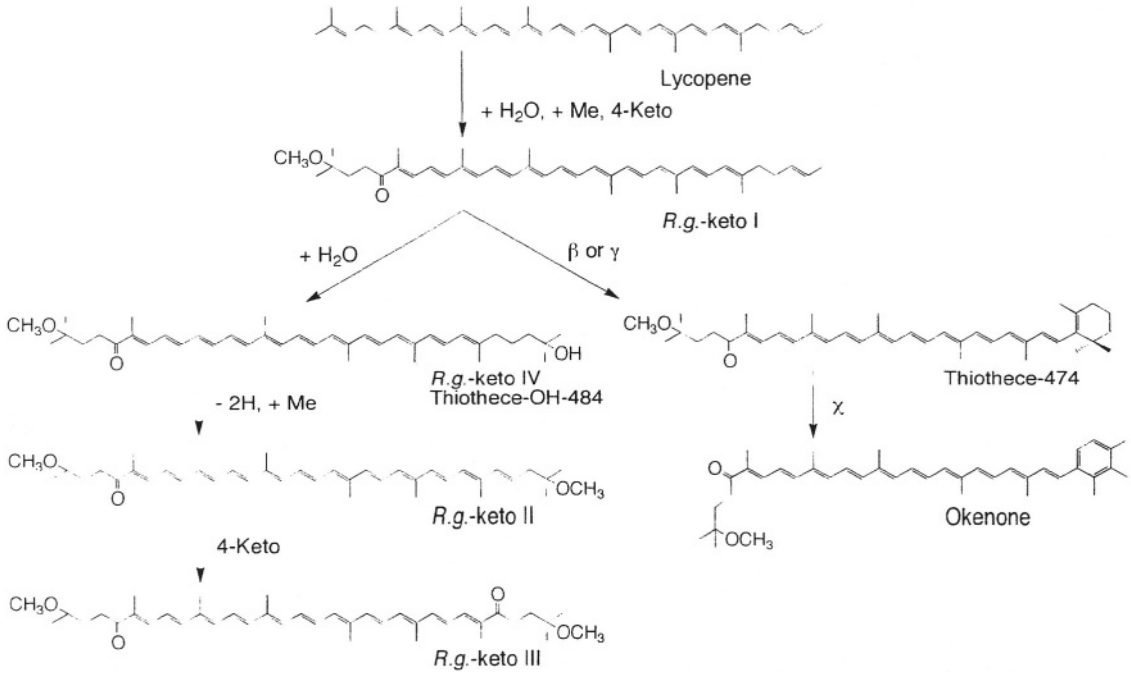

Fig. 7. The predicted pathway for the biosynthesis of okenone and *R.g.*-keto carotenoids.

is in the single bond *trans*-conformation around the conjugated double bond (Fig. 7; Fujii et al., 1998). The conformations at the C-4 keto group of other carotenoids have not been investigated. *R.g.*-Keto III is a symmetrical carotenoid having end groups the same as one end of okenone. The biosynthesis of both of these carotenoids may be closely related (Schmidt, 1978), and these pathways may be distinguished at the level of the cyclase, lycopene cyclase or γ-carotene synthase; it could be present (okenone pathway) or absent (*R.g.*-keto carotenoid pathway).

A small amount of lycopene is found in *Rpi. globiformis* (Table 3; S. Takaichi, unpublished) and in the diphenylamine-inhibited cultures of *Chr. okenii* (Schmidt et al., 1963). However in diphenylamine-inhibited cultures of *Rpi. globiformis,* lycopene was not reported (Schmidt and Liaaen-Jensen, 1973). Although small amounts of the intermediates of phytoene desaturase are usually found in photosynthetic bacteria, if the activity of the C-1,2 hydratase is high, lycopene as the substrate may not be found. Therefore, the carotenogenesis pathways of okenone and *R.g.*-keto carotenoids could possibly start from lycopene rather than from neurosporene (Fig. 7). Nothing is known about how the keto group is introduced under the anaerobic conditions.

F. Biosynthesis of Isorenieratene

1. Isorenieratene and Chlorobactene Pathways

Aromatic carotenoids with the φ end group (Fig. 1) are found only in the Chlorobiaceae. With respect to their carotenogenesis, these bacteria can be divided into two types: the isorenieratene and the chlorobactene pathways (Fig. 8; Schmidt, 1978). In the isorenieratene pathway, both end groups are cyclized by lycopene cyclase to yield β-carotene and further aromatized to yield β-isorenieratene and isorenieratene. In the chlorobactene pathway, monocyclic chlorobactene is always a predominant product, and small amounts of a hydroxylated compound, OH-chlorobactene, are also found. Therefore, two pathways may be distinguished at the level of cyclization of lycopene, although it is unknown whether γ-carotene is synthesized by lycopene cyclase or γ-carotene synthase. *Streptomyces griseus,* a non-photosynthetic Actinomycetes, also produces isorenieratene. In this case, a methyltransferase gene, *crtT,* and a dehydrogenase gene, *crtU,* have been cloned. The combination of these genes has been reported to convert β-carotene to isorenieratene (Schumann et al., 1996). *Chp. thalassium* may have an unusual chlorobactene pathway due to low activity of the aromatization step.

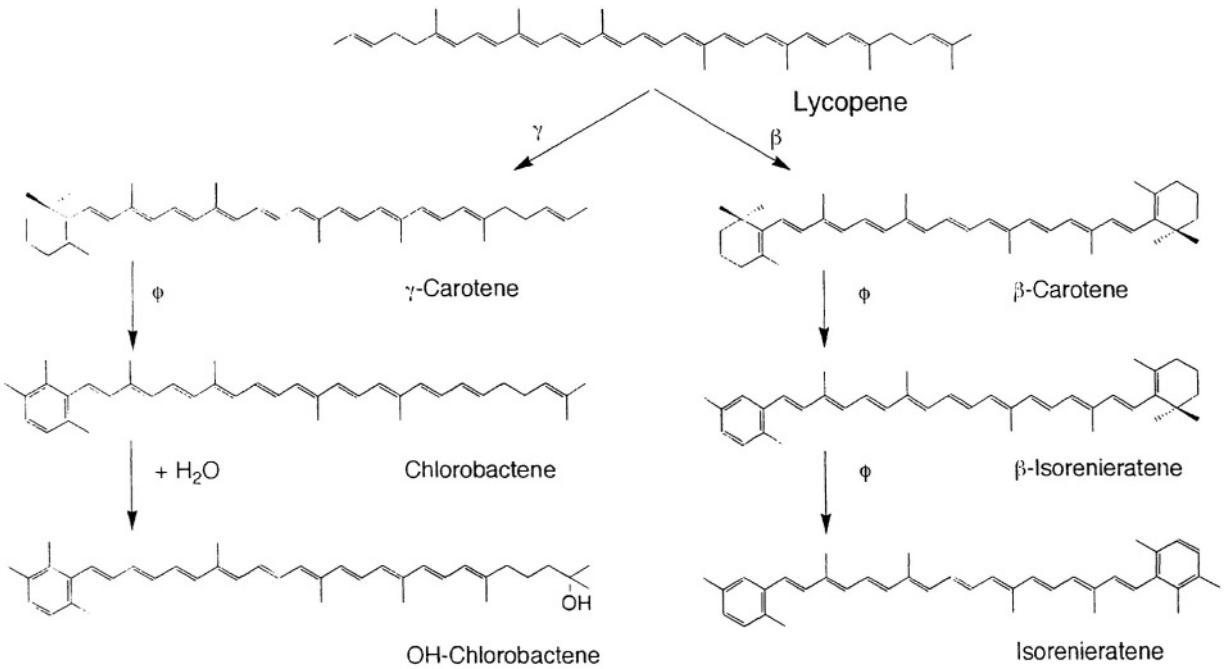

Fig. 8. The predicted pathway for the biosynthesis of isorenieratene and chlorobactene.

Chl. tepidum, a thermophilic Chlorobiaceae, has somewhat different carotenoid components (Fig. 9; Takaichi et al., 1997a). A carotenoid mutant, strain TNO, derived from the type strain LTS has **γ-carotene,** chlorobactene and their C-1,2 dihydro derivatives (**1′,2′-dihydro-γ-carotene** and 1′,2′-dihydrochlorobactene) as dominant components (Table 6). In lesser amounts, **OH-γ-carotene,** OH-chlorobactene and their glucoside esters are also found. The only esterified fatty acid present is laurate. In other strains, including the type strain, the same carotenoids are found, although the compositions vary from strain to strain. Carotenoids with the **1,2-dihydro-ψ** end group, 1,2-dihydroneurosporene and 1,2-dihydro-3,4-dehydrolycopene (Fig. 12), have also been found in *Bla. viridis* (Malhotra et al., 1970). The functions of such **1,2-dihydro-ψ** end group in photosynthesis are not known.

G. Biosynthesis of γ- and β-Carotene

γ-Carotene and **β-carotene,** found in the Chloroflexaceae, are not the typical end products of carotenogenesis in photosynthetic bacteria. These pigments are more characteristic of cyanobacteria, algae, higher plants and non-photosynthetic bacteria. In *Cfl. aurantiacus,* **γ-carotene** and **β-carotene** are the main carotenoids (Table 7; Takaichi et al., 1995). Further, **OH-γ-carotene, OH-γ-carotene** glucoside and **OH-γ-carotene** glucoside esters (Fig. 12) are also found (Fig. 10). The major fatty acids esterified are hexadecanoate and hexadecenoate. Halfen et al. (1972) found the additional 4-keto derivatives, but missed carotenoid glucoside esters probably due to saponification, which hydrolyzes carotenoid glycoside esters to carotenoid glycosides and fatty acids. In a green algae *Haematococcus pluvialis,* molecular oxygen is used for the insertion of the keto group (Breitenbach et al., 1996). A small amount of **β-carotene** has also be reported in two species of the Rhodospirillaceae, *Rmi. vannielii* (Ryvarden and Liaaen-Jensen, 1964; Britton et al., 1975) and *Rps. acidophila* strain 7050 (Schmidt, 1971), however Gardiner (1992) and S. Takaichi (unpublished) did not find it in *Rps. acidophila* strain 7050.

H. Biosynthesis of Diapocarotene

The Heliobacteriaceae only have C_{30} acyclic carotenes, 4,4′-diapocarotenes, instead of the usual C_{40} carotenoids (Fig. 11; Takaichi et al., 1997b). 4,4′-Diaponeurosporene is the major carotene, and diapophytoene, diapophytofluene, **diapo-ζ-carotene** and diapolycopene are also found as minor components. Two genes encoding enzymes in the early steps of diapocarotene biosynthesis have been

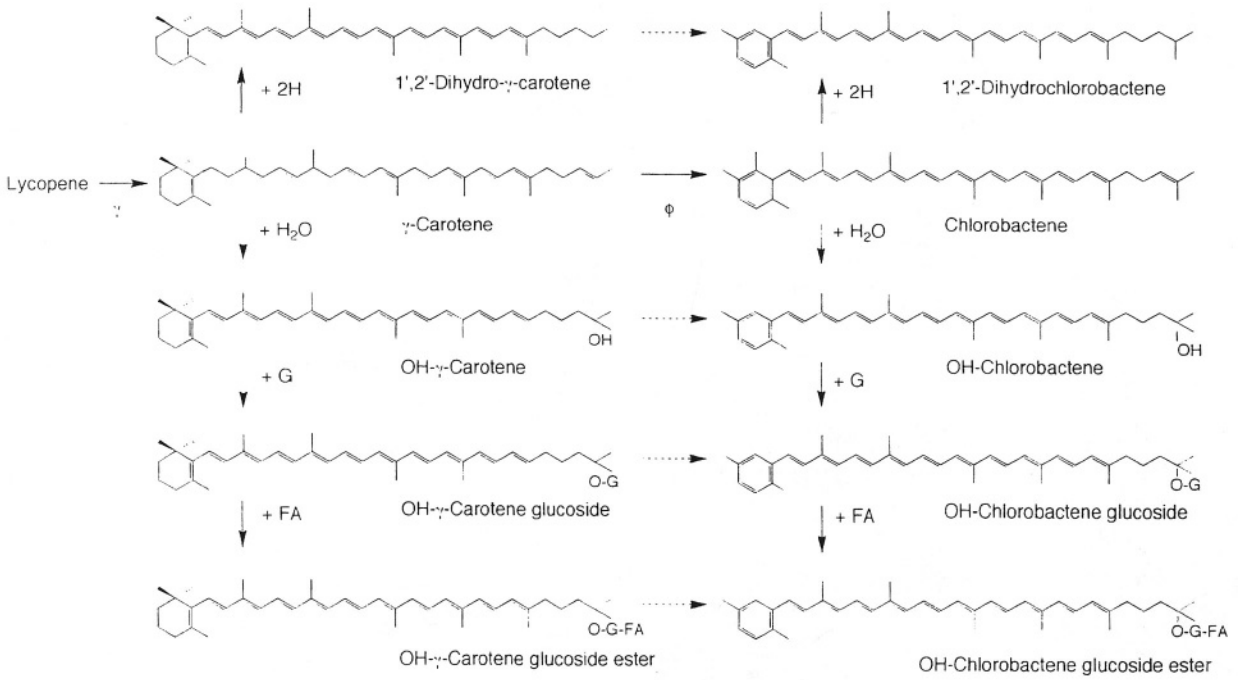

Fig. 9. The predicted pathway for the biosynthesis of C-1,2 dihydro carotenoids and carotenoid glucoside esters in *Chl. tepidum*. Dashed arrows indicate possible pathways.

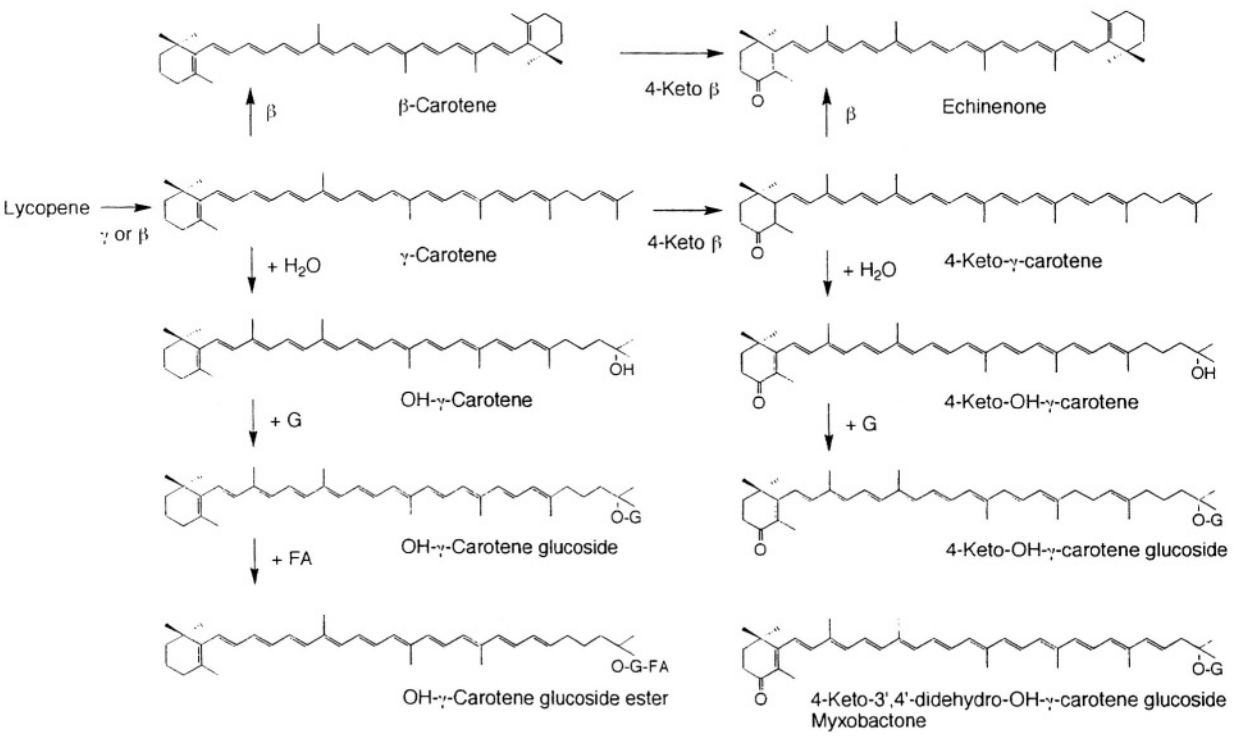

Fig. 10. The predicted pathway for the biosynthesis of OH-γ-carotene glucoside ester of *Cfl. aurantiacus*.

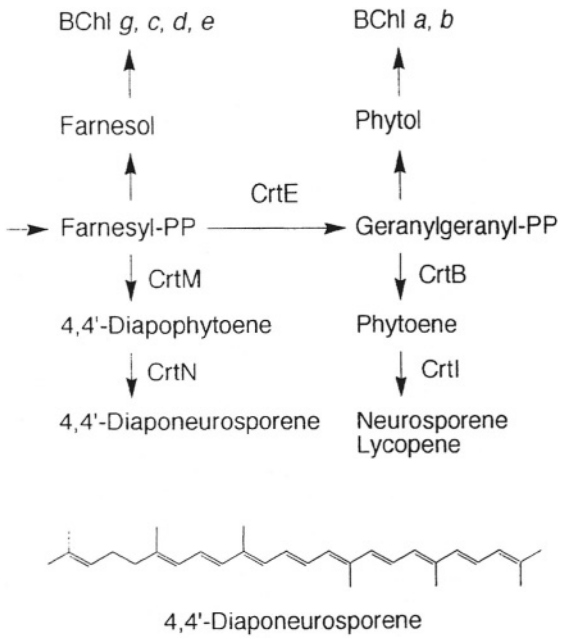

Fig. 11. The predicted pathway for the biosynthesis of diapocarotene in the Heliobacteriaceae with that of C_{40}-type carotenoids, and the esterified alcohol of BChls. CrtE, CrtB and CrtI are found in *Rhodobacter* (Armstrong et al., 1989; Lang et al., 1995), CrtM and CrtN in *Staphylococcus* (Wieland et al., 1994), and CrtM in *Hba. mobilis* (Xiong et al., 1998).

cloned and characterized from *Staphylococcus aureus,* a gram-positive non-phototroph (Wieland et al., 1994). Dehydrosqualene synthase (CrtM) converts two molecules of farnesyl pyrophosphate (C_{15}) into 4,4´-diapophytoene in a similar way to the one in which phytoene synthase (CrtB) combines two C_{20} units in the production of phytoene. Diapophytoene is then successively desaturated by diapophytoene desaturase (CrtN) to yield 4,4´-diaponeurosporene, analogous to the activity of phytoene desaturase (CrtI). Thus, the Heliobacteriaceae may well have the genes which are homologous to *crtM* and *crtN* found in *S. aureus.* Recently, *crtM* has been cloned from *Hba. mobilis* (Xiong et al., 1998).

Diapocarotene containing two carboxylic groups and its diglucosyl ester, di(acyl-β-D-glucopyranosyl)-4,4´-diapocarotene-4,4´-dioate (Fig. 12), are found in aerobic photosynthetic bacteria, *Rsc. thiosulfatophilus* (Yurkov et al., 1993) and *Methylobacterium rhodinum* (previously, *Pseudomonas rhodos*; Kleinig et al., 1979). The biosynthesis of these diapocarotene derivatives have not yet been investigated.

I. Biosynthesis of Carotenoid Glucoside and Its Fatty Acid Ester

The occurrence of carotenoid glucosides and their fatty acid esters in photosynthetic bacteria was regarded as unusual, however more recently, the wide distribution of such carotenoid derivatives among various species has been demonstrated. They have also been described in some non-photosynthetic bacteria and cyanobacteria. *Rps. acidophila* has three carotenoid glucosides; rhodopin, rodopinol and rodopinal glucosides (Schmidt et al., 1971), and the total glucoside contents are 20 to 70% of total carotenoids depending on the culture conditions and the strains (Gardiner, 1992). Rhodopin glycoside has also been found in *Rsp. fulvum* (Table 3; S. Takaichi, unpublished). Furthermore, two species of *Halorhodospira* have dihydroxylycopene diglycoside and its diester (Table 5; S. Takaichi, unpublished). *Chl. tepidum* has OH-γ-carotene glucoside ester and OH-chlorobactene glucoside ester (Takaichi et al., 1997a), and *Cfl. aurantiacus* and *Cfl. aggregans* have OH-γ-carotene glucoside ester (Takaichi et al., 1995). Myxobactone (Fig. 10) was found from *Htr. oregonensis* (Pierson et al., 1984) after the saponification procedure. *Rsc. thiosulfatophilus* (Yurkov et al., 1993) and *Methylobacterium rhodinum* (Kleinig et al., 1979) have di(acyl-glucosyl)-diapocarotene-dioate (Fig. 12).

In all known cases, the hydroxyl or the carboxylic groups of carotenoids form a glycosidic linkage with β-D-glucoside, and often a fatty acid is esterified at the C-6 hydroxyl group of glucoside (Fig. 12). In vitro experiments with *Erwinia herbicola,* UDP-glucose is the substrate for the formation of zeaxanthin glucoside (Hundle et al., 1992). Although the localization of rhodopin glucoside in the LH complex of *Rps. acidophila* has been described (McDermott et al., 1995), the functions of glucoside and its ester moieties in photosynthesis are still unknown.

III. Distribution of Carotenoids in Photosynthetic Bacteria

A. Anaerobic Photosynthetic Bacteria

1. Rhodospirillaceae

The Rhodospirillaceae are purple nonsulfur bacteria and belong to the α- and the β-subclass of the

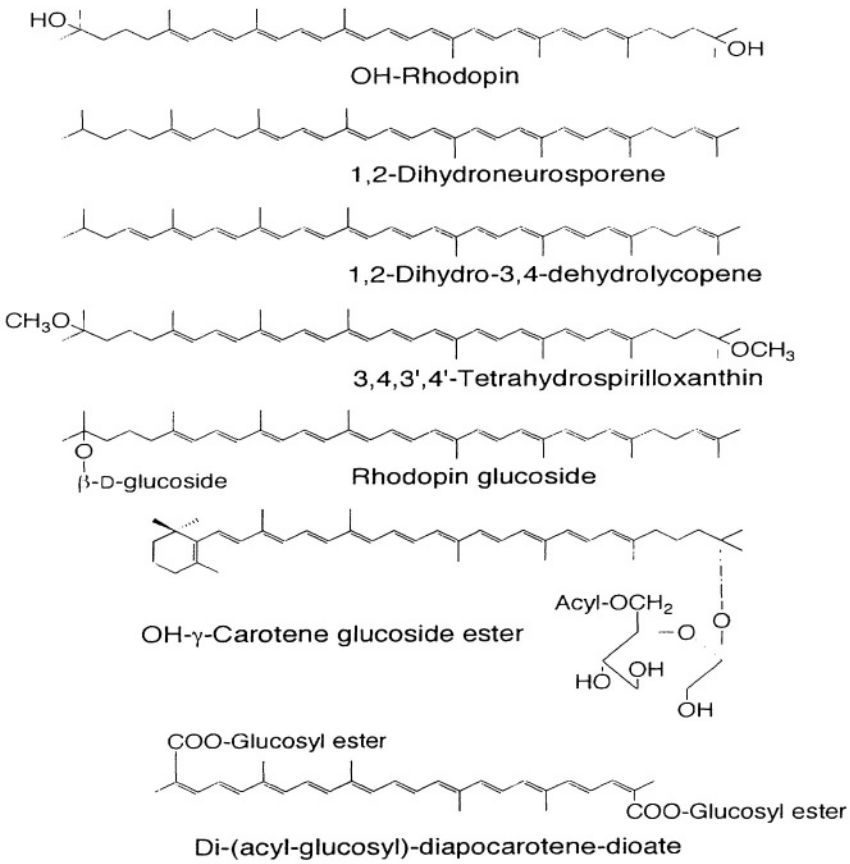

Fig. 12. Structures of some unusual carotenoids found in photosynthetic bacteria.

Proteobacteria (Imhoff, 1995). The functions of carotenoids in photosynthetic bacteria have been investigated in most detail in the Rhodospirillaceae (other chapters in this book). Their RC resembles that of PS II of green plants. Their major BChl is BChl *a* or *b*. The RC was firstly crystallized from *Bla.* (previously, *Rhodopseudomonas*) *viridis,* and the localization of one carotenoid, 1,2-dihydroneurosporene, four BChl *b* and two bacteriopheophytin *b* molecules was determined (Deisenhofer et al., 1995). A similar localization of spheroidene in the RC of *Rba. sphaeroides* has also been described (Yeates et al., 1988; Ermler et al., 1994). The fine crystal structure of the LH II antenna complex from *Rps. acidophila* strain 10050 has shown the localization of one rhodopin glucoside and three BChl *a* molecules per $\alpha\beta$ monomer (McDermott et al., 1995). A similar localization of lycopene in the LH II complex from *Rsp. molischianum* has also described (Koepke et al., 1996). Although two-dimensional crystallization of the LH I-RC complex from *Rsp. rubrum* has been described, the localization of carotenoid has not indicated (Walz and Ghosh, 1997). These are described in detail in Chapter 4 (Cogdell et al.).

The spirilloxanthin pathway is found in all the Rhodospirillaceae except for one genus, *Rhodopila,* which has the okenone pathway (Tables 1 and 3). Most genera have the normal spirilloxanthin or the unusual spirilloxanthin pathways. The spheroidene pathway is found only in genera from the α3-subclass of the Rhodospirillaceae, *Rhodobacter* and *Rhodovulum. Rhodoferax* and *Rubrivivax,* which belong to the β-subclass of the Rhodospirillaceae, have both the normal spirilloxanthin and the spheroidene pathways. All of the carotenogenesis genes have been cloned in two species of *Rhodobacter* (Armstrong et al., 1989; Lang et al., 1995). The carotenal pathway is found in *Rhodocyclus* and *Rps. acidophila.* The *R.g.*-keto carotenoid pathway is found only in *Rpi. globiformis.* β-carotene is found only in

Rmi. vannielii. Carotenoid glucoside is found in *Rsp. fulvum* and *Rps. acidophila.* The 1,2-dihydro-ψ end group is found in *Bla. viridis.*

2. Chromatiaceae

The Chromatiaceae are purple sulfur bacteria and belong to the γ-subclass of the Proteobacteria (Imhoff, 1995). Their RC resembles that of PS II of green plants. Their major BChl is BChl *a* or *b.*

The Chromatiaceae have either the spirilloxanthin pathway (normal spirilloxanthin, unusual spirilloxanthin and carotenal pathways) or okenone of the okenone pathway except for one species, *Tca. halophila,* which has both pathways (Tables 1 and 4). Even in the same genus, some species have the spirilloxanthin pathway and others have the okenone pathway. Therefore, the carotenogenesis pathways are not well related to the bacteria's classification in the Chromatiaceae.

3. Ectothiorhodospiraceae

The Ectothiorhodospiraceae are a group of haloalkaliphilic purple sulfur bacteria and belong to the γ-subclass of the Proteobacteria (Imhoff, 1995). Their RC resembles that of PS II of green plants. Their major BChl is BChl *a* or *b.*

Only the spirilloxanthin pathway is found (Tables 1 and 5). Some species have the unusual spirilloxanthin pathway. *Hlr. halochloris* and *Hlr. abdelmalekii* contain in addition carotenoid glycosides and their esters as major components.

4. Chlorobiaceae

The Chlorobiaceae are green sulfur bacteria. They forms a tight phylogenetic group, and grow only under strictly anaerobic conditions (Imhoff, 1995). Their RC resembles that of PS I of green plants. Their major BChl is Bchl *c, d* or *e.*

The Chlorobiaceae have the isorenieratene pathway only and can be divided the isorenieratene and the chlorobactene pathways (Tables 1 and 6). The species which mainly contain isorenieratene always have BChl *c* or *d* as major component, and those which chlorobactene always have BChl *e* (Imhoff, 1995). *Chl. tepidum* contains additional carotenoid glucoside esters. Mostly the carotenes are located in chlorosomes, accompanied by BChl *c*, while carotenoid glucoside esters are mainly located in the membranes and RC (S. Takaichi, unpublished).

5. Chloroflexaceae

The Chloroflexaceae are green filamentous bacteria. They form a deep division in the eubacterial line and have an interesting combination of the characteristics found in very different and diverse groups of photosynthetic bacteria (Pierson and Castenholz, 1995). Their RC resembles that of PS II of green plants. Their major BChl is BChl *a, c* or *d* depending on the species.

The Chloroflexaceae only have the γ- and β-carotene pathway (Tables 1 and 7). In *Chloroflexus,* most of carotenes and BChl *c* are located in the chlorosomes, which are very similar to those of the Chlorobiaceae, while the carotenoid glucoside esters, which are also found, are mainly located in the membranes and the envelope of chlorosomes (Tsuji et al., 1995). Except for *Chloroflexus,* analysis of carotenoids in this group needs a lot more work.

6. Heliobacteriaceae

The Heliobacteriaceae are heliobacteria. They are strictly anaerobic photosynthetic bacteria that contain BChl *g* as a major pigment. Their RC resembles that of PS I of green plants (Madigan and Ormerod, 1995).

All the Heliobacteriaceae only have C_{30} carotenes, 4,4´-diapocarotenes (Tables 1 and 8). 4,4´-Diaponeurosporene is the dominant pigment and trace amounts of C_{30} diapocarotenes are also present. Furthermore, the esterifying alcohol of BChl *g* is farnesol (C_{15}) instead of the usual phytol (C_{20}) of BChls *a* and *b*. Both phytoene and phytol are produced from geranylgeraniol (C_{20}). It is thus likely that the Heliobacteriaceae are unable to produce geranylgeraniol from farnesol (Fig. 11).

B. Aerobic photosynthetic Bacteria

More than ten genera including about 30 species of aerobic photosynthetic bacteria have now been found (Table 9). They are distinguished from typical anaerobic photosynthetic bacteria in that they synthesize BChl only under the aerobic conditions and can not grow without O_2 even in the light. In some species, photosynthetic activities have been demonstrated. The low content of BChl, unique composition of carotenoids, and presence of 'non-

Table 6. Carotenoids in Chlorobiaceae

Genus (abbreviation) [a] Species strain	Carotenogenesis type [b]	Carotenoids (% of total)	Ref. No.
Chlorobium (*Chl.*)			
limicola 6330=DSM245	Chlorobactene	chlorobactene	1
limicola f. sp. *thiosulfatophilum* 6230=DSM249	Chlorobactene	phytoene (1), phytofluene (1), lycopene (1), γ-carotene (8), chlorobactene (74), OH-chlorobactene (1)	2,3
vibrioforme 6030=DSM260	Chlorobactene	lycopene (3), rhodopin (1), chlorobactene (91), OH-chlorobactene (5)	2,3
vibrioforme f. sp. *thiosulfatophilum* 1930=DSM265	Chlorobactene	phytoene (2), phytofluene (2), neurosporene (4), lycopene (7), chlorobactene (77), OH-chlorobactene (12)	2,3
phaeobacterioides 2430=DSM266	Chlorobactene & isorenieratene	chlorobactene (5), β-carotene (1), β-isorenieratene (14), isorenieratene (80)	2,4
phaeovibrioides 2631=DSM269	Chlorobactene & isorenieratene	chlorobactene (6), β-carotene (7), β-isorenieratene (38), isorenieratene (49)	2,4
chlorovibrioides DSM1377	Chlorobactene	chlorobactene	1
tepidum TLS=ATCC49652	Chlorobactene & G-FA	γ-carotene (3), chlorobactene (65), dihydrochlorobactene (21), OH-chlorobactene (2), OH-chlorobactene glucoside ester (8)	5
TNO	Chlorobactene & G-FA	γ-carotene (24), dihydro-γ-carotene (22), OH-γ-carotene (2), chlorobactene (20), dihydrochlorobactene (23), OH-chlorobactene (2), OH-γ-carotene glucoside ester (5), OH-chlorobactene glucoside ester (3)	5
Prosthecochloris (*Ptc.*)			
aestuarii SK413=DSM271	Chlorobactene	chlorobactene or its hydroxyl derivative, hydroxyl derivative of rhodopin or lycopene	6
phaeoasteroides MG-1	Isorenieratene	isorenieratene	1
Ancalochloris (*Anc.*)			
perfilievii		no data	
Pelodictyon (*Pld.*)			
luteolum 2530=DSM273	Chlorobactene	phytoene (1), lycopene (1), γ-carotene (11), chlorobactene (72), OH-chlorobactene (1)	2,3
clathratiforme 2730	Chlorobactene		1
phaeum WS6=DSM728	Isorenieratene	isorenieratene	1
phaeoclathratiforme BU1=DSM5477	Isorenieratene	β-isorenieratene, isorenieratene	7
Chloroherpeton (*Chp.*)			
thalassium ATCC35110	Chlorobactene	γ-carotene (>80)	1

[a] Recommended 3-letter abbreviations for genera (Trüper and Imhoff, 1999).

[b] See Table 1.

1, Pfennig and Trüper, 1989; 2, Schmidt, 1978; 3, Schmidt and Schiburr, 1970; 4, Liaaen-Jensen, 1965; 5, Takaichi et al., 1997a; 6, Swarthoff et al., 1982; 7, Overmann and Pfennig, 1989.

Table 7. Carotenoids in Chloroflexaceae

Genus (abbreviation)[a] Species strain	Carotenogenesis type[b]	Carotenoids (% of total)	Ref. No.
Chloroflexus (*Cfl.*)			
aurantiacus J-10-fl=ATCC29366	γ+ β, G-FA	γ-carotene (25), β-carotene (28), OH-γ-carotene (4), OH-γ-carotene glucoside (3), OH-γ-carotene glucoside ester (40)	1
aggregans MD66=DSM9485	γ+ β, G-FA	γ-carotene (37), β-carotene (25), OH-γ-carotene (22), OH-γ-carotene glucoside (1), OH-γ-carotene glucoside ester (9), keto-OH-γ-carotene (2), keto-OH-γ-carotene glucoside (4)	2
Heliothrix (*Htr.*)			
oregonensis IS/F-1	γ+ β, G	keto-OH-γ-carotene, keto-3′,4′-didehydro-OH-γ-carotene, myxobactone (total 90)	3
Chloronema (*Cln.*)			
giganteum		no data	4
Oscillochloris (*Osc.*)			
chrysea		no data	4
trichoides Dg6	γ + β	γ-carotene, β-carotene	4
Clathrochloris (*Clt.*)			
sulfurica	no data		

[a] Recommended 3-letter abbreviations for genera (Trüper and Imhoff, 1999).
[b] See Table 1.
1, Takaichi et al., 1995; 2, S. Takaichi, unpublished; 3, Pierson et al., 1984; 4, Pfennig and Trüper, 1989.

Table 8. Carotenoids in Heliobacteriaceae

Genus (abbreviation) [a] Species strain	Carotenogenesis type [b]	Carotenoids (% of total)	Ref. No.
Heliobacterium (*Hbt.*)			
chlorum ATCC35205	Diapocarotene	diapophytoene, diapophytofluene, diapo-ζ-carotene, diaponeurosporene (>95)	1
modesticaldum ATCC51547	Diapocarotene	diapophytoene, diapo-ζ-carotene, diaponeurosporene (>95), diapolycopene	1
gestii ATCC43375	Diapocarotene	diapophytoene, diapophytofluene, diapo-ζ-carotene, diaponeurosporene (>95), diapolycopene	1
Heliobacillus (*Hba.*)			
mobilis ATCC43427	Diapocarotene	diapophytoene, diapophytofluene, diapo-ζ-carotene, diaponeurosporene (>95), diapolycopene	1
Heliophilum (*Hph.*)			
fasciatum ATCC51790	Diapocarotene	diapophytoene, diapophytofluene, diapo-z-carotene, diaponeurosporene (>95), diapolycopene	1

[a] Recommended 3-letter abbreviations for genera (Trüper and Imhoff, 1999).
[b] See Table 1.
1, Takaichi et al., 1997b.

Table 9. Carotenoids in aerobic photosynthetic bacteria

Genus (abbreviation)[a] Species strain	Carotenogenesis or carotenoid type[b]	Carotenoids (% of total)	Ref. No.
α1-Subclass			
Acidiphilium			
cryptum ATCC33463	Spirilloxanthin	rhodovibrin (4), spirilloxanthin (96)	1
rubrum ATCC35905	Spirilloxanthin	spirilloxanthin (100)	1,2
angustum ATCC35903	Spirilloxanthin	spirilloxanthin (100)	1
organovorum ATCC43141	Spirilloxanthin	rhodovibrin (6), spirilloxanthin (94)	1
multivorum AIU301=JCM8867	Spirilloxanthin	spirilloxanthin (100)	1
acidophilum ATCC27897	Spirilloxanthin	spirilloxanthin (100)	1
Roseococcus (*Rsc.*)			
thiosulfatophilus DSM8511	C_{30}-Acid, G-FA	diapocarotene-dioic acid, di(acyl-glucosyl)-diapocarotene-dioate (total 95)	3
Craurococcus			
roseus NS130=JCM9933	Spirillo & Acid	spirilloxanthin, carotenoic acids (major)	4
Paracraurococcus			
ruber NS89=JCM9931	Spirillo & Acid	spirilloxanthin, carotenoic acids (major)	4
α2-Subclass			
Methylobacterium			
extorquens NCIB9399	Spirillo & Acid	spirilloxanthin, carotenoic acids (major)	5,6
rhodesianum NR-1	Spirillo & Acid	spirilloxanthin, carotenoic acids (major)	6
radiotolerans MD-1	Spirillo & Acid	anhydrorhodovibrin (3), rhodovibrin (1), spirilloxanthin (17), carotenoic acids (79)	5
zatmanii NCIB12243		no data	
fujisawaense TK39		no data	
rhodinum NCIB9421	C_{30}-Acid, G-FA	diapocarotenoic acid (8), acyl-glucosyl-diapocarotenoate-oic acid (60), di(acyl-glucosyl)-diapocarotene-dioate (32)	7
Rhizobium BTAi1	Spirilloxanthin	spirilloxanthin (100)	8
Bradyrhizobium ORS278	Spirillo & canthaxanthin	echinenone (4), canthaxanthin (86), spirilloxanthin (6)	8
α3-Subclass			
Roseobacter (*Rsb.*)			
litoralis OCh149=ATCC49566	Spheroidene	spheroidenone	9
denitrificans OCh114=ATCC33942	Spirilloxanthin & spheroidene	2,2′-diketospirilloxanthin (1), spheroidenone (97), OH-spheroidenone (2)	10

α4-Subclass			
Erythrobacter (*Erb.*)			
longus OCh101=IFO14126 [c]	Erb-type	erythroxanthin sulfate (69), caloxanthin sulfate (1), phytoene (<1), phytofluene (<1), asymmetrical-ζ-carotene (<1), neurosporene (<1), lycopene (<1), β-carotene (<1), β-cryptoxanthin (<1), zeaxanthin (11), caloxanthin (6), nostoxanthin (1), γ-carotene (<1), bacteriorubixanthin (<1), bacteriorubixanthinal (12), spirilloxanthin (<1)	11,12,13
litoralis DSM8509	Erb-type	erythroxanthin sulfate, bacteriorubixanthinal	14
Porphyrobacter (*Por.*)			
neustonensis ACM2844	Erb-type	carotenoid sulfates (81), caloxanthin (3), nostoxanthin (9), bacteriorubixanthinal (6), spirilloxanthin (1)	6
tepidarius DSM10595 [c]	Erb-type	carotenoid sulfates (69), β-carotene (<1), caloxanthin (4), nostoxanthin (20), bacteriorubixanthinal (6), OH-spirilloxanthin (<1), spirilloxanthin (1)	6,15
Erythromicrobium (*Erm.*)			
ramosum E5=DSM8510	Erb-type	erythroxanthin sulfate (major), β-carotene, zeaxanthin, adonixanthin, caloxanthin, erythroxanthin, nostoxanthin, keto-nostoxanthin (major), bacteriorubixanthinal (major), spirilloxanthin	3
ezovicum E-1		no data	
hydrolyticum E4(1)		no data	
Sandaracinobacter			
sibiricus RB16-17		no data	
Erythromonas			
ursincola KR-99	Spheroidene	spheroidene	16
β-Subclass			
Roseateles			
depolymerans 61A=DSM11813	Spirilloxanthin	3,4-didehydrorhodopin (1), anhydrorhodovibrin (8), OH-spirilloxanthin (2), spirilloxanthin (89)	17

[a] Recommended 3-letter abbreviations for genera (Trüper and Imhoff, 1999).

[b] See Table 1; Acid: carotenoic acid; C_{30}: 4,4′-diapocarotene derivatives; Erb-type: carotenoid sulfate(s), β-carotene and its hydroxyl derivatives, γ-carotene and its cross-conjugated aldehyde, and spirilloxanthin type.

[c] Since these bacteria contain many kinds of Erb-type carotenoids, carotenoids less than 1% are also indicated.

1, Hiraishi et al., 1998; 2, Wakao et al., 1996; 3, Yurkov et al., 1993; 4, Saitoh et al., 1998; 5, Saitoh et al., 1995; 6, S. Takaichi, unpublished; 7, Kleinig et al., 1979; 8, Lorquin et al., 1997; 9, Shiba, 1991; 10, Harashima and Nakada, 1983; 11, Takaichi et al., 1988; 12, Takaichi et al., 1990; 13, Takaichi et al., 1991a; 14, Yurkov et al., 1994; 15, Hanada et al., 1997; 16, Yurkov et al., 1992; 17, Suyama et al., 1998.

photosynthetic' carotenoids, which have no photosynthetic activities, are also marked characteristics. Phylogenetically, they are not classified into a single group. Species are distributed rather widely within the α-subclass of the Proteobacteria (Shimada, 1995), furthermore one species belonging to the β-subclass has recently been found (Suyama et al., 1998). The presence of the active RCs was first discovered in *Rsb. denitrificans* and *Erb. longus* by Harashima et al. (1982). The purified RC complexes have been obtained from *Rsb. denitrificans* (Shimada et al., 1985; Takamiya et al., 1987) and more recently from *Acidiphilium rubrum* (Shimada et al., 1999). These are similar to those of the more typical purple bacteria. The RC-LH I complexes have been found in most species, while not many species also contain the LH II complexes. The properties of these antenna complexes are also similar to those of the more typical purple bacteria (Shimada, 1995).

In some species, identification of the pigments is very secure, while in others the carotenoids were not even analyzed. The only BChl found was phytol BChl *a*. Exceptionally, the acidophilic genus *Acidiphilium* has Zn-BChl *a,* where central metal is zinc instead of the usual magnesium. A small amount of usual Mg-BChl *a* is also present (Wakao et al., 1996; Hiraishi et al., 1998).

The carotenoid compositions of most of these bacteria are different from those of the more typical purple bacteria (Table 9). Most species so far investigated contain spirilloxanthin, the content of which varies from low to high depending on the species. These bacteria can be classified into five groups based upon their carotenoid composition. The first group has spirilloxanthin and its precursors, and spirilloxanthin is dominant. *Acidiphilium* (α1), *Rhizobium* (α2) and *Roseateles* (β) belong to this group. The second has spheroidene and its derivatives, and spheroidenone is dominant. *Roseobacter* (α3) and *Erythromonas* (α4) belong to this group. The third has a small amount of spirilloxanthin and large amounts of other carotenoids. *Craurococcus* (α1), *Paracraurococcus* (α1) and *Methylobacterium* (α2) contains unidentified carotenoic acids, and *Bradyrhizobium* (α2) contains canthaxanthin. The fourth group includes species such as *Rsc. thiosulfatophilus* (α1) and *Methylobacterium rhodinum* (α2), has the diapocarotene derivative, di(acyl-glucosyl)-diapocarotene-dioate (Fig. 12). Unidentified carotenoic acids in the third group seem to be different from this

	R2	R3	R4	R2'	R3'
β-Carotene	H	H	H_2	H	H
β-Cryptoxanthin	H	OH	H_2	H	H
Zeaxanthin	H	OH	H_2	H	OH
Caloxanthin	OH	OH	H_2	H	OH
Nostoxanthin	OH	OH	H_2	OH	OH
Caloxanthin sulfate	OH	OH	H_2	H	O-SO_2OH
Erythoxanthin sulfate	H	O-SO_3OH	O	OH	OH

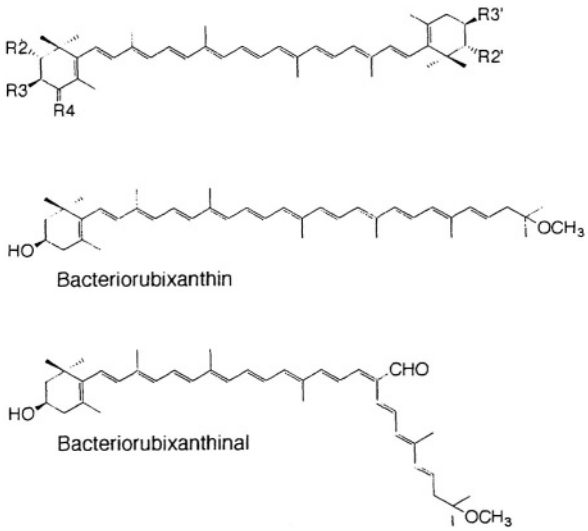

Fig. 13. Major carotenoids found in Erb-type carotenoids.

diapocarotene derivative (S. Takaichi, unpublished). The fifth group has unique Erb-type carotenoids including spirilloxanthin and its precursors, γ-carotene and its cross-conjugated aldehyde derivative, β-carotene and its poly-hydroxyl derivatives, and carotenoid sulfates. This group is found only in the α4-subclass of the Proteobacteria: *Erythrobacter, Porphyrobacter* and *Erythromicrobium.*

Erb. longus produces the typical Erb-type carotenoids. More than 20 different carotenoids have been identified including some novel ones (Fig. 13; Takaichi and Shimada, 1992; Takaichi et al., 1988, 1990, 199la). About 70% of the total are the novel carotenoid sulfates, erythroxanthin sulfate and caloxanthin sulfate. Carotenoid sulfates from *Porphyrobacter* seem to be different from these ones (S. Takaichi, unpublished). The presence of such carotenoid sulfates is very rare in the nature (Kull and Pfander, 1995). In *Erb. longus,* these carotenoid sulfates do not function as the LH pigments (Noguchi et al., 1992), indeed they can not bind to either the RC or the LH I complexes (Shimada et al., 1985). The carotenoid bonds to the RC-LH I complex of *Erb. longus* are less polar ones. Among them,

bacteriorubixanthinal is a very unique and novel carotenoid (Fig. 13). It has the cross-conjugated aldehyde group at C-19´, whose position is not known in other organisms. The ψ end group is methoxylated and 3,4-desaturated in contrast to the other carotenals described above. One end group is the 3-hydroxyl-β end group, which is a typical end group of plant carotenoids. β-Carotene and its poly-hydroxyl derivatives, caloxanthin and nostoxanthin, are also found in the RC-LH I complex. It should be noted that spirilloxanthin, which is a typical carotenoid in purple bacteria, is also found in this RC-LH I complex, although the amount is small. Bacteriorubixanthinal, and zeaxanthin or nostoxanthin are the major components in the RC-LH I complex of the Erb-type bacteria. Interestingly, these carotenoids seem to share the same binding site in the complex despite their structural differences (K. Shimada, personal communication).

In *Methylobacterium radiotolerans* (previously, *Pseudomonas radiora*), spirilloxanthin is the dominant component in the RC-LH I complex (Saitoh et al., 1995), while carotenoic acids are found in the outer membranes accompanied by no BChls and have no photosynthetic functions (S. Saitoh, personal communication). Two species of *Methylobacterium* have also similar carotenoic acids with *M. radiotolerans,* and two species of the forth group described above have polar carotenoids, diapocarotenoic acid derivatives. These highly polar carotenoids in the third, the forth and the fifth groups may be ' nonphotosynthetic' carotenoids, which are not bound to the photosynthetic pigment-protein complexes (Shimada, 1995). Although their functions are not known, there is the possibility that they protect the photosynthetic apparatus from the outside aerobic conditions.

The carotenoid composition of the first and the second groups is somewhat different from other groups, since they lack 'non-photosynthetic' carotenoids. The RC-LH I complex of *Acidiphilium rubrum* (Wakao et al., 1996; Shimada et al., 1999) and the RC-LH I and the LH II complexes of *Rsb. denitrificans* (Shimada et al., 1985) contain all the cellular carotenoids. It should be noted that the reduction of a significant part of spheroidenone to 3,4-dihydrospheroidenone upon illumination in *Rsb. denitrificans* is observed under anaerobic conditions (Takaichi et al., 1991b).

In conclusion, most aerobic photosynthetic bacteria have the purple bacteria-like photosynthetic apparatus including BChl *a,* and many species have spirilloxanthin, as well as additional polar 'non-photosynthetic' carotenoids.

Acknowledgments

The author wishes to thank R. J. Cogdell, K. Harashima and K. Shimada for reading the manuscript, and R. J. Cogdell, M. Doi, E. Halloren, S. Hanada, J. F. Imhoff, M. T. Madigan, K. Matuura, H. Oh-oka, A. Oren, S. Saitoh, K. Sato, K. Shimada and Z. -Y. Wang for cultivation of samples analyzed specially for this review.

References

Albrecht M, Ruther A and Sandmann G (1997) Purification and biochemical characterization of a hydroxyneurosporene desaturase involved in the biosynthetic pathway of the carotenoid spheroidene in *Rhodobacter sphaeroides.* J Bacteriol 179: 7462–7467

Armstrong GA (1995) Genetic analysis and regulation of carotenoid biosynthesis: Structure and function of the *crt* genes and gene products. In: Blankenship RE, Madigan MT and Bauer CE (eds) Anoxygenic Photosynthetic Bacteria, pp 1135–1157. Kluwer Academic Publishers, Dordrecht

Armstrong GA (1997) Genetics of eubacterial carotenoid biosynthesis: a colorful tale. Annu Rev Microbiol 51: 629–659

Armstrong GA, Alberti M, Leach F and Hearst JE (1989) Nucleotide sequence, organization, and nature of the protein products of the carotenoid biosynthesis gene cluster of *Rhodobacter capsulatus.* Mol Gen Genet 216: 254–268

Blankenship RE, Madigan MT and Bauer CD (eds) (1995) Anoxygenic Photosynthetic Bacteria. Kluwer Academic Publishers, Dordrecht

Breitenbach J, Misawa N, Kajiwara S and Sandmann G (1996) Expression in *Escherichia coli* and properties of the carotene ketolase from *Haematococcus pluvialis.* FEMS Microbiol Lett 140: 241–246

Britton G, Singh RK, Goodwin TW and Ben-Aziz A (1975) The carotenoids of *Rhodomicrobium vannielii* (Rhodospirillaceae) and the effect of diphenylamine on the carotenoid composition. Phytochemistry 14: 2427–2433

Caumette P, Baulaigue R and Matheron R (1988) Characterization of *Chromatium salexigens* sp. nov., a halophilic *Chromatiaceae* isolated from mediterranean salinas. Syst Appl Microbiol 10: 284–292

Caumette P, Baulaigue R and Matheron R (1991) *Thiocapsa halophila* sp. nov., a new halophilic phototrophic purple sulfur bacterium. Arch Microbiol 155: 170–176

Caumette P, Imhoff JF, Süling J and Matheron R (1997) *Chromatium glycolicum* sp. nov., a moderately halophilic purple sulfur bacterium that uses glycolate as substrate. Arch Microbiol 167: 11–18

Davies BH (1970) A novel sequence for phytoene dehydrogenation in *Rhodospirillum rubrum.* Biochem J 116: 93-99

Deisenhofer J, Epp O, Sinning I and Michel H (1995) Crystallographic refinement at 2.3 Å resolution and refined model of the photosynthetic reaction centre from *Rhodopseudomonas viridis.* J Mol Biol 246: 429–457

Dilling W, Liesack W and Pfennig N (1995) *Rhabdochromatium marinum* gen. nom. rev., sp. nov., a purple sulfur bacterium from a salt marsh microbial mat. Arch Microbiol 164: 125–131

Drews G (1981) *Rhodospirillum salexigens*, spec. nov., an obligatory halophilic phototrophic bacterium. Arch Microbiol 130: 325–327

Eichler B and Pfennig N (1986) Characterization of a new platelet-forming purple sulfur bacterium, *Amoebobacter pedioformis* sp. nov. Arch Microbiol 146: 295–300

Eichler B and Pfennig N (1988) A new purple sulfur bacterium from stratified freshwater lakes, *Amoebobacter purpureus* sp. nov. Arch Microbiol 149: 395–400

Eimhjellen KE, Steensland H and Traetteberg J (1967) A *Thiococcus* sp. nov. gen., its pigments and internal membrane system. Arch Mikrobiol 59: 82–92

Ermler U, Fritzsch G, Buchanan SK and Michel H (1994) Structure of the photosynthetic reaction centre from *Rhodobacter sphaeroides* at 2.65 Å resolution: Cofactors and protein-cofactor interactions. Structure 2: 925–936

Francis GW and Liaaen-Jensen S (1970) Bacterial carotenoids: XXXIII. Carotenoids of Thiorhodaceae: 9. The structures of the carotenoids of the rhodopinal series. Acta Chem Scand 24: 2705–2712

Frank HA, Chadwick BW, Taremi S, Kolaczkowski S and Bowman MK (1986) Singlet and triplet absorption spectra of carotenoids bound in the reaction centers of *Rhodopseudomonas sphaeroides* R26. FEBS Lett 203: 157–163

Fujii R, Chen CH, Mizoguchi Tand Koyama Y (1998)^{1}H NMR, electronic-absorption and resonance-Raman spectra of isomeric okenone as compared with those of isomeric β-carotene, canthaxanthin, β-apo-8´-carotenal and spheroidene. Spectrochim Acta A54: 727–743

Gardiner AT (1992) Peripheral antenna complexes from *Rhodopseudomonas acidophila*: Structure, function and genetic manipulation. Ph. D. Thesis, University of Glasgow

Gardiner AT, Cogdell RJ and Takaichi S (1993) The effect of growth conditions on the light-harvesting apparatus in *Rhodopseudomonas acidophila.* Photosynth Res 38: 159–167

Goodwin TW (1956) The carotenoids of photosynthetic bacteria: II. The carotenoids of a number of non-sulphur purple photosynthetic bacteria (Athiorhodaceae). Arch Mikrobiol 24: 313–322

Guyoneaud R, Mat heron R, Liesack W, Imhoff JF and Caumette P (1997) *Thiorhodococcus minus,* gen. nov., sp. nov., a new purple sulfur bacterium isolated from coastal lagoon sediments. Arch Microbiol 168: 16–23

Guyoneaud R, Süling J, Petri R, Matheron R, Caumette P, Pfennig N and Imhoff JF (1998) Taxonomic rearrangements of the genera *Thiocapsa* and *Amoebobacter* on the basis of 16S rDNA sequence analyses and description of *Thiolamprovum* gen. nov. Int J Syst Bacteriol 48: 957–964

Halfen LN, Pierson BK and Francis GW(1972) Carotenoids of a gliding organism containing bacteriochlorophylls. Arch Mikrobiol 82: 240–246

Hanada S, Kawase Y, Hiraishi A, Takaichi S, Matsuura K, Shimada K. and Nagashima KVP (1997) *Porphyrobacter tepidarius* sp. nov., a moderately thermophilic aerobic photosynthetic bacterium isolated from a hot spring. Int J Syst Bacteriol 47: 408–413

Harashima K and Nakada H (1983) Carotenoids and ubiquinone in aerobically grown cells of an aerobic photosynthetic bacterium, *Erythrobacter* species OCh 114. Agric Biol Chem 47: 1057–1063

Harashima K, Nakagawa M and Murata N (1982) Photochemical activities of bacteriochlorophyll in aerobically grown cells of aerobic heterotrophs, *Erythrobacter* species (OCh 114) and *Erythrobacter longus* (OCh 101). Plant Cell Physiol 23: 185–193

Hiraishi A and Ueda Y (1994) *Rhodoplanes* gen. nov., a new genus of phototrophic bacteria including *Rhodopseudomonas rosea* as *Rhodoplanes roseus* comb. nov. and *Rhodoplanes elegans* sp. nov. Int J Syst Bacteriol 44: 665–673

Hiraishi A and Ueda Y (1995) Isolation and characterization of *Rhodovulum sirictum* sp. nov. and some other purple nonsulfur bacteria from colored blooms in tidal and seawater pools. Int J Syst Bacteriol 45: 319–326

Hiraishi A, Hoshino Y and Satoh T(1991) *Rhodoferax fermentans* gen. nov., sp. nov., a phototrophic purple nonsulfur bacterium previously referred to as the *'Rhodocyclus gelatinosus-like'* group. Arch Microbiol 155: 330–336

Hiraishi A, Muramatsu K and Urata K (1995a) Characterization of new denitrifying *Rhodobacter* strains isolated from photosynthetic sludge for wastewater treatment. J Ferment Bioeng 79: 39–44

Hiraishi A, Urata K and Satoh T (1995b) A new genus of marine budding phototrophic bacteria, *Rhodobium* gen. nov., which includes *Rhodobium orientis* sp. nov. and *Rhodobium marinum* comb. nov. Int J Syst Bacteriol 45: 226–234

Hiraishi A, Nagashima KVP, Matsuura K, Shimada K, Takaichi S, Wakao N and Katayama Y (1998) Phylogeny and photosynthetic features of *Thiobacillus acidophilus* and related acidophilic bacteria: Its transfer to the genus *Acidiphilium* as *Acidiphilium acidophium* comb. nov. Int J Syst Bacteriol 48: 1389–1398

Hundle BS, O'Brien DA, Alberti M, Beyer P and Hearst JE (1992) Functional expression of zeaxanthin glucosyltransferase from *Erwinia herbicola* and a proposed uridine diphosphate binding site. Proc Natl Acad Sci USA 89: 9321–9325

Igarashi N, Shimada K, Matuura K and Nagashima KVP (1999) Photosynthetic gene cluster in purple bacterium, *Rubrivivax gelatinosus.* In: Garab G (ed) Photosynthesis: Mechanisms and Effects, Vol IV, pp 2889–2892. Kluwer Academic Publishers, Dordrecht

Imhoff JF (1983) *Rhodopseudomonas marina* sp. nov., a new marine phototrophic purple bacterium. Syst Appl Microbiol 4: 512–521

Imhoff JF (1995) Taxonomy and physiology of phototrophic purple bacteria and green sulfur bacteria. In: Blankenship RE, Madigan MT and Bauer CE (ed) Anoxygenic Photosynthetic Bacteria, pp 1–15. Kluwer Academic Publishers, Dordrecht

Imhoff JF and Süling J (1996) The phylogenetic relationship among Ectothiorhodospiraceae: A reevaluation of their taxonomy on the basis of 16S rDNA analyses. Arch Microbiol 165: 106–113

Imhoff JF, Petri R and Süling J (1998a) Reclassification of

species of the spiral-shaped phototrophic purple non-sulfur bacteria of the α-*Proteobacteria*: Description of the new genera *Phaeospirillum* gen. nov., *Rhodovibrio* gen. nov., *Rhodothalassium* gen. nov. and *Roseospira* gen. nov. as well as transfer of *Rhodospirillum fulvum* to *Phaeospirillum fulvum* comb, nov., of *Rhodospirillum molischianum* to *Phaeospirillum molischianum* comb. nov., of *Rhodospirillum salinarum* to *Rhodovibrio salinarum* comb. nov., of *Rhodospirillum sodomense* to *Rhodovibrio sodomensis* comb. nov., of *Rhodospirillum salexigens* to *Rhodothalassium salexigens* comb. nov. and of *Rhodospirillum mediosalinum* to *Roseospira mediosalina* comb. nov. Int J Syst Bacteriol 48: 793–798

Imhoff J F, Silling J and Petri R (1998b) Phylogenetic relationships among the *Chromatiaceae,* their taxonomic reclassification and description of the new genera *Allochromatium, Halochromatium, Isochromatium, Marichromatium, Thiococcus, Thiohalocapsa,* and *Thermochromatium.* Int J Syst Bacteriol 48: 1129–1143

IUPAC Commission on Nomenclature of Organic Chemistry and the IUPAC-IUB Commission on Biochemical Nomenclature (1975) Nomenclature of carotenoids. Pure Appl Chem 41: 407–431

Kawasaki H, Hoshino Y, Kuraishi H and Yamasato K (1992) *Rhodocista centenaria* gen. nov., sp. nov., a cyst-forming anoxygenic photosynthetic bacterium and its phylogenetic position in the *Proteobacteria* alpha group. J Gen Appl Microbiol 38: 541–551

Keppen OI and Gorlenko VM (1975) A new species of purple budding bacteria containing bacteriochlorophyll *b.* Mikrobiologiya 44: 258–264

Kleinig H, Schmitt R, Meister W, Englert G and Thommen H (1979) New C_{30}-carotenoic acid glucosyl esters from *Pseudomonas rhodos. Z* Naturforsch 34c: 181–185

Koepke J, Hu X, Muenke C, Schulten K. and Michel H (1996) The crystal structure of the light-harvesting complex II (B800-B850) from *Rhodospirillum molischianum.* Structure 4: 581–597

Komori M, Ghosh R, Takaichi S, Hu Y, Mizoguchi T, Koyama Y and Kuki M (1998) A null lesion in the rhodopin 3,4-desaturase of *Rhodospirillum rubrum* unmasks a cryptic branch of the carotenoid biosynthetic pathway. Biochemistry 37: 8987–8994

Kompantseva EI (1985) New halophilic purple bacteria, *Rhodobacter euryhalinus* sp. nov. Mikrobiologiya 54: 974–982

Kompantseva EI and Gorlenko VM (1984) A new species of moderately halophilic purple bacterium, *Rhodospirillum mediosalinum* sp. nov. Mikrobiologiya 53: 954–961

Kull D and Pfander H (1995) Appendix: List of new carotenoids. In: Britton G, Liaaen-Jensen S and Pfander H (eds) Carotenoids, Vol 1A: Isolation and Analysis, pp 295–317. Birkhäuser, Basel

Lang H P, Cogdell RJ, Takaichi S and Hunter CN (1995) Complete DNA sequence, specific Tn5 insertion map, and gene assignment of the carotenoid biosynthesis pathway of *Rhodobacter sphaeroides.* J Bacteriol 177: 2064–2073

Liaaen-Jensen S (1965) Bacterial carotenoids: XVIII. Arylcarotenes from *Phaeobium.* Acta Chem Scand 19: 1025–1030

Lorquin J, Molouba F and Dreyfus BL (1997) Identification of the carotenoid pigment canthaxanthin form photosynthetic *Bradyrhizobium* strains. Appl Environ Microbiol 63: 1151 – 1154

Madigan MT (1986) *Chromatium tepidum* sp. nov., a thermophilic photosynthetic bacterium of the family *Chromatiaceae.* Int J Syst Bacteriol 36: 222–227

Madigan MT and Ormerod JG (1995) Taxonomy, physiology and ecology of heliobacteria. In: Blankenship RE, Madigan MT and Bauer CE (eds) Anoxygenic Photosynthetic Bacteria, pp 17–30. Kluwer Academic Publishers, Dordrecht

Malhotra HC, Britton G and Goodwin TW (1970) A novel series of 1,2-dihydro carotenoids. Int J Vit Res 40: 315–322

Matsumura H, Takeyama H, Kusakabe E, Burgess JG and Matsunaga T (1997) Cloning, sequencing and expressing the carotenoid biosynthesis genes, lycopene cyclase and phytoene desaturase, from the aerobic photosynthetic bacterium *Erythrobacter longus* sp. strain OCh 101 in *Escherichia coli.* Gene 189: 169–174

Matuura K and Shimada K (1993) Electrochromic spectral band shift of carotenoids in the photosynthetic membranes of *Rhodospirillum molischianum* and *Rhodospirillum photometricum.* Biochim Biophys Acta 1140: 293–296

McDermott G, Prince SM, Freer AA, Hawthornthwaite-Lawless AM, Papiz MZ, Cogdell RJ and Isaacs NW (1995) Crystal structure of an integral membrane light-harvesting complex from photosynthetic bacteria. Nature 374: 517–521

Misawa N, Nakagawa M, Kobayashi K, Yamano S, Izawa Y, Nakamura K and Harashima K (1990) Elucidation of the *Erwinia uredovora* carotenoid biosynthetic pathway by functional analysis of gene products expressed in *Escherichia coli.* J Bacteriol 172: 6704–6712

Misawa N, Kajiwara S, Kondo K, Yokoyama A, Satomi Y, Saito T, Miki W and Ohtani T (1995) Canthaxanthin biosynthesis by the conversion of methylene to keto groups in a hydrocarbon β-carotene by a single gene. Biochem Biophys Res Commun 209: 867–876

Noguchi T, Hayashi H, Shimada K, Takaichi S and Tasumi M (1992) In vivo states and functions of carotenoids in an aerobic photosynthetic bacterium, *Erythrobacter longus.* Photosynth Res 31: 21–30

Ouchane S, Picaud M, Vernotte C, Reiss-Husson F and Astier C (1997a) Pleiotropic effects of *puf* interposon mutagenesis on carotenoid biosynthesis in *Rubrivivax gelatinosus.* J Biol Chem 272: 1670–1676

Ouchane S, Picaud M, Vernotte C and Astier C (1997b) Photooxidative stress stimulates illegitimate recombination and mutability in carotenoid-less mutants of *Rubrivivax gelatinosus.* EMBO J 16: 4777–4787

Overmann J and Pfennig N (1989) *Pelodictyon phaeoclathratiforme* sp. nov., a new brown-colored member of the Chlorobiaceae forming net-like colonies. Arch Microbiol 152: 401–406

Overmann J, Fischer U and Pfennig N (1992) A new purple sulfur bacterium from saline littoral sediments, *Thiorhodovibrio winogradskyi* gen. nov. and sp. nov. Arch Microbiol 157:329–335

Pfennig N and Trüper HG (1989) Anoxygenic phototrophic bacteria. In: Staley JT, Bryant MP, Pfennig N and Holt JG (eds) Bergy's Manual of Systematic Bacteriology, Vol 3, pp 1635–1709. Wiliams and Wilkins, Baltimore

Pfennig N, Markham MC and Liaaen-Jensen S (1968) Carotenoids of *Thiorhodaceae*: 8. Isolation and characterization of a *Thiothece, Lamprocystis* and *Thiodictyon* strain and their carotenoid pigments. Arch Mikrobiol 62: 178–191

Pfennig N, Lünsdorf H, Süling J and Imhoff JF (1997) *Rhodospira trueperi* gen. nov., spec. nov., a new phototrophic Proteobacterium of the alpha group. Arch Microbiol 168: 39–45

Pierson BK and Castenholz (1995) Taxonomy and physiology of filamentous anoxygenic phototrophs. In: Blankenship RE, Madigan MT and Bauer CE (eds) Anoxygenic Photosynthetic Bacteria, pp 31–47. Kluwer Academic Publishers, Dordrecht

Pierson BK, Giovannoni SJ and Castenholz RW (1984) Physiological ecology of a gliding bacterium containing bacteriochlorophyll *a.* Appl Environ Microbiol 47: 576–584

Raisig A, Bartley G, Scolnik P and Sandmann G (1996) Purification in an active state and properties of the 3-step phytoene desaturase from *Rhodobacter capsulatus* overexpressed in *Escherichia coll.* J Biochem 119: 559–564

Ryvarden L and Liaaen-Jensen S (1964) Bacterial carotenoids: XIV. The carotenoids of *Rhodomicrobium vannielii.* Acta Chem Scand 18: 643–654

Saitoh S, Takaichi S, Shimada K and Nishimura Y (1995) Identification and subcellular distribution of carotenoids in the aerobic photosynthetic bacterium, *Pseudomonas radiora* strain MD-1. Plant Cell Physiol 36: 819–823

Saitoh S, Suzuki T and Nishimura Y (1998) Proposal of *Craurococcus roseus* gen. nov., sp. nov. and *Paracraurococcus ruber* gen. nov., sp. nov., novel aerobic bacteriochlorophyll *a*-containing bacteria from soil. Int J Syst Bacteriol 48: 1043–1047

Sandmann G (1994) Carotenoid biosynthesis in microorganisms and plants. Eur J Biochem 223: 7–24

Sandmann G (1997) High level expression of carotenogenic genes for enzyme purification and biochemical characterization. Pure Appl Chem 69: 2163–2168

Schmidt K (1971) Carotenoids of purple nonsulfur bacteria: Composition and biosynthesis of the carotenoids of some strains of *Rhodopseudomonas acidophila, Rhodospirillum tenue,* and *Rhodocyclus purpureus.* Arch Mikrobiol 77: 231–238

Schmidt K (1978) Biosynthesis of carotenoids. In: Clayton RK and Sistrom WR (eds) The Photosynthetic Bacteria, pp 729–750. Prenum Press, New York

Schmidt K and Liaaen-Jensen S (1973) Bacterial carotenoids: XLII. New keto-carotenoids from *Rhodopseudomonas globiformis* (Rhodospirillaceae). Acta Chem Scand 27: 3040–3052

Schmidt K and Schiburr R (1970) The carotenoids of the green sulphur bacteria: carotenoid composition in 18 strains. Arch Mikrobiol 74: 350–355

Schmidt K and Trüper HG (1971) Carotenoid composition in the genus *Ectothiorhodospira* Pelsh. Arch Mikrobiol 80: 38–42

Schmidt K, Liaaen-Jensen S and Schlegel HG (1963) Die Carotinoide der Thiorhodaceae: I. Okenon als Hauptcarotinoid von *Chromatium okenii* Perty. Arch Mikrobiol 46: 117–126

Schmidt K, Pfennig N and Liaaen-Jensen S (1965) Carotenoids of Thiorhodaceae: IV. The carotenoid composition of 25 pure isolates. Arch Mikrobiol 52: 132–146

Schmidt K, Francis GW and Liaaen-Jensen S (1971) Bacterial carotenoids: XXXVI. Remarkable C_{43}-carotenoid artifacts of cross-conjugated carotenals and new carotenoid glucosides from Athiorhodaceae spp. Acta Chem Scand 25: 2476–2486

Schumann G, Nürnberger H, Sandmann G and Krügel H (1996) Activation and analysis of cryptic *crt* genes for carotenoid biosynthesis from *Streptomyces griseus.* Mol Gen Genet 252: 658–666

Schwerzmann RU and Bachofen R (1989) Carotenoid profiles in pigment-protein complexes of *Rhodospirillum rubrum.* Plant Cell Physiol 30: 497–504

Scolnik PA, Walker MA and Marrs BL (1980) Biosynthesis of carotenoids derived from neurosporene in *Rhodopseudomonas capsulata.* J Biol Chem 255: 2427–2432

Shiba T (1991) *Roseobacter litoralis* gen. nov., sp. nov., and *Roseobacter denitrificans* sp. nov., aerobic pink-pigmented bacteria which contain bacteriochlorophyll *a.* System Appl Microbiol 14: 140–145

Shimada K (1995) Aerobic anoxygenic phototrophs. In: Blankenship RE, Madigan MT and Bauer CE (eds) Anoxygenic Photosynthetic Bacteria, pp 105–122. Kluwer Academic Publishers, Dordrecht

Shimada K, Hayashi H and Tasumi M (1985) Bacteriochlorophyll-protein complexes of aerobic bacteria, *Erythrobacter longus* and *Erythrobacter* species OCh 114. Arch Microbiol 143: 244–247

Shimada K, Itoh S, Iwaki M, Nagashima KVP, Matuura K, Kobayashi M and Wakao N (1999) Reaction center complex based on Zn-bacteriochlorophyll from *Acidiphilium rubrum.* In: Garab G (ed) Photosynthesis: Mechanisms and Effects, Vol II, pp 909–912. Kluwer Academic Publishers, Dordrecht

Shneour EA (1962a) Carotenoid pigment conversion in *Rhodopseudomonas spheroides.* Biochim Biophys Acta 62: 534–540

Shneour EA (1962b) The source of oxygen in *Rhodopseudomonas spheroides* carotenoid pigment conversion. Biochim Biophys Acta 65: 510–511

Singh RK, Britton G and Goodwin TW (1973) Carotenoid biosynthesis in *Rhodopseudomonas spheroides*: *S*-adenosylmethionine as the methylating agent in the biosynthesis of spheroidene and spheroidenone. Biochem J 136: 413–419

Straub O (1987) Key to Carotenoids. Pfander H (ed). Birkhauser, Basel

Suyama T, Shigematsu T, Takaichi S, Nodasaka Y, Fujikawa S, Hosoya H, Tokiwa Y, Kanagawa T and Hanada S (1999) *Roseateles depolymerans* gen. nov., sp. nov., a New Bacteriochlorophyll *a*-Containing Obligate Aerobe Belonged to the β Subclass of the Proteobacteria. Int J Syst Bacteriol 49: in press

Swarthoff T, Kramer HJM and Amesz J (1982) Thin-layer chromatography of pigments of the green photosynthetic bacterium *Prosthecochloris aestuarii.* Biochim Biophys Acta 681: 354–358

Takaichi S and Shimada K (1992) Characterization of carotenoids in photosynthetic bacteria. Methods Enzymol 213: 374–385

Takaichi S, Shimada K and Ishidsu J (1988) Monocyclic cross-conjugated carotenal from an aerobic photosynthetic bacterium, *Erythrobacter longus.* Phytochemistry 27: 3605–3609

Takaichi S, Shimada K and Ishidsu J (1990) Carotenoids from the aerobic photosynthetic bacterium, *Erythrobacter longus*: β-carotene and its hydroxyl derivatives. Arch Microbiol 153: 118–122

Takaichi S, Furihata K, Ishidsu J and Shimada K (1991a) Carotenoid sulphates from the aerobic photosynthetic bacterium, *Erythrobacter longus.* Phytochemistry 30: 3411–3415

Takaichi S, Furihata K and Harashima K (1991b) Light-induced changes of carotenoid pigments in anaerobic cells of the

aerobic pliotosynthetic bacterium, *Roseobacter denitrificans* (*Erythrobacter* species OCh 114): reduction of spheroidenone to 3,4-dihydrospheroidenone. Arch Microbiol 155: 473–476

Takaichi S, Tsuji K, Matsuura K and Shimada K (1995) A monocyclic carotenoid glucoside ester is a majorcarotenoid in the green filamentous bacterium *Chloroflexus aurantiacus.* Plant Cell Physiol 36: 773–778

Takaichi S, Wang Z-Y, Umetsu M, Nozawa T, Shimada K and Madigan MT (1997a) New carotenoids from the thermophilic green sulfur bacterium *Chlorobium tepidum*: 1´,2´-dihydro-γ-carotene, 1´,2´-dihydrochlorobactene, and OH-chlorobactene glucoside ester, and the carotenoid composition of different strains. Arch Microbiol 168: 270–276

Takaichi S, Inoue K, Akaike M, Kobayashi M, Oh-oka H and Madigan MT (1997b) The major carotenoid in all known species of heliobacteria is the C_{30} carotenoid 4,4´-diaponeurosporene, not neurosporene. Arch Microbiol 168: 277–281

Takamiya K, Iba K and Okamura K (1987) Reaction center complex from an aerobic pliotosynthetic bacterium, *Erythrobacter* species OCh 114. Biochim Biophys Acta 890:127–133

Tanaka A, Ito H, Tanaka R, Tanaka NK, Yoshida K and Okada K (1998) Chlorophyll *a* oxygenase (CAO) is involved in chlorophyll *b* formation from chlorophyll *a.* Proc Natl Acad Sci USA 95: 12719–12723

Triiper HG and Imhoff JF (1999) International Committee on Systematic Bacteriology, Subcommittee on the Taxonomy of Phototrophic Bacteria, 10 September 1997.Int J Syst Bacteriol 49: in press

Tsuji K, Takaichi S, Matsuura K and Shimada K (1995) Specificity of carotenoids in chlorosomes of the green filamentous bacterium, *Chloroflexus aurantiacus.* In: Mathis P (ed) Photosynthesis: From Light to Biosphere, Vol IV, pp 99–102. Kluwer, Dordrecht

Wakao N, Yokoi N, Isoyama N, Hiraishi A, Shimada K, Kobayashi M, Kise H, Iwaki M, Itoh S, Takaichi S and Sakurai Y (1996) Discovery of natural photosynthesis using Zn-containing bacteriochlorophyll in an aerobic bacterium *Acidiphilium rubrum.* Plant Cell Physiol 37: 889–893

Walz T and Ghosh R (1997) Two-dimensional crystallization of the light-harvesting I-reaction center photounit from *Rhodospirillum rubrum.* J Mol Biol 265: 107–111

Weedon BCL and Moss GP (1995) Structure and nomenclature. In: Britton G, Liaaen-Jensen S and Pfander H (eds) Carotenoids, Vol 1 A: Isolation and Analysis, pp 27–70. Birkhäuser, Basel

Wieland B, Feil C, Gloria-Maercker E, Thumm G, Lechner M, Bravo J-M, Poralla K and Gotz F (1994) Genetic and biochemical analyses of the biosynthesis of the yellow carotenoid 4,4´-diaponeurosporene of *Staphylococcus aureus.* J Bacteriol 176: 7719–7726

Xiong J, Inoue K and Bauer CE (1998) Tracking molecular evolution of photosynthesis by characterization of a major photosynthesis gene cluster from *Heliobacillus mobilis.* Proc Natl Acad Sci USA 95: 14851–14856

Yeates TO, Komiya H, Chirino A, Rees DC, Allen JP and Feher G (1988) Structure of the reaction center from *Rhodobacter sphaeroides* R-26 and 2.4.1: Protein-cofactor (bacteriochlorophyll, bacteriopheophytin, and carotenoid) interactions. Proc Natl Acad Sci USA 85: 7993–7997

Yeliseev AA and Kaplan S (1997) Anaerobic carotenoid biosynthesis in *Rhodobacter sphaeroides* 2.4.1: H_2O is a source of oxygen for the 1-methoxy group of spheroidene but not for the 2-oxo group of spheroidenone. FEBS Lett 403: 10–14

Yurkov VV, Gorlenko VM and Kompantseva EI (1992) A new type of freshwater aerobic orange-colored bacterium *Erythromicrobium* gen. nov., containing bacteriochlorophyll *a.* Mikrobiologiya 61: 256–260

Yurkov V, Gad'on N and Drews G (1993) The major part of polar carotenoids of the aerobic bacteria *Roseococcus thiosulfatophilus* RB3 and *Erythromicrobium ramosum* E5 is not bound to the bacteriochlorophyll *a*-complexes of the photosynthetic apparatus. Arch Microbiol 160: 372–376

Yurkov V, Stackebrandt E, Holmes A, Fuerst JA, Hugenholtz P, Golecki J, Gad'on N, Gorlenko VM, Kompantseva EI and Drews G (1994) Phylogenetic positions of novel aerobic, bacteriochlorophyll *a*-containing bacteria and description of *Roseococcus thiosufatophilus* gen. nov., sp. nov., *Erythromicrobium ramosum* gen. nov., sp. nov., and *Erythrobacter litoralis* sp. nov. Int J Syst Bacteriol 44: 427–434

This page intentionally left blank

Chapter 4

The Structure and Function of the LH2 Complex from *Rhodopseudomonas acidophila* Strain 10050, with Special Reference to the Bound Carotenoid

Richard J. Cogdell*, Paul K. Fyfe*, Tina D. Howard*, Niall Fraser*, Neil W. Isaacs+, Andy A. Freer+, Karen McKluskey+ and Stephen M. Prince+

Division of Biochemistry and Molecular Biology and +Department of Chemistry, University of Glasgow, Glasgow G12 8QQ, Scotland, U.K.

Summary

The structure of the LH2 complex from *Rps. acidophila* is presented, with special emphasis on the detailed arrangement of the pigments (BChl *a* and the carotenoid, rhodopin-glucoside). The BChl *a*/s are arranged into two distinct groups, 9 monomeric ones absorbing at 800 nm and 18 tightly coupled ones absorbing of ~860 nm. The carotenoids connect these two groups of BChl *a*/s. Recent fs and ps time-resolved energy transfer experiments, designed to probe the mechanism of carotenoid to BChl *a*, singlet-singlet energy transfer in LH2 are described. Possible mechanisms of these energy transfer events are discussed.

I. Introduction

For those people who are interested in understanding how carotenoids act as accessory light-harvesting pigments in photosynthesis now is a very exciting time. The past few years have seen the determination of high-resolution structures of several different antenna complexes where the three dimensional arrangement of the carotenoids and the chlorophyll (bacteriochlorophyll) pigments have been clearly visualized (Kühlbrandt et al., 1994; McDermott et al., 1995; Koepke et al., 1996; Hoffman et al., 1996). This structural information, together with fs and ps time-resolved studies, has made it possible for the first time to probe the detailed molecular mechanisms involved in the light-harvesting function of carotenoids.

In this chapter we shall summarize the structure of the LH2 (B800-850) antenna complex from the purple non-sulfur photosynthetic bacterium *Rhodopseudomonas acidophila* strain 10050, placing special emphasis on the carotenoids. We will then review what is currently known about the details of the carotenoid's light-harvesting role in this system.

H. A. Frank, A. J. Young, G. Britton and R. J. Cogdell (eds): The Photochemistry of Carotenoids, pp. 71–80.

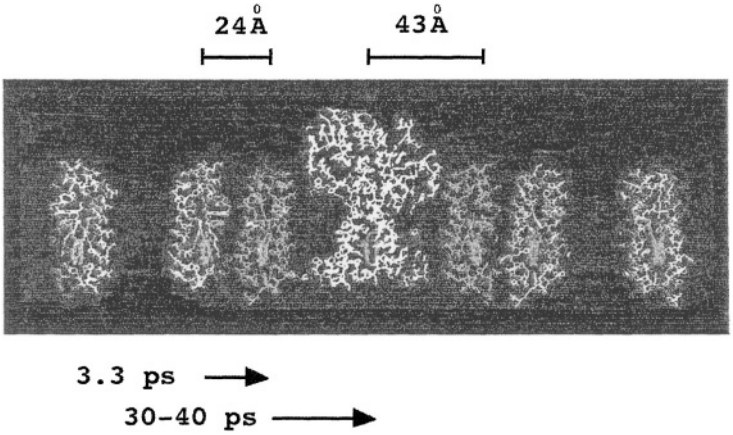

Fig. 1 A pictorial representation of a section through the purple bacterial photosynthetic unit normal to the presumed membrane plane. In Color Plate 4 the representation is LH2 - blue, LH1 - green, RC - yellow. The tightly coupled rings of BChl *a* in LH2 and LH1 and the primary dimer BChl *a*/s in the RC are shown in red. The times shown represent the rate constants for energy transfer from LH2 to LH1 and from LH1 to the RC respectively. This figure was adapted from Papiz et al., (1996). See also Color Plate 4.

II. The LH2 Complex from *Rhodopseudomonas acidophila*

A. The Purple Bacterial Photosynthetic Unit and the Composition of LH2

A typical purple bacterial photosynthetic unit consists of two types of antenna complexes, called LH1 and LH2, which transfer absorbed solar radiation to the reaction center, where the light-energy is 'trapped' and converted into useful chemical energy (for reviews see Zuber and Cogdell, 1995; Cogdell et al., 1996; Papiz et al., 1996; Hu et al., 1998). The LH1 complexes surround the RC and form the so-called 'core' complex. The LH2 complexes are arranged more peripherally around the 'core' complexes (Fig. 1).

The absorption spectrum of the LH2 complex from *Rps. acidophila* is shown in Fig. 2. In the NIR two strong absorption peaks due to the Qy transition of BChl *a* are seen, one at ~800 nm and the other at ~860 nm (this complex is also called by the generic name B800-850). There are also two other prominent absorption bands due to BChl *a*, the Qx band at ~590 nm and the Soret band at ~380 nm. The three bands seen between 450–550 nm arise from the carotenoid, rhodopin-glucoside, which has 11 conjugated double bands. The BChls and the carotenoids are non-covalently bound to two low molecular weight, very hydrophobic apoproteins, called α and β. These apoproteins have been sequenced (Bissig et al., 1998) and the α-apoprotein contains 53 amino acids and the β-apoprotein, 41. The intact antenna complex is an oligomer of $\alpha\beta$ pairs, where each $\alpha\beta$ pair binds three molecules of BChl *a* and one or two molecules of rhodopin-glucoside.

Abbreviations: BChl *a* – bacteriochlorophyll *a*; RC – reaction center

B. The Overall Structure

In 1995 the structure of the LH2 complex from *Rps. acidophila* was determined by X-ray crystallography (McDermott et al., 1995; Prince et al., 1996) to a resolution of 2.5Å. This has now been improved to 2Å (Prince, Howard and Papiz, unpublished). The overall structure is an $\alpha_9\beta_9$ nonamer and is rather like a thick-walled cylinder (Fig. 3). The central trans-membrane helices of the α-apoproteins are closely packed, side-by-side, and form the inner wall of the cylinder with a radius of 14Å. The nine trans-membrane helices of the β-apoproteins are arranged radially around the α-apoproteins to form the outer wall with a radius of 34Å. The α-apoprotein helices lie nearly perpendicular to the presumed membrane plane whereas the β-apoprotein helices are more inclined at an angle of ~15° to the normal to the membrane plane. The structure is closed off or 'capped', top and bottom by the N- and C- termini folding over and interacting with each other. All of the pigments are housed within these two rings of apoproteins.

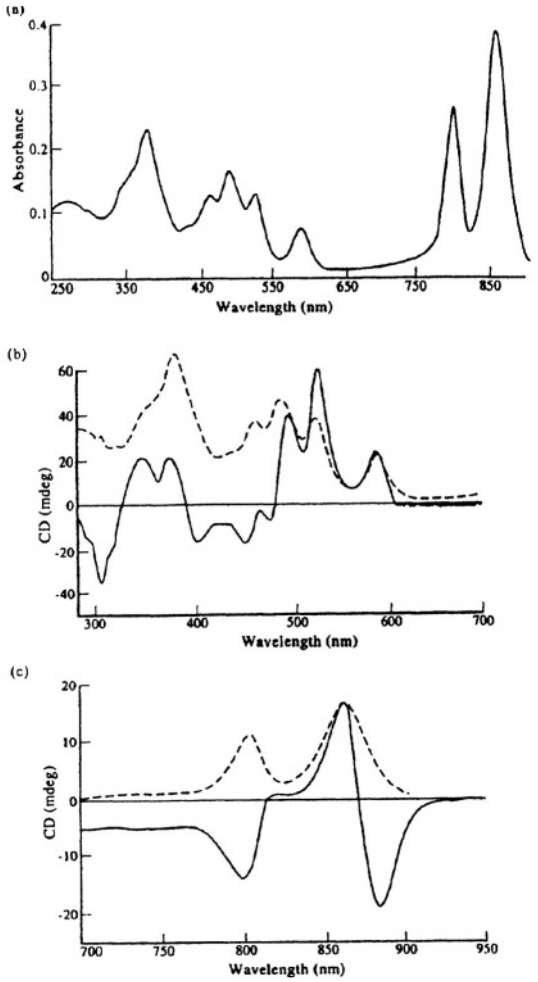

Fig. 2. The absorption spectrum and CD spectrum of the LH2 complex from *Rhodopseudomonas acidophila* strain 10050. (a) The abs spectrum of the LH2 complex. (b) A comparison of the abs spectrum (dash line) and the CD spectrum (light line) of the LH2 complex in the visible region of the spectrum. (c) A comparison of the abs spectrum (dash line) and the CD spectrum (light line) of the LH2 complex in the NIR region of the spectrum. These data were measured on the BBSRC CD facility at Stirling University, UK with the skilled assistance of Professor Nick Price and Dr Sharon Kelly.

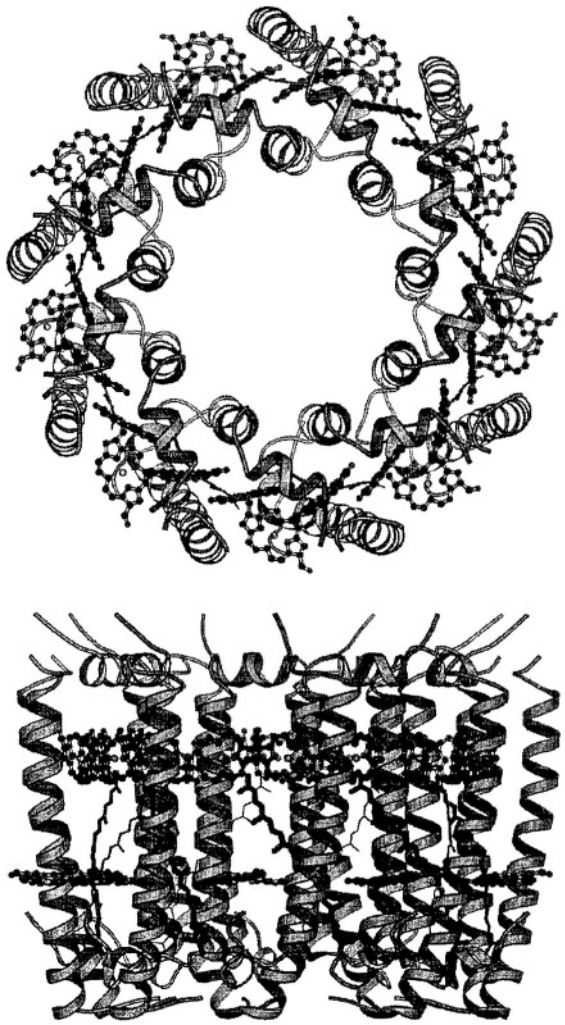

Fig. 3. A simplified structural representation of the LH2 complex from *Rhodopseudomonas acidophila* 10050. Top - A view from the periplasmic surface of the membrane. Bottom - A view from within the membrane. The polypeptide chains are shown as ribbons The α-apoproteins are on the inside of the nonameric structure and the β-apoproteins are on the outside The pigments are depicted with only the photoactive portions of the chromophores shown. This figure was produced using the package 'MOLSCRIPT" (Kraulis, 1991).

C. The Structure and Organization of the BChls

The BChl *a* molecules are organized into two distinct groups (Fig. 4). Nine, well separated (center to center distance ~21Å) peripherally arranged BChls lie between the β-apoproteins. These BChls have their central Mg^{++} atom ligated to the N-terminal extension of the N-terminal methionine residue of the α-apoproteins. In the original description of this structure this extension was modeled as a formyl group (McDermott et al., 1995). This, however, is no longer consistent with the improved 2·0Å resolution data and its identity is currently not certain. The plane of the bacteriochlorin rings of this group of BChls is rather parallel to the presumed membrane surface. Based upon a detailed characterization of the LH2 complex by absorption and CD spectroscopy (Cogdell and Scheer, 1985; Sauer et al., 1996) this group of BChls have been assigned to those which absorb at ~800 nm.

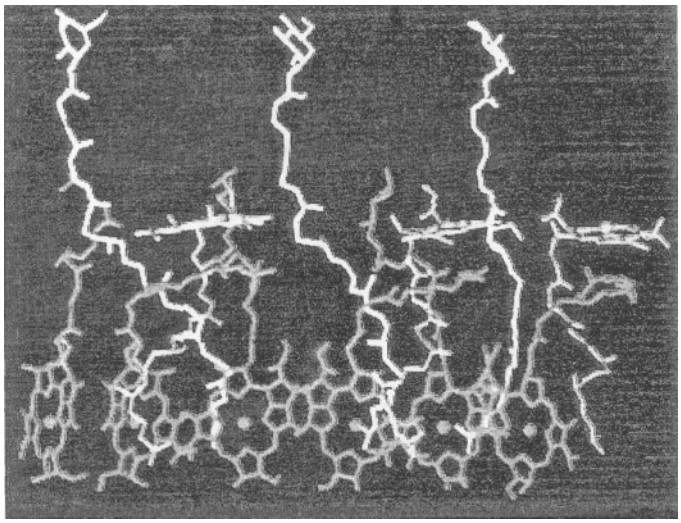

Fig. 4. A section of the structure of the LH2 complex from *Rhodopseudomonas acidophila* strain 10050 only showing the pigment. In Color Plate 5 the representation is B850 BChl *a*/s – red, B800 BChl *a*/s – green, rhodopin glucoside – yellow. This figure was redrawn from McDermott et al. (1995). See also Color Plate 5.

Further towards the center of the complex there is a second group of 18 tightly-coupled BChls. These BChls have their central Mg^{++} atoms liganded to conserved histidine residues, α-(His31) and β-(His30). Their bacteriochlorin rings lie parallel to the transmembrane helices. The individual environments and conformations of these 18 BChls are not all equivalent. Within an $\alpha\beta$ apoprotein pair, one BChl is complexed to α- and one to β- and the two BChl *a* molecules have a Mg^{++} distance of 9.53Å, whereas the Mg^{++}-Mg^{++} distance to the next BChl *a* is the ring, outside this $\alpha\beta$ pair, is 9.45Å. The face of the bacteriochlorin ring of the α-bound BChl *a* which is presented to the inside of the complex is opposite to that of the β-bound BChl *a*. This means that the BChls alternate in their orientation going round the ring. Within an $\alpha\beta$ apoprotein pair the two BChl *a* bacteriochlorin macrocycles overlap at rings C and E, while between adjacent $\alpha\beta$ apoprotein pairs the overlap is at ring A. Based upon extensive spectroscopic analysis these 18 tightly coupled BChls have been assigned to those which absorb at ~860 nm (i.e. the B850 BChls). As described in detail elsewhere (Prince et al., 1996; Cogdell et al., 1997) each of the different types of BChl *a* show distinct different conformations of their macrocycles. For example the β-bound B850 bacteriochlorin is in a 'saddle' conformation with significant 'bowing' along the direction of the Qy transition, while the B800 bacteriochlorin is slightly 'domed.' The possible spectroscopic consequences of these asymmetries are currently under investigation.

In the purple bacterial photosynthetic unit energy transfer from the antenna complexes is 'directed' to the RC because of the differences in the energy levels of the Qy absorptions of the different groups of BChls in LH2 and LH1 (Hunter et al., 1989; Olsen and Hunter 1994; Pullerits and Sundström 1996). The BChls in LH2 absorb at 800 and ~850 nm, while those in LH1 at ~875 nm. Therefore light absorbed at 800 nm is transferred within LH2 to the B850 molecules, and then goes from LH2 to LH1. In each case it is the same BChl *a* molecules involved and it is therefore important to try to understand from the structure what causes these different spectral shifts. Comparison of the amino acid sequences of the B800-850 and B800-820 forms of LH2 (Brunisholz and Zuber 1988), together with the site-directed mutagenesis studies of Fowler et al., (Fowler et al., 1992, 1994), suggested a role of hydrogen bonds from α-(Tyr44) and α-(Tryp45) to the acetyl group of the BChl *a* macrocycle in modulating where those Qy absorptions are located. The crystal structure clearly shows that α-(Tryp45) is hydrogen bonded to the acetyl carbonyl oxygen of ring A of the α-bound B850 BChl and α-(Tyr44) is hydrogen bonded to the same acetyl carbonyl oxygen of ring A of the β-bound B850 BChl *a*. Very recently we have determined the structure of the B800-820 complex from *Rps. acidophila* strain 7050 (McKluskey, Prince,

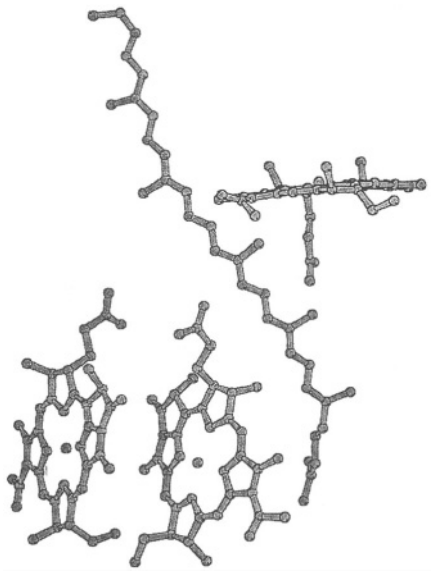

Fig. 5. A schematic representation of the arrangement of the pigments in the LH2 complex from *Rhodopseudomonas acidophila* strain 10050 within one $\alpha\beta$ apoprotein pair. The rhodopin glucoside molecule can be seen coming into contact with the edge of the B800 BChl *a* molecule and passing over the face of the α-bound B850 BChl *a* molecule.

Isaacs and Cogdell, unpublished). In this structure the acetyl carbonyl oxygen from ring A of the α-bound B820 BChl is now hydrogen bonded to α-(Tyr41) while that of the same acetyl carbonyl oxygen of ring A of the β-bound B820 BChl is free and not hydrogen bonded. A detailed analysis of this structure in comparison with that of the B800-850 complex is currently underway to try to pin-point the reason(s) for this spectral shift of the strongly coupled ring of BChls from 850 nm to 820 nm.

The distance between a B800 BChl *a* and the B850 BChls is 17.4Å to the α-bound B850 BChl and 18.2Å to the β-bound B850 BChl.

D. The Structure and Organization of the Carotenoids

The initial description of the structure of LH2 (McDermottt et al., 1995) resolved a single molecule of rhodopin glucoside per $\alpha\beta$ apoprotein pair (Fig. 5). It has an extended sigmoidal shaped conformation and spans the whole depth of the complex. This conformation is a typical all-*trans* conformation (Fig.

Fig. 6. A space filling model of the structure of rhodopin-glucoside in the LH2 complex from *Rhodopseudomonas acidophila* strain 10050. (Top) A side view; (Bottom) A view looking down the long axis of the carotenoid.

6) and confirms the previous assignment of this from resonance Raman spectroscopy (Robert and Lutz 1985). The carotenoid begins with its glucosyl ring in one $\alpha\beta$ apoprotein pair then runs through the complex, crossing over into the next $\alpha\beta$ apoprotein pair. The glucosyl ring interacts with polar residues on the N terminal side [in particular α-(Lys5) and α-(Thr9)]. The non-polar hydrocarbon chain then passes close to the edge of the B800 BChl macrocycle, then passes on to run over the face of the α-bound B850 BChl *a* macrocycle in the next pair of $\alpha\beta$-apoproteins

(Fig. 5). The closest approach of the carotenoid to the edge of the B800 BChl *a* macrocycle is 3·42Å and to the face of the α-bound B850 BChl *a* macrocycle is 3·57Å. This carotenoid shows a strong induced CD spectrum (Fig. 2) when it is bound into LH2, whereas in solution in organic solvent it is CD inactive. When the carotenoid is viewed down its long axis, from end to end, it can be seen to be twisted into about half a turn of a helix (Fig. 6). This may well be the origin of the strong CD signal. Apart from the polar interactions with the glucosyl head group the binding pocket of the carotenoid is very hydrophobic. Table 1 gives a list of the main apoprotein contacts to the rhodopin glucoside molecule.

In the original description of LH2 (McDermott et al., 1995) there was some extra electron density which was modeled as a bound molecule of the detergent β-octyl glucoside. The structure has been re-determined with crystals where the only detergent 'seen' by the LH2 complex was LDAO. Again the identical density was seen. Disappointing even at the higher resolution of 2Å, no real improvement in the details of this extra density is seen. It may be that this extra density represents another carotenoid molecule, however, we only see about one third the length of density that would be required if this is true. We cannot at present distinguish between this representing low occupancy of a second carotenoid (of which only part) is well enough ordered to be seen, or that another, as yet unknown molecule such as a lipid. Unfortunately, until now, the analysis of the pigment content of LH2 has produced equivocal results, mainly because of the relatively low precision at which the extinction coefficient for rhodopin-glucoside is known. Interestingly, a projection map of 2D crystals of LH2 from *R. sulfidophilus* shows extra density in an outer groove in the LH2 structure (Montoya et al., 1995). If the extra density was a carotenoid with a similar orientation as the well-resolved one, it would fit snuggly in this groove. Montoya et al. (1995) suggested that this could represent a second carotenoid per αβ-apoprotein pair.

It is worthwhile re-emphasizing that the well-ordered carotenoid interlinks two αβ apoprotein pairs, suggesting that it may to play a key structural role. This may well explain the long observed fact that carotenoid deletion mutants usually lack LH2 (Lang and Hunter, 1994), due to their inability to assemble LH2 in the absence of a carotenoid. In *Rb.*

Table 1. The contacts that the antenna apoproteins in the LH2 complex from *Rhodopseudomonas acidophila* strain 10050 make with the rhodopin glycoside chromophore

Rhodopin glycoside atom	Residue	Atom	Distance Å
C4	Ile (-)α6	CA	3.81
CM3	Lys (-)α5	O	3.78
C6	Val (-)α9	CG2	3.70
CM4	Tyr β14	CD2	3.43
C12	Leu β14	CD2	4.10
C13	Gln (-)α3	OE1	3.54
CM3	Val β15	O	3.87
C14	Leu α20	CD2	3.82
C15	Gly β18	O	3.66
C18	Thr β19	OG1	3.37
C25	Phe β22	CB	4.26
CM8	Val α23	CG2	3.64
C27	Ile α26	CG2	3.73
	Ala (+)α27	CB	4.06
	Ile (+)α28	CG1	4.02
	His (+)α31	NE2	4.11

This data was taken from Prince et al. (1997) and the carotenoid numbering scheme used is described in Freer et al.,(1996).

sphaeroides, for example, the LH2 apoproteins are synthesized but rapidly turned over (degraded) in the absence of carotenoids (Lang and Hunter, 1994).

III. Energy Transfer Between Carotenoids and BChl in LH2

Energy transfer between carotenoids and BChl in LH2 takes place in both directions. Singlet-singlet energy transfer occurs from carotenoid to BChl (the light-harvesting role of carotenoids) and triplet-triplet energy transfer occurs from BChl to carotenoid (the photoprotective function of carotenoids). This section will only deal with the singlet-singlet energy transfer, the triplet transfer is covered in Chapter 11 (Angerhofer).

The light-harvesting role of rhodopin glucoside in the LH2 from *Rps. acidophila* is rather easy to demonstrate by measuring the fluorescence excitation spectrum of the fluorescence emission from the B850 BChl *a* band (Angerhofer et al., 1985). In this case the efficiency of energy transfer from the carotenoid to the BChl is about 55% (Angerhofer et al., 1985). With some other LH2 complexes this energy transfer efficiency can be close to 100% (Cogdell et al., 1991). Surprisingly, therefore, it may seem strange that this process has been difficult to understand. The problem arises because the quantum yield of fluorescence of most carotenoids found in LH2 complexes is very low, usually in the order of 10^{-6} or 10^{-5}. Due to the relationship of lifetime of the excited singlet state and fluorescence yield, these low values translate into excited state lifetimes of between 100 and 200 fs (for recent reviews, see Frank and Cogdell 1996; Koyama et al., 1996). This is a very short time in which to have such efficient singlet-singlet energy transfer. How then is it possible for these carotenoids be such efficient accessory light-harvesters? Carotenoids, as described in great detail in Chapter 8, Christensen and 13, Frank), have rather unusual photochemical properties. The allowed singlet transition from the ground state (which is responsible for their strong absorption bands in the visible region of the spectrum) is due to the second excited singlet state (S_2) (Hudson et al., 1982). The ground state has Ag symmetry while the S_2 state has Bu symmetry. A lower lying excited singlet state also exists, the 2^1Ag state, but a one photon transition to this state directly from the ground state is forbidden for symmetry reasons. When carotenoids are excited to the S_2 state they relax in a few 100 fs into the S_1 state. The S_1 state then decays in a few ps to the ground state (Koyama et al., 1996). This fast transition from S_2 to S_1 is promoted by vibronic coupling (Noguchi et al., 1990; Kuki et al., 1994; Macpherson and Gillbro, 1998). The S_2 and S_1 states of many of the carotenoids have been characterized (Chapter 8, Christensen; 13, Frank) yet there are two major questions to be addressed in trying to understand the detailed molecular mechanisms involved in the light-harvesting role of carotenoids. Firstly, which of the two excited singlet states of the carotenoid are involved as energy donors and which of the two spectroscopic forms of BChl *a* (B800 and/or B850) are the energy acceptors? Then secondly, what is the detailed physical mechanism of these energy transfer events?

Figure 7 shows the structural context in which this energy transfer reaction must be considered. This figure shows the direction of the transition dipole moments (Qx and Qy) of the B800 and B850 BChls in LH2. Assuming that the transition dipole moments of the S_2 and S_1 states of the carotenoid run up and down the long axis of the polyene chain then it can be seen that only the Qx transition of the B850 BChls is well oriented for energy transfer via the Förster weak interaction dipole-dipole exchange mechanism i.e. parallel to the direction of the transition dipole moments of the carotenoid's singlet states. The best estimates of the energy levels of the S_2 and S_1 states rhodopin glucoside are ~19,500 cm^{-1} and 13,200 cm^{-1} respectively (Frank and Cogdell, 1996; Koyama et al., 1996). This would then suggest, purely on energy grounds, that energy transfer from S_2 would most readily go via the Qx band of BChl (~17,000 cm^{-1}) and from S_1 via the Qy band of BCh1 (~12,700 cm^{-1} for B800 and 11,800 cm^{-1} for B850). In this way, the spectral overlap term would be maximized.

Several papers have now been published where the singlet-singlet energy transfer from the carotenoid to bacteriochlorophyll in LH2 has been investigated on the fs and ps timescales (for example see Shreve et al., 1991; Krueger et al., 1998; Andersson et al., 1996), but, perhaps the most comprehensive study, especially with LH2 from *Rps. acidophila* is the very recent study of Macpherson et al., (Macpherson et al., 1999). The absorption of carotenoids and the emission from their S_2 state in vitro is strongly solvent dependent (Andersson et al., 1991). The absorption and emission spectra shift to the red as the polarizability of the solvent increases. Macpherson

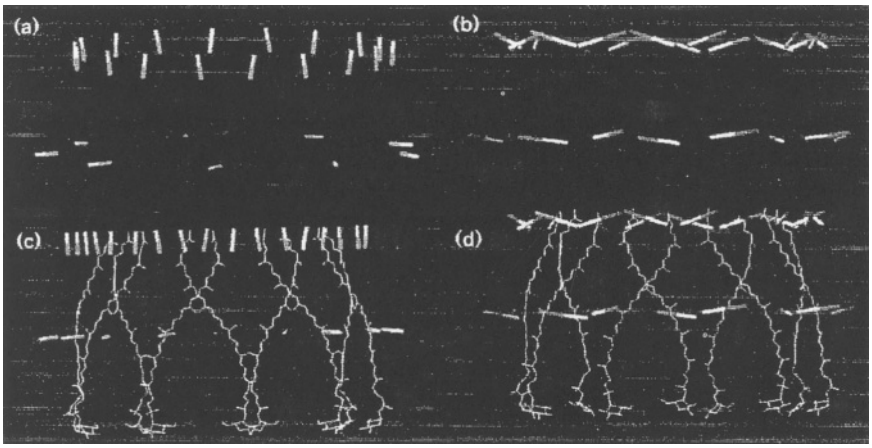

Fig. 7. A diagrammatic representation of the relative orientation of the BChl *a* Qx and Qy transitions and the carotenoids within the LH2 structure. (a) The Qx transition; (b) The Qy transition; (c) (a) together with the carotenoid; (d) (b)together with the carotenoid. This figure was redrawn from Freer et al. (1996).

et al. (1999), therefore, compared the lifetime of the fluorescence of the rhodopin glucoside in LH2 with that in benzyl alcohol, (which most closely matches the absorption spectrum of rhodopin glucoside in LH2). Using fs fluorescence up-conversion the S_2 fluorescence lifetime of rhodopin glucoside in benzyl alcohol is 132 fs while in LH2 it is shortened to 61 fs. Although the S_2 lifetime could be shortened per se on rhodopin glucoside being bound to the protein, this reduction in the lifetime by about 50% is suggestive of energy transfer from the S_2 state. In order to test whether this interpretation was correct the rise kinetics of the emission of the LH2 B850 BChl *a* were measured with an excitation pulse in the region of the carotenoid's absorption. The rise kinetics showed two phases, a very fast rise which represented 68% of the total change (and whose rise time was wavelength dependant) and a slower rise of ~820 fs (32%) which is the same time as the energy transfer rate of the B800 → B850 transfer (Macpherson et al., 1999). The fast rise was 63 fs at 851 nm and slowed down to ~180 fs at 900 nm. The fastest rise is essentially identical to the decay of the S_2 state of rhodopin glucoside when bound to LH2. The fact that the rise kinetics are so fast at 851 nm clearly shows that the internal relaxation from the Qx band of BChl which initially receives the energy from the S_2 state of the carotenoid to the Qy and is very fast. The second slower phase of the energy transfer is lost when the B800 BChls are removed from LH2 (Macpherson et al., 1999), demonstrating that it is indeed due to B800 → B850 energy transfer, and moreover that the S_2 of rhodopin glucoside gives its energy to both groups of BChl *a*.

In order to determine whether any energy transfer also occurs from the S_1 state of rhodopin glucoside, the decay kinetics of its S_1 state were measured in vitro and in the LH2 complex. Its decay time was 4.1 ps in benzyl alcohol and 3.6 ps in LH2. If all of this lifetime shortening was due to energy transfer from S_1 to the BChl then the efficiency would be about 12% of that available from S_1. When this is added to the efficiency of the energy transfer from S_2, it gives a total carotenoid to BChl efficiency in this LH2 complex of ~55%, which matches closely that previously determined by slow fluorescence excitation experiments (Macpherson et al., 1999). However in other LH2 complexes, for example from *Rb. sphaeroides* strain G1C, the efficiency of energy transfer from the carotenoid is nearly 100% and in this case the S_1 state energy is also efficiently harvested (Macpherson, Arellano, Gillbro, Fraser and Cogdell unpublished).

Up to a few years ago singlet-singlet energy transfer from the carotenoid to the BChl was always discussed in terms of two general mechanisms (Cogdell and Frank, 1987). If the energy came from the carotenoid's S_2 state, in general, Förster's dipole-dipole exchange mechanism was usually considered. While on the other hand, if the energy donor was the S_1 state the Dexter electron exchange mechanism was usually invoked. More recently, now that there is both structural information and fs kinetic data, the attempts to understand the mechanisms of energy transfer

involved have become more sophisticated. It is now generally accepted in most theoretical calculations that the electron exchange mechanism is too slow to account for the measured kinetics even from the S_1 state (Nagae et al., 1993; Krueger et al., 1998). Most researchers now favor higher order coulombic mechanisms. It may well be though that the exact mechanism will depend upon exactly which antenna complex is being studied, which of the S_2 or S_1 (or indeed both) states is the energy donor which carotenoid is present, and which of the BChl *a*/s is the acceptor. Moreover a further note of caution should be expressed concerning the theoretical studies since a lot of the important parameters in the energy transfer equations have only been estimated rather than actually determined. What is urgently needed from the theoreticians are ideas of how to critically test, by experiment, whether a proposed mechanism does actually work.

Acknowledgments

Some of the work described in this Chapter was supported by grants from the BBSRC. Karen McKluskey thanks the BBSRC for a Ph.D. studentship; Niall Fraser thanks the Gatsby Foundation for a Ph.D. scholarship; RJC thanks Drs Gillbro, Macpherson and Arellano for permission to quote some joint unpublished studies that were funded by the Human Frontiers of Science Program.

References

Andersson PO, Gillbro T, Ferguson L and Cogdell RJ (1991) Absorption spectral shifts of carotenoids related to medium polarizability J Photochem Photobiol 54: 353–360

Andersson PO, Cogdell RJ and Gillbro T (1996) Femtosecond dynamics of carotenoid to bacteriochlorophyll *a* energy transfer in the light harvesting antenna complexes from the purple bacterium *Chromatium purpuratum.* Chem Phys 210: 195–217

Angerhofer A, Cogdell RJ and Hipkins MF (1985) A spectral characterisation of the light-harvesting pigment-protein complexes from *Rhodopseudomonas acidophila.* Biochim Biophys Acta 848: 833–841

Bissig I, Brunisholz RA, Cogdell RJ and Zuber H (1988) The complete amino acid sequences of the B800-850 antenna polypeptides from *Rhodopseudomonas acidophila* strain 7750 Z Naturforsch 43c: 77–83

Brunisholz RA and Zuber H (1988) Primary structure analyses of bacterial antenna polypeptides: Correlation of aromatic amino acids with spectral properties structural similarities with reaction centre polypeptides. In: Scheer H and Schneider S (eds) Photosynthetic Light-Harvesting Systems, pp 103–116. Walter de Gruyter, Berlin

Cogdell RJ and Frank HA (1987) The function of carotenoids in photosynthesis. Biochim Biophys Acta 63: 1–17

Cogdell RJ and Scheer H (1985) Circular dichroism of light-harvesting complexes from purple photosynthetic bacteria. Photochem Photobiol 42: 669–678

Cogdell RJ, Hipkins MF, MacDonald W and Truscott TG (1981) Energy transfer between the carotenoid and bacteriochlorophyll within the B800-850 light-harvesting pigment-protein complex of *Rps sphaeroides.* Biochim Biophys Acta 634: 191–202

Cogdell RJ, Fyfe PK, Barrett SJ, Prince SM, Freer AA, Isaacs NW, McGlynn P and Hunter CN (1996) The purple bacterial photosynthetic unit. Photosynth Res 48: 55–63

Cogdell RJ, Isaacs NW, Freer AA, Arellano J, Howard T, Papiz MZ, Hawthornthwaite-Lawless AM and Prince SM (1997) The structure and function of the LH2 (B800-850) complex from the purple photosynthetic bacterium *Rhodopseudomonas acidophila* strain 10050. Proc Biophys Molec Biol 68:1–27

Fenna RE and Matthews BW (1975) Chlorophyll arrangements in a bacteriochlorophyll protein from *Chlorobium limicola.* Nature 25: 573–577

Fowler GJS, Sockalingum GD, Robert B, Grief GG and Hunter CN (1994) Blueshifts in bacteriochlorophyll absorbance correlate with changed hydrogen bonding patters in light-harvesting LH2 mutants of *Rhodobacter sphaeroides* with alterations of αTyr44 and αTyr45.Biochem J 299:695–700

Fowler GJS, Visschers RW, Grief GG, van Grondelle R and Hunter CN (1992) Genetically modified photosynthetic antenna complexes with blue-shifted absorbance bands. Nature 355: 848–850

Frank HA and Cogdell RJ (1996) Carotenoids in photosynthesis. Photochem Photobiol 63: 257–264

Hoffman E, Wrench PM, Charples FP, Hiller RG, Welte W and Diedrichts K (1996) Structural basis of light-harvesting by carotenoids: Peridinin-chlorophyll-protein from *Amphidinium carterae.* Science 272: 1788–1791

Hu X, Damjanovic A, Ritz T and Schulten K (1998) Architecture and mechanism of the light-harvesting apparatus of purple bacteria. Proc Natl Acad Sci USA 95: 5935–5941

Hudson BS, Kohler BE and Schulten K (1982) Linear polyene electronic structure and potential surfaces. In: Lim EC (ed) Excited States, Vol 6, pp 22–95. Academic Press, New York

Hunter CN, van Grondelle R and Olsen JP (1989) Photosynthetic antenna proteins: 100 ps before photochemistry starts. Tends Biochem Sci 14: 72–76

Koepke J, Hu X, Muenke C, Schulten K and Michel H (1996) The crystal structure of the light-harvesting complex II (B800-850) from *Rhodospirillum molischianum.* Structure 4: 581–597

Koyama Y, Kuki M, Andersson P-O and Gillbro T (1996) Singlet excited states and the light-harvesting function of carotenoids in bacterial photosynthesis. Photochem Photobiol 63: 243–256

Kraulis PJ (1991) MOLSCRIPT-a program to produce both detailed and schematic plots of protein structures. J Appl Cryst 24: 946–950

Krueger BP, Scholes GD and Fleming GR (1998) Calculation of couplings and energy-transfer pathways between pigments of LH2 by the *abinitio* transition density cube method. J Phys Chem B 102: 5378–5386

Krueger BP, Scholes GD, Jiminez R and Flemiong GR (1998) Electronic excitation transfer from carotenoid to bacteriochlorophyll in the purple bacterium *Rhodopseudomonas acidophila.* J Phys Chem B 102: 2284–2292

Kühlbrandt W, Wang DN and Fukiyoshi Y (1994) Atomic model of plant light-harvesting complex by electron crystallography. Nature 367: 614–621

Kuki M, Nagae H, Cogdell RJ, Shimada K and Koyama Y (1994) Solvent effect on spheroidene in non-polar and polar solutions and the environment of spheroidene in the light-harvesting complexes of *Rhodobacter sphaeroides* 241 as revealed by the energy of the $^1Ag^- \rightarrow {}^1Bu^+$ absorption and the frequencies of the vibronically coupled C = C stretching Raman lines in the $^1Ag^-$ and 2^1Ag^- states. Photochem Photobiol 59: 116–124

Lang HP and Hunter CN (1994) The relationship between carotenoid biosynthesis and the assembly of the light-harvesting LH2 complex in *Rhodobacter sphaeroides.* Biochem J 298: 197–205

Macpherson AN and Gillbro T (1998) Solvent dependence of the ultrafast S_2-S_1 internal conversion rate of β-carotene. J Phys Chem A 102: 5049–5058

Macpherson AN, Arellano JB, Fraser NJ, Cogdell RJ and Gillbro T (1999) Ultrafast energy transfer from rhodopin glucoside in the light-harvesting complex of *Rps acidophila.* In: Garab G (ed) Photosynthesis: Mechanisms and Effects, Vol I, pp 9–14. Kluwer Academic Publishers, Dordrecht

McDermott G, Prince SM, Freer AA, Hawthornthwaite-Lawless AM, Papiz MZ, Cogdell RJ and Isaacs NW (1995) Crystal structure of an integral membrane light-harvesting complex from photosynthetic bacteria. Nature 374: 517–521

Montoya G, Cyrklaff M and Sinning I (1995) Two-dimensional crystallisation and preliminary structure analysis of light-harvesting II (B800-850) complex from the purple bacterium *Rhodovilum sulphidophilum.* J Mol Biol 250: 1010

Nagae H, Kikitani T, Katoh T and Mimuro M (1993) Calculation of excitation transfer matrix elements between the S_2 and S_1 states of carotenoids and the S_2 and S_1 states of bacteriochlorophyll. J Phys Chem 98: 8012–8023

Noguchi T, Nayashi H, Tasumi M and Atkinson GH (1990) Frequencies of the Frank-Condon active ag C=C stretching mode in the 2*´Ag- excited state of carotenoids. Chem Phys Lett 175: 159–169

Olsen JD and Hunter CN (1994) Protein structure modelling of the bacterial light-harvesting complex. Photochem Photobiol 60: 521–535

Papiz MZ, Prince SM, Hawthornthwaite-Lawless AM, Mcdermott G, Freer AA, Isaacs NW and Cogdell RJ (1996) A model for the photosynthetic apparatus of purple bacteria. Trends Plant Sci I: 198–206

Prince SM, Papiz, MZ, Freer AA, McDermott G, Hawthornthwaite-Lawless AM, Cogdell RJ and Isaacs NW (1977) Apoprotein structure in the LH2 complex from *Rhodopseudomonas acidophila* strain 10050: Modular assembly and protein pigment interactions. J Mol Biol 268: 412–423

Pullerits T and Sundström V (1996) Photosynthetic light-harvesting pigment-protein complexes: Toward understanding how and why. Acc Chem Res 29: 381–389

Robert B and Lutz M (1985) Structure of antenna complexes of several Rhodospirillales from their resonance Raman spectra. Biochim Biophys Acta 807: 10–23

Sauer K, Cogdell RJ, Prince SM, Freer AA, Isaacs NW and Scheer H (1996) Structure based calculations of the optical spectra of the LH2 bacteriochlorophyll-protein complex from *Rhodopseudomonas acidophila.* Photochem Photobiol 64:564–576

Shreve AP, Trautman JK, Frank HA, Owens TG and Albrecht AC (1991) Femtosecond energy transfer processes in the B800-880 light-harvesting complex of *Rhodobacter sphaeroides* 241. Biochim Biophys Acta 1058: 280–288

Zuber H and Cogdell RJ (1995) Structure and organisation of purple bacterial antenna complexes. In: Blankenship RE, Madigan MT and Bauer CT (eds) Anoxygenic Photosynthetic Bacteria, pp 315–348. Kluwer Academic Publishers, Dordrecht

Chapter 5

Carotenoids as Components of the Light-harvesting Proteins of Eukaryotic Algae

Roger G. Hiller
Biological Sciences, Macquarie University, NSW Australia 2113

Summary

Studies of light harvesting proteins which contain carotenoids as the principal components absorbing light in the spectral region from 450 nm to 550 nm have three principal aims. These may be summarized as: how do these proteins work at the structure/function level; how do they adapt to different environmental conditions and how did they evolve. At the structural level the emphasis has shifted, perhaps prematurely, from studies of pigment composition and basic biochemistry to a consideration of atomic structures and viewing carotenoids in action directly by means of time resolved spectroscopy. The only caroteno-Chl protein from eukaryotic algae for which a high resolution structrue is available is soluble peridinin chlorophyll *a*-protein (sPCP). PCP is the protein with the highest carotenoid:Chl ratio and has the potential to greatly advance our understanding of photosynthetic energy transfer through site directed mutagenesis and in vitro reconstitution from heterologously expressed protein and purified pigments.

Application of molecular biological techniques has yielded derived amino acid sequences of intrinsic light-harvesting proteins from all major and some minor groups of algae. These sequences can all accommodate the basic structural pattern determined for higher plants , that is, three transmembrane structure helices with key

H. A. Frank, A. J. Young, G. Britton and R. J. Cogdell (eds): The Photochemistry of Carotenoids, pp. 81–98.

Chl *a* molecules conserved on the crossed first and third helices. However, the positioning of carotenoid molecules in this class of antenna complexes is still uncertain. Isolation of light-harvesting genes, especially from diatoms, brown algae and dinoflagellates, has also provided molecular tools to integrate basic pigment composition data with the synthesis/degradation of specific mRNAs and their corresponding proteins. Sufficient LHC sequences are now available that evolutionary relationships between the different groups of algae can be delineated and these can be compared with those deduced from 16sRNA and other conserved features. The diatoms and brown algal sequences form a related group but *Isochrysis,* although containing fucoxanthin, is as distant from the former as is that of dinoflagellates. The origin of the sPCP genes remains obscure.

I. Introduction

Early biochemical studies of light-harvesting complexes in eukaryotic algae attempted to apply the SDS-polyacrylamide 'green gel' techniques successfully pioneered in higher plants by Thornber (Thornber et al., 1994). These proved unreliable as much pigment was stripped from the complexes and that which remained, especially in the case of the carotenoids such as fucoxanthin (Fig. 1), was not functional in energy transfer. Use of digitonin or any of a large number of glycosidic detergents combined with sucrose gradient separation, now permits isolation of intact light-harvesting complexes of 120 to 350 kDa, which contain functional carotenoids (as shown by efficient energy transfer to Chl *a*) and extended absorbance into the green region of the spectrum characteristic of intact thylakoids. Unfortunately, the availability of large amounts of functional, but probably heterogeneous, LHC has only been accompanied by few additional purification steps (although these seem to be quite feasible). Consequently our knowledge of amino-acid and DNA sequences far outstrips our knowledge of the biochemistry of LHCs.

Although all chlorophyll-protein complexes isolated to date, whether they are associated with PS I or II, contain carotenoids, it is only in two classes of complexes that carotenoids play the major light-harvesting role. These two classes are the unique soluble peridinin-chlorophyll *a*-proteins (sPCPs) of dinoflagellates and the membrane-bound light-harvesting complexes of eukaryotic algae, which are related to the chlorophyll *b*-binding proteins of higher plants and green algae. Much of the earlier data, indicating a large number of distinct light-harvesting protein types, mostly from western blots using polyclonal antibodies, as well as variation in apparent molecular mass, can now be rationalized. This has come has come about as a result of the rapid in increase in DNA-derived sequences, part of the general penetration of the techniques of molecular biology into the traditional realms of plant physiology and biochemistry. It is now well established that all intrinsic light-harvesting proteins, no matter what their carotenoid composition, Chl composition, or molecular mass of their subunit or complex, can be accommodated by the Kühlbrandt three transmembrane helix model (Kühlbrandt et al., 1994). This model was derived from electron diffraction studies of two-dimensional crystals of the Pea light-harvesting Chl *a*-*b*-binding protein, also known as LHC II. It should, however, be mentioned that for none of the intrinsic carotenoid-containing proteins to be reviewed in this chapter is there a structure at high resolution. Structural information is largely the result of spectroscopic studies, especially that of circular dichroism and time resolved energy transfer. Notwithstanding the rapid advance in sequence data, there remain many areas where traditional approaches relating to variation of pigment composition with changes in light intensity or spectral quality are still required, so that the roles of the many genes and their products now known to be involved can be assigned. This chapter will not attempt to document every eukaryotic algal LHC which contains carotenoid. It will concentrate on those systems, especially the PCPs and FCPs for which information on the role of carotenoids is available from a number of different

Abbreviations: Cab protein – chlorophyll *a/b*-binding protein; Chl – chlorophyll; DGDG – digalactosyl diglyceride; FCP – Fucoxanthin-Chlorophyll Protein; HLIP – High Light Induced Protein; iPCP–intrinsic Peridinin Chlorophyll *a*-Protein; LHC–light-harvesting complex; MFPCP – Mainform Peridinin Chlorophyll *a*-Protein; PCP – Peridinin Chlorophyll *a*-Protein; PCR – polymerase chain reaction; pI – isoelectric point; PS I – Photosystem I; PS II – Photosystem II; RT-PCR – reverse transcriptase-polymerase chain reaction; Rubisco – ribulose 1,5-biscarboxylase; sPCP – soluble Peridinin Chlorophyll *a*-Protein

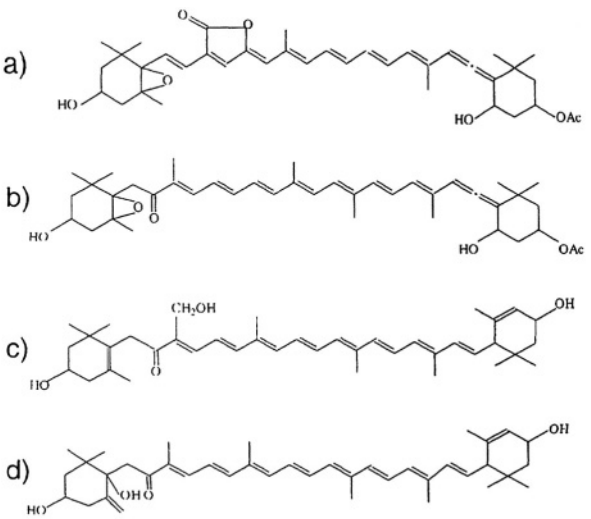

Fig. 1. Structures of some carotenoids known to play a major role in light-harvesting in eukaryotic algae: a) peridinin; b) fucoxanthin; c) siphonaxanthin; d) prasinoxanthin.

experimental viewpoints.

This chapter also distinguishes between the photoprotective role of carotenoids and the light-harvesting role and concentrates on the latter. It should be noted, however, that this distinction is largely artificial as the distance and geometry constraints of the two processes are similar. General aspects of light-harvesting in algae have been comprehensively reviewed recently by Larkum and Howe (1997) and in earlier work by Hiller, Anderson and Larkum (1991).

II. Water Soluble Proteins

A. The Soluble Peridinin Chlorophyll a*-Protein (sPCP) of Dinoflagellates*

Peridinin-chlorophyll *a*-proteins (sPCPs) have the highest carotenoid to chlorophyll ratio of any protein. They were first purified in 1976 (Haxo et al., 1976) and a great deal of data relating to their occurrence and variation has accumulated (Prezelin, 1987; Iglesias et al., 1991; Jovine et al., 1992). In the past four years the field has advanced rapidly with derived amino acid sequences from a wide variety of peridinin-containing dinoflagellates being determined (Triplett et al., 1993; Norris and Miller, 1994; Hiller et al., 1995; Li et al., 1997) . The recent publication of the atomic structure of PCP determined at 2.0Å by X-ray crystallography has given this aspect of eukaryotic light-harvesting proteins added impetus (Hofmann et al., 1996).

The water soluble sPCPs contain between 25% and 80% of the peridinin content of the cell. There are two distinct types, which will be designated mainform PCP (MFPCP) and highsalt PCP (HSPCP), in the absence of an agreed nomenclature. MFPCPs contain eight peridinin and two Chl *a* molecules in total mol mass of ~40kDa determined by gel filtration chromatography in dilute solution. Higher peridinin:Chl *a* ratios have also been reported (Haxo et al., 1976; Ogata and Smayda, 1993), but these have not been independently confirmed. The pigments are bound either to a single polypeptide of 32 kDa or to two polypeptides of 16 kDa. Most species contain only one type of apoprotein but this may reflect the relatively small number of species studied in clonal isolates. Polyclonal antibodies raised to purified MFPCP from one species cross react with all others and it was generally accepted, even before amino acid sequences became available, that the monomeric form reflected gene duplication and fusion rather than any fundamental difference in organization from the dimeric form. A remarkable feature of all MFPCPs is the existence of several to many forms which differ in isoelectric point but whose spectroscopic properties are essentially identical (Prézelin, 1987). The pattern of pIs is fairly constant for a given dinoflagellate isolate, sufficiently so for its use in distinguishing different species. The origin of this variation is undoubtedly genetic (see below) although additional post translational proteolytic modification cannot be excluded (Ogata et al., 1994).

The spectral properties of purified PCP of one predominant isoform are illustrated in Fig. 2, together with the spectrum of the detached pigments in 80% acetone. The interaction of peridinin with the apoprotein gives a prominent shoulder at about 525 nm and results in a significant increase in relative absorbance at all wavelengths beyond 500 nm. The CD spectrum indicates a strong interaction between pairs of peridinin molecules, which were originally modeled at right angles to each other and arranged in two pairs as a square around each chlorophyll (Koka and Song 1975). It is now known that the paired peridinins cross at an angle of ~55°. Light absorbed by the peridinin molecules is transferred with high efficiency to Chl *a* and the fluorescence emission is at 670 nm.

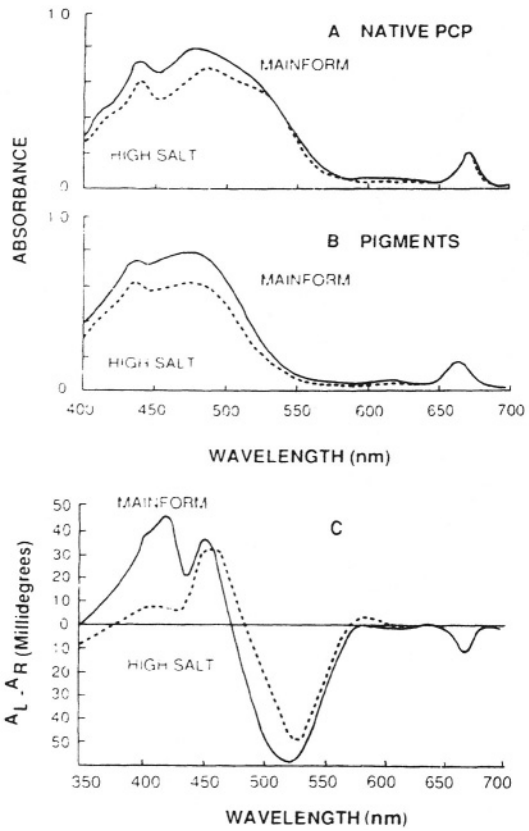

Fig. 2. Absorbance and circular dichroism spectra of sPCP from *Amphidinium carterae*. Mainform PCP represents the greater part of total sPCP, whereas HighSalt PCP is a minor form of high PI. a) native proteins; b) isolated pigments in 80% acetone; c) circular dichroism. The spectra have been normalized to the Chl *a* Q_y absorbance at 670 nm or 663 nm respectively, or to the negative CD at 670 nm. (Sharples et al., 1996)

1. Amino Acid Sequences of Mainform PCPs (MFPCPs)

The amino acid sequences of complete amino acid sequences including the putative chloroplast-directing N-terminal extensions, from three different, distantly related species are shown in Fig. 3. The three sequences of the mature proteins are ~80% identical. A feature of the mature protein sequence is the division into N- and C-terminal domains consistent with the origin of the 32 kDa forms by gene duplication and fusion. Each domain is 55% identical/ 70% similar and contains a pair of histidines. One of the pair binds Chl via a water molecule as the fifth ligand of the Mg atom (Hofmann et al., 1996). Also shown in Fig. 3 is the amino acid sequence of the mature 16kDa form from *Heterocapsa,* which has been arbitrarily aligned with the C-terminal domain of the other PCPs. It is 63% identical/74% similar to the 32 kDa forms. It should be noted that the original report (Triplett et al., 1993, see also Fig. 3A of Li et al., 1997) of the *Heterocapsa* sequence suggested that the 16 kDa forms of PCP showed identity with the 32 kDa forms over only a very limited region. However, in the original report the start codon was incorrectly identified and the error compounded by a reading frame error at the 3´ end. There are two regions of marked difference between the *Heterocapsa* sequence and the others, but these lie in trimer contact regions rather than dimer contact regions.

In an investigation of PCP by means of optically detected magnetic resonance (ODMR) it was shown that Chl triplets were readily produced and these populated the peridinin triplet states (Carbonera et al., 1996). At low temperature (2 K) *Amphidinium* PCP shows evidence for two triplet populations possibly arising from the two pigment clusters, but this was not observed *in Heterocapsa* PCP. Although the spectral properties of the monomeric form of PCP from *Amphidinium* are very similar to those of the dimeric form from *Heterocapsa,* there is a marked difference in the rate of spin exchange of the lowest triplet state of the peridinins between the pigment clusters. In *Heterocapsa* this is an order of magnitude faster than it is in *Amphidinium* PCP (Carbonera et al., 1996). Since the amino acid sequences around the pigments is conserved in both PCPs, the difference in spin exchange must reflect a subtle difference in geometry or distance between the pigment clusters in each case.

2. Gene Organization of MFPCPs

The original reports (Triplett et al., 1993, Norris and Miller, 1994) of PCP amino acid sequences noted the existence of several cDNA species but the differences between them were trivial and unable to account for the range of pIs already noted. Southern blotting, however, indicated a large number of genes. A wider range of gene sequences was also shown by a combination of direct protein sequencing and genomic and RT-PCR with at least two genes connected in series (Sharples et al., 1996). A detailed study (Li et al., 1997) of the copy number in *Gonyaulax* gave the astonishing 5,800 PCP genes per cell, probably connected in series with the intergenic space averaging 1 kb. The sequence variation in this high copy number was not investigated. No introns were present, neither were any characteristic eukaryotic promoter or poly A sites

```
      1                                                          60
pcpa  MVRSGKKAVV LAAVAFCATS VVQKSHGFVP SPLRQRAAAA GAAAASAATM FAPAAFADEI
pcps  ***GAR**IA VG-**VAVAC GL**HLN*** G*RH----** PV***A*SM* M*********
pcpx  *G*TVRALAT GVV*LAATRC HKPAN*S*** G***RN*-*P A*********LA*********

      61                                                         120
pcpa  GDAAKKLGDA SYAFAKEVDW NNGIFLQAPG KLQPLEALKA IDKMIVMGAA ADPKLLKAAA
pcps  ********** **S******* ********** *F******** *****E**** *******D**
pcpx  *********S ********** ********** *F******** ********VQ **********

      121                                                        180
pcpa  EAHHKAIGSV SGPNGVTSRA DWDNVNAALG RVIASVPENM VMDVYDSVSK ITDPKVPAYM
pcps  D********I ********** ***S****** ********AT *****N***G ****A*****
pcpx  *********I ********** ***A****I* **V****KAK **A*****TA ****G*****

      181                                                        240
pcpa  KSLVSGADAE KAYEGFLAFK DVVKKSQVTS AAGPATVPSG DKIGVAAQQL SEASYPFLKE
pcps  ****N***** ********** ****R***ST **A*P**SAS *A**E**KK* **Q******D
pcpx  ****N*P*** ***Q***E** ***E*N**AT *SA**V**** ****E**KA* *D*****I*D
pcph  .......... ..........   .......  .......... ***AD**KK* **********

      241                                                        300
pcpa  IDWLSDVYMK PLPGVSAQQS LKAIDKMIVM GAQADGNALK AAAEAHHKAI GSIDATGVTS
pcps  *N****I*L* ***DATISKK AI******I* **K****L** ***Q***Q** *****N****
pcpx  ******I*L* ****KT*PET ********** **KM***L** ********** **********
pcph  ***T****A* -*XTANPFDV ********** **AM*SA*** *GA******* S****K***T

      301                                                        360
pcpa  AADYAAVNAA LGRVIASVPK STVMDVYNAM AGA-TDTSIP LNMFSKVNPL DANAAAKAFY
pcps  L***S***** ****V***** KM******S* *SL-VAPTV* N***AS**** **********
pcpx  ****E***** I**LV***** T*******S* **V-V*S*V* N*L******* **V****G**
pcph  L***E***** I*HMV**AGE *KT******F **FNLGKDVG PY*M****AA **S**Y***L

      361
pcpa  TFKDVVQAAQ R
pcps  ******ASQV A
pcpx  ******E*S* *
pcph  E***A*K*S* R
```

Fig. 3. Alignment of amino acid sequences of MFPCPs. pcpa, *Amphidinium (*Hiller et al., 1995*);* pcps *Symbiodinium* (Norris and Miller 1994); pcpx *Gonyaulax* (Li et al., 1997)*;* pcph *Heterocapsa,* bold face Edman-derived N-terminal sequence, ordinary face cDNA sequence (Pisano, Crossley and Hiller unpublished). Mature proteins begin at residue 58 (D). * identity with top sequence; - a space.

present and it is possible that the particular gene sequenced is not expressed. However a similar lack of characteristic eukaryotic 5´ signals has been noted in both Rubisco (Rowan et al., 1996) and LHC genes (R. G. Hiller, F. P. Sharpies and P. Wrench, unpublished) in Dinoflagellates.

3. Structure of MFPCPs

MFPCPs purified to one predominant isoform by either ammonium sulfate precipitation and cation exchange chromatography or by chromatofocusing followed by gel filtration chromatography, readily form crystals which diffract X-rays well (Steck et al., 1990) and have enabled the structure (Hoffman et al., 1996) to be solved at 2.0Å (Brookhaven protein data base ID code 1PPR). The basic structure is a non-crystallographic trimer 100Å long × 40Å in thickness (Fig. 4), consistent with its proposed location (Norris and Miller, 1994) in the thylakoid lumen. Each monomer within the trimer has a twofold pseudo-symmetry axis delineating similar N-terminal and C-terminal domains. The predominantly **α-helical** structure forms a hydrophobic interior in which two pigment clusters are located. In each cluster (Fig. 5) there are two pairs of peridinins which cross at 55°. One peridinin of each pair is parallel to either the Qx or Qy transition of the Chl and each peridinin is at some point in van der Waals contact with the Chl macrocycle as well as with its pair. Light absorbed by any peridinin can be passed to its pair or to Chl by excitonic energy transfer within a few ps and then equilibrated with other Chls within the trimer by Förster dipole-dipole interaction before transfer to either, the intrinsic light-harvesting complex, or to the inner antenna of PS II, CP43/CP47. A surprising observation is that part of the hydrophobic environment of surrounding each Chl is provided by a digalactosyl diacyl glycerol molecule and its tempting to speculate that in some forms of MFPCP this could be replaced by peridinin. This might account for those results where a nine or ten peridinin:2 Chl a ratio has been reported.

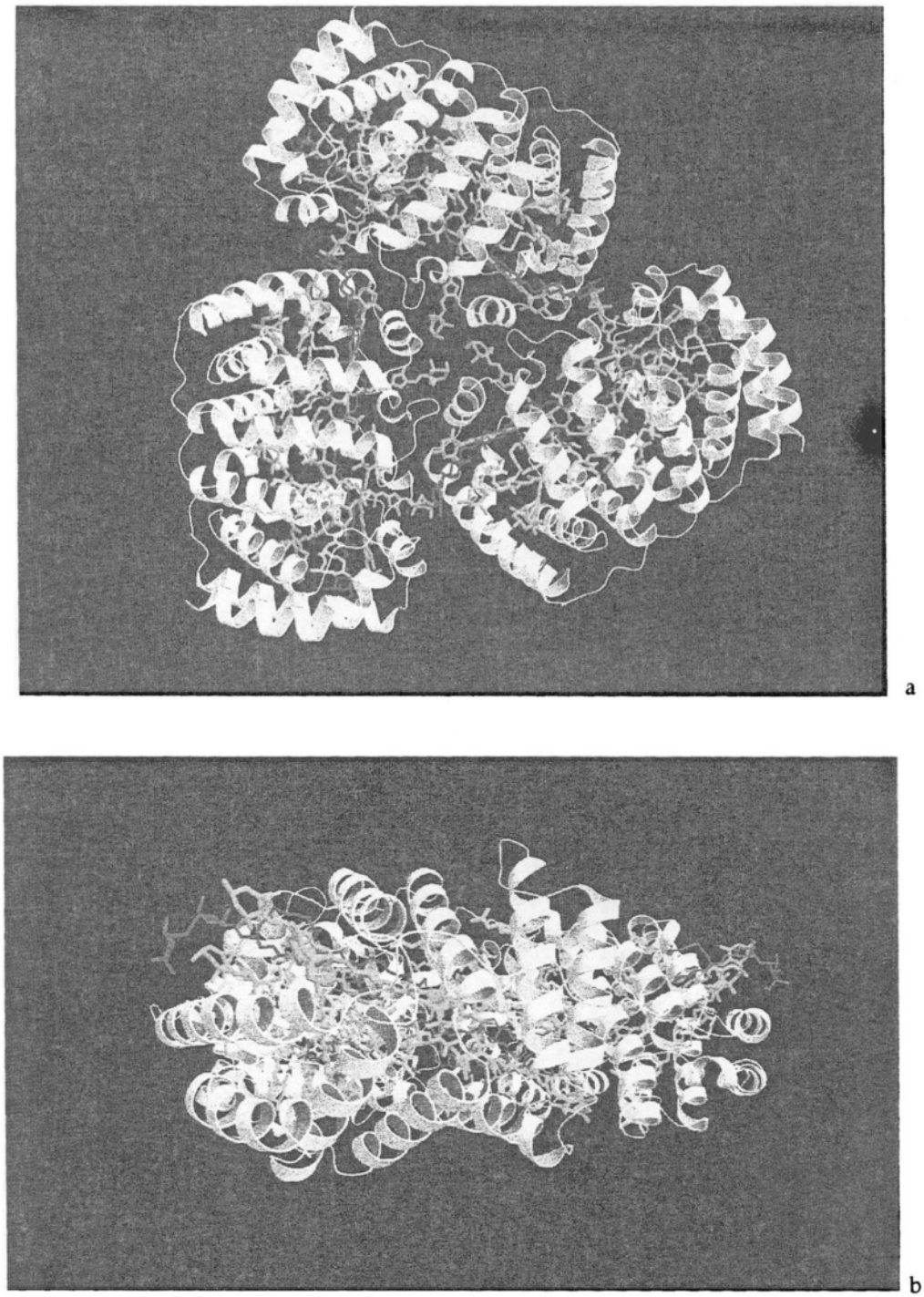

Fig. 4. a) Top and b) side views of trimeric PCP. (See also Color Plate 6)

4. Minor forms of sPCP

During purification of large amounts of MFPCP from *Amphidinium* for crystallization experiments, a minor component (2%) eluted from the cation exchange column at higher salt concentrations (hence HSPCP). This had an apoprotein of 34 kDa vs. the 32kDa of MFPCPs and N-terminal protein sequenc-

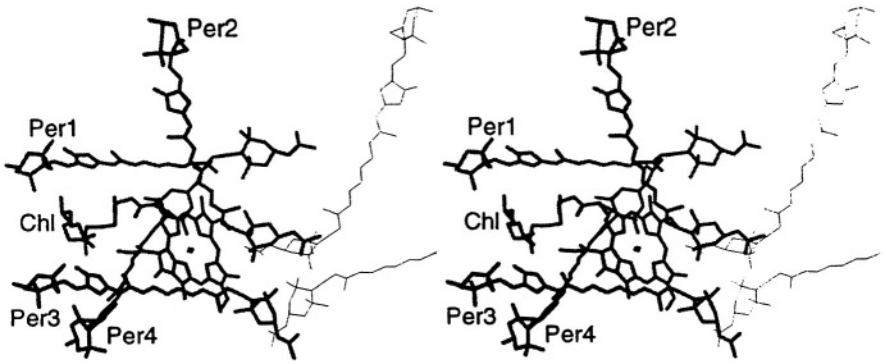

Fig. 5. Stereo view of the four peridinins and one Chl *a* in a pigment cluster in sPCP. The thin lines show a peridinin pair from the adjacent cluster within the monomer (Hoffman et al., 1996).

ing indicated substantial differences compared to MFPCP which was confirmed by further protein and DNA sequencing (Sharples et al., 1996). The HSPCP and MFPCP sequences are only 31% identical/52% similar (c.f. the 80% identity of monomeric MFPCP forms between species) but the two domain structure is preserved with a single histidine residue in each (Sharples et al., 1996). Pigment analysis showed that HSPCP has only 6 peridinins:2 Chl *a* with the reduced peridinin content being accompanied by a marked change in CD. The positive CD component in the 440 nm region is much reduced (Fig. 2) and the zero crossing point is at 490nm rather than 477nm of MFPCP. HSPCP shows efficient energy transfer from peridinin to Chl *a* with the fluorescence emission maximum moving to ~5nm longer wavelengths. It has been hypothesized that it may play a linker role between MFPCPs and other light-harvesting components of the photosystems (Sharples et al., 1996).

III. Intrinsic Thylakoid Proteins

A. The Intrinsic Light-Harvesting Harvesting Complex (iPCP) of Dinoflagellates

Much of the early work on dinoflagellate LHCs was based on non-denaturing gels in the presence of varying amounts of SDS (Boczar et al., 1980; Boczar and Prezelin,1986; Knoetzel and Rensing, 1990) These techniques resulted in a seemingly large number of complexes with poor energy transfer from carotenoids to Chl *a* and containing multiple subunits including that of apoPCP. With the application of digitonin or mild glycosidic detergents to thylakoid solubilization, most of the membrane-bound peridinin could be recovered on sucrose gradients as a single band containing only one or two polypeptides of ~19 kDa (Hiller et al., 1993; Iglesias-Prieto et al., 1993; Jovine et al., 1995). These preparations showed excellent energy transfer from peridinin to Chl *a* which was readily disrupted with mild heating or SDS treatment. Some spectroscopic properties of these complexes are illustrated in Fig. 6. The absorbance spectrum shows clearly the presence of peridinin and two forms of Chl *c* absorbing at 633 nm and 646 nm. The normalization of absorbance and the fluorescence excitation spectrum indicated that some carotenoid was ineffective in energy transfer (Iglesias-Prieto et al., 1993). It was suggested this might indicate a photoprotective role but may also indicate partial denaturation during isolation. There is strong excitonic interaction between carotenoid molecules as shown by the CD spectrum between 380 nm and 560 nm but the interpretation is difficult due to spectral overlap with the Soret bands of Chl *a* and *c*. There is some similarity with the CD spectrum of HSPCP, but less with MFPCP, nevertheless it may be suggested that the paired arrangement of peridinins seen in the PCP crystal structure also operates in the LHCs. There is an intriguing contrast between the dinoflagellate CD spectrum and that of the FCPs (compare Fig. 6b and 10b). In the former the long wavelength shoulder of the peridinin is associated with strong negative dichroism whereas in the latter no dichroism is associated with the shoulder at ~530nm but there is a strong positive CD at shorter wavelengths, so it is possible that the dimeric association of the carotenoids is a special characteristic of peridinin in LHCs.

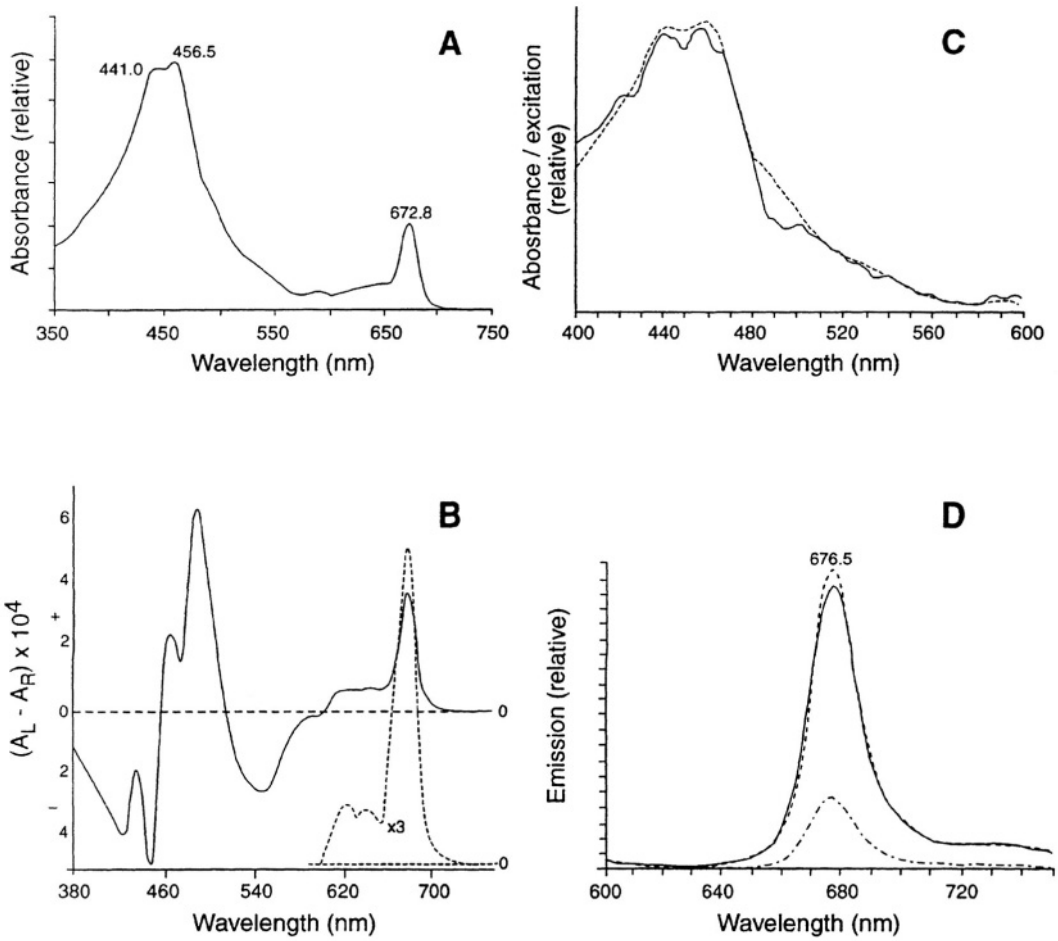

Fig. 6. Spectroscopic characteristics of iPCP from Dinoflagellates. a) absorbance spectrum, b) circular dichroism spectrum, c) fluorescence excitation spectra monitored at 676 nm, d) fluorescence emission spectra. In c the solid line is the fluorescence spectrum and the dashed line the normalized absorbance spectrum. (Hiller et al., 1993, Iglesias-Prieto et al., 1993)

1. Amino Acid Sequences of iPCPs

Sequences of the intrinsic LHC are available only for those of *Amphidinium,* six are shown in Fig. 7 but it is not known how many genes are represented by them as the iPCP gene(s) encodes a polyprotein (Hiller et al., 1995). However, as three of the above sequences were obtained by RT-PCR, and two by genomic DNA sequencing and a fourth is a consensus of direct protein sequencing, there is little doubt that a number of different types of 19 kDa apoprotein occur in the LHC and there are probably a number of genes. Regions of sequence showing low variability are often in putative transmembrane regions (Fig. 8). Owing to the sequence variation shown in Fig. 8, only a summary of the relationships to LHCs of other algal groups and higher plants will be given (see also Table 1 and Fig. 9). The closest relationship is with LHCs containing fucoxanthin (FCPs), especially towards the N-terminus where the identity is ~50% (Fig. 9). With all other groups, including the Euglenoids, the relationship is much more distant, the degree of identity being of the order of 20–25% after the insertion of variable numbers of gaps. The highest degree of identity is with the first transmembrane helix and its adjacent N-terminal residues and transmembrane helix 3 but there is little or no identity with the poorly defined second helix. Despite these limitations conserved Chl *a* binding sites can be identified in Dinoflagellates just as they can be in the complexes containing fucoxanthin (Fig. 7). A major deficiency in modeling the dinoflagellate LHC on the Kühlbrandt higher plant structure is the lack of detail in the model for loops between the helices and the loss of carotenoids from the two dimensional crystals. Despite the similarities in sequence between

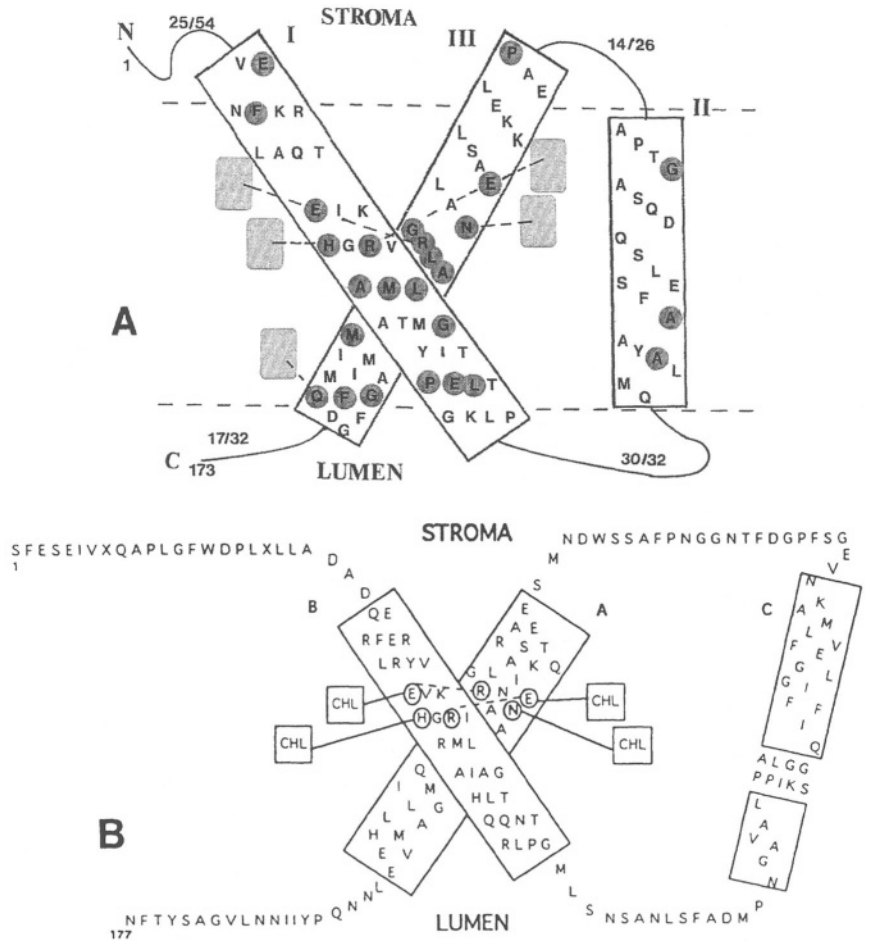

Fig. 7. Hypothetical structures of a) iPCP from *Amphidinium* (Hiller et al., 1995) and b) FCP from *Laminaria* (Caron et al., 1995) based on the three transmembrane model of higher plant LHCII (Kühlbrandt et al., 1994). Squares or dashed lines show the attachment points of conserved Chl *a* molecules and circles identical residues to those in LHCII.

dinoflagellate LHCs and those containing fucoxanthin there is a major difference in gene organization. In *Amphidinium* the sequences encoding the individual 19 kDa subunits are contiguous within the gene and are synthesized as a polyprotein. This polyprotein may contain up to ten subunits without any spacer polypeptides and is cleaved at a C-terminal arginine residue of the preceding 19 kDa subunit after transfer to the chloroplast (Hiller et al.,1995). A similar situation has been demonstrated in *Euglena* (Muchal and Scwartzbach, 1992) but is probably independently derived in view of the distantly related amino acid sequences and different polyprotein cleavage mechanism, which involves the excision of ten residue

Table 1. Comparison of various mature chromophyte light-harvesting protein sequences using the program Bestfit (Wisconsin Package, 1994). The sequences used are – *Macrocystis,* Apt et al., 1995; *Phaeodactylum*, Bhaya and Grossman 1993; *Giraudyopsis*, Passequet and Lichtlé, 1995; *Isochrysis* LaRoche et al., 1994; *Amphidinium,* Hiller et al., 1995. Figures are % identity/ % similarity.

	Phaeodactylum	*Giraudyopsis*	*Isochrysis*	*Amphidinium*
Macrocystis	62/79	72/83	22/47	39/63
Phaeodactylum		55/74	26/52	33/54
Giraudyopsis			28/49	43/63
Isochrysis				33/54

```
  1                                                  50
a XFENERGVQD PVGFFDPLGF TADGSVENFK RLAQTEIKHG RVAMLATMGY
b a**s*l***a *t*******l ss****d*** *rras***** **********
c a****l**aa *t**w****l ak***mka** *rras***** *i********
d              ****** *ke*n*d*** *rra****** *I********
e a********* ********** ********** *rr******* **********
f a**s*****p ********** *k**n****t *rra****** *I********

  51                                                 I00
a ITPEITGKLP GYLSPSTGVK YDDIPNGLGA ISKVPAAGWG QMIAYAAFSE
b m*****a*f* ****y*qss* fa*v****a* m****vl**a *va**g*vcd
c ****l***f* ******m*l* *e******** *******v*a *il***fyc*
d ****l#frfd ****r*a*** *a******a* f****fv**v **v**cllv-
e ********** ****r***** ********** ********* ********c*
f ****l#frfd ****r*a*** *v******** f****fv**v **v**cllv*

  101                                                150
a LSQDQSAGTP AAEGDFGFKV LTSSDPAELE KKLSAELANG RLAMMAIIGM
b v********* g*a******* I**e*eet*k r**ns***** *********l
c q*****e*sa gea******* ***k*eeg** r**ns*I*** **********
d I*****q*a* *q#******* ********k* ***r****** **********
e ********** ********** ********** ******s*** **********
f I*****q*a* sq#******* ****n***k* ***r****** **********

  151                  170
a FFQDGLTGSA WGDWASYTAS PL
b ********g* y****n**d* **r
c ********** y****nf*** **r
d ********** *****n**e* **r
e ********** ********** **r
f ********** *****n**d* **r
```

Fig. 8. Amino acid sequences of mature dinoflagellate iPCP proteins. Sequence a is a consensus sequence obtained by direct protein sequencing, b,c and d by RT-PCR and e and f from genomic sequencing (Hiller et al.,1995 and R. G.Hiller and P.M. Wrench, unpublished). # a space; * identity.

polypeptide from between each subunit.

2. Effect of Light Intensity and Quality on the Peridinin-Containing Light-Harvesting Proteins

In common with most photosynthetic systems, a low light environment results in a diversion of resources towards the production of the light-harvesting proteins with their associated pigments. The PCPs are no exception and it has been reported that in low light conditions up to 90% of the soluble protein may be associated with sPCP (Prézelin, 1987) although the peridinin content of the LHC may have been under estimated. From studies of in vitro protein synthesis, Roman et al., (1988) concluded that sPCP levels in *Heterocapsa* correlated with mRNA abundance. Growth in different wavelengths of light also affects the light-harvesting proteins with sPCP forms of low pI predominating under blue light, however no corresponding mRNA s have been identified (Jovine et al., 1992). These observations were extended by ten Lohuis and Miller (1998) who estimated that sPCP mRNA increased about 80 times when *Amphidinium* was transferred from growth at 100 μmol $m^{-2}s^{-1}$ PAR to 2 μmol m^{-2} s^{-1}. The LHC mRNAs also increased significantly, especially on the transfer to intermediate (20μmol m^{-2} s^{-1}) light intensities. An especially intriguing observation was that besides the quantitative change in the LHC mRNA, the predominant mRNA species were 6 kb and 3 kb at low and intermediate light regimes, but only 3 kb at high light. It was suggested that the large gene (or genes) which encodes the polyprotein can be processed at the 3´end so that LHC forms appropriate to the conditions can be preferentially expressed. This hypothesis is supported by the conserved intron positions within individual coding units of the LHC gene. (R. G. Hiller and P. M. Wrench, unpublished).

B. Light-Harvesting Complexes Containing Fucoxanthin (FCPs) of Diatoms, Brown Algae and Prymnesiophytes

Although these complexes are distributed over a wide range of taxonomically distinct algae, all the available evidence suggests they are quite closely related (with the possible exception of *Isochrysis*) in structure and amino acid sequence. Typical

```
          1                                                  50
girau     AFEDAEGAQA PLGFFDPLGL LNDADQERFD RLRYVEVKHG RISMLAIAGH
macpy     S**NEI**** ****W***** *A****DG*E ********** **A*******
phatr     ***NEI***Q ****W***** VA*GN**K*D ********** **C***V**Y
acart     ***NER*VQ* *VG******F TA*GSV*N*K **AQT*I*** *VA***TM*Y

          51                                                 100
girau     LVQQ.NVRLP GYLSISENIK FTDVPNGLAA FSKIPAAGIA QLVAFIGFLE
macpy     ****.*A*** *M**N*A*LS *A*M***V** L****P**L* *IF*******
phatr     *T*EAGI*** *DIDY*GT.S *ESI***F** L*AV*G**** *II*****F*
acart     ITPEITGK** ****PSTGV* YD*I****G* I*******WG *MI*YAAFS*

          101                                                150
girau     LAVMQQVEGS .TPGDMNRFG ENSTWASWD. ..EETQSRKA SIELNNGR.A
macpy     ****KNVEGS .F***FT.L* G*PFGAS**A MS****AS*R A*******A*
phatr     ****KDIT*G EFV**...*R N*YLDFG**T FS*DKKLQ*R A****Q**A*
acart     *SQD*SAGTP AAE**F.... GFKVLTSS*P AEL*K...*L *A**A***L*

          151                                181
girau     QMGILALMVH EQLNGRPYII NDILGQAYTW N
macpy     ********** *E**NK**V* **LVGA***F *
phatr     ********** ***GVSILP. .. .. .. . .
acart     M*A*IGMFFQ DGLTGSAWGD WASYTASPL. .
```

Fig. 9. Alignment of four chromophyte intrinsic light-harvesting proteins using the programme Pileup. girau *Giraudyopsis* (Passequet and Lichtlé, 1995); mapyr *Macrocystis* (Apt et al., 1995); phatr *Phaeodactylum* (Bhaya and Grossman, 1993); acart *Amphidinium* (Hiller et al., 1995). The approximate position of putative transmembrane helices are underlined. * = identity with top sequence; . a space.

absorbance spectra of FCPs are shown in Figs. 10a and c. The absorbance spectrum of native *Dictyota* FCP illustrates (Fig. 10a) the typical long wavelength shoulder of fucoxanthin absorbance at ~535nm which is lost when then the protein is exposed to heat or excess detergent. This spectral change is associated with loss of energy transfer, as well as CD and LD features. Most studies report on the pigment content as ratios with respect to Chl *a,* and typically indicate equal amounts of Chl a and fucoxanthin together with smaller amounts of violaxanthin. The last may participate in the protective xanthophyll cycle (Table 2). Unfortunately many of the recent excellent molecular studies have not included basic information on pigment/protein ratios so the data above may be rather unrepresentative. Data are especially needed on *Isochrysis* (Chrysophyta) and *Pavlova* (Prymesiophyta) (Fawley et al., 1987; Hiller et al., 1988) as there is some doubt as to whether the predominant carotenoid is universally fucoxanthin or 19´-hexanoyloxyfucoxanthin in the Prymnesiophytes (Larrido and Zapata, 1998). Although there is little doubt the proteins of these complexes are encoded by a family of genes (*Isochrysis* is an exception), no gene product has been associated with a spectroscopically specific form of LHC. Caron et al. (1996) separated several different FCP forms by ion exchange or isoelectric focusing chromatography following the initial separation by sucrose gradient centrifugation. One form, which was made by both

Table 2. The pigment composition of LHCs containing fucoxanthin. Figures are relative to 100 Chl *a* together with estimates of the (number) of molecules per subunit.

Organism	Chl *a*	Fucoxanthin	Chl *c*	Other carotenoids	Reference
Phaeodactylum	100 (5)*	102 (5)	48 (2.5)		Fawley et al., 1987
Phaeodactylum	100 (2)*	250 (5)	33 (1)		Friedman and Alberte, 1984
Dictyota	100 (5)* ◇	77 (3)	23 (1)	4 violax	Katoh et al., 1989
Giraudyopsis	100 (5)#	84 (4)	25 (1)	4 violax	Lichtlé, et al., 1995
Laminaria	100 (4)# □	96 (4)	26 (1)	9 violax	Caron et al., 1995

* based on protein estimation. # based on sequence conservation compared to LHCII, ◇ based on an assumed apoprotein of 20kDa instead of 54 kDa in the original paper; □ A subsequent paper (Caron et al., 1996) found seven conserved putative Chl-binding sites: violax., violaxanthin.

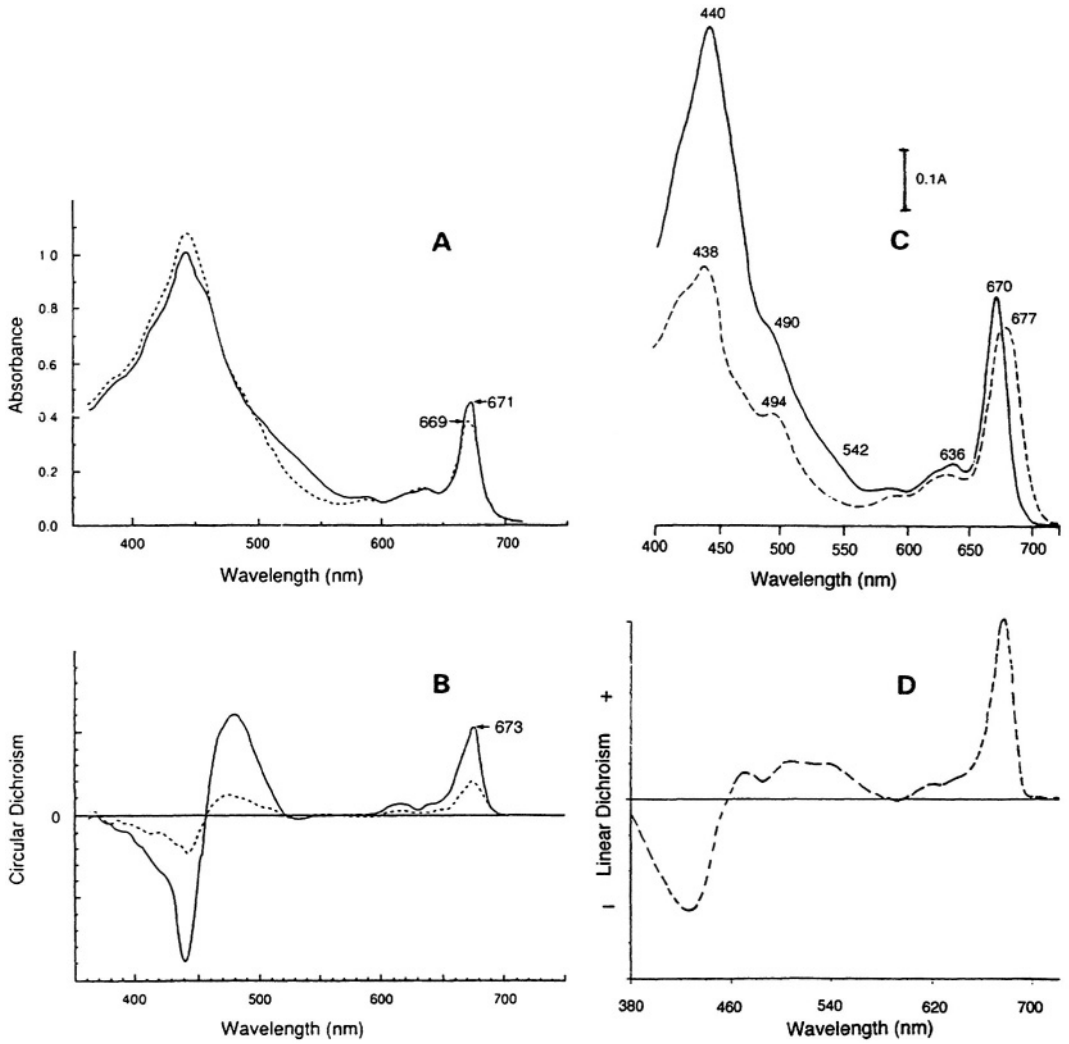

Fig. 10. Spectroscopic properties of FCPs from *Dictyota dichotoma* (a and b, Mimuro et al., 1990a) and *Pavlova lutherii* (c and d, Hiller et al., 1988 and Hiller and Breton, 1992) a) absorbance spectrum b) CD spectrum. (In both a and b the broken line is the dissociated form of the complex) c, absorbance spectrum of FCP (solid line) and PS I (broken line) d, LD spectrum of FCP in the thylakoids.

methods, lacked violaxanthin but was otherwise similar in pigment composition to the native LHC used as starting material. These authors also found an LHC form enriched in violaxanthin and lacking Chl *c,* but the status of this is uncertain as energy transfer from fucoxanthin to Chl *a* had been destroyed.

1. Amino Acid Sequences and Gene Organization

In *Phaeodactylum,* FCPs are encoded by at least two gene families whose members are closely aligned without introns (Bhaya and Grossman, 1993) and a similar arrangement is found in *Macrocystis.* Apt et al. (1995), investigated the level of several FCP mRNAs from *Macrocystis* under different light regimes. Although a particular FCP protein was not associated with the most divergent FCP gene, northern blots showed that this gene was preferentially transcribed under low blue light conditions, opening the way to elucidate the function of specific LHC forms. All FCPs, as well as PCPs are nuclear encoded, synthesized on cytosolic ribosomes and transported to the chloroplast. During transport a leader sequence is proteolytically removed. This leader sequence invariably has a hydrophobic N-terminal region of 15–30 residues with characteristics of a signal sequence. It is believed that this directs the preprotein

initially into the endoplasmic reticulum with subsequent import into the chloroplast stroma. Support for this is the demonstration that *Phaeodactylum* preFCP can be imported into canine microsomes (Bhaya and Grossman, 1991). Unfortunately nothing is known about either the assembly of these proteins, or the precise pathway of carotenoid biosynthesis and the location of its enzymes.

2. Structure

Information on structure is available only indirectly. Amino-acid sequences suggest that the three *trans* membrane helix structure of higher plant LHC can be applied to all the FCPs (e.g. Fig. 8) but the sequences are invariably shorter being 165–210 residues in length compared with ~250 residues in the Cab proteins. Since the helices are conserved, the differences are in the loops, especially that of the N-terminal domain and that between helices 2 and 3 which is much shorter. An unexplained feature is that although four or five conserved Chl binding sites can be identified (Fig. 8), the overall chlorophyll/protein ratio of FCPs (~5–6 per subunit) is much lower than that of Pea LHCII (14 per subunit, all helix-associated). Perhaps fucoxanthin displaces some of the Chl. In contrast to the FCPs, the *Amphidinium* iPCP has been reported (Hiller et al., 1993) to contain eleven Chl and ten carotenoids per subunit. This difference is surprising in view of the degree of sequence similarity between the iPCPs and FCPs, especially in the transmembrane helices. No part of the sequences has, however, been associated with carotenoids but based on the sPCP structure it may be expected that hydrophobic R-groups from several loops/helices will contribute to binding of carotenoids, that the acetylated cyclohexane ring (Fig. 1) will be buried and that the epoxy cyclohexane ring will be towards the outside of the membrane. Our only insights into the pigment organization come from a few polarized spectroscopy studies. CD can provide information on pigments in close proximity, i.e. in van der Waals contact and in appropriate orientation, whereas LD provides information on the direction of pigment dipoles with respect to the plane of the membrane or direction of the applied force in aligned isolated proteins. In FCP of *Dictyota* the CD spectrum (Fig. 9b) shows a positive band due to Chl *a* peaking at 673 nm and a stronger split band with a positive peak at 440 nm, negative peak at 480 nm and crossing at 455 nm much of which may be attributed to fucoxanthin. Interpretation is, however, difficult because of contributions from the Soret bands of Chl *a* and Chl *c*. This result is typical, as FCPs from *Phaeodactylum* and *Pavlova* are very similar (R. G. Hiller, and E. Nabedryk, unpublished). In both FCPs and iPCPs there are only weak interactions between Chl *c* molecules whereas there are strong CD signals from Chl *b* in higher plants and green algae. In contrast to the CD data, LD spectroscopy, especially the data for LD of thylakoid preparations (Fig. 9d) suggest that the 540 nm component of fucoxanthin is strongly oriented and this transition lies in the membrane plane (Hiller and Breton, 1992). Isolated FCP complexes often show a complete reversal of the LD signals with respect to the membrane plane or direction of applied force (Hsu and Lee, 1987; Mimuro et al., 1990) but this may be an artifact of the sample preparation (Hiller and Breton, 1992).

3. Time-Resolved Energy Transfer Studies

In vitro fluorescence from three of the carotenoids, peridinin, fucoxanthin and siphonaxanthin, whose structures are shown in Fig. 1, is from the optically forbidden S_1 state (Mimuro et al., 1992) but with a very low yield (efficiency $1–5 \times 10^{-5}$). It is generally accepted that this S_1 state emission which overlaps the Chl *a* Qy absorbance band is the species active in energy transfer in the LHCs containing peridinin or fucoxanthin. The decay of the S_2 state to the S_1 state has a time constant of less than 200 fs whereas the energy is not transferred to Chl a until ~2 ps (Akimoto et al., 1996). The S_1 life time of excited fucoxanthin and peridinin in organic solvents is 40 ps (Katoh et al., 1991; Shreve et al., 1991) and 15 ps (J. A. Bautista, R. G. Hiller, F. P. Sharples, D. Gosztola, M. Wasielewski and H. A. Frank, unpublished) respectively, although longer values for the latter have been reported (Akimoto et al., 1996). Akimoto et al. (1996) were not able to measure the S_1 lifetime of peridinin in PCP but noted that the rise of the Chl *a* fluorescence was less than 3 ps as expected given the energy transfer efficiency from carotenoid to Chl *a* of 85%—almost 100%.

The transfer time from carotenoids to Chl *a* in *Phaeodactylum* thylakoids has been measured as 0.9 ps for a one channel model and 0.5 ps and 2.0 ps for a two channel model (Trautman et al., 1989, 1990) consistent with the known high efficiency of energy transfer, whereas the S_2 to S_1 transition is less than 100 fs. (In the Eustigmatophyte *Nannochloropsis,* the transfer to Chl *a* was best described a

single exponential with a time constant of 0.24 ps.) Curiously the calculated efficiencies in *Phaeodactylum* were wavelength dependent, being considerably reduced with excitation at 490 nm compared to 540 nm. Mimuro et al., (1990b) investigated energy transfer in whole cells of the dinoflagellate *Protogonyaulax* by following the fluorescence emission kinetics at 77 K at several different wavelengths from 649 nm to 698 nm; energy was transferred initially from peridinin to Chl *a* 670 nm. They concluded that there was no evidence for Chl *c* as an intermediate between peridinin and Chl *a* and estimated the transfer time to be less than 18 ps at low temperature but considerably shorter at room temperature. These experiments are difficult to interpret as the time resolution was only 6 ps and by using whole cells, peridinin associated with both sPCP and iPCP would have been excited.

C. The Intrinsic Light-Harvesting Complex of Pleurochloris

This Xanthophycean alga has the carotenoids heteroxanthin, diadinoxanthin and vaucheraxanthin ester as components of its LHC (Wilhelm et al., 1988) and make up a combined carotenoid: Chl *a* ratio of 1:2. From fluorescence studies it is apparent that the carotenoids extend the range of light-harvesting beyond that of the Soret band of Chl *c* with a strong absorbance peak at 490nm. An interesting observation is that with time in vitro, the isolated complex changes and excitation at 490 nm excites Chl *c*. This has been interpreted as energy transfer from the carotenoids. If this is correct it implies that carotenoids and Chl *c* are in close proximity and that the energy transfer pathway is unusual in this organism. Subsequent studies have suggested that the LHC associated with PS I is different from the main LHC associated with PS II. The CD of the main LHC complex (Buchel and Garab, 1997) showed only weak signals in the region of 480–520 nm suggesting the organization of the light-harvesting xanthophylls is different from that of either fucoxanthin or peridinin in their respective complexes as detailed above.

D. The Intrinsic Light-Harvesting Complex of Mantoniella squamata

This alga is remarkable for containing a Chl *c*-like pigment, as well as Chl *b* (Wilhelm and Lenartz-Weiler, 1987). Its thylakoid organization is similar to that of chromophyte algae with the thylakoids paired or in threes and stacking, as in higher plants, is absent. The LHC has been sequenced from cDNA clones (Rhiel and Morschel, 1993; Jiao and Fawley, 1994) as well as directly (Schmitt et al., 1994) and is clearly more closely related to the green algal type than it is to FCPs or iPcps. Following a more elaborate purification protocol than that usually employed, crystals have been obtained (Welte et al., 1995) but no structural details are available. The carotenoids contained in the LHC are neoxanthin, violaxanthin, and prasinoxanthin. In spectra of the intact algae there is clear indication of a red shifted carotenoid component at 500–540 nm but this is missing from the LHC which was isolated on polyacrylamide gels using LIDS to solubilize the thylakoids. (Fawley et al., 1986) Recently, a detailed analysis of the pigment composition of the LHC has been reported (Wilhelm et al., 1997); the stoichiometry being six Chl *a,* six Chl *b,* two Chl *c*-like and two prasinoxanthin per polypeptide. Seven other carotenoids were found but none in stoichiometric amounts and the authors suggest that this results from the formation of trimers made up of heterogeneous polypeptides containing different carotenoids. This is particularly intriguing as so far, fewer genes coding for the LHC have been found in *Mantoniella* than in any other Chl *b*-containing alga. The possibility that the minor carotenoids of iPCPs and FCPs could also be incorporated as components of mixed trimers or other oligomers has not been seriously considered, although a hint of its possibility comes from the work of Caron et al., (1996) cited above. This is partly because the green (perhaps it should be brown!) gel technique is not effective in separating LHCs, so trimers are either not present (Durnford and Green, 1994) or are very unstable. The multiplicity of iPCP and FCP sequences may be associated with binding the minor carotenoids as well as peridinin and fucoxanthin. Although the minor carotenoids and their role in LHCs has been largely ignored, it is worth noting that they may comprise 25% of the total carotenoids and exceed Chl *c* on a mol to mol basis!

E. The Intrinsic LHCs of the Siphonous Green Algae, Bryopsis *and* Codium

These sub-littoral algae exist in an environment where harvesting of light in the green region of the spectrum is an advantage. Both species have an unusual LHC

in which a very low Chl *a*/Chl *b* ratio is accompanied by the replacement of lutein with siphonaxanthin and siphonein. Interaction of siphonaxanthin with protein extends the effective absorbing wavelength range well into the green region of the spectrum in a similar manner to fucoxanthin in the FCPs (Chu and Anderson, 1985; Nakayama et al., 1987). The pigment ratios in the LHC are 6 Chl *a*:8 Chl *b:3* siphonaxanthin:l siphonein: 1neoxanthin per polypeptide. Nakayama and Mimuro (1994) showed that excitated siphonaxanthin could transfer energy primarily to Chl *a* forms absorbing at 672 nm and based on time resolved fluorescence emission propose that the pigment organization in *Bryopsis* is similar to that in spinach chloroplasts and LHCII. There was no evidence of any energy transfer from carotenoids to Chl *b* (Nakayama et al., 1994).

IV. Evolution

The evolutionary relationships between intrinsic light-harvesting proteins have been determined largely by analysis of their amino acid sequences. A current view is that precursors of intrinsic LHCs occur in the cyanobacteria in the form of HLIP proteins with two putative membrane-spanning helices. These in turn evolved at an early stage into a protein (CP 22 or PsbS) with four membrane spanning helices which in its turn was the ancestor of the present day LHCs (Green and Pichersky, 1994). In this scenario most of the major extant algal groups would have acquired the specific carotenoids independently as a compensation either for loss of phycobilins (e.g. in diatoms, brown algae and dinoflagellates) or as a specific means of extending existing carotenoid absorbance further into the green spectral regions (e.g. siphonous green algae). If this is correct we may expect to find that the carotenoid binding sites are not conserved and will only have in common the necessity of localizing the carotenoid within van der Waals contact of Chl *a*.

In dinoflagellates it might be hypothesized that iPCP was the original LHC as it contains introns and acquired peridinin, whereas sPCP, whose protein has no clear provenance but may have been acquired by lateral gene transfer, was able to utilize the pre-existing peridinin. In contrast to iPCP, neither of the distinct sPCP form genes contains introns. Caron et al. (1996) analyzed the relationships between all intrinsic LHC amino acid sequences from heterokont algae. They concluded that there was no evidence for distinct sequences associated with PS I or PS II as occurs in higher plants. An unrooted parsimony tree grouped all the diatom sequences on a separate branch from the brown algae and placed those of *Heterosigma* and *Isochrysis* close to the branch point of the chlorophyte and heterokont lines. A surprising result in view of the degree of identity with FCPs, was the placing of *Amphidinium* iPCP with no bias towards either of the above lines. At the base of such evolutionary trees, however, the confidence levels are not very great and the branch positions may be affected by the particular sequence selected from the multigene family for the comparison. A similar evolutionary analysis by Durnford and Green (1996) placed *Amphidinium* on the chromophyte line, although separate from the fucoxanthin-containing algae. Caron et al., (1996) also noted that in *Laminaria* there is an intron of ~900bp in the N-terminal leader sequence, which may have unusual exon/intron borders, but so few genomic LHC sequences are available the evolutionary implications remain to be determined.

V. Future Directions

With the exception of sPCP we have no detailed knowledge of the geometry of carotenoid/Chl interaction in algae, so a clear picture of an intrinsic LHC with fucoxanthin or peridinin would be a major advance but the crystallization of membrane proteins suitable for X-ray crystallography is still very difficult. Sub picosecond spectroscopy is now a reliable technique in several laboratories so the pathway of energy from carotenoid to specific spectroscopically distinct Chl *a* forms should be defined in all groups of algae as it has in higher plant LHCs. Transformation systems for diatoms (Apt et al., 1996) and dinoflagellates (ten Lohuis and Miller, 1998) are now available, so that light-harvesting systems can be manipulated to over express distinct gene products whose effects can be monitored spectroscopically in cells, thylakoids and purified LHCs. Heterologous protein expression combined with in vitro pigment reconstitution is likely to be applied in several laboratories and in combination with site directed mutagenesis will greatly enhance our knowledge of specific pigment/amino acid interactions. This is especially the case for sPCP whose heterologously expressed N-terminal domain spontaneously refolds

around purified pigments to give a product indistinguishable from native PCP (F. P. Sharples, R. G. Hiller, J. Catmull and D. J. Miller, unpublished). Molecular probes for all the cDNAs of these proteins will be available and can be used to monitor environmentally altered light-harvesting strategies.

Acknowledgements

I am grateful to Dr D. J. Miller for providing preprints of papers, to the Australian Research Council for support of my research on dinoflagellate light-harvesting proteins, to Eckhard Hofmann for Fig. 4 and to Pamela Wrench for her comments on the manuscript.

References

Akimoto S, Takaichi S, Ogata T, Nishinura Y, Yamazaki I and Mimuro M (1996) Excitation transfer in carotenoid-chlorophyll protein complexes probed by femtosecond fluorescence decays Chem Phys Lett 260: 147–152

Apt KE, Glendennen SK, Powers DA and Grossman AR (1995) The gene family encoding the fucoxanthin chlorophyll proteins from the brown alga *Macrocystis pyrifera.* Mol Gen Genet 246: 455–464

Apt KE, Kroth-Pancic PG and Grossman AR (1996) Stable transformation nuclear transformation of the diatom *Phaeodactylum tricornutum.* Mol Gen Genet 252: 572–579

Bhaya D and Grossman AR (1991) Targeting proteins to diatom plastids involves transport through an endoplasmic reticulum. Mol Gen Genet 229: 400–404

Bhaya D and Grossman AR (1993) Characterization of gene clusters encoding the chlorophyll proteins in the diatom *Phaeodactylum tricornutum.* Nucl Acids Res. 21: 4458–4466

Boczar BA and Prezelin BB (1986) Light and $MgCl_2$-dependendent characteristics of four chlorophyll-protein complexes isolated from the marine dinoflagellate, *Glenodinium sp.* Biochim Biophys Acta 850: 300–309

Boczar BA, Prezelin BB, Markwell J and Thornber JP (1980) A chlorophyll *c*-containing pigment-protein complex from the marine dinoflagellate, *Glenodinium sp.* FEBS Lett 120: 243–247

Büchel C and Garab G (1997) Organisation of the pigment molecules in the chlorophyll *a/c* light-harvesting complex of *Pleurochloris meirengis* (Xanthophyceae). Characterisation with circular dichroism and absorbance spectroscopy J Photochem, Photobiol B: Biology 37: 118–124

Büchel C and Wilhelm C (1993) Isolation and characterization of a Photosytem I-associated antenna (LHCI) and a Photosystem I-core complex from the chlorophyll *c*-containing alga *Pleurochloris meirengis.* J Photochem Photobiol 20: 87–93

Carbonera D, Giacometti G and Segre U (1996) Carotenoid interactions in peridinin chlorophyll *a* proteins from dinoflagellates. Evidence for optical excitons and triplet migration. J Chem Soc Faraday Trans 92: 989–993

Caron L, Douady D, Rousseau B, Quinet-Szely M and Berkaloff C (1995) Light-harvesting complexes from a brown alga. Biochemical and molecular study. In: Mathis P (ed) Photosynthesis: From Light to Biosphere, Vol I, pp 175–178, Kluwer Academic Publishers, Dordrecht

Caron L, Douady D, Quinet-Szely M, de Goer S and Berkaloff C (1996) Gene structure of a chlorophyll *a/c*-binding protein from a brown alga: Presence of an intron and phylogenetic implications. J Mol Evol 43: 270–280

Chu Z-X and Anderson JM (1985) Isolation and characterization of a siphonaxanthin-chlorophyll *a/b* complex from a *Codium* species (Siphonales). Biochim Biophys Acta 806: 154–160

Durnford DG and Green BR (1994) Characterisation of the light-harvesting proteins of the chromophyte alga, *Olisthodiscus luteus (Heterosigma carterae).* Biochim Biophys Acta 1184: 118–123

Fawley MW, Morton JS, Steward KD and Mattox KR (1987) Evidence for a common evolutionary origin of light-harvesting fucoxanthin chlorophyll *a/c* protein complexes of *Pavlova gyrans* (Prymnesiophyceae) and *Phaeodactylum tricornutum* (Bacillariophyceae). J Phycol 23: 377–381

Friedman AL and Alberte RS (1984) A diatom light-harvesting pigment protein complex: Purification and characterization. Plant Physiol 76: 483–489

Garrido JL and Zapata M (1998) Detection of new pigments from *Emiliana huxleyi* (Prymnesiophyceae) by high-performance liquid chromatography, liquid chromatography-mass spectrometry, visible spectroscopy and fast atom bombardment mass spectrometry. J Phycol 34: 70–78

Govind NS, Roman SJ, Iglesias-Prieto R, Trench RK, Triplett EL and Prézelin BB (1990) An analysis of the light-harvesting peridinin-chlorophyll *a*-binding protein from dinoflagellates by immunoblotting techniques. Proc Roy Soc Lond B 240: 187–195

Haxo FT, Kycia, JH, Somers GF, Bennet A and Siegelman HW (1976) Peridinin-chlorophyll *a*-binding protein of the dinoflagellate *Amphidinium carterae* (Plymouth 450). Plant Physiol 57: 297–303

Hiller RG and Breton J (1992) A linear dichroism study of photosynthetic pigment organisation in two fucoxanthin-containing algae. Biochim Biophys Acta 1102: 365–370

Hiller RG, Bardin AM and Nabedryk E (1987) The secondary structure content of pigment-protein complexes of two chromophyte algae. Biochim Biophys Acta 894: 365–369

Hiller RG, Larkum AWD and Wrench PM (1988) Chlorophyll-proteins of the prymnesiophyte *Pavlova lutherii* (Droop) comb. Nov.: Identification of the major light harvesting complex. Biochim Biophys Acta 932: 223–231

Hiller RG, Anderson JM and Larkum AWD (1991) The chlorophyll-protein complexes of algae. In: Scheer H (ed) The Chlorophylls, pp 529–547. CRC Publications, Boca Raton

Hiller RG, Wrench PM and Sharples FP (1995) The light-harvesting chlorophyll *a-c*-binding protein of Dinoflagellates: A putative polyprotein. FEBS Lett 363: 175–178

Hofmann E, Wrench PM, Sharples FP, Hiller RG, Welte W and Diedereichs K (1996) Structural basis of light harvesting by carotenoids: Peridinin chlorophyll-*a*-protein from *Amphidinium carterae.* Science 272: 1788–1791

Hsu BD and Lee JY (1987) Orientation of pigments and pigment-protein complexes in the diatom *Cylindrotheca fusiformis.* A

linear dichroism study. Biochim. Biophys. Acta. 893, 572–577

Iglesias-Prieto R, Govind NS and Trench RK, (1991) Apoprotein composition and spectroscopic characterisation of the water-soluble peridinin-chlorophyll *a*-proteins from three symbiotic dinoflagellates. Proc Roy Soc Lond B 246: 275–283

Iglesias-Prieto R, Govind NS and Trench RK, (1993) Isolation of 3 membrane-bound chlorophyll-protein complexes from 4 dinoflagellate species. Philos Trans Roy Soc Lond Ser B 340: 381–392

Jiao S and Fawley MW (1994) A cDNA clone encoding a light-harvesting protein from *Mantoniella squamata.* Plant Physiol. 104: 797–798

Jovine RVM, Triplett EL Nelson NB and Prezelin BB (1992) Quantification of chromophore pigments, apoprotein abundance and isoelectric variants of peridinin-chlorophyll *a*-protein complexes (PCPs) in the dinoflagellate *Heterocapsa pygmaea* grown under variable light conditions Plant Cell Physiol 33: 733–741

Jovine RVM, Johnsen G and Prezelin BB (1995) Isolation of a membrane bound light-harvesting complexes from the dinoflagellates *Heterocapsa pygmaea and Prorocentrum minimum.* Photosynth Res 44: 127–138

Katoh T, Mimuro M and Takaichi S (1989) Light-harvesting particles isolated from a brown alga *Dictyota dichotoma.* A supramolecular assembly of fucoxanthin-chlorophyll-protein complexes. Biochim Biophys Acta 976: 233–240

Katoh T, Nagashima U and Mimuro M (1991) Fluorescence properties of the allenic carotenoid fucoxanthin: Implications for energy transfer in photosynthetic systems. Photosynth Res 27: 221–226

Knoetzel J and Rensing L (1990) Characterisation of the photosynthetic apparatus from the marine dinoflagellate *Gonyaulax polyedra* I. Pigment and polypeptide composition of the pigment-protein complexes. J Plant Physiol 136: 271–279

Kühlbrandt W, Wang DN and Fujiyoshi Y (1994) Atomic model of plant light-harvesting complex by electron crystallography. Nature 367: 614–621

Larkum T and Howe CJ (1997) Molecular aspects of light-harvesting processes in algae. In: Callow J.A. (ed) Adv Bot Res, Vol 27, pp 257–330. Academic Press, New York

La Roche J, Henery D, Wyman K, Sukenic A and Falkowski P (1994) Cloning and nucleotide sequence of a cDNA encoding a major fucoxanthin chlorophyll *a/c*- containing protein from the chrysophyte *Isochrysis galbana*: implications for evolution of the cab gene family. Plant Mol Biol 25: 355–368

Le QH, Markovic P, Hastings JW, Jovine RV and Morse D. (1997) Structure and organization of the peridinin-chlorophyll *a*-binding protein from the dinoflagellate *Gonyaulax polyedra.* Mol Gen Genet 255: 595–604

Lichtle C, Arsalane W, Duval JC and Passequet C (1995) Characterization of the light-harvesting complex of *Giraudyopsis stelliferer* Dageard (Chrysophyceae) and effects of light stress. J Phycol 31: 380–387

Mimuro M, Katoh T and Kawai H (1990a) Spatial arrangements of pigments and their interaction in the fucoxanthin-chlorophyll *a/c* protein assembly (FCPA) isolated from the brown alga *Dictyota dichotoma.* Analysis by means of polarised spectroscopy. Biochim Biophys Acta 1015: 450–456

Mimuro M, Tamai N, Ishimara T and Yamazaki I (1990b) Characteristic fluorescence components of photosynthetic pigment system of a marine dinoflagellate, *Protogonyaulax tamarensis,* and energy flow among them. Studies by means of steady state and time-resolved fluorescence spectroscopy Biochim Biophys Acta 1016: 280–287

Mimuro M, Nagashima U, Takaichi S, Nishimura Y, Yamazaki I and Katoh T (1992) Molecular structure and optical properties of carotenoids for the in vivo transfer function of the algal photosynthetic pigment system. Biochim Biophys Acta 1098: 271–274

Muchal US and Schwartzbach SD (1992) Characterization of a *Euglena* gene encoding a polyprotein precursor to the light-harvesting chlorophyll *a/b* protein of Photosytem II. Plant Mol Biol 18: 287–299

Nakayama K and Mimuro M (1994) Chlorophyll forms and excitation energy transfer pathways in light-harvesting chlorophyll *a/b* protein complexes isolated from the siphonous green alga, *Bryopsis maxima.* Biochim Biophys Acta 1184: 103–110

Nakayama K, Itagaki T and Okada M (1986) Pigment composition of chlorophyll-protein complexes from the green alga, *Bryopsis maxima.* Plant Cell Physiol 27: 311–317

Nakayama K, Mimuro M, Nishimura Y, Yamazaki I and Okada M (1994) Kinetic analysis of energy transfer in LHCII isolated from the siphonous green alga, *Bryopsis maxima* with the use of picosecond fluorescence spectroscopy. Biochim Biophys Acta 1188: 117–124

Norris BJ and Miller DJ (1994) Nucleotide sequence of a cDNA clone encoding the precursor of the peridinm-chlorophyll *a*-binding protein from the dinoflagellate *Symbiodinium* sp. Plant Mol Biol 24: 673–677

Ogata T and Kodama M (1993) Peridinin chlorophyll *a*-protein of toxic dinoflagellates. In: Smayda T and Shimizu Y (eds.) Toxic Phytoplankton Blooms in the Sea, pp 901–905. Elsevier New York

Ogata T, Kodama M, Nomura S, Kobayashi M, Nozawa T, Katoh T and Mimuro M (1994) A novel peridinin-chlorophyll *a*-binding protein from the marine dinoflagellate *Alexandrium cohorticula:* A high pigment content and spectral forms of peridinin and chlorophyll *a.* FEBS Lett 356: 367–371

Owens TG and Wold ER (1986) Light-harvesting function in the diatom *Phaeodactylum tricornutum.* Plant Physiol 80: 732–738

Passequet C and Lichtlé C (1995) Molecular study of a light-harvesting apoprotein of *Giraudyopsis stelliferer* (Chrysophyceae). Plant Mol Biol 29–135–148

Prézelin BB (1987) Photosynthetic physiology of dinoflagellates. In: Taylor FJR (ed) The Biology of Dinoflagellates, pp 174–223. Blackwell, Oxford

Prézelin BB and Haxo FT (1976) Purification and characterization of peridinin-chlorophyll *a*-proteins of *Glenodinium sp* and *Gonyaulax polyedra.* Planta 130: 251–256

Rhiel E and Mörschel E (1993) The atypical chlorophyll *a/b/c* light-harvesting complex of *Mantoniella squamata*: molecular cloning and sequence analysis. Mol Gen Genet 240: 403–413

Rhiel E, Lage W and Morschel E (1993) The unusual the light-harvesting complex of *Mantoniella squamata:* supramolecular composition and assembly. Biochim Biophys Acta 1143: 163–172

Rowan R, Whitney SM, Fowler A and Yellowlees D (1996) Rubisco in marine symbiotic dinoflagellates: Form II enzymes in eukaryotic oxygenic phototrophs encoded by a nuclear gene

family. Plant Cell 8: 539–553

Sharples FP, Wrench PM and Hiller RG (1996) Two distinct forms of the peridinin-chlorophyll *a*-protein (PCP) from *Amphidinium carterae.* Biochim Biophys Acta 1276: 117–123.

Shreve AP, Trautmann TG, Owens TG and Albrecht AC (1991) A femtosecond study of electronic state dynamics of fucoxanthin and implications for photosynthetic carotenoid to chlorophyll energy transfer mechanisms. Chem Phys 154: 171–178

Song PS, Koka P, Prézelin BB and Haxo FT (1976) Molecular topology of the photosynthetic light-harvesting pigment complex, peridinin-chlorophyll *a*-binding protein from marine dinoflagellates. Biochemistry 15: 4422–4427

Steck K, Wacker T, Welte W, Sharples FP and Hiller RG (1990) Crystallization and preliminary X-ray analysis of a peridinin-chlorophyll a protein from *Amphidinium carterae.* FEBS Lett 268: 48–50

ten Lohuis MR and Miller DJ (1998a) Light-regulated transcription of genes encoding peridinin chlorophyll *a*-proteins and the major intrinsic light-harvesting complex proteins in the dinoflagellate *Amphidinium carterae* Hulburt (Dinophyceae). Plant Physiol 117: 189–197

ten Lohuis MR and Miller DJ (1998b) Genetic transformation of dinoflagellates (*Amphidinium* and *Symbiodinium*): Expression of GUS in microalgae using heterologous promoter constructs. Plant J (1998) 13: 427–435

Thornber JP, Cogdell RJ, Chitnis P, Morishige DT, Peter GF, Gomez SM, Anandan S, Preiss S, Dreyfuss BW, Lee A, Takeuchi T and Kerfield C (1994) Antenna pigment-protein complexes of higher plants and purple bacteria. In: Barber J (ed) Advances in Molecular and Cell Biology, Vol 10, pp 55–118. JAI Press, Greenwich CT

Trautmann JK, Shreve AP, Owens TG and Albrecht AC (1990) Femtosecond dynamics of carotenoid-to-chlorophyll energy transfer in thylakoid membrane preparations of *Phaeodactylum tricornutum* and *Nannachloropsis* sp. Chem Phys Lett 166: 369–374

Triplett EL, Jovine RVM, Govind NS, Roman SJ, Chang SS and Prézelin BB (1993) Characterization of two full length cDNA sequences encoding for apoproteins peridinin-chlorophyll *a*-protein (PCP) sequences. Mol Mar Biol Biotech 2: 246–254

Welte C, Nickel R and Wild A (1995) Three dimensional crystallisation of the light-harvesting complex from *Mantoniella squamata* requires an adequate purification procedure. Biochim Biophys Acta 1231: 265–274

Wilhelm C and Lenartz-Weiler I (1987) Energy transfer and pigment composition in three chlorophyll *b*-containing light-harvesting complexes isolated from *Mantoniella squamata* (Prasinophyceae), *Chlorella fusca* (Chlorophyceae) and *Sinapsis alba.* Photosynth Res 13: 101–107

Wilhelm C, Buchel C and Rousseau B (1988) The molecular organization of chlorophyll-protein complexes in the Xanthophycean alga *Pleurochloris meiringensis.* Biochim Biophys Acta 934: 220–226

Wilhelm C, Kolt S, Meyer M, Scmitt A, Zuber H, Egeland ES and Liaaen-Jensen S (1997) Refined carotenoid analysis of the major light-harvesting complex of *Mantoniella squamata.* Photosynthetica 33: 161–171

Wisconsin Package (1994) Program Manual for the Wisconsin Package Version 8, August 1994, Genetics Computer Group, 575 Science Drive, Madison, Wisconsin, USA 53711

Chapter 6

The Structure of Reaction Centers from Purple Bacteria

Günter Fritzsch and Andreas Kuglstatter
Max-Planck-Institut für Biophysik, Heinrich-Hoffmann-Str. 7, 60528 Frankfurt, Germany

Summary

The function of photosynthetic bacterial reaction centers (RCs) is closely related to their structure. In the last 15 years a wealth of structural data has been accumulated on bacterial RCs, mainly through X-ray structure analysis of three-dimensional RC crystals. In this chapter, the arrangement of protein subunits and cofactors in the RC complexes of the non-sulfur purple bacteria *Rhodobacter (Rb.) sphaeroides* and *Rhodopseudomonas (Rp.) viridis* are delineated. A prominent feature of the bacterial RCs is their location in the photosynthetic membrane. Inside the RC complex, a finely tuned arrangement of amino acid residues and cofactors maintains a highly ordered system. The positions and likely functions of hydrogen bonds are described, since they play a key role in protein-cofactor interactions. Special emphasis is placed on the symmetry relations in the RC and on the functional asymmetry of electron and proton transfer that contradicts the observed pseudo two-fold structural symmetry.

The structures of the RCs from *Rb. sphaeroides* and *Rp. viridis* show a striking identity, apart from the cytochrome-*c* subunit found only in the latter RC. The core regions around the bacteriochlorophylls and bacteriopheophytins, including the carotenoid, are particularly similar. New observations of water clusters close to the primary and secondary quinones are described and their impact on proton transfer processes is discussed. These findings help elucidate the intermeshed processes of electron-proton coupling in the RC.

H. A. Frank, A. J. Young, G. Britton and R. J. Cogdell (eds): The Photochemistry of Carotenoids, pp. 99–122.

I. Introduction

Life on earth depends on solar light. Photosynthesis is the process that converts the energy of light into chemical free energy. It requires protein complexes that stabilize highly ordered arrangements of cofactors with finely tuned spectral properties. As primary players in a complex bioenergetic machinery, the photosynthetic proteins supply energy to numerous biochemical processes. A clear understanding of the underlying principles of photosynthesis requires detailed knowledge of the protein-cofactor complexes.

The primary processes of charge separation in photosynthetic bacteria and higher plants take place in so-called reaction centers (RCs). These are integral membrane protein complexes which bind pigments like (bacterio)chlorophylls, (bacterio)pheophytins, carotenoids, and quinones. In the membrane, the RCs are embedded in ring-like structures of light-harvesting (LH) proteins (antennae). The antennae also contain (bacterio)chlorophylls and carotenoids which absorb light and transfer the excitation energy to the RCs. Thus, the RCs are able to absorb light directly from the environment as well as excitation energy from the neighboring antennae, and they facilitate subsequent electron and proton transfer reactions.

The proteins most relevant to photosynthesis are membrane-bound and are therefore difficult to crystallize for structural analysis. Nevertheless, the RC from the purple bacterium *Rhodopseudomonas (Rp.) viridis* was the first membrane-bound protein from which well-ordered three-dimensional crystals were grown (Michel, 1982). The structure of this RC was solved by the multiple isomorphous replacement method to 2.3 Å resolution (Deisenhofer et al., 1984, 1985, 1995). The prerequisite for crystallization was the development of a systematic strategy (Michel, 1983) that involved the handling of membrane proteins in suitable detergent micelles. It was necessary to reduce the size of the detergent micelle surrounding the protein to a size that no longer inhibited the formation of crystals of protein-detergent complexes. Subsequently, the structure of the *Rhodobacter (Rb.) sphaeroides* RC was determined by several groups which used three types of crystals: orthorhombic (Allen et al., 1986; Chang et al., 1986; Arnoux et al., 1989), trigonal (Ermler et al., 1994), and tetragonal (Allen, 1994). So far, several X-ray structures of photosynthetic RCs have been described and these are deposited in the Brookhaven Protein Data Bank (Bernstein et al., 1977). Table 1 shows selected crystallographic data for both RCs from a list presented by Lancaster et al. (1995).

In recent years, the X-ray structures of two further photosynthetic membrane-bound proteins have been analyzed by studying three-dimensional crystals: the light-harvesting antenna complexes from *Rp. acidophila* (McDermott et al., 1995) and *Rhodospirillum (Rs.) molischianum* (Koepke et al., 1996), and the Photosystem I reaction center (Krauss et al., 1996). Apart from photosynthetic proteins, few other membrane proteins have been structurally resolved by X-ray crystallography.

The most surprising result from the crystallographic analysis of the bacterial RC was the discovery of the local two-fold symmetry of the cofactor arrangement. Successful structural analysis has also allowed more detailed analysis of RC functions. An important initial result was obtained by applying polarized absorption spectroscopy to crystals from *Rp. viridis* RC. Zinth et al. (1985) and Kirmaier et al. (1985) determined that only one of the two symmetrically related branches of cofactors is used in electron transfer (ET). The bacterial RCs have now become a paradigm for the study of electron and proton transfer processes in proteins. Compendiums of structural and functional analyses of bacterial RCs can be found in several monographs: Michel-Beyerle (1985, 1990, 1996), Breton and Verméglio (1988, 1992), Deisenhofer and Norris (1993), and Blankenship et al. (1995).

Abbreviations: Φ_A – bacteriopheophytin (A branch); Φ_B – bacteriopheophytin (B branch); A – active branch; B – inactive branch; B_A – accessory bacteriochlorophyll (A branch); B_B – accessory bacteriochlorophyll (B branch); D – primary electron donor ('special pair'); D* – excited state of D; D^+ – oxidation state of D; D_A – bacteriochlorophyll of the primary donor (A branch); D_B – bacteriochlorophyll of the primary donor (B branch); ET – electron transfer; FTIR – Fourier transform infrared; H – subunit of the reaction center; HQH – quinol (dihydroxyquinone); L – subunit of the reaction center; LDAO – N,N-dimethyl-dodecylamine-N-oxide; LH – light-harvesting protein; M – subunit of the reaction center; PEG – polyethylene glycol; PS II – Photosystem II; Q_A – primary electron acceptor quinone (A branch); Q_B – secondary electron acceptor quinone (B branch); *Rb.* – *Rhodobacter*; RC – reaction center; *Rc.* – *Rhodocyclus*; *Rp.* – *Rhodopseudomonas*; *Rs.* – *Rhodospirillum*

Table 1. Reaction Center Structures

PDB entry code[a]	Crystal type	Resolution limit [Å]	No. of unique reflections	completeness [%]	n_{obs}/n_{par}[b]	R_{cryst} (R_{free})	Mean coordinate error [Å] (Luzzati, 1952)	Reference
Rp. viridis								
1PRC	tetragonal	2.3	95,762	75.4	2.38	19.3	0.26	Deisenhofer & Michel, 1989b
2PRC	tetragonal	2.45	79,397	76.5	1.83	18.2 (22.9)	0.26	Lancaster & Michel, 1997
6PRC	tetragonal	2.3	102,117	81.4	2.43	18.5	0.22	Lancaster & Michel, 1998b
Rb. sphaeroides								
2RCR	orthorhombic	3.1	13,493	50.8	0.63	22.0	0.5	Chang et al., 1991
4RCR	orthorhombic	2.8	21,992	60.0	0.81	22.7	0.4	Yeates et al., 1988
1PSS	orthorhombic	3.0	21,518	68.9	0.79	22.3	0.5	Chirino et al., 1994
1PCR	trigonal	2.65	56,141	90.4	1.91	18.6	0.3	Ermler et al., 1994
1AIJ[c]	tetragonal	2.2	112,234	86.0	1.53	21.6 (27.0)	-	Stowell et al., 1997
1AIG[d]	tetragonal	2.6	71,316	88.0	0.99	21.5 (29.9)	-	Stowell et al., 1997

[a] Name of the entry code in the Brookhaven data bank. [b] Number of observed unique reflections/number of parameters necessary to define the model. [c] Neutral (dark) state. [d] Charge separated state (light).

II. Preparation of Three-Dimensional Crystals

In this chapter, procedures for protein isolation and crystallization will be described briefly. Cells of *Rb. sphaeroides* and *Rp. viridis* grow photoheterotrophically in sodium succinate medium (Claus et al., 1983). After about one week, the cells reach the late log phase and are harvested. From now on all samples are kept in the dark. After disrupting the bacteria by ultrasonication, the chromatophores are usually layered onto sucrose gradients and isopycnic centrifugation is performed. The bands containing the RCs are washed and solubilized with the non-ionic detergent N,N-dimethyldodecylamine-N-oxide (LDAO), with 0.5% and 6% LDAO applied for the RCs of *Rb. sphaeroides* and *Rp. viridis*, respectively. The RCs from *Rb. sphaeroides* are usually further purified by anion exchange chromatography (Diethylaminoethyl (DEAE)-Sepharose) and molecular sieve chromatography (Fractogel) (Allen and Feher, 1991). This approach has frequently been modified. The RCs from *Rp. viridis* were isolated using only molecular sieve chromatography (Michel, 1982). A survey of the methods for isolation and crystallization of the RCs from *Rb. sphaeroides* and *Rp. viridis* is presented in Fritzsch (1998).

Orthorhombic crystals from *Rb. sphaeroides* RCs are obtained in sitting drops by the vapour diffusion method using polyethylene glycol 4000 (PEG^{4000}) as precipitant and 1,2,3-heptanetriol as additive (Allen et al., 1986). The detergent LDAO may be exchanged for β-octyl glucoside (Chang et al., 1986). Under appropriate conditions $6 \times 0.5 \times 0.5$ mm^3 large, needle-like crystals of space group $P2_12_12_1$ grow after several days or weeks. They diffract to 2.8 Å. However, the ratio n_{obs}/n_{par} (number of observed unique reflections divided by the number of parameters to be refined) is 0.8 or less, meaning that the number of experimental data is too low for an objective refinement of the model. Trigonal crystals from *Rb. sphaeroides* RC are obtained with potassium phosphate as precipitant and a mixture of 1,2,3-heptanetriol and 1,2,3-hexanetriol as additive (Buchanan et al., 1993; Fritzsch, 1998). The crystals of space group $P3_121$ can reach 4 mm in length and 1.5 mm in diameter. They are more stable than the orthorhombic crystals and diffract to 2.4 Å resolution with a ratio $n_{obs}/n_{par} = 3.0$ (Kapaun, 1998). In Fig. 1 a trigonal crystal with hexagonal cross-section is shown. Finally, tetragonal crystals from *Rb. sphaeroides* RC grow in the presence of the detergent β-octyl glucoside, the precipitant PEG^{4000} and the additives benzamidine hydrochloride and 1,2,3-heptanetriol (Allen, 1994). The tetragonal crystals belong to space group $P4_32_12$ and diffract to 2.2 Å (Stowell et al., 1997). Crystals from *Rp. viridis* RC are exclusively tetragonal and little smaller than the crystals from *Rb. sphaeroides* RC. They diffract to 2.0 Å (Lancaster and Michel, 1999a,b).

The *Rb. sphaeroides* RC is much more hydrophobic

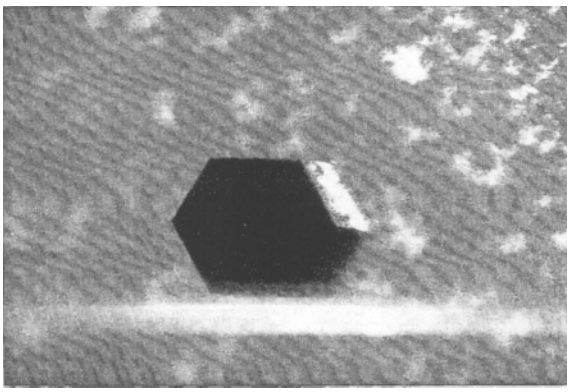

Fig. 1. Trigonal crystal of the RC from *Rb. sphaeroides*. The hexagonal cross-section is oriented parallel to the x- and y-axes. The crystal is about 1 mm long (perpendicular to the plane of the page) and the distance between opposite vertices is about 0.6 mm. (From Buchanan et al., 1993)

than the RC from *Rp. viridis,* since it leaks a hydrophilic subunit equivalent to the cytochrome-*c* subunit that is characteristic for the *Rp. viridis* RC (see below). The RC molecules from *Rb. sphaeroides* interact with each other via hydrophilic surface domains projecting from the cytoplasmic and periplasmic sides. Nevertheless, the crystal packing density is high enough to form stable crystals. As can be seen in Fig. 2, the trigonal crystals of *Rb. sphaeroides* contain 'holes' filled with buffer and detergent (white) and interconnected parts of RC protein (black).

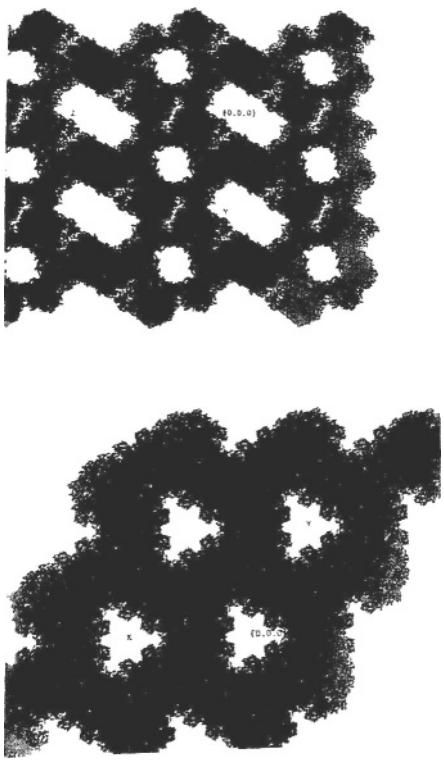

Fig. 2. Views into the trigonal crystal of *Rb. sphaeroides* RC. The calculated model of the RC in the crystal lattice is shown in black. The white domains are holes in the crystals filled with solvent and detergent. The unit cell is marked with thin lines. Upper: View along the crystalline x-axis. Lower: View along the crystalline z-axis. (From Fritzsch et al., 1996)

III. Survey of Structure and Function

Overall the X-ray structures of RCs from *Rb. sphaeroides* and *Rp. viridis* are very similar. Figure 3 shows a schematic view of the *Rp. viridis* RC complex together with the light-harvesting protein, the cytochrome-bc_1 complex, and the soluble cytochrome c_2. The pathway of ET is indicated by black dots. Figure 4 presents a model of the RC from *Rp. viridis* where the protein matrix is represented by a grey ribbon diagram and the cofactors are shown in color. Both RC species have a core that is formed by two integral membrane proteins, L and M, each containing five membrane-spanning helices. These subunits are related by a pseudo two-fold symmetry with the symmetry axis oriented perpendicular to the plane of the membrane. Another more hydrophilic subunit, H, is located at the cytoplasmic side of the membrane. The RC from *Rp. viridis* possesses an additional tetraheme *c*-type cytochrome that is tightly bound to the L-M core and that extends to the periplasm. Ten cofactors sit in the core. They are arranged in two branches, the active (A) and the inactive one (B). The point of origin of the dual branches is a bacteriochlorophyll dimer, D, which comprises two components, D_A and D_B (red in Fig. 4). The center of gravity of the two macrocycles is located on the two-fold symmetry axis. Two additional bacteriochlorophylls, B_A and B_B (green in Fig. 4), are positioned next to D_A and D_B, but lie deeper in the membrane. The local symmetry is broken close to the B molecules, since the carotenoid molecule (lilac in Fig. 4) is associated only with the B branch, a corresponding 'mirror object' in the A branch is missing. The bacteriochlorophyll monomers are followed by the bacteriopheophytins, Φ_A and Φ_B (yellow in Fig. 4), which lie in the middle of the

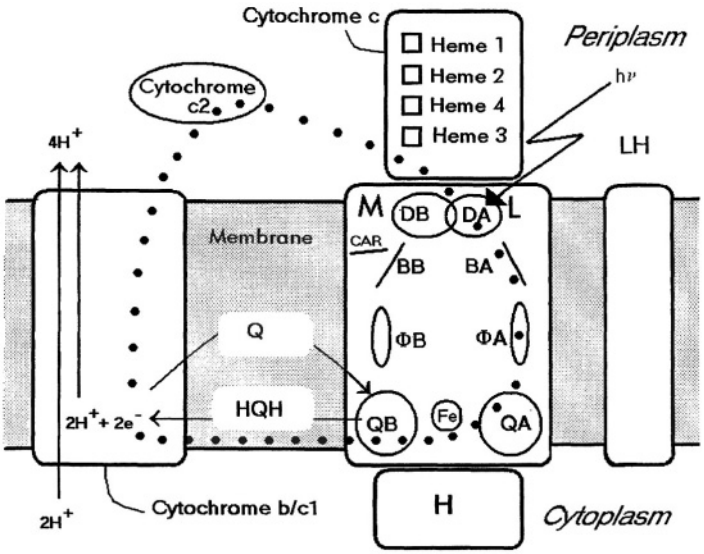

Fig. 3. Schematic view of the bacterial RC. The M- and L-subunits of the RC are embedded in the membrane while the H- and the cytochrome-subunit are bound at the cytoplasmic and periplasmic side of the RC, respectively. The pathway of electron transfer is indicated by black dots. Q: quinone, HQH: quinol.

membrane. The primary (Q_A) and secondary (Q_B) quinones (orange in Fig. 4) are located close to the cytoplasmic side of the RC. Between them the non-heme iron, Fe^{2+}, is positioned precisely on the two-fold symmetry axis (cyan in Fig. 4). The four heme groups of the cytochrome-*c* subunit in the *Rp. viridis* RC (blue in Fig. 4) are arranged in a nearly linear chain pointing to D. Only the heme next to D is located on the symmetry axis. The other hemes have a separate local symmetry that are described in Chapter 5 (Hiller).

Although the core of the protein displays a striking symmetry, the pathway of ET is asymmetric (Kirmaier et al., 1985; Zinth et al., 1985). Upon either transfer of excitation energy from the LH complexes or direct illumination, the special pair D is excited to D* and an electron is transferred exclusively along branch A to B_A. The time constant is 3.5 ps for both RCs; in a second step, the electron interacts with the electron acceptor, Φ_A, with a time constant of 0.9 and 0.65 ps for the RCs of *Rb. sphaeroides* and *Rp. viridis,* respectively (Zinth et al., 1996). The electron from Φ_A is transferred to the primary quinone Q_A in about 200 ps. Q_A is a so-called 'one-electron gate' which releases the electron within 10 to 100 μs to the secondary quinone Q_B. Before this step occurs, the oxidized primary donor (D^+) is reduced by a secondary electron donor which is heme 3 of the cytochrome-*c* subunit in the RC of *Rp. viridis* (about 200 ns) (Ortega and Mathis, 1993). In the RC of *Rb. sphaeroides* the re-reduction depends firstly on the docking of the cytochrome c_2 onto the RC, and secondly on the electron transfer process itself that takes about 1 μs (Mathis, 1994). The arrival of the electron at Q_B gives the state $DQ_AQ_B^-$ and a second electron can be transferred after another photon is absorbed. This leads to the diradical state $DQ_A^-Q_B^-$. In this state a proton is taken up from the cytoplasm and a second electron is transferred to Q_B. A second proton is taken up and the secondary quinone changes finally to the ubiquinol form (Q_BH_2). Ubiquinol has a low affinity for the Q_B binding site; it therefore diffuses within the membrane from the RC to the cytochrome-bc_1 complex.

The free energy gained from the quinol oxidation in the cytochrome-bc_1 complex allows further proton transfer from the cytoplasm to the periplasm. The bc_1-complex also mediates ET to the periplasmic side. There, soluble cytochromes c_2 accept the electrons and transport them back to the RC to reduce D^+. The electron transfer is cyclic and therefore does not cause transmembrane potential. This potential is generated by the electrogenic proton translocation in the cytochrome-bc_1 complex. The electrochemical proton gradient is utilized by the ATP-synthase to form adenosine triphosphate from adenosine diphosphate and phosphate.

Fig. 4. Overall view of the RC structure. The C_α chains of the protein are shown as grey ribbons. Refer to color plate 7 for the colors of the cofactors which are represented as: blue (heme groups), red (special pair), green (accessory bacteriochlorophylls), lilac (carotenoid), yellow (bacteriopheophytins), orange (quinones) and cyan (non-heme iron). (See also Color Plate 7)

IV. Subunits L, M, and H

The primary function of the RC apoprotein is to stabilize the finely tuned arrangement of cofactors that facilitate light absorption and the transfer of electrons and protons. There is another function of the protein domains surrounding the pigments: Special distortions of nuclear configurations are required for ET that is consequently an energy consuming process. It has been postulated that the amount of the so-called reorganization energy is particularly low in a suitable protein environment (Sharp, 1998). The core of the RC consists of two hydrophobic subunits, L and M, which bind ten cofactors. In both subunits, five long helices span the membrane and their amino termini are located on the cytoplasmic side of the membrane. Except for small parts of their mass, the L- and M-subunits are related by a two-fold rotational symmetry axis that is oriented perpendicular to the plane of the membrane. The lengths of the RCs (as measured perpendicular to the membrane) are 70 Å for the RC of *Rb. sphaeroides* and 130 Å for the RC of *Rp. viridis.* The projection of the core perpendicular to the membrane is elliptical with axes of about 70 and 30 Å for both RCs.

In *Rp. viridis* RC, the overall sequence homology of L and M is 25% (Michel et al., 1986a). The histidines ligated to metal ions are highly conserved while other residues that interact with the cofactors differ between L and M. Sequence identity of the L-subunits in the RCs of *Rp. viridis, Rb. sphaeroides* and *Rb. capsulatus* extends to almost 60% whereas it is about 50% in the M-subunit (Michel et al., 1986a). The sequence differences between L and M are mostly conservative, indicating that the structures of the reaction centers of the non-sulfur purple bacteria are very similar.

In the *Rp. viridis* RC the helical residues of the L- and M-subunits are: L33-L53 (LA), L84-L111 (LB), L116-L139(LC), L171-L198(LD), L226-L249(LE) and M52-M76 (MA), M111-M137 (MB), M143-M166 (MC), M198-M223 (MD), M260-M284 (ME) (Deisenhofer and Michel, 1989a,b). The longest membrane-spanning helices consist of 28 amino acids (LB and LD) while the shortest (LA) contains 21 amino acids. Some shorter helical stretches exist between these dominant helices, they are described by small letters like cd. The most frequently observed amino acids are leucine, alanine, and glycine. Several prolines are observed at each end of the helices. All helices include segments of at least 19 side chains which lack ionizable residues. Some helices possess acidic or basic side chains proximal to the cytoplasmic or periplasmic end, but not at both ends simultaneously. A few helices are tilted by up to 38°. At the periplasmic end, only one ionizable amino acid residue is found whereas several acidic or basic residues occur at the cytoplasmic ends (Deisenhofer and Michel, 1989a,b). In Fig. 5, the structures of the L- and M-subunits are represented, respectively. The M-subunit in Fig. 5 (upper right) has been superimposed on the L-subunit in order to illustrate the degree of similarity of these polypeptides. A perfectly symmetric arrangement of the L- and M-subunits would allow two pathways of ET along

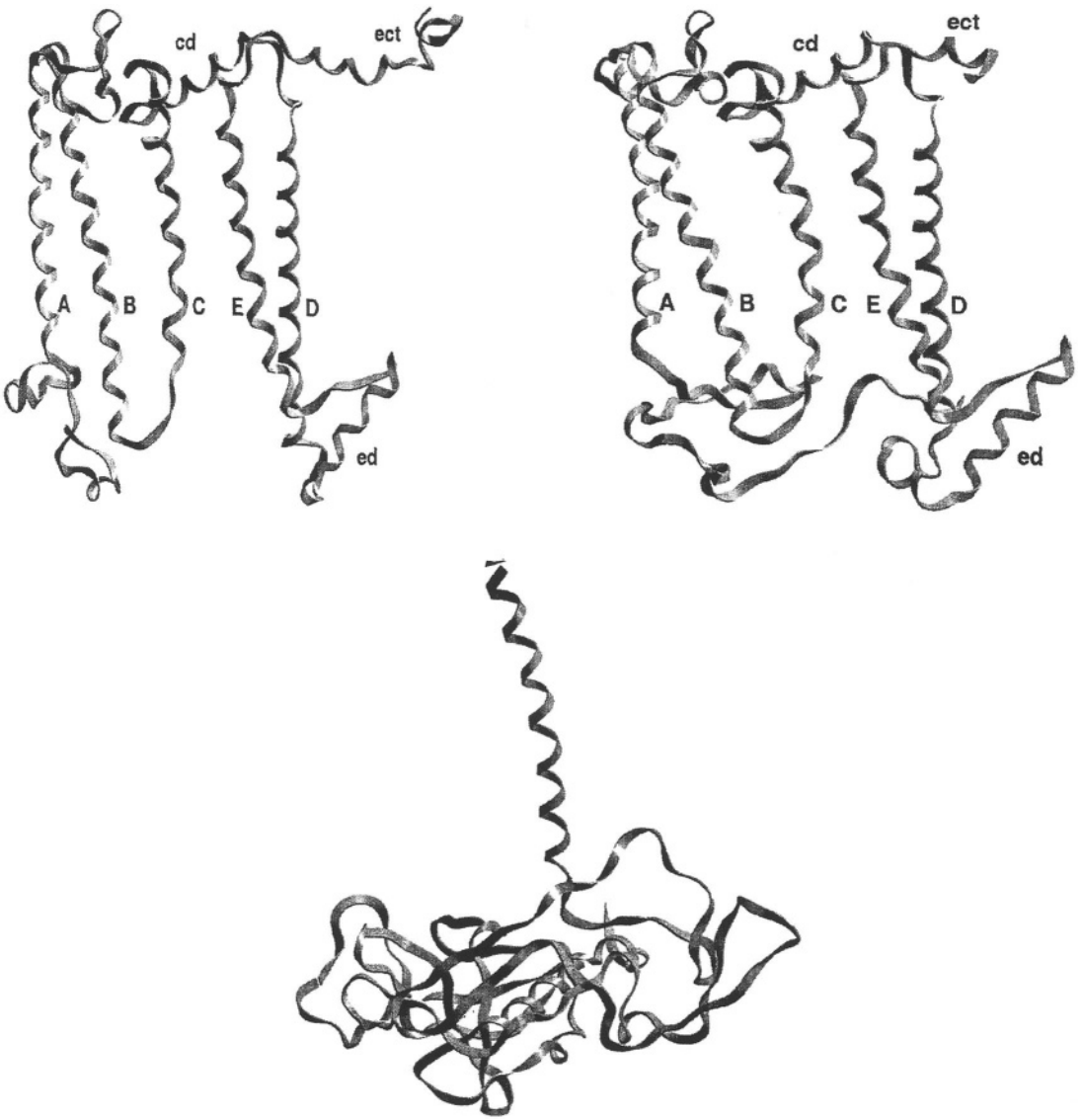

Fig. 5. Backbone representation of the subunits L (upper left), M (upper right) and H (lower). The M-subunit has been superimposed on the L-subunit to emphasize the high degree of identity of these polypeptides. (ect: helical segment between E and the C-terminal.)

two *symmetrically* related branches. In fact, the ET in the RC occurs unidirectionally, i. e. in an *asymmetric* mode along only one branch. This is achieved by a special asymmetric distribution of amino acid residues among L and M, mainly in the vicinity of the pigments.

The H-subunit (Fig. 5, lower) forms a large cytoplasmic domain with a more hydrophilic surface than the L- and M-subunits. Unlike the L- and M-subunits, it does not participate in cofactor binding and its removal does not interrupt the electron transfer (Feher and Okamura, 1978; Wiemken and Bachofen, 1984). The H-subunit is anchored in the membrane by a single transmembrane α-helix that has contacts with the antiparallel E helix of M. Salt bridges play an important role in the binding of the H-subunit to the core region. In *Rb. sphaeroides* RC about one-third of all salt bridges are observed as interchain bridges between the H-polypeptide and the L-M core (Chang et al., 1991). In Fig. 6, a view along the local symmetry axis shows the positions of the H helix, together with the other five plus five helices from L and M. The two bacteriochlorophylls of the primary donor, D_A and D_B, are indicated in black.

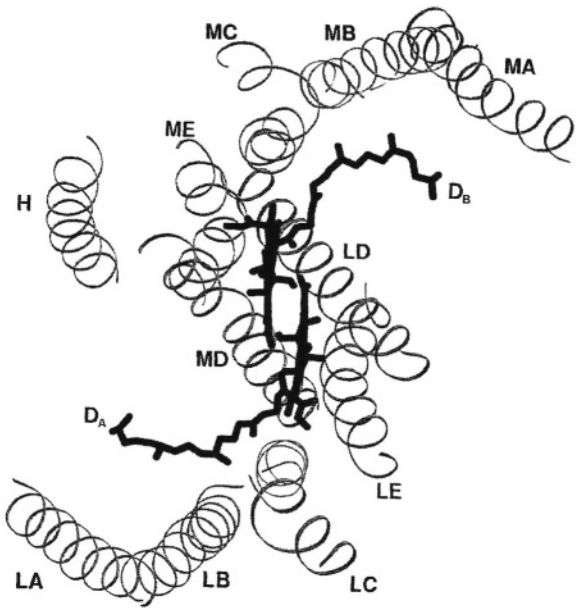

Fig. 6. A view through the *Rb. sphaeroides* RC along the local symmetry axis showing the helical transmembrane segments from the L-, M- and H-subunits. The two parallel macrocycles of the primary donor, D_A/D_B, are shown in black.

Three structural regions characterize the H-subunit of *Rb. sphaeroides* and *Rp. viridis* RCs. The segment at the NH_2-terminus forms the single transmembrane helix with 24 residues followed by a cluster of seven charged residues in the *Rp. viridis* RC and only three in the *Rb. sphaeroides* RC. The next segment consists of about 70 residues and is attached to the L-M complex. This contact probably stabilizes the binding of the H-subunit. The third and longest part of H starts about at H105 and forms a globular domain consisting of a system of parallel and antiparallel β-sheets. This domain forms a pocket with strongly hydrophobic interior walls (Deisenhofer and Michel, 1989a,b).

Several amino acid residues of H form electrostatically coupled clusters of ionizable residues near Q_B (Lancaster et al., 1996). In the *Rb. sphaeroides* RC, Glu H173 is a member of a cluster which also includes Asp L213, a residue required for proton uptake by Q_B (see below). Mutation of Glu H173 to Gln retards both the kinetics of the first electron transfer and of the proton-linked second electron transfer (Takahashi and Wraight, 1996). Another characteristic for the region proximal to Q_A and Q_B are clusters of firmly bound water molecules (Abresch et al., 1998; Fritzsch et al., 1998). Several side chains of the H-subunit contribute a system of ionizable amino acid residues that are in extensive contact with the water molecules of these clusters.

V. Cytochrome Subunit

In addition to subunits L, M, and H, the RCs of several purple bacteria such as *Rp. viridis, Rhodocyclus (Rc.) gelatinosus,* and *Chromatium vinosum* contain a tightly bound tetraheme cytochrome-*c* subunit which donates electrons to D. In *Rp. viridis,* this subunit does not possess intramembranous segments, but it has an N-terminal cysteine that is linked to a glycerol residue via a thioether bond (Weyer et al., 1987). Such a bond has also been found at the N-terminus of the major outer membrane lipoprotein of *Escherichia coli* (Hantke and Braun, 1973) in which the fatty acids form a lipid-type membrane anchor.

The cytochrome subunit is the largest subunit in the *Rp. viridis* RC and consists of 336 residues. It contains four *c*-type heme groups, which form a linear chain pointing to D and which are in van der Waals contact with their neighbors. Two pairs of protein segments bind the four heme groups: One contains hemes 1 and 2, the other one hemes 3 and 4, where the numbering of the groups is defined according to their location along the protein primary sequence. The planes of the two outer heme groups 1 and 3 are aligned almost parallel to the z-axis of the *Rp. viridis* RC crystal, while the inner groups 2 and 4 are oriented almost perpendicular to z. The heme-binding segments are related by a local two-fold symmetry that is, however, not related to the central symmetry mentioned before. Each segment includes a helix of about 17 residues and the typical cytochrome-*c* consensus sequence Cys-X-Y-Cys-His where the cysteine residues are connected to the hemes by thioether linkages (Deisenhofer and Michel, 1989a,b). The sixth ligands of all the hemes are methionines, except heme 4 which is ligated with histidine. In Fig. 7, a stereo view of the backbone (grey) and the four heme groups (black) shows the relative positions of the hemes. The helices of the heme-binding segments can clearly be seen. The hemes are not completely buried in the apoprotein, parts of the hemes are in contact with the periplasmic environment. Polarized absorption spectroscopy of redox poised crystals (Fritzsch et al., 1989) has yielded the following assignment of the absorption

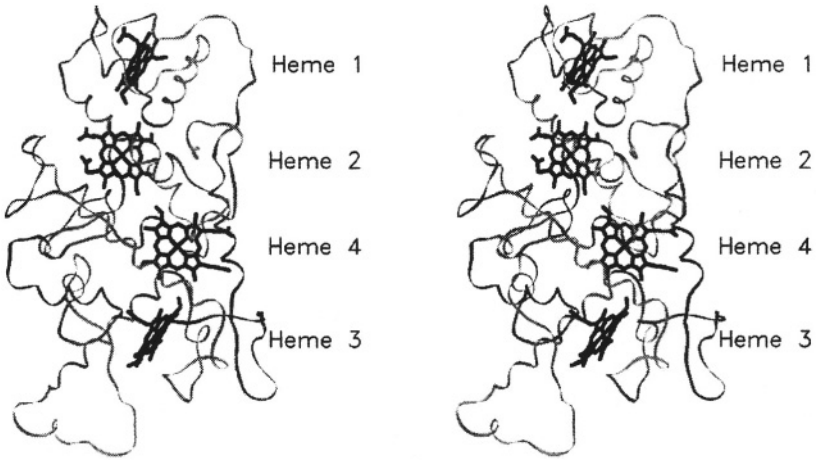

Fig. 7. Stereo representation of the cytochrome C_α chain (grey) and the four heme groups (black) of the *Rp. viridis* RC. The best view of the heme-binding helical segment is seen close to heme 1.

wavelengths and redox potentials of hemes 1 to 4: Heme 1 (552.5 nm/–60 mV), heme 2 (556.0 nm/ +300 mV), heme 4 (552.0 nm/+10 mV), and heme 3 (558.5 nm/+370 mV).

A highly conserved tyrosine (Tyr L162) is positioned halfway between heme 3 and the primary donor. The distance between the Fe atom of heme 3 and the nearest edge of the primary donor is about 14 Å. It seems Tyr L162 contributes to the fast ET. Studies with mutant RCs where the tyrosine has been replaced by methionine, phenylalanine, tryptophan, leucine, glycine or threonine, show modestly slower fast phases of electron transfer (but less than factor 10). These results indicate that the highly conserved Tyr L162 is not essential for fast electron transfer. It was concluded that Tyr L162 may support efficient docking of the cytochrome to the L- and M-subunits (Dohse et al., 1995).

In *Rb. sphaeroides* RCs, the primary donor in state D^+ is re-reduced via the soluble cytochrome c_2. The structural interaction between cytochrome c_2 and the RC has been studied in an X-ray diffraction experiment with co-crystals of the RC from *Rb. sphaeroides* and cytochrome c_2 at 4.5 Å resolution (Adir et al., 1996). The structure obtained for the complex shows the cytochrome c_2 interacting with the RC at the periplasmic surface of the M-subunit. Recent studies provide evidence for an RC with two cytochrome-*c* subunits in the purple sulfur bacterium *Chromatium minutissimum* (Chamorovsky et al., 1998). A gel-electrophoretic assay yields five rather than four RC subunits. These have molecular masses of 37, 34, 25, 19, and 17 with the 37- and 19-kDa subunits assigned as cytochromes. Redox titrations revealed six heme mid-point potentials where those of 210 mV and 100 mV are not observed in the *Rp. viridis* RC.

VI. Bacteriochlorophylls, Bacteriopheophytins, and Carotenoid

The cofactors are held in a highly ordered arrangement by numerous interactions with the protein scaffold. Table 2 summarizes the specific interactions between the protein and the cofactors of the RCs from *Rb. sphaeroides* and *Rp. viridis*. As described in Ermler et al. (1994), these interactions are rather similar in both RCs.

A. The Primary Donor

In bacterial RCs, the light-driven reactions are initiated by a non-covalently linked dimeric primary electron donor, D, also called a 'special pair'. The existence of such a dimer was first postulated from spin-resonance experiments (Norris et al., 1971). This special pair was identified as a homodimeric bacteriochlorophyll *a* (*Rb. sphaeroides*) or *b* (*Rp. viridis*) complex. Its position is close to the periplasmic side at the L and M polypeptide interface. In the *Rp. viridis* RC the dimer is located close to heme 3 of the cytochrome-*c* subunit. The helices C, D, E, and cd of both, L- and M-subunits, stabilize the

Table 2. Interactions between apoprotein and the cofactors in the RCs of *Rb. sphaeroides* and *Rp. viridis*

	Rhodobacter sphaeroides			*Rhodopseudomonas viridis*		
	Atom of cofactor	Atom of apoprotein	D...A dist. (Å)	Atom of cofactor	Atom of apoprotein	D...A dist. (Å)
D_A	Mg^{2+}	HisL173-NE2	2.3	Mg^{2+}	HisL173-NE2	2.1
	Ring-I keto-O	HisL168-NE2	3.1	Ring-I keto-O	HisL168-NE2	2.7
	Ring-V ester-O	CysL247-SG	3.5	Ring-V keto-O	ThrL248-OG1	2.9
D_B	Mg^{2+}	HisM202-NE2	2.2	Mg^{2+}	HisM200-NE2	2.0
				Ring-I keto-O	TyrM195-OH	2.7
B_A	Mg^{2+}	HisL153-NE2	2.2	Mg^{2+}	HisL153-NE2	2.1
	Ring-V keto-O	w59a	2.6	Ring-V keto-O	w302a	3.1
B_B	Mg^{2+}	HisM182-NE2	2.2	Mg^{2+}	HisM180-NE2	2.1
	Ring-V ester-O	w62	3.1			
Φ_A	Ring-V ester-O	TrpL100-NE1	3.0	Ring-V ester-O	TrpL100-NE1	3.0
	Ring-V keto-O	GluL104-OE1	2.6	Ring-V keto-O	GluL104-OE1	2.7
Φ_B	Ring-V ester-O	TrpM129-NE1	2.8	Ring-V ester-O	TrpM127-NE1	2.7
Q_A	Prox. keto-O	HisM219-ND1	2.9	Prox. keto-O	HisM217-ND1	2.9
	Dist. keto-O	AlaM260-N	3.0	Dist. keto-O	AlaM258-N	3.1
Q_B	Prox. keto-O	HisL190-ND1	6.9*	Prox. keto-O	HisL190-ND1	2.6
	Dist. keto-O	GlyL225-N	4.7*	Dist. keto-O	GlyL225-N	2.9
	Dist. keto-O	IleL224-N	2.4	Dist. keto-O	IleL224-N	3.0
	Dist. keto-O	TyrL222-O	3.3	Dist. keto-O	TyrL222-O	5.5*
Non-heme iron	Fe^{2+}	HisL190-NE2	2.0	Fe^{2+}	HisL190-NE2	2.0
	Fe^{2+}	HisL230-NE2	2.1	Fe^{2+}	HisL230-NE2	2.3
	Fe^{2+}	HisM219-NE2	2.0	Fe^{2+}	HisM217-NE2	2.0
	Fe^{2+}	HisM266-NE2	2.0	Fe^{2+}	HisM264-NE2	2.0
	Fe^{2+}	GluM234-OE1	2.0	Fe^{2+}	GluM232-OE1	2.2
	Fe^{2+}	GluM234-OE2	2.2	Fe^{2+}	GluM232-OE2	2.0

* No hydrogen bond; D: donor; A: acceptor. The data for *Rb. sphaeroides* RC are taken from an improved structure obtained from trigonal crystals (Kapaun, 1998), the data for *Rp. viridis* RC are from Lancaster et al. (1997), PDB entry code 2PRC.

dimer in its position. The monomeric components, D_A and D_B, interact with the L- and M-subunit. The crystallographic B-factors of D are low compared with those of the other cofactors. Rigidity within the A branch is higher than in the B branch, e.g., in the *Rp. viridis* RC the tetrapyrrole ring of D_A has an average B-factor of 10.3 $Å^2$ compared with 21.1 $Å^2$ for D_B (Deisenhofer and Michel, 1989a,b). As shown by a detailed comparison of several RCs, the agreement of the coordinates from D and Φ_A is significantly higher than that of other cofactors (Arnoux and Reiss-Husson, 1996). These results emphasize the importance of a highly ordered relationship between D and Φ_A for a proper RC function.

The excitonic interaction of the dimer D is stabilized by a system of aromatic residues. In the RC of *Rp. viridis,* five phenylalanines, three tryptophans, and three tyrosines interact with the tetrapyrrole rings of D, where Tyr L162 is located between the dimer and heme 3 of the cytochrome subunit as mentioned before. The macrocycles are aligned nearly in parallel, with a minimum distance of about 3.2 Å. In the projection perpendicular to the planes of D_A and D_B, both monomers overlap with their pyrrole rings I. The overlapping area is slightly larger in the RC from *Rp. viridis* than in the one of *Rb. sphaeroides* (Ermler et al., 1994). The positions of the macrocycles of D_A and D_B are almost perfectly symmetric, and the bacteriochlorophyll rings are oriented nearly parallel to the symmetry axis. Figure 8 shows a superposition of the special pairs from both types of RCs. A high degree of structural identity is observed. In the *Rp. viridis* RC optimum superposition of tetrapyrrole rings is achieved by a 179.7° rotation (Deisenhofer and Michel, 1989a,b), which is very close to perfect symmetry. The phytyl side chain of D_B, which interacts with the M-subunit is partly disordered while that of D_A is well ordered.

The ring I acetyl group of D_A is in close contact

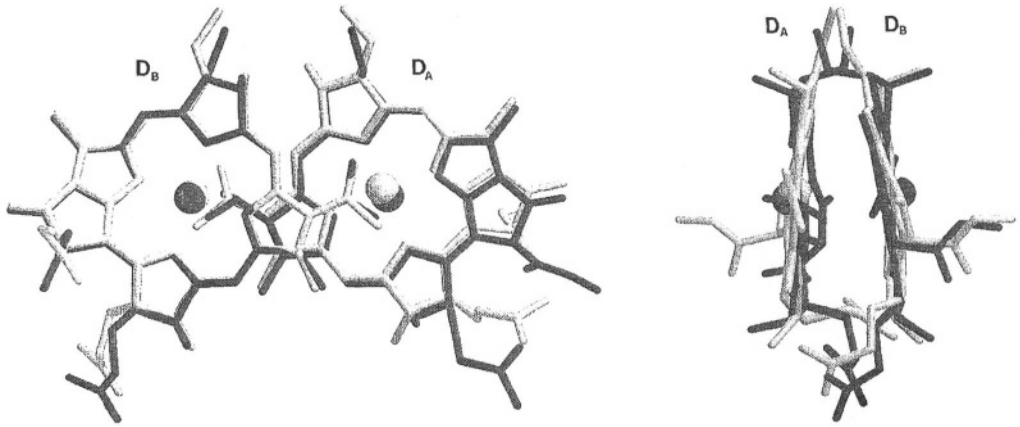

Fig. 8. Superposition of the special pairs of the RCs from *Rb. sphaeroides* (shown in Color Plate 8 in red) and *Rp. viridis* (shown in Color Plate 8 in green) represented without their phytyl chains. left: View perpendicular to the planes of the macrocycles. right: View rotated by 90°. The superposition shows the high degree of structural identity of both RCs. As shown in b, the ester methyl groups of ring V have different orientations in both RCs. (See also Color Plate 8)

with the central Mg^{2+} of D_B and *vice versa,* but there is no ligation between them. The Mg^{2+} ions are pentacoordinated. Their fifth ligands are His L173 and His M202/M200 (*Rb. sphaeroides* RC/*Rp. viridis* RC), with a distance of about 2.2 Å between the Nε2 atoms of the histidines and the Mg^{2+} ions. Crystal structures of mutant RCs from *Rb. sphaeroides,* in which His L173 and His M202 were replaced by leucines, show bacteriopheophytins in place of the bacteriochlorophylls. The lack of the magnesium atoms, however, does not cause significant structural perturbations of the surrounding polypeptides (Chirino et al., 1994). In both RCs, His L168 forms a hydrogen bond to the ring I aceryl carbonyl of D_A, with distances of 3.2 Å (*Rb. sphaeroides*) and 2.8 Å (*Rp. viridis*).

In the regions around ring V of D_A and D_B, remarkable conformational differences are observed between the RCs of *Rp. viridis* and *Rb. sphaeroides.* While the *Rb. sphaeroides* RC ring V of D_A approaches helix C, it is bent towards helix D in *Rp. viridis* RC. In particular, the positions of the ring V ester methyl groups differ by 5.3 Å. This change is related to a different distribution of bulky side chains in the two bacterial RCs. Moreover, in the *Rp. viridis* RC the residues Gly L247 and Thr L248 are sandwiched between ring V of D_A and the D helix of the L-subunit, thereby allowing a close contact between these two structural units. The hydroxyl group of Thr L248 forms a hydrogen bond to the ester carbonyl oxygen of ring V from D_A. At the opposite side of ring V, Met L127 and the ethylidene group of B_A support the strong bending of ring V towards the LD helix. In the *Rb. sphaeroides* RC, however, the more bulky Cys L247 and Met L248 side chains project ring V away from LD and towards the LC helix. In addition, L127 is an alanine instead of a methionine, further facilitating the positioning of ring V towards LC. The conformation of the ethylidene group in B_A also favors the position of ring V (Ermler et al., 1994). The porphyrin groups of D_A and D_B are not perfectly planar, but show characteristic out-of-plane conformations. D_B is more deformed than D_A and the strongest conformational differences occur at ring V. Thus, the ester methyl groups of D_B ring V are displaced by only 1.0 Å in the RCs of both bacterial species compared with 5.3 Å for D_A as described above. No polar interactions between ester or keto carbonyl oxygens and the polypeptide chain are observed (Ermler et al., 1994).

Hydrogen bond formation has a strong impact on the physical and chemical properties of D. *Rb. sphaeroides* mutant RCs were used to show that the introduction of new hydrogen bonds between the polypeptide chain and D changes the donor mid-point redox potential (Williams et al., 1992). The mutations Leu L131 to His and Leu M160 to His near the ring V keto carbonyl of D_A and D_B, respectively, have different effects on the primary donor: The mid-point potential increases up to 80 mV, the initial rate of electron transfer is slowed down up to a factor of 4, and the rate of charge recombination between Q_A and the donor is about 30% higher in both mutants compared to the wild type. The effect of a nonconserved hydrogen bond that interacts with D in the RC of *Rp. viridis* but not

of *Rb. sphaeroides* was tested by introducing the mutation Phe M197 → Tyr in the RC of *Rb. sphaeroides* (Wachtveitl et al., 1993). The mutation was expected to generate a hydrogen bond comparable to that in *Rp. viridis* wild type RC where, at this position, a tyrosine is hydrogen bonded to the acetyl carbonyl oxygen of ring I at D_B. Fourier transform resonance Raman spectroscopy of the mutant RC Phe M197 → Tyr indicates the formation of a new hydrogen bond near the 2-acetyl group of D_B. X-ray crystallographic analysis of the *Rb. sphaeroides* mutant RC Phe M197 → Tyr at 2.7 Å resolution does not allow an unambiguous assignment of the acetyl carbonyl oxygen group in ring I of D_B. According to Ippolito et al. (1990), however, one of the possible alternative conformations of the acetyl carbonyl oxygen of ring I displays an optimal geometry for hydrogen bond acceptance (Kuglstatter et al., 1998).

Little is known about the interactions between D and the protein matrix in other photosynthetic bacteria. In a comparative study, the RCs from *Rs. rubrum, Rs. centenum, Rb. sphaeroides,* and *Rb. capsulatus* have been analyzed using optical spectroscopy (Wang et al., 1994). Although the four RC species have different spectral characteristics, the general spectral features of the initial charge separated state are almost identical. This result implies a similar pattern of protein-cofactor interactions in RCs that extends beyond *Rb. sphaeroides* and *Rp. viridis.*

B. The Carotenoid

The bacterial RCs contain a non-covalently bound carotenoid molecule that is located at the B branch. The lacking of a symmetrically related cofactor in the A branch introduces an element of asymmetry into the RC's architecture. The structural effect of this asymmetry on the C_α chains of the L- and M-subunits is not drastic as can be seen in Fig. 5. The carotenoid is spheroidene in the RC of *Rb. sphaeroides* and 1,2-dihydroneurosporene in the RC of *Rp. viridis.* In both RCs, the carotenoids interact with helices A, B, C (see below) and cd of the M-subunit and the plane spanned by the carotenoid molecule is oriented parallel to the plane of the membrane. The carotenoid shows a *cis*-geometric isomeric form and its binding pocket is mainly formed by hydrophobic residues, especially in the *Rb. sphaeroides* RC where six phenylalanines and five tryptophans are found within a radius of 5 Å around the spheroidene molecule. In the *Rp. viridis* RC only three phenylalanines and two tryptophans are observed within this distance. The orientation of the spheroidene could be determined reliably due to its non-identical two ends (Ermler et al., 1994).

A 13,14-*cis* configuration was initially deduced for 1,2-dihydroneurosporene from the electron density map of the *Rp. viridis* RC (Deisenhofer et al., 1995). The structure analysis of the *Rb. sphaeroides* RC using trigonal crystals, however, could not discriminate between either a 13,14-*cis* or a 15,15´-*cis* configuration (Ermler et al., 1994). A recent analysis performed by Lancaster and Michel (1998) strongly favors a 15-15´-*cis* configuration for 1,2-dihydroneurosporene in *Rp. viridis* RC. In that study, models with 13 -14-*cis* and 15 -15´-*cis* configurations have been compared using techniques of simulated annealing omit maps for the removal of model bias (Hodel et al., 1992), individual B-factor refinement analysis, and analysis of the deviation from ideal geometry. The 15-15´-*cis* configuration yields the best fit. This finding agrees with Raman (Lutz et al., 1987; Koyama et al., 1990) and NMR (De Groot et al., 1992) spectroscopy studies of *Rb. sphaeroides* RCs. Recent spectroscopic and photochemical experiments with locked 15,15´-*cis*-spheroidene incorporated into *Rb. sphaeroides* RC did not show differences compared to the *Rb. sphaeroides* wild type RCs (Bautista et al., 1998), indicating no functional reason for the preference of a 15,15´-*cis*-isomer in the natural RC.

In bacterial RCs the carotenoids are not directly involved in ET. They protect, however, the bacteriochlorophylls from photodestruction by quenching the triplet states of D (Monger et al., 1976; Lous and Hoff, 1989; Frank and Cogdell, 1996). The excited state energy is dissipated as heat. The photoprotecting function requires a close proximity of the carotenoid to other cofactors. In the *Rb. sphaeroides* RC, the nearest distance between the carotenoid and B_B is about 4 Å suggesting an energy transfer from D to the carotenoid via B_B. The existence of a strong interaction between both cofactors has been confirmed by different experiments (Frank et al., 1993). In *Rb. sphaeroides* RC, the binding affinity of spheroidene depends on the existence of B_B. As has been shown by Frank et al. (1988) the removal of B_B is accompanied by loss of the carotenoid.

The protective effect of the carotenoid has not been observed in the *Rp. viridis* RC. This is probably due to the fact that the resident bacteriochlorophyll *b*

has a triplet state of lower energy than bacteriochlorophyll *a*. Thus, the energy gap between the triplet states of D and B_B is higher and the triplet transfer is more inhibited (Takiff and Boxer 1988a,b). The triplet energy transfer can be influenced by structural changes of the protein matrix. As shown by Laible et al. (1998), mutations of Phe L181 and Tyr M208 effect significantly the efficiency of the triplet transfer. For a fuller description of the triplet-triplet ET reaction in RCs see Chapter 11, Angerhofer.

The stereo pairs in Fig. 9 shows the carotenoid molecules of the RCs from *Rb. sphaeroides* (red) (Ermler et al., 1994) and *Rp. viridis* (green) (Lancaster and Michel, 1997). Upper: View perpendicular to the plane of the membrane, Lower: View into the 'planes' of the carotenoids. The aromatic amino acid residues that form the carotenoid binding site are also presented. In Fig. 10, the spheroidene molecule of the *Rb. sphaeroides* RC is displayed in a stereo representation together with the cofactors D, B, and Φ.

C. The Accessory Bacteriochlorophylls

Two bacteriochlorophyll monomers, B_A and B_B, are located next to the primary donor D, but they are buried deeper in the membrane. Their positions are fixed by helices B, C, D, and de of the L- and M-subunits, respectively. How these so-called accessory bacteriochlorphylls are involved in the ET has been the subject of a long debate (Holzapfel et al., 1990; Kirmaier and Holten, 1991). Some evidence for their function as true electron carriers has been provided by subpicosecond absorption spectroscopy (Arlt et al., 1993; Zinth et al., 1996). The B_B molecule facilitates the triplet energy transfer between D and the carotenoid (Frank and Violette, 1989). B_A and B_B follow the local c_2 symmetry. Their tetrapyrrole rings are superimposed by a rotation (M on L) of –175.8° (Deisenhofer and Michel, 1989a,b) which is not as perfect as for the D_A/D_B pair. As in the case of D_B, the phytyl side chain of B_B interacts with the M-subunit

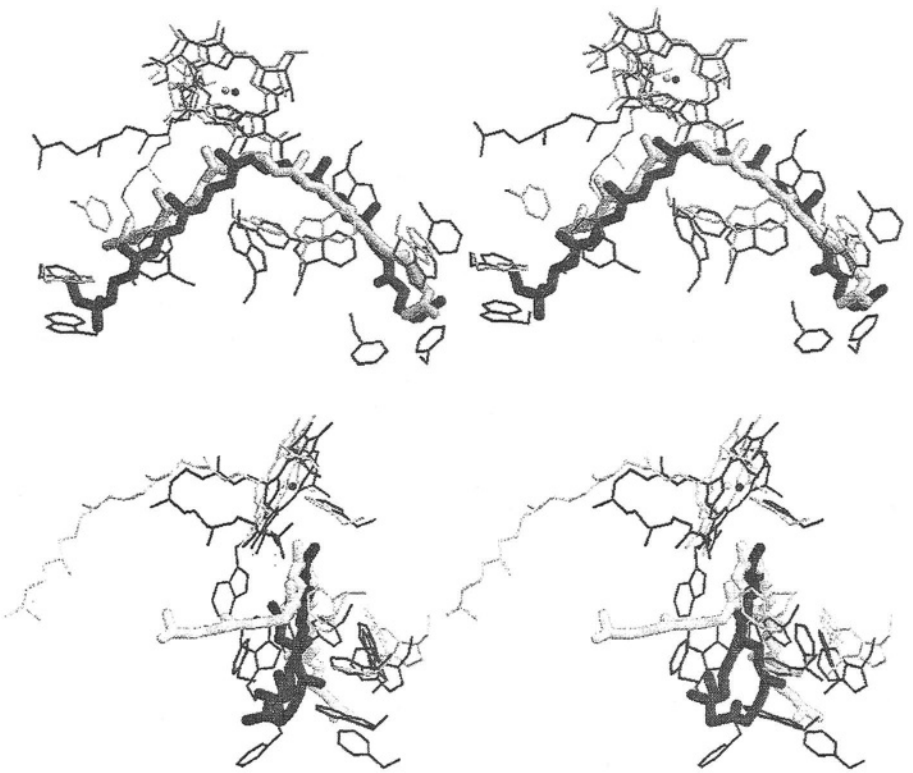

Fig. 9. The carotenoids. Superposition of the spheroidene and 1,2-dihydroneurosporene molecules from *Rb. sphaeroides* (shown in Color Plate 9 in red) and *Rp. viridis* (shown in Color Plate 9 in green) RC. The binding pocket is formed by six (three) phenylalanines and five (two) tryptophans in the *Rb. sphaeroides* (*Rp. viridis*) RC. Upper: View perpendicular to the planes of the carotenoids. Lower: View rotated by 90°. (See also Color Plate 9)

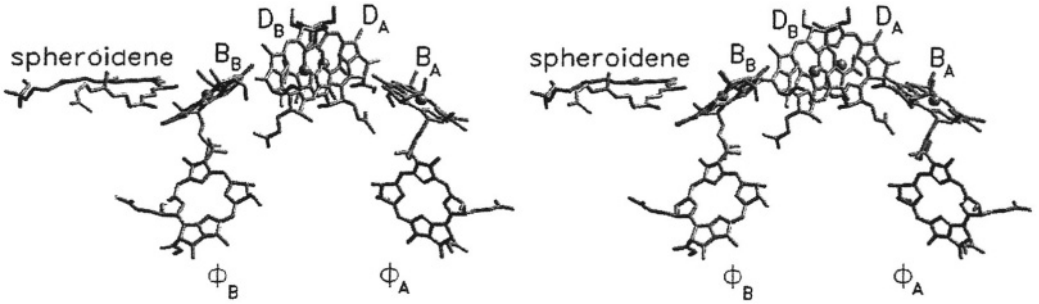

Fig. 10. Stereo view of the primary donor D, the accessory bacteriochlorophylls B, the bacteriopheophytins Φ, and the carotenoid (spheroidene) in the RC from *Rb. sphaeroides*.

and is partly disordered, whereas B_A is well ordered. B_A and B_B are in van der Waals contact with D as well as with Φ_A and Φ_B, respectively. The central Mg^{2+} ion of B_A is stabilized through a hydrogen bond contact to His L153 (Nε2), with distances of 2.2 Å for the *Rp. viridis* and 2.3 Å for the *Rb. sphaeroides* RCs. B_B makes contact with His M180 (2.1 Å) in *Rp. viridis* and His M182 (2.2 Å) in *Rb. sphaeroides* RC. His L153 forms additional hydrogen bonds involving its Nδ atom and the peptide carbonyl oxygens of Gly L149 and Ile L 150.

Similar to the primary donor, additional hydrogen bonds to B_A and B_B change their functional properties significantly. In order to introduce possible hydrogen bond donor groups for the ring V keto carbonyl of each bacteriochlorophyll, mutations were introduced in *Rb. sphaeroides* RCs at positions L177 (Ile to Asp) and M203 (Gly to Asp) near B_A and B_B, respectively. The mutations near B_B change the mid-point potential of D^+ by 25 mV or less and the mutation near B_A causes a roughly 3-fold decrease in the rate of the initial electron transfer (Williams et al., 1992).

D. The Bacteriopheophytins

The bacteriopheophytin on the A branch, Φ_A, is an intermediary electron acceptor while Φ_B is inactive in ET. Since the bacteriopheophytins lack a central magnesium ion, they are not bound to the polypeptide chain via histidine ligands. The sequence positions that correspond to the histidines in B_A and B_B, are methionine and leucine, respectively. Φ_A and Φ_B are surrounded by the transmembrane helices B, C, D, and E of the L- and M-subunit, respectively, and the interactions with the polypeptide chain are exclusively non-covalent. Φ_A (Φ_B) is sandwiched at van der Waals distances between B_A (B_B) and Q_A (Q_B). The shortest distance between the conjugated ring systems of D_A and Φ_A is 10 Å (Deisenhofer and Michel, 1989a, b). As is the case for the bacteriochlorophylls they obey close two-fold symmetry and are related by a –173.2° rotation when tetrapyrrole ring superposition is optimized.

The different properties of Φ_A and Φ_B can be derived from their environment. As shown for the special pair, the occurrence of aromatic residues is also asymmetric at the level of the bacteriopheophytins where the neighborhood of Φ_A is rich in aromatic residues. They render the Φ_A binding site rigid, stabilizing the position and orientation of the Φ_A molecule that lacks metal coordination by histidines. The Φ_B binding site, however, is formed by smaller amino acid residues. The structural features that derive from perfect symmetry are very similar in both types of RC (Ermler et al., 1994) except for the side chain at position 4 of the pyrrole ring II, which is an ethyl group in bacteriopheophytin *a* (*Rb. sphaeroides*) and an ethylidene group in bacteriopheophytin *b* (*Rp. viridis*). Hydrogen bonds with contact distances of about 2.9 Å are formed between the indole nitrogens of Trp L100 and Trp M129 (M127 in *Rp. viridis*) and the ester carbonyl oxygens of ring V. In Φ_A an additional hydrogen bond is observed between the ring V keto-O and the carboxyl group of Glu L104, which is most likely in its protonated state. Since the homologously related amino acid residue on B branch is threonine, it was postulated that Glu L104 has a special function. However, mutations of Glu L104 have no significant influence on the dynamics or unidirectionality of ET (Bylina et al., 1988).

Using the double mutant Gly M201 → Asp / Leu M212 → His of *Rb. capsulatus* it was possible to test the effect of the protein environment near B_A and Φ_A

on functional properties. Φ_A is replaced by a bacteriochlorophyll molecule because His M212 allows hydrogen bond contact be made between Asp M201 and the ring V of B_A. In this mutant only 70% of the yield of charge separation is directed towards the A branch, 15% is rapidly deactivated to the ground state, and 15% is directed to the B branch. This means that unidirectionality is perturbed in this double mutant RC (Heller et al., 1995a). Two phenylalanines are located between B_A and Φ_A, indicating a special involvement in ET. Replacement of these phenylalanines by site directed mutagenesis, however, does not significantly effect the charge separation process (Heller et al., 1995b). Resonance Raman spectroscopic methods demonstrate a temperature sensitivity of [Phi uc]$_A$ structure in *Rb. sphaeroides* RC (Peloquin et al., 1990 and 1991).An upshift of the skeletal mode of Φ_A by~4 cm^{-1} indicates a flattening of the macrocycle at low temperatures. It is assumed that the structural change influences the electron-transfer rates in the RC.

VII. Quinones and Non-Heme Iron

On its path through the RC, the electron is transferred from the intermediary electron acceptor Φ_A to the 'primary electron acceptor' quinone Q_A, and then to the 'secondary' acceptor Q_B. The quinones are stable electron acceptors. Q_A functions as a one-electron gate whereas Q_B becomes doubly reduced and can leave the RC in the form of quinol (dihydroquinone). In *Rb. sphaeroides* RCs both quinones are ubiquinone-10 molecules while in *Rp. viridis* RCs Q_A is a menaquinone-9 and Q_B a ubiquinone-9 molecule. Although the two types of quinones differ in structure, the Q_A binding pocket is very similar in both RCs. The quinones of several other bacterial RCs have been characterized (Agalidis et al., 1997):Q_A (Q_B) is menaquinone-7 (ubiquinone-7) in *Chromatium tepidium,* menaquinone-8 (ubiquinone-8) in *Rc. tenuis* and *Rubrivivax gelatinosus,* menaquinone-10 (menaquinone-10) in *Chloroflexus aurantiacus.* In these bacteria, the lengths of the Q_B quinone tails are as long as the tails of the Q_A molecules. For the RCs of *Rs. rubrum, Rs. centenum, Rb. sphaeroides,* and *Rb. capsulatus,* differences in the interactions between quinones and nearby protonatable residues have been postulated (Wang et al., 1994). Kinetic measurements have shown different pH dependences of charge recombination rates in these RCs. These findings indicate different properties of the Q_A and Q_B binding sites giving rise to imperfect symmetry at the level of the quinones.

A. The Primary Quinone

The binding pocket for Q_A is located on the A branch, although it is bound by amino acid residues of the M polypeptide. Q_A is situated proximally to the cytoplasmic side of the RC in a strongly hydrophobic domain of M. The isoprenoid side chain of Q_A is folded along the interface between L and M. A globular domain of the H polypeptide shields the Q_A binding pocket from the cytoplasm (Deisenhofer and Michel, 1989a,b). Q_A is kept in this position by two hydrogen bonds. The keto-oxygen (1-C=O) on the distal side (referred to the iron atom) is hydrogen bonded to the peptide nitrogen of Ala M260 in *Rb. sphaeroides* RC and Ala M258 in *Rp. viridis* RC with distances of 3.0 and 3.1 Å, respectively. The proximal (relative to the non-heme iron) keto-oxygen (4-C=O) forms a hydrogen bond to His M219/M217 with a distance of 2.9 Å in both RCs. This histidine is coordinated with the non-heme iron ion. The distances observed in the X-ray structures indicate a nearly symmetric binding of the Q_A molecule. This contradicts Fourier-transform infrared (FTIR) measurements of site-specific isotopically labeled ubiquinone-10 in R26 *Rb. sphaeroides* RCs. These studies show very strong interaction of the proximal keto-oxygen with His M219/217, but weak interaction of the distal keto-oxygen (Brudler et al., 1994; Breton et al., 1994).

Crucial for the electron transfer between Φ_A and Q_A is tryptophan M252/M250. The indole ring of this amino acid is in van der Waals contact with both cofactors. Its ring system is oriented parallel to the Q_A head group. Tryptophan M252/M250 is the only amino acid residue lying on the potential electron path between Φ_A and Q_A. In both RCs the symmetry-related position in the L polypeptide is occupied by a phenylalanine. A detailed mutagenesis and kinetic study of this tryptophan in *Rb. sphaeroides* RC is presented in Stilz et al. (1994). The mutants M252 Trp $\rightarrow$ Phe and Trp $\rightarrow$ Tyr grow under photosynthetic conditions with a rate comparable to the wild type, but Q_A is less firmly bound to its binding site. Following a method developed by Okamura et al. (1975) several types of quinones have been inserted into *Rb. sphaeroides* RCs (Sebban, 1988). The Anthraquinone, e.g., possesses two additional

benzene rings compared to ubiquinone; nevertheless, it is easily tolerated in the binding pocket (Kuglstatter, 1999). In *Rp. viridis* RCs, the native Q_A can be replaced by high concentrations of an extraneous quinone (Breton, 1997). FTIR spectroscopy shows that the Q_A pocket of this RC has similar bonding interactions for vitamin K_1 as the one from *Rb. sphaeroides* whereas the interactions for ubiquinones are significantly different (Breton, 1997).

B. The Non-Heme Iron

The ferrous non-heme iron is located between the two quinones on the cytoplasmic side of the RC and is positioned close to the two-fold symmetry axis. It is kept in its position by five side chain residues, the four histidines L190, L230, M219/217 (*Rb. sphaeroides/Rp. viridis*) and M266/264 and the glutamate M234/232. His L190 and M219/217 interact with Q_A and Q_B, respectively. The histidines are located at the D and E helices of M and L. They are conserved in both bacterial and plant systems. Glu M234/232, a residue of helix de in M is conserved in bacterial RCs. The non-heme iron is the central component of the Q_B-HisL190-Fe-HisM219-Q_A system which represents the segment of ET where the electrons are transferred parallel to the membrane (Fig. 11). Surprisingly, removal of the iron has no drastic effects on the function of the RC. The iron depleted RCs do work, but the rate of ET from Q_A^- to Q_B is slower by a factor of 2. Reconstitution of the iron binding site with Mn^{2+}, Co^{2+}, Ni^{2+}, Cu^{2+}, or Zn^{2+} barely changes the characteristics of the native RC (Debus et al., 1986). In the RC of *Rb. sphaeroides* strain Y a Mn^{2+} occupies this place. It is coordinated in the same way as the Fe^{2+} in the other RCs (Arnoux et al., 1995). A superposition of the RCs from *Rb. sphaeroides* and *Rp. viridis* in a region around the Fe^{2+} shows a high level of identity consistent with the importance of the iron-histidine complex (Ermler et al., 1994).

The environment of the iron is a distorted octahedron with axial ligands His L230 and His M266/264, and equatorial ligands His L190, His 219/217, and Glu M234/232 (Deisenhofer and Michel, 1989a,b). Surprisingly, a specific function for the iron atom in ET has yet to be observed. Its coordination with histidines of the L- and M-polypeptide implies a structural role: to stabilize the relative position of L and M. The carboxylate group of M234/232 acts as a bidentate ligand.

C. The Secondary Quinone

The loss of more than 50% of native Q_B during purification of bacterial RCs causes unreliable modeling of Q_B in terms of its position and hydrogen bonding. Although located in the domain of the B branch, the Q_B molecule is hydrogen bonded exclusively with the L polypeptide in a position close to the H polypeptide and to the cytoplasmic side of the RC. Symmetric with Q_A, the Q_B molecule is embedded in a domain formed by helices D, E, de, and a loop segment of the L-subunit. With respect to

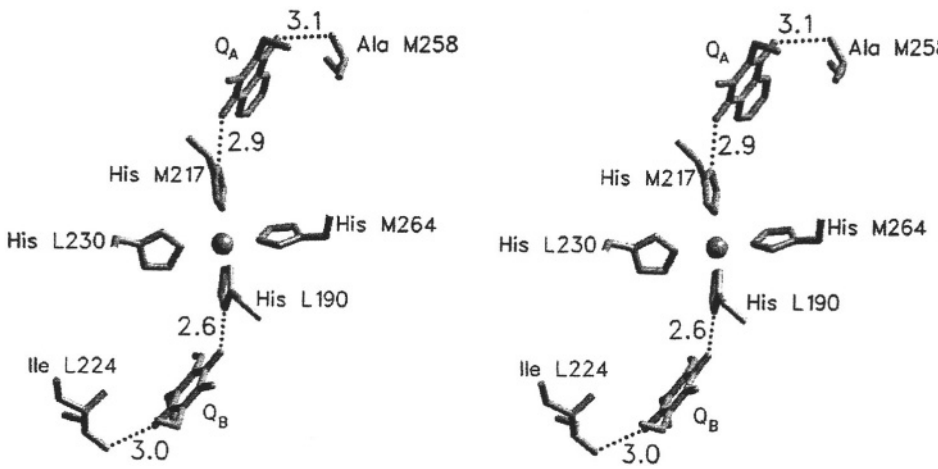

Fig. 11. Stereo view of the Q_A–Fe–Q_B cluster in the *Rp. viridis* RC. The hydrogen bonding of the proximal and distal keto-oxygens from both quinones, the non-heme iron and its four histidine ligands is illustrated. A straight line extends from the proximal Q_A keto-oxygen to the proximal Q_B keto-oxygen via the non-heme iron.

other structural and functional aspects, striking differences exist between the two quinones. Thus, the environment of Q_B is strongly polar while it is rather apolar around Q_A.

A thorough analysis of the Q_B pocket structure is presented in Lancaster and Michel (1997). A difference of 5 Å was observed in two positions between the Q_B head-groups from *Rb. sphaeroides* and *Rp. viridis* RC (Ermler et al., 1994). A reinvestigation of the original data set of the *Rp. viridis* RC by Lancaster and Michel (1997) showed that the native Q_B, in contrast to the earlier analysis (Deisenhofer et al., 1995), is dominantly localized in the distal position. The two positions of Q_B are represented in Fig. 12 where Q_{BD} (Q_{BP}) means the distal (proximal) position of Q_B. The distal position of the secondary quinone is also observed in a 2.2 Å resolution structure of the RC from the *Rb. sphaeroides* R-26 strain obtained with tetragonal crystals exposed to X-rays at cryogenic temperature (Stowell et al., 1997; Abresch et al., 1998). The peptide nitrogen of Ile L224 forms a hydrogen bond to the distal keto-O of Q_B in its distal position. It is the only hydrogen bond that is observed in the distal as well as in the proximal position. The transition between both Q_B positions includes a 180° flip of the quinone around its isoprenoid tail (Lancaster and Michel, 1997). The occurrence of such a ring flip is confirmed by the analysis of light-induced structural changes observed with tetragonal crystals of *Rb. sphaeroides* R-26 RCs (Stowell et al., 1997) at cryogenic temperatures where the native ubiquinone was partially replaced by ubiquinone-2. The position of Q_B in the charge neutral state is distal whereas that of the charge separated state corresponds to the proximal position of Q_B as described for the *Rp. viridis* RC with exchanged ubiquinone-2. Stowell et al. (1997) postulate that the quinone, before its reduction to ubisemiquinone, makes a '180° propeller twist' and moves towards the cytoplasm.

The crystallographic refinement of a *Rp. viridis* RC in which the Q_B molecule was reconstituted by ubiquinone-2 shows a well defined proximal position of the ubiquinone-2 molecule (Lancaster and Michel, 1997). This ubiquinone is shorter and less hydrophobic than the native ubiquinone-9 and can move more proximal to the non-heme iron. In the refined structure of this RC, three hydrogen bonds of ubiquinone-2 can be assigned: His L190 (coordinated with the non-heme iron) forms a hydrogen bond

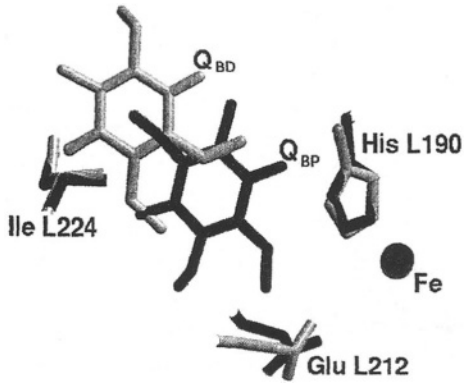

Fig. 12. The two positions of the secondary quinones in both RCs. The distal position (Q_{BD}) is shown in grey, the proximal (Q_{BP}) in black. The two positions reflect two different states of this molecule in the RC. The distal position has been found, e.g., for RCs with native Q_B (*Rb. sphaeroides* RC in Ermler et al. (1994), *Rp. viridis* RC in the reinvestigated structure of Lancaster and Michel, (1997)). The proximal position is found for the ubiquinone-2 reconstituted *Rp. viridis* RC (Lancaster and Michel, 1997).

(2.6 Å) to the proximal keto-oxygen of Q_B, and the distal keto-oxygen accepts two hydrogen bonds from Ile L224 and Gly L225 peptide nitrogens. A more difficult assignment is a hydrogen bond to Ser L223 which, according to its position, can interact either with the distal keto-oxygen of Q_B or with Asn L213. Conclusions from studies with the Ser L223 → Ala mutant in *Rb. sphaeroides* (Paddock et al., 1990) and *Rb. capsulatus* RC (Bylina and Wong, 1992) support the idea of a Ser L223–Asn L213 hydrogen bond in the *Rp. viridis* RC as has been discussed by Lancaster and Michel (1997). An important constituent of the Q_B binding pocket is Phe L216 that is oriented parallel to the quinone molecule and separated from it by about 3.5 Å, shielding the hydrophobic Q_B head group against the polar environment. Evidence for this role of the phenylalanine was provided by the mutant Phe L216 → Ser in *Rp. viridis* RC where the affinity for quinone binding is decreased (Sinning et al., 1989).

Michel et al. (1986b) describe two X-ray structures of *Rp. viridis* RCs where the competitive inhibitors terbutryn [2-(methylthio)-4-(ethylamino)-6-(*tert*-butylamino)-*s*-triazine] and *o*-phenanthroline are bound into the Q_B pocket. Terbutryn interacts with the protein via hydrogen bonds to Ser L223 and Ile L224 and is located close to the hydrophobic 'entrance' of the Q_B binding site. *o*-Phenanthrolin is situated nearer the 'bottom' of the Q_B pocket and

forms a hydrogen bond with His L190 Nδ. The structure of the quinone depleted binding site for the *Rp. viridis* RC has been analyzed by Lancaster and Michel (1997). Q_B is replaced by a detergent (LDAO) molecule and a cluster of five or six water molecules which are bridged with the LDAO molecule and with the hydrogen bonding donors for Q_B. Another pattern of hydrogen bonding has been revealed by an X-ray structure analysis of a *Rp. viridis* RC where Q_B was substituted by the Q_B site inhibitor stigmatellin A (Lancaster and Michel, 1997). The hydrogen bonds of ubiquinone-2 are maintained with the stigmatellin molecule. In addition, the proximal methoxy oxygen atom of stigmatellin is in hydrogen bond distance to His L190 Nδ, and the stigmatellin hydroxyl group can act as a hydrogen donor to the Ser L223 Oγ atom. This extensive hydrogen bonding pattern explains the high affinity of stigmatellin.

By evaluating the richness of structural data from the *Rp. viridis* RC, Lancaster and Michel (1997) have proposed a mechanistic model of electron and proton coupling that is consistent with all relevant structural results of the Q_B site presented so far. The neutral Q_B binds to the distal position; at this time the proximal position is filled with several water molecules. Then the Q_B molecule flips around its isoprenoid chain and moves towards the proximal position displacing several water molecules. In this state, an electron is transferred from Q_A to Q_B giving Q_B^-. After accepting a second electron and one proton, the monoprotonated, doubly reduced intermediate Q_BH^- is assumed to occupy the proximal binding position. It accepts a second proton forming ubiquinol (Q_BH_2) which leaves the Q_B pocket that is subsequently filled by five or six water molecules. X-ray crystallographic studies with *Rb. sphaeroides* R-26 RC in the dark and under illumination (Stowell et al,, 1997 and Abresch et al., 1998) are in agreement with this model.

The structures of the Q_B binding sites from other purple bacteria are not known, but flash-induced absorbance spectroscopical methods provide evidence for structural differences between the RCs from *Rb. capsulatus* and *Rb. sphaeroides.* Measurements of the pH dependence of $P^+Q_B^-/PQ_B$ recombination rates for wild type and mutant RCs from *Rb. capsulatus* reveal effects thought to be caused by structural differences (Baciou et al., 1993).

VIII. Clusters of Firmly Bound Water Molecules and Proton Transfer

While the structural conditions for light absorption and electron transfer in photosynthetic RCs have been studied in considerable detail, less is known about the transfer of protons over a distance of several Å. Such transfer is thought to be facilitated by suitable arrangements of protonatable amino acid residues and firmly bound water molecules, since the protein matrix is usually considered as an insulator of proton conduction. Numerous firmly bound water molecules are observed in the *Rb. sphaeroides* RC domain close to the cytoplasm (Ermler et al., 1994; Fritzsch et al., 1996, 1998; Stowell et al., 1997; Abresch et al., 1998). Clusters consisting of several interconnected water molecules are located close to the primary and secondary quinones where they are associated with parts of the L-, M-, and H-subunit. One water cluster has been identified close to Q_A (Fritzsch et al., 1998) (Fig. 13). The shortest distance between the cluster and the quinone is 5 Å, which is too long for an interaction mediated by hydrogen bonding. One water molecule approaches the surface of the RC to about 4 Å. It is assumed that this water cluster is involved in the partial proton uptake by the RC upon reduction.

The other water clusters are connected to amino acid residues that are crucial for the protonation of Q_B. One chain-like cluster is oriented perpendicular to the membrane and extends from the cytoplasm to Glu L212 (Q_B-glu cluster) (Fig. 14 left). It is about 20 Å long. In the structure refined from trigonal crystals, this cluster consists of 12 water molecules and contacts the surface of the RC. In the structure from tetragonal crystals this chain has two branches with both contacting the protein surface (Abresch et al., 1998). Another water cluster runs almost parallel to the membrane and is in contact with Asp L213 (Q_B-asp cluster) (Fig. 14 right). It is more bulky than the Q_B-glu cluster and has also contact with the surface of the protein. The shortest hydrogen-bonded pathway between Q_B and the surrounding of the RC is 7 Å long and connects Asp L213 with Asp M17 that is located at the surface of the RC. The X-ray structure of *Rp. viridis* RC reveals similar water clusters near the cytoplasm (Lancaster et al., 1996; Lancaster and Michel, 1996, 1997). Further examples of membrane-bound proteins containing interconnected water

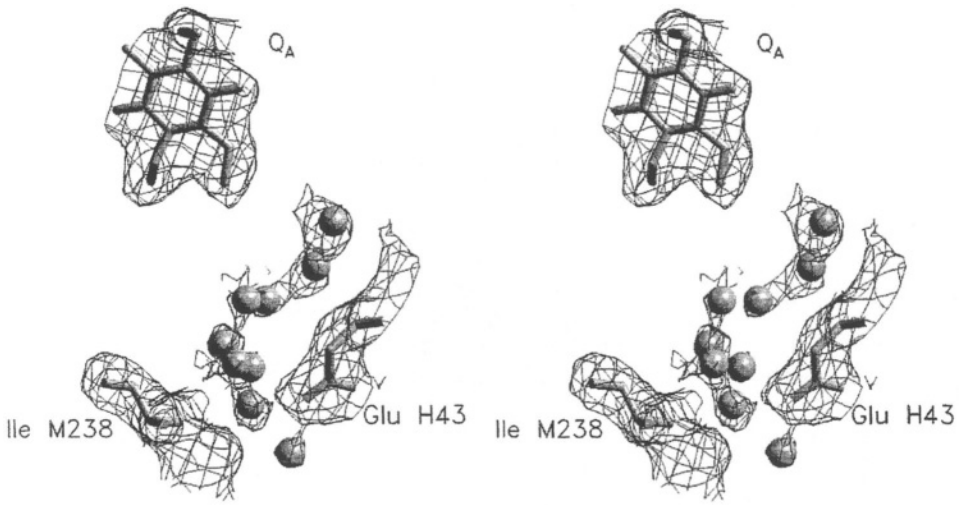

Fig. 13. Stereo view of nine water molecules from the Q_A cluster. The electron density is contoured at a level of 1.0 σ above the mean density of the map.

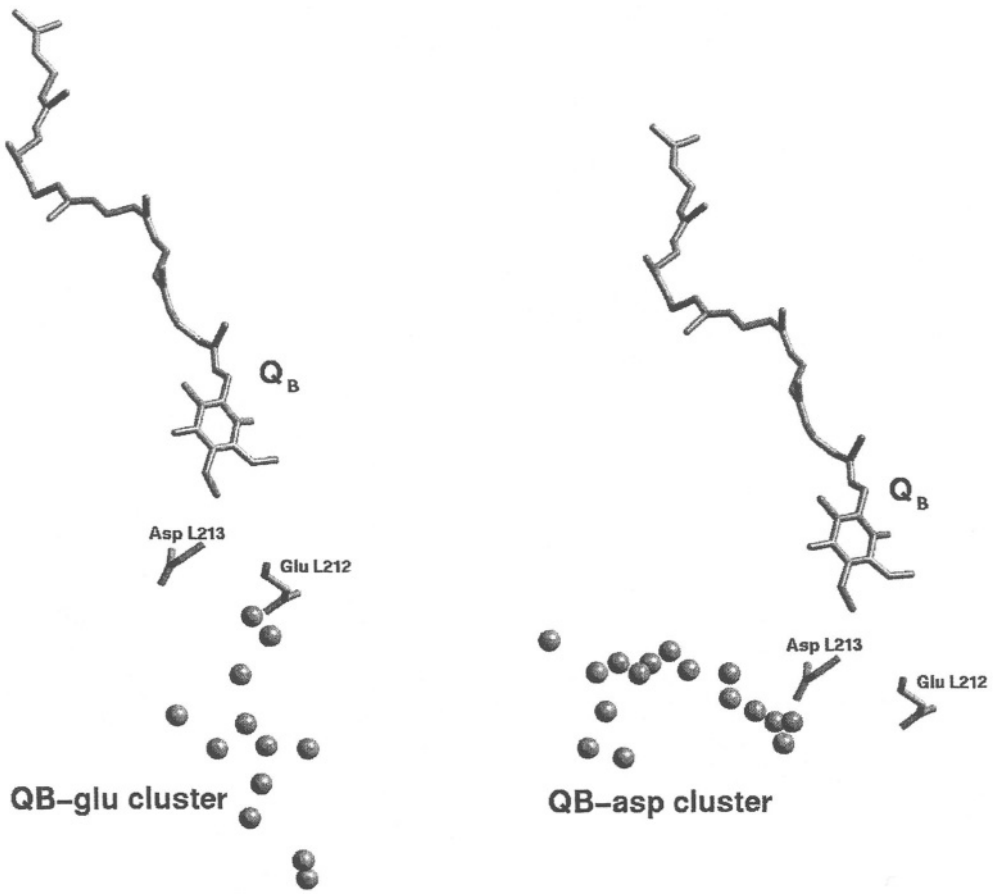

Fig. 14. Water clusters proximal to Q_B. Left: The Q_B-glu cluster which is oriented perpendicular to the plane of the membrane. Right: The Q_B-asp cluster which is oriented almost parallel to the plane of the membrane.

molecules are the *f* subunit of chloroplast cytochrome b_6f complex (Martinez et al., 1996) and the cytochrome *c* oxidase from *Paracoccus denitrificans* (Ostermeier et al., 1997). The water clusters provide paradigms for the analysis of proton transfer involving water molecules and ionizable amino acid residues.

IX. Comparison with Photosystem II

Sequence comparisons between the L- and M-subunits from bacterial RCs, on the one hand, and the D1 - and D2-subunits from cyanobacteria, algae, and higher plants, on the other, reveal similarity indicative of a close evolutionary relationship (Michel and Deisenhofer, 1988). The function of the D1- and D2-subunits at the core of Photosystem II (PS II), the site of primary charge separation, was confirmed by biochemical experiments with a PS II complex from spinach grana thylakoids consisting of D1, D2, and cytochrome *b*-559 (Nanba and Satoh, 1987). It seems most likely that the relatives of cyanobacteria have 'acquired' the bacterial RC and supplemented it with a water splitting apparatus. Amino acids with structural functions like histidines, glycines, prolines, and arginines are conserved (Deisenhofer and Michel, 1989 b). Also conserved is the tyrosine close to D (Tyr L162 in bacterial RCs). This residue probably plays a role in the re-reduction of D^+. Amino acids that are not conserved include those involved in the binding of B_A and B_B plus the glutamic acid that functions as a bidentate ligand for the non-heme iron. Primary sequence analysis suggests the occurrence of five helices in both D1 and D2, just like the L- and M-subunits of bacterial RCs. A new cryoelectron microscopic structure determination from two-dimensional crystals of a PS II sub-core complex yielded a projection map at 8 Å resolution (Rhee et al., 1997). A projected density map of the L- and M-subunits from *Rp. viridis* RC shows similarity to a certain domain of the PS II projection structure as demonstrated by cross-correlation of the two maps. From this analysis likely positions of D1 and D2 in the PS II structure are concluded.

X. Outlook

The bacterial RC is arguably the best analyzed membrane protein. A wealth of structural information has elucidated essential functional details of bacterial light-driven electron and proton transfer. These results have greatly impacted research on biological energy transduction. To date only static structures of the RC from non-sulfur purple bacteria have been determined by X-ray structure analysis. However, photosynthetic processes involve time-dependent structural changes that are triggered by charge separation, electron transfer and proton transfer. For example, trypsination of *Rb. sphaeroides* RCs (Brzezinski and Andréasson, 1995) showed protein conformational changes after charge separation. Tiede et al. (1996) describe temperature-dependent conformational changes that are associated with the electron transfer from Q_A to Q_B. It is assumed that temporary structural changes are needed to stabilize certain intermediate states and to facilitate otherwise energetically unfavorable processes. Analysis of those structural changes by time-resolved techniques is a big challenge for future studies of bacterial RCs.

Acknowledgments

We thank Dr. C.R.D. Lancaster, Prof. H. Michel, Dr. B.C. Monk, and Dr. C. S. Wright for reading the manuscript. In this article, the graphics program SETOR (Evans, 1993) has been used for the preparation of Figures 4–14.

References

Abresch EC, Paddock ML, Stowell MHB, McPhillips TM, Axelrod HL, Soltis SM, Rees DC, Okamura MY and Feher G (1998) Identification of proton transfer pathways in the X-ray crystal structure of the bacterial reaction center from *Rhodobacter sphaeroides.* Photosynth Res 55: 119–125

Adir N, Axelrod HL, Beroza P, Isaacson RA, Rongey SH, Okamura MY and Feher G (1996) Co-crystallization and characterization of the photosynthetic reaction center cytochrome *c*-2 complex from *Rhodobacter sphaeroides.* Biochemistry 35: 2535–2547

Agalidis I, Ivancich A, Mattioli TA and Reiss-Husson F (1997) Characterization of the *Rhodocyclus tenuis* photosynthetic reaction center. Biochim Biophys Acta 1321: 31–46

Allen JP (1994) Crystallization of the reaction center from *Rhodobacter sphaeroides* in a new tetragonal form. Proteins 20: 283–286

Allen JP and Feher G (1991) Crystallization of reaction centers from *Rhodobacter sphaeroides.* In: Michel H (ed) Crystallization of Membrane Proteins, pp 137–153. CRC Press, Boca Raton, Ann Arbor, Boston

Allen JP, Feher G, Yeates TO, Deisenhofer J, Michel H and Huber R (1986) Structural homology of reaction centers from

Rhodobacter sphaeroides and *Rhodopseudomonas viridis* as determined by X-ray diffraction. Proc Natl Acad Sci USA 83: 8589–8593

Arlt T, Schmidt S, Kaiser W, Lauterwasser C, Meyer M, Scheer H and Zinth W (1993) The accessory bacteriochlorophyll: A real electron carrier in primary photosynthesis. Proc Natl Acad Sci USA 90: 11757–11761

Arnoux B and Reiss-Husson F (1996) Pigment-protein interactions in *Rhodobacter sphaeroides* Y photochemical reaction center; comparison with other reaction center structures. Eur Biophys J 24: 233–242

Arnoux B, Ducruix A, Reiss-Husson F, Lutz M, Morris J, Schiffer M and Chang CH (1989) Structure of spheroidene in the photosynthetic reaction center from *Rhodobacter sphaeroides* Y. FEBS Lett 258: 47–50

Arnoux B, Gaucher JF, Ducruix A and Reiss-Husson F (1995) Structure of the photochemical reaction centre of a spheroidene-containing purple bacterium, *Rhodobacter sphaeroides* Y, at 3 Å resolution. Acta Cryst D51: 368–379

Baciou L, Bylina EJ and Sebban P (1993) Study of wild type and genetically modified reaction centers from *Rhodobacter capsulatus*: Structural comparison with *Rhodopseudomonas viridis* and *Rhodobacter sphaeroides.* Biophys J 65: 652–660

Bautista JA, Chynwat V, Cua A, Jansen FJ, Lugtenburg J, Gosztola D, Wasiliewski MR and Frank H (1998) The spectroscopic and photochemical properties of locked-15, 15′-*cis*-spheroidene in solution and incorporated into the reaction center of *Rhodobacter sphaeroides* R-26.1. Photosynth Res 55: 49–65

Bernstein FC, Koetzle TF, Williams GJB, Meyer EF, Brice MD, Rodgers JR, Shimanouchi T and Tasumi M (1977) The Protein Data Bank: A computer-based archival file for macromolecular structures. J Mol Biol 112: 535–542

Blankenship RE, Madigan MT and Bauer CE (eds) (1995) Anoxygenic Photosynthetic Bacteria. Kluwer Academic Publishers, Dordrecht

Breton J (1997) Efficient exchange of the primary quinone acceptor Q-A in isolated reaction centers of *Rhodopseudomonas viridis.* Proc Natl Acad Sci USA 94: 11318–11323

Breton J and Verméglio A (eds) (1988) The Photosynthetic Bacterial Reaction Center: Structure and Dynamics. Plenum Press, New York

Breton J and Verméglio A (eds) (1992) The Photosynthetic Bacterial Reaction Center II, NATO-ASI Series A, Life Sciences 237. Plenum Press, New York

Breton J, Boullais C, Burie J-R, Nabedryk E and Mioskowski C (1994) Binding sites of quinones in photosynthetic bacterial reaction centers investigated by light-induced FTIR difference spectroscopy: Assignment of the interactions of each carbonyl of Q_A in *Rhodobacter sphaeroides* using site-specific ^{13}C-labeled ubiquinone. Biochemistry 33: 14378–14386

Brudler R, de Groot HJM, van Liemt WBS, Steggerda WF, Esmeijer R, Gast P, Hoff AJ, Lugtenburg J and Gerwert K (1994) Asymmetric binding of the 1-and 4-C=O groups of Q_A in *Rhodobacter sphaeroides* R26 reaction centres monitored by Fourier transform infra-red spectroscopy using site-specific isotopically labelled ubiquinone-10. EMBO J 13: 5523–5530

Brzezinski P and Andréasson L-E (1995) Trypsin treatment of reaction centers from *Rhodobacter sphaeroides* in the dark and under illumination: Protein structural changes follow charge separation. Biochemistry 34: 7498–7506

Buchanan SKB, Fritzsch G, Ermler U and Michel H (1993) New crystal form of the photosynthetic reaction centre from *Rhodobacter sphaeroides* of improved diffraction quality. J Mol Biol 230: 1311–1314

Bylina EJ and Wong R (1992) Analysis of spontaneous herbicide resistant revertants derived from *Rhodobacter capsulatus* in which Ser L223 of the reaction center is replaced with alanine. In: Murata N (ed) Research in Photosynthesis, Vol 1, pp 369–372. Kluwer Academic Publishers, Dordrecht

Bylina EJ, Kirmeier C, McDowell L, Molten D and Yuovan DC (1988) Influence of an amino-acid residue on the optical properties and electron transfer dynamics of a photosynthetic reaction centre complex. Nature 336: 182–184

Chamorovsky SK, Zakhorova NI, Remennikov SM, Sabo YA and Rubin AB (1998) The cytochrome subunit structure in the photosynthetic reaction center of *Chromatium minutissimum.* FEBS Lett 422: 231–234

Chang CH, Tiede D, Tang J, Smith U, Norris J and Schiffer M (1986) Structure of *Rhodobacter sphaeroides* R-26 reaction center. FEBS Lett 205: 82–86

Chang CH, El Kabbani O, Tiede D, Norris J and Schiffer M (1991) Structure of the membrane-bound protein photosynthetic reaction center from *Rhodobacter sphaeroides.* Biochemistry 30: 5352–5360

Chirino AJ, Lous EJ, Huber M, Allen JP, Schenck CC, Paddock ML, Feher G and Rees DC (1994) Crystallographic analyses of site-directed mutants of the photosynthetic reaction center from *Rhodobacter sphaeroides.* Biochemistry 33: 4584–4593

Claus D, Lack P and New B (1989) Catalogue of Strains, 4. Edition, p 280. DSM–Deutsche Sammlung von Mikroorganismen und Zellkulturen GmbH, Braunschweig, Germany

Debus RJ, Feher G and Okamura MY(1986) Iron-depleted reaction centers from *Rhodobacter sphaeroides* R-26: Characterization and reconstitution with Fe^{2+}, Mn^{2+}, Co^{2+}, Ni^{2+}, Cu^{2+}, and Zn^{2+}. Biochemistry 25: 2276–2287

De Groot HJM, Gebhard R, van der Hoef I, Hoff AJ, Lugtenburg J, Violette CA and Frank HA (1992) ^{13}C Magic angle spinning NMR evidence for a 15,15′-*cis* configuration of the spheroidene in the *Rhodobacter sphaeroides* photosynthetic reaction center. Biochemistry 31: 12446–12450

Deisenhofer J and Michel H (1989a) The photosynthetic reaction center from the purple bacterium *Rhodopseudomonas viridis.* Science 245: 1463–1473

Deisenhofer J and Michel H (1989b) The photosynthetic reaction centre from the purple bacterium *Rhodopseudomonas viridis.* EMBO J 8: 2149–2170

Deisenhofer J and Norris JR (eds) (1993) The Photosynthetic Reaction Center. Academic Press, San Diego

Deisenhofer J, Epp O, Miki K, Huber R and Michel H (1984) X-ray structure analysis of a membrane protein complex: electron density map at 3 Å resolution and a model of the chromophores of the photosynthetic reaction center from *Rhodopseudomonas viridis.* J Mol Biol 180: 385–398

Deisenhofer J, Epp O, Miki K, Huber R and Michel H (1985) Structure of the protein subunits in the photosynthetic reaction center of *Rhodopseudomonas viridis* at 3 Å resolution. Nature 318, 618–642

Deisenhofer J, Epp O, Sinnig I and Michel H (1995) Crystallographic refinement at 2.3 Å resolution and refined model of the photosynthetic reaction center from *Rhodopseudomonas viridis.* J Mol Biol 246: 429–457

Dohse B, Mathis P, Wachtveitl J, Laussermair E, Iwata S, Michel H and Oesterhelt D (1995) Electron transfer from the tetraheme cytochrome to the special pair in the *Rhodopseudomonas viridis* reaction center: Effects of mutations of tyrosine L162. Biochemistry 34: 11335–11343

Ermler U, Fritzsch G, Buchanan SK and Michel H (1994) Structure of the photosynthetic reaction centre from *Rhodobacter sphaeroides* at 2.65 Å resolution: Cofactors and protein-cofactor interactions. Structure 2: 925–936

Evans SV (1993) SETOR: Hardware lighted three-dimensional solid model representations of macromolecules. J Mol Graphics 11: 134–138

Feher G and Okamura MY (1978) Chemical composition and properties of reaction centers. In: Clayton RC and Sistrom WR (eds) The Photosynthetic Bacteria, pp 349–386. Plenum Press, New York

Frank HA and Cogdell RJ (1996) Carotenoids in photosynthesis. Photochem Pholobiol 63: 257–264

Frank HA and Violette CA (1989) Monomeric bacteriochlorophyll is required for the triplet energy transfer between the primary donor and the carotenoid in photosynthetic bacterial reaction centers. Biochim Biophys Acta 976: 222–232

Frank HA, Taremi SS, Knox JR and Mäntele W (1988) Single crystals of the photochemical reaction center from *Rhodobacter sphaeroides* wild type strain 2.4.1 analyzed by polarized light. In: Breton J and Verméglio A (eds) The Photosynthetic Bacterial Reaction Center, pp 27–32. Plenum Press, New York

Frank HA, Chynwat V, Hartwich G, Meyer M, Katheder I and Scheer H (1993) Carotenoid triplet state formation in *Rhodobacter sphaeroides* R-26 reaction centers exchanged with modified bacteriochlorophyll pigments and reconstituted with spheroidene. Photosynth Res 37: 193–203

Fritzsch G (1998) Obtaining crystal structures from bacterial photosynthetic reaction centers. Methods Enzymol 297: 57–77

Fritzsch G, Buchanan S and Michel H (1989) Assignment of cytochrome hemes in crystallized reaction centers from *Rhodopseudomonas viridis*. Biochim Biophys Acta 977: 157–162

Fritzsch G, Ermler U, Merckel M and Michel H (1996) Crystallization and structure of the photosynthetic reaction centres from *Rhodobacter sphaeroides*—wild type and mutants. In: Michel-Beyerle M-E (ed) Reaction Centers of Photosynthetic Bacteria. Structure and Dynamics, pp 3–13. Springer-Verlag, Berlin

Fritzsch G, Kampmann L, Kapaun G and Michel H (1998) Water clusters in the reaction centre of *Rhodobacter sphaeroides*. Photosynth Res 55: 127–132

Hantke K and Braun V (1973) Covalent binding of lipid to protein. Eur J Biochem 34: 284–296

Heller B A, Holten D and Kirmaier C (1995a) Control of electron transfer between the L- and M-sides of photosynthetic reaction centers. Science 269: 940–945

Heller B A, Holten D and Kirmaier C (1995b) Characterization of bacterial reaction centers having mutations of aromatic residues in the binding site of the bacteriopheophytin intermediary electron carrier. Biochemistry 34: 5294–5302

Hodel A, Kim SH and Brünger AT (1992) Model bias in macromolecular crystal structures. Acta Crystallogr A 48: 851–858

Holzapfel W, Finkele U, Kaiser W, Oesterhelt D, Scheer H, Stilz HU and Zinth W (1990) Initial electron-transfer in the reaction center from *Rhodobacter sphaeroides*. Proc Natl Acad Sci USA 87: 5168–5172

Ippolito JA, Alexander RS and Christianson DW (1990) Hydrogen bond stereochemistry in protein structure and function. J Mol Biol 215: 457–471

Kapaun G (1998) Röntgenkristallographische Untersuchungen am Reaktionszentrum von *Rb. sphaeroides*: hochaufgelöste Wildtypstruktur und Cofaktor-Austausch. Diploma thesis, Johann Wolfgang Goethe-Universität, Frankfurt

Kirmaier C and Holten D (1991) An assessment of the mechanism of initial electron transfer in bacterial reaction centers. Biochemistry 30: 609–613

Kirmaier C, Holten D and Parson WW (1985) Picosecond-photodichroism studies of the transient states in *Rhodopseudomonas sphaeroides* reaction centers at 5 K. Effects of electron transfer on the six bacteriochlorin pigments. Biochim Biophys Acta 810: 49–61

Koepke J, Hu X, Muenke C, Schulten K and Michel H (1996) The Crystal Structure of the Light-Harvesting Complex II (B800-850) from *Rhodospirillum molischianum*. Structure 4: 581–597

Koyama Y, Takatsuka I, Kanaji M, Tomimoto K, Kito M, Shimamura T, Yamashita J, Saiki K and Tsukida K (1990) Configurations of carotenoids in the reaction center and light-harvesting complex of *Rhodospirillum rubrum*. Natural selection of carotenoid configurations by pigment protein complexes. Photochem Photobiol 51: 119–128

Krauss N, Schubert WD, Klukas O, Fromme P, Witt T and Saenger W (1996) Photosystem I at 4 Å resolution represents the first structural model of a joint photosynthetic reaction centre and core antenna system. Nature Struct Biol 3: 965–973

Kuglstatter A (1999) Röntgenkristallographische Untersuchungen am photosynthetischen Reaktionszentrum des Purpurbakteriums *Rhodoabcter sphaeroides*: Punktmutationen und Kofaktoraustausch. Diploma thesis, Johann Wolfgang Geothe-Universität, Frankfurt

Kuglstatter A, Fritzsch G and Michel H (1999) Crystallographic analysis of the mutant reaction center M 197 (FY) from *Rhodobacter sphaeroides*. In: Garab G (ed) Photosynthesis: Mechanisms and Effects, Vol II, pp 699–702. Kluwer Academic Publishers, Dordrecht

Laible PD, Chynwat V, Thurnauer MC, Schiffer M, Hanson DK and Frank H (1998) Protein modifications affecting triplet energy transfer in bacterial photosynthetic reaction centers. Biophys J 74: 2623–2637

Lancaster CRD and Michel H (1996) New insights into the X-ray structure of the reaction center from *Rhodopseudomonas viridis*. In: Michel-Beyerle ME(ed) Reaction Centers of Photosynthetic Bacteria. Structure and Dynamics, pp 23–35. Springer-Verlag, Berlin

Lancaster CRD and Michel H (1997) The coupling of light-induced electron transfer and proton uptake as derived from crystal structures of reaction centres from *Rhodopseudomonas viridis* modified at the binding site of the secondary quinone, Q_B. Structure 5: 1339–1359

Lancaster CRD and Michel H (1999a) The structure of the *Rhodopseudomonas viridis* reaction centre—an overview and recent advances. In: Garab G (ed) Photosynthesis: Mechanisms and Effects, Vol II, pp 673–678. Kluwer Academic Publishers, Dordrecht

Lancaster CRD and Michel H (1999b) Refined crystal structures of reaction centres from *Rhodopseudomonas viridis* in complexes with the herbicide atrazine and two chiral atrazine derivatives also lead to a new model of the bound carotenoid. J Mol Biol 286: 883–898

Lancaster CRD, Ermler U and Michel H (1995) The structures of photosynthetic reaction centers from purple bacteria as revealed by X-ray crystallography. In: Blankenship RE, Madigan MT and Bauer CE (eds) Anoxygenic Photosynthetic Bacteria, pp 503–526. Kluwer Academic Publishers, Dordrecht

Lancaster CRD, Michel H, Honig B and Gunner MR (1996) Calculated coupling of electron and proton transfer in the photosynthetic reaction centre of *Rhodopseudomonas viridis*. Biophys J 70: 2469–2492

Lous EJ and Hoff AJ (1989) Isotropic and linear dichroitic triplet-minus-singlet absorbance difference spectra of two carotenoid-containing bacterial photosynthetic reaction centers in the temperature range 10–288 K. An analysis of the bacteriochlorophyll-carotenoid triplet-transfer. Biochim Biophys Acta 974: 88–103

Lutz M, Szponarski W, Berger G, Robert B and Neuman JM (1987) The stereoisomerism of bacterial, reaction-center-bound carotenoids revisited: an electronic absorption, resonance Raman and ^{1}H-NMR study. Biochim Biophys Acta 894: 423–433

Luzzati PV (1952) Traitement statistique des erreurs dans la détermination des structures cristallines. Acta Crystallogr 5: 802–810

Martinez SE, Huang D, Ponomarev M, Cramer WA and Smith JL (1996) The heme redox center of chloroplast cytochrome *f* is linked to a buried five-water chain. Protein Science 5: 1081–1092

Mathis P (1994) Electron transfer between cytochrome c_2 and the isolated reaction center of purple bacterium *Rhodobacter sphaeroides*. Biochim Biophys Acta 1187: 177–180

McDermott G, Prince SM, Freer AA, Hawthornwaite-Lawless AM, Papiz MZ, Cogdelt RJ and Isaacs NW (1995) Crystal structure of an integral membrane light-harvesting complex from photosynthetic bacteria. Nature 374: 517–521

Michel H (1982) Three-dimensional crystals of a membrane protein complex. J Mol Biol 158: 567–572

Michel H (1983) Crystallization of membrane proteins. Trends Biochem Sci 8:56–59

Michel H and Deisenhofer J (1988) Relevance of the photosynthetic reaction center from purple bacteria to the structure of Photosystem II. Biochemistry 27: 1–7

Michel H, Weyer KA, Gruenberg K, Dunger I, Oesterhelt D and Lottspeich F (l986a) The 'light' and 'medium' subunits of the photosynthetic reaction centre from *Rhodopseudomonas viridis*: Isolation of the genes, nucleotide and amino acid sequence. EMBO J 5: 1149–1158

Michel H, Epp O and Deisenhofer J (1986b) Pigment-protein interactions in the photosynthetic reaction centre from *Rhodopseudomonas viridis*. EMBO J 5: 2445–2451

Michel-Beyerle ME (ed) (1985) Antennas and Reaction Centers of Photosynthetic Bacteria. Structure, Interactions, and Dynamics. Springer-Verlag, Berlin

Michel-Beyerle ME (ed) (1990) Reaction Centers of Photosynthetic Bacteria. Springer-Verlag, Berlin

Michel-Beyerle ME (ed) (1996) Reaction Centers of Photosynthetic Bacteria. Structure and Dynamics. Springer-Verlag, Berlin

Monger TG, Cogdell RJ and Parson WW (1976) Triplet states of bacteriochlorophyll and carotenoids in chromatophores of photosynthetic bacteria. Biochim Biophys Acta 449: 136–159

Nanba O and Satoh K (1987) Isolation of a Photosystem II reaction center consisting of D-1 and D-2 polypeptides and cytochrome *b*-559. Proc Natl Acad Sci USA 84: 109–112

Morris JR, Uphaus RA, Crespi HL and Katz JJ (1971) Electron spin resonance of chlorophyll and the origin of signal I in photosynthesis. Proc Natl Acad Sci USA 68: 625–628

Okamura MY, Isaacson RA and Feher G (1975) Primary acceptor in bacterial photosynthesis: Obligatory role of ubiquinone in photoactive reaction centers of *Rhodobacter sphaeroides*. Proc Natl Acad Sci USA 72: 3491–3495

Ortega JM and Mathis P (1993) Electron transfer from the tetraheme cytochrome to the special pair in isolated reaction centers of *Rhodopseudomonas viridis*. Biochemistry 32: 1141–1151

Ostermeier C, Harrenga A, Ermler U and Michel H (1997) Structure at 2.7 Å resolution of the *Paracoccus denitrificans* two-subunit cytochrome *c* oxidase complexed with an antibody F_V fragment. Proc Natl Acad Sci USA 94:10547–10553

Paddock ML, McPherson PH, Feher G and Okamura MY (1990) Pathway of proton transfer in bacterial reaction centers: Replacement of serine-L223 by alanine inhibits electron and proton transfers associated with reduction of quinone to dihydroquinone. Proc Natl Acad Sci USA 87: 6803–6807

Peloquin JM, Violette CA, Frank HA and Bocian DF (1990) Temperature dependent conformational changes in the bacteriopheophytins of *Rhodobacter sphaeroides* reaction centers. Biochemistry 29: 4892–4898

Peloquin JM, Bylina EJ, Youvan DC and Bocian DF (1991) Effects of pigment-protein interactions on the conformation of the primary electron acceptor in *Rhodopseudomonas capsulatus* reaction centers. Biochim Biophys Acta 1065: 85–88

Rhee KH, Morris EP, Zheleva D, Hankamer B, Kühlbrandt W and Barber J (1997) Two-dimensional structure of plant Photosystem II at 8-Å resolution. Nature 389: 522–526

Sebban P (1988) pH effect on the biphasicity of the $P^+Q_A^-$ charge recombination kinetics in the reaction centers from *Rhodobacter sphaeroides,* reconstituted with anthraquinones. Biochim Biophys Acta 936: 124–132

Sharp KA (1998) Calculation of electron transfer reorganization energies using the finite difference Poisson-Boltzmann model. Biophys J 73: 1241–1250

Sinning I, Michel H, Mathis P and Rutherford AW (1989) Characterization of four herbicide-resistant mutants of *Rhodopseudomonas viridis* by genetic analysis, electron paramagnetic resonance and optical spectroscopy. Biochemistry 28: 5544–5553

Stilz HU, Finkele U, Holzapfel W, Lauterwasser C, Zinth W and Oesterhelt D (1994) Influence of M subunit Thr222 and Trp252 on quinone binding and electron transfer in *Rhodobacter sphaeroides* reaction centres. Eur J Biochem 223: 233–242

Stowell MHB, McPhillips TM, Rees DC, Soltis SM, Abresch E and Feher G (1997) Light-induced structural changes in photosynthetic reaction center: Implications for mechanism of electron-proton transfer. Science 276: 812–816

Takahashi E and Wraight CA (1996) Potentiation of proton transfer function by electrostatic interactions in photosynthetic reaction centers from *Rhodobacter sphaeroides*: First results

from site-directed mutation of the H subunit. Proc Natl Acad Sci USA 93: 2640–2645

Takiff L and Boxer SG (1988a) Phosphorescence from the primary electron donor in *Rhodobacter sphaeroides* and *Rhodopseudomonas viridis* reaction centers. Biochim. Biophys. Acta 932: 325–334

Takiff L and Boxer SG (1988b) Phosphorescence spectra of bacteriochlorophylls. J Am Chem Soc 110: 4425–4426

Tiede DM, Vázquez J, Córdova J and Marone PA (1996) Time-resolved electrochromism associated with the formation of quinone anions in the *Rhodobacter sphaeroides* R26 reaction center. Biochemistry 35: 10763–10775

Wachtveitl J, Farchaus JW, Das R, Lutz M, Robert B and Mattioli TA (1993) Structure, spectroscopic, and redox properties of *Rhodobacter sphaeroides* reaction centers bearing point mutations near the primary electron donor. Biochemistry 32: 12875–12886

Wang S, Lin S, Lin X, Woodbury NW and Allen JP (1994) Comparative study of reaction centers from purple photosynthetic bacteria: Isolation and optical spectroscopy. Photosynth Res 42: 203–215

Weyer KA, Schäfer W, Lottspeich F and Michel H (1987) The cytochrome subunit of the photosynthetic reaction center from *Rhodopseudomonas viridis* is a lipoprotein. Biochemistry 26: 2909–2914

Wiemken V and Bachofen R (1984) Probing the smallest functional unit of the reaction center of *Rhodospirillum rubrum* G-9 with proteinases. FEBS Lett 166: 155–159

Williams JC, Alden RG, Murchison HA, Peloquin JM, Woodbury NW and Allen JP (1992) Effects of mutations near the bacteriochlorophylls in reaction centers from *Rhodobacter sphaeroides.* Biochemistry 31: 11029–11037

Yeates TO, Komiya H, Chirino A, Rees DC, Allen JP and Feher G (1988) Structure of the reaction center from *Rhodobacter sphaeroides* R-26 and 2.4.1: Protein-cofactor bacteriochlorophyll bacteriopheophytin and carotenoid interactions. Proc Natl Acad Sci USA 85: 7993–7997

Zinth W, Knapp EW, Fischer SF, Kaiser W, Deisenhofer J and Michel H (1985) Correlation of structural and spectroscopic properties of a photosynthetic reaction center. Chem Phys Lett 119: 1–4

Zinth W, Arlt T, Schmidt S., Penzkofer H, Wachtveitl J, Huber H, Nägele T, Hamm P, Bibikova M, Oesterhelt D, Meyer M and Scheer H (1996) The first femtoseconds of primary photosynthesis—the process of the initial electron transfer reaction. In: Michel-Beyerle ME (ed) The Reaction Center of Photosynthetic Bacteria, pp 160–173. Springer-Velag, Berlin

Chapter 7

Carotenoids and the Assembly of Light-harvesting Complexes

Harald Paulsen
Institut fürAllgemeine Botanik der Universität Mainz, Müllerweg 6, D-55099 Mainz, Germany

Summary

Carotenoids are constitutive components of all light-harvesting complexes in plants and many such complexes in bacteria. In the crystal structures of several light-harvesting complexes, carotenoids are seen to span the lipid bilayer and connect components of the complex on both membrane surfaces and/or to mediate the interaction of transmembrane protein helices. This important stabilizing function suggests that these pigments are also actively involved in the assembly of light-harvesting complexes. Verification of this notion appears too ambitious a goal at present, as the question of how the pigment-protein complexes of the photosynthetic apparatus are assembled is still open. However, information is emerging about which light-harvesting complexes depend on the presence of carotenoids during their assembly, and which carotenoids are specifically required. This information comes from experiments in which all or some carotenoids are missing during biogenesis of the photosynthetic apparatus, due either to inhibitors of carotenoid biosynthesis or mutations in carotenoid biosynthesis pathways. Further information comes from reconstitution experiments in vitro in

H. A. Frank, A. J. Young, G. Britton and R. J. Cogdell (eds): The Photochemistry of Carotenoids, pp. 123–135.

which light-harvesting complexes are assembled from their apoproteins and a pigment mixture containing a restricted or heterologous selection of carotenoids.

One important result of such studies is that the peripheral light-harvesting complex in bacteria, LH2, but not the core antenna LH1, is dependent on carotenoids for stable assembly. The chlorophyll-*a/b* light-harvesting complexes in plants also assemble only when carotenoids are present. In some organisms, lutein appears to play a particularly important role: when lutein is missing, at least some of the chlorophyll-*a/b* complexes do not assemble. On the other hand, in other organisms the lack of lutein has no obvious effect on the chlorophyll-*a/b* antenna. An explanation may come from in-vitro reconstitution experiments: light-harvesting complexes in which luteins presumably are replaced with other carotenoids exhibit lower stabilities than those reconstituted with the authentic pigment, and different organisms may vary in their ability to tolerate this reduced complex stability.

I. Introduction: Possible Structural Role of Carotenoids in the Assembly of Light-harvesting Complexes

Carotenoids in light-harvesting complexes fulfill three major functions: (i) they collect light energy, mostly in the blue-green wavelength range, which is then transferred to the photosynthetic reaction centers, (ii) they stabilize light-harvesting complexes as structural components, and (iii) they provide photoprotection by quenching excited triplet states in bacteriochlorophyll (BChl) or chlorophyll (Chl) molecules and singlet states in oxygen. Whereas the light-harvesting function can be exerted only in the partially or fully assembled state of the photosynthetic apparatus when light-harvesting complexes are coupled to the reaction centers, the other two functions are likely to play a role already during the assembly of light-harvesting complexes as well. A number of molecular structures of light-harvesting complexes have been elucidated in the last few years. Therefore, as a starting point for considering the implication of carotenoids in the assembly of light-harvesting complexes, it may be worthwhile to have a look at structural carotenoid contributions in the fully assembled state of these complexes. This is the major subject of other chapters in this book (Chapter 4, Cogdell and Chapter 5, Hiller) and also of a recent review (Moskalenko and Karapetyan, 1996); therefore, only a few more general aspects will be touched upon here. The possible importance of carotenoids for photoprotection during the assembly of light-harvesting complexes will be discussed in the last section of this chapter.

With only a limited number of molecular structures of carotenoid-containing complexes available, it seems impossible as yet to define the contributions that carotenoids can make to the stability of such complexes. However, the following features can be extracted from several of the known structures.

(a) Carotenoids span the lipid membrane and connect structural elements located at the two surfaces. In the known structure of LH2 from *Rhodopseudomonas acidophila,* the one carotenoid per α,β protein pair connect the B800 and B850 BChl rings (Cogdell et al., 1996). In the major LHCII of higher plants, too, at least some of the carotenoids form a bridge between groups of Chls: the head groups of the two carotenoids visible in the structure interact with the Chl clusters situated near the membrane surfaces. Specifically, each cyclohexane ring is in van-der-Waals distance of a different Chl molecule, assigned to be a Chl *a* molecule. Moreover, the carotenoid head groups are in H-bonding distance to hydrophilic loop domains of the protein or, on the stromal side, to the hydrophilic extension of the trans-membrane α helices (Kühlbrandt et al., 1994). A consensus motif WFDPL has been suggested to bind lutein headgroups; this motif is found or at the ends of the closely interacting protein α helices in all apoproteins of LHCI and LHCII (Pichersky and Jansson, 1996).

By contrast, the carotenoids in the bacterial reaction centers of *Rhodobacter sphaeroides* and *Rhodopseudomonas viridis* do not span the membrane. They are in a kinked conformation because of a cis double bond in position 15, and oriented roughly perpendicular to the trans-membrane helices (Ermles et al., 1994; Lancaster and Michel, 1996) The carotenoids interact mostly with hydrophobic amino

Abbreviations: BChl – bacteriochlorophyll; Chl – chlorophyll; CP29, CP26, and CP24 – pigment complexes of Lhcb4, Lhcb5, and Lhcb6, respectively; LH1 and LH2–bacterial light-harvesting complexes 1 and 2, respectively; LHCI and LHCII – plant light-harvesting complexes of Photosystems I and II, respectively; Major LHCII – pigment complex of Lhcb1 and Lhcb2.

acids via their polyene chain, and the cis double bond is in van-der-Waals distance to one of the BChls; there is no visible interaction between the hydrophilic head group and the protein components. Clearly, the positioning of components on opposite faces of the membrane is not a function of these reaction center carotenoids.

(b) Carotenoids mediate the interaction of trans-membrane α-helical protein domains. In LH2 from *Rp. acidophila,* the trans-membrane α helices apparently do not form direct contacts with one another; these α helices are interfaced by carotenoids and BChls (McDermott et al, 1995; Cogdell et al., 1996). The polyene chain of the carotenoid predominantly interacts with aromatic and hydrophobic amino acids, like it is seen for spheroidene in the reaction center of *Rhodobacter sphaeroides* (Ermles et al., 1994). Similarly, in the major LHCII of higher plants, the superhelix formed by the trans-membrane α helices A and B seems to be stabilized by two carotenoid molecules bound into the grooves of the superhelix (Kühlbrandt et al, 1994). Hydrophobic interactions with these carotenoids may be an essential factor for stablizing the arrangement of α helices in this complex, as there are relatively few ionic helix-helix interactions in the major LHCII as compared to other complexes like bacterio-rhodopsin or the bacterial reaction center.

In the water-soluble peridinin-Chl complex of dinoflagellates, the peridinin molecules also connect protein α helices. In this case, however, the carotenoids do not undergo hydrophobic interactions with the α helices but link α-helical protein domains on the surface of the complex through their expoxy-cyclohexane rings (Hofmann et al., 1996).

If carotenoids are believed to stabilize helix-helix interactions in membrane protein complexes, this function may also assist the assembly process of these complexes and the folding of the apoproteins. In a proposed general folding scheme of membrane proteins, Popot et al. described a two-step process in which trans-membrane α helices are formed in the first step and then, during the second step, juxtaposed and arranged properly (Popot and Engelmann, 1990; Popot, 1993). It may be a general function of carotenoids to help in this second step, namely to arrange hydrophobic protein α helices in their native position in the membrane. Simultaneously, carotenoids as membrane-spanning structures may be of general importance during the assembly of membrane-located pigment-protein complexes in that they help to position structural features on opposite sides of the membrane that would otherwise have some freedom of motion along the surface of the membrane, like hydrophilic protein loops or ligands such as (B)Chl molecules.

An important experimental approach to assessing the structural importance of carotenoids during the assembly of light-harvesting complexes is to study organisms in which all or some of the carotenoids are missing, due to mutations in the carotenoid biogenesis pathways, or to inhibitors of single steps in carotenoid biosynthesis. An alternative possibility is to analyze the reconstitution of light-harvesting complexes in vitro in the presence or absence of various carotenoids. The information that such experiments have yielded for the assembly of light harvesting complexes in purple bacteria and in higher plants is outlined in Sections II and III, respectively. Section IV then summarizes what we know (or rather what we do not know) about the light-protective function of carotenoid during the assembly of light-harvesting complexes.

II. Light-harvesting Complexes of Purple Bacteria

A. Mutants with Deficient or Changed Carotenoid Compositions

The carotenoid requirement of the peripheral antenna complex in purple bacteria, LH2, seems to be higher than that of the core antenna LH1, as mutants deficient in carotenoids assemble the RC and LH1 but not LH2 complexes (Griffith and Stanier, 1956; Brand and Drews, 1997). A carotenoid-minus mutant of *Rhodobacter capsulatus* assembles mRNA coding for LH2 polypeptides and, as shown in pulse-chase experiments, even synthesizes the polypeptides and incorporates them into the membrane where they are then, however, rapidly degraded (Oberlé et al, 1990; Brandt and Drews, 1997). Similar observations have been made with a carotenoid-deficient mutant of *Rb. sphaeroides* (Lang and Hunter, 1994). These data suggest that the LH2 polypeptides are instable when they cannot be properly assembled due to the absence of carotenoids. On the other hand, about half of the carotenoids can be extracted from LH2 from *Rb. capsulatus.* The B800 absorption is lost whereas B850 is only somewhat red-shifted, and the complex becomes less stable (Zurdo et al., 1995).

Why carotenoids in LH1 play a less essential role in the assembly or stabilization will hopefully become clearer when the molecular structure of this complex becomes available at higher resolution. The physical environment of carotenoids in these two complexes appears to be rather different, as indicated, e.g., by their much higher polarizability in LH2 as compared to LH1 (Kuki et al., 1994). The dissociation of LH1 complexes of non-sulfur bacteria into B820 subunits seems to be always accompanied by the loss of carotenoid (unless the LH1 is from a carotenoid-deficient strain) (Visschers et al., 1992). By contrast, the B820 subunits of *Chromatium purpuratum,* a marine sulfur purple bacterium, retains its carotenoid. However, whereas other, carotenoid-free B820 subunits can be re-associated to form the B870 holocomplex, this is not possible with B820 from *C. purpuratum*, suggesting that the carotenoid still bound is inhibiting the re-association of subunits (Kerfeld et al., 1994).

B. Reconstitution of Light-harvesting Complex in Vitro

Consistent with the notion that carotenoids are not structurally essential in LH1 complexes, LH1 polypeptides of several purple bacteria can be reconstituted with BChl, in the absence of carotenoids, in detergent solution, resulting in B820 and B875 at virtually 100% yield (Loach et al., 1994). If carotenoids are included in this reconstitution procedure, they are efficiently reconstituted into the complexes as judged from spectral shifts of both carotenoid and BChl absorption bands, CD signals, energy transfer from carotenoids to BChls and photoprotection by carotenoids being very similar to those of the native carotenoid-containing LH1 complexes (Davis et al., 1995).

Heterologous reconstitution experiments show some structural restraints: Spheroidene from *Rb. sphaeroides* can be reconstituted into a complex with LH1 polypeptides from *Rhodospirillum rubrum,* restoring spectral properties of native *Rs. rubrum* LH1 and carotenoid-BChl energy transfer whereas spirilloxanthin is unable to incorporate into a reconstituted complex with LH1 apoproteins from *Rb. sphaeroides* (Davis et al., 1995).

Reconstitution experiments with LH1 from *Rubriviviax gelatinosus* show that carotenoids do play a more important role in the assembly of this complex: Only in the presence hydroxyspheroidene, the carotenoid found in native LH1 from this organism, did the B875 complex form from the carotenoid-free B820 subunits. Other carotenoids like spheroidene, spheroidenone, neurosporene, spirilloxanthin, although structurally closely related, did not support significant oligomerization of the antenna, indicating a very specific structural role of the carotenoid in stabilizing this complex (Jirsakova and Reiss-Husson).

An astonishing plasticity in accommodating carotenoids is shown by *Rb. sphaeroides* LH1 and LH2 polypeptides in an 'in-vivo reconstitution' system: A mutant expressing carotenoid biosynthesis genes from *Erwinia herbicola,* accumulating only the foreign carotenoids β-carotine, zeaxanthin and cryptoxanthin instead of spheroidene and its derivatives, is still able to accumulate light-harvesting complexes, although the amounts of complexes per cell are reduced, particularly for LH2. Apparently, the heterologous carotenoids, although structurally quite different from the homologous ones, are even able to transfer light energy to the reaction centers (Hunter et al., 1994).

Another large group of photosynthesizing bacteria, the green sulfur bacteria, also contain carotenoids in their light-harvesting apparatus, the chlorosome (Olson, 1998). However, carotenoids seem to be largely dispensable for the assembly, stability, or function of chlorosomes: reduction of colored carotenoid amounts by 90%, due to treatment of *Chloroflexus auranthiacus* with 2-hydroxybiphenyl, did not significantly change the accumulation of chlorosomes or the organization of their BChl *c* molecules (Foidl et al., 1997; Frese et al., 1997).

III. Light-harvesting Chlorophyll-*a*/*b* Complexes

The impact of Chls on the assembly of light-harvesting Chl *a/b* complexes can be easily investigated by studying the greening process of, e.g., etiolated plant leaves where the light-induced accumulation of Chls allows the examination of Chl-controlled assembly processes. The role of carotenoids in the assembly process is more difficult to establish, as carotenoids are accumulated in the dark and do not appear to be limiting components in the assembly of the photosynthetic apparatus under normal circumstances (although the dependence of LHC assembly on carotenoid biosynthesis has been

proposed, Plumley and Schmidt, 1995). Therefore, in order to examine the importance of carotenoids in the biosynthesis of light-harvesting Chl *a/b* complexes, one has to limit the supply either by using inhibitors of carotenoid biosynthesis or by looking at mutants that are deficient in (some) carotenoids. Another possibility is to study the assembly process in reconstitution systems in vitro where the input of pigments can be controlled.

A. Inhibitors of Carotenoid Biosynthesis

Norfluorazon is an often-used inhibitor of carotenoid biosynthesis, interfering with the step of phytoene desaturation (Sandmann, 1994). Norflurazon treatment of mustard seedlings showed that PS II assembly is more sensitive to reduced levels of carotenoids than PS I assembly (Markgraf and Oelmüller, 1991). The assembly of D1 into the PS II reaction center appears to be dependent on β-carotene. Upon treatment of *Chlamydomonas reinhardtii* with phytoene desaturase inhibitors, D1 degraded during photoinhibition cannot be replaced (Trebst and Depka, 1997).

Lysed chloroplasts from norflurazon-treated pea plants, containing only 5% of their normal carotenoid contents, stably inserted less than 10% of Lhcb1 into their thylakoid membranes compared to control experiments with non-treated plants (Dahlin and timko, 1994). This indicates either that the low amounts of carotenoids (and/or Chl *b*) in these chloroplasts were insufficient to stabilize newly inserted Lhcb1, or that the lack of pigments inhibited the insertion of Lhcb1 into the thylakoid. Carotenoid deficiency due to norfluorazon treatment appears also to impair protein import into isolated chloroplasts.

B. Mutations in the Carotenoid Biosynthesis Pathway

Light-harvesting Chl *a/b* complexes contain carotenoids of the β-β type (β-carotene, violaxanthin, antheraxanthin, zeaxanthin, neoxanthin) and of the β-ε type (lutein). Some higher plants like lettuce contain an ε,ε-carotenoid, lactucaxanthin, both in the major and in minor Chl *a/b* complexes which may replace either lutein or other xanthophylls (Phillip and Young, 1995). Among β,β-carotenoids, violaxanthin, antheraxanthin, and neoxanthin contain epoxides whereas the others do not. In order to establish specific roles of these epoxides in the assembly of the pigment-protein complexes, it is therefore instructive to compare mutations resulting in a general deficiency of carotenoids with those affecting only the biosynthesis of either β,β- or β,ε-carotenoids, or the epoxidase/de-epoxidase pathway.

1. Carotenoid-deficient Mutants

Chlamydomonas mutants that are entirely deficient in colored carotenoids do not accumulate reaction centers or light-harvesting complexes of Photosystem I or Photosystem II (Herrin et al., 1992). The accumulation of the mRNAs does not seem to be affected, so the failure in protein accumulation must be either due to inhibition of translation or rapid degradation of the proteins that cannot be assembled in the absence of carotenoids. Chl is also synthesized but very rapidly degraded in these mutants.

Mutants of *Scenedesmus obliquus* have been described that are carotenoid-deficient when grown in the dark because of a lack of phytoene synthase activity (Sandmann et al., 1997). These mutants behave differently from the *Chlamydomonas* mutants in that they assemble a functional PS I but no PS II and no Chl *a/b* complexes (Humbeck et al., 1989; Römer et al., 1995). Upon illumination, carotenoids are formed and, concomitantly, PS II activity and light-harvesting complexes appear (Römer et al., 1990). A comparison of the accumulation kinetics of different carotenoids with the appearance of PS I suggested that lutein and possibly also β-carotene are the limiting carotenoid species.

2. Mutants Deficient in β,ε-Carotenoids

Two *lut* mutants in *Arabidopsis* that have defects in the ε-cyclase and in the ε-ring hydroxylase, accumulate Chl *a/b* complexes, Chl and total carotenoids to the same levels as wild-type plants (Pogson et al., 1996). Interestingly, zeaxanthin and antheraxanthin are accumulated to much higher levels than in the wildtype in the absence of light stress. They are not epoxidized to violaxanthin, suggesting that they are located in a position where they are not accessible to the epoxidase. This may indicate that they are incorporated into positions normally occupied by lutein.

By contrast, in *Scenedesmus obliquus* a deficiency in β,ε-carotenoids causes dramatically reduced levels of Chl *b* and Chl *a/b*-protein complexes. In these

mutants, β-carotene, violaxanthin, and zeaxanthin are accumulated to higher levels than in the wildtype (Bishop et al., 1995). Also, the remnant LHCII, which is in a monomeric rather than trimeric state in these mutants, contains raised levels of β-carotene, violaxanthin and zeaxanthin. Apparently, these carotenoids cannot structurally and functionally replace lutein in light-harvesting complexes of *Scenedesmus* (Bishop, 1996). A more detailed analysis of a similar *Scenedesmus* mutant revealed that the absence of β,ε-carotenoids causes the predominant LHCII subunits in *Scenedesmus* to disappear altogether, whereas some minor subunits, particularly those with a relatively low Chl *b* content, are accumulated to the same or even enhanced levels as compared to the wildtype. These subunits then have a much higher relative content of violaxanthin, antheraxanthin, and zeaxanthin in their remaining LHCII (Heinze et al., 1997). These authors conclude that the β,ε-carotenoids including lutein are essential for the accumulation of some but not all of the LHCII subunits in *Scenedesmus,* as lutein can be functionally replaced with xanthophyll cycle pigments in some of the minor LHCII subunits.

Chlamydomonas seems to be more similar to *Scenedesmus* than to *Arabidopsis* with respect to the consequences of β-ε carotenoid deficiency. In the *lut1* mutant, an increased Chl *a:b* ratio indicates a partial defect in the assembly or stability of Chl *a/b* complexes (Eichenberger et al., 1986). However, at least some of the LHCII subunits are still assembled. Since these complexes are thought to contain lutein in the wildtype, this means that β-carotene-type xanthophylls are probably able to replace lutein during the assembly and in stabilizing these complexes (Niyogi et al., 1997b).

3. Mutants Deficient in Epoxidized or De-epoxidized Carotenoids

The *aba* mutant of *Arabidopsis* is impaired in epoxy-carotenoid biosynthesis and thus, makes zeaxanthin but not violaxanthin, antheraxanthin, and neoxanthin (Rock and Zeevaart, 1991; Rock et al., 1992). The pigment stoichiometries indicate a 1:1 replacement of neoxanthin and violaxanthin by zeaxanthin. The lutein content decreases compared to wildtype *Arabidopsis,* indicating a reduced Chl *a/b* antenna. Also comparing the composition of the antenna changes, there is less of the major LHCII and more of the minor Chl *a/b* complexes (Hurry et al., 1997). The photosynthetic performance of the mutant does not change significantly under non-stress light conditions. However, the major LHCII isolated from this mutant appears less stable, as it dissociates more easily from the trimeric to the monomeric state and also into protein and unbound pigments (Tardy and Havaux, 1996). It may be this reduced amount and/or the reduced stability of trimeric LHCII in the *aba* mutant that is responsible for its reduced thylakoid stacking (Rock et al., 1992).

Chlamydomonas mutants have been isolated that are deficient either in violaxanthin de-epoxidase or zeaxanthin epoxidase. Using these mutants, it could be demonstrated that only part of the non-photochemical quenching observed in *Chlamydomonas* is dependent on the formation of zeaxanthin (Niyogi et al., 1997a). It will be interesting to see whether the absence of xanthophyll epoxidase or de-epoxidase products has an effect on the assembly of light-harvesting complexes in these mutants.

C. Reconstitution of Chlorophyll-a/b Complexes

About ten years ago, Plumley and Schmidt (1987) demonstrated that the pigment-binding step in the assembly of the major LHCII can be reproduced in vitro by placing the detergent-denatured complex, still in detergent solution, into renaturing conditions. This reconstitution procedure was then extended to bacterially expressed plant apoprotein (Paulsen et al., 1990; Cammarata and Schmidt, 1992) and to recombinant apoproteins of minor Chl *a/b* complexes (Giuffra et al., 1996) and of LHCI (Schmidt et al., 1997). The reconstituted complexes were found to be very similar to their native counterparts with regard to their biochemical and spectroscopic properties. Therefore, the reconstitution of Chl *a/b* complexes in vitro has been exploited to yield much valuable information on the role of carotenoids in the assembly of these complexes.

1. Major LHCII

The first publication on the reconstitution of the major LHCII complex already contained some information on the role of specific carotenoids (Plumley and Schmidt, 1987). When carotenoids were altogether omitted from the reconstitution mixture, no reconstitution of stable complexes was observed, so carotenoids are essential. However, not all three carotenoids found in native LHCII were

needed: lutein or violaxanthin could be omitted from the mixture without much effect. Reconstitutions with lutein as the only carotenoid had a lower yield, violaxanthin promoted complex formation when the level of Chl was raised, but when neoxanthin was present as the only carotenoid, no reconstitution was observed.

Similar results were obtained with recombinant LHCII apoproteins: no stable recombinant LHCII can be formed without carotenoids (Paulsen et al., 1990; Cammarata and Schmidt, 1992). The carotenoid specificities observed in this study were slightly different from the original report on reconstitution (Plumley and Schmidt, 1987) in that only violaxanthin or neoxanthin could be omitted from the carotenoid mixture with some or significant loss, respectively, in complex yields. However, these differences reflect only gradual variations in complex stabilities. When the stringency during the isolation of reconstituted complexes is lowered, allowing the isolation of recombinant complexes with decreased stability, it is possible to obtain versions of the major LHCII with all carotenoid combinations, including reconstitutions with either lutein, violaxanthin, or neoxanthin as the only carotenoid component. (S. Hobe and H. Paulsen, unpublished). Among these, the lutein-only complexes appear more stable than reconstitution products containing violaxanthin or neoxanthin as the only carotenoids. Although these complexes dissociate more easily than wildtype major LHCII (or the reconstitution product including all three carotenoids), pigment stoichiometries indicate that the carotenoids fill true binding sites, rather than just being attached non-specifically to the membrane complex. Studies are underway to measure the affinities of various binding sites for individual carotenoids in competition experiments (H. Niemeier, S. Hobe, and H. Paulsen, unpublished).

In order to define the carotenoid structures necessary for LHCII assembly and stabilization, a number of different carotenoids have been used in reconstitution assays with only one carotenoid component present. Not only the xanthophyll cycle carotenoids zeaxanthin and antheraxanthin turned out to promote reconstitution but also heterologous carotenoids as diverse structurally as astaxanthin, okenone, and fucoxanthin. In general, a hydroxyl group in position 3 of at least one of the cyclohexane ring seems to be important for complex formation (D. Phillip, S. Hobe, A. Young, and H. Paulsen, unpublished). Similarly, the major LHCII from *Chlorella fusca,* reconstituted from the heat-denatured native complex, accommodated some prasinoxanthin when this was added to the reconstitution mix but not peridinin (Meyer and Wilhelm, 1993).

No attempts to specifically mutagenize the supposedly lutein-binding protein motifs (Pichersky and Jansson, 1996) have been published yet. Interestingly, however, N-terminal deletions of the protein, removing one of these motifs (GWDTA), did not appreciably change the stability of the reconstituted complex (Ammarata and Schmidt, 1992; Paulsen and Hobe, 1992). A possible explanation is that, among other interactions binding the carotenoid into the complex, the one with the caroteinoid-binding motif is not essential.

2. *Minor Chlorophyll-a/b Complexes and LHCI*

Other Chl *a/b* complexes can be reconstituted with pigments under very similar conditions as the major LHCII complex. When reconstituting CP29 with varying combinations of carotenoids, only lutein proves to be indispensable. When either violaxanthin or neoxanthin is omitted from the pigment mixture, the complexes appear about as stable as complexes reconstituted with the full complement of carotenoids (Giuffra et al., 1996).

Only limited specificity with regard to carotenoids is seen in reconstituted CP26 (Ros et al., 1998). All reconstitutions with two out of the three native xanthophylls and even with only one xanthophyll give reconstitution yields between 40 and 80%. Comparing the reconstitutions with only one of the carotenoids missing, neoxanthin appears to be somewhat more efficient for obtaining higher yields, which is surprising as neoxanthin is present in substoichiometric amounts in native CP26. Another interesting observation is that recombinant CP26 with violaxanthin as the only carotenoid is about as stable as complexes formed with lutein only or neoxanthin only. Both CP29 and major LHCII reconstituted with violaxanthin as the only carotenoid are clearly less stable than the lutein-only complexes. This contribution of violaxanthin to CP26 stability may correlate with the dominant role that CP26 (together with CP24) is thought to play in the xanthophyll cycle (Jahns and Schweig, 1995; Ruban et al., 1996).

The heterodimeric complex of Lhca1 and Lhca4, one of the subunits of LHCI, has recently been reconstituted from recombinant apoprotein and

pigments in vitro (Schmid et al., 1997). No detailed analysis of carotenoid requirements for LHCI reconstitution has been performed yet. Preliminary data indicate that in the absence of lutein the formation of the monomeric complexes of Lhca1 and Lhca4 is impaired (V Schmid, personal communication).

Little is known about the role of carotenoids in the assembly of Chl *c*-containing algal light-harvesting complexes. The Chl *a,b,c*-containing LHCII of the prasinophyte *Mantoniella squamata* has been reconstituted in vitro from the denatured native complex. This complex contains prasinoxanthin, violaxanthin, and neoxanthin but can also bind some externally added lutein (Meyer and Wilhelm, 1993).

D. Which Carotenoids Are Essential for Assembling Chl a/b *Complexes?*

Both for the accumulation in vivo and for the assembly in vitro of Chl *a/b* complexes, carotenoids are essential. However we have no way of telling yet whether the carotenoids are actively involved in the assembly process itself or whether they play a merely structural role in stabilizing the complexes. Studies of the protein's circular dichroism during in vitro reconstitution experiments with the major LHCII suggested that the folding of the denatured protein into its native structure is triggered by the binding of pigments (Paulsen et al., 1993). Specifically, when reconstitution is attempted in the presence of Chl *a* and Chl *b* but without carotenoids, the protein does not fold. If the cooperative binding of pigments to light-harvesting protein triggers protein folding also in vivo, this may be the driving force for the insertion of the protein into the thylakoid membrane (Kuttkat et al., 1997; Paulsen, 1997).

An involvement of carotenoids in the thylakoid insertion of light-harvesting proteins has also been concluded from a pulse-chase measurement of the rate of protein insertion into membranes that have reduced amounts of carotenoids, due to norflurazon treatment (Dahlin and Timko, 1997). It should be kept in mind that carotenoids may also control other biosynthetic steps in the synthesis and assembly of light-harvesting complexes such as the import of the protein precursors into plastids (Dahlin, 1993; Dahlin and Franzén, 1997).

Additional information about the actual contribution of carotenoids to the assembly of light-harvesting pigment-protein complexes may also be obtained by measuring complex formation in a time-resolved fashion. This allows the reaction steps that are or are not controlled by carotenoids to be distinguished. Fluorescence kinetic measurements in the millisecond to minute time range during the formation of the major LHCII in vitro showed that the reaction steps leading to a stable pigment-protein complex took place only when both carotenoids and Chls were present (Booth and Paulsen, 1996). This confirmed the notion that the complex is cooperatively stabilized by these pigments (Paulsen, 1997).

In the crystal structure of major LHCII from pea only two carotenoids are visible (Kühlbrandt et al., 1994), although biochemical studies show that there are more than two carotenoids bound to the complex (Jansson, 1994). The other carotenoids may be only peripherally bound and, therefore, less well resolved in the 2D crystal structure. Most pigment analyses of Chl *a/b* complexes agree that there are two luteins bound per apoprotein in all members of the family (Bassi et al., 1993). Consequently, it appears reasonable to assume that the two carotenoids seen to stabilize two *trans*-membrane helices in the atomic structure are in fact luteins (Kühlbrandt et al., 1994), although this assumption is still awaiting direct experimental proof. If these assumptions are valid, one would expect lutein to be more strictly required for the assembly of light-harvesting complexes than the other carotenoids.

This idea is consistent with a specific requirement of lutein in some reconstitutions (Plumley and Schmidt, 1987; Paulsen et al., 1990; Giuffra et al., 1996) and also with the failure of *Scenedesmus* mutants lacking lutein to assemble light-harvesting complexes (Bishop, 1996). However, the finding that *Arabidopsis* and *Chlamydomonas* mutants deficient in β,ε-carotenoids do assemble functional light-harvesting complexes (Pogson et al., 1996; Niyogi et al., 1997b) clearly shows that lutein is not absolutely essential. If lutein in fact plays an important structural role in light-harvesting complexes, then it can be functionally replaced by β,β-carotenoids.

Reconstitutions in vitro of Chl *a/b* light-harvesting complexes with non-native sets of carotenoids show gradual differences in the stability of the complexes formed. These complexes either can or cannot then be isolated, depending on the stringency applied during reconstitution and subsequent isolation of the complexes. Different organisms may tolerate reduced stabilities of various light-harvesting complexes to varying degrees. This may also explain why similar mutations, such as a deficiency of β,ε-carotenoids,

Table 1. Carotenoid requirement for reconstituting different Chl *a/b* proteins. Data from different studies are compiled on the reconstitution of Chl *a/b* proteins in vitro with the reduced carotenoid set shown in addition to Chl *a* and Chl *b*. Stabilities of reconstituted complexes are estimated on the basis of reconstitution yields. +++, complexes about as stable as the native complexes; ++, complexes significantly less stable than native complexes; +, complexes rather instable, must be isolated under low-stringency conditions; nd, not determined; lut, lutein; neo, neoxanthin; vio, violaxanthin.

Chl *a/b* protein	lut + neo	vio + neo	vio
Lhca1[a]	+++	+	+
Lhca4[a]	+++	+	+
Lhcb1[b]	+++	+	+
Lhcb4[c]	+++	+	n.d.
Lhcb5[d]	+++	+++	++

[a] V.H.R. Schmid, G.W. Schmidt, and H. Paulsen, unpublished

have such different effects on light-harvesting complex assembly in different organisms, such as *Arabidopsis* and *Scenedesmus* (see Section III.B.2).

The fact that the lack of β,ε-carotenoids in *Scenedesmus* and *Chlamydomonas* strongly impairs the accumulation of the major LHCII but leaves some minor Chl *a/b* complexes unaffected indicates that in these complexes lutein can be more easily replaced with β,β-carotenoids (Section III.B.2). Consistent with this notion, the minor Chl *a/b* protein Lhcb5 (CP26) reconstituted with pigment mixtures lacking lutein is more stable than the major Chl *a/b* protein reconstituted with the same pigments (Section III.C, Table 1).

Whereas the structural role in stabilizing Chl *a/b* complexes played by (presumably) tightly bound carotenoids appears quite obvious from the crystal structure of the major LHCII, the contribution of more weakly bound carotenoids to the assembly of these complexes is less clear. Carotenoids that only interact weakly with the protein complexes or are unbound, may influence the assembly of pigment-protein complexes by modifying the fluidity of the lipid bilayer(Tardy and Havaux, 1997). Lipids changing the bending rigidity of the lipid bilayer have recently been shown to alter the folding behavior of bacteriorhodopsin in a lipid-micelle model system (Booth et al., 1997). All-*trans* carotenoids spanning the bilayer are likely to have an effect on the bending rigidity of the thylakoid membrane and thus may influence the assembly of pigment-protein complexes even without binding directly to them.

E. Assembly of Light-harvesting Complexes into Larger Units

1. Oligomerization and Aggregation

Many light-harvesting complexes assemble into oligomers. Whereas LH1 and LH2 in bacteria form 16-meric and 8- or 9-meric ring structures, respectively, most or all of the major LHCII in plants is organized into trimers and the LHCI complexes are thought to be dimeric. In the bacterial LH2, the oligomeric structure quite obviously is stabilized by carotenoids; in LH1 this structural contribution of carotenoids cannot be essential as these complexes are stable without carotenoids (see Section II.A). On the other hand, the crystal structure of the major LHCII suggests a merely intra-molecular stabilization by the two visible carotenoids (Kühlbrandt et al., 1994). Of course, the interaction between the membrane-spanning helices A and B that is presumably stabilized by these carotenoids may in turn influence the trimer formation of the complex. However, it is also possible that the additional carotenoid(s), known to be part of the complex from biochemical data but not visible in the crystal structure, stabilize trimers. This can be suggested from the observation that in the *aba* mutant of *Arabidopsis* where zeaxanthin appears to replace violaxanthin and neoxanthin, the major LHCII dissociates more easily into monomers when isolated under partially denaturing conditions (Tardy and Havaux, 1996). A closer biochemical inspection of the major LHCII in various carotenoid-deficient plant and algae mutants will be necessary to assess the impact of carotenoids on the formation of trimeric LHCII. Another experimental approach will be to study how the variation of the carotenoid components influences the reconstitution of trimeric LHCII in vitro (Hobe et al., 1994).

Carotenoids may also influence the aggregation behavior of LHCII in the thylakoid membrane. In fact, a model for explaining the involvement of xanthophyll cycle carotenoids in non-photochemical quenching is based on such an effect. When isolated major LHCIIb is solubilized at detergent concentrations close to where aggregation of the complex starts, the aggregation can be initiated by adding zeaxanthin. Conversely, violaxanthin inhibits this aggregation (Ruban et al., 1997). A possible explanation is that zeaxanthin, due to its conjugated double bonds extending into the head groups, is a

near planar molecule whereas in violaxanthin, the rings are tilted out of the plain of the carbon chain into a perpendicular position. The flat structure of zeaxanthin may somehow favor oligomerization/ aggregation of LHCII trimers (see Chapter 15, Horton et al.).

2. Assembly into the Holo-Antennae of Photosystems

In PS II, the Chl *a/b* complexes are arranged in a well-defined and highly ordered fashion as demonstrated, for example, by the structural data now emerging from PS II crystals (Rhee et al., 1997). So far it is entirely unclear how the individual subcomplexes recognize their correct neighbors and find their place within this architecture. One can only guess at this point that carotenoids may be involved in this final step of the assembly of the PS II light-harvesting complex. The fact that a large number of carotenoids are functionally coupled to light-harvesting complexes (since they are capable of transferring energy to the reaction centers) but are biochemically only weakly linked to the pigment-protein complexes (since they appear as free pigments as soon as the photosystems are dissociated into subcomplexes under weakly denaturing conditions) may indicate that (some) carotenoids are bound at the interface of individual subcomplexes of PS II. Similar considerations possibly apply for PS I.

IV. Photoprotection During Assembly

There are good reasons to believe that protection by carotenoids against photodynamic damage is even more important during the assembly of light-harvesting complexes than in the functional photosynthetic apparatus. As long as the antenna complexes are not functionally integrated into the photosystems yet, the excited states of their light-harvesting Chl or BChl molecules cannot be quenched photochemically by energy transfer to the reaction centers, and therefore pose a higher risk for the generation of potentially damaging singlet oxygen. It is therefore, reasonable to suggest that carotenoids are involved in photoprotection in all stages of the assembly of (B)Chl-protein complexes, at least under aerobic conditions.

Unfortunately, our knowledge of how pigments are assembled into the pigment-protein complexes of the photosynthetic apparatus is very limited. It is not even clear where light-harvesting complexes are assembled. Studies with greening mutants of *Chlamydomonas* suggest that LHCII is assembled in the envelope rather than in the thylakoid (Park and Hoober, 1997; Wolfe et al., 1997). It is clear therefore that we are far from understanding how the Chl (precursor) molecules, that need to be protected against photodynamic activity, find their way from their site of biogenesis to light-harvesting proteins (Paulsen, 1997). A number of proteins have been suggested as possible Chl carriers such as ELIP, the early light-inducible protein (Adamska, 1997) and PsbS, a member of the extended cab protein family with four rather than three membrane-spanning domains (Funk et al., 1995; Lindahl et al., 1997). Both of these proteins have been reported to bind Chls and carotenoids. Further work along these lines will hopefully reveal how carotenoids help to avoid photodynamic damage during the assembly of light-harvesting complexes.

Acknowledgments

I thank several colleagues for communicating their results prior to publication. Work in the author's laboratory has been funded by Deutsche Forschungsgemeinschaft and Fonds der Chemischen Industrie.

References

Adamska I (1997) Elips: Light induced stress proteins. Physiol Plant 100: 794–805

Bassi R, Pineau B, Dainese P and Marquardt J (1993) Carotenoid-binding proteins of Photosystem II. Eur J Biochem 212: 297–303

Bishop NI (1996) The β,ε carotenoid, lutein, is specifically required for the formation of the oligomeric forms of the light harvesting complex in the green alga, *Scenedesmus obliquus.* J Photochem Photobiol B Biol 36: 279–283

Bishop NI, Urbig T and Senger H (1995) Complete separation of the β,ε-and β,β-carotenoid biosynthetic pathways by a unique mutation of the lycopene cyclase in the green alga, *Scenedesmus obliquus.* FEBS Lett 367: 158–162

Booth PJ and Paulsen H (1996) Assembly of light-harvesting chlorophyll *a/b* complex in vitro. Time-resolved fluorescence measurements. Biochemistry 35: 5103–5108

Booth PJ, Riley ML, Flitsch SL, Templer RH, Farooq A, Curran AR, Chadborn N and Wright P (1997) Evidence that bilayer bending rigidity affects membrane protein folding. Biochemistry 36: 197–203

Brand M and Drews G (1997) The role of pigments in the

assembly of photosynthetic complexes in *Rhodobacter capsulatus.* J Basic Microbiol 37: 235–244

Cammarata KV and Schmidt GW (1992) In-vitro reconstitution of a light-harvesting gene product—deletion mutagenesis and analyses of pigment binding. Biochemistry 31: 2779–2789

Cogdell RJ, Fyfe PK, Barrett SJ, Prince SM, Freer AA, Isaacs NW, Mcglynn P and Hunter CN (1996) The purple bacterial photosynthetic unit. Photosynth Res 48: 55–63

Dahlin C (1993) Import of nuclear-encoded proteins into carotenoid-deficient young etioplasts. Physiol Plant 87: 410–416

Dahlin C and Franzén LG (1997) Carotenoid deficient young wheat etioplasts are able to bind precursor proteins on the plastid surface but are impaired in their translocation ability. Physiol Plant 99: 279–285

Dahlin C and Timko MP (1994) Integration of nuclear-encoded proteins into pea thylakoids with different pigment contents. Physiol Plant 91: 212–218

Davis CM, Bustamante PL and Loach PA (1995) Reconstitution of the bacterial core light-harvesting complexes of *Rhodobacler sphaeroides* and *Rhodospirillum rubrum* with isolated alpha- and beta-polypeptides, bacteriochlorophyll *a*, and carotenoid. J Biol Chem 270: 5793–5804

Eichenberger W, Boschetti A and Michel HP (1986) Lipid and pigment composition of a chlorophyll *b*-deficient mutant of *Chlamydomonas reinhardttii.* Physiol Plant 66: 589–594

Ermler U, Fritzsch G, Buchanan SK and Michel H (1994) Structure of the photosynthetic reaction centre from *Rhodobacter sphaeroides* at 2,65 Å resolution: Cofactors and protein-cofactor interactions. Structure 2: 925–936

Foidl M, Golecki JR and Oelze J (1997) Phototrophic growth and chlorosome formation in *Chloroflexus aurantiacus* under conditions of carotenoid deficiency. Photosynth Res 54: 219–226

Frese R, Oberheide U, van Stokkum I, van Grondelle R, Foidl M, Oelze J and van Amerongen H (1997) The organization of bacteriochlorophyll *c* in chlorosomes from *Chloroflexus aurantiacus* and the structural role of carotenoids and protein—An absorption, linear dichroism, circular dichroism and Stark spectroscopy study. Photosynth Res 54: 115–126

Funk C, Schröder WP, Napiwotzki A, Tjus SE, Renger G and Andersson B (1995) The PS II-S protein of higher plants: A new type of pigment-binding protein. Biochemistry 34: 11133–11141

Giuffra E, Cugini D, Croce R and Bassi R (1996) Reconstitution and pigment-binding properties of recombinant CP29. Eur J Biochem 238: 112—120

Griffith DE and Stanier RY (1956) Some mutagene changes in the photosynthetic system of *Rhodpseudomonas sphaeroides.* J Gen Microbiol 14: 698–715

Havaux M (1998) Carotenoids as membrane stabilizers in chloroplasts. Trends Plant Sci 3: 147–151

Heinze I, Pfündel E, Huhn M and Dau H (1997) Assembly of light harvesting complexes II(LHC II) in the absence of lutein: A study on the alpha carotenoid free mutant C 2a´ 34 of the green alga *Scenedesmus obliquus.* Biochim Biophys Acta 1320: 188–194

Herrin DL, Battey JF, Greer K and Schmidt GW (1992) Regulation of chlorophyll apoprotein expression and accumulation—requirements for Carotenoids and chlorophyll. J Biol Chem 267: 8260–8269

Hobe S, Prytulla S, Kühlbrandt W and Paulsen H (1994) Trimerization and crystallization of reconstituted light-harvesting chlorophyll *a/b* complex. EMBO J 13: 3423–3429

Hofmann E, Wrench PM, Sharpies FP, Hiller RG, Welte W and Diederichs K (1996) Structural basis of light harvesting by Carotenoids: Peridinin-chlorophyll-protein from *Amphidinium carterae.* Science 272: 1788–1791

Humbeck K, Römer S and Senger H (1989) Evidence for an essential role of carotenoids in the assembly of an active Photosystem II. Planta 179: 242–250

Hunter CN, Hundle BS, Hearst JE, Lang HP, Gardiner AT, Takaichi S and Cogdell RJ (1994) Introduction of new carotenoids into the bacterial photosynthetic apparatus by combining the carotenoid biosynthetic pathways of *Erwinia herbicola* and *Rhodobacter sphaeroides.* J Bacteriol 176: 3692–3697

Hurry V, Anderson JM, Chow WS and Osmond CB (1997) Accumulation of zeaxanthin in abscisic acid deficient mutants of *Arabidopsis* does not affect chlorophyll fluorescence quenching or sensitivity to photoinhibition in vivo. Plant Physiol 113: 639–648

Jahns P and Schweig S (1995) Energy-dependent fluorescence quenching in thylakoids from intermittent light grown pea plants: Evidence for an interaction of zeaxanthin and the chlorophyll *a/b* binding protein CP26. Plant Physiol Biochem 33: 683–687

Jansson S (1994) The light-harvesting chlorophyll *a/b* binding proteins. Biochim Biophys Acta 1184: 1–19

Jirsakova V and Reiss-Husson F (1994) A specific carotenoid is required for reconstitution of the *Rubrivivax gelatinosus* B875 light harvesting complex from its subunit form B820. FEBS Lett 353: 151–154

Karrasch S, Bullough PA and Ghosh R (1995) The 8.5 Å projection map of the light-harvesting complex I from *Rhodospirillum rubrum* reveals a ring composed of 16 subunits. EMBO J 14: 631–638

Kerfeld CA, Yeates TO and Thornber JP (1994) Biochemical and spectroscopic characterization of the reaction center LH1 complex and the carotenoid-containing B820 subunit of *Chromatium purpuratum.* Biochim Biophys Acta 1185: 193–202

Kühlbrandt W, Wang DN and Fujiyoshi Y (1994) Atomic model of plant light-harvesting complex by electron crystallography. Nature 367: 614–621

Kuki M, Nagae H, Cogdell RJ, Shimada K and Koyama Y (1994) Solvent effect on spheroidene in nonpolar and polar solutions and the environment of spheroidene in the light-harvesting complexes of *Rhodobacter sphaeroides* 2.4.1 as revealed by the energy of the $^1A_g^- \rightarrow {}^1B_u^+$ absorption and the frequencies of the vibronically couple C=C stretching Raman lines in the $^1A_b^-$ and $2^1A_b^-$ states. Photochem Photobiol 59: 116–124

Kuttkat A, Edhofer 1, Eichacker LA and Paulsen H (1997) Light harvesting chlorophyll *a/b* binding protein stably inserts into etioplast membranes supplemented with Zn pheophytin *a/b.* J Biol Chem 272: 20451–20455

Lancaster CRD and Michel H (1996) Three-dimensional structures of photosynthetic reaction centers. Photosynth Res 48: 65–74

Lang HP and Hunter CN (1994) The relationship between carotenoid biosynthesis and the assembly of the light-harvesting LH2 complex in *Rhodobacter sphaeroides.* Biochem J 298: 197–205

Lindahl M, Funk C, Webster J, Bingsmark S, Adamska I and Andersson B (1997) Expression of ELIPs and PS II-S protein in spinach during acclimative reduction of the Photosystem II antenna in response to increased tight intensities. Photosynth Res 54: 227–236

Loach PA, Parkes-Loach PS, Davis CM and Heller BA (1994) Probing protein structural requirements for formation of the core light-harvesting complex of photosynthetic bacteria using hybrid reconstitution methodology. Photosynth Res 40: 231–245

Markgraf T and Oelmüller R (1991) Evidence that carotenoids are required for the accumulation of a functional photosystem-II, but not photosystem-I in the cotyledons of mustard seedlings. Planta 185: 97–104

McDermott G, Prince SM, Freer AA, Hawthornthwaite-Lawless AM, Papiz MZ, Cogdell RJ and Isaacs NW (1995) Crystal structure of an integral membrane light-harvesting complex from photosynthetic bacteria. Nature 374: 517–521

Meyer M and Wilhelm C (1993) Reconstitution of light-harvesting complexes from *Chlorella fusca* (*Chlorophyceae*) and *Mantoniella squamata* (*Prasinophyceae*). Z Naturforsch C 48: 461–473

Moskalenko AA and Karapetyan NV (1996) Structural role of carotenoids in photosynthetic membranes. Z Naturforsch C 51: 763–771

Olson JM (1998) Chlorophyll organization and function in green photosynthetic bacteria. Photochem Photobiol 67: 61–75

Niyogi KK, Bjorkman O and Grossman AR (1997a) *Chlamydomonas* xanthophyll cycle mutants identified by video imaging of chlorophyll fluorescence quenching. Plant Cell 9: 1369–1380

Niyogi KK, Bjorkman O and Grossman AR (1997b) The roles of specific xanthophylls in photoprotection. Proc Natl Acad Sci USA 94: 14162–14167

Oberlé B, Tichy HV, Hornberger U & Drews G (1990) Regulation of formation of photosynthetic light-harvesting complexes in *Rhodobacler capsulatus.* In: Drews G and Dawes EA (eds) Molecular Biology of Membrane-Bound Complexes in Phototrophic Bacteria, pp. 77–84. Plenum Press, New York.

Park H and Hoober JK (1997) Chlorophyll synthesis modulates retention of apoproteins of light-harvesting complex II by the chloroplast in *Chlamydomonas reinhardtii.* Physiol Plant 101: 135–142

Paulsen H (1997) Pigment ligation to proteins of the photosynthetic apparatus in higher plants. Physiol Plant 100: 760–768

Paulsen H, Rümler U and Rüdiger W (1990) Reconstitution of pigment-containing complexes from light-harvesting chlorophyll *a/b*-binding protein overexpressed in *E. coli.* Planta 181: 204–211

Paulsen H, Finkenzeller B and Kühlein N (1993) Pigments induce folding of light-harvesting chlorophyll *a/b*-binding protein. Eur J Biochem 215: 809–816

Phillip D and Young AJ (1995) Occurrence of the carotenoid lactucaxanthin in higher plant LHC II. Photosynth Res 43: 273–282

Pichersky E and Jansson S (1996) The light-harvesting chlorophyll *a/b*-binding polypeptides and their genes in angiosperm and gymnosperm species. In: Ort DR and Yocum CF (eds) Oxygenic Photosynthesis: The Light Reactions, pp. 507–521. Kluwer Academic Publishers, Dordrecht

Plumley FG and Schmidt GW (1995) Light-harvesting chlorophyll *a/b* complexes: Interdependent pigment synthesis and protein assembly. Plant Cell 7: 689–704

Plumley FG and Schmidt GW (1987) Reconstitution of chlorophyll *a/b* light-harvesting complexes: Xanthophyll-dependent assembly and energy transfer. Proc Natl Acad Sci USA 84: 146–150

Pogson B, McDonald KA, Truong M, Britton G and DellaPenna D (1996) *Arabidopsis* carotenoid mutants demonstrate that lutein is not essential for photosynthesis in higherplants. Plant Cell 8: 1627–1639

Popot JL (1993) Integral membrane protein structure: Transmembrane alpha-helices as autonomous folding domains. Curr Opin Struct Biol 3: 532–540

Popot JL and Engelman DM (1990) Membrane protein folding and oligomerization: The two-stage model. Biochemistry 29: 4031–4037

Rhee KH, Morris EP, Zheleva D, Hankamer B, Kühlbrandt W and Barber J (1997) Two dimensional structure of plant Photosystem II at 8 Å resolution. Nature 389: 522–526

Rock CD and Zeevaart JAD (1991) The *aba* mutant of *Arabidopsis thaliana* is impaired in epoxy-carotenoid biosynthesis. Proc Natl Acad Sci USA 88: 7496–7499

Rock CD, Bowlby NR, Hoffmann-Benning S and Zeevaart JAD (1992) The *aba* mutant of *Arabidopsis thaliana* (L) Heynh. has reduced chlorophyll fluorescence yields and reduced thylakoid stacking. Plant Physiol 100: 1796–1801

Römer S, Humbeck K and Senger H (1990) Relationship between biosynthesis of carotenoids and increasing complexity of Photosystem I in mutant C-6D of *Scenedesmus obliquus.* Planta 182: 216–222

Römer S, Senger H and Bishop NI (1995) Characterization of the carotenoidless strain of *Scenedesmus obliquus,* mutant C-6E, a living Photosystem I model. Bot Acta 108: 80–86

Ros F, Bassi R and Paulsen H (1998) Pigment binding properties of the recombinant Photosystem II subunit CP26 reconstituted in vitro. Eur J Biochem, in press

Ruban AV, Young AJ and Morton P (1996) Dynamic properties of the minor chlorophyll *a/b* binding proteins of Photosystem II, an in vitro model for photoprotective energy dissipation in the photosynthetic membrane of green plants. Biochemistry 35: 674–678

Ruban AV, Phillip D, Young AJ and Horton P (1997) Carotenoid dependent oligomerization of the major chlorophyll *a/b* light harvesting complex of Photosystem II of plants. Biochemistry 36: 7855–7859

Sandmann G (1994) Carotenoid biosynthesis in microorganisms and plants. Eur J Biochem 223: 7–24

Sandmann G, Bishop NI and Senger H (1997) The carotenoid deficient mutant, C 6E, of *Scenedesmus obliquus* is blocked at the site of phytoene synthase. Physiol Plant 99: 391–394

Schmid VHR, Cammarata KV, Bruns BU and Schmidt GW (1997) In vitro reconstitution of the Photosystem I light harvesting complex LHCI 730: Heterodimerization is required for antenna pigment organization. Proc Nat. Acad Sci USA 94: 7667–7672

Tardy F and Havaux M (1996) Photosynthesis, chlorophyll fluorescence, light-harvesting system and photoinhibition resistance of a zeaxanthin-accumulating mutant of *Arabidopsis thaliana.* J Photochem Photobiol B-Biol 34: 87–94

Tardy F and Havaux M (1997) Thylakoid membrane fluidity and thermostability during the operation of the xanthophyll cycle

in higher-plant chloroplasts. Biochim Biophys Acta 1330: 179–193

Trebst A and Depka B (1997) Role of carotene in the rapid turnover and assembly of Photosystem II in *Chlamydomonas reinhardtii.* FEBS Lett 400: 359–362

Visschers RW, Nunn R, Calkoen F, van Mourik F, Hunter CN, Rice DR and van Grondelle R (1992) Spectroscopic characterization of B820 subunits from light-harvesting complex I of *Rhodospirillum rubrum* and *Rhodobacter sphaeroides* prepared with the detergent *n*-octyl-*rac*-2,3-dipropyl-sulfoxide. Biochim Biophys Acta 1100: 259–266

Wolfe GR, Park H, Sharp WP and Hoober JK (1997) Light harvesting complex apoproteins in cytoplasmic vacuoles in *Chlamydomonas reinhardtii* (*Chlorophyta*). J Phycol 33: 377–386

Zurdo J, Centeno MA, Odriozola JA, Fernandez-Cabrera C and Ramirez JM (1995) The structural role of the carotenoid in the bacterial light-harvesting protein 2 (LH2) of *Rhodobacter capsulatus.* A Fourier transform Raman spectroscopy and circular dichroism study. Photosynth Res 46: 363–369

This page intentionally left blank

Chapter 8

The Electronic States of Carotenoids

Ronald L. Christensen
Department of Chemistry, Bowdoin College, Brunswick, Maine 04011, U.S.A.

Summary

The photochemistry of Carotenoids is determined by the electronic structures of their low energy, excited states. This chapter first relates the optical spectroscopy of carotenoids to current theoretical descriptions of polyene electronic states. Highly detailed spectroscopic information now available for model polyenes leads to a simple, three-level energy scheme: $S_2(1^1B_u) > S_1(2^1A_g) > S_0(1^1A_g)$. Optical studies of polyenes and carotenoids of intermediate length demonstrate that increases in conjugation lengths invariably result in $S_2 \rightarrow S_0$ emissions replacing the characteristic $S_1 \rightarrow S_0$ emissions of short polyenes. This cross–over to S_2 fluorescence can be accounted for by the energy gap law: decreases in S_1 energies lead to sharp increases in the rates of $S_1 \rightarrow S_0$ nonradiative decay with increasing conjugation. The dominance of S_2 emissions in long polyenes means that the S_1 states of the carotenoids employed by photosynthetic systems are difficult to locate using fluorescence detection. Even less information is available regarding the energies of carotenoid T_1 states due, in large part, to the absence of confirmed phosphorescence in any polyene or carotenoid. This chapter critically examines the use of extrapolation procedures, including applications of the energy gap law, in estimating the S_1 and T_1 energies of long, non–emissive carotenoids. In spite of the inherent limitations of extrapolations, estimates of S_1 energies in molecules such as spheroidene and β-carotene now are adequate for understanding the

H. A. Frank. A. J. Young, G. Britton and R. J. Cogdell (eds): The Photochemistry of Carotenoids, pp. 137–159.

mechanisms of singlet energy transfer in photosynthetic systems. Outstanding issues still to be addressed include: the development of a more quantitative understanding of the effects of conjugation, substitution, isomeric structure, and solvent environment on the energies and dynamics of S_1 and S_2 states; the extension of the limited data base of T_1 energies to longer polyenes and carotenoids; the evaluation of the effects of conformational disorder on carotenoid spectroscopy and photochemistry; and the consideration of additional low-lying singlet states in the energy level diagram.

I. Introduction: Low Lying Excited Singlet and Triplet States in Carotenoids

The roles of carotenoids as light-harvesting and photoprotective pigments and their use as visual chromophores ultimately are determined by the energies, structures, and dynamics of their low-energy, excited electronic states. An accurate description of these states thus is the crucial first step in explaining carotenoid photochemistries and for understanding the interactions between carotenoids and other molecules in photobiological processes. The primary focus of this chapter is the energetics of carotenoid excited electronic states and their dependence on conjugation length, the presence of substituents, isomeric structure, and solvent environments. Issues regarding excited state dynamics, e.g., the rates of radiative and nonradiative decay, also will be discussed to the extent that they contribute to our understanding of carotenoid spectroscopy. Other chapters describe the importance of carotenoids in photobiological processes and provide further motivation for understanding their excited states.

A great deal of what we know about the low energy excited states of the carotenoids involved in photobiology can be traced to the high-resolution optical spectroscopy of model polyenes. The organization of this chapter parallels the recent evolution of the field and, in large part, follows the progression toward structural complexity illustrated by Fig. 1. Incremental increases in conjugation lengths and the addition of substituents provide a relatively continuous transition from the electronic states of octatetraene to molecules such as spheroidene and β-carotene. It comes as no surprise that the level of precision in understanding and describing polyene excited states decreases with increasing molecular complexity. Nevertheless, the experimental data on the longer carotenoids now is of sufficient quality to allow careful answers to questions regarding the energies of carotenoid singlet and triplet states and the ability of these states to serve as energy donors or acceptors in photosynthetic systems.

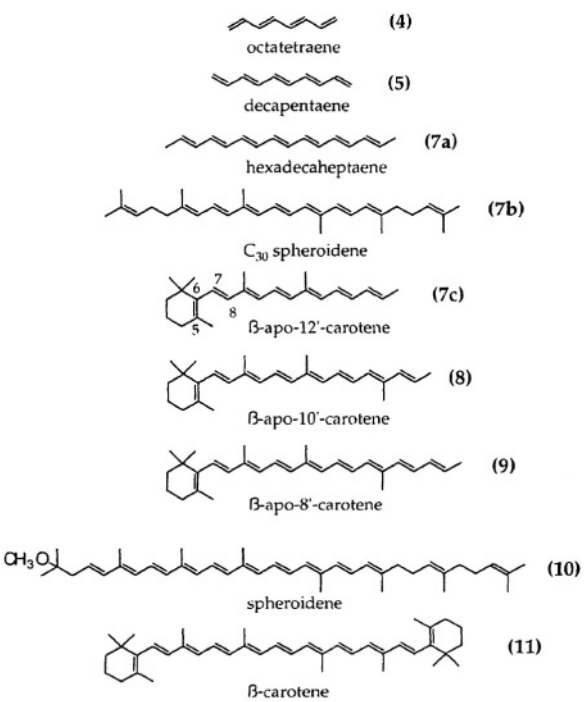

Fig. 1. Representative polyenes and carotenoids. Boldfaced numbers refer to the number of conjugated double bonds.

Abbreviations: (0-0) – transition between zero-point vibrational levels of two electronic states (= electronic origin); HOMO – highest occupied molecular orbital; LUMO – lowest unoccupied molecular orbital; PPP-CI – PPP-MO Theory which includes configuration interaction; PPP-MO– Pariser Parr Pople Molecular Orbital Theory; S_0, S_1, S_2 – ground (S_0) and excited (S_1, S_2) electronic singlet states; T_1, T_2 – excited electronic triplet states; λ_{max} – wavelength of maximum absorption or maximum emission intensity for an electronic transition (in general, $\lambda_{max} \neq \lambda_{(0-0)}$) λ_{max} refers to a vertical transition, i.e., an electronic transition between states with the same geometry.

II. Low-Energy, Excited Singlet States in Polyenes

A. Theoretical Descriptions of Polyene Singlet States

Theoretical descriptions of polyene/carotenoid excited electronic states have been well summarized in several recent reviews (Hudson et al., 1982; Orlandi et al., 1991; Kohler, 1993a,b; Frank and Cogdell, 1996; Koyama et al., 1996). Most, if not all, of our current understanding of the photochemistry of carotenoid singlet states can be described in terms of the simple energy level scheme given in Fig. 2. Transitions to higher energy singlet states (S_3, S_4, etc.) also are observed in carotenoid spectroscopy, e.g., the intensity of '*cis*-peaks' provides a useful diagnostic tool in identifying isomers (Zechmeister, 1962). However, the photochemistry of carotenoids is dominated by processes originating from low-lying energy levels, and this chapter will restrict its attention to the singlet states depicted in Fig. 2. Symmetry labels for the electronic states are based on the C_{2h} geometry of simple *all-trans*-polyenes. These designations and their implications for transition intensities, radiative lifetimes, etc. also work remarkably well for a wide range of unsymmetric, *cis* and *trans* polyenes and carotenoids, and the A_g and B_u labels will be used throughout this review.

The $S_2(1^1B_u)$ states are well described by simple molecular orbital treatments as being of HOMO → LUMO parentage, and the symmetry-allowed, $S_0(1^1A_g) \rightarrow S_2(1^1B_u)$ transitions have long been appreciated to be responsible for the colors of long polyenes and carotenoids. Indeed, the realization that the $S_0 \rightarrow S_2$, infinite-polyene limit of ~600–700 nm (Kohler, 1993b; Kohler and Samuel, 1995) is related to the alternation of carbon-carbon bond lengths was one of the early accomplishments of the application of simple Hückel and free-electron models to linearly-conjugated, π-electron systems (Kuhn, 1948; Labhart, 1957; Murrell, 1963). However, satisfactory descriptions of the $S_1(2^1A_g)$ states demand a detailed consideration of the correlation of electron-electron interactions. Within molecular orbital theory, even a qualitative explanation of why $E(2^1A_g) < E(1^1B_u)$ requires the interaction of both singly (e.g., HOMO − 1 → LUMO and HOMO → LUMO + 1) and doubly (e.g., HOMO, HOMO → LUMO, LUMO) excited configurations (D-CI). Quantitative agreement between theoretical and experimental 2^1A_g energies requires even more extensive configuration interaction. For example, the inclusion of all single through quadruply excited configurations (Q-CI) explains the slight increase in $(E(1^1B_u) - E(2^1A_g))$ as a function of increasing polyene length (Tavan and Schulten, 1979). However, the computational effort for calculations at this level of CI increases exponentially with the number of π-electrons, and high level CI calculations have proven prohibitive for polyenes with more than five or six double bonds.

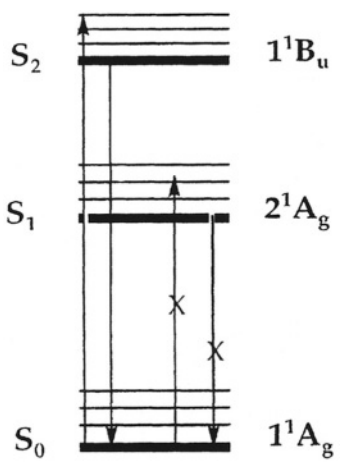

Fig. 2. The ordering of low-energy singlet states in polyenes and carotenoids. Labels refer to molecules belonging to the C_{2h} point group. Arrows with x's refer to symmetry-forbidden electronic transitions.

For longer polyenes, multireference double excitation configuration interaction (MRD-CI) approximations have been employed which select the most important electronic configurations and 'balance' the effects of electron correlation in the ground and excited states. The MRD-CI methods provide results comparable to Q-CI or full -CI calculations on short polyenes (Zoos and Ramasesha, 1984) and have allowed calculations to be extended to molecules with up to eight double bonds (Tavan and Schulten, 1986). These calculations also predict a small increase in the $(E(1^1B_u) - E(2^1A_g))$ energy gap with increasing conjugation. The calculated energy gaps (~6300 cm^{-1} for octatetraene; ~7100 cm^{-1} for hexadecaoctaene) are in reasonable agreement with gas phase experimental values (6604 cm^{-1} for octatetraene (Petek et al., 1994); ~9000 cm^{-1} for hexadecaoctaene (Snyder et al., 1985). However, quantitative comparisons between calculations and spectra are not straightforward: 1.) Calculations of electronic

energy differences refer to 'vertical transitions' in which excited states retain ground state geometries, whereas the experimentally observed energies refer to transitions between the zero-point vibrational levels ((0-0) bands). Vertical transition energies can be converted to (0-0) energies in specific cases, though the corrections depend both on the transition involved and the length of conjugation. 2.) Theoretical calculations presumably refer to isolated molecules, while the experimental data available for longer polyenes generally are limited to spectra obtained in solutions. Solvation causes a significant reduction in the $(E(1^1B_u) - E(2^1A_g))$ energy difference due to the preferential stabilization of the 1^1B_u state. For example, ΔE decreases from 6604 cm^{-1} (Petek et al., 1994) to 3540 cm^{-1} when gaseous *all-trans*-octatetraene (4) is placed into a substitutional site in a crystal of 4.2 K n-octane (Granville et al., 1980). (Note that *all-trans*-octatetraene is the only polyene for which the $S_0(1^1A_g) \rightarrow S_1(1^1A_g)$ and $S_0(1^1A_g) \rightarrow S_2(1^1B_u)$ electronic origins have been directly observed in both the gas and condensed phases. In fact, a great deal of what we know about the low energy, excited electronic states of polyenes and carotenoids is based on the highly detailed spectroscopic studies of this prototype.) For longer polyenes and carotenoids, for which gas phase spectral measurements are not feasible, it is possible to estimate corrections to transition energies for solvent effects (see below) to allow direct comparison with theoretical calculations. One additional consideration is that the parameters used in the PPP-MRD-CI and other semi-empirical methods may in part be based on spectra of molecules in condensed phases. 3.) Comparison of theory with carotenoid electronic energy differences is further complicated by the differential effects of substitution (e.g., methyl groups and β-ionylidene rings) on the S_0, S_1, and S_2 states. Some attempts have been made to empirically account for the effects of substitution (Kohler, 1993a,b). However, this is complicated by limitations in the accuracy of data available for the zero-point 2^1A_g energies of longer polyenes and problems in correcting 1^1B_u and 2^1A_g energies for comparisons in common solvents and temperatures.

In summary, theory gives at least a semi-quantitative explanation for why Fig. 2 applies to a wide range of polyene systems and provides a useful guide for understanding relative energies, the symmetry-forbidden nature of the $S_0 \leftrightarrow S_1$ transitions, and the re-arrangement of π-bond orders in carotenoid excited states (Schulten et al., 1976). Nevertheless, the further development of an accurate catalog of 2^1A_g energies will continue to rely on their spectroscopic detection, especially for carotenoids employed in photobiological processes. Identification of (0-0) energies is particularly important, since the zero-point vibrational states are the starting points for photochemistry and energy transfer in thermally equilibrated systems.

B. The Experimental Observation of Polyene Singlet States

1. One-Photon Spectroscopy/Vibronic Structure

The connection between experiment and the energy level diagram summarized in Fig. 1 is illustrated by the low temperature absorption and fluorescence spectra of *all-trans*-hexadecaheptaene (Fig. 3). The vibronic structure exhibited in these spectra generally is broadened in spectra of carotenoids, particularly for molecules such as β-carotene where non-planarities between the central polyene chain and terminal cyclohexenylidene rings result in a distribution of absorbing and emitting species (Christensen and Kohler, 1973; Hemley and Kohler, 1977). The well-resolved spectra of unsubstituted, model polyenes facilitates the unambiguous identification of electronic origins ((0-0) bands) and the precise measurement of 1^1B_u and 2^1A_g electronic energies. Most characteristic of spectra of short, model polyenes is the gap between the onsets ((0-0)'s) of the strongly allowed, $1^1A_g \rightarrow 1^1B_u$ absorption (molar absorptivities of $\sim 10^5$ L $mole^{-1}$ cm^{-1}) and the $2^1A_g \rightarrow 1^1A_g$ emission. Although the fluorescence quantum yield for hexadecaheptaene has not been measured, the $S_1 \rightarrow S_0$ yields show a steady fall-off with increasing conjugation, ranging from ~1 in octatetraene (Gavin et al., 1978) to $<10^{-5}$ in molecules such as β-carotene (Bondarev and Knyukshto, 1994; Andersson et al.,1995).

The vibronic features of these spectra are worth noting. (Higher-resolution versions of the hexadecaheptaene spectra, obtained in low-temperature, mixed crystals, have been discussed by Simpson, et al. (1987)). The absorption and emission spectra presented in Fig. 3 are dominated by combinations of totally symmetric (a_g) C-C and C=C stretching modes with vibrational frequencies of ~1200 and ~1600 cm^{-1}. These details are more easily identified in the $S_1(2^1A_g) \rightarrow S_0(1^1A_g)$ fluorescence spectrum which is

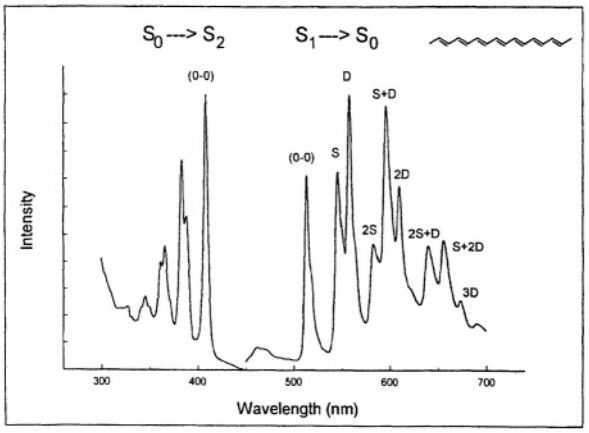

Fig. 3. Fluorescence and fluorescence excitation spectra of *all-trans*-hexadecaheptaene (7a) in 77 K n-pentadecane. The fluorescence excitation spectrum was obtained by exciting at 414 nm, and the fluorescence excitation spectrum monitored the emission intensity at 558 nm. Vibronic structure in the fluorescence spectrum has been assigned to combinations of carbon-carbon single (S) and double (D) bond stretching vibrations.

better-resolved and shows Franck-Condon maxima that characteristically involve at least one quantum of the double bond stretch. In broader spectra the vibronic features corresponding to single and double bond stretches often coalesce into progressions in what appear to be a single, intermediate frequency of 1300–1400 cm^{-1}, depending on the length of conjugation and the transition involved. Note that the absorption spectrum of the heptaene has its maximum intensity in the (0-0) band, most likely reflecting the smaller geometry change experienced in the $S_0(1^1A_g) \rightarrow S_2(1^1B_u)$ transition. This is consistent with theory which predicts a more significant transposition of π-bond orders in the 2^1A_g state (Schulten et al., 1976). It also is important to note that the vibronic features in Fig. 3, those seen in low-temperature spectra of mixed crystals (Simpson et al., 1987), and the highly detailed vibronic development observed in high-resolution spectra of isolated tetraenes in supersonic expansions (Petek et al., 1995) all are consistent with planar 2^1A_g and 1^1B_u excited states in longer polyenes. There is no evidence in long polyenes and carotenoids for the substantial deviations from planarity experienced by the excited states of dienes and trienes (Dormans et al., 1987; Zerbetto and Zgierski, 1990; Orlandi et al., 1991).

The characteristic Franck-Condon envelopes and vibronic signatures of polyene transitions observed in the fluorescence spectra of molecules such as hexadecaheptaene prove to be critical in interpreting the weaker, more poorly resolved emissions of longer carotenoids. It also is important to understand why the (0-0) band is so prominent (Fig. 3) in this supposedly forbidden $S_1(2^1A_g) \rightarrow S_0(1^1A_g)$ transition. First, it should be noted that other than in high resolution experiments (e.g., Simpson et al., 1987; Kohler et al., 1988), the $S_0(1^1A_g) \rightarrow S_1(2^1A_g)$ transitions generally are too weak (with transition dipoles and integrated extinction coefficients $\sim 10^{-2}$–10^{-3} those of allowed polyene transitions) to be detected in standard absorption or fluorescence excitation measurements. The weakness of these bands confirms that they truly are due to symmetry-forbidden, $g \rightarrow g$ transitions. On the other hand, the selection rules also imply that the (0-0) band should be weak (or nonexistent) with the major part of the spectral intensity built on nontotally symmetric (b_u) 'promoting' modes that mix the 2^1A_g and 1^1B_u electronic states (Geldof et al., 1971).

High-resolution experiments on model polyenes explain the apparent contradiction of observing relatively strong (0-0) bands in symmetry-forbidden electronic transitions. Under isolated-molecule conditions (e.g., supersonic jets) or in the small number of cases where polyenes have been incorporated into crystals that rigorously retain their inversion centers, the $S_0 \leftrightarrow S_1$ (0-0)'s are indeed missing with transitions being built on b_u false origins (Petek et al., 1995). However, the most prominent b_u promoting vibrations are in-plane bending modes of very low frequency, < 100 cm^{-1} in long polyenes. Therefore, even for polyenes or carotenoids that retain idealized C_{2h} symmetries, the distinctions between (0-0) bands and b_u false origins will not be detectable, even in relatively well-resolved $S_1 \rightarrow S_0$ spectra such as presented in Fig. 3. In addition, small distortions from C_{2h} symmetry, either due to asymmetric substitutions or solvent perturbations, tend to give the (0-0) bands intensities that are comparable to those of false origins (Christensen and Kohler, 1976; Petek et al., 1995). Furthermore, these bands undergo inhomogeneous solvent shifts due to the distribution of local solvent environments. As a result, the electronic origins of $S_0 \leftrightarrow S_1$ spectra of polyenes in solutions and glasses should be viewed as due to a complicated, unresolved collection of distorted and undistorted molecules all of which contribute to the '(0-0)' bandshapes in typical spectra.

2. Two-Photon Spectroscopy

Two-photon spectra of *all-trans* octatetraene, both in n-octane (which provides centrosymmetric mixed-crystal sites) and for isolated molecules in supersonic jets, furnish the most direct proof that the lowest energy transition must be assigned to a $g \rightarrow g$ transition (Granville et al., 1979; Petek et al., 1995). The $S_0 \rightarrow S_1$ transitions are allowed under two-photon excitation conditions, giving relatively intense (0-0) bands and spectra dominated by totally symmetric (a_g) vibrations. Furthermore, in two-photon experiments $g \rightarrow u$ transitions are forbidden, thus enhancing the ability of this technique to locate 2^1A_g states in molecules whose π-electron densities maintain at least an approximate center of inversion. This technique found early success in locating low-energy 2^1A_g states in retinol, retinal, and a retinal Schiff base (Birge et al., 1978). However, there has been remarkably little additional exploitation of two-photon methods to locate 2^1A_g states in other polyenes or carotenoids. This is due, in part, to the weak $S_1 \rightarrow S_0$ emissions from longer polyenes and carotenoids which preclude the detection of their two-photon $S_0(1^1A_g) \rightarrow S_1(2^1A_g)$ absorptions using fluorescence excitation techniques. In addition, the low energies of $S_0(1^1A_g) \rightarrow S_1(2^1A_g)$ transitions in carotenoids requires two-photon experiments to be conducted in the near infrared where one-photon-allowed overtones of solvent vibrations can cause significant interferences (R. R. Birge, personal communication).

3. Solvent Effects

The $S_0(1^1A_g) \rightarrow S_1(2^1A_g)$ and $S_0(1^1A_g) \rightarrow S_2(1^1B_u)$ transitions undergo shifts to lower energy when gaseous molecules are solvated. Understanding these shifts is important in relating theoretical calculations to transition energies obtained from typical solution spectra. Solvent effects also provide a useful diagnostic tool for distinguishing between allowed and forbidden transitions. The analysis of solvent effects in polyene spectroscopy has been well described by Hudson et al. (1982). For nonpolar polyenes in nonpolar solvents the transition energies should exhibit a linear dependence on solvent polarizability:

$$\tilde{\nu}(\text{solvent}) = \tilde{\nu}(\text{gas}) - k(n^2 - 1)/(n^2 + 2) \quad \text{Eq. (1)}$$

where $\tilde{\nu}$ refers to the transition energy (typically the (0-0) band expressed in cm^{-1}), n is the refractive index of the solvent, and k is constant for a given polyene transition. As discussed by Hudson et al. (1982),

$$k \propto a^{-3}(M + E(\alpha_e - \alpha_g)) \quad \text{Eq. (2)}$$

where a is an effective solute cavity radius, M_{ge} is the electric dipole transition moment for the transition, E is the average transition energy, and $(\alpha_e - \alpha_g)$ is the increase in the polarizability of the polyene upon excitation.

These equations have been tested for several short polyenes and for β-carotene (Sklar et al., 1977; Snyder et al., 1985; Andersson et al., 1991). For $S_0(1^1A_g) \rightarrow S_2(1^1B_u)$ transitions, k's are typically 10^4 cm^{-1}. In addition to the linear dependence of transition energies on solvent polarizability, another critical test of Eq. (1) is its ability to predict gas phase (n=1) transition energies. For the $S_0(1^1A_g) \rightarrow S_2(1^1B_u)$ transitions of diphenylpolyenes with one to four double bonds, extrapolations of solution data and transition energies obtained from gas phase measurements agree within experimental error (Hudson et al., 1976,1982). Equation 1 also accounts for the shifts in spectra in the few cases where solvent studies have been carried out on vibronically-resolved $S_1(2^1A_g) \rightarrow S_0(1^1A_g)$ transitions. The k's are considerably smaller but not insignificant, ~1000–2000 cm^{-1} for unsubstituted polyenes (Snyder et al., 1985). In the one case (all-trans-octatetraene) where the gas phase $S_1(2^1A_g) \rightarrow S_0(1^1A_g)$ electronic origin is accurately known (28,949 cm^{-1}, Petek et al., 1995), the solution phase data provide an excellent extrapolation (28,970 ± 100 cm^{-1}) to n=1 (Snyder et al., 1985). The data available for short polyenes and diphenyl polyenes in nonpolar solvents thus validate the use of the solvent model described by in Eqs. (1 and 2). This solvent model is particularly important for understanding how the S_1 and S_2 energies are modified when carotenoids are placed in biological matrices, e.g., the protein environments of reaction centers and light-harvesting antenna.

For carotenoids, Andersson et al. (1991) have suggested that the $E(\alpha_e - \alpha_g)$ term dominates the transition dipole term in determining k for the $S_0(1^1A_g) \rightarrow S_2(1^1B_u)$ absorption. Although there is considerably less solvent effect information available for $S_1(2^1A_g) \rightarrow S_0(1^1A_g)$ transitions (See Snyder et al. (1985) for a

summary.), their relatively large k's and relatively small transition moments imply that polarizability changes also govern the solvent dependence of these transitions, at least for shorter polyenes. It is somewhat surprising that the k's do not exhibit a systematic dependence on polyene length (Sklar et al., 1977; Hudson et al., 1982; Snyder et al., 1985). The transition dipole moment and the change in polarizability for the $S_0(1^1A_g) \rightarrow S_2(1^1B_u)$ transition both are expected to increase with increasing conjugation (Kohler, 1990; Anderson et al., 1991). However, the k's (at least for the $S_0(1^1A_g) \rightarrow S_2(1^1B_u)$ transitions) are essentially independent of conjugation length, cf. $k = 11{,}700\ cm^{-1}$ for β-carotene (Andersson et al., 1991) and $k = 10{,}900\ cm^{-1}$ for octatetraene (Snyder et al., 1985). A plausible explanation is that the increases in transition moments and polarizability upon optical excitation are counteracted by comparable increases in molecular volumes ($\propto a^3$) that also should scale with the length of conjugation.

III. Low-Energy, Excited Singlet States in Carotenoids

Extending the spectroscopic investigations of polyene singlet states to the carotenoids employed in photobiology is hampered by several 'deficiencies' of longer, more highly substituted conjugated systems. Foremost is the marked decrease in fluorescence quantum yields with increasing conjugation. The dominance of non-radiative decay processes makes it increasingly difficult to detect the symmetry-forbidden, $S_1(2^1A_g) \rightarrow S_0(1^1A_g)$ transitions, let alone to confirm their identity using standard fluorescence excitation techniques. Furthermore, increasing the conjugation length leads to a predominance of higher energy, $S_2(1^1B_u) \rightarrow S_0(1^1A_g)$ emissions with low-energy, vibronic tails that mask the $S_1 \rightarrow S_0$ fluorescence. In addition to issues of fluorescence intensity, the electronic spectra of naturally occurring carotenoids tend to be significantly broadened, making it even more difficult to observe and identify the weak fluorescence signals from these systems. These problems often are exacerbated by interferences from the relatively strong emissions of shorter polyene breakdown products and other impurities.

A. The Electronic Spectroscopy of Short Carotenoids

Some of the differences between the electronic spectroscopy of simple polyenes and that of carotenoids are illustrated in Fig. 4 which compares the low-temperature absorption and fluorescence spectra of three heptaenes: hexadecaheptaene (7a), a synthetic C_{30} spheroidene (7b), and an apo-carotene (7c). Spectra of hexadecaheptaene are well resolved with well-defined electronic origins, allowing the accurate measurement of the $S_1(2^1A_g)$ and $S_2(1^1B_u)$ electronic energies. The addition of methyl substituents to form the isoprenoid, C_{30} spheroidene (7b) results in broadening of the vibronic bands and systematic shifts of transitions to lower energy. The $S_0(1^1A_g) \rightarrow S_2(1^1B_u)$ transition is considerably more sensitive to methyl substitution than the $S_0(1^1A_g) \rightarrow S_1(2^1A_g)$ transition. This is a common feature of polyene/carotenoid spectroscopy, mirroring .the relative sensitivities of the 2^1A_g and 1^1B_u energies to solvent perturbations. Introduction of the terminal β-ionylidene ring in the apo-carotene further broadens the spectra and shifts the $S_0(1^1A_g) \rightarrow S_2(1^1B_u)$ transition to substantially higher energy relative to the absorption spectrum of the corresponding C_{30} spheroidene. The apo-carotene $S_1(1^1A_g) \rightarrow S_0(2^1A_g)$ bands experience a significantly smaller blue shift relative to the spheroidene.

The loss of resolution in the apo-carotene spectra can be traced to repulsions between methyl groups on the β-ionylidene ring and the hydrogen atom at the end of the C_{7-8} double bond (Fig. 1) in the polyene chain (Christensen and Kohler, 1973; Hemley and Kohler, 1977). These interactions twist the C_{6-7} single bond, forcing the double bond in the ring (C_{5-6}) out of the plane formed by the other carbon-carbon double bonds. X-ray structures of carotenoid single crystals provide a direct measure of the significant (and variable) nonplanarities between rings and side chains in retinoic acid and retinal (Stain and MacGillavry, 1963; Gilardi, et al., 1971). The potential energy along the 5-6-7-8 dihedral angle apparently is both shallow and flat, resulting in a distribution of conformations in solutions and glasses. As a result, solutions of apo-carotenes, β-carotene, etc. typically contain a distribution of conformers with a range of effective conjugation lengths and transition energies. This simple model not only accounts for the relative broadness of carotenoid optical spectra but also

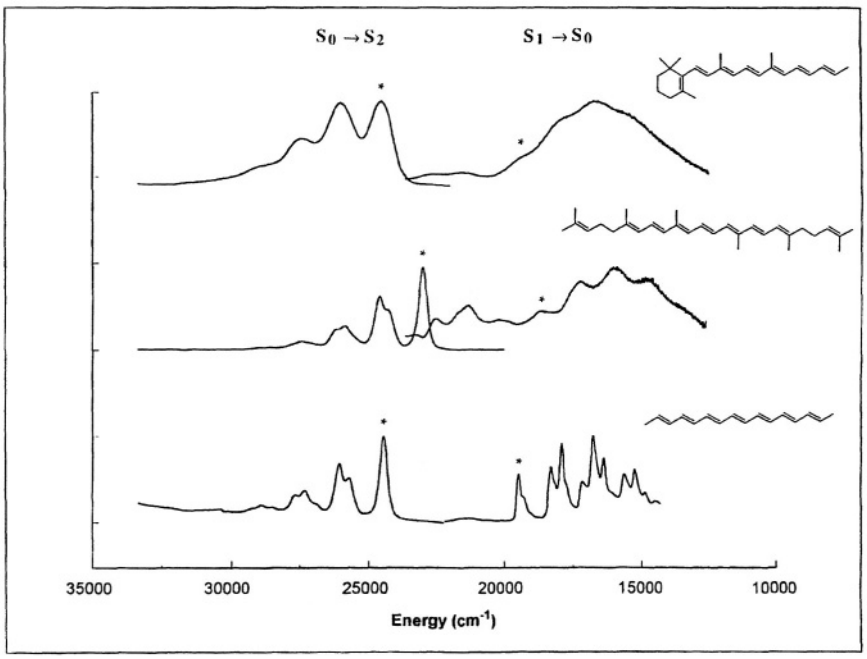

Fig. 4. Comparison of absorption and fluorescence spectra of hexadecaheptaene (7a), a C_{30} spheroidene (7b), and β-apo-12′-carotene (7c). Spectra were obtained at 77 K in an EPA glass (ether/isopentane/ethanol, 5/5/2, v/v/v). Electronic origins are designated by asterisks.

explains the significant blue shift in the apo-carotene (7a) relative to the spheroidene (7b). The C_{30} spheroidene enjoys the full effect of seven conjugated double bonds, while the apo-carotene spectrum is due to a distribution of conjugation lengths which average between six (90° rotation about $C_{6\text{-}7}$) and seven (no rotation) conjugated bonds. Empirical estimates of the average loss in effective conjugation due to the presence of a β-ionylidene ring range from 0.15 (Kohler, 1993) to 0.8 (Hirayama, 1955). These effects also explain the small red shift in the $S_0 \rightarrow S_2$ absorption spectrum of lycopene relative to that of β-carotene and our perception of differences in the colors of these pigments in plants. In addition, this model accounts for the systematic increase in the resolution of carotenoid $S_0 \rightarrow S_2$ spectra with increasing conjugation length. The leveling-off of $S_0 \rightarrow S_2$ transition energies for large N implies that nonplanarities of the terminal double bonds have a decreasing impact on the spread in transition energies (Hemley and Kohler, 1977).

Comparison of the spectra of hexadecaheptaene (7a) and the apo-heptaene (7c) show fortuitous agreements in $S_0(1^1A_g) \rightarrow S_2(1^1B_u)$ and $S_1(2^1A_g) \rightarrow S_0(1^1A_g)$ transition energies. For heptaenes the red shift induced by methyl substituents is effectively counterbalanced by the blue shift due to non-planarities and the loss in effective conjugation length. This suggests that model polyenes may provide reasonable models for estimating the excited state energies of apo-carotenes (including molecules such as β-carotene) with the same formal number of double bonds, though more work is needed to better understand the effects of substituents on the 2^1A_g and 1^1B_u energies of longer carotenoids.

B. The Electronic Spectroscopy of Long Carotenoids

1. Cross-Over from $S_1 \rightarrow S_0$ to $S_2 \rightarrow S_0$ Emissions in Carotenoids and Polyenes of Intermediate Length

The major differences between the optical spectroscopy of model polyenes and short apo-carotenes and the longer, more conjugated carotenoids employed in photobiology are illustrated in Fig. 5. Most striking is the cross-over from the $S_1(2^1A_g) \rightarrow S_0(1^1A_g)$ emission observed for the apo-heptaene (7c) to the dominant, $S_2(1^1B_u) \rightarrow S_0(1^1A_g)$ fluorescence of the analogous apo-nonaene (9). Similar changes from $S_1 \rightarrow S_0$ to $S_2 \rightarrow S_0$ emissions have been noted in

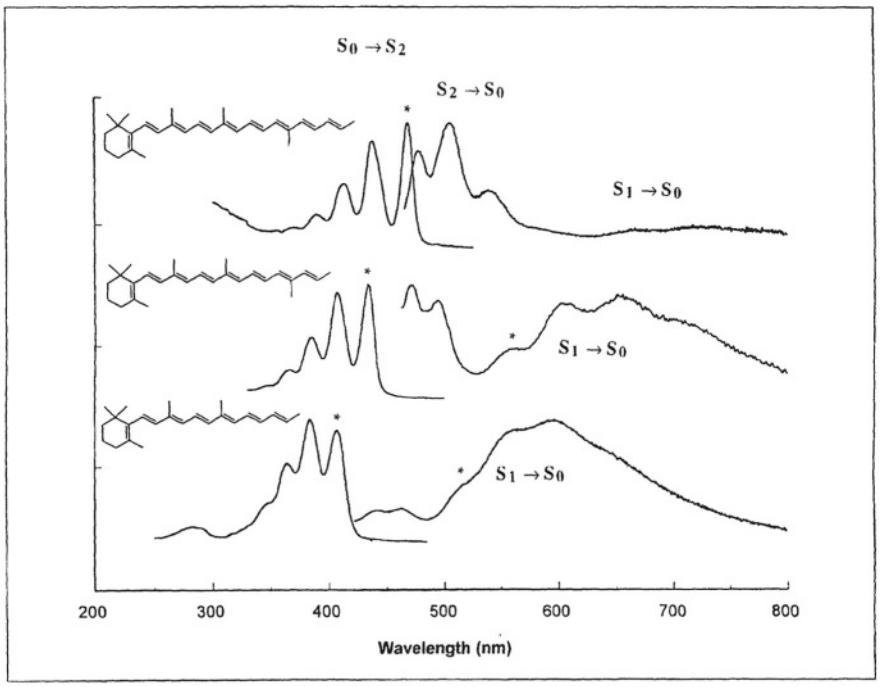

Fig. 5. Comparison of absorption and fluorescence spectra of β-apo-12′-carotene (7c), β-apo-10′-carotene (8), and β-apo-8′-carotene (9). Spectra were obtained at 77 K in an EPA glass. Electronic origins are designated by asterisks.

simple polyenes (Snyder et al., 1985), apo-carotenols (Cosgrove et al., 1990), spheroidenes (DeCoster et al., 1992), and analogs of β-carotene (Anderson et al., 1995). Fluorescence quantum yields are sensitive to structural details, though the relatively abrupt change to $S_2 \rightarrow S_0$ emissions invariably occurs for molecules with seven or eight conjugated bonds. This has the important practical consequence for photobiology that the 2^1A_g states of molecules such as spheroidene (10) and β-carotene (11) are difficult to detect using routine fluorescence techniques.

The characteristic change from $S_1 \rightarrow S_0$ to $S_2 \rightarrow S_0$ emissions in longer polyenes originally was attributed (Snyder et al., 1985; Cosgrove et al., 1990) to the increase in the S_2-S_1 energy difference with increasing conjugation length. This presumably results in a decrease in the rate of $S_2 \rightarrow S_1$ internal conversion following the well-known 'energy-gap law' (Englman and Jortner, 1970). For large energy gaps internal conversion rates become sufficiently small to allow the strongly allowed $S_2 \rightarrow S_0$ fluorescence to compete with radiationless decay processes, leading to violations of Kasha's Rule (Turro, 1978; Wayne, 1991). (Kasha's Rule states that for large molecules in condensed phases, radiationless processes from higher energy excited states (S_2, S_3, ...; T_2, T_3, ...) are so rapid that all radiative and photochemical processes originate from the lowest energy electronic state of a given multiplicity, i.e., S_1 or T_1.) The energy gap model accounts for $S_2 \rightarrow S_0$ emissions in several aromatic molecules all of which are characterized by large S_2-S_1 energy differences (Englman and Jortner, 1970).

Long polyenes and carotenoids, at first glance, are likely violators of Kasha's Rule. The S_2-S_1 energy difference at which $S_2 \rightarrow S_0$ fluorescence is observed ($> 5000\ cm^{-1}$) is consistent with the thresholds for S_2 emissions in a variety of organic and inorganic systems. However, the rather abrupt changeover from $S_1 \rightarrow S_0$ to $S_2 \rightarrow S_0$ emissions is not easily reconciled with the very modest changes in S_2-S_1 energy differences in previously studied polyene/carotenoid series (Snyder et al., 1985; Cosgrove et al., 1990; DeCoster et al., 1992; Anderson et al., 1995). Indeed, the three apo-carotenes whose spectra are presented in Fig. 5 have S_2-S_1 energy gaps that are almost identical ($5100 \pm 150\ cm^{-1}$, R. Christensen, unpublished). Given a constant S_2-S_1 energy gap, the rate of $S_2 \rightarrow S_1$ radiationless decay should be relatively insensitive to conjugation length. In fact, the expected increase in the density of vibrational 'accepting' modes in longer apo-carotenes (generally thought to

be C-C stretches, Orlandi et al., 1991) argues that $S_2 \rightarrow S_1$ internal conversion rates should *increase* in longer apo-carotenes. Recent investigations of $S_2 \rightarrow S_0$ fluorescence quantum yields in carotenes (Andersson et al., 1995) and spheroidenes (Frank et al., 1997) indicate $S_2 \rightarrow S_1$ internal conversion rates that are remarkably insensitive to conjugation length over the range N=5 to N=13. The 'cross-over' to $S_2 \rightarrow S_0$ fluorescence in these systems and in the longer apo-carotenes (Fig. 5) thus is most easily explained by increases in the rates of $S_1 \rightarrow S_0$ nonradiative decay due to a combination of smaller S_1-S_0 energy gaps and the increased density of S_0 accepting modes in larger molecules. This leads to the disappearance of $S_1 \rightarrow S_0$ fluorescence, allowing the weak, residual $S_2 \rightarrow S_0$ fluorescence to dominate the emissions of longer carotenoids. Further insights on $S_2 \rightarrow S_1$ internal conversion rates in spheroidenes and carotenes are provided by Andersson et al. (1995) and Frank et al. (1997).

2. Extrapolation of $S_2 \leftrightarrow S_0$ and $S_1 \leftrightarrow S_0$ Transition Energies to Long Carotenoids: The Infinite Polyene Limit

The absence of detectable $S_1 \rightarrow S_0$ emissions from long carotenoids thwarts the direct detection of the 2^1A_g states in molecules such as violaxanthin (N=9), antheraxanthin (N=10), spheroidene (N=10), zeaxanthin (N=11), β-carotene (N=11), spirilloxanthin (N=13), etc. Since an accurate knowledge of 2^1A_g energies is essential for understanding the roles these molecules play in photosynthetic systems, it has been tempting to extrapolate from the 2^1A_g energies of shorter, more fluorescent systems. Fig. 6 shows the (0-0) energies as a function of the number of double bonds for methyl-substituted polyenes and spheroidenes (DeCoster et al., 1992; Fujii et al., 1998). Simple extrapolations of these kinds of plots prove useful in analyzing the weak $S_1 \rightarrow S_0$ emissions from longer, more conjugated systems, particularly in estimating the positions of (0-0) bands in weak and/or poorly resolved spectra. For example, simple linear extrapolations of S_2-S_1 energy gaps combined with measurements of $S_0 \rightarrow S_2$ (0-0)'s or the more elaborate extrapolation schemes described below should provide reliable estimates of the S_1 energies of carotenoids employed in photosynthetic systems, i.e., for $9 \leq N \leq 13$.

More systematic extrapolation approaches have relied on theoretical models which suggest that

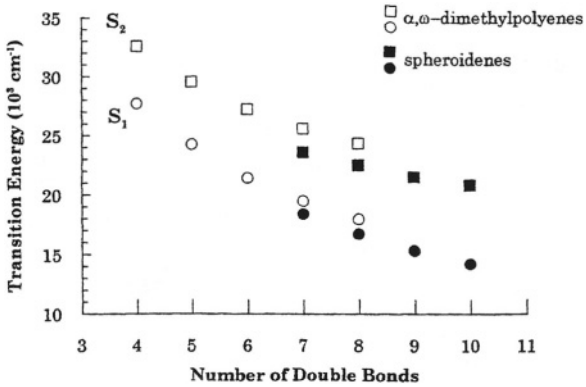

Fig. 6. $S_1 \rightarrow S_0$ ($1^1A_g \rightarrow 2^1A_g$) and $S_0 \rightarrow S_2$ ($1^1A_g \rightarrow 1^1B_u$) transition energies for α,ω-dimethylpolyenes and spheroidenes as a function of conjugation length. Transition energies are the electronic origins (0-0 bands) observed for $S_1 \rightarrow S_0$ and $S_0 \rightarrow S_2$ transitions in room temperature methanol. (The S_1 energy of spheroidene (N = 10) was obtained in n-hexane by Fujii et al. (1998).) Dimethylpolyene data are from Morey and Christensen (unpublished) and Kohler et al. (1988). Spheroidene data are from DeCoster et al. (1992) and from Fujii et al. (1998). S_2 energies are known to ± 50 cm^{-1}. S_1 energies have uncertainties of ± 100 cm^{-1} for the dimethylpolyenes, ± 200 cm^{-1} for the spheroidenes.

transition energies should vary as N^{-1} where N is the number of conjugated double bonds. The simplest versions of the free electron and Hückel MO models predict that, in the absence of bond alternation, the one-electron, $S_0(1^1A_g) \rightarrow S_2(1^1B_u)$ transition energies should exhibit a simple $(2N + 1)^{-1}$ dependence on polyene length with transition energies approaching zero for infinite polyenes (Kuhn, 1948; Murrell, 1963). Bond alternation and the resulting asymptotic approach to non-zero transition energies suggest that the $S_0 \leftrightarrow S_2$ transition energies of long polyenes should be modeled by $E = A + BN^{-1}$ (or $E = A + B(2N+1)^{-1}$). Tavan and Schulten (1987) have argued that similar dispersion relations should apply to $S_1 \leftrightarrow S_0$ transition energies, though extending the form of the $S_0 \leftrightarrow S_2$ extrapolations to transitions involving correlated, $1^1A_g \rightarrow 2^1A_g$ excitations has no a priori justification. Nevertheless, the limited amount of reliable data for the 2^1A_g energies of short polyenes does show a linear dependence on N^{-1}, and these fits have been extended to estimate 2^1A_g energies in longer, nonfluorescent polyenes. An interesting by-product of such fits is their use to predict 2^1A_g energies and $S_2 - S_1$ energy gaps in infinite polyenes, spheroidenes, and carotenes.

A review of recent extrapolations is summarized

in Table 1. The substantial variation in extrapolated ($N=\infty$) 2^1A_g and 1^1B_u energies illustrates the perils of such extrapolations, particularly for 2^1A_g states for which there is so little theoretical or experimental guidance on how transition energies should depend on the length of conjugation. Table 1 also reformulates the as yet unresolved issue of the differences between the electronic energies of simple polyenes and carotenoids, in particular the extent to which methyl substituents and terminal, β-ionylidene rings modify the energies for a particular N.

The early work of Hemley and Kohler (1977) used $E = A + B/N$ to fit the $S_0(1^1A_g) \rightarrow S_2(1^1B_u)$, (0-0) transition energies of unsubstituted polyenes with four through ten double bonds in a common hydrocarbon solvent (isooctane). This later proved to be consistent with Kohler's simple theoretical model (1990) which empirically adjusted the configuration interaction matrix elements used to calculate the 2^1A_g and 1^1B_u energies for unsubstituted, α,ω-dialkyl substituted, and α,ω-diphenyl substituted polyenes. The only molecules considered in the data set were those for which (0-0) transition energies were precisely known from low-temperature, mixed-crystal spectra in n-alkane solvents. Using an iterative, least squares procedure that corrected conjugation lengths for the effects of alkyl and phenyl substitution, Kohler reproduced ~25 $S_0(1^1A_g) \rightarrow S_2(1^1B_u)$ and $S_0(1^1A_g) \leftrightarrow S_1(2^1A_g)$ (0-0) transition energies. The empirically derived, best-fit parameters then were applied to calculate the infinite polyene transition energies presented in Table 1.

Kohler (1993b) later used simple N^{-1} fits and the concept of an 'effective' conjugation length ($N_{eff} = N \pm \delta N_{substituent}$) to develop universal fits of the 2^1A_g and 1^1B_u energies of different polyenes series. The goal of this work was to develop empirical equations with well-defined rules for calculating N_{eff} that would account for (and predict) the 2^1A_g and 1^1B_u energies of any substituted polyene or carotenoid. For example,

Table 1. Extrapolations of carotenoid/linear polyene transition energies to the infinite polyene limit

2^1A_g ($n = \infty$) in cm^{-1}	1^1B_u ($n = \infty$) in cm^{-1}	
	16,500[a]	unsubstituted polyenes in iso-octane ($E = A + B/N$)
	14,400[b]	α,ω-*tert*-butyl polyenes in pentane ($E = A + B/N$)
8,710[c]	15,878[c]	least squares fit to Hückel model with empirical adjustment of configuration-interaction matrix elements to account for the effects of α,ω-dialkyl substitution (based on data obtained in low temperature, n-alkane solvents)
6,800[d]	14,250[d]	$E = A + B/N_{eff}$ where N_{eff} attempts to correct for the effects of a wide range of substituents (Solvents and temperatures are not clearly specified.)
		unsubstituted and methyl-substituted polyenes in polar and nonpolar solvents and over a range of temperatures
6,500[e]		$E = A + B/(2N+1)$
		carotenoids and spheroidenes in a variety of solvents and temperatures
4,800[e]		$E = A + B/(2N+1)$
		carotenes in 3-methyl pentane glasses S_1 energies of long carotenes were extrapolated from the energy gap law.
7,790[f]	13,630[f]	$E = A + B/N$
3,470[f]	10,980[f]	$E = A + B/N + C/N^2$
		spheroidenes in methanol and n-alkanes S_1 energies of long spheroidenes were extrapolated from the energy gap law.
3,802[g]	10,955[g]	$E = A + B/(N + C)$
		diphenylpolyenes in toluene (N = 2–7)
–4,200[h]	2,400[h]	$E = A + B/(N + C)^D$

[a] Hemley and Kohler, 1977; [b] Knoll and Schrock, 1998; [c] Kohler, 1990; [d] Kohler, 1993b; [e] Koyama et al., 1996; [f] Andersson and Gillbro, 1995; [g] Frank et al., 1997; [h] Bachilo et al., 1998

to rationalize the 1^1B_u energies of molecules such as β-carotene, N was reduced to $N_{eff} = N - 0.3$ to account for the loss of effective conjugation due to the out-of-plane rotations of the terminal β-ionylidene rings. Similar empirical corrections were made for alkyl and phenyl substituents. Although the resulting fits of E vs. N^{-1} are generally of good quality, the discrepancies with the parameters (e.g., $N=\infty$ energies) obtained from data on simple, unsubstituted polyenes (Hemley and Kohler, 1977: Kohler, 1990) indicates some systematic shortcomings in accounting for substituents in this manner. One of the problems with this approach is illustrated in the difference between using $N_{eff} = N - 0.3$ for the 1^1B_u energies and $N_{eff} = N + 0.5$ for the 2^1A_g energies to correct for the presence of double bonds rings in molecules such as β-carotene. It is plausible that effective conjugation lengths may not be the same for every electronic transition, but an *increase* in conjugation length in 2^1A_g due to nonplanarity has no physical basis nor any support from spectra such as presented in Fig. 4. In spite of these obvious shortcomings, further development of universal 1^1B_u and 2^1A_g energy curves has considerable appeal. Refinement of this approach will require that energies be related to a common solvent and temperature and clearly awaits more reliable spectroscopic data on 2^1A_g (0-0) transition energies in longer polyenes and carotenoids.

Recent attempts at extrapolating carotenoid energies require careful examination. Andersson and Gillbro (1995) combined estimates of (0-0) energies obtained from the fluorescence spectra of short, mini-carotenes (including β-carotene) with estimates of 2^1A_g energies of homologous, longer members of this series, obtained from lifetime measurements and empirical extrapolations of the energy-gap law (see below). The 2^1A_g and 1^1B_u energies then were fit to both two and three term expansions in 1/N to obtain estimates of the long polyene limits for the two states. The two-term ($E = A + B/N$) expansions give parameters that are comparable with those of Kohler. However, it is noteworthy that the two-term extrapolation of Andersson and Gillbro leads to a $1^1B_u - 2^1A_g$ energy gap that is essentially independent of carotenoid length. In order to improve the fits to the (0-0)'s for the longer members of the series (whose energies were estimated from extrapolations based on the energy gap law- see below), a three term expansion was used which significantly lowered the 2^1A_g and 1^1B_u energies in the long polyene limit. It is important to stress that there is no theoretical justification for a three term expansion and that the inclusion of the additional term largely appears to have been dictated by the only two carotenoids whose 2^1A_g energies could not be determined directly.

Frank et al. (1997) obtained comparable data for a homologous series of spheroidenes with seven to thirteen double bonds. It is significant that the $S_1(2^1A_g) \rightarrow S_0(1^1A_g)$ (0-0) band can be directly observed only for the shortest three of the seven molecules in this series with the remaining (0-0) energies being estimated from energy-gap law extrapolations. These energies as well as the $S_0(1^1A_g) \rightarrow S_2(1^1B_u)$ (0-0)'s then were fit to A+B/(N+C) with the results indicated in Table 1. The large (~5000 cm^{-1}) differences between the long chain ($N = \infty$) 2^1A_g and 1^1B_u energies of simple polyenes (Kohler, 1990, 1993b) and the energies obtained by Andersson and Gillbro and by Frank et al. have been attributed to the stabilizing effects of the methyl substituents in the carotenoid systems. However, there is little support for substituent effects of this magnitude (e.g., $C \approx 2$ for the $S_0 \rightarrow S_2$ transitions) in the spectra of shorter model systems (Fig. 4).

At this point, most of the discrepancies in the long-polyene/long-carotenoid extrapolations summarized in Table 1 should be attributed to the differences in the fitting functions rather than fundamental differences in the data. It is important to reiterate that there is no theoretical basis for either of the three parameter extrapolations employed for the carotene or spheroidene data. The recent use of four parameter functions to fit the S_2 and S_1 energies of diphenylpolyenes (Bachilo et al., 1998) further illustrates the limitations of arbitrary, phenomenological functions to describe polyene/carotenoid electronic energies. In this later case, the large N extrapolations lead to negative S_1 energies, providing a strong reminder of the lack of a physical basis for such fits. At a minimum, it will be important to subject simple polyenes and carotenoids to the same analysis to explore the systematic effects of substitution and conjugation length on the electronic energies of these systems. Careful use of extrapolation procedures also must consider the relative weights of data points. There are substantial differences in the uncertainties of S_1 energies obtained from well-resolved spectra and those estimated from energy gap extrapolations. These uncertainties should be

reflected in the statistical weights used in least squares fits to properly evaluate how electronic energies depend on the length of conjugation.

3. Use of Lifetime Measurements and the Energy-Gap Law to Estimate 2^1A_g Energies in Long Carotenoids.

The reduction of $S_1 - S_0$ energy differences and the increased density of S_0 vibrational accepting modes work together to enhance the rates of $S_1 \rightarrow S_0$ radiationless decay in longer polyenes and carotenoids. As described above, this accounts for the steady fall-off in $S_1 \rightarrow S_0$ fluorescence yields in going from octatetraene ($\phi_f \sim 1$ in low temperature glasses (Gavin et al., 1978)) to molecules such as β-carotene ($\phi_f < 10^{-5}$, Andersson et al., 1995). The extremely weak $S_1(2^1A_g) \rightarrow S_0(1^1A_g)$ emissions in polyene/carotenoids with N > 9, i.e., in almost all Carotenoids of photobiological interest, has required other approaches for estimating the 2^1A_g energies of these molecules. In particular, the weak-coupling limit of the energy-gap law developed by Englman and Jortner (1970) appears to be well suited for describing $S_1 \rightarrow S_0$ nonradiative decay (internal conversion) in long polyenes: $E(S_1) - E(S_0) = \Delta E$ is large and internal conversion is dominated by a single type of vibrational accepting mode, i.e., symmetric C=C stretches. A simplified version of this model is summarized as follows:

$$k_{ic} = C \exp(-\gamma \Delta E/h\nu) \qquad \text{Eq. (3)}$$

where k_{ic} is the rate of $S_1 \rightarrow S_0$ internal conversion (in most cases the reciprocal of the S_1 lifetime), ΔE is the energy difference between the S_0 and S_1 states, and $h\nu$ is the energy of the S_0 accepting vibrations ($\sim 1600\ cm^{-1}$). C and γ are assumed to have only a mild dependence on ΔE, $h\nu$, the number of accepting modes, and the displacement between the S_0 and S_1 potential energy surfaces. C, γ, and $h\nu$ often are treated as constants in fits relating k_{ic} to ΔE for different carotenoids. (See Chynwat and Frank (1995) and Andersson et al. (1995) for further discussion of these assumptions.) These simplifications lead to a linear version of the energy-gap law:

$$\ln k_{ic} = \ln C - B\Delta E \qquad \text{Eq. (4)}$$

Andersson et al. (1995) applied the energy-gap law to a series of carotenes, Frank et al. (1993) and Chynwat and Frank (1995) carried out a similar study on spheroidenes and other carotenoids, and Bachilo et al (1998) studied S_1 internal conversion rates in diphenylpolyenes. The rates of S_1 nonradiative decay (determined from fluorescence lifetime or transient absorption measurements) and the $S_1(2^1A_g) \rightarrow S_0(1^1A_g)$ (0-0) transition energies (determined (or estimated) from spectroscopic measurements) appear to obey the energy-gap law, e.g., plots of $\ln k_{ic}$ vs. ΔE tend to obey equation 4 with $\ln C \sim 35$–40 and $1/B$ ($= h\nu/\gamma$) ~ 1100–$1500\ cm^{-1}$ for a wide range of polyenes and carotenoids (Frank et al., 1993; Andersson et al., 1995; Bachilo et al., 1998). More sophisticated applications of the energy-gap law have been discussed by Chynwat and Frank (1995). Parameters obtained from molecules for which both ΔE and k_{ic} are known then are used to extrapolate $\Delta E = E(2^1A_g)$ for longer carotenoids for which only k_{ic} can be experimentally determined. This approach has been used to estimate the 2^1A_g energies of several nonfluorescent carotenoids that play important roles in photobiological systems (Frank et al, 1993, 1997; Chynwat and Frank, 1995).

The value of energy gap extrapolations depends both on the applicability of the model to the range of molecules being considered and the quality of data used to determine the empirical relationships between k_{ic} and ΔE. One of the most fundamental limitations in applying energy gap analysis to carotenoids can be traced to unresolved optical spectra and the somewhat arbitrary assignment of ΔE values in various solvents. Andersson et al. (1995) obtained S_1 lifetimes of a series of molecules homologous to **β-carotene,** and $S_1(2^1A_g) \rightarrow S_0(1^1A_g)$ (0-0)'s (ΔE's) were based on fluorescence spectra obtained in 77 K, 3-methylpentane glasses (Andersson et al., 1992). Even under low temperature conditions, the carotene spectra are essentially unresolved. The (0-0) bands for $S_0 \rightarrow S_2$ and $S_1 \rightarrow S_0$ transitions only could be estimated from absorption maxima, with errors of $\pm$ $1000\ cm^{-1}$ reported for the mini-5, mini-7, and mini-9 (0-0) transitions (Andersson et al., 1992). In a recent application of the energy-gap law to this series, Andersson et al. (1995) use S_1 depopulation rates in room temperature hexane and Eq. (4) to extrapolate the S_1 energies for two longer, nonfluorescent carotenoids (with N = 15 and N = 19) whose S_1 lifetimes were obtained by transient absorption techniques. The 77 K mini-carotene $S_1 \rightarrow S_0$ transition

energies were systematically lowered by 1000 cm^{-1} to estimate the ΔE's in room temperature hexane. This adjustment plus the uncertainties in locating the (0-0)'s in the 77 K glasses give rise to considerable uncertainties in the ΔE's used to determine the parameters in Eq. (4).

The energy gap studies of Frank et al. (Chynwat and Frank, 1995; Frank et al., 1997) are based on $S_1 \rightarrow S_0$ fluorescence spectra and S_1 lifetime measurements of three synthetic spheroidenes (DeCoster et al., 1992), two mini-carotenes (Andersson and Gillbro, 1992), and fucoxanthin (Katoh et al., 1991; Shreve et al., 1991; Mimuro et al., 1992). Problems regarding the uncertainties in the 2^1A_g (0-0) energies are partially overcome, e.g., the vibronic resolution is sufficient to locate $S_1 \rightarrow S_0$ electronic origins in the two shorter spheroidenes and in fucoxanthin. However, the (0-0) energies must be estimated for the other three molecules, including two of the mini-carotenes discussed above. Lifetimes ($\sim 1/k_{ic}$) were obtained in diethylether for the spheroidenes, CS_2 for fucoxanthin, and n-hexane for the mini-carotenes. Corresponding ΔE's were obtained in methanol, CS_2 and 77 K 3-methylpentane glasses (Andersson et al., 1992). Unlike Andersson et al. (1995), Frank et al. retain the ΔE's estimated from the original 77 K spectra of the two mini-carotenes and relate these energies to lifetimes obtained in room temperature solutions. Future applications of the energy-gap law to estimate S_1 energies in nonfluorescent carotenoids should carefully consider how k_{ic} and ΔE (and the parameters obtained from Eqs. (3) and (4)) depend both on solvent and on temperature.

Another consideration is the appropriateness of applying energy-gap law fits to molecules with significantly different structures. Whereas the studies by Andersson et al. were confined to a homologous series, Frank et al. employed a range of carotenoids in their extrapolations. A survey of recent energy-gap law fits to spheroidenes (Frank et al., 1993), carotenes (Andersson et al., 1995), and diphenyl polyenes (Bachilo et al., 1998) shows systematic differences in parameters (B and C in Eq. (4)) which may be related to differences in molecular structure. Furthermore, a previous study of the gas phase fluorescence of simple tetraenes and pentaenes showed significant increases in $S_2 \rightarrow S_1$ internal conversion rates upon methyl-substitution where the $E(S_2) - E(S_1)$ difference remained constant (Bouwman et al., 1990). The acceleration of internal conversion was attributed to the increased density of S_1 vibronic states in methyl-substituted compounds. Similar effects may modify $S_1 \rightarrow S_0$ internal conversion rates in carotenoids, e.g., B and C in equation 4 may be different for carotenes and spheroidenes and/or depend on the length of conjugation. Typical parameters ($1/B \approx 1100$–1500 cm^{-1}) indicate that changing k_{ic} by a factor of two (e.g., by modifying the solvent, temperature, or molecular structure) changes ΔE by 750–1050 cm^{-1}. This argues for caution in applying the energy-gap law to a wide range of conjugated molecules under different solvent conditions, even if k_{ic} and ΔE both can be accurately determined. These limitations should cause particular pause in using lifetime-based estimates of 2^1A_g energies to extrapolate to infinite carotenes or spheroidenes (Table 1).

4. Recent Attempts at the Direct Detection of the 2^1A_g State in β-Carotene and Other Long Carotenoids

Due largely to its photobiological importance and the availability of high purity samples, β-carotene has been a popular target for the initial application of a wide variety of spectroscopic techniques to elucidate the energies and properties of 'long carotenoid' electronic states. Recent publications include the observation of a relatively strong absorption at 14,200 cm^{-1} in zeolite, detected by reflectance spectroscopy (Haley et al., 1992). The authors argue that the symmetry-forbidden, $g \rightarrow g$ transition is made allowed by distortion of β-carotene by asymmetric sites in the zeolite host. However, a 14,120 cm^{-1} peak in the reflectance spectrum of a 4.2 K single crystal of β-carotene was attributed to an experimental artifact (Gaier et al., 1991). In this same study, Gaier et al. reported low energy features in the pre-resonance Raman excitation spectra of β-carotene single crystals that were assigned to $S_0(1^1A_g) \rightarrow S_1(2^1A_g)$ absorption. Analysis of these bands leads to an 13,600 cm^{-1} estimate for the (0-0). Another intriguing result was the observation of a weak absorption background in the inverse Raman (Raman loss) spectrum of canthaxanthin (Jones et al., 1992) which shows evidence for a low lying absorption at ~600–700 nm. However, there is little support for the identification of this feature with the $S_0(1^1A_g) \rightarrow S_1(2^1A_g)$ transition. Rohlfing et al. (1996) have investigated the electric-field-induced change in the absorption (electroabsorption) of β-carotene and a model octaene in polystyrene matrices. Electroabsorption is directly

related to the third-order nonlinear susceptibilities of these molecules. A weak, low-energy feature in the electroabsorption spectrum of the octaene at 2.65 eV (21,400 cm^{-1}) was associated with $1^1A_g \rightarrow 2^1A_g$ absorption activated by the symmetry-breaking effect of the applied electric field. A similar but weaker response was reported for β-carotene. All of the studies on β-carotene would benefit from more systematic extensions to shorter polyenes/carotenoids for which the energies of the 2^1A_g states can be unambiguously established by detection of vibronically resolved, $S_1 \rightarrow S_0$ fluorescence. This would allow straightforward evaluation of the ability of these alternate techniques to detect $1^1A_g \rightarrow 2^1A_g$ transitions in molecules such as β-carotene.

The most promising of recent efforts to detect the 2^1A_g state in long carotenoids began with the report by Bondarev and Knyukshto (1994) of a very weak ($\phi_f \sim 10^{-5}$) and very broad, $S_1 \rightarrow S_0$ emission in β-carotene. These authors somewhat arbitrarily assigned the $S_1(2^1A_g) \rightarrow S_0(1^1A_g)$ (0-0) energy as 13,200 ± 300 cm^{-1} in n-hexane, toluene, and carbon disulfide. Andersson et al. (1995) later repeated the results of Bondarev and Knyukshto but reported sufficient vibronic structure in carbon disulfide to place the (0-0) transition at 14,200 cm^{-1}. However, Andersson et al. did not present fluorescence excitation spectra, a critical issue in proving that the weak, long-wavelength emissions belonged to β-carotene. Koyama and Fujii (Chapter 9) and Fujii et al. (1998) recently extended these earlier studies to detect weak, $S_1(2^1A_g) \rightarrow S_0(1^1A_g)$ (0-0) transitions in *all-trans* isomers of β-carotene (14,500 cm^{-1}), spheroidene (14,200 cm^{-1}), and neurosporene (15,300 cm^{-1}) in n-hexane. These assignments are supported by fluorescence excitation spectra that are in excellent agreement with the $S_0 \rightarrow S_2$ absorption spectra. The locations of the (0-0) bands confirm previous estimates (Cosgrove et al., 1990; Andersson et al., 1992; DeCoster et al., 1992; Frank et al, 1993, 1997; Chynwat and Frank, 1995) based on extrapolations from shorter, more fluorescent analogs.

These recent experiments demonstrate that it should be possible to use fluorescence to detect resolved, $S_1 \rightarrow S_0$ emissions in other long carotenoids, although such studies will require samples of high purity and should include a careful analysis of fluorescence excitation spectra to confirm the source of any weak, low energy emissions. The extremely low $S_1 \rightarrow S_0$ fluorescence yields ($<10^{-5}$ for molecules such as β-carotene) put heavy demands both on the quality of the samples and the interpretation of the experiments in order to exclude the possibility of interferences from other emissive species. Thus, for example, the original claims of 2^1A_g emissions in spheroidene (Watanabe et al., 1993) later were showed to be due to chlorophyll *a* impurities in the spheroidene preparations (Koyama et al., 1996; Frank et al,, 1997; Fujii et al., 1998)

Finally, it is important to comment on the very recent report (Sashima et al (1998)) of the detection of the 2^1A_g state in solid *all-trans*-spheroidene using resonance Raman excitation techniques. The potential of using resonance Raman excitation spectra to detect resolved $S_0 \rightarrow S_1$ absorptions in carotenoids provides a tantalizing alternative to the detection of weak fluorescence signals and/or the use of extrapolation techniques (energy gap and other approaches). However, the application of resonance Raman excitation techniques to carotenoids has a tortuous past. See DeCoster et al. (1992) and Frank and Christensen (1995) for a discussion of previous attempts to use Raman excitation techniques to locate the S_1 state in β-carotene, starting with the early reports of Thrash et al. (1977, 1979). It thus will be important to see if the experiments reported by Sashima et al. on spheroidene can be readily extended to shorter polyenes and carotenoids for which the $S_0 \leftrightarrow S_1$ (0-0)'s have been unambiguously located by fluorescence techniques. Similar features in the resonance Raman excitation profiles of 4.2 K single crystals of β-carotene (Gaier et al., 1991) were only cautiously assigned to $S_0 \rightarrow S_1$ absorptions. The vibronic progressions in the excitation profiles of Sashima et al. appear to depend on the vibrational mode monitored (C-C or C=C symmetric stretch), whereas the excitation profiles of Gaier et al. do not depend on the Raman mode monitored. It also should be noted that the excitation profiles reported by Gaier et al. and by Sashima et al. both show maximum intensities in what are identified as the (0-0) and (0-1) bands of the $S_0 \rightarrow S_1$ transitions. This is in stark contrast to the steep, monotonic rises in $S_0 \rightarrow S_1$ vibronic intensities observed in high resolution spectra of model polyenes (Simpson et al., 1987; Kohler et al., 1988; Petek et al., 1991). To the extent that the forbidden, $S_0 \rightarrow S_1$ transitions are made 'allowed' by vibronic interactions between 2^1A_g and 1^1B_u, $S_0 \rightarrow S_1$ (0-0) bands are typically rather weak compared to vibronic transitions to S_1 vibrational states that are closer to the zero-point energy of $S_2(1^1B_u)$. A careful examination of relative vibronic

intensities thus should be part of any assignment of low-energy features in carotenoid electronic spectra.

IV. Triplet States in Polyenes and Carotenoids: Spectroscopic Observations and Theory

Compared to excited singlet states, considerably less experimental information is available regarding the energies of polyene/carotenoid triplet states. This, in large part, is due to their lack of confirmed phosphorescence. This presents a major barrier to understanding the energies and properties of triplets, particularly of longer polyenes and of the carotenoids involved in photobiological processes. Evans' pioneering experiments using high pressure, oxygen perturbation techniques to enhance $S_0 \rightarrow T_1$ absorption spectra (1960, 1961, 1972) provided the first direct observations of low-lying triplet states in ethylene, butadiene, hexatriene, and octatetraene. Evans (1960) also detected $S_0 \rightarrow T_1$ transitions in octatrienal, decatetraenal, and dodecapentaenal. This work was extended to retinal by Raubach and Guzzo (1973), though their assignment of the 803 nm band as the $S_0 \rightarrow T_1$ electronic origin probably is in error. (Evans' work on dodecapentaenal indicates that the (0-0) band for retinal most likely is at ~900 nm.) Electron-impact spectroscopy (Kuppermann, 1979; Allan et al. 1984) later provided complementary information on the low-lying excited triplet states of the short polyenes. The results of these measurements and the gas-phase measurements of the $S_0 \rightarrow S_1$ and $S_0 \rightarrow S_2$ transitions in these simple polyenes are summarized in Table 2.

There is strong theoretical support for assigning the lowest lying triplet state in polyenes (T_1) as ^3B_u (Allen et al. 1984; Zoos and Ramasesha 1983). It is important to note the distinctions between data obtained in solution versus that obtained in the gas-phase and whether there is sufficient resolution to allow the unambiguous identification of electronic origins as opposed to estimates of the Franck-Condon maxima of 'vertical' transitions. Data obtained by electron-impact and oxygen perturbation techniques are in excellent agreement. This not only provides confidence in the measurements, but also confirms that the spin-forbidden, $S_0 \rightarrow T_1$ transitions are relatively insensitive to solvent perturbations. It is significant that very little additional spectroscopic information regarding polyene triplets has been obtained since the early work of Evans. True to form, octatetraene provides the most accurate, most complete set of data for the singlet and triplet electronic energies of any polyene. The vibronic features of all $S_0 \rightarrow T_1$ spectra are very similar to those observed for corresponding $S_0 \rightarrow S_1$ and $S_0 \rightarrow S_2$ transitions. Vibronic intervals of 1400–1500 cm^{-1} can be traced to unresolved combinations of C=C and C-C symmetric stretching vibrations. $S_0 \rightarrow T_1$ (0-0) bands are typically weak, suggesting a more significant change in geometry than for low energy S $\rightarrow$ S transitions. The characteristic vibronic signatures of polyene spectra again provide an useful tool for assigning electronic transitions.

Little, if any reliable spectroscopic information is available regarding the T_1 energies of polyenes or carotenoids with more than six conjugated double bonds. As a result, it has been necessary to rely on indirect measurements and/or extrapolations to estimate the T_1 energies of carotenoids employed in photosynthetic systems. One such approach has been outlined by Bensasson et al. (1976, 1993) and discussed by Frank and Cogdell (1993). A plot of the reciprocal of the triplet energies (from Table 2) as a

Table 2. Energies (in cm^{-1}) of low-lying electronic states of simple polyenes. Vertical transition energies (Franck-Condon maxima) are given in parentheses. Other energies refer to the electronic origins (0-0 bands) of $S_0 \rightarrow T_1$ and $S_0 \rightarrow S_n$ transitions. The O_2 perturbation spectra were obtained in chloroform; all other energies refer to the gas phase.

	O_2 perturbation[a]	electron impact[b]		
	1^3B_u	1^3B_u	2^1A_g	1^1B_u
ethylene	<28,700 (37,000)	(34,800)		~48,000[f]
butadiene	20,830 (26,000)	(26,000)	~43,500[c]	46,260[g]
hexatriene	16,450 (20,800)	(21,000)	<34,038[d]	39,786[g]
octatetraene	13,750 (17,000)	13,900 (16,900)	29,949[e]	35,553[g]

[a] Evans (1960,1961); [b] Allan et al. (1984); Kuppermann et al. (1979); [c] Chadwick et al. (1985); [d] Buma et al. (1990); [e] Petek et al. (1995); [f] Ziegler et al. (1983); [g] Vaida (1984)

function of the number of double bonds gives a linear fit that has been used to extrapolate to the triplet energies of more extensively conjugated molecules such as spheroidene and β-carotene. There is little justification for extrapolating from N = 4 to N = 11. Nevertheless, this procedure (or a plot of triplet energies vs. N^{-1}, cf. Table 1) predicts T_1 energies for longer carotenoids, e.g., ~ 6200–6800 cm^{-1} for β-carotene, depending on assumptions regarding the effective length of conjugation (Bensasson, 1976, 1993). These energies are consistent with those estimated from quenching experiments in which molecules of known triplet energy are used to sensitize the formation of β-carotene triplets. Detailed quenching experiments, particularly involving the quenching of singlet oxygen (Bensasson, 1993), place the T_1 level of β-carotene to be almost isoenergetic with that of excited, singlet oxygen (~7900 cm^{-1}).

Extensive use also has been made of the approximation from the simple valence bond description of polyene energy levels that the lowest triplet level in polyenes/carotenoids (1^3B_u) should have an energy approximately one half that of the lowest singlet state (2^1A_g) (Hudson et al., 1982). The limited data given in Table 2 indicates that this relationship is approximately true for short polyenes. Though there is only qualitative theoretical support for this statement, valence bond theory has yet to provide a quantitative accounting of the energies of low-lying singlet states in long or short polyenes.), the lack of alternate spectroscopic information has allowed the ($E(1^1A_g \rightarrow 1^3B_u) = E(1^1A_g \rightarrow 2^1A_g)/2$) 'rule of thumb' to find wide use in estimating the energies of carotenoid triplets. (See, for example, Haley et al 1992) As discussed in section III, recently improved estimates of the 2^1A_g energy in β-carotene (Cosgrove et al. 1990; Frank et al., 1993, 1997; Bondarev and Knyukshto 1994; Andersson et al. 1995, Koyama and Fujii, Chapter 9) converge on an 2^1A_g energy of 14,500 ± 500 cm^{-1}. The rule of thumb leads to a 1^3B_u (T_1) energy of ~7,250 cm^{-1} which is consistent with the results of quenching experiments and the extrapolation of Evans' data on short polyenes.

Bachilo (1995) recently used transient absorption techniques to detect a weak $T_1 \rightarrow T_n$ transition at 8100 cm^{-1} in β-carotene. This places T_n (^3B_u or ^3A_g?) at almost the same energy as S_1. Assuming (as appears to be the case for shorter polyenes (Allan et al. 1984)) that the lowest triplet state is ^3B_u and that there is a nominal splitting between 2^1A_g and its corresponding triplet, there must be an undetected ^3A_g state lying somewhere between T_1(1^3B_u ~7000 ± 1000 cm^{-1}) and S_1(2^1A_g ~ 14,500 cm^{-1}). Understanding the energies and symmetry labels of these low-lying triplet states will be important in more fully describing spin-orbit coupling and triplet quenching in this well-studied molecule.

Marston et al. (1995) reported the detection of phosphorescence from β-carotene in the near IR using Fourier transform techniques, placing T_1 at ~7400 cm^{-1}. This study would have benefited by systematic application to longer and shorter conjugated systems, the time-honored way to demonstrate that the energies of carotenoid excited states depend inversely on the length of conjugation. Furthermore, the phosphorescence spectrum reported by Marston shows vibronic structure with ~500 cm^{-1} spacings. This is not consistent with the higher frequency C-C and C=C stretches that dominate polyene singlet ↔ singlet spectra (Section II.B. 1 and Fig. 3) as well as the vibronic patterns observed in the $S_0 \rightarrow T_1$ transitions of short polyene hydrocarbons (Evans 1960, 1961; Allan et al. 1984).

In contrast to the wide-ranging efforts to detect triplet states in β-carotene, very little effort has been expended on other carotenoids such as spheroidene. Our understanding of low-lying triplet energies in these systems is limited to quenching experiments (Farhoosh et al., 1994, 1997), estimates based on extrapolations from the triplet energies of shorter polyenes, and the use of the $E(1^3B_u) \approx E(2^1A_g)/2$ approximation. It is important to reiterate that the use of extrapolations or the rule-of-thumb requires critical scrutiny, especially for carotenoids for which this is the only means of estimating triplet energies.

V. Conclusions and Unresolved Issues

The primary focus of this chapter has been the connection between the spectroscopy of simple polyenes and the low-lying, excited electronic states of carotenoids involved in photobiological processes, A survey of recent work indicates the crucial significance of 'high-resolution' spectroscopic experiments: first, in establishing the existence of low energy 2^1A_g states in model systems and subsequently, in understanding how the energies of these states change with increasing conjugation, the presence of substituents, and different solvent environments. The simple geometries of unsubstituted molecules allow their incorporation into low

temperature mixed crystals, and the relatively high vapor pressures of short polyenes permit their detailed study as low-temperature, isolated molecules in supersonic jets. These experiments (resolutions of <1 cm^{-1} in supersonic jets, <10 cm^{-1} in n-alkane crystals) and to a lesser extent, experiments carried out in low temperature glasses (resolutions of > 100 cm^{-1}, e.g., see Figs. 4 and 5), provide sufficient vibronic resolution to allow the unambiguous identification of electronic origins as well as a detailed look at other vibrational states accessed by both symmetry-allowed and symmetry-forbidden electronic transitions.

The major challenges in extending the experiments on short polyenes to the longer, more complicated carotenoids employed in photobiology are the precipitous decreases in $S_1 \rightarrow S_0$ fluorescence yields combined with the losses in spectral resolution. (High-resolution mixed crystal and gas phase techniques are not easily applied to molecules such as β-carotene.). The limited experimental data available for longer carotenoids and the subsequent need for ad hoc extrapolations leads to 'low-resolution' estimates of the 2^1A_g energies (uncertainties of hundreds of cm^{-1}), in contrast to the much higher precisions to which electronic and vibrational energies can be determined for shorter polyenes. On the other hand, such low-resolution estimates may be quite sufficient for understanding the mechanisms of energy transfer in photosynthetic systems. For example, it now seems clear that the 2^1A_g state of spheroidene (E ~ 14,200 cm^{-1} in n-hexane) lies well above the $S_1(Q_y)$ state of bacteriochlorophyll *a* (e.g., E ~ 12,500 cm^{-1} in the B800 monomer of the light harvesting complex (LH2) of *Rhodobacter sphaeroides* (Sauer, 1978)), allowing efficient spheroidene $(S_1) \rightarrow$ bacteriochlorophyll *a* (S_1) energy transfer in the antenna complexes of typical photosynthetic bacteria.

In other situations, more accurate estimates of carotenoid electronic energies may be required. The $S_1(2^1A_g)$ state of β-carotene (E ~ 14,500 cm^{-1} in n-hexane) appears to lie somewhat below the $S_1(Q_y)$ state of chlorophyll *a* (e.g., E ~ 14,700 cm^{-1} in the light-harvesting complex of Photosystem II (Kwa et al. 1992). This suggests that the S_2 state of β-carotene must be involved in energy transfer (Cosgrove et al., 1990; DeCoster et al., 1992; Frank and Christensen, 1995), as originally proposed by Snyder et al. (1985). However, more accurate estimates of the in vivo $S_1(2^1A_g)$ energies of β-carotene are required to fully understand the relative roles of the carotenoid S_2 and S, states in a variety of photosynthetic antennae. Similarly, one attempt to explain how excess energy is dissipated by plants under conditions of high photon fluxes relies on subtle (~500–1000 cm^{-1}) differences between the 2^1A_g energies of three xanthophylls (violaxanthin (N = 9), antheraxanthin (N = 10), and zeaxanthin (N = 11)) found in the light-harvesting machinery of plants (Frank et al., 1994). More reliable estimates of 2^1A_g energy differences in biological environments would be helpful in understanding the interactions between the xanthophylls and chlorophyll. Note also that the population of low frequency vibrations and phonons results in a significant fraction of states $(\sim e^{-\Delta E/kT})$ within a few kT (~200 cm^{-1} at 25 °C) of the electronic origins. Thermal effects thus need to be considered in understanding the interactions between closely separated carotenoid and chlorophyll excited states. This also suggests that kT might be an appropriate experimental goal for the accuracy of electronic energy determinations of carotenoids employed in photobiological processes.

In spite of the inherent difficulties in locating 2^1A_g states in weakly fluorescent samples, no better approach has emerged that yields unambiguous assignments of $S_0 \leftrightarrow S_1$ electronic origins in long polyenes or carotenoids. Two-photon spectroscopy, reflectance spectroscopy, resonance Raman excitation spectroscopy, consecutive two-photon absorption, electroabsorption, etc. have failed to improve on (or, in many cases, even to reproduce) data obtained from fluorescence experiments on shorter carotenoids and polyenes. A fundamental problem with techniques based on one-photon absorption (i.e., almost all the techniques listed above) is the difficulty in locating the extremely weak $S_0 \rightarrow S_1$ (0-0) bands hi other than high resolution experiments. Polyene $1^1A_g \rightarrow 2^1A_g$ absorptions show steep rises in vibronic intensities in approaching the $1^1A_g \rightarrow 1^1B_u$ origins due to a $(\Delta E)^{-2}$ dependence on vibronic mixing/intensity borrowing between the 2^1A_g and 1^1B_u states (Petek et al., 1991). This effect is particularly evident in high-resolution spectra of model heptaenes and octaenes (Simpson et al., 1987; Kohler et al., 1988). The current lack of suitable spectroscopic alternatives means that extrapolation procedures, e.g., the use of the energy-gap law to estimate 2^1A_g energies in nonfluorescent carotenoids, will continue to be used. Extrapolations, including the fitting of experimental energies to various functions of N, would very much benefit from a careful analysis of uncertainties in the original data (including corrections for solvent

perturbations) and the propagation of these errors into estimates of 2^1A_g energies for larger N.

Outstanding issues to be addressed by more accurate information on the electronic energies of long polyenes and carotenoids include a quantitative understanding of the differences between the $S_0 \leftrightarrow S_1$ and $S_0 \leftrightarrow S_2$ transition energies of simple polyenes, spheroidenes, and carotenoids. Although a relevant comparison for N=7 is provided by Fig. 4, more comprehensive studies are needed for larger N to understand the effects of conjugation length and substituents (both methyl groups and terminal β-cyclohexenyl rings) on S_1 and S_2 energies. An interesting sidelight of these studies will be a better understanding of the effects of substitution on S_1 and S_2 energies in the long/infinite polyene limit and the resolution of the discrepancies summarized in Table 1.

Our understanding of the effects of solvents on S_1 energies is limited to the application of Eqs. (1) and (2) to the transition energies of short, model polyenes. A systematic look at both $S_0 \leftrightarrow S_1$ and $S_0 \leftrightarrow S_2$ solvent shifts (i.e., the determination of k's in Eqs. (1) and (2)) in longer carotenoids would be useful in exploring systematic changes as a function of conjugation length. This not only would be helpful in evaluating and comparing transition energies obtained in different solvents (including biological matrices), but also will be essential in allowing more accurate extrapolations of transition energies to infinite polyenes and carotenoids.

Any extension of the spectroscopic investigations of energy levels naturally should be coupled with systematic investigations of S_1 and S_2 dynamics to develop a better understanding of substituent effects and isomeric structure on radiative and nonradiative processes. Such studies would include more detailed tests of the energy-gap law for specific homologous series and quantitative investigations of differences in the rates of radiationless processes due to details of molecular structure, e.g., the differences between spheroidenes and carotenes. Recent studies on spheroidene (Ricci et al., 1996) and β-carotene (Macpherson and Gillbro, 1998) show that their S_2 internal conversion rates are strongly dependent on solvent. Parallel investigations of the effect of solvent environment (including temperature) on S_1 dynamics also will be important in understanding the interplay between energetics and solvent effects in determining the rates of radiative and nonradiative decay.

The spectroscopic catalog of polyene T_1 triplet energies (Table 2) has expanded very little since the early 1960s (Evans, 1960, 1961). Given the importance of these states (and their energies) to the protective function of carotenoids and the increase sophistication of spectroscopic techniques, it is remarkable that so little new information is available concerning triplet energies in longer polyenes or carotenoids. The $E(T_1) \sim E(S_1)/2$ rule-of-thumb is based almost entirely on data from simple polyenes with N = 1-4. A systematic look at longer polyenes is needed to refine and extend this approximation to carotenoids of biological significance.

Kohler and Samuel (1995) recently examined the absorption spectra of long, synthetic polyenes (N=20-240) and noted that these molecules absorb at wavelengths significantly shorter than those predicted by the extrapolation of spectra of shorter, model systems (Table 1). Effects of conformational disorder were invoked to explain the spectra, leading to a distinction between 'conjugation length' and 'chain length' in long polyenes. According to this model (Kohler and Woehl, 1995), twists about polyene single bonds break the chain into a distribution of shorter polyene segments with statistical (entropy) considerations predicting a dominance of short conjugation length segments in room temperature solutions. The analysis of these effects strongly suggests that conformational disorder also should be important for polyenes of intermediate length, including naturally occurring carotenoids. It is important to stress that there currently is no evidence for such effects in the spectroscopy of short polyenes or the carotenoids discussed in this review. Nevertheless, conformational disorder would have far-reaching implications for understanding the spectroscopy and photochemistry of carotenoids, and this hypothesis warrants careful consideration.

This chapter has focused almost exclusively on the electronic structures and dynamics associated with carotenoids in *all-trans* configurations. Although *all-trans* carotenoids often are selected by light-harvesting complexes, *cis*-isomers tend to be employed by photosynthetic reaction centers, and it is important to understand both how the energetics and the kinetics are modified for *cis* conformers. One obvious problem in carrying out such studies, at least in vitro, is the thermal and photochemical instability of the *cis* forms. Nevertheless, the importance of these isomers in vision and in photoprotection provides strong motivation for extending spectroscopic and time-resolved studies to these systems.

This chapter has adopted the approach that all of

the singlet state photochemistry of *cis* and *trans* carotenoids can be explained using the energy level diagram presented in Fig. 1. It is important to mention that there is both experimental and theoretical support for the incursion of other electronic states into the low energy regions of this figure. For example, nonlinear optical measurements on *all-trans-β*-carotene indicate the existence of a ^1A_g state ~ 1000 cm^{-1} above the 1^1B_u state (van Beek et al., 1992). In addition, the PPP-MRD-CI calculations of Tavan and Schulten suggest the presence of another low-lying 'covalent' state ($^1B_u^-$) which for N > 5 lies below the 'ionic' 1^1B_u state ($^1B_u^+$) identified as S_2 throughout this review. Although there is at present very little experimental support for additional, electronic levels ($(^1B_u^-)$ or otherwise) with energies less than $E(S_2)$, improvements in spectroscopic techniques eventually should allow a more rigorous search for these states in longer carotenoids.

Acknowledgments

The author acknowledges the Kenan Fellowship Program, administered by Bowdoin College, for supplemental sabbatical leave support. Acknowledgment also is made to the donors of the Petroleum Research Fund, administered by the American Chemical Society, for support of this research. The author thanks Beverly DeCoster for her help in preparing the manuscript and Professor Johan Lugtenburg for the gift of the C_{30} synthetic spheroidene. Finally, the author thanks Dr. Garry Rumbles and the Department of Chemistry at Imperial College for their hospitality during the preparation of this chapter.

References

Allan M, Neuhaus L and Haselbach E (1984) (All-E)-1,3,5,7-octatetraene: Electron-energy loss and electron-transmission spectra. Helv Chim Acta 67: 1776–1782

Andersson PO and Gillbro T (1995) Photophysics and dynamics of the lowest excited singlet state in long substituted polyenes with implications for the very long chain limit. J Chem Phys 103:2509–2519

Andersson PO, Gillbro T, Ferguson L and Cogdell RJ (1991) Absorption spectral shifts of carotenoids related to medium polarizability, Photochem Photobiol 54: 353–360

Andersson PO, Gillbro T, Asato AE and Liu RSH (1992) Dual singlet-state emission in a series of mini-carotenes. J Luminescence 51: 11–20

Andersson PO, Bachilo SM, Chen RL and Gillbro T (1995) Solvent and temperature effects on dual fluorescence in a series of carotenes. Energy gap dependence of the internal conversion rate. J Phys Chem 99: 16199–16209

Bachilo SM (1995) *β*-carotene triplet state absorption in the near-IR range. J Photochem Photobiol A: Chemistry 91: 111–115

Bachilo SM, Spangler CW and Gillbro T (1998) Excited state energies and internal conversion in diphenylpolyenes: From diphenylbutadiene to diphenyldecaheptaene. Chem Phys Lett 283:235–242

Bensasson R, Land EJ and Maudinas B (1976) Triplet states of carotenoids from photosynthetic bacteria studied by nanosecond ultraviolet and electron pulse irradiation. Photochem Photobiol 23: 189–193

Bensasson RV, Land EJ and Truscott TG (1993) Excited States and Free Radicals in Biology and Medicine. Oxford University Press, Oxford

Birge RR (1986) Two photon spectroscopy of protein-bound chromophores. Acc Chem Res 10: 138–146

Birge R, Bennett JA, Fang HL and Leroi GE (1978) The two photon spectroscopy of all-trans retinal and related polyenes. In: Zewail AH (ed) Springer Series in Chem Phys, Vol 3, pp 347–354. Springer, Berlin

Bondarev SL and Knyukshto VN (1994) Fluorescence from the S_1 (2^1A_g) state of *all-trans-β*-carotene. Chem Phys Lett 225: 346–350

Bondarev SL, Dvornikov SS and Bachilo SM (1988) Fluorescence of *β*-carotene at 77 K and 4.2 K. Opt Spectrosc (USSR) 64: 268–270

Bondarev SL, Bachilo SM, Dvornikov SS and Tikhomorov SA (1989) $S_2 \nrightarrow S_0$ fluorescence and transient $S_n \infty S_0$ absorption of *all-trans-β*-carotene in solid and liquid solutions. Photochem Photobiol, A: Chemistry 46: 315–322

Bouwman W, Jones A, Phillips D, Thibodeau P, Friel C and Christensen R (1990) Fluorescence of gaseous tetraenes and pentaenes. J Phys Chem 94: 7429–7434

Bredas JL, Silbey R, Boudreaux DS and Chance RR (1983) Chain-length dependence of electronic and electrochemical properties of conjugated systems: Polyacetylene, polyphenylene, polythiophene, and polypyrrole. J Am Chem Soc 105:6555–6559

Buma WJ, Kohler BE and Song K (1990) Location of the ^1A_g state in hexatriene. J Chem Phys 92: 4622–4623

Chadwick RR, Gerrity DP and Hudson BS (1985) Resonance Raman spectroscopy of butadiene: Demonstration of a 2^1A_g state below the 1^1B_u V state. Chem Phys Lett 115: 24–28

Christensen RL and Kohler BE (1973) Low resolution optical spectroscopy of retinyl polyenes: Low lying electronic levels and spectral broadness. Photochem Photobiol 18: 293–301

Christensen RL and Kohler BE (1975) Vibronic coupling in polyenes: High resolution optical spectroscopy of 2,10-dimethylundecapentaene. J Chem Phys 63: 1837–1846

Christensen RL and Kohler BE (1976) High resolution optical spectroscopy of polyenes related to the visual chromophore. J Phys Chem 80: 2197–2200

Chynwat V and Frank H A (1995) Application of the energy gap law to the S_1 energies and dynamics of carotenoids. Chem Phys 194:237–244

Cosgrove SA, Guite MA, Burnell TB and Christensen RL (1990) Electronic relaxation in long polyenes. J Phys Chem 94:8118–8124

D'Amico KL, Manos C and Christensen RL (1980) Electronic energy levels in a homologous series of unsubstituted linear polyenes. J Am Chem Soc 102: 1777–1782

DeCoster B, Christensen RL, Gebhard R, Lugtenburg J, Farhoosh R and Frank H (1992) Low lying electronic states of carotenoids. Biochim Biophys Acta 1102: 107–114

Dormans GJM, Groenenboom GC and Buck HM (1987) Dynamical calculations on the photoisomerization of small polyenes in a nonadiabatic formalism. J Chem Phys 86:4895–4909

Englman R and Jortner J (1970) The energy gap law for radiationless transitions in large molecules. Mol Phys 18:145–164

Evans DF (I960) Magnetic perturbations of singlet-triplet transitions. Part IV. Unsaturated compounds. J Chem Soc 1735–45

Evans DF (1961) Magnetic perturbations of singlet-triplet transitions. Part VI. Octa-1,3,5,7-tetraene. J Chem Soc 2566–2569

Evans DF and Tucker JN (1972) Magnetic perturbations of singlet-triplet transitions. J Chem Soc Faraday Trans II 54: 174–176

Farhoosh R, Chynwat V, Gebhard R, Lugtenburg J and Frank HA (1994) Triplet energy transfer between bacteriochlorophyll and carotenoids in B850 light-harvesting complexes of *Rhodobacter sphaeroides* R-26.1. Photosynth Res 42: 157–166

Farhoosh R, Chynwat V, Gebhard R, Lugtenburg J and Frank HA (1997) Triplet energy transfer between the primary donor and carotenoids in *Rhodobacter sphaeroides* R-26.1 reaction centers incorporated with spheroidene analogs having different extents of π-electron conjugation. Photochem Photobiol 66: 97–104

Frank HA (1993) Carotenoids in photosynthetic bacterial reaction centers: Structure, spectroscopy, and photochemistry. In: The Photosynthetic Reaction Center pp 221–237. Academic Press, New York

Frank HA and Christensen RL (1995) Singlet energy transfer from carotenoids to bacteriochlorophylls. In: Blankenship RE, Madigan MT and Bauer CE (eds) Anoxygenic Photosynthetic Bacteria, Advances in Photosynthesis pp 373–384. Kluwer Academic Publishers, Dordrecht

Frank HA and Cogdell RJ (1993) Photochemistry and function of carotenoids in photosynthesis. In: Young A and Britton G (eds) Carotenoids in Photosynthesis, pp 252–326. Chapman and Hall, London

Frank HA and Cogdell RJ (1996) Carotenoids in photosynthesis. Photochem Photobiol 63: 257–264

Frank HA, Farhoosh R, Gebhard R, Lugtenburg J, Gosztola D and Wasielewski MR (1993) The dynamics of the S_1 excited states in carotenoids. Chem Phys Lett 207: 88–92

Frank HA, Cua A, Chynwat V, Young A, Gosztola D and Wasielewski MR (1994) Photophysics of the carotenoids associated with the xanthophyll cycle in photosynthesis. Photosynth Res 41: 389–395

Frank HA, Chynwat V, Desamero RZB, Farhoosh R, Erickson J and Bautista J (1997) On the photophysics and photochemical properties of carotenoids and their role as light-harvesting pigments in photosynthesis. Pure & Appl Chem 69: 2117–2124

Frank HA, Desamero RZB, Chynwat V, Gebhard R, van der Hoef I, Jansen FJ, Lugtenburg J, Gosztola D and Wasielewski MR (1997) Spectroscopic properties of spheroidene analogs having different extents of π-electron conjugation. J Phys Chem A 101: 149–157

Fujii R, Onaka K, Kuki M, Koyama Y and Watanabe Y (1998) The $2A_g^-$ energies of *all-trans*-neurosporene and spheroidene as determined by fluorescence spectroscopy. Chem Phys Lett 288:847–853

Gaier K, Angerhofer A and Wolf HC (1991) The lowest excited electronic singlet states of *all-trans*-β-carotene single crystals. Chem Phys Lett 187: 103–109

Gavin, Jr. RM, Weisman C, McVey JK and Rice SA (1978) Spectroscopic properties of polyenes. III. 1,3,5,7-octatetraene. J Chem Phys 68: 522–529

Geldof PA, Rettschnick RPH and Hoytink G (1971) Vibronic coupling and radiative transitions. Chem Phys Lett 10: 549–558

GillbroTand Cogdell RJ (1989) Carotenoid fluorescence. Chem Phys Lett 158: 312–316

Gilardi R, Karle IL, Karle J and Sperling W (1971) Crystal structures of the visual chromophores, 11-cis and all-trans retinal. Nature 232: 187–188

Granville MF, Holtom GR, Kohler BE, Christensen RL and D'Amico KL (1979) Experimental confirmation of the dipole forbidden character of the lowest excited singlet state in 1,3,5,7-octatetraene. J Chem Phys 70: 593–594

Granville MF, Holtom GR and Kohler BE (1980) High-resolution one and two photon excitation spectra of *trans,trans*-1,3,5,7-octatetraene. J Chem Phys 72: 4671–4675

Haley JL, Fitch AN, Goyal R, Lambert C, Truscott TG, Chacon JN, Stirling D and Schlach W (1992) The S_1 and T_1 energy levels of *all-trans*-β-carotene. J Chem Soc, Chem Comm 1992:1175–76

Hemley R and Kohler B (1977) Electronic structure of polyenes related to the visual chromophore: a simple model for the observed band shapes. Biophysical Journal 20: 377–382

Hirayama K (1955) Absorption spectra and chemical structures I. Conjugated polyenes and p-polyphenyls. J Am Chem Soc 77:373–379

Hudson BS and Kohler BE (1972) A low lying weak transition in the polyene α,ω-diphenyloctatetraene. Chem Phys Lett 14: 299–304

Hudson BS and Kohler BE (1973) Polyene spectroscopy: the lowest energy excited singlet state of diphenyloctatetraene and other linear polyenes. J Chem Phys 59: 4984–5002

Hudson BS and Kohler BE (1974) Linear polyene electronic structure and spectroscopy. Ann Rev Phys Chem 25:437–460

Hudson BS and Kohler BE (1984) Electronic structure and spectra of finite linear polyenes. Synthetic Metals 9: 241–253

Hudson BS, Ridyard JN and Diamond J (1976) Polyene spectroscopy. Photoelectron spectra of the diphenylpolyenes. J Am Chem Soc 98: 1126–1129

Hudson BS, Kohler BE and Schulten K (1982) Linear polyene electronic structure and potential surfaces. In: Lim EC (ed) Excited States, Vol 6, pp 1–95. Academic Press, New York

Jones PF, Jones WJ and Davies B (1992) Direct observation of the $2^1A_g^-$ electronic state of carotenoid molecules by consecutive two-photon absorption spectroscopy. Photochem Photobiol A: Chem, 68: 59–75

Katoh T, Nagashima U and Mimuro M (1991) Fluorescence properties of the allenic carotenoid fucoxanthin: Implication for energy transfer in photosynthetic pigment systems. Photosyn

Res 27:221-229
Knoll K and Schrock RR (1989) Preparation of *tert*-butyl-capped polyenes containing up to 15 double bonds. J Am Chem Soc 111: 7989–8004
Kohler BE (1990) A simple model for linear polyene electronic structure. J Chem Phys 93: 5838–5842
Kohler BE (1991) Electronic properties of linear polyenes. In: Bredas JL and Silbey R (eds) Conjugated Polymers: The novel science and technology of conducting and nonlinear optically active materials, pp 405–434. Kulver Press, Dordrecht
Kohler BE (1993a) Octatetraene photoisomerization. Chem Rev 93:41–54
Kohler BE ()993b) Carotenoid electronic structure. In: Pfander H, Liaaen-Jensen S and Britton G (eds) Carotenoids, Vol. IB, pp 1-1 2 Birkhäuser Verlag AG, Basel
Kohler BE and Samuel IDW (1995) Experimental determination of conjugation lengths in long polyene chains. J Chem Phys 103:6248–6252
Kohler BE and Woehl JC (1995) A simple model for conjugation lengths in long polyene chains. J Chem Phys 103:6253-6256
Kohler BE, Spiglanin TA, Hemley RJ and Karplus M (1984) Vibrational analysis of the lowest ^1B state of 1,3,5,7-octatetraene. J Chem Phys 80: 23–30
Kohler BE, Spangler C and Westerfield C (1988) The 2^1A_g state in the linear polyene 2,4,6,8,10,12,14,16-octadecaoctaene. J Chem Phys 89: 5422–5428
Koyama Y, Kuki M, Andersson PO and GillbroT(1996) Singlet excited states and the light harvesting function of carotenoids in bacterial photosynthesis. Photochem Photobiol 63: 243–256
Kuhn H (1948) Free-electron model for absorption spectra of organic dyes. J Chem Phys 16: 840-841
Kuhn H (1949) A quantum mechanical theory of light absorption of organic dyes and similar compounds. J Chem Phys 17: 1198–1212
Kupperman A, Flicker WM and Mosher OA (1979) Electronic spectroscopy of polyatomic molecules by low-energy, variable-angle electron impact. Chem Rev 79: 77–90
Kwa SLS, Groeneveld FG, Dekker JP, van Grondelle R, van Amerongen H, Lin S and Struve WS (1992) Steady-state and time-polarized light spectroscopy of the green plant light-harvesting complex II. Biochim Biophys Acta 1101: 143–146
Labhart H (1957) FE theory including an elastic σ skeleton I. Spectra and bond lengths in long polyenes. J Chem Phys 27: 957-962
Macpherson AN and Gillbro T (1998) Solvent dependence of the ultrafast $S_2 \rightarrow S_1$ internal conversion rate of β-carotene. JPhys Chem A 102: 5049–5058
Marston G, Truscott TG and Wayne RP (1995) Phosphorescence of β-carotene. J Chem Soc Faraday Trans 91: 4059–4061
Mimuro M, Nagashima U, Nagaoka S, Takaichi S, Yamazaki I, Nishimura Y and Katoh T (1993) Direct measurement of the low-lying singlet excited (2^1A_g) state of a linear carotenoid, neurosporene, in solution. Chem Phys Lett 204: 101–105
Murrell JN (1963) The Theory of the Electronic Spectra of Organic Molecules. Methuen and Co Ltd, London, pp 67–90
Ohmine I, Karplus M and Schulten K (1978) Renormalized configuration interaction method for electron correlation in the excited states of polyenes. J Chem Phys 68: 2298–2318
Orlandi G, Zerbetto F and Zgterski MZ (1991) Theoretical analysis of spectra of short polyenes, Chem Rev 91: 867-891
Petek H, Bell AJ, Choi YS, Yoshihara K and Christensen RL (1991) Spectroscopic and dynamical studies of the S_1 and S_2 states of decatetraene in supersonic molecular beams. J Chem Phys 95: 4739–4750
Petek H, Bell AJ, Choi YS, Yoshihara K, Tounge BA and Christensen RL (1995) One- and two-photon fluorescence excitation spectra of the 2^1A_g states of linear tetraenes in free jet expansions. J Chem Phys 102: 4726–4739
Ramasesha S and Zoos ZG (1984) Correlated states in linear polyenes, radicals, and ions: Exact PPP transition moments and spin densities. J Chem Phys 80: 3278–3287
Raubach RA and Guzzo AV (1973) Singlet-triplet absorption spectrum of *all-trans*-retinal. J Phys Chem 75: 983-984
Ricci M, Bradforth SE, Jimenez R and Fleming G (1996) Internal conversion and energy transfer dynamics of spheroidene in solution and in the LH-1 and LH-2 light-harvesting complexes. Chem Phys Lett 259: 381–390
Rohlfing F, Bradley DDC, Eberhardt A, Müllen K, Cornil J, Beljonne D, and Brédas JL (1996) Electroabsorption spectroscopy of β-carotene and α,ω-bis(1,1-dimethylheptyl)-1,3,5,7,9,11,13,15-hexadecaoctaene. Synthetic Metals 76:35–38
Rossi G, Chance RR and Silbey R (1989) Conformational disorder in conjugated polymers. J Chem Phys 90: 7594–7601
Sashima T, Shiba M, Hashimoto H, Nagae H and Koyama Y (1998) The $^1A_g^-$ energy of *all-trans*-spheroidene as determined by resonance-Raman excitation profiles. Chem Phys Lett 290: 36–42
Sauer K (1978) Photosynthetic membranes. Acc Chem Res 11: 257–264
Schulten K and Karplus M (1972) On the origin of a low-lying forbidden transition in polyenes and related molecules. Chem Phys Lett 14:305-309
Schulten K, Ohmine I and Karplus M (1976) Correlation effects in the spectra of polyenes. J Chem Phys 64: 4422–4441
Shreve AP, Trautman JK, Owens TG and Albrecht AC (1991) A femtosecond study of electronic state dynamics of fucoxanthin and implications for photosynthetic carotenoid-to-chlorophyll energy transfer mechanisms. Chem Phys 154: 171-178
Simpson JH, McLaughlin L, Smith DS and Christensen RL (1987) Vibronic coupling in polyenes: High resolution optical spectroscopy of *all-trans*-2,4,6,8,10,12,14-hexadecaheptaene. J Chem Phys 87: 3360–3365
Sklar IA, Hudson BS, Petersen M and Diamond J (1977) Conjugated polyene fatty acids on fluorescence probes: Spectroscopic characterization. Biochem 16: 813-819
Snyder R, Arvidson E, Foote C, Harrigan L and Christensen RL (1985) Electronic energy levels in long polyenes: $S_2 \rightarrow S_0$ emission in *all-trans*-1,3,5,7,9,11,13-tetradecaheptaene. J Am Chem Soc 107:4117–4122
Stam CH and MacGillavry CH (1963) The crystal structure of the triclinic modification of Vitamin-A acid. Acta Cryst B16: 62–68
Tavan P and Schulten K(1979) The 2^1A_g–1^1B_u energy gap in the polyenes: an extended configuration interaction study. J Chem Phys70: 5407–5413
Tavan P and Schulten K (1986) The low-lying electronic excitations in long polyenes: a PPP-MRD-CI study. J Chem Phys 85: 6602–6609
Tavan P and Schulten K (1987) Electronic excitations in finite and infinite polyenes. Phys Rev B 36: 4337–4358

Trash RJ, Fang H and Leroi GE (1977) The Raman excitation profile spectrum of β-carotene in the preresonance region: Evidence for a low-lying singlet state. J Chem Phys 76: 5930–5933

Trash RJ, Fang H and Leroi GE (1979) On the role of forbidden low-lying excited states of light-harvesting carotenoids in energy transfer in photosynthesis. Photochem Photobiol 29: 1049–1050

Turro NJ (1978) Molecular Photochemistry. Benjamin/Cummings, Menlo Park, California

Vaida V (1986) Electronic spectroscopy of jet-cooled molecules. Acc Chem Res 19: 114–120

van Beck JB, Kajzar F and Albrecht AC (1992) Third-harmonic generation in *all-trans* β-carotene: The vibronic origins of the third-order nonlinear susceptibility in the visible region. Chem Phys 161: 299–311

Watanabe Y, Kameyana T, Miki Y, Kuki M and Koyama Y (1993) The $2^1A_g^-$ state and two additional low-lying electronic states of spheroidene newly identified by fluorescence and fluorescence excitation spectroscopy at 170 K. Chem Phys Lett 206: 62–68

Wayne RP (1991) Principles and Applications of Photochemistry. Oxford University Press, Oxford

Zechmeister L (1962) *Cis-Trans* Isomeric Carotenoids, Vitamins A and Arylpolyenes. Academic Press, New York

Zerbetto F and Zgierski MZ (1990) The missing fluorescence of *s-trans* butadiene. J Chem Phys 93: 1235–1245

Zerbetto F and Zgierski MZ (1994) Franck-Condon modeling of the structure of the $S_0 \rightarrow S_2$ transition of *trans,trans-, cis,trans-,* and *cis,cis*-octatetraene. J Chem Phys 93: 1842–1851

Ziegler LD and Hudson BS (1983) Resonance Raman scattering of ethylene. Evidence for a twisted geometry in the V state. J Chem Phys 79: 1197–1202

Zoos ZG and Ramasesha S (1984) Valence bond theory of linear Hubbard and Pariser-Parr-Pople models. Phys Rev B 29: 5410–5422

This page intentionally left blank

Chapter 9

Cis-Trans Carotenoids in Photosynthesis: Configurations, Excited-State Properties and Physiological Functions

Yasushi Koyama and Ritsuko Fujii
Faculty of Science, Kwansei Gakuin University, Uegahara, Nishinomiya 662-8501, Japan

H. A. Frank, A. J. Young, G. Britton and R. J. Cogdell (eds): The Photochemistry of Carotenoids, pp. 161–188.

Summary

Correlations between the ^{1}H-NMR, electronic-absorption and resonance-Raman spectra and the *cis-trans* configurations have been identified for β-carotene and other carotenoids: (1) the chemical shifts of the olefinic ^{1}Hs in NMR, (2) the wavelength of the $A_g^- \rightarrow B_u^+$ absorption and the relative intensity of the $A_g^- \rightarrow A_g^+$ vs. the $A_g^- \rightarrow B_u^+$ absorption in electronic absorption, and (3) the C=C stretching frequency, the relative intensity of the C10–C11 vs. the C14–C15 stretching vibration and the appearance of key modes in resonance Raman can be used to identify the all-*trans* or a mono-*cis* configuration.

The natural selection of the carotenoid configurations is described; i.e., the all-*trans* configuration is selected by the light-harvesting complexes (LHCs), whereas the 15-*cis* configuration is selected by the reaction centers (RCs). The excited-state properties of the all-*trans* and the 15-*cis* configurations are attempted to be correlated with their physiological functions. The conjugated system of the all-*trans* carotenoids in the LHCs have approximate C_{2h} symmetry, giving rise to two distinct low-lying excited states denoted B_u^+ and $2A_g^-$. Characterization of these singlet states leads to the conclusion that they provide two channels for singlet-energy transfer to (bacterio)chlorophyll. The 15-*cis* configuration has a unique property of extremely-efficient isomerization toward the all-*trans* configuration upon triplet excitation. This is based on the characterization of the singlet and triplet species of β-carotene and the products of isomerization. Resonance Raman spectroscopy, together with normal-coordinate analysis of the RC-bound spheroidene, has revealed twisting and large changes in bond order of the conjugated backbone upon triplet excitation, which is proposed to enhance the rate of relaxation to the ground state and the dissipation of triplet energy.

I. Introduction

Natural selection of carotenoid configurations in photosynthetic systems, i.e., the all-*trans* configuration is selected by the light-harvesting complexes (LHCs), whereas the 15-*cis* configuration is selected by the reaction centers (RCs), has been established by determination of the configurations of carotenoids in the pigment-protein complexes of various photosynthetic organisms. Only all-*trans* carotenoids are bound to the LHCs (LH1 and LH2) of purple non-sulfur bacteria (Lutz et al., 1978; Koyama et al, 1988a, 1990; McDermott et al., 1995; Koepke et al., 1996; Ohashi et al., 1996; Lancaster and Michel, 1997), and all-*trans* carotenoids are the major component in the LHC II of spinach, although *cis* carotenoids also have been found as minor components (Gruszecki et al., 1997; Bialek-Bylka et al., 1998a). On the other hand, 15-*cis* carotenoids have been identified in the quinone-type RCs of purple bacteria (Koyama et al., 1982, 1983, 1988a, 1990; Arnoux et al., 1989; Jiang et al., 1996; Ohashi et al., 1996) and of spinach Photosystem (PS) II (Bialek-Bylka et al., 1995). Further, 15-*cis* carotenoids have been found also in the iron sulfur-type RC of a green sulfur bacterium (Bialek-Bylka et al., 1998b) and of the PS I of spinach (Bialek-Bylka et al., 1996) and a cyanobacterium (Bialek-Bylka et al., 1998b). In relation to this natural selection of the carotenoid configurations, we can assume that the light-harvesting function is more important for the LHC-bound all-*trans* carotenoid, whereas the photoprotective function for the RC-bound 15-*cis* carotenoid.

What is the reason for the natural selection of the 15-*cis* configuration by the RCs? Indeed, is there physiological relevance to the natural selection? One naive interpretation is that a 15-*cis* carotenoid was bound, by chance, to an ancestor RC, and then, inherited by the RCs of all the succeeding photosynthetic organisms. The other interpretation is that the photosynthetic organisms have tried all the *cis-trans* configurations in the history of their development, and chosen the 15-*cis* configuration because of functional advantage under the physiological conditions on this planet. The same argument can be made for the all-*trans* configuration in the

Abbreviations: BChl – bacteriochlorophyll; *Cb.* – *Chlorobium*; DMF – dimethylformamide; H – ^{1}H; HPLC – high-pressure liquid chromatography; k – stretching force constant; LHCs – light-harvesting complexes; n – number of conjugated double bonds; *n* – solvent refractive index; PPP-SD-CI – Pariser-Parr-Pople calculation including the singly- and doubly-excited configurational interactions; PS – photosystem; *Rb.* – *Rhodobacter;* RCs – reaction centers; *Rs.* – *Rhodospirillum*; S_0 – the ground state; S_1 – the first singlet-excited state; S_2 – the second singlet-excited state; *Sc.* – *Synechococcus;* T_1 – the lowest triplet-excited state; ε – molar extinction coefficient; ν_1 C=C stretching mode; ν_2 C–C stretching mode

LHCs. The correct interpretation should emerge when the configurations of carotenoids in the RC and the LHC of all the typical photosynthetic organisms are precisely determined, and when the detailed mechanisms of photo-protective and light-harvesting functions are revealed in both types of pigment-protein complexes.

This goal will be reached by the following steps: First, the dependence of the ground-state physical properties on the *cis-trans* configurations of carotenoids need to be determined. The different chromatographic and spectroscopic properties of a set of *cis-trans* isomers can be used to identify *cis-trans* carotenoids in the extract from a LHC or a RC complex. Spectroscopic techniques probe the in situ configuration of carotenoids bound to pigment-protein complexes. Second, the dependence of the singlet and triplet excited-state properties on the *cis-trans* configurations may provide a key to natural selection in relation to the functions of light-harvesting and photo-protection. Third, the mechanisms of singlet-energy transfer from all-*trans* carotenoid to chlorophyll in the LHCs, of triplet-energy transfer from (bacterio)chlorophyll to 15-*cis* carotenoid, and of dissipation of triplet energy in the RCs need to be determined. Finally, the photo-protective function of all-*trans* carotenoids in the LHCs and the light-harvesting function of 15-*cis* carotenoids in the RCs need to be examined to establish the implication of the natural selection.

Our series of investigations is at an early stage of the third step, and this chapter will summarize the results so far obtained. Section II describes the dependence of the ground (S_0), first singlet-excited (S_1) and first triplet-excited (T_1) state properties on the *cis-trans* configurations of β-carotene as a representative carotenoid. Regarding the spectroscopic properties in the ground state, the results from other carotenoids also are summarized to aid in the determination of configurations. Section III describes the properties of the two low-lying singlet states of all-*trans*-β-carotene and spheroidene, a bacterial carotenoid, in relation to their light-harvesting function. Finally, Section IV describes the unique T_1-state properties of 15-*cis*-β-carotene and spheroidene, and describes the concept of the 'triplet-excited region.' A possible mechanism of triplet-energy dissipation is proposed.

The authors of this chapter hope that the tables and figures will be a valuable resource and reference for researchers. Previously unpublished results are also presented. Earlier stages of these investigations have been summarized (Koyama, 1991; Koyama and Hashimoto, 1993; Koyama and Mukai, 1993; Koyama et al., 1996).

II. Dependence of the Ground-State and the Excited-State Properties on the Configuration of the Carotenoid

A. The Ground-State Properties of β-Carotene and Other Carotenoids

1. Structures of Typical Carotenoids from Photosynthetic Systems and HPLC Analyses of Their Cis-Trans *Isomers*

Figure 1 shows the chemical structures of carotenoids which will be dealt with in this Section. The length and position of the conjugated system are different from one carotenoid to another. All the carotenoids, except for β-apo-8′-carotenal, neurosporene, and spheroidene, contain a complete central structural motif which is terminated by the 6 and 6′ carbon atoms. The dependence of the ^{1}H-NMR, electronic absorption and resonance-Raman spectroscopic properties on the *cis-trans* configurations of the symmetric β-carotene molecule can change when there is a lack of a complete central structural motif in a carotenoid or when the carotenoid is asymmetric. In the following three subsections, the spectroscopic properties of the carotenoid, β-carotene, will be described first, and then those of other carotenoids will be mentioned.

Figure 2 shows several all-*trans* and mono-czs isomers of β-carotene which have been identified. The all-*trans* isomer is unique in that it contains a stretched conjugated system with C_{2h} symmetry. The symmetry notations of nA_g^+, nA_g^-, nB_u^+ and nB_u^- are appropriate for this structure (Tavan and Schulten, 1987), but this notation will also be used for convenience in *cis* isomers. The mono-*cis* isomers can be classified either as peripheral-*cis* (7-*cis* and 9-*cis*) or central-*cis* (13-*cis* and 15-*cis*) isomers, or as unmethylated-cis (7-*cis*, 11-*cis* and 15-*cis*) or methylated-*cis* (9-*cis* and 13-*cis*) isomers. The unmethylated-*cis* isomers have been considered to be unstable because of steric interaction in the concave side of the *cis* bend (Zechmeister, 1962). Actually, the 7-*cis* isomer can be formed from the all-*trans* isomer by thermal isomerization (Tsukida et al.,

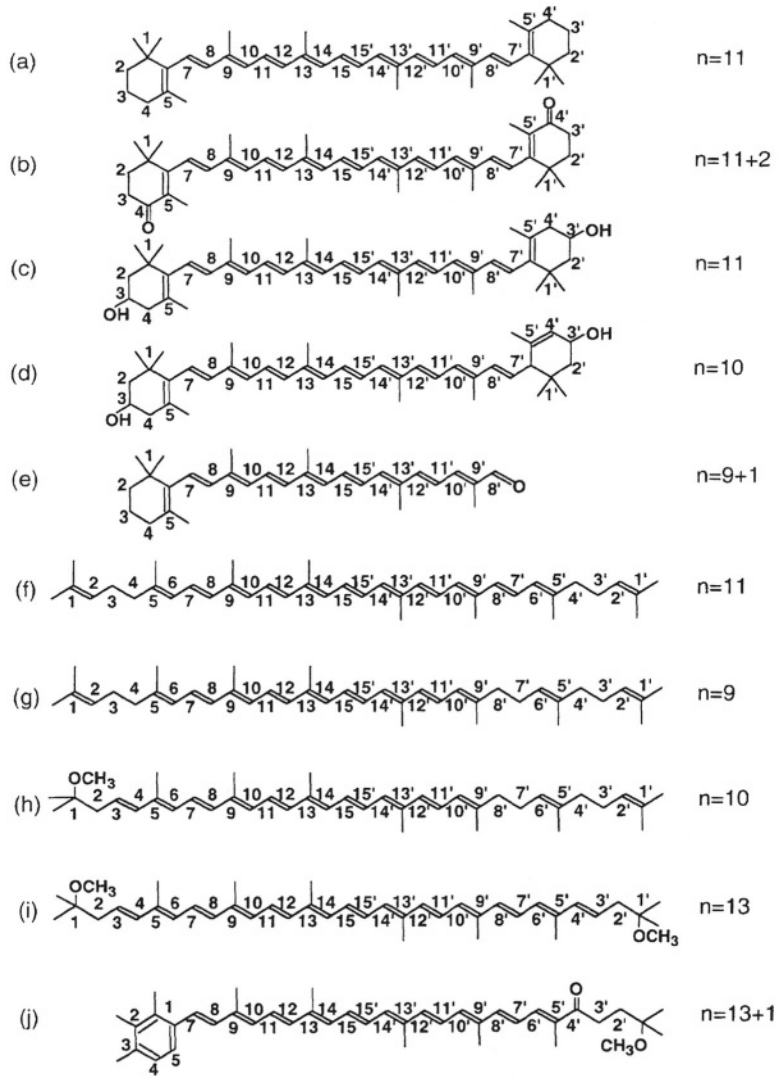

Fig. 1. Chemical structures of carotenoids, the dependence of the ground-state properties on their *cis-trans* configurations being described in Sec. II. (a) β-Carotene, (b) canthaxanthin, (c) zeaxanthin, (d) lutein, (e) β-apo-8′-carotenal, (f) lycopene, (g) neurosporene, (h) spheroidene, (i) spirilloxanthin and (j) okenone. For each carotenoid, the number of conjugated C=C plus C=O bonds is shown.

1982), and is the most stable among the mono-*cis* isomers (Kuki et al., 1991). The 11-*cis* isomer can be formed synthetically, but it thermally isomerizes into the all-*trans* isomer (Hu et al., 1997). The 15-*cis* isomer thermally isomerizes into the all-*trans* isomer, and the reverse thermal isomerization also takes place to reach an equilibrium (Kuki et al., 1991).

Figure 3 shows a high-pressure liquid chromatography (HPLC) elution pattern of isomeric β-carotene (Koyama et al., 1988b; Hu et al., 1997). The mono-*cis* isomers elute in the order from the central-*cis* to the peripheral-*cis* isomers, the retention time being in the order, 15-*cis* < 13-*cis*< 11-*cis* <9-*cis* < 7-*cis*. Di-*cis* isomers tend to elute earlier than the component mono-*cis* isomers. HPLC of the isomers of each carotenoid is extremely important in characterizing their spectroscopic properties. For the set of carotenoids shown in Fig. 1, the HPLC techniques can be found in the references attached to Tables 1–4.

2. ^{1}H-NMR Spectroscopy

a. β-Carotene

Table 1 (top left) and Table 2 (extreme left) show the

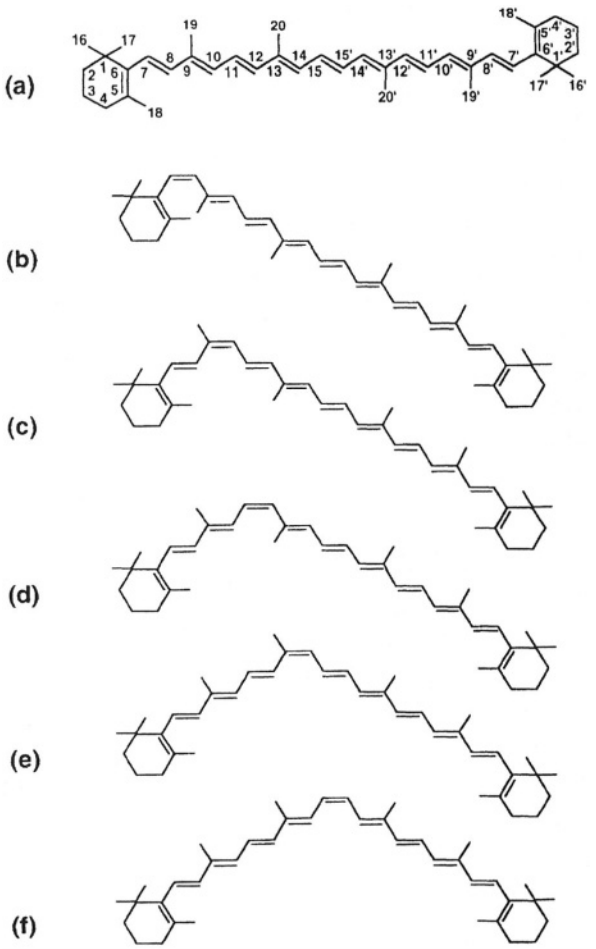

Fig. 2. The configurations of the (a) all-*trans*, (b) 7-*cis*, (c) 9-*cis*, (d) 11-*cis*, (e) 13-*cis* and (f) 15-*cis* isomers of β-carotene.

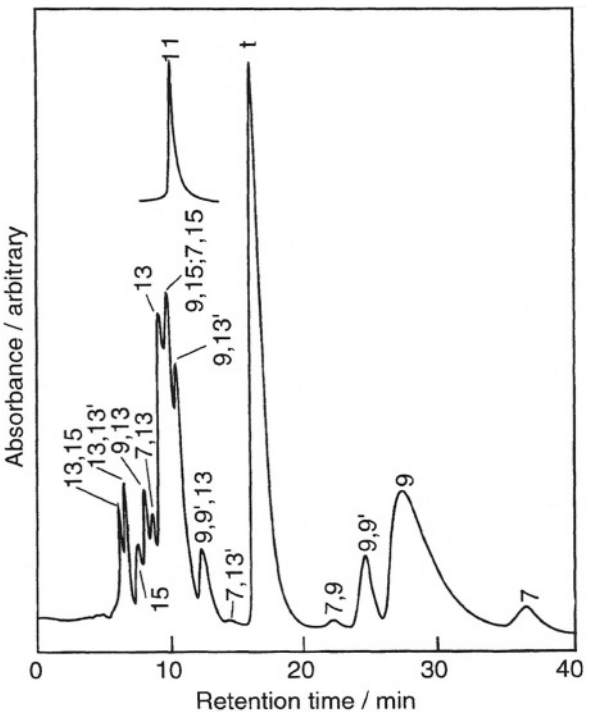

Fig. 3. An HPLC elution profile of isomeric β-carotene; the configurational assignment of each peak is given. HPLC conditions: a 4 mm × 300 mm column packed with calcium hydroxide; eluent, 0.1 % acetone in *n*-hexane; flow rate, 0.5 $ml \cdot min^{-1}$; and detection at 450 nm.

^{1}H (abbreviated as H) chemical shifts of all-*trans*-β-carotene in benzene and chloroform solutions (Koyama et al., 1989). The chemical shifts can be explained in terms of the H-H steric interaction (see Fig. 2a for the structure). Because of the severe steric interaction between 11H (11′H) and both 19Me and 20Me (19′Me and 20′Me), the 11H (11′H) signal appears in the lowest field. Because of the less severe steric interaction between 15H and 20Me (15′H and 20′Me), the 15H (15′H) signal appears in the second-lowest field, and the rest of the H signals appear at higher field. Tables 1 and 2 also show isomerization shifts which are defined as changes in the H chemical shifts in reference to the H chemical shifts of the all-*trans* isomer. When a *cis*-bend is introduced, the high-field-shifts take place on the convex side because of decrease in the steric interaction, whereas the low-field-shifts take place on the concave side because of increase in the steric interaction. Thus, the 7-*cis* configuration is characterized by high-field-shifts of 7H and 8H, the 9-*cis* configuration by a high-field-shift of 10H and low-field shifts of 8H and 11H, the 11-*cis* configuration by high-field-shifts of 11H and 12H and a low-field shift of 10H, the 13-*cis* configuration by a high-field-shift of 14H and low-field shifts of 12H and 15H, and the 15-*cis* configuration by a high-field-shift of 15H and a low-field shift of 14H (Englert, 1982, 1995; Koyama et al., 1989). These isomerization shifts are underlined in the tables.

b. Other Carotenoids

Tables 1 and 2 also list the H chemical shifts of the all-*trans* isomers of other carotenoids. The chemical-shift values in the region from 10H to 10′H are conserved for carotenoids having a complete central structural motif in either benzene or chloroform solution. Even in β-apo-8′-carotenal, neurosporene and spheroidene that lack this structural motif, the chemical-shift values are conserved in the complete

Table 1. H chemical shifts (ppm) for the all-*trans* isomer and isomerization shifts[a] for *cis* isomers in benzene-d_6 at 281K

	β-carotene						canthaxanthin[d]				lutein[e]			β-apo-8'-carotenal[f]				
	all-*trans*[b]	7-*cis*[b]	9-*cis*[b]	11-*cis*[c]	13-*cis*[b]	15-*cis*[b]	all-*trans*	9-*cis*	13-*cis*	15-*cis*	all-*trans*	9-*cis*	13-*cis*	all-*trans*	7-*cis*	9-*cis*	13-*cis*	15-*cis*
7 H	6.33	–0.39					6.15				6.23			6.38	–0.40			
7′H	6.33						6.15				5.46			6.38				
8 H	6.40	–0.14	+0.69				6.38	+0.75			6.35	+0.73		6.34	–0.07	+0.74		
8′H	6.40						6.38				6.22			9.45				
10 H	6.35	+0.07	–0.14	+0.63			6.29	–0.07			6.35	–0.13		6.32	+0.16	–0.13		–0.13
10′H	6.35						6.29				6.29			6.52				
11 H	6.79		+0.26	–0.34			6.73	+0.20			6.80	+0.25		6.81		+0.27		+0.06
11′H	6.79						6.73				6.76			6.48				
12 H	6.48			–0.37	+0.60		6.50	–0.08	+0.55		6.51	–0.06	+0.56	6.45			+0.56	+0.09
12′H	6.48						6.50				6.53			6.43				
14 H	6.32			+0.13	–0.19	+0.54	6.36		–0.20	+0.54	6.34		–0.20	6.27			–0.18	+0.59
14′H	6.32						6.36				6.34			6.32				+0.55
15 H	6.68		–0.06	–0.06	+0.25	–0.22	6.70		+0.24	–0.23	6.70		+0.25	6.73			+0.25	–0.21
15′H	6.68				–0.07		6.70		–0.07		6.70		–0.07	6.57			–0.06	–0.23

	neurosporene[g]				spheroidene[h]					spirilloxanthin[i]			okenone[j]				
	all-*trans*	9-*cis*	13'-*cis*	15-*cis*	all-*trans*	9-*cis*	13-*cis*	13'-*cis*	15-*cis*	all-*trans*	13-*cis*	15-*cis*	all-*trans*	7-*cis*	9-*cis*	13-*cis*	
7 H	6.66				6.76					6.79	–0.08		7.05	–0.39			
7′H	6.66				6.76					6.79			6.59				
8 H	6.42	+0.66			6.53	+0.63				6.53			6.95	–0.52	+0.68		
8′H	6.42				6.53					6.53			6.43				
10 H	6.34	–0.18			6.38	–0.22				6.39	–0.06		6.44	–0.11	–0.16		
10′H	6.14				6.17					6.39			6.38				
11 H	6.75	+0.26			6.76	+0.27				6.78			6.85		+0.31		
11′H	6.66				6.68					6.78			6.72				
12 H	6.48	–0.06			6.52	–0.07	+0.56			6.54	+0.52		6.56	–0.07	–0.07	+0.57	
12′H	6.42		+0.56		6.45			+0.56		6.54			6.58				
14 H	6.33			+0.57	6.35		–0.23		+0.56	6.38	–0.25	+0.54	6.39			–0.23	
14′H	6.33		–0.23		6.33			–0.20	+0.55	6.38			6.38				
15 H	6.69		–0.10	–0.22	6.70		+0.22	–0.08	–0.23	6.73	+0.21	–0.26	6.72			+0.31	
15′H	6.69		+0.26		6.70		–0.06	+0.25		6.73	–0.12		6.75			–0.14	

[a] Isomerization shifts whose absolute values larger than 0.05 are shown.
[b] Koyama et al., 1989
[c] Hu et al., 1997
[d] Hashimoto et al., 1988b
[e] Bialek-Bylka et al., 1998a
[f] Hashimoto et al., 1993
[g] Katayama et al., 1990
[h] Jiang et al., 1996
[i] Koyama et al., 1990
[j] Fujii et al., 1998a

Table 2. H chemical shifts (ppm) for the all-*trans* isomer and isomerization shifts[a] for *cis* isomers in $CDCl_3$

	β-carotene[b]					lutein[c]			zeaxanthin[d]					lycopene[e]				
	all-*trans*	7-*cis*	9-*cis*	13-*cis*	15-*cis*	all-*trans*	9-*cis*	13-*cis*	all-*trans*	7-*cis*	9-*cis*	13-*cis*	15-*cis*	all-*trans*	7-*cis*	9-*cis*	13-*cis*	15-*cis*
7 H	6.17	–0.34				6.12			6.11	–0.32				6.49	–0.33			
7′H	6.17					5.43			6.11					6.49				
8 H	6.12		+0.54			6.12	+0.55		6.13		+0.54			6.25	–0.39	+0.54		
8′H	6.12					6.15			6.13					6.25				
10 H	6.14	+0.07	–0.10			6.16	–0.09		6.16	+0.06	–0.09			6.18	+0.06	–0.14		
10′H	6.14					6.14			6.16					6.18				
11 H	6.64		+0.10			6.64	+0.10		6.64	–0.08	+0.10			6.64		+0.16		
11′H	6.64					6.62			6.64					6.64				
12 H	6.34		+0.06	+0.53	+0.07	~6.36	–0.06	+0.54	6.36		–0.06	+0.51	+0.07	6.35		–0.07	+0.53	+0.08
12′H	6.34					~6.36			6.36					6.35				
14 H	6.24			–0.15	+0.41	~6.26		–0.12	~6.26			–0.15	+0.41	6.25			–0.14	+0.43
14′H	6.24					~6.26			~6.26					6.25				
15 H	6.62		–0.06	+0.17	–0.24	~6.63		+0.17	~6.63			+0.16	–0.23	6.62			–0.18	–0.22
15′H	6.62			–0.07		~6.63		–0.07	~6.63			–0.07		6.62				

[a] Isomerization shifts whose absolute values larger than 0.05 are shown.
[b] Koyama et al., 1989
[c] Kachik et al., 1992
[d] Englert et al., 1991
[e] Hengartner et al., 1992

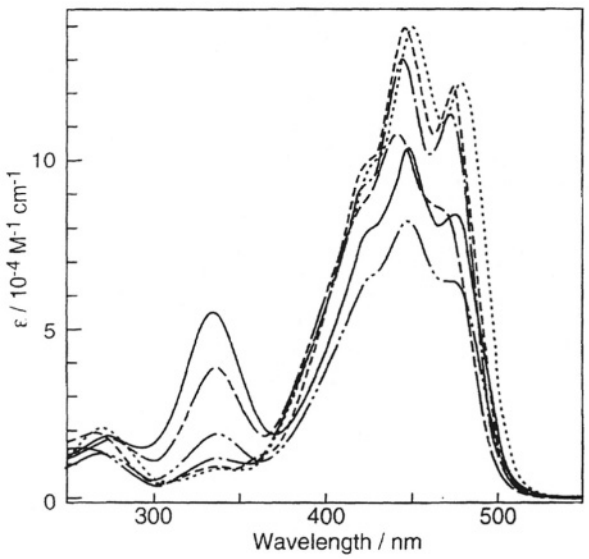

Fig. 4. Electronic-absorption spectra of isomeric β-carotene: all-*trans* (·····), 7-*cis* (- - - -), 9-*cis* (— · — · —), 11-*cis* (— ·· — ·· —), 13-*cis* (— - - — - - —) and 15-*cis* (———).

side (Fujii et al., 1998a). The results indicate that the H chemical shifts are determined primarily by H-H steric interactions. The isomerization shifts are also conserved for the isomers of these carotenoids in both benzene and chloroform solutions. However, it is to be noted that *cis* isomers are more stable in the non-polar solvent, benzene, especially just above the freezing point which is 8 °C.

Thus, the H chemical shifts and the isomerization shifts are very useful to identify the all-*trans* or a *cis* configuration, but measurements of nuclear Overhauser effects (NOE) are necessary to determine the configurations precisely.

3. Electronic Absorption Spectroscopy

a. β-Carotene

Figure 4 shows the electronic absorption spectra of several isomers of β-carotene (Koyama et al., 1983; Hu et al., 1997). The $A_g^- \rightarrow B_u^+$ absorption with the (0-0), (0-1) and (0-2) vibrational features having a transition moment along the resultant sum of π-electron conjugation (the long axis) is often called the main absorption. An $A_g^- \rightarrow A_g^+$ absorption appears upon *trans*-to-*cis* isomerization on the shorter-wavelength side and has a transition moment perpendicular to the long axis. This absorption band is called the *cis* peak. The intensity ratio of the $A_g^- \rightarrow A_g^+$ band to the $A_g^- \rightarrow B_u^+$ band (the *cis* peak vs. the main absorption) increases in the order from the all-*trans* isomer < peripheral-cis isomer < central-cis isomer (see Fig. 2 for the configurations). Actually, the relative intensity for isomeric β-carotene listed in Table 3 increases in the order, all-*trans* -1-*cis* < 9-*cis* < 11 -*cis* < 13-*cis* < 15-*cis*. Even in the 11 -*cis* isomer which gives rise to a very low molar extinction coefficient (ε) due to the distortion of the conjugated backbone (see Fig. 4), the relative intensity follows the above order (Hu et al., 1997). It is also to be noted that the $A_g^- \rightarrow B_u^+$ (0-0) absorption shifts to the blue with the λ_{max} value appearing in the order, all-*trans* > 7-*cis* > 9-*cis* > 13-*cis*, a fact which indicates a decrease in the effective conjugation when a *cis* bend is introduced from the peripheral to the center of the conjugated chain. The 15-*cis* isomer does not follow this trend probably owing to its C_{2v} (C_2) symmetry which may cause electronic coupling between both ends.

b. Other Carotenoids

Table 3 shows that the ratio of the intensity of the $A_g^- \rightarrow A_g^+$ band to the $A_g^- \rightarrow B_u^+$ band increases in the order from the all-*trans* isomer < peripheral-*cis* isomer < central-*cis* isomer for all the carotenoids except for lutein and β-apo-8′-carotenal. In these exceptions, however, the difference between the values is small. The wavelength of the $A_g^- \rightarrow B_u^+$ (0-0) absorption is in the order, all-*trans* > 9-*cis* > 13-*cis*, and this is found for many other carotenoids. Thus, a combination of the relative intensity of the $A_g^- \rightarrow A_g^+$ vs. the $A_g^- \rightarrow B_u^+$ absorption and the position of the wavelength of the $A_g^- \rightarrow B_u^+$ (0-0) absorption can be used to identify mono-*cis* isomers (other than 15-*cis*) for many carotenoids (Fujii et al., 1998a).

4. Resonance Raman Spectroscopy

a. β-Carotene

Figure 5 shows the Raman spectra of several isomers of β-carotene (Koyama et al., 1983; Hu et al., 1997), each of which exhibits a unique spectral pattern. The Raman lines can be correlated to the *cis-trans* configurations as follows (Koyama et al. 1988c; Hu et al., 1997): (1) The frequency of the strongest Raman line due to the in-phase C=C stretchings is configuration-sensitive; the C=C stretching frequency increases in the order, all-*trans* < 7-*cis* < 9-*cis* < 13-

Table 3. The wavelength (nm) of the $A_g^- \rightarrow B_u^+(0\text{-}0)$ absorption (isomerization shift in parentheses) and the relative intensity of the $A_g^- \rightarrow A_g^+$ vs. $A_g^- \rightarrow B_u^+$ absorption for isomeric carotenoids in *n*-hexane solution

	β-carotene		canthaxanthin[c]		lutein[d]		*β*-apo-8'-carotenal[e]		zeaxanthin[d]	
	$A_g^- \rightarrow B_u^+(0\text{-}0)$ wavelength / nm (isomerization shift)	$\frac{A_g^- \rightarrow A_g^+}{A_g^- \rightarrow B_u^+}$ relative intensity	$A_g^- \rightarrow B_u^+(0\text{-}0)$ wavelength / nm (isomerization shift)	$\frac{A_g^- \rightarrow A_g^+}{A_g^- \rightarrow B_u^+}$ relative intensity	$A_g^- \rightarrow B_u^+(0\text{-}0)$ wavelength / nm (isomerization shift)	$\frac{A_g^- \rightarrow A_g^+}{A_g^- \rightarrow B_u^+}$ relative intensity	$A_g^- \rightarrow B_u^+(0\text{-}0)$ wavelength / nm (isomerization shift)	$\frac{A_g^- \rightarrow A_g^+}{A_g^- \rightarrow B_u^+}$ relative intensity	$A_g^- \rightarrow B_u^+(0\text{-}0)$ wavelength / nm (isomerization shift)	$\frac{A_g^- \rightarrow A_g^+}{A_g^- \rightarrow B_u^+}$ relative intensity
all-*trans*	478 (0)[a]	0.06[a]	~505	0.15	473 (0)	0.13	480 (0)	0.01	477 (0)	0.09
7-*cis*	474 (4)[a]	0.06[a]					480 (0)	0.03		
9-*cis*	473 (5)[a]	0.09[a]		0.17	468 (5)	0.12	477 (3)	0.02	473 (4)	0.18
11-*cis*	475 (3)[b]	0.25[b]								
13-*cis*	467 (11)[a]	0.36[a]		0.45	466 (7)	0.44	474 (6)	0.41	470 (7)	0.46
15-*cis*	475 (3)[a]	0.52[a]			469 (4)	0.55	475 (5)	0.48	474 (3)	0.58

	neurosporene[f]		spheroidene[g]		spirilloxanthin[h]		okenone[i]		*α*-carotene[j]	
	$A_g^- \rightarrow B_u^+(0\text{-}0)$ wavelength / nm (isomerization shift)	$\frac{A_g^- \rightarrow A_g^+}{A_g^- \rightarrow B_u^+}$ relative intensity	$A_g^- \rightarrow B_u^+(0\text{-}0)$ wavelength / nm (isomerization shift)	$\frac{A_g^- \rightarrow A_g^+}{A_g^- \rightarrow B_u^+}$ relative intensity	$A_g^- \rightarrow B_u^+(0\text{-}0)$ wavelength / nm (isomerization shift)	$\frac{A_g^- \rightarrow A_g^+}{A_g^- \rightarrow B_u^+}$ relative intensity	$A_g^- \rightarrow B_u^+(0\text{-}0)$ wavelength / nm (isomerization shift)	$\frac{A_g^- \rightarrow A_g^+}{A_g^- \rightarrow B_u^+}$ relative intensity	$A_g^- \rightarrow B_u^+(0\text{-}0)$ wavelength / nm (isomerization shift)	$\frac{A_g^- \rightarrow A_g^+}{A_g^- \rightarrow B_u^+}$ relative intensity
all-*trans*	468 (0)	0.03	484 (0)	0.09	526 (0)	0.10	516 (0)	0.11	474 (0)	~0
7-*cis*							508 (8)	0.13		
9-*cis*	461 (7)	0.20	476 (8)	0.20			511 (5)	0.19	469 (5)	0.09
11-*cis*										
13-*cis*			474 (10)	0.32	520 (6)	0.55	506 (10)	0.53	465 (9)	0.42
15-*cis*	464 (4)	0.48	482 (2)	0.45	524 (2)	0.65				

[a] Koyama et al., 1989
[b] Hu et al., 1997
[c] H. Hashimoto unpublished
[d] Khachik et al., 1992
[e] Hashimoto et al., 1993
[f] Katayama et al., 1990
[g] Jiang et al., 1996
[h] Koyama et al., 1990
[i] Fujii et al., 1998a
[j] Emenhiser et al., 1996

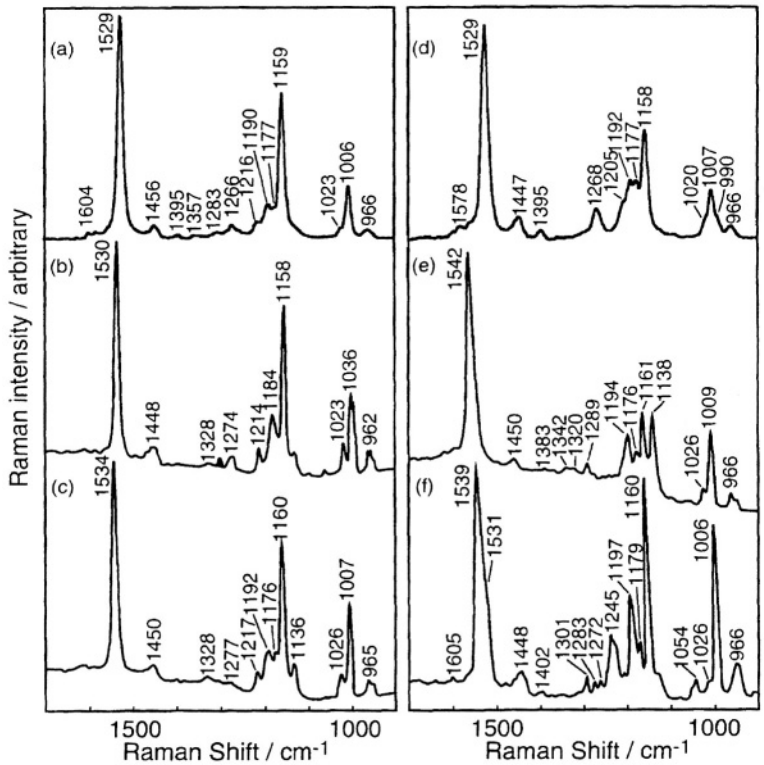

Fig. 5. Resonance-Raman spectra of isomeric β-carotene (at 77 K, 488.0 nm probe): (a) all-*trans*, (b) 7-*cis*, (c) 9-*cis*, (d) 11-*cis*, (e) 13-*cis* and (f) 15-*cis*.

cis, due to decrease in conjugation when a *cis* bend is introduced from the peripheral part toward the central part (see also Table 4). (2) The frequencies and intensities of the Raman lines in the 1200–1100 cm^{-1} region due to the C–C stretchings coupled with the C–H in-plane bending are also configuration-sensitive. Actually, the relative intensity of the C10-C11 stretching around 1140 cm^{-1} vs. the C14–C15 stretching around 1160 cm^{-1} increases in the order, all-*trans* < 7-*cis* < 9-*cis* < 13-*cis* (Table 4). This observation can be explained by a general trend that a normal mode taking place at the center of an all-*trans* fragment gives rise to the highest Raman intensity (Koyama et al., 1988c). Fig. 2 shows that, when the position of *cis* double bond shifts to the center from 7-*cis* to 13-*cis,* the position of the C14–C15 (C10–C11) bond becomes a peripheral (central) bond in the all-*trans* fragment(s). The 11-*cis* and the 15-*cis* isomers do not follow this rule because of the distortion of the conjugated backbone and the changes in the normal modes due to the C_{2v} (C_2) symmetry, respectively (Hu et al., 1997). (3) The coupled vibration of the C–H in-plane bending and the C=C stretching of an unmethylated-cw group, called the UC mode, gives rise to a key Raman line of the unmethylated-ctt group (Koyama et al., 1988c; Koyama and Mukai, 1993). The 1274 cm^{-1} Raman line of the 7-*cis* isomer, the 1268 cm^{-1} Raman line of the 1 l-*cis* isomer, and the 1245 cm^{-1} line of the 15-*cis* isomer are regarded as key Raman lines for these particular unmethylated-*cis* configurations.

b. Other Carotenoids

Essentially the same observations as β-carotene were made for other carotenoids (Fujii et al., 1998a) (see Table 4). (1) The C=C stretching Raman line shifts to the higher frequencies in the order, all-*trans* < 7-*cis* < 9-*cis* < 13-*cis.* This holds true in all sets of carotenoids except for spheroidene. (2) An increase in the relative intensity of the C10–C11 stretching mode vs. the C14–C15 stretching mode holds true for all the other carotenoids. (3) The key Raman line of the 15-*cis* configuration appears at the following frequencies: β-carotene (1245 cm^{-1}), β-apo-8′-carotenal (1246 cm^{-1}), neurosporene (1240 cm^{-1}),

Table 4. The frequency of the C=C stretching Raman line and the relative intensity of the C10-C11 stretching vs. the C14-C15 stretching Raman line

	β-carotene		canthaxanthin[c]		lutein[d]		β-apo-8'-carotenal[e]	
	C=C stretching frequency / cm^{-1} (isomerization shift)	C10-C11 str. / C14-C15 str. relative intensity	C=C stretching frequency / cm^{-1} (isomerization shift)	C10-C11 str. / C14-C15 str. relative intensity	C=C stretching frequency / cm^{-1} (isomerization shift)	C10-C11 str. / C14-C15 str. relative intensity	C=C stretching frequency / cm^{-1} (isomerization shift)	C10-C11 str. / C14-C15 str. relative intensity
all-*trans*	1529 (0)[a]	~0[a]	1523 (0)	0.09	1535 (0)	~0	1530 (0)	~0
7-*cis*	1530 (1)[a]	0.20[a]					1535 (5)	0.11
9-*cis*	1534 (5)[a]	0.35[a]	1529 (6)	0.23	1536 (1)	0.26	1538 (8)	0.23
11-*cis*	1529 (0)[b]	~0[b]						
13-*cis*	1542 (13)[a]	0.99[a]	1537 (14)	0.67	1545 (10)	0.74	1548 (18)	0.91
15-*cis*	1539 (10)[a]	0.12[a]					1542 (12)	0.44

	neurosporene[f]		spheroidene[g]		spirilloxanthin[h]		okenone[i]	
	C=C stretching frequency / cm^{-1} (isomerization shift)	C10-C11 str. / C14-C15 str. relative intensity	C=C stretching frequency / cm^{-1} (isomerization shift)	C10-C11 str. / C14-C15 str. relative intensity	C=C stretching frequency / cm^{-1} (isomerization shift)	C10-C11 str. / C14-C15 str. relative intensity	C=C stretching frequency / cm^{-1} (isomerization shift)	C10-C11 str. / C14-C15 str. relative intensity
all-*trans*	1532 (0)	~0	1529 (0)	~0	1508 (0)	0.08	1518 (0)	~0
7-*cis*							1519 (1)	~0
9-*cis*			1541 (12)	0.57			1526 (8)	0.31
11-*cis*								
13-*cis*			1539 (10)	0.75	1520 (12)	0.44	1532 (14)	1.54
15-*cis*	1539 (7)	0.16	1536 (7)	0.10	1516 (8)	0.27		

[a] Koyama et al., 1982
[b] Hu et al., 1997
[c] Hashimoto and Koyama, 1991
[d] Y. Sakano, unpublished
[e] Hashimoto et al., 1993
[f] Koyama et al., 1988a
[g] Jiang et al., 1996
[h] Koyama et al., 1990
[i] Fujii et al., 1998a

spheroidene (1244 cm^{-1}) and spirilloxanthin (1242 cm^{-1}) (see references attached to Table 4).

Thus, the frequency of the C=C stretching Raman line as well as the relative intensity of the C10–C11 stretching vs. the C14–C15 stretching are able to distinguish the all-*trans* or a peripheral-cw configuration *(7-cis* and 9-*cis*) from a central-*cis* (13-*cis*) configuration. The UC modes can be used to identify the 7-*cis* and the 15-*cis* configurations. The 11-*cis* configuration is not present in Nature.

5. Thermal Isomerization of β-Carotene

Figures 6a–e show thermal isomerization of *β*-carotene at 80°C starting from the all-*trans* and mono-*cis* isomers and it can be characterized as follows (Kuki et al., 1991): (1) The efficiency of thermal isomerization defined as a decrease in the starting isomer is in the order, all-*trans* < 7-*cis* < 9-*cis* < 13-*cis* < 15-*cis,* among the naturally occurring isomers; (2) the '*trans*-to-*cis*' isomerization predominates in the central part of the all-*trans* or a peripheral-*cis* isomer, whereas the *cis*-to-*trans* isomerization predominates in the central-*cis* isomers; and (3) the *cis*-to-*cis* isomerization takes place only in the central part of the central-*cis* isomers. Because of the first characteristic the all-*trans* isomer is much more stable than the 15-*cis* isomer, and the 15-*cis* isomer is the least stable among the naturally-occurring isomers. Because of the second and the third characteristics, all-*trans* isomerizes into 13-*cis* and 15-*cis,* whereas 15-*cis* isomerizes into all-*trans* and 13-*cis.* Fig. 6f compares thermal isomerization at 38°C starting from the 15-*cis* and the 11-*cis* isomers (Hu et al., 1997). One-way *cis*-to-*trans* isomerization takes place very efficiently in the 11-*cis* isomer.

B. Excited-State Properties of β-Carotene

1. The S_1 ($2A_g^-$) State

The $S_1 \rightarrow S_n$ absorption spectra of the all-*trans,* 9-*cis,*

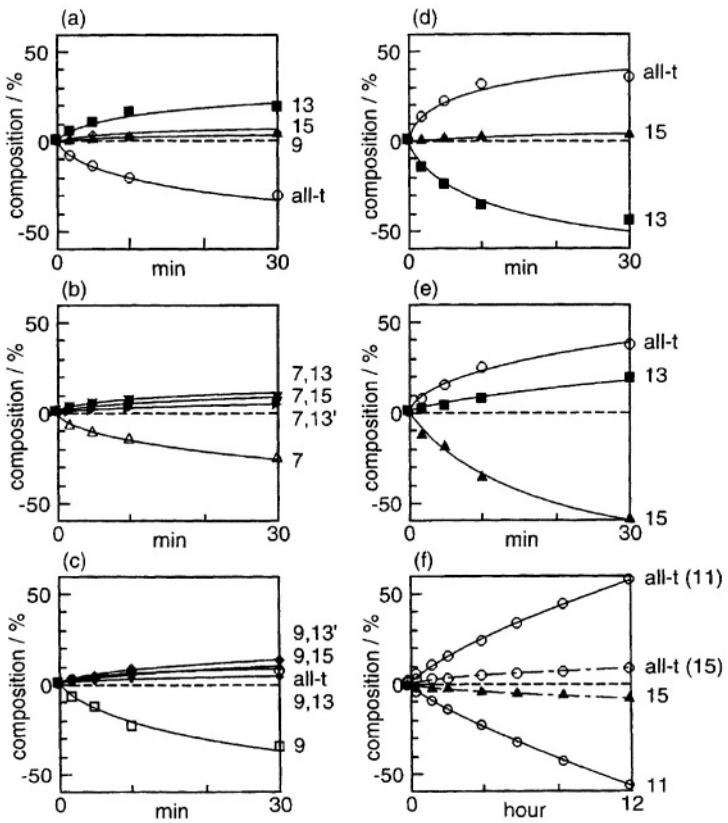

Fig. 6. Thermal isomerization of *β*-carotene at 80 °C starting from the (a) all-*trans*, (b) 7-*cis*, (c) 9-*cis*, (d) 13-*cis* and (e) 15-*cis* isomers. (f) Thermal isomerization at 38 °C of the 11-*cis* isomer is also compared with that of the 15-*cis* isomer.

13-*cis* and 15-*cis* isomers of β-carotene were recorded by using 20–25 ps, 355 nm-pump and white continuum-probe pulses (Hashimoto et al., 1991). Each isomer exhibited a different absorption maximum: all-*trans,* 556 nm; 9-*cis,* 565 nm; 13-*cis*, 560 nm; and 15-*cis,* 562 nm. Thus, the all-*trans* and each *cis* S_1 species were detected. No time-dependent shifts of the $S_1 \rightarrow S_n$ absorption were detected, a fact which indicates that no isomerization takes place in the S_1 state. The quantum yields of intersystem crossing were determined to be on the order of 10^{-3}.

The S_1 Raman spectra of the same set of isomers of β-carotene were recorded by using 355 nm-pump and 532 nm-probe pulses (Hashimoto and Koyama, 1989; Hashimoto et al., 1991). Each S_1 species exhibited the C=C stretching Raman line as high as 1777–1790 cm^{-1}. Since this strongly Raman-active mode is to be assigned to an a_g-type C=C stretching mode, and since its abnormally high frequency can be ascribed to the vibronic coupling with the ground (A_g^-) state, the S_1 state probed by transient-Raman spectroscopy was assigned to the $2A_g^-$ state (Hashimoto and Koyama, 1989). The spectral patterns in the most configuration-sensitive 1300–1100 cm^{-1} region were different from one isomer to another, a fact which indicates that no isomerization takes place in the S_1 state (Hashimoto et al., 1991).

2. The T_1 (B_u^+) State

Figure 7 shows the electronic-absorption spectra of the T_1 (lowest-lying triplet) species generated from the set of *cis-trans* isomers of β-carotene (Hashimoto et al., 1989). The all-*trans,* 7-*cis,* 9-*cis* and 13-*cis* isomers show different spectral patterns, a fact which indicates that the T_1-state isomerization, if any, is not efficient for these isomers. The wavelength of the $T_1 \rightarrow T_n$ absorption (nm) and the decay rate ($k_d \times 10^{-5}$ s^{-1}) for each T_1 species have been determined as follows: all-*trans,* 520 and 2.1;7-*cis*, 510 and 1.6; 9-*cis,* 520 and 2.7; and 13-*cis,* 522 and 2.8. However, the T_1 species generated from the 15-*cis* isomer shows exactly the same $T_1 \rightarrow T_n$ absorption pattern and decay rate as that generated from the all-*trans* isomer (the all-*trans* T_1).

Figure 8 shows the transient Raman spectra of T_1 species generated from the same set of isomers of β-carotene (Hashimoto and Koyama, 1988). The spectral patterns are very similar to one another, but differences are seen in the 1250–1150 cm^{-1} region. The all-*trans,* 7-*cis,* 9-*cis* and 13-*cis* isomers show

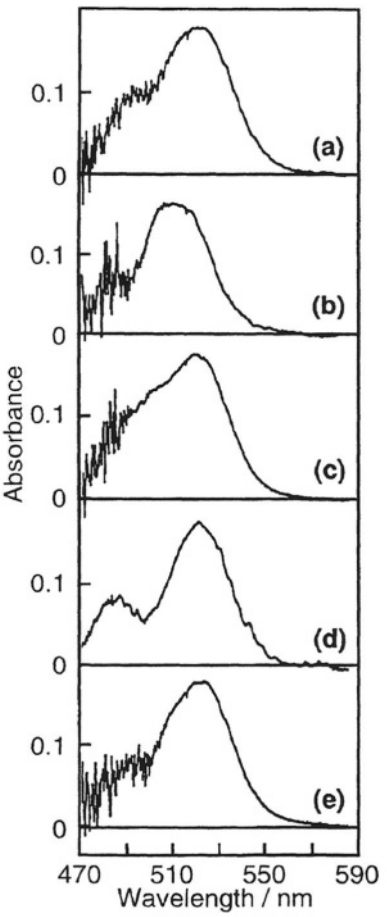

Fig. 7. Electronic-absorption spectra of the T_1 species of β-carotene generated from the (a) all-*trans*, (b) 7-*cis*, (c) 9-*cis*, (d) 13-*cis* and (e) 15-*cis* isomers (1.8 μs after excitation of the sensitizer, anthracene, at 355 nm).

unique T_1 spectral patterns, supporting the above conclusion. Here again, the T_1 species generated from the 15-*cis* isomer shows a Raman spectrum which is identical to that of the T_1 species generated from the all-*trans* isomer.

Figure 9 shows the pathways of triplet-sensitized isomerization starting from each *cis-trans* isomer and the relative quantum yields. Quantum yield is defined as the amount of isomerization per T_1 species generated (Kuki et al., 1991). The length of each arrow is proportional to the quantum yield along the particular pathway. A thicker arrow indicates that the quantum yield should be multiplied by 10 to compare with a thinner arrow. The results show extremely efficient one-way isomerization from 15-*cis* to all-*trans* via the T_1 state. The quantum yields of isomerization defined as a decrease in the starting

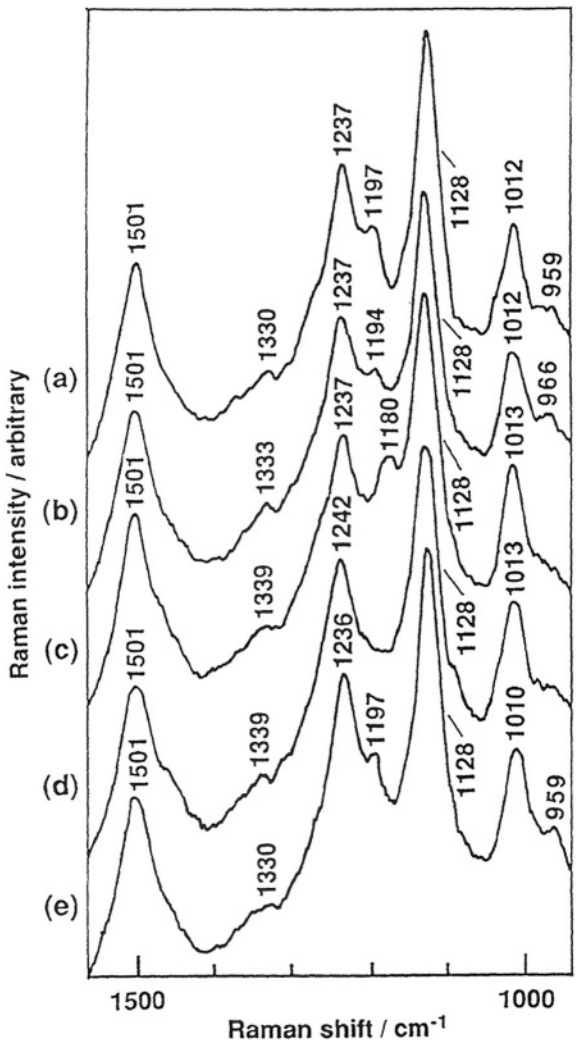

Fig. 8. Resonance-Raman spectra of T_1 spices of β-carotene generated from the (a) all-*trans*, (b) 7-*cis*, (c) 9-*cis*, (d) 13-*cis* and (e) 15-*cis* isomers (1.8 μs after excitation of the sensitizer, anthracene, at 337 nm).

isomer are all-*trans*, 0.044; 7-*cis*, 0.12; 9-*cis*, 0.15; 13-*cis*, 0.82; and 15-*cis*, 0.98.

The excited-state properties of the all-*trans* and the 15-*cis* isomers can be summarized as follows: In the S_1 state, no isomerization was found in any of the isomers. In the T_1 state, the 15-*cis* isomer exhibits extremely efficient isomerization into the all-*trans* isomer. In other words, the 15-*cis* T_1 is too short-lived to be detected, and the resultant all-*trans* T_1 alone can be detected by time-resolved spectroscopy. The T_1-state isomerization of the all-*trans* isomer is much less efficient.

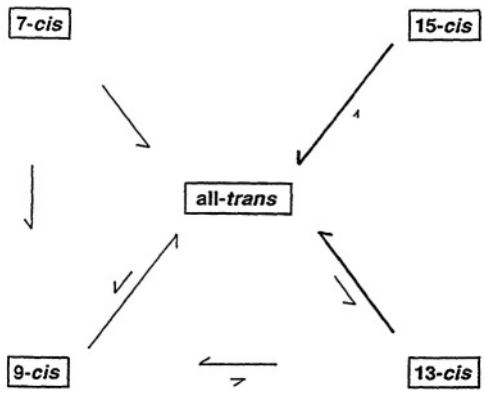

Fig. 9. Pathways of triplet-sensitized isomerization of β-carotene starting from the all-*trans*, 7-*cis*, 9-*cis*, 13-*cis* and 15-*cis* isomers. The length of each arrow is proportional to the quantum yield of isomerization (per triplet species generated); the length of a thicker arrow should be multiplied by 10 to compare with a thinner arrow.

III. Light-Harvesting Function of All-*Trans* Carotenoids in the LHC

A. The Singlet-State Properties of All-Trans-β-Carotene and Spheroidene

1. The B_u^+ State

a. Energy

Figure 10 shows the dependence of the B_u^+ energies of β-carotene and spheroidene on the solvent polarizability (Nagae et al., 1994; Kuki et al., 1994): The B_u^+ energy exhibits, in both nonpolar and polar solvents, a linear dependence on $R(n) = (n^2 - 1)/(n^2 - 2)$, where n is the solvent refractive index. In β-carotene, the B_u^+ energy (absorption maximum in cm^{-1}) can be expressed as $\nu(B_u^+)^{(N)} = 24976 - 12178\,R(n)$ in non-polar solvents and $\nu(B_u^+)^{(P)} = 23787 - 8268\,R(n)$ in polar solvents; in spheroidene, the B_u^+ energies are expressed as $\nu(B_u^+)^{(N)} = 24846 - 12130\,R(n)$ and $\nu(B_u^+)^{(P)} = 23800 - 8668\,R(n)$. Thus, in each carotenoid, $\nu(B_u^+)^{(P)}$ is lower than $\nu(B_u^+)^{(N)}$ in the limit of $R(n) \to 0$ (n = 1, i.e., in vacuum) and the line for polar solvents shows a gentler slope; as a result, it crosses the line for non-polar solvents at $R(n) \approx 0.3$. A theory was developed to explain this observation (Nagae et al., 1994; Nagae, 1997): In polar solvents, an electric field which is generated by fluctuation of the solvent dipoles affects the conjugated chain of the carotenoid in a long spheroidal cavity; it stabilizes the B_u^+ energy through the polarization effect

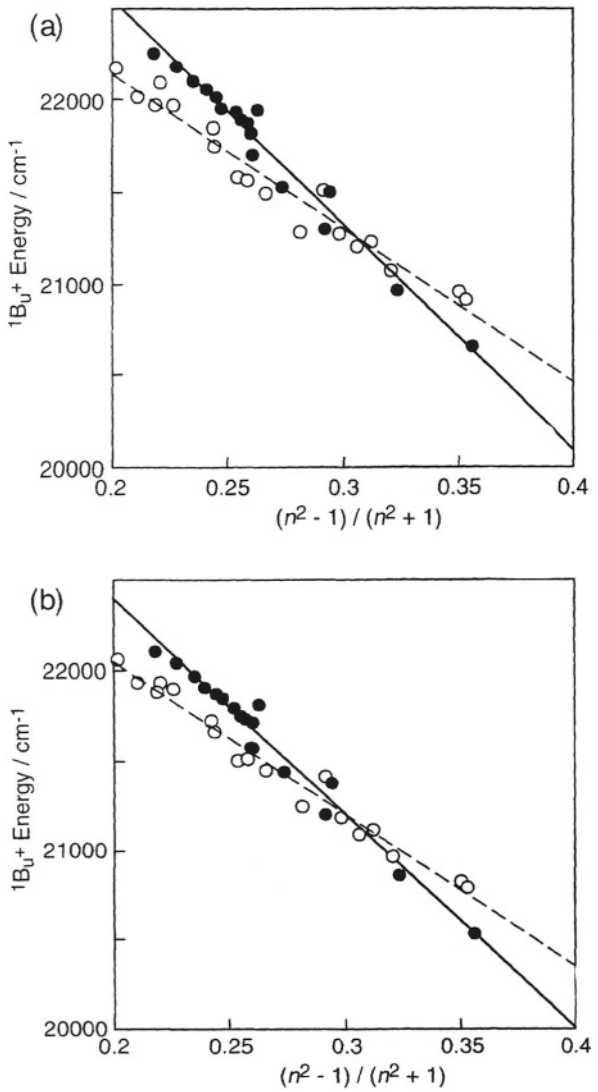

Fig. 10. Relation between the B_u^+ energy (absorption maximum) and the solvent polarizability, $R(n) = (n^2 - 1) / (n^2 + 2)$, where n is the refractive index of the solvent. (a) All-*trans*-β-carotene and (b) all-*trans*-spheroidene in nonpolar (closed circles) and polar (open circles) solvents.

(stabilization at $R(n) \rightarrow 0$) and substantially reduces the dispersive interaction (causing a gentler slope). It is to be noted that the B_u^+ energy can be changed, as large as by 1500 cm^{-1}, in an ordinary range of the solvent polarizability.

b. Lifetime

Table 5 lists the B_u^+ lifetimes of β-carotene and spheroidene (Kandori et al., 1994; Ricci et al., 1996), which were determined precisely by the fluorescence up-conversion technique. No dependence of the lifetime on the probing wavelength was observed in either carotenoid, an observation which is consistent with the proposed intramolecular relaxation time shorter than 50 fs (Watanabe et al., 1993). In spheroidene, the B_u^+ lifetime was found to be strongly dependent on the solvent polarizability (Ricci et al., 1996); similar observation has been obtained for β-carotene as well (A.N. McPherson and T. Gillbro, unpublished).

Table 5. The $1B_u^+$ lifetimes and energies of β-carotene and spheroidene

carotenoid	solvent	τ_2 (fs)	$1B_u^+$ (cm^{-1})
β-carotene[a]	*n*-hexane	195 ± 10	21000
spheroidene	*n*-pentane	245 ± 10[b]	20700[c]
	CS_2	155 ± 10[b]	19200[c]
	LH1	55 ± 20[b]	19800[c]
	LH2	80 ± 20[b]	19400[c]

[a] Kandori et al., 1994
[b] Ricci et al., 1996
[c] Kuki et al., 1994

2. The $2A_g^-$ State

a. Energy

Although the $2A_g^-$ state is 'optically-forbidden', efficient B_u^+ to $2A_g^-$ internal conversion causes fluorescence from the $2A_g^-$ state when the conjugated chain is short enough. When the conjugated chain becomes longer, the energy gap between the B_u^+ and $2A_g^-$ states increases, and then, the crossover from the $2A_g^-$ fluorescence to the B_u^+ fluorescence takes place. Therefore, the detection of the $2A_g^-$ fluorescence becomes extremely difficult when the number of the conjugated double bonds (n) exceeds 9.

Figure 11 a shows the electronic absorption, fluorescence and fluorescence-excitation spectra of all-*trans*-β-carotene (Y. Watanabe et al., unpublished), whereas Fig. 11b shows that of all-*trans*-spheroidene (Fujii et al., 1998b). In each case, the $B_u^+ \rightarrow A_g^-$ fluorescence constitutes a complete mirror image with respect to the $A_g^- \rightarrow B_u^+$ absorption. In addition, extremely weak $2A_g^-$ fluorescence appears on the lower-energy side when the ordinate scale is expanded. The fluorescence spectra were analyzed by a deconvolution method based on the vibronic transitions from both the B_u^+ (0) and the $2A_g^-$ (0) states. When the vibrational structure was not apparent, a similar spacing was assumed for each

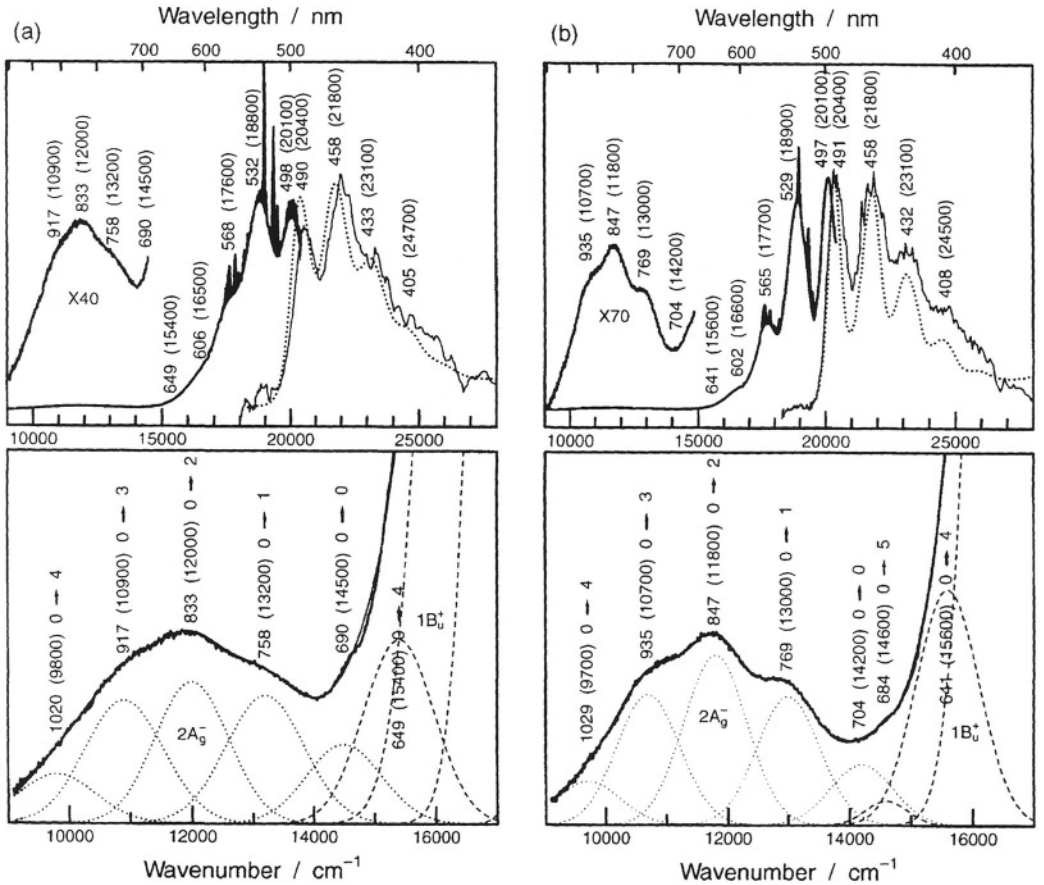

Fig. 11. Electronic-absorption (dotted line), fluorescence (thicker solid line) and fluorescence-excitation (thinner solid line) spectra; Raman lines are painted in black. Lower panels show the results of deconvolution in the low-energy region. (a) All-*trans*-β-carotene at 170 K, excitation at 488 nm and probing at 770 nm for the fluorescence and fluorescence-excitation measurements; (b) all-*trans*-spheroidene at 200 K, excitation at 488 nm and probing at 770 nm for the fluorescence and fluorescence-excitation measurements.

vibrational progression. The results of deconvolution shown in the lower panels of Fig. 11a and 11b indicate that the vibronic origin of the $2A_g^-$ state is 14500 cm^{-1} for β-carotene and 14200 cm^{-1} for spheroidene. A similar analysis of the fluorescence spectrum of neurosporene identified the $2A_g^-$ (0-0) origin at 15300 cm^{-1} (Fujii et al., 1998b). In each carotenoid, the same spacings in both the B_u^+ and the $2A_g^-$ progressions (1000-1400 cm^{-1}) reflect the S_0-state vibrational levels. The presence of a spacing other than the above (900 and 400 cm^{-1} in all-*trans*-β-carotene and spheroidene, respectively) provides us with a clue to identify the $2A_g^-$ (0-0) origin.

Fluorescence spectroscopy can be applied, in principle, to carotenoids having a longer conjugated chain. However, the most serious problem is the identification of the (0-0) origin, because the $2A_g^-$ fluorescence becomes broader with increasing chain length (Y. Watanabe et al., unpublished). The method of resonance-Raman excitation profile avoids this problem. This method measures the excitation energy-dependence of the Raman intensity for a single vibrational mode, and therefore, resolution is always high(Koyama, 1995). Fig. 12a shows the resonance-Raman excitation profile for the a_g-type C=C stretching (ν_1) mode of crystalline all-*trans*-β-carotene. The peak at 14500 cm^{-1} was proposed to be the $2A_g^-$ (0-0) origin (Hashimoto et al., 1997) in agreement with the above fluorescence result.

The resonance-Raman excitation profile of carotenoid in the $2A_g^-$ state can be explained by the A term of the Albrecht theory (Tang and Albrecht, 1970) that is applicable to the totally-symmetric (a_g-type) modes when the electronic transition dipole is not completely zero (Sashima et al., 1998a). The results lead us to the conclusion that the observed

peaks are due to the $A_g^-(0) \rightarrow 2A_g^-(v)$transitions with $v = 0, 1, 2....$ Thus, the resonance-Raman excitation-profiles for both the C=C stretching (ν_1) and the C–C stretching (ν_2) a_g-type modes facilitate the identification of the $2A_g^-$ (0-0) origin, from which both of the vibrational progressions having different spacings start. Figures 12b and c show the resonance-Raman excitation profiles of the pair of modes for crystalline spheroidene (Sashima et al., 1998a). The ν_1 resonance-Raman excitation profile exhibits three peaks at 14200, 15700 and 17250 cm^{-1} (spacings 1500 and 1550 cm^{-1}), whereas the ν_2 resonance-Raman excitation profile exhibits two clear peaks at 14200 and 15350 cm^{-1} (spacing 1150 cm^{-1}) and an additional broad profile. Thus, the common 14200 cm^{-1} peak can be definitely assigned to the $2A_g^-$ (0-0) origin. Again, this result agrees with that of the above fluorescence spectroscopy.

In each carotenoid, the $2A_g^-$ (0-0) energy for the absorptive transition determined by resonance-Raman excitation profile in the crystalline state is in *complete* agreement with that for the emissive transition determined by fluorescence spectroscopy in *n*-hexane solution, a fact which strongly suggests that neither the Stokes shift nor the dependence on the polarizabiliry of the environment (in *n*-hexane solution vs. in crystal) is present in this particular electronic state.

Figure 13 (open circles) shows the $2A_g^-$ energies of the shorter analogs of spheroidene, neurosporene and spheroidene determined by fluorescence spectroscopy (DeCoster et al., 1992; Fujii et al., 1998b) as a function of 1 / (2n + 1), where n is the number of conjugated double bonds (Koyama et al., 1996). It is interesting to note that the $2A_g^-$ energy(in cm^{-1}) is expressed by a straight line, $\nu\ (2A_g^-) = 220946 / (2n + 1) + 3681$. The $2A_g^-$ energy for the infinite chain in this analysis is 3681 cm^{-1}.

b. Lifetime

Table 6 lists the $2A_g^-$ lifetimes of the β-carotene and spheroidene analogs (references attached to the table). The lifetime decreases when n increases, a fact which is in accord with the decrease in the energy gap between the $2A_g^-$ and the A_g^- states. After establishing the relation between the $2A_g^-$ energy determined by fluorescence spectroscopy and the $2A_g^-$ lifetime determined by time-resolved absorption spectroscopy in terms of the energy-gap law (Englman and Jortner, 1970) for carotenoids having a shorter conjugated

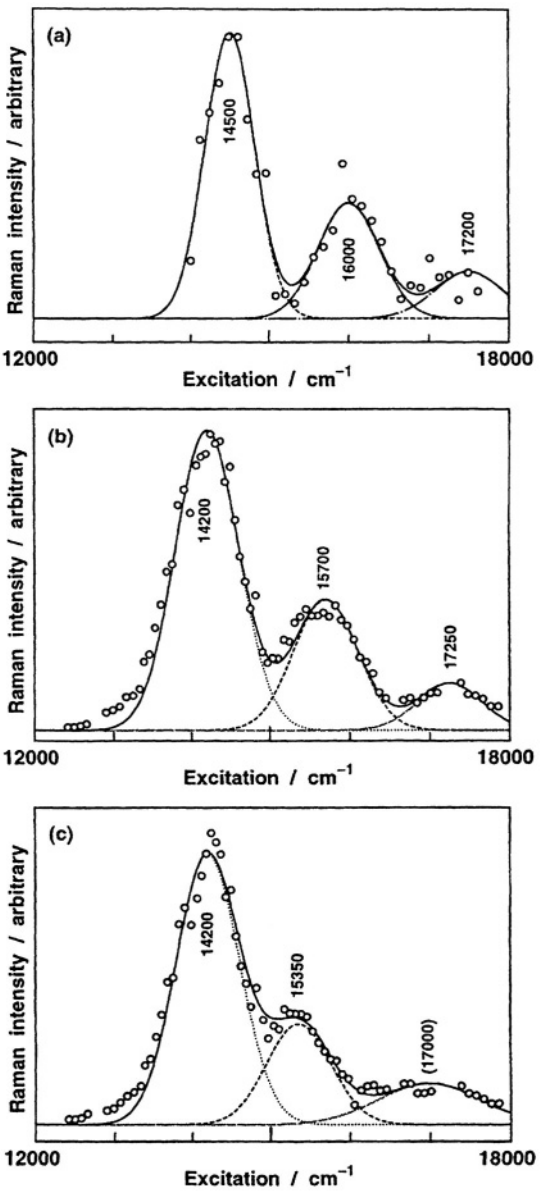

Fig. 12. Resonance-Raman excitation profiles (at 77 K) of (a) the C=C stretching (ν_1) mode of crystalline all-*trans*-β-carotene, and (b) the C=C stretching (ν_1) mode and (c) the C–C stretching (ν_2) mode of crystalline all-*trans*-spheroidene.

chain, the $2A_g^-$ energy of a carotenoid having a longer conjugated chain can be estimated; the estimated values are listed in Table 6 (in parentheses). It is to be noted that the $2A_g^-$ energy of spheroidene which has been predicted to be 14200 cm^{-1} (Frank et al., 1997) is now proved by the spectroscopic methods described above. It is also noted that the predicted $2A_g^-$ energies of the spheroidene analogs having n =

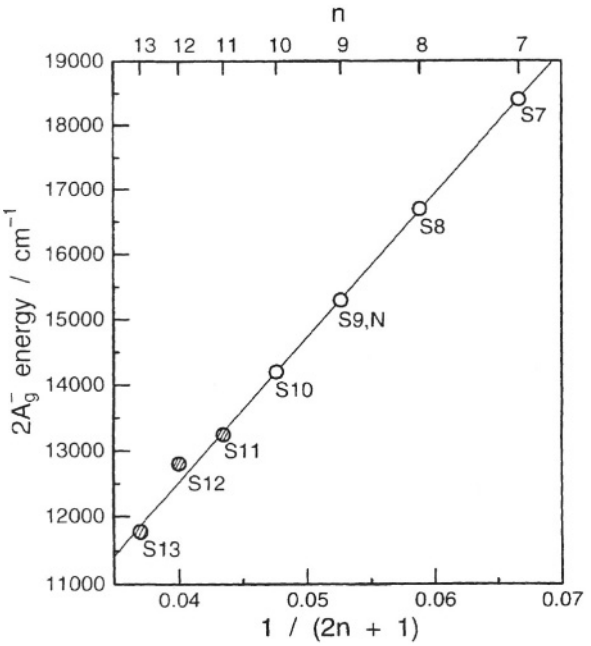

Fig. 13. The $2A_g^-$ (0-0) energy as a function of 1 / (2n + 1), where n is the number of conjugated double bonds. The $2A_g^-$ energies include those of the shorter analogs of spheroidene (S7–S9) and those of neurosporene (N9) and spheroidene (S10) determined by fluorescence spectroscopy (open circles). The $2A_g^-$ energies of the longer analogs of spheroidene which have been predicted by using their $2A_g^-$ lifetimes based on the energy-gap law are shown for comparison (shaded circles).

11,12 and 13 (Frank et al., 1997) are approximately on the straight line in Fig. 13 (see the shaded circles). The result supports the idea that the $2A_g^-$ energies predicted by the energy-gap law for spheroidene analogs are reliable, although the $2A_g^-$ energies need to be determined eventually by direct spectroscopic methods described above.

B. Unique B_u^+- and $2A_g^-$-State Properties of All-Trans Carotenoids and the Mechanisms of Singlet Energy transfer

The conjugated chain of all-*trans* carotenoids in the LHCs has C_{2h} symmetry, which gives rise to the low-lying, symmetrically-independent B_u^+ and $2A_g^-$ states. One of the unique features of the carotenoid-to-BChl singlet-energy transfer is that it uses these two electronic states as two different channels. (In most pigment systems, singlet-energy transfer takes place only from the lowest singlet-excited state.) The two channels are facilitated by the situation that *direct* internal conversion from the B_u^+ to the $2A_g^-$ state is forbidden within the framework of Pariser-Parr-Pople approximation (*vide infra*). This is most probably the reason why this particular configuration is selected by the LHCs for the light-harvesting function. Fig. 14 shows an energy diagram for the LH2 complex of *R. sphaeroides*. The B_u^+ vibronic levels and the Q_x and Q_y levels of the B800 and B850 BChls were determined by electronic absorption spectroscopy of

Table 6. The $2A_g^-$ lifetimes and energies (values estimated by the energy-gap law in parentheses) of β-carotene and spheroidene analogs

conjugated	β-carotene analogs		spheroidene analogs	
double bonds (n)	lifetime (s)	energy (cm^{-1})	lifetime (s)	energy (cm^{-1})
5	2.7×10^{-9} [a]	22700[d]		
6				
7	2.82×10^{-10} [a]	19900[d]	4.07×10^{-10} [e]	18400[e]
8	9.6×10^{-11} [a]	17500[c]	8.5×10^{-11} [e]	16700[e]
9	5.2×10^{-11} [a]	16600[d]	2.54×10^{-11} [e]	15300[e]
10			8.7×10^{-12} [f]	(14200[f])
11	8.1×10^{-12} [b]	14500[c]	3.9×10^{-12} [f]	(13200[f])
12			2.7×10^{-12} [f]	(12800[f])
13			1.1×10^{-12} [f]	(11800[f])
15	1.1×10^{-12} [c]	(11300[c])		
19	5×10^{-13} [c]	(10200[c])		

[a] In *n*-hexane, Andersson et al., 1995
[b] In 3-methyl pentane, Wasielewski et al., 1989
[c] In 3-methyl pentane and *n*-hexane, Andersson and Gillbro,1995
[d] In 3-methyl pentane, Andersson et al., 1992
[e] In *n*-hexane, DeCoster et al., 1992
[f] In *n*-hexane, Frank et al., 1997

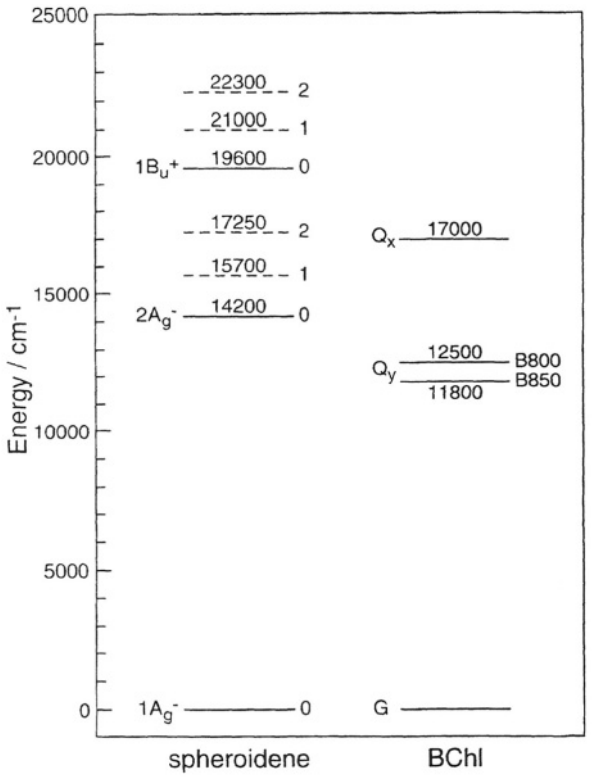

Fig. 14. An energy diagram of spheroidene and BChl *a* in the LH2 complex of *Rb. sphaeroides* 2.4.1. The B_u^+ vibronic energies of spheroidene and the Q_x and Q_y energies of B800 and B850 BChls have been determined by electronic absorption spectroscopy, and the $2A_g^-$ vibronic energies are taken from those of crystalline all-*trans*-spheroidene shown in Fig. 12b.

the complex, and the $2A_g^-$ vibronic levels are transferred from those of crystalline all-*trans*-spheroidene (Fig. 12b). The energy diagram shows that the two channels of singlet-energy transfer, i.e., one from the B_u^+ state of carotenoid to the Q_x state of BChl and the other from the $2A_g^-$ state of carotenoid to the Q_y state of BChl, are energetically feasible. Another unique feature of the carotenoid-to-BChl energy transfer is that it takes place rapidly within the lifetimes of the B_u^+ and the $2A_g^-$ state (0.2 and 10 ps in spheroidene; see Tables 5 and 6). (In ordinary pigments, the S_1 lifetime is on the order of 1-100 ns.) These short lifetimes are very important to efficiently dissipate the excess singlet energy. In this chapter, the mechanisms facilitating such short lifetimes in the two electronic states will be described.

The unique energetic and dynamic properties of the B_u^+ and the $2A_g^-$ states of carotenoids have been discussed in relation to the light-harvesting function in purple photosynthetic bacteria (Koyama et al., 1996). However, the finding of a new electronic level (the B_u^- state) in-between the B_u^+ and the $2A_g^-$ states in crystalline all-*trans* spheroidene (Sashima et al., 1998b) has revealed that the energy-transfer mechanisms can be much more complicated than anticipated. A discussion based on the detailed X-ray structures of the LH2 complexes is given by R. Cogdell in Chapter 4.

1. The B_u^+ State

In general, the rate of internal conversion is proportional to the square of vibronic-coupling constant, which is expressed by $V_{ij} = \langle \psi_i \mid \partial H/\partial Q \mid \psi_j \rangle$, where H is the molecular Hamiltonian, Q is a normal coordinate, and ψ_i and ψ_j are the electronic wavefunctions of the relevant states. Here, within the framework of the Pariser-Parr-Pople method, the vibronic-coupling constant becomes 0 if ψ_i and ψ_j have different Pariser's ± labels (Pariser, 1956) in alternant hydrocarbons (Callis et al., 1983), a rule which indicates that the vibronic coupling between the B_u^+ and the $2A_g^-$ states, and as a result, the B_u^+ to $2A_g^-$ internal conversion, is symmetrically forbidden. Then, a question arises why this internal conversion can take place on the order of 0.2 ps in spheroidene, for example? There must be some mechanism to facilitate this internal conversion process. Most recently, the measurements of resonance-Raman excitation profiles of the ν_1 and ν_2 Raman lines for crystalline all-*trans*-spheroidene in KBr disc at 77 K (Sashima et al., 1998b) identified a new singlet state at 17600 cm^{-1} that is located in-between the $2A_g^-$ state (14200 cm^{-1}) and the B_u^+ state (19700 cm^{-1}). This particular state was assigned to the B_u^- state on the basis of the extrapolation of the PPP-MRD-CI calculations for the low-lying singlet states of shorter polyenes (Tavan and Schulten, 1986). This state must mediate the B_u^+ to $2A_g^-$ internal conversion because (1) the selection rule for the B_u^+ to B_u^- internal conversion (forbidden) can break down because of the proximity of the two electronic states (energy difference, 2100 cm^{-1}), and (2) the B_u^- to $2A_g^-$ internal conversion (energy difference, 3400 cm^{-1}) is now allowed, when vibronic coupling through a b_u-type vibration is present. Thus, the extremely short lifetime of the B_u^+ state is explained.

2. The $2A_g^-$ State

The presence of vibronic coupling between the $2A_g^-$

and A_g^- states of carotenoid was first evidenced by transient Raman spectroscopy of all-*trans*-β-carotene (Hashimoto and Koyama, 1989). A transient Raman line which appeared as high as 1777 cm^{-1} in benzene solution was ascribed to the in-phase C=C stretching mode in the $2A_g^-$ state, which is pushed to the higher frequencies due to the vibronic coupling with the A_g^- (ground) state (see Sec. II.B.1). The role of this vibronic coupling in dissipating the excess energy by enhancing the $2A_g^-$ to A_g^- internal conversion was then suggested (Hashimoto and Koyama, 1989).

The small effects of deuteration and of lowering temperature on the $2A_g^-$ lifetime of all-*trans*-β-carotene in 3-methyl-pentane solution lead to a similar conclusion (Wasielewski et al., 1989). The lifetime increased slightly from 8.1 ± 0.5 ps to 10.5 ± 0.6 ps at 294 K by perdeuteration, and it was increased only by a factor of two by lowering the temperature from 100 to 20 K. These results exclude the possible involvement of the C-H stretching or the low-frequency skeletal modes in the particular internal-conversion process. Calculated changes in bond order upon excitation from the A_g^- to the $2A_g^-$ state also suggested a large Frank-Condon factor of the C=C stretching mode to enhance this process (Wasielewski et al., 1989).

Most recently, the mechanism of internal conversion from the $2A_g^-$ state to the A_g^- state of all-*trans*-β-carotene was examined by the use of isotope effects (Nagae et al., unpublished): (1) Picosecond transient Raman spectroscopy determined the frequencies of the totally-symmetric, vibronically-coupled C=C stretching (ν_1) mode in the $2A_g^-$ and A_g^- states, i.e., $\nu_1(S_1)$ and $\nu_1(S_0)$, of the unlabeled and the totally ^2H- and ^{13}C-labeled species (hereafter called as [NA], [^{2}H] and [^{13}C]). When the difference, $\Delta\nu_1 = \nu_1(S_1) - \nu_1(S_0)$, was taken as a measure of the squared vibronic-coupling constant, it became in the ratio, [NA] : [^{2}H] : [^{13}C] = 1 : 1.20 : 0.88. (2) An equation was developed to express the vibronic coupling constants in terms of the transition bond-order (bond transition-density) matrix and the L matrix in the normal-coordinate analysis (Nagae et al., 1993). It predicted the relative squared vibronic-coupling constant to be [NA] : [^{2}H] : [^{13}C] = 1 : 1.17 : 0.86, which agrees well with the above observed ratio. (3) A simplified form of the Englman-Jortner equation (Englman and Jortner, 1970), i.e., $k = 4\pi^2 / \sqrt{\Delta E h\nu^0} \cdot C^2 \cdot \exp(-2\pi\gamma\Delta E / h\nu^0)$ predicted the ratio of the internal conversion rate to be [NA] : [^{2}H] : [^{13}C] = 1 : 0.96 : 0.68, when $\nu^0 = [\nu(S_1) + \nu(S_0)] / 2$ and $2\pi\gamma = 1$ were assumed and the above relative coupling constants were used. This ratio is in good agreement with the ratio, [NA] : [^{2}H] : [^{13}C] = 1 : 0.93 : 0.70, determined by subpicosecond time-resolved absorption spectroscopy. The results indicate that the vibronic coupling through the totally-symmetric C=C stretching mode plays a major role in facilitating the $2A_g^-$ to A_g^- internal conversion (energy difference, 14200 cm^{-1}). Thus, the short lifetime of the $2A_g^-$ state is explained in terms of vibronic coupling through the a_g-type ν_1 mode.

IV. Photo-Protective Function of 15-*Cis* Carotenoids in the RC

A. Universal Presence of 15-Cis Carotenoids in the RCs of Photosynthetic Organisms

The RCs in photosynthetic organisms have been classified into two groups, i.e., quinone-type and iron sulfur-type. The quinone-type RCs are present in purple non-sulfur bacteria as well as in the PS II of cyanobacteria and chloroplasts (of algae and higher plants), whereas the iron sulfur-type RCs are present in green and purple sulfur bacteria as well as in the PS I of cyanobacteria and chloroplasts (Blankenship, 1992; Hauska et al., 1995).

1. Purple Non-Sulfur Bacteria

The presence of a *cis* carotenoid in the RCs of purple non-sulfur bacteria was first detected by resonance-Raman spectroscopy (Lutz et al., 1976,1978). It was shown also that the binding of an all-*trans* carotenoid to the RC of a carotenoidless mutant caused the formation of the *cis* carotenoid (Agalidis et al., 1980). A 15-*cis* configuration was predicted based on comparison of the Raman spectra of RCs with those of isomeric β-carotene (Koyama et al., 1982; 1983). Definitive determination of the 15-*cis* configuration has been based on the HPLC analysis of the extract from the RC, the configurational determination by ^{1}H-NMR spectroscopy of the major component in the extract, and comparison of the Raman spectrum of the 15-*cis* isomer thus identified with the Raman spectrum of the RC (Koyama et al., 1988a, 1990; Jiang et al., 1996; Ohashi et al., 1996). The 15-*cis* configurations in the RCs were determined by solid-

state NMR spectroscopy (Gebhard et al., 1991) and by X-ray crystallography (Arnoux et al., 1989; Lancaster and Michel, 1997).

Figure 15 shows the case of spheroidene in *Rb. sphaeroides* 2.4.1 (Ohashi et al., 1996). Comparison of (a) the Raman spectrum of the LH2 complex with (b) that of the all-*trans* isomer in solution shows that the carotenoid is in a rigid, planar all-*trans* configuration with in-plane distortion of the conjugated backbone. This conclusion is based on the observations that the C–H in-plane bending mode (1286 cm^{-1}) is sharpened and that additional methyl in-plane rockings (1032 and 1015 cm^{-1}) appear. Comparison of (c) the Raman spectrum of the RC with (d) that of the 15-*cis* isomer shows that the carotenoid is in a rigid, 15-*cis* configuration with a twisting around the –C15H=C15´H– group. This conclusion is based on the intensity enhancement of the C–H out-of-plane wagging mode at 954 cm^{-1}. Appearance of the additional C–H in-plane bending modes suggests some in-plane distortion of the conjugated system, as well.

Figure 16a shows an HPLC elution profile of the acetone extract from the RC of *Rb. sphaeroides* 2.4.1. The first major component was purified by HPLC, and its configuration was determined to be 15-*cis* by H-NMR spectroscopy (Jiang et al., 1996). The assignments of the rest of components were based on the HPLC analysis of isomeric spheroidenes and their electronic-absorption spectra (Jiang et al., 1996). The HPLC analysis of a 15-*cis* isomer in the extract is always accompanied by the generation of both the 13-*cis* and the all-*trans* isomers through thermal isomerization and/or porphyrin-sensitized photo-isomerization. The HPLC analysis, together with the above Raman spectroscopy, has established that 15-*cis*-spheroidene is bound to the RC of *Rb. sphaeroides* (Jiang et al., 1996; Ohashi et al., 1996). The same technique was applied to neurosporene in the RC of *Rb. sphaeroides* G1C (Koyama et al., 1988a) and spirilloxanthin in the RC of *Rhodospirillum (Rs.) rubrum* S1 (Koyama et al., 1990).

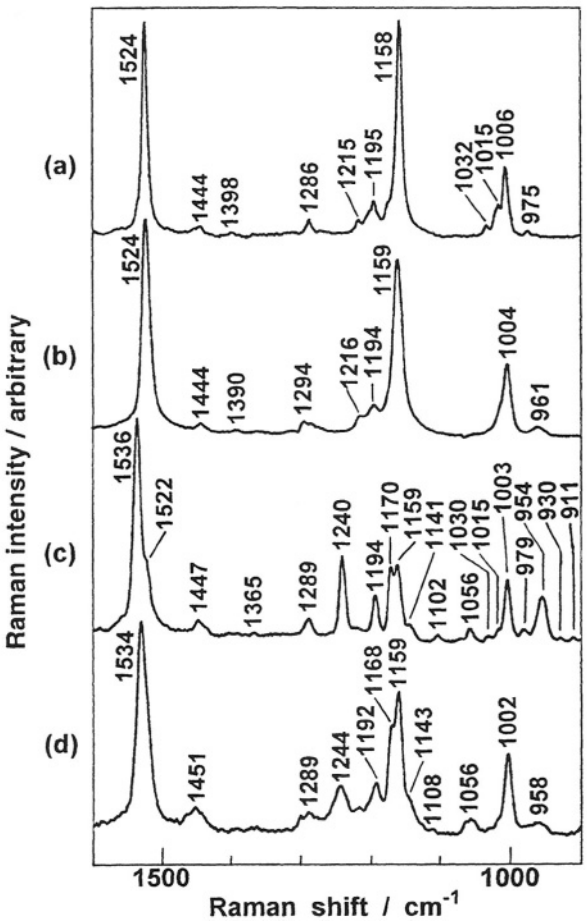

Fig. 15. S_0 Raman spectra of all-*trans*-spheroidene (a) bound to the LH2 complex of *Rb. sphaeroides* 2.4.1 and (b) free in *n*-hexane solution, and those of 15-*cis*-spheroidene (c) bound to the RC of *Rb. sphaeroides* 2.4.1 and (d) free in *n*-hexane solution (at 77 K, probing at 514.5 nm).

2. The Photosystem II of Spinach Chloroplasts

Solvent extraction at ~4 °C in complete darkness, and subsequent analysis by HPLC using an apparatus equipped with a two-dimensional diode-array detector spectroscopically identified **15-*cis*-β-carotene** in the RC of spinach PS II (Bialek-Bylka et al., 1995). Fig. 16b shows an HPLC elution profile of the acetone extract. The vibrational structures of the $A_g^- \rightarrow B_u^+$ absorption of the first component agreed with those of purified **15-*cis*-β-carotene** (see Fig. 4 and Table 3). The following plateau and shoulder in the elution profile can be ascribed to the isomerization products, 13-*cis*- and **all-*trans*-β-carotene.** Extraction by using dimethylformamide (DMF) enabled the detection of the strong *cis*-peak ($A_g^- \rightarrow A_g^+$ absorption) of the 15-*cis* isomer (Fig. 4 and Table 3). This result called into question the previous conclusion that only all-*trans*-**β-carotene** is bound to the PS II RC (Fujiwara et al., 1987). When enough precaution was not taken against thermal isomerization (~4 °C) and porphyrin-sensitized photo-isomerization (complete darkness), the 15-*cis* component disappears completely (Bialek-Bylka et al., 1995).

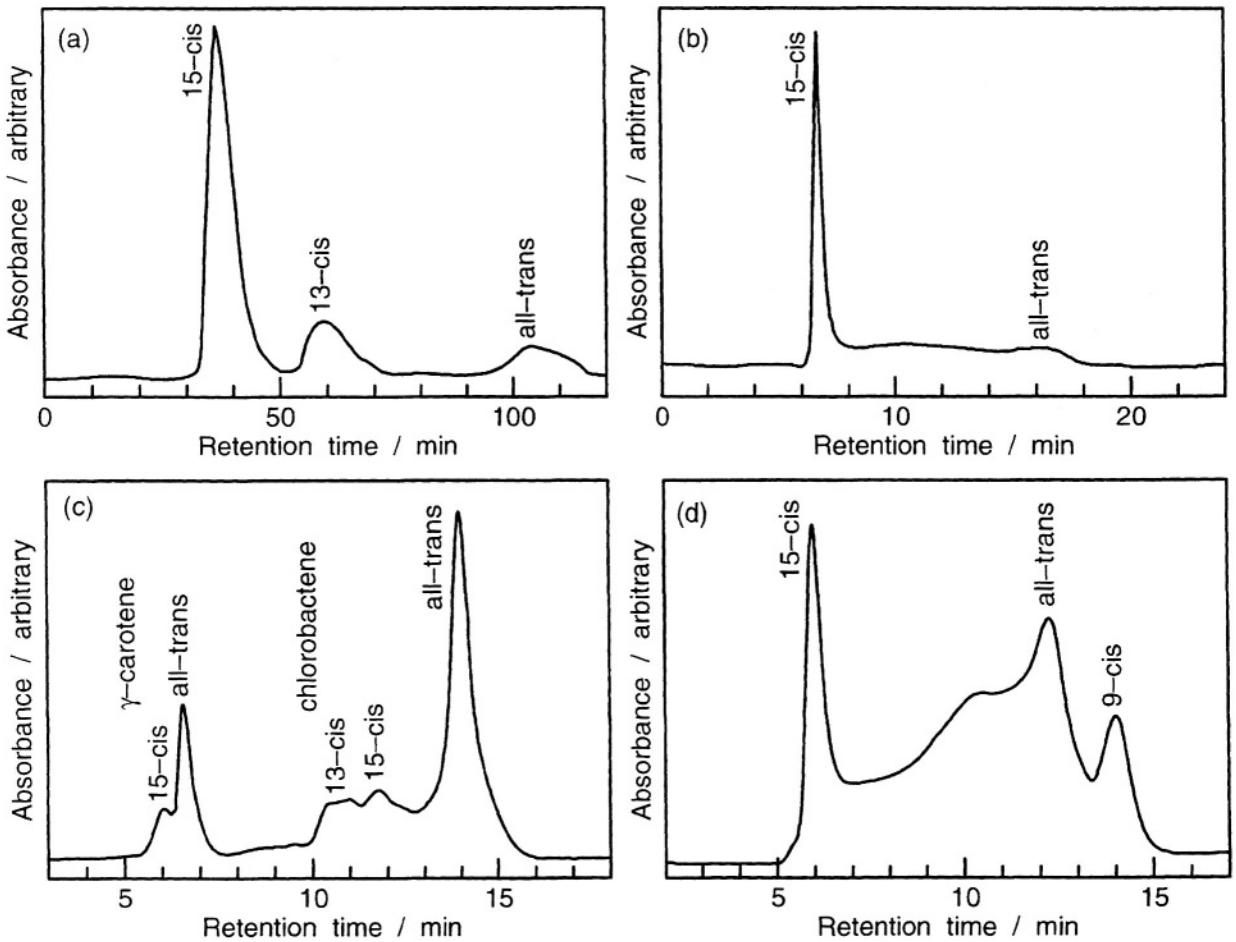

Fig. 16. HPLC elution profiles of (a) spheroidene extracted from the RC of *Rb. sphaeroides* 2.4.1 (acetone extract, detection at 450 nm), (b) β-carotene extracted from the PS II RC of spinach (acetone extract, detection at 450 nm), (c) γ-carotene and chlorobactene extracted from the RC of *Cb. tepidum* (DMF extract, detection at 460 nm), and (d) β-carotene extracted from the PS I RC of *Sc. vulcanus* (acetone extract, detection at 450 nm).

3. A Green-Sulfur Bacterium

The same analysis described above was applied to the RC of *Chlorobium (Cb.) tepidum* (Bialek-Bylka et al., 1998b). Extraction of the carotenoids was performed under the nitrogen atmosphere by using DMF. Fig. 16c shows an HPLC elution profile of the extract from the RC. An HPLC analysis and structural determination by ^{1}H-NMR spectroscopy of the isomers of γ-carotene and chlorobactene which were extracted from the cells of *Cb. limicola* lead to the assignments of these carotenoids. The assignments of the peaks due to the all-*trans* isomers of γ-carotene and chlorobactene were based on a comparison of their absorption spectra with those from the literature, whereas the assignments of the 15-*cis* isomers of γ-carotene and chlorobactene were based on the intensity ratios of the $A_g^- \rightarrow A_g^+$ absorption band to the $A_g^- \rightarrow B_u^+$ band. The numbers are 0.51 for γ-carotene and 0.48 for chlorobactene (see Table 3 for comparison with other carotenoids). It has been proposed that the RC of *Cb. limicola* contains 3 ± 1 carotenoids (Oh-oka et al., 1995). If this is the case for *Cb. tepidum,* then the mole ratio of γ-carotene to chlorobactene which is 1:3 (S. Takaichi and H. Oh-oka, unpublished) leads to the conclusion that one γ-carotene and three chlorobactenes are bound to the RC. The results indicate that at least one of each carotenoid should have a 15-*cis* configuration in the RC.

4. Photosystem I of a Cyanobacterium and Spinach Chloroplasts

The same analysis described above was applied to PS I RCs of *Synechococcus* (*Sc.*) *vulcanus* (Bialek-Bylka et al., 1998b). Each of the Psa A and Psa B subunits is believed to contain 5–7 or 6–8 β-carotene molecules (Thornber et al., 1991; Golbeck, 1992). Fig. 16d shows an HPLC elution profile for the acetone extract from the RC of *Sc. vulcanus.* The wavelengths of the vibrational structures of the $A_g^- \rightarrow B_u^+$ absorption recorded at the retention time of 5.70 min were identical to those of purified 15-*cis*-β-carotene. Further, the strong *cis*-peak (Fig. 4) could be identified using the DMF extract (relative intensity 0.42). Thus, it was concluded that at least one β-carotene molecule out of 5–8 has a 15-*cis* configuration, 15-*Cis*-β-carotene was identified in the PS I RC of spinach, as well (Bialek-Bylka et al., 1996).

Figure 17 summarizes the 15-*cis* carotenoids identified in the RCs so far (see above for references). The 15-*cis* isomers of neurosporene, spheroidene and spirilloxanthin have been identified in the quinone-type RCs of purple bacteria, i.e., *Rb. sphaeroides* G1C, 2.4.1 and *Rs. rubrum* S1, respectively. 15-*Cis*-γ-carotene and 15-*cis*-chlorobactene are found in the iron sulfur-type RC of a green sulfur bacterium, *Cb. tepidum.* 15-*Cis*-β-carotene have been identified in the quinone-type PS II RC of spinach, and also in the iron sulfur-type PS I RCs of a cyanobacterium, *Sc. vulcanus* and from spinach.

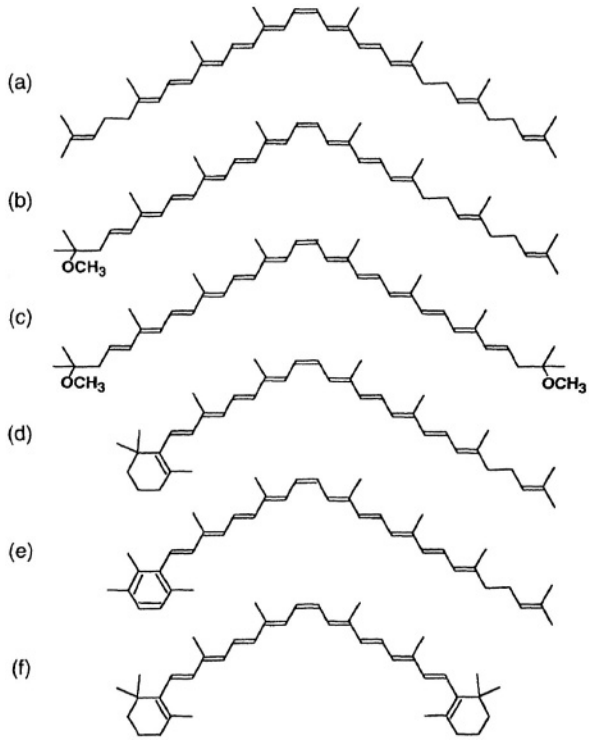

Fig. 17. 15-*Cis*-carotenoids identified so far in the RCs of various photosynthetic organisms: (a) neurosporene, (b) spheroidene and (c) spirilloxanthin in the quinone-type RC of purple non-sulfur bacteria, *Rb. sphaeroides* G1C, 2.4.1 and *Rs. rubrum* S1; (d) γ-carotene and (e) chlorobactene in the iron sulfur-type RC of green sulfur bacterium, *Cb. tepidum*; and (f) β-carotene in the quinone-type PS II RC of spinach chloroplasts as well as in the iron sulfur-type PS I RC of a cyanobacterium, *Sc. vulcanus*, and spinach chloroplasts.

*B. Unique T_1-State Properties of 15-*Cis *Carotenoids and the Mechanism of Energy Dissipation*

*1. Extremely Efficient 15-*Cis *to All-*Trans *Isomerization in the Triplet-Excited Region*

The triplet-excited region is defined as a region where changes in bond order take place upon triplet excitation, i.e., double bonds become single bond-like, whereas single bonds become double bond-like (Koyama et al., 1992). It has a span of approximately six conjugated double bonds, it is localized in the central part of a conjugated chain, and it triggers *cis* to *trans* isomerization in the T_1 state. The triplet-excited region was first found in the analysis of the T_1 Raman spectra of retinal homologs having different lengths of the conjugated chain (Hashimoto et al., 1988a; Mukai et al., 1990), and then proved for retinal by the determination of a set of stretching force constants by the normal-coordinate analysis of variously deuterated retinal (Mukai et al., 1995). This concept explained the T_1-state isomerization of isomeric retinal that was characterized by efficient isomerization of the central-*cis* isomers and by inefficient isomerization of the peripheral-*cis* isomers (Mukai et al., 1990). The Pariser-Parr-Pople calculations including the singly- and doubly-excited configurational interactions (PPP-SD-CI calculations) of model polyenes having different chain lengths supported this idea (Kuki et al., 1991).

Figure 18a shows the results of the PPP-SD-CI calculation of the π-bond orders for a model β-carotene (docosaundecaene) (Kuki et al., 1991). In

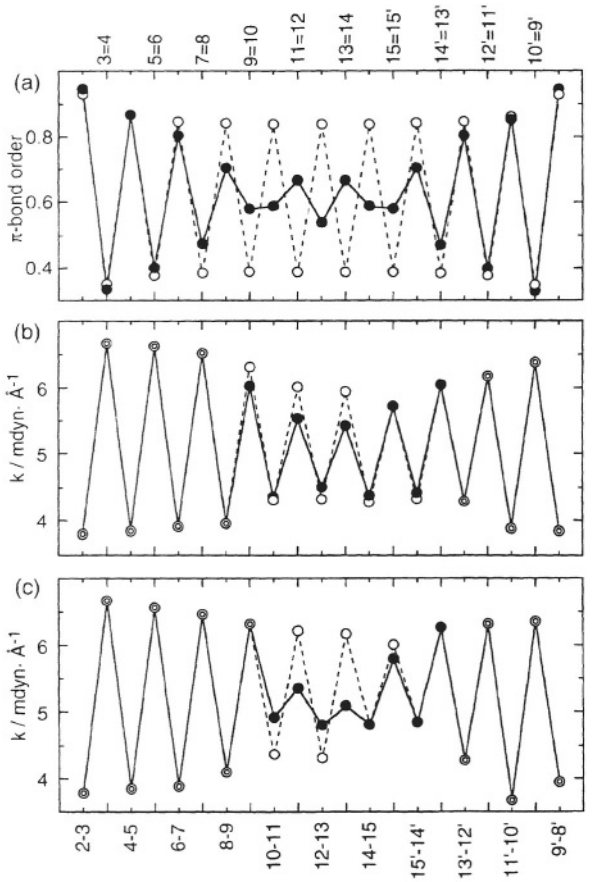

Fig. 18. (a) PPP-SD-CI calculations of π-bond orders in the S_0 (open circles) and T_1 (closed circles) states for a model of all-*trans*-β-carotene (docosaundecaene). The S_0-state (open circles) and the T_1-state (closed circles) stretching force constants (k) determined for (b) all-*trans*-spheroidene in *n*-hexane solution and (c) 15-*cis*-spheroidene bound to the RC of a carotenoidless mutant *Rb. sphaeroides* R26 are also shown. Double circles indicate those force constants assumed for both the S_0 and the T_1 states.

the S_0 state (open circles), bond alternation is clearly seen with slight decrease (increase) in bond order in the central conjugated double bonds (single bonds). Upon triplet excitation, the central double bonds become single bond-like, where as the central single bonds become double bond-like. The changes in bond order are very small on both peripheral parts. Because a decrease in bond order of a double bond causes its elongation and a decrease in the barrier of internal rotation, and then the efficient T_1-state isomerization of the central-*cis* isomers is expected (see Fig. 9). In particular, the inversion of bond order is predicted for the central 15=15′ bond. This must facilitate the extremely rapid one-way isomerization from 15-*cis* to all-*trans* in the T_1 state (Figs. 7–9). The normal-coordinate analysis of the T_1 Raman spectra of deuterated β-carotenes is ongoing to determine the set of stretching force constants for this symmetric carotenoid.

Figure 18b shows a preliminary result of normal-coordinate analysis of the S_0 and T_1 Raman spectra of seven deuterated homologs (10D, 12D, 14D, 15D, 15,15′D_2, 15′D and 14′D) of all-trans-spheroidene, an asymmetric bacterial carotenoid (Y. Mukai et al., unpublished; a collaboration with J. Lugtenburg). Because of the limited number of the deuterated species, the stretching force constants (k) in both peripherals were assumed to be the same between the S_0 and T_1 states (shown in double circles). Interestingly, the S_0-state force constants (open circles) are symmetric with respect to the 15=15′ bond, whereas the T_1-state force constants are symmetric with respect to the center of the conjugated chain (the 12–13 or the 13=14 bond). In other words, the triplet-excited region is shifted to the left-hand-side of the molecular skeleton of this carotenoid (see Fig. 1h). (Note that the S_0 and T_1 force constants are overlapped in the figure for the C15=C15′ and the C14′=C13′ bonds.)

2. The Structure of the RC-Bound Spheroidene in the T_1 State and a Possible Mechanism of Triplet-Energy Dissipation

Figure 19c shows the T_1 Raman spectrum of spheroidene bound to the RC of *Rb. sphaeroides* 2.4.1 (Ohashi et al., 1996). The following conclusions can be drawn based on this difference spectrum concerning the molecular structure of the RC-bound T_1 spheroidene: (1) The low-frequency shift of the C=C stretching Raman line and the high-frequency shift of the C–C stretching Raman line indicate a decrease in the C=C bond order and an increase in the C–C bond order, respectively; (2) the large enhancement and the low-frequency shift of the Raman line due to the C–H out-of-plane wagging coupled with the C=C torsion ($956 \rightarrow 935$ cm^{-1}) indicates that substantial twisting around a central double bond (presumably around the C15=C15′ bond) is taking place; and (3) The strong enhancement of the methyl in-plane rocking Raman line ($1004 \rightarrow 1008$ cm^{-1}) indicates a large in-plane distortion of the conjugated backbone. The above results suggest that large changes in the C=C and C–C bond orders, substantial twisting around a C=C bond(s), and a large in-plane distortion take place in the conjugated

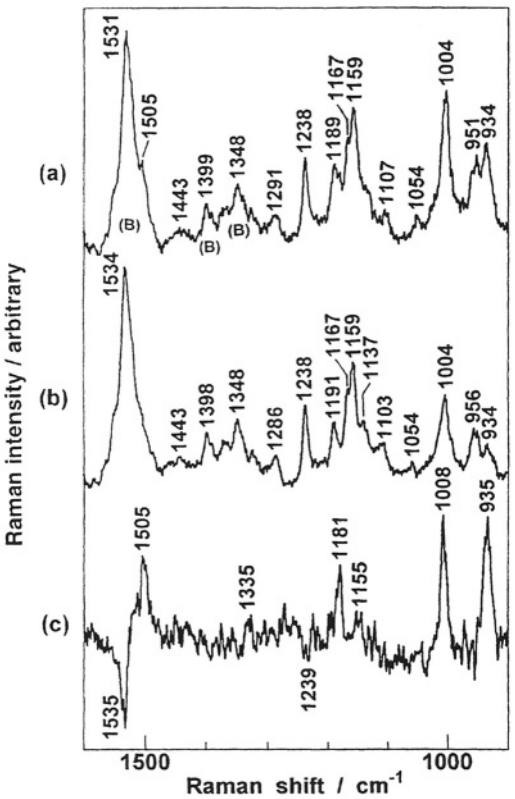

Fig. 19. Transient Raman spectrum of the RC of *Rb. sphaeroides* 2.4.1 obtained at 100 K by the use of 600-nm pump and 532-nm probe 5 ns pulses: (a) with-pump and (b) without-pump spectra, and (c) the difference spectrum of spectrum a minus spectrum b. The difference spectrum is due to the generation of the T_1-state spheroidene bound to the RC.

chain upon triplet excitation starting from a slightly-twisted configuration in the S_0 state (Sec. IVA. 1).

In order to determine the S_0-state and the T_1-state structures of the RC-bound spheroidene, six deuterated analogs (12D, 14D, 15D, 15,15′D_2, 15′D and 14′D) were bound to the RC of *Rb. sphaeroides* R26 (a carotenoidless mutant), their S_0 and T_1 Raman spectra were recorded, and the normal-coordinate analysis of those spectra was performed to determine a set of stretching force constants (Y. Mukai et al., unpublished; a collaboration with J. Lugtenburg, and R. Cogdell). Fig. 18c shows a preliminary result. A large decrease in bond order takes place for the 11=12 and the 13=14 bonds, whereas large increase in bond order takes place for the 10–11 and the 12–13 bonds. Substantial twisting (~60°) around the C15=C15′ bond was necessary to achieve the low-frequency shift of the C–H out-of-plane wagging coupled with the C=C torsion ($956 \rightarrow 935\ cm^{-1}$).

The above results suggest that a large change in the molecular structure takes place upon triplet excitation of the RC-bound spheroidene. This structural change must originate from the intrinsic properties of 15-*cis* carotenoids in solution in which large changes in bond order and isomerization toward all-*trans* take place for the central double bond(s). However, the intermolecular interaction with the apo-protein must apply a structural constraint on the carotenoid, resulting in changes in the bond orders and in the rotational angle(s) mentioned above. In particular, the internal-rotation or twisting motion may cause a change in the orbital angular momentum due to changes in the mixing of the s and p orbitals on each C nuclei and as a result, a change in the spin angular momentum (in other words, the T_1 to S_0 intersystem crossing), when the total angular momentum is conserved. The above intermolecular interaction may then cause another structural change back to the initial configuration in the process of relaxation to the S_0 state. This cyclic change in the structure of the RC-bound carotenoid is now proposed as a possible mechanism of triplet-energy dissipation.

Bautista et al. (1998) incorporated locked-15,15′-*cis* spheroidene into the RC of *R. sphaeroides* R26.1, and determined the rise and decay time constants of its triplet state to be 25 ± 1 ns and 7 ± 1 μs. They compared these values with those of the RC-bound spheroidene, i.e., 10 ns and 4-5 μs (Cogdell et al. 1975), and concluded that the isomerization (internal rotation) around the 15=15′ bond should not be the mechanism of triplet-energy dissipation. In the authors' opinion, this observation not necessarily denies our proposal because much faster structural changes in the extended triplet-excited region can still take place. The final conclusion must await for the determination of the quenching rate of triplet BChl and the rate of the structural change. Information concerning the structural change will be obtained when the above normal-coordinate analysis of the Raman spectra of the RC-bond carotenoid in the T_1 state is completed.

Acknowledgments

The authors thank Dr. Grazyna Bialek-Bylka, Dr. Hideki Hashimoto and Dr. Jian-Ping Zhang for reading this manuscript and criticism. Editing the manuscript by Dr. Harry Frank is gratefully acknowledged. This work has been supported by

Human Frontier Science Program and a grant (# 6239101) from the Ministry of Education, Science, Sports and Culture, Japan.

References

Agalidis I, Lutz M and Reiss-Husson F (1980) Binding of carotenoids on reaction centers from *Rhodopseudomonas sphaeroides* R26. Biochim Biophys Acta 589: 264–274

Andersson PO and Gillbro T (1995) Photophysics and dynamics of the lowest excited singlet state in long substituted polyenes with implications to the very long-chain limit. J Chem Phys 103:2509–2519

Andersson PO, Gillbro T, Asato AE, and Liu RSH (1992) Dual singlet state emission in a series of mini-carotenes. J Lumin 51: 11–20

Andersson PO, Bachilo SM, Chen R-L and Gillbro T (1995) Solvent and temperature effects on dual fluorescence in a series of carotenes. Energy gap dependence of the internal conversion rate. J Phys Chem 99: 16199–16209

Arnoux B, Ducruix A, Reiss-Husson F, Lutz M, Norris J, Schiffer M and Chang C-H (1989) Structure of spheroidene in the photosynthetic reaction center from Y *Rhodobacter sphaeroides.* FEBS Lett 258: 47–50

Bautista JA, Chynwat V, Cua A, Jansen FJ, Lugtenburg J, Gosztola D, Wasielewski MR and Frank HA (1998) The spectroscopic and photochemical properties of locked-15,15´-*cis*-spheroidene in solution and incorporated into the reaction center of *Rhodobacter sphaeroides* R-26.1. Photosynth Res 55: 49–65

Bialek-Bylka GE, Tomo T, Satoh K and Koyama Y (1995) 15-*Cis*-β-carotene found in the reaction center of spinach Photosystem II. FEBS Lett 363: 137–140

Bialek-Bylka GE, Hiyama T, Yumoto K and Koyama Y (1996) 15-*Cis*-β-carotene found in the reaction center of spinach Photosystem I. Photosynth Res 49: 245–250

Bialek-Bylka GE, Sakano Y, Mizoguchi T, Shimamura T, Phillip D, Koyama Y and Young AJ (1998a) Central-*cis* isomers of lutein found in the major light-harvesting complex of Photosystem II (LHC IIb) of higher plants. Photosynth Res 56: 255–264

Bialek-Bylka GE, Fujii R, Chen C-H, Oh-oka H, Kamiesu A, Satoh K, Koike H and Koyama Y (1998b) 15-*Cis*-carotenoids found in the reaction center of a green sulfur bacterium *Chlorobium tepidum* and in the Photosystem I reaction center of a cyanobacterium *Synechococcus vulcanus.* Photosynth Res 58: 1–8

Blankenship RE (1992) Origin and early evolution of photosynthesis. Photosynth Res 33: 91–111

Callis PR, Scott TW and Albrecht AC (1983) Perturbation selection rules for multiphoton electronic spectroscopy of neutral alternant hydrocarbons. J Chem Phys 78: 16–22

Cogdell RJ, Monger TG and Parson WW (1975) Carotenoid triplet states in reaction centers from *Rhodopseudomonas sphaeroides* and *Rhodospirillum rubrum.* Biochim Biophys Acta 408: 189–199

DeCoster B, Christensen RL, Gebhard R, Lugtenburg J, Farhoosh R and Frank HA (1992) Low-lying electronic states of carotenoids. Biochim Biophys Acta 1102: 107–114

Emenhaiser C, Englert G, Sander LC, Ludwig B and Schwartz SJ (1996) Isolation and structural elucidation of the predominant geometrical isomers of α-carotene. J Chromatogr A 719:333–343

Englert G (1982) N.M.R. of carotenoids. In: Britton G and Goodwin TW (eds) Carotenoid Chemistry and Biochemistry, pp 107–134. Pergamon Press, Oxford

Englert G (1995) NMR spectroscopy. In: Britton G, Liaaen-Jensen S and Pfander H (eds) Carotenoids, Vol 1B, pp 147–260. Birkhauser Verlag, Basel

Englert G, Noack K, Broger EA, Glinz E, Vecchi M and Zell R (1991) Synthesis, isolation, and full spectroscopic characterization of eleven (Z)-isomers of (3R, 3′R)-zeaxanthin. Helv Chim Acta 74: 969-982

Englman R and Jortner J (1970) Energy gap law for radiationless transitions in large molecules. Mol Phys 18: 145–164

Frank HA, Desamero RZB, Chynwat V, Gebhard R, van der Hoef I, Jansen FJ, Lugtenburg J, Gosztola D and Wasielewski MR (1997) Spectroscopic properties of spheroidene analogs having different extents of π-electron conjugation. J Phys ChemA 101: 149–157.

Fujii R, Chen C-H, Mizoguchi T and Koyama Y (1998a) ^{1}H-NMR, electronic-absorption and resonance-Raman spectra of isomeric okenone as compared with those of isomeric β-carotene, canthaxanthirf β-apo-8´-carotenal and spheroidene. Spectrochim Acta Part A 54: 727–743

Fujii R, Onaka K, Kuki M, Koyama Y and Watanabe Y (1998b) The $2A_g^-$ energies of all-*trans*-neurosporene and spheroidene as determined by fluorescence spectroscopy. Chem Phys Lett 288: 847–853

Fujiwara M, Hayashi H, Tasumi M, Kanaji M, Koyama Y and Sato K (1987) Structural studies on a Photosystem II reaction-center complex consisting of D-1 and D-2 polypeptides and cytochrome *b*-559 by resonance Raman spectroscopy and high-performance liquid chromatography. Chem Lett: 2005–2008

Gebhard R, van der Hoef K, Violette CA, de Groot HJM, Frank HA and Lugtenburg J (1991) ^{13}C Magic angle spinning NMR evidence for a 15,15´-Z configuration of the spheroidene chromophore in the *Rhodobacter sphaeroides* reaction center; synthesis of ^{13}C- and ^{2}H-labelled spheroidenes. Pure Appl Chem 63: 115–122

Golbeck JH (1992) Structure and function of Photosystem I. Annu Rev Plant Physiol Plant Mol Biol, 43: 293–324

Gruszecki WI, Matula M, Ko-chi N, Koyama Y and Krupa Z (1997) *Cis-trans*-isomerization of violaxanthin in LHC II: Violaxanthin isomerization cycle within the violaxanthin cycle. Biochim Biophys Acta 1319: 267–274

Hashimoto H and Koyama Y (1988) Time-resolved resonance Raman spectroscopy of triplet β-carotene produced from all-*trans,* 7-*cis,* 9-*cis,* 13-m, and 15-*cis* isomers and high-pressure liuid chromatography analyses of photoisomerization via the triplet state. J Phys Chem 92: 2101–2108

Hashimoto H and Koyama Y (1989) The C=C stretching Raman lines of β-carotene isomers in the S_1 state as detected by pump-probe resonance Raman spectroscopy. Chem Phys Lett 154: 321–325

Hashimoto H and Koyama Y (1991) The S_0 and T_1 states of isomeric canhaxanthin as compared with those of β-carotene: effect of the terminal carbonyl groups detected by Raman

spectroscopy. Photochem Photobiol 54: 67–73

Hashimoto H, Mukai Y and Koyama Y (1988a) Transient Raman spectra of all-*trans,* 7-*cis,* 9-*cis,* 11 -*cis* and 13-*cis* retinylidene-acetaldehyde. Structures of triplet species as revealed by Raman spectroscopy. Chem Phys Lett 152: 319–324

Hashimoto H, Koyama Y and ShimamuraT(1988b) Isolation of *cis-trans* isomers of canthaxanthin by high-performance liquid chromatography using a calcium hydroxide column and identification of their configurations by ^{1}H NMR spectroscopy. J Chromatogr 448: 182–187

Hashimoto H, Koyama Y, Ichimura K and Kobayashi T (1989) Time-resolved absorption spectroscopy of the triplet state produced from the all-*trans,* 7-*cis,* 9-*cis,* 13-*cis*, and 15-*cis* isomers of β-carotene. Chem Phys Lett 162: 517–522

Hashimoto H, Koyama Y, Hirata Y and Malaga N (1991) S_1 and T_1 species of β-carotene generated by direct photoexcitation from the all-*trans*, 9-*cis,* 13-*cis*, and 15-*cis* isomers as revealed by picosecond transient absorption and transient Raman spectroscopies. J Phys Chem 95: 3072–3076

Hashimoto H, Miki Y, Kuki M, Shimamura T, Utsumi H and Koyama Y (1993) Isolation by high-pressure liquid chromatography of the *cis-trans* isomers of β-apo-8′-carotenal. Determination of their S_0-state configurations by NMR spectroscopy and prediction of their S_1- and T_1-state configurations by transient Raman spectroscopy. J Am Chem Soc 115: 9216–9225

Hashimoto H, Koyama Y and Mori Y (1997) Mechanism activating the 2^1A_g state in all-*trans*-β-carotene crystal to resonance Raman scattering. Jpn J Appl Phys 36: 916–918

Hauska G, Hager-Braun C, Schneebauer N, Schütz M, Zimmermann R and Nelson N (1995) Biochemical aspects of the reaction center in green sulfur bacteria—comparison with other FeS-types. In: Mathis P(ed) Photosynthesis: From Light to Biosphere, Vol 11, pp 11–16. Kluwer Academic Publishers, Dordrecht

Hengartner U, Bernhard K and Meyer K (1992) Synthesis, isolation, and NMR-spectroscopic characterization of fourteen (Z)-isomers of lycopene and of some acetylenic didehydro- and tetrahydrolycopenes. Helv Chim Acta 75: 1848–1865

Hu Y, Hashimoto H, Moine G, Hengartner U and Koyama Y (1997) Unique properties of the 11 -*cis* and 11,11′-di-*cis* isomers of β-carotene as revealed by electronic absorption, resonance Raman and ^{1}H and ^{13}C NMR spectroscopy and by HPLC analysis of their thermal isomerization. J Chem Soc Perkin Trans 2: 2699–2710

Jiang Y-S, Kurimoto Y, Shimamura T, Ko-chi N, Ohashi N, Mukai Y and Koyama Y (1996) Isolation by high-pressure liquid chromatography, configurational determination by ^{1}H-NMR, and analyses of electronic absorption and Raman spectra of isomeric spheroidene. Biospectroscopy 2: 47–58

Kandori H, Sasabe H and Mimuro M (1994) Direct determination of a lifetime of the S_2 state of β-carotene by femtosecond time-resolved fluorescence spectroscopy. J Am Chem Soc 116: 2671–2672

Katayama N, Hashimoto H, Koyama Y and Shimamura T (1990) High performance liquid chromatography of *cis-trans* isomers of neurosporene: Discrimination of *cis* and *trans* configurations at the end of an open conjugated chain. J Chromatogr 519: 221–227

Khachik F, Englert G, Daitch CE, Beecher GR and Tonucci LH (1992) Isolation and structural elucidation of the geometrical isomers of lutein and zeaxanthin in extracts from human plasma. J Chromatogr 582: 153–166

Koepke J, Hu X, Muenke C, Schulten K and Michel H (1996) The crystal structure of the light-harvesting complex II (B800-850) from *Rhodospirillum molischianum.* Structure 4: 581–597

Koyama Y (1991) Structures and functions of carotenoids in photosynthetic systems. J Photochem Photobiol B: Biol 9: 265–280

Koyama Y (1995) Resonance Raman spectroscopy. In: Briton G, Liaaen-Jensen S and Pfander H (eds) Carotenoids, Vol 1B Spectroscopy, pp 135–146. Birkhäuser Verlag, Besel

Koyama Y and Hashimoto H (1993) Spectroscopic studies of carotenoids in photosynthetic systems. In: Young A and Britton G (eds) Carotenoid in Photosynthesis, pp 327–408. Chapman and Hall, London

Koyama Y and Mukai Y (1993) Excited states of retinoids, carotenoids and chlorophylls as revealed by time-resolved, electronic absorption and resonance Raman spectroscopy. In: Clark R and Hester R (eds) Biomolecular Spectroscopy Part B, pp 49–137. John Wiley and Sons Ltd, Chichester

Koyama Y, Kito M, Takii T, Saiki K, Tsukida K and Yamashita J (1982) Configuration of the carotenoid in the reaction centers of photosynthetic bacteria: Comparison of the resonance Raman spectrum of the reaction center of *Rhodopseudomonas sphaeroides* G1C with those of *cis-trans* isomers of β-carotene. Biochim Biophys Acta 680: 109–118

Koyama Y, Takii T, Saiki K and Tsukida K (1983) Configuration of the carotenoid in the reaction centers of photosynthetic bacteria. (2) Comparison of the resonance Raman lines of the reaction centers with those of the 14 different *cis-trans* isomers of β-carotene. Photobiochem Photobiophys 5: 139–150

Koyama Y, Kanaji M and Shimamura T (1988a) Configurations of neurosporene isomers isolated from the reaction center and the light-harvesting complex of *Rhodobacter sphaeroides* G1C. A resonance Raman, electronic absorption, and ^{1}H NMR study. Photochem Photobiol 48: 107–114

Koyama Y, Hosomi M, Miyata A, Hashimoto H, Reames SA, Nagayama K, Kato-Jippo T and Shimamura T (1988b) Supplementary and revised assignment of the peaks of the 7,9-, 9,9′-, 13,13′-, 9,13′-di-*cis* and 9,9′,13-tri-*cis* isomers of β-carotene in high-performance liquid chromatography using a column of calcium hydroxide. J Chromatogr 439: 417–422

Koyama Y, Takatsuka I, Nakata M and Tasumi M (1988c) Raman and infrared spectra of the all-*trans,* 7-*cis,* 9-*cis,* 13-cis and 15-*cis* isomers of β-carotene: Key bands distinguishing stretched or terminal-bent configurations from central-bent configurations. J Raman Spectrosc 19: 37–49

Koyama Y, Hosomi M, Hashimoto H and Shimamura T (1989) ^{1}H NMR spectra of the all-*trans,* 7-*cis,* 9-*cis,* 13-*cis* and 15-*cis* isomers of β-carotene: Elongation of the double bond and shortening of the single bond toward the center of the conjugated chain as revealed by vicinal coupling constants. J Mol Struct 193: 185–201

Koyama Y, Takatsuka I, Kanaji M, Tomimoto K, Kito M, Shimamura T, Yamashita J, Saiki K and Tsukida K (1990) Configurations of carotenoids in the reaction center and the light-harvesting complex of *Rhodospirillum rubrum.* Natural selection of carotenoid configurations by pigment protein complexes. Photochem Photobiol 51: 119–128

Koyama Y, Mukai Y and Kuki M (1992) Excited-state properties

and physiological functions of biological polyenes: 'The triplet-excited region' of retinoids and carotenoids. SPIE (Laser Spectroscopy of Biomolecules) 1921: 191–202

Koyama Y, Kuki M, Andersson PO and Gillbro T (1996) Singlet excited states and the light-harvesting function of carotenoids in bacterial photosynthesis. Photochem Photobiol 63: 243–256

Kuki M, Koyama Y and Nagae H (1991) Triplet-sensitized and thermal isomerization of all-*trans*, 7-*cis*, 9-*cis*, 13-*cis* and 15-*cis* isomers of β-carotene: Configurational dependence of the quantum yield of isomerization via the T_1 state. J Phys Chem 95:7171–7180

Kuki M, Nagae H, Cogdell RJ, Shimada K and Koyama Y (1994) Solvent effect on spheroidene in nonpolar and polar solutions and the environment of spheroidene in the light-harvesting complexes of *Rhodobacter sphaeroides* 2.4.1 as revealed by the energy of the $^1A_g^- \rightarrow {}^1B_u^+$ absorption and the frequencies of the vibronically coupled C=C stretching Raman lines in the $^1A_g^-$ and $2^1A_g^-$ states. Photochem Photobiol 59: 116–124

Lancaster CRD and Michel H (1997) The coupling of light-induced electron transfer and proton uptake as derived from crystal structures of reaction centres from *Rhodopseudomonas viridis* modified at the binding site of the secondary quinone, Q_B. Structures: 1339–1359

Lutz M, Kleo J and Reiss-Husson F (1976) Resonance Raman scattering of bacteriochlorophyll, bacteriopheophytin and spheroidene in reaction centers of *Rhodopseudomonas spheroides*. Biochem Biophys Res Commun 69: 711–717

Lutz M, Agalidis I, Hervo G, Cogdell RJ and Reiss-Husson F (1978) On the state of carotenoids bound to reaction centers of photosynthetic bacteria: A resonance Raman study. Biochim Biophys Acta 503: 287–303

McDermott G, Prince SM, Freer AA, Hawthornthwaite-Lawless AM, Papiz MZ, Cogdell RJ and Isaacs NW (1995) Crystal structure of an integral membrane light-harvesting complex from photosynthetic bacteria. Nature 374: 517–521

Mukai Y, Hashimoto H and Koyama Y (1990) Dependence of the triplet potential of retinal homologues on the chain length: Resonance Raman spectroscopy and analysis of triplet-sensitized isomerization. J Phys Chem 94: 4042–4051

Mukai Y, Abe M, Katsuta Y, Tomozoe S, Ito M and Koyama Y (1995) Structure of *all -trans*-retinal in the T_1 state as determined by Raman spectroscopy: A set of carbon-carbon and carbon-oxygen stretching force constants determined by the normal coordinate analysis of the T_1 Raman lines of the undeuterated and variously deuterated retinals. J Phys Chem 99: 7160–7171

Nagae H (1997) Theory of solvent effects on electronic absorption spectra of rodlike or disklike solute molecules: Frequency shifts. J Chem Phys 106: 5159–5170

Nagae H, Kakitani T, Katoh T and Mimuro M (1993) Calculation of the excitation transfer matrix elements between the S_2 or S_1 state of carotenoid and the S_2 or S_1 state of bacteriochlorophyll. J Chem Phys 98: 8012–8023

Nagae H, Kuki M, Cogdell RJ and Koyama Y (1994) Shifts of the $^1A_g^- \rightarrow {}^1B_u^+$ electronic absorption of carotenoids in nonpolar and polar solvents. J Chem Phys 101: 6750–6765

Oh-oka H, Kakutani S, Kamei S, Matsubara H, Iwaki M and Itoh S (1995) Highly purified photosynthetic reaction center (PscA/cytochrome $c_{551})_2$ complex of the green sulfur bacterium *Chlorobium limicola*. Biochemistry 34: 13091–13097

Ohashi N, Ko-chi N, Kuki M, Shimamura T, Cogdell RJ and Koyama Y (1996) The structures of S_0 spheroidene in the light-harvesting (LH2) complex and S_0 and T_1 spheroidene in the reaction center of *Rhodobacter sphaeroides* 2.4.1 as revealed by Raman spectroscopy. Biospectroscopy 2: 59–69

Pariser R (1956) Theory of the electronic spectra and structure of the polyacenes and of alternant hydrocarbons. J Chem Phys 24:250–268

Ricci M, Bradforth SE, Jimenez R and Fleming GR (1996) Internal conversion and energy transfer dynamics of spheroidene in solution and in the LH-1 and LH-2 light-harvesting complexes. Chem Phys Lett 259: 381–390

Sashima T, Shiba M, Hashimoto H, Nagae H and Koyama Y (1998a) The $2A_g^-$ energy of crystalline all-trans-spheroidene as determined by resonance-Raman excitation profiles. Chem Phys Lett 290: 36–42

Sashima T, Nagae H, Kuki M and Koyama Y (1998b) A new singlet-excited state of all-trans-spheroidene as detected by resonance-Raman excitation-profiles. Chem Phys Lett 299: 187–194

Tang J and Albrecht AC (1970) Developments in the theories of vibrational Raman intensities. In: Szymanski HA (ed) Raman Spectroscopy Theory and Practice, Vol 2, pp 33–68. Plenum Press, New York

Tavan P and Schulten K (1986) The low-lying electronic excitations in long polyenes: A PPP-MRD-CI study. J Chem Phys 85: 6602–6609

Tavan P and Schulten K (1987) Electronic excitations in finite and infinite polyenes. Phys Rev B 36: 4337–4358

Thornber JP, Morishige DT, Anandan S and Peter GF (1991) Chlorophyll-carotenoid proteins of higher plant thylakoids. In: Scheer H (ed) Chlorophylls, pp 549–585. CRC Press, Boca Raton

Tsukida K, Saiki K, Takii T and Koyama Y (1982) Separation and determination of *cis/trans*-β-carotenes by high-performance liquid chromatography. J Chromatogr 245: 359–364

Wasielewski MR, Johnson DG, Bradford EG and Kispert LD (1989) Temperature dependence of the lowest excited singlet-state lifetime of all-*trans*-β-carotene and fully deuterated all-*trans*-β-carotene. J Chem Phys 91: 6691–6697

Watanabe J, Takahashi H, Nakahara J and Kushida T (1993) Subpicosecond dynamic Stokes shift in β-carotene solution probed by excitation energy dependence of fluorescence spectrum. Chem Phys Lett 213: 351–355

Zechmeister L (1962) *Cis-trans* isomeric carotenoids vitamins A and arylpolyenes. Academic Press, New York

Chapter 10

The Electronic Structure, Stereochemistry and Resonance Raman Spectroscopy of Carotenoids

Bruno Robert
Section de Biophysique des protéines et des membranes,
DBCM/CEA and URA 2096/CNRS, C.E. Saclay, 91191 Gif/Yvette Cedex France

Summary

Resonance Raman Spectroscopy yields information on the conformation and the configuration of carotenoid molecules, whether isolated in solvents or embedded in soluble or membrane proteins. Deviations of the conjugated polyene chain from linearity indeed results in the appearance of new Raman bands, arising from modes which have become allowed by the change in molecular symmetry. By making use of time-resolved Raman techniques, it is possible to extend these studies to the singlet and triplet states of carotenoids, and to gain insights into the nature of these excited states. After a short introduction to the physical principles that govern resonance Raman Spectroscopy, a detailed characterization of resonance Raman spectra of carotenoids is described in this chapter, together with the experiments which helped in determining to which structural parameter each Raman band is sensitive. Applications of this technique on the carotenoid molecules involved in the photosynthetic process are then reviewed. In particular the molecular conformation and configuration of carotenoids bound to photochemical reaction centers and to light-harvesting proteins of the different photosynthetic organisms is discussed in the light of resonance Raman results.

H. A. Frank. A. J. Young. G. Britton and R. J. Cogdell (eds): The Photochemistry of Carotenoids, pp. 189–201.

I. Introduction

The first resonance Raman spectra of carotenoid molecules were reported well before the first lasers were conceived, at a time where spectroscopists were still using powerful Xenon lamps to record the Raman scattering on photographic plates (Szymansky, 1962) (actually only a few years after the Raman effect was observed (Raman, 1928)). Since that time, although the sensitivity of the set-ups has increased by many orders of magnitude, carotenoids have always been considered as objects of choice for Raman spectroscopy. The popularity of these molecules among the Raman community may be easily explained by the fact that they yield very intense resonance signals as they constitute, without doubt, one of the most efficient Raman scatterers among organic molecules. Due to the linear structure of carotenoids, their Raman spectra contain only a small number of intense bands. These bands are surprisingly insensitive to the molecular environment. For example, the resonance Raman spectra of isolated carotenoids dissolved in hexane are nearly identical to those obtained from protein-bound molecules (Gill et al., 1970), even when these are involved in strong excitonic couplings (Pascal et al., 1998, and spectra therein). On the other hand, any deviation of the conjugated, polyene, chain from linearity, i.e. any change in the molecular conformation and/or configuration, will result in the appearance of new Raman bands, arising from modes which have become allowed by the change in molecular symmetry. Resonance Raman has thus been extensively used for determining, in vitro as well as in vivo, carotenoid conformations and configurations.

Carotenoids play multiple roles in the photosynthetic process. On one hand, they harvest incoming photons at wavelengths that chlorophyll molecules do not absorb and, on the other, they are capable of accepting the energy of chlorophyll triplet states, which otherwise could induce formation of harmful singlet oxygen species. Both these functions require a precise positioning of the carotenoids relative to the chlorophyll molecules, as well as a fine tuning of their ground and excited electronic levels, in order to optimize the efficiency of these energy transfer events (Frank and Cogdell, 1993). Moreover, it has recently become more and more obvious that carotenoids molecules have a structural role, i.e. that they participate in stabilizing the folded, fully active, state of several photosynthetic proteins (Jirzakova and Reiss-Husson, 1994; Zurdo et al., 1995). This role seems particularly obvious when considering the recent three-dimensional structures of LHCII of higher plants (Kühlbrandt et al., 1994) and/or LHII from purple bacteria (McDermott et al., 1995). The properties of carotenoids are tuned by different mechanisms, including molecular conformational changes.

The aim of this chapter is to review the contribution of resonance Raman spectroscopy to our knowledge of the stereochemistry and electronic structure of carotenoid molecules involved in photosynthesis. However, a precise understanding of the information provided by resonance Raman about carotenoids requires the description of those relevant experiments, which were performed in vitro (usually in organic solvents), and which are at the foundation of our current interpretations of the Raman signals. In order to keep this review article as concise as possible, these will be presented after a short introduction on the method itself, and I will focus only on biologically relevant results.

Abbreviations: NMR – Nuclear Magnetic Resonance; PS – Photosystem; Rb. – *Rhodobacter;* RC – reaction center; Rps. – *Rhodopseudomonas*

II. Principles of Raman Spectroscopy

A. The Raman Effect

The Raman effect is the phenomenon of a change of frequency of light when it is scattered by polyatomic molecules. This phenomenon may only happen if some energy is exchanged between the incoming photon and the scattering molecule. As the energy levels of the scattering molecule are discrete, if the frequency of the incident light is ν_o and that of the scattered light is ν_r, the energy $h . \Delta\nu = h . (\nu_o - \nu_r)$ must correspond to that of a transition between molecular energy levels. In the following, we'll only uniquely consider vibrational energy levels of the scattering molecules. Raman spectroscopy thus yields information on the energy of the vibrational levels of a given electronic state, usually the ground state, but it can be any excited electronic state in time-resolved Raman spectroscopy. As the vibrational levels of a particular molecule intimately depends on its structure, i.e. the nature of its constituent atoms, the bonds between these atoms, and its molecular

symmetry, Raman spectroscopy can be used as an analytical method for determining the chemical structure of molecules, as well as their conformation. The Raman effect is a very low probability process, and a major drawback of Raman spectroscopy is that the signal measured is usually very weak. On the other hand, since Raman-active molecular vibrations are those involving change in molecular polarizability, the Raman signal of water thus seldom interferes with that of the biological molecules being studied. This constitutes an important advantage for the Raman technique over infra-red absorption spectroscopy.

B. The Resonance Effect

In classical Raman spectroscopy, the signal only depends on the frequency ν_0 of the light used for inducing the Raman effect because it is a scattered signal, and it thus varies according to the fourth power of this frequency ν_0^4. However, when this frequency matches an electronic transition of the irradiated molecule, an enhancement of a subset of Raman-active modes is observed which may reach six orders of magnitude. This is the resonance effect. In resonance Raman spectroscopy, it is thus possible to selectively observe a molecule in a complex medium, provided that this molecule possesses an absorption transition, the energy of which matches the energy of the incoming photons. It then becomes possible to study the interactions assumed by or the conformation of chromophores within proteins, even though these proteins are still embedded in a biological membrane or are poorly purified. This very specific aspect of Raman spectroscopy has been extensively used on biological chromophores, such as hemes, iron-sulfur clusters, chlorophylls and carotenoid molecules (Carey, 1982).

In resonance conditions, the signal arising from only a fraction of the vibrational modes of the scattering molecule is enhanced. More precisely, in the simplest case when only one electronic state is involved in the resonance phenomenon, the enhanced signal arises from the vibrational modes involving nuclei motions which correspond to distortions experienced by the molecule during transition between the ground- and the excited state used for inducing the resonance (Albrecht, 1961). This intra-mode selection may thus constitute a limitation, for example if a domain of the molecule is not involved in the electronic transition, resonance Raman will not yield any information about this domain. However, for most biological chromophores the functional part of the molecule consists of those atoms which are conjugated with the electronic transition, and resonance Raman will therefore yield selective information on these biologically active structures. The analysis of the resonance Raman-active modes observed upon excitation with a given electronic transition will thus yield information about the nature of this transition. In short, the position of bands in Raman spectra will yield information about the vibrational structure of the low-energy electronic state involved in the transition used for inducing the resonance, while the intensity of these peaks will yield information about the higher energy electronic state involved in this transition.

III. Resonance Raman Spectroscopy and Carotenoid Stereochemistry

A. Introduction: The Raman Spectra of β-Carotene

Resonance Raman spectra of all-trans, planar, β-carotene molecules are generally obtained in resonance conditions with their main electronic transition (corresponding to ^1B_u[left arrow]^1A_g transition of the polyene chain) or in preresonance conditions with this transition. They contain about 40 bands between 90 and 1610 cm^{-1}, among which three groups are very intense, at ca. 1530 (ν_1), 1120–1200 (ν_2), and 1000(ν_3) cm^{-1} (Fig. 1). When exciting with ultra-violet lasers in the 260 nm region, in resonance with the $2^1B_u \leftarrow {}^1A_g$ transition, spectra are then dominated by an intense band at about 1590 cm^{-1} (Saito et al., 1983). The enhancement of all these bands correspond to A-type resonance, i.e. involving only one excited electronic level.

In the early 1970s based on a model derived from an infinite polyenic chain, it was concluded that the intense bands observed in Raman spectra of carotenoids arose from modes involving nuclear coordinates of the conjugated chain of these molecules (Rimai et al., 1973). In the frame of this model, these authors attributed ν_1 to the stretching modes of the conjugated C=C bonds, ν_2 to a mixture of C=C and of C–C bond stretching modes with C-H bending modes, and ν_3 to stretching modes of C–CH_3 bonds between the main-chain and the side methyl carbon. The weak band at ca 950 cm^{-1} (ν_4) was

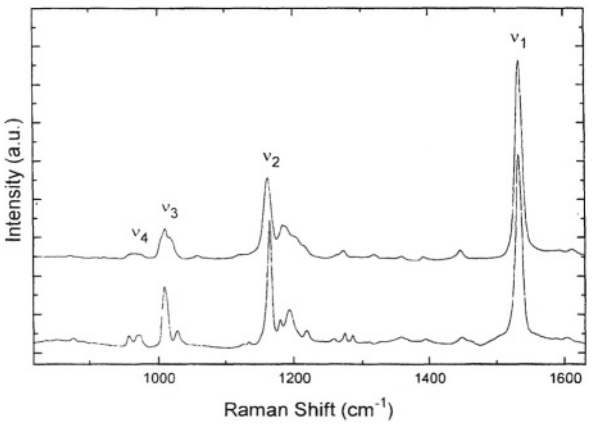

Fig. 1. Resonance Raman spectra (800–1620 cm^{-1}) of CP 47-bound β-carotene (bottom) and FCP-bound fucoxanthin (top). Excitation conditions: 488.0 nm. Temperature: 77 K

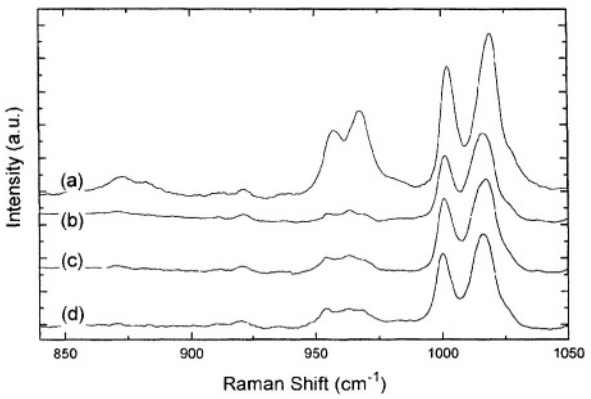

Fig. 2. Resonance Raman spectra (840–1050 cm^{-1}) of FCP-bound fucoxanthin molecules. Excitation lines 514.5, 476.5, 488.0 and 528.7 nm (a-d).

attributed to out-of-plane C-H modes (formally forbidden for planar molecules) (Rimai et al., 1973). During the same period, it was shown by the same authors that the frequency of these modes was strongly dependent on the molecular conformation of these polyenes. This was achieved in particular by studying retinal molecules in the all-*trans* and *cis* conformations (Rimai et al., 1971). Due to the very high resonance enhancement of the carotenoid Raman signal, it is possible to study the conformation of these molecules when they are bound to proteins without interference of the Raman signals from other biological macromolecules.

B. Influence of the Chemical Structure of Carotenoids on Raman Spectra

Carotenoid molecules, although constituting a very broad family of diverse chemical structures, exhibit remarkably similar resonance Raman spectra. The precise frequency of the ν_1 band depends on their molecular structure, since it decreases with the length of the polyene chain. This has been interpreted as resulting from an equalization phenomenon between the C–C and C=C bonds (Rimai et al., 1973), indicating that the degree of delocalization of the π electrons increases when the chain length decreases. The other bands contributing to the Raman spectra are very similar for all carotenoid molecules. This indicates that these spectra are only weakly dependent on the groups present at each side of the polyene chain, even though these most often determine their chemical structure. Chemical modifications involving the polyene chain of these molecules would be expected to influence their resonance Raman spectra, but carotenoids exhibiting such molecular structures are seldom encountered in photosynthesis. There are, however, a few examples of allenic carotenoids, which possess a C≡C bond conjugated with the polyene chain. Resonance Raman spectra of the allenic fucoxanthin molecules, the main carotenoid found in some brown algal species, such as *Laminaria,* have been reported recently (Pascal et al., 1998). They do not differ drastically from other carotenoid spectra other than in the ν_3 region, where it is clear that more modes are contributing (Figs. 1 and 2). Since a similar splitting of the ν_3 band is observed for vauscheriaxanthin, which is an allenic carotenoid synthesized by an other brown algae (L. Caron, J. C. Duval, A. A. Pascal and B. Robert, unpublished), these additional modes in the ν_3 band are likely to arise from the influence of the C≡C triple bond on the carotenoids vibrational modes.

C. Resonance Raman and Molecular Conformation of β-Carotene

The influence of the molecular conformation on the resonance Raman spectra of β-carotene was systematically determined for 14 different *cis-trans* isomers in the early 1980s (Koyama et al., 1982, 1983, 1988a). The conformation of 8 of these 14 isomers was determined by NMR spectroscopy, allowing the comparison of resonance Raman spectra

of the following conformations: all-trans, 7-*cis,* 9-*cis,* 13-*cis*, 15-*cis*, 9–13-di*cis*, 9–15di*cis*, 9–13′-di*cis* and 13–15-di*cis*. It was concluded that *cis* isomerization generally induces an upshift of the ν_1 band. This effect is small when the isomerization occurs near the end of the molecule (1 and 5 cm^{-1} for the 7- and 9-cis isomers, respectively), becomes larger for the central isomers (10 and 13 cm^{-1} for the 15- and 13-*cis,* respectively) and is even larger for di-*cis* isomers. The frequency of this band appears to be slightly dependent on the excitation wavelength when the experiments are conducted at low temperature. Shifts as large as 4 cm^{-1} may be observed when shifting this excitation from 457.9 to 514.5 nm (Koyama et al., 1982). As these displacements are of the same order of magnitude as some of the differences observed between isomers, it is often difficult to be certain about the assignments of the molecular conformation of carotenoid molecules just by measuring the frequency of this band. More precise attributions may be achieved by analyzing the 1100–1300 cm^{-1} region, where bands characteristic of the 15-and 13-*cis* isomers contribute. Indeed, resonance Raman spectra of all the isomers of β-carotene containing a C_{15}=$C_{15'}$ bond in a *cis* conformation contain a strong band at ca 1245 cm^{-1} (1254 cm^{-1} for the 13–15-di*cis* conformation), and those of the molecules containing a C_{13}=C_{14} bond in a *cis* conformation exhibit an intense band at ca 1138 cm^{-1}. Since both these bands are absent or very weak in resonance Raman spectra of the other isomers, they may be safely used as fingerprints for these conformations (Koyama et al., 1982, 1983).

Besides the intense ν_1 to ν_3 bands, a number of weak bands in the lower frequency region are sensitive to carotenoid conformation. This is particularly the case for the bands located between 825 and 900 cm^{-1} (Lutzetal., 1978; Saito et al., 1983), which experience shifts as large as 25 cm^{-1} upon 15–15 *cis-trans* isomerization. At lower frequencies, most of the bands seem sensitive to carotenoid conformation,, however, as these modes are weak, their use for establishing the molecular structure in vivo is often difficult. Among these, bands between 470 and 530 cm^{-1} exhibit sensitivity to *cis-trans* isomerization in terms of both intensity and position. Because of their intensity changes, these bands may be more useful conformational reporters slightly easier to use in vivo (Lutz et al., 1978).

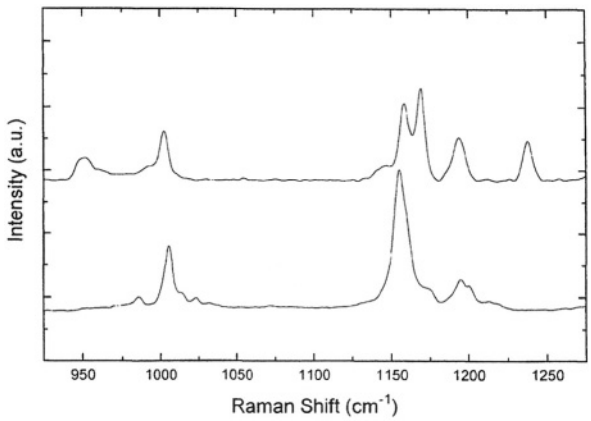

Fig. 3. Resonance Raman spectra (940–1260 cm^{-1}) of spheroidenone bound to LHII (bottom) and reaction centers of *Rhodobacter sphaeroides*.

D. Resonance Raman and Molecular Configuration of Carotenoids

Non-planar configurations of carotenoid molecules, involving rotations around C–C bonds are not stable in solution at room temperature. It is thus not possible to study in vitro the influence of these configurations on resonance Raman spectra. As described above, it was predicted as early as 1971 that the intensity of the ν_4 band should be sensitive to out-of-plane deviations of carotenoid molecules. This has been experimentally verified by studying protein-bound carotenoid molecules, namely spheroidene when bound to reaction centers of purple bacteria. In this particular case, it was found that, when the carotenoid is bound to its host protein, the intensity of the ν_4 band is of the same order of magnitude as that of the ν_3 or ν_2 bands (Fig. 3). The ν_4 band is usually five to ten times less intense in resonance Raman spectra of isolated carotenoids in equivalent resonance conditions (Lutz et al., 1976,1978). Upon carotenoid extraction, this band loses most of its intensity, while the ν_1 to ν_3 bands change very little if at all (Lutz et al., 1987). This was interpreted as resulting from the relaxation of a molecular torsion around a C–C bond, induced by the protein binding site. This has also been suggested by ESR studies (Chadwick and Frank, 1986). Since the intensity of the ν_4 band is only very weakly sensitive to the excitation conditions, the presence of strong bands around 960 cm^{-1} may be considered as a reliable indication that the configuration adopted by the carotenoid molecule involves

out-of-plane torsions around C–C bonds. It should also be noted that such an out-of-plane configuration of the carotenoid is not accompanied by frequency changes of the ν_1 to ν_3 bands, i.e. it has little if any influence if at all on the bands arising from the vibrational modes which are localized on the polyene chain portion of the molecule.

Further analysis of resonance Raman spectra of reaction center-bound spheroidene demonstrated that other bands, in the 830–900 cm^{-1} region, were sensitive to the molecular configuration of this molecule (Lutz et al., 1978, 1987). Three bands, at 889, 849 and 829 cm^{-1} show drastic intensity changes upon relaxation of the out-of-plane configuration of the carotenoid molecule. In a more recent study, where a similar out-of-plane configuration was demonstrated for a protein-bound fucoxanthin molecule, a similar increase of intensity was observed for the bands located in this same spectral region, together with a drastic increase of the intensity of the ν_4 band (Pascal et al., 1998). These bands therefore constitute an additional indicator for carotenoid out-of-plane configurations and they can also be used for determining the position of the twisted C–C bond (see below).

E. Normal Coordinate Analysis of β-Carotene

Normal coordinate analysis of β-carotene isomers was performed in 1983 by Saito and Tasumi (1983) using force constants derived from those calculated for *all-trans* retinal, which were further refined taking into account the experimental spectra (both infra-red and resonance Raman) of all-trans β-carotene. These calculations led to a number of new assignment of bands which has proved extremely useful for interpreting resonance Raman spectra in terms of molecular structures. Not only were the previous assignments of the main bands ν_1 to ν_4 confirmed, but it also became possible to show, from these calculations, which nuclear coordinates were the origin of each mode and in what proportion. The weaker bands present in resonance Raman spectra of carotenoid molecules could also be attributed. It was shown, in particular that while the C=C stretching had a strong in-phase character, this character was lost in C–C stretching because of the presence of the CH_3 at positions C_9, C_{13} and $C_{13'}$. According to these calculations, the most intense band in the ν_2 region (1160 cm^{-1}) was attributed mainly to C_{14}-C_{15} and $C_{14'}$-C_{15} stretching, with little if any involvement of the nuclear coordinates of the other carbon atoms of the chain, this mode being mixed with C_{15}-H, $C_{15'}$-H in-plane bending. By contrast, in the 15–15 *cis* isomer, the same band arises from the in-phase stretching of the C_{10}-C_{11}, C_{14}-C_{15}, $C_{15'}$-$C_{14'}$ and $C_{11'}$-$C_{10'}$ bonds. Such a difference in mode localization, occurring for the same bands for two different isomers of the same molecule, could well explain anomalous results obtained on carotenoid triplet states (see below). Of particular interest were the attributions of the bands characteristic of the 15–15′ *cis* and of the 13–14 *cis* forms, at 1241 and 1138 cm^{-1}. These were attributed to skeletal stretching and C-H bending of the bent central region, and to the C_{10}-C_{11} ($C_{10'}$-$C_{11'}$) stretching modes, respectively (Saito and Tasumi, 1983).

Components of the ν_4 band at 950 and 960 cm^{-1} were attributed to a mixture of C_{11}-C_{12} torsion (with respect to C_7-C_8) and to out-of plane wagging of the C_{12}-bound H (with respect to the out-of-plane wagging modes of the C_8- and C_7-bound H atoms) (attribution of these modes were inverted in Saito and Tasumi, 1983; M. Tasumi, personal communication). Similarly, weak bands in the lower frequency range at 848,825 and 775 cm^{-1} have been mainly attributed to out-of-plane wagging of the H atoms bound to C_8, C_{12} and C_{15}, respectively, while the 868 cm^{-1} band was attributed to the in-plane rocking mode of the C_9-bound methyl group. It is worth noting that this latter mode was shown, in 1987 (Lutz et al., 1987), not to change intensity upon relaxation of an out-of-plane configuration of spheroidene, while the three other did, fully confirming their out-of-plane and in-plane character, respectively.

More recently, applying these calculations, which were originally performed on the symmetric β-carotene molecule, to other carotenoids has been questioned. Resonance Raman spectra of spheroidene molecules selectively enriched in either ^{13}C or ^{2}H were performed, and they led to quite surprising results. It was in particular shown that the 15-^{13}C substitution had nearly no effect on spheroidene's resonance Raman spectra, while the 14 ^{13}C substitution resulted in dramatic spectral perturbations (Kok et al., 1994). This is in good agreement with the conclusions drawn from normal mode analysis of all-trans β-carotene, that the C_{15}=$C_{15'}$ stretch is decoupled from the other C=C stretches However, the same calculations led to the conclusion that the main 1540 cm^{-1} observed in the 15-*cis* isomers arises principally from the C_{15}=$C_{15'}$ stretching

mode. ^{13}C substitution experiments clearly indicate this is not the case, and that this particular bond contributes only weakly to the ν_1 of 15-*cis* spheroidene. More recently, resonance Raman spectra of spheroidene isotopically enriched in D at positions 14, 14´, 15 and 15´ were reported (Kok et al., 1997). These experiments showed that the 1241 cm^{-1} band characteristic of the 15–15´ isomers involves coordinates from the C_{12} and C_{13} atoms. It is clear that these studies, combining selective isotopic exchange and resonance Raman, will provide a very firm basis for new, more precise, normal mode calculations.

IV. Resonance Raman Spectroscopy of Excited States of Carotenoids

A. Triplet States

The first resonance Raman spectra of β-carotene in its triplet state were obtained in 1979, using excitation at 531 nm which is located near the main T←T absorption transition at 515 nm. The triplet state was accumulated by pulse radiolysis, using naphthalene as a sensitizer, and this was one of the first examples of time-resolved resonance Raman spectroscopy applied to a molecular excited state (Dallinger et al., 1979). Resonance Raman spectra of triplet carotenoid mainly differ from those of ground state molecules in the ν_1 and ν_2 bands, i.e. in those bands arising from modes delocalized over the molecule. The ν_1 band generally downshifts by more than 25 cm^{-1}. Thus, while this band is seen at 1530 cm^{-1} in spectra of ground-state β-carotene, it is at 1509 cm^{-1} when this molecule is in its triplet excited state (Dallinger et al., 1979). This downshift was interpreted as reflecting the delocalization of the triplet throughout the conjugated system. This should result in an increase in conjugation. This downshift should thus been accompanied by an upshift of the frequency of the C–C stretching modes, as the decrease in π order of the C=C bonds should correspond to an increase in those of the C–C single bonds. This is not observed as the main ν_2 band also downshifts from 1164 to 1125 cm^{-1} (Wilbrandt et al., 1980, Hashimoto and Koyama, 1989). This apparently anomalous behavior may be easily explained, since this band was not attributed to a pure C–C stretching mode, but rather to a complex mixture of C–C and C=C stretching and C–H bending modes. However, given the fact that the precise origin of this band seems to differ depending on the isomer studied, it is equally possible that the new 1125 cm^{-1} band does not involve the same nuclear coordinate as the 1164 cm^{-1} band. In particular, it was proposed, for *all-trans* β-carotene, that the 1125 cm^{-1} band might arise from stretching of the C_{15}=$C_{15'}$ central bond, present in the triplet state as an elongated C_{15}-C_{15} bond (Hashimoto and Koyama, 1988). Most of the other resonance Raman bands are weakly sensitive to the ground-state to triplet transition of carotenoid molecules: the ν_3 upshifts from 1003 to ca 1012 cm^{-1}, which confirms its main attribution to C-(CH_3) stretching modes, and the ν_4 frequency remains unchanged between the ground- and triplet states (Wilbrandt and Jensen, 1981). The influence of the molecular conformation on these bands has not yet been precisely defined, although systematic studies of the resonance Raman spectra of different isomers of β-carotene isomers in their triplet states have been performed. Moreover, these molecules rapidly change conformation when excited to their triplet state, and resonance Raman of the *all-trans* and 9-*cis* isomers have been observed in vitro (Hashimoto and Koyama, 1988). As in the ground-state therefore, resonance Raman spectra of the carotenoid triplet state are also only poorly sensitive to the molecular environment (Conn et al., 1993).

B. Singlet States

The intense optical absorption of polyenes in general, and of β-carotene in particular, arises from an allowed electronic transition from the ^1A_g ground-state to a ^1B_u excited state. Until 1972, it was assumed that this state was the low-lying excited singlet state of these molecules. However, evidence of a lower, forbidden, singlet excited state with A_g symmetry was provided in short polyene molecules. The first evidence of the existence of this state for carotenoids came from measurements of the excitation profile of the resonance Raman scattering of all-*trans* β-carotene in cyclohexane (Thrash et al., 1977). The value deduced for this forbidden transition (17230 cm^{-1}), has however since been questioned by many authors (Koyama et al., 1996), and it is probably located at lower energies, i.e. between 12 000 and 14 000 cm^{-1}. Discovery of such a forbidden state is of particular interest, as its energy matches, for many carotenoids found in photosynthesis, with that of the Q_x transition of (bacterio)chlorin pigments. It has been suggested therefore that carotenoid to chlorophyll singlet-singlet

transfer could occur between these two states and thus play an important role in light-harvesting. The lifetimes of these 2^1A_g states are in general shorter than 100 picoseconds for carotenoids found in vivo (Frank et al., 1993), which means that the carotenoid to bacteriochlorophyll transfer would then be in competition with the very fast deexcitation of these states. It should be noted though that this is much slower than that of the B_u state, which generally takes place within a few hundreds of femtoseconds (Shreve et al., 1991). Although particularly difficult to measure, the resonance Raman spectra of β-carotene, spirilloxanthin and spheroidene in their S^1 states have been obtained using picosecond time-resolved lasers with excitation at 532 or 567 nm (Hashimoto et al., 1989a; Hayashi et al., 1990; Kuki et al., 1990; Noguchi et al., 1991). These spectra contain an intense band at high frequencies (>1750 cm^{-1}) which has been attributed to an a_g-type C=C stretching mode. In contrast, the 1530 cm^{-1} C=C stretching mode of the carotenoid ground-state, the frequency of this mode appears to be highly sensitive to the polarity of the carotenoid environment. Shifts as large as 10 cm^{-1} were observed in different solvents (Noguchi et al., 1991). By contrast, the frequency of this band is poorly sensitive to the molecular conformation, suggesting that it involves nuclear coordinates located at the end of the carotenoid molecules (Hashimoto and Koyama, 1989b). Interestingly, the mechanism of deexcitation of the 2^1A_g to the ^1A_g state could be demonstrated by anti-Stokes resonance Raman measurements to involve vibrational coupling, and this gives a picture of these vibrational excited states populated after the formation of the 2^1A_g state (Hayashi et al., 1991b).

V. Resonance Raman of Carotenoid Molecules In Vivo: Light-Harvesting Proteins

A. Light-Harvesting Proteins from Purple Bacteria

Resonance Raman studies have been conducted on carotenoid molecules bound to light-harvesting proteins (the core and peripheral complexes), isolated from a large number of bacterial species including those either synthesizing carotenoids from the spheroidene or the spirilloxanthin series. In general, Raman spectra of LH-bound carotenoids are extremely similar to those of *all-trans* carotenoid in hexane (Fig. 3), showing unambiguously that these molecules are all in the *all-trans* conformation in vivo (Lutz et al., 1976; Robert, 1983). Carotenoid molecules from the spheroidene series are in a planar configuration, as indicated by the low intensity of the ν_4 band in their resonance Raman spectra. However, this band is slightly more intense in spectra of LH-bound carotenoid than in hexane for carotenoids from the spirilloxanthin series, and it was proposed that these molecules are more distorted when they are bound to antenna complexes of purple bacteria (Iwata et al., 1985). In the three-dimensional structures of peripheral light-harvesting proteins deduced from X-ray crystallography (Mc Dermott et al., 1995; Koepke et al., 1996) carotenoid molecules are *all-trans* in a planar configuration, at least at the level of their conjugated chain, and there does not seem significant differences in conformation between carotenoids from the spirilloxanthin or the spheroidene series. It should be noted that, in both these structures, it is not clear whether there are two carotenoid molecules bound per protein subunit. However, only one is visible in the structures. It could thus well be that the other carotenoid molecule, which is not seen in the X-ray structure, is slightly more distorted in antenna proteins binding carotenoid molecules from the spirilloxanthin series.

When LHII proteins from *Rb. sphaeroides* or *Rps. acidophila* are treated with Li- or SDS detergents, one of their absorption transitions in the infrared region, at 800 nm, progressively disappears. This results from a progressive loss of one of their bound bacteriochlorophylls, and it is accompanied by a small but significant blue-shift of the absorption of the carotenoid(s ?) bound to the protein. It was shown, at least in the case of *Rps. acidophila,* that this absorption shift was accompanied by a small (a few wavenumbers) upshift of the ν_1 carotenoid Raman band, together with the appearance of a new, weak band in the ν_4 region (Robert and Frank, 1988). These changes indicate that detergent treatment induces a slight change in the structure of the LHII-bound carotenoid, which most likely affecting the conformation of the end(s) of the conjugated chain, as well as its planarity. It should be noted that these changes are observed under different excitation conditions, i.e. LHII-bound carotenoid molecules seem to behave as a single pool from a resonance Raman point of view, suggesting the presence of on carotenoid molecule only per protein subunit.

Time-resolved resonance Raman spectra of the

excited singlet and triplet states have been measured in light-harvesting proteins, either embedded in the whole intracytoplasmic membrane, or as purified complexes (Kuki et al., 1990, 1994, Hayashi et al., 1991). In the spectra of the S1 state of antenna-bound carotenoid molecules, the frequency of the highest frequency band arising from the C=C stretching modes is lower in the peripheral than in the core antennae (Kuki et al., 1994). Since the structures of these two classes of proteins are closely related (they all derive from the annular assembly of rather homologous polypeptides) the polarizability of the carotenoid environment is not likely to be so different in these two proteins. This frequency shift was thus rather interpreted in terms of differences in vibronic couplings between the 2^1A_g and 3^1A_g electronic states, as well as a displacement of the energy level of the latter state (Kuki et al., 1994).

B. Light-Harvesting Complexes from Oxygen-Evolving Organisms

Most of the Raman studies of light-harvesting proteins from oxygen-evolving organisms have involved the major peripheral antenna from Photosystem II (LHCIIb). This is in part due to the intrinsic complexity of inner antennae of these systems (CP47 and CP43 contain no less than 5 and 4 β-carotene molecules each), and also because minor antenna proteins from these organisms have proved difficult to purify in large amounts until recently. LHCIIb contains six lutein, three neoxanthin and a viola-xanthin molecules per trimer. Neoxanthin, as an allenic carotenoid molecule, should yield characteristic Raman features in the ν_3 region (see above), but these have not yet been observed. It was proposed, from a combination of methods, including resonance Raman spectroscopy, that a light-induced viola-xanthin *cis-trans* isomerization occurs in these complexes (Gruszecki et al., 1997). However, it was also reported that there was no detectable differences between Raman spectra of LHCIIb preparation isolated from light- or dark-adapted thylakoids (Ruban et al., 1995). More work is clearly needed to reconcile these apparently contradictory results. Recent, extensive, experiments conducted on LHCIIb, did not reveal the presence of any *cis* carotenoids in these complexes, at any stage of the violaxanthin cycle (Pascal and Robert, unpublished).

Isolated LHCIIb may exist, depending on the detergent concentration, as protein trimers or as large polypeptide aggregates. When these proteins are in their aggregated state, a quenching of chlorophyll fluorescence is observed, which has been proposed to be related to the important process of non-photochemical quenching in vivo (Horton et al., 1991). This interesting model has been studied by a number of techniques, and, in particular, the effect of the protein aggregation state on the conformation and configuration of the LHCIIb-bound carotenoid molecules has been investigated by resonance Raman spectroscopy (Ruban et al., 1995). It was shown that none of the bands in the ν_1 to ν_3 region was affected by LHCIIb aggregation, however in the ν_4 region, one additional, weak, band is observed in the resonance Raman spectra of the trimeric state. It thus seems that the configuration of at least one lutein molecule is aggregation dependent, being in a more constrained, planar configuration in LHCIIb aggregates, and in a slightly twisted configuration in LHCIIb trimers.

Recently, the antenna from a brown algae (*Laminaria*) was extensively studied by resonance Raman spectroscopy (Pascal et al., 1998). This protein, called the fucoxanthin-chlorophyll *a/c* protein (FCP), contains six chlorophyll *a,* two chlorophyll *c* and eight fucoxanthin molecules, i.e. it exhibits a much higher carotenoid content that LHCIIb from plants. Excitation wavelengths in the range from 441.8 to 530 nm were used, i.e. throughout the absorption transition of the protein-bound fuco-xanthin. It was shown that most of the Raman spectra obtained were identical to those of *all-trans* fucoxanthin in cyclohexane, although the absorption of these molecules are drastically perturbed when these are bound to the antenna proteins, most likely due to intermolecular excitonic coupling.. At 514.5 nm, however, a dramatic increase of the intensity of the ν_4 band is observed, as well as of bands located between 700 and 900 cm^{-1}. This is typical of the presence of a carotenoid molecule which has lost its planar configuration due to a twist around a C–C bond (Lutz et al., 1987). It was thus concluded that all the fucoxanthin molecules present in FCP proteins were *all-trans,* and that a fraction of them (probably two out of eight) were distorted. Since the distorted molecules can only be observed with a single excitation wavelength, this particular work illustrates the importance of using various excitation conditions when studying proteins containing many carotenoid molecules.

VI. Resonance Raman of Carotenoid Molecules In Vivo: Reaction Centers

A. Reaction Centers from Purple Bacteria

Reaction centers (RC) of purple bacteria consist of three integral membrane proteins which bind four bacteriochlorophyll and two bacteriopheophytin molecules, as well as a carotenoid. It was reported in 1976 that this reaction center-bound molecule had an unusual resonance Raman signal (Lutz et al., 1976). This signal was found in reaction centers purified from different purple bacteria (Lutz et al., 1978), and it was proposed that the reaction center carotenoid assumed a particular, *cis* configuration. As there is an intense band at 1242 cm^{-1} in the Raman spectra of the RC-bound carotenoids (Fig. 3), it was proposed that the spheroidene bound to the reaction center-from *Rb sphaeroides* was in the 15–15´ cis configuration as these conformations only are associated with the presence of this Raman band (Koyama et al., 1982). Nuclear magnetic resonance experiments performed on the carotenoid extracted from the reaction centers confirmed this configuration (Lutz et al., 1987). However, during the extraction procedure (which was performed in complete darkness), the unusually high intensity of the ν_4 is lost in the resonance Raman spectra, suggesting that the conformation of the molecule is modified (Lutz et al., 1987). It was therefore concluded that an additional twist of the polyene chain exists in the structure of the RC-bound carotenoid. Relying on calculations performed by Saito and Tasumi (1983), Lutz et al. proposed that this twisting of the carotenoid bound to the reaction centers should be in the C_8-C_{12} and/or $C_{8'}-C_{12'}$ regions (Lutz et al., 1987). Since the resonance Raman spectra of the carotenoid bound to reaction centers from a range of purple bacteria all exhibit the same features, this configuration is likely to be a general characteristic of RC-bound carotenoid. This has been confirmed by NMR studies on neurosporene in *Rb. sphaeroides* strain G1C (Koyama et al., 1988b). When a carotenoid molecule is bound to the reaction centers from carotenoidless mutants, their Raman spectra becomes similar to that of RC-bound carotenoid molecule. This led to the conclusion that this particular conformation and configuration are imposed by the protein binding site (Agalidis et al., 1980). It was recently proposed that the spirilloxanthin molecule bound to the reaction centers of *Rhodospirillum rubrum* experiences a *cis-trans* isomerization when these reaction centers are poised at low redox potential (Kuki et al., 1995), but other authors have observed 15–15′ *cis* spirilloxanthin in similar conditions, using resonance Raman spectroscopy (Zhou et al., 1987). The precise conditions necessary for this spirilloxanthin *cis-trans* isomerization are not yet clear.

Resonance Raman spectra of the RC-bound carotenoid in its triplet state were first recorded using pulsed lasers (Lutz et al., 1983). Later on, it was shown that it was possible to accumulate the carotenoid triplet state in the reaction centers with continuous illumination, by making use of the fact that this triplet state is usually produced in these proteins with a high yield when the electron transfer is blocked (Robert et al., 1989; see Fig. 4). From these experiments it was concluded that the particular, 15–15´-*cis*, twisted, structure of the carotenoid is conserved when these molecules are in the triplet state. In particular, resonance Raman spectra of the RC-bound carotenoid in their triplet states exhibit an unusually intense ν_4, which likely reveals that the molecule is not planar (Lutz et al., 1983, Robert et al., 1989).

B. Photosystems I and II

Photosystem I and II of oxygen-evolving organisms generally have extremely complex membrane architecture, involving a large number of polypeptides, and binding many β-carotene and chlorophyll molecules. However, a subparticle from PS II was isolated in 1987, called the D1D2 complex, as it contains, among others things, the so-called the D1 and D2 polypeptides (Nanba and Satoh, 1987). This particle contains a small number of subunits, five or six chlorophyll and one or two carotenoid molecules. Partial primary charge separation is still achievable in these samples. This particle has been the object of many studies, including an investigation of the conformation of the carotenoid molecule(s) by resonance Raman spectroscopy. Although the presence of one carotenoid molecule in a *cis*-conformation has once been suggested (Bialek-Bylka et al., 1995), most groups which have studied this type of sample obtained resonance Raman spectra very similar if not identical to the spectra of all-trans β-carotene (de Paula et al., 1990; Moenne-Locoz et al., 1990; Picorel, R. personal communication). It seems therefore that, although the PS II reaction centers share many similarities with bacterial reaction

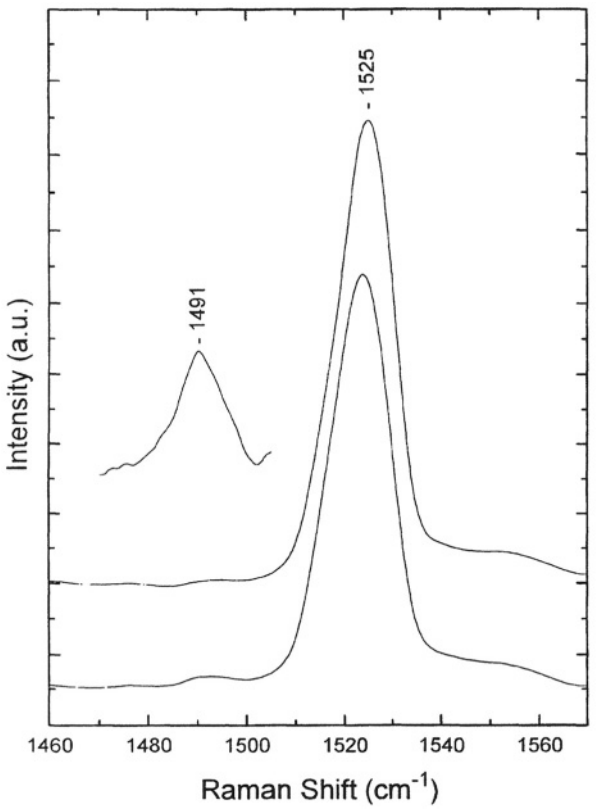

Fig. 4. Resonance Raman spectra (1460–1570 cm^{-1}) of spheroidenone bound to reaction centers of *Rhodobacter sphaeroides* 2.4.1. poised at a low redox potential. Excitation line: 568.1 nm. Bottom 100 K, mid: 20 K. Top: computed difference (enlarged 20×) between spectra recorded at 100K and 20 K, showing the contribution of the ν_1 of spheroidenone in its triplet state.

centers, they do not bind a 15–15′ *cis* carotenoid molecule.

The core of Photosystem I consists of two large subunits, which each bind many chlorophyll and carotenoid molecules. It is thus impossible to prepare, by mild biochemical treatments alone, a PS I subparticle which only binds a small number of carotenoid and chlorophyll molecules. After pigment extraction with cold ether, it is however possible to obtain a PS I preparation that only retains 6 chlorophyll a and a reduced number of carotenoid molecules. Resonance Raman studies performed on such samples led to the conclusion that the carotenoid still bound to PS I were in an *all-trans* conformation (P. Moenne-Loccoz and B. Robert, unpublished data). It thus seems that β-carotene is always *all-trans* in reaction centers from oxygen-evolving organisms.

VII. Perspectives

While resonance Raman spectroscopy has been of immense utility in providing precise molecular information regarding carotenoids, these molecules have played an equally important role in the development of this spectroscopic method. The use of selective isotopic enrichment of these molecules, together with new methods for calculating the vibrational sublevels of conjugated molecules, should in the near future provide a much deeper understanding of the Raman spectra of carotenoids. With the recent developments in laser technology, new light sources are available which are continuously tunable over the whole UV-Visible range, and which therefore allow precise measurements of resonance Raman profiles. Thus it is clear that resonance Raman spectroscopy will continue to be an essential technique in the years to come for understanding structure-function relationships and the photochemistry of carotenoid molecules involved in photosynthesis.

Acknowledgments

The author wishes to thank Andy Pascal and Andrew Gall for their constant help during the writing of this manuscript.

References

Agalidis I, Lutz M and Reiss-Husson F (1980) Binding of carotenoid on reaction centers from *Rhodopseudomonas sphaeroides*. Biochim Biophys Acta 589: 264–274

Albrecht AC (1961) On the theory of Raman intensities. J Chem Phys 34:1476–1484

Szymansky HA (1962) Raman Spectroscopy, Theory and Practice. Plenum Press, New York

Bialek-Bylka GE, Tomo T, Satoh K and Koyama Y (1995) 15-cis β-carotene found in the reaction center of spinach Photosystem II. FEBS Lett 363: 137–140

Carey PR (1982) Biochemical applications of Raman and Resonance Raman spectroscopies. Academic Press, New York

Chadwick BW and Frank HA (1986) Electron-spin resonance studies of carotenoids incorporated into reaction centers of *Rhodobacter sphaeroides* R26.1. Biochim Biophys Acta 851: 257–266

Conn PF, Haley J, Lambert CR, Truscott TG and Parker AW (1993) Time-resolved resonance Raman spectroscopy of carotenoids in triton X-100 micellar solution. J Chem Soc Faraday Trans 89: 1753–1757

Dallinger RF, Guanci JJ, Woodruff WH and Rodgers MA (1979)

Vibrational spectroscopy of the electronically excited state: pulse radiolysis/time-resolved resonance Raman study of the triplet β-carotene. J Am Chem Soc 101: 1355–1357

De Paula JC, Ghanotakis DF, Bowlby NR, Dekker JP, Yocum CF and Babcock GT (1990) Chlorophyll-protein interactions in Photosystem II. Resonance Raman spectroscopy of the D1 D2-cytochrome b_{559} complex and the 47 kDa protein. In: Baltscheffsky M (ed) Current Research in Photosynthesis, pp 643–646, Kluwer Academic Publishers, Dordrecht

Frank HA and Cogdell RJ (1993) Photochemistry and functions of carotenoids in Photosynthesis. In: Young A and Britton G (eds) Carotenoids in Photosynthesis, pp 252–326. Chapman & Hall, London

Frank HA, Farhoosh R, Gebhard R, Lugtenburg J, Gosztola D and Wasielewski MR (1993) The dynamics of the S_1 states of carotenoids. Chem Phys Lett 207: 88–92

Gill D, Kilponen RG and Rimai L (1970) Resonance Raman scattering of laser radiation by vibrational modes of carotenoid pigment molecules in intact plant tissues. Nature, 227: 743–744

Gruszecki WI, Matula M, Ko-chi N, Koyama Y and Krupa Z (1997) *Cis-trans* isomerization of violaxanthin in LHCII: violaxanthin isomerization within the violaxanthin cycle. Biochim Biophys Acta 1319: 267–274

Hashimoto H and Koyama Y (1988) Time-resolved Raman spectroscopy of triplet β-carotene produced from all-trans, 7-is, 13-cis and 15-cis isomers and high-pressure liquid chromatography analyses of photoisomerisation via the triplet state. J Phys Chem 92: 2101–2108

Hashimoto H and Koyama Y (1989a) Raman spectra of all-trans β-carotene in the S1 and T1 states produced by direct photoexcitation. Chem Phys Lett 163: 251–256

Hashimoto H and Koyama Y (1989b) The C=C stretching Raman lines of β-carotene isomers in the S_1 state as detected by pump-probe resonance Raman spectroscopy. Chem Phys Lett 154: 321–325

Hayashi H, Kolaczkowski SV, Noguchi T, Blanchard D and Atkinson GH (1990) Picosecond time-resolved resonance Raman scattering and absorbance changes of carotenoids in light-harvesting systems of photosynthetic bacterium *Chromatium vinosum.* J Am Chem Soc 112: 4664–4670

Hayashi H, Brack TL, Noguchi T, Tasumi M and Atkinson GH (1991) Vibrational relaxation in carotenoids in vivo and in vitro: picosecond time-resolved anti-Stokes resonance Raman spectroscopy. J Phys Chem 95: 6797–6802

Horton P, Ruban AV, Rees D, Pascal AA, Noctor G and Young AJ (1991) Control of the light-harvesting function of chloroplast membranes by aggregation of the LHCII chlorophyll-protein complex. FEBS Lett 292: 1–4

Iwata K, Hayashi H and Tasumi M (1985) Resonance Raman studies of the conformations of all-trans carotenoids in light-harvesting systems of photosynthetic bacteria. Biochim Biophys Acta 810: 269–273

Jirsakova V and Reiss–Husson F(1994) A specific carotenoid is required for reconstitution of the *Rubrivivax gelatinosus* B875 light harvesting complex from its subunit form B820. FEBS Lett 353: 151–154

Koepke J, Hu X, Münke C, Schulten K and Michel H (1996) The crystal structure of the light-harvesting complex II (B8000–850) from *Rhodospirillum molischianum.* Structure 4: 581–597

Kok P, Koehler J, Groenen EJJ, Gebhard R, van der Hoef I, Lugtenburg J, Hoff AJ, Farhoosh R and Frank HA (1994) Towards a vibrational analysis of spheroidene. Resonance Raman spectroscopy of 13C-labeled spheroidenes in petroleum ether and in the Rhodobacter sphaeroides reaction center. Biochim Biophys Acta 1185: 188–192

Kok P, Koehler J, Groenen EJJ, Gebhard R, van der Hoef I, Lugtenburg J, Hoff AJ, Farhoosh R and Frank HA (1997) Resonance Raman spectroscopy of 2H-labeled spheroidenes in petroleum ether and in the Rhodobacter sphaeroides reaction center. Spectrochim Acta 53A: 381–392

Koyama Y, Takii T, Saiki K, Tsukida K and Yamashita KJ (1982) Configuration of the carotenoid in the reaction centers of photosynthetic bacteria. Comparison of the resonance Raman spectrum of the reaction centers of Rhodopseudomas sphaeroides G1C with those of *cis-trans* isomers from β-carotene. Biochim Biophys Acta 680: 109–118

Koyama Y, Takii T, Saiki K and Tsukida K (1983) Configuration of the carotenoid in the reaction centers of photosynthetic bacteria. 2) Comparison of the resonance Raman lines of the reaction centers with those of the 14 different *cis-trans* isomers of β-carotene. Photobiochem Photobiophys 5: 139–150

Koyama Y, Takatsuka I, Nakata M and Tasumi, M (1988a) Raman and infra-red spectra of the all-*trans,* 7-*cis,* 9-*cis,* 13-*cis* and 15-*cis* isomers of β-carotene: Key bands distinguishing stretched or terminal bent configurations from central-bent configurations. J Raman Spectrosc 19: 37–49

Koyama Y, Kanaji M, and Shimamura T (1988b) Configurations of neurosporene isomers isolated from the reaction center and the light-harvesting complex of *Rhodobacter sphaeroides* G1C. A resonance Raman, electronic absorption and proton NMR study. Photochem Photobiol 48: 107–114

Koyama Y, Kuki M, Andersson PO and Gillbro T (1996) Singlet excited states in the light-harvesting function of carotenoids in bacterial photosynthesis. Photochem Photobiol 63: 243–256

Kühlbrandt W, Wang DN and Fujiyoshi Y (1994) Atomic model of plant light-harvesting complex by electron crystallography. Nature 367: 614–621

Kuki M, Hashimoto H & Koyama Y (1990) The 2^1A_g state of a carotenoid bound to the chromatophore membrane of Rhodobacter sphaeroides 2.4.1. as revealed by transient resonance Raman spectroscopy. Chem Phys Lett 165: 417–422

Kuki M, Nagae R, Cogdell RJ, Shimada K and Koyama Y (1994) Solvent effect on spheroidene in non-polar and polar solutions and the environment of spheroidene in the light-harvesting complexes of Rhodobacter sphaeroides 2.4.1. as revealed by the energy of the $^1A_g \rightarrow {}^1B_u$ absorption and the frequency of the vibronically coupled C=C stretching Raman line in the ^1A_g and 2^1A_g states. Photochem Photobiol 59: 116–124

Kuki M, Naruse M, Kakuno T and Koyama Y (1995) Resonance Raman evidence for 15-*cis* to *all trans* photoisomerisation of spirilloxanthin bound to a reduced form of the reaction centers of *Rhodospirillum rubrum* S1. Photochem Photobiol 62: 502–507

Lutz M, Kleo J and Reiss-Husson F (1976) Resonance Raman scattering of bacteriochlorophyll, bacteriopheophytin and spheroidene in reaction centers of *Rhodopseudomonas spheroides.* Biochem Biophys Res Comm 69: 711–717

Lutz M, Agalidis A, Hervo G, Cogdell RJC and Reiss-Husson F (1978) On the state of the carotenoids bound to reaction

centers of photosynthetic bacteria: A resonance Raman study. Biochim Biophys Acta 503: 387–303

Lutz M, Chinsky L and Turpin PY (1983) Triplet states of carotenoid bound to the reaction centers of photosynthetic bacteria. Time resolved resonance Raman spectroscopy. Photochem Photobiol 36: 503–513

Lutz M, Szponarski W, Berger G, Robert B and Neumann JM (1987) The stereoisomerism of bacterial, reaction center bound carotenoids revisited: an electronic absorption, resonance Raman and 1H-NMR study. Biochim Biophys Acta 894:423–433

Mc Dermott G, Prince SM, Freer AA, Hawthornthwaite-Lawless AM, Papiz MZ, Cogdell RJ and Isaacs NW (1995) Crystal structure of an integral membrane light-harvesting complex from photosynthetic bacteria. Nature 374: 517–521

Moenne-Loccoz P, Robert B and Lutz M (1990) Structure of the primary reactants in Photosystem II: resonance Raman studies of D1D2 particles. In: Baltscheffsky M (ed) Current Research in Photosynthesis, pp 423–426, Kluwer Academic Publishers, Dordrecht,

Nanba O and Satoh K (1987) Isolation of a Photosystem II reaction center consisting of D1 and D2 polypeptides and cytochrome b_{559}. Proc Natl Acad Sci USA 84: 109–112

Noguchi T, Hayashi H, Tasumi M and Atkinson GH (1991) Solvent effects on the a_g stretching mode in the 2^1A_g-excited state of β-carotene and two derivatives:picosecond time-resolved resonance Raman spectroscopy. J Phys Chem 95: 3167–3172

Pascal AA, Caron L, Rousseau B, Lapouge K, Duval JC and Robert B (1998) Resonance Raman spectroscopy of a light-harvesting protein from the brown Alga Laminaria saccharina. Biochemistry 37: 2450–2457

Raman CV and Krishnan KS (1928) A new type of secondary radiation. Nature 121: 501–502

Rimai L, Gill D and Parson JL (1971) Raman spectra of dilute solutions of some stereoisomers of vitamin A-type molecules. J Am Chem Soc 93: 1353–1357

Rimai L, Heyde ME and Gill D (1973) Vibrational spectra of some carotenoids and related linear polyenes. A Raman spectroscopic study. J Am Chem Soc 95: 4493–4501

Robert B (1983) Etude par diffusion Raman de resonance de complexes proteine-pigment antennes des Rhodospirillales. These Doct. 3ème Cycle, Université Pierre et Marie Curie, Paris

Robert B and Lutz M (1985) Structures of antenna complexes of several Rhodospirillales from their resonance Raman spectra. Biochim Biophys Acta 807: 10–23

Robert B and Frank HA (1988) A resonance Raman investigation of the effect of lithium dodecyl sulfate on the B800–850 light-harvesting protein of *Rhodopseudomonas acidophila* 7750. Biochim Biophys Acta 934: 401–405

Robert B, Nabedryk E and Lutz M (1989) Vibrational spectroscopy of transient states in photosynthetic bacterial reaction centers. In: Clark RJH and Hester RE (eds) Time-resolved spectroscopy, pp 301–333. John Wiley and Sons, New York

Ruban AV, Horton P and Robert B (1995) Resonance Raman spectroscopy of the Photosystem II light-harvesting complexes of green plants. A comparison of the trimeric and aggreggated states Biochemistry 34: 2333–2337

Saito S, Tasumi M and Eugster CH (1983) Resonance Raman spectra ($5800–40\ cm^{-1}$) of all-trans and 15–*cis* isomers of βcarotene in the solid state and in solution. Measurements with various laser lines from ultraviolet to red. J Raman Spectrosc 14: 299–309

Saito S and Tasumi M (1983) Normal-coordinate analysis of β-carotene isomers and assignments of the Raman and infrared bands. J Raman Spectrosc 14: 310–321

Shreve AP, Trautman JK, Owens TG and Albrecht CA (1991) Determination of the S_2 lifetime of β-carotene. Chem Phys Lett 178: 89–96

Thrash RJ, Fang HLB and Leroi GE (1977) The Raman excitation profile spectrum of β-carotene in the preresonance region: Evidence for a low-lying singlet state. J Chem Phys 67:5929–5931

Wilbrandt R, Jensen NH, Pagsberg P, Sillesen AH and Hansen KB (1980) Time-resolved resonance Raman spectroscopy: the triplet state of all-trans β-carotene and related compounds. In: Murphy WF (ed) Proceedings of the 7^{th} International Conference on Raman Spectroscopy, pp 632–633. NRCC, Ottawa

Zhou Q, Robert B and Lutz M (1987) Intergeneric structural variability of the primary donor of photosynthetic bacteria: Resonance Raman spectroscopy of reaction centers from two *Rhodospirillum* and *Rhodobacter* species. Biochim Biophys Acta 890: 368–376

Zurdo J, Centeno MA, Odriozola JA, Fernandez-Cabrera C, and Ramirez JM (1995) The structural role of the carotenoid in the bacterial light-harvesting protein II (LHII) of *Rhodobacter capsulatus.* A Fourier transform Raman spectroscopy and circular dichroism study. Photosynth Res 46: 363–369

This page intentionally left blank

Chapter 11

Electron Magnetic Resonance of Carotenoids

Alexander Angerhofer
The University of Florida, Department of Chemistry,
Box 117200, Gainesville, FL 32611, U.S.A.

Summary

Carotenoids function in photosynthesis as quenchers of chlorophyll triplet states to prevent their harmful reaction with oxygen. Current research has mainly focused on their detection and identification, the determination ofkinetic parameters, and the elucidation ofthe triplet energy transfer pathways in both photosynthetic antenna and reaction centers. Since carotenoids do not take part in the photosynthetic electron transfer reactions, their paramagnetic radical species occur to a lesser extent in vivo, although they may play a role in the photoprotection of Photosystem II.

This chapter reviews the work ofthe last five to six years on paramagnetic states ofcarotenoids using electron magnetic resonance. Mainly radical cation and neutral molecular triplet states are treated. Part of this chapter deals with paramagnetic states ofcarotenoids in model systems. These have been synthesized in order to mimic both electron and energy transfer processes in the natural photosynthetic systems. Consequently, the electron magnetic resonance (EMR) spectroscopy of carotenoid triplet and radical states yields important information about their photochemistry. Finally, the EMR spectroscopy on carotenoid radicals is reviewed. It serves to establish the database on their intrinsic properties which is necessary for the analysis of carotenoid radicals in vivo.

H. A. Frank, A. J. Young, G. Britton and R. J. Cogdell (eds): The Photochemistry of Carotenoids, pp. 203–222.

I. Introduction

The use of solar energy by photosynthetic organisms depends on their ability to safely dissipate excess energy and to quench chlorophyll triplet states in the event that they are formed in order to prevent them from sensitizing harmful singlet oxygen. This important function is performed in most photosynthesizing organisms by the carotenoids, a group of pigments that can be divided into two main classes: carotenes and xanthophylls. Apart from their role as photoprotectors they also serve as accessory antenna pigments that widen the wavelength range of photon energy usable for photosynthesis.

Some of the important questions that one might ask about the dual role of the carotenoids and the mechanisms by which these roles are performed in vivo are: What are the structures of the carotenoids in vivo? How does the structure determine or modify their biological activities? What are the mechanisms of triplet quenching and which are the pathways for triplet energy transfer? What are the mechanisms for radical reactions with carotenoids? How do they quench singlet oxygen? The answers to these questions lie in the understanding of their molecular features, i.e., structure and conformations, electronic ground and excited states, and the dynamics of the intra- and intermolecular processes that they might undergo. Structural information is obtained from X-ray and electron diffraction studies on reaction center (RC) and antenna complexes which have become available in recent years. The electronic structure of the pigments as well as their dynamic behavior as isolated molecules or in pigment-protein complexes is investigated by a host of spectroscopic methods, including absorption, fluorescence, resonance Raman, nuclear magnetic resonance, electron magnetic resonance (EMR), and fast transient optical spectroscopy, as well as by computational methods. This chapter deals with recent accomplishments mainly in the application of EMR and its related techniques (ENDOR and ODMR) to the investigation of carotenoids.

Abbreviations: ADMR – absorption detected magnetic resonance; ATP – adenosine triphosphate; BChl – bacteriochlorophyll; BPh – bacteriopheophytin; Car – carotenoid; Chl – chlorophyll; CIDEP – chemically induced electron spin polarization; CV – cyclic voltammetry; EMR – electron magnetic resonance (the general expression that includes ESR and EPR and electron cyclotron resonance); END OR – electron nuclear double resonance; EPR – electron paramagnetic resonance; ESEEM – electron spin echo envelope modulation; ESR – electron spin resonance; FDMR – fluorescence detected magnetic resonance; FT-EPR – Fourier transform EPR; FTIR – Fourier transform infrared; ISC – inter-system crossing; LHC-II – light harvesting complex II; MIA – microwave-induced absorption; MODS – magneto-optical difference spectroscopy; NMR – nuclear magnetic resonance; ODMR – optically detected magnetic resonance; PCP – peridinin-chlorophyll-protein-complex; PS II – Photosystem II; RC – reaction center; RCs – reaction centers; SEEPR – simultaneous electrochemistry and EPR; TREPR – time-resolved EPR

II. Photosynthetic Systems

EMR or ODMR of carotenoids in photosynthetic pigment-protein complexes have mainly focused on the meta-stable light-induced triplet states after the initial work of Mathis and co-workers and Wolff and Witt who demonstrated that carotenoids act as triplet quenchers for chlorophylls in plants (Mathis, 1966; Mathis and Galmiche, 1967; Wolff and Witt, 1969). The photoprotective function of the carotenoids is mainly based on this quenching reaction and has been reviewed many times in the literature (Cogdell, 1985; Siefermann-Harms, 1985, 1987; Frank, 1992, 1993; Frank and Cogdell, 1996). It is operative in vivo based on the vicinity between carotenoid (Car) and chlorophyll (Chl) molecules (Cogdell et al., 1997) whereas in vitro triplet quenching is a diffusion controlled reaction (Borland et al., 1989). Another photoprotective mechanism, the xanthophyll cycle, operates mainly at the singlet exciton level and regulates excitation density in the Chl antenna system (Young, 1991; Arsalane et al., 1994; Frank et al., 1994; Pfündel and Bilger, 1994; Demmig-Adams and Adams, III, 1996; Frank et al., 1996a; Young and Frank, 1996; Ambarsari et al., 1997).

A. Carotenoid Triplet States in Photosynthetic Antenna Complexes

1. Purple Photosynthetic Bacteria

BChl triplet states are generated in the antenna complex of photosynthetic bacteria and subsequently quenched by the carotenoids within about 20 ns (Monger et al., 1976; Renger and Wolff, 1977). The quantum yields of antenna carotenoid triplet formation in wild-type chromatophores of various purple bacteria is of the order of 2–5% but increases to 20% if the reaction centers are closed (Monger et al., 1976; Rademaker et al., 1980). There have been some reports in the literature citing evidence for the

generation of carotenoid triplet states by singlet fission upon direct excitation of the S_2 (^1B_u) state with relatively high quantum yields (approx. 30%) and fast triplet formation times (approx. 100 ps) (Rademaker et al., 1980; Nuijs et al., 1984, 1985). From magnetic field effect and time-resolved resonance Raman experiments it was concluded that fission of a singlet excitation of the carotenoid into a triplet pair is the most probable pathway (Rademaker et al., 1980; Frank et al., 1982b; McGann and Frank, 1983; Kingma et al., 1985a,b; Naruse et al., 1991; Koyama and Mukai, 1993). In the case of homo-fission such a mechanism would require close van der Waals contact between two carotenoid molecules which is questionable given the emerging picture of the antenna X-ray structures from purple bacteria (Freer et al., 1996; Koepke et al., 1996; Papiz et al., 1996; Cogdell et al., 1997). That would point to hetero-fission as the most likely mechanism. A quick estimate of the necessary energy can be done based on the known triplet energy of the BChl molecule (7590 and 8240 cm^{-1} for RCs and BChl in vitro (Takiff and Boxer, 1988b)) and that of β-carotene (8050 or 6790 cm^{-1} for the triplet state energy obtained by singlet-oxygen quenching and photoacoustic calorimetry experiments, respectively (Gorman et al., 1988; Lambert and Redmond, 1994)). This requires the triplet pair precursor to be above 14380 cm^{-1} (695 nm) in the most favorable case, and above 16290 cm^{-1} (614 nm) in the worst case (using the largest estimates for both BChl and β-carotene triplet states). This interval is clearly above the S_1 state of spheroidene (14100 to 14500 cm^{-1} (Frank et al., 1993a, 1997; Koyama et al., 1996)), yet below the S_2 state. Thus the proposed fission mechanism would have to start out from the Car S_2 state and compete with ultrafast internal conversion from S_2 ($^1B_u^+$) to S_1 ($^2A_g^-$) which occurs on a time scale of 200 fs (Ricci et al., 1996).

The spin polarization of the antenna carotenoid triplet state has been observed by Frank et al. (1980; 1982a; 1987) in quite a number of different purple bacterial strains, and under all conditions shows an eae aea pattern (where *e* means emission and *a* absorption of microwaves) that can be explained with intersystem crossing in a BChl molecule with subsequent triplet energy transfer to the carotenoid. This seems to contradict the additional triplet formation pathway by hetero-fission of a carotenoid singlet excitation and it would therefore be of great interest to revisit the earlier time-resolved optical and magnetic field effect data and furthermore investigate the excitation wavelength dependence of the carotenoid triplet spin polarization by EMR.

Zero-field ODMR has also been used to detect and identify the triplet states of antenna carotenoids in a variety of purple bacteria (Ullrich et al., 1988, 1989; Aust et al., 1991; Angerhofer et al., 1995; Jirsakova et al., 1996a,b). Their fine structure splittings correlate linearly with the length of the polyene chain. The spin alignment favors the $2|E|$-signal as the most intense while the $|D| \pm |E|$-signals are usually weaker by an order of magnitude. A peculiar temperature dependence of the ODMR signal intensities has been noted with a dip around 50–60 K and a subsequent increase in intensity with rising temperatures to about 120 K (Ullrich et al., 1989). Similar behavior has been observed for the antenna carotenoids of dinoflagellates (Carbonera et al., 1995). Time-resolved absorption difference spectroscopy has shown only a very weak temperature dependence of the over-all triplet lifetime and consequently the sublevel decay rates are not expected to change dramatically with temperature, i.e., can not account for the peculiar behavior of the ODMR signal intensities (Groß, 1997). However, time-resolved ODMR of PCP from *Glenodinium* showed an increase in triplet sublevel relaxation at 30 K compared with 100 K which could be interpreted as due to increased spin-lattice relaxation (Groß, 1997). This may be due to an onset of triplet energy hopping between at least two of the four different peridinin sites in the complex but probably does not represent a good explanation of the observation of the same effect in purple bacterial antenna complexes where the carotenoids seem to be too far away from each other to allow for triplet exchange.

The explanation may therefore well lie in the intrinsic spin dynamics of the carotenoid molecules themselves. A clear answer would be desirable and should come from the temperature dependence of time-resolved EMR experiments, preferably at multiple field/frequency combinations.

When monitoring the microwave-induced absorption (MIA) spectra of the carotenoid triplet states specific interactions can be seen in the BChl Q_y region. This is true for practically all antenna and RC carotenoids studied so far to varying degrees (van der Vos et al., 1991; Carbonera et al., 1992b; Angerhofer et al., 1995; Hartwich et al., 1995). The case of the B830 complex from *Chromatium purpuratum* is different from the others, however,

because the interaction bands are especially strong and sharp, indicating a possible breaking of BChl excitonic interaction when the okenone triplet state is formed (Angerhofer et al., 1995).

Very few reports have appeared in the literature concerning the time-resolved behavior of the ^{3}Car* triplet sublevels, which is probably due to the generally weak EMR and/or ODMR intensities. McGann and Frank report sublevel decay rates of $(2.5 \pm 0.2) \times 10^5$, $(9.0 \pm 2.2) \times 10^4$, and $(3.9 \pm 0.1) \times 10^5$ s^{-1} for spheroidene in the bacterial RCs of *Rhodobacter (Rb.) sphaeroides* (McGann and Frank, 1985). Still faster rates have been observed by Groß in the PCP antenna complex of *Heterocapsa,* $(1.8 \pm 0.1) \times 10^5$, $(6.7 \pm 0.5) \times 10^5$, and $(1.6 \pm 0.8) \times 10^6$ s^{-1} (Groß, 1997).

What has become clear from all of these triplet studies is that carotenoid triplet state formation occurs mainly through a Dexter type exchange mechanism between BChl as the triplet donor and carotenoid pigments with at least nine conjugated double bonds as the acceptors (not all carotenoids with nine conjugated double bonds will work, see discussion below). The protective effect of the carotenoids is due to the fact that the quenching of ^{3}BChl* occurs about three orders of magnitude faster than the diffusion controlled sensitization of singlet oxygen. From the crystal structure it is clear that the carotenoids are in van der Waals contact with both B800 and B850 BChls which is consistent with the spectroscopic data (Freer et al., 1996; Koepke et al., 1996; Papiz et al., 1996; Cogdell et al., 1997).

2. Green Sulfur Bacteria

The two species that have been examined with FDMR are *Chlorobium phaeobacteroides* (containing BChl *e,* and isorenieratene as the major carotenoid) and *Chlorobium limicola* (containing BChl *c,* and chlorobactene as the major carotenoid). Car triplet states were observed with fine structure splittings of $|D| = 0.0332$ cm^{-1} and $|E| = 0.0039$ cm^{-1} for chlorobactene, and $|D| = 0.0355$ cm^{-1} and $|E| = 0.0039$ cm^{-1} for isorenieratene, and assigned to antenna carotenoids (Psencik et al., 1994). BChl triplet states were observed alongside the carotenoids which seems to indicate that at least some of the triplet energy transfer from BChl to Car can be switched off at low temperatures.

3. Dinoflagellates

ODMR work on the dinoflagellate peridinin-chlorophyll-protein (PCP) antenna complex, mainly done by the group of Giacometti in Padova has shown at least two distinct triplet sites with readily distinguishable fine structure parameters (Carbonera et al., 1995). The X-ray structure of these antenna complexes has been solved and shows four peridinin molecules per chlorophyll per subunit for *Glenodinium* or *Heterocapsa* and twice that number for *Amphidinium carterae* (Hofmann et al., 1996) (see also Chapter 5, Hiller). In both cases the peridinin triplet ODMR signals show interesting temperature dependencies with clearly visible splittings of the $|D| \pm |E|$-signals at low temperatures that merge to a single line at higher temperatures for *Amphidinium* (Carbonera et al., 1995), and frequency shifts for Glenodinium (Carbonera et al., 1996). These effects were qualitatively accounted for by the assumption of inter- and intra-cluster excitonic interactions between the peridinin molecules which will lead to Davydov-type splittings in the slow exchange regime at low temperatures but will be averaged out by faster hopping rates and increased Boltzmann population of higher lying states as temperature is increased (Carbonera et al., 1996).

4. Plant Antenna Systems

An atomic resolution model of the plant light-harvesting complex LHC-II has been published (Kühlbrandt, 1994; Kühlbrandt et al., 1994; Hunter et al., 1994b). Two xanthophyll molecules are located at the center of the complex and were identified as lutein based on the fact that this pigment is the most abundant. They apparently have a structural role in addition to their triplet quenching ability (Plumley and Schmidt, 1987; Paulsen et al., 1990; Heinze et al., 1997). The main xanthophylls are lutein, neoxanthin, and violaxanthin (Siefermann-Harms, 1985, 1990a). Time-resolved optical spectroscopy showed that at least two spectroscopically distinct xanthophylls participate in triplet quenching, apparently lutein and violaxanthin (Peterman et al., 1995, 1997).

Spin-polarized EMR spectra of the xanthophyll triplet states in LHC-II were reported by Carbonera et al. (1989). While the spectral resolution at X-band prevented the distinction of different triplet sites,

zero-field ADMR and FDMR experiments later revealed three triplet states differing in their zero field splittings (van der Vos et al., 1991; Carbonera et al., 1992a). The size of the *D*-parameter corresponds to a polyene chain of between eight and nine conjugated double bonds (Carbonera et al., 1989; Carbonera et al., 1992a). Based on the ADMR intensities, van der Vos et al. (1991) assigned the two strongest triplet states to lutein and neoxanthin rather than lutein and violaxanthin as suggested from the purely optical work by Peterman et al. (1997). The ADMR work revealed interesting interaction bands in the Chl region around 680 nm which can be explained as bleachings and/or band shifts of both Chl *a* and *b* upon xanthophyll triplet formation (van der Vos et al., 1991). Tentative models drawn up from this observation involved the close proximity and interaction between Chl monomers and the xanthophylls (van der Vos et al., 1994), the latter possibly being in a 9-*cis* conformation (van der Vos et al., 1991). However, the electron crystallographic model suggests three Chl a molecules in close proximity to the two resolved *all-trans* xanthophylls (Kühlbrandt et al., 1994). Unfortunately, an unambiguous correlation between the structural model and the available spectroscopic data is still elusive. This is in part due to the relative crude resolution (3.4 Å) at which the structure is known, and to the large number of pigments involved, i.e., 12–13 chlorophylls and 2–3 xanthophylls whose identities have only tentatively been assigned (Kühlbrandt et al., 1994).

β-carotene triplet states have been detected by ODMR in the core antenna complexes CP43 and CP47 of higher plants by Carbonera et al. (1992b). Slightly different zero field splitting parameters were found for the two preparations, and strong interaction bands with Chl a were found in the corresponding MIA spectra between 685 and 690 nm, Qualitatively, the spectra looked very similar to those found in LHC-II (van der Vos et al., 1991; Carbonera et al., 1992a).

Very recently, Siefermann-Harms and Angerhofer (1998) found evidence that the triplet quenching ability of the xanthophylls is not sufficient to protect the LHCII complex from photooxidation of its pigments. In fact, the pigment- and protein organization seems to play a crucial role in excluding oxygen from the xanthophyll sites (Siefermann-Harms, 1990b,c; Siefermann-Harms and Angerhofer, 1995, 1998). This would perhaps explain why two of them are located at the center of the complex which would be the place where oxygen is least likely to get access. It should also be noted that the xanthophylls seem to participate in the quenching of Chl *a* singlet excitation, thus decreasing the possibility of triplet formation through an alternate mechanism (Naqvi et al., 1987).

B. Carotenoid Triplet States in Photosynthetic Reaction Center Complexes

1. Purple Bacterial Reaction Centers

Carotenoids function in photosynthetic reaction centers (RC) as triplet quenchers of the primary donor chlorophyll or bacteriochlorophyll triplet states. The best studied RCs are those of purple photosynthetic bacteria where atomic models are available based on X-ray crystallography and optical as well as magnetic resonance spectroscopies have yielded a detailed picture of the flow of triplet energy transfer. Good reviews of these topics can be found in (Frank, 1992, 1993; Frank and Cogdell, 1996).

The structure of RCs of *Rb. sphaeroides* wild-type has been well described in the past and place the 15,15´-as spheroidene molecule adjacent to the monomeric BChl labeled B_B (subscript B for the electron transfer-inactive branch of the RC) and approximately 10 Å away from the primary donor P_{870} (Allen et al., 1988; Reiss-Husson and Mäntele, 1988;Yeates et al., 1988;Arnoux et al., 1989; Ermler et al., 1994a,b;Arnoux et al., 1995). This arrangement suggests that one of the functions if not the main one of B_B is to serve as a 'bridge' for triplet energy transfer from the primary donor (where the triplet state is generated via the radical-pair mechanism) to the carotenoid. Early indications for such a role came from phosphorescence experiments by Takiff and Boxer (1988a,b) who estimated the triplet energy level of B_B to be approximately 200 cm^{-1} above that of the primary donor, just in the right order of magnitude to explain the thermally activated behavior of the $^3Car^*$ quantum yield (Schenck et al., 1984), and from triplet EMR experiments on borohydride-reduced and spheroidene reconstituted RCs (Frank and Violette, 1989; Frank, 1990) (however, see the caution on borohydride treatment by Struck et al. (1991)).

The main approaches to the investigation of triplet energy transfer in the bacterial photosynthetic RC

have been the tuning of the energies of the participants, mainly B_B and carotenoid by selective pigment exchange or substitution and protein modification.

a. Exchange of the Accessory Bacteriochlophyll B_B

Using the technique of selective pigment exchange (Struck et al., 1990a,b; Struck and Scheer, 1990; Scheer and Struck, 1993) it has become possible to change the triplet energy level of the intermediate BChl, B_B, and study the influence of the modification on triplet energy transfer. The triplet EMR signals of preparations in which B_B has been exchanged with 13^2-hydroxy-[Zn]-bacteriochlorophyll *a* and [3-vinyl]13^2-hydroxy-bacteriochlorophyll *a* show equal amounts of $^3P_{870}$ and spheroidene triplet states at approx. 100 and 135 K, respectively, as compared to 35 K in unmodified RCs (Frank et al., 1993a). This attests to the rise in energy of the barrier for triplet transfer upon exchanging of B_B with pigments of higher triplet state energy, i.e., identifies it as the energy barrier that has to be overcome by a thermally activated process.

Independently, a monomeric triplet state was observed in RCs of the carotenoid-less mutant *Rb. sphaeroides* R26, and later identified with $^3B_B^*$ by its characteristic microwave induced absorption (MIA) spectrum (Angerhofer and Aust, 1993; Hartwich et al., 1995). The identification was confirmed by the interaction band which is visible in the MIA spectrum of the spheroidene triplet state (Hartwich et al., 1995). In RCs where B_B is exchanged for [3-vinyl]-13^2-hydroxy-bacteriochlorophyll *a* and then spheroidene-reconstituted, a MIA band shifts from 813 to 776 nm. This bleaching which has also been observed by MODS spectroscopy (Lous and Hoff, 1989) may be explained by a partial delocalization of the triplet excitation between spheroidene and B_B and allows the unequivocal determination of the ground state absorption of B_B (812 nm) which is obscured by the absorption of B_A (804 nm) and the upper exciton component of $P_{870}^{+\cdot}$ around 807 nm (Hartwich et al., 1995). The conclusion from these observations are that:

(i) B_B and spheroidene are in such close contact that a molecular excitation on one perturbs the optical spectrum of the other, i.e., they are in van der Waals contact as predicted from the X-ray structure, which is a necessary condition for efficient triplet energy transfer;

(ii) $^3B_B^*$ is generated, presumably via triplet energy transfer from $^3P_{870}^*$, which makes B_B a viable bridge for triplet transfer to the spheroidene molecule.

Unfortunately, ^{3}Car* was not observed in an EMR study of single crystals of RCs from *Rb. sphaeroides* 2.4.1 (wild-type) even at temperatures above 35 K (Budil et al., 1988). This would have allowed the determination of the relative orientation of the ^{3}Car* and $^3P_{870}^*$ fine structure tensors.

All of these results can be summarized in a kinetic model shown in Fig. 1 (Angerhofer, 1997). Since the time scales of $^3P_{870}^*$ decay and ^{3}Car* generation are of the order of tens of ns the primary charge separation which happens on a much shorter time-scale is not considered in the model and reduced to an initial population rate for the primary radical pair triplet state $^3[P_{870}^+ \Phi_A^-]$, $k_{1\leftarrow 0}$. Decay back to the ground state through the singlet channels is globally described by the rate $k_{0\leftarrow 1}$. $^3P_{870}^*$ population essentially takes place via the radical pair mechanism from $^3[P_{870}^+ \Phi_A^-]$ (rate $k_{2\leftarrow 1}$ and reverse process $k_{1\leftarrow 2}$). Decay of $^3P_{870}^*$ through intersystem crossing (ISC) is described by $k_{0\leftarrow 2}$. The thermally activated triplet transfer through the intermediate $^3B_B^*$ to ^{3}Car* is described by broken arrows (because their magnitudes are unknown), denoting the rates $k_{3\leftarrow 2}$, $k_{4\leftarrow 3}$, and their reverse processes, $k_{2\leftarrow 3}$ and $k_{3\leftarrow 4}$. It is assumed that $^3B_B^*$ has such a short lifetime that molecular ISC to its ground state is not efficient. On the other hand, the main relaxation pathway for ^{3}Car*, described by rate $k_{6\leftarrow 4}$, is through ISC. These rates make up what is in the rest of this article called the classical model, because it does not assume any processes in addition to the thermally activated triplet transfer via $^3B_B^*$. The hypothetical rates $k_{3\leftarrow 1}$ and $k_{4\leftarrow 2}$ are also shown in Fig. 1 to describe the 'bypass' and the 'tunneling' model for triplet energy transfer as discussed further below. A detailed discussion of this kinetic model and its implications on the observables in the transient absorption experiment was given by Angerhofer (1997).

While there can be no doubt about the role of B_B as a bridge for triplet energy transfer a number of open questions remained and have been addressed in more recent work. Using the temperature dependence of time-resolved absorption difference spectroscopy, Frank et al. (1996b) have determined the energy barriers of $^3B_B^*$ with respect to $^3P_{870}^*$ in wild-type, 13^2-hydroxy-[Zn]-bacteriochlorophyll *a*- and [3-vinyl]-13^2-hydroxy-bacteriochlorophyll *a*-exchanged (and spheroidene-reconstituted) RCs as 140± 100,380±

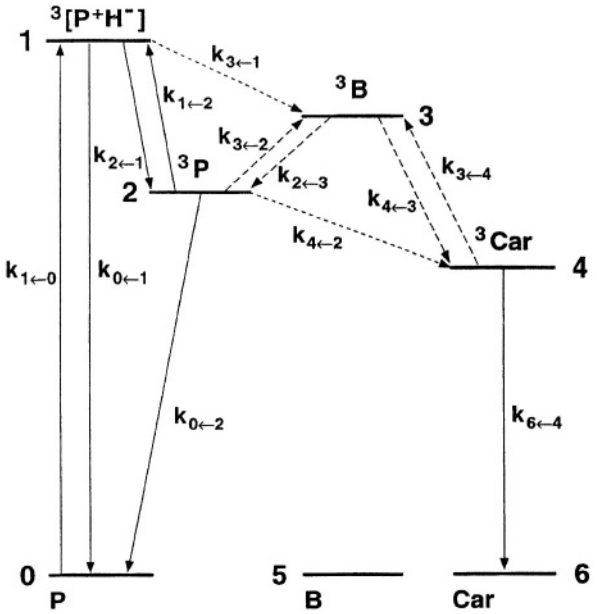

Fig. 1. The four-state model used for the description of triplet energy transfer in the RC according to Angerhofer (1997). For detailed explanation, see text. The filled arrows denote the rates that have been observed and described in the literature. The broken arrows depict rates that are either unknown (from and to $^3B_B^*$) or speculative ($k_{3\leftarrow1}$ for bypass reaction, and $k_{4\leftarrow2}$ for tunneling). The rates defined by arrows between different molecules (P, B, and Car) are in reality second order rates, i.e. they depend on the ground state concentrations of the molecule the excited state of which they point to. In the case of low excitation densities, i.e., when double excitation of the RCs can be neglected these rates can be assumed to be first order as for example done by Frank et al. (1996b).

100, and 1150 ± 400 cm^{-1}. The error bars in these values are quite large due to the noise in the experimental data and the reliance on only a few data points in the case of the [3-vinyl]-13^2-hydroxy-bacteriochlorophyll *a*-exchanged RC sample (Frank et al., 1996b). In addition to the temperature-dependent triplet formation rate a temperature-independent rate was observed in all cases around 3×10^7 s^{-1} and attributed to $^3P_{870}^*$ generation due to its feature-less spectral profile. However, a similar effect (a fast temperature independent ^{3}Car* formation in addition to a temperature dependent one) was observed by Kolaczkowski (1989) who studied a series of fully, partially and undeuterated RCs. Kolaczkowski interpreted the fast ^{3}Car* rise time as due to a fast triplet transfer reaction from a 'vibrationally hot $^3P_{870}^*$' possibly through other intermediate triplet states to ^{3}Car*. As far as the thermally activated process is concerned he measured 130 ± 20 cm^{-1} for the energy barrier and ascribed it to a librational mode of the spheroidene molecule. This interpretation has clearly been superceded by $^3B_B^*$ as the intermediate state based on the evidence discussed above. Nevertheless it proved impossible to explain the fast temperature-independent ^{3}Car* formation with the simple classical model shown in Fig. 1 (Angerhofer, 1997). Kolaczkowski rationalized it by introducing a bypass model (see Fig. 1, rate $k_{3\leftarrow1}$) while Frank et al. (1996b) dismissed its experimental evidence as an artifact that stemmed from the fast rise in $^3P_{870}^*$ population. A more recent study confirmed that the spectral profile of the fast rate observed peaks at 550 nm and follows the ^{3}Car* MIA spectrum quite nicely (Angerhofer, 1997; Angerhofer et al., 1998). However, since the light-induced difference-minus-ground-state spectrum of $^1[P^+_{870}\Phi_A^-]$ shows a bleaching of one of the bacteriopheophytins (BPh) near 546 nm, the charge recombination of the primary radical pair would yield a very similar spectral profile and its time constant would be of similar magnitude as the one observed (Shuvalov and Parson, 1981). Thus it seems still premature to make a decisive statement on the fast transient component observed as an increase in absorption at the wavelength of the spheroidene triplet-triplet absorption band at 550 nm.

Another observation of Kolaczkowski's could also not be explained by the classic model, i.e., the leveling-off of the ^{3}Car* formation rate around 2–3 x 10^6 s^{-1} below 66 K (Kolaczkowski, 1989). This is about two orders of magnitude faster than the decay rate of the primary donor triplet, $^3P_{870}^*$, to which the apparent ^{3}Car* population rate would be expected to drop if they were still observable at all. Besides, with an activation energy of more than 100 cm^{-1} it is not expected that ^{3}Car* should be present at temperatures below 35 K to a measurable extent. Nevertheless, Kolaczkowski reports the ^{3}Car* signals down to less than 15 K (Kolaczkowski, 1989), and zero-field ADMR experiments have revealed the presence of ^{3}Car* as low as 4.2 K with good signal-to-noise ratio (Ullrich, 1988; Ullrich et al., 1989; Angerhofer et al., 1992; Aust, 1995). This points to an alternative population pathway for ^{3}Car* at low temperatures when the thermally activated process is frozen out. Kolaczkowski interpreted it with tunneling based on the temperature independence of the slow ^{3}Car* formation rate below 66 K. However, this is in contradiction with the parallel observation of a much slower decay rate of $^3P_{870}^*$ of the order of 10^4 s^{-1}. A more reasonable explanation is found in the possible heterogeneity of the height of the energy barrier in

the RC samples (Angerhofer, 1997; Angerhofer et al., 1998). It was possible to simulate the observed slow ^{3}Car* formation rate at low temperatures under the assumption of a Gaussian distribution of the energy of $^3B_B^*$ with a half width of 95 cm^{-1} which corresponds to the linewidth of the pigment's Q_y-band in the singlet manifold (Angerhofer, 1997; Angerhofer et al., 1998). Strictly speaking, the assumption of a heterogeneity would make the observed triplet transfer rate non-exponential because a distribution of slightly different rates now combine to the macroscopic observable rate. However, such an effect may go unnoticed given the limited signal/noise ratio of the experiment and a sufficiently narrow distribution function. Furthermore, the assumption of a heterogeneous energy barrier would of course imply that heterogeneity is not only present in the energy of $^3B_B^*$ but also in that of the primary donor triplet $^3P_{870}^*$. With this assumption one can not only understand the peculiar behavior of the ^{3}Car* formation rate at low temperature but also the detection of spheroidene triplet states in wild-type and $^3B_B^*$ in green mutants at low temperatures: There is always a small fraction of the sample in which $^3B_B^*$ is equal or even lower in energy than $^3P_{870}^*$ which would permit triplet energy transfer without thermal activation. One could test this by taking 'excitation spectra' of either the slow ^{3}Car* formation or the spheroidene ADMR spectra at low temperatures, where the narrow band excitation wavelength would be varied across the primary donor absorption band (from 850 to 900 nm). The heterogeneity of the sample should then manifest itself by yielding more ^{3}Car* upon excitation in the blue (towards 850 nm) and less when excited in the red (towards 900 nm), since one would expect the triplet energy of the selected sites to follow the trend in the singlet manifold.

b. Substitution of Carotenoids

Farhoosh et al. (1997) have reported on the successful insertion of spheroidene and two synthetic spheroidene analogs with shorter polyene chains, 3,4-dihydrospheroidene, and 3,4,5,6-tetrahydrospheroidene, having nine and eight conjugated double bonds instead of the ten found in spheroidene. For the singlet manifold electronic absorption spectra and theoretical analysis see Frank and co-workers (Frank et al., 1997; Connors et al., 1993). The estimated triplet energies of these three carotenoids are 7050 cm^{-1}, 7650 cm^{-1}, and 8350 cm^{-1} for decreasing chain lengths. Only spheroidene was able to efficiently quench the primary donor triplet state as found from the light-induced EMR spectra of the three samples. This seems surprising because the mutant *Rb. sphaeroides* G1C contains neurosporene a carotenoid with nine conjugated double bonds which performs as a triplet quencher albeit with relatively low yield and reversible transfer (i.e., back transfer from ^{3}Car* to $^3P_{870}^*$) (Frank et al., 1982a, 1983). Another mutant, GA, containing chloroxanthin, a neurosporene analog with nine conjugated double bonds performs efficient triplet energy transfer at room temperature in both RC (Cogdell et al., 1975) and antenna complexes (Kung and DeVault, 1976). Substitution of methoxyneurosporene into RCs of the green *Rb.* mutant R26 also revealed its effectiveness as a triplet quencher at room temperature (Frank et al., 1986). This indicates that in addition to the total energies of the pigments involved, other parameters are relevant, e.g., orbital overlap which may be modified by a slightly different structural arrangement of the neurosporene analogs in the binding pocket as compared to 3,4-dihydrospheroidene. Also, the point of intersection of the energy hypersurfaces of the BChl monomer B_B and the carotenoids may be different in the two cases, which might result in an extra energy barrier for triplet transfer to 3,4-dihydrospheroidene (Farhoosh et al., 1997). It is interesting to note, however, that incorporation of methoxyneurosporene with nine conjugated double bonds in RCs of *Rb. sphaeroides* R26 resulted in essentially the same optical spectral peaks in both the singlet and triplet manifolds as observed for spheroidene with ten conjugated double bonds (Frank et al., 1986).

It is well known from both early resonance Raman data (Lutz et al., 1976, 1982) as well as the crystal structures (Allen et al., 1988; Yeates et al., 1988; Arnoux et al., 1989, 1995; Ermler et al., 1994a,b) that spheroidene occurs in the 15,15′-*cis* conformation in bacterial RCs. Since the 15-*cis* isomer has a strong tendency for triplet-sensitized *all-trans* conversion (Hashimoto and Koyama, 1988; Hashimoto et al., 1989; Kuki et al., 1991; Koyama and Mukai, 1993) and because there appeared to be indications of *cis*-to-*trans* isomerization in the RC (Boucher and Gingras, 1984), a mechanism of energy dissipation was proposed that involved the twisting of the 15,15′-*cis* double bond into an *all-trans* position (Koyama et al., 1990; Koyama, 1991). To test this

hypothesis Bautista et al. (1998) inserted a synthetic 'locked' 15,15´-*cis* spheroidene analog into RCs of *Rb. sphaeroides* R26.1. Triplet energy transfer proceeded in exactly the same way as in the wild-type or in spheroidene-reconstituted mutants R26.1. This indicates that a twisting motion of the carotenoid is not involved in either triplet transfer or relaxation, and that the 15,15´-*cis* conformation is merely a result of the size and shape of the binding pocket of the protein.

EMR spectra of the locked-15,15´-*cis*-spheroidene showed zero-field splitting values of $|D| = (294 \pm 4) \times 10^{-4}$ cm^{-1} and $|E| = (44 \pm 1) \times 10^{-4}$ cm^{-1} (Bautista et al., 1998) which are virtually identical to those observed from unlocked spheroidene in bacterial RCs (Frank et al., 1980; Chadwick and Frank, 1986). The EMR signals of this preparation, taken at 35 and 100 K, are very similar to those of wild-type RCs indicating that the thermal activation is approximately the same in both samples, i.e., the locked spheroidene performs exactly like the natural unlocked one.

Although the main 15,15´-cis conformation of the spheroidene in RCs of *Rb. sphaeroides* has been well documented, two slightly distinct triplet states appear at temperatures lower than 60 K (Kolaczkowski et al., 1988; Ullrich, 1988). They may be due to different sites that freeze out in slightly different conformations. Possible twists of the portion of the carotenoid that protrudes from the RC have been discussed in this respect. Possible twisting along the conjugated backbone of the carotenoid was indicated by resonance Raman data (Ohashi et al., 1996).

Essentially new carotenoids, e.g., plant carotenoids, can be introduced into the photosynthetic apparatus of purple bacteria by using cloned genes of the biosynthetic pathway (Bartley et al., 1994; Hunter et al., 1994a). In this way it was possible to insert β-carotene into the LH2 complex of *Rb. sphaeroides,* although neither its triplet quenching ability nor its magnetic resonance spectrum have been probed (Hunter et al., 1994a).

c. Site-Selective Mutagenesis of Amino Acid Residues in the Vicinity of B_B

Earlier reports on carotenoid triplet spectra in site-directed mutants found appreciable ^{3}Car* population at temperatures as low as 6 K in the heterodimer mutant M200(His → Leu) of *Rb. capsulatus* (Bylina et al, 1990). This agrees well with the notion of B_B acting as a bridging molecule since in the hetero-dimer mutant the primary donor triplet largely resides on the BChl-half of the special pair rather than the BPh-half, with presumably higher triplet energy than in the wild-type where the triplet wavefunction is delocalized over two BChl molecules. This would naturally lead to a lower barrier for the thermally activated triplet transfer to the carotenoid since it starts out at higher energies. On the other hand, the total triplet yield is very much decreased, owing to the different relaxation pathways in the hetero-dimer compared to the wild-type. Similar results were found for the L_{173}(His → Leu) mutant of *Rb. sphaeroides,* which is essentially the complementary hetero-dimer of the above (Frank et al., 1993b).

Very recently, Laible et al. (1998) carried out an analysis of triplet energy transfer in 21 site-directed mutants of RCs of *Rb. capsulatus.* The mutations were performed at residues L_{181}(Phe) and/or M_{208}(Tyr). Both residues are in the vicinity of the primary donor special pair as well as the two BChl monomers, B_A and B_B, and have previously been shown to influence the primary electron transfer rates, the redox potentials, and the low temperature absorption spectra of these RCs (Jia et al., 1993; DiMagno et al., 1998). Light-modulated EMR experiments demonstrated the wide variability of the efficiency of triplet energy transfer in these preparations (Laible et al., 1998): The changes in the protein may influence the distribution of the electronic wavefunction and overlap of the chromophores (in particular B_B which acts as the triplet transfer bridge) and/or adjust the thermal barrier for triplet energy transfer. In particular, replacement of L_{181}(Phe) with a lysine which donates a sixth ligand to the BChl monomer B_B reduced the transfer efficiency significantly. This may be due to an increase in its triplet energy level which is equivalent to an increased barrier energy for thermal triplet transfer. On the other hand, several polar substitutions at M_{208} increased the triplet transfer efficiency compared to the wild-type. This work is highly significant because it provides first insights into the mechanisms by which the protective function of the RC carotenoid is fine-tuned in vivo.

2. Plant Reaction Centers

The β-carotene radical cation can be induced in RCs of plant Photosystem II (PS II) by illumination of ferricyanide-treated BBY-type RC particles (Noguchi et al., 1994). The radical was observed by FTIR

spectroscopy at 80 K (Noguchi et al., 1994). However, its identification by EMR was not possible, at least not with conventional X-band EMR, due to the spectral overlap with the Chl cation radical which is another redox component of the donor side of PS II (de Paula et al., 1985). Apparently, the photoprotective action of β-carotene in PS II is due to the electron-donating ability of the carotenoid which leads to the reduction of light-induced $P^{+\cdot}_{680}$ and eventual bleaching of β-carotene due to radical formation and further reactions with oxygen (Telfer et al., 1991; De Las Rivas et al., 1993). These radicals have not been directly observed by EMR though because they are difficult to distinguish from $P^{+\cdot}_{680}$.

Carotenoid triplet formation has also been observed in Tris-treated chloroplasts (Kramer, 1980). When PS II RCs are closed (in the Q-state) and at low excitation intensities the ^{3}Car* triplet quantum yield is about 30% of that of P_{680} photooxidation. However, a clear connection of these ^{3}Car* triplet states with the radical-pair recombination mechanism has not been established and they may be actually due to energy transfer from ^{3}Chl* formed in the associated antenna complex. This is also consistent with the finding that carotenoid excited triplet states are efficient quenchers of PS II fluorescence in both plant (Sonneveld et al., 1980) and bacterial antenna systems (Monger and Parson, 1977). The PS II RC complex normally contains two β-carotene molecules. Their presence is essential to prevent rapid light-induced degradation of the PS II D1 protein (Sandmann et al., 1993; Trebst and Depka, 1997). However, they do not quench the triplet state of the primary donor, $^3P_{680}$ which appears in EMR and ODMR spectra of PS II particles and RC preparations (Demetriou et al., 1988; Frank et al., 1989; van der Vos et al., 1992; Angerhofer et al., 1993, 1994).

III. Model Systems

A. Energy Transfer Model Systems

More than a decade ago, Frank et al. (1987) reported on the light-modulated EMR of a number of synthetic porphyrin-polyene model systems that were linked by an amide group and in some cases by methylene spacers of various lengths. The triplet transfer efficiency increased as the link between the two pigments became shorter which is what one would expect, especially for Dexter type triplet exchange which requires overlap of the respective wave-functions. A highly surprising result was reported, i.e., that the ^{3}Car* triplet spin polarization, as measured by light-induced X-band EMR spectroscopy, did not depend on either geometry (ortho-, meta-, and para-substitutions of the polyene on one of the phenyl side groups gave identical results) or central metal substitution of the porphyrin (free base versus Zn-porphyrin, which gives different spin polarization of the porphyrin triplet state) (Frank et al., 1987). These findings could not be adequately explained then. However, more recent studies have revealed that the spin polarization, if not measured immediately after the laser pulse, is solely governed by the intrinsic sublevel decay properties of the carotenoids (Carbonera et al., 1997b). Four different ortho-, meta-, and para-substituted phorphyrin-carotenoid dyads as well as two carotenopyro-pheophorbide (one free base, one Zn-substituted) were investigated. The initial spin-polarization, measured within 1 μs after the laser pulse was found to be quite sensitive to the particular geometry of the compound and to the population probabilities of the triplet donor (Carbonera et al., 1997a,b). Based on the assumption of fast triplet energy transfer from the porphyrin (or pyropheophorbide) to the carotenoid on the time scale of few tens of ns, with conservation of spin angular momentum and negligible dispersion due to the intrinsic sublevel decay kinetics and/or spin lattice relaxation in the donor molecule, the early spin polarized spectra could be simulated using molecular conformations that were suggested to be particularly stable by NMR and molecular mechanics calculations. Apparently, only a selection of the energetically equivalent conformations contributes to the triplet spin polarization pattern. For example, for the para-substition the sum of the rotational angles, ϕ, between the molecular planes of the donor and acceptor pigments assumes only two of four possible energetically equivalent values (0° and 180°, but not 90° and 270°) (Carbonera et al., 1997b). For the carotenopyropheophorbide dyads the results indicate a dihedral angle between the molecular planes of 60° for the Zn-substituted molecule while an all-planar geometry is favored for the free base (Carbonera et al., 1997a).

B. Artificial Electron Transfer Models

Hasharoni et al. (1990) have reported on the observation of a coupled radical pair in a carotenoid-

porphyrin-diquinone tetrad where the cation is located on the carotenoid portion of the molecule. Using 2-pulse FT-EPR it was possible to observe at least some of the broad (compared to the narrow and hyperfine-resolved quinone anion spectra) spectral features of the carotenoid. The reaction proceeds via the singlet pathway which is attested to by the resulting spin polarization of the radical products, and the charge separated state lives for approximately one μs.

The photochemistry of a molecular triad consisting of a porphyrin covalently linked to a carotenoid polyene and a fullerene derivative has been studied at 20 K by time-resolved EMR spectroscopy following laser excitation (Carbonera et al., 1998). Excitation of the porphyrin yields a coupled radical pair with a carotenoid cation and a C_{60} anion. The exchange interation in the pair has been determined to approx. 1.2 G. It decays with a time constant of 1.2 μs into a spin-polarized triplet state of the porphyrin which mimics similar processes observed in photosynthetic RCs.

Many other supermolecules containing carotenoids have been synthesized and their photochemistry characterized (Osuka et al., 1990; Moore et al., 1994; Cardoso et al., 1996), but not yet investigated with EMR. One of these, a carotenoid- porphyrin-quinone triad has been used to demonstrate light-induced vectorial electron transfer across an artificial photosynthetic liposome membrane with subsequent production of ATP catalyzed by F_0F_1-ATPase (Steinberg-Yfrach et al., 1998).

C. Triplet States in Polyenes

A systematic study of retinal and a number of related polyenals has been reported by Groenen's group in Leiden. They applied electron spin echo spectroscopy after a laser excitation flash in both zero fields and X-band to the following polyenes: retinal, tridemethyl retinal, trimethyldodecapentaenal, dimethyldecatetraenal, dodecapentaenal, decatetraenal, octatrienal, hexadienal, 3,7-dimethyloctatrienal, and tetradecahexaenal (Ros and Groenen, 1989, 1991; Ros et al., 1992; Groenen et al., 1992; Kokand Groenen, 1995). Since the experiments were performed by incorporating the polyenals into stretched polyethylene films, it was possible to correlate the fine structure tensor with the molecular structure: the z-axis lies roughly parallel to the polyene molecular axis, y lies in the molecular plane, and x normal to the plane. This agrees with the results from EMR on single crystals of β-carotene (Frick et al., 1990). The triplet states of the polyenals are essentially $\pi\pi^*$ excitations and their population is promoted via the spin-orbit coupling between the oxygen $^1n\pi^*$ and polyene $^3\pi\pi^*$ states (Ros and Groenen, 1991).

The zero field splitting parameters as well as the triplet sublevel decay rates and population probabilities have also been reported in these studies (Ros and Groenen, 1989,1991; Ros et al., 1992; Groenen et al., 1992; Kok and Groenen, 1995). The zero field parameter $|D|$ obeys an inverse linear relationship with (n + 1):

$$|D| \sim \frac{1}{n+1} \tag{1}$$

where n is the number of conjugated double bonds in the polyene chain. Such a relationship is predicted from a simple Hückel model where the triplet wavefunction was approximated by the singly excited configuration in which one electron is promoted from the HOMO to the LUMO (Ros and Groenen, 1991). A similar inverse linear dependency with chain length was reported for the triplet states in bacterial and plant photosynthetic antenna in which the carotenoids are present in *all-trans* conformation (Ullrich et al., 1989; Aust et al., 1991; Angerhofer et al., 1995). Based on the energy gap law which predicts an exponential decrease of the Franck-Condon factors (here for triplet to ground state transitions), the logarithm of the triplet decay rates are expected to obey a similar proportionality, i.e.,

$$\ln k \sim \frac{1}{n+1} \tag{2}$$

which is indeed observed (Kok and Groenen, 1995).

The triplet spin density distribution along the polyene chain of dodecapentaenal has been calculated using the semiempirical MINDO method (Kok and Groenen, 1996). The spin density at carbon 2 has been measured with ESEEM on deuterated molecules and agrees well with these calculations and validates them (Kok and Groenen, 1996).

Essentially similar results, as far as the chain length dependence of the fine structure parameters is concerned, have been found by Bennati et al. (1996a; 1996b) for a series of thiophene oligomers with two to eight thiophene units (4 to 16 conjugated double

bonds). This suggests a similar pattern for other long chain oligomers/polymers, i.e., the localization of the triplet exciton in a confined region on a chain that may in theory be infinitely long. This corresponds to the description of the polaron and/or bipolaron states in polymers (Campbell et al., 1992; Soos et al., 1993).

Transient EMR has also been reported on the triplet state of retinal dissolved in liquid crystalline phase (Münzenmaier et al., 1992). The simulation of the transients with the stochastic Liouville equation provides the motional and order parameters of the pigment. The anisotropy of motional correlation times is high as expected for such an extended linear molecule and the correlation times could be followed with temperature over a range of two orders of magnitude in the nematic and smectic phase.

IV. Carotenoid Radicals

Carotenoids have long been recognized as potent antioxidants and related biological functions for dietary carotenoids have been postulated such as protecting cells and organisms against the harmful effects of light, air, and sensitizer pigments, but also as enhancers of the immune system (Krinsky, 1989, 1993; Rousseau et al., 1992; Bendich, 1993; Ross and Ternus, 1993; Gerster, 1997a,b). In the course of carotenoid-radical interactions (e.g., the quenching of oxygen-centered free radicals) and carotenoid autooxidation, carbon-centered carotenoid radicals may be observed by EMR or other methods (Pryor and Govindan, 1981; Truscott, 1990; Rousseau et al., 1992). As described in other chapters, carotenoid radicals may also occur in photosynthetic systems and take part in some of the photoprotective mechanisms, or may participate as integral parts in the light-induced charge separation in artificial electron transfer chains.

It follows that a detailed knowledge of the carotenoids and their oxidation products is essential to the overall understanding of these processes. For many years Kispert and his group in Tuscaloosa have devoted their efforts to this purpose and to date have carried out numerous EMR-, ENDOR-, optical, and electrochemical studies on a variety of carotenoids, including β-carotene, β-apo-8′-carotenal, and canthaxanthin and some of their derivatives (Kispert et al., 1997).

The oxidation process for β-carotene, β-apo-8′-carotenal, and canthaxanthin in organic solvents as studied by electrochemistry involves the transfer of two electrons from the electrode and subsequent oxidation of neutral carotenoids according to the comproportionation reaction (Khaled et al., 1990):

$$Car^{2+} + Car \overset{K_{com}}{\rightleftharpoons} 2Car^{+\cdot} \qquad (3)$$

The comproportionation constant K_{com} can be measured by simultaneous electrochemistry and EPR (SEEPR) and has been determined not only for the three carotenoids mentioned above (Khaled et al., 1991), but also for the xanthophylls echinenone, isozeaxanthin, and rhodoxanthin (Jeevarajan et al., 1994b). The EMR spectra of the monocations of these pigments are generally found at $g \approx 2.0026$ with a Gaussian half width of the order of 13 to 16 G.

A series of synthetic substituted phenyl-7′-apocarotenoids with varying electron donating and accepting substituents has also been investigated with similar results (Jeevarajan et al., 1994c). The comproportionation constants of these molecules were measured and it was determined that the substituents affect the redox potentials as expected. The introduction of a central triple bond into the polyene chain increases the oxidation potential by about 250 mV and decreases the EMR linewidth by as much as 2.5 G (Jeevarajan et al., 1996a). Again, the *g*-factors of the monocations are as expected for polyenic carbon-centered radicals. The dication is much more stable in the acetylenic carotenoids compared to the exclusively double bonded analogs. AM1 calculated charge distributions show a facile distribution of two excess electrons on the two halves of the polyene chain (separated by the triple bond).

Based on CV and polarography studies it became clear that other reactions take place during an oxidation-reduction cycle, such as cation and dication deprotonation with resulting neutral radicals or cations, as well as other minor and less characterized side reactions (Khaled et al., 1990; Jeevarajan et al., 1994b; Jeevarajan and Kispert, 1996). Further reactions that occur during cation radical and dication formation are geometrical isomerizations with the major isomers found in the 9-*cis* and 13-*cis* configuration (Jeevarajan et al., 1994a; Gao et al., 1996b; Wei et al., 1997). Optical absorption as well as resonance Raman spectra of some of these carotenoid cation radicals and dications have also been reported (Jeevarajan et al., 1996b,c). In the case

of the synthetic carotenoid (7E,7′Z)-diphenyl-7,7′-diapocarotene, a polymerization reaction occurs during the CV cycle with subsequent deposition of a polymer film on the electrode (Gao et al., 1996a, 1997a). Electroactive films of oxidized β-carotene adsorbed on Au electrodes have also been reported (Otero et al., 1991) as well as magnetic field effects on the photoconductivity of β-carotene single crystals (Triebel et al., 1993).

Time-resolved EPR spectroscopy (TREPR) at Q-band (35 GHz) was performed on the products of the light-induced charge separation in CCl_4 of β-carotene, 15,15′-didehydro-β-carotene, 7,7′-dicyano-7′-apo-β-carotene, and 7′-cyano-7′-ethoxycarbonyl-7′-apo-β-carotene (Jeevarajan et al., 1996d). Photoexcitation was performed by an excimer laser pulse (308 nm) and produced a solvent-separated radical ion pair between $CCl_4^{-\cdot}$ and $Car^{+\cdot}$. The polarization of the spectrum can be explained by the radical pair mechanism of CIDEP with singlet precursor. It was concluded that the charge separation is initiated by the excited singlet state of the carotenoid. The Q-band was used because it allowed the resolution of two resolved EMR lines (absorption and emission) which were not visible in X-band (Jeevarajan et al., 1993a).

Photolysis of β-carotene and canthaxanthin in frozen solutions of CCl_4, $CHCl_3$, CH_2Cl_2, and CS_2 occurs with visible to UV light in the wavelength range of 308 to 578 nm and produces paramagnetic species that are stable for days at 77 K (Konovalova et al., 1997). The resulting EMR spectra contain the lines due to carotenoid radical cations in addition to those of the solvent-derived radicals. Photoactivated oxidation and subsequent destruction was also observed using ferric chloride as a catalyst (Gao et al., 1997b).

ENDOR and NMR studies in conjunction with theoretical AM1 and/or INDO studies (in particular RHF-INDO/SP) have contributed greatly to the understanding of the carotenoid radical cation and the description of the charge delocalization along the polyene chain (Piekara-Sady et al., 1991; Hand et al., 1993; Piekara-Sady et al., 1993,1995). An improved crystal structure of β-carotene reported by Senge et al. (1992) has been used and provided the basis for the success of some of the theoretical descriptions. ENDOR studies have also been successfully performed on β-carotene and canthaxanthin radicals produced photochemically on Nafion films and silica gel (Piekara-Sady et al., 1991; Wu et al., 1991), and on β-carotene, canthaxanthin, and 8′-apo-β-carotene-8′-al on activated silica-alumina (Jeevarajan et al., 1993b). They provide strong evidence for the formation of carotenoid radical cations due to electron transfer to the Lewis acid sites on these surfaces. A specific ENDOR line at 6.5 MHz obtained for the carotenoids on solid supports and carotenoid-$AlCl_3$ solution, is attributed to the high-frequency feature of a hyperfine doublet, centered about the ^{27}Al Larmor frequency (Konovalova and Kispert, 1998). ENDOR detection of the hyperfine doublet, instead of the single line at the Larmor frequency, indicates the formation of strong complexes between carotenoid molecules and Lewis acid sites on the surface.

Spin-label substituted short polyenes have also been synthesized and their molecular structure in frozen glass determined by ENDOR spectroscopy (Mustafi et al., 1993). Nitric oxide has been shown to react with β-carotene to yield stable nitroxide radicals that can be detected and analyzed by EMR (Gabr et al., 1995).

In all these studies, one point was proven time and again: Essentially, the wavefunction of the delocalized charge in the carotenoid cation radical spreads over the polyene chain, making it a carbon-centered radical. Structural relaxation occurs in the center of the chain where the bond alternation is markedly suppressed (Kuhn, 1989; Ehrenfreund et al., 1993; Valladares et al., 1993; Loglund and Brédas, 1994; Kawashima et al., 1997). In the language of polymer and solid-state physics the cation is a positive polaron state that is localized in the center of the polyene chain. However, the areas of charge delocalization and bond relaxation are not necessarily the same as found from a study of β-carotene analogs with between 5 and 23 conjugated double bonds (Broszeit et al., 1997).

References

Allen JP, Feher G, Yeates TO, Komiya H and Rees DC (1988) Structure of the Reaction Center from *Rhodobacter sphaeroides* R-26 and 2.4.1. In: Breton J and Verméglio A (eds) The Photosynthetic Bacterial Reaction Center. Structure and Dynamics, pp 5–11. Plenum Press, New York

Ambarsari I, Brown BE, Barlow RG, Britton G and Cummings D (1997) Fluctuations in algal chlorophyll and carotenoid pigments during solar bleaching in the coral *Goniastrea aspera* at Phuket, Thailand. Marine Ecol Prog Ser 159: 303–307

Angerhofer A (1997) Triplettzustände in photosynthetischen Pigment-Protein Komplexen—Untersuchungen mit optisch nachgewiesener Resonanz und Doppelresonanz. Logos Verlag,

Berlin
Angerhofer A and Aust V (1993) A monomeric bacteriochlorophyll triplet state (^{3}B) in reaction centres of *Rhodobacter sphaeroides* R26, studied by absorption-detected magnetic resonance. J Photochem Photobiol B: Biol 20: 127–132
Angerhofer A, Aust V, Hofbauer U and Wolf HC (1992) Triplet energy transfer from bacteriochlorophyll to carotenoids in photosynthetic bacteria. In: Murata N (ed) Research in Photosynthesis, Vol 1, pp 129–132. Kluwer Academic Publishers, Dordrecht
Angerhofer A, Bernlochner D and Robert B (1993) Absorption detected magnetic resonance of D1/D2-complexes from *Pisum sativum.* Z Phys Chem 182: 167–180
Angerhofer A, Friso G, Giacometti GM, Carbonera D and Giacometti G (1994) Optically detected magnetic resonance study on the origin of the pheophytin triplet state in D1/D2-cytochrome *b*-559 complexes. Biochim Biophys Acta 1188: 35–45
Angerhofer A, Bornhäuser F, Gall A and Cogdell RJ (1995) Optical and optically detected magnetic resonance investigation on purple photosynthetic antenna complexes. Chem Phys 194: 259–274
Angerhofer A, Bornhäuser F, Aust V, Hartwich G and Scheer H (1998) Triplet energy transfer in bacterial photosynthetic reaction centres. Biochim Biophys Acta 1365: 404–420
Arnoux B, Ducruix A, Reiss-Husson F, Lutz M, Norris J, Schiffer M and Chan CH (1989) Structure of spheroidene in the photosynthetic reaction center from Y *Rhodobacter sphaeroides.* FEBS Lett 258: 47–50
Arnoux B, Gaucher JF, Ducruix A and Reiss-Husson F (1995) Structure of the photochemical reaction centre of a spheroidene-containing purple bacterium, *Rhodobacter sphaeroides* Y, at 3 Å resolution. Acta Cryst D 51: 368–379
Arsalane W, Rousseau EJ and Duval JC (1994) Influence of the pool size of the xanthophyll cycle on the effects of light stress and photoinhibition. Photochem Photobiol 60: 237–243
Aust V (1995) ADMR und transiente Absorption zum Triplettenergietransfer im bakteriellen Reaktionszentrum. PhD thesis, Universität Stuttgart
Aust V, Angerhofer A, Ullrich J, von Schütz JU, Wolf HC and Cogdell RJ (1991) ADMR of carotenoid triplet states in bacterial photosynthetic antenna and reaction center complexes. Chem Phys Lett 181: 213–221
Bartley GE, Scolnik PA and Giuliano G (1994) Molecular biology of carotenoid biosynthesis in plants. Annu Rev Plant Physiol Mol Biol 45: 287–301
Bautista JA, Chynwat V, Cua A, Jansen FJ, Lugtenburg J, Gosztola D, Wasielewski MR and Frank HA (1998) The spectroscopic and photochemical properties of locked-15,15′*cis*-spheroidene in solution and incorporated into the reaction center of *Rhodobacter sphaeroides* R-26.1. Photosynth Res 55: 49–65
Bendich A (1993) Biological functions of dietary carotenoids. In: Canfield LM, Krinsky NI and Olson JA (eds) Carotenoids in Human Health, pp 61–67. New York Academy of Sciences, New York
Bennati M, Grupp A, Mehring M and Bäuerle P (1996a) Pulsed EPR spectroscopy of the photoexcited triplet states of thiophene oligomers in frozen solution. J Phys Chem 100: 2849–2853
Bennati M, Németh K, Surján PR and Mehring M (1996b) Zero-field-splitting and π-electron spin densities in the lowest excited triplet state of oligothiophenes. J Chem Phys 105:4441–4447
Borland CF, Cogdell RJ, Land EJ and Truscott TG (1989) Bacteriochlorophyll *a* triplet state and its interactions with bacterial carotenoids and oxygen. J Photochem Photobiol B: Biol 3: 237–245
Boucher F and Gingras G (1984) Spectral evidence for photo-induced isomerization of carotenoids in bacterial photoreaction center. Photochem Photobiol 40: 277–281
Broszeit G, Diepenbrock F, Gräf O, Hecht D, Heinze J, Martin HD, Mayer B, Schaper K, Smie A and Strehblow HH (1997) Vinylogous β-carotenes: Generation, storage, and delocalization of charge in carotenoids. Liebigs Ann-Recueil 2205–2213
Budil DE, Taremi SS, Gast P, Norris JR and Frank HA (1988) Single crystal electron spin resonance studies of the photochemical reaction center from *Rhodobacter sphaeroides* wild type strain 2.4.1. Isr J Chem 28: 59–66
Bylina EJ, Kolaczkowski SV, Norris JR and Youvan DC (1990) EPR characterization of genetically modified reaction centers of *Rhodobacter capsulatus.* Biochemistry 29: 6203–6210
Campbell DK, Gammel JT, Lin HQ and Loh, Jr. EY (1992) Triplet states and optical absorptions in finite polyenes and conjugated polymers. Synth Metals 49–50: 631–646
Carbonera D, Giacometti G, Agostini G and Toffoletti A (1989) ESP spectra of a carotenoid pigment triplet in LHCII complexes. Gazz Chim Ital 119: 225–228
Carbonera D, Giacometti G and Agostini G (1992a) FDMR of carotenoid and chlorophyll triplets in light-harvesting complex LHCII of spinach. Appl Magn Reson 3: 859–872
Carbonera D, Giacometti G, Agostini G, Angerhofer A and Aust V (1992b) ODMR of carotenoid and chlorophyll triplets in CP43 and CP47 complexes of spinach. Chem Phys Lett 194: 275–281
Carbonera D, Giacometti G and Agostini G (1995) FDMR Spectroscopy of Peridinin-Chlorophyll-*a* Protein from *Amphidinium carterae.* Spectrochim Acta A 51A: 115–123
Carbonera D, Giacometti G and Segre U (1996) Carotenoid interactions in peridinin chlorophyll *a* proteins from dinoflagellates. Evidence for optical excitons and triplet migration. J Chem Soc Faraday Trans 92: 989–993
Carbonera D, Di Valentin M, Corvaja C, Giacometti G, Agostini G, Liddell PA, Moore AL, Moore TA and Gust D (1997a) Carotenoid triplet detection by time-resolved EPR Spectroscopy in carotenopyropheophorbide dyads. J Photochem Photobiol A: Chem 105: 329–335
Carbonera D, Di Valentin M, Agostini G, Giacometti G, Liddell PA, Gust D, Moore AL and Moore TA (1997b) Energy transfer and spin polarization of the carotenoid triplet state in synthetic carotenoporphyrin dyads and in natural antenna complexes. Appl Magn Res 13: 487–504
Carbonera D, Di Valentin M, Corvaja C, Agostini G, Giacometti G, Liddell PA, Kuciauskas D, Moore AL, Moore TA and Gust D (1998) EPR investigation of photoinduced radical pair formation and decay to a triplet state in a carotene-porphyrin-fullerene triad. J Am Chem Soc 120: 4398–4405
Cardoso SL, Nicodem DE, Moore TA, Moore AL and Gust D (1996) Synthesis and fluorescence quenching studies of a series of carotenoporphyrins with carotenoids of various lengths. J Braz Chem Soc 7: 19–30
Chadwick BW and Frank HA (1986) Electron-spin resonance studies of carotenoids incorporated into reaction centers of

Rhodobacter sphaeroides R26.1. Biochim Biophys Acta 851: 257–266

Cogdell RJ (1985) Carotenoids in photosynthesis. Pure Appl Chem 57: 723–728

Cogdell RJ, Monger TG and Parson WW (1975) Carotenoid triplet states in reaction centers from *Rhodopseudomonas sphaeroides* and *Rhodospirillum rubrum.* Biochim Biophys Acta 408: 189–199

Cogdell RJ, Isaacs NW, Freer AA, Arrelano J, Howard TD, Papiz MZ, Hawthornthwaite-Lawless AM and Prince S (1997) The structure and function of the LH2 (B800-850) complex from the purple photosynthetic bacterium *Rhodopseudomonas acidophila* strain 10050. Prog Biophys Molec Biol 68: 1–27

Connors RE, Burns DS, Farhoosh R and Frank HA (1993) Computational studies of the molecular structure and electronic spectroscopy of Carotenoids. J Phys Chem 97: 9351–9355

De Las Rivas J, Telfer A and Barber J (1993) Two coupled β-carotene molecules protect P680 from photodamage in isolated Photosystem II reaction centres. Biochim Biophys Acta 1142: 155–164

de Paula JC, Innes JB and Brudvig GW (1985) Electron transfer in Photosystem II at cryogenic temperatures. Biochemistry 24: 8114–8120

Demetriou C, Lockett CJ and Nugent JHA (1988) Photochemistry in the isolated Photosystem II reaction-centre core complex. Biochemical J 252: 921–924

Demmig-Adams B and Adams, III WW (1996) The role of xanthophyll cycle carotenoids in the protection of photosynthesis. Trends Plant Sci 1: 21–26

DiMagno TJ, Laible PD, Reddy NR, Small GJ, Norris JR, Schiffer M and Hanson DK (1998) Protein chromophore interactions: spectral shifts report the consequences of mutations in the bacterial photosynthetic reaction center. Spectrochimica Acta A 54: 1247–1267

Ehrenfreund E, Moses D, Lee K, Heeger AJ, Cornil J and Brédas JL (1993) Solitons in doped β-carotene films—optical absorption and ESR studies. Synth Met 57: 4707–4713

Ermler U, Michel H and Schiffer M (1994a) Structure and function of the photosynthetic reaction center from *Rhodobacter sphaeroides.* J Bioenerg Biomembr 26: 5–15

Ermler U, Fritzsch G, Buchanan SK. and Michel H (1994b) Structure of the photosynthetic reaction centre from *Rhodobacter sphaeroides* at 2.65 Å resolution: Cofactors and protein-cofactor interactions. Structure 2: 925–936

Farhoosh R, Chynwat V, Gebhard R, Lugtenburg J and Frank HA (1997) Triplet energy transfer between the primary donor and carotenoids in *Rhodobacter sphaeroides* R-26.1 reaction centers incorporated with spheroidene analogs having different extents of π-electron conjugation. Photochem Photobiol 66: 97–104

Frank HA (1990) Potassium borohydride removes the monomeric bacteriochlorophyll and the carotenoid from reaction centers *of Rhodobacter sphaeroides* wild type strain 2.4.1. Trends Photochem Photobiol 1: 1–4

Frank HA (1992) Electron paramagnetic resonance studies of carotenoids. Meth Enzymol 213: 305–312

Frank HA (1993) Carotenoids in photosynthetic bacterial reaction centers: Structure, spectroscopy, and photochemistry. In: Deisenhofer J and Norris JR(eds) The Photosynthetic Reaction Center, Vol II, pp 221–237. Academic Press, San Diego

Frank HA and Cogdell RJ (1996) Carotenoids in Photosynthesis. Photochem Photobiol 63: 257–264

Frank HA and Violette CA (1989) Monomeric bacteriochlorophyll is required for the triplet energy transfer between the primary donor and the carotenoid in photosynthetic bacterial reaction centers. Biochim Biophys Acta 976: 222–232

Frank HA, Bolt JD, de B. Costa SM and Sauer K (1980) Electron paramagnetic resonance detection of carotenoid triplet states. J Am Chem Soc 102: 4893–4898

Frank HA, Machniki J and Felber M (1982a) Carotenoid triplet states in photosynthetic bacteria. Photochem Photobiol 35: 713–718

Frank HA, McGann WJ, Machniki J and Felber M (1982b) Magnetic field effects on the fluorescence of two reaction centerless mutants of *Rhodopseudomonas capsulata.* Biochem Biophys Res Comm 106: 1310–1317

Frank HA, Machnicki J and Friesner R (1983) Energy transfer between the primary donor bacteriochlorophyll and carotenoids in *Rhodopseudomonas sphaeroides.* Photochem Photobiol 38: 451–455

Frank HA, Chadwick BW, Taremi S, Kolaczkowski S and Bowman M (1986) Singlet and triplet absorption spectra of carotenoids bound in the reaction centers of *Rhodopseudomonas sphaeroides* R26. FEBS Lett 203:157–163

Frank HA, Chadwick BW, Oh JJ, Gust D, Moore TA, Liddell PA, Moore AL, Makings LR and Cogdell RJ (1987) Triplet–triplet energy transfer in B800-850 light-harvesting complexes of photosynthetic bacteria and synthetic carotenoporphyrin molecules investigated by electron spin resonance. Biochim Biophys Acta 892: 253–263

Frank HA, Hansson Ö and Mathis P (1989) EPR and optical changes of the Photosystem II reaction center produced by low temperature illumination. Photosynth Res 20: 279–284

Frank HA, Chynwat V, Hartwich G, Meyer M, Katheder I and Scheer H (1993a) Carotenoid triplet state formation in *Rhodobacter sphaeroides* R-26 reaction centers exchanged with modified bacteriochlorophyll pigments and reconstituted with spheroidene. Photosynth Res 37: 193–203

Frank HA, Innes J, Aldema M, Neumann R and Schenck CC (1993b) Triplet state EPR of reaction centers from the $His^{L173} \rightarrow Leu^{L173}$ mutant of *Rhodobacter sphaeroides* which contains a heterodimer primary donor. Photosynth Res 38: 99–109

Frank HA, Cua A, Chynwat V, Young A, Gosztola D and Wasielewski MR (1994) Photophysics of the carotenoids associated with the xanthophyll cycle in photosynthesis. Photosynth Res 41: 389–395

Frank HA, Cua A, Chynwat V, Young A, Gosztola D and Wasielewski MR (1996a) The lifetimes and energies of the first excited singlet states of diadinoxanthin and diatoxanthin: The role of these molecules in excess energy dissipation in algae. Biochim Biophys Acta 1277: 243–252

Frank HA, Chynwat V, Posteraro A, Hartwich G, Simonin I and Scheer H (1996b) Triplet state energy transfer between the primary donor and the carotenoid in *Rhodobacter sphaeroides* R-26.1 reaction centers exchanged with modified bacteriochlorophyll pigments and reconstituted with spheroidene. Photochem Photobiol 64: 823–831

Frank HA, Desamero RZB, Chynwat V, Gebhard R, van der Hoef I, Jansen FJ, Lugtenburg J, Gosztola D and Wasielewski MR (1997) Spectroscopic properties of spheroidene analogs having different extents of π-electron conjugation. J Phys Chem A 101: 149–157

Freer A, Prince S, Sauer K, Papiz M, Hawthorhthwaite-Lawless

A, McDermott G, Cogdell R and Isaacs NW (1996) Pigment-pigment interactions and energy transfer in the antenna complex of the photosynthetic bacterium *Rhodopseudomonas acidophila.* Structure 4: 449–462

Frick J, von Schütz JU, Wolf HC and Kothe G (1990) First detection of the (nonphosphorescent) triplet state in single crystals of β-carotene. Mol Cryst Liq Cryst 183: 269–272

Gabr I, Patel RP, Symons MCR and Wilson MT (1995) Novel reactions of nitric oxide in biological systems. J Chem Soc Chem. Commun 915–9I6

Gao G, Jeevarajan AS and Kispert LD(1996a) Cyclic voltammetry and spectroelectrochemical studies of cation radical and dication adsorption behavior for 7,7′-diphenyl-7,7′ -diapocarotene. J Electroanal Chem 411: 51–56

Gao G, Wei CC, Jeevarajan AS and Kispert LD (1996b) Geometrical isomerization of carotenoids mediated by cation radical/dication formation. J Phys Chem 100: 5362–5366

Gao G, Wurm DB, Kim YT and Kispert LD (1997a) Electrochemical quartz crystal microbalance, voltammetry, spectroelectrochemical, and microscopic studies of adsorption behavior for (7E,7′ Z)-diphenyI-7,7′ -diapocarotene electrochemical oxidation product. J Phys Chem B 101: 2038–2045

Gao G, Deng Y and Kispert LD (1997b) Photoactivated ferric chloride oxidation of carotenoids by near-UV to visible light. J Phys Chem B 101: 7844–7849

Gerster H (1997a) The potential role of lycopene for human health. J Am Coll Nutr 16: 109–126

Gerster H (I997b) Vitamin A—functions, dietary requirements and safety in humans. Intl J Vit Nutr Res 67: 71–90

Gorman AA, Hamblett I, Lambert C, Spencer B and Standen MC (1988) Identification of both preequilibrium and diffusion limits for reaction of singlet oxygen, $O_2(^1\Delta_g)$, with both physical and chemical quenchers: Variable-temperature, time-resolved infrared luminescence studies. J Am Chem Soc 110: 8053–8059

Groenen EJJ, Kok P and Ros M (1992) From polyenals to retinal: An electron-spin-echo study of the triplet state. Pure Appl Chem 64: 833–839

Groß U (1997) Zeitaufgelöste ODMR an Carotinoidtriplett-zuständen in Antennenkomplexen von Dinoflagellaten. PhD thesis, Universität Stuttgart

Hand ES, Belmore KA and Kispert LD (1993) AM1 electron density and NMR spectral studies of carotenoids with a strong terminal electron acceptor. J Chem Soc Perkin Trans 2: 659–663

Hartwich G, Scheer H, Aust V and Angerhofer A (1995) Absorption and ADMR studies on bacterial photosynthetic reaction centres with modified pigments. Biochim Biophys Acta 1230: 97–113

Hasharoni K, Levanon H, Tang J, Bowman MK, Norris JR, Gust D, Moore TA and Moore AL (1990) Singlet photochemistry in model photosynthesis: Identification of charge separated intermediates by Fourier transform and CW-EPR spectroscopies. J Am Chem Soc 112: 6477–6481

Hashimoto H and Koyama Y (1988) Time-resolved resonance Raman spectroscopy of triplet β-carotene produced from *all-trans,* 7-*cis,* 9-*cis,* and 15-*cis* isomers and high pressure liquid chromatography analyses of photoisomerization via the triplet state. J Phys Chem 92: 2101–2108

Hashimoto H, Koyama Y, Ichimura K and Kobayashi T (1989) Time-resolved absorption spectroscopy of the triplet state produced from the *all-trans,* 7-*cis,* 9-*cis,* 13-cis, and 15-*cis* isomers of β-carotene. Chem Phys Lett 162: 517–522

Heinze I, Pfündel E, Hühn M and Dau H (1997) Assembly of light harvesting complexes II (LHC-II) in the absence of lutein. A study on the α-carotenoid-free mutant C-2A′-34 of the green alga *Scenedesmus obliquus.* Biochim Biophys Acta 1320:188–194

Hofmann E, Wrench PM, Sharples FP, Hiller RG, Welte W and Diederichs K (1996) Structural basis of light harvesting by carotenoids: Peridinin-chlorophyll-protein from *Amphidinium carterae.* Science 272: 1788–1791

Hunter CN, Hundle BS, Hearst JE, Lang HP, Gardiner AT, Takaichi S and Cogdell RJ (1994a) Introduction of new carotenoids into the bacterial photosynthetic apparatus by combining the carotenoids biosynthetic pathways of *Erwinia herbicola* and *Rhodobacler sphaeroides.* J Bact 176: 3692–3697

Hunter CN, Artymiuk PJ and van Amerongen H (1994b) Many chlorophylls make light work. Curr Biol 4: 344–346

Jeevarajan JA and Kispert LD(1996) Electrochemical oxidation of carotenoids containing donor/acceptor substituents. J Electroanal Chem 411: 57–66

Jeevarajan AS, Khaled M, Forbes MDE and Kispert LD (1993a) CIDEP studies of carotenoid radical cations. Z Phys Chem 182: 51–61

Jeevarajan AS, Kispert LD and Piekara-Sady L (1993b) An ENDOR study of carotenoid cation radicals on silica-alumina solid supports. Chem Phys Lett 209: 269–274

Jeevarajan AS, Wei CC and Kispert LD (1994a) Geometrical isomerization of carotenoids in dichloromethane. J Chem Soc Perkin Trans 2: 861–869

Jeevarajan AS, Khaled M and Kispert LD (1994b) Simultaneous electrochemical and electron paramagnetic resonance studies of keto and hydroxy carotenoids. Chem Phys Lett 225: 340–345

Jeevarajan AS, Khaled M and Kispert LD (1994c) Simultaneous electrochemical and electron paramagnetic resonance studies of carotenoids: Effect of electron donating and accepting substituents. J Phys Chem 98: 7777–7781

Jeevarajan JA, Jeevarajan AS and Kispert LD (1996a) Electrochemical EPR and AM 1 studies of acetylenic and ethylenic carotenoids. J Chem Soc Faraday Trans 92: 1757–1765

Jeevarajan JA, Wei CC, Jeevarajan AS and Kispert LD (1996b) Optical absorption spectra of dications of carotenoids. J Phys Chem 100: 5637–5641

Jeevarajan AS, Kispert LD, Chumanov G, Zhou C and Cotton TM (1996c) Resonance Raman study of carotenoid cation radicals. Chem Phys Lett 259: 515–522

Jeevarajan AS, Kispert LD, Avdievich NI and Forbes MDE (1996d) Role of excited singlet state in the photooxidation of carotenoids: a time-resolved Q-band EPR study. J Phys Chem 100: 669–671

Jia YW, DiMagno TJ, Chan CK, Wang Z, Du M, Hanson DK, Schiffer M, Norris JR, Fleming GR and Popov MS (1993) Primary charge separation in mutant reaction centers of *Rhodobacter capsulatus.* J Phys Chem 97: 13180–13191

Jirsakova V, Reiss-Husson F, van Dijk B, Owen G and Hoff AJ (1996a) Characterization of carotenoid triplet state in the light-harvesting complex B800-850 from the purple bacterium *Rubrivivax gelatinosus.* Photochem Photobiol 64: 363–368

Jirsakova V, Reiss-Husson F, Agalidis I, Vrieze J and Hoff AJ (I996b) Triplet-states in reaction-center, light-harvesting complex B875 and its spectral form B840 from *Rubrivivax gelatinosus* investigated by absorbency-detected electron-spin-resonance in zero magnetic-field (ADMR). Biochim Biophys Acta 1231: 313–322

Kawashima Y, Nakayama K, Nakano H and Hirao K (1997) Theoretical study of the $\pi \rightarrow \pi^*$ excited states of linear polyene radical cations and dications. Chem Phys Lett 267: 82–90

Khaled M, Hadjipetrou A and Kispert L (1990) Electrochemical and electron paramagnetic resonance studies of carotenoid cation radicals and dications: Effect of deuteration. J Phys Chem 94: 5164–4169

Khaled M, Hadjipetrou A, Kispert L and Allendoerfer RD (1991) Simultaneous electrochemical and electron paramagnetic resonance studies of carotenoid radicals and dications. J Phys Chem 95: 2438–2442

Kingma H, van Grondelle R and Duysens LNM (1985a) Magnetic-field effects in photosynthetic bacteria I. Magnetic-field-induced bacteriochlorophyll emission changes in the reaction center and the antenna of *Rhodospirillum rubrum, Rhodopseudomonas sphaeroides* and *Prosthecochloris aestuarii.* Biochim Biophys Acta 808: 363–382

Kingma H, van Grondelle R and Duysens LNM (1985b) Magnetic-field effects in photosynthetic bacteria. II. Formation of triplet states in the reaction center and the antenna of *Rhodospirillum rubrum* and *Rhodopseudomonas sphaeroides.* Magnetic-field effects. Biochim Biophys Acta 808: 383–399

Kispert LD, Gao G, Deng Y, Konovalov V, Jeevarajan AS, Jeevarajan JA and Hand E (1997) Carotenoid radical cations, dications, and radical trications. Acta Chem Scand 51: 572–578

Koepke J, Hu X, Muenke C, Schulten K and Michel H (1996) The crystal structure of the light-harvesting complex II (B800-850) from *Rhodospirillum molischianum.* Structure 4: 581–597

Kok P and Groenen EJJ (1995) The lowest triplet state of tetradecahexaenal. Recl Trav Chim Pays-Bas 114: 425–429

Kok P and Groenen EJJ (1996) The triplet spin-density distribution along a polyene chain: An electron-spin-echo study of deuterododecapentaenal. J Am Chem Soc 118: 7790–7794

Kolaczkowski SV (1989) On the mechanism of triplet energy transfer from the triplet primary donor to spheroidene in photosynthetic reaction centers from *Rhodobacter sphaeroides* 2.4.1. PhD thesis, Brown University

Kolaczkowski SV, Budil DB, Bowman MK and Norris JR (1988) Effects of deuteration on photosynthetic reaction centers: Radical pair recombination rate, triplet energy transfer, and carotenoid triplet EPR spectra. Biophys J 53: 614a

Konovalova TA and Kispert LD (1998) EPR and ENDOR studies of carotenoid-solid Lewis acid interactions. J Chem Soc Faraday Trans 94: 1465–1468

Konovalova TA, Kispert LD and Konovalov VV (1997) Photoinduced electron transfer between carotenoids and solvent molecules. J Phys Chem B 101: 7858–7862

Koyama Y (1991) Structures and functions of carotenoids in photosynthetic systems. J Photochem Photobiol B: Biol 9: 265–280

Koyama Y and Mukai Y (1993) Excited states of retinoids, carotenoids and chlorophylls as revealed by time-resolved, electronic absorption and resonance Raman spectroscopy. In: Clark RJH and Hester RE (eds) Biomolecular Spectroscopy, Vol 21, Part B, pp49–137. John Wiley and Sons Ltd, Chichester

Koyama Y, Takatsuka I, Kanaji M, Tomimoto K, Kito M, Shimamura T, Yamashita J, Saiki K and Tsukida K (1990) Configurations of carotenoids in the reaction center and the light-harvesting complex of *Rhodospirillum rubrum.* Natural selection of carotenoid configurations by pigment protein complexes. Photochem Photobiol 51: 119–128

Koyama Y, Kuki M, Andersson PO and GillbroT (1996) Singlet excited states and the light-harvesting function of carotenoids in bacterial photosynthesis. Photochem Photobiol 63: 243–256

Kramer H (1980) Quantum yield and rate of formation of the carotenoid triplet state in photosynthetic structures. Biochim Biophys Acta 593: 319–329

Krinsky NI (1989) Antioxidant functions of carotenoids. Free Rad Biol Med 7: 617–635

Krinsky NI (1993) Actions of carotenoids in biological systems. Annu Rev Nutr 13:561–587

Kühlbrandt W (1994) Structure and function of the plant light-harvesting complex LHCII. Curr Op Struct Biol 4: 519–528

Kühlbrandt W, Wang DN and Fujiyoshi Y (1994) Atomic model of plant light-harvesting complex by electron crystallography. Nature 367: 614–621

Kuhn C (1989) Solitons, polarons, and excitons in polyacetylene: Step-potential model for electron-phonon coupling in π-electron systems. Phys Rev B 40: 7776–7787

Kuki M, Koyama Y and Nagae H (1991) Triplet-sensitized and thermal isomerization of *all-trans,* 7-*cis,* 9-*cis,* 13-*cis*, and 15-*cis* isomers of β-carotene: Configurational dependence of the quantum yield of isomerization via the T_1 state. J Phys Chem 95: 7171–7180

Kung MC and DeVault D (1976) Carotenoid triplet state in *R. spheroides* GA Chromatophores. Photochem Photobiol 24: 87–91

Laible PD, Chynwat V, Thurnauer MC, Schiffer M, Hanson DK and Frank HA (1998) Protein modifications affecting triplet energy transfer in bacterial photosynthetic reaction centers. Biophys J 74: 2623–2637

Lambert C and Redmond RW (1994) Triplet energy level of β-carotene. Chem Phys Lett 228: 495–498

Löglund M and Brédas JL (1994) Theoretical analysis of the charge-storage states in diphenylpolyenes with one to seven double bonds. J Chem Phys 100: 6543–6549

Lous EJ and Hoff AJ (1989) Isotropic and linear dichroic triplet-minus-singlet absorbance difference spectra of two carotenoid-containing bacterial photosynthetic reaction centers in the temperature range 10–288 K. An analysis of bacterio-chlorophyll-carotenoid triplet transfer. Biochim Biophys Acta 974: 88–103

Lutz M, Kleo J and Reiss-Husson F (1976) Resonance Raman scattering of bacteriochlorophyll, bacteriopheophytin and spheroidene in reaction centers of *Rhodopseudomonas spheroides.* Biochem Biophys Res Comm 69: 711–717

Lutz M, Chinsky L and Turpin PY (1982) Triplet states of carotenoids bound to reaction centers of photosynthetic bacteria: Time-resolved resonance Raman spectroscopy. Photochem Photobiol 36: 503–515

Mathis P (1966) Variation d'absorption de courte durée, induite dans une suspension de chloroplastes par un éclair laser. C. R. Acad. Sci Paris D 263: 1770–1772

Mathis P and Galmiche JM (1967) Action des gaz paramagnétiques sur un état transitoire induit par un éclair laser dans une suspension de chloroplasts. C R Acad Sci Paris D 264: 1903–1906

McGann WJ and Frank HA (1983) Magnetic field effects on the fl uorescence of mutant strains of *Rhodopseudomonas capsulata.* Biochim Biophys Acta 725: 178–189

McGann WJ and Frank HA (1985) Transient electron spin resonance spectroscopy of the carotenoid triplet state in *Rhodopseudomonas sphaeroides* wild type, Chem Phys Lett 121: 253–261

Monger TG and Parson WW (1977) Singlet-triplet fusion in *Rhodopseudomonas sphaeroides* chromatophores. A probe of the organization of the photosynthetic apparatus. Biochim Biophys Acta 460: 393–407

Monger TG, Cogdell RJ and Parson WW (1976) Triplet states of bacteriochlorophyll and carotenoids in chromatophores of photosynthetic bacteria. Biochim Biophys Acta 449: 136–153

Moore TA, Gust D and Moore AL (1994) Carotenoids—natures unique pigments for light and energy processing. Pure Appl Chem. 66: 1033–1040

Münzenmaier A, Rösch N, Weber S, Feller C, Ohmes E and Kothe G (1992) Transient EPR of the spin-polarized triplet states of chlorophyll and retinal in liquid crystalline matrix: Characterization of the overall and librational pigment dynamics. J Phys Chem 96: 10646–10653

Mustafi D, Boisvert WE and Makinen MW (1993) Synthesis of conjugated polyene carbonyl derivatives of nitroxyl spin–labels and determination of their molecular structure and conformation by electron nuclear double resonance. J Am Chem Soc 115: 3674–3682

Naqvi KR, Melá TB, Raju BB, Jøvrofi T, Simidjiev I and Garab G (1987) Quenching of chlorophyll *a* singlets and triplets by carotenoids in light-harvesting complex of Photosystem II: Comparison of aggregates with trimers. Proc Natl Acad Sci USA 84: 109–112

Naruse M, Hashimoto H.Kuki M and KoyamaY (1991) Triplet excitation of precursors of spirilloxanthin bound to the chromatophores of *Rhodospirillum rubrum* as detected by transient Raman spectroscopy. J Mol Struct 242: 15–26

Noguchi T, Mitsuka T and Inoue Y (1994) Fourier transform infrared spectrum of the radical cation of β-carotene photoinduced in Photosystem II. FEBS Lett 356: 179–182

Nuijs AM, van Bochove AC, Joppe HLP and Duysens LNM (1984) Picosecond carotenoid triplet formation in the antenna of *Rhodospirillum rubrum* as measured by absorbance difference spectroscopy. In: Sybesma C (ed) Advances in Photosynthesis Research, Vol I, pp 65–68, Martinus Nijhoff Publishers, The Hague

Nuijs AM, van Grondelle R, Joppe HLP, van Bochove AC and Duysens LNM (1985) Singlet and triplet excited carotenoid and antenna bacteriochlorophyll of the purple photosynthetic bacterium *Rhodospirillum rubrum* as studied by picosecond absorbance difference spectroscopy. Biochim Biophys Acta 810: 94–105

Ohashi N, Ko-chi N, Kuki M, Shimamura T, Cogdell RJ and Koyama Y (1996) The structures of S_0 spheroidene in the light-harvesting (LH2) complex and S_0 and T_1 spheroidenein the reaction center of *Rhodobacter sphaeroides* 2.4.1 as revealed by Raman spectroscopy. Biospectroscopy 2: 59–69

Osuka A, Yamada H and Maruyama K (1990) Synthesis of conformationally restricted carotenoid-linked porphyrins. Chem Lett 1905–1908

Otero L, Silber JJ and Sereno L (1991) Electrooxidation of β-carotene in chlorinated solvents. The formation of an electroactive film on gold electrodes. J Electroanal Chem 319: 415–422

Papiz MZ, Prince SM, McDermott G, Hawthornthwaite-Lawless AM, Freer A A, Isaacs NW and Cogdell RJ (1996) A model for the photosynthetic apparatus of purple bacteria. Trends Plant Sci 1: 198–206

Paulsen H, Rümler U and Rüdiger W (1990) Reconstitution of pigment-containing complexes from light-harvesting chlorophyll *a/b*-binding protein overexpressed in *Escherichia coli.* Planta 181: 204–211

Peterman EJG, Dukker FM, van Grondelle R and van Amerongen H (1995) Chlorophyll *a* and carotenoid triplet states in light-harvesting complex II of higher plants. Biophys J 69: 2670–2678

Peterman EJG, Gradinaru CC, Calkoen F, Borst JC, van Grondelle R and van Amerongen H (1997) Xanthophylls in light-harvesting complex II of higher plants: Light-harvesting and triplet quenching. Biochemistry 36: 12208–12215

Pfündel E and Bilger W (1994) Regulation and possible function of the violaxanthin cycle. Photosynth Res 42: 89–109

Piekara-Sady L, Khaled MM, Bradford E and Kispert LD (1991) Comparison of the INDO to the RHF-INDO/SP derived EPR proton hyperfine couplings for the carotenoid cation radical: experimental evidence. Chem Phys Lett 186: 143–148

Piekara-Sady L, Jeevarajan AS and Kispert LD (1993) An ENDOR study of the canthaxanthin cation radical in solution. Chem Phys Lett 207: 173–177

Piekara-Sady L, Jeevarajan AS, Kispert LD, Bradford EG and Plato M (1995) ENDOR study of the (7′,7′-dicyano)-7′-apo-β-carotene and (7′-phenyl)-7′-apo-β-carotene radical cations formed by UV photolysis of carotenoids adsorbed on silica-gel. J Chem Soc Faraday Trans 91: 2881–2884

Plumley FG and Schmidt GW (1987) Reconstitution of chlorophyll *a/b* light-harvesting complexes: Xanthophyll-dependent assembly and energy transfer. Proc Natl Acad Sci USA 84: 146–150

Pryor W A and Govindan CK (1981) Decomposition of triphenyl phosphite ozonide in the presence of spin traps. J Org Chem 45: 4679–4682

Psencik J, Searle GFW, Hala J and Schaafsma TJ (1994) Fluorescence-detected magnetic resonance (FDMR) of green sulfur photosynthetic bacteria *Chlorobium* sp. Photosynth Res 40: 1–10

Rademaker H, Hoff AJ, van Grondelle R and Duysens LNM (1980) Carotenoid triplet yields in normal and deuterated *Rhodospirillum rubrum.* Biochim Biophys Acta 592: 240–257

Reiss-Husson F and Mäntele W (1988) Spectroscopic characterization of reaction center crystals from the carotenoid-containing wild-type strain *Rhodobacter sphaeroides* Y. FEBS Lett 239: 78–82

Renger G and Wolff C (1977) Further evidence for dissipative energy migration via triplet states in photosynthesis. The protective mechanism of carotenoids in *Rhodopseudomonas spheroides* chromatophores. Biochim Biophys Acta 460: 47–57

Ricci M, Bradforth SE, Jimenez R and Fleming GR (1996) Internal conversion and energy transfer dynamics of

spheroidene in solution and in the LH-1 and LH-2 light-harvesting complexes. Chem Phys Lett 259: 381–390

Ros M and Groenen EJJ (1989) The triplet state of dodecapentaenal: Electron spin echo spectroscopy of a polyenal. Chem Phys Lett 154: 29–33

Ros M and Groenen EJJ (1991) An electron-spin-echo study of the nonradiative triplet state of polyenals. J Chem Phys 94: 7640–7648

Ros M, Hogenboom MA, Kok P and Groenen EJJ (1992) Electronic structure of retinal and related polyenals in the lowest triplet state: an electron spin echo study. J Phys Chem 96: 2975–2982

Ross AC and Ternus ME (1993) Vitamin A as a hormone: Recent advances in understanding the actions of retinol, retinoic acid, and beta carotene. J Am Diet Assoc 93: 1285–1290

Rousseau EJ, Davison AJ and Dunn B (1992) Protection by β-carotene and related compounds against oxygen-mediated cytotoxicity and genotoxicity: Implications for carcinogenesis and anticarcinogenesis. Free Rad Biol Med 13: 407–433

Sandmann G, Kuhn M and Böger P (1993) Carotenoids in photosynthesis: Protection of D1 degradation in the light. Photosynth Res 35: 185–190

Scheer H and Struck A (1993) Bacterial reaction renters with modified tetrapyrrole chromophores. In: Deisenhofer J and Norris JR (eds) The Photosynthetic Reaction Center, Vol I, pp 157–192. Academic Press, San Diego

Schenck CC, Mathis P and Lutz M (1984) Triplet formation and triplet decay in reaction centers from the photosynthetic bacterium *Rhodopseudomonas sphaeroides.* Photochem Photobiol 39: 407–417

Senge MO, Hope H and Smith KM (1992) Structure and conformation of photosynthetic pigments and related compounds 3. Crystal structure of β-carotene. Z Naturforsch 47c: 474–476

Shuvalov VA and Parson WW (1981) Energies and kinetics of radical pairs involving bacteriochlorophyll and bacteriopheophytin in bacterial reaction centers. Proc Natl Acad Sci USA 78: 957–961

Siefermann-Harms D (1985) Carotenoids in photosynthesis. I. Location in photosynthetic membranes and light-harvesting function. Biochim Biophys Acta 811: 325–355

Siefermann-Harms D (1987) The light-harvesting and protective functions of carotenoids in photosynthetic membranes. Physiol Plantarum 69: 561–568

Siefermann-Harms D (1990a) Chlorophyll, carotenoids and the activity of the xanthophyll cycle. Environ Pollut 68: 293–303

Siefermann-Harms D (1990b) Photooxidation and pheophytin formation of chlorophyll in the light-harvesting Chl-*a/b*-protein complex exposed to fatty acids: Protective role of the intact apoprotein. In: Baltscheffsky M (ed) Current Research in Photosynthesis, Vol II, pp 245–248. Kluwer Academic Publishers, Dordrecht

Siefermann-Harms D (1990c) Protective function of the apoprotein of the light-harvesting chlorophyll-*a/b*-protein complex in pigment photo-oxidation. J Photochem Photobiol B: Biol 4: 283–295

Siefermann-Harms D and Angerhofer A (1995) An O_2-barrier in the light-harvesting Chl-*a/b*-protein complex LHCII protects chlorophylls and carotenoids from photooxidation. In: Mathis P (ed) Photosynthesis: From Light to Biosphere, Vol IV, pp 71–74. Kluwer Academic Publishers, Dordrecht

Siefermann-Harms D and Angerhofer A (1998) Evidence for an O_2-barrier in the light-harvesting chlorophyll-*a/b*-protein complex LHCII. Photosynth Res 55: 83–94

Sonneveld A, Rademaker H and Duysens LNM (1980) Transfer and trapping of excitation energy in Photosystem II as studied by chlorophyll a_2 fluorescence quenching by dinitrobenzene and carotenoid triplet. The matrix model. Biochim Biophys Acta 593: 272–289

Soos ZG, Ramasesha S, Galvnõ DS, Kepler RG and Etemad S (1993) Electronic excitations and alternation of conjugated polymers. Synth. Metals 54: 35–47

Steinberg-Yfrach G, Rigaud JL, Durantini EN, Moore AL, Gust D and Moore TA (1998) Light-driven production of ATP catalysed by F_0F_1-ATP synthase in an artificial photosynthetic membrane. Nature 392: 479–482

Struck A and Scheer H (1990) Modified reaction centers from *Rhodobacter sphaeroides* R26: Exchange of monomeric bacteriochlorophyll with 13^1-hydroxy-bacteriochlorophyll. FEBS Lett 261: 385–388

Struck A, Beese D, Cmiel E, Fischer M, Müller A and Schäfer W (1990a) Modified Bacterial Reaction Centers: 3. Chemical Modified Chromophores at Sites B_A, B_B and H_A, H_B. In: Michel-Beyerle ME (ed) Reaction Centers of Photosynthetic Bacteria, pp 313–326. Springer, Berlin

Struck A, Cmiel E, Katheder I and Scheer H (1990b) Modified reaction centers from *Rhodobacter sphaeroides* R26. 2: Bacteriochlorophylls with modified C-3 substituents at sites B_A and B_B . FEBS Lett 268: 180–184

Struck A, Müller A and Scheer H (1991) Modified bacterial reaction centers. 4. The borohydride treatment reinvestigated: comparison with selective exchange experiments at binding sites $B_{A,B}$ and $H_{A,B}$. Biochim Biophys Acta 1060: 262–270

Takiff L and Boxer SG (1988a) Phosphorescence from the primary electron donor in *Rhodobacter sphaeroides* and *Rhodopseudomonas viridis* reaction centers. Biochim Biophys Acta 932: 325–334

Takiff L and Boxer SG (1988b) Phosphorescence spectra of bacteriochlorophylls. J Am Chem Soc 110: 4425–4426

Telfer A, De Las Rivas J and Barber J (1991) β-carotene within the isolated Photosystem II reaction centre: Photooxidation and irreversible bleaching of this chromophore by oxidised P680. Biochim Biophys Acta 1060: 106–114

Trebst A and Depka B (1997) Role of carotene in the rapid turnover and assembly of Photosystem II in *Chlamydomonas reinhardtii.* FEBS Lett 400: 359–362

Triebel M, Batalov S, Frankevich E, Angerhofer A, Frick J, von Schütz JU and Wolf HC (1993) Magnetic field effects on the photoconductivity of *all-trans* β-carotene single crystals. Z Phys Chem 180: 209–221

Truscott TG (1990) The photophysics and photochemistry of the carotenoids. J Photochem Photobiol B: Biol. 6: 359–371

Ullrich J (1988) Temperaturabhängige ADMR Untersuchungen an Triplettzuständen in den Reaktionszentren photosynthetisierender Bakterien. PhD thesis, Universität Stuttgart

Ullrich J, von Schütz JU and Wolf HC (1988) Absorption detected magnetic resonance in zero magnetic field on antenna complexes from *Rps. acidophila* 7050—the temperature dependence of the carotenoid triplet state properties. In: Scheer H and Schneider S (eds) Photosynthetic Light-Harvesting Systems, pp 339–347. Walter de Gruyter and Co., Berlin

Ullrich J, Speer R, Greis J, von Schütz JU, Wolf HC and Cogdell

RJ (1989) Carotenoid triplet states in pigment-protein complexes from photosynthetic bacteria: Absorption-detected magnetic resonance from 4 to 225 K. Chem Phys Lett 155: 363–370

Valladares RM, Hayes W, Fisher AJ and Stoneham AM (1993) Defect electronic states in β-carotene and lower homologues. J Phys Condons Matter 5: 7049–7062

van der Vos R, Carbonera D and Hoff AJ (1991) Microwave and optical spectroscopy of carotenoid triplets in light-harvesting complex LHC II of spinach by absorbance-detected magnetic resonance. Appl Magn Reson 2: 179–202

van der Vos R, van Leeuwen PJ, Braun P and Hoff AJ (1992) Analysis of the optical absorbance spectra of D1-D2-cytochrome b-559 complexes by absorbance-detected magnetic resonance. Structural properties of P680. Biochim Biophys Acta 1140: 184–198

van der Vos R, Franken EM and Hoff AJ (1994) ADMR study of the effect of oligomerization on the carotenoid triplets and on triplet-triplet transfer in light-harvesting complex-II (LHC-II) of spinach. Biochim Biophys Acta 1188: 243–250

Wei CC, Gao G and Kispert LD (1997) Selected *cis/trans* isomers of carotenoids formed by bulk electrolysis and iron(III) chloride oxidation. J Chem Soc Perkin Trans 2 pp 783–786

Wolff C and Witt HT (1969) On metastable states of carotenoids in primary events of photosynthesis. Z Naturforsch 24b: 1031–1037

Wu Y, Piekara-Sady L and Kispert LD (1991) Photochemically generated carotenoid radicals on Nafion film and silica gel: An EPR and ENDOR study. Chem Phys Lett 180: 573–577

Yeates TO, Komiya H, Chirino A, Rees DC, Allen JP and Feher G (1988) Structure of the reaction center from *Rhodobacter sphaeroides* R-26 and 2.4.1: Protein-cofactor (bacterio-chlorophyll, bacteriopheophytin, and carotenoid) interactions. Proc Natl Acad Sci USA 85: 7993–7997

Young AJ (1991) The photoprotective role of carotenoids in higher plants. Physiol Plant 83: 702–708

Young AJ and Frank HA (1996) Energy transfer reactions involving carotenoids: Quenching of chlorophyll fluorescence. J Photochem Photobiol B: Biol 36: 3–15

Chapter 12

Carotenoid Radicals and the Interaction of Carotenoids with Active Oxygen Species

Ruth Edge and T. George Truscott
Chemistry Department, Keele University, Staffs, ST5 5BG, U.K.

Summary

Carotenoid radicals are generated from the interaction of a wide range of carotenoids with several oxy-radicals, such as $CCl_3O_2^{\bullet}$, $RSO_2^{\bullet}$, $NO_2^{\bullet}$, and various aryl peroxyl radicals, while less strongly oxidizing radicals, such as alkyl peroxyl radicals, can lead to hydrogen atom transfer, thereby generating the neutral carotene radical. Comparison of the relative abilities of many pairs of carotenoids to donate/accept electrons: $CAR1^{\bullet+} + CAR2 \rightarrow CAR1 + CAR2^{\bullet+}$, has allowed the relative oxidation potentials to be established, showing that lycopene is the easiest carotenoid to oxidize to its cation radical and astaxanthin is the most difficult.

The interaction of carotenoids and carotenoid radicals with other anti-oxidants is of importance with respect to anti-oxidative and possibly pro-oxidative reactions of carotenoids. All the radical cations of the carotenoids studied reacted with vitamin C so as to 'repair' the carotenoid (e.g. in methanol, $CAR^{\bullet+} + AscH_2 \rightarrow CAR + AscH^{\bullet} + H^+$). In polar environments the vitamin E radical cation is deprotonated ($TOH^{\bullet+} \rightarrow TO^{\bullet} + H^+$) and $TO^{\bullet}$ does not react with carotenoids, whereas in non-polar environments, $TOH^{\bullet+}$ is converted into TOH by hydrocarbon carotenoids. In all solvents studied, singlet oxygen is efficiently quenched by carotenoids that have appropriate low-lying triplet energy levels $^1O_2^* + CAR \rightarrow {}^3O_2 + {}^3CAR^*$. However, such reactions are still to be observed in vivo.

H. A. Frank, A. J. Young, G. Britton and R. J. Cogdell (eds): The Photochemistry of Carotenoids, pp. 223–234.

I. Introduction

Of the 600 or so carotenoids found in nature, about 40 are regularly consumed by humans. Carotenoids are commonly found in yellow, orange and green fruit and vegetables, and naturally occurring carotenoids, either synthetic or from natural sources, are added to food to enhance color. Amongst the carotenoids often used as colorants are β-carotene, lycopene, lutein, astaxanthin and canthaxanthin.

Interest in the radicals of carotenoids is partly due to a possible role in photosynthesis; they are certainly detected under conditions when the Photosystem II reaction center is photoactivated and $P680^{\bullet+}$ can accumulate. Under these conditions there is an electron transfer reaction from β-carotene to $P680^{\bullet+}$ and the β-carotene is oxidized to its radical cation $CAR^{\bullet+}$ (Telfer et al., 1991). Carotenoid radicals arise in systems designed to model the processes that occur in the reaction center (Gust et al., 1993; Steinberg-Yfrach et al., 1997). However, the major reason for the current interest in carotenoid radicals is their formation following quenching of free radicals by the carotenoid. It has been shown that both anti-oxidative and pro-oxidative processes can arise from such reactions (Burton and Ingold, 1984). The proposed role of the dietary carotenoids in man with respect to disease prevention and the use of carotenoids as food supplements and colorants may well be related to such reactions.

It is well known that carotenoids can act as anti-oxidants by quenching singlet oxygen or photo-sensitizer triplet states and that this protective role of carotenoids is important in photosynthesis and probably in the treatment of the acute skin photosensitivity associated with a hereditary form of porphyric disease known as erythropoietic proto-porphyria (epp). In epp protoporphyrin accumulates in the skin and the use of β-carotene can ameliorate the photosensitivity presumably by quenching either or both the protoporphyrin triplet state and singlet oxygen. The mechanism of the singlet oxygen quenching process is well established and such reactions have recently been extended to the protection of human lymphocyte cells by membrane bound dietary carotenoids (Tinkler et al., 1994). However, the role of carotenoids as free radical quenchers is far less well understood, as is the reason for the switch in behavior of carotenoids from anti-oxidants to pro-oxidants under some conditions.

For many years it has been accepted that the epidemiological evidence suggests that a diet rich in β-carotene (and according to more recent reports, lycopene) is associated with decreased incidence of many important diseases including cancer, athero-sclerosis, age-related macular degeneration (ARMD) and multiple sclerosis. It is suggested that this may occur via prevention of lipid peroxidation. The carotenoids in the eye are the xanthophylls, zeaxanthin and lutein. The reason for this selectivity of carotenoids in the macula of the eye is not clear but is discussed below, as is the surprising claim that the ingestion of increased amounts of lycopene, which is not detected in the eye, offers protection against ARMD. The general acceptance of a beneficial role of carotenoids has been seriously challenged by the recent results from clinical trials that suggest deleterious effects of administered β-carotene in certain groups such as heavy smokers, (see, for example, The α-tocopherol, β-carotene cancer prevention study group, 1994; Omenn et al., 1996). Consequently, an area of current activity is associated with establishing the molecular mechanisms of anti-oxidative and pro-oxidative activity of carotenoids in an attempt to understand these surprising epidemiological results.

Radicals are species with an odd electron, and may or may not carry a formal charge. Thus, radicals of a carotenoid CAR are most simply obtained by adding or removing an electron to generate the radical anion and cation respectively, ($CAR^{\bullet-}$ and $CAR^{\bullet+}$). For example a process involving a peroxyl radical ($ROO^{\bullet}$) can be written as:

$$ROO^{\bullet} + CAR \rightarrow ROO^{-} + CAR^{\bullet+}$$

The carotene radical cation can formally lose a proton to yield a neutral radical $CAR^{\bullet}$ (strictly this should be written to show the loss of the hydrogen, but $CAR^{\bullet}$ is used for convenience). This neutral radical can, of course, be produced via H-atom transfer such as:

Abbreviations: 77DH – 7,7′-dihydro-β-carotene (7,8–Dihydro-8′,7-retro-β,β-carotene); ARMD – age-related macular degeneration; $AscH_2$ – ascorbic acid; ASTA – astaxanthin; CAR – carotenoid; β-CAR – β-carotene; ENDOR – electron nuclear double resonance; epp – erythropoietic protoporphyria; EPR – electron paramagnetic resonance; FTIR – Fourier transform infrared; LUT – lutein; LYC – lycopene; MO/CI – molecular orbital/charge interaction; TOH–vitamin E; TX-100–Triton X-100; ZEA – zeaxanthin

$$ROO^{\bullet} + CAR \rightarrow ROOH + CAR^{\bullet}(-H).$$

Radicals can also arise by addition processes such as:

$$CAR + ROO^{\bullet} \rightarrow [ROO\text{-}CAR]^{\bullet}.$$

Other radical species such as dimer cations (Badger and Brocklehurst, 1969) and various ion-pairs (Ebrey et al., 1967) can arise, but these will not be discussed.

The absorption spectra of a wide range of carotenoid radical cations and anions were first established by nanosecond pulse radiolysis under conditions of mono-electronic processes (Dawe and Land, 1975;Lafferty et al., 1977). This work reported the spectra in hexane for the radical cations and in hexane and methanol for the radical anions. Subsequently, such studies for the radical cations have been extended to other solvents (Hill et al., 1995; Edge et al., 1998). Table 1 gives a selection of λ_{max} values for carotenoid radical cations in four solvents.

As can be seen there is a marked bathochromic shift for radical cations in non-polar solvents compared with the polar solvent methanol. This shift is much less marked for the parent carotenoid. Also, hydroxy-group substitution comparing zeaxanthin with β-carotene, e.g., has little effect on the position of the absorption maxim. As with the parent carotenoids, the λ_{max} for the radical cations shifts to longer wavelength with increasing number of conjugated C=C bonds, n, but, in contrast to the parent molecule, there is no limiting wavelength. Of particular note is the comparison of λ_{max} for β-carotene in the neutral detergent Triton X-100 with that in polar and non-polar solvents. Clearly, the values suggest that the β-carotene radical cation is in a micro-environment akin to the aqueous polar region rather than the non-polar region which would be the expected location of the parent molecule. This may be of importance in the possible interaction of carotenoid radal cations in biological environments with aqueous reducing agents such as ascorbic acid (see later). Perhaps, rather surprisingly, there is little or no difference between the λ_{max} of the radical anion of β-carotene in Triton X-100 and hexane (Hill, 1994).

As well as the λ_{max} values given in Table 1, Bally et al. (1992) have stabilized the radical cations of carotenoids via tert-butyl capping and reported the corresponding absorption spectra in freon matrices. These agree well with the earlier pulse radiolysis data given above but also show an additional weak absorbance at longer wavelengths, for example, for β-carotene this additional band is near 2000 nm. These results, for molecules up to n = 19, were discussed in terms of a simple MO/CI model.

While the majority of the studies of carotenoid radicals have been based on monitoring the strong near infrared absorption bands, other techniques, including time resolved resonance Raman spectroscopy (Jeevarajan et al., 1996), FTIR spectroscopy (Noguchi et al., 1994), EPR (Grant et al., 1988), ENDOR (Piekarasady et al., 1995), and cyclic voltametry (Grant et al., 1988) have also been used.

While the generation of carotenoid radical cations was originally achieved by radiolytic processes they have now been prepared photochemically (Tinkler et al., 1996), chemically (Ding et al., 1988), and via electrochemical methods (Grant et al., 1988). In the electrochemical study both one-electron and two-electron oxidation was observed with the two-electron oxidation subsequently producing the radical cation via reactions of the type:

$$CAR^{2+} + CAR \rightleftharpoons 2CAR^{\bullet+}$$

Of course, if carotenoid radicals are formed in vivo their subsequent fate is of interest although this has been little studied. For a wide range of carotenoid radicals Böhm et al. (1997) have shown that the carotenoid radical is converted into the parent carotenoid (a 'repair' reaction) by ascorbic acid. Of course, it may be that hydrocarbon carotenoids such as β-carotene and lycopene are unlikely to encounter water-soluble vitamin C in the environment in vivo. On the other hand the radical cations are likely to be more polar than the parent carotenoid and Moore et al. (T. A. Moore, personal communication) have shown that, in model membrane systems, hydrocarbon carotenoid radicals in the non-polar membrane react efficiently with ascorbic acid.

II. Electron Transfer Between Carotenoids and Carotenoid Radicals

Pulse radiolysis studies (Edge et al., 1998) have been used to determine the electron transfer rate constants between various pairs of dietary carotenoids, one of which is present as the radical cation:

Table 1. Absorption maxima (λ_{max},nm) and number of conjugated C=C double bonds (n) for carotenoid radical ions.

Carotenoid (n)	λ_{max} (nm) of $CAR^{\bullet+}$ in various solvents			
	Hexane	Benzene	Methanol	Triton X-100
β-Carotene (11)	1040	1020	920	936
Septapreno-β-carotene[1] (9)	915	–	820	850
Canthaxanthin (11)	960	940	840	862
Astaxanthin (11)	940	920	840	875
Zeaxanthin (11)	1040	1000	910	936
Lutein (10)	973	950	860	900
8′-Apo-β-caroten-8′-al (9)	890	880	820	–
Lycopene (11)	1070	1050	950	–
Decapreno-β-carotene[1] (15)	1250	–	–	–
7,7′Dihydro-β-carotene[2] (8)	830	–	760	–

[1] Septapreno-β-carotene and decapreno-β carotene are the C_{35} ($C_{20} + C_{15}$) and C_{50} ($C_{25} + C_{25}$) analogues, respectively, of β-carotene ($C_{20} + C_{20}$)
[2] 7,8-Dihydro-8′-7-retro-β,β-carotene

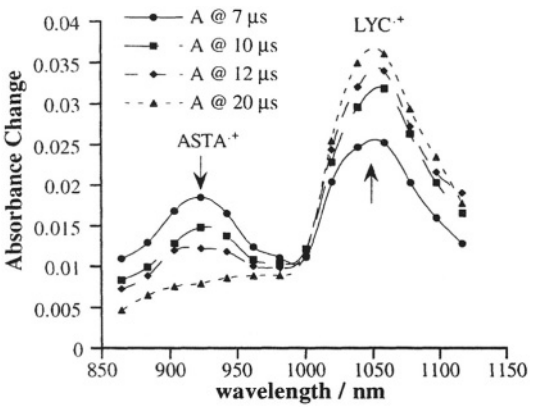

Fig. 1. Electron transfer from the radical cation of astaxanthin to lycopene measured by absrobance (A).

$$CAR1^{\bullet+} + CAR2 \rightarrow CAR1 + CAR2^{\bullet+}$$

Typical experimental results for astaxanthin and lycopene are shown in Fig. 1.

These and related results involving electron transfer to vitamin E have suggested the order of relative reduction potentials, $E(CAR^{\bullet+} / CAR)$ of seven carotenoid radical cations as:

Astaxanthin > 8′-Apo-β-caroten-8′-al > Canthaxanthin > Lutein > Zeaxanthin > β-Carotene > Lycopene

Lycopene is therefore the strongest reducing agent (the most easily oxidized) and astaxanthin is the weakest. Rather similar results have been reported recently, obtained by less direct methods (Miller et al., 1996; Mortensen and Skibsted, 1997a,b).

It is noteworthy that Edge et al. (1998) showed that the radical cations of the carotenoids found in the eye, lutein (LUT) and zeaxanthin (ZEA), are reduced by lycopene (LYC) but not by β-carotene (β-CAR). This may be relevant to the claim that lycopene reduces the onset of age-related macular degeneration even though there is no lycopene or β-carotene in the eye.

III. Interactions Involving Radicals of Carotenoids and Vitamins C and E

A. Vitamin C

Böhm et al. (1997) showed that all the carotenoid radical cations studied reacted efficiently with ascorbic acid ($AscH_2$) in both methanol and Triton X-100 micelles to regenerate (presumably) the parent carotenoid.

$$CAR^{\bullet+} + AscH_2 \rightarrow CAR + AscH^{\bullet} + H^{+}$$

$$CAR^{\bullet+} + AscH^{-} \rightarrow CAR + AscH^{\bullet-} + H^{+}$$

with the second order rate constants in the region

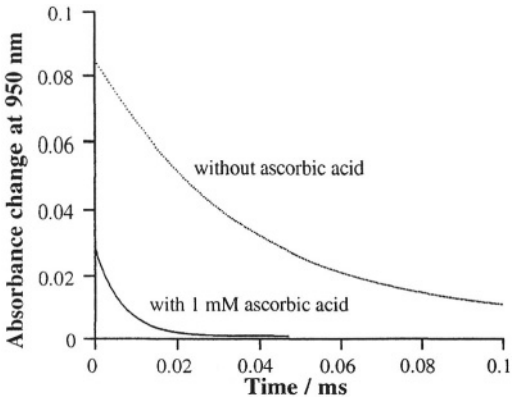

Fig. 2. Kinetic profile of the decay of lycopene$^{\bullet+}$ following laser flash photolysis of 70 μM lycopene in methanol in the absence and presence of 1 mM ascorbic acid.

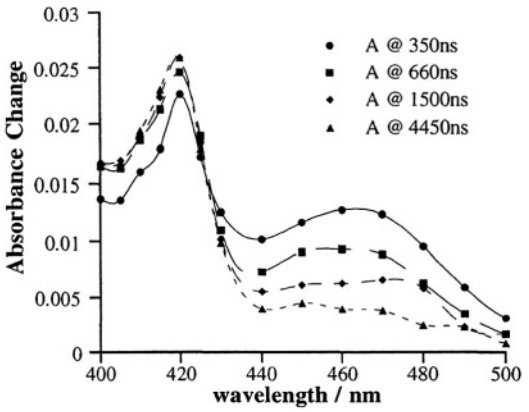

Fig. 3. The decay of the cation radical of vitamin E (TOH$^{\bullet+}$) at 460 nm and the growth of the deprotonated TO$^{\bullet}$ monitored at 420 nm by absrobance (A) Solvent is hexane flushed with N_2O.

$10^9 M^{-1}s^{-1}$ in methanol. A typical example of such quenching is given in Fig. 2.

There is much current debate about the relevance of such 'carotenoid repair' processes to hydrocarbon carotenoids such as **β-carotene** and lycopene in vivo where the parent carotenoid is unlikely to encounter the polar ascorbic acid. However, the cation radical, with a positive charge, may be sufficiently polar and long-lived for such interactions to be possible. For the carotenoids found in the macula, where an efficient anti-oxidant process is crucial, the hydroxy carotenoids zeaxanthin, meso zeaxanthin and lutein are likely to be in a membrane orientation such that the corresponding cation radicals are efficiently repaired by the vitamin C (cf. vitamin E, below).

B. Vitamin E

Ingold and co-workers (Valgimigli et al., 1997) have shown there is no reaction between the deprotonated cation radical of vitamin E (TO$^{\bullet}$) and **β-carotene,** whereas Mortensen and Skibsted (1997b) showed that the **β-carotene** cation radical reacts with vitamin E (TOH):

$$\beta\text{-car}^{\bullet+} + \text{TOH} \rightarrow \beta\text{-car} + \text{TO}^{\bullet} + \text{H}^{+}$$

Work with 7,7′ **dihydro-β-carotene** (7,8-dihydro-8′,7-retro-**β,β-carotene,** 77DH) and vitamin E has allowed Edge et al. (1998) to gain a better understanding of the interaction of the vitamin E radicals with carotenoids. Figure 3 shows the transient absorption spectrum at various times following pulse radiolysis of vitamin E in hexane flushed with N_2O. As can be seen, there are two peaks (420 nm and 460 nm maxima) but the kinetics associated with these absorption maxima are clearly quite different. The species with λ_{max} = 420 nm is long-lived. However, the species at 460 nm decayes with two lifetimes of about 250 ns and 6 ms. The shorter of these may be related to geminate processes. The species absorbing at 460 nm is the radical cation (TOH$^{\bullet+}$) and that at 420 nm is the neutral radical (TO$^{\bullet}$). These results are consistent with the conclusion that the decay of the TOH$^{\bullet+}$ is, in part, due to deprotonation with a corresponding growth in the species absorbing at 420 nm and show that the lifetime of TOH$^{\bullet+}$ in non-polar environments is markedly longer than had been previously suggested.

On adding 77DH the decay rate of the slow component of the species absorbing at 460 nm was markedly increased corresponding to a second-order rate constant of ~$10^{10} M^{-1}s^{-1}$. Figure 4 compares the kinetics of the formation of the 77DH radical cation at 830 nm in the absence and presence of vitamin E (1×10^{-2} M).

These, and related results confirm the electron transfer process:

$$\text{TOH}^{\bullet+} + \text{CAR} \rightarrow \text{TOH} + \text{CAR}^{\bullet+}$$

However, Edge et al. (1998) also show different behavior for astaxanthin, a carotenoid containing both carbonyl and hydroxy groups, such that the

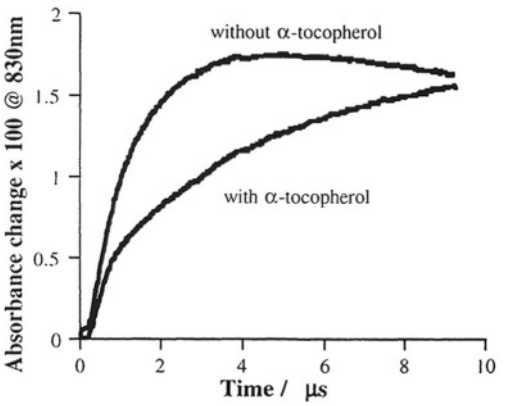

Fig. 4. Representative kinetics profile of the formation of 77DH$^{\bullet+}$ following pulse radiolysis of 10 mM 77DH in the absence and presence of 100 mM α-tocopherol.

astaxanthin cation radical has a reduction potential that is higher than that of tocopherol ($TOH^{\bullet+}/TOH$). Mortensen and Skibsted (1997b) have also shown a quenching of $TOH^{\bullet+}$ by astaxanthin.

These interactions of carotenoids with vitamins C and E, taken with the varying reduction potentials of the carotenoids discussed above, may well be relevant to the possible synergistic effects of some combinations of anti-oxidants.

IV. Interactions of Carotenoids with Free Radicals

As noted above in the introduction, in principle, carotenoids can react with free radicals in a number of ways, namely electron transfer, hydrogen atom transfer and addition:

$$ROO^{\bullet} + CAR \rightarrow ROO^{-} + CAR^{\bullet+}$$

$$ROO^{\bullet} + CAR \rightarrow ROOH + CAR^{\bullet}(-H^{+})$$

$$ROO^{\bullet} + CAR \rightarrow [ROO - CAR]^{\bullet}$$

However, the mechanism and rate of scavenging of oxy-radicals by carotenoids is strongly dependent on the nature of the oxidizing species but much less dependent on the carotenoid structure (Mortensen et al., 1997).

A. Electron Transfer and Addition Reactions

Some oxy-radicals lead to both electron transfer reactions and addition to the carotenoid. The most well studied is the trichloromethylperoxyl radical $CCl_3OO^{\bullet}$, a peroxyl radical which is known to cause hepatotoxity and other types of tissue injury (Packer et al., 1981; Hill et al., 1995). Packer et al. (1981) showed that, in the presence of β-carotene, there was a fast bleaching of the carotene ground state absorption with a rate constant of $1.5 \times 10^9\ M^{-1}s^{-1}$. The loss of absorption at 450 nm was accompanied by an increase in absorption in the near infrared region (950–1000 nm), indicating that the reaction produces the β-carotene radical cation.

Hill et al. (1995) studied the reaction of $CCl_3OO^{\bullet}$ with a range of carotenoids in aqueous Triton X 100 micelles, at pH 7. They observed two peaks in the absorption spectra produced for all six carotenoids studied and noted that these two peaks had different kinetics, with the species at shorter wavelength decaying into the other species. For β-carotene, the peaks were observed at 820 nm and 920 nm. The longer-wavelength peak is assigned to the radical cation produced as shown in the following scheme:

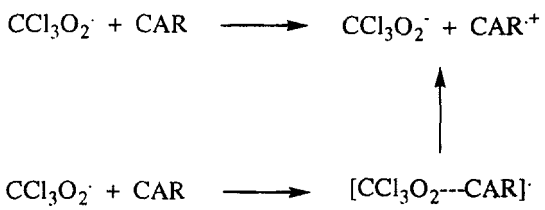

However, the nature of the species absorbing at shorter wavelengths in the infra red is not known with certainty. Indeed, Mortensen et al. (1997) suggest that the radical addition complex $[CCl_3O_2—CAR]^{\bullet}$ does not absorb in the red region but absorbs in the same spectral region as the parent carotenoid, whereas the intermediate in the above scheme (absorbing at about 820 nm for β-carotene) is an ion pair. Hill et al. (1995) noted that oxygen-centered radicals are required for the production of such adducts because, without oxygen present, the $CCl_3^{\bullet}$ radicals react with carotenoid to give only the carotenoid radical cation. Hill et al. (1995) rule out the formation of carotenoid dications because only one-electron oxidation reactions were initiated, despite the fact that the

dications are blue-shifted compared to the radical cations. Recently, Liebler and McLure (1996) have oxidized β-carotene with radicals resulting from the thermal decomposition of azo-bis-(2,4-dimethyl valero nitrile) (AN=NA) and have studied the structure of the adducts formed by Atmospheric Pressure Chemical Ionization mass spectrometry. In benzene the AN=NA thermally decomposes to 2A$^{\bullet}$ (carbon-centred radicals, $(CH_3)_2CHCH_2C{\cdot}CH_3CN$) and N_2 and the A$^{\bullet}$ radicals react in the presence of oxygen to yield peroxyl (AOO$^{\bullet}$) and alkoxyl (AO$^{\bullet}$) radicals. 'Substitution' products formed by replacement of a carotenoid hydrogen by one radical, and 'addition' products in which β-carotene and two radical fragments are linked, were detected. Certainly, the precise nature of the intermediates formed in such processes needs further study.

The work by Hill et al. (1995) also showed differences for astaxanthin compared with the other carotenoids studied. Its radical cation was not formed initially from $CCl_3O_2^{\bullet}$, but was formed solely through the proposed addition radical. Unfortunately, lycopene could not be studied due to its insolubility in TX 100 micelles. However, since lycopene appears, from its quenching of singlet oxygen, to be (marginally) the most efficient natural carotenoid anti-oxidant, this work has been investigated by using 4% TX 405 : TX 100 (4:1) mixed micelles for both β-carotene and lycopene (R. Edge, D. J. McGarvey and T. G. Truscott, unpublished). Lycopene behaves in a different way to the other carotenoids, as there appears to be no conversion of the 'adduct' into the radical cation. However, this may be due to the properties of the mixed micelle and further work is required.

The sulfonyl radical $CH_3SOO^{\bullet}$ also reacts with carotenoids to generate both the cation radical and some pre-cation radical intermediate species (Everett et al., 1996; Mortensen et al., 1997). In the recent study the loss of the ground state absorption led to complex kinetics and these results seem best interpreted by considering that an intermediate (possibly an ion pair) leads to the carotene radical and the adduct $[CAR{-}{-}RSO_2]^{\bullet}$, which has absorption overlapping that of CAR, then undergoes a bimolecular process to give some unidentified product(s).

The phenoxyl radical also gives two routes to the carotene cation radical (Mortensen and Skibsted, 1996a). Using laser flash photolysis, these workers generated $C_6H_5O^{\bullet}$ (absorbing near 400 nm) and the reaction between this radical and β-carotene was interpreted as involving adduct formation as well as direct electron transfer to CAR$^{\bullet+}$. Since the phenoxyl radical can be regarded as a model of tyrosine, such reaction sequences may suggest that some carotenoids can act as anti-oxidants via recycling (repairing) one-electron-oxidized tyrosine.

Mortensen and Skibsted (1996b) have shown that laser flash photolysis of carotenoids in chloroform leads to immediate bleaching of the carotene absorption and the concomitant formation of two near infrared absorbing species ($\lambda_{max} \approx 920$ nm and 1000 nm for β-carotene). The species absorbing at about 1000 nm is the carotene radical cation (β-car$^{\bullet+}$) and, as with the carotene/$CCl_3O_2^{\bullet}$ system noted above, the β-car$^{\bullet+}$ is formed from the other species. The nature of the other species is not defined although an adduct/ion pair or a neutral carotene radical is proposed.

Presumably these reactions arise from reaction of the extremely short-lived photo-excited carotenoid with $CHCl_3$ (in high concentration as the solvent) in processes such as:

$$CAR^* + CHCl_3 \rightarrow CAR^+ + CHCl_3^-$$

and

$$CAR^* + CHCl_3 \longrightarrow [CAR{-}{-}{-}CHCl_3]$$

$$[CAR{-}{-}{-}CHCl_2]^{\cdot} + Cl^{\cdot} \longrightarrow CAR^{\cdot+} + CHCl_2^-$$

These observations have recently been extended to carotenoids containing keto, hydroxy and aldehyde groups in halogenated solvents. Following laser excitation all the xanthophylls produce a transient species in $CHCl_3$ absorbing in the 850–960 nm region and this transient decays by first-order kinetics to another species (the radical cation) which absorbs at longer wavelengths (870–1040 nm). In contrast, the authors note that whilst carotenoids are also bleached in CCl_4 no near infrared absorbing species arise on laser excitation in this solvent. Possibly the neutral radical, CAR$^{\bullet}$, is produced via hydrogen atom transfer, and this does not absorb in the near infrared e.g.

$$CAR^* + CCl_4 \rightarrow CAR^{\bullet} + HCl + CCl_3^{\bullet}.$$

B. Electron Transfer

Some radicals appear to lead only to electron transfer reactions with carotenoids ($ROO^{\bullet} + CAR$, $ROO^{-} + CAR^{\bullet+}$) and not to addition/intermediate species. Of course, if such addition/intermediate species are extremely short lived and decay to the $CAR^{\bullet+}$ they would not be detected.

A particularly interesting example is nitrogen dioxide ($NO_2^{\bullet}$), which is an air pollutant and which arises from cigarette smoke. Böhm et al. (1995) showed that both β-carotene and lycopene protected human lymphocyte cells from $NO_2^{\bullet}$ with lycopene being the more efficient anti-oxidant. More recently, Böhm et al. (1998) have investigated the abilities of α-tocopherol, ascorbic acid and β-carotene to protect human lymphocytes from membrane damage caused by the nitrogen dioxide radical and found a synergistic protective effect when the anti-oxidants were bound to the lymphocyte cells, with only 5.3% of cells killed compared to 53% without any added anti-oxidants. In addition, Cooney et al. (1994) have suggested that light-mediated reduction of $NO_2^{\bullet}$ to NO by carotenoids may be an important mechanism for preventing damage in plants exposed to $NO_2^{\bullet}$.

Mortensen et al. (1997) and Everett et al. (1996) used pulse radiolysis to generate $NO_2^{\bullet}$ and showed that, for the five carotenoids studied (β-carotene, astaxanthin, lutein, zeaxanthin and lycopene), only electron transfer could be observed:

$$NO_2^{\bullet} + CAR \rightarrow NO_2^{-} + CAR^{\bullet+}$$

with no evidence of radical adducts $[CAR\text{-}NO_2]^{\bullet}$. The rate constants reported ($\sim 10^7 M^{-1}s^{-1}$ in t-butanol/water) varied by a rather small factor for the five carotenoids studied.

Another radical species which reacts with carotenoids to give only the carotenoid radical cation is the superoxide radical anion ($O_2^{\bullet-}$), although there have been few studies and there is some confusion in the literature. β-Carotene was shown by Conn et al. (1992) to react with superoxide. Pulse radiolysis of β-carotene, in oxygen-saturated aqueous 2%TX-100 micelles containing sodium formate, produced a species with λ_{max} at 940 nm. This was originally assigned to a superoxide-β-carotene addition product but later re-interpreted as the formation of β-carotene radical cation, i.e.

$$O2^{\bullet-} + CAR + 2H+ \rightleftharpoons CAR^{\bullet+} + H_2O_2$$

This is consistent with the data of Hill et al. (1995) who have shown that the λ_{max} of $\beta\text{-car}^{\bullet+}$ in TX 100 is blue-shifted by 104 nm to 936 nm compared with 1040 nm in hexane (Dawe and Land, 1975). Such differences were found for all the carotenoids studied by Hill et al. (1995).

Another group of molecules which lead only to electron transfer processes are the aryl peroxy radicals (M. Burke, R. Edge, E. J. Land, L. Mulroy, D. J. McGarvey and T. G. Truscott, unpublished). These were generated via pulse radiolysis by using reductive dehalogenation of the corresponding aryl bromide (ArBr) in methanol as shown in the following equations:

$$ArBr + e^-_{sol} \rightarrow Ar^{\bullet} + Br^-$$

$$Ar^{\bullet} + O_2 \rightarrow ArO_2^{\bullet}$$

Three such peroxyl radicals (9-phenanthrylperoxyl, 1-naphthylperoxyl and 2-naphthylperoxyl) have been studied in methanol and the rate constants obtained for their electron transfer reaction with the carotenoids zeaxanthin and lutein are given in Table 2.

As can be seen, there is a marked variation of values for the different peroxyl radicals as the structure (and, hence, the oxidation potential) varies but much less variation between the two values obtained with the xanthophylls studied (as noted above).

C. Radical Addition

Probably the best example of this class of reactions involves thiyl radicals ($RS^{\bullet}$) such as glutathione. Mortensen et al. (1997) used pulse radiolysis to generate $RS^{\bullet}$ from RSH via H atom transfer to a carbon-centred radical ($^{\bullet}CH_2(CH_3)_2COH$). The two thiyl radicals studied were the glutathione radical and the 2-mercaptoethanol thiyl radical ($HOCH_2CH_2S^{\bullet}$) in reaction with carotenoids. In each case there was a loss of ground state absorption due to the parent carotenoid but no corresponding absorption was detected at wavelengths longer than 600 nm. The

Table 2. Second-order rate constants for the reaction of $ArO_2^{\bullet}$ with zeaxanthin and lutein

Peroxyl radical	$k / 10^8$ dm^3 mol^{-1} s^{-1}	
	Zeaxanthin	Lutein
9-Phenanthrylperoxyl	3.0	4.0
1-Naphthylperoxyl	1.3	0.9
2-Naphthylperoxyl	0.2	0.5

pressured adduct formed was found to absorb in a spectral region close to that of the parent carotenoid The bleaching in this spectral region was biphasic with a fast step due to the addition process:

$$CAR + RS^{\cdot} \rightarrow [RS\text{–}CAR]^{\cdot}$$

and a slower bimolecular step due to the decay of this adduct:

$$2[RS\text{–}CAR]^{\cdot} \rightarrow \text{product/s}$$

It has been suggested that nitric oxide (NO), which is a radical, bleaches β-carotene presumably by forming addition complexes (Gabr et al., 1995). However, we have found no interaction between NO and β-carotene when oxygen is rigorously excluded from the system.

D. Hydrogen Atom Transfer

It was noted above that laser flash photolysis of β-carotene in chloroform as solvent, led to carotenoid cation radical production and a corresponding transient absorption in the infrared. However, Mortensen and Skibsted (1996b) have also shown that, in carbon tetrachloride as solvent, whilst the parent carotenoid was bleached, no infrared absorbing species arose. Possibly the neutral carotene radical (CAR$^{\cdot}$) was produced via hydrogen atom transfer:

$$CAR^{*} + CCl_4 \rightarrow CAR^{\cdot} + HCl + CCl_3^{\cdot}$$

Very recently Mortensen and Skibsted (1998) have reported a study of the ability of β-carotene to scavenge three alkylperoxyl radicals, namely the cyclohexylperoxyl, the tetrahydrofuranperoxyl and the t-butanylperoxyl radicals, by use of laser flash photolysis and steady-state techniques. Only very slow reaction rates could be detected, corresponding to second-order rate constants of less than $10^6\ M^{-1}\ s^{-1}$, and it was suggested that this slow reaction was due to either addition or hydrogen atom transfer reactions.

Overall it is interesting to compare the different series of peroxyl radicals discussed above. The alkylperoxyl radicals react only very slowly to yield adducts and/or neutral carotene radicals by hydrogen atom transfer, the arylperoxyl radicals and $NO_2^{\cdot}$ give carotenoid radical cations only and $CCl_3O_2^{\cdot}$ and $CH_3SOO^{\cdot}$ give carotenoid cation radicals and, for most carotenoids, an intermediate which decays to the carotenoid cation radical; the nature of this intermediate is not established. The reaction pathway can be expected to depend on several factors including the reduction potential difference between the radical and the carotenoid. Thus, for example, $CCl_3O_2^{\cdot}$ reacts with all the carotenoids studied, except astaxanthin, to give the cation radical and a pre-cation radical intermediate. For astaxanthin, the most difficult of these carotenoids to oxidize (see above and Edge et al., 1998), no direct electron abstraction to yield astaxanthin radical cation could be detected (Hill et al., 1995).

V. Reactions between Carotenoids and Singlet Oxygen

The quenching of singlet molecular oxygen ($^1O_2^*$) by carotenoids and the mechanism by which this reaction protects against $^1O_2^*$ mediated photo-oxidation reactions have been much discussed.

In biological systems, sensitizers such as porphyrins, chlorophylls and riboflavin can sensitize $^1O_2^*$ production:

$$^3sens^* + {}^3O_2 \xrightarrow{k_{et}} sens + {}^1O_2^*$$

and this can lead to deleterious effects including DNA damage and lipid peroxidation.

The first demonstration that β-carotene could inhibit photosensitized oxidation and was, therefore, an efficient quencher of $^1O_2^*$ was reported by Foote and Denny (1968). Wilkinson and Ho (1978) showed that quenching by electron exchange energy transfer to produce the carotenoid triplet state (^{3}CAR) is the principal mechanism of carotenoid photoprotection against $^1O_2^*$:

$$^1O_2^* + CAR \longrightarrow {}^3O_2 + {}^3CAR^*$$

although chemical quenching (reaction) also occurs, leading to destruction of the carotenoid. Once produced, ^{3}CAR can easily return to the ground state, dissipating the energy as heat, or it can be quenched physically via enhanced intersystem crossing by $^3O_2$. Thus, the carotenoid acts as a catalyst, deactivating $^1O_2^*$.

Table 3. Singlet oxygen quenching rate constants for various carotenoids in benzene

Carotenoid	n	k_q / $\times 10^9$ $M^{-1}s^{-1}$
Dodecapreno-β-carotene[1]	19	23.0
Decapreno-β-carotene[2]	15	20.0
3,4,3′,4′-Tetradehydrolycopene	15	10.7
Astaxanthin	11 (+2, C=O)	14.0
Lycopene	11	17.0
all-*trans*-β-Carotene	11	13.0
15-*cis*-β-Carotene	11	11.0
9-*cis*-β-Carotene	11	11.0
Zeaxanthin	11	12.0
α-Carotene	10	12.0
Lutein	10	6.64
8'-Apo-β-carotenal	9(+1 C=O)	5.27
Violaxanthin	9	16.0
Septapreno-β-carotene[2]	9	1.38
7,7'-Dihydro-β-carotene[2]	8	0.3

[1] The C_{60} (C_{30}+ C_{30}) analogue of β-carotene
[2] See footnotes to Table 1.

Many different carotenoids have been studied to investigate the influence of different structural characteristics on the ability to quench $^1O_2^*$.

Much of this work has been carried out in organic solvents. Some typical results, taken from Conn et al. (1991) and Rodgers and Bates (1980), together with some unpublished data are shown in Table 3.

As the number of conjugated double bonds increases, the energies of the excited states (S_2, S_1, T_1) decrease and this is reflected in the dependence of the $^1O_2^*$ quenching rate constant on carotenoid chain length. For example, the results of Conn et al. (1991) and Edge et al. (R Edge, DJ McGarvey and TG Truscott, unpublished) indicate that the ability to quench $^1O_2^*$ increases with increasing chain length n, reflecting increased exothermicity in the energy transfer. For example, $k_q = 0.3 \times 10^9$ $M^{-1}s^{-1}$ for 7,7′-dihydro-β-carotene (n = 8) and 23×10^9 $M^{-1}s^{-1}$ for dodecapreno-β-carotene (n = 19), with intermediate values for the other carotenoids following the trend (see Table 3). Interestingly, the two carotenoids present in the eye, zeaxanthin and lutein, have very different quenching rate constants with respect to $^1O_2^*$. Zeaxanthin (n = 11) appears to be at least twice as effective as lutein (n = 10) and this may indicate that they have different roles in the protection of the eye.

Di Mascio et al. (1989) used a mixed solvent system (ethanol:chloroform:water, 50:50:1) in which there is a possibility of carotenoid aggregation and they found, as did other workers (Conn et al., 1991), that lycopene is the naturally occurring carotenoid that quenches $^1O_2^*$ most efficiently, although, their k_q value for lycopene is higher than that determined by Conn et al. (1991). This indicates that the presence of the acyclic end group rather than the β- rings has a positive effect on $^1O_2^*$ quenching; the value found by Di Mascio et al. (1989) for γ-carotene, which has one β-ring and one acyclic end group, is between the values for β-carotene and lycopene.

In systems which more closely resemble the in vivo environment Anderson and Krinsky (1973) showed that incorporation of carotenoids into liposomal membranes gave good protection against the effects of oxidation sensitized by toluidine blue, with β-carotene offering better protection than canthaxanthin. They could not however, determine whether the carotenoids were acting exclusively as $^1O_2^*$ quenchers, or as radical quenchers. Also, Telfer et al. (1994) have shown that β-carotene can act as an efficient quencher of singlet oxygen generated within isolated Photosystem II reaction centers. This work demonstrated the direct role of singlet oxygen in causing photo-oxidative damage within a biological environment. However, reactions such as these have not been observed in vivo.

Acknowledgments

We thank the American Institute for Cancer Research (AICR), EPSRC and The Wellcome Trust for financial support. Much of the pulse radiolysis data discussed in this chapter were obtained at the Paterson Institute for Cancer Research Free Radical Research Facility, Christie Hospitial NHS Trust, Manchester, U.K. The facility is supported by the European Commission TMR Programme—Access to Large Scale Facilities.

References

Anderson SM and Krinsky NI (1973) Protective action of carotenoid pigments against photodynamic damage to liposomes. Photochem Photobiol 18: 403–408

Badger B and Brocklehurst B (1969) Absorption spectra of dimer cations. Trans Faraday Soc 65: 2576–2581

Bally T, Roth K, Tang W, Schrock RR, Knoll K and Park LY (1992) Stable polarons in polyacetylene oligomers: Optical spectra of long polyene radical cations. J Amer Chem Soc 114: 2440–2446

Böhm F, Tinkler JH and Truscott TG (1995) Carotenoids protect against cell membrane damage by the nitrogen dioxide radical.

Nature Med 1: 98–99
Böhm F, Edge R, Land EJ, McGarvey DJ and Truscott TG (1997) Carotenoids enhance vitamin E anti-oxidant efficiency. J Am Chem Soc 119: 621–622
Böhm F, Edge R, McGarvey DJ and Truscott TG (1998) β-Carotene with vitamins E and C offer synergistic cell protection against NO_x. FEBS Lett 436: 387–389
Burton GW and Ingold KU (1984) β-Carotene: An unusual type of lipid anti-oxidant. Science 224: 569–573
Conn PF, Schalch W and Truscott TG (1991) The singlet oxygen and carotenoid interaction. J Photochem Photobiol B: Biol 11: 41–47
Conn PF, Lambert CR, Land EJ, Schalch W and Truscott TG (1992) Carotene-oxygen radical interactions. Free Rad Res Comms 16: 401–408
Cooney RV, Harwood PJ, Custer LJ and Franke AA (1994) Light-mediated conversion of nitrogen dioxide to nitric oxide by carotenoids. Environ Health Perspect 102: 460–462
Dawe EA and Land EJ (1975) Radical ions derived from photosynthetic polyenes. J Chem Soc Farad Trans I 71: 2162–2169
Di Mascio P, Kaiser S and Sies H (1989) Lycopene as the most efficient biological carotenoid singlet oxygen quencher. Arch Biochem Biophys 274: 532–538
Ding R, Grant JL, Metzger RM and Kispert LD (1988) Carotenoid cation radicals produced by the interaction of carotenoids with iodine. J Amer Chem Soc 92: 4600–4606
Ebrey TG (1967) Charge transfer complexes of polyenes. J Phys Chem 71: 1963–1964
Edge R, Land EJ, McGarvey D, Mulroy L and Truscott TG (1998) Relative one-electron reduction potentials of carotenoid radical cations and the interactions of carotenoids with the vitamin E radical cation. J Amer Chem Soc 120: 4087–4090
Everett SA, Dennis MF, Patel KB, Maddix S, Kundu SC and Willson RL (1996) Scavenging of nitrogen dioxide, thiyl, and sulphonyl free radicals by the nutritional anti-oxidant β-carotene. J Biol Chem 271: 3988–3994
Foote CS and Denny RW (1968) Chemistry of singlet oxygen. VIII. Quenching by β-carotene. J Am Chem Soc 90: 6233–6235
Gabr I, Patel RP, Symons MCR and Willson MT (1995) Novel reactions of nitric oxide in biological systems. J Chem Soc Chem Comm 915–916
Grant JL, Kramer VJ, Ding R and Kispert LD (1988) Carotenoid cation radicals: Electrochemical, optical and EPR study. J Amer Chem Soc 110: 2151–2157
Gust D, Moore TA, Moore AL, Jori G and Reddi E (1993) The photochemistry of Carotenoids: Some photosynthetic and photomedical aspects. Ann New York Acad Sci 691: 32–47
Hill TJ, Land EJ, McGarvey DJ, Schalch W, Tinkler JH and Truscott TG (1995) Interactions between carotenoids and the $CCl_3O_2^{\bullet}$ radical. J Am Chem Soc 117: 8322–8326
Jeevarajan AS, Kispert LD, Chumanov G, Zhou C and Cotten TM (1996) Resonance Raman study of carotenoid radical cations. Chem Phys Lett 259: 515–522
Lafferty J, Roach AC, Sinclair RS, Truscott TG and Land EJ (1977) Absorption spectra of radical ions of polyenes of biological interest. J Chem Soc Farad Trans I 73: 416–429
Liebler DC and McClure TD (1996) Anti-oxidant reactions of β-carotene: Identification of carotenoid-radical adducts. Chem Res Toxicol 9: 8–11
Miller NJ, Sampson J, Candeias LP, Bramley PM and Rice-Evans CA (1996) Anti-oxidant activities of carotenes and xanthophylls. FEBS Lett 384: 240–242
Mortensen A and Skibsted LH (1996a) Kinetics of parallel electron transfer from β-carotene to phenoxyl radical and adduct formation between phenoxyl radical and β-carotene. Free Rad Res 25: 515–523
Mortensen A and Skibsted LH (1996b) Kinetics of photobleaching of β-carotene in chloroform and formation of transient carotenoid species absorbing in the near infrared. Free Rad Res 25:355–368
Mortensen A and Skibsted LH (1997a) Importance of carotenoid structure in radical-scavenging reactions. J Agric Food Chem 45: 2970–2977
Mortensen A and Skibsted LH (1997b) Relative stability of carotenoid radical cations and homologue tocopheroxyl radicals. A real time kinetic study of anti-oxidant hierarchy. FEBS Lett 417: 261–266
Mortensen A and Skibsted LH (1998) Reactivity of β-carotene towards peroxyl radicals studied by laser flash and steady-state photolysis. FEBS Lett 426: 392–396
Mortensen A, Skibsted LH, Sampson J, Rice-Evans C and Everett SA (1997) Comparative mechanisms and rates of free radical scavenging by carotenoid anti-oxidants. FEBS Lett 418: 91–91
Noguchi T, Mitsuka T and Inoue Y (1994) Fourier-transform infrared-spectrum of the radical-cation of β-carotene photoinduced in photosystem-II. FEBS Lett 356: 179–182
Omenn GS, Goodman GE, Thornquist MD, Balmes J, Cullen MR, Glass A, Keogh JP, Meyskens FL Jr, Valanis B, Williams JH, Barnhart S and Hammar S (1996) Effects of a combination of β-carotene and vitamin A on lung cancer and cardiovascular disease. New Eng J Med 334: 1150–1155
Packer JE, Mahood JS, Mora-Arellano VO, Slater TF, Willson RL and Wolfenden BS (1981) Free radicals and singlet oxygen scavengers: Reaction of a peroxy-radical with β-carotene, diphenyl furan and 1,4-diazobicyclo-(2,2,2)-octane. Biochem Biophys Res Comm 98: 901–906
Piekarasady L, Jeevarajan AS, Kispert LD, Bradford EG and Plato M (1995) ENDOR study of the (7′,7′-dicyano)-7′-apo-β-carotene and (7′-phenyl)-7′-apo-β-carotene radical cations formed by UV photolysis of carotenoids adsorbed on silica-gel. J Chem Soc Farad Trans 91: 2881–2884
Rodgers MAJ and Bates AL (1980) Kinetic and spectroscopic features of some carotenoid triplet states: Sensitization by singlet oxygen. Photochem Photobiol 31: 533–537
Steinberg-Yfrach G, Liddell PA, Hung S-C, Moore AL, Gust D and Moore TA (1997) Conversion of light energy to proton potential in liposomes by artificial photosynthetic reaction centres. Nature 385: 239–241
Telfer A, De Las Rivas J, and Barber J (1991) β-Carotene within the isolated Photosystem II reaction centre: photooxidation and irreversible bleaching of this chromophore by oxidized P680. Biochim Biophys Acta 1060: 106–114
Telfer A, Dhami S, Bishop SM, Phillips D and Barber J (1994) β-carotene quenches singlet oxygen formed by isolated Photosystem II reaction centers. Biochemistry 33: 14469–14474
The α-tocopherol, β-carotene cancer prevention study group (1994) The effect of vitamin E and β-carotene on the incidence of lung cancer and other cancers in male smokers. New Eng J

Med 330: 1029–1035
Tinkler JH, Böhm F, Schalch W and Truscott TG(1994) Dietary carotenoids protect human cells from damage, J Photochem Photobiol B:Biol 26: 283–285
Tinkler JH, Tavender SM, Parker AW McGarvey DJ, Mulroy L and Truscott TG (1996) Investigation of carotenoid radical cations and triplet states by laser flash photolysis and time-resolved resonance Raman spectroscopy: Observation of competitive energy and electron transfer. J Am Chem Soc 118: 1756–1761
Valgimigli L, Lucarini M, Pedulli GF and Ingold KU (1997) Does β-carotene really protect vitamin E from oxidation? J Am Chem Soc 119: 8095–8096
Wilkinson F and Ho W-T (1978) Electronic energy transfer from singlet molecular oxygen to carotenoids. Spectroscopy Lett 11: 455–436

Chapter 13

Incorporation of Carotenoids into Reaction Center and Light-Harvesting Pigment-protein Complexes

Harry A. Frank
University of Connecticut, Department of Chemistry, 55 North Eagleville Road, Storrs, CT 06269-3060, U.S.A.

Summary

A wide variety of natural and synthetic carotenoids including locked-*cis*-geometric isomers and specific isotopically labeled molecules can be readily incorporated into reaction center and light-harvesting pigment-protein complexes isolated from Carotenoidless mutants of photosynthetic bacteria. Experiments on these samples provide the means to study systematically the effect of varying the structure, extent of π-electron conjugation, energy levels, spectral overlap, and dynamics on the spectroscopic properties and the light-harvesting and photoprotection roles of carotenoids in photosynthesis. In this chapter, steady state and transient optical and magnetic resonance spectroscopic studies are described that examine the photochemical behavior of the pigment-protein complexes containing the incorporated carotenoids. The biochemical procedures for incorporating exogenous carotenoids into the reaction centers and the B850 antenna complex from *Rhotobacter sphaeroides* R26.1 are given in detail.

H. A. Frank, A. J. Young, G. Britton and R. J. Cogdell (eds): The Photochemistry of Carotenoids, pp. 235–244.

I. Introduction

Carotenoids are bound non-covalently in discrete locations within antenna and reaction center (RC) protein complexes and with specific structures that facilitate their carrying out several important roles in photosynthesis. Carotenoids may act as: (i) Light-harvesting agents, absorbing light energy and then transferring the energy to chlorophyll (Chl) using excited singlet states (Cogdell and Frank, 1987; Frank and Cogdell, 1993); (ii) Protective devices, either quenching chlorophyll triplet states before they sensitize singlet oxygen formation or scavenging any singlet oxygen that may be produced (Krinsky, 1968, 1971); (iii) Energy flow regulators, dissipating excess energy not used for photosynthesis (Demmig-Adams, 1990); (iv) Structure stabilizers, promoting the proper folding, assembly and stabilization of some pigment-protein complexes in the photosynthetic apparatus (Jirsakova and Reiss-Husson, 1994; Lang and Hunter, 1994; Chapter 7, Paulsen).

The first three of these roles directly involve excited electronic states. The pioneering work in this area derives from optical spectroscopic experiments carried out on model polyenes (Hudson et al., 1982, 1984; Kohler, 1991). The studies have shown that polyenes and Carotenoids possess two low-lying excited singlet states, denoted S_1 and S_2, and one low-lying triplet state, denoted T_1, that account for much of their photochemical behavior (Cogdell and Frank, 1987; Frank and Cogdell, 1993, Frank and Christensen, 1995). The ground state, denoted S_0, and the S_1 excited state of these molecules possess A_g symmetry in the idealized C_{2h} point group. Electronic transitions between these states, i.e. $S_0 \rightarrow S_1$ ($1^1A_g \rightarrow 2^1A_g$) absorption or $S_1 \rightarrow S_0$ ($2^1A_g \rightarrow 1^1A_g$) fluorescence, are symmetry forbidden. In contrast, the transitions, $S_0 \rightarrow S_2$ ($1^1A_g \rightarrow 1^1B_u$) and $S_2 \rightarrow S_0$ ($1^1B_u \rightarrow 1^1A_g$), to and from S_0 and the second excited state, S_2, which has B_u symmetry, are allowed. The $S_0 \rightarrow S_2$ ($1^1A_g \rightarrow 1^1B_u$) transition is responsible for the characteristic strong absorption in the visible region associated with all polyenes and Carotenoids. Much less is known about the nature of the excited triplet states of Carotenoids, although it is certain that the longer Carotenoids (>10 conjugated carbon-carbon double bonds) have triplet states sufficiently low to quench bacteriochlorophyll (BChl) triplets in both antenna and RC pigment-protein complexes (Cogdell and Frank, 1987).

In analyzing the mechanisms responsible for the roles of carotenoids, it has been proven useful to compare strains of bacteria containing carotenoids with those obtained from carotenoidless mutants. The carotenoidless mutants, *Rhodobacter (Rb.) sphaeroides* R-26 and *Rhodospirillum (Rs.) rubrum* G9, have been used extensively in this manner (Boucher et al. 1977; Feher and Okamura, 1978; Budil and Thurnauer 1991). The observation that these mutants are unable to be grown photosynthetically in the presence of oxygen was one of the first pieces of evidence that carotenoids protect the photosynthetic apparatus from oxidative damage (Griffiths et al., 1955; Krinsky 1971). A comparison of the steady state and kinetic properties of the pigment-protein complexes prepared from the various carotenoid-containing strains with those of the carotenoidless mutants has provided information on the structure, geometry, dynamics and interactions of the carotenoids in the complexes (Cogdell et al. 1975; Monger et al., 1976; Parson and Monger, 1976; Frank et al., 1983; Koyama et al., 1983; Schenck et al., 1984). This comparative approach is limited, however, by the fact that only a small number of bacterial strains are available from which to isolate similar proteins having systematically varied carotenoid compositions. Indeed, many of these naturally-occurring protein complexes contain complex mixtures of carotenoids depending on growth conditions. This can complicate the interpretation of the data.

This chapter describes experiments on RC and light-harvesting pigment-protein complexes that have been isolated from carotenoidless mutants and then constituted with exogenous carotenoids. Our group and others have shown that several carotenoids can readily be incorporated into these proteins (Boucher et al., 1977; Davidson and Cogdell, 1981; Chadwick and Frank, 1986; Agalidis et al., 1990). For example, when spheroidene (Fig. 1) is incorporated into RCs of the carotenoidless mutant *Rb. sphaeroides* R-26.1, it behaves spectroscopically and functionally precisely like natural spheroidene in RCs from the *Rb. sphaeroides* wild type strain 2.4.1 (Chadwick and Frank, 1986; Frank and Violette, 1989). This

Abbreviations: BChl – bacteriochlorophyll; CD – circular dichroism, EPR – electron paramagnetic resonance; HPLC – high performance liquid chromatography; NMR – nuclear magnetic resonance; P–870 – primary donor; RC – reaction center

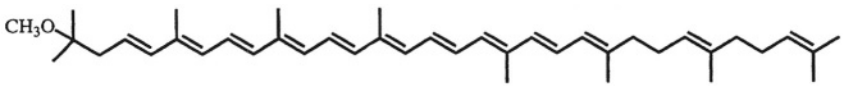

Fig. 1. The structure of spheroidene.

suggests that structurally modified carotenoids may be incorporated into the proteins to probe the effect the modifications have on the spectroscopic behavior, photochemistry and function. In this chapter, experiments on naturally-occurring and synthetic carotenoids, including specifically isotopically-labeled and locked-cis geometric isomers of carotenoids, will be described. The procedures for incorporating exogenous carotenoids into RCs and the B850 antenna complex from *Rb. sphaeroides* R26.1 will be given in detail.

II. Reaction Centers

A. Incorporation of Exogenous Carotenoids into Reaction Centers from Carotenoidless Mutants

Boucher et al. (1977) were the first to report that exogenous carotenoids could be incorporated into RCs from carotenoidless bacteria. Using the G9 strain from *Rs. rubrum,* these authors demonstrated that four carotenoids, spirilloxanthin, spheroidene, spheroidenone and chloroxanthin could be incorporated with nearly 1:1 mol ratios with respect to the primary donor (P–870). The authors showed that the bound carotenoids protected BChl against photodynamic bleaching. An analysis of the absorption and circular dichroism (CD) spectra of the bound carotenoids lead the authors to conclude that the carotenoids adopted a central mono-*cis* configuration, a conclusion later confirmed by X-ray diffraction studies on *Rhodopseudomonas viridis* and *Rb. sphaeroides* (Yeates et al., 1988; Arnoux, 1989; Deisenhofer and Michel, 1989; Ermler et al. 1994; Chapter 6, Fritsch).

Agalidis et al. (1980) showed that the carotenoidless RCs from *Rb. sphaeroides* R-26 were able to bind either spheroidene or spheroidenone in nearly 1:1 mol ratios with respect to P-870. Neither **β-carotene** nor spirilloxanthin could be bound in appreciable amounts, however, suggesting steric interactions are important in determining the type of carotenoids that could be bound. Resonance Raman investigations of the bound carotenoids carried out by these authors indicated that the carotenoids were bound in a *cis* isomeric configurations very similar to that adopted by spheroidene in wild-type RCs.

One of the important roles of carotenoids in RC complexes is to quench triplet states of the primary donor before they lead to the formation of singlet oxygen (Krinsky, 1971). Although Boucher et al. (1977) demonstrated that the bound carotenoids protected BChl against photodestruction, their work did not include experiments that directly probed triplet state formation. For this, electron paramagnetic resonance (EPR) and transient absorption spectroscopy have been used (Chadwick and Frank, 1986; Frank et al. 1986; Chapter 11, Angerhofer). Chadwick and Frank (1986) showed that the triplet state |D| and |E| zero-field splitting parameters of spheroidene incorporated into RCs of *Rb. sphaeroides* R-26.1 are precisely the same as those observed from spheroidene in wild type RCs. Frank et al. (1986) also showed that the triplet absorption spectra were the same for the two preparations, and Frank and Violette (1989) measured the lifetime of the triplet state of spheroidene to be 10.8 μs in wild type RCs and precisely the same value for spheroidene incorporated into *Rb. sphaeroides* R26.1 RCs. These authors also examined the absorption and CD spectra of spheroidene in both wild type and R-26.1 RCs containing spheroidene. They argued that the spheroidene molecules in both proteins are bound in a single site, in the same environment and with the same structure (Fig. 2).

Kolaczkowski (1989) incorporated perdeuterospheroidene into protonated and deuterated RCs and explored the role of vibrational terms in the mechanism of triplet energy transfer from the primary donor to the carotenoid. Mechanisms of triplet energy transfer have been postulated to involve specific electronic and/or vibrational states and/or structural changes in the protein to account for the activated nature of the process (Frank et al., 1983, 1993a, 1996; Takiff and Boxer, 1988a,b; Kolaczkowski, 1989; Lous and Hoff, 1989).

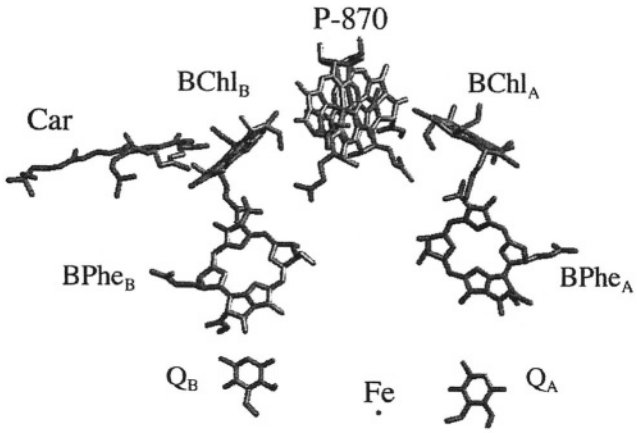

Fig. 2. The structure of the reaction center from *Rhodobacter sphaeroides* wild type. The figure was adapted using the coordinates 1PCR deposited in the Brookhaven Protein Data Bank by Ermler, et al. (1994). The phytol tails of the BChls and BPhes and the alkane chains of the quinones were removed for clarity.

B. Incorporation of Carotenoids Having Different π-Electron Chain Lengths

Work by Farhoosh et al. (1997) sought to explore systematically the effect of changing the extent of π-electron conjugation of the carotenoid bound in the RC and its consequence on the yield and dynamics of triplet energy transfer from the primary donor. The authors analyzed three carotenoids, spheroidene, 3,4-dihydrospheroidene and 3,4,5,6-tetrahydrospheroidene incorporated into *Rb. sphaeroides* R-26.1 RCs. These molecules have extents of π-electron conjugation from 8 to 10 carbon-carbon double bonds. The dynamics of the triplet states of the primary donor and carotenoid were measured at room temperature by flash absorption spectroscopy. The carotenoid, spheroidene, was observed to quench the primary donor triplet state. No quenching ofprimary donor triplet states by 3,4-dihydrospheroidene was seen in the *Rb. sphaeroides* R-26.1 RCs incorporated with that molecule nor in the R-26.1 RCs incorporated with 3,4,5,6-tetrahydrospheroidene. Triplet state EPR was also carried out on the same samples. The spectra showed carotenoid triplet state signals in the *Rb. sphaeroides* R-26.1 RCs incorporated with spheroidene, indicating that the primary donor triplet is indeed quenched by the carotenoid. However, no carotenoid signals were observed from *Rb. sphaeroides* R-26.1 RCs incorporating 3,4-dihydrospheroidene nor in RCs incorporating 3,4,5,6-tetrahydrospheroidene. CD and steady state absorbance bandshifts accompanying the primary photochemistry in the RC confirmed that the carotenoids were bound in the RCs and interacting with the primary donor. The authors hypothesized that of the three carotenoids incorporated into the RC, only spheroidene had a triplet state low enough to quench the primary donor triplet state in high yield.

C. The Mechanism of Triplet Energy Transfer from the Primary Donor-to-Carotenoids in Chemically Modified Reaction Centers

Sodium borohydride-treated *Rb. sphaeroides* R-26 RCs are known to have the bridging BChl$_B$ molecule removed or dislocated (Ditson et al. 1984; Maroti et al. 1985; Struck, 1991). Frank and Violette (1989) incorporated spheroidene into these RCs and demonstrated that compared to untreated RCs, the primary donor-to-carotenoid triplet energy transfer was inhibited. This suggested that the process of triplet energy transfer was dependent on the triplet state energy of the bridging BChl$_B$ molecule as postulated by Takiff and Boxer (1988a,b) from phosphorescence studies and Schenk et al. (1984) from transient absorption measurements. If the triplet energy of the bridging BChl$_B$ molecule is truly the source of the activated temperature dependence of the transfer process, experiments on RCs having BChl molecules with altered triplet energies in that site should show different temperature dependencies. The modified RCs allowed a test of the role of the BChl$_B$ pigment in the mechanism of triplet energy transfer.

Scheer and coworkers (Struck and Scheer, 1990; Struck et al., 1990a,b; Harwich et al., 1995) reported

a procedure for exchanging the native BChls at the accessory BChl ($BChl_A$ and $BChl_B$) binding sites for modified BChl pigments. By incorporating modified pigments, the effect of the structural change on the activation energy, dynamics, and efficiency of primary donor-to-carotenoid triplet energy transfer may be studied.

Frank et al. (1996) measured the dynamics of triplet energy transfer between the primary donor and the carotenoid on photosynthetic bacterial RC preparations from *Rb. sphaeroides* R26.1 exchanged with 13²-hydroxy-[Zn]-BChl at the accessory BChl sites and constituted with spheroidene, and R26.1 RCs exchanged with [3-vinyl]-13²-hydroxy-BChl at the accesssory BChl sites and also constituted with spheroidene. For the samples containing carotenoids, all of the decay times corresponded well to the previously observed times for spheroidene. The rise times of the carotenoid triplets were found in all cases to be bi-exponential and comprised of a strongly temperature dependent component and a temperature independent component. From a comparison of the behavior of the carotenoid containing samples with that from the RC of the carotenoidless mutant *Rb. sphaeroides* R-26.1, the temperature independent component was assigned to the build-up of the primary donor triplet state resulting from charge recombination in the RC. Arrhenius plots of the rate constant for the buildup of the carotenoid triplet state were used to determine the activation energies for triplet energy transfer from the primary donor to the carotenoid. These activation energies were observed to be different for the different RC preparations. The data showed clearly that the activation barrier for triplet energy transfer is dependent on the triplet state energy of the accessory BChl pigment, $BChl_B$.

*D. Locked-*cis *Carotenoids Incorporated into* Rb. sphaeroides *R-26 Reaction Centers*

It has been suggested (Koyama et al. 1990, Kuki et al. 1995) that *cis* carotenoid isomers, and specifically the 15-*cis* isomer, exists in the RC to enhance the ability of the carotenoid to dissipate triplet energy via *cis*-to-*trans* isomerization. Bautista et al. (1998) tested this mechanism using locked-15,15´-*cis*-spheroidene. By a comparison of the behavior of the locked-15,15´-*cis*-spheroidene with the unlocked spheroidene incorporated into RCs, and also comparing these samples with wild type RCs, it was possible to determine whether *cis*-to-*trans* isomerization is a factor contributing to the mechanism of triplet energy transfer. If a *cis*-to-*trans* isomerization of the carotenoid is involved in the mechanism of triplet trapping and energy dissipation, the process should be either inhibited or altered in some manner in the RC sample containing the locked-15,15´-*cis*-spheroidene.

The spectroscopic and photochemical properties of the synthetic carotenoid, locked-15,15´-*cis*-spheroidene, were studied by absorption, fluorescence, CD, fast transient absorption and EPR spectroscopies in solution and after incorporation into the RC of *Rb. sphaeroides* R-26.1. High performance liquid chromatography (HPLC) purification of the synthetic molecule reveal the presence of several di-*cis* geometric isomers in addition to the mono-*cis* isomer of locked-15,15'-*cis*-spheroidene. In solution, the absorption spectrum of the purified mono-*cis* sample was red-shifted and showed a large *cis*-peak at 351 nm compared to unlocked all-*trans* spheroidene. Spectroscopic studies of the purified locked-15,15´-mono-*cis* molecule in solution revealed a more stable manifold of excited states compared to the unlocked spheroidene. Molecular modeling and semi-empirical calculations revealed that geometric isomerization and structural factors affect the room temperature spectra. RCs of *Rb. sphaeroides* R-26.1 in which the locked-15,15´-*cis*-spheroidene was incorporated showed no difference in either the spectroscopic properties or photochemistry compared to RCs in which unlocked spheroidene was incorporated or to *Rb. sphaeroides* wild type strain 2.4.1 RCs which naturally contain spheroidene. The data indicate that the natural selection of a *cis*-isomer of spheroidene for incorporation into native RCs of *Rb. sphaeroides* wild type strain 2.4.1 was probably more determined by the structure or assembly of the RC protein than by any special quality of the *cis*-isomer of the carotenoid that would affect its ability to accept triplet energy from the primary donor or to carry out photoprotection.

E. Solid-State Magic Angle Spinning NMR on Isotopically-Labeled Carotenoids in Rb. sphaeroides *Reaction Centers*

The ability to incorporate carotenoids into pigment protein complexes allowed solid-state magic angle spinning (MAS) nuclear magnetic resonance (NMR) experiments to be carried out on isotopically-labeled

carotenoids in *Rb. sphaeroides* RCs. DeGroot et al. (1992) analyzed the configuration around the central (15,15′) double bond of the RC-bound carotenoid, spheroidene, using low-temperature MAS ^{13}C NMR. RCs from the carotenoidless mutant *Rb. sphaeroides* R-26 were constituted with spheroidene specifically isotopically labeled with ^{13}C at the C-14′ or C-15′ position and the signals from the labels were separated from the natural abundance background using ^{13}C MAS NMR difference spectroscopy. The resonances were observed to shift upfield upon incorporation of the carotenoids into the protein complex, similar to the upfield shifts occurring in β-carotene upon *trans* to 15,15′-*cis* isomerization. Hence, the MAS NMR revealed a *cis*-configuration about the 15,15′ double bond. This study was the first MAS ^{13}C NMR investigation of a carotenoid in a pigment-protein complex. It demonstrated the feasibility of MAS NMR as an important non-destructive spectroscopic probe of components of the RC.

F. Resonance Raman Spectroscopy on Isotopically-Labeled Carotenoids Incorporated into Rb. sphaeroides *R-26 Reaction Centers*

Resonance Raman spectroscopy carried out on carbon-specific, isotopically-labeled carotenoids can provide an important means to assign the Raman spectral bands and, upon incorporation of the carotenoid into RCs, can aid greatly in elucidating structural features not evident from X-ray diffraction studies and in understanding the effect of the protein on the vibrational activity of the carotenoid. Kok et al. (1994,1997) have examined the resonance Raman spectra of several ^{13}C- and ^{2}H-labeled spheroidenes incorporated into *Rb. sphaeroides* R26.1 RCs. 14-^{2}H, 15-^{2}H, 15′-^{2}H, 14′-^{2}H, 14,15′-^{2}H and 15,15′-^{2}H spheroidenes were examined in petroleum ether and except for 14,15′-^{2}H spheroidene, also incorporated in the *Rb. sphaeroides* R26.1 RC. The data show evidence for out-of-plane distortion of the RC-bound carotenoid in the central C_{14} to C'_{14} region.

G. Method for Reconstitution of Carotenoids into Reaction Centers of Rb. sphaeroides *R-26.1*

For the incorporation of carotenoids, RCs from *Rb. sphaeroides* R-26.1 are introduced into a small (8 ml) vial, and 1% of Triton X-100 in 15 mM Tris buffer, pH 8, is added to obtain a final solution of 0.67% Triton X-100. A 15-fold molar excess of the carotenoid in petroleum ether relative to BChl is layered onto the surface of the RC solution. The petroleum ether is then evaporated with a steam of nitrogen. The resulting mixture is sonicated for 30–45 min at room temperature in the dark. The solution is then diluted 1:5 with 15 mM Tris buffer, pH 8.0, and loaded onto a 1 x 8 cm DEAE Sephacel column. The RCs now containing the carotenoid, are washed using a buffer containing 15 mM Tris, 0.1% Triton X-100 and 100 mM NaCl at pH 8.0 to remove the excess unbound carotenoids. The purified RCs are then eluted using a buffer containing 15 mM Tris, 0.1 % Triton X-100 and 300 mM NaCl at pH 8.0, and then dialyzed overnight using Spectrapor standard cellulose dialysis tubing (25 mm, M.W. cutoff 12,000–14,000 D) against 15 mM Tris buffer containing 0.03%Triton X-100, atpH 8.0. Finally, the RCs with the carotenoid incorporated are concentrated for subsequent use by centrifugation at 3,000 x g using an Amicon microconcentrator (MW cutoff of 10,000 D). The absorption spectrum of *Rb. sphaeroides* R26.1 RCs before and after spheroidene incorporation are shown in Fig. 3.

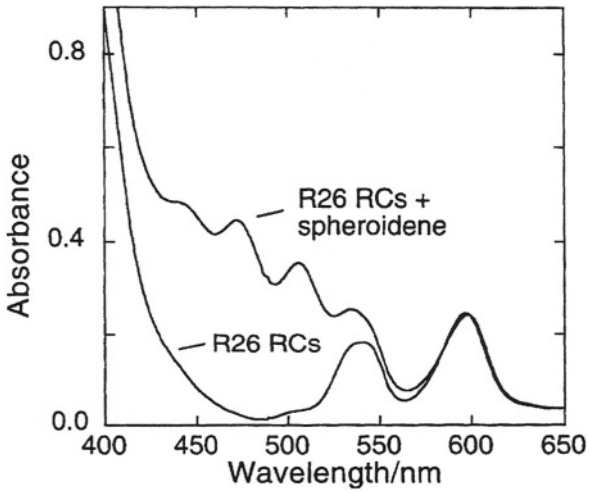

Fig. 3. The absorption spectra of *Rb. sphaeroides* R26 RCs with and without spheroidene incorporated.

III. Light-Harvesting Complexes

A. Incorporation of Exogenous Carotenoids into Light-Harvesting Complexes from Carotenoidless Mutants

The absorption spectrum of cells of *Rb. sphaeroides* R-26 when it was first described in 1963, displayed a peak at 870 nm and, in comparison with the wild type

strain, was shown to lack the B800-850 (or LH2) protein (Crounse et al., 1963). As time passed, it was found that the 870 nm absorption band attributable to the antenna complex had moved between 5 and 10 nm to shorter wavelength. A comparative analysis (Davidson and Cogdell, 1981; Theiler et al., 1984) revealed a partial revertant of the original R-26 had resulted in the bacterium regaining the LH2 protein. The revertant was denoted R-26.1 and the α and β subunits of the LH2 protein complex sequenced and compared with the standard form of the LH2 complex from *Rb. sphaeroides* wild type strain 2.4.1. It was found that a single replacement of a phenylalanine in the R26.1 LH2 complex for a valine at position 24 in the α-subunit of the wild type complex had occurred. The LH2 complex from *Rb. sphaeroides* R-26.1 is a B800-850-type of protein, having high sequence homology with the LH2 complex from *Rb. sphaeroides* wild type strain 2.4.1, but lacking the 800 nm absorbing BChl. For this reason, the LH2 complex from *Rb. sphaeroides* R-26.1 is sometimes referred to as the B850 complex.

Davidson and Cogdell (1981) showed that two carotenoids, neurosporene and spheroidene, could be incorporated into the B850 light-harvesting complex from *Rb. sphaeroides* R-26.1 by mixing the carotenoids with freeze-dried chromatophore membranes. They showed that carotenoids incorporated in this manner were able to transfer energy to BChl and also protect the complex from the photodynamic reaction.

In a study aimed at exploring the factors controlling the efficiency of energy transfer from carotenoids to BChl in purple photosynthetic bacteria, Hayashi et al., (1989) and Noguchi et al., (1990) incorporated several carotenoids into antenna complexes from *Chromatium (Ch.) vinosum* and into the B870 antenna pigment-protein from the original *Rb. sphaeroides* R-26. Using absorption, fluorescence excitation, and resonance Raman spectroscopy the authors found a correlation between the appearance of an out-of-plane CH wagging mode at 965 cm^{-1} in the Raman spectrum and a reduced efficiency of singlet energy transfer between carotenoids and BChl. They argued that the distortion of the π-electron chain of the carotenoid which is more pronounced for carotenoids bound in the pigment-protein complex from *Ch. vinosum* than in *Rb. sphaeroides* led to a decrease in the efficiency of light-harvesting. Also, they found that carotenoids having 11 to 13 carbon-carbon double bonds showed lower efficiencies of energy transfer, <50%, presumably due to their higher propensity to be distorted than spheroidene which has ten carbon–carbon double bonds and exhibits a fairly high, >90%, energy transfer efficiency to BChl.

B. Incorporation of Carotenoids Having Different π-Electron Chain Lengths

To examine the effect of π-electron conjugated chain length on singlet energy transfer, Frank et al. (1993b) and Farhoosh et al. (1994) incorporated 3,4,7,8-tetrahydrospheroidene, 3,4,5,6-tetrahydrospheroidene, 3,4-dihydrospheroidene, and spheroidene into the B850 complex of the carotenoidless mutant *Rb. sphaeroides* R-26.1. In this group of molecules the extent of π-electron conjugation increases incrementally from seven to ten conjugated carbon-carbon double bonds. The experiments probed the effects of energy levels, spectral overlap, and dynamics on the efficiency of energy transfer. Desamero et al. (1998) extended this work by incorporating spheroidene analogs having extents of π-electron conjugation ranging from 10 to 13 carbon-carbon double bonds into the same B850 light-harvesting complex from *Rb. sphaeroides* R-26.1. The spheroidene analogs used in that study were 5′,6′-dihydro-7′,8′-didehydrospheroidene, 7′,8′-didehydrospheroidene, and 1′,2′-dihydro-3′,4′,7′,8′-tetradehydrospheroidene and the data, taken together with the results of the studies by Farhoosh et al. (1994) provided a large range of molecules for understanding the molecular features that determine the mechanism of energy transfer from carotenoids to BChl in photosynthetic bacterial light-harvesting complexes. The authors used steady-state absorption, fluorescence, fluorescence excitation, resonance Raman, and time-resolved absorption spectroscopy in their investigations. The sub-picosecond dynamics data were interpreted in conjunction with the carotenoid-to-BChl energy transfer efficiencies measured by steady state fluorescence excitation methods and suggested that only carotenoids having ten or fewer carbon-carbon double bonds transfer energy via their 2^1A_g (S_1) states to BChl to any significant degree. The data further suggested that energy transfer via the 1^1B_u (S_2) state of the carotenoid becomes more important than the S_1 route as the number of conjugated carbon-carbon double bonds increases above ten. Finally, the results suggested that the S_2 state associated with the Q_x transition of the B850 BChl, is the most likely acceptor state for energy transfer originating from both the 2^1A_g (S_1) and 1^1B_u (S_2) states of all carotenoids.

C. Incorporation of Carotenoids into Higher Plant Light-Harvesting Complexes

One of the roles of carotenoids is to act as energy flow regulators, dissipating excess energy not used for photosynthesis (Demmig-Adams, 1990). This effect manifests itself as a quenching of Chl fluorescence (Horton et al., 1996). One approach used to study the effect of carotenoids on Chl fluorescence is to examine the effect of exogenous pigments on quenching in the isolated light-harvesting system. This has been done using the bulk light-harvesting complex, LHC IIb (Phillip et al., 1996), and, more recently, the minor PS II light-harvesting complexes (Ruban et al., 1996). The main conclusion from these studies was that the addition of violaxanthin and zeaxanthin affected the aggregation state of the complex and had quite different effects on fluorescence quenching. The addition of violaxanthin to isolated LHC IIb inhibited quenching and this carotenoid could in fact be considered to be acting as an 'anti-quencher.' In contrast, zeaxanthin acted to stimulate the quenching of Chl fluorescence. Interestingly, this effect was most pronounced in the minor complexes rather than the bulk complex, again highlighting their possible key role in non-photochemical quenching. A key observation was the pH-dependence of this effect in vitro, adding further support to the activation (i.e. low pH requirement) of quenching by stimulating the formation of LHC II aggregates. These studies using exogenous carotenoids in higher plant complexes are described in detail in Chapter 15, Horton et al.

D. Method for Reconstitution of Carotenoids into the B850 Complex of Rb. sphaeroides *R-26.1*

This method for constituting carotenoids into the B850 light-harvesting complex from *Rb. sphaeroides* R-26.1 uses a procedure outlined by Noguchi et al. (1990) with some modifications introduced by Frank et al. (1993b). Before the carotenoids can be incorporated into the B850 light-harvesting complex, the detergent in the solution should be exchanged from 0.1% LDS to 2% deoxycholate (5β-cholan-24-oic acid-3α, 12α-diol). This is done by dialyzing the purified B850 light-harvesting solution overnight against 15 mM Tris buffer, pH 8.0, containing 2% deoxycholate. The carotenoid dissolved in petroleum ether is layered on the surface of the B850 light-harvesting complex in a molar ratio of 15:1 carotenoid-to-BChl. A stream of nitrogen gas is then passed over the surface of the solution until all of the petroleum ether had evaporated and the carotenoid is deposited as a thin film on the side of the vial. The mixture is then sonicated 30–45 min at 4 °C in the dark, after which an additional 15-fold molar excess of carotenoid in petroleum ether is added. Again, the petroleum ether can be evaporated using the stream of nitrogen gas and the mixture sonicated in the dark. Excess carotenoids can be removed by the application of the solution to a discontinuous sucrose density gradient, consisting of 0.75 M, 1.5 M and 2 M sucrose solutions, and subsequent ultracentrifugation at 150,000 x *g* and 4 °C for 18 hours. The purified carotenoid-constituted B850 light-harvesting complex should then be dialyzed overnight against 15 mM Tris buffer, pH 8.0, with 0.02% deoxycholate to remove the sucrose from the solution.

Acknowledgments

The author wishes to thank several of his present and former students, Mila Aldema, James Bautista, Barry Chadwick, Agnes Cua, Ruel Desamero, John Machnicki, William McGann, Shane Taremi, and Carol Violette, postdoctoral associates, Veeradej Chynwat, Jennifer Innes, and Pierre Parot, and collaborators, David Bocian, Ronald Christensen, Richard Cogdell, Huub DeGroot, Ronald Gebhard, Edgar Groenen, David Gosztola, Frans Jos Jansen, Johan Lugtenburg, Ineke van der Hoef, and Michael Wasielewski, without whose efforts these studies would not have been possible. Work on carotenoids and xanthophylls in the author's laboratory is supported by grants from the National Institutes of Health (GM-30353), the National Science Foundation (MCB-9816759), and the University of Connecticut Research Foundation.

References

Agalidis I, Lutz M and Reiss-Husson F (1980) Binding of carotenoids on reaction centers from *Rhodopseudomonas sphaeroides* R–26. Biochim Biophys Acta 589: 264–274

Arnoux B, Ducruix A, Reiss-Husson F, Lutz M, Morris J, Schiffer M and Chang CH (1989) Structure of spheroidene in the photosynthetic reaction center from Y *Rhodobacter sphaeroides.* FEBS Letters 258: 47–50

Bautista JA, Chynwat V, Cua A, Jansen FJ, Lugtenburg J, Gosztola D, Wasielewski MR and Frank HA (1998) The

spectroscopicand photochemical properties of locked-15,15′-cis-spheroidene in solution and incorporated into the reaction center of *Rhodobacter sphaeroides* R-26.1. Photosyn Res 55: 49–65

Boucher F, van der Rest M and Gingras G (1977) Structure and function of carotenoids in the photoreaction center from *Rhodospirillum rubrum.* Biochim Biophys Acta 461:339–357

Budil DE and Thurnauer MC (1991) The chlorophyll triplet state as a probe of structure and function in photosynthesis. Biochim Biophys Acta 1057: 1–41

Chadwick W and Frank HA (1986) Electron-spin resonance studies of carotenoids incorporated into reaction centers of *Rhodobacter sphaeroides* R-26.1. Biochim Biophys Acta 851: 257–266

Cogdell RJ and Frank HA (1987) How carotenoids function in photosynthetic bacteria. Biochim Biophys Acta 895: 63–79

Cogdell RJ, Monger TG and Parson WW (1975) Carotenoid triplet states in reaction centers from *Rhodopseudomonas sphaeroides* and *Rhodospirillum rubrum.* Biochim Biophys Acta 408: 189–199

Crounse JB, Feldman RP and Clayton RJ (1963) Accumulation of polyene precursors of neurosporene in mutant strains of *Rhodopseudomonas spheroides.* Nature 198: 1227–1228

Davidson E and Cogdell RJ (1981) Reconstitution of carotenoids into the light-harvesting pigment-protein complex from the carotenoidless mutant of *Rhodopseudomonas sphaeroides* R-26. Biochim Biophys Acta 635: 295–303

De Groot HJM, Gebhard R, van der Hoef I, Hoff AJ, Lugtenburg J, CA Violette and Frank HA (1992) ^{13}C magic angle spinning NMR evidence for a 15,15′-cis configuration of the spheroidene in the *Rhodobacter sphaeroides* photosynthetic bacterial reaction center. Biochemistry 31: 12446–12450

Deisenhofer J and Michel H (1989) The photosynthetic reaction centre from the purple bacterium *Rhodopseudomonas sphaeroides* and *Rhodospirillum rubrum.* Chemica Scripta 29: 205–220

Demmig-Adams B (1990) Carotenoids and photoprotection in plants: A role for the xanthophyll zeaxanthin. Biochim Biophys Acta 1020: 1–24

Desamero RZB, Chynwat V, van der Hoef I, Jansen FJ, Lugtenburg J, Gosztola D, Wasielewski MR, Cua A, Bocian DF and Frank HA (1998) The mechanism of energy transfer from carotenoids to bacteriochlorophyll: Light-harvesting by carotenoids having different extents of π-electron conjugation incorporated into the B850 antenna complex from the carotenoidless bacterium *Rhodobacter sphaeroides* R-26.1. J Phys Chem l02: 8151–8162

Ditson S, Davis RC and Pearlstein RM (1984) Relative enrichment of P–870 in photosynthetic reaction centers treated with sodium borohydride. Biochim Biophys Acta 766: 623–629

Ermler U, Fritzsch G, Buchanan SK and Michel H (1994) The structure of the photosynthetic reaction centre from *Rhodobacter sphaeroides* at 2.65 angstroms resolution: Cofactors and protein-cofactor interactions. Structure 2: 925–936

Farhoosh R, Chynwat V, Gebhard R, Lugtenburg J, Frank HA (1994) Triplet energy transfer between bacteriochlorophyll and carotenoids in B850 light-harvesting complexes of *Rhodobacter sphaeroides* R-26.1. Photosynth Res 42: 157–166

Farhoosh R, Chynwat V, Gebhard R, Lugtenburg J and Frank HA (1997) Triplet energy transfer between the primary donor and carotenoids in *Rhodobacter sphaeroides* R-26.1 reaction centers incorporated with spheroidene analogs having different extents of π-electron conjugation. Photochem Photobiol 66:97–104

Feher G and Okamura Y (1978) Chemical composition and properties of reaction centers. In: Clayton RK and Sistrom WR (eds) The Photosynthetic Bacteria, pp 349–386. Plenum Press, New York

Frank HA and Christensen RL (1995) Singlet Energy Transfer from Carotenoids to Bacteriochlorophylls. In: Blankenship RE, Madigan MT and Bauer CE (eds) Anoxygenic Photosynthetic Bacteria, Advances in Photosynthesis, pp 373–384. Kluwer Academic Publishing, Dordrecht

Frank HA and Cogdell RJ (1993) Photochemistry and functions of carotenoids in photosynthesis. In: Young A and Britton G (eds) Carotenoids in Photosynthesis, pp 252–326. Springer–Verlag, London

Frank HA and Violette CA (1989) Monomeric bacteriochlorophyll is required for triplet energy transfer between the primary donor and the carotenoid in photosynthetic bacterial reaction centers Biochim Biophys Acta 976: 222–232

Frank HA, Machnicki J and Friesner R (1983) Energy transfer between the primary donor bacteriochlorophyll and carotenoids in *Rhodopseudomonas sphaeroides.* Photochem Photobiol 38: 451–456

Frank HA, Chadwick BW, Taremi S, Kolaczkowski S and Bowman M (1986) Singlet and triplet absorption spectra of carotenoids bound in the reaction centers of *Rhodopseudomonas sphaeroides* R-26. FEBS Lett 203: 157–163

Frank HA, Chynwat V, Hartwich G, Meyer M, Katheder I and Scheer H (1993a) Carotenoid triplet state formation in *Rhodobacter sphaeroides* R-26 reaction centers exchanged with modified–bacteriochlorophyll pigments and reconstituted with spheroidene. Photosynth Res 37: 193–203

Frank HA, Farhoosh R, Aldema ML, DeCoster B, Christensen RL, Gebhard R and Lugtenberg J (1993b) Carotenoid-to-bacteriochlorophyll singlet energy transfer in carotenoid-incorporated B850 light-harvesting complexes of *Rb. sphaeroides* R-26.1. J Photochem Photobiol 57: 49–55

Frank HA, Chynwat V, Posteraro A, Hartwich G, Simonin I and Scheer H (1996) Triplet state energy transfer between the primary donor and the carotenoid in *Rhodobacter sphaeroides* R-26.1 reaction centers exchanged with modified bacteriochlorophyll pigments and reconstituted with spheroidene. Photochem Photobiol 64: 823–831

Griffiths M, Sistrom WR, Cohen-Bazire G and Stanier RY (1955) Function of carotenoids in photosynthesis. Nature 176: 1211–1214

Hartwich G, Scheer H, Aust V and Angerhofer A (1995) Absorption and ADMR studies on bacterial photosynthetic reaction centers with modified pigments. Biochim Biophys Acta 1230: 97–113

Hayashi H, Noguchi T and Tasumi M (1989) Studies on the interrelationship among the intensity of a Raman marker band of carotenoids, polyene chain-structure, and efficiency of the energy transfer from carotenoids to bacteriochlorophyll in photosynthetic bacteria. Photochem Photobiol 49: 337–343

Horton P, Ruban AV and Walters RG (1996) Regulation of light harvesting in green plants. Annu Rev Plant Physiol Mol Biol 47:655–684

Hudson BS and Kohler BE (1984) Electronic structure and

spectra of finite linear polyenes. Synthetic Metals 9: 241–253
Hudson BS, Kohler BE and Schulten K (1982) Linear polyene electronic structure and potential surfaces. In: Lim EC (ed) Excited State, Vol 6, pp 1–95. Academic Press, New York
Jirsakova V and Reiss-Husson F (1994) A specific carotenoid is required for reconstitution of the Rubrivivax gelatinosus B875 light harvesting complex from its subunit form B820. FEBS Lett 353: 151–154
Kohler BE (1991) Electronic properties of linear polyenes. In: Brédas JL and Silbey R (eds) Conjugated Polymers: The novel science and technology of highly conducting and nonlinear optically active materials, pp 405–434. Kluwer Press, Dordrecht
Kok P, Köhler J, Groenen EJJ, Gebhard R, van der Hoef I, Lugtenburg J, Hoff AJ, Farhoosh R and Frank HA (1994) Towards a vibrational analysis of spheroidene. Resonance Raman spectroscopy of ^{13}C-labeled spheroidenes in petroleum ether and in the *Rhodobacter sphaeroides* reaction centre. Biochim Biophys Acta 1185: 188–192
Kok P, Köhler J, Groenen EJJ, Gebhard R, van der Hoef I, Lugtenburg J, Farhoosh R and Frank HA (1997) Resonance Raman spectroscopy of ^{2}H-labeled spheroidenes in petroleum ether and in the *Rhodobacter sphaeroides* reaction centre. Spectr Chim Acta A Biomolec Spectros 53: 381–392
Kolaczkowski SV (1989) On the mechanism of triplet energy transfer from the primary donor to spheroidene in photosynthetic reaction centers from *Rhodobacter sphaeroides* 2.4.1. Ph.D. Thesis, Brown University
Koyama Y, Takii T, Saiki K and Tsukida K (1983) Configuration of the carotenoid in the reaction centers of photosynthetic bacteria-2. Comparison of the resonance Raman lines of the reaction centers with those of 14 different cis-trans isomers of β-carotene. Photobiochem Photobiophys 5: 139–150
Koyama Y, Takatsuka I, Kanaji M, Tomimoto K, Kito M, Shimamura T, Yamashita J, Saiki K and Tsukida K (1990) Configurations of carotenoids in the reaction center and the light-harvesting complex of *Rhodospirillum rubrum*: Natural selection of carotenoid configurations by pigment-protein complexes. Photochem Photobiol 51: 119–128
Krinsky NI (1968) The protective function of carotenoid pigments. In: Giese AC (ed) Photophysiology, Vol III, pp 123–195. Academic Press, New York
Krinsky NI (1971) Function. In: Isler O, Guttman G and Solms U (eds) Carotenoids, pp 669–716. Birkhauser Verlag, Basel
Kuki M, Naruse M, Kakuno T and Koyama Y (1995) Resonance Raman evidence for 15-*cis* to all-*trans* photoisomerization of spirilloxanthin bound to a reduced form of the reaction center of *Rhodospirillum rubrum* S1. Photochem Photobiol 62: 502–508
Lang HP and Hunter CN (1994) The relationship between carotenoid biosynthesis and the assembly of the light-harvesting LH2 complex in *Rhodobacter sphaeroides*. Biochem J 298: 197–205
Lous EK and Hoff AJ (1989) Isotropic and linear dichroic triplet-minus-singlet absorbance difference spectra of two carotenoid-containing bacterial photosynthetic reaction centers in the temperature range 10–288 K. An analysis of bacteriochlorophyll-carotenoid triplet transfer. Biochim Biophys Acta 974: 88–103
Maroti P, Kirmaier C, Wraight C, Holten D and Pearlstein RM (1985) Photochemistry and electron transfer in borohydride-treated photosynthetic reaction centers. Biochim Biophys Acta 810: 132–139
Monger T, Cogdell RJ and Parson WW (1976) Triplet states of bacteriochlorophyll and carotenoids in chromatophores of photosynthetic bacteria. Biochim Biophys Acta 449: 136–153
Noguchi T, Hayashi H and Tasumi T (1990) Factors controlling the efficiency of energy transfer from carotenoids to bacteriochlorophyll in purple photosynthetic bacteria. Biochim Biophys Acta 1017: 280–290
Parson WW and Monger TG (1976) Interrelationships among excited states in bacterial reaction centers. Brookhaven Symp Biol 28: 195–212
Phillip D, Ruban AV, Horton P, Asato A and Young AJ (1996) Quenching of chlorophyll fluorescence in the major light-harvesting complex of photosystem II: Effect of carotenoid S_1 energy. Proc Natl Acad Sci USA 93: 1492–1497
Ruban AV, Young AJ and Horton P (1996) Dynamic properties of the minor chlorophyll *a/b* binding proteins of Photosystem II—an in vitro model for photoprotective energy dissipation in the photosynthetic membrane of green plants. Biochemistry 35: 674–678
Schenck CC, Mathis P and Lutz M (1984) Triplet formation and triplet decay in reaction centers from the photosynthetic bacterium *Rhodopseudomonas sphaeroides*. Photochem Photobiol 39:407–417
Struck A and Scheer H (1990) Modified reaction centers from Rb. sphaeroides R-26. Exchange of monomeric bacteriochlorophyll with 13^2-hydroxy-bacteriochlorophyll. FEBS Lett 261: 385–388
Struck A, Beese D, Cmiel E, Fischer M, Müller A, Schäfer W and Scheer H (1990a) Modified bacterial reaction centers: 3. Chemical modified chromophores at sites B_A, B_B, and H_A, H_B. In: Michel-Beyerle (ed) Springer Series in Biophysics: Reaction Centers of Photosynthetic Bacteria, Vol 6, pp 313–326. Springer, Berlin
Struck A, Cmiel E, Katheder I and Scheer H (1990b) Modified reaction centers from Rb. sphaeroides R-26: 2: Bacteriochlorophylls with modified C-3 substituents at sites B_A and B_B. FEBS Lett 268: 180–184
Struck A, Müller A and Scheer H (1991) Modified bacterial reaction centers. 4. The borohydride treatment reinvestigated: comparison with selective exchange experiments at binding sites $B_{A,B}$ and $H_{A,B}$. Biochim Biophys Acta 1060: 262–270
Takiff L and Boxer SG (1988a) Phosphorescence from the primary electron donor in *Rhodobacter sphaeroides* and *Rhodopseudomonas viridis* reaction centers. Biochim Biophys Acta 932: 325–334
Takiff L and Boxer SG (1988b) Phosphorescence spectra of bacteriochlorophylls. J Am Chem Soc 110: 4425–4426
Theiler R, Suter F, Zuber H and Cogdell RJ (1984) A comparison of the primary structures of the two B800-850-apoproteins from wild-type *Rhodopseudomonas sphaeroides* strain 2.4.1 and carotenoidless mutant strain R26.1. FEBS Lett 175: 231–237
Yeates TO, Komiya H, Chirino A, Rees DC, Allen JP and Feher G (1988) Structure of the reaction center from *Rhodopseudomonas sphaeroides* R-26 and 2.4.1: Protein-cofactor (bacteriochlorophyll, bacteriopheophytin, and carotenoid) interactions. Proc Natl Acad Sci USA 85: 7993–7997

Chapter 14

Ecophysiology of the Xanthophyll Cycle

Barbara Demmig-Adams, William W. Adams III, Volker Ebbert, and Barry A. Logan
Department of Environmental, Population, and Organismic Biology,
University of Colorado, Boulder, CO 80309-0334, U.S.A.

Summary

This chapter seeks to illustrate the impressive range of environmental modulation of the xanthophyll cycle in terrestrial plants in their natural habitats, where the demand for thermal energy dissipation can change within seconds or between seasons and vary from a moderate to a very large fraction of the absorbed light. Plants from habitats with concomitant xanthophyll cycle conversions and changes in energy dissipation activity are included as well as examples from habitats in which zeaxanthin and antheraxanthin (Z+A) persist and energy dissipation is modulated largely via their rapid engagement and disengagement. The well-characterized, rapidly inducible and reversible form of xanthophyll cycle-dependent energy dissipation is contrasted with the sustained maintenance of higher levels of (Z+A)-dependent thermal dissipation under various environmental

H. A. Frank. A. J. Young, G. Britton and R. J. Cogdell (eds): The Photochemistry of Carotenoids, pp. 245–269.

stresses with an emphasis on seasonally low temperatures. Furthermore, the association of Z+A retention with the phenomenon of photoinhibition of Photosystem II (and alterations in the stoichiometry of proteins associated with PS II) is discussed as well as a possible involvement of thylakoid protein phosphorylation in sustained (Z+A)-dependent energy dissipation. An integrative understanding is sought by comparing acclimation patterns of thermal energy dissipation as well as overall foliar antioxidant capacity with those of photosynthetic and respiratory metabolism of whole plants. It is proposed that acclimation of all of these processes responds to whole plant source-sink relationships.

I. Introduction

The intensity of solar irradiance, the energy source for all photosynthetic organisms, varies dramatically in nature. Very different light environments are experienced by leaves at different positions in the canopy of a plant or individual plants growing at the extremes of deep shade or full sunlight; and even individual leaves routinely experience large fluctuations in irradiance levels over the course of a single day. While whole plant photosynthesis rates may very well increase proportionally up to full sunlight, photosynthesis rates of individual leaves do not. Instead, at the level of the individual leaf, only a portion of full sunlight can be utilized for photochemistry and photosynthesis. Sun leaves at noon typically absorb much of the incident solar radiation resulting in a considerable excess of excitation energy. This unutilized and excess excitation energy has the potential to decay via pathways leading to dangerous reactive intermediates such as singlet oxygen formed from triplet chlorophyll in the pigment bed. To prevent an increased deexcitation via these undesirable pathways, excess excitation energy is dissipated harmlessly as heat via an alternative pathway—by deexcitation of excess singlet excited chlorophyll directly. This process is used by all species of higher plants examined to date and, as will be illustrated below, is employed routinely each day by leaves of most plant species.

The photoprotective dissipation of excess excitation energy is typically catalyzed by a combination of two factors, the association of the xanthophylls zeaxanthin and antheraxanthin (Z+A) with proteins of the light-collecting pigment bed (see Chapter 16, Yamamoto) and the protonation of these proteins. The initial proposal of a role of the xanthophyll cycle in energy dissipation (Demmig et al., 1987) was followed by a decade of intense research into the relationship among the three processes, (i) energy dissipation, (ii) xanthophyll cycle deepoxidation, and (iii) thylakoid acidification (for selected recent reviews see Demmig-Adams et al., 1996a; Demmig-Adams and Adams, 1996a; Horton et al., 1996; Eskling et al., 1997; Gilmore, 1997). Recently, elegant studies with mutants of the xanthophyll cycle (Niyogi et al., 1998; see Chapter 2, DellaPenna) as well as studies dissecting the role of protonation versus xanthophyll deepoxidation in vivo (for a review see Gilmore, 1997) have provided convincing evidence for an obligatory role of xanthophylls in energy dissipation. In higher plants, the majority of thermal energy dissipation depends on the presence of Z+A of the xanthophyll cycle while the actual engagement of thermal dissipation is induced by thylakoid acidification as the signal for the presence of excess light (Gilmore et al., 1998).

The molecular mechanism of (Z+A)/pH-dependent thermal energy dissipation remains to be established in vivo. However, based on determinations of the S_1 energy levels of these molecules (Frank et al., 1994; Phillip et al., 1996) a simple and direct singlet-singlet energy transfer downhill from $^1Chl^*$ to zeaxanthin (and possibly antheraxanthin) has now been shown to be energetically feasible (see Chapters 13, Frank and 15, Horton et al.).

Abbreviations: A–antheraxanthin; APX–ascorbate peroxidase; α-C – α-carotene; β-C – β-carotene; $^1Chl^*$ – singlet excited chlorophyll; CP–minor chlorophyll-binding protein; D–fraction of excitation energy absorbed by chlorophyll associated with PS II that is dissipated thermally; D1 – D1 protein of the PS II reaction center; F_o – minimal level of fluorescence at open PS II units; F_m, F_m' – maximal level of fluorescence at open PS II units in darkness and during illumination, respectively; F_v/F_m, F_v'/F_m' – efficiency of open PS II units in darkness and during illumination, respectively; GR – glutathione reductase; L – lutein; La – lactucaxanthin; LHC – light-harvesting chlorophyll-binding proteins; LHCII–peripheral, major light-harvesting chlorophyll–binding protein of PSII; N–neoxanthin; NPQ–nonphotochemical quenching of chlorophyll fluorescence as a measure of thermal energy dissipation, $F_m/F_m' - 1$; P – fraction of excitation energy absorbed by chlorophyll associated with PS II that is processed photochemically; PFD – photon flux density (400–700 nm); PS II – Photosystem II; $\Phi_{open\ PS\ II}$ – efficiency of open PS II units; SOD – superoxide dismutase; V – violaxanthin; VAZ – xanthophyll cycle carotenoids; Z – zeaxanthin

In the present chapter the impressive dynamic range of the response of thermal energy dissipation to contrasting environments in nature will be explored. Examples will be shown where xanthophyll cycle conversions and modulation of energy dissipation, presumably by acidification, vary largely concomitantly such as over the course of a sunny day in exposed habitats under otherwise favorable environmental conditions. Furthermore, environmental conditions will be identified under which Z+A persist and energy dissipation is modulated solely via their rapid engagement and disengagement in response to presumed changes in thylakoid acidification. Under yet other conditions, a sustained maintenance of both a highly deepoxidized state of the xanthophyll cycle as well as apparently of thylakoid acidification can be involved in acclimation to environmental stress. While many of the findings in this first part of the chapter have been discussed elsewhere (Björkman and Demmig-Adams, 1994; Demmig-Adams and Adams, 1996a; Demmig-Adams et al., 1996a, 1997), the second part will explore the role of Z+A in the phenomenon of the 'photoinhibition of photosynthesis' under prolonged light stress and the less well charted area of the association between sustained (Z+A)-dependent energy dissipation and the turnover and composition of Photosystem II (PS II). We will furthermore propose that whole plant source-sink relationships are involved in the modulation of a persistent form of (Z+A)-dependent energy dissipation, perhaps via modulation of thylakoid protein phosphorylation. Lastly, the role of xanthophyll cycle-dependent energy dissipation will be placed into perspective with other foliar defense systems that are involved in the detoxification of various reactive oxygen species.

II. Environmental Modulation of the Xanthophyll Cycle

A. Concomitant Operation of the Xanthophyll Cycle and Modulation of Energy Dissipation: Diurnal Changes in Sunny Habitats Without Additional Environmental Stresses

Changes in xanthophyll cycle conversion and energy dissipation over the course of sunny days under environmental conditions favorable for growth have now been examined in many different plant species, and in all cases pronounced diurnal changes were reported. From controlled studies it is known that excess light induces the deepoxidation of violaxanthin (V) by violaxanthin deepoxidase to zeaxanthin via antheraxanthin whereas under non-excessive, limiting light reconversion of Z+A to V by zeaxanthin epoxidase is favored (Chapter 16, Yamamoto). Under field conditions the greatest degree of deepoxidation and highest level of energy dissipation typically coincide with the highest level of solar irradiance (or incident PFD = photon flux density), and occur at different times of day depending on the orientation of the leaf (Adams et al., 1989, 1992; Adams and Demmig-Adams, 1992; Björkman and Demmig-Adams, 1994; Demmig-Adams and Adams, 1996b; Barker and Adams, 1997; Adams and Barker, 1998; Barker et al., 1998). In Fig. 1 south-facing leaves are shown that experienced maximal incident PFDs at noon. As is typical for plants under conditions that do not inhibit growth, leaves of both plants began the day with a rather epoxidized xanthophyll cycle, formed Z+A as the levels of incident PFD increased, and returned to a largely epoxidized xanthophyll cycle in the late afternoon.

Thermal energy dissipation activity is commonly estimated from decreases in the yield of chlorophyll fluorescence, often termed nonphotochemical quenching (NPQ; Fig. 1). When excitation energy is dissipated as heat (leading to increases in NPQ) before it reaches the reaction center of PS II, the efficiency of open PS II units decreases. This efficiency can be assessed from chlorophyll fluorescence as F_v'/F_m' ($\Phi_{open\ PS\ II}$) during sun exposure (Fig. 1) and its decrease can serve as another measure of the increased thermal energy dissipation. In fact, diurnal changes in the efficiency of PS II were reported (Adams, 1988; Adams et al., 1987, 1988) before it was realized that this can reflect thermal energy dissipation in PS II antennae and before the involvement of the xanthophyll cycle was recognized. Furthermore, changes in F_v'/F_m' can be used to estimate the fractions of light absorbed in PS II antennae that are allocated to photochemistry versus thermal energy dissipation (Fig. 1; Demmig-Adams et al., 1996b). In Fig. 1, the diurnal characteristics of two plant species with different maximal photosynthesis rates are compared; while sunflower has high rates of photosynthesis and utilizes a large fraction of the absorbed light for photosynthesis over the course of the day, the ornamental shrub *Euonymus kiautschovicus* has lower maximal photosynthesis rates and utilizes a lesser fraction of the absorbed light for

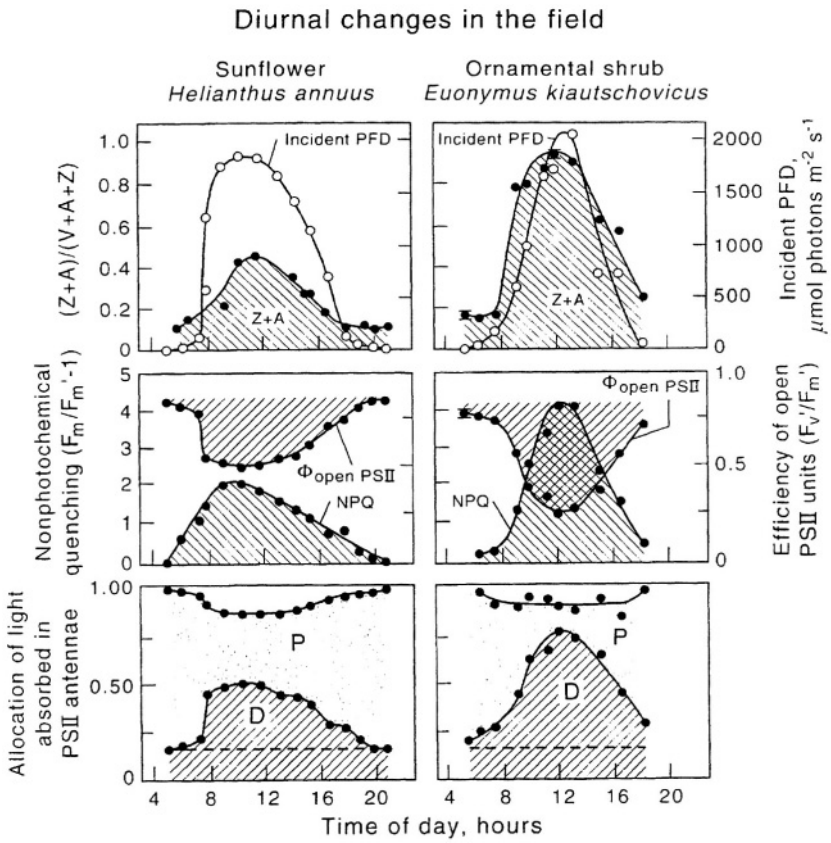

Fig. 1. Diurnal characterization of (top panels) incident PFD and the fraction of the xanthophyll cycle converted to Z+A, (middle panels) energy dissipation activity quantified as nonphotochemical quenching of F_m and the efficiency of open PS II units, and (bottom panels) the fractional allocation of excitation energy absorbed in PS II to photochemistry (P) and thermal energy dissipation (D). The area below the dashed lines in the bottom two panels represents thermal dissipation associated with the inherent inefficiency of energy transfer within the PS II complex, whereas D above the dashed line represents the regulated thermal dissipation dependent upon Z+A. Plants were characterized in Boulder, Colorado in the summer of 1993 (sunflower) or the summer of, 1995 (*Euonymus kiautschovicus*). The data for sunflower are redrawn from Demmig-Adams and Adams (1996a) and Demmig-Adams et al. (1997), whereas the data for *Euonymus kiautschovicus* were redrawn from Verhoeven et al. (1998).

photosynthesis, particularly at noon. These differences in photosynthetic utilization lead to concomitant differences in the degree of Z+A formation at peak PFD, with greater levels of Z+A formed in the species (*E. kiautschovicus*) that utilized less of the absorbed energy in photosynthesis and thus dissipated more as heat (Adams and Demmig-Adams, 1992; Winter and Lesch, 1992; Demmig-Adams and Adams, 1996b,c; Demmig-Adams et al., 1996b). It might therefore be appropriate to view the process of thermal energy dissipation as affording photoprotection while allowing plants to keep the investment in photosynthetic capacity to the level required to support the growth rate permitted by inherent genetic constraints and environmental conditions (Poorter, 1990; Koch, 1996).

It can be concluded that under these conditions favorable for growth of plants, the operation of the xanthophyll cycle as well as the presumed level of thylakoid acidification resulting in engagement of Z+A in energy dissipation both follow the changes in excess excitation energy over the course of the day. However, it has been noted that there is hysteresis in the PFD response of the levels of Z+A when ascending PFDs in the morning and descending PFDs in the afternoon are compared (Adams and Demmig-Adams, 1992; Schindler and Lichtenthaler, 1996). During descending PFD the disengagement of Z+A in energy dissipation, presumably in response to rapidly falling levels of thylakoid acidification, tracks PFD closely. In contrast, the actual reconversion of Z+A to V via epoxidation in the xanthophyll cycle

takes a bit longer on the order of minutes to hours. These field observations are consistent with the known rates of (fast) deepoxidation and (slower) epoxidation under experimental conditions (Chapter 16, Yamamoto).

Another mechanism that allows leaves to avoid overexcitation, and particularly overheating at peak PFD is variation of the leaf angle. It has been reported that leaves with the lowest (most horizontal) leaf angles, absorbing the greatest levels of light, also displayed the largest xanthophyll cycle (VAZ) pools relative to chlorophyll and the greatest conversion to Z+A at peak PFD (Adams et al., 1992; Lovelock and Clough, 1992; Demmig-Adams and Adams, 1996b). Furthermore, leaves with a dense layer of epidermal wax that reflects much of the incident PFD possessed smaller VAZ pools and lesser conversion to Z+A than leaves without such a layer (Robinson and Osmond, 1994).

B. Modulation of Energy Dissipation Against the Background of Sustained Xanthophyll Cycle Deepoxidation in Highly Variable Light Environments

Most leaves in nature probably do not experience the day-long exposure to unattentuated sunlight discussed in the previous section. Instead, leaves in the understory or lower in the canopy of a single plant typically experience variable light environments including periods of shading and periods of exposure to direct sunlight. Several questions come to mind: How common is the absorption of excess light by leaves other than those that are fully sun-exposed? Can leaves in highly variable light environments keep up with the rapidly changing demands for energy dissipation during direct exposure and maximal light utilization upon return to low PFDs?

Figures 2 and 3 show diurnal changes in xanthophyll cycle conversion and PS II characteristics for understory leaves experiencing intermittent sunflecks. Growing on the deeply shaded floor of a multilayered subtropical rainforest, leaves of the very shade-tolerant species *Alocasia brisbanensis* experienced only two sunflecks of low intensity during the whole day (Fig. 2). In contrast, the vine *Stephania japonica* which can be found in sites ranging from full sun to deep shade was characterized in an understory site where it experienced multiple, high-intensity sunflecks over the course of the day (Fig. 3). Despite these profound differences in sunfleck frequency and intensity, all leaves showed certain common responses: In all leaves a considerable increase in the degree of deepoxidation of the xanthophyll cycle occurred during the first sunfleck(s) of the day, and this was followed by a maintenance of these elevated Z+A levels throughout subsequent periods in the shade and subsequent sunflecks. Thus elevated levels of Z+A were already in place during all subsequent sunflecks. In contrast to the persistent elevated Z+A levels, the levels of energy dissipation (NPQ) increased sharply during the sunflecks and returned rapidly to low levels during shaded periods between sunflecks. Thus the level of energy dissipation closely tracked these extremely rapid changes in incident PFD. It can be concluded that understory leaves routinely experience excess light during sunflecks and that, even in environments with the lowest light levels conducive for plant growth, sunflecks of low PFDs can represent excess light for the plants that grow there. Therefore there is a strong selective pressure for the retention of this xanthophyll cycle-dependent energy dissipation process in species that grow in the lowest of light environments.

Furthermore, understory leaves appear to be able to achieve both high levels of thermal energy dissipation when needed during the sunflecks as well as a rapid return to high levels of PS II efficiency subsequent to sunflecks. It is likely that these understory leaves achieve full photoprotection during all sunflecks subsequent to the first of the day (which often turns out to be one of low intensity). Considering the strong evidence for an obligatory role of the xanthophyll cycle in energy dissipation and the modulating role of thylakoid acidification, it is likely that the rapid modulation of energy dissipation activity in response to the rapidly fluctuating PFD is via changes in thylakoid acidification against the background of persistent high Z+A levels, leading to rapid engagement and disengagement of Z+A in dissipation. However, since we have obtained evidence (see Section II.H.) that sustained LHCII phosphorylation is involved in sustained NPQ/Z retention, a possible role of rapidly modulated thylakoid protein phosphorylation in rapidly modulated NPQ cannot be excluded.

If modulation of e.g. thylakoid acidification in response to excess light alone can modulate energy dissipation activity sufficiently, why wouldn't leaves just maintain a background level of zeaxanthin at all times? Or phrased differently, why do chloroplasts have the xanthophyll cycle at all? Upon closer

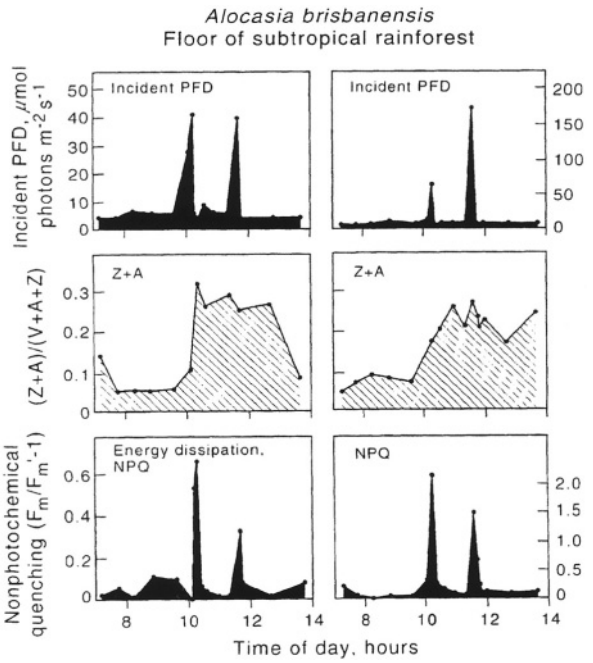

Fig. 2. Diurnal characterization of (top panels) incident PFD, (middle panels) the fraction of the xanthophyll cycle converted to Z+A, and (bottom panels) energy dissipation activity quantified as nonphotochemical quenching of F_m in leaves of *Alocasia brisbanensis* on the floor of a subtropical rainforest in Dorrigo National Park in Australia during June of 1994. Data from Logan et al. (1997).

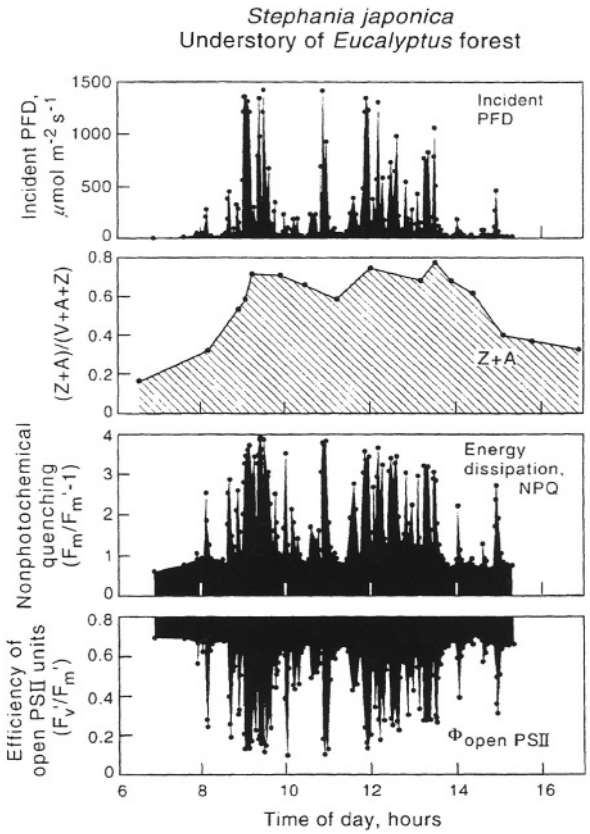

Fig. 3. Diurnal characterization of incident PFD, the fraction of the xanthophyll cycle converted to Z+A, energy dissipation activity quantified as nonphotochemical quenching of F_m, and the efficiency of open PS II units in leaves of *Stephania japonica* growing in the understory of an open *Eucalyptus* forest in Australia during June of 1994. Data from Adams et al. (1999).

examination of Figs. 2 and 3, it is evident that, although energy dissipation levels dropped rapidly subsequent to a sunfleck, they did not quite return to zero nor did the efficiency of open PS II quite return to the typical maximal levels of 0.8 or above in the leaves that retained considerable levels of Z+A (Fig. 3). It is thus possible that a return to the very maximal PS II efficiencies would require removal of zeaxanthin as well. This is consistent with the finding of Niyogi et al. (1998) that *Arabidopsis* mutants with constitutively high Z levels exhibited slowed relaxation kinetics of NPQ compared to wildtype. While maintenance of elevated Z+A levels subsequent to sunflecks was observed in the above-described studies, either a lesser or no long-term retention was found in other studies (Watling et al., 1997; Thiele et al., 1998). Interestingly, in the latter studies a single experimental exposure to high PFD was used (Watling et al., 1997) or a single cluster of sunflecks occurred naturally during the day (Thiele et al., 1998). It may also be relevant that the studies described above (Figs. 2 and 3) were conducted during the cooler winter season.

Furthermore, pools of the xanthophyll cycle (both relative to Chl and relative to the total carotenoid pool) for understory and gap leaves experiencing intermittent exposure to elevated PFDs were intermediate between those of leaves growing in deep shade and full sun (Demmig-Adams et al., 1995; Königer et al., 1995; Logan et al., 1996; Demmig-Adams, 1998; Adams et al., 1999). This suggests a continuous acclimation of leaves to increasing sun exposure with respect to xanthophyll cycle-dependent energy dissipation. However, in addition to a longer-term acclimation of the VAZ pool size to gap environments, there may also be very rapid changes in VAZ pool size upon exposure of understory leaves to sunflecks, perhaps related to a rapid conversion of existing β-carotene to Z (Depka et al., 1998; Adams et al., 1999).

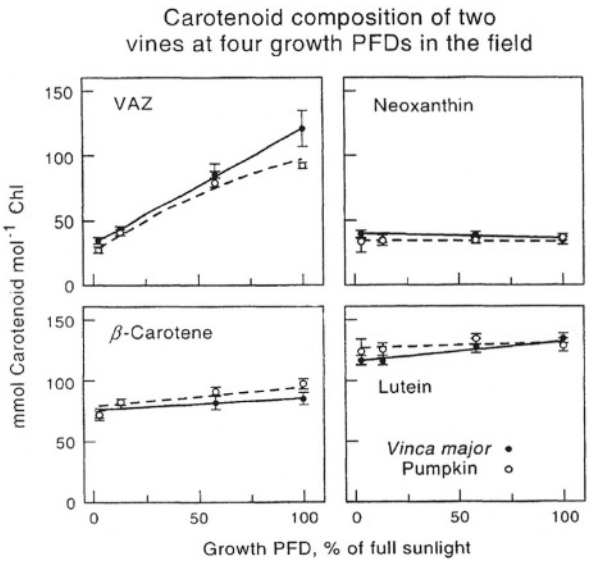

Fig. 4. The effect of growth PFD on the foliar carotenoid composition of *Vinca major* (closed circles and solid lines) or pumpkin (open circles and dashed lines) grown in the field in Boulder, Colorado during the summer of 1995. Data from Logan et al. (1998).

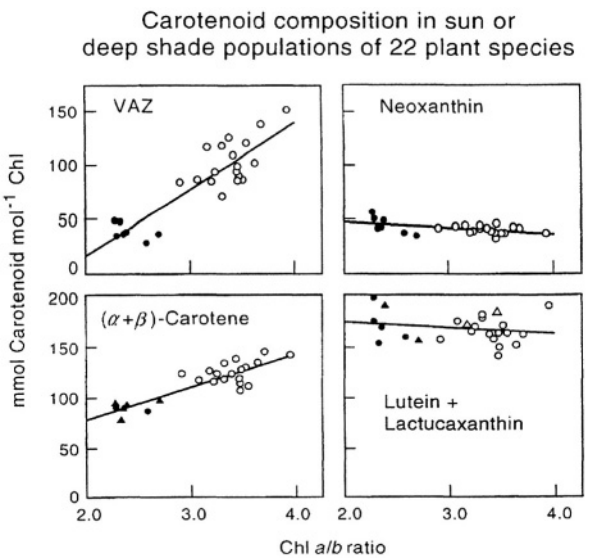

Fig. 5. Relationship between the Chl *a/b* ratio and the sum of the carotenoids of the xanthophyll cycle (V+A+Z), neoxanthin, the sum of [α-carotene + β-carotene], and the sum of [lutein + lactucaxanthin] in the leaves of 22 species surveyed from deep shade (closed symbols) and sun-exposed (open symbols) habitats in Boulder, Colorado during the summer of 1993. Triangles denote those species that contained α-carotene in addition to β-carotene or those species that contained lactucaxanthin in addition to lutein. Data from Demmig-Adams (1998).

C. Sun/Shade Acclimation, PS II Composition, and Functional Relevance of Xanthophyll Cycle Pool Size and Conversion State

Increasing growth PFD affects leaf carotenoid composition predominantly via a strong increase in the pool size of the xanthophyll cycle (Fig. 4; see also Figs. 5–7). These plants were grown in the field in full sunlight and at different levels of shading; a similar previous study with cotton cotyledons yielded similar results (Björkman and Demmig-Adams, 1994), except that in the latter study some increase in β-carotene levels with increasing growth PFD was also found. Increasing growth PFD in the field results in very similar responses in a wide range of different plant species (Fig. 5), as long as the sum of [α-carotene + β-carotene] or the sum of [lutein + lactucaxanthin] is considered in those plant species containing α-carotene and/or lactucaxanthin. This suggests that α-carotene may replace β-carotene and lactucaxanthin may replace lutein in certain ones of their respective binding sites (Demmig-Adams and Adams, 1996b; Demmig-Adams, 1998 and references therein). In Fig. 5, carotenoid composition is plotted versus Chl *a/b* ratio to allow interspecies comparison, but no functional relationship based upon this ratio should be implied. Similar differences as seen among leaves grown over a range of different growth PFDs were also observed for a cross-section of a single thick leaf (Robinson and Osmond, 1994).

It has been speculated that the increase in VAZ pool size with increasing growth PFD may be the consequence of an altered stoichiometry of PS II protein complexes. While carotenes are bound preferentially to photosystem core complexes, xanthophylls are bound to light-harvesting complexes, among which VAZ is thought to be enriched relative to Chl in the inner 'CP' complexes (Yamamoto and Bassi, 1996). Thus a lower ratio of outer, major light-harvesting complexes (LHCs) to inner CPs and cores might be expected to result in increased VAZ pools relative to Chl or total carotenoids. Such an effect is responsible for the large increase in VAZ pool size in chlorophyll-deficient mutants that nevertheless showed very similar energy dissipation characteristics as the wildtype (Gilmore et al., 1996) and may also contribute to the greater VAZ pool relative to Chl in sun versus shade leaves (Thayer and Björkman, 1990; Logan et al., 1997; see also below). On the other hand the ratio of total carotenes to total

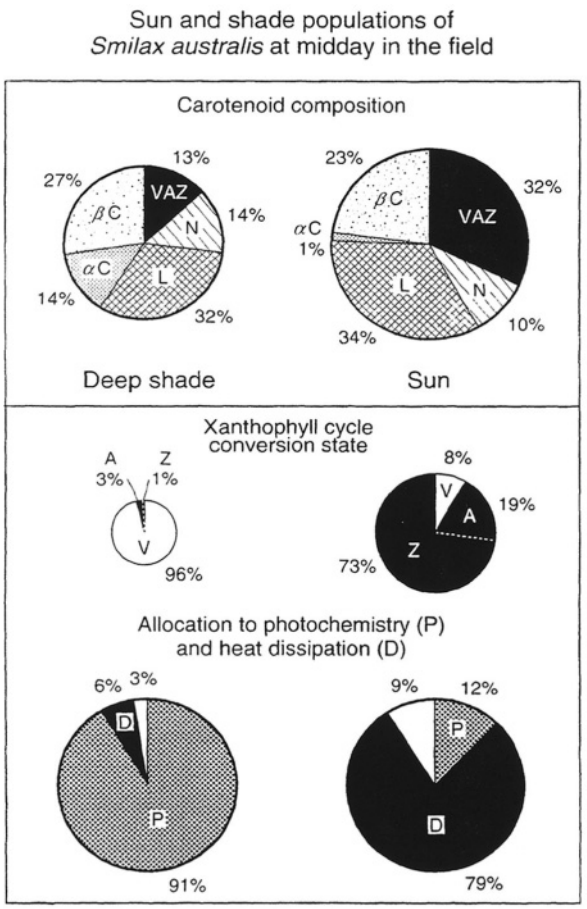

Fig. 6. Fractional carotenoid composition (expressed relative to foliar chlorophyll content; top panel) and (bottom panel) the midday conversion state of the xanthophyll cycle (fractionally expressed relative to foliar chlorophyll content) as well as the allocation of excitation energy absorbed by PS II to photochemistry (P) and dissipation (D) in leaves of *Smilax australis* growing in a deeply shaded (midday PFD = 30 μmol photons m^{-2} s^{-1}) or a fully exposed (midday PFD = 1500 μmol photons m^{-2} s^{-1}) habitat in Australia during June of 1994. Data from Adams et al. (1999).

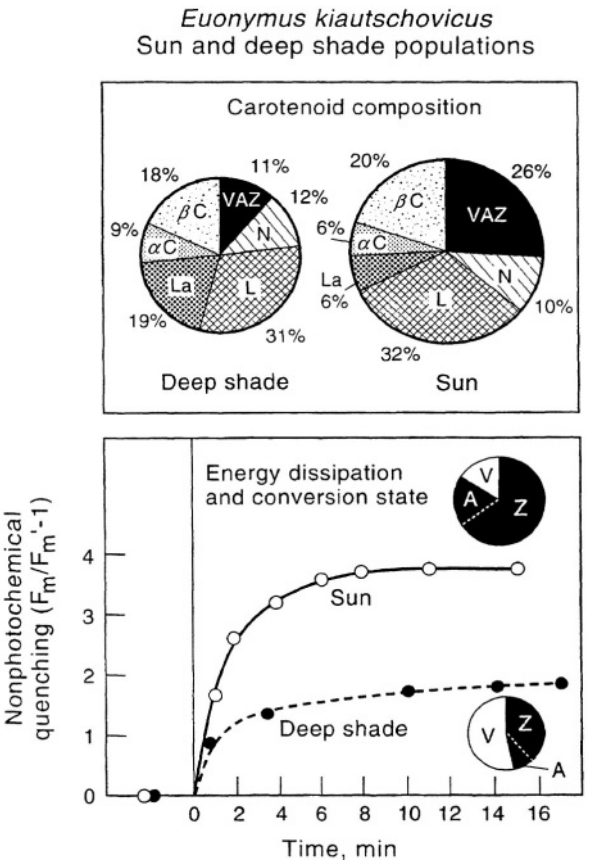

Fig. 7. Fractional carotenoid composition (expressed relative to foliar chlorophyll content; top panel) and (bottom graph) time-course of changes in energy dissipation activity quantified as nonphotochemical quenching of F_m upon the transition from darkness to 2050 μmol photons m^{-2} s^{-1} at 25 °C as well as the conversion state of the xanthophyll cycle (fractionally expressed relative to foliar chlorophyll content) determined at the end of each exposure from leaves of *Euonymus kiautschovicus* collected from plants growing in deep shade or in a fully exposed site in Boulder, Colorado. Data from Demmig-Adams et al. (1995).

xanthophylls does not increase much from shade to sun leaves (Demmig-Adams, 1998), and this would be consistent with binding of greater levels of VAZ to the protein complexes in sun compared to shade leaves.

Thus what, if any, is the functional significance of the greater VAZ pool size in sun leaves? In the field, sun leaves allocate a much greater fraction of the light absorbed at peak PFD to thermal energy dissipation than shade leaves (Fig. 6). At the same time sun leaves exhibit both larger VAZ pools and a greater degree of deepoxidation to Z+A at peak PFD in the field. Sun leaves of many plant species also show a greater level of deepoxidation to Z+A and a greater level of thermal energy dissipation (NPQ) than shade leaves during short-term experimental exposures to high PFDs (Fig. 7; Demmig-Adams and Adams, 1992, 1994; Brugnoli et al., 1994; Demmig-Adams et al., 1995; Demmig-Adams, 1998). In addition, similar differences were also observed for the upper exposed halves versus the lower shaded halves of thick leaves (Adams et al., 1996; see also Robinson and Osmond, 1994). Greater levels of rapidly attainable Z+A and NPQ as well as a lower efficiency of open PS II units (F_v'/F_m') upon exposure to high PFD in sun leaves compared to

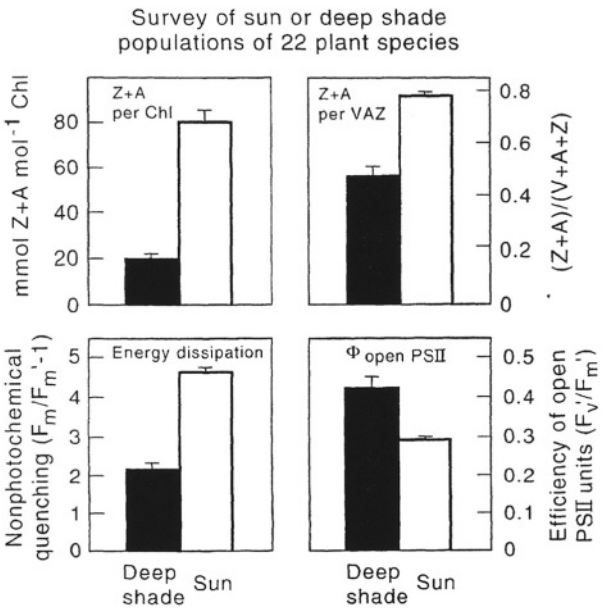

Fig. 8. Degree of conversion of the xanthophyll cycle to Z+A (top panel), relative to either total chlorophyll content or total xanthophyll cycle content, as well as (bottom panels) the level of energy dissipation activity quantified from the nonphotochemical quenching of F_m and the efficiency of open PS II units following illumination with a high PFD of between 1800 and 2050 μmol photons m^{-2} s^{-1} for 10 to 15 min. Data are means (±SE) of means from 7 species growing in deep shade (solid bars) and 18 species growing in full sunlight (open bars) in Boulder, Colorado. Data from Demmig-Adams (1998).

shade leaves (Fig. 8) indicate that sun leaves have a greater ability to increase thermal energy dissipation activity rapidly during a transfer to high light. Gilmore (1997) has suggested that the functionally relevant concentration of Z+A is that in quenching centers in specific sites among the light-harvesting proteins of PS II, and that a few strategically placed Z+A molecules may be sufficient for maximal thermal dissipation. It is possible that sun leaves possess a greater number of quenching sites than shade leaves or that binding of Z+A to these sites is favored in sun leaves.

D. Increased Conversion to Zeaxanthin + Antheraxanthin (Z+A) and Increased Allocation of Absorbed Light to Thermal Energy Dissipation in Response to Additional Environmental Stresses

Any condition that lowers photosynthesis rates at a given PFD without a change in light absorption results in a greater level of excess absorbed light. Lowering leaf temperature over the short term results in lower rates of photochemistry and increased levels of Z+A formation and thermal energy dissipation as demonstrated e.g. in cotton (Bilger and Björkman, 1991). Compared to plants acclimated to warm temperatures, cotton grown in growth chambers at slightly suboptimal temperatures (Königer and Winter, 1991) as well as several overwintering plant species in the field (Oberhuber and Bauer, 1991; Adams et al., 1995a; Adams and Barker, 1998; Verhoeven et al., 1998,1999) also exhibited greater levels of Z+A and higher levels of thermal energy dissipation at midday as judged from lower efficiencies of open PS II units. Other stress factors that lower photosynthesis rates more than light absorption have also been reported to induce an increase in the conversion state of the xanthophyll cycle to Z+A and in (Z+A)-dependent energy dissipation, such as iron (Morales et al., 1994) and nitrogen deficiency (Verhoeven et al., 1997), drought stress (Björkman and Demmig-Adams, 1994; Saccardy et al., 1998), and desiccation (Casper et al., 1993).

E. Modulation of Energy Dissipation Against the Background of Sustained Xanthophyll Cycle Deepoxidation by Subfreezing Temperatures in the Winter

Acclimation of overwintering plant species to winter conditions involves a low temperature-induced maintenance of PS II in a state primed for energy dissipation. Figure 9 shows diurnal changes of xanthophyll cycle composition and the efficiency of open PS II units monitored directly in the field on a very cold and a warm day in February for overwintering leaves of the perennial shrub *E. kiautschovicus* in the Front Range of the Rocky Mountains. On the cold day high levels of Z+A and low levels of PS II efficiency persisted throughout the day and night cycle. In this situation NPQ (as light-induced quenching) cannot be computed since PS II remained primed for thermal energy dissipation overnight rather than inducing this state only upon illumination (Adams and Demmig-Adams, 1995; Adams et al., 1995b; Verhoeven et al., 1996). High levels of (Z+A)-dependent energy dissipation were apparently maintained in both sun and shade leaves. In contrast, on the warm winter day six days later shade leaves in the field had fully returned to the low levels of (Z+A)-dependent energy dissipation typical

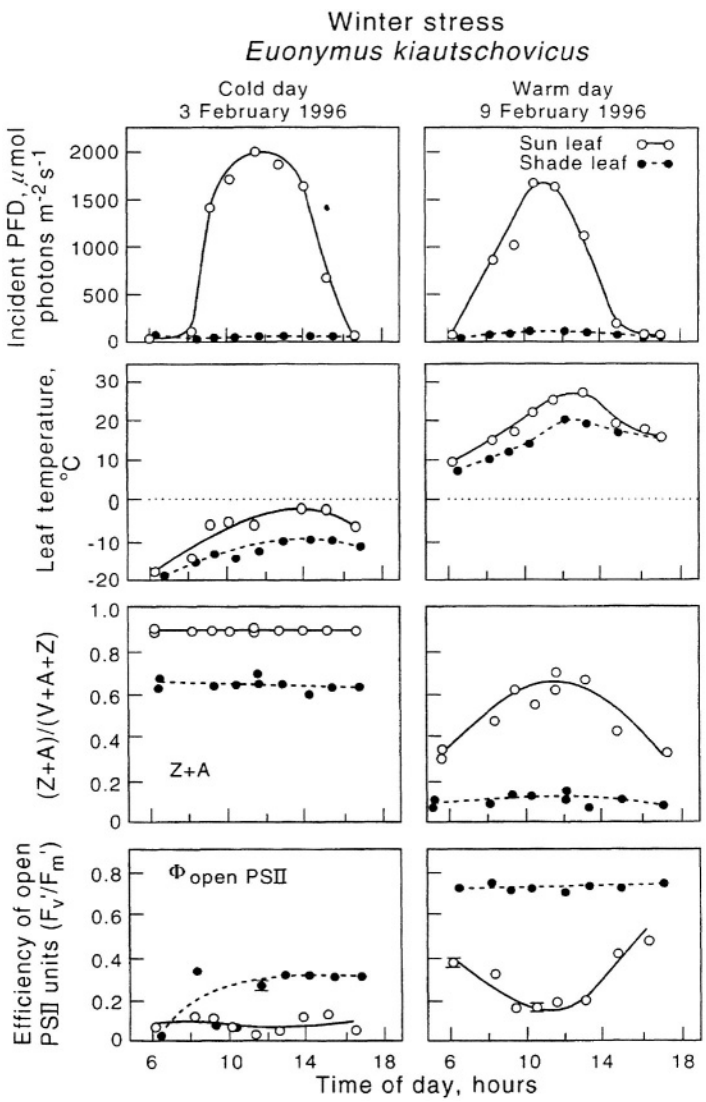

Fig. 9. Diurnal characterization of (top four panels) incident PFD and leaf temperature as well as (bottom four panels) the fraction of the xanthophyll cycle converted to Z+A and the efficiency of open PS II units from leaves of deep shade (closed circles and dashed lines) or fully sun-exposed (open circles and solid lines) plants of *Euonymus kiautschovicus* growing in Boulder, Colorado during the winter of 1996. Redrawn from Verhoeven et al. (1998).

for summer conditions whereas sun leaves showed diurnal xanthophyll cycle conversions that were less pronounced than those in summer (Fig. 1)—since some overnight retention of Z+A was still present. Within minutes upon warming of leaves collected from the field at the end of a cold winter night, PS II efficiency returned to high levels in shade leaves and to intermediately high levels in sun leaves (Fig. 10). It is an attractive possibility that these pronounced changes in PS II properties that persist in the cold and relax instantly upon warming may reflect modulation of (Z+A)-dependent energy dissipation activity by virtue of nocturnal maintenance of thylakoid acidification.

Since even engaged Z+A can be subject to epoxidation (Gilmore et al., 1994), a slowing of the epoxidation process may also contribute to nocturnal engagement in the winter. This could involve a simple effect of low temperature on epoxidase activity, and possibly on the ability of xanthophylls to move within the membrane to allow epoxidation of both end groups (D. Kramer, personal communication), but

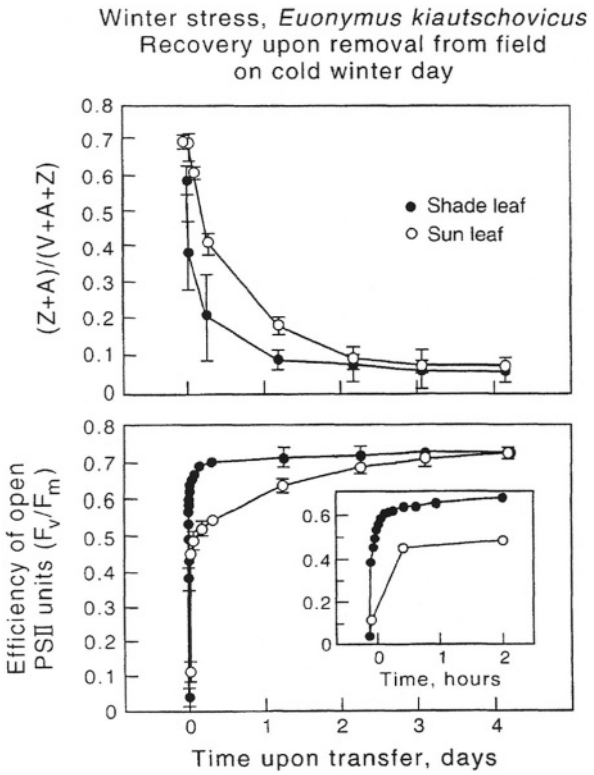

Fig. 10. Changes in (top panel) the fraction of the xanthophyll cycle present as Z+A and (bottom panel) the efficiency of open PS II units upon the warming of shade (closed circles) or sun (open circles) leaves of *Euonymus kiautschovicus* experiencing winter stress in Boulder, Colorado. Leaves were characterized in the field (data points at time 0 obtained predawn on 26 January, 1996, when the nocturnal minimum was −14 °C) and subsequently upon transfer to room temperature and low PFD. Redrawn from Verhoeven et al. (1998).

may also involve other aspects. The phenomenon suggested by Kramer might be consistent with the observation of unusually large amounts of A in cold stressed leaves (Adams et al., 1995a).

In warm-grown leaves, lowering leaf temperature experimentally subsequent to a high light exposure resulted in a maintenance of high Z+A levels as well as a maintenance of PS II in a state primed for energy dissipation (dark-sustained NPQ) for prolonged periods in low light or darkness (Gilmore and Björkman, 1994, 1995). This dark-sustained NPQ could be reversed by the uncoupler nigericin. It is interesting to note that maintenance of (Z+A)-dependent energy dissipation was observed only at subfreezing temperatures in the field in winter-acclimated leaves whereas for warm-grown leaves similar effects were reported already at much higher temperatures of e.g. +5° in lettuce (Gilmore and Björkman, 1995) to +15 °C in a chilling-sensitive mangrove species and cotton (Gilmore and Björkman, 1994). One may speculate that a cold-induced tightening of the thylakoid membrane may be important e.g. for reducing proton leakage (see Gilmore, 1997), and that the cold-hardening process lowers the temperature threshold for this event considerably.

Gilmore and Björkman (1995) also proposed the possibility that maintenance of high levels of (Z+A)-dependent energy dissipation at low leaf temperatures may involve ATP-dependent reverse proton pumping though the thylakoid ATP synthase (coupling factor) into the lumen. However, the pronounced lowering of PS II efficiency in *E. kiautschovicus* at cold temperatures—which relaxed instantly upon warming (Fig. 10)—was not associated with elevated ATP/ADP ratios (Verhoeven et al., 1998) as a prerequisite to reverse the direction of the ATP synthase-catalyzed reactions (see Gilmore and Björkman, 1995).

At low temperatures in the field, nocturnal maintenance of PS II in a state primed for instantaneous high levels of (Z+A)-dependent energy dissipation upon illumination is likely of ecological importance. In the Colorado Rockies where many overwintering species were characterized, the sun frequently rises over a frozen landscape, and leaves would presumably be unable to form Z+A sufficiently rapidly for photoprotection—had they not simply retained them overnight! We have shown that, even in cold-hardened plants, deepoxidation is indeed slow at low temperatures (Adams et al., 1995b, but see also Bilger and Björkman, 1991). Therefore, a cold-maintained high level of (Z+A)-dependent energy dissipation that disengages rapidly upon warming is an elegantly regulated process that offers protection when needed but relaxes immediately upon a cessation of cold stress.

It appears that all leaves (i.e. sun and shade leaves) of all species examined uniformly exhibited a strong lowering of PS II efficiency associated with sustained Z+A retention on cold days (and nights) in the field. However, the extent to which the component that relaxes instantly upon warming (Fig. 10) contributed to this varied widely among plant species (see Section II.F). We will examine a variety of cases below in which sustained (Z+A)-dependent dissipation persists at warm temperatures and will discuss whether or not this may constitute any limitation to plant growth.

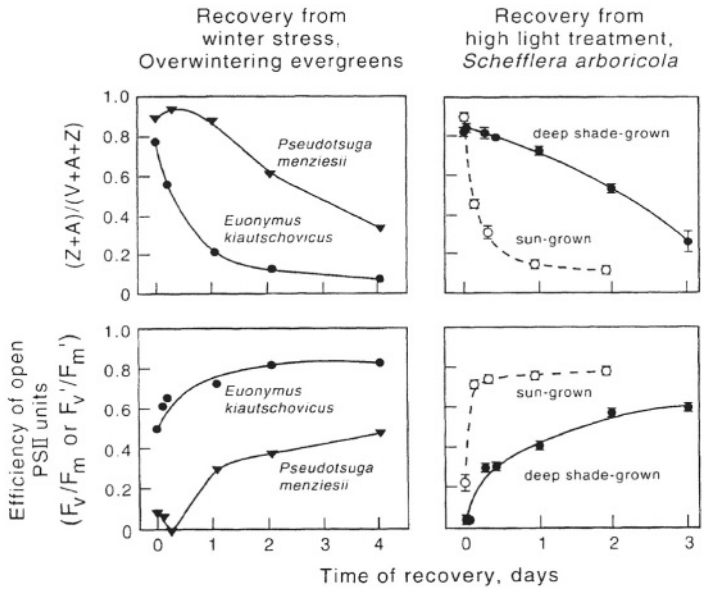

Fig. 11. Changes in (top two panels) the fraction of the xanthophyll cycle present as Z+A and (bottom two panels) the efficiency of open PS II units during recovery from high light and winter stress in needles of Douglas fir or leaves of *Euonymus kiautschovicus* removed from the field (predawn on 10 January, 1994, nocturnal minimum of −3.3 °C) and transferred to room temperature and low light, or during recovery upon transfer of *Schefflera arboricola* leaves to low light following exposure to 1100 to 1200 μmol photons m^{-2} s^{-1} for 24 h. Data for Douglas fir and *Euonymus kiautschovicus* from Verhoeven et al. (1996), and data for *Schefflera arboricola* from Demmig-Adams et al. (1998).

F. Concomitant Retention of Z+A and Persistent Low PS II Efficiency at Warm Temperatures: Role of Retained Z+A in Photoinhibition

1. As a Result of Low Temperature or Other Environmental Stresses

While PS II efficiency in shade leaves of the overwintering shrub *E. kiautschovicus* rapidly returned to maximally high levels upon warming, sun leaves still showed some depression of PS II efficiency that persisted after warming either in the field (Fig. 9) or upon removal of leaves from the field (Fig. 10). Such effects were most pronounced in sun leaves of overwintering evergreen sclerophytes (Fig. 11). The relationship between sustained Z+A retention and persistently lowered PS II efficiency in overwintering leaves after transfer to warm conditions was strikingly similar to the relationship between (rapidly removable) *Z+A* and (rapidly relaxing) changes in PS II efficiency of open units during exposure to the sun in summer (Fig. 12). This is quite remarkable considering that energy dissipation during the summer day in the field, leading to the lowering of PS II efficiency, is presumably a function of [Z+A] and thylakoid pH (Gilmore and Yamamoto, 1993) while the bulk pH gradient across the thylakoid membrane has presumably dissipated during the warming of leaves collected in the winter. An attractive possibility accounting for these similarities is to assume that the protein conformational change leading to Z+A engagement in dissipation can become 'locked in,' perhaps via a stable form of protonation or via another mechanism (Ruban and Horton, 1995; see Chapter 15, Horton et al.). For overwintering leaves two forms of persistent Z+A engagement have thus been identified, with one persisting exclusively at subfreezing temperature and the second being stable even at warm temperatures (Verhoeven et al., 1998,1999).

Does this stable form of (Z+A)-dependent energy dissipation (or associated changes in PS II) that persists at warm temperatures limit plant productivity during warm periods in the winter? We favor the view that sustained maintenance of high levels of (Z+A)-dependent thermal dissipation is a consequence of an overall downregulation of photosynthesis in those plant species that cease growth during the winter. Comparison of the direction of seasonal acclimation of photosynthetic capacity revealed profound differences between mesophytic herbs and sclerophytes (Fig. 13). Mesophytes such

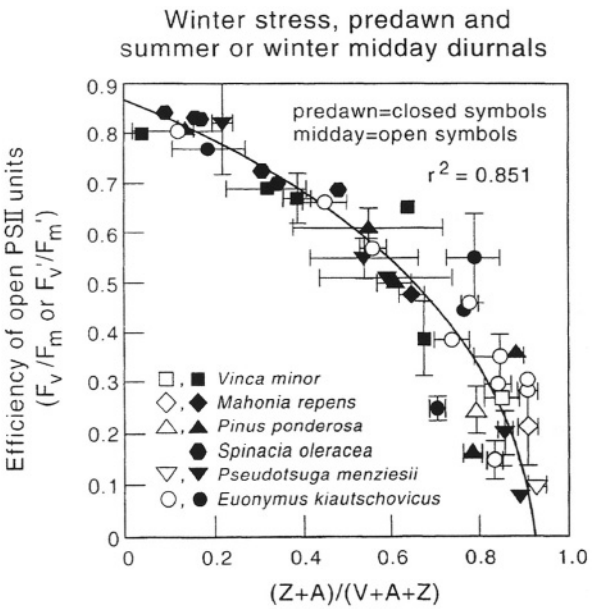

Fig. 12. Relationship between the fraction of the xanthophyll cycle present as Z+A and the efficiency of open PS II units (F_v/F_m predawn or F_v'/F_m' at midday) from leaves of six species removed from the field prior to sunrise on cold days in the winter and assayed at warm temperatures (closed symbols) or *in situ* during maximal exposure to sunlight on cold days in the winter (open symbols), except for the open circles of *Euonymus kiautschovicus*. The latter represent a range of leaves experiencing PFDs between 6 and 2000 μmol photons m^{-2} s^{-1} on a warm day in the summer, with the exception of the open circle with a PS II efficiency below 0.2 that was sampled midday in the winter. Error bars represent standard deviations (n = 3). Data plotted from Adams and Demmig-Adams (1994, 1995) and Adams et al. (1995a,b).

as overwintering *Malva neglecta* (Fig. 13) or spinach (Adams et al., 1995b) exhibited increased photosynthetic capacities in the winter as has also been reported for cereals (Hurry et al., 1995) acclimated to low temperatures in growth chambers. In contrast, overwintering sclerophyllous evergreens such as Scots pine (Ottander and Öquist, 1991), Ponderosa pine (Fig. 13), or *Vinca minor* (Fig. 13) as well as other evergreen shrubs and trees (Oberhuber and Bauer, 1991; Bauer et al., 1994) exhibited pronounced apparent downregulation of photosynthesis. Whereas in *M. neglecta* new leaves continued to emerge during warm periods in the winter, the conifers and *V. minor* apparently ceased growth during the winter.

Consistent with this difference, *M. neglecta* returned quickly to high PS II efficiency on warm days during the winter whereas e.g. Ponderosa pine—particularly when examined in late winter—did not (Verhoeven et al., 1999). In addition, the day-to-day changes in predawn PS II efficiency and Z+A retention in *M. neglecta* were associated with pronounced changes in nocturnal ATP/ADP ratio whereas no seasonal or day-to-day change in ATP/ADP ratio were detected in the evergreen sclerophytes Ponderosa pine or *E. kiautschovicus* (Verhoeven et al., 1998, 1999). Below we propose that sustained elevated phosphorylation of LHCII can be involved in sustained (Z+A)-dependent energy dissipation at warm temperatures (see Section II.H.). It is an attractive possibility that sustained thylakoid protein phosphorylation may also be involved in the maintenance of high levels of (Z+A)-dependent energy dissipation in overwintering leaves. One may speculate that the high nocturnal ATP/ADP ratios in

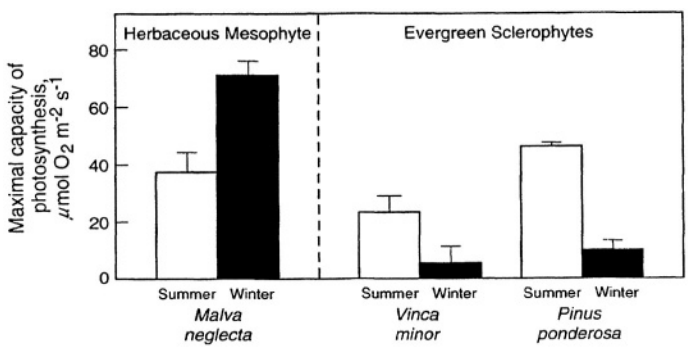

Fig. 13. Seasonal changes in the maximal capacity for photosynthetic oxygen evolution in the mesophytic herb *Malva neglecta* versus the evergreen sclerophytes *Vinca minor* (Periwinkle) and *Pinus ponderosa* (Ponderosa pine). To express photosynthesis rates of Ponderosa pine on a leaf area basis, needles were aligned beside each other and taped together. Data from Verhoeven et al. (1999) and TN Rosenstiel, WW Adams III, B Demmig-Adams, unpublished

Malva neglecta (Verhoeven et al., 1999) could inactivate thylakoid phosphatase(s). Inhibition of LHCII dephosphorylation by ATP has been shown by Carlberg and Andersson (1996), and is a common feature of phosphatases (Ballou and Fisher, 1986; Cohen, 1989).

An association between Z+A retention and high NPQ or low PS II efficiency sustained at warm temperatures has been reported for plants experiencing high light in combination with a host of different environmental stresses. These include not only winter stress (Oberhuber and Bauer, 1991; Adams and Demmig-Adams, 1994,1995; Adams et al., 1995a; Ottander et al., 1995; Verhoeven et al., 1996; Adams and Barker, 1998; Barker et al., 1998), and low growth temperatures under controlled conditions (Fryer et al., 1995; Haldimann et al., 1995; Jung and Steffen, 1997), but also insufficient iron supply in the field (pear trees; Morales et al., 1994), drought stress (Demmig et al., 1988; Maxwell et al., 1994), and nitrogen-deficiency (spinach; Verhoeven et al., 1997).

2. As a Result of Photoinhibitory Light Treatments

Persistent high levels of Z+A that mirror persistent low levels of the efficiency of open PS II units have also been observed for plants experiencing high light stress alone. Elevated Z+A levels were maintained for days during the recovery of a deep shade-acclimated leaf of the shade-tolerant plant *Schefflera arboricola* subsequent to an exposure to approximately half of full sunlight (or 120× its growth PFD; Fig. 11). Similar observations have been made for a variety of other systems, including leaves of other shade-grown species transferred to high light (Demmig-Adams et al., 1989), brown algae acclimated to low light and transferred to high PFD (Uhrmacher et al., 1995), as well as intermittent light-grown plants transferred to continuous light (Jahns and Miehe, 1996). In all of these systems an accumulation and retention of large amounts of Z+A was accompanied by persistent low PS II efficiency, often addressed as 'photoinhibition' of PS II, and the level of retained Z+A thus correlated positively with the degree of photoinhibition. This phenomenon led various authors to conclude that accumulation of large amounts of Z did not confer increased tolerance to photoinhibition (Hurry et al., 1992; Ciompi et al., 1997; Jung and Steffen, 1997). However, we propose that a key feature of this phenomenon of photoinhibition in intact plants is the persistent (Z+A)-dependent energy dissipation (Adams et al., 1995a) affording photoprotection under conditions where whole plant demand for photosynthate (sink strength) is presumably low (see below).

Whereas stress-induced retention of Z+A appears to be extremely common, persistent low PS II efficiency is associated with this for many but not all plant species and conditions. Although shade-grown leaves of all plant species transferred to high PFD exhibited a very pronounced sustained retention of Z+A, leaves of the sclerophyllous, perennial species *Monstera deliciosa* and *Rhizophora mangle* showed concomitant strong and persistent effects on PS II efficiency of open units, while the annual mesophyte cotton (Demmig-Adams et al., 1989) exhibited only small effects on PS II efficiency. Furthermore, while *Nerium oleander* showed a combination of both phenomena under drought stress, two species of *Yucca* showed strong nocturnal retention of Z+A but little persistent PS II depressions during the dry, hot summer in the Mojave desert (D. Barker, W Adams, B. Demmig-Adams, B. Logan, and A. Verhoeven, unpublished; see also Maxwell et al., 1995). These observations indicate that Z+A retention and their persistent engagement in energy dissipation are two distinct, albeit often co-occurring, phenomena.

G. Associations between Z+A Retention, Carotene/Xanthophyll Ratio, and PS II Composition and Function

In the past, associations between persistent changes in PS II efficiency and either PS II protein turnover or Z+A retention have often been characterized in isolation. In this section, studies comparing all of these processes are discussed.

1. Seasonal Transitions in the Field

One of the few available studies considering both xanthophyll cycle conversions and PS II composition and function—as the two processes that have been implicated in the phenomenon of 'photoinhibition' (Osmond, 1994; Adams et al., 1995a; Anderson et al., 1997)—is the study by Ottander et al. (1995) of seasonal transitions in the field in Scots pine (*pinus silvestris*). Scots pine ceases growth during the winter season and downregulates overall photosynthetic

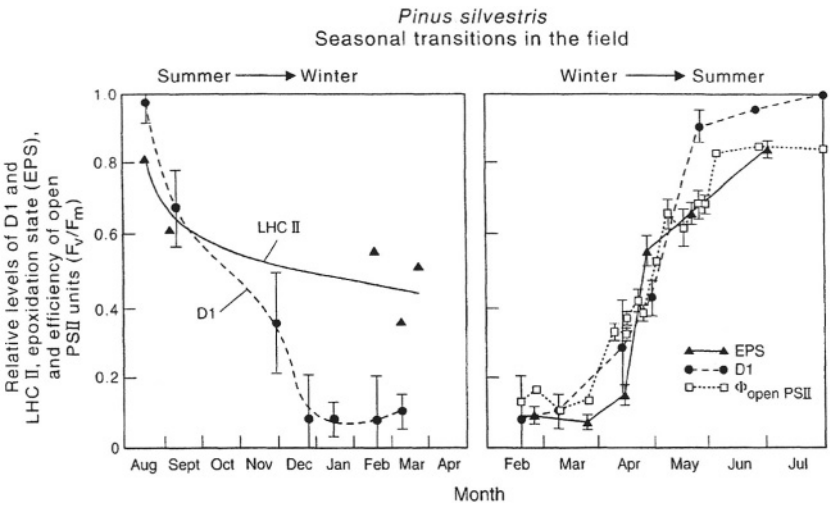

Fig. 14. Characterization of (left panel) the relative levels of the D1 and LHCII proteins during the transition from summer to winter (1993 to 1994), and (right panel) the relative level of the D1 protein, the epoxidation state, EPS, of the xanthophyll cycle (0.5A+V)/(V+A+Z), and the efficiency of open PS II units (F_v/F_m determined after a 30 min period of dark adaptation) during the transition from winter to summer (1994) from needles of Scots pine growing in Sweden. Data redrawn from Ottander et al. (1995).

capacity (Ottander and Öquist, 1991). During transition to winter, Scots pine exhibited depletion of PS II proteins with a preferential removal of the core protein D1 relative to the less pronounced decrease in the level of LHCII (Fig. 14). In addition, in winter the xanthophyll cycle remained highly converted to Z+A (Ottander et al., 1995). Upon return to the summer, levels of PS II proteins increased again and a general association was observed between D1 re-insertion, removal of retained Z+A, and return to high efficiency of open PS II units (Fig. 14). Thus during seasonal transitions changes in PS II composition coincided with changes in the degree of Z+A retention. Ottander and coworkers concluded that PS II is downsized during the winter and restructured to allow preservation of a portion of the LHCII, presumably in a highly photoprotected form involving elevated levels of Z+A that are retained as long as winter stress lasts.

The conclusion that LHCs can be preserved during the winter while cores are degraded is consistent with observations that the levels of β-carotene (preferentially bound to photosystem cores) decreased at low temperature while the levels of lutein and neoxanthin remained similar and the levels of VAZ increased (Fig. 15). This observation is also consistent with the assumption that additional VAZ, and in particular additional Z+A, may be formed from the existing pool of β-carotene in the thylakoid membrane (Demmig-Adams et al., 1989; Depka et al., 1998).

2. Other Examples

Drought stress in pea seedlings led to a depletion of PS II cores while LHCs were maintained, resulting in one-half the number of cores relative to LHCs in drought compared to pre-drought conditions (Giardi et al., 1996). In other studies where changes in carotenoid composition were observed (see below), a more rapid decrease in β-carotene levels relative to xanthophylls also suggests a preferential degradation of photosystem cores while components of the light-harvesting system persist. A greater decrease in β-carotene and Chl relative to xanthophylls under light stress had been reported long ago by Sironval and Kandler (1958) and had been attributed to a differential sensitivity to photooxidation. It now appears that this may reflect adjustment in the number of PS II cores and photoprotection of persisting components of PS II. These preferential decreases in β-carotene content were associated with accumulation and retention of Z+A under various conditions representing excess light (see below; Falbel et al., 1994). However, it should be noted that there are also cases in which all carotenoids and chlorophylls are depleted in similar proportions, for example in spinach grown under limiting nitrogen in the soil (Verhoeven et al., 1997). Such a proportional depletion was associated with only little retention of Z+A and persistent lowering of PS II efficiency.

Sudden transfer of a shade-grown plant of

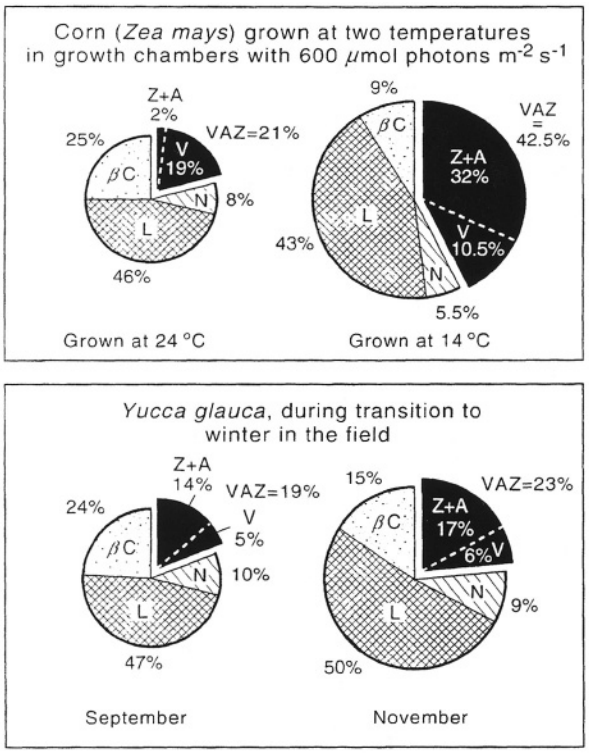

Fig. 15. The influence of growth temperature on the foliar carotenoid composition (expressed relative to chlorophyll content) of corn grown at 24 °C or 14 °C and of *Yucca glauca* growing in the field in Colorado at the end of September (mean minima and maxima of 6 ± 2 °C and 21 ± 5 °C for the week preceding characterization) or at the end of November (mean minima and maxima of −9 ± 10 °C and 5 ± 10 °C for the week preceding characterization) in 1993. Data for corn from Haldimann et al. (1995), and data for *Yucca glauca* from Adams and Barker (1998).

Schefflera arboricola to a PFD far exceeding its growth PFD induced decreases in β-carotene, increases in the VAZ pool (that had been small at low PFD), but little change in the other xanthophylls lutein and neoxanthin (Fig. 16). This transition also resulted in an increased accumulation of Z+A that was retained during recovery and was mirrored by persistent decreases in the efficiency of open PS II units. Furthermore, the carotenoid biosynthesis inhibitor SAN 9785 (taken up by the roots of spinach sun plants) induced decreases in carotenoid levels among which that in β-carotene was again the most pronounced, followed — in descending order of severity—by VAZ, lutein, and neoxanthin (Fig. 16). This was again associated with an increased accumulation and retention of Z+A. Such findings suggest that a low synthesis rate of various PS II core components (e.g. either D1, β-carotene [Depka et al., 1998], or chlorophyll [Falbel et al., 1994]) under excess light somehow triggers Z+A retention. In cases where the number of photosystem cores decreases preferentially, retained Z+A may once again serve in the photoprotection of preserved light-harvesting complexes. We localized retained Z+A preferentially in the isolated fraction of thylakoid proteins containing light-harvesting complexes (and among these clearly in LHCII trimers) but not in PS II cores from photoinhibited leaves of the shade plant *Monstera deliciosa* (unpublished). In a study by Färber et al. (1997), retained Z+A was localized in a fraction containing CP26 and PS II cores that could not be separated from each other.

H. Conclusions and Speculations: Z+A retention, Photoinhibition, and Whole Plant Source-Sink Relationship

Many aspects of photosynthesis have now been shown to be influenced by the source/sink balance within the plant or within particular organs. Leaves are the primary source organs, producing the carbohydrates that are exported to the rest of the plant. Sink strength refers to the capacity of newly developing, growing, storing, and metabolizing tissues to utilize or store the carbohydrates provided by the source organs. Under conditions where the demand for carbohydrates is high relative to the supply, i.e. when plants possess a high sink strength, the levels of photosynthetic proteins are upregulated in the source leaves in order to increase the capacity for photosynthesis (Koch, 1996; Jang and Sheen, 1997). On the other hand, when sink strength is low relative to the capacity to supply carbohydrates, many proteins involved in photosynthesis are downregulated. The signals sensed may include some aspect of carbohydrate metabolism or export, plant hormones, and leaf energy status (Koch, 1996; Van der Werf, 1996; Jang and Sheen, 1997). Photosynthetic proteins regulated in this manner include those involved in light collection (e.g. LHCII; Krapp and Stitt, 1995) and photochemistry (e.g. D1; Kilb et al., 1996) in addition to others in electron transport and carbon fixation and export. The relative source/sink balance within a plant is determined by both genetic factors governing growth and development, as well as environmental factors that influence both source and sink activity. Under favorable conditions for growth, rapidly growing mesophytes have higher rates of photo-

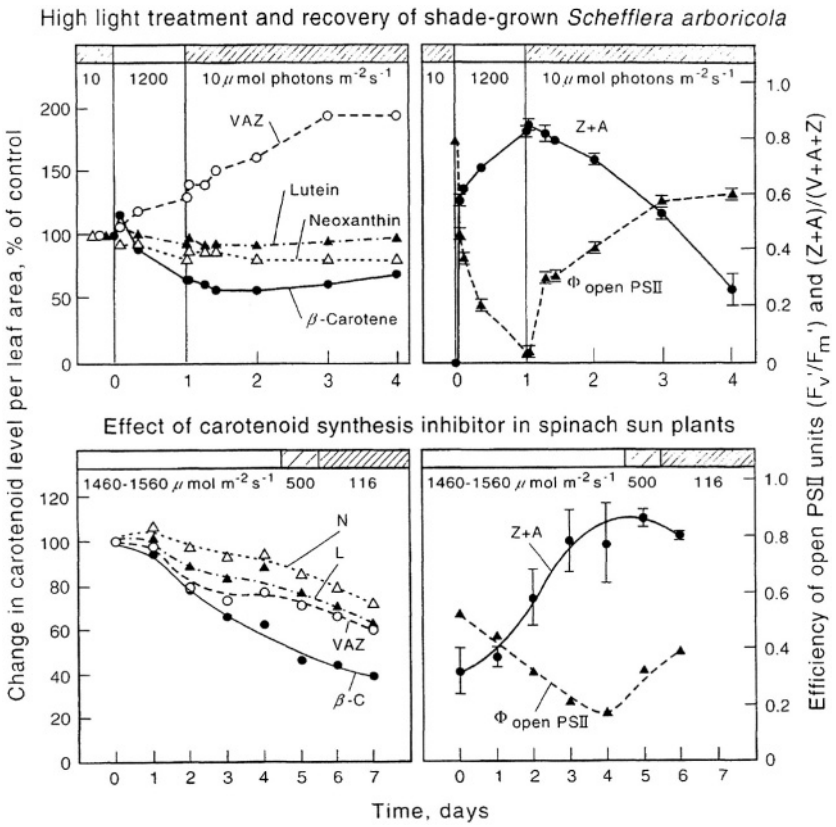

Fig. 16. Characterization of (two left panels) the carotenoid composition and (two right panels) the efficiency of open PS II units as well as (Z+A)/(V+A+Z) in shade leaves of *Schefflera arboricola* exposed to high PFD (1200 μmol photons m^{-2} s^{-1}) for 24 h followed by recovery at low PFD (10 μmol photons m^{-2} s^{-1}; Demmig-Adams et al., 1998) and in leaves of spinach from plants watered daily with the carotenoid synthesis inhibitor SAN 9785 (0.1 mM) in a fully exposed greenhouse (B Demmig-Adams and AS Verhoeven, unpublished).

synthesis than more slowly growing sclerophytes. As conditions become less favorable for growth (limiting water, limiting nutrients, extremes in temperature, etc.), growth, and thus sink strength, decreases and photosynthesis in source leaves is downregulated.

The classic conditions that induce photoinhibition—transfer of plants to PFDs exceeding their growth PFD and additional environmental stresses (Powles, 1984)—are all conditions under which whole plant sink strength is likely to be temporarily or permanently limiting. Shade-acclimated plants are likely to possess a low sink activity level matched by the low rates of carbon flow from source leaves to the sink tissues of the plant under the low growth PFD. Upon sudden transfer to an increased PFD, the production of carbohydrates likely exceeds the plant's capacity to export and utilize these increased levels of carbohydrates. We have observed that during photoinhibitory treatments of whole shade plants high levels of carbohydrates accumulate in the leaves and do not appear to be exported (unpublished; Roden et al., 1997). One clearly has to conclude that in these photoinhibited leaves a step other than PS II activity is limiting plant productivity. Furthermore, for the case of sun-grown plants various additional environmental stresses are likely to inhibit growth directly thus also affecting source-sink relationships. For example, under limiting N supply foliar carbohydrate levels rise strongly (e.g. Paul and Driscoll, 1997). We propose that, in addition to a downsizing of light collecting and photochemical capacity, sink limitation can also induce a transformation of (Z+A)-dependent thermal energy dissipation from a rapidly modulated to a sustained form that persists until sink to source ratio increases again.

We have obtained evidence that during recovery from high light treatments, sustained phosphorylation of LHCII is involved in sustained zeaxanthin retention

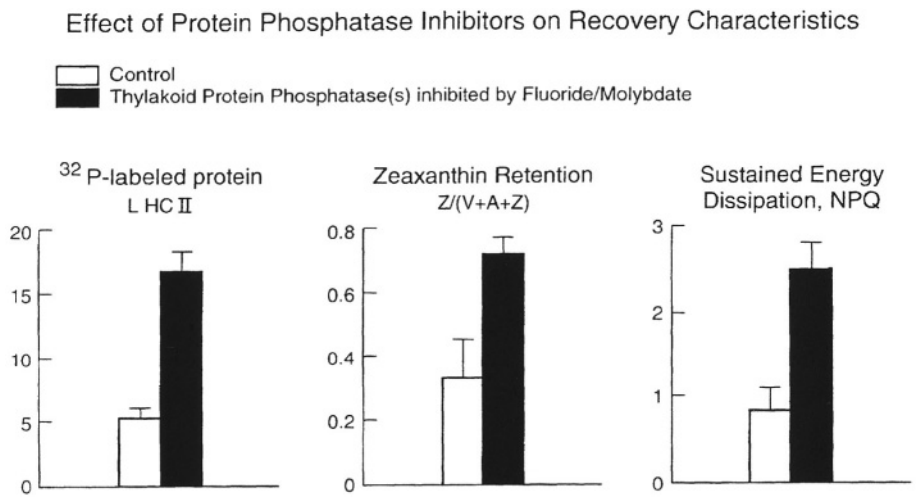

Fig. 17. Effect of a mix of the protein phosphatase inhibitors fluoride and molybdate on (left graph) LHCII phosphorylation as well as (middle graph) zeaxanthin retention and (right graph) sustained thermal energy dissipation (NPQ) in leaf discs of *Parthenocissus quinquefolia* (Virginia creeper). Leaf discs were vacuum-infiltrated with ^{32}P-labeled orthophosphate and a mix of 10 mM NaF and 10 mM Na_2MoO_4. Leaf discs were prelabeled at 50 μmol photons m^{-2} s^{-1} for 1 h and subsequently were exposed to a PFD of 1800 μmol photons m^{-2} s^{-1} for 1 h after which time the PFD was lowered again to 50 μmol photons m^{-2} s^{-1}. After 1 h of recovery at 50 μmol photons m^{-2} s^{-1} samples were taken for the analysis of the parameters shown. Phosphorylation level was determined by quantifying optical density by laser densitometry of autoradiograms from thylakoid protein phosphorylation patterns determined by SDS-PAGE electrophoresis (Laemmli, 1970). The labeling intensity of each band was compared to all other bands in all other lanes as a fraction of the sum of the optical densities of all bands combined. ^{32}P-labeled bands included LHCII, D1/D2, and CP43 among which only LHCII showed a treatment effect. Data shown are means of three independent experiments ±SD for ^{32}P-labeling (n = 3), fluorescence (n = 6), and pigments (n = 3). (V Ebbert, B Demmig-Adams, WW Adams III, unpublished)

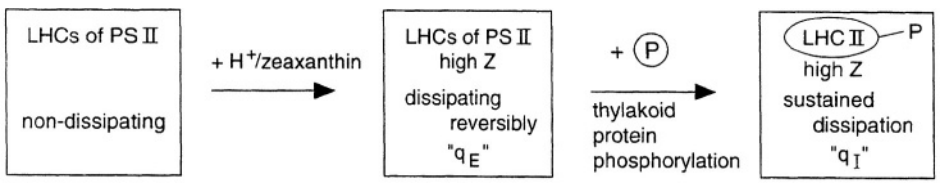

Fig. 18. Schematic model of the presumed mechanism for rapidly reversible nonphotochemical quenching (q_E) and the proposed mechanism for sustained NPQ (q_I). LHCs = light-harvesting complexes of PS II; LHCII = major, peripheral light-harvesting complex of PS II; LHCII-P = phosphorylated LHCII; Z = zeaxanthin

and its persistent engagement in thermal energy dissipation (sustained NPQ or 'q_I'; Figs. 17 and 18). Treatment with inhibitors of thylakoid protein phosphatase(s) induced retention of Z as well as sustained NPQ (Fig. 17) during the recovery of *Parthenocissus quinquefolia* (Virginia creeper) leaves from high light treatments. Structural changes resulting from the phosphorylation of LHCII may induce a stable engagement of Z+A. in energy dissipation (Fig. 18). In the case of thylakoid protein phosphorylation an ever more sophisticated regulation system is being unraveled, involving e.g. chloroplast redox state and ATP level (for recent reviews see Allen and Nilsson, 1997; Gal et al., 1997; Vener et al., 1998), both of which respond to source/sink balance. The characterization of signal transduction in response to whole plant source/sink balance and the specific aspects of xanthophyll cycle synthesis, operation, and engagement in energy dissipation affected should prove an exciting field for future study.

III. Associations Between (Z+A)-Dependent Dissipation, Photosynthesis, and Foliar Antioxidant Levels

Under a wide variety of environmental conditions representing an increased excess of light, (Z+A)-dependent thermal dissipation typically increases while both photosynthetic capacity and overall leaf antioxidant capacity can either increase or decrease.

A. Growth Photon Flux Density (PFD)

With increasing growth PFD up to full sunlight in the field, photochemistry rates, xanthophyll cycle-dependent energy dissipation, and foliar levels of various antioxidant enzymes all increased (Fig. 19). The foliar levels of reduced ascorbate (Vitamin C) closely followed the patterns for xanthophyll cycle-dependent energy dissipation and changes in the levels of ascorbate peroxidase (APX), consistent with ascorbate's dual role in the reductive deepoxidation of V to Z+A and as cofactor of APX (Nakano and Asada, 1981; Bratt et al., 1995). In contrast to ascorbate, α-tocopherol (Vitamin E) levels did not show a growth PFD-dependent trend (see also Grace and Logan, 1996). Both α-tocopherol and carotenoids are lipophilic antioxidants capable of catalyzing a host of protective responses in vitro including deexcitation and detoxification of triplet excited Chl and singlet excited oxygen. The ubiquitous carotenoids other than VAZ, including β-carotene, lutein, and neoxanthin, exhibited very similar trends as α-tocopherol, i.e. no or little growth PFD-dependent differences (Figs. 4 and 5). The taxonomically restricted carotenoids α-carotene and lactucaxanthin were present mostly in shade leaves and levels typically decreased with increasing growth PFD (Demmig-Adams and Adams, 1996b; Demmig-Adams, 1998). In those cases where β-carotene levels increased somewhat with increasing growth PFD this is likely to reflect increased numbers of photosystem cores. Thus it appears that generally the same conclusion can be drawn for carotenoids (other than VAZ) and for α-tocopherol, i.e. that there is no adjustment in the levels of these antioxidants in response to increasing levels of light stress with increasing growth PFD. This suggests that xanthophyll cycle-dependent energy dissipation effectively prevents a growth PFD-dependent increase in triplet Chl or singlet oxygen formation, but that there may be some constitutive level of singlet oxygen formed at all PFDs.

Foliar levels of the enzymes APX, superoxide dismutase (SOD), glutathione reductase (GR), and catalase, that are all involved in the scavenging of reduced reactive oxygen species, increased with increasing growth PFD (Fig. 19). This suggests that, in contrast to singlet oxygen, production of these reduced oxygen species does increase with an increase in growth PFD. This could include increased oxygen reduction in both photosynthetic electron transport and mitochondrial respiration, as well as other cellular processes. Both photosynthesis and respiration rates tend to increase with increasing growth PFD (Björkman, 1981). In addition to these general concomitant trends for increases in photosynthesis, respiration, and foliar scavenging capacity forreduced reactive oxygen, there were also additional, superimposed trends of contrasting changes. While in *Vinca major* saturation of photochemistry rates occurred considerably below full sunlight, in pumpkin these rates continued to increase up to full sunlight (Fig. 19). In turn, *V. major* exhibited a greater increase in thermal energy dissipation at full sunlight as well as higher activities of the predominantly chloroplast-localized (Gillham and Dodge, 1986) ascorbate peroxidase relative to pumpkin. In contrast to APX, catalase activities were higher at full sunlight and increased more from 58% to full sunlight in pumpkin relative to *V. major,* which may be consistent with a role of catalase in the photorespiratory cycle and with presumed higher photorespiration rates in pumpkin relative to *V. major.*

B. Nitrogen Limitation under High PFD

Growth with limiting N supply in the soil resulted in a lower capacity for photosynthetic electron transport as well as lower Chl levels and thus presumably less light absorption compared with N-replete controls (Fig. 20). A greater degree of excess light was apparently nevertheless still absorbed in N-limited leaves and dissipated via the xanthophyll cycle. This depletion/downsizing of the photosynthetic apparatus under limiting N was accompanied by lower levels of most enzymatic and other leaf antioxidants on a leaf area basis, including all carotenoids (VAZ, L, N, and β-carotene decreased in strict proportion; see also Verhoeven et al., 1997), APX, GR, and reduced ascorbate (Fig. 20). In contrast, respiration rates — as well as SOD activities—were similar in N-limited and control leaves. These data suggest that under N limitation, lower rates of photosynthetic electron transport on a leaf area basis may be associated with

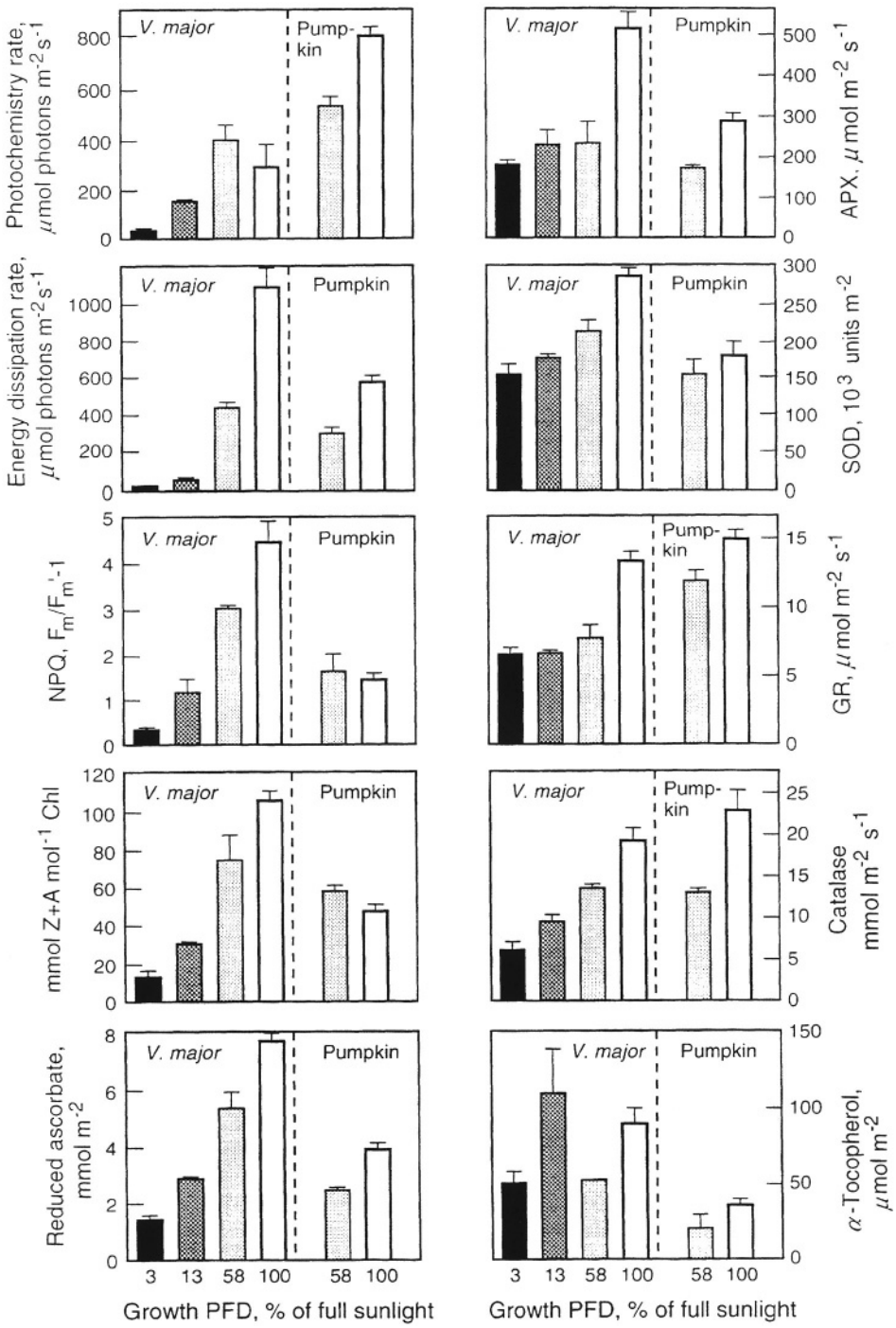

Fig. 19. In situ estimates of the rate of photochemistry, the rate of thermal energy dissipation, and the level of energy dissipation activity from the nonphotochemical quenching of F_m, and the levels or activities of Z+A, reduced ascorbate, ascorbate peroxidase (APX), superoxide dismutase (SOD), glutathione reductase (GR), catalase, and α-tocopherol in leaves of *Vinca major* growing under four different PFDs or pumpkin growing under two PFDs in the field in Boulder, Colorado during the summer of 1995. Data from Logan et al. (1998).

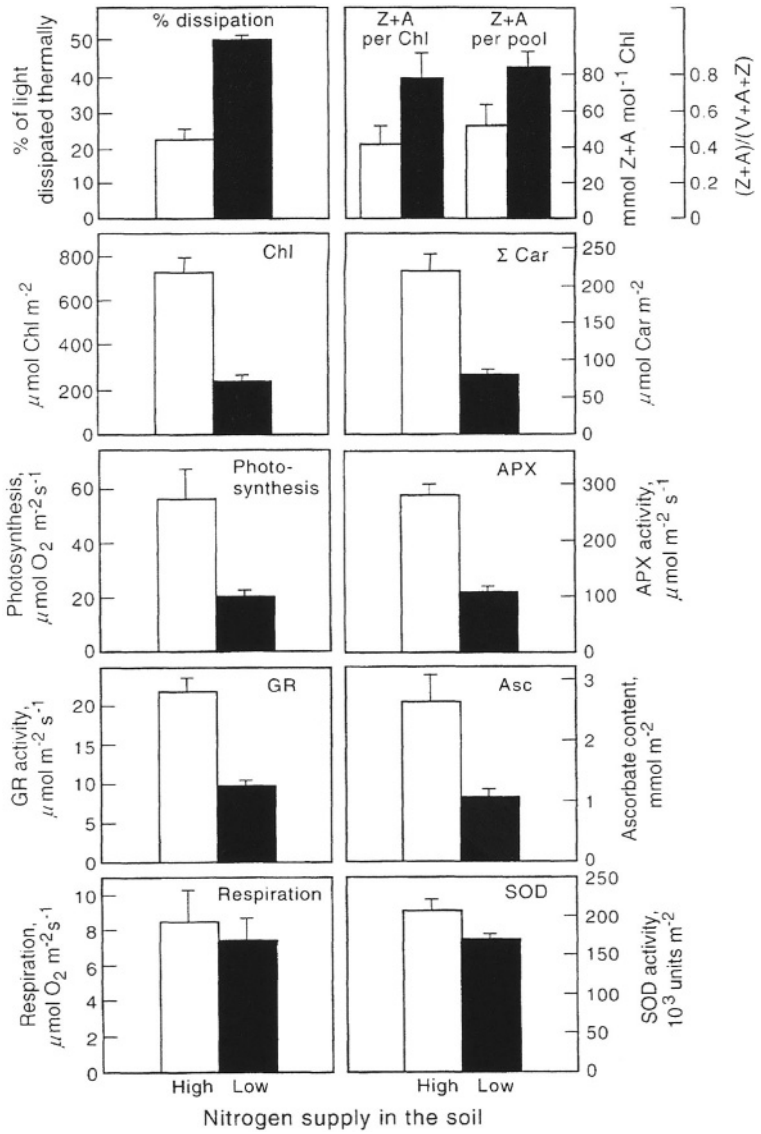

Fig. 20. Influence of nitrogen nutrition (high = 14 mM nitrate and low = 0.25 mM nitrate in the nutrient sol...) on (top two panels) the fraction of excitation energy absorbed by PS II dissipated thermally and foliar levels of Z+A, (second two panels) chlorophyll and total carotenoids, (third and fourth sets of panels) the capacity for photosynthetic oxygen evolution and the foliar activities of ascorbate peroxidase (APX) and glutathione reductase (GR) as well as the foliar ascorbate content, and (bottom two panels) the rate of respiratory oxygen consumption and the foliar activity of superoxide dismutase (SOD) in spinach grown in a fully exposed greenhouse. (B. A. Logan, B. Demmig-Adams, W. W. Adams III, T. N. Rosenstiel, unpublished).

lower absolute rates of photoreduction of oxygen, thus requiring lower levels of scavengers of reactive reduced oxygen species in the chloroplast. In contrast, unaltered rates of mitochondrial respiration may have been associated with an unaltered capacity to scavenge superoxide via SOD.

C. Conclusions

During the acclimation of whole plants to contrasting environments an integration of the response of the metabolic processes of photosynthesis and respiration with that of protective processes such as (Z+A)-dependent energy dissipation and oxygen scavenging is evident. (Z+A)-dependent energy dissipation appears to effectively counteract any environmentally-modulated changes in reactive oxygen production in the Chl pigment bed. Levels of antioxidants involved in the scavenging of reduced reactive oxygen can apparently respond to excess light as well as be

coordinated with changes in overall electron transport capacity during up- or down-regulation of photosynthesis (or respiration). The latter may, once again, point to a regulation by source/sink balance. And once again, the identification of signals involved in this concerted response should be a target of future research.

Acknowledgments

The work in our laboratory has been supported by a Fellowship from the David and Lucile Packard Foundation to BD-A, the National Science Foundation (award numbers IBN-9207653 and IBN-9631064), the United States Department of Agriculture (award number 94-37100-0291), and a Visiting Fellowship from the Australian National University.

References

Adams WW III (1988) Photosynthetic acclimation and photoinhibition of terrestrial and epiphytic CAM tissues growing in full sunlight and deep shade. Austr J Plant Physiol 15: 123–134

Adams WW III and Barker DH (1998) Seasonal changes in xanthophyll cycle-dependent energy dissipation in *Yucca glauca* Nuttall. Plant Cell Environ 21: 501–511

Adams WW III and Demmig-Adams B (1992) Operation of the xanthophyll cycle in higher plants in response to diurnal changes in incident sunlight. Planta 186: 390–398

Adams WW III and Demmig-Adams B (1994) Carotenoid composition and down regulation of Photosystem II in three conifer species during the winter. Physiol Plant 92: 451–458

Adams WW III and Demmig-Adams B (1995) The xanthophyll cycle and sustained thermal energy dissipation activity in *Vinca minor* and *Euonymus kiautschovicus* in winter. Plant Cell Environ 18: 117–127

Adams WW III, Smith SDand Osmond CB (1987) Photoinhibition of the CAM succulent *Opuntia basilaris* growing in Death Valley: evidence from 77K fluorescence and quantum yield. Oecologia 71: 221–228

Adams WW III, Terashima I, Brugnoli E and Demmig B (1988) Comparisons of photosynthesis and photoinhibition in the CAM vine *Hoya australis* and several C_3 vines growing on the coast of eastern Australia. Plant Cell Environ 11: 173–181

Adams W W III, Díaz M and Winter K. (1989) Diurnal changes in photochemical efficiency, the reduction state of Q, radiationless energy dissipation, and nonphotochemical fluorescence quenching from cacti exposed to natural sunlight in northern Venezuela. Oecologia 80: 553–561

Adams WW III, Volk M, Hoehn A and Demmig-Adams B (1992) Leaf orientation and the response of the xanthophyll cycle to incident light. Oecologia 90: 404—410

Adams WW III, Demmig-Adams B, Verhoeven AS and Barker DH (1995a) 'Photoinhibition' during winter stress: Involvement of sustained xanthophyll cycle-dependent energy dissipation. Austr J Plant Physiol 22: 261–276

Adams WW III, Hoehn A and Demmig-Adams B (1995b) Chilling temperatures and the xanthophyll cycle. A comparison of warm-grown and overwintering spinach. Austr J Plant Physiol 22:75–85

Adams WW III, Demmig-Adams B, Barker DH and Kiley S (1996) Carotenoids and Photosystem II characteristics of upper and lower halves of leaves acclimated to high light. Austr J Plant Physiol 23: 669–677

Adams WW III, Demmig-Adams B, Logan BA, Barker DH and Osmond CB (1999) Rapid changes in xanthophyll cycle-dependent energy dissipation and Photosystem II efficiency in two vines, *Stephania japonica* and *Smilax australis,* growing in the understory of an open *Eucalyptus* forest. Plant Cell Environ 22: 125–136

Allen JF and Nilsson A (1997) Redox signalling and the structural basis of regulation of photosynthesis by protein phosphorylation. Physiol Plant 100: 863–868

Anderson JM, Park Y-I and Chow WS (1997) Photoinactivation and photoprotection of Photosystem II in nature. Physiol Plant 100:214–223

Ballou LM and Fischer EH (1986) Phosphoprotein phosphatases. In: Boyer P and Krebs EG (eds) The Enzymes, Vol 17, pp 311–361. Academic Press, Orlando

Barker DH and Adams WW III (1997) The xanthophyll cycle and energy dissipation in differently oriented faces of the cactus *Opuntia macrorhiza.* Oecologia 109: 353–361

Barker DH, Adams WW III, Logan BA and Demmig-Adams B (1998) Photochemistry and xanthophyll cycle-dependent energy dissipation in differently oriented cladodes of *Opuntia stricta* during the winter. Austr J Plant Physiol 25: 95–104

Bauer H, Nagele M, Comploj M, Caller V, Mair M and Unterpertinger E (1994) Photosynthesis in cold acclimated leaves of plants with various degrees of freezing tolerance. Physiol Plant 91: 403–412

Bilger W and Björkman O (1991) Temperature dependence of violaxanthin de-epoxidation and non-photochemical fluorescence quenching in intact leaves of *Gossypium hirsutum* L. and *Malva parviflora* L. Planta 184: 226–234

Björkman O (1981) Responses to different quantum flux densities. In: Lange OL, Nobel PS, Osmond CB and Ziegler H (eds) Encyclopedia of Plant Physiol, NS, Vol. 12A, Physiological Plant Ecology I, pp 57–107. Springer, Berlin

Björkman O and Demmig-Adams B (1994) Regulation of photosynthetic light energy capture, conversion, and dissipation in leaves of higher plants. In: Schulze E-D and Caldwell MM (eds) Ecophysiology of Photosynthesis, pp. 17–47. Springer, Berlin

Bratt CE, Arvidsson P-O, Carlsson M, Åkerlund H-E (1995) Regulation of violaxanthin de-epoxidase activity by pH and ascorbate concentration. Photosynth Res 45: 169–175

Brugnoli E, Cona A and Lauteri M (1994) Xanthophyll cycle components and capacity for non-radiative energy dissipation in sun and shade leaves of *Ligustrum ovalifolium* exposed to conditions limiting photosynthesis. Photosynth Res 41: 451–463

Carlberg I, Andersson B (1996) Phosphatase activities in spinach thylakoid membranes—effectors, regulation and location. Photosynth Res 47: 145–156

Casper C, Eickmeier WG and Osmond CB (1993) Changes in fluorescence and xanthophyll pigments during dehydration in the resurrection plant *Selaginella lepidophylla* in low and medium light intensities. Oecologia 94: 528–533

Ciompi S, Castagna A, Ranieri A, Nali C, Lorenzini G and Soldatini GF (1997) CO_2 assimilation, xanthophyll cycle pigments and PS II efficiency in pumpkin plants as affected by ozone fumigation. Physiol Plant 101: 881–889

Cohen P (1989) The structure and regulation of protein phosphatases. Annu Rev Biochem 58:453–508

Demmig B, Winter K, Krüger A and Czygan F-C (1987) Photoinhibition and zeaxanthin formation in intact leaves. A possible role of the xanthophyll cycle in the dissipation of excess light energy. Plant Physiol 84: 218–224

Demmig B, Winter K, Krüger A and Czygan F-C (1988) Zeaxanthin and the heat dissipation of excess light energy in *Nerium oleander* exposed to a combination of high light and water stress. Plant Physiol 87: 17–24

Demmig-Adams B (1998) Survey of thermal energy dissipation and pigment composition in sun and shade leaves. Plant and Cell Physiology 39: 474–482

Demmig-Adams B and Adams III WW (1992) Carotenoid composition in sun and shade leaves of plants with different life forms. Plant Cell Environ 15: 411–419

Demmig-Adams B and Adams WW III (1994) Capacity for photoprotective energy dissipation in leaves with different xanthophyll cycle pools. Austr J Plant Physiol 21: 575–588

Demmig-Adams B and Adams WW III (1996a) The role of xanthophyll cycle carotenoids in the protection of photosynthesis. Trends Plant Sci 1: 21–26

Demmig-Adams B and Adams WW III (1996b) Chlorophyll and carotenoid composition in leaves of *Euonymus kiautschovicus* acclimated to different degrees of light stress in the field. Austr J Plant Physiol 23: 649–659

Demmig-Adams B and Adams WW III (1996c) Xanthophyll cycle and light stress in nature: uniform response to excess direct sunlight among higher plant species. Planta 198: 460–470

Demmig-Adams B, Winter K, Winkelmann E, Krüger A and Czygan F-C (1989) Photosynthetic characteristics and the ratios of chlorophyll, β-carotene, and the components of the xanthophyll cycle upon a sudden increase in growth light regime in several plant species. Bot Acta 102: 319–325

Demmig-Adams B, Adams WW III, Logan BA and Verhoeven AS (1995) Xanthophyll cycle-dependent energy dissipation and flexible PS II efficiency in plants acclimated to light stress. Austr J Plant Physiol 22: 249–260

Demmig-Adams B, Gilmore AM and Adams III WW (1996a) In vivo functions of carotenoids in higher plants. FASEB J 10: 403–412

Demmig-Adams B, Adams WW III, Barker DH, Logan BA, Verhoeven AS and Bowling DR (1996b) Using chlorophyll fluorescence to assess the allocation of absorbed light to thermal dissipation of excess excitation. Physiol Plant 98: 253–264

Demmig-Adams B, Adams WW III and Grace SC (1997) Physiology of light tolerance in plants. Hort Rev 18: 215–246

Demmig-Adams B, Moeller DL, Logan BA, Adams WW III (1998) Positive correlation between levels of retained zeaxanthin + antheraxanthin and degree of photoinhibition in shade leaves of *Schefflera arboricola* (Hayata) Merrill. Planta 205: 367–374

Depka B, Jahns P and Trebst A (1998) β-carotene to zeaxanthin conversion in the rapid turnover of the D1 protein of Photosystem II. FEBS Letts 424: 267–270.

Eskling M, Arvidsson P-O and Åkerlund H-E (1997) The xanthophyll cycle, its regulation and components. Physiol Plant 100:806–816

Falbel TG, Staehelin LA and Adams WW III (1994) Analysis of xanthophyll cycle carotenoids and chlorophyll fluorescence in light intensity-dependent chlorophyll-deficient mutants of wheat and barley. Photosynth Res 42:, 191–202

Färber A, Young AJ, Ruban AV, Horton P and Jahns P (1997) Dynamics of xanthophyll-cycle activity in different antenna subcomplexes in the photosynthetic membranes of higher plants. The relationship between zeaxanthin conversion and nonphotochemical fluorescence quenching. Plant Physiol 115: 1609–1618

Frank HA, Cua A, Chynwat V, Young A, Gosztola D and Wasielewski MR (1994) Photophysics of the carotenoids associated with the xanthophyll cycle in photosynthesis. Photosynth Res 41: 389–395

Fryer MJ, Oxborough K, Martin B, Ort DR and Baker NR (1995) Factors associated with depression of photosynthetic quantum efficiency in maize at low growth temperature. Plant Physiol 108: 761–767

Gal A, Zer H and Ohad I (1997) Redox-controlled thylakoid protein phosphorylation. News and views. Physiol Plant 100: 869–885

Giardi MT, Cona A, Geiken B, Kucera T, Masojidek J and Mattoo AK (1996) Long-term drought stress induces structural and functional reorganization of Photosystem II. Planta 199: 118–125

Gillham DJ and Dodge AD (1986) Hydrogen peroxide scavenging systems in pea chloroplasts. Planta 167: 246–251

Gilmore AM (1997) Mechanistic aspects of xanthophyll cycle-dependent photoprotection in higher plant chloroplasts and leaves. Physiol Plant 99: 197–209

Gilmore AM and Björkman O (1994) Adenine nucleotides and the xanthophyll cycle in leaves. 1. Effects of CO_2- and temperature-limited photosynthesis on adenylate energy charge and violaxanthin de-epoxidation. Planta 192: 526–536

Gilmore AM and Björkman O (1995) Temperature-sensitive coupling and uncoupling of ATPase-mediated, nonradiative energy dissipation: Similarities between chloroplasts and leaves. Planta 197: 646–654

Gilmore AM and Yamamoto HY (1993) Linear models relating xanthophylls and lumen acidity to non-photochemical fluorescence quenching. Evidence that antheraxanthin explains zeaxanthin-independent quenching. Photosynth Res 35: 67–78

Gilmore AM, Mohanty N and Yamamoto HY (1994) Epoxidation of zeaxanthin and antheraxanthin reverses non-photochemical quenching of Photosystem II chlorophyll *a* fluorescence in the presence of a trans-thylakoid ΔpH. FEBS Letts 350: 271–274

Gilmore AM, Hazlett T, Debrunner PG and Govindjee (1996) Photosystem II chlorophyll *a* fluorescence lifetimes are independent of the antennae size difference between barley wild-type and *chlorina* mutants. Comparison of xanthophyll-cycle dependent and photochemical quenching. Photosynth Res 48:171–187

Gilmore A, Shinkarev VP, Hazlett TL and Govindjee (1998)

Quantitative analysis of the effects of intrathylakoid pH and the xanthophyll cycle pigments on chlorophyll *a* fluorescence lifetime distributions and intensity in thylakoids. Biochemistry 37:13582–13593

Grace SC and Logan BA (1996) Acclimation of foliar antioxidant systems to growth irradiance in three broad-leaved evergreen species. Plant Physiol 112: 1631–1640

Haldimann P, Fracheboud Y and Stamp P (1995) Carotenoid composition in *Zea mays* developed at sub-optimal temperature and different light intensities. Physiol Plant 95: 409–414

Horton P, Ruban AV and Walter RG (1996) Regulation of light harvesting in green plants. Annu Rev Plant Physiol Plant Mol Biol 47: 655–684

Hurry VM, Krol M, Öquist G and Huner NPA (1992) Effect of long-term photoinhibition on growth and photosynthesis of cold-hardened spring and winter wheat. Planta 188: 369–375

Hurry VM, Keerberg O, Pärnik T, Gardeström P and Öquist G (1995) Cold-hardening results in increased activity of enzymes involved in carbon metabolism in leaves of winter rye (*Secale cereale* L). Planta 195: 554–562

Jahns P and Miehe P (1996) Kinetic correlation of recovery from photoinhibition and zeaxanthin epoxidation. Planta 198: 202–210

Jang J-C and Sheen J (1997) Sugar sensing in higher plants. Trends Plant Sci 2: 208–214

Jung S and Steffen KL (1997) Influence of photosynthetic photon flux densities before and during long-term chilling on xanthophyll cycle and chlorophyll fluorescence quenching in leaves of tomato (*Lycopersicon hirsutum*). Physiol Plant 100: 958–966

Kilb B, Wietoska H and Godde D (1996) Changes in the expression of photosynthetic genes precede the loss of photosynthetic activities and chlorophyll when glucose is supplied to mature spinach leaves. Plant Sci 115: 225–235

Koch KE (1996) Carbohydrate-modulated gene expression in plants. Annu Rev Plant Physiol Plant Mol Biol 47: 509–540

Krapp A and Stitt M (1995) An evaluation of direct and indirect mechanisms for the 'sink-regulation' of photosynthesis in spinach: changes in gas exchange, carbohydrates, metabolites, enzyme activities and steady-state transcript levels after cold-girdling source leaves. Planta 195: 313–323

Königer M and Winter K (1991) Carotenoid composition and photon-use efficiency of photosynthesis in *Gossypium hirsutum* L. grown under conditions of slightly suboptimum leaf temperatures and high levels of irradiance. Oecologia 87:349–356

Königer M, Harris GC, Virgo A and Winter K (1995) Xanthophyll-cycle pigments and photosynthetic capacity in tropical forest species: A comparative field study on canopy, gap and understory plants. Oecologia 104: 280–290

Laemmli UK (1970) Cleavage of structural proteins during assembly of the head of bacteriophage T4. Nature 227: 680–685

Logan BA, Barker DH, Demmig-Adams B and Adams WW III (1996) Acclimation of leaf carotenoid composition and ascorbate levels to gradients in the light environment within an Australian rainforest. Plant Cell Environ 19: 1083–1090

Logan BA, Barker DH, Adams WW III and Demmig-Adams B (1997) The response of xanthophyll cycle-dependent energy dissipation in *Alocasia brisbanensis* to sunflecks in a subtropical rainforest. Austr J Plant Physiol 24: 27–33

Logan BA, Demmig-Adams B, Adams WW III and Grace SC (1998) Antioxidation and xanthophyll cycle-dependent energy dissipation in *Cucurbita pepo* L. and *Vinca major* L. acclimated to four growth PPFDs in the field. J Exp Bot 49: 1869–1879

Lovelock CE and Clough BF (1992) Influence of solar radiation and leaf angle on leaf xanthophyll concentrations in mangroves. Oecologia 91: 518–525

Maxwell C, Griffiths H and Young AJ (1994) Photosynthetic acclimation to light regime and water stress by the C_3-CAM epiphyte *Guzmania monostachia:* gas-exchange characteristics, photochemical efficiency and the xanthophyll cycle. Funct Ecol 8: 746–754

Maxwell C, Griffiths H, Borland AM, Young AJ, Broadmeadow MSJ and Fordham MC (1995) Short-term photosynthetic responses of the C_3-CAM epiphyte *Guzmania monostachia* var. *monostachia* to tropical seasonal transitions under field conditions. Austr J Plant Physiol 22: 771–781

Morales F, Abadia A, Belkhodja R and Abadia J (1994) Iron deficiency-induced changes in the photosynthetic pigment composition of field-grown pear (*Pyrus communis* L.) leaves. Plant Cell Environ 17: 1153–1160

Nakano Y and Asada K (1981) Hydrogen peroxide is scavenged by ascorbate-specific peroxidase in spinach chloroplasts. Plant Cell Physiol 22: 867–880

Niyogi KK, Grossman AR and Björkman O (1998) Arabidopsis mutants define a central role for the xanthophyll cycle in the regulation of photosynthetic energy conversion. Plant Cell 10: 1121–1134

Oberhuber W and Bauer H (1991) Photoinhibition of photosynthesis under natural conditions in ivy (*Hedera helix* L.) growing in an understory of deciduous trees. Planta 185: 545–553

Osmond CB (1994) What is photoinhibition? Some insights from comparisons of shade and sun plants. In: Baker NR and Bowyer JR (eds) Photoinhibition of Photosynthesis from Molecular Mechanisms to the Field, pp 1–24. Bios Scientific Publishers, Oxford

Ottander C and Öquist G (1991) Recovery of photosynthesis in winter-stressed Scots pine. Plant Cell Environ 14: 345–349

Ottander C, Campbell D and Öquist G (1995) Seasonal changes in Photosystem II organisation and pigment composition in *Pinus sylvestris*. Planta 197: 176–183

Paul MF and Driscoll SP (1997) Sugar repression of photosynthesis: The role of carbohydrates in signalling nitrogen deficiency through source:sink imbalance. Plant Cell Environ 20:110–116

Phillip D, Ruban AV, Horton P, Asato A and Young AJ (1996) Quenching of chlorophyll fluorescence in the major light-harvesting complex of Photosystem II: A systematic study of the effect of carotenoid structure. Proc Natl Acad Sci USA 93: 1492–1497

Poorter H (1990) Interspecific variation in relative growth rate: on ecological causes and physiological consequences. In: Lambers H, Cambridge ML, Konings H and Pons TL (eds) Causes and Consequences of Variation in Growth Rate and Productivity of Higher Plants, pp 45–68. SPB Academic Publishing, The Hague

Powles SB (1984) Photoinhibition of photosynthesis induced by visible light. Annu Rev Plant Physiol 35: 15–44

Robinson SA and Osmond CB (1994) Internal gradients of chlorophyll and carotenoid pigments in relation to photo-

protection in thick leaves of plants with crassulacean acid metabolism. Austr J Plant Physiol 21: 497–506

Roden JS. Wiggins DJ and Ball MC (1997) Photosynthesis and growth of two rain forest species in simulated gaps under elevated CO_2. Ecology 78: 385–393

Ruban AV and Horton P(1995) An investigation of the sustained component of nonphotochemical quenching of chlorophyll fluorescence in isolated chloroplasts and leaves of spinach. Plant Physiol 108:721–726

Saccardy K, Pineau B, Roche O and Cornic G (1998) Photochemical efficiency of Photosystem II and xanthophyll cycle components in *Zea mays* leaves exposed to water stress and high light. Photosynth Res 56: 57–66

Schindler C and Lichtenthaler HK (1996) Photosynthetic CO_2-assimilation, chlorophyll fluorescence and zeaxanthin accumulation in field grown maple trees in the course of a sunny and a cloudy day. J Plant Physiol 148: 399–412

Sironval C and Kandler O (1958) Photoxidation processes in normal green *Chlorella* cells. I. The bleaching process. Biochim Biophys Acta 29: 359–368

Thayer SS and Björkman O (1990) Leaf xanthophyll content and composition in sun and shade determined by HPLC. Photosynth Res 23:331–343

Thiele A, Krause GH and Winter K (1998) In situ study of photoinhibition of photosynthesis and xanthophyll cycle activity in plants growing in natural gaps of the tropical forest. Austr J Plant Physiol 25: 189–195

Uhrmacher S, Hanelt D and Nultsch W (1995) Zeaxanthin content and the degree of photoinhibition are linearly correlated in the brown alga *Dictyota dichotoma.* Marine Biol 123: 159–165

Van der Werf A (1996) Growth analysis and photoassimilate partitioning. In: Zamski E and Schaffer AA (eds) Photoassimilate Distribution in Plants and Crops Source-Sink Relationships, pp 1–20. Marcel Dekker, New York

Vener AV, Ohad I and Andersson B (1998) Protein phosphorylation and redox sensing in chloroplast thylakoids. Curr Opin Plant Biol 1/3:217–223

Verhoeven AS, Adams WW III and Demmig-Adams B (1996) Close relationship between the state of the xanthophyll cycle pigments and Photosystem II efficiency during recovery from winter stress. Physiol Plant 96: 567–576

Verhoeven AS, Demmig-Adams B and Adams WW III (1997) Enhanced employment of the xanthophyll cycle and thermal energy dissipation in spinach exposed to high light and nitrogen stress. Plant Physiol 113: 817–824

Verhoeven AS, Adams WW III and Demmig-Adams B (1998) Two forms of sustained xanthophyll cycle-dependent energy dissipation in overwintering *Euonymus kiautschovicus.* Plant Cell Environ 21: 893–903

Verhoeven AS, Adams WW III and Demmig-Adams B (1999) The xanthophyll cycle and acclimation of *Pinus ponderosa* and *Malva neglecta* to winter stress. Oecologia 118: 277–287

Watling JR, Robinson SA, Woodrow IE and Osmond CB (1997) Responses of rainforest understorey plants to excess light during sunflecks. Austr J Plant Physiol 24: 17–25

Winter K and Lesch M (1992) Diurnal changes in chlorophyll *a* fluorescence and carotenoid composition in *Opuntia ficus-indica,* a CAM plant, and in three C_3 species in Portugal during summer. Oecologia 91: 505–510

Yamamoto HY and Bassi R (1996) Carotenoids: localization and function. In: Ort DR and Yocum CF (eds) Oxygenic Photosynthesis: The Light Reactions, pp 539–563. Kluwer Academic Publishers, Dordrecht

This page intentionally left blank

Chapter 15

Regulation of the Structure and Function of the Light Harvesting Complexes of Photosystem II by the Xanthophyll Cycle

Peter Horton, Alexander V. Ruban
Robert Hill Institute, Department of Molecular Biology and Biotechnology, University of Sheffield, Western Bank, Sheffield S10 2TN, U.K.

Andrew J. Young
School of Biological and Earth Sciences, Liverpool John Moores University, Byrom St, Liverpool L3 3AF, U.K.

H. A. Frank, A. J. young, G. Britton and R. J. Cogdell (eds): The Photochemistry of Carotenoids, pp. 271–291.

Summary

The xanthophyll cycle is a relatively simple process whereby the interconversion of violaxanthin into zeaxanthin in the light harvesting complexes serves to regulate light harvesting and subsequent energy dissipation in different light environments. In order to determine how these carotenoids can regulate such processes it is first important to ascertain what differences exist between these two xanthophylls. De-epoxidation brings about significant changes in the structures and hence the properties of these carotenoids. Thus when the conjugated chain length is increased from nine to eleven conjugated double bonds this in turn affects their S_1 energies but also alters the molecule's size and shape. The 'Molecular Gear Shift Model' describes the direct quenching of chlorophyll fluorescence by singlet-singlet energy transfer to zeaxanthin, while violaxanthin can only act to transfer its energy to chlorophyll. However this model does not account for the ability of these molecules to profoundly affect structure and organization of light harvesting complexes. Differences in carotenoid structure affect their interactions with the complexes so that violaxanthin and zeaxanthin play an important role in determining their structure and function by controlling its inter-subunit structure. In the presence of violaxanthin, complexes are optimized for light utilization and are resistant to ΔpH-dependent quenching. De-epoxidation into zeaxanthin allows a different state to be formed in which ΔpH formation readily triggers conversion to a strongly quenched state in which sub-unit interactions are increased.

I. Introduction

Under light limiting conditions the light harvesting system of Photosystem II transfers absorbed excitation energy efficiently to the reaction center so that the quantum yield of electron transfer, even in a leaf in the field, approaches the maximum theoretical value (Björkman and Demmig, 1987). The high quantum yield of photosynthesis is maintained at low irradiances, but the electron transfer and metabolic reactions of CO_2 fixation begin to saturate as the light level increases (Fig. 1). The decline in gradient of the photosynthesis vs. irradiance curve frequently occurs at around the growth light intensity (Anderson and Osmond, 1987). Further increases in irradiance saturate these dark reactions and a ceiling level, the Pmax, is reached. Light saturation of photosynthesis is a common occurrence in nature; it occurs in fast growing crop plants under tropical conditions (Murchie et al., 1999), at moderate light levels at low temperature (Falk et al., 1996) and generally if photosynthetic capacity is decreased either by sub-optimal environmental conditions or by metabolic or developmental constraints such as carbohydrate build-up or leaf senescence.

Under conditions when photosynthesis is light saturated, the photosynthetic pigments continue to absorb light, the level of excitation increasing linearly with increased irradiance — much of this excitation energy is in excess of that needed for photosynthesis. The greater the light intensity is above saturation, the greater the excess energy. Excess excitation energy means the density of excited states in the light harvesting system of PS II will increase, increasing the probability of pigment and protein damage through triplet formation, free radical production and photo-oxidation (Krause, 1988). More specifically, the rate of excitation of the PS II reaction centers will be higher, increasing the probability of damaging events and leading to photoinhibition (Park et al., 1995; Andersson and Barber, 1996).

Light saturation of photosynthesis is expected to lead to an increased frequency of closed PS II reactions. However, it was observed from measurements of photochemical fluorescence quenching, qP, that PS II was relatively oxidized even though photosynthesis was saturated (Weis and Berry, 1987). This indicated that in some way the excess energy level was not being 'seen' by PS II. The increased degree of saturation of photosynthetic electron transfer was found to be accompanied by an increase in the level of non-photochemical quenching of chlorophyll fluorescence, suggesting that excess energy was being quenched, by non-radiative

Abbreviations: DCCD – dicyclhexylcarbodimmide; DEPS – de-epoxidation state; LHCII – light harvesting complexes of Photosystem II; PFD – photon flux density; Pmax – light saturated rate of photosynthesis; PS II – Photosystem II; qE – non-photochemical quenching of chlorophyll fluorescence dependent upon the transthylakoid proton gradient; qN – non-photochemical quenching of chlorophyll fluorescence; VDE – violaxanthin de-epoxidase; ΔpH – transthylakoid pH gradient;

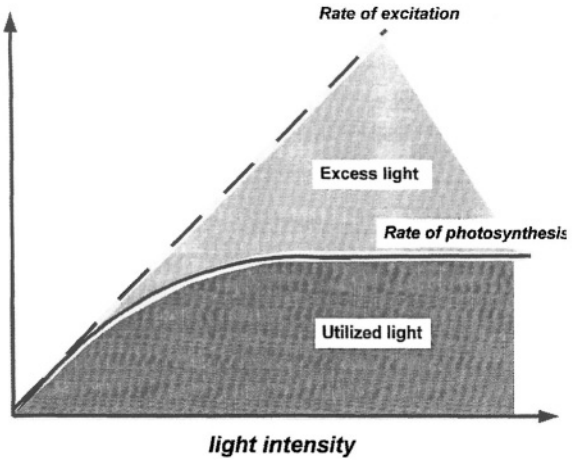

Fig. 1. Light intensity dependence of the rate of excitation of the light harvesting system of the chloroplast and the rate of photosynthesis. Below the photosynthesis curve is the utilized light and above the curve is the (potentially damaging) excess.

dissipation. This was recognized as an example of feed-back control over light harvesting by Photosystem II (Horton, 1989). Non-photochemical quenching was therefore viewed as an adaptive mechanism that brings about dissipation of excess energy, bringing the light and dark reactions of photosynthesis into balance, thereby protecting against photodamage (Horton and Ruban, 1992).

Non-photochemical quenching consists of a number of processes, with different relaxation times in darkness, arising from different molecular processes in the thylakoid membrane (Horton, 1996). During most periods of excess illumination, the main part of qN relaxes within minutes of return to low light or darkness. This rapidly relaxing quenching process is referred to as qE, because it is dependent obligatorily on the energization of the thylakoid in the form of the transthylakoid pH gradient (Briantais et al., 1979). Sometimes qE can persist for extended periods after illumination if the ΔpH is maintained (Gilmore and Björkman, 1994).

Although the molecular mechanism of qE has yet to be elucidated, a number of features are supported by a variety of experimental evidence:

1. The ΔpH causes quenching mainly through the acidification of the thylakoid lumen. qE can be titrated against lumen pH, measured using pH indicators such as 9-aminoacridine or neutral red (Krause et al., 1988; Noctor and Horton, 1990).

2. qE is associated with a conformational change that is the cause of an absorbance change at 535 nm (Bilger and Björkman, 1994; Noctor et al., 1993; Ruban et al., 1993b). Inhibition of ΔA_{535} accompanies the blocking of qE by antimycin A (Horton et al., 1991), and the recently described *npq4* mutant of *Arabidopsis thaliana* does not show either qE or ΔA_{535} (Björkman and Niyogi, 1999) Although ΔpH formation and relaxation occur within seconds, both qE and Δ_{535} are much slower (Noctor et al., 1991, 1993), and conditions which lead to fast qE kinetics are associated with similarly altered kinetics of ΔA_{535} (Ruban et al., 1993b).

3. qE occurs in the light harvesting system of Photosystem II, LHCII. LHCII comprises the products of the six Lhcb genes (Lhcb1-6) that are assembled into four types of complexes known as LHCIIa, LHCIIb, LHCIIc and LHCIId (Peter and Thornber, 1991; Jansson, 1994). LHCIIb is a trimeric complex binding approximately 60% of PS II chlorophyll. LHCIIa, LHCIIc and LHCIId are monomeric complexes more widely known as CP29, CP26 and CP24, respectively. The evidence that qE occurs in one or more of these complexes has been comprehensively reviewed (Horton and Ruban., 1992, 1994; Horton et al., 1996) but includes the fact that qE is reduced when Lhcb polypeptides are absent (Jahns and Krause, 1994). The involvement of the xanthophyll cycle (see below) is strong evidence that LHCII is the site of qE. More recent evidence includes the elimination of qE when the LHCII associated xanthophylls zeaxanthin and lutein are missing in *Chlamydomonas* double mutants (Niyogi et al., 1997a,b) and the identification of binding sites for the qE-antagonist DCCD on Lhcb polypeptides (Walters et al., 1994, 1996; Pesaresi et al., 1997). Spectroscopic measurements provided evidence of preferential quenching of excitation in LHCII rather than in the PS II reaction center or the core-antenna complexes CP47 and CP43 (Ruban and Horton, 1994). The final line of evidence supporting the participation of LHCII is the capacity for all isolated LHCII components to show in vitro quenching resembling in vivo qE (see Section IV.B.2). There is considerable debate concerning whether there is a specific quenching site residing in one type of LHCII; it has been suggested that the minor complexes CP29 and CP26 may contain

the quenching sites (Horton and Ruban, 1992; Bassi et al., 1994; Crofts and Yerkes, 1994; Gilmore et al., 1996; Pesaresi et al., 1997), although there is as yet no proof of this.

4. Strong correlations between the levels of zeaxanthin and qE indicate that the reversible de-epoxidation of violaxanthin via the xanthophyll cycle has a major controlling role in qE (Demmig-Adams, 1990; Demmig-Adams and Adams, 1992; Demmig-Adams et al., 1995b). The ΔpH and zeaxanthin together control the induction of quenching (Horton et al; 1991, 1996;Noctor et al., 1991; Gilmore and Yamamoto, 1992; Ruban and Horton, 1995; Gilmore et al., 1998). There is disagreement of how the xanthophyll cycle is involved, and in particular whether there is an obligatory requirement for zeaxanthin for qE (see Chapter 14, Demmig-Adams et al.).

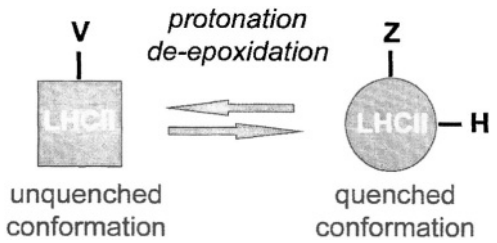

Fig. 2. Simple two state 'allosteric' model for qE in which the switch between quenched and unquenched conformation is driven by the effect of protonation and de-epoxidation. In this model LHCII can exist in two states, an unquenched conformation and a quenched conformation. Because the affinity of proton and zeaxanthin binding is greater in the quenched state, the ΔpH and de-epoxidation state will determine the equilibrium between these states. The existence of co-operativity indicates that these two states consist of a group of LHCII subunits which interact and change conformation in concert. The changed conformation, and intersubunit interaction, may give rise to quenching process itself. In this model one or more of the different LHCII components may be involved.

II. General Model for Non-Photochemical Quenching

The induction of qE as a result of ΔpH and violaxanthin de-epoxidation leads to a general model for qE based on changes in conformation of LHCII (Horton et al., 1991). A simplified version of this model is shown in Fig. 2. An unprotonated LHCII system binding violaxanthin is the state that provides maximum efficiency in light harvesting. Protonation and zeaxanthin binding results in a state in which energy is dissipated as heat. These states were suggested to be conformationally different, explaining the close association between qE and ΔA_{535} described above. Modeling of steady state chlorophyll fluorescence yield (Walters and Horton, 1993) and measurement of chlorophyll fluorescence lifetimes (Gilmore et al., 1995) provided evidence for the existence of these two different states of the PS II antenna.

This general formulation makes various predictions about qE, which have been confirmed by experimental observation. Synergism between DEPS and ΔpH has been found: in the de-epoxidized state, the ΔpH requirement for qE is reduced compared to the epoxidized state; at high ΔpH maximum quenching can be observed even at very low DEPS and at low ΔpH the stimulation of qE by DEPS is greatest (Rees et al., 1989; Noctor et al., 1991). Violaxanthin de-epoxidation 'activates' the ΔpH-dependent qE. The effect of this activation is found in the kinetics of the induction of quenching: the rate of induction of proton-dependent quenching is increased at high compared to low DEPS (Ruban and Horton, 1998). This effect can be observed in leaves, isolated chloroplasts and isolated LHCII (Fig. 3).

These kinetic features of qE are the same as shown by many other oligomeric proteins having a regulatory function. Thus LHCII could be viewed as a multisubunit enzyme whose 'product' is heat (Horton and Ruban, 1995). The rate of reaction is determined by violaxanthin/zeaxanthin and proton concentration. In fact, the dependency of qE on proton concentration indicates co-operative binding, with n = 4–6 (Schoenknecht et al., 1996; Heinze and Dau, 1996). In our own experiments, a Hill coefficient of approx. 7 was found in dark adapted zeaxanthin-free chloroplasts, whereas in the presence of zeaxanthin, this co-operativity is reduced to n = 0.9 and the reaction more closely matches hyperbolic Michaelis-Menton kinetics (Fig. 4). Such data shows positive co-operativity of qE with respect to H^+ binding, and the behavior of the increased zeaxanthin/violaxanthin ratio as an allosteric activator, shifting the ΔpH requirement and removing co-operative kinetics. The simplest explanation for these kinetics is that the sub-units of LHCII interact and the transition between the unquenched and quenched conformations proceeds in a concerted manner. This model explains

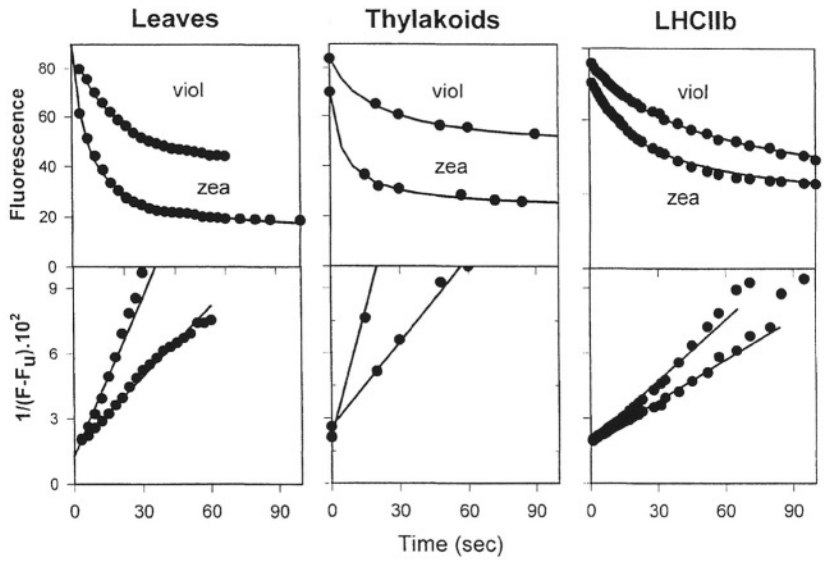

Fig. 3. Kinetics of chlorophyll fluorescence quenching in leaves, thylakoids and LHCIIb from spinach. Leaf samples were dark adapted (viol) or pre-illuminated (zea) as described by Noctor et al. (1991), and the thylakoids and LHCIIb isolated from the leaves as described by Ruban et al. (1994b). For leaves and thylakoids, quenching was initiated by illumination, for LHCIIb by dilution to low pH (Ruban et al., 1998a,b). Solid lines are a second order rate equation. Data are redrawn from Ruban and Horton (1998).

all existing data on qE. The high Hill coefficient, may indicate that the number of interacting units is high. As a typical LHCII system contains 4–5 trimers and three minor complexes, this could suggest that interaction throughout this group of subunits contributes to the observed high Hill coefficient. Consistent with this idea, the Hill coefficient and extent of co-operativity are reduced in mutants lacking LHCIIb (Schoenknecht et al., 1996). Recent structural analysis of large PS II units shows how the LHCII sub-units are assembled in close proximity to each other (Hankamer et al., 1997; Boekema et al., 1998), and this could provide an opportunity for co-operative changes in conformation.

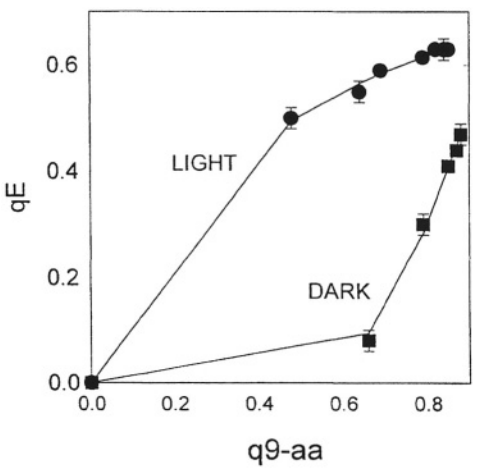

Fig. 4. pH dependency of qE in chloroplasts with (L) and without zeaxanthin (D). Data was obtained as in Noctor et al. (1991). q9-aa refers to the proportional quenching of 9-aminoacridine fluorescence. Using the equation $qE = (q9aa)^n/[(q9aa)^n + Q^n]$, where n is the Hill Coefficient and Q the relative proton binding affinity, the data shown indicate n = 0.98 and 7.48 and Q = 0.49 and 0.98 for L and D respectively.

III. Unanswered Questions Concerning the Roles of the Xanthophyll Cycle in Non-photochemical Quenching

Central to elucidating the mechanism of qE is to understand the role of the xanthophyll cycle. First it is necessary to obtain information on where within the LHCII system the 'active' xanthophyll carotenoids are bound. Information on the structural features of violaxanthin and zeaxanthin that determine their binding to LHCII is needed, just as such information is vital to understanding other allosteric effectors in biology. Then, information about the nature of the protein binding sites themselves is needed. With such biochemical information it may then be possible to understand how these carotenoids control quenching. For this to be achieved there is a

Table 1. Pigment composition of LHCII, thylakoid membranes and Photosystem II BBY particles

Sample	%/MR	lut	neo	vio	β-car
LHCIIb	MR	1.9	1.0	0.2	
CP26	MR	1.2	1.0	0.9	
CP29	MR	0.9	0.6	1.2	
PS II (est)	MR	34	17	<7	10
	%	50	25	<10	15
BBY	%	47	21	19	13
PS II (corr)	MR	36	17	15	10

LHCIIb, CP29 and CP26 were prepared by IEF of BBY PS II particles. *PS II (est)* refers to that predicted from the composition of individual complexes. *PS II (corr)* is the composition required to match the measured composition of BBY particle. *%*, carotenoid content as a % of total; *MR*, estimated molar ratio; *lut*, lutein; *neo*, neoxanthin; *vio*, violaxanthin; *β-car*, β-carotene. For the estimate of PS II pigment content, it was assumed that one PS II consisted of one D1/D2, 1 CP47, 1 CP43, 1 CP29, 1 CP26, 1 CP24, and 5 trimers of LHCIIb.

requirement to develop new experimental approaches since simple correlative measurements on intact leaves and chloroplasts have so far not given any clear information on mechanism. In the remainder of this chapter these important questions will be discussed.

A. Violaxanthin Binding Sites on Light Harvesting Complexes of Photosystem II

Although it is agreed that PS II-associated violaxanthin is bound to LHCII rather than core complexes, the reported number of pigments bound is variable (Peter and Thornber, 1991; Bassi et al., 1993; Ruban et al., 1994b; Phillip and Young, 1995, Sandona et al, 1998; Ruban et al., 1999). The minor complexes CP29, CP26 and CP24 are enriched in violaxanthin relative to LHCIIb, which has been reported to be almost completely deficient in this carotenoid (Bassi et al., 1993). Such data have led to suggestions that the site of qE must be in the minor complexes. While the location of DCCD-binding sites on CP29 and CP26 (Walters et a., 1994) also support this location for qE, re-examination of the violaxanthin binding data is warranted. Based on the carotenoid composition of purified complexes the composition of PS II can be predicted (Table 1). This approach indicates that at most there are 7 violaxanthin molecules per PS II. Whereas these calculations accurately predict the content of lutein, neoxanthin and β-carotene, the measured value for violaxanthin is 19%, nearly double the predicted value. Hence, at least eight violaxanthin molecules in PS II are not accounted for by the measurements on purified complexes.

With the specific aim of isolating the xanthophyll cycle from PS II, more gentle detergent treatments were used (Ruban et al., 1999) and it was then found that approx. 0.8 mol violaxanthin was bound by each LHCIIb monomer. It was concluded that all LHCII monomers bind one violaxanthin per monomer. Depending on the number of LHCIIb trimers in PS II, this predicts between 15 and 20 violaxanthin molecules are bound to PS II, the majority of which are associated with LHCIIb, similar to the measured content. Violaxanthin is bound only loosely to LHCIIb. A systematic study of the removal of different pigments from LHCII complexes allowed quantitation of the apparent binding affinity. For the pigments of LHCII the strength of binding decreases in the order chlorophyll *b* > neoxanthin > chlorophyll *a* > lutein > zeaxanthin > violaxanthin. Comparing the different complexes, violaxanthin is most strongly held by CP29 and most weakly by LHCIIb (Fig. 5a). The ease with which violaxanthin is removed from LHCIIb suggests it is bound on the periphery of the complex. Conversely for CP29 in which one of the two centrally located luteins is missing, at least a part of the violaxanthin is bound internally. It is likely that loose binding is essential if violaxanthin is to be available to the de-epoxidase (Chapter 16, Yamamoto). The low de-epoxidation state for CP29 compared to LHCIIb suggests the violaxanthin tightly bound to the interior of the complex is not available for de-epoxidation (Fig. 5b). The conclusion from these observations is that the violaxanthin active in qE is bound to the periphery of LHCII. An alternative view has been put forward by Bassi and co-workers,

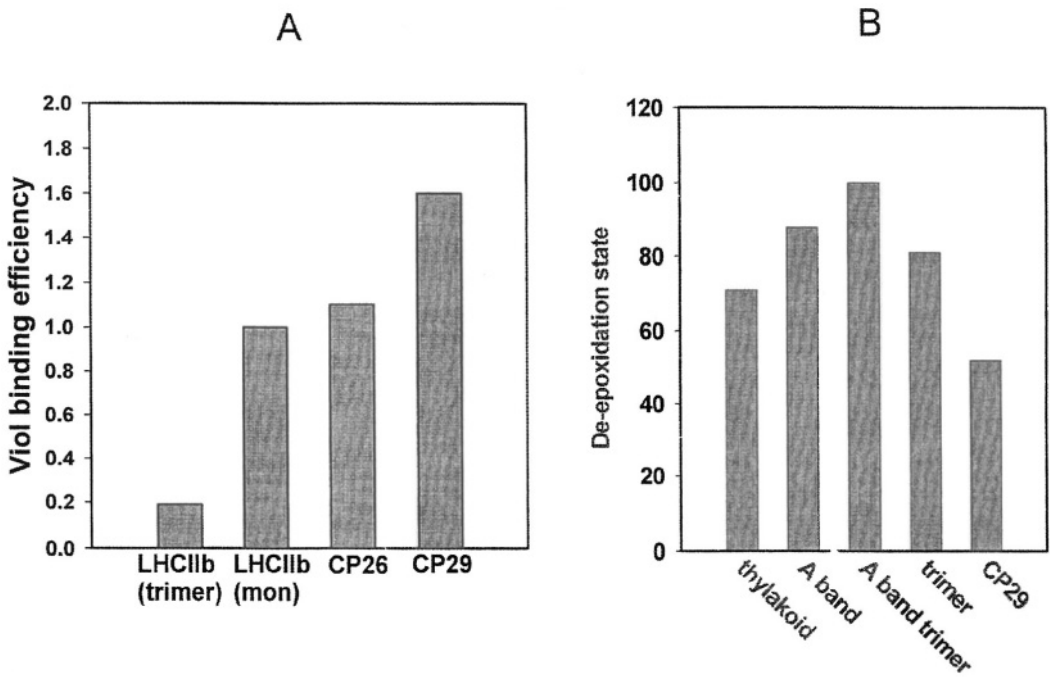

Fig. 5. Determination of the relative efficiency of binding of violaxanthin to different LHCII complexes (A) and the de-epoxidation states of CP29 compared to thylakoids, and different preparations of LHCIIb (B). A-band refers to an oligomeric LHCII preparation prepared by gentle detergent solubilization of thylakoids, and A-band trimer, the LHCIIb trimer prepared from it (Ruban et al., 1999).

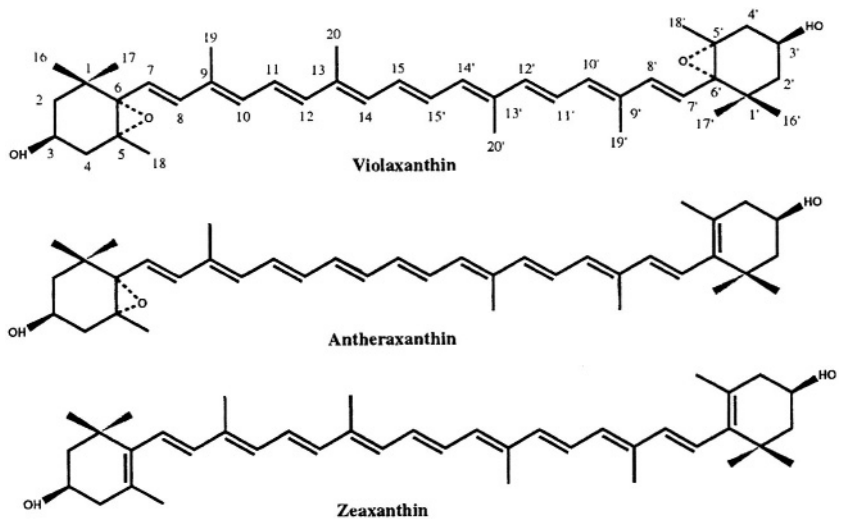

Fig. 6. Structures of the carotenoids involved in the xanthophyll cycle in higher plants and in algae.

who propose that a zeaxanthin bound internally in CP29 is directly involved in non-photochemical quenching (Sandonà et al., 1998).

B. Differences Between Violaxanthin and Zeaxanthin

In addition to determining the site of quenching and the binding sites of the carotenoids involved in the xanthophyll cycle (see above) it is also important to consider carefully the structures and associated properties of these carotenoids. The processes of de-epoxidation of violaxanthin into zeaxanthin (via antheraxanthin) and subsequent epoxidation (Fig. 6) has the effect of altering the structure of these pigments. These structural effects as determined by

3D-modeling of these xanthophylls are outlined below. Changes to carotenoid structure (which will in turn will alter the physico-chemical properties of these molecules; Britton, 1995) directly result from the lengthening (de-epoxidation) or shortening (epoxidation) of the conjugated double bond system (which ranges from 9 to 11 carbon-carbon double bonds in violaxanthin and zeaxanthin, respectively). The implications of such changes to the chromophore are two-fold: (i) first, the extent of the conjugated double bond system in polyenes and carotenoids affects both the energies and lifetimes of their excited states; (ii) second, the extension of the conjugated double bond system into the β-end-group of carotenoids (for one end-group in antheraxanthin and for both end-groups in zeaxanthin) introduces conformational changes in these molecules. Similar effects would be predicted for the one-step de-epoxidation/epoxidation of diadinoxanthin and diatoxanthin seen in some algae.

1. Energy Levels

The photochemical and spectroscopic properties of carotenoids are derived from their low-lying energy states (for a more detailed review see Chapter 8, Christensen). The low-lying singlet states of carotenoids are denoted the 1^1B_u (S_2) and the 2^1A_g (S_1) states and their energies and lifetimes govern their behavior in photosynthetic systems. The visible absorption spectra of carotenoids arises from an electronic transition from the ground state (1^1A_g or S_0) to the S_2 state (which has B_u symmetry). The energy and lifetimes of the S_2 state can be readily determined and are dependent upon the extent of π-electron conjugation of the carotenoid (an increase in conjugation results in a decrease in S_2 energy). The S_1 state possesses A_g symmetry in the idealized C_{2h} point group. The ground state also has A_g symmetry and as a result the $S_0 \rightarrow S_1$ transition is forbidden. Determination of the energies of the S_1 states has been achieved for a few carotenoids by measuring the rather weak fluorescence spectra of compounds (due to the $S_1 \rightarrow S_0$ transition) which have less than nine conjugated double bonds (e.g. Andersson et al., 1992). For longer chromophores the $S_2 \rightarrow S_0$ electronic transition dominates and, as a result, the determination of the S_1 energy level has been difficult to establish (Frank et al., 1997). Locating the S_1 energies in the xanthophyll cycle carotenoids has instead relied on the extrapolation of data observed using the lifetimes of the S_1 states in conjunction with the energy gap law for radiationless transitions (Engelman and Jortner, 1970; Frank et al., 1994, 1996; Chynwat and Frank, 1995; see Chapter 8, Christensen for details).

Differences in the extent of the conjugated double bond system of the xanthophyll cycle carotenoids (violaxanthin n = 9 conjugated double bonds, antheraxanthin n = 10 and zeaxanthin n = 11) directly affect their S_1 energies. Based on the S_1 fluorescence of a range of acyclic carotenoids the energy-gap law for non-radiative transitions was applied to the xanthophyll cycle carotenoids (Frank et al., 1994). S_1 state lifetimes of τ = 23.9 ps for violaxanthin, τ = 14.4 ps for antheraxanthin and τ = 9.0 ps for zeaxanthin were used to calculate energies for the S_1 levels. The energies for the xanthophyll cycle carotenoids were estimated to be 15,290 cm^{-1}, 14,720 cm^{-1} and 14,170 cm^{-1} for violaxanthin, antheraxanthin and zeaxanthin, respectively (Young et al., 1997; Fig. 7). The potential significance of these values in photosynthetic energy dissipation is discussed below.

It should however be emphasized that there is a great deal of uncertainty in the estimation of the S_1 energy of carotenoids, so that for example recent estimations of the S_1 energy of β-carotene have varied considerably (Andersson and Gillbro, 1995). In addition, the fact that the S_1 energies of all the carotenoids present in the photosynthetic tissues of higher plants lie very close to the Q_y transition of chlorophyll has raised questions as to whether this state has enough singlet energy to participate in singlet energy transfer to chlorophyll *a* or, more importantly in the context of the xanthophyll cycle, participate in singlet energy transfer from chlorophyll to carotenoid (Frank et al., 1997). It should also be noted that the predicted absorption spectrum of this excited state is thought to be very wide thus there may be considerable overlap between chlorophyll and carotenoid spectra. Thus the carotenoid spectrum for compounds with ten or more conjugated double bonds *may* also be able to act as quenchers of chlorophyll fluorescence (e.g. lutein, antheraxanthin; Frank et al., 1996; Young and Frank, 1996). Similarly it may be possible for violaxanthin to quench as it is thought that its spectrum will overlap that of chlorophyll *a*, although this reaction is not preferred (in solution violaxanthin can indeed quench chlorophyll fluorescence (Frank et al., 1995)).

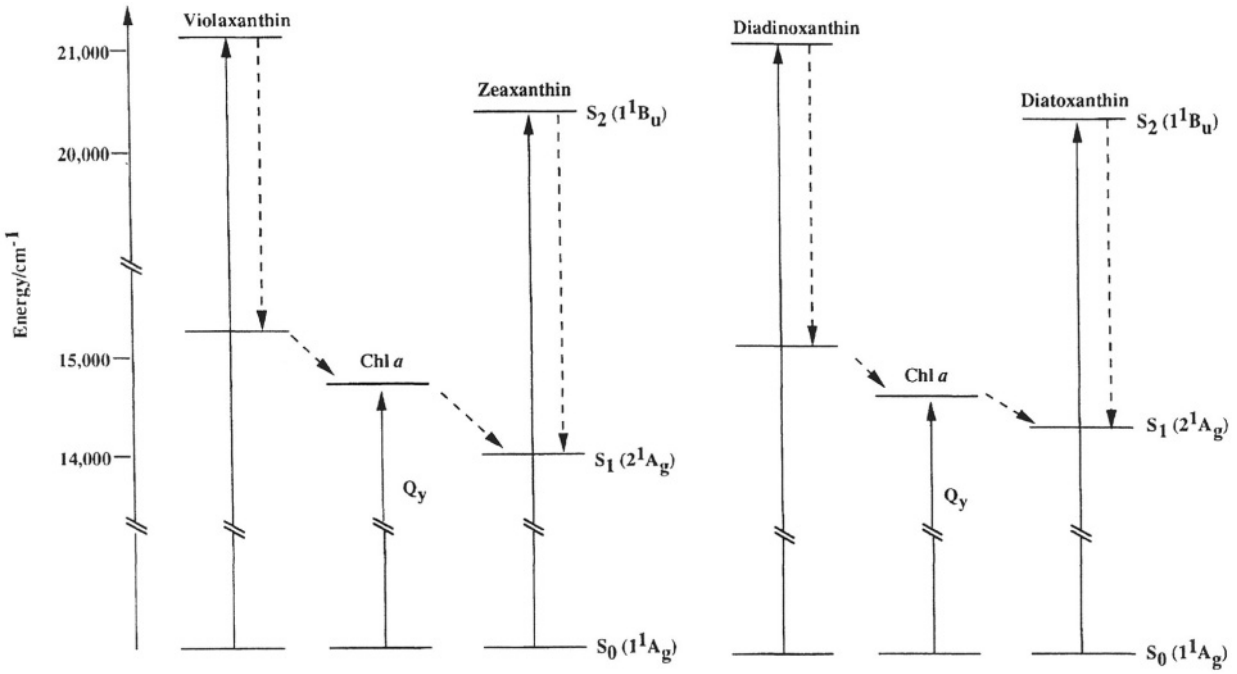

Fig. 7. The 'Molecular Gear Shift' model showing the positions of the S_1 energies of the xanthophyll cycle carotenoids relative to chlorophyll *a*. Antheraxanthin and lutein (not shown) are isoenergetic with chlorophyll *a* (Frank et al., 1994, 1996).

2. Structure

The stereo or 3D structures of carotenoids can be determined by examination of their crystal structures or by NMR spectroscopy, although only a few molecules have been studied to date (Mo, 1995). The 3D structures of a number of carotenoids including all-*trans* violaxanthin and all-*trans* zeaxanthin (determined with C_1 and C_2 symmetry) have recently been determined by use of semi-empirical molecular orbital calculations using the AM1 Hamiltonian (H. Hashimoto, T. Yoda and A. J. Young, unpublished). As illustrated in Fig. 6, conversion from violaxanthin into zeaxanthin is achieved by de-epoxidation of both end groups, and this will, in turn, affect their stereo-structures, especially around the C5-C6 torsion angle. The C5=C6-C7=C8 dihedral angle is greatly affected by the presence or absence of epoxide groups. The most stable conformers result from a dihedral angle of –48° for zeaxanthin and 92° for violaxanthin. The most stable structures for these two carotenoids are shown in Fig. 8.

The structures of violaxanthin and zeaxanthin and in particular the length and angles adopted by certain carbon-carbon bonds are predicted to be quite different (H. Hashimoto, T. Yoda and A. J. Young, unpublished). Thus, the presence of the epoxide group at C5-C6 alters the length of the C5-C6 and C18-C5 bonds and induces elongation of the C4-C5 and C6-C1 bonds in violaxanthin. Also the epoxide groups in violaxanthin decrease the C5-C6-C7, C18-C5-C6 and C6-C7-C8 bond angles compared to zeaxanthin. The C4-C5-C6-C7 dihedral angle is slightly decreased in the case of violaxanthin but the most pronounced effects are the increase in the C5-C6-C7-C8 angle and especially the very large decrease in the C18-C5-C6-C7 dihedral angle in violaxanthin. Comparison with other carotenoids suggests that these effects are primarily due to the presence of the epoxide groups. The structures of the carotenoids involved in the xanthophyll cycle are therefore significantly different, particularly the overall shape (planarity) of the molecules and ring-to-chain conformation. Such differences have previously been suggested to be responsible, at least in part, for the behavior of these carotenoids with respect to the xanthophyll cycle (Ruban et al., 1994a, 1996, 1997b, 1998b; Horton et al., 1996; Young et al., 1997). This data does not however really illustrate what may be significant differences in the ability of the end-groups to rotate around the C6-C7 bond: in zeaxanthin the extension of the conjugation together

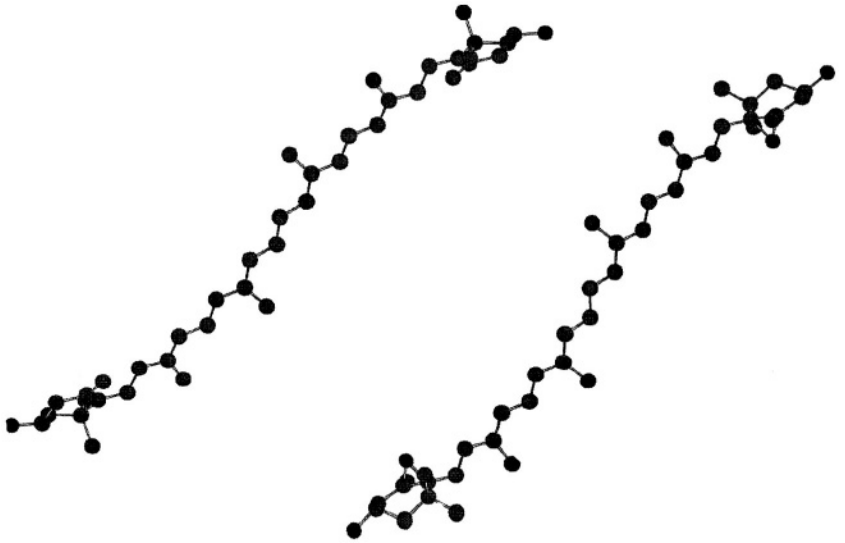

Fig. 8. Stereo-structures of violaxanthin (right) and zeaxanthin (left) as determined by geometry optimization using the AM1 Hamiltonian (Mopac). For clarity the hydrogen atoms are omitted (H. Hashimoto, T. Yoda and A. J. Young, unpublished).

with steric hindrance effects would restrict the molecule to a near-planar conformation while in violaxanthin the lack of conjugation may allow greater rotation.

The physico-chemical properties of a carotenoid molecule are linked to its structure and this should therefore be an important consideration when considering the biological role of the xanthophyll cycle carotenoids (Ruban et al., 1993a; Britton, 1995). For example, the tendency of carotenoids to aggregate (forming H-type aggregates) in ethanol/water solutions has been determined to rely on their structure and in particular appears to be dependent upon the ring-to-chain conformation of these pigments and not their polarity per se (Ruban et al., 1993a). Thus, it requires less energy to aggregate carotenoids with two β-end-group such as β-carotene and zeaxanthin than carotenoids that possess either e-end-groups (e.g. lactucaxanthin) or 5,6-epoxides (e.g. violaxanthin). The inter-conversion of violaxanthin and zeaxanthin will also affect the behavior of these molecules in a membrane (see below).

IV. Mechanisms of the Xanthophyll Cycle in Controlling qE

There are currently two main schools of thought concerning the nature of the mechanism by which a relatively simple alteration to the carotenoid composition of the LHC affects the efficiency of, or balance between light-capture and energy dissipation in different light environments (Horton et al., 1996; Young et al., 1997). The first describes a theoretical model based on direct singlet-singlet energy transfer from chlorophyll to carotenoid resulting in quenching of chlorophyll fluorescence and dissipation of excitation energy. The second hypothesis concerns the role of the xanthophyll cycle carotenoids in controlling the organization of LHCII. Both of these are discussed in some detail in the following sections.

A. Direct Quenching

The possibility that differences in the S_1 energies of violaxanthin and zeaxanthin might account for the operation of the xanthophyll cycle in terms of dissipation of excitation energy was first proposed by Demmig-Adams (1990) and later by Owens et al. (1992). They suggested that zeaxanthin would be expected to have an S_1 energy identical to that of β-carotene as these molecules are essentially isoelectronic (both molecules have 11 conjugated double bonds). This state would lie below that of chlorophyll *a* allowing the carotenoid molecule to act as a sink for excitation energy. However it was not until Frank and colleagues (1994, 1996) determined the S_1 energies of the xanthophyll cycle carotenoids that a clear picture of this theoretical mechanism for the regulation of light-harvesting and energy dissipation emerged.

The energy of the lowest excited singlet state

(denoted S_1) of chlorophyll *a* in the light-harvesting complex of Photosystem II has been estimated to be in the region 14,700–15,000 cm^{-1} (based on a maximum fluorescence of 680 nm; Kwa et al., 1992). The significance of this is clear when compared to the S_1 energies of the xanthophyll cycle carotenoids (Fig. 7): the value of 14,700 cm^{-1} for chlorophyll *a* is lower than that determined for the S_1 state of violaxanthin but higher than that of zeaxanthin. This would suggest that it is energetically possible for the S_1 state of zeaxanthin to quench chlorophyll fluorescence via deactivation of the chlorophyll excited singlet state. In contrast, the higher S_1 level of violaxanthin would only permit it to function as a light-harvesting pigment, transferring its excitation energy onto chlorophyll *a*. It is possible that zeaxanthin may also function as a light-harvesting pigment using energy transfer from its S_2 state to chlorophyll.

The term 'Molecular Gear Shift' was originally used to describe the model in which the interconversion of violaxanthin into zeaxanthin serves to alter their S_1 energies and hence their interaction with chlorophyll (Frank et al., 1994). Thus at high PFDs when dissipation of excess excitation energy is required, zeaxanthin is formed within LHCII. Its presence serves to deactivate the excited singlet state of chlorophyll *a* (resulting in a reduction in chlorophyll fluorescence) and dissipate excitation energy harmlessly as heat. Once their energies were determined it was found that this model could also be applied to diatoxanthin and diadinoxanthin (Frank et al., 1996).

These data support the notion that the enzymatic de-epoxidation/epoxidation reactions of the diatoxanthin/diadinoxanthin and zeaxanthin/violaxanthin xanthophyll cycles appear to be acting as regulators of light flow in the pigment protein complexes (Frank et al., 1994; Young and Frank, 1996). It has been further suggested that antheraxanthin and indeed lutein (which both posses ten conjugated double bonds) can act to quench chlorophyll fluorescence via singlet-singlet energy transfer (Niyogi et al., 1997b). This may explain the observation that quenching can take place in the absence of zeaxanthin, although the S_1 energy of lutein is consistent with its predicted role in highly efficient energy transfer to chlorophyll (Frank et al., 1997). For lutein or antheraxanthin to be involved in energy dissipation they would have to rely on the rather broad spectra that are predicted for the S_1 states of these carotenoids.

The quenching of chlorophyll fluorescence by carotenoids (e.g. β-carotene) in organic solvents suggests that carotenoids could play a role in regulating the flow of energy between chlorophylls and carotenoids in photosynthetic antenna (Beddard et al., 1977). However, the mechanism of quenching of chlorophyll excited states by carotenoids is not understood and may occur by one or more of several plausible energy dissipation routes. In organic solvents such as benzene chlorophyll and carotenoid can interact in a number of ways, with different associations between these pigment molecules potentially giving rise to two different types of quenching processes with different Stern-Volmer behavior, namely static and dynamic quenching of chlorophyll fluorescence (Frank et al., 1995). Further studies have shown however that the predicted carotenoid-chlorophyll interaction or association seen in benzene may be weak (Egorova-Zachernyuk et al., 1996). Such in vitro studies have shown zeaxanthin to be a slightly better quencher of chlorophyll fluorescence than violaxanthin, probably as a result of the increased spectral overlap between chlorophyll fluorescence and zeaxanthin $S_0 \rightarrow S_1$ absorption compared to violaxanthin. The spectral overlap of violaxanthin is expected to be less owing to the fact that its S_1 state is estimated to be higher in energy than zeaxanthin by ~1,200 cm^{-1}. The small preferential quenching ability of zeaxanthin over violaxanthin in vitro was not, however, large enough to account for the zeaxanthin content and fluorescence quenching in vivo.

It is important to emphasize that the S_1 energies and lifetimes of the xanthophyll-cycle carotenoids have not been determined in vivo and as yet, no direct evidence to show that singlet-singlet energy transfer from chlorophyll to carotenoid occurs in the photosynthetic apparatus itself. The 'Molecular Gear Shift' hypothesis described above only suggests that such carotenoid-chlorophyll direct quenching may be a possible route of deactivation. Indeed, recent data has demonstrated that carotenoids that are predicted to have a much higher S_1 energy than zeaxanthin (e.g. the furanoid auroxanthin with seven conjugated double bonds) can bring about quenching of chlorophyll fluorescence in vitro (see below; Ruban et al., 1998b).

For carotenoids such as zeaxanthin to be involved in energy dissipation in vivo relies on several factors, including the position and nature of their energy states, the orientation of the transition dipoles, spectral overlap and the dynamics of their excited states (Frank et al., 1997). Therefore taken overall the

'Molecular Gear Shift' hypothesis only serves to describe the tendency of a particular carotenoid molecule to be involved in energy transfer to or from chlorophyll. Thus, diadinoxanthin would be predicted to be 1.7 times more likely to transfer its energy from its S_1 state to chlorophyll than is diatoxanthin. In contrast, chlorophyll a would be 0.6 times less likely to transfer its energy to diadinoxanthin (Frank et al., 1996). A similar trend would be expected for violaxanthin and zeaxanthin although with these molecules differences in spectral overlap would be larger.

B. Indirect Quenching

The structural differences between violaxanthin and zeaxanthin may provide an explanation of how the xanthophyll cycle could indirectly control qE. De-epoxidation would change the interaction between LHCII and the xanthophyll. Violaxanthin would stabilize the unquenched conformation and zeaxanthin the quenched conformation (see Fig. 2). But what is the evidence for this kind of indirect control of qE?

1. Quenching in the Absence of Zeaxanthin

Experiments with isolated chloroplasts showed that zeaxanthin was not required for quenching (Noctor et al., 1991). A similar conclusion could be made from the occurrence of qE in *Chlamydomonas* mutants lacking VDE activity (Niyogi et al., 1997a,b). In this case it was suggested that lutein fulfils the quenching role. Such an explanation is not inconsistent with an indirect role of the xanthophyll cycle since this model does not specify the quenching mechanism — it could well involve a chlorophyll-lutein interaction in the central domains of the complexes. Since zeaxanthin and lutein are bound to different sites, direct quenching would have to involve specific ΔpH-dependent interactions at two locations in the complex.

It has been suggested that quenching in the absence of zeaxanthin could be explained by the presence of the small amount of antheraxanthin invariably present in most dark-adapted, zeaxanthin-free samples (Gilmore et al., 1998). One percent of carotenoid, would be approx. one molecule per PS II. This would have to be very tightly bound and induce, or be itself, a strong quencher. The proposition is that a high ΔpH could increase the strength of xanthophyll binding to the active site such that only a low concentration of antheraxanthin would be necessary as a 'quencher.' However, such ΔpH-dependent changes in binding affinity have not been demonstrated. In fact, the apparent dependency of qE on low amounts of antheraxanthin can also be readily explained by the allosteric model in Fig. 2 and does not imply that this xanthophyll is acting as a direct quencher.

2. Quenching in Isolated Light Harvesting Complexes

The strongest evidence supporting the indirect mechanism comes from experiments with isolated LHCII (Ruban and Horton., 1992; Ruban et al., 1992a; 1994a; 1996; 1998b; Phillip et al., 1996). When LHCII components are removed from the membrane and purified they are in detergent micelles, the detergent shielding the hydrophobic membrane-facing domains of the complex from the aqueous phase. In this state the fluorescence yield is high, and approaches that of free chlorophyll. Upon dilution of the detergent, there is an increased tendency for the hydrophobic parts of the complex to be exposed to the aqueous phase; this tendency will be offset by structural changes which minimize the exposure of hydrophobic areas to the aqueous phase. Such changes may be conformational transitions within a single LHCII subunit or the formation of new hydrophobic interactions between complexes, leading to aggregation. The latter leads to a very strong chlorophyll fluorescence quenching (Ruban and Horton, 1992). It was suggested that similar aggregation or conformational transitions could be the basis for qE (Horton et al., 1991) and may be linked to the gross changes in membrane structure observed under qE conditions: the membrane becomes thinner, and the interior more hydrophobic (Murakami and Packer, 1970).

Direct experimental evidence supports the view that the in vitro system provides a good model for qE.

a. pH-Dependency

Lowering pH stimulates quenching in LHCIIb, CP29 and CP26 (Ruban et al., 1996; 1998a). This effect is only observed if the detergent concentration is carefully chosen. In vivo the LHC antenna is 'properly balanced,' it is protected by lipids, interaction with the other proteins and possibly carotenoids against the permanent collapse into the 'quenched state.' In

vitro with too low a detergent concentration, quenching is rapid and spontaneous and no control by pH or other external factors can be observed. Conversely if the detergent is too high, changes in protein structure cannot be induced because these depend on the alteration in hydrophobic/hydrophilic forces discussed above. For LHCIIb the apparent pKa is at pH 5.0, whereas for CP26 it is at approx. 6.0 (Ruban and Horton, 1998). These pHs are in the range expected for lumen pH in vivo. DCCD, an inhibitor of qE (Ruban et al., 1992b, Walters et al, 1994) is an inhibitor of pH-dependent quenching in CP29 and CP26, but not LHCIIb (Ruban et al., 1996, 1998a). The covalent binding of DCCD to specific carboxyl residues on these complexes was correlated with the inhibition of fluorescence quenching for a range of complexes, including recombinant CP29 in which putative DCCD-binding sites had been replaced (Ruban et al., 1998a). Since complexes without DCCD binding all showed pH-dependent quenching it is clear that, at least in vitro, the DCCD sites are not the only H^+ binding sites involved in quenching. One serious deficiency of this in vitro system is the lack of sidedness and protonation of the 'stromal' surface of the complexes may lead to non-physiological effects. Indeed, if these complexes have a H^+ channel function (Jahns and Junge, 1990), such behavior will be obscured in vitro.

b. Inhibitors and Enhancers

In addition to DCCD, other agents control qE in thylakoids. Most notably, antimycin A is a strong qE inhibitor (Oxborough and Horton, 1987) and dibucaine a qE stimulator (Noctor et al., 1993). Antimycin A is an inhibitor of quenching of LHCIIb in vitro (Horton et al., 1991; Ruban et al., 1992a), and in particular reduced the tendency for aggregation of the complexes in a low detergent environment. In terms of the model in Fig. 2 this is consistent with antimycin A stabilizing the unquenched form of the LHCII system. The mechanisms of this effect of antimycin is not understood, although there is evidence that it may arise from the protonophoric effect (Yerkes and Crofts, 1995), perhaps *removing* protons from sites within LHCII. Dibucaine has the opposite effect to antimycin—it promotes the adoption of the quenched state—qE is induced more rapidly in thre presence of dibucaine. There is evidence that qE is also induced at lower ΔpH (Noctor et al., 1993), but this observation is complicated by the interference between dibucaine and 9-amino-acridine fluorescence (Gilmore and Yamasaki, 1998). Dibucaine is a potent stimulator of quenching in all complexes. Again the mechanism is unknown, but may relate to the potential of this reagent to *donate* protons to key sites in LHCII.

c. Violaxanthin De-Epoxidation

The most striking similarity between qE and in vitro quenching is the differential effects of violaxanthin and zeaxanthin. As discussed below, exogenous violaxanthin is an inhibitor of quenching, whereas violaxanthin is a stimulator. Most significantly, if LHCIIb is isolated from leaves with a high DEPS, zeaxanthin binding is retained. Compared to samples with just violaxanthin present, the zeaxanthin containing LHCIIb had a greater tendency for quenching (Ruban and Horton., 1998), displaying more rapid quenching (Fig. 3) and a shift to lower pH requirement. It is important to emphasize that zeaxanthin exerts no effect on either the fully quenched or unquenched states, only on the transition between them. Therefore the reported absence of effects of DEPS on the fluorescence lifetimes of LHCIIb are not inconsistent with these more recent observations (Mullineaux et al., 1993).

d. Kinetics of Quenching

The kinetics of induction of quenching in leaves, thylakoids and isolated LHCII are remarkably similar. For LHCIIb, a good fit to the quenching kinetics was obtained with a single second order hyperbolic function (Fig. 3). This function was found to adequately describe the more complex in vivo data. Most significantly, in all three cases, the increase in DEPS could be described by the same alterations in kinetics: an increased rate constant for induction of quenching and an increase in the total amount of fluorescence quenched.

e. Spectroscopic Indicators

Quenching in LHCIIb is accompanied by changes in photophysical properties of bound pigments, as will be discussed in more detail below. Principal among these are the absorbance changes in the Soret and red region of the spectrum. Similar absorbance changes have been observed in isolated chloroplasts and leaves (Fig. 9).

3. Control of Quenching by Exogenous Carotenoids

If the xanthophyll binding sites effective in quenching are peripheral to the LHCII complexes it would be expected that carotenoids added to the complexes in vitro would exert effects on quenching. In fact, such effects are found, and yield the clearest information on the mechanism of action of the xanthophyll cycle.

a. Violaxanthin as a Quenching Inhibitor

Violaxanthin inhibits in vitro quenching in LHCIIb, CP29 and CP26 (Ruban et al 1994a, 1996; 1998; Phillip et al., 1996). As for the effect of endogenous DEPS, the effect is to control the rate constant and amplitude of quenching (Fig. 10B). Maximum effect was found with approx. 1 molecule violaxanthin per chlorophyll but this is the amount added, not bound.

b. Zeaxanthin as a Quenching Stimulator

Zeaxanthin has the opposite effect to violaxanthin: it stimulates quenching in LHCIIb, CP29 and CP26 (Ruban et al 1994a, 1996; 1998; Phillip et al., 1996). Again, the effect is to increase the rate constant for formation of quenching (Fig 10A). At carefully chosen detergent concentration, addition of zeaxanthin to isolated CP29 causes a large, and immediate quenching of fluorescence (Fig. 11). Prior addition of violaxanthin diminishes the effect of zeaxanthin.

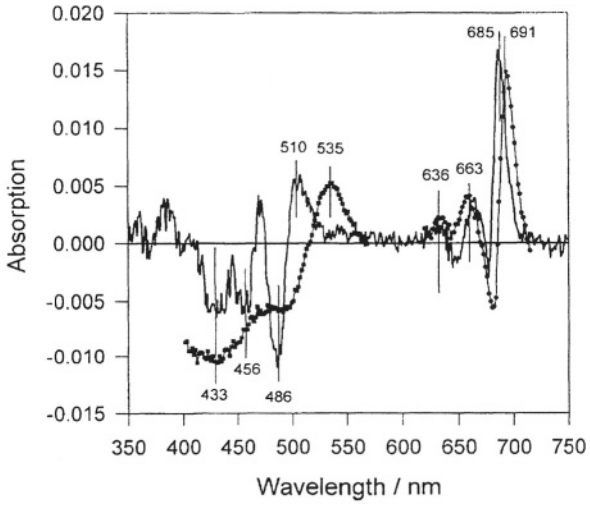

Fig. 9. Absorption difference spectra for qE in a leaf (dotted lines) and for DCCD-dependent quenching in isolated CP29. Note the broad similarities in the spectrum in the Soret and red regions.

c. Specificity of Xanthophyll Effects on LHCII

The nature of the interaction between the xanthophyll cycle carotenoids and LHCIIb has been investigated by testing the effects of a variety of externally added

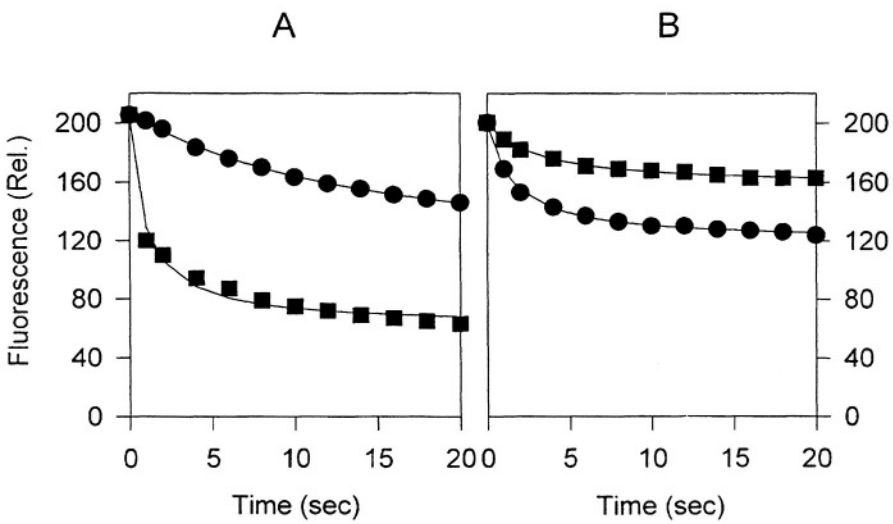

Fig. 10. Kinetics of quenching in isolated CP26. Quenching was induced by dilution to low detergent concentration. A. Effect of zeaxanthin, circles – control; squares – plus zeaxanthin. B. Effect of violaxanthin, circles – control; squares – plus violaxanthin. Solid lines are theoretical second order equations.

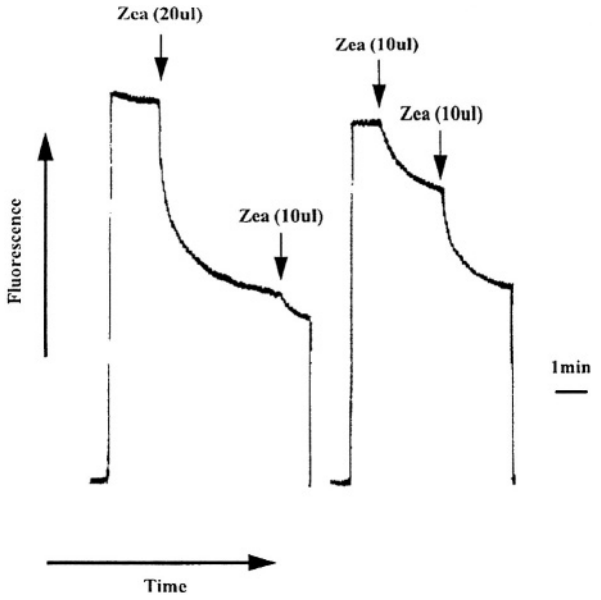

Fig. 11. Effect of addition of zeaxanthin on fluorescence quenching in isolated CP29. Note the stable fluorescence level before zeaxanthin (zea) addition and the rapid and saturatable response.

carotenoids with different structures. An inhibitory effect on quenching could be observed with a variety of carotenoids in which the length of the conjugated carbon double chain is less than nine. Similarly, the stimulatory effect was observed when there were greater than 11 carbon double bonds (Phillip et al., 1996). This data suggested the importance of the S_1 energy level of the carotenoid, although it was pointed out that it was hard to incorporate this into the fact that the effects were on the kinetics of the induction of quenching rather than the extent of quenching. Moreover, the observation that violaxanthin and other short chain carotenoids inhibit quenching is not predicted from the stand point of direct quenching. These observations were explained by the idea that all carotenoids have the ability to prevent quenching by binding to the hydrophobic domains of the complex. However, this 'anti-quenching' could be offset by their tendency to accept energy from chlorophyll and be quenchers of fluorescence.

However, this view has been challenged by two subsequent experiments. The first involved observation of the effects on LHCIIb structure (see d, below). The second arose from the effects of a different set of carotenoids in which the relative importance of the structural and energetic aspects of the molecules could be explored (Fig. 12). The furanoid carotenoid auroxanthin is a di-epoxy carotenoid similar to violaxanthin but it has a conjugated chain length of seven because the epoxides are in the C5,8 configuration and not C5,6 as in violaxanthin. Its S_1 energy level is predicted to be much higher than violaxanthin. The end groups of this molecule are predicted to lie in the plane of the carbon double

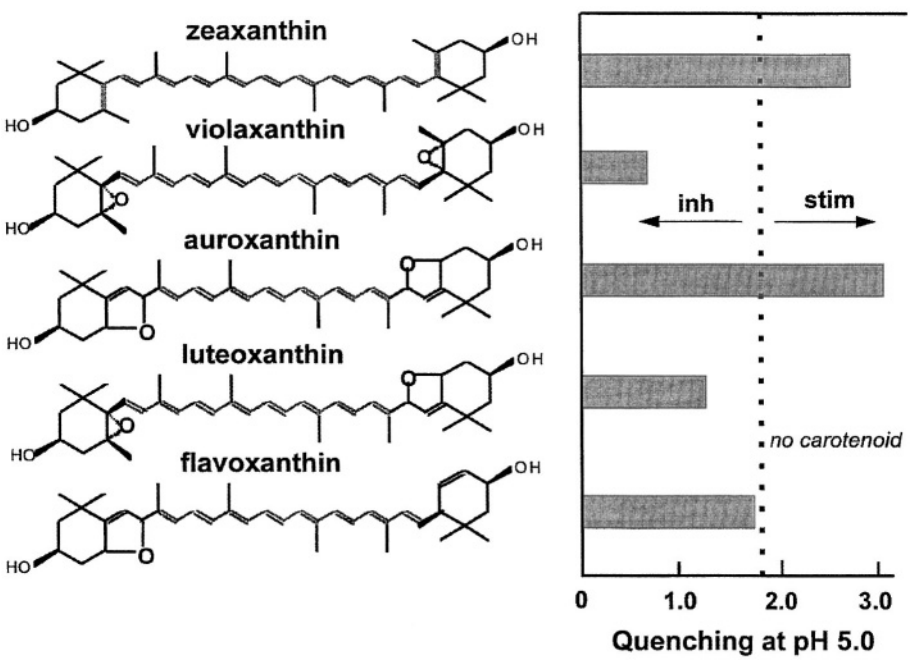

Fig. 12. Effectiveness of different epoxy carotenoids on quenching at pH 5.0 in LHCIIb. Experiment carried out as in Ruban et al. (1998).

bond chain (rather like zeaxanthin). Auroxanthin is a stimulator of quenching, therefore suggesting that the action of zeaxanthin is not due to its altered S_1 energy but to the end-group orientation (Ruban et al., 1998). In luteoxanthin, one end-group is predicted to be out-of-plane (as a violaxanthin) and the other in plane (as in auroxanthin) and this molecule is a mild inhibitor of quenching. Flavoxanthin, with one in plane and the other tending to be out of plane, was neutral. Hence the opposing effects of end-group orientation on inhibition and stimulation of quenching can be observed. Calculations on the structures of violaxanthin and zeaxanthin suggest that the actual shape of the molecule may not fully explain these effects: the big difference in polarity of violaxanthin compared to zeaxanthin may be a very important feature which determine the type and strength of their interaction with LHCII.

d. Effects of Xanthophyll Cycle on LHCII Structure

The model for non-photochemical quenching is the quenching that occurs upon aggregation of LHCII in vitro. If this model is applicable to in vivo qE, then it would be predicted that violaxanthin and zeaxanthin should control the aggregation process. Direct evidence of this has been obtained by observing the behavior of LHCIIb after centrifugation on sucrose gradients; samples pre-incubated with violaxanthin showed reduced aggregation compared to a control, and zeaxanthin-treated samples showed increased aggregation (Ruban et al., 1997b). In this experiment the LHCIIb aggregates were smaller than in earlier work and are approx. 5–6 LHCIIb trimers. These experiments unequivocally demonstrate that the different structures of violaxanthin and zeaxanthin cause them to exert dramatically different effects on LHCIIb; these effects can fully explain their effects on fluorescence quenching without the need to invoke additional direct quenching.

4. Mechanism of Quenching in Isolated LHCII

It has not been possible to elucidate the exact physical mechanism of quenching in isolated LHCII. Spectroscopic investigations of LHCIIb have revealed a number of specific alterations in a small proportion (one or two molecules) of bound pigments. An absorbance change in the chlorophyll a band with a λ_{max} in the difference spectrum of 683 nm indicates formation of a new absorbing species, such as a chlorophyll dimer or at least a change in interaction between a chlorophyll and its environment (Ruban and Horton, 1992, Ruban et al., 1996; 1998a; Horton and Ruban, 1994). This 683 nm band is correlated with quenching. Other changes in the absorption spectrum point to an altered chlorophyll *b* and a carotenoid. LD and CD spectra confirm the changes in a sub-set of pigments, and most clear is a change in orientation of one chlorophyll *b* and one chlorophyll a upon aggregate formation (Ruban et al., 1997a). These changes are also detected as formation of new H bonds to the protein matrix, and the twisting of one of the bound xanthophylls (Ruban et al., 1995b).

Aggregation of LHCIIb, CP29 and CP26 are all associated with an alteration in the shape of the fluorescence emission band at 77 K (Ruban et al., 1996). In the unquenched, unaggregated state the λ_{max} is around 682 nm and upon aggregation there is a shift to long wavelengths, typically with λ_{max} around 700 nm. Analysis of the spectrum shows the presence of several long wavelength species in aggregated LHCIIb, with λ_{max} ranging from 681 to 710 nm (Ruban et al., 1995a). As the temperature is lowered towards 4 Kthe fluorescence yield rises as the energy is trapped on emitters at shorter wavelength. This energy transfer to the long wavelength species could be a part of the quenching process, involving one or two chlorophylls, which either directly quench fluorescence or transfer energy to another quencher (Mullineaux et al., 1993). In this case, zeaxanthin is excluded from being the quenching molecule, because the quenching in aggregated LHCIIb is observed in the absence of this xanthophyll. The formation of the red-shifted chlorophyll forms in aggregates is accompanied by increased intensity of vibronic satellite bands, and it was suggested that these represents the routes of non-radiative decay (Ruban and Horton, 1992). Indeed, in the condensed state, such as aggregated LHCII, where distances between chlorophylls are approaching the van der Waals distance (Kühlbrandt et al., 1994) it could be expected that collective excitations could easily take place. Evidence for this comes from some excitonic features in OD, LD and CD spectra described above. On the other hand, vibrational spectroscopy revealed some strong change in the chlorophyll environment (Ruban et al., 1995b). Therefore, factors such as formation of excitonic states and the effect of the medium

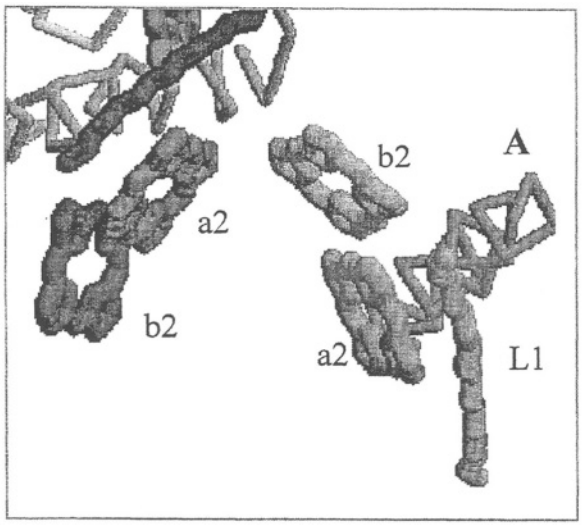

Fig. 13. Segment of the LHCIIb structural model to show the close proximity between chlorophylls. Shown are regions containing Chl b2 and Chl a2, lutein (L1) and a portion of the A-helix, for two associated LHCIIb trimers. The distance between Chl a2 and Chl b2 is 4.06 Å.

(protein, xanthophyll and chlorophyll) can be new important features, which determine the excitation lifetime in LHCII. For example, examination of the structural model for LHCIIb (Kühlbrandt et al., 1994) reveals numerous possibilities for strong interaction between chlorophylls and adjacent pigments (both chlorophyll and carotenoid) and the protein (Fig. 13). These types of interactions can alter the probability of the transition of electronic energy directly into the lattice (environment) vibrations and heat. By nature, this energy dissipation channel is temperature dependent, since the medium superimposes the temperature dependent molecular displacements upon those brought by the electronic excited state. The stronger chlorophyll interacts with the environment, the shorter the excitation lifetime. In cases when optical, π-electrons are preferentially influenced by interaction with the environment, much stronger non-radiative energy dissipation is expected. Therefore, alteration of the type and strength of chlorophyll co-ordination could be an important mechanism for modulation of quenching. The lattice type of quenching is most likely in systems with strong spectral shifts in absorption and fluorescence. The very strong temperature dependence of the fluorescence and existence of a number of new red-shifted emitters in LHCII are therefore highly consistent with energy dissipation through lattice vibrations.

IV. Conclusions

A. Xanthophylls May Control Intra and Intersubunit Structure in LHCII

Xanthophylls play an important role in determining the structure and function of LHCII. Tightly bound to internal sites they stabilize the intrasubunit structure of the light-harvesting system by means of binding sites on the lumen and stromal surfaces, and also act as chlorophyll triplet quenchers, preventing photooxidation (Kühlbrandt et al., 1994). In addition, at weaker binding sites peripheral to the complexes, violaxanthin and zeaxanthin are bound. These carotenoids control the *inter subunit* structure of the light harvesting system (Horton et al., 1991; 1996) De-epoxidation allows the switch between two different states of organization: in the presence of violaxanthin, complexes are resistant to ΔpH-dependent quenching, being optimized for energy utilization. De-epoxidation to zeaxanthin poises the system such that ΔpH formation triggers conversion to a strongly quenched state where sub-unit interactions are increased. Thus, the control of the packing of LHCII in the thylakoid membrane may be a result of the DEPS and ΔpH. The control of the 2-D organization of the thylakoid probably relates to the observation that zeaxanthin formation is associated with an increased stability of the thylakoid at higher temperatures; a decreased membrane fluidity could result from the tighter packing of LHCII in the thylakoid (Sarry et al, 1994).

B. Changes in Xanthophyll Cycle Pool Size

A key feature of the regulation of the xanthophyll cycle is that the size of the pool of violaxanthin, antheraxanthin and zeaxanthin is higher in plants grown at higher irradiance (Demmig-Adams and Adams, 1992; Ruban et al., 1993b; Björkman and Demmig-Adams, 1995a; Demmig-Adams et al., 1995). Often, but not always, this is accompanied by an increase in chlorophyll *a/b* ratio arising from a decline in LHCIIb content. The size of the pool, as a % total carotenoid varies from 15% to 30%. The upper limit might be defined by the number of binding sites on LHCII. It has been estimated that PS II in spinach (chlorophyll *a/b* = 3.5) has a binding site capacity of 18–21 xanthophyll cycle carotenoids Ruban et al., 1999). Measurements indicate

approx. 15 of these are occupied. Under shade conditions it is predicted that occupancy will be lower, and under sun conditions, higher. But, why does the pool size depend upon irradiance in this way? The increased level of zeaxanthin could simply be needed to give the higher level of qE also associated with growth in high light. However, a large pool of zeaxanthin, as in the *aba* mutants of *Arabidopsis* (Hurry et al., 1997) does not seem to confer greater quenching capacity. Rather, it is suggested that increased quenching capacity results from a change in PS II macrostructure that allow a greater number of quenching interactions to take place. Perhaps the important feature is not the larger pool of zeaxanthin per se but the larger amount of violaxanthin — this is needed to stabilize the LHCII system to maintain high quantum yield under limiting light. De-epoxidation then allows deep quenching to be attained, enhancing the dynamic range of light harvesting function.

C. Prospects for Future Research

From the standpoint of this chapter, a complete understanding of regulation of light harvesting will require not only information at atomic resolution about protein structure, but also an elucidation of the key features of the macro-structure of PS II units. Time resolved spectroscopy (Connelly et al., 1997; Gradinaru et al., 1998) and protein crystallography (Kühlbrandt et al., 1994; Rhee et al., 1997) are close to revealing the details of processes occurring within each complex. Vibrational, site-selection and hole burning spectroscopy along with the crystallographic data will be able to describe the specificity of the chlorophyll environment in the quenched state of LHCII and lead to the identification of the quencher. Electron microscopy of carefully prepared 'super complexes' is starting to reveal details of macro-organization (Boekema et al., 1996; 1998; Hankamer et al., 1997). Application of these dual approaches, combined with further development of in vitro systems in which the functional state of LHCII has been selected, promises to finally reveal the mechanism of this key regulatory process. Then it will be possible to definitively interpret the results obtained from a genetic approach in which qE has been eliminated by random mutagenesis (Niyogi et al., 1997a,b; 1998, 1999) or the complement of the LHCII proteins altered by antisense expression (Zhang et al., 1997). In turn, this offers the opportunity of genetic manipulation of crop plants with a view to improving photosynthetic performance.

Acknowledgments

We wish to thank Mark Wentworth for making available the data shown in Figs. 10 and 11. The work described in this article was supported by grants from the UK Biotechnology and Biological Sciences Research Council.

References

Anderson JM, and Osmond CB (1987) Shade-sun responses: Compromises between acclimation and photoinhibition. In: Kuyle DJ, Osmond CB and Arntzen CJ (eds) Photoinhibition pp 1–38, Elsevier Science Publishers, The Hague

Andersson B and Barber J (1996) Mechanisms of photodamage and protein degradation during photoinhibition of Photosystem II. In: Baker NR (ed) Photosynthesis and the Environment, pp 101–121, Kluwer Academic Publishers, Dordrecht

Andersson PO and Gillbro T (1995) Photophysics and dynamics of the lowest excited singlet-state in long substituted polyenes with implications to the very long chain limit. J Chem Phys 103:2509–2519

Andersson PO, Gillbro T, Asato AE and Liu RSH (1992) Dual singlet state emission in a series of mini-carotenes. J Luminescence 51: 11–20

Bassi R, Pineau B, Dainese P and Marquardt J (1993) Carotenoid-binding proteins of Photosystem II. Eur J Biochem 212: 297–303

Beddard GS, Davidson RS and Trethewey KR (1977) Quenching of chlorophyll fluorescence by β-carotene. Nature 267: 373–374.

Bilger W and Björkman O (1994) Relationships among violaxanthin deepoxidation, thylakoid membrane conformation, and nonphotochemical chlorophyll fluorescence quenching in leaves of cotton *Gossypium hirsutum.* L. Planta 193: 238–246

Björkman O and Demmig B (1987) Photon yield of O_2 evolution and chlorophyll fluorescence characteristics at 77 K among plants of diverse origins. Planta 170: 489–504

Björkman O and Demmig-Adams B. (1995) Regulation of Photosynthetic Light Energy Capture, Conversion, and Dissipation in Leaves of Higher Plants. Ecophysiology of Photosynthesis Ecological Studies. Vol 100: 14–47

Björkman O and Niyogi K (1999) Xanthophylls and excess-energy dissipation: A genetic dissection in Arabidopsis. In: Garab G (ed) Photosynthesis: Mechanisms and Effects, Vol III, pp 2085–2090. Kluwer Academic Publishers, Dordrecht

Boekema EJ, Hankamer B, Bald D, Kruip J, Nield J, Boostra AF, Barber J and Rogner M. (1996) Supramolecular organisation of the Photosystem II complex from green plants and cyanobacteria. Proc Nat. Acad Sci USA 92: 175–179

Boekema EJ, van Roon H and Dekker JP (1998) Specific

association of Photosystem II and light harvesting complex II in partially solubilised Photosystem II membranes. FEBS Lett 424: 95–99

Briantais J-M, Vernotte C, Picaud M and Krause GH (1979) A quantitative study of the slow decline of chlorophyll *a* fluorescence in isolated chloroplasts. Biochim Biophys Acta 548: 128–138

Britton G (1995) Structure and properties of carotenoids in relation to function. FASEB J 9: 1551–1558.

Chynwat V and Frank HA (1995) The application of the energy gap law to the S_1 energies and dynamics of carotenoids. Chem Phys 194: 23 7–244.

Connelly JP, Muller, MG, Gatzen G, Mullineaux C, Ruban AV, Horton P and Holzwarth AR (1997) Ultrafast spectroscopy of trimeric light harvesting complex II from higher plants. J Chem Phys 101:1902–1909

Crofts AR and Yerkes CT (1994) A molecular mechanism for qE-quenching. FEBS Lett 352: 265–270

Demmig-Adams B (1990) Carotenoids and photoprotection: a role for the xanthophyll zeaxanthin. Biochim Biophys Acta 1020: 1–24

Demmig-Adams B and Adams III WW (1992) Photoprotection and other responses of plants to high light stress. Annu Rev Plant Physiol Plant Mol Biol 43: 599–626

Demmig-Adams B, Adams III WW, Logan BA and Verhoevan AS (1995a) Xanthophyll cycle-dependent energy dissipation and flexible Photosystem II efficiency in plants acclimated to light stress. Aust J Plant Physiol 22: 249–60

Demmig-Adams B, Gilmore AM and Adams III WW (1995b) Changing views of in vivo functions of carotenoids in higher plants. FASEB J 10:403–412

Egorova-Zachernyuk TA, Raap J, Oschkinat H, Gast P, Frank HA and de Groot, HJM (1996) β-Carotene/chlorophyll a interactions in solution. Abstract. 11th International Symposium on Carotenoids, Leiden

Engleman R and Jortner J (1970) The energy gap law for radiationless transitions in large molecules. Mol Phys 18:145–164.

Falk S, Maxwell DP, Laudenbach DE and Huner NPA (1996) Photosynthetic adjustments to temperature. In: Baker NR (ed) Photosynthesis and the Environment, pp 367–385, Kluwer Academic Publishers, Dordrecht

Frank HA, Cua A, Chynwat V, Young AJ, Goztola D and Wasielewski MR (1994) Photophysics of the carotenoids associated with the xanthophyll cycle in photosynthesis. Photosynth Res 41: 38–395

Frank HA, Cua A, Chynwat V, Young AJ, Zhu J and Blankenship RE (1995) Quenching of chlorophyll excited states by carotenoids. In: Mathis P (ed) Photosynthesis: From Light to Biosphere, Vol IV, pp. 3–7. Kluwer Academic Publishers, Dordrecht

Frank HA, Cua A, Chynwat V, Young AJ, Goztola D and Wasielewski M R (1996) The lifetimes and energies of the first excited singlet states of diadinoxanthin and diatoxanthin: The role of these molecules in excess energy dissipation in algae. Biochim Biophys Acta 1277: 243–252

Frank HA, Chynwat V, Desamero RZB, Farhoosh R, Erickson J and Bautista J (1997) On the photophysics and photochemical properties of carotenoids and their role as light-harvesting pigments in photosynthesis. Pure Appl Chem 69: 2117–2124

Gilmore AM and Björkman O. (1994) Adenine nucleotides and the xanthophyll cycle in leaves II. Comparison of the effects of CO_2- and temperature-limited photosynthesis on Photosystem II fluorescence quenching, the adenylate energy charge and violaxanthin de-epoxidation in cotton. Planta 192: 537–544

Gilmore AM and Yamamoto HY (1992) Linear models relating xanthophylls and lumen acidity to non-photochemical fluorescence quenching. Evidence that antheraxanthin explains zeaxanthin-independent quenching. Photosynth Res 35: 67–78

Gilmore AM and Yamasaki H (1998) 9-aminoacridine and dibucaine exhibit competetive interactions and complicated inhibitory effects that interfere with measurements of ΔpH and xanthophyll cycle-dependent Photosystem II energy dissipation. Photosynth Res 57: 159–174

Gilmore AM, Hazlett TL and Govindjee (1995) Xanthophyll cycle dependent quenching of Photosystem II chlorophyll *a* fluorescence: Formation of a quenching complex with a short lifetime. Proc Nat Acad Sci USA 92: 2273–2277

Gilmore AM, Hazlett TL, Debrunner PG and Govindjee (1996) Photosystem II chlorophyll *a* fluorescence lifetimes and intensity are independent of the antenna size differences between wild type and *chlorina* mutants: Photochemical and xanthophyll cycle-dependent quenching of fluorescence. Photosynth Res 48: 171–187

Gilmore AM, Shinkarev VP, Hazlett TL and Govindjee (1998) Quantitative analysis of the effects of intrathylakoid pH and xanthophyll cycle pigments on chlorophyll *a* fluorescence lifetime distributions and intensity in thylakoids. Biochemistry 37, 13582–13593

Gradinaru CC, Pascal AA, van Mourik F, Robert B, Horton P, van Grondelle H and van Amerongen H (1998) Ultrafast evolution of the excited states in the chlorophyll *a/b* complex CP29 from green plants studied by energy-selective pump-probe spectroscopy. Biochemistry 37: 1143–1149

Hankamer B, Barber J and Boekema EJ (1997) Structure and membrane organisation of Photosystem II in green plants. Annu Rev Plant Physiol Plant Mol Biol 48: 641–671

Heine I and Dau H (1997) The pH-dependence of the Photosystem II fluorescence:co-operative transition to a quenching state. Berichte der Bunsen-Gesellschaft-Physical Chemistry 100: 2008–2013

Horton P (1989) Interactions between electron transport and carbon assimilation: Regulation of light harvesting and photochemistry. In: Briggs W (ed) Photosynthesis, Plant Biology, Vol 9, pp 393–406. A. Liss Inc., New York

Horton P (1996) Nonphotochemical quenching of chlorophyll fluorescence. In: Jennings RC, Zucchelli G, Ghetti F and Colombetti G (eds) Light as an Energy Source and Information Carrier in Plant Physiology, pp 99–111. Plenum Press, New York

Horton P and Ruban AV (1992) Regulation of Photosystem II. Photosynth Res 34: 375–385

Horton P and Ruban AV (1994) The role of LHCII in energy quenching. In: Baker NR and Bowyer JR (eds) Photoinhibition of Photosynthesis—From Molecular Mechanisms to the Field. pp 111–128. Bios Scientific Publishers, Oxford

Horton P, Ruban AV, Rees D, Pascal AA, Noctor G and Young AJ (1991) Control of the light-harvesting function of chloroplast membranes by aggregation of the LHCII chlorophyll-protein

complex. FEBS Lett 292: 1–4

Horton P, Ruban AV and Walters RG (1996): Regulation of light harvesting in green plants. Annu Rev Plant Physiol Plant Mol Biol 47: 65–84

Hurry V, Anderson JM, Chow WS, Osmond CB (1997) Accumulation of zeaxanthin in abscisic acid-deficient mutants of *Arabidopsis* does not affect chlorophyll fluorescence quenching or sensitivity to photoinhibition in vivo. Plant Physiol 113, 639–648

Jahns P and Junge W. (1990) Dicyclohexyl carbodiimide-binding proteins related to the short circuit of the proton pumping activity of Photosystem II. Eur J Biochem 193: 731–736

Jahns P and Krause GH. (1994) Xanthophyll cycle and energy-dependent fluorescence quenching in leaves from pea plants grown under intermittent light. Planta 1922: 176–182

Jansson S (1994) The light harvesting chlorophyll *a/b* binding proteins. Biochim Biophys Acta 1184: 1–19

Krause GH (1988) Photoinhibition of photosynthesis. An evaluation of the damaging and protective mechanisms. Physiol Plant 74: 566–574

Krause GH, Laasch H and Weis E (1988) Regulation of thermal dissipation of absorbed light energy in chloroplasts indicated by energy-dependent fluorescence quenching. Plant Physiol Biochem 26: 445–52

Kühlbrandt W, Wang DN and Fujiyoshi Y (1994) Atomic model of plant light-harvesting complex by electron crystallography. Nature 367: 614–621

Kwa SLS, Vanamerongen H, Lin S, Dekker JP, Van Grondelle R and Struve WS (1992) Ultrafast energy transfer in LHC-II trimers from the Chl *a/b* light-harvesting antenna of photosystem-II. Biochim Biophys Acta 1102: 202–212.

Mo F (1995) X-ray crystallographic studies. In: Britton G, Liaaen-Jensen S and Pfander H (eds) Carotenoids, Vol. 1B. Spectroscopy, pp 321–342. Birkhauser, Basel.

Mullineaux CW, Pascal AA, Horton P and Holzwarth AR (1992) Excitation energy quenching in aggregates of the LHCII chlorophyll-protein complex: a time-resolved fluorescence study. Biochim Biophys Acta. 1141: 23–28

Murakami S and Packer L (1970) Protonation and chloroplast membrane structure. J Cell Biol 47: 332–351

Murchie EH, Chen Y, Hubbart S, Peng S and Horton P (1999) Interactions between senescence and leaf orientation determine in situ patterns of photosynthesis and photoinhibition in field grown rice. Plant Physiol 119: 553–563

Niyogi KK, Björkman O and Grossman AR (1997a) *Chlamydomonas* xanthophyll cycle mutants identified by video imaging of chlorophyll fluorescence quenching. Plant Cell 9: 1369–1380

Niyogi KK, Björkman O and Grossman AR (1997b) The roles of specific xanthophylls in photoprotection. Proc Nat Acad Sci USA 94: 14162–14167

Niyogi KK, Grossman AR and Björkman O(1998) Arabidopsis mutants define a central role for the xanthophyll cycle in the regulation of photosynthetic energy conversion. Plant Cell 10: 1121–1134

Noctor G and Horton P (1990) Uncoupler titration of energy-dependent chlorophyll fluorescence and Photosystem II photochemical yield in intact pea chloroplasts. Biochim Biophys Acta 1016: 228–234

Noctor G, Rees D, Young AJ and Horton P (1991) The relationship between zeaxanthin, energy-dependent quenching of chlorophyll fluorescence and the transthylakoid pH-gradient in isolated chloroplasts. Biochim Biophys Acta 1057: 320–330

Noctor G, Ruban AV and Horton P (1993) Modulation of ΔpH-dependent nonphotochemical quenching of chlorophyll fluorescence in isolated chloroplasts. Biochim Biophys Acta 1183: 339–344

Owens TG, Shreve AP and Albrecht AC (1992) Dynamics and mechanism of singlet energy transfer between carotenoids and chlorophylls: Light harvesting and nonphotochemical fluorescence quenching. In: Murata N (ed) Research in Photosynthesis, Vol 4, pp 179–186. Kluwer Academic Publishers, Dordrecht

Oxborough K and Horton P (1987) Characterisation of the effects of antimycin A upon the high energy state quenching of chlorophyll fluorescence qE in spinach and pea chloroplasts. Photosynth Res 12: 119–128

Park YI, Chow WS and Anderson J (1995) Light inactivation of functional Photosystem II in leaves of peas grown in moderate light depends on photon exposure. Planta 196: 401–411

Pesaresi P, Sandona D, Giuffra E and Bassi R (1997) A single point mutation (E166Q) prevents dicychlohexylcarbodiimide binding to the Photosystem II subunit CP29. FEES Lett 402: 151–156

Peter GF and Thornber P (1991) Biochemical composition and organisation of higher plant Photosystem II light harvesting proteins. J Biol Chem 266: 16745–16754

Phillip D and Young AJ (1995) Occurrence of the carotenoid lactucaxanthin in higher plant LHCII. Photosynth Res 43: 273–282

Phillip D, Ruban AV, Horton P, Asato A and Young AJ (1996) Quenching of chlorophyll fluorescence in the major light harvesting complex of Photosystem II. Proc Nat Acad Sci USA, 93: 1492–1497

Rees D, Young AJ, Noctor G, Britton G and Horton P (1989) Enhancement of the ΔpH-dependent dissipation of excitation energy in spinach chloroplasts by light activation: Correlation with the synthesis of zeaxanthin. FEBS Lett 256: 85–90

Rhee K-H, Morris EP, Zhaleva D, Hankamer B, Kühlbrandt W, and Barber J (1997) Two-dimensional structure of plant Photosystem II at 8 Å resolution. Nature 389: 522–526

Ruban AV and Horton P (1992) Mechanism of ΔpH-dependent dissipation of absorbed excitation energy by photosynthetic membranes I. Spectroscopic analysis of isolated light-harvesting complexes. Biochim Biophys Acta 1102: 30–38

Ruban AV and Horton P (1994) Spectroscopy of non-photochemical and photochemical quenching of chlorophyll fluorescence in leaves; evidence for a role of the light harvesting complex of Photosystem II in the regulation of energy dissipation. Photosynth Res 40: 181–190

Ruban AV, and Horton P (1995) Regulation of non-photochemical quenching of chlorophyll fluorescence in plants. Aust J Plant Physiol 22: 21–30

Ruban AV and Horton P (1998) The xanthophyll cycle modulates the kinetics of nonphotochemical energy dissipation in isolated light harvesting complexes, intact chloroplasts and leaves. Plant Physiol 119: 531–542

Ruban AV, Rees D, Pascal AA and Horton P (1992a) Mechanism of ΔpH-dependent dissipation of absorbed excitation energy by photosynthetic membranes II. The relationships between LHCII aggregation in vitro and qE in isolated thylakoids.

Biochim Biophys Acta 1102: 39–44

Ruban AV, Waiters RG and Horton P (1992b) The molecular mechanism of the control of excitation energy dissipation in chloroplast membranes; inhibition of ΔpH-dependent quenching of chlorophyll fluorescence by dicyclohexylcarbodiimide. FEES Lett. 309: 175–179

Ruban AV, Horton P and Young AJ (1993a) Aggregation of higher plant xanthophylls: Differences in absorption spectra and in the dependency on solvent polarity. J. Photobiol. Photobiochem. B. Biol. 21: 229–234

Ruban AV, Young AJ and Horton P (1993b) Induction on nonphotochemical energy dissipation and absorbance changes in leaves. Evidence for changes in the state of the light harvesting system of Photosystem II in vivo. Plant Physiol 102: 741–750

Ruban AV, Young AJ and Horton P (1994a) Modulation of chlorophyll fluorescence quenching in isolated light harvesting complex of Photosystem II. Biochim Biophys Acta 1186: 123–127

Ruban AV, Young AJ, Pascal AA and Horton P (1994b) The effects of illumination on the xanthophyll composition of the Photosystem II light harvesting complexes of spinach thylakoid membranes. Plant Physiol 104: 227–234

Ruban AV, Dekker JP, Horton P and van Grondelle R. (1995a) Temperature dependence of chlorophyll fluorescence from the light harvesting complex of higher plants. Photochem Photobiol 61: 216–221

Ruban AV, Horton P and Robert B (1995b) Resonance Raman spectroscopy of the Photosystem II light harvesting complex of green plants. A comparison of the trimeric and aggregated states. Biochemistry. 34: 2333–2337

Ruban AV, Young AJ and Horton P (1996) Dynamic properties of the minor chlorophyll *a/b* binding proteins of Photosystem II, an in vitro model for photoprotective energy dissipation in the photosynthetic membrane of green plants. Biochemistry 35: 674–678

Ruban AV, Calkoen F, Kwa SLS, van Grondelle R, Horton P and Dekker JP(1997a) Characterisation of LHCII in the aggregated state by linear and circular dichroism spectroscopy. Biochim Biophys Acta 1321: 61–70

Ruban AV, Philip D, Young AJ and Horton P (1997b) Carotenoid-dependent oligomerisation of the major light harvesting complex of Photosystem II in plants. Biochemistry 36: 7855–7859.

Ruban AV, Pesaresi P, Wacker U, Irrgang K-D, Bassi R and Horton P (1998a) The relationship between the binding of dicyclohexylcarbodiimide and pH-dependent quenching of chlorophyll fluorescence in the light harvesting proteins of Photosystem II. Biochemistry 37: 11586–11591

Ruban AV, Philip D, Young AJ and Horton P (1998b) Excited state energy level does not determine the differential effect of violaxanthin and zeaxanthin on chlorophyll fluorescence quenching in isolated light harvesting complex of Photosystem II. Photochem Photobiol 68: 829–834

Ruban A V, Young AJ and Horton P (1999) Determination of the stoichiometry and strength of binding of xanthophylls to the Photosystem II light harvesting complexes. J Biol Chem, in press

Sandonà D, Croce R, Pagano A, Crimi M and Bassi R (1998) Higher plants light harvesting proteins. Structure and function as revealed by mutation analysis of either protein or chromophore moieties. Biochim Biophys Acta 1365: 207–214

Sarry JE, Montillet JL, Sauvaire Y and Havaux M (1994) The protective function of the xanthophyll cycle in photosynthesis. FEBS Lett 353: 147–150

Schonknecht G, Neimanis S, Gerst U and Heber U. (1996) The pH dependent regulation of photosynthetic electron transport in leaves. In: Mathis P (ed) Photosynthesis: From Light to the Biosphere, pp 843–846. Kluwer Academic Publishers, Dordrecht

Walters RG and Horton P (1993) Theoretical assessment of alternative mechanisms for non-photochemical quenching in barley leaves. Photosynth Res 27: 121–133

Walters RG, Ruban AV and Horton P (1994) Light-harvesting complexes bound by dicyclohexylcarbodiimide during inhibition of protective energy dissipation. Eur J Biochem 226: 1063–1069

Walters RG, Ruban AV and Horton P (1996) Identification of proton-active residues in a higher plant light-harvesting complex. Proc Nat Acad Sci USA 93: 14204–14209

Weis E and Berry J (1987) Quantum efficiency of Photosystem II in relation to energy dependent quenching of chlorophyll fluorescence. Biochim Biophys Acta 894: 198–208

Yerkes CT and Crofts AR (1995) Antimycin inhibits qE quenching by a protonophoric mechanism. In: Mathis P (ed) Photosynthesis: From Light to the Biosphere, Vol III, pp 115–118. Kluwer Academic Publishers, Dordrecht

Young AJ and Frank HA (1996) Energy transfer reactions involving carotenoids: quenching of chlorophyll fluorescence. J Photochem Photobiol 36: 3–15

Young AJ, Phillip D, Frank HA, Ruban AV and Horton P (1997). The xanthophyll cycle and carotenoid mediated dissipation of excess excitation energy in photosynthesis. Pure Appl Chem 69: 2125–2130

Zhang H, Goodman HM and Jansson S (1997) Antisense inhibition of the Photosystem I antenna protein Lhca4 in *Arabidopsis thaliana.* Plant Physiol 115: 1525–1531

This page intentionally left blank

Chapter 16

Biochemistry and Molecular Biology of the Xanthophyll Cycle

Harry Y. Yamamoto, Robert C. Bugos and A. David Hieber
Department of Plant Molecular Physiology, University of Hawaii at Mãnoa, 3190 Maile Way, Honolulu, HI 96822, U.S.A.

Summary

The xanthophyll cycle is the cyclical interconversion of violaxanthin, antheraxanthin and zeaxanthin in plants and green algae. The existence of the cycle has been known for many years but has attracted renewed interest because of its role in protection of plants against the potentially harmful effects of excess light by enhancing the dissipation of excess energy as heat. The cycle is catalyzed by two enzymes that are localized on opposite sides of the thylakoid membrane. The de-epoxidase that converts violaxanthin to zeaxanthin by way of the intermediate, antheraxanthin, is localized in the thylakoid lumen. The epoxidase that catalyzes the resynthesis of violaxanthin is bound to the stromal side of the membrane. The extent and rate of zeaxanthin and antheraxanthin formation (de-epoxidation) are affected by at least four factors, namely, (i) pool size, (ii) availability, (iii) ascorbate, and (iv) lumen pH. The mechanism for de-epoxidation is assumed to be reduction followed by dehydration. Factors affecting the recovery of violaxanthin (epoxidation) include levels of NADPH, ferredoxin, ferredoxin-oxidoreductase and FAD. The mechanism of epoxidation is assumed to be similar to other monooxygenases wherein hydroperoxyflavin is involved and one oxygen atom from molecular oxygen is incorporated. Recently, the cDNAs for both enzymes were isolated and catalytic activities of the expressed proteins demonstrated. Analyses of the deduced polypeptide sequences indicate that both proteins belong to the lipocalin family. The lipocalins are a diverse group of proteins with a conserved barrel structure that bind small hydrophobic molecules. This chapter summarizes the biochemistry of the xanthophyll cycle and examines recent advances in the molecular biology of the cycle.

H. A. Frank, A. J. Young, G. Britton and R. J. Cogdell (eds): The Photochemistry of Carotenoids, pp. 293–303.

I. Introduction

The xanthophyll cycle, also known as the violaxanthin cycle, is present in all higher plants and green algae examined to date. The cycle is also present in brown and some red algae but not blue-green algae. This distribution suggests that the xanthophyll cycle evolved relatively late overall among photosynthetic organisms but early in the evolution of higher plants. The cycle involves de-epoxidation and re-epoxidation reactions that interconvert violaxanthin (V), antheraxanthin (A) and zeaxanthin (Z) (Yamamoto et al., 1962). A similar cycle involving the xanthophylls diadinoxanthin and diatoxanthin (D) is present in *Euglena,* diatoms, and some other algae (Hager and Stransky, 1970). Current interest in the xanthophyll cycle focuses on its role in protecting plants against the potentially damaging effects of excess light, the condition wherein irradiance is higher than can be used photosynthetically. The condition of excess irradiance varies with plant species, degree of light adaptation and other factors such as water stress that can affect photosynthetic capacity. The de-epoxidized pigments (Z and A or D) enable excess energy absorbed by chlorophyll to be harmlessly dissipated as heat.

The mechanism for the dissipation of excess energy by xanthophylls (measured as non-photochemical fluorescence quenching, NPQ) is controversial. There are two prevailing hypotheses. One proposes a direct role for the de-epoxidized xanthophyll formed by the cycle in forming quenching complexes with light-harvesting complexes (Gilmore, 1997). Another proposes an indirect role whereby de-epoxidation enhances formation of aggregated light-harvesting complexes that are highly quenched (Young et al., 1997). The former hypothesis is consistent with the relative energetic levels of the implicated xanthophyll and chlorophylls (Frank et al., 1994) as well as the short lifetime species formed by de-epoxidation (Gilmore et al., 1995,1996). The alternate hypothesis is supported by evidence that violaxanthin has an anti-quenching effect on isolated LHCII in model systems (Noctor et al., 1991; Ruban et al., 1994). Regardless of mechanism, there is general agreement that the xanthophyll cycle provides plants with a means of modulating the dissipation of excess energy. For further discussions on the xanthophyll–cycle mediated NPQ and the xanthophyll cycle itself, readers are referred to Chapter 15 (Horton et al.), Chapter 2 (Della Penna) and Chapter 14 (Demmig-Adams et al.) and a recent review by Eskling et al. (1997). In addition to a role in NPQ, the cycle also has been implicated in stomatal opening (Srivastava and Zieger, 1995). This chapter focuses mainly on the biochemistry and molecular biology of the violaxanthin cycle in higher plants and algae.

Abbreviations: A –antheraxanthin; ABA–abscisic acid; CaMV – cauliflower mosaic virus; D – diatoxanthin; DGDG – digalactosyldiacylglyceride; DTT–dithiothreitol; Elips – early light-induced proteins; FAD–flavin-adenine dinucleotide; 1EF–isoelectric focusing; IML – intermittent light; LHC – light-harvesting complex; LHCI – light-harvesting complex of Photosystem 1; LHCII–light-harvesting complex of Photosystem 11; MGDG – monogalactosyldiacylglyceride; NPQ – non-photochemical quenching; PFD – photon-flux density; V – violaxanthin; VDE–violaxanthin de-epoxidase; Z–zeaxanthin; ZE – zeaxanthin epoxidase

II. Biochemistry

A. De-Epoxidation

The xanthophyll cycle has a long history. Sapozhnikov et al. (1957) observed that violaxanthin levels in leaves responded dynamically to light-dark treatments. Later, Yamamoto et al. (1962) showed that the effect was due to the cyclical pathway involving stoichiometric changes between V, A, and Z now known as the xanthophyll or violaxanthin cycle. The cycle is localized in chloroplasts and organized transmembrane across the thylakoid with de-epoxidation situated on the lumenal side and epoxidation on the stromal side of the membrane (Fig. 1). This organization is concluded based on the biochemical properties of de-epoxidation and epoxidation, especially their pH optima. De-epoxidase activity has a pH optimum of around 5.0 and in chloroplasts is induced under high light conditions that result in acidification of the lumen by the proton pump (Hager, 1969). In contrast, epoxidase activity has a pH optimum of around 7.5 (Hager, 1975; Siefermann and Yamamoto, 1975a). Importantly, it is possible to shift the activity from de-epoxidation to epoxidation while maintaining the ΔpH across the membrane (Gilmore et al., 1994).

Violaxanthin de-epoxidase (VDE) carries out the reaction sequence $V \rightarrow A \rightarrow Z$, the step- wise removal of the 5-6 epoxide presumably by reductive dehydration. The extent of de-epoxidation depends on at least four factors, namely, (i) pigment pool size, (ii) the fraction of violaxanthin in this pool that is

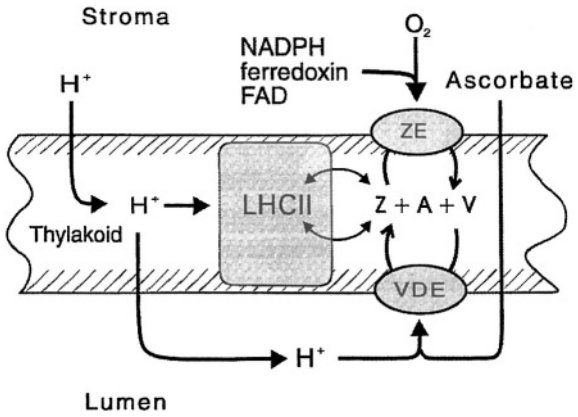

Fig 1. Schematic of the trans-thylakoid organization of the violaxanthin cycle. De-epoxidation (VDE) and epoxidation (ZE) activities are depicted as taking place on free pigments in the lipid phase. The pigments of the xanthophyll cycle (V, A, and Z) are shown as exchanging between the lipid phase and LHCII, under light or temperature stress. It is speculated that carrier proteins may facilitate this exchange. Zeaxanthin in conjunction with the transthylakoid ΔpH leads to NPQ in LHCII. The role of membrane- localized protons in NPQ is controversial.

'available' for de-epoxidation, (iii) induction of a lumen pH, and (iv) the presence of ascorbate. Pool size is the relative concentration of violaxanthin cycle pigments to chlorophyll, reaction centers or thylakoid proteins. Pool size varies depending on species and growth conditions, generally increasing under high light or other imposed stresses that affect photosynthetic activity (Thayer and Björkman, 1990; Bilger et al, 1995; Demmig-Adams and Adams, 1996; Verhoeven et al., 1997). Pool size does not depend directly on the amount of LHCII as demonstrated with intermittent light (IML) grown peas which have only the minor LHCII and lack chlorophyll *b* (Jahns, 1995). Availability is the fraction of the violaxanthin pool that maximally can be de-epoxidized. This fraction varies with species and growth-light conditions (Thayer and Björkman, 1990), ranging from less than 10% to more than 90%, generally increasing with increasing levels of light stress (Demmig-Adams and Adams, 1996). The actual fraction that is de-epoxidized is modulated by light intensity up to the maximum availability (Siefermann and Yamamoto, 1974, 1975b). Availability is also affected by. temperature stress, increasing by decreased (Bilger and Björkman, 1991) or increased temperature (Havaux and Tardy, 1996; Arvidsson et al., 1997). Availability was reported to be nearly 100% in IML-grown plants that have reduced LHC (Jahns, 1995; Härtel et al., 1996; also see Chapter 14, Demmig-Adams et al.).

In thylakoids, the required lumen pH for de-epoxidation is generated by the photosynthetic proton pump. Generally, the lumen acidity required to support de-epoxidation is achieved under conditions where light intensity exceeds photosynthetic capacity, consistent with the concept of excess light. In vitro, the pH optimum for VDE activity shifts to <pH 5.0 at low ascorbate concentrations, apparently because it is the acid form that binds to VDE (Bratt et al., 1995). Ascorbate concentrations are apparently high enough in high-light acclimated plants to support optimal VDE activity (Logan et al., 1996). The ascorbate requirement suggests that the mechanism for de-epoxidation is reduction followed by dehydration; however, direct evidence for this mechanism is lacking. Ascorbate also has an additional function of supporting the required lumen acidification. If limiting photosynthesis defines the condition of excess-light, how is the necessary electron transport for the proton pump supported? A possibility is pseudocylic electron flow mediated by the Mehler-ascorbate-peroxidase reaction. This reaction has been demonstrated to support both de-epoxidation and NPQ (Neubauer and Yamamoto, 1992).

VDE is firmly bound to thylakoids at <pH 6.0. It can be extracted from thylakoids at neutral pH by sonication (Yamamoto and Higashi, 1978) or freeze-thaw (Hager and Holocher, 1994). In vitro, VDE binds at pH 5.2 to monogalactosyldiacylglyceride (MGDG), the principle lipid in thylakoids (Rockholm and Yamamoto, 1993). This property was used to purify VDE to apparent homogeneity and peptide sequences of the purified protein were used to isolate a VDE cDNA (Rockholm and Yamamoto, 1996; Bugos and Yamamoto, 1996). VDE can de-epoxidize other xanthophylls besides violaxanthin and antheraxanthin that have the appropriate stereo configuration (3-hydroxy and 5-6 epoxide in a 3R, 5S, 6R) and are all-*trans* in the polyene chain. Thus, *all-trans* neoxanthin, diadinoxanthin, β-cryptoxanthin epoxide, and lutein epoxide are de-epoxidized but not *9-cis* neoxanthin and *9-cis* violaxanthin or violeoxanthin (Yamamoto and Higashi, 1978). The fact that only all-*trans* pigments are active suggests that the VDE active center is within a narrow cylindrically-shaped cavity. Indeed, as discussed below, the protein structure of VDE inferred from the deduced polypeptide sequence from the cDNA is consistent with this idea.

The activities against the various epoxy-xanth-

ophyll substrates mentioned above were observed in model systems wherein the pigments were incorporated into MGDG micelles (Yamamoto and Higashi, 1978). MGDG is a so-called hexagonal-two phase lipid which does not form bilayers but instead inverse micelles wherein the hydrophobic lipid tails are oriented outward (Williams et al., 1984). Violaxanthin, thus suspended, shows a room-temperature absorbance spectrum typical for this xanthophyll in organic solvent. De-epoxidation of V suspended with MGDG is rapid and complete. In contrast, VDE is inactive against violaxanthin suspended without MGDG or V in detergent-purified LHCII (Yamamoto, Thornber and Lee, unpublished). Moreover, VDE can de-epoxidize violaxanthin that is facing the stroma side of the thylakoid (Arvidsson et al., 1997). These results suggests that, in vivo, VDE acts mainly and possibly exclusively, on violaxanthin that is in the lipid phase of thylakoids. If that is the case, it follows that violaxanthin that is associated with LHCH is in equilibrium with the lipid phase. The availability phenomenon (Siefermann and Yamamoto, 1974) may then reflect the shift in the relative distribution of violaxanthin from protein bound to lipid phase induced by light or temperature stress. The characteristics of the xanthophyll cycle in intermittent-light (IML) grown plants are consistent with this view. Such plants have high levels of violaxanthin and high convertibility to zeaxanthin while having little chlorophyll *a/b*-binding proteins (Jahns, 1995). When IML-grown plants are re-greened, the convertible fraction decreased as antenna proteins increased (Färber and Jahns, 1998). It has also been reported that in the unicelluar green alga *Dunaliella bardawil,* Z is bound to Cbr, a homolog of the early light-induced proteins (Elips) of higher plants, which in turn binds to the minor LHCII's (Levy et al., 1993). In barley *chlorina f2* mutants grown under IML, LHC is not formed but Elips are present as is a considerable amount of violaxanthin (Król et al., *1995).* Thus, LHC is not required for accumulation of xanthophyll-cycle pigments. Nevertheless, light-induced changes in xanthophyll cycle pigments are reflected in the composition of pigment-protein complexes, mainly in the minor LHCII (Bassi et al., 1993). As discussed earlier in this Chapter, IML-grown plants contain only minor LHCII.

Recently, Gruszecki et al. (1997) reported that V is bound to LHCII in the *15-15' cis* configuration and that, in liposomes, light induces the detachment of *15-15' cis V* from LHCII to the lipid phase as all-*trans* violaxanthin. They suggested *cis* to all-*trans* isomerization was a mechanism for the phenomenon of light-induced availability. However, there is contrasting evidence that most violaxanthin in thylakoids is all-*trans.* In isolated chloroplasts, de-epoxidation proceeds in the dark at pH 5 to an equivalent degree as when light induced (Yamamoto et al., 1971). Since *cis* to *trans* isomerization is not expected under dark reaction conditions, these results suggest that violaxanthin is predominantly *all-trans* in thylakoid. Nevertheless, a fraction of the total violaxanthin in LHCII is apparently in the *cis* configuration. According to A. Young (personal communication), in dark-adapted *Hordeum,* violaxanthin is mostly all-*trans* but there is a small amount of *9-cis* present. Subsequent light treatment for two hours induced formation of 13-*cis* violaxanthin with little to no decrease of *9-cis* violaxanthin. These results suggest a light-induced *trans* to *cis* isomerization.

B. Epoxidation

The reverse epoxidation sequence, V ← A ← Z, occurs in the dark or under dim light after induction of de-epoxidation and is slow relative to the forward de-epoxidation. The epoxide is derived from molecular oxygen (Takeguchi and Yamamoto, 1968). Epoxidation is affected by conditions of the requisite initial de-epoxidation as well as the general growth condition or status. Under low actinic light, Z forms initially and thereafter slowly cycles back to starting V levels (Siefermann, 1971; Jahns and Miehe, 1996). This can be understood as due to the activation of CO_2 fixation which results in a decrease of lumen acidity and de-epoxidase activity, thus allowing epoxidase activity to restore V to starting levels. Under excess light, depending on light intensity, various steady-state levels of Z are attained. Complete epoxidation of the Z formed may take several hours or, under some conditions appears inhibited (Adams and Demmig-Adams, 1995).

Preformed zeaxanthin is epoxidized in the presence of NADPH and FAD at around pH 7.5 (Hager, 1975; Siefermann and Yamamoto, 1975a;Büch et al., 1995). Importantly, epoxidase activity continues even in the presence of a light-induced acidified lumen, confirming that the epoxidation system must be on

the stromal-side of the thylakoids and that the xanthophyll cycle is organized transmembrane (Gilmore et al., 1994). Zeaxanthin epoxidase (ZE) has not been isolated directly from plants. Its cDNA was cloned from *Nicotiana plumbaginifolia, Capsicum annuum* and *Lycopersicon esculentum* and the enzyme expressed in *Escherichia coli* (Marin et al., 1996, Bouvier et al., 1996; Burbidge et al., 1997). The availability of the expressed epoxidase has significantly advanced our understanding of its mechanism of action. In addition to NADPH, the presence of ferredoxin and 'ferredoxin-like' reductives are required for activity; bacterial rubredoxin can substitute for plant ferredoxin. ZE epoxidized β-cryptoxanthin, zeaxanthin, antheraxanthin but not β-carotene or α-cryptoxanthin; therefore, the epoxidase is a β-cyclohexenyl monooxygenase (Bouvier et al., 1996). It is noted that the epoxidase activities were carried out in a reaction system that included the major thylakoid lipids MGDG and DGDG (digalactosyldiacylglyceride). The presumed lipid requirement and apparent specificity for 3-hydroxy β-cyclohexenyl ring is similar to violaxanthin de-epoxidase (Yamamoto and Higashi, 1978). We therefore speculate that the epoxidase may also require the *all-trans* configuration in the polyene chain as does the de-epoxidase. Finally, although ZE activity is closely associated with the presence of LHCII (Gruszecki and Krupa, 1993; Härtel et al., 1996; Färber and Jahns, 1998), the deduced protein sequences for ZE show that LHCII is not the epoxidase.

Violaxanthin and neoxanthin are precursors of abscisic acid (ABA)(Parry and Horgan, 1991. Thus, mutants impaired in epoxy carotenoid synthesis accumulate zeaxanthin and display, to varying degrees, classical symptoms of ABA deficiency (Rock and Zeevaart, 1991). The Arabidopsis *aba*-4 mutant accumulates high levels of zeaxanthin and has reduced fluorescence and thylakoid stacking compared to wild-type (Rock et al., 1992). Recently, it was shown that higher zeaxanthin levels in *aba*-mutants do not result in higher levels of NPQ or improved resistance to photoinhibition, suggesting that only a few molecules of zeaxanthin are needed for these effects (Hurry et al., 1997) or that zeaxanthin has no role in these processes (Tardy and Havaux, 1996).

III. Molecular Biology

A. Violaxanthin De-epoxidase

Early attempts to purify VDE from spinach (Hager and Perz, 1970) and lettuce (Yamamoto and Higashi, 1978) chloroplasts resulted in only partially purified fractions. Rockholm and Yamamoto (1993, 1996) added an anion-exchange chromatography step using Mono Q and a novel lipid-affinity precipitation step with MGDG to achieve 15,000-fold purification of VDE from romaine lettuce (*Lactuca, sativa* L. cv. Romaine). This procedure yielded one major polypeptide of about 43 kDa with a pI of 5.4 as observed by two-dimensional IEF/SDS-PAGE. Similarly, spinach VDE was also recently purified over 10,000-fold as compared to thylakoids using a modification of the method of Hager and Perz (1970) with an additional anion exchange chromatography step (Åkerlund et al., 1995, Arvidsson et al., 1996). Although the spinach VDE was not purified to a single major fraction, VDE activity also correlated with a 43 kDa protein. The N-terminus of the spinach VDE was sequenced and was 90% identical to the lettuce VDE N-terminus (Arvidsson et al., 1996; Rockholm and Yamamoto, 1996).

A fragment of the lettuce VDE cDNA was amplified from lettuce cDNA by PCR and used to isolate a near full-length cDNA for lettuce VDE (Bugos and Yamamoto, 1996). The cDNA encoded a polypeptide of 473 amino acids with a calculated molecular mass of 54.4 kDa. This was confirmed from in vitro transcription/translation of the VDE cDNA which produced a 55 kDa polypeptide when analyzed by SDS-PAGE. The deduced preprotein contained a 125 amino acid bipartite transit peptide for transport into the chloroplast and thylakoid lumen. Based on the N-terminal sequence of the purified VDE from lettuce, which indicates the transit peptide cleavage site, the mature VDE protein is encoded by 348 amino acids with a calculated molecular mass of 39.9 kDa, close to the reported molecular mass of 43 kDa for purified VDE from lettuce and spinach. Further verification of the VDE cDNA was accomplished by expression of active VDE in *Escherichia coli* and demonstrating that the addition of DTT, a strong inhibitor of VDE activity (Yamamoto and Kamite, 1972), abolished all activity (Bugos and Yamamoto, 1996). Analysis of the reaction products of de-epoxidation by the *E. coli* expressed VDE

showed the presence of both antheraxanthin and zeaxanthin demonstrating unequivocal evidence that the same enzyme catalyzes both steps in the de-epoxidation reaction.

The lettuce cDNA was used as a probe to isolate VDE cDNAs from tobacco and *Arabidopsis* (Bugos et al., 1998). A database search has revealed that the VDE gene is located on chromosome 1 in *Arabidopsis,* adjacent to the *KNOLLE* gene (Lukowitz et al., 1996). Sequence alignments of the mature VDE proteins indicate high conservation among dicotyledonous plants and the sequences share roughly 90% similarity and 82% identity. In the mature proteins only nine amino acid positions have different amino acids in all three proteins. All three VDE proteins share three characteristic domains: a) a cysteine-rich domain, b) a lipocalin signature and c) a highly charged domain (Fig. 2A) (Bugos and Yamamoto, 1996). In the first domain 11 of the total 13 cysteines are localized in this region which may be a putative site for inhibition by DTT. All 13 of these cysteines are invariant in the three VDE sequences. The second domain, a lipocalin signature, is a motif identified in a number of proteins (referred to as the lipocalin family) that bind small hydrophobic molecules (Pervaiz and Brew, 1987; Flower, 1996). Three-dimensional crystal structures for a number of the lipocalin proteins exhibit a highly conserved folding pattern consisting of a single eight-stranded β-sheet that forms a continuously hydrogen bonded barrel (Flower, 1996). This suggests that the VDE protein may have a β-barrel type structure in which the xanthophyll pigment is inserted and the de-epoxidation reaction is catalyzed at the bottom of the barrel. Interestingly, a well-like structure for VDE was speculated nearly two decades earlier for the active site of VDE (Yamamoto and Higashi, 1978). Pigments in the *all-trans* form were de-epoxidized whereas no de-epoxidation was observed with pigments in the 9- *cis* configuration, suggesting that steric hindrance of the *9-cis* forms may prevent the pigment from reaching the active site at the bottom of the well. The third domain is a highly charged region that contains a high concentration of glutamic acid residues. It was proposed that partial protonation of these residues possibly increases binding to the thylakoid membrane.

The VDE mRNA transcript level was analyzed in market romaine lettuce by northern hybridization. The younger leaf tissues (yellow leaves and rapidly expanding green leaves) had low levels of transcript present (Bugos and Yamamoto, 1996). Since there was some transcript detected in the immature yellow leaves, this may suggest there is some constitutive level of expression of VDE in tissue having no developed chloroplasts. In support of this finding, VDE activity was detected in etiolated bean *(Phaseolus vulgaris* L. van Commodore) leaves, a tissue lacking an active photosynthetic apparatus (Pfündel and Strasser, 1988). Greater levels of VDE mRNA were detected in mature green leaf tissue. This increased level of transcript may suggest higher expression in tissues with a higher density of fully developed chloroplasts or regulation by light intensity since the mature outer leaves of lettuce receive a higher light intensity than the inner younger leaves.

To assess the impact of a reduced level of VDE in a plant species, an antisense construct was prepared using the tobacco VDE cDNA under the control of the CaMV 35S promoter and integrated into the tobacco *(Nicotiana tabacum* cv. Xanthi) genome by *Agrobacterium*-mediated transformation (Bugos, Chang and Yamamoto, unpublished). A total of 40 transgenic plants were grown in a shaded greenhouse in which light intensity was never greater than 300 μmoles photons m^{-2} sec^{-1}. The plants were screened by illuminating leaf discs from dark-adapted leaves with 1800 μmoles photons m^{-2} sec^{-1} white light for 20 min and the pigments were analyzed and quantified by HPLC (Gilmore and Yamamoto, 1991) to determine the level of de- epoxidation. A total of 18 plants had various levels of inhibition of de-epoxidation with two plants having more than a 90% reduction in de-epoxidation. Seeds were collected from these plants, germinated under antibiotic selection and grown under controlled conditions in a growth chamber with a light intensity of 350 μmoles photons m^{-2} sec^{-1}. No phenotypic differences were observed with the transgenic plants as compared to wild-type tobacco. The plants were analyzed by measuring VDE specific activity in a leaf where the peak VDE activity is known to occur. The specific activity of VDE varied greatly among the plants giving a wide range of values with the best antisense plants having VDE reduced by over 95%. Currently, the tobacco plants having the most reduced levels of VDE are being grown both in a growth chamber and under field conditions to determine what impact the reduced level of enzyme will have on NPQ, photosynthesis, adaptation to increased light intensity and plant growth.

A novel approach using digital video imaging of

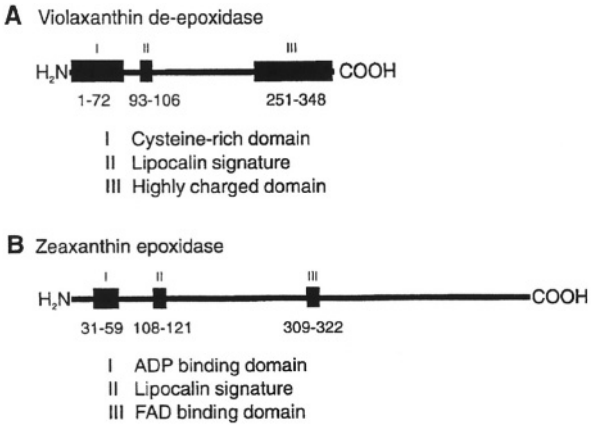

Fig 2. Schematic illustrating domains identified within the coding sequence of the deduced amino acid sequences for violaxanthin de-epoxidase and zeaxanthin epoxidase. (A) Violaxanthin de-epoxidase from *Lactuca sativa* (Bugos and Yamamoto, 1996). (B) Zeaxanthin epoxidase from *Nicotiana plumbaginifolia* (Marin et al., 1996). The domains for each sequence are illustrated (I-III) with the amino acid sequence spanning regions indicated below. The amino acid numbering is from the N-terminus of the mature protein.

chlorophyll fluorescence was developed to isolate nonphotochemical fluorescence quenching (NPQ) mutants in *Chlamydomonas reinhardtii* (Niyogi et al., 1997a). Approximately 15,000 mutagenized colonies were screened with the video imaging system under high-light conditions (1200 μmoles photons m^{-2} sec^{-1}) to induce NPQ. Mutants defective in NPQ were recovered at a frequency of approximately 1% and secondary screening using pigment analysis identified two mutants defective in the xanthophyll cycle; the *npq1* mutant was unable to de-epoxidize violaxanthin whereas the *npq2* mutant was unable to epoxidize zeaxanthin. Chlorophyll fluorescence analysis demonstrated that the *npq1* mutant had only 20% less NPQ than wild-type cells. In addition, photoautotrophic growth of the *npq1* mutant under light conditions of 100 and 500 μmoles photons m^{-2} sec^{-1} showed no difference relative to wild-type cells. Under these conditions, de-epoxidation of violaxanthin was not required for survival of *Chlamydomonas.* This suggests that in addition to A and Z dependent NPQ, other processes are involved in the dissipation of excess light energy in *Chlamydomonas.*

To further analyze the effect of impaired pigment synthesis in *Chlamydomonas,* a double mutant was prepared by crossing *npq1* with *lor1,* a *Chlamydomonas* mutant defective in the synthesis of α-carotene, lutein and loroxanthin (Niyogi et al., 1997b). This double mutant exhibited almost no reversible NPQ on exposure to high light (1160 μmoles photons m^{-2} sec^{-1}). Growth of the *npq1 lor1* double mutant at low light (50 μmoles photons m^{-2} sec^{-1}) was similar to wild-type cells; however, growth at high light (500 μmoles photons m^{-2} sec^{-1}) was reduced and the cells rapidly bleached as compared to wild-type cells. The *npq1* and *lor1* single mutants grew relatively normal under both light conditions. These results suggest that in *Chlamydomonas* lutein or other protective factors may contribute to the dissipation of excess light energy and photoprotection.

B. Zeaxanthin Epoxidase

The isolation of the cDNA encoding a zeaxanthin epoxidase (ZE) was first identified from *Nicotiana plumbaginifolia* as a gene involved in ABA biosynthesis. Using insertional mutagenesis with the maize *Activator* (*Ac*) element, a mutant exhibiting precocious seed germination and a severe wilty phenotype, characteristic of *aba* mutants, was isolated (Marin et al. 1996). In plants the synthesis of ABA involves carotenoid precursors including zeaxanthin, violaxanthin and neoxanthin (Parry and Morgan, 1991). The carotenoid content of the mutant and wild-type plants was analyzed by HPLC to determine at what step the ABA biosynthetic pathway was impaired. It was found that zeaxanthin content accumulated in the mutant but not in the wild-type leaves. In addition, violaxanthin and neoxanthin were not detected in mutant leaves. Therefore, it was concluded that the mutant was impaired in the epoxidation of zeaxanthin. DNA sequence information from the regions flanking the *Ac* insertion site was then used to screen a cDNA library and a gene encoding a chloroplast imported protein was isolated and subsequently identified to be a zeaxanthin epoxidase.

The cDNA from *N. plumbaginifolia* was used to isolate cDNAs encoding ZE from pepper *(Capsicum annuum* L. cv. Yolo Wonder) and from a wilt-related tomato *(Lycopersicon esculentum* Mill.) (Bouvier et al., 1996, Burbidge et al., 1997). All three are members of the Solanaceae family. The *N. plumbaginifolia* ZE encodes a polypeptide of 663 amino acids with a mature protein estimated at 613 amino acids. As already noted, unlike the de-epoxidase, the native epoxidase has not been purified and therefore, the N-terminal amino acid has not been identified directly. The proposed N-terminal amino acid is based on a

possible chloroplast processing site. In vitro transcription/translation products of the ZE cDNA were used to verify localization of ZE in the chloroplast and showed a processed molecular weight of 67 kDa, supporting that estimated from sequence analysis (Marin et al., 1996). The predicted amino acid sequence of ZE from *N. plumbaginifolia* has 88% and 90% identity with amino acid sequences of ZE from pepper and tomato, respectively.

A number of domains have been identified in the derived amino acid sequence. The ZE sequences contain a consensus sequence known to be involved in ADP binding (amino acids 31–59) (Fig 2B). ZE also contains a FAD binding domain (amino acids 309–322) which was also identified in squalene epoxidases from yeast and rat (Jandrositz et al., 1991; Sakakibara et al., 1995). FAD was previously demonstrated to enhance ZE activity (Büch et al., 1995). Detailed analysis of the sequence reveals the presence of a lipocalin motif (amino acids 108–121) (Bugos et al., 1998). This motif was also described for the violaxanthin de-epoxidase. Apart from this motif, which would imply a similar tertiary structure, there are no other common sequences between the two proteins. It is realistic to consider that the de-epoxidase and the epoxidase enzymes might have the same basic tertiary structure considering that they both function on the same molecule (antheraxanthin). Sequence analysis of the pepper ZE cDNA also showed that it contained possible PEST domains, conserved regions identified in rapidly degraded proteins (Rogers et al., 1986).

The only other sequence for a ZE, not from the Solanaceae family, is a partial sequence from an expressed sequence tag in *Arabidopsis* (accession number T45502) (Newman et al., 1994). Identified by sequence homology it has a predicted open reading frame of 79 amino acids and displayed 64% identity with the *N. plumbaginifolia* and tomato deduced polypeptide sequences and 50% identity with the pepper polypeptide. Based on this homology, further experiments showed the T45502 sequence to be mapped to a region on chromosome 5 in *Arabidopsis.* This position correlated with the previously reported locus for an ABA-deficient wilty mutant of *Arabidopsis* (*aba1*) (Koornneef et al., 1982). The *aba* mutants were shown to be impaired in the epoxidation of zeaxanthin (Rock and Zeevaart, 1991). Complementation experiments not only demonstrated that the *N. plumbaginifolia* ZE cDNA could restore a normal phenotype to the original *Nicotiana* mutant (*aba 2*) but also that the ZE cDNA could restore the wild type phenotype in the *Arabidopsis aba1-1* mutant (Marin et al., 1996).

Although the native ZE protein has not been purified, there is growing evidence supporting the cloned ZE as the epoxidase of both the xanthophyll cycle and the ABA biosynthetic pathway. This includes some preliminary data demonstrating the upregulation of ZE mRNA in pepper seedlings subjected to photooxidative stress either through use of carotenoid inhibitors or the use of photooxidative stress-inducing herbicides (Bouvier et al., 1996). Interestingly, an *Arabidopsis* mutant *(npq2)* specifically isolated to be defective in the xanthophyll cycle showed no epoxidation of Z, exhibited the same phenotype as the Arabidopsis *aba1* mutants and failed to complement the *Arabidopsis aba1* mutation (K. Niyogi, personnel communication). This independent evidence, together with the previously described complementation of the *Arabidopsis aba1* mutation with the ZE cDNA from *N. plumbaginifolia,* support this gene as being the epoxidase both for the xanthophyll cycle and ABA biosynthesis.

Acknowledgments

We thank W. Adams, B. Demmig-Adams, P. Jahns, K. Niyogi and A. Young for advance copies of their work. This work was supported in part by USDA Research Initiative Competitive Grant No. 97-35100-4851 and U. S. Department of Energy Grant No. DE-FG03-92-ER20078.

References

Adams WW III and Demmig-Adams B (1995) The xanthophyll cycle and sustained thermal energy dissipation activity in *Vinca minor* and *Euonymus kiautschovicus* in winter. Plant Cell Environ 18: 117–127

Åkerlund H-E, Arvidsson P-O, Bratt CE and Carlsson M (1995) Partial purification of the violaxanthin de-epoxidase. In: Mathis P (ed) Photosynthesis From Light to Biosphere, Vol. IV, pp 103–106. Kluwer Academic Publishers, Dordrecht

Arvidsson P-O, Bratt CE, Carlsson M and Åkerlund H-E (1996) Purification and identification of the violaxanthin de-epoxidase as a 43 kDa protein. Photosynth Res 49: 119–129

Arvidsson P-O, Carlsson M, Stefánsson H, Albertsson P-Å and Åkerlund H-E (1997) Violaxanthin accessibility and temperature dependency for de-epoxidation in spinach thylakoid membranes. Photosynth Res 52: 39–48

Bassi R, Pineau B, Dainese P and Marquardt J (1993) Carotenoid-

binding proteins of Photosystem II. Eur J Biochem 212: 297–303

Bilger W and Björkman O (1991) Temperature dependence of violaxanthin de-epoxidation and non-photochemical fluorescence quenching in intact leaves of *Gossypium hirsutum* L. and *Malva parviflora* L. Planta 184:226–234

Bilger W, Fisahn J, Brummet W, Kossmann J and Willmitzer L (1995) Violaxanthin cycle pigment contents in potato and tobacco plants with genetically reduced photosynthetic capacity. Plant Physiol 108:1479–1486

Bouvier F, d'Harlingue A, Hugueney P, Marin E, Marion-Poll A and Camara B (1996) Xanthophyll biosynthesis: Cloning, expression, functional reconstitution, and regulation of β-cyclohexenyl carotenoid epoxidase from pepper (*Capsicum annuum*). J Biol Chem 271: 28861– 28867

Bratt CE, Arvidsson P-O, Carlsson M and Åkerlund H-E (1995) Regulation of violaxanthin de-epoxidase activity by pH and ascorbate concentration. Photosynth Res 45: 169–175

Büch K, Stransky H and Hager A (1995) FAD is a further essential cofactor of the NAD(P)H and O2-dependent zeaxanthin-epoxidase. FEBS Lett 376: 45–48

Bugos RC and Yamamoto HY (1996) Molecular cloning of violaxanthin de-epoxidase from romaine lettuce and expression in *Escherichia coli.* Proc Natl Acad Sci USA 93: 6320–6325

Bugos RC, Hieber AD and Yamamoto HY (1998) Xanthophyll-cycle enzymes are members of the lipocalin family, the first identified from plants. J Biol Chem 273: 15321–15324

Burbidge A, Grieve T, Terry C, Corlett J, Thompson A and Taylor 1 (1997) Structure and expression of a cDNA encoding zeaxanthin epoxidase, isolated from a wilt-related tomato (*Lycopersicon esculentum* Mill.) library. J Exp Bot 48: 1749–1750

Demmig-Adams B and Adams WW III (1996) The role of Xanthophyll cycle carotenoids in the protection of photosynthesis. Trends Plant Sci 1: 21–26

Eskling M, Arvidsson P-O and Åkerlund H-E (1997) The xanthophyll cycle, its regulation and components. Physiol Plant 100: 806–816

Färber A and Jahns P (1998) The xanthophyll cycle of higher plants: Influence of antenna size and membrane organization. Biochim Biophys Acta 1363:47–58

Flower, DR (1996) The lipocalin protein family: Structure and function. Biochem J 318: 1–14

Frank HA, Cua A, Chynwat V, Young A, Gosztola D and Wasielewski MR (1994) Photophysics of the carotenoids associated with the xanthophyll cycle in photosynthesis. Photosyn Res 41: 389–395

Gilmore AM (1997) Mechanistic aspects of xanthophyll cycle-dependent photoprotection in higher plant chloroplasts and leaves. Physiol Plant 99: 197–209

Gilmore AM and Yamamoto HY (1991) Resolution of lutein and zeaxanthin using a non- endcapped, lightly carbon-loaded C_{18} high-performance liquid chromatographic column. J Chromatogr 543: 137–145

Gilmore AM, MohantyN and Yamamoto HY (1994)Epoxidation of zeaxanthin and antheraxanthin reverses non-photochemical quenching of photosystem II chlorophyll *a* fluorescence in the presence of trans-thylakoid ΔpH. FEBS Lett 350: 271 –274

Gilmore AM, Hazlett TL and Govindjee (1995) Xanthophyll cycle-dependent quenching of Photosystem II chlorophyll *a* fluorescence: Formation of a quenching complex with a short fluorescence lifetime. Proc Natl Acad Sci USA 92:2273–2277

Gilmore AM, Hazlett TL, DebrunnerPG and Govindjee (1996) Photosystem II chlorophyll *a* fluorescence lifetimes and intensity are independent of the antenna size differences between barley wild-type and *chlorina* mutants: Photochemical quenching and xanthophyll cycle-dependent nonphotochemical quenching of fluorescence. Photosynth Res 48:171–187

Gruszecki WI and Krupa Z (1993) LHCII, the major light-harvesting pigment-protein complex, is a zeaxanthin epoxidase. Biochim Biophys Acta 1144: 97–101

Gruszecki WI, Matula M, Ko-Chi N, Koyama Y and Krupa Z (1997) *Cis-trans*-isomerization of violaxanthin in LHC II: Violaxanthin isomerization cycle within the violaxanthin cycle. Biochim Biophys Acta 1319: 267–274

Hager A (1969) Lichtbedingte pH-erniedrigung in einem chloroplasten-kompartiment als ursache der enzymatischen violaxanthin → zeaxanthin-umwandlung; beziehungen zur photophosphorylierung. Planta 89: 224–243

Hager A (1975) Die reversiblen, lichtabhängigen xanthophyllumwandlungen im chloroplasten. Ber Deutsch Bot Ges Bd 88: 27–44

Hager A and Holocher K (1994) Localization of the xanthophyll-cycle enzyme violaxanthin de-epoxidase within the thylakoid lumen and abolition of its mobility by a (light-dependent) pH decrease. Planta 192: 581–589

Hager A and Perz H (1970) Veränderung der lichtabsorption eines carotinoids im enzym (de-epoxidase)-substrat (violaxanthin)-komplex. Planta 93: 314–322

Hager A and Stransky H (1970) Das carotinoidmuster und die verbreitung des lichtinduzierten xanthophyll-cyclus in verschiedenen algenklassen V. Einzelne vertreter der Cryptophyceae, Euglenophyceae, Bacillariophyceae, Chrysophyceae und Phaeophyceae. Archiv Mikrobiol 73: 77–89

Härtel H, Lokstein H, Grimm B and Rank B (1996) Kinetic studies on the xanthophyll cycle in barley leaves: Influence of antenna size and relations to nonphotochemical chlorophyll fluorescence quenching. Plant Physiol 110: 471–482

Havaux M and Tardy F (1996) Temperature-dependent adjustment of the thermal stability of Photosystem II in vivo: Possible involvement of xanthophyll-cycle pigments. Planta 198:324–333

Hurry V, Anderson JM, Chow WS and Osmond CB (1997) Accumulation of zeaxanthin in abscisic acid-deficient mutants of *Arabidopsis* does not affect chlorophyll fluorescence quenching or sensitivity to photoinhibition in vivo. Plant Physiol 113: 639–648

Jahns P (1995) The xanthophyll cycle in intermittent light-grown pea plants: Possible functions of chlorophyll *a/b*-binding proteins. Plant Physiol 108: 149–156

Jahns P and Miehe B (1996) Kinetic correlation of recovery from photoinhibition and zeaxanthin epoxidation. Planta 198: 202–210

Jandrositz A, Turnowsky F and Högenauer G (1991) The gene encoding squalene epoxidase from *Saccharomyces cerevisiae:* cloning and characterization. Gene 107: 155–160

Koornneef M, Jorna ML, Brinkhorst-van der Swan DLC and Karssen CM (1982) The isolation of abscisic acid (ABA) deficient mutants by selection of induced revertants in non-germinating gibberellin sensitive lines of *Arabidopsis thaliana* (L.) Heynh. Theor Appl Genet 61: 385–393

Król M, Sprangfort MD, Huner NPA, Öquist G, Gustafsson P

and Jansson S(1995)Chlorophyll *a/b*-bindingproteins,pigment conversions, and early light-induced proteins in a chlorophyll *b*-less barley mutant. Plant Physiol 107: 873–883

Levy H, Tamar T, Shaish A and Zamir A (1993) Cbr, an algal homolog of plant early light-induced proteins, is a putative zeaxanthin binding protein. J Biol Chem 268: 20892–20896

Logan BA, Barker DH, Demmig-Adams B and Adams WW III (1996) Acclimation of leaf carotenoid composition and ascorbate levels to gradients in the light environment within an Australian rain forest. Plant Cell Environ 19: 1083–1090

Lukowitz W, Mayer U and Jürgens G (1996) Cytokinesis in the *Arabidopsis* embryo involves the syntaxin-related *KNOLLE* gene product. Cell 84: 61–71

Marin E, Nussaume L, Quesada A, Gonneau M, Sotta B, Hugueney P, Frey A and Marion-Poll A (1996) Molecular identification of zeaxanthin epoxidase of *Nicotiana plumbaginifolia,* a gene involved in abscisic acid biosynthesis and corresponding to the *ABA* locus of *Arabidopsis thaliana.* EMBO J 15: 2331–2342

Neubauer C and Yamamoto HY (1992) Mehler-peroxidase reaction mediates zeaxanthin formation and zeaxanthin-related fluorescence quenching in intact chloroplasts. Plant Physiol 99:1354–1361

Newman T, de Bruijn FJ, Green P, Keegstra K, Kende H, McIntosh L, Ohlrogge J, Raikhel N, Somerville S, Thomashow M, Retzel E and Somerville C (1994) Genes galore: A summary of methods for accessing results from large-scale partial sequencing of anonymous *Arabidopsis* cDNA clones. Plant Physiol 106: 1241–1255

Niyogi KK, Björkman O and Grossman AR (1997a) *Chlamydomonas* xanthophyll cycle mutants identified by video imaging of chlorophyll fluorescence quenching. Plant Cell 9: 1369–1380

Niyogi KK, Björkman O and Grossman AR (1997b) The roles of specific xanthophylls in photoprotection. Proc Natl Acad Sci USA 94: 14162–14167

Noctor G, Rees D, Young A and Horton P (1991) The relationship between zeaxanthin, energy-dependent quenching of chlorophyll fluorescence, and trans-thylakoid pH gradient in isolated chloroplasts. Biochim Biophys Acta 1057: 320–330

Parry AD and Horgan R (1991) Carotenoids and abscisic acid (ABA) biosynthesis in higher plants. Physiol Plant 82: 320–326

Pervaiz S and Brew K (1987) Homology and structure-function correlations between α_1-acid glycoprotein and serum retinol-binding protein and its relatives. FASEB J 1: 209–214

Pfündel E and Strasser RJ (1988) Violaxanthin de-epoxidase in etiolated leaves. Photosynth Res 15: 67–73

Rock CD and Zeevaart JAD (1991) The *aba* mutant of *Arabidopsis thaliana* is impaired in epoxy-carotenoid biosynthesis. Proc Natl Acad Sci USA 88: 7496–7499

Rock CD, Bowlby NR, Hoffmann-Bennig S and Zeevaart JAD (1992) The *aba* mutant of *Arabidopsis thaliana* (L.) Heynh. has reduced chlorophyll fluorescence yields and reduced thylakoid stacking. Plant Physiol 100: 1796–1801

Rockholm DC and Yamamoto HY (1993) Purification of violaxanthin de-epoxidase by lipid affinity precipitation. In: Yamamoto HY and Smith CM (eds) Photosynthetic Responses to the Environment, p 237. American Society of Plant Physiologists, Rockville

Rockholm DC and Yamamoto HY (1996) Violaxanthin de-epoxidase: Purification of a 43-kilodalton lumenal protein from lettuce by lipid-affinity precipitation with mono-galactosyldiacylglyceride. Plant Physiol 110: 697–703

Rogers S, Wells R and Rechsteiner M (1986) Amino acid sequences common to rapidly degraded proteins: The PEST hypothesis. Science 234: 364–368

Ruban AV, Young A and Horton P (1994) Modulation of chlorophyll fluorescence quenching in isolated light harvesting complex of Photosystem II. Biochim Biophys Acta 1186: 123–127

Sakakibara J, Watanabe R, Kanai Y and Ono T (1995) Molecular cloning and expression of rat squalene epoxidase. J Biol Chem 270:17–20

Sapozhnikov DI, Krasovskaya TA and Maevskaya AN (1957) Change in the interrelationship of the basic carotenoids of the plastids of green leaves under the action of light. Dokl Akad Nauk 113:465–467

Siefermann D (1971) Kinetic studies on the xanthophyll cycle of *Lenma gibba* L.—influence of photosynthetic oxygen and supplied reductor. In: Forti G, Avron M and Melandri A (eds) Proceedings IInd International Congress on Photosynthesis Research, pp 629–635. Dr. W Junk N.V. Publishers, The Hague

Siefermann D and Yamamoto HY (1974) Light-induced de-epoxidation of violaxanthin in lettuce chloroplasts. III. Reaction kinetics and effect of light intensity on de-epoxidase activity and substrate availability. Biochim Biophys Acta 357: 144–150

Siefermann D and Yamamoto HY (1975a) Properties ofNADPH and oxygen-dependent zeaxanthin epoxidation in isolated chloroplasts. Arch Biochem Biophys 171: 70–77

Siefermann D and Yamamoto HY (1975b) Light-induced de-epoxidation of violaxanthin in lettuce chloroplasts. IV. The effects of electron-transport conditions on violaxanthin availability. Biochim Biophys Acta 387: 149–158

Srivastava A and Zeiger E (1995)The inhibitor of zeaxanthin formation, dithiothreitol, inhibits blue-light-stimulated stomatal opening in *Vicia faba.* Planta 196: 445-449

Takeguchi CA and Yamamoto HY (1968) Light-induced $^{18}O_2$ uptake by epoxy xanthophylls in New Zealand spinach leaves (*Tetragonia expansa*). Biochim Biophys Acta 153: 459–465

Tardy F and Havaux M (1996) Photosynthesis, chlorophyll fluorescence, light-harvesting system and photoinhibition resistance of a zeaxanthin-accumulating mutant of *Arabidopsis thaliana* . J Photochem Photobiol B: Biol 34: 87–94

Thayer SS and Björkman O (1990) Leaf xanthophyll content and composition in sun and shade determined by HPLC. Photosynth Res 23: 331–343

Verhoeven AS, Demmig-Adams B and Adams WW III (1997) Enhanced employment of the xanthophyll cycle and thermal energy dissipation in spinach exposed to high light and N stress. Plant Physiol 113: 817–824

Williams WP, Gounaris K and Quinn PJ (1984) Lipid-protein interactions in the thylakoid membranes of higher plant chloroplasts. Adv Photosyn Res 3: 123–130

Yamamoto HY and Higashi RM (1978) Violaxanthin de-epoxidase. Lipid composition and substrate specificity. Arch Biochem Biophys 190: 514–522

Yamamoto HY, Kamite L and Wang YY (1971) An ascorbate-induced absorbance change in chloroplasts from violaxanthin de-epoxidation. Plant Physiol 49: 224–228

Yamamoto H Y and Kamite L (1972) The effects of dithiothreitol on violaxanthin de-epoxidation and absorbance changes in the 500 nm region. Biochim Biophys Acta 267: 538–543

Yamamoto HY, Nakayama TOM and Chichester CO (1962) Studies on the light and dark interconversions of leaf xanthophylls. Arch Biochem Biophys 97: 168–173

Young AJ, Phillip D, Ruban AV, Horton P and Frank HA (1997) The xanthophyll cycle and carotenoid-mediated dissipation of excess excitation energy in photosynthesis. Pure Appl Chem 69:2125–2130

This page intentionally left blank

Chapter 17

Relationships Between Antioxidant Metabolism and Carotenoids in the Regulation of Photosynthesis

Christine H. Foyer
Department of Biochemistry and Physiology, Institute of Arable Crops Research (IACR), Rothamsted, Harpenden, Herts AL5 2JQ, U.K.

Jeremy Harbinson
ATO/DLO, Bornsesteeg 59, Postbus 17, NL-6700 AA Wageningen, The Netherlands

Summary

The large driving forces produced in photosynthesis require precise control and regulation to prevent potentially destructive side reactions involving active oxygen species that damage pigments and proteins. Oxygen can be activated either by energy transfer, yielding singlet oxygen, or by reduction, yielding superoxide or hydrogen peroxide. At Photosystem I, the lifetime of the excited chlorophyll singlet state within the antenna pigment bed is short and little threat is posed by formation of highly reactive singlet oxygen. The situation is completely different in Photosystem II. Here, the lifetime of singlet chlorophyll is sufficiently long to allow significant formation of chlorophyll triplet states able to transfer energy to ground state triplet oxygen, generating singlet oxygen. Carotenoids intervene to control these processes in at least two important ways. First, pigments such as β-carotene are capable of directly quenching both triplet chlorophyll and singlet oxygen states (the so-called triplet valve mechanism). Second, the xanthophyll cycle is involved in lowering the yield of triplet chlorophyll formation by pre-emptive quenching of excited singlet state chlorophyll, a mechanism that can have a high quantum yield value for energy dissipation. The chief difference between these two mechanisms is that the xanthophyll cycle is inducible and subject to regulation, whereas the triplet valve pathway is constitutive and unregulated. Although formation of singlet oxygen must be avoided or controlled, chloroplasts

H. A. Frank, A. J. Young, G. Britton and R. J. Cogdell (eds): The Photochemistry of Carotenoids, pp. 305–325.

have exploited the potential of oxygen chemistry to drive and regulate metabolism while minimizing the deleterious effects of uncontrolled interactions with oxygen. Hence, while the potential of the chloroplast as a source of oxidative stress is large, in reality this organelle offers minimal risk because of pre-emptive regulation and effective defense. The production of superoxide and hydrogen peroxide by the thylakoid membranes is limited by efficient control of electron transport. This regulation limits the potential for oxidative damage and prevents high rates of electron transport to oxygen. Effective antioxidant defense ensrures rapid elimination of active forms of oxygen further preventing oxidative damage.

I. Introduction

In this chapter we explore the role of carotenoids in photosynthesis. An important aspect of this description is the role of the thermodynamic (or kinetic) driving forces generated within the photosynthetic machinery. The severity of stresses associated with photosynthesis is determined by the responses, within genetically determined limits, of photosynthetic driving forces to environmental factors such as irradiance or temperature, acting independently or (more commonly) in concert. Of these stresses, the best known are those associated with formation of the active oxygen species (AOS) superoxide and singlet molecular oxygen by PS I and PS II, respectively.

The presence of photodynamic pigments in the thylakoid membranes commits the chloroplast to light absorption. The energy of the absorbed radiation is then used to oxidize water and produce the NADPH required to reduce CO_2 to the level of sugar phosphate. Intrinsic to this process is the generation of a transmembrane proton potential difference that not only produces the ATP needed for CO_2 assimilation but also regulates the flux of electrons. Prior to the evolution of the cyanobacteria, the earth's atmosphere contained very low concentrations of oxygen (Berkner and Marshall, 1965). The evolution of organisms able to perform hydrolytic photosynthesis meant that energy contained within a weak yet abundant reductant, water, could be used to drive anabolic reactions. It also entailed the development of biological systems able not only to cope with life in high oxygen tensions, but also to exploit the metabolic and physiological opportunities of the oxidizing potential of oxygen. This oxidizing potential has entailed the accompanying necessary evolution of a battery of antioxidant defenses (Fridovich, 1995). Since redox reactions are central to energy flow in plant cells, it is not surprising that evolution has led to the integration of these antioxidants into every major cellular process. Nowhere is this more evident than in the case of photosynthesis. Antioxidants prevent uncontrolled oxidation, regulate electron transport processes, participate in and control enzymatic reactions, and direct acclimation and development through control of gene expression. The principal soluble antioxidants of the chloroplast stroma, ascorbate and glutathione, interact directly with the xanthophyll cycle by providing the reducing power for zeaxanthin production and indirectly by participating in the acidification of the thylakoid lumen that activates violaxanthin deepoxidase (VDE).

Abbreviations: A_1 – secondary electron acceptor in rc_1; AA – ascorbic acid; AOS – active oxygen species; APX – ascorbate peroxidase; Ci–intracellular CO_2 concentrations; $^1Chl^*$ – chlorophyll singlet state; DHA–dehydroascorbate; DHAR–dehydroascorbate reductase; ϕ_{exc} –yield of photochemistry by rc_{II} withoxidized Q_A; F–Faraday constant; Fd–ferredoxin; F_m –relative yield or intensity of chlorophyll fluorescence whenall Q_A is reduced in the dark-adapted state; F_m' – as F_m but under conditions of irradiation; FNR – ferredoxin-NADP reductase; F_o – relative yield or intensity of fluorescence when all Q_A is oxidized; F_v – relative change in fluorescence yield or intensity produced by completely reducing the Q_A pool in the dark-adapted state; F_v' –as F_v but under conditions of irradiation; F_x – third electron acceptor in rc_1; $F_{x/B}$– fourth electron acceptor in rc_1; GR – glutathione reductase; GSH – reduced glutathione; GSSG – glutathione disulfide; $J_{PS\,I}$– index of PS I electron transport, the product of $\Phi_{PS\,I}$ and irradiance; LHCII – light-harvesting chlorophyll *a/b*-binding protein associated with PS II; MDHA –monodehydroascorbate; MDHAR–monodehydroascorbate reductase; NPQ– non-photochemical quenching of variable chlorophyll *a* fluorescence; P_{680} – chlorophyll pair that forms the primary electron donor in the reaction center of PS II; P_{700} – chlorophyll pair that forms the primary electron donor in the reaction center of PS I; PQ – plastoquinone; PS – photosystem; $\Phi_{PS\,I}$ –quantum yield for PS I electron transport; $\Phi_{PS\,II}$ – quantum yield for PS II electron transport; Q_A– primary stable electron acceptor to PS II; Q_B–terminal electron acceptor of the PS II reaction center; q_Q– probability that an exciton in PS II will encounter a rc_{II} with anoxidized Q_A; R–universal gas constant (8.31 $JK^{-1}mol^{-1}$); rc_I– reaction center of PS I; rc_{II}– reaction center of PS II; Rubisco – ribulose-1,5-bisphosphate carboxylase/oxygenase; RuBP – ribulose-1,5-bisphosphate; SOD – superoxide dismutase; T – absolute temperature; $\Delta\mu_{H^+}$ – transthylakoid proton potential; VDE – violaxanthin deepoxidase

A. Role of Carotenoids in the Efficient Operation of Photosynthetic Electron Transport

Photosynthesis is a process in which a significant amount of the free-energy of absorbed quanta is used to drive otherwise endothermic chemical reactions. It can be compared to a machine using light to generate and sustain driving forces that can power assimilatory processes. These driving forces are formed by differences between the redox potentials of electron transport component pools, or differences in the electrochemical potential of H^+ ion pools on opposite sides of membranes. Though fundamental to the useful function of photosynthesis, these driving forces are also an Achilles' Heel, for they may also drive other, less desirable reactions that result in damage and loss of function. Much of the regulation of photosynthetic systems seems directed towards ensuring that the necessary driving forces are sustained, without becoming excessive. In this regard carotenoids play two opposing roles. On the one hand they act to increase the capacity of the photosynthetic system to harvest the primary driving force for photosynthesis, i.e., light. On the other hand they act, in co-operation with other regulatory processes, either to quench damaging side reactions or to reduce the magnitude of driving forces formed directly or indirectly within the photosynthetic machinery following light absorption (Fig. 1). With special attention to the roles of the carotenoids, we will describe the current understanding of how photosynthesis is regulated in order to balance opposing goals: efficient metabolism, which needs a driving force, and stress avoidance, which, in the limit, requires there to be no driving force.

B. Organization of Chlorophyll-Based Light-Harvesting and Electron Transport Processes

All photosynthetic systems share common features. The conversion of light energy to a metabolically usable form is achieved by means of: 1. light-absorbing pigment-protein complexes, 2. electron transport components that produce vectorial electron transport within and around membrane bound compartments, 3. membrane bound protein complexes, such as ATPases, that couple the relaxation of a transmembrane $\Delta\mu_{H^+}$ to transport or synthesis, e.g. of ATP, and 4. reductases that reduce stable electron or hydrogen carriers that can be used to drive reductive

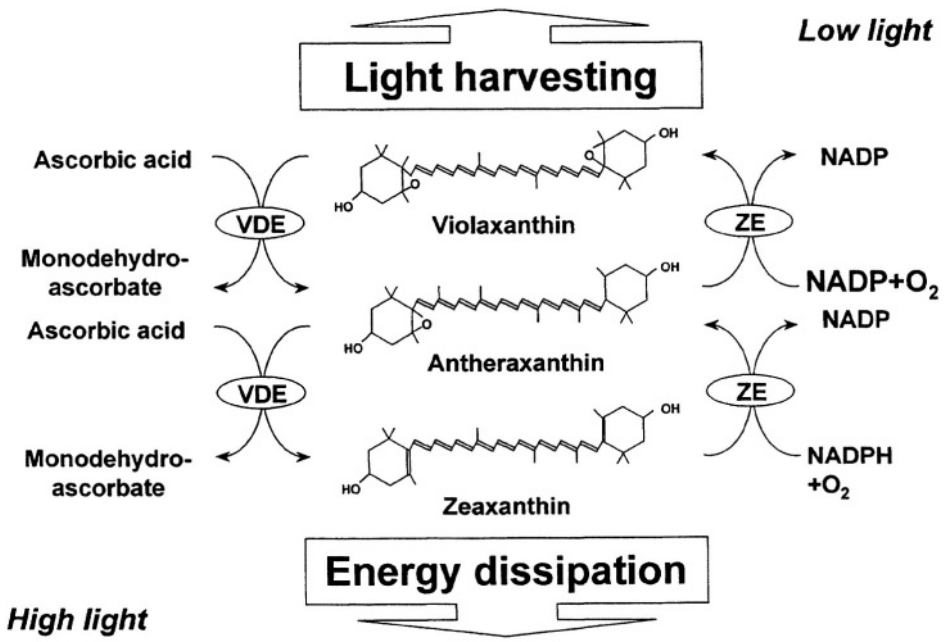

Fig. 1. The xanthophyll cycle and its effects on light-harvesting and energy dissipation within the photosynthetic apparatus. The enzyme violaxanthin de-epoxidase (VDE) catalyzes the sequential conversion of violaxanthin to zeaxanthin via antheraxanthin using ascorbic acid (AA) as a reductant and generating monodehydroascorbate (MDHA). The epoxidation of zeaxanthin to violaxanthin in the reverse reaction sequence is catalyzed by the enzyme zeaxanthin epoxidase (ZE).

metabolic processes. In the photosynthetic embryophytes (the multicellular green plants) the photosynthetic machinery is particularly well characterized. Light is absorbed by a diverse range of protein-bound pigments, which are chlorophylls *a* and *b,* carotenes and xanthophylls (Alfonso et al., 1994; Jansson, 1994; Simpson and Knoetzel, 1996; Yamamoto and Bassi, 1996). The organization of pigments within those protein/pigment complexes shows their stoichiometry to be exact and their structure to be highly ordered, so that once a quantum has been absorbed by a pigment to form an excited state the 'exciton' can move quickly between the pigments (Hastings et al., 1994; Savikhin et al., 1994; Van Grondelle et al., 1994; DiMagno et al., 1995; Kleima et al., 1997; Palsson et al., 1998). This capacity for movement is essential for the operation of photosynthesis as it allows the exciton to move from the site of absorption to specialized chlorophyll molecules in structures called reaction centers.

Quanta absorbed by photosynthetic pigments produce several accessible excited states, but, at least in the chlorophylls, these states relax to the lowest excited singlet state prior to transfer to another pigment. In common with nearly all oxygenic photosynthetic organisms, long-range transfer of the excited state to the reaction center is carried out by transfer between chlorophyll *a* molecules (only *Acaryochloris,* which uses chlorophyll *d,* is known to be different; Miyashita et al., 1997). Rapid movement between pigments increases the potential quantum yield of photosynthesis by increasing the likelihood that the excited state will arrive at the reaction center and produce successful charge separation rather than decaying to the ground state by another non-photochemical route, such as fluorescence, singlet-triplet conversion or internal conversion to heat. A high quantum yield for photosynthesis is advantageous in light-limiting (i.e., low light) conditions.

In reaction centers the excitation energy associated with the excited state of chlorophyll *a* is used to produce charge separation and thence electron transport. The association of the light-harvesting pigment/protein complexes with the reaction centers is highly ordered. In oxygenic photosynthetic organisms two types of reaction centers have been identified, and each type is associated with its own types of pigment-protein complexes producing the two Photosystems, I and II. The stoichiometries of some pigment/protein complexes with the reaction center complexes are fixed, whereas for others it appears to be adaptive, depending on irradiance (Jansson, 1994; Melis, 1996; Simpson and Knoetzel, 1996; Yamamoto and Bassi, 1996). Some pigment/protein complexes may be capable of associating with both types of photosystem (McCormac et al., 1994; Samson and Bruce, 1995). By virtue of its simple structure and its similarity to the reaction center of the photosynthetic purple bacterium *Rhodopseudomonas viridis,* which has been crystallized and mapped to a high resolution using X-ray crystallography (Deisenhofer and Michel, 1993; Lancaster and Michel, 1996), the structure of the reaction center of PS II (rc_{II}) is at least partially understood. The reaction center of PS I (rc_I) has also been crystallized, the X-ray structure providing important information on the function of individual components.

Reaction centers cannot support repeated charge separation, and thus sustained electron transport, in the absence of other electron components; there must ultimately be a source of reductant and a sink for reductant (i.e., a source of oxidant). Following charge separation, an oxidized primary electron donor (special chlorophyll *a* pairs: P_{680} in PS II and P_{700} in PS I) is formed, along with a reduced primary acceptor (a phaeophytin in rc_{II} and a chlorophyll *a* in rc_I). The primary donor must be re-reduced before it can be re-oxidized by the next photoact. Similarly, the primary acceptor must be re-oxidized. In non-cyclic electron flow (Fig. 2) electrons are carried from the terminal electron acceptor of rc_{II} (Q_B) to the initial electron donor to rc_I (plastocyanin) by the plastoquinone, cytochrome b_6f and unbound plastocyanin pools (Haehnel, 1984). This process requires an electron source, water, and an electron acceptor such as CO_2. Non-cyclic electron transport flux is coupled to the deposition of protons within the thylakoid lumen due to, first, water oxidation to O_2 and H^+ and, second, by the oxidation of plastoquinol to plastoquinone through the concerted action of the Rieske FeS and b_6 of the cytochrome b_6f complex (Witt, 1979; Kramer and Crofts, 1993). PS I may also participate in cyclic electron transport in which the path from the rc_I electron acceptor chain leads back to the rc_I primary donor. The different cyclic mechanisms which have been proposed (Bendall and Manasse, 1995; Scheller, 1996) involve the reduction and oxidation of plastoquinol, leading to transthylakoid proton transport, and the development of a $\Delta\mu_{H^+}$. It seems unlikely, however, that cyclic electron transport plays a quantitatively significant

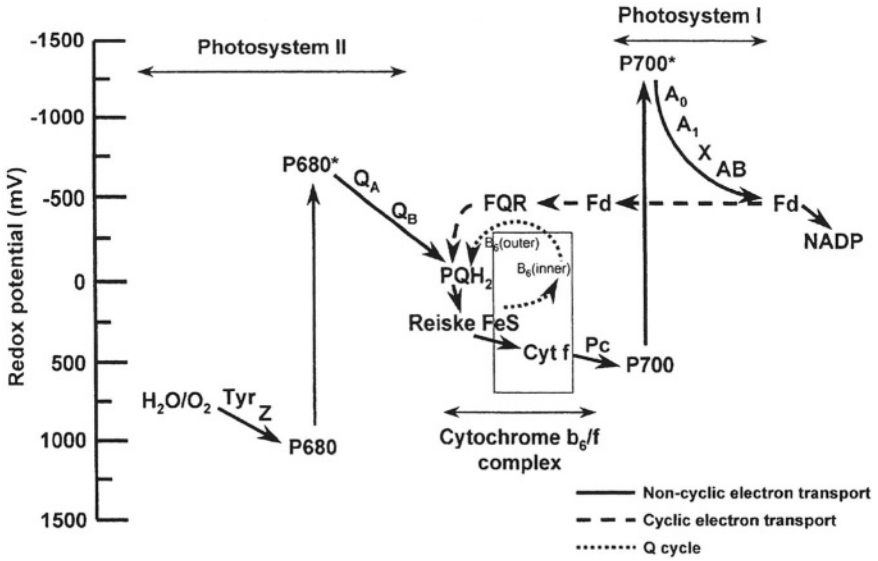

Fig. 2. the Z-scheme model of photosynthetic electron flow showing non-cyclic, cyclic and pseudocyclic paths of electron transport.

role in C_3 photosynthesis in vivo (Genty and Harbinson, 1996). Cyclic electron transport pathways have been reported for PS II, but their in vivo activity does not appear to be significant.

1. Role of Chlorophyll Singlets

Light absorption by photosynthetically active pigments produces chlorophyll *a* singlet states (^{1}Chl*). The fate of the ^{1}Chl* pool in photosynthetic pigment beds is important because of the possibility of chlorophyll triplet formation. At physiological temperatures, ^{1}Chl* states are unstable; the intrinsic lifetime of the S_1 state of chlorophyll *a* is 15 ns, and actual average lifetimes differ in vivo between the photosystems and depend on their condition. In PS I with P_{700} in the non-oxidized state, a fluorescence lifetime of 23 ps has been measured in PS II-free *Synechocystis* (Hecks et al., 1994) and a chlorophyll *a* lifetime of 40 ps has been measured in thylakoids (Nuijs et al., 1986). However, the effect of changes in the condition of rc_I on the lifetime is not known in detail. In vitro, variable fluorescence is produced from P_{700}-enriched particles under reducing conditions (Ikegami, 1976; Kleinherenbrink et al., 1994; Trissl, 1997). Under conditions where the electron acceptors of rc_I are oxidized the lifetime of the ^{1}Chl* was similar whether P_{700} is oxidized or non-oxidized (Nuijs et al., 1986; Hecks et al., 1994). Recently, however, Trissl (1997) has shown a 10% increase in the fluorescence from PS I upon oxidizing P_{700}. Although variable PS I fluorescence, leading to changes in the lifetime of ^{1}Chl*, may occur, these are small effects.

In PS II the lifetime of chlorophyll *a* fluorescence increases from about 0.3 ns (Genty et al., 1992) when all Q_A is oxidized in dark-adapted material (the F_o state of chlorophyll fluorescence) to about 1.9 ns with all Q_A reduced and in the absence of any non-photochemical quenching (NPQ) of chlorophyll fluorescence (the F_m state of fluorescence; Genty et al., 1992). NPQ is a mechanism that quenches ^{1}Chl* by an internal conversion, with the result that all the energy associated with the singlet is converted to heat (Gilmore et al., 1995, 1996a,b). It has a rate constant which allows it to compete with photochemistry in PS II, and is thus an effective means of controlling the rate of photochemistry by open PS II reaction centers (Genty et al., 1992; Gilmore et al., 1998).

Although the consequences of NPQ for regulation of PS II are understood, the underlying mechanisms are less clear. The establishment of a transthylakoid pH difference is obligatory for heat dissipation to occur but conversion of violaxanthin to zeaxanthin in the xanthophyll cycle is also involved (Demmig-Adams, 1990; Horton et al., 1996). Regulated increases in the rate of thermal energy dissipation of excess excitation energy correlate with the conversion of the carotenoid pigment violaxanthin to zeaxanthin (Fig. 1). This reaction is catalyzed by the enzyme VDE, which has a pH optimum of about 5, and uses

ascorbic acid as a co-factor (Hager, 1969; Hager and Holocher, 1994). The xanthophyll cycle pigments are present in the antenna systems of PS I and PS II. Conversion of zeaxanthin to violaxanthin also forms part of the synthetic pathway of abscisic acid, and enzymes catalyzing the two successive epoxidation reactions are found in both the chloroplast envelope and in the thylakoid membranes (Siefermann and Yamamoto, 1975). It is therefore possible that similar epoxidase isoenzymes are involved in both the xanthophyll cycle and epoxy-carotenoid biosynthesis leading to abscisic acid formation. Since abscisic acid is implicated in the control of stomatal aperture and transpiration, as well as adaptation to environmental stresses, the epoxidation state of the xanthophyll cycle may modify photosynthesis indirectly as well as directly, by participation in the synthesis of a hormone which controls the availability of CO_2 for photosynthesis.

When violaxanthin is present in the light-harvesting antennae complexes they are efficient light-harvesting systems (Fig. 1; Siefermann-Harms, 1987; Koyama, 1991). Conversion to zeaxanthin favors energy dissipation (Fig. 1), for example, by direct quenching of chlorophyll excited states by energy transfer to zeaxanthin (Frank et al., 1994). A precise mechanism by which zeaxanthin quenches chlorophyll singlet states has yet to be elucidated. The different number of conjugated carbon-carbon double bonds in zeaxanthin and violaxanthin may be significant. Violaxanthin has nine double bonds and a lowest energy level of 1.89 eV. This energy level corresponds to a wavelength of 655 nm, allowing violaxanthin to donate energy efficiently to any pigment with an absorption peak at longer wavelength. The introduction of additional double bonds by de-epoxidation decreases the lowest energy level, so that the corresponding absorption peaks are at 680 nm for antheraxanthin (ten double bonds) and 704 nm for zeaxanthin (eleven double bonds). Zeaxanthin will therefore function more efficiently as an energy acceptor than as an energy donor. It should be noted that changes in the xanthophyll de-epoxidation states alone are not sufficient to bring about quenching but they may control the interactions between the proteins in the light-harvesting antennae (Ruban et al., 1997).

Although the exact mechanisms acting to control NPQ await elucidation, the ΔpH and zeaxanthin act together to increase the rate of thermal dissipation within PS II, and thus reduce its photochemical efficiency (Gilmore et al., 1998). An increase of NPQ causes a reduction of the singlet lifetime proportional to the reduction of ϕ_{exc} (Genty et al., 1992). The lifetime of $^1Chl^*$ in PS II is variable and dependent on the operational state of the photosynthetic system and is always much longer than that in PS I.

In ethanolic solution, the yield of fluorescence from $^1Chl^*$ is about 32% and that of triplet formation is 68%. Shipman (1980) has calculated a rate constant for chlorophyll triplet formation from $^1Chl^*$ of $1.9 \times 10^8\ s^{-1}$, compared to the rate constant for fluorescence emission of $6.5 \times 10^7\ s^{-1}$. Measurements on isolated thylakoids also indicate that the yield of chlorophyll *a* triplet formation is twice that of fluorescence decay (Kramer and Mathis, 1980), with a triplet yield of 0.15 (calculated over all PS I and PS II chlorophylls) when all rc_{II} was in the Q_A^- state. More recent studies on purified PS II pigment-protein complexes show that for CP47 at 4 K the yield of fluorescence is 0.11 ± 0.03 and that of triplets is 0.16 ± 0.03 (Groot et al., 1995), which is consistent with a triplet:fluorescence yield ratio of about two. There is no means by which chlorophyll triplets can be detected in functioning photosynthetic systems in vivo, but the relationship with chlorophyll fluorescence, or $^1Chl^*$ lifetime, allows an estimate of their formation to be made. In PS I with a $^1Chl^*$ lifetime of 23 ps the yield will be 0.003 whereas, in the absence of NPQ, PS II will show yields of 0.04 (all Q_A oxidized) and 0.25 (all Q_A reduced). Clearly, the greatest yield of triplet formation is in PS II, and the small $^1Chl^*$ lifetime dependency that may occur in PS I has no significant effect on the total yield of triplets.

Chlorophyll triplet states alone pose no danger, since they decay to the ground state by phosphorescence or internal conversion. They are a threat in the presence of molecular oxygen, which has a biradical triplet ground state. This is relatively unreactive but when it interacts with another triplet state, such as a chlorophyll triplet, it can form singlet oxygen. At least partial protection against this reaction is conferred by the close proximity of β-carotene and chlorophylls in photosynthetic pigment/protein complexes. These permit the triplet state to be transferred from a chlorophyll to an adjacent carotene from which it can decay to the ground state by internal conversion. In LHCIIb, for example, luetins and chlorophyll *a* are in close association (Kühlbrandt et al., 1994) and transfer occurs very efficiently. In LHCIIb at room temperature 92% (±7) of the triplets formed on chlorophyll *a* are transferred to carotenes

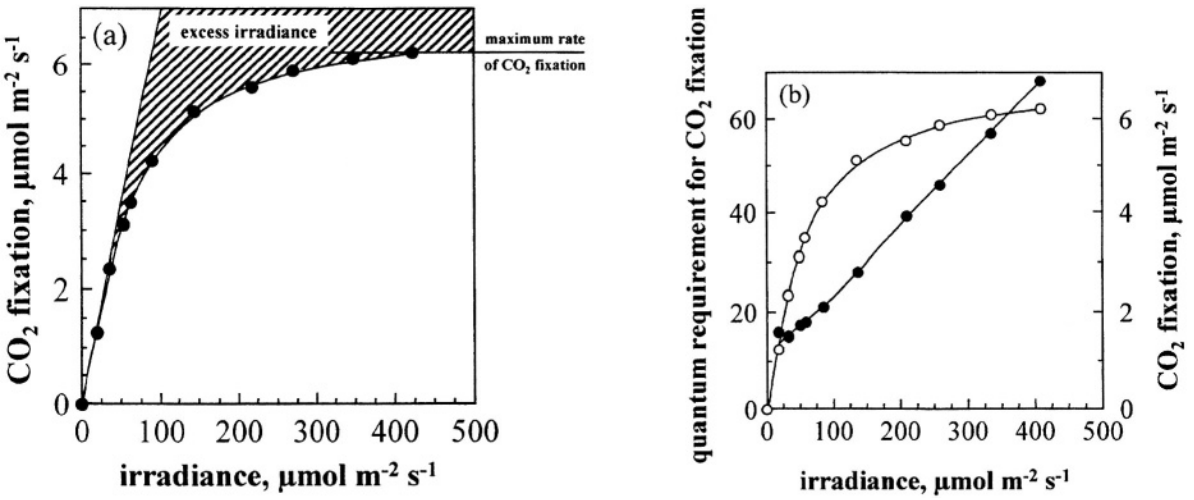

Fig. 3. (A) The irradiance response curve of CO_2 assimilation under non-photorespiratory conditions (350 ppm CO_2, 2% O_2, and N_2. The solid line represents the response as it would be if the quantum yield for CO_2 fixation remained at a maximum value. Excess irradiance (quanta which cannot be used for photochemistry) is a consequence of the loss of quantum yield for CO_2 fixation shown by the difference between the actual and maximum responses. (B) The irradiance dependencies of the quantum requirement for CO_2 fixation (●) and CO_2 fixation (○) for a leaf of *Juanulloa aurantiaca*.

(Barzda et al., 1998). This transfer of triplets from chlorophyll to carotene, and its subsequent harmless dissipation as heat, has been termed the triplet valve mechanism (Witt, 1979). Based on estimates of triplet yield, this mechanism is much more important in PS II than in PS I. In isolated PS II complexes β-carotene failed to provide complete protection against photodamage from chlorophyll triplets, probably because P_{680} is highly oxidizing (+1.1V) and may oxidize any closely-bound carotenoid pigment.

The protective mechanisms associated with carotenoids, especially NPQ, are commonly described as being involved with the dissipation of excess excitation energy. This usage introduces a terminology problem connected with the processes of energy dissipation. Energy storage by the reaction centers 1.4 μs after a 677 nm flash is 83% for PS I and 65% for PS II (Nitsch et al., 1988), and that of CO_2 fixation as a whole is only about 35% (Hill and Rich, 1983). In blue irradiance about 35% of the energy is dissipated thermally before the exciton reaches the reaction center. Even at maximum quantum yield (Genty and Harbinson, 1996) photosynthetic systems are predominantly energy dissipating systems. Thus it is pertinent to distinguish between the energy losses intrinsic to the photosynthetic system and inducible protective processes which divert quanta to a path where they are converted to heat without coupling to energy storing processes.

2. Control of Photosynthesis

Photosynthetic light-harvesting and electron transport systems must be regulated because large driving forces are associated with low quantum yields and with increased flux through damaging side reactions. According to Ohm's law, flux is a function of the product of driving force and conductance (or its inverse, resistance). Regulation of the driving force in a system may involve an increase in the conductance. An increase in conductance must be accompanied by a decreased driving force to maintain a given flux. If conductance cannot be decreased then the driving force must be attenuated or the damaging side reactions must be tightly managed. These strategies occur in photosynthesis and several involve carotenoid pigments (Genty and Harbinson, 1996).

Under conditions of low photorespiration, about 90% of photochemical product is allocated to CO_2 fixation. The progression from light limitation to light saturation in photosynthesis is illustrated in Fig. 3 A which shows a typical light saturation curve for photosynthesis illustrated in the shrub *Juanulloa aurantiaca*. The quantum requirement per mole CO_2 fixed (on an incident irradiance basis) increases as the irradiance and rate of CO_2 assimilation increase. The higher the flux the lower the efficiency of CO_2 assimilation (Fig. 3B). As the ATP and NADPH requirements for CO_2 fixation are independent of

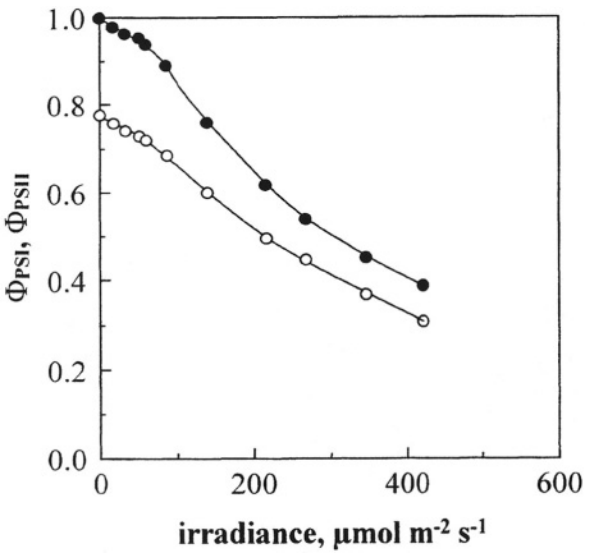

Fig. 4. The effect of irradiance on the quantum yield for electron transport by Photosystems I (●) and II (○) measured simultaneously with the irradiance response of CO_2 assimilation (Fig. 3a) in *Juanulloa aurantiaca*.

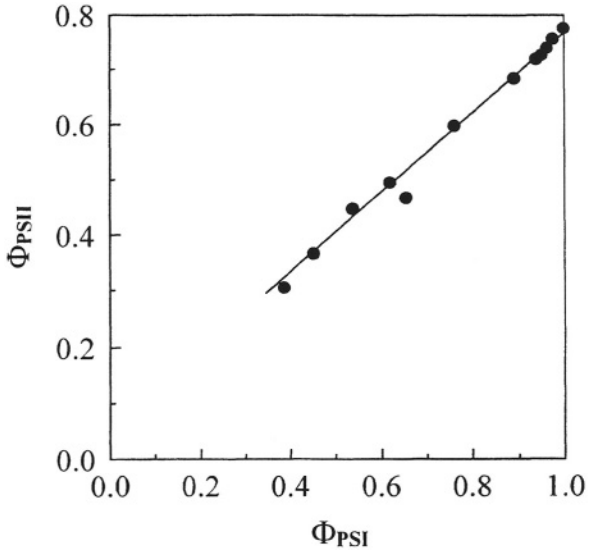

Fig. 5. The relationship between the quantum efficiencies for electron transport by Photosystems I and II (Φ_{PSI}, Φ_{PSII})*whose* irradiance response is shown in Fig. 4.

irradiance, the increased inefficiency requires greater dissipation of excitons. Both $\Phi_{PS\,I}$ and $\Phi_{PS\,II}$ decrease with increasing irradiance (Fig. 4). There is a linear correlation between $\Phi_{PS\,I}$ and $\Phi_{PS\,II}$ (Fig. 5), implying a dominant role for non-cyclic electron transport (Genty and Harbinson, 1996).

Under conditions where photorespiration occurs, the effect of oxygen on the stoichiometry between $\Phi_{PS\,I}$ or $\Phi_{PS\,II}$ and Φ_{CO2} is comparable to that predicted from models of CO_2 fixation based on the biochemistry of Rubisco (Peterson, 1989; Cornic and Briantais, 1991). This is consistent with a tight coupling between metabolism and electron transport as illustrated in Fig. 6. Increased redox driving forces, produced as Q_A become more reduced and the P_{700} pool more oxidized, are linearly related to the index of PS I electron transport $J_{PS\,I}$ (the product of $\Phi_{PS\,I}$ and irradiance; Fig. 7). The relationship between driving force and flux varies with environment, for example, $J_{PS\,I}$ increases more gradually with increasing redox gradient in the shade plant, *Begonia luzonensis* and for the more high light tolerant *J. aurantiaca* (Fig. 7).

As the quantum inefficiency within PS I with increasing irradiance under steady-state conditions arises through increases in $[P^+_{700}]/([P^+_{700}]+[P^0_{700}])$ due to a donor-side limitation of electron transport, changes in the chlorophyll *a* singlet lifetime are small or nil. Chlorophyll triplet formation in the PS I pigment bed is low. Under certain conditions,

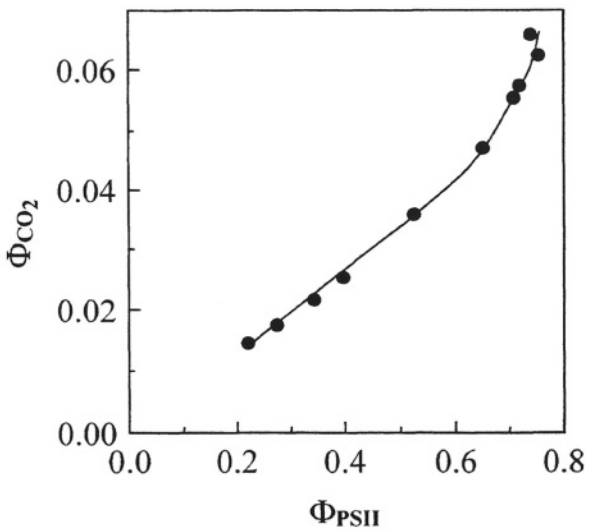

Fig. 6. The relationship between the quantum efficiency for CO_2 assimilation (Φ_{CO_2}) and the quantum efficiency for Photosystem II electron transport (Φ_{PSII}) measured at each irradiance simultaneously with CO_2 fixation.

however, PS I efficiency is limited by an acceptor side limitation of electron transport. In leaves in air, this type of restriction can transiently follow sudden increases in irradiance (Foyer et al., 1992; Harbinson and Hedley, 1993; Klughammer and Schreiber, 1993); more persistent acceptor side limitation may occur in leaves irradiated in an atmosphere of 2% O_2 and less

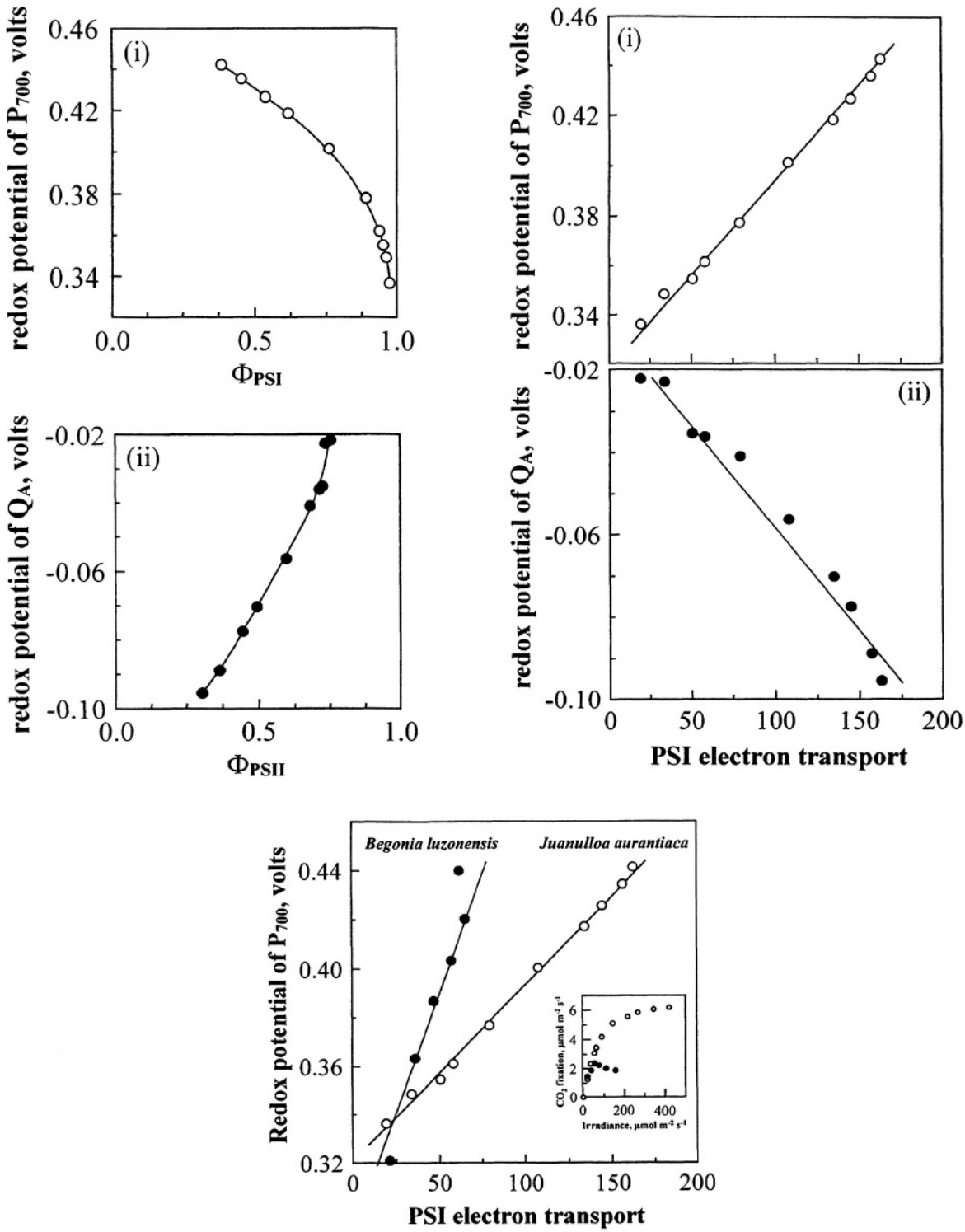

Fig. 7. (A) The relationship between (i) the redox potential of the P_{700} pool and Φ_{PSI} and (ii) the redox potential of Q_A pool (calculated from measurements of q_Q) and Φ_{PSII}. (B) The relationship between Photosystem I electron transport and (i) the redox potential of the P_{700} pool and (ii) the redox potential of Q_A. (C) The relationship between Photosystem I electron transport and the redox potential of the P_{700} pool. Inset figure: The effect of irradiance on CO_2 assimilation under non-photorespiratory conditions in the *Begonia* (●) and *Juanulloa* (○) leaves.

than 100 ppm CO_2 (Genty and Harbinson, 1996). In these conditions, the electron acceptors on the reducing side of PS I become highly reduced, potentially leading to an increase of O_2^- formation by the Mehler reaction (Foyer and Harbinson, 1994).

Back-reactions from PS I electron acceptors to P^+_{700} may occur, entailing high-yield formation of the triplet state of P_{700} (Polm and Brettel, 1998). In contrast to those formed in the antenna, chlorophyll triplets in the reaction center may pose a serious threat. Under conditions of acceptor side limitation of electron transport, photoaccumulation of $F^-_{A/B}$ and F^-_X is likely. Once F^-_X accumulates the back-reaction within rc_I will occur between A_1^- and P^+_{700}, generating triplet P_{700} with a yield of over 85% (Polm and Brettel, 1998).

Damage to the PS II reaction center can occur as a consequence of singlet oxygen formation (Telfer et al., 1991, 1994a,b; De las Rivas et al., 1993). While protection of reaction centers by quenching singlet oxygen via β-carotene appears to be the preferred protective mechanism, β-carotene bound to the PS II reaction center cannot completely protect against photodamage caused by chlorophyll triplet formation. This may be because P_{680} is highly oxidizing (+1.1 V) and would be expected to oxidize any carotenoid pigment bound in close proximity. Exogenous antioxidants do not protect the reaction center from damage but altering the amount of β-carotene does affect the yield of singlet oxygen and is clearly linked to photoprotection.

Active oxygen species have been implicated in PS I photoinhibition (Sonoike and Terashima, 1994; Terashima et al., 1994; Sonoike 1996a,b) and methyl viologen, a powerful PS I electron acceptor, protects against photoinhibition (Sonoike, 1996a), though this may also prevent reduction of O_2 by reduced PS I acceptors (Sonoike et al., 1997). Under most atmospheric conditions, however, photosynthetic electron transport is quickly limited at the PQH_2/cytochrome b_6f transfer step to ensure that no significant acceptor side limitation persists. During the photosynthetic induction of a dark-adapted leaf, for example, the acceptor side limitation only lasts for a few tens of seconds (Foyer et al., 1992; Harbinson and Hedley, 1993). It is not known how stress, such as temperature extremes or water shortage, affects the speed of the this response, though low temperatures would be expected to increase it. It is noteworthy that photoinhibition of PS I has largely been detected in leaves illuminated at low temperatures (Sonoike and Terashima, 1994; Sonoike, 1996b). Fluctuations in irradiance are not unusual under field conditions (Chazdon and Pearcy, 1991).

The responses of PS II to increasing irradiance are more complex because of changes that occur in NPQ. With increasing irradiance both q_Q and ϕ_{exc} decrease (Fig. 8). The decrease in q_Q is associated with the increasing reduction of Q_A, and the loss of ϕ_{exc} is associated with the increase of NPQ, which also causes a decrease of ^{1}Chl* lifetime under standardized conditions; e.g., conditions at F'_m or F'_o (Genty et al., 1992). The effect of increasing NPQ on the quantum yields of the inducible and constitutive dissipation pathways for PS II (calculated by the method of Laisk et al., 1997) can be seen in Fig. 8. Even in the absence of photochemistry and NPQ, the excitons within PS II still decay to the ground state. There is thus a constitutive dissipation path, distinct from the inducible dissipative pathway associated with zeaxanthin synthesis and ΔpH. In stressed leaves there is arguably a third dissipative mechanism based upon the loss of F_v/F_m caused by photoinhibition (Crofts and Yerkes, 1994). Though photoinhibition involves damage to PS II (Aro et al., 1993a,b; Baker and Bowyer, 1994; Andersson and Barber, 1996), a slowly reversible zeaxanthin-linked quenching, which modulates ^{1}Chl* lifetimes in PS II and consequently regulates the driving force for linear electron transport, is also found (Verhoeven et al., 1996).

The relative yield of chlorophyll fluorescence under steady-state conditions is a measure of the relative lifetime of ^{1}Chl* in PS II (Krause and Weis, 1991). With increasing irradiance the steady-state fluorescence yield remains almost constant and close to the F_o level, even though large changes in $\Phi_{PS\ II}$ occur (Foyer and Harbinson, 1994). This implies that the ^{1}Chl* lifetime is constant with increasing irradiance, though the density of ^{1}Chl* in PS II, the product of lifetime and the rate of singlet formation, will increase because of the increasing irradiance (Fig. 9). If the inducible NPQ were not to develop, then as $\Phi_{PS\ II}$ decreased due to decreases in q_Q alone, the steady-state fluorescence yield and thus the ^{1}Chl* lifetime would increase (Fig. 9). The ^{1}Chl* density in PS II under these circumstances would increase logarithmically with increasing irradiance (Fig. 9), with parallel increases in the rate of chlorophyll triplet formation and singlet oxygen generation. Another consequence of modulating ^{1}Chl* lifetime is that the degree of reduction of the Q_A pool with increasing irradiance is less than would develop in the absence

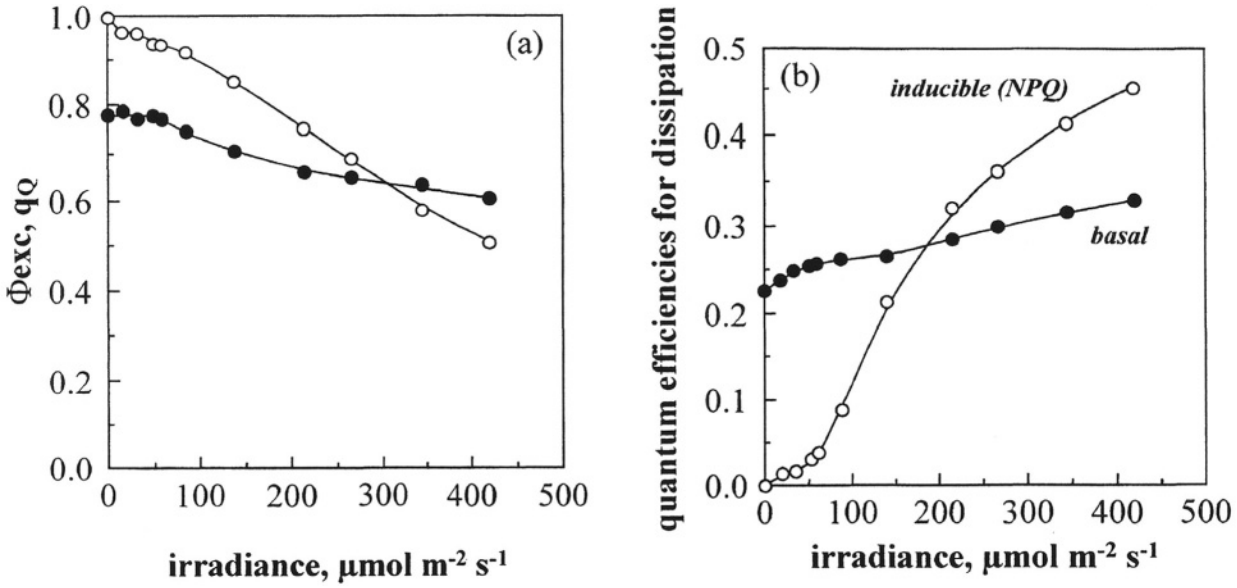

Fig. 8. (a) The irradiance dependency of q_Q (○) and the quantum efficiency of electron transport by open Photosystem II reaction centres (ϕ_{exc}; ●). (b) the irradiance dependency of the quantum efficiencies for de-excitation by the basal, constitutive pathway and the inducible (NPQ or non-photochemical quenching) pathway; at each irradiance the sum of these de-excitation pathways and the quantum yield for Photosystem II electron transport is one.

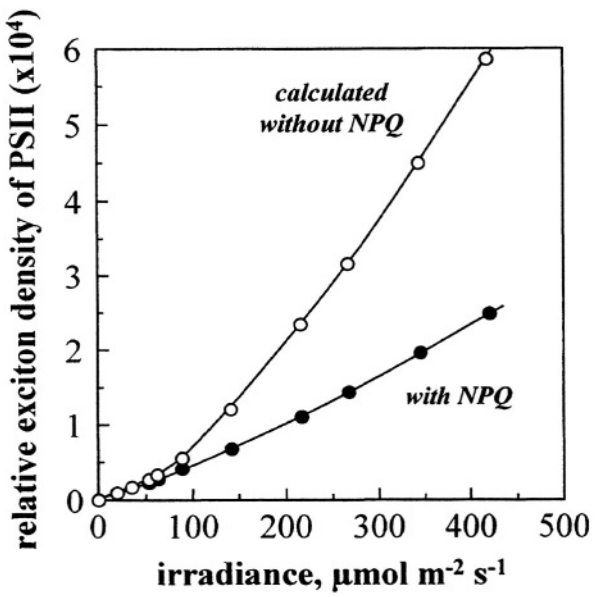

Fig. 9. The irradiance dependency of the relative exciton density in Photosystem II, calculated as the product of the irradiance and the relative, steady-state fluorescence yield (in arbitrary units) in the presence of NPQ, the natural situation, and estimated in the absence of NPQ.

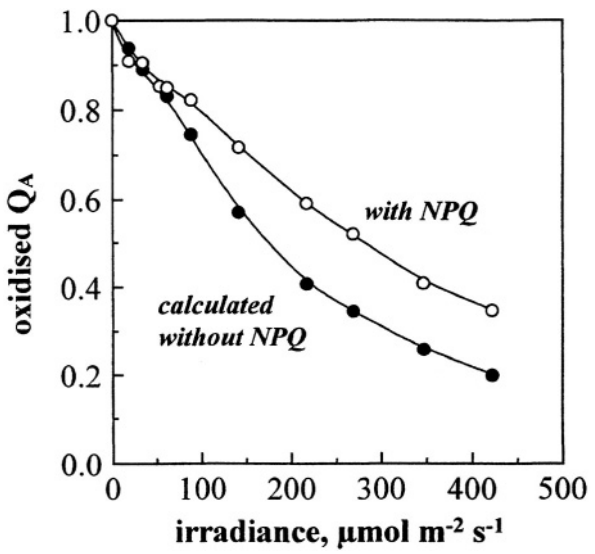

Fig. 10. The effect of NPQ on the irradiance dependency of the relative degree of oxidation of Q_A (Calculated from q_Q).

of NPQ (Fig. 10); this is because increasing NPQ decreases the probability that a $^1Chl^*$ will produce charge separation. Regulation of Q_A reduction reduces the likelihood of photoinhibition caused by damage to rc_{II}. Decreased Q_A reduction is equivalent to a less negative redox potential.

The mechanism of acceptor side photoinhibition of PS II is founded on the formation of triplet P_{680}, as a result of the back-reaction between reduced phaeophytin and P^+_{680}, under conditions where the Q_A is doubly reduced or absent (Van Mieghem et al., 1989, 1995). With rc_{II} in this state the triplet P_{680} is

relatively stable with a lifetime of about 1 ms in the absence of oxygen, decreasing to 33 μs in the presence of oxygen. This quenching of the triplet state by oxygen suggested that highly reactive singlet oxygen could be formed as a by-product and that this could cause irreversible damage to rc_{II}. Singlet oxygen formation in isolated reaction center cores of PS II has been detected under conditions favoring triplet P_{680} formation. Some protection of the reaction center from the damage that can arise following double reduction of Q_A is conferred by cytochrome b_{559} which has been postulated to re-oxidize doubly reduced Q_A (Whitmarsh et al., 1994). Acting in parallel with this, increases in NPQ will act to decrease Q_A reduction and thus the risk of double reduction of Q_A. This mechanism may, however, have a negative consequence for the efficiency of photosynthetic electron transport. As a result of the restriction of Q_A^- formation (Fig. 10), the driving force for linear electron transport is reduced (Fig. 11). The correlation between the redox potential of Q_A and the electron transport flux (Fig. 7) suggests that this would lead to a decreased rate of electron transport. However, effects of NPQ-induced changes on the rate or rate-constant for non-cyclic electron transport remain to be demonstrated. However, the rate constant of the reaction between plastoquinol and the Rieske FeS of the cytochrome b_6f complex is dependent on the plastoquinol concentration (Bendall, 1982; Rich, 1982; Hope et al., 1988) and changes in Q_A redox potential would be expected to affect plastoquinol redox potential.

It has been postulated that β-carotenes bound to the PS II and PS I reaction centers are in the 15-*cis* configuration (see Chapter 9, Koyama and Fujii). The 15-*cis* configuration may allow more efficient energy transfer between chlorophyll and carotenoid. β-carotene turnover in the reaction centers may lead directly to the formation of zeaxanthin as suggested recently by the group of Trebst (Trebst and Depka, 1997). Xanthophyll pigments in the light harvesting complex (LHCII) are primarily bound in the -*trans* form (Kühlbrandt et al., 1994). This does not mean that these xanthophyll pigments do not undergo triplet reactions. Triplets have been found in all major xanthophylls in plants, including lutein, neoxanthin and violaxanthin and xanthophyll triplets have been observed in isolated LHC (Peterman et al., 1995).

The control of zeaxanthin-linked NPQ is unclear. Although this form of NPQ is dependent on both ΔpH and zeaxanthin synthesis, its effect on ϕ_{exc} is

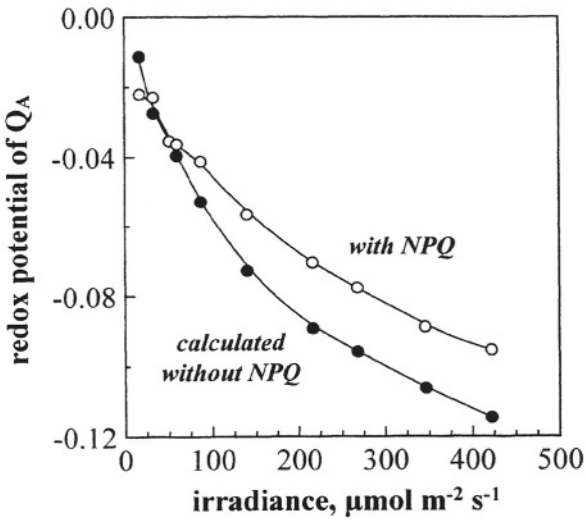

Fig. 11. The effect of NPQ on the irradiance dependency of the redox potential of Q_A (calculated from q_Q).

surprisingly consistent between different leaves under different conditions. For example, the effect of increasing irradiance on light-harvesting efficiency can be compared in a *Begonia luzonensis* leaf and a *Juanulloa aurantiaca* leaf. The observed decreases in ϕ_{exc} with increasing irradiance are quite different, NPQ in the *Begonia* leaf being activated more strongly with increasing irradiance. If, however, the $\Phi_{PS\,II}$ and ϕ_{exc} irradiance responses of these leaves are compared to their $\Phi_{PS\,I}$ irradiance response (Fig. 12A) it is clear that the co-ordination between the loss of $\Phi_{PS\,II}$ and ϕ_{exc}, in relation to the loss of $\Phi_{PS\,I}$, is identical. Thus, with regard to the internal relationship between photochemical and dissipative efficiencies, NPQ does not work any better in the *Begonia* leaf than in the *Juanulloa* leaf. It is not clear how the ΔpH or the intrathylakoid pH changes with increasing irradiance. In both these species under these conditions of measurement the rate constant for linear electron transport does not increase with increasing irradiance (Fig. 12B), as is commonly found (Genty and Harbinson, 1996) over a range of irradiances where ϕ_{exc} is decreasing and NPQ is increasing. Since the rate constant for linear electron transport is sensitive to the intrathylakoid pH (Tikhonov et al., 1984; Nishio and Whitmarch, 1993), an unchanged rate constant has been interpreted to imply that the intrathylakoid pH either remains constant or changes only slightly with increasing irradiance (Genty and Harbinson, 1996). It is therefore not clear how proposed control of NPQ by ΔpH might function in

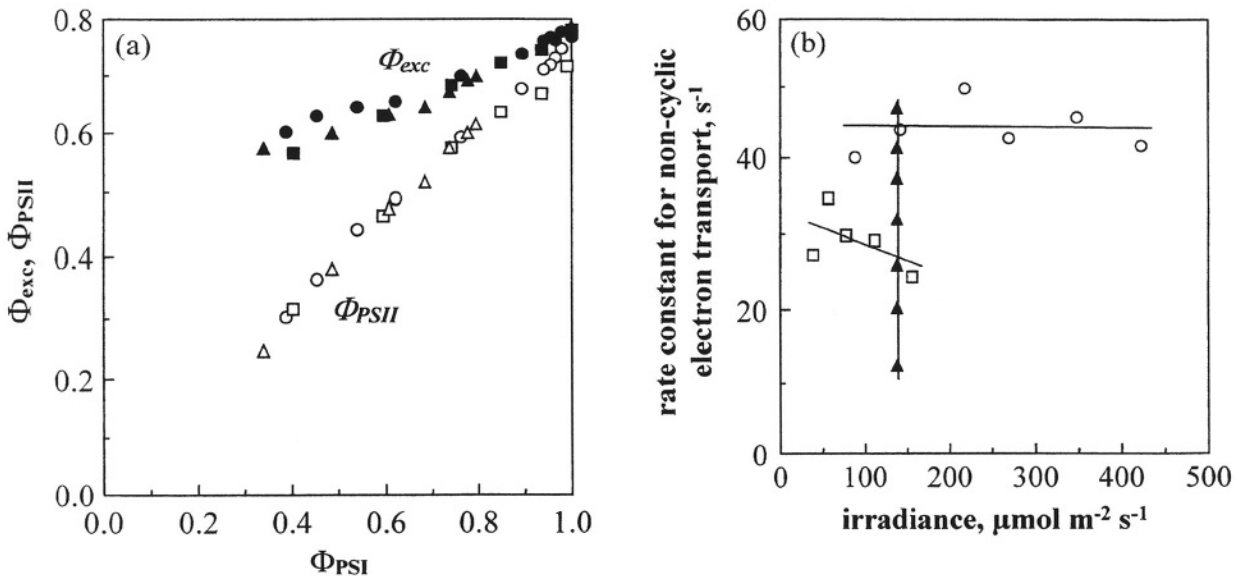

Fig. 12. (a) The relationship between the quantum efficiency of Photosystem I electron transport (Φ_{PSI}) and the quantum efficiencies for Photosystem II electron transport (Φ_{PSII}) and the quantum efficiencies for open Photosystem II reaction centers (Φ_{exc}). These data were obtained from leaves of *Juanulloa aurantiaca* (●, ○) and *Begonia luzonensis* (■, □) under conditions of increasing irradiance and a leaf of *Juanulloa aurantiaca* kept at constant irradiance, but subjected to decreasing CO_2 concentrations (350–35 ppm) in a non-photorespiratory atmosphere (▲, △). (b) The irradiance response of the rate constants for non-cyclic electron transport.

vivo. One possibility is that zeaxanthin acts to amplify NPQ at a given ΔpH (Noctor et al., 1991). Control by ΔpH could then be mediated via large effects of small changes in ΔpH both on zeaxanthin synthesis and on the sensitized zeaxanthin-dependent NPQ. Pfündel and Bilger (1994) suggested that sensitive control of ΔpH over zeaxanthin synthesis might result from a sharp increase in VDE activity with decreasing pH. In leaves under non-photorespiratory conditions and a constant irradiance, decreasing CO_2 concentrations result in decreased rates of CO_2 fixation, $\Phi_{PS\ II}$, $\Phi_{PS\ I}$, q_Q and ϕ_{exc} (Harbinson, 1994) and decreased rate constants for electron transport (Genty and Harbinson, 1996). This represents clear evidence of photosynthetic control of electron transport. Since decreasing q_Q indicates a more reduced Q_A pool, it is likely that this control was effected by decreasing intrathylakoid pH. However, in a *Juanulloa* leaf subjected to such a treatment, the internal relationship between $\Phi_{PS\ I}$, $\Phi_{PS\ II}$ and ϕ_{exc} is the same as that observed in leaves under changing irradiance conditions (Fig. 12). This illustrates the incomplete nature of our current understanding of the control of NPQ.

II. Active Oxygen Species and Photosynthesis

Singlet oxygen, superoxide and hydrogen peroxide can be generated within PS II complexes (Wydrzynski et al., 1989; Fine and Frisch, 1990; Macpherson et al., 1993; Ananyev et al., 1994). While several components associated with PS II have antioxidant activity (Ananyev et al., 1994; Hundal et al., 1995; Miller et al., 1996), AOS formation in PS II can initiate photoinhibitory damage (Kyle et al., 1985; Kyle, 1987; Mishra et al., 1993; Hideg et al., 1994). Degradation of D1 protein may commence by radical attack but it also involves the activation of a specific protease (Mattoo et al., 1989; Barber and Andersson, 1992; Aro et al., 1993). Redox control of mRNA abundance and mRNA-binding proteins involved in D1 synthesis as well as that of the light-harvesting antenna proteins have been reported (Danon and Mayfield, 1994; Escoubas et al., 1995; Maxwell et al., 1995). Changes in the turnover of D1 may be a general adaptive response to environmental stress mediated by the redox poise of the chloroplasts (Huner et al., 1996; Giardi et al., 1997). While redox signaling has been shown to regulate the expression of several genes coding for chloroplast proteins

(Pearson et al., 1993; Escoubas et al., 1995; Henkow et al., 1996) photoinhibition has also been shown to cause changes in the expression of genes coding for cytosolic proteins (Karpinski et al., 1997).

A. Electron Transport to Oxygen

While NADP is the preferred electron acceptor in photosynthesis, oxygen can also accept electrons from the photosynthetic electron transport chain (Mehler, 1951; Mehler and Brown, 1952; Allen, 1975, 1992; Egneus et al., 1975; Marsho et al., 1979). Molecular oxygen contains two unpaired electrons with parallel spins. As a consequence O_2 is most easily reduced by single electron additions because divalent reduction of O_2 (to H_2O_2) requires a spin inversion (Cadenas, 1989). The addition of an electron to oxygen by the photosynthetic electron transport chain produces superoxide (Asada et al., 1974). The reduction of molecular oxygen by the photosynthetic electron transport system is called the 'Mehler reaction' (Mehler, 1951; Mehler and Brown, 1952) and electron transport from water to molecular O_2 is called 'pseudocyclic electron flow' (Allen, 1975, 1977). Reported values for O_2 concentrations required to half-saturate the rate of the Mehler reaction are between 2 and 60 μM (Robinson, 1988) which corresponds to 0.17 to 5% O_2 in air at 25 °C.

Carriers within the photosynthetic electron transport chain that have electrochemical potentials commensurate with the reduction of molecular oxygen exist in both PS II and PS I (Asada et al., 1974; Allen, 1977; Wydrzynski et al., 1989). Oxygen reduction by the electron transport components does not appear to be a deleterious event per se but rather serves a useful function in preventing over-reduction of the electron transport chain and 'poising' electron carriers for more efficient functioning particularly during induction (Arnon and Chain, 1975; Egneus et al., 1975; Heber et al., 1978;Ziem-Hanck and Heber, 1980; Polle, 1996). While components of PS II are capable of reducing O_2 (Wydrzynski et al., 1989; Ananyev et al., 1994), the major flux of electrons to oxygen appears to occur on the reducing side of PS I (Asada, 1994, 1996). Superoxide formation can occur within the thylakoid membrane (Takahashi and Asada, 1988; Hormann et al., 1993; Asada, 1994) or at the membrane surface (Allen, 1977; Badger, 1985). Numerous components involved in electron transfer on the acceptor side of PS I have been shown to be autoxidizable, i.e., they can reduce oxygen to superoxide. These include the FeS centers (X, A and B), thylakoid-bound and stromal ferredoxin, FNR, and other flavin-containing dehydrogenases such as monodehydroascorbate reductase (MDHAR) and glutathione reductase (GR) (Misra and Fridovich, 1971; Asada et al., 1974; Allen, 1977; Goetze and Carpentier, 1994; Miyake et al., 1996). The contribution of flavoenzyme-mediated superoxide production in vivo is unknown since the endogenous electron acceptors for these enzymes suppress superoxide formation. As discussed earlier in this chapter, the re-reduction of P^+_{700} is the rate-limiting step of linear electron transport under many conditions and significant limitations on the acceptor side of PS I are not common. We may therefore conclude that electron acceptors such as $NADP^+$ will normally be available for electron transport, minimizing superoxide production via components associated with PS I.

B. Mehler-Peroxidase Reaction Sequence

Photosynthesis and photorespiration produce substantial amounts of superoxide and H_2O_2 as metabolic intermediates (Zelitch, 1973, 1990; Asada, 1994; Willekens et al., 1997). Superoxide production in the stroma contributes to stromal alkalinization and the formation of the transthylakoid ΔpH. Protons are consumed when superoxide is reduced to H_2O_2 by ascorbate (Buettner and Jurkiewicz, 1996) or is dismutated to H_2O_2 and O_2, a reaction catalyzed by chloroplastic SODs (Asada et al., 1973; Salin, 1988). Since the chloroplastic ascorbate concentration is very high (10–50 mM; Foyer et al., 1983), ascorbate-mediated superoxide reduction may compete effectively with the dismutation pathway. Chloroplastic H_2O_2 produced from either reaction is rapidly destroyed by the action of ascorbate peroxidases (APX; Asada et al., 1973; Asada, 1992, 1994). Continuous elimination of superoxide and H_2O_2 prevents production of both singlet O_2 and hydroxyl radical (OH·) (Khan and Kasha, 1994). Hydroxyl radicals can be formed by interaction of superoxide and hydrogen peroxide, particularly in the presence of transition metal ions (Elstner et al., 1978; Youngman and Elstner, 1981; Cadenas, 1989). While hydroxyl radical formation at PS II was found to be relatively high in *Euglena gracilis* (Tschiersch and Ohmann, 1993), spinach chloroplasts only produced substantial amounts of this radical when the

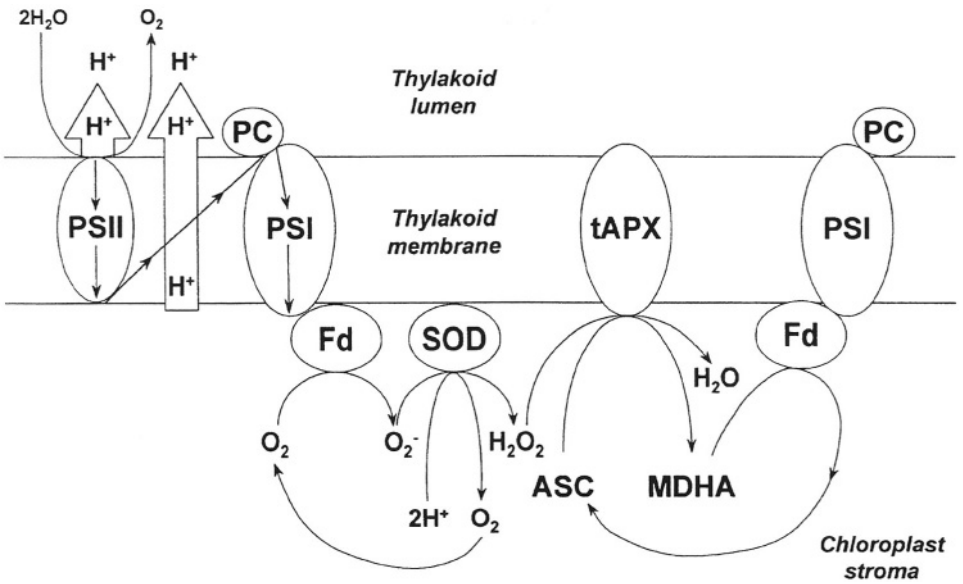

Fig. 13. The Mehler-peroxidase cycle. ASC – ascorbate; MDHA – monodehydroascorbate; Fd – ferredoxin; PC – plastocyanin; PS I – Photosystem I; PS II – Photosystem II; SOD – superoxide dismutase; tAPX – thylakoid bound ascorbate peroxidase.

endogenous antioxidant system was impaired (Jakob and Heber, 1996). Under most conditions, SOD and APX appear to function efficiently to control superoxide and H_2O_2, thereby minimizing hydroxyl radical formation. Any hydroxyl radicals that are formed can be de-activated by antioxidants of low molecular weight such as ascorbate (Halliwell, 1987) or, under certain stress conditions, mannitol (Shen et al., 1997). Since the lifetime of the highly reactive hydroxyl radical is extremely short, the most important requirements for effective scavenger molecules is that they be present at high concentration and in proximity to the site of radical production (Halliwell, 1987).

Because oxygen reduction via the Mehler reaction is tightly coupled to the production and destruction of H_2O_2 by APX (Groden and Beck, 1979; Anderson et al., 1983a,b), this reaction sequence is known as the 'Mehler-peroxidase cycle' (Fig. 13; Neubauer and Schreiber, 1989; Neubauer and Yamamoto, 1992). For ascorbate to continue to serve as a reductant in this pathway, it must be regenerated from monodehydroascorbate (MDHA), the immediate product of the peroxidase reaction (Miyake and Asada, 1992; Grace et al., 1995). MDHA is itself a powerful electron acceptor that may be reduced by ferredoxin (Miyake and Asada, 1994) or by NADPH in a reaction catalyzed by the stromal enzyme, MDHAR. The Mehler-peroxidase cycle therefore consists of (a) electron transfer from water through the photosynthetic electron transport chain to oxygen, producing superoxide at PS I, (b) the dismutation of the superoxide radical by SOD to form H_2O_2, (c) the reduction of H_2O_2 to water by APX and (d) the regeneration of ascorbate from MDHA.

This sequence not only performs an essential protective function in preventing oxidative stress but also contributes to the control of photosynthetic electron transport. First, it is coupled to the generation of a transthylakoid pH gradient and, second, it prevents excessive reduction of the PS I acceptor pools (Foyer et al., 1990; Polle, 1996; Foyer and Harbinson, 1997). These effects reduce the risk of harmful back reactions within PS II that increase the probability of singlet oxygen formation (see above). In this way, the production and destruction of AOS is directly involved in the regulation of photosynthetic electron transport. Any MDHA escaping re-reduction in the Mehler peroxidase cycle will rapidly disproportionate to ascorbate and dehydroascorbate. The dehydroascorbate thus formed can be recycled to ascorbate via the ascorbate-glutathione cycle (Fig. 14); this cycle uses NADPH derived from photosynthetic electron transport and, hence, remains a coupled process contributing to the formation of a *trans*-thylakoid proton gradient and ATP formation.

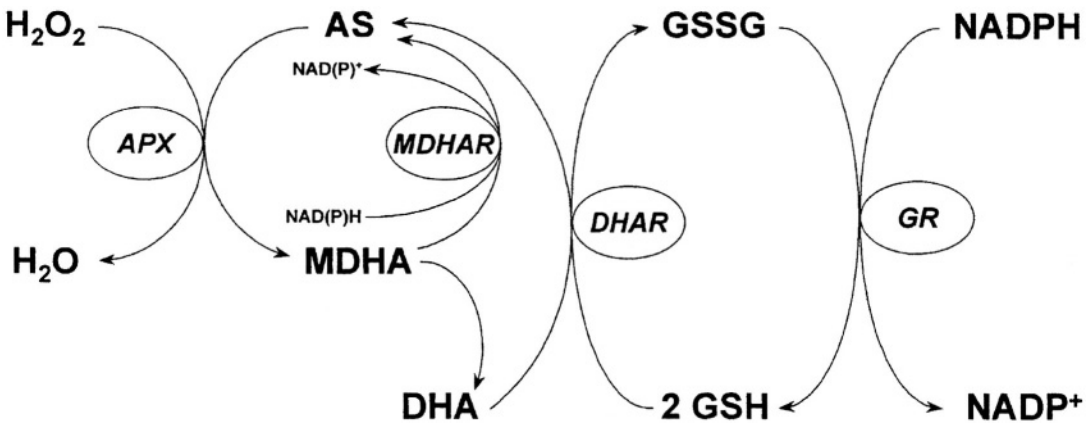

Fig. 14. The ascorbate-glutathione cycle. APX – ascorbate peroxidase; DHA – dehydroascorbate; DHAR – dehydroascorbate reductase; GR – glutthione reductase; GSH – reduced glutathione; GSSG – glutathione disulfide; MDHR – monodehydroascorbate reductase.

C. Ascorbate Transport

While ascorbate is transported into isolated intact chloroplasts (Anderson et al., 1983b; Beck et al., 1983; Foyer and Lelandais, 1996), the thylakoid membranes appear to have no carrier system to transport ascorbate into the thylakoid lumen (Foyer and Lelandais, 1996). This is surprising since the enzyme VDE, located inside the thylakoid, requires ascorbate to convert violaxanthin to zeaxanthin (Fig. 2). Upon illumination the pH of the lumen falls and VDE binds to the lumenal side of the thylakoid membrane and becomes active (Hager and Holocher, 1994; Rockholm and Yamamoto, 1996). The affinity of VDE for ascorbate is strongly dependent on pH, because ascorbic acid is the true substrate of the enzyme (Bratt et al., 1995). The addition of H_2O_2 to illuminated thylakoid membrane preparations induces a transient inhibition of zeaxanthin formation (Neubauer and Yamamoto, 1992), suggesting competition for ascorbate between the Mehler-peroxidase cycle and the VDE reaction. Since the ascorbate pool in the chloroplast stroma is substantial (10–50 mM), sufficient amounts of ascorbic acid may be able to cross the membrane by diffusion (Foyer et al., 1983; Foyer, 1993; Foyer and Lelandais, 1995). However, if the permeability of the thylakoid membrane for ascorbate restricts the rate of zeaxanthin formation it could have important consequences for thermal energy dissipation. Furthermore, at low lumenal pH in the light, when highest rates of zeaxanthin formation are expected to occur, a greater proportion of the lumenal ascorbate pool will be present as ascorbic acid. The uncharged form will tend to diffuse out of the lumen more readily than the ionized form, exacerbating the problem of ascorbate availability.

D. Antioxidants and Xanthophyll Cycle-Dependent Energy Dissipation

In the present analysis of the roles of antioxidants and carotenoid pigments in the regulation of photosynthetic electron transport, we have presented evidence for the involvement of these processes in protecting against light- and stress-induced damage. A complex relationship between xanthophyll cycle-dependent energy quenching and the formation of AOS occurs in photosynthetic systems. Clearly, both processes are increased at high light or when plants grown under moderate irradiances are subject to stress. Increases in the activities or contents of foliar antioxidants occur in response to environmental stresses (Grace and Logan, 1996; Logan et al., 1998a). Correlations between growth irradiance and various antioxidant enzyme activities and metabolite contents have been reported in both field-grown plants and those grown in controlled environments (Gillham and Dodge, 1987; Grace and Logan, 1996; Logan et al., 1998b). Stress situations also lead to increased xanthophyll cycle-dependent energy dissipation (Khamis et al., 1990; Bilger and Björkman, 1991). Both processes serve to prevent over-reduction of the photosynthetic electron transport chain and hence decrease the likelihood of photoinhibition stress-induced increases in antioxidants mitigate oxidative

damage to proteins and other membrane components. These systems operate in parallel but have numerous points of interaction, particularly with regard to the central role of ascorbate. It is probable that similar systems of signal transduction, leading to the induction of gene expression, occur for the two systems; such processes are largely unexplored at present and remain to be elucidated.

Acknowledgment

We are deeply indebted to Graham Noctor for critical reading of the manuscript.

References

Alfonso M, Montoya G, Cases R, Rodriguez R and Picorel R (1994) Core antenna complexes, CP43 and CP47, of higher plant Photosystem II. Spectral properties, pigment stoichiometry, and amino acid composition. Biochemistry 33: 10494–10500

Allen JF (1975) Oxygen reduction and optimum production of ATP in photosynthesis. Nature 256: 599–600

Allen JF (1977) Oxygen—a physiological electron acceptor in photosynthesis? Curr Adv Plant Sci 29: 459–468

Allen JF (1992) Protein phosphorylation in regulation of photosynthesis. Biochim Biophys Acta 1098: 275–335

Ananyev G, Renger G, Wacker U and Klimov V (1994) The photoproduction of superoxide radicals and the superoxide dismutase activity of Photosystem II. The possible involvement of cytochrome b_{559}. Photosynth Res 41: 327–338

Anderson JW, Foyer CH and Walker DA (1983a) Light-dependent reduction of hydrogen peroxide by intact spinach chloroplasts. Biochim Biophys Acta 724: 69–74

Anderson JW, Foyer CH and Walker DA (1983b) Light-dependent reduction of dehydroascorbate and uptake of exogenous ascorbate by spinach chloroplasts. Planta 158: 442–450

Andersson B and Barber J (1996) Mechanisms of photodamage and protein degradation during photoinhibition of Photosystem II. In: Baker NR (ed) Photosynthesis and the Environment, pp 101–121. Kluwer, Dordrecht

Arnon DI and Chain RK (1975) Regulation of ferredoxin-catalysed photosynthetic phosphorylations. Proc Natl Acad Sci USA 72: 4961–4965

Aro E-M, McCaffery S and Anderson JM (1993a) Photoinhibition and D_1 protein degradation in peas acclimated to different growth irradiances. Plant Physiol 103: 835–843

Aro E-M, Virgin I and Andersson B (1993b) Photoinhibition of Photosystem II. Inactivation, protein damage and turnover. Biochim Biophys Acta 1143: 113–134

Asada K (1992) Ascorbate peroxidase—a hydrogen peroxide scavenging enzyme in plants. Physiol Plant 85: 235–241

Asada K (1994) Production and action of active oxygen species in photosynthetic tissues. In: Foyer CH, Mullineaux PM (eds) Causes of Photooxidative Stress and Amelioration of Defense Systems in Plants, pp 77–104. CRC Press, Baton Rouge

Asada K (1996) Radical production and scavenging in the chloroplasts. In: Baker NR (ed) Photosynthesis and the Environment, pp 128–150. Kluwer Academic Publishers, Dordrecht

Asada K, Urano M and Takaliashi M (1973) Subcellular location of superoxide dismutase in spinach leaves and preparation and properties of crystalline spinach superoxide dismutase. Eur J Biochem 36: 257–266

Asada K, Kiso K and Yoshikawa K (1974) Univalent reduction of molecular oxygen by spinach chloroplasts on illumination. J Biol Chem 247: 2175–2181

Badger MR (1985) Photosynthetic oxygen exchange. Ann Rev Plant Physiol 36: 27–53

Baker NR and Bowyer JR (eds) (1994) Photoinhibition of photosynthesis. From molecular mechanisms to the field. Bios, Oxford

Barber J and Andersson B (1992) Too much of a good thing: Light can be bad for photosynthesis. Trends Biochem Sci 17: 61–66

Barzda V, Peterman EJG, Van Grondelle R and Van Amerongen H (1998) The influence of aggregation on triplet formation in light-harvesting chlorophyll *a/b* pigment-protein complex II of green plants. Biochemistry 37: 546–551

Beck E, Burkert A and Hofmann M (1983) Uptake of L-ascorbate by intact chloroplasts. Plant Physiol 73: 41–45

Bendall DS (1982) Photosynthetic cytochromes of oxygenic organisms. Biochim Biophys Acta 683: 119–152

Bendall DS and Manasse RS (1995) Cyclic photophosphorylation and electron transport. Biochim Biophys Acta 1229: 23–38

Berkner LV and Marshall LC (1965) On the origin and rise of oxygen concentration in the earth's atmosphere. J Atmos Sci 22: 225–261

Bilger W and Björkman O (1990) Role of the xanthophyll cycle in photoprotection elucidated by measurements of light-induced absorbance changes, fluorescence and photosynthesis in leaves of *Hedera canariensis*. Photosynth Res 25: 173–185

Bratt CE, Arvidsson P-O, Carlsson M and Akerlund H-E (1995) Regulation of violaxanthin de-epoxidase by pH and ascorbate concentration. Photosynth Res 45: 169–175

Buettner GR and Jurkiewicz BA (1996) Chemistry and biochemistry of ascorbic acid. In: Cadenas E, Packer L (eds) Handbook of Antioxidants, pp 91–115. Marcel Dekker Inc., New York

Cadenas E (1989) Biochemistry of oxygen toxicity. Ann Rev Biochem 58: 79–110

Chazdon RL and Pearcy RW (1991) The importance of sunflecks for forest understory plants. BioScience 41: 760–766

Cornic G and Briantais J-M (1991) Partitioning of photosynthetic electron flow between CO_2 and O_2 reduction in a C_3 leaf (*Phaseolus vulgaris* L.) at different CO_2 concentrations and during drought stress. Planta 183: 178 –184

Crofts AR and Yerkes CT (1994) A molecular mechanism for q_E quenching. FEBS Lett 352: 265–270

Danon A and Mayfield SP (1994) Light-regulated translation of chloroplast messenger RNAs through redox potential. Science 266: 1717–1719

Deisenhofer J and Michel H (1993) Three-dimensional structure of the photosynthetic reaction centre from *Rhodopseudomonas viridis*. In: Deisenhofer J and Norris JR (eds) The Photosynthetic Reaction Center, Vol 2, pp 541–558. Academic Press, London

De las Rivas J, Telfer A and Barber J (1993) 2-coupled β-carotene molecules protect p860 from photodamage in isolated Photosystem II reaction centers. Biochim Biophys Acta 1142: 155–164

Demmig-Adams B (1990) Carotenoids and photoprotection in plants: A role for the xanthophyll zeaxanthin. Biochim Biophys Acta 1020: 1–24

DiMagno L, Chan C-K, Jia Y, Lang MJ, Newman JR, Mets L, Fleming GR and Haselkorn R (1995) Energy transfer and trapping in Photosystem I reaction centers from cyanobacteria. Proc Natl Acad Sci USA 92: 2715–2719

Egneus H, Heber U, Matthiesen U and Kirk M (1975) Reduction of oxygen by the electron transport chain of chloroplasts during assimilation of carbon dioxide. Biochim Biophys Acta 408: 252–268

Elstner EF, Saran M, Bors W and Lengfelder E (1978) Oxygen activation in isolated chloroplasts. Mechanism of ferredoxin-dependent ethylene formation from methionine. Eur J Biochem 89: 61–66

Escoubas J-M, Lomas M, LaRoche J and Falkowski PG (1995) Light intensity regulates cab gene expression via the redox state of the plastoquinone pool in the green alga *Dunaliella tertiolecta.* Proc Natl Acad Sci USA 92: 10237–10241

Fine PL and Frisch WD (1990) The mechanism of H_2O_2 production by the S_2 state of the oxygen-evolving complex. In: Baltscheffsky M (ed) Current Research in Photosynthesis I. pp 905–908, Kluwer Academic Publishers, Dordrecht

Foyer CH (1993) Interactions between electron transport and carbon assimilation in leaves: Co-ordination of activities and control. In: Abrol Y, Mohanty P, Govindjee (eds), Photosynthesis. Photoreactions to Plant Productivity, pp 199–224. Oxford and IBH publishing Co. PVT Ltd, New Delhi

Foyer CH and Harbinson J (1994) Oxygen metabolism and the regulation of photosynthetic electron transport. In: Foyer CH, Mullineaux PM (eds) Causes of Photo-oxidative Stress and Amelioration of Defense Systems in Plants, pp 1–42. CRC Press, Boca Raton

Foyer CH and Harbinson J (1997) The photosynthetic electron transport system: efficiency and control. In: Foyer CH, Quick WP (eds), A molecular approach to primary metabolism in higher plants, pp 3–39. Taylor and Francis, London, UK

Foyer CH and Lelandais M (1995) Ascorbate transport into protoplasts, chloroplasts and thylakoid membranes of pea leaves. In: Mathis P (ed), Photosynthesis: From light to Biosphere, Vol V, pp 511–514. Kluwer Academic Publishers, Dordrecht

Foyer CH and Lelandais M (1996) A comparison of the relative rates of transport of ascorbate and glucose across the thylakoid, chloroplast and plasmalemma membranes of pea leaf mesophyll cells. J Plant Physiol 148: 391–398

Foyer CH, Rowell J and Walker D (1983) Measurement of the ascorbate content of spinach leaf protoplasts and chloroplasts during illumination. Planta 157: 239–244

Foyer CH, Furbank R, Harbinson J and Horton P (1990) The mechanisms contributing to photosynthetic control of electron transport by carbon assimilation in leaves. Photosynth Res 25: 83–100

Foyer CH, Lelandais M and Harbinson J (1992). Control of the quantum efficiencies of Photosystems I and II, electron flow and enzyme activation following dark-to-light transitions in pea leaves. Plant Physiol 99: 979–986

Frank HA, Cua A, Chynwat V, Young A, Gosztola D and Wasielewski MR (1994) Photophysics of the carotenoids associated with the xanthophyll cycle in photosynthesis. Photosynth Res 41: 389–395

Fridovich I (1995) Superoxide radical and superoxide dismutases. Ann Rev Biochem 64: 97–112

Genty B and Harbinson J (1996) The regulation of light utilization for photosynthetic electron transport. In: Baker NR (ed) Photosynthesis and the Environment, pp 67–99. Kluwer Academic Press, Dordrecht

Genty B, Goulas Y, Dimon B, Peltier JM and Moya I (1992) Modulation efficiency of primary conversion in leaves, mechanisms involved in PS II. In: Murata N (ed) Research in Photosynthesis, Vol 4, pp 603–610. Kluwer Academic Publishers, Dordrecht

Giardi MT, Masojídek J and Godde D (1997) Effects of abiotic stresses on the turnover of the D_1 reaction centre II protein. Physiol Plant 101: 635–642

Gillham DJ and Dodge AD (1987) Chloroplast superoxide and hydrogen peroxide scavenging systems from pea leaves: Seasonal variations. Plant Sci 50: 105–109

Gilmore AM, Hazlett TL and Govindjee (1995) Xanthophyll cycle-dependent quenching of Photosystem II chlorophyll *a* fluorescence: Formation of a quenching complex with a short fluorescence lifetime. Proc Natl Acad Sci USA 92: 273–2277

Gilmore AM, Hazlett TL, Debrunner PG and Govindjee (1996a) Photosystem II chlorophyll *a* fluorescence lifetimes and intensity are independent of the antenna size differences between barley wild-type and *chlorina* mutants: Photochemical quenching and xanthophyll cycle dependent non-photochemical quencing of fluorescence. Photosynth Res 48: 171–187

Gilmore AM, Hazlett TL, Debrunner PG and Govindjee (1996b) Comparative time-resolved Photosystem II chlorophyll *a* fluorescence analyses reveal distinctive differences between photoinhibitory reaction center damage and xanthophyll cycle dependent energy dissipation. Photoschem Photobiol 64: 552–563

Gilmore AM, Shinkarev VP, Hazlett TL and Govindjee (1998) Quantitative analysis of the effects of intrathylakoid pH and the xanthophyll cycle pigments on chlorophyll *a* fluorescence lifetime distributions and intensity in thylakoids. Biochemistry 37: 13582–13593

Goetze DC and Carpentier R (1994) Ferredoxin $NADP^+$ reductase is the site of oxygen reduction in pseudocyclic electron transport. Can J Bot 72: 256–260

Grace S and Logan BA (1996) Acclimation of foliar antioxidant systems to growth irradiance in three broad-leaves evergreen species. Plant Physiol 112: 1631–1640

Grace S, Pace R and Wydrzynski T (1995) Formation and decay of monodehydroascorbate radicals in illuminated thylakoids as determined by ERR spectroscopy. Biochim Biophys Acta 1229: 155–165

Groden D and Beck E (1979) H_2O_2 destruction by ascorbate-dependent systems from chloroplasts. Biochim Biophys Acta 546: 426–435

Groot M-L, Peterman EJG, Van Stokkum IHM, Dekker JP and Van Grondelle R (1995) Triplet and fluorescing states of the CP47 antenna complex of Photosystem II studied as a function of temperature. Biophys J 68: 281–290

Haehnel W (1984) Photosynthetic electron transport in higher plants. Annu Rev Plant Physiol 35: 659–683

Hager A (1969) Lichtbedingte pH-erniederigung in einem chloroplasten-kompartiment als Ursache der enzymatischen Violaxanthin → Zeaxanthin-Umwandlung, Beziehungen zur Photophosphorylierung. Planta 89: 224–243

Hager A and Holocher K (1994) Localisation of the xanthophyll cycle enzyme violaxamthin deepoxidase within the thylakoid lumen and abolition of its mobility by a (light-dependent) pH decrease. Planta 192: 581–589

Halliwell B (1987) Oxidative damage, lipid peroxidation and antioxidant protection in chloroplasts. Chemistry and Physics of Lipids 44: 327–340

Harbinson J (1994) The responses of thylakoid electron transport and light utilisation efficiency to sink limitation of electron transport. In: Baker NR and Bowyer JR (eds) Photoinhibition of Photosynthesis, pp 273–295. Bios Scientific Publishers, Oxford

Harbinson J and Hedley CL (1993) Changes in P-700 oxidation during the early stages of the induction of photosynthesis. Plant Physiol 103: 649–660

Hastings G, Kleinherenbrink FAM, Lin S and Blankenship RE (1994)Time-resolved fluorescence and absorption spectroscopy of Photosystem I. Biochemistry 33: 3185–3192

Heber U, Egneus H, Hanch Jensen M and Köster S (1978) Regulation of photosynthetic electron transport and photophosphorylation in intact chloroplasts and leaves of *Spinacia oleracea* L. Planta 143: 41–49

Hecks B, Wulf K, Breton J, Leibl W and Trissl HW (1994) Primary charge separation in Photosystem I: A two-step electrogenic charge separation connected with $P_{700}^{+} A_0^{-}$ and $P_{700}^{+} A_1^{-}$ formation. Biochemistry 33: 8619–8624

Henkow L, Strid Å, Berglund T, Rydstöm J and Ohlsson AB (1996) Alteration of gene expression in Pisum sativum tissue cultures caused by the free radical-generating agent 2,2′-azobis (2-amidinopropane) dihydrochloride. Physiol Plant 96: 6–12

Hideg E, Spetea C and Vass I (1994) Singlet oxygen and free radical production during acceptor- and donor-side-induced photoinhibition. Studies with spin trapping ERR spectroscopy. Biochim Biophys Acta 1186: 143–152

Hill R and Rich PR (1983) A physical interpretation for the natural photosynthetic process. Proc Natl Acad Sci USA 80: 978–982

Hope AB, Liggins J and Matthews DB (1988) The kinetics of reactions in and near the cytochrome *b/f* complex of chloroplast thylakoids. I. Proton deposition. Aust J Plant Physiol 15: 695–703

Hormann H, Neubauer C, Asada K and Schreiber U (1993) Intact chloroplasts display pH 5 optimum of O_2-reduction in the absence of methyl viologen. Indirect evidence for a regulatory role of superoxide protonation. Photosynth Res 37: 69–89

Horton P, Ruban AV and Walters RG (1996) Regulation of light harvesting in green plants. Annu Rev Plant Physiol Plant Mol Biol 47: 655–84.

Hundal T, Forsmark-Andrée P, Ernster L and Andersson B (1995) Antioxidant activity of reduced plastoquinone in chloroplast thylakoid membranes. Arch Biochem Biophys 324: 117–122

Huner NPA, Maxwell DP, Gray GR, Savitch LV, Krol M, Ivanov AG and Falk S (1996) Sensing environmental temperature change through imbalances between energy supply and energy consumption: Redox state of Photosystem II. Physiol Plant 98: 358–364

Ikegami I (1976) Fluorescence changes related in the primary photochemical reaction in the P_{700} enriched particles isolated from spinach chloroplasts. Biochim Biophys Acta 449: 245–258

Jakob B and Heber U (1996) Photoproduction and detoxification of hydroxyl radicals in chloroplasts and leaves in relation to photoinactivation of Photosystems I and II. Plant Cell Physiol 37: 629–635

Jansson S (1994) The light-harvesting chlorophyll *a/b*-binding proteins. Biochim Biophys Acta 1184: 1–19

Karpinski S, Escobar C, Karpinska B, Crerssen G and Mullineaux PM (1997) Photosynthetic electron transport regulates the expression of cytosolic ascorbate peroxidases genes in *Arabidopsis* during excess light stress. Plant Cell 9: 627–640

Khamis S, Lamaze T, Lemoine Y and Foyer C (1990) Adaptation of the photosynthetic apparatus in maize leaves as a result of nitrogen limitation. Plant Physiol 94: 1436–1443

Khan AU and Kasha M (1994) Singlet molecular oxygen in the Haber-Weiss reaction. Proc Natl Acad Ser USA 91: 12365–12367

Kleima FJ, Gradinaru CC, Calkoen F, Van Stokkum IHM, Van Grondelle R and Van Amerongen H (1997) Energy transfer in LHCII monomers at 77K studied by sub-picosecond transient absorption spectroscopy. Biochemistry 36: 15262–15268

Kleinherenbrink FAM, Hastings G, Wittmershaus BP and Blankenship RE (1994) Delayed fluorescence from Fe-S type photosynthetic reaction centers at low redox potential. Biochemistry 33: 3096–3105

Klughammer C and Schreiber U (1993) An improved method, using saturating light pulses, for the determination of Photosystem I quantum yield via $P\text{-}700^{+}$-absorbance changes at 830 nm. Planta 192: 261–268

Koyama Y (1991) Structures and functions of carotenoids in photosynthetic systems. J Photochem Photobiol B Biol 9: 265–280

Kramer DM and Crofts AR (1993) the concerted reduction of the high and low potential chains of the *bf* complex by plastoquinol. Biochim Biophys Acta 1183: 72–84

Kramer H and Mathis P (1980) Quantum yield and rate of formation of the carotenoid triplet state in photosynthetic structures. Biochim Biophys Acta 593: 319–329

Krause GH and Weis E (1991) Chlorophyll fluorescence and photosynthesis: The basics. Annu Rev Plant Physiol Plant Mol Biol 42: 313–349

Kühlbrandt W, Wang DN and Fujiyoshi Y (1994) Atomic model of plant light-harvesting complex by electron crystallography. Nature 367: 614–621

Kyle DJ (1987) The biochemical basis for photoinhibition of Photosystem II. In: Kyle DJ, Osmond CB and Arntzen CJ (eds) Photoinhibition. Photoinhibition, Topics of Photosynthesis, pp 197–226. Elsevier, Scientific Press, Amsterdam

Kyle DJ, Ohad I and Arntzen CJ (1985) Molecular mechanisms of compensation to light stress in chloroplast membranes. In: Key JL and Kosuge T (eds) Cellular and Molecular Biology of Plant Stress, pp 51–69. Liss, New York

Laisk A, Oja V, Rasulov B, Eichelmann H and Sumberg A (1997) Quantum yields and rate constants of photochemical and non-photochemical excitation quenching—Experiment and model. Plant Physiol 115: 803–815

Lancaster CRD and Michel H (1996) Three-dimensional structures

of photosynthetic reaction centers. Photosynth Res 48: 65–74
Logan BA, Grace SC, Adams WW III and Demmig-Adams B (1998a) Seasonal differences in xanthophyll cycle characteristics and antioxidants in *Mahonia repens* growing in different light environments. Oecologia 116: 9–17
Logan BA, Demmig-Adams B, Adams WW III and Grace SC (1998b) Antioxidants and xanthophyll cycle-dependent energy dissipation in *Cucurbita pepo* L.and *Vinca major* L. acclimated to four growth PPFDs in the field. J Exp Bot 49: 1869–1879
Macpherson AN, Telfer A, Barber J and Truscott TG (1993) Direct detection of singlet oxygen from isolated Photosystem II reaction centres. Biochim Biophys Acta 1143: 301–309
Marsho TV, Behrens PW and Radmer RJ (1979) Photosynthetic oxygen reduction in isolated intact chloroplasts and cells from spinach. Plant Physiol 64: 656–659
Mattoo AK, Marder JB and Edelman M (1989) Dynamics of the Photosystem II reaction center. Cell 56: 241–246
Maxwell DP, Laudenbach DE and Huner NPA (1995) Redox regulation of light-harvesting complex II and cab mRNA abundance in *Dunaliella salina.* Plant Physiol 109: 787–795
McCormac DJ, Bruce D and Greenberg BM (1994) State transitions, light-harvesting antenna phosphorylation and light-harvesting antenna migration in vivo in the higher plant *Spirodela oligorrhiza.* Biochim Biophys Acta Bioener 1187: 301–312
Mehler AH (1951) Studies on reactions of illuminated chloroplasts. I. Mechanisms of the reduction of oxygen and other Hill reagents. Arch Biochem Biophys 33: 65–77
Mehler AH and Brown AH (1952) Studies on reactions of illuminated chloroplasts. III. Simultaneous photoproduction and consumption of oxygen studied with oxygen isotopes. Arch Biochem Biophys 38: 365–370
Melis A (1996) Excitation energy transfer: functional and dynamic aspects of Lhc (cab) proteins. In: Ort DR and Yocum CF (eds) Oxygenic Photosynthesis, pp 523–538. Kluwer Academic Publishers, Dordrecht
Miller NJ, Sampson J, Candeias LP, Bramley PM and Rice-Evans CA (1996) Antioxidant activities of carotenes and xanthophylls. FEBS Lett 384: 240–242
Mishra NP and Fridovich I (1971) The generation of superoxide radical during the autooxidation of ferredoxin. J Biol Chem 246: 6886–6890
Mishra NP, Mishra RK and Singhal GS (1993) Involvement of active oxygen species in photoinhibition of Photosystem II: protection of photosynthetic efficiency and inhibition of lipid peroxidation by superoxide dismutase and catalase. J Photochem Photobiol B Biol 19: 19–24
Miyake C and Asada K (1992) Thylakoid-bound ascorbate peroxidase in spinach chloroplasts and photoreduction of its primary oxidation product monodehydroascorbate radicals in thylakoids. Plant Cell Physiol 33: 541–553
Miyake C and Asada K (1994) Ferredoxin-dependent photoreduction of the monodehydroascorbate radical in spinach thylakoids. Plant Cell Physiol 35: 539–549
Miyake C, Schreiber U, Hormann H, Sano S and Asada K (1996) Monodehydroascorbate radical reductase-dependent photoreduction of oxygen in chloroplast thylakoids. Plant Cell Physiol 37: s284
Miyashita H, Adachi K, Kurano N, Ikemoto H, Chihara M and Miyachi S (1997) Pigment composition of a novel oxygenic photosynthetic prokaryote containing chlorophyll *d* as the major chlorophyll. Plant Cell Physiol 38: 274–281
Neubauer C and Schreiber U (1989) Photochemical and non-photochemical quenching of chlorophyll fluorescence induced by hydrogen peroxide. Z Naturforsch 44C: 262–270
Neubauer C and Yamamoto HY (1992) Mehler-peroxidase reduction mediates zeaxanthin formation and zeaxanthin-related fluorescence quenching in intact chloroplasts. Plant Physiol 99: 1354–1361
Nishio JN and Whitmarsh J (1993) Dissipation of the proton electrochemical potential in intact chloroplasts. II. The pH gradient monitored by cytochrome *f* reduction kinetics. Plant Physiol 101: 89–96
Nitsch C, Braslavsky SE and Schatz GH (1988) Laser-induced optoacoustic calorimetry of primary processes in isolated Photosystem I and Photosystem II particles. Biochim Biophys Acta 934: 201–212
Noctor G, Rees D, Young A and Horton P (1991) The relationship between zeaxanthin, energy-dependent quenching of chlorophyll fluorescence and *trans*-thylakoid pH gradient in isolated chloroplasts. Biochim Biophys Acta 1057: 320–330
Nuijs AM, Shuvalov VA, van Gorkom HJ, Plijter JJ and Duysens LNM (1986) Picosecond absorbance difference spectroscopy on the primary reactions and the antenna excited states in Photosystem I particles. Biochim Biophys Acta 850: 310–318
Palsson LO, Flemming C, Gobets B, Grondelle R van, Dekker JP and Schlodder E (1998) Energy transfer and charge separation in Photosystem I: P700 oxidation upon selective excitation of the long wavelength antenna chlorophylls of *Synechococcus elongatus.* Biophys J 74: 2611–2622
Pearson CK, Wilson SB, Schaffer R and Ross AW (1993) NAD turnover and utilisation of metabolites for RNA synthesis in a reaction sensing the redox state of the cytochrome b_6/f complex in isolated chloroplasts. Eur J Biochem 218: 397–404
Peterman EJG, Dukker FM and van Amerongen H (1995) Chlorophyll *a* and carotenoid triple states in light-harvesting complex II of higher plants. Biophys J 69: 2670–2678
Peterson RB (1989) Partitioning of noncyclic photosynthetic electron transport to O_2-dependent dissipative processes as probed by fluorescence and CO_2. Plant Physiol 90: 1322–1328
Pfundel E and Bilger W (1994) Regulation and possible function of the violaxanthin cycle. Photosynth Res 42: 89–109
Polle A (1996) Mehler Reaction: Friend or Foe in Photosynthesis. Bot Acta 109: 84–89
Polm M and Brettel K(1998)Secondary pair charge recombination in Photosystem I under strongly reducing conditions: Temperature dependence and suggested mechanism. Biophys J 74: 3173–3181
Rich P (1982) A physicochemical model of quinone-cytochrome bc complex electron transfers. In: Trumpower BL (ed) Function of Quinones in Energy Conserving Systems, pp 73–86. Academic Press, New York
Robinson JM (1988) Does O_2 photoreduction occur within chloroplasts in vivo? Physiol Plant 72: 666–680
Rockholm DC and Yamamoto HY (1996) Violaxanthin de-poxidase. Purification of a43-kilodalton lumenal protein from lettuce by lipid-affinity precipitation with monogalactosyl-diacylglyceride. Plant Physiol 110: 697–703
Ruban AV, Phillip D, Young AJ and Horton P (1997) Carotenoid-dependent oligomerisation of the major chlorophyll *a/b* light-harvesting complex of Photosystem II of plants. Biochemistry 36: 7855–7859

Salin ML (1988) Toxic oxygen species and protective systems of the chloroplast. Physiol Plant 72: 681–689

Samson G and Bruce D (1995) Complementary changes in absorption cross-sections of Photosystems I and II due to phosphorylation and Mg^{2+}-depletion in spinach thylakoids. Biochim Biophys Acta 1232: 21–26

Savikhin S, Van Amerongan H, Kwa SLS, Van Grondelle R and Struve WS (1994) Low-temperature energy transfer in LHC-II trimers from the Chl *a/b* light-harvesting antenna of Photosystem II. Biophys J 66: 1597–1603

Scheller HV (1996) In vitro cyclic electron transport in barley thylakoids follows two independent pathways. Plant Physiol 110:187–194

Shen B, Jensen RG and Bohuent HJ (1997) Mannitol protects against oxidation byhydroxyl radicals. Plant Physiol 115: 527–532

Shipman LL (1980) A theoretical study of excitons in chlorophyll *a* photosystems on a picosecond timescale. Photochem Photobiol 31: 157

Siefermann D and Yamamoto HY (1975) Properties of NADPH and oxygen-dependent zeaxanthin apoxidation in isolated chloroplasts. Arch Biochem Biophys 171: 70–77

Siefermann-Harms D (1987) The light-harvesting and protective functions of carotenoids in photosynthetic membranes. Physiol Plant 69: 561–568

Simpson DJ and Knoetzel J (1996) Light-harvesting complexes of plants and algae: Introduction, survey and nomenclature. In: Ort DR and Yocum CF (eds) Oxygenic Photosynthesis: The Light Reactions, pp 493–506. Kluwer, Dordrecht

Sonoike K (1996a) Degradation of psaB gene product, the reaction center subunit of Photosystem I, is caused during photoinhibition of Photosystem I: Possible involvement of active oxygen species. Plant Sci (Shannon) 115: 157–164

Sonoike K (1996b) Photoinhibition of Photosystem I—Its physiological significance in the chilling sensitivity of plants. Plant Cell Physiol 37: 239–247

Sonoike K and Terashima I (1994) Mechanism of Photosystem I photoinhibition in leaves of *Cucumis sativus* L. Planta 194: 287–293

Sonoike K, Hamo M, Hihara Y, Hiyama T and Enami I (1997) The mechanism of the degradation of psaB gene products, one of the photosynthetic reaction center subunits of Photosystem I, upon photoinhibition. Photosynth Res 53: 55–63

Takahashi M and Asada K (1988) Superoxide production in the aprotic interior of chloroplast thylakoids. Arch Biochem Biophys 267: 714–722

Telfer A, Rivas JD and Barber J (1991) β-carotene within the isolated Photosystem-II reaction center—photooxidation and irreversible bleaching of this chromophore by oxidized P_{680}. Biochim Biophys Acta 1060: 106–114

Telfer A, Bishop SM, Phillips D and Barber J (1994a) Isolated photosynthetic reaction-center of Photosystem II as a sensitizer for the formation of singlet oxygen—detection and quantum yield determination using a chemical trapping technique. J Biol Chem 269: 13244–13253

Telfer A, Dhami S, Bishop SM, Phillips D and Barber J (1994b) β-carotene quenches singlet oxygen formed by isolated Photosystem II reaction centers. Biochemistry 33: 14469–14474

Terashima I, Funayama S and Sonoike K (1994) The site of photoinhibition in leaves of *Cucumis sativus* L at low temperatures is Photosystem I, not Photosystem II. Planta 193: 300–306

Tikhonov AN, Khomutov GB and Ruuge EK (1984) Electron transport control in chloroplasts. Effects of magnesium ions on the electron flow between two photosystems. Photobiochem Photobiophys 8: 261–269

Trebst A and Depka B (1997) Role of carotene in the rapid turnover and assembly of Photosystem II in *Chlamydomonas reinhardtii.* FEBS Lett 400: 359–362

Trissl HW (1997) Determination of the quenching efficiency of the oxidized primary donor of Photosystem I, P_{700}^{+}: Implications for the trapping mechanism. Photosynth Res 54: 237–240

Tschiersch H and Ohmann E (1993) Photoinhibition in *Euglena gracilis.* Planta 191: 316–323

Van Grondelle R, Dekker JP, Gillbro T and Sundström V (1994) Energy transfer and trapping in photosynthesis. Biochim Biophys Acta 1187: 1–65

Van Mieghem F, Nitschke W, Mathis P and Rutherford AW (1989) The influence of the quinone-iron electron acceptor complex on the reaction centre photochemistry of Photosystem II. Biochim Biophys Acta 977: 207–214

Van Mieghem F, Brettel K, Hillman B, Kamlowski A, Rutherford AW and Schlodder E (1995) Charge recombination reactions in Photosystem II. 1. Yields, recombination pathways, and kinetics of the primary pair. Biochemistry 24: 4798–4813

Verhoeven AS, Adams, WW, III and Demmig-Adams B (1996) Close relationship between the state of the xanthophyll cycle pigments and Photosystem II efficiency during recovery from winter stress. Physiologia Plantarum 96: 567–576

Whitmarsh J, Samson, G and Poulson M (1994) Photoprotection in Photosystem II—the role of cytochrome b_{559}. In: Baker NR, Bowyer JR (eds), Photoinhibition of Photosynthesis, pp 75–93, Bios, Oxford

Willekens H, Chamnongpol S, Davey M, Schraudner M, Langebartels C, Van Montagu M, Inzé D and Van Camp W (1997) Catalase is a sink for H_2O_2 and is indispensable for stress defense in C_3 plants. EMBO J 16: 4806–4816

Witt HT (1979) Energy conversion in the functional membrane of photosynthesis. Analysis by light pulse and electric pulse methods. The central role of the electric field. Biochim Biophys Acta 505: 355–427

Wydrzynski T, Ångström J and Vänngård T (1989) H_2O_2 formation by Photosystem II. Biochim Biophys Acta 973: 23–28

Yamamoto HY and Bassi R (1996) Carotenoids: localization and function. In: Ort DR and Yocum CF (eds) Oxygenic Photosynthesis: The Light Reactions, pp 539–563. Kluwer Academic Publishers, Dordrecht

Youngman RJ and Elstner EF (1981) Oxygen species in paraquat toxicity: The crypto-OH radical. FEBS Lett 129: 265–268

Zelitch I (1973) Plant productivity and the control of photorespiration. Proc Natl Acad Sci USA 10: 579–584

Zelitch I (1990) Oxygen resistant photosynthesis in tobacco plants selected for oxygen resistant growth. In: Zelitch I (ed), Perspectives in Biochemical and Genetic Regulation of Photosynthesis, pp 239–252. Alan R Liss Inc., New York

Ziem-Hanck K and Heber U (1980) Oxygen requirement of photosynthetic CO_2 assimilation. Biochim Biophys Acta 951: 266–274

This page intentionally left blank

Chapter 18

Novel and Biomimetic Functions of Carotenoids in Artificial Photosynthesis

Thomas A. Moore, Ana L. Moore and Devens Gust
Department of Chemistry and Biochemistry and Center for the Study of Earlay Events in Photosynthesis, Arizona State University, Tempe, AZ 85287-1604, U.S.A.

Summary

In addition to their universal occurrence in photosynthetic organisms, carotenoid pigments are important components of biomimetic photosynthetic constructs. Much of the photophysics and photochemistry including singlet energy transfer, triplet energy transfer, sequential electron transfer, radical pair recombination, spin states and spin dynamics observed in natural photosynthetic reaction centers and antennas can be mimicked by these constructs. In addition to playing a role in biomimetic energy and electron transfer processes, carotenoid pigments are essential components of artificial photosynthetic membranes where they participate in a redox-loop-based light-driven proton pump.

H. A. Frank, A. J. Young, G. Britton and R. J. Cogdell (eds): The Photochemistry of Carotenoids, pp. 327–339.

I. Introduction

Carotenoid pigments are found in organisms from many phyla and in all wild type photosynthetic bacteria, algae and higher plants examined to date. They are photochemically active in photosynthetic organisms and photochemically inert as pigments responsible for cryptic coloration in other living things (Moore et al., 1994). There is mounting evidence that in certain plants carotenoids may be the elusive blue light photoreceptors (Quiñones, 1996).

Within the last 25 years the salient features of carotenoid photophysics have been established and form a basis for understanding the varied role of these pigments in photobiology (Frank and Cogdell, 1987,1996; Koyama et al., 1996). This review focuses on photochemical studies of carotenoid-containing supramolecular structures that have been designed to mimic natural carotenoid functions and to explore roles for these pigments in the nascent field of molecular-level devices (Gust, 1994; Gust et al., 1994, 1997a; Leatherman, 1998). We begin with a brief review of carotenoid photophysics and function in photosynthetic membranes and follow with examples of biomimetic model systems. In the last section an artificial photosynthetic membrane is described in which the lipophilic nature of a carotenoid is used to direct assembly of the membrane and carotenoid redox chemistry is used to drive proton translocation by a quinone-based redox loop.

II. Carotenoid Photophysics

This discussion applies to the genre of carotenoid pigments having nine or more conjugated double bonds including oxy- and hydroxy-substituted compounds, although there are certainly small differences between pigments. The absorption of light in the 400–550 nm spectral region gives rise to their intense yellow-orange color. Carotenes typically have very high extinction coefficients ($\sim 10^5 M^{-1}cm^{-1}$) in this region. This strongly electric dipole allowed transition is from the ground state (S_0) to the *second* excited singlet state, S_2, of the carotenoid. As one would expect for an upper excited singlet state, the S_2 species has a very short lifetime (on the order of 200 fs or less)(Truscott, 1990; Shreve, et al., 1991, 1992; Kandori, et al., 1994; Macpherson and Gillbro, 1998). Because of the short lifetime, the quantum yield of fluorescence emission from this state is very low ($< 10^{-4}$) in spite of the strongly allowed nature of the transition and its correspondingly large radiative rate constant ($\sim 10^9$ s^{-1}). Surprisingly, this state is important as an energy donor in photosynthesis (Trautman et al., 1990; Ricci et al., 1996).

The transition from S_0 to the lowest excited singlet state of carotenoids, S_1, is electric dipole forbidden (Kohler, 1991), and is not observed in the usual single-photon absorption experiment. S_1 is readily populated by relaxation from S_2. The lifetime of the S_1 state, as measured by transient absorption techniques, is on the order of 10–40 ps for most carotenoids (Wasielewski and Kispert, 1986; Trautman et al., 1990). The state decays almost totally via internal conversion. Fluorescence from S_1 is virtually undetectable (quantum yield $<10^{-4}$), and intersystem crossing to the triplet state is not observed. Because the forbidden nature of the $S_0 \rightarrow S_1$ transition makes it very difficult to detect, the energy of the S_1 state is uncertain for most of the carotenoids involved in photosynthesis. The S_1 level of β-carotene has been reported at various values between ~650 and ~700 nm, based on different experimental techniques (Jones et al., 1992; Koyama et al., 1996)

Although carotenoid triplet states are not formed in appreciable yield by the usual intersystem crossing pathway, they can be produced via triplet-triplet energy transfer from other species or by radical pair recombination processes in artificial reaction centers (Gust et al., 1992; Liddell et al., 1997; Carbonera et al., 1998). Thus, their transient absorption characteristics are well known (Mathis and Kleo, 1973; Bensasson et al., 1976). Typically, they have strong absorption maxima at about 540 nm ($\varepsilon_T - \varepsilon_G \sim 1 = 10^5$ $M^{-1}cm^{-1}$). In most organic solvents in the absence of oxygen, carotenoid triplet states have lifetimes of 5–10 μs. Phosphorescence from these triplets has not been reported, and therefore the energies of the carotenoid triplet states have not been spectroscopically measured. Energy transfer studies have demonstrated that the energy of the lowest-lying carotenoid triplet is below that of singlet oxygen at ~ 1 .0 eV. Results from our laboratory obtained using a hybrid spectroscopic-calorimetric technique (photoacoustic spectroscopy) have located the lowest-

Abbreviations: ADP – adenosinediphosphate; ATP adenosinetriphosphate; Car – carotenoid; Chl – chlorophyll; EPR – electron paramagnetic resonance; Pi – inorganic phosphate

lying triplet state of a representative carotenoid (see structure **5** below) at 0.65 ±0.04 eV (Lewis et al., 1994). Thus, the expected origin of the phosphorescence would be about 1900 nm. In keeping with the dearth of emission from other carotenoid excited states, and in view of the rather low triplet energy and therefore strong nonradiative coupling to the ground state, it is unlikely that phosphorescence will be observed.

IV. Carotenoids in Natural Photosynthesis

A. Antenna Function

In the photosynthetic process Carotenoids play some roles that are ancillary to the basic energy conversion reactions and crucial to the protection of photosynthetic membranes from photochemical damage (Cohen-Bazire and Stanier,1958; Sieferman-Harms, 1987; Frank and Cogdell, 1996). As accessory light harvesting pigments carotenoids are found in the chlorophyll binding antenna proteins of photosynthetic organisms where they absorb light in the blue-green spectral region and transfer energy to nearby chlorophylls (Eqs. (1) and (2)).

$$\mathrm{Car} \xrightarrow{h\nu} {}^1\mathrm{Car} \qquad (1)$$

$${}^1\mathrm{Car} + \mathrm{Chl} \rightarrow \mathrm{Car} + {}^1\mathrm{Chl} \qquad (2)$$

Light energy collected in this way is funneled to special structures in the membranes known as reaction centers where energy conversion to electrochemical potential takes place.

B. Photoprotection

Under certain conditions most photosynthetic organisms unavoidably generate chlorophyll triplet excited states when exposed to light. Often, these are produced in the reaction center via recombination of charge-separated states. Chlorophyll triplet states are excellent sensitizers for formation of singlet oxygen from the oxygen ground-state triplet as per Eq. (3):

$${}^3\mathrm{Chl} + {}^3\mathrm{O}_2 \rightarrow \mathrm{Chl} + {}^1\mathrm{O}_2. \qquad (3)$$

Singlet oxygen, with an energy ~1 eV above the ground state, is a highly reactive species which can react with and destroy lipid bilayer membranes and other vital components of cells. Clearly, singlet oxygen production in photosynthetic organisms is potentially injurious (Krinsky, 1979; Cogdell and Frank, 1993). Such organisms have developed dual defense mechanisms based upon the low energy of the carotenoid triplet state mentioned above. Carotenes can quench chlorophyll triplet states at a rate which precludes singlet oxygen generation via a triplet-triplet energy transfer process (Eq. (4)). Additionally, carotenoids can quench singlet oxygen itself through energy transfer (Eq. (5)) or chemical reaction (Foote et al., 1970).

$${}^3\mathrm{Chl} + \mathrm{Car} \rightarrow \mathrm{Chl} + {}^3\mathrm{Car} \qquad (4)$$

$${}^1\mathrm{O}_2 + \mathrm{Car} \rightarrow {}^3\mathrm{O}_2 + {}^3\mathrm{Car}. \qquad (5)$$

Because the carotenoid triplet state is much lower in energy than singlet oxygen, it returns harmlessly to the ground state with the liberation of heat.

From this overview it is readily appreciated that carotenoids were selected by the evolving photosynthetic apparatus because of their unique photophysical properties. Their strong absorption is closely matched to the maximum of the solar flux yet their triplet levels are well below the energy of singlet oxygen.

C. Carotenoid Regulation of Photosynthesis

It has been found that carotenoid polyenes are involved in a mechanism whereby some photosynthetic organisms dissipate excess chlorophyll singlet excitation energy (Yamamoto, 1979; Demmig-Adams, 1992; Yamamoto and Bassi 1995; Horton et al., 1996). This process is sometimes referred to as non-photochemical quenching and it is measured by in vivo fluorescence spectroscopy of plant leaves. It comes into play at high light levels and evidently helps protect the organism from light-induced damage. Non photochemical quenching is signaled by the conversion of violaxanthin to zeaxanthin, but the details of the quenching process are as yet not understood.

V. Carotenoids in Biomimetic Systems

A. Mimicry of the Antenna Function of Carotenoids

As indicated in Eq. (2), in order to act as antennas for gathering light carotenoid pigments must transfer singlet excitation energy to nearby chlorophyll molecules. Singlet energy transfer from carotenoid to chlorophyll can occur by at leat two different pathways. At one limit, following absorption of light and internal conversion from S_2, the S_1 level of the carotenoid is populated and then transfers energy to the Q_y (S_1) of the chlorophyll. At the other limit, energy transfer from the S_2 level of the carotenoid to the Q_x (S_2) of the chlorophyll competes with internal coversion in the carotenoid. The short lifetime of the S_2 state of the carotenoid does not a priori exclude the second possibility. Indeed, detailed spectroscopic studies on the subpicosecond time scale of antenna protein complexes that make up the light-harvesting antennas of photosynthetic organisms suggest that in some cases energy transfer from the carotenoid to the chlorophyll or bacteriochlorophyll may occur from the carotenoid S_2 level rather that from the lower energy excited S_1 state as predicted by Kasha's Rule (Trautman et al., 1990; Shreve et al., 1991; Koyama, et al., 1996; Ricci et al., 1996; Krueger et al., 1998). The two pathways are shown schematically in Fig. 1.

However, the complexity of the natural systems containing multiple chromophores and the difficulty of the measurements on such a short time scale make the pathway assignments uncertain. Compounds **1** and **4** are examples of simple, well defined molecular dyads which were designed to help in the understanding of the carotenoid to chlorophyll singlet-singlet energy transfer process in natural systems.

Transient absorption and fluorescence experiments on **1** and **4** and the model carotenoid pigments **3** and **6** yielded convincing results about the energy transfer pathway (Fig 1) (A.L. Moore et al., unpublished). In **1**, the lifetime of S_2 was measured by fluorescence upconversion to be 45 fs, whereas the S_2 lifetime of model carotenoid **3** is 160 fs. The S_1 lifetime was 8 ps in both **1** and **3**. Moreover, the S_1 rise time for tetrapyrrole **2** was found to be 62 fs by fluorescence upconversion. Therefore, only the carotenoid S_2 state was quenched by the attached tetrapyrrole. The observation that the time constant associated with the decay of the energy donor(carotenoid S_2) matches

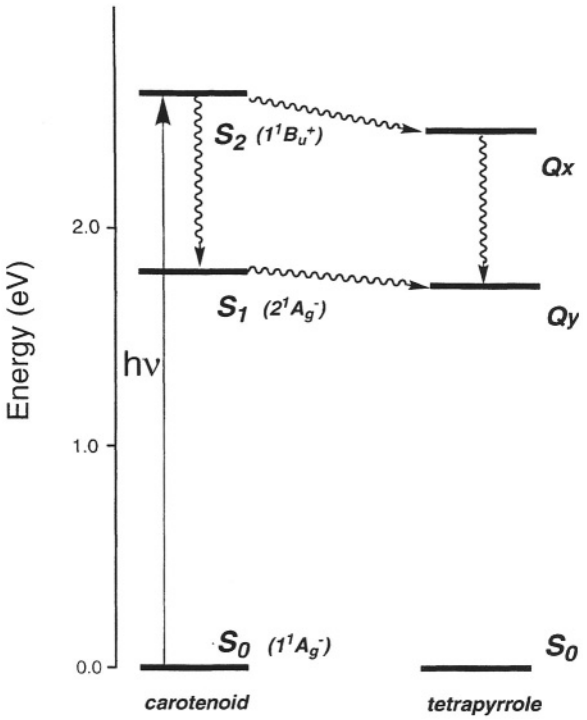

Fig. 1. Approximate energy levels for dyads **1** and **4** illustrating the two pathways for singlet energy transfer from the carotenoid to the tetrapyrrole moiety. The carotenoid S_1 levels have not been measured and the small difference between the levels of tetrapyrroles **2** and **5** is not shown.

that associated with the energy arrival at the acceptor (tetrapyrrole S_1) solidly demonstrates the S_2 energy transfer pathway. (The difference between carotenoid S_2 decay at 45 fs and tetrapyrrole S_1 rise at 62 fs is undoubtedly due to the delay associated with relaxation to the fluorescent state in the tetrapyrrole.) Quantitatively, quenching of the carotenoid S_2 state from 160 fs to 45 fs by energy transfer results in an efficiency of 70% which matches that measured by steady state fluorecence excitation spectroscopy.

Dyad **4** illustrates that both pathways can be active. In initial experiments on dyad **4** the attached tetrapyrrole was found to quench the carotenoid S_2 state of **6** from 95 to 28 fs and its S_1 level from 12 to 9 ps. The rise of the S_1 level of tetrapyrrole **5** as measured by fluorescence upconversion required a major exponential component (74%) of 41 fs^{-1} and a minor component (26%) of 4 ps^{-1}. While the match between the 9 ps decay of the carotenoid S_1 and the 4 ps rise component of the tetrapyrrole S_1 is only qualitative, these prelimenary experiments do provide evidence that both states can be energy donors.

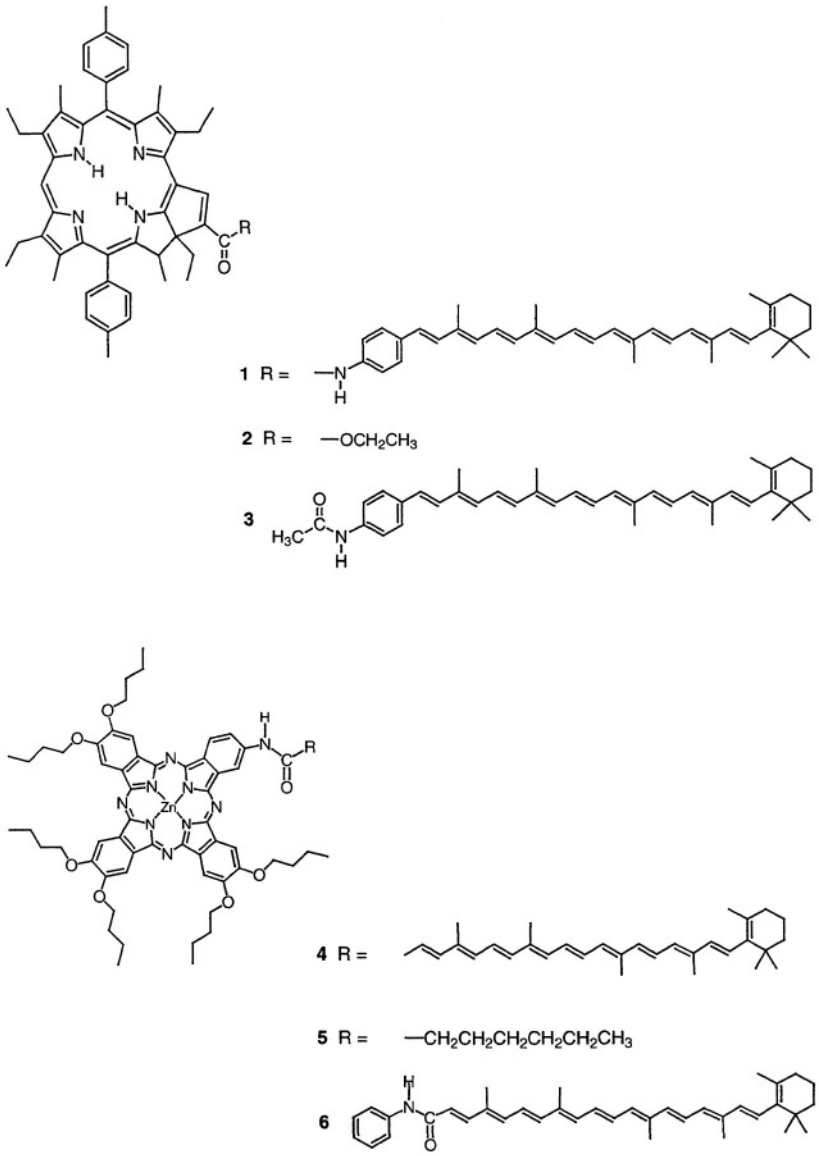

Taken together, the carotenoid S_2 and S_1 kinetic data give an overall quantum yield of energy transfer of ~ 80%, in qualitative agreement with that observed by steady state fluorescence excitation spectroscopy.

Why is the yield of the S_1 pathway different in **1** and **4**? There are undoubtedly subtle differences in the electronic coupling between the chromophores and the energy transfer energetics could be different. The S_1 level of the tetrapyrrole in **4** is about 270 cm^{-1} higher than that of **1**. Considering this small energy difference, the fact that the S_1 carotenoid band is expected to be rather broad (Frank et al., 1996), and that the S_1 levels of these carotenoids have not been measured but should be similar, the role of thermodynamics in controlling these energy transfer processes remains speculative.

B. Carotenoid Antennas for Non-photosynthetic Pigments

One of the clearest examples of the increased absorption cross section for a photochemical process provided by carotenoid pigments is that observed in carotenoid-buckminsterfullerene dyad **7** (Imahori et al., 1995). The carotenoid absorption spectrum is distinct and much stronger than that of the underlying C_{60} bands. Upon excitation of the carotenoid moiety of **7** with a 150 fs pulse of 600 nm laser light, the

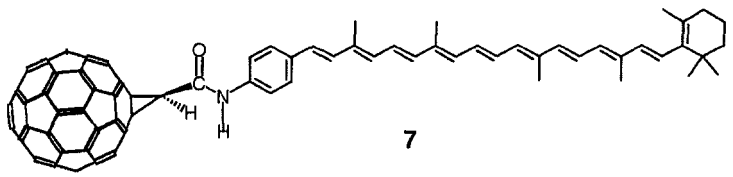

7

carotenoid radical cation forms in ~800 fs via photoinduced electron transfer to the fullerene to yield $C^{\bullet+}$-$C_{60}^{\bullet-}$. The charge separated species has a lifetime of ~500 ps and decays partially to the carotenoid triplet. Excitation of the carotenoid pigment leads to two routes to the charge separated species: energy transfer from the carotenoid to the C_{60} followed by photoinduced electron transfer to the C_{60} S_1 and direct photoinduced electron transfer from the carotenoid S_1 level. Although the contributions of the two pathways leading to $C^{\bullet+}$-$C_{60}^{\bullet-}$ could not be separated, the overall quantum yield for the formation of $C^{\bullet+}$-$C_{60}^{\bullet-}$ is unity. These results illustrate one way that primary photochemistry with a high yield can occur upon excitation of a carotenoid pigment and keep the door open to the suggestion that carotenoids can serve as blue light photoreceptors (Quiñones, 1996).

C. Mimicry of the Triplet Energy Transfer Relay and Charge Recombination to a Molecular Triplet.

Synthetic carotenoids incorporated into multicomponent sutructures such as triad **8** have been used as spectroscopic labels to follow the flow of triplet energy and the spin dynamics in model photosynthetic reaction centers. Excitation of the porphyrin moiety in **8** yields C-^{1}P-C_{60} which decays by photoinduced electron transfer to yield C-$P^{\bullet+}$-$C_{60}^{\bullet-}$. This state rapidly evolves into the final charge separated state, $C^{\bullet+}$-P-$C_{60}^{\bullet-}$ (Liddell et al., 1997). The fact that both electron transfer steps in **8** occur even in a glassy matrix at 77K has made it possible to observe some unusual and biologically relevant triplet-triplet energy transfer phenomena in the triads (Gust et al., 1997b). In triad **8** triplet energy is transfered from the fullerene moiety of C-P-$^3C_{60}$ (generated by intersystem crossing) to the carotenoid polyene, yielding ^{3}C-P-C_{60}. The transfer has been studied both in toluene at ambient temperatures and in 2-methyltetrahydrofuran at lower temperatures. The energy transfer is an activated process, with $E_a = 0.17$ eV. This is consistent with transfer by a triplet energy transfer relay, whereby energy first migrates from C-P-$^3C_{60}$ to the porphyrin, yielding C-^{3}P-C_{60} in a slow, thermally activated step. Rapid energy transfer from the porphyrin triplet to the carotenoid gives the final state. Triplet relays of this general kind have been observed in photosynthetic reaction centers, and are part of the system that protects the organism from damage by singlet oxygen, whose production is sensitized by chlorophyll triplet states (Gust et al., 1993; Krasnovsky et al., 1993).

As explained above, the $C^{\bullet+}$-P-$C_{60}^{\bullet-}$ state decays at 77 K to give the carotenoid triplet. EPR investigation of the signal from this triplet state shows that the spin polarization of ^{3}C-P-C_{60} is characteristic of a triplet formed by charge recombination of a singlet-derived radical pair. The kinetics of the decay of ^{3}C-P-C_{60} to the ground state were also determined, and the decay constants for the three triplet sublevels were measured. Similar spin states and dynamics which are the signature of radical pair recombination reactions have been observed in photosynthetic reaction centers but are unique to **8** (and close relatives) in the area of photosynthetic model systems (Carbonera et al., 1998). To aid in the interpretation of the EPR spectra

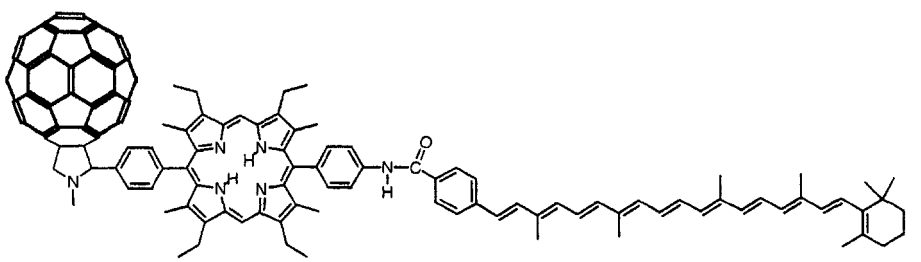

8

of the triads, we carried out several other studies on the EPR properties of carotene-porphyrin dyads (Carbonera, 1997a; Carbonera, 1997b).

D. Mimicry of Non-photochemical Quenching

Regarding the role of carotenoid pigments in non-photochemical quenching of photosynthesis mentioned in the introduction, it is interesting to compare **1** and **4**. Both demonstrate a high level of antenna function as measured by energy tranfer efficiencies of 70 to 80% which are similar to those observed in many natural systems. Regarding the tetrapyrrole singlet energies, the S_1 level of **1** is slightly lower than that of **4**. Although the carotenoid moities in **1** and **4** are different, and their S_1 levels are not known, there is no evidence from the observed absorption into S_2 that there are significant differences in their singlet energy levels. Interestingly, in **4** the tetrapyrrole fluorescence is quenched (by the attached carotenoid) ca. three-fold over that of **1**. This is consistent with a simple description of the tetrapyrrole energetics in that energy transfer quenching from the tetrapyrrole S_1 to the carotenoid would be more likely in **4** because its S_1 level is above that of the tetrapyrrole of **1**, and therefore more likely to be above that of the carotenoid S_1. However, this interpretation is inconsistent with the carotenoid S_1 state acting as an energy donor in **4** and not in **1**. If tetrapyrrole to carotenoid energy transfer in **4** is downhill, then carotenoid to tetrapyrrole energy transfer must be uphill and is more uphill in **4** than in **1**. Although we do not have an explanation for the quenching effect and enigmatic energy transfer behavior, **1** and **4** do illustrate that subtle changes in parameters such as the coupling between the pigments, their redox levels and their spectroscopic energies can modulate and direct the energy flow between carotenoids and tetrapyrroles.

What is the role of energy or electron transfer in the quenching of tetrapyrrole fluorescence by carotenoids? In other model studies the redox levels of a porphyrin-carotenoid dyad have been shown to influence the quenching mechanism to the extent that electron transfer from the carotenoid to the excited porphyrin was shown to occur (Hermant et al., 1993). However, in a series of carotenoid-porphyrin dyads in which the number of conjugated carbon-carbon double bonds in the carotenoid moiety was systematically increased from 7 to 11, quenching could not be assigned uniquely to either electron or energy transfer processes (Cardoso, 1996). Unfortunately, these model studies have not produced a definitive answer to the electron/energy transfer question.

E. Mechanistic Considerations

Regarding the role of carotenoids as antenna pigments, energy transfer from them to chlorophylls can be brought about by a variety of interactions. If the distance between the chromophores is larger than their transition dipole lengths and if the transition dipoles have sufficient strength and the correct orientation, and if the donor state has sufficient lifetime (usually expressed as fluorescence quantum yield), energy transfer may be decribed by the Förster mechanism (Förster, 1948). As the chromophores are brought closer together higher order electrostatic terms must be included in the electronic coupling matrix elements. The inclusion of these terms can relax the need for strong, dipole-allowed transitions and relatively long lived states in the donor and can satifactorily account for the carotenoid S_1 and S_2 levels acting as donor states (Nagae et al., 1993; Krueger et al., 1998). If the chromophores are brought into van der Waals contact so that there is orbital overlap between the donor and the acceptor, the Dexter electron exchange mechanism becomes important (Dexter, 1953).

The Dexter mechanism does not depend on dipole or mutipole strengths and is the accepted mechanism for triplet-triplet energy transfer. How fast can Dexter-mediated energy transfer be and to what extent do electron exchange-based electronic coupling matrix elements contribute to singlet energy transfer in these systems? In dyads **1** and **4** and several other carotenoid-containing multichromophoric molecules energy tranfer from the triplet tetrapyrrole to populate the carotenoid triplet state is remarkably fast. Due to kinetic constraints inherent to these dyads the actual rate cannot be determined. This is illustrated in Fig. 2(a) which presents the rise of the carotenoid triplet species (measured at 540 nm, spectrum shown in 2(b) taken 4 ns after excitation) following excitation of the porphyrin moiety of dyad **1** in methyl-tetrahydrofuran solution with a ~100 fs pulse of 510 nm light. The 1.50 ns rise time fit to the data is shown by the solid line. The fluorescence lifetime of **1** under the same conditions is 1.51 ns. The agreement between

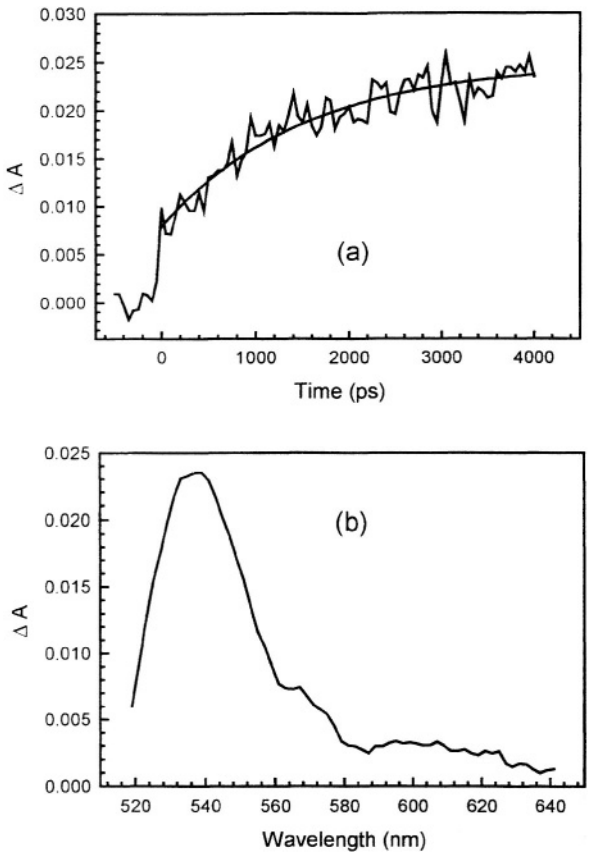

Fig. 2. (a) Rise of the carotenoid triplet species in dyad **1** following excitation with a ~ 100 fs pulse of 510 nm light. The sample was dissolved in 2-methyltetrahydrofuran at ~ 1 mM concentration and the triplet measured at 540 nm. (b) Spectrum of the carotenoid triplet species in dyad **1** taken 4 ns after excitation under the conditions of (2a).

the rise time of the triplet energy acceptor and the singlet lifetime of the triplet energy donor indicates that intersystem crossing in the donor is the rate limiting step in the flow of energy from the singlet of the donor to the triplet of the acceptor. In other words, the true rise time of the triplet carotenoid is much faster than intersystem crossing in the tetrapyrrole so that the carotenoid triplet is observed to rise with the singlet lifetime of the tetrapyrrole.

The final answer to the second part of the question awaits detailed quantum chemical calculations. In the mean time, it has been addressed experimentally in one study of three isomeric carotenoporphyrins in which singlet-singlet energy transfer efficiency (albeit at much lower efficiency than observed in dyads **1** and **4**) and triplet-triplet energy transfer rates were found to depend in the same way on the electronic structure of the interchromophore linkage group (Gust et al., 1992). Because the triplet energy transfer process is mediated by the linkage group via the Dexter mechanism, the simplest interpretation is that in those dyads the singlet energy transfer is also electron exchange mediated.

VII. The Evolution of Carotenoid Function in Photosynthesis

One may assume that carotenoids were selected by the evolving photosynthetic apparatus because of their unique photophysical properties. Three properties can be identified that stand out in this regard: a highly allowed absorption band in the 450 to 500 nm range where the solar flux is high for efficient light harvesting, an S_1 energy level that is highly forbidden (vide supra), and a lowest excited triplet state that is well below the energy of singlet oxygen ($^1\Delta_g$, 0.98 eV) so that Eq. (5) is irreversible. Notwithstanding the fact that the highly allowed absorption band near the solar irradiance maximum accounts for between one fourth and one half of the sunlight that drives photosynthesis on the earth, the crucial role of carotenoids in photosynthesis today is undoubtedly to protect photosynthetic organisms from the deleterious effects of singlet oxygen.

It is interesting to speculate about the evolutionary origin of photoprotection and the link between photoprotection and the highly forbidden carotenoid S_1 level (Moore et al., 1990). From the earliest photosynthetic organisms until the evolution of oxygen production (2.2 ~ 3.5 billion years ago), atmospheric oxygen levels were extremely low; there would have been no need for protection from singlet oxygen under these conditions. However, it is almost certain that photosynthetic organisms evolving during this time used carotenoids as light harvesting pigments. In order to do so, chlorophyll and carotenoid binding proteins evolved in which singlet energy transfer from carotenoids to chlorophylls was efficient. Because of the forbidden nature of the carotenoid S_1 level efficient energy transfer required extensive electronic coupling between the pigments. In fact, it appears that efficient energy transfer required electronic coupling sufficient to allow energy transfer from S_2 with a rate constant $\geq 10^{13} s^{-1}$. In order to achieve this coupling, the pigments had to be essentially in contact with one another which, as it

turns out, is exactly the requirement for triplet energy transfer by the Dexter mechanism. Thus, even before it was needed to suppress singlet oxygen sensitization, triplet-triplet energy transfer as shown in Eq. (4) was fast. In other words, because of the forbidden nature of S_1 (and the short lifetime of S_2) the evolutionary pressure to acquire efficient singlet energy transfer drove the system into a coupled state in which Dexter-based triplet energy transfer is facile.

VIII. Carotenoids in Artificial Photosynthesis

A. Carotenoids in Artificial Reaction Centers

The conversion of solar energy to chemical potential in photosynthetic reaction centers begins with photoinduced electron transfer. A prototype reaction center must contain pigments capable of absorbing visible light and either reducing an electron acceptor (A) or oxidizing an electron donor (D). In a dyad in which the pigment acts as the donor, excitation yields, for example, ^{1}D-A, which undergoes photoinduced electron transfer to give $D^{\bullet+}$-$A^{\bullet-}$. Such systems can generate charge separation with a quantum yield of essentially unity while preserving a large part of the photon energy as intramolecular redox potential. However, rapid charge recombination to the ground state, which usually occurs on the subnanosecond time scale, releases the stored energy as heat; it is difficult to imagine intermolecular energy-conserving processes that can compete with this degradation.

In the early 1980s we designed an artificial photosynthetic reaction center that overcomes this problem by using a multistep electron transfer strategy such as that found in natural reaction centers (Moore et al, 1984). More recently, molecular triad **9** which consists of a porphyrin chromophore (P) bound covalently to a naphthoquinone derivative (NQ) and a carotenoid electron donor (C) was designed both to undergo multistep electron transfer and to organize itself in a bilayer lipid membrane. These two characteristics are discussed below.

Excitation of the porphyrin moiety of **9** leads to C–^{1}P-NQ, which decays by photoinduced electron transfer to give C-$P^{\bullet+}$-$NQ^{\bullet-}$ with a quantum yield near unity. Competing with charge recombination, a second electron transfer from the carotenoid to the porphyrin radical cation occurs, yielding a $C^{\bullet+}$-P-$NQ^{\bullet-}$ charge-separated state. In this state, the radicals are separated by the neutral porphyrin moiety, and therefore charge recombination is slower by several orders of magnitude than that of a comparable dyad. We have used this strategy in a variety of other reaction center mimics, some of which rival the natural systems in terms of quantum yield, fraction of energy stored, and lifetime for charge separation (Gust and Moore, 1991; Gust et al., 1993).

It has been demonstrated that under certain conditions triad **9** inserts unidirectionally into a liposomal phospholipid bilayer membrane (Steinberg-Yfrach, 1997). How can this observation be rationalized? Triad **9** is highly amphiphilic due to the hydrophobic carotenoid pigment distal to the carboxylate group which is attached to the naphthoquinone. When a small amount of **9** dissolved in a suitable solvent such as tetrahydofuran is added to an aqueous solution of liposomes the amphiphilic molecules associate with the membrane. It is likely that the most stable association is with the hydrophobic carotenoid moiety in the low-dielectric interior of the bilayer and the hydrophilic carboxylate group at or near the aqueous interface. Because **9** is added from the bulk aqueous phase on the outside of the liposomal bilayer, the expected initial arrangement would be vectorial with the majority of triads having their carboxylate-bearing naphthoquinones near the bulk aqueous phase as shown schematically in Fig. 3. The energetic cost of transporting the carboxylate across the bilayer would slow, but not prevent, flip-flop diffusion which would ultimately randomize the orientation.

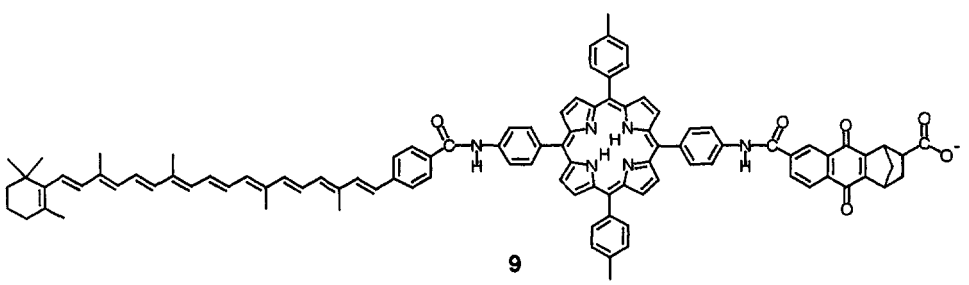

9

B. Artificial Proton Pump

The availability of artificial reaction centers which self assemble vectorially into bilayer lipid membranes makes it possible to design a proton pump which would generate a transmembrane gradient in proton electrochemical potential (pmf), the next step in converting solar energy to a biologically useful form (Steinberg-Yfrach, 1997). In order to couple the vectorial redox potential in the species $C^{\bullet+}$-P-$NQ^{\bullet-}$ to proton translocation, a lipophilic collateral quinone (2,5-diphenylbenzoquinone, Qs) was incorporated into the liposomal bilayer where it functions as a shuttle for protons across the bilayer. As shown diagrammatically in Fig. 3, excitation of **9** generates the $C^{\bullet+}$-P-$NQ^{\bullet-}$ charge-separated state via the multistep electron transfer process described above. The redox potential of $C^{\bullet+}$-P-$NQ^{\bullet-}$ drives a redox loop in which the reduced (protonated) form of Qs carries protons inwards and the oxidized (unprotonated) form of Qs completes the loop by equilibrating across the membrane. Proton import has been monitored both by trapping a pH-sensitive fluorescent dye, pyranine trisulfonate, inside the liposome and by the use of 8-aminoacridine to measure ΔpH directly. Illumination of the liposomes with light absorbed by the porphyrin moiety of **9** leads to a change in the fluorescence of the dye, which signals import of protons into the liposome to establish a pmf across the bilayer. Fluorescence quenching of the 9-aminoacridine indicates that a ΔpH of ca. 2 is readily attained. The pH gradient thus generated can be relaxed by addition of an ionophore such as FCCP. The photochemical import of protons is enhanced by the addition of potassium and valinomycin which presumably reduce the uncompensated charge buildup in the intraliposomal volume. Thus, a photocyclic transmembrane proton pump has been assembled.

C. ATP Synthesis

In order to demonstrate that the pmf generated by the artificial photosynthetic membrane is sufficient to carry out biochemical work, the CF_0F_1-ATP synthase from spinach chloroplast thylakoids was reconstituted into liposomes containing the components of the light-driven proton pump discussed above (Steinberg-Yfrach, 1998). As illustrated in Fig. 3, the enzyme is inserted into the bilayer with the ATP-synthesizing portion extending out into the external aqueous solution. Thioredoxin is added to activate the enzyme, and ADP, Pi and an initial amount of ATP are added to the external phase. The liposomes are illuminated for various periods of time with laser light at 633 nm, which is absorbed only by the triad. Illumination is terminated, and the ATP produced is measured using a calibrated luciferin/luciferase luminescence assay.

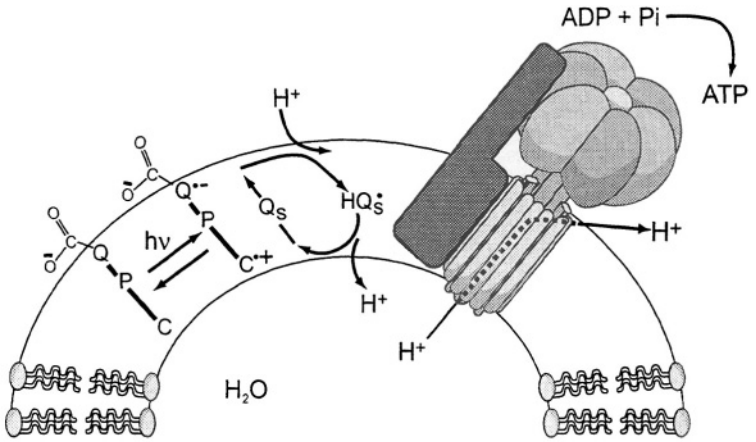

Fig. 3. Schematic diagram of a liposome-based artificial photosynthetic membrane including the photocycle that pumps protons into the interior of the liposome and the CF_0F_1-ATP synthase enzyme. The detailed mechanism of the redox-loop-based proton pump has not been established. The steps presented in Fig. 3 merely illustrate the function of the photocycle and are not intended to preclude the involvement of other oxidation states of these species or the transport of hydrogen atoms by self-exchange reactions among the Qs molecules. Each proteoliposome contained ~1 spinach chloroplast CF_0F_1-ATPase, ~1×10^3 molecules of triad **9**, and ~ 500 molecules of Qs. The liposomes were prepared from a mixture of egg phosphatidylcholine and egg phosphatidic acid (10:1 by weight) plus cholesterol (20 mole percent). The bulk aqueous phase contained 16 mM Na_2SO_4 and 2.5 mM $MgSO_4$, and was buffered by 16 mM tricine and 5 mM KH_2PO_4 to a pH of 8. The intraliposomal volume contained 2 mM tricine and 40 mM Na_2SO_4 with the pH adjusted to 8 prior to liposome formation. Oxygen was removed from the cuvette by flowing argon.

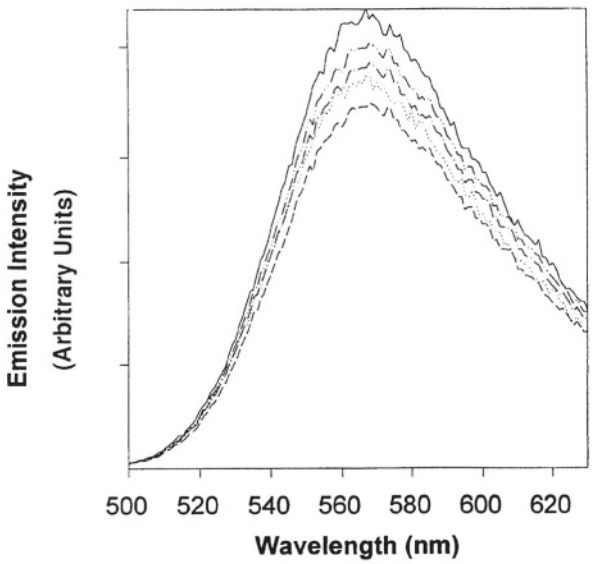

Fig. 4. The [ATP]-dependent steady-state luminescence of oxyluciferin measured as a function of liposome irradiation times of 0 min (-----), 17 min (·····), 30 min (–·–·–·), 45 min (–··–··–··), and 60 min (——). The irradiation source was a 5 mW beam of 633 nm light from a HeNe laser, and the sample volume was 250 μL. The laser beam diameter was expanded to ~ 10 mm, but no effort was made to provide uniform intensity across the cuvette; this level of actinic light saturated the rate of synthesis of ATP. In this experiment, the ATP and ADP concentrations prior to irradiation were ~ 2×10^{-4} M and Pi was 5×10^{-3} M. Oxygen was removed from the cuvette by flowing argon.

The results of a typical experiment are shown in Fig. 4. In this experiment, both the ATP and ADP concentrations prior to illumination were 200 μM, and the Pi concentration was 5 mM. The figure shows the oxyluciferin luminescence spectrum recorded as a function of illumination time. The increase in luminescence with exposure to actinic light is clear evidence of an increase in ATP concentration with illumination.

Quantitative measurements show that at low levels of illumination, where ATP synthesis is limited by light absorption, the quantum yield of ATP is about 15% (assuming approximately 50% of the light is absorbed by the scattering liposome solutions). Assuming that four protons must be transported out of the liposome by ATP synthase per molecule of ATP produced, the yield of the proton pump must be ~0.6. The turnover number for the enzyme, measured under saturating illumination and optimal conditions, is ca. 40 molecules of ATP per CF_0F_1-ATP synthase per second.

The liposome system can synthesize ATP against considerable ATP chemical potential. Under the conditions of 200 mM ATP, 200μM ADP and 5 mM Pi, ATP is synthesized against a potential of ~15 kcal/mol. By increasing the ratio of [ATP]/[ADP] until the net synthesis of ATP ceases for thermodynamic reasons, a limiting ΔG of ~ 16 kcal/mol was determined. Similar experiments using thylakoid membranes isolated from spinach yielded essentially the same limiting ΔG for ATP synthesis. Remarkably, the artificial membrane converts light energy to chemical potential under conditions similar to those of the energy transducing membranes of living organisms.

IX. Conclusions

Carotenoids play myriad roles in photobiology and are crucial components of photosynthetic membranes. The key photophysical functions of Carotenoids in photosynthesis have been mimicked in model systems. Furthermore, it is possible to mimic the basic features of energy conversion in bacterial photosynthetic membranes in a mostly artificial, 'bionic' construct which employs carotenoid pigments as essential components of artificial reaction centers. Optimization of such systems could provide solar biological 'power packs' that might be used to drive the enzymatic synthesis of other high-energy or high-value compounds, or power natural or artificial nanoscale 'machines.' Both scientific and practical uses of such modules can be envisioned.

Acknowledgments

The authors gratefully acknowledge the contributions of the students, colleagues and collaborators who helped carry out this research and who are listed as authors of the cited references. This work was supported by grants from the Office of Basic Energy Sciences, U. S. Department of Energy (DE-FG03-93ER14404) and the National Science Foundation (CHE-9709272).

References

Bensasson R, Land EJ and Maudinas B (1976) Triplet states of carotenoids from photosynthetic bacteria studied by nanosecond ultraviolet and electron pulse irradiation. Photochem Photobiol 23: 189–193

Cardoso SL, Nicodem DE, Moore TA, Moore AL and Gust D (1996) Synthesis and fluorescence quenching studies of a

series of carotenoporphyrins with carotenoids of various lengths. J Braz Chem Soc 7: 19–29

Carbonera D, Di Valentin M, Corvaja C, Giacometti G, Agostini G, Liddell PA, Moore AL, Moore TA and Gust D (1997a) Carotenoid triplet detection by time resolved EPR spectroscopy in carotenopyropheophorbide dyads. *J* Photochem Photobiol A: Chem 105: 329–335

Carbonera D, De Valentin M, Agostini G, Giacometti G, Liddell PA, Gust D, Moore AL and Moore TA (1997b) Energy transfer and spin polarization of the carotenoid triplet state in synthetic carotenoporphyrin dyads and in natural antenna complexes. Applied Magn Reson 13: 487–504

Carbonera D, Di Valentin M, Corvaja C, Agostini G, Giacometti G, Liddell PA, Kuciauskas D, Moore AL, Moore TA and Gust D. (1998) EPR investigation of photoinduced radical pair formation and decay to a triplet state in a carotene-porphyrin-fullerene triad. J Am Chem Soc 120: 4398–4405

Cogdell RJ and Frank HA (1993) Photochemistry and function of carotenoids in photosynthesis. In: Young A and Britton G (eds) Carotenoids in Photosynthesis, pp 252–326. Chapman and Hall, London

Demmig-Adams B (1992) Operation of the xanthophyll cycle in higher plants in response to diurnal changes in incident sunlight. Planta 186: 390–398

Dexter DL (1953) A theory of sensitized luminescence in solids. J Chem Phys 21: 836–860

Foote CS, Chang YC and Deeny RW (1970) Chemistry of singlet oxygen. X. Carotenoid quenching parallels biological protection. J Am Chem Soc 92: 5216–5218

Frank HA and Cogdell RJ (1987) How carotenoids function in photosynthetic bacteria. Biochim Biophys Acta 895: 63–79

Frank HA and Cogdell RJ (1996) Carotenoid in photosynthesis. Photochem Photobiol 63: 257–264

Frank H, Cua A, Chynwat V, Young A, Gosztola D and Wasiele wski M R (1996) The lifetimes and energies of the first excited singlet states of diadinoxanthin and diatoxanthin: the role of these molecules in excess energy dissipation in algae. Biochim Biophys Acta 1277 243–252

Förster T (1948) Intermolecular energy transfer and fluorescence. Ann Phys 2: 55–75

Cohen-Bazire G and Stanier RY (1958) Inhibition of carotenoid synthesis in photosynthetic bacteria. Nature 181: 250–252

Gust D (1994) Molecular wires and girders. Nature 372: 133–134

Gust D and Moore TA (1991) Mimicking photosynthetic electron and energy transfer. Advances in Photochemistry 16: 1–65

Gust D, Moote TA and Moore AL(1993) Molecular mimicry of photosynthetic energy and electron transfer. Ace Chem Res 26: 198–205

Gust D, Moore TA, Moore AL, Devadoss C, Liddell PA, Hermant R, Nieman RA, Demanche LJ, DeGraziano JM and Gouni I (1992) Triplet and singlet energy transfer in carotene-porphyrin dyads: the role of the linkage bonds. J Am Chem Soc 114: 3590–3603

Gust D, Moore TA, Moore AL, Krasnovsky AA, Jr, Liddell PA, Nicodem D, DeGraziano JM, Kerrigan P, Makings LR and Pessiki PJ (1993) Mimicking the photosynthetic triplet energy transfer relay. J Am Chem Soc 115: 5684–5691

Gust D, Moore TA and Moore AL(1994) Photosynthesis mimics as molecular electronic devices. IEEE Engineering in Medicine and Biology, February/March pp 58–66

Gust D, Moore TA and Moore AL (1997a) Photosynthesis as a paradigm for molecular-scale electronics. Molecular Nanotechnology—Biological Approaches and Novel Applications, IBC, Southborough, MA, Ch. 2.1, 2.1.1–2.1.39

Gust D, Moore TA, Moore AL, Kuciauskas D, Liddell PA and Halbert BD (1997b) Mimicry of carotenoid photoprotection in artificial photosynthetic reaction centers: Triplet-triplet energy transfer by a relay mechanism. *J.* Photochem Photobiol 43: 209–216

Hermant RM., Liddell PA, Lin S, Alden RG, Kang HK, Moore A, Moore TA and Gust D (1993) Mimicking carotenoid quenching of chlorophyll fluorescence. J Am Chem Soc 115: 2080–2081

Horton P, Ruban AV and Walters RG (1996) Regulation of light harvesting in green plants. Annu Rev Plant Physiol Plant Mol Biol 47: 655–684

Imahori H, Cardoso S, Tatman D, Lin S, Macpherson AN, Noss L, Seely GR, Sereno L, Chessa de Silber J, Moore TA, Moore AL and Gust D (1995) Photoinduced electron transfer in a carotenobuckminsterfullerene dyad. Photochem Photobiol 62: 1009–1014

Jones PF, Jones WJ and Davies BH (1992) Direct observation of the $2.^1A_g^-$ electronic state of carotenoid molecules by consecutive two-photon absorption spectroscopy. *J.* Photochem Photobiol A: Chem. 68: 59–75

Kandori H, Sansabe H, and Mimuro M, (1994) Direct determination of the lifetime of the S_2 state of β-carotene by femtosecond time-resolved fluorescence spectroscopy. J Am Chem Soc 116: 2671–2672

Kohler BE (1991) Electronic properties of linear polyenes. In Bredas JL and Silbey R, (eds) Conjugated Polymers, pp 405–434. Kluwer Academic Publishers, Dodrecht

Koyama Y, Kuki M, Andersson PO and Gillbro T (1996) Singlet excited states and the light-harvesting function of carotenoids in bacterial photosynthesis. Photochem Photobiol 63: 243–256

Krasnovsky Jr, AA, Cheng P, Blankenship RE, Moore TA and Gust D (1993) The photophysics of monomeric bacterio–chlorophylls *c* and *d* and their derivatives: Properties of the triplet state and singlet oxygen photogeneration and quenching. Photochem Photobiol 57: 324–330

Krinsky NI (1979) Carotenoid protection against oxidation. Pure Appl Chem 51: 649–660

Krueger BP, Scholes GD, Jimenez R, and Fleming GR (1998) Electronic excitation transfer from carotenoid to bacterio-chlorophyl in the purple bacterium Rhodopseudomonas acidophila. J Phys Chem, 102: 2284–2292

Leatherman G, Durantini EN, Gust D, Moore TA, Moore AL, Stone S, Zhou Z, Rez P, Liu Y, and Lindsay SM (1999) Carotene as a molecular wire: Conducting atomic force microscopy. J Phys Chem, in press

Lewis JE, Moore TA, Benin D, Gust D, Nicodem D and Nonell S (1994) The triplet energy of a carotenoid pigment determined by photoacoustic calorimetry. Photochem Photobiol 59S: 35S

Liddell PA, Kuciauskas D, Sumida JP, Nash B, Nguyen D, Moore AL, Moore TA, and Gust D (1997) Photoinduced Charge Separation and Charge Recombination to a Triplet State in a Carotene-Porphyrin-Fullerene Triad. J Am Chem Soc 119: 1400–1405

Macpherson AN and Gillbro T (1998) Solvent dependence of the ultrafast S_2-S_1 internal conversion rate of β-carotene. J Phys

Chem 102: 5049–5058
Mathis P and Kleo J (1973) The triplet state of β-carotene and of analog polyenes of different length. Photochem Photobiol 18: 343–346
Moore TA, Gust D, Mathis P, Mialocq J-C, Chachaty C, Bensasson RV, Land EJ,. Doizi D, Liddell PA, Lehman WR, Nemeth GA, and Moore AL (1984) Photodriven charge separation in a carotenoporphyrin-quinone triad. Nature 307: 630–632
Moore TA, Gust D and Moore AL (1990) The function of carotenoid pigments in photosynthesis and their possible involvement in the evolution of higher plants. In: Krinsky NI, Mathews-Roth MM and Taylor RF, (eds) Carotenoids: Chemistry and Biology, pp. 223–228. Plenum Press, New York
Moore TA, Gust D and Moore AL (1994) Carotenoids: Nature's unique pigments for light and energy processing. Pure Appl Chem 66: 1033–1040
Nagae H, Kakitani T, Katoh T, and Mimuro M (1993) Calculation of the excitation transfer matrix elements between the S_2 or S_1 state of carotenoid and the S_2 or S_1 state of bacteriochlorophyll. J Chem Phys 98: 8012–8023
Quiñones MA, Lu Z and Zeiger E (1996) Close correspondence between the action spectra for the blue light responses of the guard cell and coleoptile chloroplasts, and the spectra for blue light-dependent stomatal opening and coleoptile phototropism. Proc Natl Acad Sci USA 93: 2224–2228
Ricci M, Bradforth SE, Jimenez R, and Fleming GR. (1996) Internal conversion and energy transfer dynamics of spheroidene in solution and in the LH-1 and LH-2 light-harvesting complexes. Chem Phys Lett 259: 381–390
Shreve AP, TrautmanJK, Owens TG, and Albrecht AC (1991) Determination of the S_2 lifetime of β-carotene. Chem Phys Lett 178: 89–96
Shreve AP, Trautman JK, Frank HA, Owens TG, and Albrecht AC (1991) Femtosecond energy-transferprocesses in the B800-850 light-harvesting complex of *Rhodobacter sphaeroides* 2.4.1. Biochim Biophys Acta 1058: 280–288
Shreve AP, Trautman JK, Frank HA, Owens TG, van Beek JB and Albrecht AC (1992) On subpicosecond excitation energy transfer in light harvesting complexes (LHC): The B800-B850 LHC of *Rhodobacter sphaeroides* 2.4.1. J Lumin 53: 179–186
Steinberg-Yfrach G, Liddell PA, Hung S-C, Moore AL, Gust D and Moore TA (1997) Conversion of light energy to proton potential in liposomes by artificial photosynthetic reactions centres. Nature 385: 239–241
Steinberg-Yfrach G, Rigaud J-L, Durantini EN, Moore AL, Gust D and Moore TA (1998) Light-driven production of ATP catalyzed by F_oF_1-ATP synthase in an artificial photosynthetic membrane. Nature 392: 479–482
Sieferman-Harms D (1987) The light-harvesting and protective functions of carotenoids in photosynthetic membranes. Physiol Plant 69: 561–568
Trautman JK, Shreve AP, Owens TG and Albrecht AC (1990) Femtosecond dynamics of carotenoid-to-chlorophyll energy transfer in thylakoid membrane preparations. Chem Phys Lett 166: 369–374
Truscott TG (1990) The photophysics and photochemistry of the carotenoids. Photochem Photobiol B Biol 6: 359–371
Wasielewski MA and Kispert LD (1986) Direct measurement of the lowest excited singlet state lifetime of all-trans-β-carotene and related carotenoids. Chem Phys Lett 128: 238–243
Yamamoto H Y and Bassi R (1995) Carotenoids: localization and function. In Oxygenic Photocynthesis: The Light Reactions Ort DR and Yocum CF (eds) Advances in Photosynthesis, Kluwer Academic Publishers, Dordrecht
Yamamoto HY (1979) Biochemistry of the violaxanthin cycle. Pure Appl Chem 51: 639–64

This page intentionally left blank

Chapter 19

Physical Properties of Carotenoids in the Solid State

Hideki Hashimoto
Department of Materials Science and Chemical Engineering, Faculty of Engineering, Shizuoka University, 5-1 Johoku 3-chome, Hamamatsu 432-8561, Japan

H. A. Frank, A. J. Young, G. Britton and R. J. Cogdell (eds): The Photochemistry of Carotenoids, pp. 341–361.

Summary

Physical properties of carotenoids in solid states are introduced and the effect induced by intermolecular interactions is discussed. Phenomena which can only be identified in the crystals are emphasized. First, the physical properties of carotenoids in thin-solid films are shown. Simple but reliable methods to determine the optical constants of two familiar thin-solid films, i.e., a spin-coated film and a Langmuir-Blodgett film, are shown, and molecular orientation in these films is discussed. Second, X-ray crystallography on all-*trans*-β-carotene single crystals is shown, and the effect induced by raising the crystal temperature is discussed. Third, optical properties of all-*trans*-β-carotene in the condensed phase are shown, and the effect of intermolecular interactions is discussed. In addition, observation of the optically forbidden $2^1A_g \leftarrow A_g$ transition specifically in the crystals is demonstrated. Finally, transient optical properties of all-*trans*-β-carotene single crystals are shown. Observation of solitonlike excitations, which have been found in one-dimensional conducting polymers and play the crucial roles of energy- and charge-carrying excitations, is demonstrated.

I. Introduction

Photosynthetic systems can be thought of as bio-devices which can effectively convert the light energy into chemical potential. They also have a protective function against the drastic change of the environment, i.e., the dissipation of excess energy as heat. It is well-known that photosynthesis is a reaction that produces carbohydrates and oxygen from water and carbon dioxide utilizing light energy from the sun. In order to perform this function effectively, biological molecules such as carotenoids and chlorophylls, which have specific chain-lengths and ring structures, are selected. These photosynthetic pigments bind to apo-proteins and form pigment-protein complexes needed to perform the physiological functions. Crystallographic analyses on light-harvesting complexes (Kühlbrandt et al., 1994; Karrasch et al., 1995; McDermott et al., 1995) and reaction centers (Deisenhofer and Michel, 1989) enabled us to visualize the structures of these complexes. It was shown that the specific spatial arrangement of the pigment molecules, is important in performing the effective physiological functions. Understanding of the effect of intermolecular interactions which governs the spatial arrangement of the pigment molecules is one of our primary objectives. One of the ways to examine the intermolecular interactions is to determine the structures of pigment molecules in the condensed phase and to correlate them with the physical properties.

Molecular properties of carotenoids are well studied because of their physiological significance in photosynthesis as mentioned above. However, their physical properties in the condensed phase have yet to be explored. This chapter is intended to introduce the readers in a concise way to these properties of carotenoids. Results of solid samples fabricated using all-*trans*-β-carotene. In Section II, the physical properties of carotenoids in thin-solid films are introduced. Simple but reliable methods to determine the optical constants of two familiar thin-solid films, i.e., a spin-coated film and a Langmuir-Blodgett film, are shown, and molecular orientation in these films is discussed. In Section III, X-ray crystallography on all-*trans*-β-carotene single crystals is shown, and the effect induced by raising the crystal temperature is discussed. In Section IV, optical properties of all-*trans*-β-carotene in the condensed phase are shown, and the effect of the intermolecular interactions is discussed. In addition, observation of the optically forbidden $2^1A_g \leftarrow A_g$ transition specifically in the crystals is demonstrated. Finally, in Section V, transient optical properties of all-*trans*-β-carotene single crystals are shown. Observation of solitonlike excitations, which have been found in one-dimensional conducting polymers and play the crucial roles of energy- and charge-carrying excitations, is demonstrated

Abbreviations: EPR – electron paramagnetic resonance; HE – high-energy; IPS–isopentane solution; LB–Langmuir-Blodgett; LE – low-energy; MCD – microcrystals dispersed in a KBr disk; ORTEP – Oak Ridge thermal ellipsoid plot; ROC – randomly oriented crystals; SC – spin-coated; SCF – spin-coated film

II. Physical Properties of Carotenoids in Thin-Solid Films

In recent years, various organic thin-solid films have

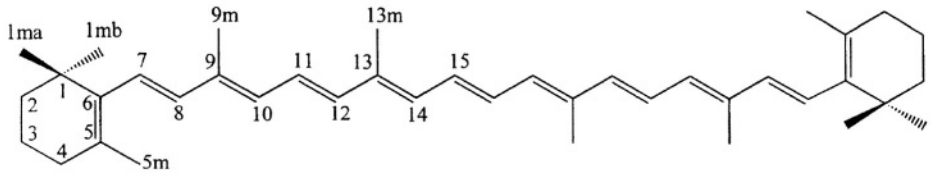

Fig. 1. Chemical structure of all-*trans*-β-carotene.

been fabricated and their physical properties have been examined in a search for novel electric and nonlinear optical devices. Carotenoid molecules can be good candidates for this purpose, because they have large nonlinear optical susceptibilities (Marder et al., 1997). Most familiar thin-solid films are either spin-coated (SC) films or Langmuir-Blodgett (LB) films. As the first step in determining the physical properties of these films, it is necessary to measure the optical constants, refractive indices and extinction coefficients, and thickness of the films. In this section, simple but reliable methods to determine these constants are introduced. Further, by using these methods one can also determine the molecular orientation in the films.

The methods were developed by the present author and coworkers (Hashimoto et al., 1996), and were applied to the SC and LB films of all-*trans*-β-carotene. Figure 1 shows the chemical structure of all-*trans*-β-carotene, which is one of the most studied carotenoids (Koyama and Hashimoto 1993). Its structure is characterized by an extended polyene chain composed of alternating carbon-carbon single and double bonds. Due to the π electrons in the polyene chain, all-*trans* β-carotene molecules give rise to a strong absorption band in the 400–500 nm spectral region. The origin of this particular absorption band is assigned to $^1B_u^+ \leftarrow {}^1A_g^-$ transition using the representations on the C_{2h} symmetry group which is polarized parallel to the long molecular axis. Therefore, if we use linearly polarized light which is in resonance with this particular transition, we can obtain information about the molecular orientation of the all-*trans*-β-carotene molecules.

A. Experimental Procedures

1. Optical Characterization

All optical measurements were performed at room temperature and in air. Figure 2 defines the Cartesian coordinate system on the glass substrate (26 mm x 76 mm x 1 mm) which was used for fabricating the

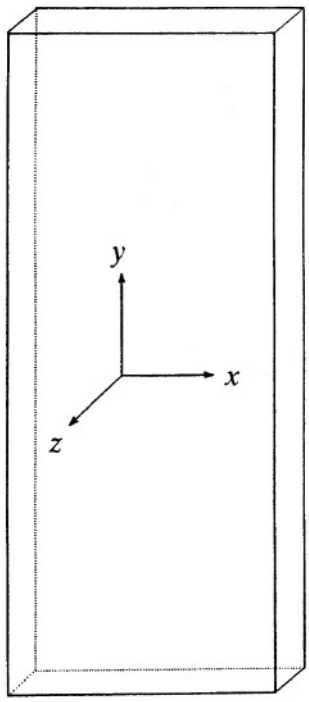

Fig. 2. A schematic description of the Cartesian coordinate on the plane of a glass substrate. The short side of the glass substrate is set to the *x*-axis, and the long side to the *y*-axis. The *z*-axis corresponds to the normal of the substrate.

film samples. We define the short side of the glass substrate as the *x*-axis, and the long side as the *y*-axis. The film sample was fabricated on the *x*-*y* plane of the substrate, and a measuring light was irradiated through this plane of the substrate. The *z*-axis corresponds to the normal of the substrate, and the substrate was rotated around *x*-axis during measurements of the angular dependence. The angular dependence of reflectance, transmittance or absorbance of the film was measured using a linearly polarized and collimated light (beam diameter = 1 mmϕ) from a 40 W tungsten-halogen lamp passed through a monochromator (JACSO, CT-25C). A silicon detector (Hamamatsu, S1227-66BQ) and a lock-in amplifier (EG and G, Model 5105) were used to detect the light intensity. The output signal of the

lock-in amplifier was digitized, accumulated and analyzed by a micro-computer (NEC, PC9801-UV).

2. Fabrication of Films

All the fabrication steps were performed in a dust-free environment and under dim red light. The SC film of all-*trans*-β-carotene was prepared using a spin-coating apparatus fabricated by us. An aliquot (about 20 μl) of a chloroform solution of all-*trans*-β-carotene (0.02 M) was spread onto the glass substrate rotating at 2500 rpm, and the solvent was evaporated in air. The film thus fabricated was immediately subjected to optical measurements.

The mixed LB film composed of all-*trans*-β-carotene with barium stearate (1:10) was prepared at 18 °C using a trough made of acrylic acid resin fabricated by us. The entire surface of the trough was covered with paraffin prior to use. A benzene solution containing both β-carotene (2×10^{-4} M) and stearic acid (2×10^{-3} M) was spread onto the surface of a buffer sublayer (pH = 7.3 – 8.5) composed of barium chloride (3×10^{-5} M) and potassium hydrogen carbonate (4×10^{-4} M). Surface pressure was controlled by moving a barrier made of paraffin at a speed of 20 mm/min. Surface pressure was determined using a Wilhelmy-type float made of mica (35.5 mm × 73.0 mm × 0.25 mm) and a torsion balance (Shimadzu). The readings of the torsion balance were corrected independently against various standards, e.g., oleic acid and ethyl myristate. The glass substrate was dipped into and raised along the *y*-axis, which was set normal to the plane of the buffer sublayer, at a speed of 6 mm/s (vertical method), and the monolayer on the buffer sublayer was transferred onto the x-y plane of the substrate. A total of 200 monolayers were transferred onto the substrate at a surface pressure of 30 mN/m. The mixed LB films were thus fabricated on both sides of the glass substrate. The film on one side of the substrate was rinsed with chloroform to dissolve β-carotene, and the film on the other side was subjected to subsequent optical measurements.

B. Results

The all-*trans*-β-carotene molecule has a transition moment that is parallel to its molecular axis in the visible spectral region. Therefore, it is expected that we can determine the molecular orientation in the solid materials on irradiation with linearly polarized light which excites this transition moment.

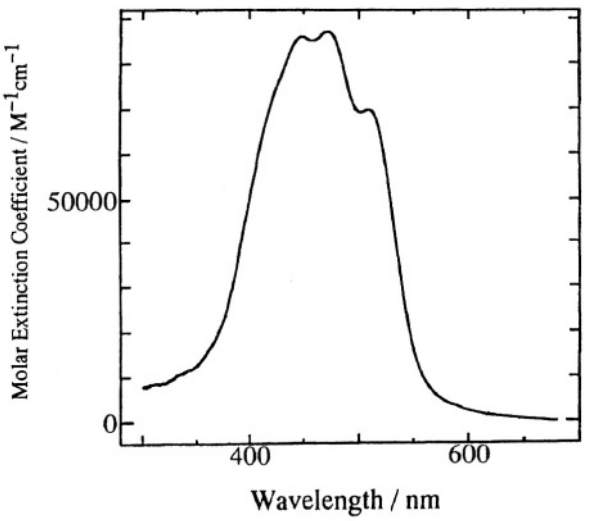

Fig. 3. Optical absorption spectrum of the spin-coated film of all-*trans*-β-carotene measured at room temperature on normal irradiation with linearly polarized light.

1. Spin-Coated Film

Figure 3 shows the optical absorption spectrum of the all-*trans*-β-carotene SC film measured on normal irradiation with linearly polarized light. The optical absorption spectrum of the SC film obtained on irradiation with linearly polarized light parallel to the *x*-axis of the substrate showed exactly the same spectral pattern and intensity with that parallel to the *y*-axis at all points on the film, suggesting that the SC film is uniform and the transition moment due to the β-carotene molecule distributes isotropically in the plane of the substrate within the resolution of 1 mm judging from the beam diameter (1 mmϕ). Furthermore, we could not observe any microcrystals with grain size larger than 5 μm in the SC film using an optical microscope with 500× magnification.

Figure 4 shows the plots of the (a) reflectance and (b) transmittance of the SC film detected on irradiation with 445 nm light at all incident angles. Filled circles represent the results obtained on irradiation with *s*-polarized light, and open circles represent those with *p*-polarized light. We can determine the Brewster's angle of the film β to be 58° in Fig. 4(a), and relative intensity of reflectance at β for the *s*- and *p*-polarizations is $R_\beta = R_p(\beta)/R_s(\beta) = 0.186$.

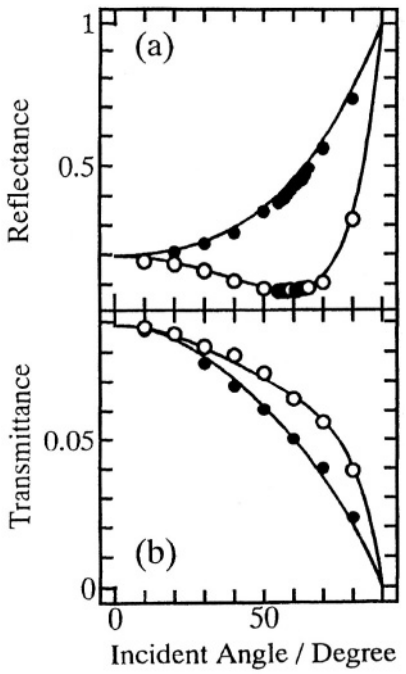

Fig. 4. Plots for the (a) reflectance and (b) transmittance of the spin-coated film of all-*trans*-β-carotene detected on irradiation with 445 nm light at all incident angles. Filled circles represent the results obtained on irradiation with *s*-polarized light, and open circles represent those with *p*-polarized light. Solid lines in (a) show the results of the theoretical calculations assuming n = 1.38 and κ = 1.09. Solid lines in (b) show the results of the theoretical calculations assuming n = 1.38, κ = 1.09, and d = 82.5 nm.

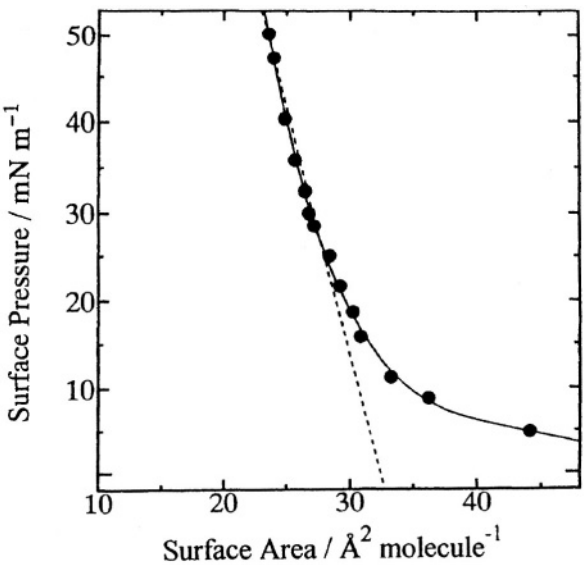

Fig. 5. π-A isotherm at 18 °C of the mixed Langmuir monolayer composed of all-*trans*-β-carotene and barium stearate (1:10) at the air/water interface. A broken line shows a linear extrapolation of the steep rise of the π-A isotherm.

2. Langmuir-Blodgett Film

Figure 5 shows the π-A isotherm of the mixed Langmuir monolayer composed of all-*trans*-β-carotene with barium stearate (1:10) at the air/water interface. The π-A isotherm shows a steep rise at the surface pressure above 15 mN/m. This observation confirms that the molecules in the monolayer are closely packed at the surface pressure of 30 mN/m, the value which corresponds to the fabricating condition when transferring the monolayer to the glass substrate. The limiting area, which corresponds to the area occupied by one molecule at the air/water interface, can be extrapolated from the steep part of the π-A isothermto be 32 Å² /molecule (see broken line in Fig. 5). This value is larger than that reported previously (18 Å² /molecule) (Leblanc and Orger, 1972) for a neat β-carotene Langmuir monolayer where the molecules are perpendicular to the water subphase. This means that the β-carotene molecule is tilted at the air/water interface in our fabrication (vide infra). An independent determination showed that the limiting area of the barium stearate Langmuir monolayer was 26 Å²/molecule. This value is in good agreement with that reported previously (20 Å² /molecule) (Kawai et al., 1989), which confirms that barium stearate molecules are closely packed in our fabrication.

Figure 6 shows the optical absorption spectra of the mixed LB film of all-*trans*-β-carotene with barium stearate (1:10) measured on normal irradiation with light polarized parallel to the *x*- or *y*-axis of the substrate. The intensities of these spectra clearly show anisotropy in the plane of the substrate between these two polarizations, although their shapes are identical within the limit of experimental uncertainties.

Figure 7 shows the plots for the absorbance of the mixed LB film detected on irradiation with 445 nm light at any incident angles. Filled circles represent the results obtained on irradiation with *s*-polarized light, and open circles represent those with *p*-polarized light; correction for multiple reflection at the air/film, film/glass, and glass/air interfaces was performed. When using the *p*-polarized light, the observed absorbance shows weak dependence on the incident angles, while clear angular dependence is seen when using the *s*-polarized light.

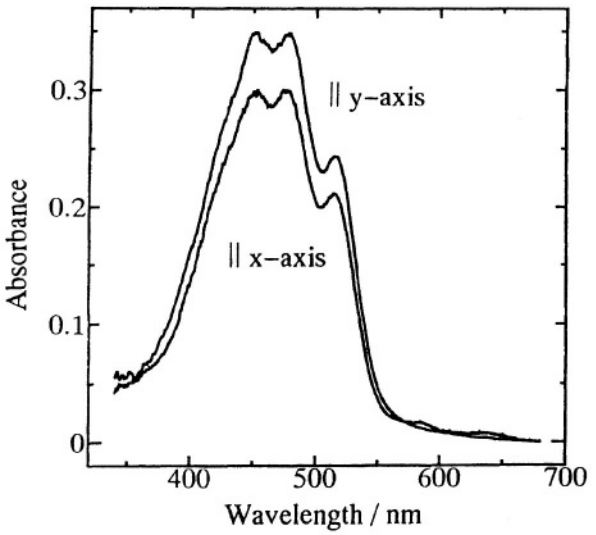

Fig. 6. Optical absorption spectra of the mixed Langmuir-Blodgett film of all-*trans*-β-carotene with barium stearate (1:10) measured at room temperature on normal irradiation with light polarized parallel to the *x*- or *y*-axis of the substrate.

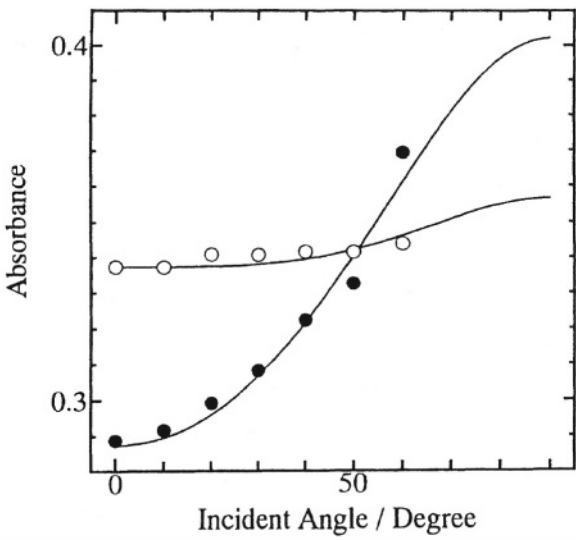

Fig. 7. Plots for the absorbance of the mixed Langmuir-Blodgett film of all-*trans*-β-carotene with barium stearate (1:10) detected on irradiation with 445 nm light at any incident angles. Filled circles represent the results obtained on irradiation with s-polarized light. Solid lines show the results of the theoretical calculations based on the axis model assuming $n = 1.46$ and $C_x/C_y = 0.5$

C. Analyses

1. Determination of Optical Constants, Thickness and Density of the Spin-Coated Film

Assuming the SC film to be 'an isotropic absorbing medium', the optical constants of the film, i.e., a refractive index n and an extinction coefficient κ, both of which define a complex refractive index $\tilde{n} = n + i\kappa$, can be determined according to the method described by Humphreys-Owen (1961). With $p = n^2 + \kappa^2$, $q = n^2 - \kappa^2$, and $Q^2 = 4R_\beta/(1 + R_\beta)^2$, p and q can be analytically solved as shown in Eqs. (1) and (2).

Therefore, we can determine n and κ as $n = \sqrt{(p+q)/2}$ and $\kappa = \sqrt{(p-q)/2}$, respectively. According to the results obtained in Section II.B.1 ($\beta = 58°$, $R_\beta = 0.186$), we obtain $n = 1.38$ and $\kappa = 1.09$; these results are consistent with those reported by Babaev and A1'perovich (1973).

The above analysis deals with reflection only at the air/film interface and ignores the effect of multiple reflection at the air/film, film/glass and glass/air interfaces. Therefore, such an analysis is valid only for the thick film which shows a large optical density at the monitoring wavelength (445 nm). In order to examine the validity of the analysis, we theoretically calculated reflectance as a function of incident angle using above values of n and κ, and checked the agreement with experimental results shown in Fig. 4(a).

As illustrated in Fig. 8, we denote the refractive index of the air as n_1, that of the SC film as $\tilde{n}_2$, and that of the glass substrate as n_3. If we express $\tilde{n}_2 = n_2(1 + i\kappa_2)$ and define the refractive angle of the light in the SC film as θ_2, we can express as $n_2\cos\theta_2 = u_2 + iv_2$. Here, new valuables u_2 and v_2 can be related with the incident angle θ_1 and the refractive index n_2 and the

$$p^2 = \frac{\sin^2\beta\cdot\tan^2\beta}{2\left(1-Q^2\cos^2\beta\right)}\left[2+\tan^2\beta-2Q^2\cos 2\beta+\tan^2\beta\sqrt{1+8Q^2\cos^2\beta}\right] \tag{1}$$

$$q = \frac{p^2\left(1+2\cos^2\beta-p^2\cot^4\beta\right)}{2\sin^2\beta} \tag{2}$$

$$2u_2^2 = n_2^2(1-\kappa_2^2) - n_1^2\sin^2\theta_1 + \sqrt{\left[n_2^2(1-\kappa_2^2) - n_1^2\sin^2\theta_1\right]^2 + 4n_2^4\kappa_2^2} \tag{3}$$

$$2v_2^2 = -\left[n_2^2(1-\kappa_2^2) - n_1^2\sin^2\theta_1\right] + \sqrt{\left[n_2^2(1-\kappa_2^2) - n_1^2\sin^2\theta_1\right]^2 + 4n_2^4\kappa_2^2} \tag{4}$$

(s-polarization)

$$\rho_{12} = \frac{(n_1\cos\theta_1 - u_2)^2 + v_2^2}{(n_1\cos\theta_1 + u_2)^2 + v_2^2} \tag{5}$$

(p-polarization)

$$\rho_{12} = \frac{\left[n_2^2(1-\kappa_2^2)\cos\theta_1 - n_1u_2\right]^2 + \left[2n_2^2\kappa_2^2\cos\theta_1 - n_1v_2\right]^2}{\left[n_2^2(1-\kappa_2^2)\cos\theta_1 + n_1u_2\right]^2 + \left[2n_2^2\kappa_2^2\cos\theta_1 + n_1v_2\right]^2} \tag{6}$$

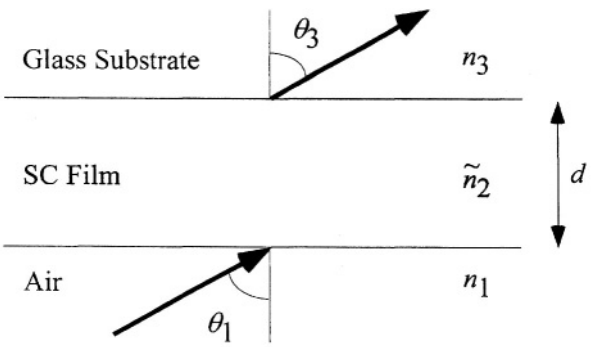

Fig. 8. A schematic drawing of the spin-coated film on glass substrate.

extinction coefficient κ_2 of the SC film according to the Snell's law as shown in Eqs. (3) and (4).

According to the geometrical optics treatment (Born and Wolf, 1980), the angular dependence of reflectance ρ_{12} at the air/film interface for s- and p-polarized light is described by Eqs. (5) and (6), respectively.

Solid lines in Fig. 4(a) show the results of the calculations. The calculated curves are in good agreement with the experimental results, which supports the validity of the above analysis and the assumption of the isotropic SC film.

In order to determine the thickness d of the SC film, we analyzed the angular dependence of transmittance. Using the thickness d and the wavelength λ_0 of the incident radiation, we introduced a new parameter $\eta = 2\pi d/\lambda_0$. Again, according to the geometrical optics treatment (Born and Wolf, 1980), the angular dependence of transmittance T for the s- and p-polarized lights is described by Eqs. (7) and (8), respectively, for the isotropic absorbing medium.

Here, τ_{12} and τ_{23} show the transmittance at the air/film and film/glass interfaces, respectively, ρ_{23} shows the reflectance at the film/glass interface, and ϕ_{12} and ϕ_{23} show the phase differences at the air/film and film/glass interfaces, respectively. (For the analytical

(s-polarization)

$$T = \frac{n_3\cos\theta_3}{n_1\cos\theta_1} \cdot \frac{\tau_{12}^2\tau_{23}^2\exp(-2v_2\eta)}{1+\rho_{12}^2\rho_{23}^2\exp(-4v_2\eta) + 2\rho_{12}\rho_{23}\exp(-2v_2\eta)\cos(\phi_{12}+\phi_{23}+2u_2\eta)} \tag{7}$$

(p-polarization)

$$T = \frac{n_1\cos\theta_3}{n_3\cos\theta_1} \cdot \frac{\tau_{12}'^2\tau_{23}'^2\exp(-2v_2\eta)}{1+\rho_{12}^2\rho_{23}^2\exp(-4v_2\eta) + 2\rho_{12}\rho_{23}\exp(-2v_2\eta)\cos(\phi_{12}+\phi_{23}+2u_2\eta)} \tag{8}$$

solutions of these new valuables, see the reference by Born and Wolf (1980).) Equations (7) and (8) contain the effect of multiple reflection, and three parameters, i.e., $n\,(=n_2)$, $\kappa\,(=\kappa_2)$ and d, are used for the calculation. Since we have already determined n and κ in the previous analysis, we can now fit the theoretical curves to the experimental results with d as a single parameter. The simulated curves are shown by solid lines in Fig. 4(b). The best fit was obtained when d = 82.5 nm. It is to be noted that this analysis is very sensitive to the parameter d, and we can determine the thickness of the film within an accuracy of ±0.3 nm. Using d thus obtained, we can calculate the density ρ of the film. Since the molar extinction coefficient at 450 nm of all-*trans*-β-carotene in a *n*-hexane solution is 139000 $M^{-1}cm^{-1}$ (Tsukida et al., 1982), the number of molecules which occupy the unit area in the film can be determined by dissolving the film into *n*-hexane and by measuring its optical density. Therefore, we can determine the density of the film $\rho = 0.835$ g/cm^3, which is in good agreement with the earlier report by Babaev and Al'perovich (1973) (0.863 g /cm^3).

2. Axis Model Applied to Langmuir-Blodgett Film

The molecular orientation of all-*trans*-β-carotene in the mixed LB film with barium stearate can be analyzed by the use of the axis model. This model was first proposed by Schmidt and Reich (1972) to analyze the molecular orientation of all-*trans*-lutein in the mixed LB film with cadmium arachidate. In their investigation, they only examined the absorbance at 45° incidence. In our investigation, we measured more fully the angular dependence of the absorbance at other than 45° incidence. Therefore, we believe that our analysis is more reliable than theirs.

All-*trans*-β-carotene is a one-dimensional polyene molecule which has a transition moment parallel to its molecular axis in the visible region. The 445 nm light used in determining the angular dependence of absorbance excites this particular transition moment. Denoting the molar concentration of β-carotene in the film whose transition moment is parallel to the *x*-, *y*-, or *z*-axis of the substrate to be C_x, C_y, or C_z, respectively, then the total concentration C can be described as

$$C = C_x + C_y + C_z \tag{9}$$

According to the- Lambert-Beer's law, the absorbance of the film detected on normal irradiation with light linearly polarized parallel to the *x*- or *y*-axis of the substrate can be described as

$$A_x = \varepsilon C_x d \tag{10}$$

$$A_y = \varepsilon C_y d \tag{11}$$

using thickness d of the film and the molar extinction coefficient ε at 445 nm. Therefore, according to the observed results shown in Fig. 6, we can calculate the ratio C_x/C_y to be 0.85.

In the following analysis, we assume that the mixed LB film is a non-absorbing medium for the following two reasons: (1) Since the molar ratio of β-carotene to barium stearate is 1:10 in the mixed LB film, the number of the barium stearate molecules predominates in the film; (2) The angular dependence of reflectance for the mixed LB film fits the theoretical curves for the non-absorbing medium calculated using the refractive index of barium stearate (1.462) (Blodgett, 1935).

If we rotate the substrate around the *x*-axis, incident radiation makes an angle θ relative to the *z*-axis of the substrate. In this case, we can define a real refraction angle α according to Snell's law as

$$\alpha = \sin^{-1}\left(\frac{1}{n}\sin\theta\right) \tag{12}$$

using the incident angle θ and the refractive index n of the film. Using α thus obtained and the thickness d of the film, we can describe an optical path length L in the film as

$$L = \frac{d}{\cos\alpha} \tag{13}$$

Therefore, we can describe the absorbance of the film detected on irradiation with *s*- or *p*-polarized light as

$$A_s = A_x \frac{L}{d} \tag{14}$$

$$A_p = A_y\left(\cos^2\alpha + \frac{C_z}{C_y}\sin^2\alpha\right)\frac{L}{d} \tag{15}$$

Hence, by fitting Eqs. (14) and (15) to the experimental results shown in Fig. 7, we can determine the refractive index $n = 1.46$ and the ratio $C_z/C_y = 0.5$. It is noteworthy that the refractive index thus determined is in good agreement with that reported for the LB film of barium stearate (1.462) (Blodgett, 1935), which also confirms our assumption of the mixed LB film as the non-absorbing medium.

D. Molecular Orientation of β-Carotene in the Spin-Coated Film and in the Langmuir-Blodgett Film

1. Spin-Coated Film

It was shown that the transition moment of the β-carotene molecule is isotropically distributed in the plane of the SC film. As regards the normal direction of the film, the observed angular dependence of both reflectance and transmittance was in excellent agreement with the theoretical curves calculated assuming the isotropic absorbing medium. This means that the refractive index of the SC film is isotropic in the normal of the film. Since the refractive index can be directly related to the polarizability of a molecule using Clausius-Mosotti's law and a transition moment linearly depends on the polarizability, the present investigation reveals that the transition moment of the β-carotene molecule is isotropically distributed both in the plane and in the normal of the SC film. The transition moment lies parallel to the molecular axis of β-carotene, hence we can conclude that the β-carotene molecules are randomly oriented in the SC film.

2. Langmuir-Blodgett Film

According to the π-A isotherms, the limiting areas were determined to be 26 and 32 Å²/molecule, respectively, for the Langmuir monolayer of barium stearate and for that of β-carotene with barium stearate (1:10). Based on these observations, we can calculate the averaged occupation area of a single β-carotene molecule at the air/water interface to be 92 Å²/molecule. The limiting area when the β-carotene molecule is perpendicular to the air/water interface was reported to be 18 Å²/molecule (Lebranc and Orger, 1972), and the area of the β-carotene molecule along the molecular axis was calculated to be 230 Å²/molecule based on the molecular model (Ohnishi et al., 1978). Therefore, based on these data and assuming all the β-carotene molecules are oriented along the same direction in the monolayer, we can calculate the angle between the molecular axis and the water surface to be 71° in our Langmuir monolayer.

According to the analysis based on the axis model, we determined that $C_x/C_y = 0.85$ and $C_z/C_y = 0.5$. This shows that $C_z/C = 0.21$. Since the angle γ between the molecular axis of β-carotene and the z-axis of the substrate is related as

$$Cz = C \cdot \cos^2\gamma \qquad (16)$$

we can determine $\gamma = 63°$. Hence, the molecular axis of β-carotene in the mixed LB film makes an angle of 27° relative to the plane of the substrate. This means that β-carotene molecule is more tilted in the mixed LB film than that at the air/water interface. However, it makes a substantial angle relative to the plane of the substrate, and this finding completely contradicts the earlier report by Ohnishi et al. (1978), who suggested that β-carotene molecules are parallel to the surface of the substrate.

It has long been believed that polar substituent groups such as a hydroxyl group are necessary in order that a carotenoid molecule makes a substantial angle relative to the plane of the substrate in the mixed LB film (Schmidt and Reich, 1972; Palacin et al., 1989). However, our present investigation reveals that this is not the case, since nonpolar β-carotene makes a substantial angle relative to the plane of the substrate. Therefore, the present investigation highlights a possibility that we can control the molecular orientation in the mixed LB film even for nonpolar carotenoids.

III. X-Ray Crystallography of Carotenoids

Hundreds of carotenoid molecules are found in nature (Otto, 1987), but crystal structures are reported for only three of them, i.e., all-*trans*-β-carotene (Sterling, 1964; Senge et al., 1992), all-*trans*-canthaxanthin (Bart and MacGillavry, 1968) and all-*trans*-β-apo-8′-carotenal (Drikos et al., 1988). This is due to the difficulty of growing single crystals of sufficient quality and due to the degradation of the crystals by X-ray irradiation. In order to avoid the latter difficulty, a most promising method is to determine the crystallographic structures at low temperatures. However, improvements in technology make it possible to collect diffraction data with minimum

X-ray irradiation, hence we can determine the crystallographic structures sufficiently well at room temperature. Because the crystal structure analysis has fundamental importance for any quantitative analyses, accumulation of the structural data is necessary in the search for practical applications of carotenoid molecular crystals. In this section, growth and structures of all-*trans*-β-carotene single crystals are introduced.

A. Growth of All-trans-β-Carotene Single Crystals

The single crystals of all-*trans*-β-carotene were grown by means of (1) a diffusion-zone method (Vaala et al., 1973; Madjid, 1975) or (2) simple crystallization from a benzene solution. For the former method, a container covered with a sheet of parchment paper (Shin-Ohjiseishi Co., Ltd., P-parchment S45) was filled with a saturated benzene solution of all-*trans*-β-carotene. The container was then dipped in methanol, and kept at room temperature for one month .Since the solubility of β-carotene in methanol was much lower than that of β-carotene in benzene, methanol passing through the parchment paper lowered the solubility of β-carotene in the benzene solution and single crystals were gradually grown in the container. As for the latter method, the single crystals were grown by recrystallization from a benzene solution at 8 °C or by slow evaporation of a solvent at room temperature. The single crystals thus grown were hexagonal and typically, 3 mm x 6 mm × 0.3 mm in size. It is to be noted that by using the diffusion-zone method we sometimes could grow a crystal whose size is 3 cm long along the long side of the crystal.

B. Crystallographic Structure of all-trans-β-Carotene Single Crystal at Room Temperature

There are two reports of the crystal structure of all-*trans*-β-carotene (Sterling, 1964;Senge et al., 1992). These two reports show essentially the same monoclinic crystal structure, however, a slight difference is seen for the assignment of the space group. Sterling (1964) assigned the space group to be $P2_1/c$, while Senge et al. (1992) assigned it to be $P2_1/n$. Therefore, redetermination of the crystal structure is appropriate. The previous examination of the crystal structure was performed only at low temperature. Since we have performed the optical characterization of the single crystals at room temperature (vide infra), it is important to also know the crystal structure at this particular temperature.

Table 1 shows space group information and unit cell parameters with their estimated standard deviations for the all-*trans*-β-carotene single crystal at 130 K reported by Senge et al. (1992) and at 293 K determined by the present author and coworkers (Hashimoto et al., 1998). In our determination, the space group of the single crystal is $P2_1/n$, and two independent molecules exist in each unit cell, a finding that supports the previous determination by Senge et al. (1992). As expected, comparison of volumes (V) and calculated densities (D_{calc}) of the unit cells at 130 K and at 293 K shows the expansion of the crystal on raising the temperature. However, comparison of the lattice constants, i.e., *a*, *b*, *c* and β, shows that the expansion of the crystal is not isotropic; elongation of the unit cell length occurs in the order $a > b > c$, and decrease of monoclinic angle β is seen on raising the temperature. This anisotropy must be due to intermolecular interactions between each β-carotene molecule in the crystal. The intermolecular interaction may also affect the structure of component β-carotene molecules. Hence, we further compared bond lengths, bond angles and dihedral angles of β-carotene molecules at 130 K and at 293 K.

Table 2 gives the atomic coordinates and equivalent isotropic displacement coefficients (B_{eq}) of carbon atoms with their estimated standard deviations for the all-*trans*-β-carotene single crystal at 293 K (see Fig. 1 for numbering of carbon atoms). In Table 2, coordinates for only half of the carbon atoms are listed since the all-*trans*-β-carotene molecule has C_i symmetry in the crystal. B_{eq}'s of C(2) and C(3) atoms are larger values than those of other carbon atoms, which indicates the fluctuation of these atoms in the crystal. This observation is consistent with that of Senge et al. (1992).

Table 3 gives the bond lengths, bond angles and dihedral angles of all-*trans*-β-carotene molecules in the single crystal at 130 K and at 293 K. Δ is the difference between the values at 130 K and 293 K (values greater than double the standard deviation are underlined). Concerning the bond lengths and the dihedral angles, considerable displacements caused by raising the temperature can be seen in the peripheral part of the polyene backbone. On the other hand, significant displacements can be seen in the central part for the bond angles. These

Table 1. Comparison of space group information and unit cell parameters for all-*trans*-β-carotene single crystals at 130 K and at 293 K

130 K[a)]	293 K[b)]
Space group information	
Symbol: $P2_1/n$	Symbol: $P2_1/n$
number: 14 (centric)	number: 14 (centric)
Z value: 2	Z value: 2
Unit cell parameters	
a: 7.656(2) Å	*a*: 7.790(2) Å (+0.134(3) Å; +1.75 %)
b: 9.445(5) Å	*b*: 9.500(3) Å (+0.055(6) Å; +0.58 %)
c: 23.536(15) Å	*c*: 23.738(2) Å (+0.202(15) Å; +0.86 %)
β: 93.41(2) °	β: 92.70(2) ° (–0.71(3)°; –0.76 %)
V: 1698.8(15) Å^3	V: 1754.8(7) Å^3 (+56.0(17) Å^3; +3.3 %)
D_{calc}: 1.050 g/cm^3	D_{calc}: 1.016 g/cm^3 (–0.034 g/cm^3; –3.2 %)

[a)] Senge et al., 1992

[b)] Hashimoto et al., 1998

Table 2. Atomic coordinates and equivalent isotropic displacement coefficients for all-*trans*-β-carotene

atom	*x*	*y*	*z*	B_{eq} [a)]
C(1)	1.1761(6)	0.6519(5)	0.1825(2)	5.5(1)
C(1ma)	1.116(1)	0.7721(8)	0.1431(4)	10.5(3)
C(1mb)	1.3310(10)	0.5801(9)	0.1585(4)	9.9(3)
C(2)	1.228(1)	0.720(1)	0.2378(3)	12.1(3)
C(3)	1.181(1)	0.675(1)	0.2883(3)	12.2(3)
C(4)	1.0161(8)	0.5980(7)	0.2923(2)	6.4(2)
C(5)	0.9471(5)	0.5335(5)	0.2370(2)	5.3(1)
C(5m)	0.7902(8)	0.4456(8)	0.2441(3)	8.1(2)
C(6)	1.0270(5)	0.5481(4)	0.1888(2)	4.7(1)
C(7)	0.9757(6)	0.4699(5)	0.1364(2)	5.1(1)
C(8)	0.9386(6)	0.3341(5)	0.1332(2)	4.8(1)
C(9)	0.8942(5)	0.2547(4)	0.0819(2)	4.5(1)
C(9m)	0.9081(8)	0.3262(6)	0.0258(2)	5.8(1)
C(10)	0.8421(5)	0.1192(5)	0.0865(2)	5.0(1)
C(11)	0.7865(5)	0.0252(5)	0.0420(2)	4.8(1)
C(12)	0.7249(6)	–0.1041(5)	0.0503(2)	4.8(1)
C(13)	0.6578(5)	–0.2014(4)	0.0086(2)	4.7(1)
C(13m)	0.6552(8)	–0.1571(7)	–0.0525(2)	5.9(1)
C(14)	0.5990(6)	–0.3273(5)	0.0247(2)	5.2(1)
C(15)	0.5276(6)	–0.4373(4)	–0.0094(2)	5.3(1)

[a)] $B_{eq} = \frac{8}{3}\pi^2\left(U_{11}(aa^*)^2 + U_{22}(bb^*)^2 + U_{33}(cc^*)^2 + 2U_{13}aa^*cc^*\cos\beta\right)$

observations are crucial to understanding of the effect of intermolecular interactions in the crystal, and should be discussed in detail separately.

Finally, Fig. 9 shows an ORTEP (Oak Ridge thermal ellipsoid plot) view of the unit cell projected against the (001) plane (*ab* plane) of the single crystal. As can be expected based on this result, the transition moment induced by the irradiation polarized along the *b*-axis must be larger than that induced by the irradiation polarized along the *a*-axis. This molecular arrangement induces anisotropy in the absorption spectrum of the single crystal in the visible spectral region as shown in the following section.

Table 3. Bond lengths (Å), bond angles (°) and dihedral angles (°)[a] of all-*trans*-β-carotene in the single crystals at 130 K and at 293 K.

atom position	6	7	8	9	10	11	12	13	14	15	15′
					130 K[b]						
Bond length	1.449(5)	1.352(5)	1.445(5)	1.352(5)	1.442(5)	1.352(5)	1.444(5)	1.353(5)	1.441(5)	1.346(8)	
Bond angle		126.7(3)	127.2(3)	119.1(3)	127.3(3)	123.0(3)	126.1(4)	117.7(4)	127.7(4)	123.0(5)	
Dihedral angle	−42.51(3)	−176.2(3)	−175.2(2)	177.7(4)	−175.0(2)	175.7(2)	−179.8(5)	179.4(12)	177.9(4)	180.0	
					293 K						
Bond length	1.487(5)	1.324(6)	1.460(5)	1.355(5)	1.436(6)	1.337(6)	1.435(5)	1.343(6)	1.419(6)	1.350(8)	
Δ[c]	+0.038(7)	−0.028(8)	+0.015(7)	+0.003(7)	−0.006(8)	−0.015(8)	−0.009(7)	−0.010(8)	−0.022(8)	+0.004(11)	
Bond angle		125.8(4)	126.5(4)	118.9(4)	127.8(5)	124.1(4)	127.7(5)	119.7(4)	128.5(5)	125.7(6)	
Δ[c]		−0.9(5)	−0.7(5)	−0.2(5)	+0.5(6)	+1.1(5)	+1.6(6)	+2.0(6)	+0.8(6)	+2.7(8)	
Dihedral angle	−45.0(7)	−177.6(4)	−173.1(5)	177.3(4)	−174.8(5)	176.2(4)	−179.2(5)	179.7(4)	179.2(6)	180.0	
Δ[c]	−2.4(8)	−1.4(5)	+2.1(5)	−0.4(6)	+0.2(5)	+0.5(4)	+0.6(7)	+0.3(13)	+1.3(7)	±0.0	

[a] Dihedral angle around the C6-C7 bond is determined using the C5-C6-C7-C8 backbone.
[b] Senge et al, 1992
[c] Values greater than double the standard deviations are underlined.

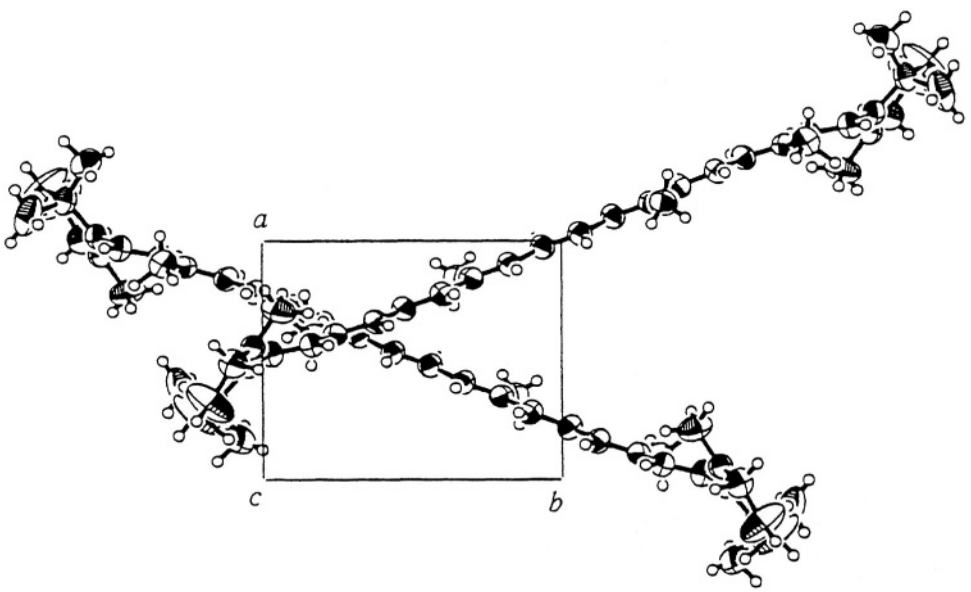

Fig. 9. An ORTEP projection on to the (001) plane of the all-*trans*-β-carotene single crystal.

IV. Optical Properties of all-*trans*-β-Carotene in the Condensed Phase

A. Optical Absorption Spectra of all-trans-β-Carotene Single Crystals in the Visible Spectral Region

As shown in the previous section, the single crystals of β-carotene are hexagonal plates. The short side of the crystal corresponds to the *a*-axis, while the long side corresponds to the *b*-axis (Chapman et al., 1967). Exact direction of the crystal axes is determined by measuring the angular dependence of reflectance. Since β-carotene molecules have a large molar extinction coefficient (139,000 $M^{-1}cm^{-1}$ at 450 nm in *n*-hexane) (Tsukida et al., 1982), it is difficult to measure directly the optical absorption spectra of the crystals in the visible region. Instead, they are obtained through the Kramers-Kronig transformation of reflection spectra.

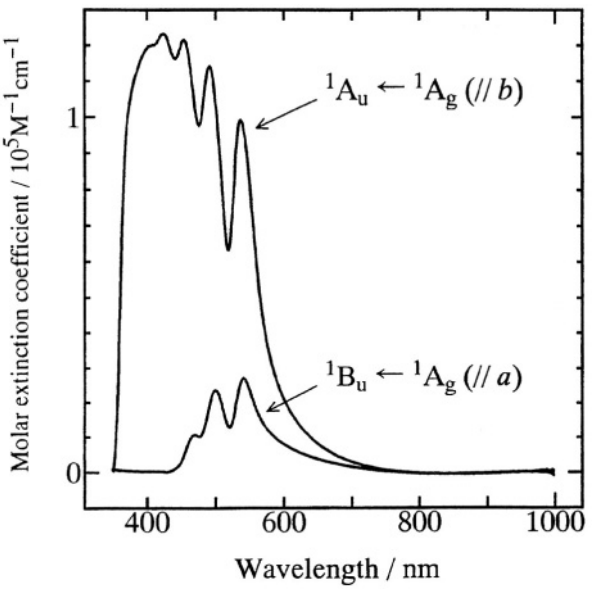

Fig. 10. Optical absorption spectra of the single crystal of all-*trans*-β-carotene measured at room temperature on irradiation with linearly polarized light parallel to the *a*- or *b*-crystal axis. They were obtained by the Kramers-Kronig transformation of the reflection spectra.

Figure 10 shows the optical absorption spectra of the single crystal of all-*trans*-β-carotene measured upon irradiation with linearly polarized light parallel to the *a*- or *b*-crystal axis. Large optical anisotropy for the molar extinction coefficient is seen in these spectra. This observation can be explained in terms of the molecular orientation of β-carotene in the crystal (see Fig. 9). Since the molecular axis of β-carotene is almost parallel to the *b*-axis, the molar extinction coefficients along *b*-axis should appear larger than those along *a*-axis. Based on the symmetry considerations, these spectra can be assigned to the transitions to the ^1A_u (//*b*-axis) and ^1B_u (//*a*-axis) molecular excitons, as illustrated in Fig. 10 (Chapman et al., 1967).

Table 4 compares the peak wavelengths as well as the band widths of the optical absorption spectra of the single crystal together with those of the *n*-hexane solution, mixed LB film and SC film (see Section II). The single crystal shows the largest values among these samples for both the peak wavelength of the $0 \leftarrow 0$ transition and the bandwidth. The peak wavelength of the $0 \leftarrow 0$ transition along the *a*-axis (540 nm) is red-shifted from that along the *b*-axis (535 nm). This observation corresponds to the Davydov splitting in the crystal due to two nonequivalent molecules in each unit cell (Davydov, 1962; 1971). We determined the peak energies of the $0 \leftarrow 0$ transition, and found the energy of the Davydov splitting E_D to be 170 ± 60 cm^{-1}. This energy corresponds to that of resonance interaction of two β-carotene molecules in each unit cell. Therefore, by taking the energy of 25 °C (kT = 207 cm^{-1}) into consideration, excitations are freely moving among β-carotene molecules in the crystal at room temperature (production of free excitons).

B. Intermolecular Interaction of β-Carotene in the Condensed Phase

Figure 11 compares the optical absorption spectra of all-*trans*-β-carotene in (a) 10^{-5} M *n*-hexane solution, (b) mixed LB film with barium stearate, (c) SC film and (d) single crystal (absorption spectrum parallel to *b*-axis is shown). The peak energies of $0 \leftarrow 0$ transitions are in the order (Solution, 20700 cm^{-1}) > (LB film, 19300 cm^{-1}) ≈ (SC film, 19300 cm^{-1}) > (Crystal, 18700 cm^{-1}). The band widths of the spectra are in the order (Solution, 4270 cm^{-1}) < (LB film, 5830 cm^{-1}) < (SC film, 6510 cm^{-1}) < (Crystal, 9720 cm^{-1}).

The optical absorption spectra of organic molecular solids are characterized by two kinds of intermolecular interaction energy, i.e., the Coulombic energy and the resonance interaction energy (Davydov, 1962, 1971). The former energy induces

Table 4. Peak wavelengths (nm) and bandwidths (cm^{-1}) of the optical absorption spectra of all-*trans*-β-carotene

	Peak wavelength / nm				Bandwidth/cm^{-1}
	$0 \leftarrow 0$	$1 \leftarrow 0$	$2 \leftarrow 0$	$3 \leftarrow 0$	
n-Hexane soln.	482	450	422		4270
LB Film	520	482	450		5830
SC Film	519	477	445		6510
Single Crystal					
a-axis	540	500	465		3060
b-axis	535	493	456	426	9720

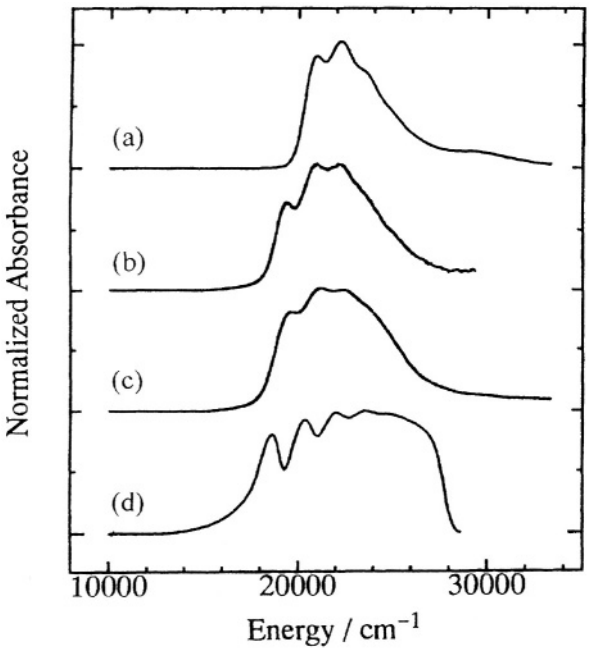

Fig. 11. Optical absorption spectra of all-*trans*-β-carotene at room temperature for the (a) 10^{-5} M *n*-hexane solution, (b) mixed Langmuir-Blodgett film with barium stearate (1:10), (c) spin-coated film, and (d) single crystal (parallel to the *b*-axis).

the site-energy shift, and causes the lower energy shift of the $0 \leftarrow 0$ absorption transition compared to that of the isolated molecule. The latter energy induces the Davydov splitting. The density of β-carotene molecules in the *n*-hexane solution can be estimated from the concentration ($\sim 10^{-5}$ M) of the solution to be 5×10^{-6} g/cm^3, while that in the mixed LB film can be calculated from the molar ratio of β-carotene and barium stearate (1:10) and the thickness of the film (5160 Å) to be 0.072 g/cm^3. (The thickness of the mixed LB film can be estimated from the thickness of the single monolayer of barium stearate (25.8 Å) (Mann and Kuhn, 1971)). The density of β-carotene molecules in the SC film was determined to be 0.835 g/cm^3 as shown in Section II, while that in the single crystal was determined to be 1.016 g/cm^3 as shown in Section III. Based on the estimated densities, the strengths of the intermolecular interaction H_i in the above four samples are in the order H_i(Solution) < H_i(LB film) < H_i(SC film) < H_i(Crystal). This order is consistent with that of the $0 \leftarrow 0$ peak energies and that of the bandwidths in these samples. This trend is also found for the frequencies of ν_1 (C=C stretching) Raman lines (Hashimoto et al., 1997).

The above discussion deals only with the $0 \leftarrow 0$ peak energies and the bandwidths. In what follows, we discuss the band shapes of the absorption spectra in view of microscopic molecular order for the condensed samples. Among the four samples described above, we can define the molecular order in two of them, namely, that in the *n*-hexane solution and that in the single crystal. We know definitely that molecules are isolated (random orientation and arrangement) in the solution, while both the orientation and the arrangement are ordered in the single crystal. These two samples show the weakest and the strongest intermolecular interactions, respectively. The remaining two samples, i.e., the mixed LB film and the SC film, are found in-between these samples, judging from the strengths of the intermolecular interaction. However, it is interesting to note that besides the $0 \leftarrow 0$ peak energies and the bandwidths, the overall shape of the optical absorption spectrum for the mixed LB film and that for the SC film are different from that of the isolated molecule in solution and they approach that of the single crystal in the order solution → LB film → SC film → single crystal. This may imply that the molecular order of β-carotene which is seen in the single crystal partially exists in the mixed LB film and in the SC film. If we can classify the molecular order into short- and long-range orders, both of them are lacking in the solution but are present in the crystal. The long-range order of the orientation partially exists in the mixed LB film, while it does not exist in the SC film. Hence, the above similarity of the absorption band shapes of the mixed LB film and the SC film to that of the single crystal suggests that the short-range order similar to that of the single crystal exists in the mixed LB film and in the SC film.

As described above, the β-carotene molecules are randomly oriented in the SC film, but the above discussion suggests that the short-range order similar to that in of the single crystal exists in the SC film. Therefore, we can now conclude definitely that the SC film is an amorphous film, and this conclusion supports the assumption by Babaev and A1'perovich (1973). As for the LB film, the optical absorption spectrum measured on normal irradiation with light polarized parallel to the *x*-axis of the substrate showed exactly the same spectral pattern with that parallel to the *y*-axis, although the intensities of these spectra were apparently different. This shows that there is only one transition moment in the mixed LB film. Saito et al. (1991 a,b) reported the optical absorption spectra of various molecular aggregates in the

interface-adsorbed complex LB films of arachidic acid and water-soluble cyanine dyes. They classified the dye aggregates in the complex LB film into four types, i.e., J-aggregate, H-aggregate, Davydov aggregate and 'monomer'. Here, the term 'monomer' does not necessarily mean that the dye molecules are isolated in the LB film but it includes the weak aggregate whose size is too small to be classified as either J-, H-, or Davydov aggregate. In order to denote this, the term is expressed with a set of single quotation marks. The J-aggregate (H-aggregate) gives rise to a sharp red-shifted (blue-shifted) absorption band compared to that of the isolated molecule in solution. The absorption spectrum of the Davydov aggregate shows large in-plane anisotropy both in the optical density and in the spectral band shape; it consists of two absorption bands, one which shows a red-shift and the other which shows a blue- shift relative to that of the isolated molecule in solution. The 'monomer' has only one transition moment and shows small in-plane anisotropy only in the optical density. Therefore, according to Saito et al.'s classification, the absorption spectra of the mixed LB film of β-carotene with barium stearate (1:10) shown in Fig. 6 correspond to that of the 'monomer' which is weakly perturbed by the short-range order in the film as discussed above.

The difference of the spectral band shape of the mixed LB film from that of the solution is not due to the intermolecular interaction between β-carotene and barium stearate. This is deduced from the fact that all-*trans*-lutein in the mixed LB film with L-α-phosphatidylcholine-β-oleyl-γ-stearoyl showed a similar absorption spectrum with that in an ethanol solution (N'soukpoé-Kossi et al., 1988), hence, all-*trans*-lutein is reported to be isolated in the mixed LB film. As described above, the short-range order similar to that of the single crystal also exists in the mixed LB film. Therefore, we can conclude that the β-carotene molecules are weakly aggregated in the mixed LB film; however, the size of the aggregate is too small to be identified as the J-, H-, or Davydov aggregate. In this sense, we classify the aggregate in the mixed LB film as the 'monomer' according to the classification for the cyanine dye aggregates. This interpretation is similar to that of Ohnishi et al. (1978) who reported that the β-carotene molecules are stacked in card pack manner in the mixed LB film. However, their interpretation seems to be inadequate since such a kind of aggregate is assigned to the H-aggregate in the cyanine dye aggregates (Saito et al., 1991a) and it may show the blue shift of the absorption band. Actually, the blue-shifted absorption band of the H-aggregate peaking around 400 nm has been reported for all-*trans*-lutein, all-*trans*-zeaxanthin or all-*trans*-astaxanthin in an aqueous solution (Salares et al., 1977), and the transformation of the H-aggregate (card-packed aggregate) to the J-aggregate (head-to-tail aggregate) of all-*trans*-astaxanthin was demonstrated by the present author and coworkers (Mori et al., 1996).

C. Resonance Raman Spectroscopy of all-trans-β-Carotene in the Condensed Phase

We investigated the mechanism activating the forbidden transition and the 2^1A_g energy for all-*trans*-β-carotene crystals by comparing resonance Raman excitation profiles in the 13990–21840 cm^{-1} region for randomly oriented crystals (ROC) with ones for a spin-coated amorphous film (SCF, see Section II), microcrystals dispersed in a KBr disk (MCD) and an isopentane solution (IPS) (Hashimoto et al., 1997). All-*trans*-β-carotene exhibits an intense Raman line around 1520 cm^{-1}, which is assigned to the a_g-type C=C stretching vibrational mode (hereafter referred to as ν_1). We found that the frequency of the ν_1 Raman line is structure sensitive; ν_1 frequencies of IPS at 160 K, SCF at 11 K, and ROC at 11 K were determined to be 1526.2 ± 1.1, 1524.8 ± 0.8, and 1516.5 ± 0.7 cm^{-1}, respectively.

Figure 12 shows excitation profiles for the ν_1 Raman lines of (a) IPS at 160 K, (b) SCF at 11 K, and (c) ROC at 11 K as well as their optical absorption spectra; in Fig. 12(c), the optical absorption spectrum of MCD is used as a substitute for that of ROC because the peak energies of vibrational progression for MCD are quite similar to those for the single crystal observed (see Section IV. A). In the excitation profiles of IPS and SCF, clear peaks due to rigorous resonance to the $^1B_u \leftarrow {}^1A_g$ (0,0) transition are observed. For ROC (Fig. 12(c)), an additional intense peak at 14500 cm^{-1} and a shoulder at around 16000 cm^{-1} are clearly observable in the excitation profile below the $^1B_u \leftarrow {}^1A_g$ transition; the result is very similar to that obtained for a single crystal by Gaier et al. (1991). The additional peak was not detected in MCD, SCF nor IPS.

The results shown in Fig. 12 indicate that the peak at 14500 cm^{-1}, which was found by Gaier et al. (1991) and was attributed to the forbidden transition to 2^1A_g, is observed only in the case of ROC; the

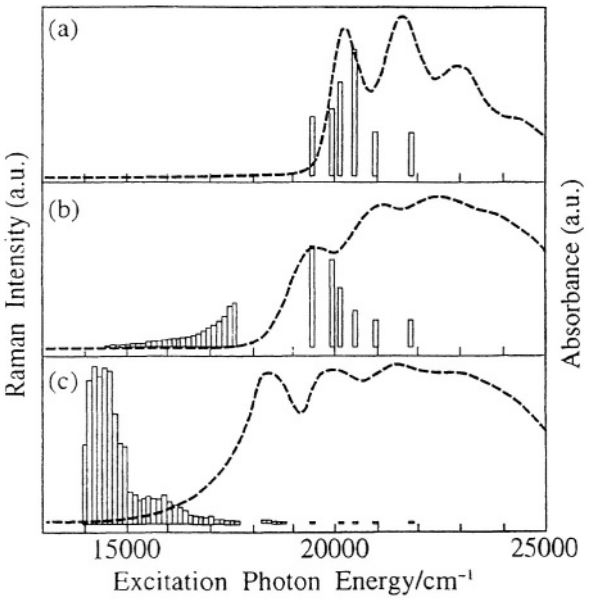

Fig. 12. Excitation profiles of the ν_1 Raman lines of all-*trans*-β-carotene for the (a) isopentane solution at 160 K, (b) spin-coated film at 11 K, and (c) randomly oriented crystals (grain size < 1 mm) at 11 K (bar graphs) as well as their optical absorption spectra (broken lines). The optical absorption spectrum in (c) is taken from that of microcrystals dispersed in a KBr disk.

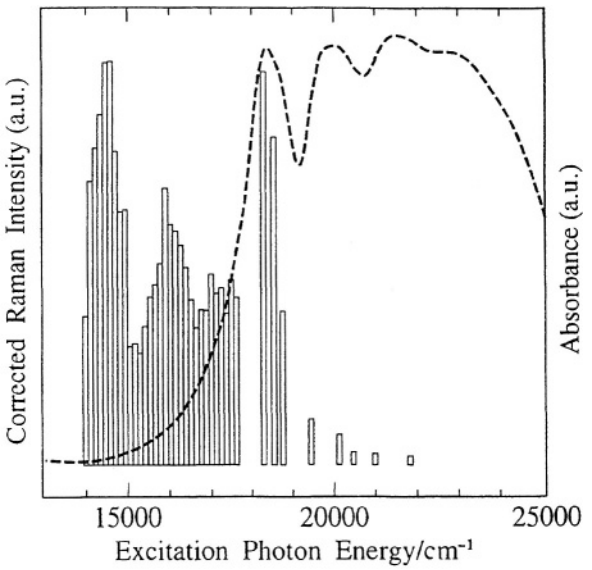

Fig. 13. Excitation profile of the ν_1 Raman line of all-*trans*-β-carotene for randomly oriented crystals at 11 K, which was corrected against the re-absorption of Raman scattering (bar-graph). The optical absorption of the microcrystals dispersed in a KBr disk is also shown for comparison.

constancy of the ν_1 frequencies supports the idea that the enhancement is intrinsic to the crystal.

We will discuss the intensity of the 14500 cm^{-1} peak. Since the measured Raman intensity in ROC is affected by the re-absorption of the Raman scattering, we try to eliminate this effect using the following equation

$$i_c(\nu) = a \cdot I(\nu) \cdot [\varepsilon(\nu_0) + \varepsilon(\nu)] \qquad (17)$$

where a is a constant, $i_c(\nu)$ and I(v) are the corrected and measured Raman intensities, and $\varepsilon(\nu_0)$ and $\varepsilon(\nu)$ are the absorption coefficients of the incident and scattered light at the frequencies of ν_0 and v, respectively. Equation (17) was derived for the backscattering geometry assuming an absorption so strong that there in no transmission of excitation light across the sample.

Figure 13 shows both the corrected excitation profile of the ν_1 Raman line for ROC and the optical absorption spectrum of MCD. Clear peaks are noted at 14500 and 16000 cm^{-1}, although the intensity of the peak at 18400 cm^{-1} relative to their intensities is increased substantially after this correction. Even a third peak at around 17500 cm^{-1} can be identified. Based on the spacings between these three peaks, these structures can be assigned to the vibrational progression of the $2^1A_g \leftarrow 1^1A_g$ transition. In addition, this observation suggests that the enhancement of Raman intensity in resonance with the 2^1A_g state can be ascribed to the A-term of the Albrecht theory, which is applicable to symmetric modes when the electronic transition dipole is not zero (Tang and Albrecht, 1970). Because a resonance Raman excitation profile originating from the B-term of the Albrecht theory, which is applicable to an asymmetric mode giving rise to vibronic coupling between two electronic excited states, is expected to generate the $2A_g(v) \leftarrow 1A_g(0)$ vibrational structures with v = 0 and 1 alone (Carey, 1982)

On the basis of a theoretical analysis of the resonance Raman excitation profile of all-*trans*-β-carotene using the A term (Inagaki et al., 1974), we can obtain the following relation for the Raman intensity when the Raman process is in resonance with the $0 \leftarrow 0$ transition,

$$I_b^{00}/I_a^{00} = [(f_b/f_a)(E_a/E_b)(\gamma_a/\gamma_b)]^2 \qquad (18)$$

where I_a^{00} and I_b^{00} are the Raman intensities, f_a and f_b are the oscillator strengths, E_a and E_b are the resonance energies, and γ_a and γ_b are the damping constants for

the transitions to the *a*-th and *b*-th stares. Hereafter, we define the *a*-th and *b*-th states as the 2^1A_g and ^1B_u states, respectively.

It is reported that the f_b value of the $^1B_u \leftarrow {}^1A_g$ transition of all-*trans*-β-carotene in solution is approximately 1 (Frank and Cogdell, 1993), and that the value is conserved in the crystal. When the values of $E_a/E_b = 14500/18400$, $\gamma_a/\gamma_b = (150 \times 10^{-15})/(10 \times 10^{-12})$ (adopted from the ratio between the lifetimes of the states of β-carotene solution (Hashimoto et al., 1991; Kandori et al., 1994) and $I_a^{00}/I_b^{00} = 0.97$ (taken from Fig. 13) are applied to Eq. (18), the f_a value of the $2^1A_g \leftarrow {}^1A_g$ transition can be estimated as 1×10^{-2}. This small value supports the assignment of the 14500 cm^{-1} peak to an optically forbidden transition, which is very likely to be 2^1A_g as proposed by Gaier et al. (1991).

Using the above results of the lifetimes together with the radiative relaxation times estimated from f_a and f_b, we can estimate the intensity ratio $R(2^1A_g/{}^1B_u)$ of the fluorescence from the 2^1A_g level to that from the ^1B_u level. The estimated value of 0.4 agrees with the experimental result of 0.8. The agreement supports the validity of the estimated f_a above.

Since the 14500 cm^{-1} peak is not observed in SCF, it is natural to check whether the intermolecular interaction between β-carotene molecules might be the mechanism allowing this transition. SCF was proved to be an amorphous film and its density was determined as $\rho = 0.835$ g /cm^3 (see Section II). The density of the single crystal was determined to be 1.016 g/cm^3 (see Section III). We can estimate an average interaction strength H_i in ROC compared with that in SCF from the density of the solids. The ratio of the H_i values of ROC to SCF is somewhat around the ratio of the densities (1.016/0.835). The $2^1A_g \leftarrow {}^1A_g$ transition was not detected in SCF, which means that its signal in SCF must be at least three orders of magnitude weaker than that in ROC. This difference in intensity is too large to be consistent with the ratio of H_i. Consequently, the mechanism activating the forbidden transition is not simply relevant to intermolecular interaction.

The above consequence suggests that some degradation of the symmetry takes place in ROC to allow the forbidden transition. The difference in the Raman excitation profiles between ROC and MCD indicate that the Raman excitation profile depends on the crystal size (we confirmed experimentally the lack of the additional peak in the microcrystals powder). This result, together with the SCF result, means that the degradation can occur only when both requirements of periodic molecular arrangement and crystal size are fulfilled.

The degradation induced in ROC may be an asymmetric distortion in the molecular crystal, and this distortion could be either time-independent (static) or time-dependent (vibration), the latter being the case for benzene (Ziegler and Hudson, 1980) and the interpretation adopted by Gaier et al. (1991). However, it is unlikely that the difference in ROC from both SCF and MCD causes such an essential difference in vibrational structure; therefore, the latter can be ruled out. We propose that the symmetry degradation is due to a static distortion in the crystal at 11 K. Actually, X-ray crystallography of all-*trans*-β-carotene showed a disorder in the C(2) and C(3) atoms (see Section III). This result suggests that the coupling of the electron with non-totally symmetric mode in all-*trans*-β-carotene may be weak compared with that in benzene, and that the peak energy of 14500 cm^{-1} corresponds to the 2^1A_g electron energy. Our recent study on the crystals of all-*trans*-spheroidene supported this conclusion (Sashima et al., 1998).

V. Transient Optical Properties of all-trans-β-Carotene Single Crystals

One dimensional conducting polymers are well known as synthetic metals because of their wide-range of controllability of electrical conductivity. They have attracted considerable attention, since the study of these systems has given rise to entirely new scientific concepts as well as promising new technologies. A simple example of the class of conducting polymer is *trans*-polyacetylene. It consists of a weakly coupled chain of CH units forming a pseudo-one-dimensional lattice. Its chainlike structure leads to strong coupling of electronic states, and conformational excitations, such as 'solitons' peculiar to the one-dimensional system, are generated.

Upon photoexcitation of the film of *trans*-polyacetylene, it gives rise to two induced-absorption bands in the gap state, i.e., a high-energy (HE) band at 1.4 eV and a low-energy band at 0.5 eV Based on time-resolved absorption measurements in the femtosecond to millisecond time regime, as well as EPR (electron paramagnetic resonance) measurements, it is now well established that the elementary excitations which give rise to the HE band are neutral

solitons, while those giving rise to the LE band are charged solitons (Verdeny, 1993). These solitons are reported to extend over 5 to 10 C=C bonds (Heeger et al., 1988), and they are thought to play the crucial role of energy- and charge-carrying excitations.

All-*trans*-β-carotene has a similar structure with *trans*-polyacetylene, and it is often referred to as a model compound of *trans*-polyacetylene. It is one of the longest conjugated oligomers (a finite polyene), with a chain length long enough to accommodate the solitons. Although powder crystals of all-*trans*-β-carotene show photoconductivity which increase upon doping oxygen and extends to the near-infrared region (Mori et al., 1995), the mechanisms of the generation and transportation of the carriers have not been clarified.

Keeping all these things in mind, it is intriguing to address the following two questions. (1) Why do all-*trans*-β-carotene crystals give rise to photoconductivity that extends to the near-infrared region? (2) Is it possible to find metastable states in all-*trans*-β-carotene crystals that corresponds to the solitons in *trans*-polyacetylene? In order to answer these questions, we have applied photoinduced and time-resolved absorption spectroscopies to the all-*trans*-β-carotene single crystals (Hashimoto et al., 1998).

A. Experimental Procedures for Optical Characterization

Optical absorption spectra of the single crystals in the infrared spectral region were recorded at room temperature using a single-beam monochromator (JASCO, CT-25C), PbS (Hamamatsu, P394) and InSb (Hamamatsu, P839-07) detectors which have sensitivity in the infrared spectral regions, and a lock-in amplifier (EG and G, Model 5101). The output signals of the lock-in amplifier were digitized and accumulated in a personal computer (NEC, PC9801-UV).

The single crystals were placed in a cryostat and were kept at cryogenic temperature for the photoinduced and time-resolved absorption measurements. Both pump and probe beams polarized along the *b*-crystal axis were exposed onto the *ab*-plane of the crystals. As regards the photoinduced absorption measurements, we used an Ar^+-laser (Lexel, Model 95) and a CW dye laser (Spectra-Physics 375) for excitation. A probe beam was derived from a 40 W tungsten halogen lamp, dispersed by a monochromator (JASCO, CT-25C) in the spectral range of 950 to 1700 nm. The power of the pump beam was set as low as possible (approx. 20 $\mu W/cm^2$) in order to eliminate the effect of heating of the crystals. The pump beam was modulated by a chopper with a frequency of 1 kHz. The probe transmission T and its modulated changes of ΔT were measured using an InGaAs detector (Hamamatsu, G3476-05) and a lock-in amplifier (EG and G, Model 5101). The spectra were normalized in the form of $\Delta T/T$, that is proportional to the induced absorption. As regards the time-resolved absorption measurements, we used a pulsed dye laser (PTI, PL202, 120 μJ/pulse, 500 ps, 1 Hz) pumped by a nitrogen laser (PTI, PL2300) for excitation. The time dependence of ΔT was measured using an InGaAs detector (Hamamatsu, G3476-05) and a digital oscilloscope (Tektronix, TDS-302). The time resolution of the apparatus was set to be 1 μs.

*B. Optical Absorption Spectra of all-*trans*-β-Carotene Single Crystals in the Infrared Spectral Region*

Optical absorption spectra of all-*trans*-β-carotene single crystal in the visible region were shown in Fig. 10. According to these spectra, the single crystals give rise to strong absorptions in the visible region, and the near-infrared region seems to be transparent. However, we found new absorption bands in the near- to mid-infrared region by directly measuring the absorption spectra of the single crystals.

Figure 14 shows optical absorption spectra of the single crystals recorded at room temperature in the spectral range of 600 to 4000 nm. Together with sharp absorption bands due to intramolecular phonons, we can see broad and anisotropic absorption bands that show a gradual increase from the near- to mid-infrared region as the background of the sharp phonon lines. This observation indicates that there exist substantial energy levels in the near- to mid-infrared region of the single crystals. The presence of these infrared absorption bands is supported by the photoinduced absorption measurements described below.

*C. Photoinduced Bleaching of the Infrared Absorption Bands and Its Recovery as Observed for all-*trans*-β-Carotene Single Crystals*

Figure 15 shows the photoinduced absorption (bleaching) spectrum of the single crystals of all-

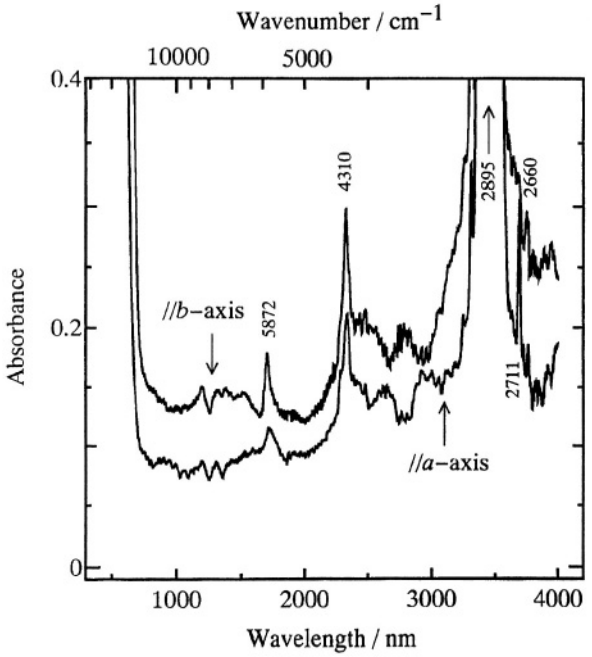

Fig. 14. Optical absorption spectra of all-*trans*-β-carotene single crystals in the visible to mid-infrared region recorded at room temperature by irradiating light polarized along *a* or *b* crystal axis.

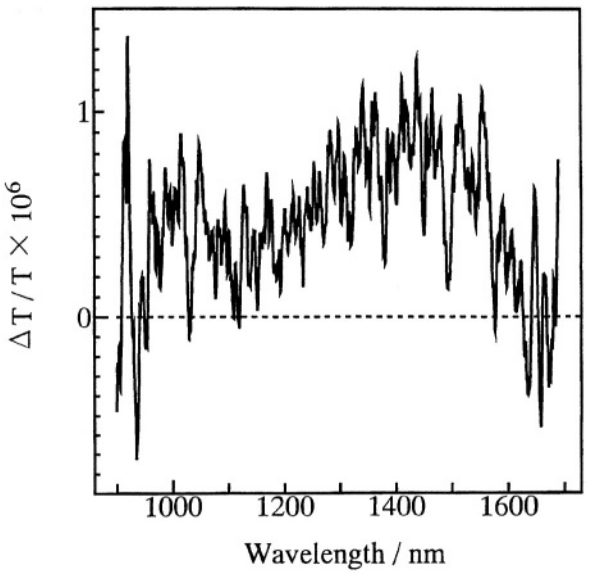

Fig. 15. Photoinduced bleaching of the infrared absorption band of an all-*trans*-β-carotene single crystal recorded at 11 K and excited at 575 nm.

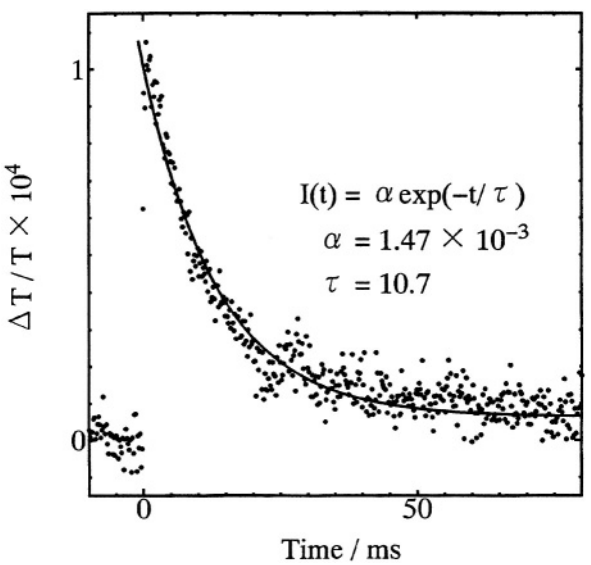

Fig. 16. Single-exponential recovery of the photoinduced bleaching of a single crystal of all-*trans*-β-carotene recorded at 77 K. The crystal was excited at 575 nm and the recovery was probed at 1300 nm.

trans-β-carotene at 11 K when excited at 575 nm and probed in the spectral range of 950 to 1700 nm. The spectrum shows weak but apparent bleaching of the infrared absorption band due to the photoexcitation of the visible absorption band. This observation confirms the presence of energy levels in the infrared region of the single crystals, and shows that the energy levels which give rise to the infrared absorption bands are closely related to the energy levels which give rise to the visible absorption bands. We further examined the recovery of this bleaching by time-resolved absorption spectroscopy.

We examined the recovery when excited at 575 nm and probed at 1300 nm for many crystals, and found typically a single-exponential recovery with a lifetime of ~10 ms, as illustrated in Fig. 16. This observation strongly suggests the generation and the relaxation of a metastable state after the photoexcitation of the single crystals. Furthermore, depending on the crystals, we could observe other two types of recovery, as illustrated in Fig. 17. In Figs. 17(a) and 17(b), we could identify, respectively, stretched-exponential [$\alpha\exp(-(t/\tau)\beta)$, $\tau = 2.42 \times 10^{-5}$ s, $\beta = 0.19$] and power-law [$\alpha t^{-\beta}$, $\beta = 1.02$] recoveries. These observations correspond to the intrinsic phenomena upon photoexcitation of the single crystals, and possibilities due to the heating of the crystals or thermal lens effect are excluded based on the experimental evidences (Hashimoto et al., 1998).

At this stage, it is speculative to assign the origins of the above recoveries but it may be worthwhile to compare the above recoveries to those of *trans*-polyacetylene. As already mentioned, *trans*-

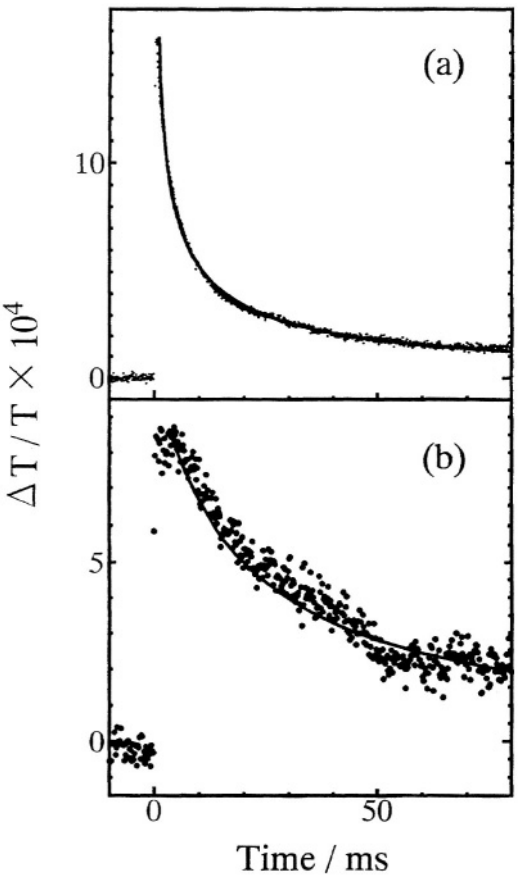

Fig. 17. (a) Stretched-exponential and (b) power-law recoveries of the bleaching of the infrared absorption bands of all-*trans*-β-carotene single crystals recorded at 77 K. The crystals were excited at 575 nm and the recoveries were probed at 1300 nm.

polyacetylene film exhibits two photoinduced absorption bands. Based on the time-resolved absorption measurements for oriented films of *trans*-polyacetylene in the femtosecond to millisecond time regime, it has been reported that the HE band decays in the stretched-exponential mode ($\beta = 0.3$ at 80 K), and the decay is attributed to the recombination of the neutral soliton-antisoliton pairs (Verdeny, 1993). On the other hand, the LE band decays in the power-low mode ($\beta < 1$), and the decay is attributed to the recombination of charged solitons (Verdeny, 1993). Slow relaxation of the LE band in the millisecond time regime is attributed to the recombination of the charged solitons involving three-dimensional interchain carrier hopping. By inference based on the similarity of the recovery types of all-*trans*-β-carotene single crystals to the decay patterns of the HE and LE bands of *trans*-polyacetylene, the stretched-exponential and power-low recoveries of the infrared absorption bands of all-*trans*-β-carotene single crystals may be attributed to the recombination of photogenerated carriers such as solitons in *trans*-polyacetylene. The idea for the generation of solitonlike excitations in a finite chain of all-*trans*-β-carotene are supported by the theoretical calculations (Hashimoto et al., 1998).

The questions set forth here are answered as follows: First, broad and anisotropic absorption bands where found to gradually increase from the near- to mid-infrared region of all-*trans*-β-carotene single crystals. Second, the stretched-exponential and power-law recoveries of the photoinduced bleaching of the infrared absorption bands may correspond to the recombination of the solitonlike excitations in all-*trans*-β-carotene single crystals.

References

Babaev TB and Al'perovich LI (1973) Optical characteristics of β-carotene films. Zh Prikl Spectrosk 18: 513–515

Bart JCJ and MacGillavry CH (1968) The crystal and molecular structure of canthaxanthin. Acta Cryst B24: 1587–1606

Blodgett K (1935) Films built by depositing successive monolayers on a solid surface. J Am Chem Soc 57: 1007–1022

Bom M and Wolf E (1980) Principles of Optics. Pergamon Press, Oxford

Carey PR (1982) Biochemical Applications of Raman and Resonance Raman Spectroscopies. Academic, Tokyo

Chapman D, Cherry RJ and Morrison A (1967) Spectroscopic and electrical studies of all-*trans*-β-carotene crystals. Proc Roy Soc A 301: 173–193

Davydov AS (1962) Theory of Molecular Excitons: Kasha M and Oppenheimer Jr. M (transl). McGraw Hill, New York

Davydov AS (1971) Theory of Molecular Excitons: Dresner S.B. (transl). Plenum Press, New York

Deisenhofer J and Michel H (1989) The photosynthetic reaction center from the purple bacterium *Rhodopseudomonas viridis.* Science 245: 1463–1473

Drikos G, Dietrich H and Rüppel H (1988) The polarized UV-absorption spectra and the crystal structure of two different monoclinic crystal forms of the retinal homologue β-8'-apocarotenal. Eur. Biophys J 16: 193–205

Frank HA and Cogdell RJ (1993) The photochemsitry and function of carotenoids in photosynthesis. In: Young A and Britton G (eds) Carotenoids in Photosynthesis, pp 252–326. Chapman and Hall, London

Gaier K, Angerhofer A and Wolf HC (1991) The lowest excited electronic singlet states of all-*trans*-β-carotene single crystals. Chem Phys Lett 187: 103–109

Hashimoto H, Koyama Y, Hirata Y and Mataga N (1991) S_1 and T_1 species of β-carotene generated by direct photoexcitation from the all-*trans,* 9-*cis,* 13-*cis* and 15-*cis* isomers as revealed by picosecond transient absorption and transient Raman spectroscopies. J Phys Chem 95: 3072–3076

Hashimoto H, Kiyohara D, Kamo Y, Komuta H and Mori Y (1996) Molecular orientation of all-*trans*-β-carotene in spin-coated film and in Langmuir-Blodgett film as detected by polarized optical absorption and reflection spectroscopies. Jpn J Appl Phys 35: 281–289

Hashimoto H, Koyama Y and Mori Y (1997) Mechanism activating the 2^1A_g state in all-*trans*-β-carotene crystal to resonance Raman scattering. Jpn J Appl Phys 36: L916–L918

Hashimoto H, Sawahara Y, Okada Y, Hattori K, Inoue T and Matsushima R (1998) Observation of solitonlike excitations in all-*trans*-β-carotene single crystals. Jpn J Appl Phys: 37: 1911–1918

Heeger AJ, Kivelson S, Schrieffer JR and Su W-P (1988) Solitons in conducting polymers. Rev Mod Phys 60: 781–850

Humphreys-Owen SPF (1961) Comparison of reflection methods for measuring optical constants without polarimetric analysis, and proposal for new methods based on the Brewster angle. Proc Phys Soc 77: 949–957

Inagaki F, Tasumi M and Miyazawa T (1974) Excitation profile of the resonance Raman effect of β-carotene. J Mol Spectrosc 50: 286–303

Kandori H, Sasabe H and Mimuro M (1994) Direct determination of the S_2 state of β-carotene by femtosecond time-resolved fluorescence spectroscopy. J Am Chem Soc 116: 2671–2672

Karrasch S, Bullough PA and Ghosh R (1995) The 8.5 Å projection map of the light-harvesting complex I from *Rhodospirillum rubrum* reveals a ring composed of 16 subunits. EMBO J 14: 631–638

Kawai T, Umemura J and Takenaka T (1989) Non-resonance Raman studies on spread monolayers of stearic acid-d_{35} and cadmium stearate-d_{35} on water surfaces and thin LB films. Chem Phys Lett 162: 243–247

Koyama Y and Hashimoto H (1993) Spectroscopic studies of carotenoids in photosynthetic systems. In: Young A and Britton G (eds) Carotenoids in Photosynthesis, pp 327–408. Chapman and Hall, London

Külbrandt W, Wang DN and Fujimori Y (1994) Atomic model of plant light-harvesting complex by electron crystallography. Nature 367: 614–621

Lebranc RM and Orger BH (1972) β-Carotene film at water-air interface. Biochim Biophys Acta 275: 102

Madjid AH (1975) Diffusion zone process, a new method for growing crystals. Phys Teach 13: 176–179

Mann B and Kuhn H (1971) Tunneling through fatty acid salt monolayers. J Appl Phys 42: 4398–4405

Marder SR, Torruellas WE, Blanchard-Desce M, Ricci V, Stegeman GI, Gilmour S, Brédas J-L, Li J, Bublitz GU and Boxer SG (1997) Large molecular third-order optical nonlinearities in polarized carotenoids. Science 276: 1233–1236

McDermott G, Prince SM, Freer AA, Hawthornthwaite-Lawless AM, Papiz MZ, Cogdell RJ and Isaacs NW (1995) Crystal structure of an integral membrane light-harvesting complex from photosynthetic bacteria. Nature 374: 517–521.

Mori Y, Hosokawa K, Teramoto H and Hashimoto H (1995) Photoconductivity of all-*trans*-β-carotene and all-*trans*-β-apo-8'-carotenal. Proc SPIE 2362: 231–239

Mori Y, Yamano K and Hashimoto H (1996) Bistable aggregate of all-*trans*-astaxanthin in an aqueous solution. Chem Phys Lett 254: 84–88

N'soukpoé-Kossi CN, Sielewiesiuk J, Leblanc RM, Bone RA and Landrum JT (1988) Linear dichroism and orientational studies of carotenoid Langmuir-Blodgett films. Biochim Biophys Acta 940: 255–265

Ohnishi T, Hatakeyama M, Yamamoto N and Tsubomura H (1978) Electrical and spectroscopic investigations of molecular layers of fatty acids including carotene. Bull Chem Soc Jpn 51: 1714–1716

Otto S (1987) Key to Carotenoids. Pfander H, Gerspacher M, Rychener M and Schwabe R (eds) 2nd enlarged and revised edition. Birkhäuser Verlag, Basel

Palacin S, Blanchard-Desce M, Lehn JM and Barraud A (1989) Well organized Langmuir-Blodgett films based on push-pull carotenoids. Thin Sold Films 178: 387–392

Saito K, Ikegami K, Kuroda S, Saito M, Tabe Y and Sugi M (1991a) Modification of aggregate formation in arachidic-acid–cysanine-dye complex Langmuir-Blodgett films by substituent groups. J Appl Phys 69: 8291–8297

Saito K, Ikegami K, Kuroda S, Tabe Y and Sugi M (1991b) Formation of herringbone structure with Davydov splitting in cyanine dye-adsorbed Langmuir-Blodgett films. Jpn J Appl Phys 30: 1836–1840

Salares VR, Young NM, Carey PR and Bernstein HJ (1977) Excited state (exciton) interaction in polyene aggregates. J Raman Spectrosc 6: 282–288

Sashima T, Shiba M, Hashimoto H, Nagae H and Koyama Y (1998) The $2^1A_g^-$ energy of crystalline all-*trans*-spheroidene as determined by resonance-Raman excitation profiles. Chem Phys Lett: 290: 36–42

Senge MO, Hope H and Smith KM (1992) Structure and conformation of photosynthetic pigments and related compounds 3. Crystal structure of β-carotene. Z Naturforsch 47c: 474–476

Schmidt S and Reich R (1972) Über den Einfluß elektrischer Felder auf das Absorptionsspektrum von Farbstoffinolekülen in Lipidschichten. III Electrochromie eines Carotinoids (Lutein). Ber. Bunsenges. Phys Chem 76: 1202–1208

Sterling C (1964) Crystal-structure analysis of β-carotene. Acta Cryst 17: 1224–1228

Tang J and Albrecht AC (1970) Developments in the theories of vibrational Raman intensities. In: Szymanski HA (ed) Raman Spectroscopy, Vol 2, pp 33–68. Plenum, New York

Tsukida K, Saiki K, Takii T and Koyama Y (1982) Separation and determination of *cis*/*trans*-β-carotenes by high-performance liquid chromatography. J Chromatogr 245: 359–364

Vaala AR, Madjid AH and Torrado MT (1973) On the growing of large single crystals of the biological carotenoid pigment, β-carotene. J Crystal Growth 18: 39–44

Vardeny ZV (1993) Evolution of photoexcitations in poly-acetylene and related polymers from femtoseconds to milliseconds. In: Kobayashi T (ed) Relaxation in Polymers, pp. 166–214. World Scientific, Singapore

Ziegler LD and Hudson B (1981) Resonance Raman scattering of benzene and benzene-d_6 with 212.8 nm excitation. J Chem Phys 74: 982–992

This page intentionally left blank

Chapter 20

Carotenoids in Membranes

Wieslaw I. Gruszecki
Department of Biophysics, Institute of Physics,
Marie Curie-Sklodowska University, 20-031 Lublin, Poland

Summary

Membranes of bacteria, plants and animals contain carotenoid pigments as direct constituents of their lipid phase. The rod-like structure of a carotenoid molecule, often terminated with polar groups and the molecular dimensions of a typical carotenoid matching the thickness of the hydrophobic membrane core, are directly responsible for the localization and orientation of pigment molecules within the membrane and for effects on the membrane properties. Model studies have revealed several effects of carotenoids on structure and dynamics of lipid membranes. Restrictions to the motional freedom of lipids due to the hydrophobic interactions with rigid rod-like molecules of Carotenoids are the main cause of the effects on the membrane properties such as the increase in the membrane rigidity and thermostability or the increase in the penetration barrier to molecular oxygen and other small molecules. These and other effects on the membrane properties are reviewed and discussed with regard to the carotenoid biological functions in biomembranes including those already well established and experimentally proven, such as in the membranes of bacteria, those currently studied, like the effects of the xanthophyll pigments on the thylakoid membranes as well as those predictable on the basis of the results of the experiments carried out in model systems, awaiting confirmation from detailed physiological studies.

H. A. Frank, A. J. Young, G. Britton and R. J. Cogdell (eds): The Photochemistry of Carotenoids, pp. 363–379.

I. Are Carotenoids Present in Lipid Membranes?

According to a general, current view, physiologically active carotenoid pigments in biomembranes are functionally attached to membrane proteins. Such a statement applies in particular to the photosynthetic membranes comprising chlorophyll- and carotenoid-containing light-harvesting pigment-proteins and protein complexes of reaction centers (see other chapters). On the other hand, there are several indications that a certain pool of carotenoid pigments is directly present in a lipid phase of membranes. This holds true for the membranes of the retina (Bone and Landrum, 1984; Bone et al., 1992), other photoreceptors (Anton-Erxleben and Langer, 1987), membranes of bacteria (Huang and Haug, 1974; Omata and Murata, 1984; Gombos and Vigh, 1986; Gombos et al., 1987; Chamberlain et al., 1991; Yurkov et al., 1993) but also for the photosynthetic membranes. The light-dependent interconversion of photosynthetic xanthophyll pigments: violaxanthin, antheraxanthin and zeaxanthin in higher plants in the reactions of the so-called xanthophyll cycle (Chapter 16, Yamamoto) requires uncoupling of these pigments from proteins and their diffusion in the thylakoid membranes where the main xanthophyll cycle enzymes are localized and spatially separated. A transient but direct xanthophyll presence in the photosynthetic membranes is not only an idea following directly from the transmembrane organization of the xanthophyll cycle (Siefermann and Yamamoto, 1975; Hager and Holocher, 1994) but also has an experimental support as will be discussed in section V.

This chapter presents research on the organization of carotenoid-lipid membranes. Diverse experimental techniques show a pronounced influence of carotenoid pigments on structural and dynamic properties of membranes. It is, however, a matter of debate whether all these effects are physiologically relevant. The problem of a physiological importance of carotenoids in membranes will be pointed out in the last section of this chapter, but also it appears in other chapters of this publication.

Abbreviations: DBPC–dibehanoylphosphatidylcholine; DGDG – digalactosyldiacylglycerol; DLPC – dilauroylphosphatidylcholine; DMPC – dimyristoylphosphatidylcholine; DOPC – dioleoylphosphatidylcholine; DPPC– dipalmitoylphosphatidylcholine; DSPC – distearoylphosphatidylcholine; EYPC – egg yolk phosphatidylcholine; MGDG – monogalactosyldiacyl–glycerol; PC – phosphatidylcholine; SASL – stearic acid spin label

II. Localization of Carotenoids in Lipid Membranes

Carotenes are entirely lipophyllic molecules and may be expected to be located in a hydrophobic core of a membrane. The same localization may be expected for xanthophylls, largely hydrophobic molecules with their polar groups located at the opposite sides of a long rod-like non-polar skeleton. On the other hand, the process of energy minimization requires xanthophyll polar groups to be placed outside the membrane hydrophobic core in the water phase or more likely in the polar head-group region of a membrane. Such a condition to be fulfilled in the case of xanthophylls would obviously limit orientational freedom of a pigment molecule with respect to a membrane. The expectation that carotenoid chromophores are localized in a hydrophobic environment of a membrane has experimental support from the measurements of the position of electronic absorption spectra of these pigments in different organic solvents and while incorporated into lipid membranes (Milon et al., 1986a; Gruszecki and Sielewiesiuk, 1990; Andersson et al., 1991). The determination of pigment localization is based on the correlation of a position of absorption maximum and dielectric properties of a chromophore moiety represented by solvent polarizability which is a function of the appropriate refractive index. Figure 1 presents such a correlation for zeaxanthin dissolved in several organic solvents and incorporated into DPPC liposomes. As stated above, the location of polar groups with respect to a lipid bilayer is the second main determinant of the organization of carotenoid-lipid membranes. The requirement of polar groups of carotenoids to be displaced out of the membrane hydrophobic core implies two essentially different pigment orientations with respect to the membrane: one in which polar groups located at the opposite side of a molecule are placed in two different head-group zones and the other in which both polar sides of a pigment molecule are in contact with the same polar region of a membrane. In principle both orientations are possible taking into account geometry of a membrane and the molecular dimension of a typical C40 carotenoid, although stereochemical conditions would imply

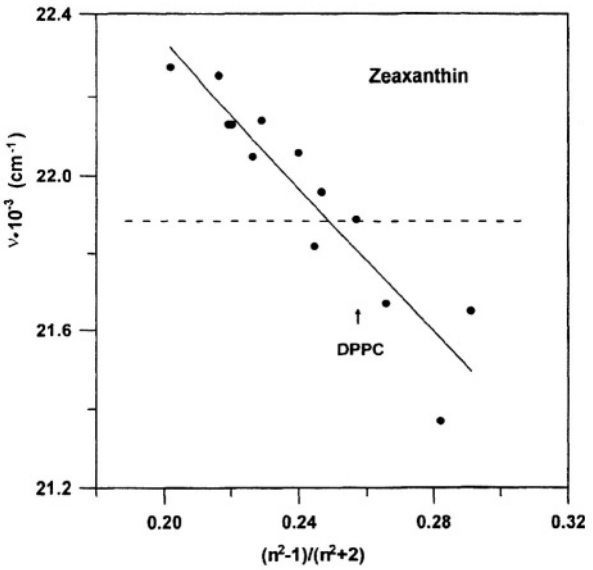

Fig. 1. Dependence of the position of the main electronic absorption maximum of zeaxanthin dissolved in several organic solvents of the refractive index n on the polarizability term. The position of the absorption maximum of zeaxanthin embedded to DPPC liposomes indicated with the dashed line and the value of a polarizability term of phosphatidylcholine hydrophobic core indicated with the arrow. Data for the plot were taken from Milon et al. (1986a), Britton (1995b) and from own measurements.

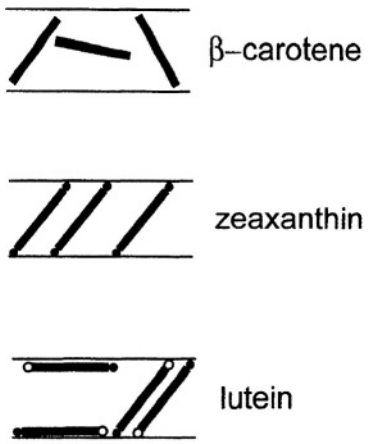

Fig. 2. Schematic representation of the hydrophobic core of the lipid bilayer and the carotenoid pigments oriented differently depending on their stereochemical structure. The picture refers to EYPC membrane and different pigments indicated. For details see Table 1.

some orientations to be more preferable, as will be discussed below for zeaxanthin and lutein as examples. A membrane-spanning orientation of a typical xanthophyll molecule seems to be a direct consequence of reasonably good matching of the thickness of the hydrophobic core of biomembranes (about 3 nm in the case of thylakoid membranes, Kühlbrandt and Wang, 1991) and the distance between opposite polar groups (between 3 and 3.2 nm depending on the exact location of oxygen atoms in a carotenoid, Milon et al., 1986a). Such a concept is depicted in Fig. 2: the thickness of the hydrophobic core of a membrane smaller than the distance of polar groups forces a xanthophyll molecule to adopt a tilted orientation with respect to the axis normal to the membrane. The opposite proportion of the dimensions of a membrane and a pigment molecule influences predominantly the thickness of a membrane (see DPPC, Table 1). Owing to the well-defined orientation of a dipole-transition moment with respect to rod-like-shaped molecule orientation, carotenoids may be examined by means of a linear dichroism technique in ordered lipid-layer samples. Table 1 presents data on the thickness of a hydrophobic core of membranes formed with different lipid components as well as the expected and experimentally determined carotenoid orientations. It may be seen from Table 1 there is no general rule in the orientation of β-carotene within a lipid bilayer. On the one hand, hydrophobic interactions with acyl fatty acid chains would orient the carotenoid molecule parallel with respect to the normal to the membrane, especially in the gel state of a lipid phase and on the other hand, lack of any polar groups able to be anchored in head-group regions provides no conditions for carotenoid orientational order based on hydrogen bonding. This dualism is represented by the coexistence of two differently oriented pools of β-carotene in membranes formed with DMPC or DGDG or by an orientation close to the magic angle (54.7°) in membranes formed with EYPC which is consistent with the random orientation of chromophores within the membrane. As it may be expected all polar carotenoids examined, tend to adopt an orientation defined by the acute angle between the molecular axis and the axis normal to the membrane, clearly lower than the magic angle. The condition of matching the distance between polar groups and the thickness of the membrane hydrophobic core leads to relatively good predictions of a carotenoid orientation, in particular in the case of fluid membranes formed with unsaturated lipids (EYPC). A striking exception to this rule is an orientation of lutein. The mean angle between molecules and the normal to the membrane plane are much wider than the predicted one. Such a discrepancy does not appear

Table 1. Orientation of carotenoid pigments in lipid bilayers

Lipid component	Thickness of the hydrophobic core[a] [nm]	Carotenoid	Predicted orientation[b] [deg]	Determined orientation[b,c] [deg]
EYPC	2.26			
	2.17	β-carotene	45–90	55 [d]
	2.17	β-carotene		0 and 90 [f]
	2.26	zeaxanthin	45	44
	2.33	lutein	45	67
	2.33	β-cryptoxanthin	–	38
	2.25	canthaxanthin	> 25	29
	2.21	astaxanthin	25	26
	2.30	lycopene	45–90	74
		1,2,1′,2′ tetrahydro-lycopene-1,1′-diol	45–52	48
1-oleoyl-sn-glycerol		β-carotene		90 [e]
polyglycerol monolaurate		β-carotene		90 [e]
DOPC		β-carotene		~ 90 [f]
SBPC		β-carotene		~ 0 [f]
		crocetin		0 and 90 [f]
DMPC	2.54			
	2.74	violaxanthin	33	22
	2.76	zeaxanthin	33	25
		β-carotene		0 and 90 [f]
DPPC	3.22			
	3.05	zeaxanthin	16	36
	3.05	lutein	16	57
Outer membrane of *Synechocistis* PCC6714		zeaxanthin myxoxanthophyll and other minor xanthophylls		~ 90 [g]
DGDG		violaxanthin		28
		zeaxanthin		9
MGDG		violaxanthin		35
		zeaxanthin		17

[a] The thickness of the membrane hydrophobic core determined in the author's laboratory on the basis of the diffractometric measurements at 25 °C. For details see Gruszecki and Sielewiesiuk (1990, 1991) and Gruszecki et al. (1994).
[b] The angle formed by the axis defined by the conjugated double bond chain and the axis normal to the plain of the membrane.
[c] The typical experimental error in determining carotenoid orientation on the basis of 3–5 experiments is lower than 10%.
[d] if not indicated, determinations were made in the author's laboratory at 25 °C. Some of them are published (Gruszecki and Sielewiesiuk, 1991, 1992) or unpublished (A.A. Woodall et al.).
[e] reported by Johansson et al. (1981).
[f] reported by Van de Ven et al. (1984).
[g] reported by Jürgens and Mäntle (1991).

in the case of zeaxanthin. In this case the predicted orientation is reasonably close to the one found in the experiment. The different behavior observed for lutein and zeaxanthin is somewhat surprising considering that both pigments are C40 xanthophylls with hydroxyl groups located at the 3 and 3′ positions. Zeaxanthin and lutein differ in the position of a terminal ring double bond which is located between the carbon atoms 4′ and 5′ in lutein and between the carbon atoms 5′ and 6′ in zeaxanthin. Such a difference results not only in the altered spectroscopic properties of both pigments related directly to the length of the conjugated double bond system, but also in the stereochemical conformations of the molecules. The essential molecular feature of lutein different from zeaxanthin is the potential of the entire terminal ring to rotate round about the 6′-7′ single bond. This provides the possibility of interaction of both hydroxyl groups located at the 3 and 3′ positions with the same polar zone of the

membrane. A direct consequence of such a pigment localization is its orientation which may be parallel to the plane of the membrane. A relatively large mean orientation angle of lutein may be interpreted as an expression of the existence of two essentially different pools of pigment molecules; one oriented parallel to the plane of the membrane and the second having the same orientation as zeaxanthin. The angle of 67° reported in Table 1 for lutein incorporated into membranes formed with EYPC corresponds to a population of 71 % of a pigment pool oriented parallel to the plane of the membrane and the remaining 29% having the same orientation as zeaxanthin (44°). This proportion is different in membranes formed with entirely saturated lecithin, DPPC: 48% parallel and 52% perpendicular to the membrane.

Additional information concerning the organization of carotenoid-pigmented lipid membranes may be obtained from a comparison of the thickness of the hydrophobic core of a membrane with and without a pigment component (Table 1). The differences are significant in membranes formed with saturated lipids, DMPC and DPPC. As it may be seen, a presence of xanthophyll pigments in the hydrophobic core of a membrane increases its thickness when it is smaller than the distance between opposite polar groups in a membrane-spanning pigment molecule (the case of DMPC) and slightly decreases its thickness when it is larger than the distance between opposite polar groups (the case of DPPC). Such a phenomenon reflects a strong interaction of rigid, rod-like molecules of carotenoid pigments and hydrophobic core-forming lipid alkyl chains. It may be expected that this type of interaction influences molecular dynamic properties of lipid membranes.

III. Solubility of Carotenoids in Lipid Membranes

Largely lipophyllic molecules of carotenoids are well miscible with lipids (Borel et al., 1996) and like lipids they are well soluble in most organic solvents (some carotenoids require special solvent mixtures to yield efficient solubilization with lipids). This property of both lipids and carotenoids is most frequently applied to prepare carotenoid-pigmented model lipid membranes. It involves the evaporation of a carotenoid lipid mixture followed by the hydration of a thin dry film. There are several different approaches to address the problem of the solubility of carotenoids within lipid membranes. The selection of an appropriate experimental procedure as well as instrumental technique depends on a particular approach. The kind of information obtained, concerning solubility of carotenoids in lipid membranes depends also on a selected method. One approach is based on the observation of incorporation of carotenoids present in a water phase, in most cases in a microcrystalline form, into the lipid phase of membranes, in most cases unilamellar or multilamellar liposomes. (Gruszecki, 1986,1990a;Takagi et al., 1987).This method is based on the removal of non-incorporated pigment molecules remaining as microcrystals via selective centrifugation, frequently combined with liposome filtration and on the differences in spectroscopic characteristics of carotenoids in lipid and water phases. On the other hand, the spectra of carotenoids remaining in a water phase in a form of molecular aggregates (Hager, 1970) are exceptionally close to those formed directly in lipid membranes (Mendelsohn and Van Holten, 1979; Gruszecki, 1990b) due to a very similar organization pattern of both carotenoid crystals and small molecular aggregates (Gruszecki, 1991). The presence of aggregated forms of a xanthophyll pigment, lutein, within a lipid phase of DPPC membranes may be deduced from the comparison of the absorption spectra presented in Fig. 3 and Fig. 4. Figure 3 presents the absorption spectra of lutein in ethanol (monomeric form) and in 10% ethanol in water (aggregated form) while Fig. 4 presents the absorption spectra of 4 mol% lutein and zeaxanthin in liposomes formed with DPPC. Another approach to study carotenoid-lipid miscibility is to form pigmented liposomes directly, by the method of the evaporation of lipid solution in chloroform or other organic solvent containing different molar fraction of a carotenoid followed by the step of hydration, vortexing and/or sonication or by the method of organic solution injection into the water phase. Carotenoid-pigmented liposomes may be then analyzed by a variety of experimental techniques with a particular attention paid to the process of aggregation of carotenoids within a lipid phase due to a miscibility threshold. The most representative of these methods are the following: spectrophotometric measurements of a card pack aggregation-related hypsochromic shift of electronic absorption bands (Kolev and Kafalieva, 1986; Milon et al., 1986a; Gruszecki 1990b), resonance Raman-based detection

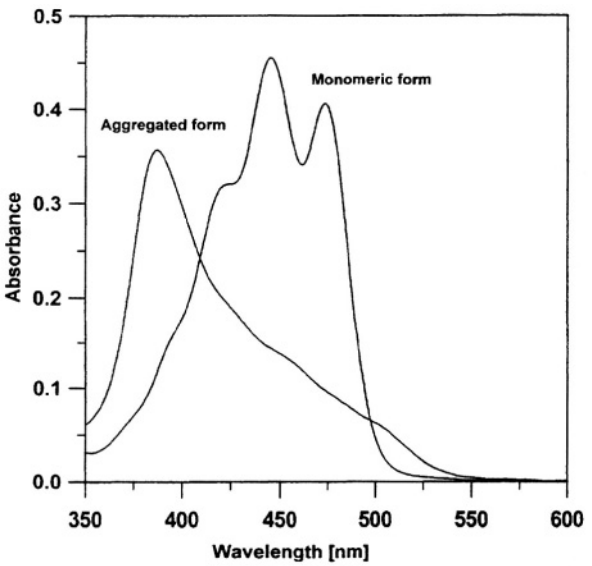

Fig. 3. Electronic absorption spectra of lutein dissolved in ethanol in a monomeric form and hydrated ethanol (90% water) in an aggregated form.

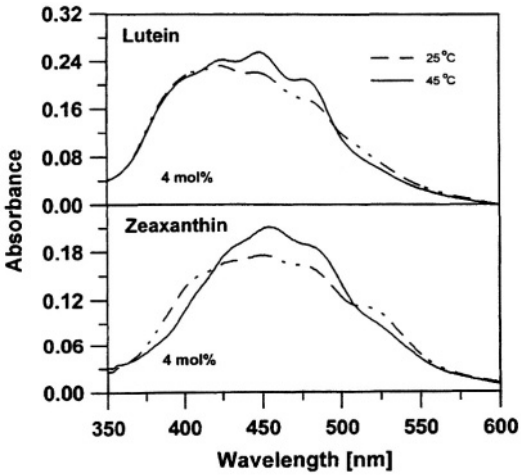

Fig. 4. Electronic absorption spectra of DPPC liposomes containing 4 mol% lutein (upper panel) or zeaxanthin (lower panel) recorded at 25 °C (dashed line) and 45 °C (solid line).

of exciton interaction-induced shifts of the main vibration frequencies of carotenoid molecules organized into molecular aggregates (Salares et al., 1977; Mendelsohn and Van Holten, 1979) or calorimetric technique-monitored phase separation within a lipid phase (Kolev and Kafalieva, 1986). Changes of physical properties of a lipid membrane upon the incorporation of carotenoids were also used to follow the process of carotenoid-lipid miscibility with application of magnetic resonance techniques: NMR (Gabrielska and Gruszecki, 1996) and ESR (Wisniewska and Subczynski, 1998). All the techniques presented above show that the process of the aggregation of carotenoid pigments in membranes is highly dependent on the physical state of a lipid phase. In particular the main thermotropic phase transition of phosphatidylcholines resulting in the membrane fluidization ($P_{\beta'} - L_{\alpha}$) has a pronounced effect in solubility of carotenoid aggregates in membranes (Yamamoto and Bangham, 1978; Mendelsohn and Van Holten, 1979; Brody, 1984, Gruszecki, 1986; Kolev and Kafalieva, 1986) as may be also seen from Fig. 5. A direct consequence of such a strong relationship is the dependency of carotenoid solubility in membranes upon the temperature which is one of the major factors responsible for a physical state of a membrane. This dependency was applied to probe the physical state of a membrane following spectroscopic changes of carotenoids in model systems (Mendelsohn and Van Holten, 1979) and natural membranes (Gombos and Vigh, 1986; Gombos et al., 1987; Masamoto and Furukawa, 1997). The solubility of different carotenoid pigments in membranes composed of several lipids at different temperatures are summarized in Table 2. It is difficult to compare directly the solubility thresholds obtained in different laboratories, with the application of different experimental techniques, under different conditions. These parameters are interpreted by some authors as a molar fraction of the pigment corresponding to its presence in a lipid phase in the entire monomeric form, sometimes to a molar fraction corresponding to the massive pigment aggregation and sometimes to those increasing pigment fractions still not leading to any abrupt changes of physical properties of a membrane represented by diverse empirical parameters. Despite these different interpretations the miscibility thresholds reported from different laboratories (see Table 2) are close to each other under comparative experimental conditions. The data show that in a fluid phase of most of the membrane systems studied, carotenoid pigments are largely in an aggregated state while they are present at concentrations higher than 10 mol% with respect to lipid. As reported, pigment solubility is usually not that efficient at temperatures below the main phase transition and pretransition of lipid membranes

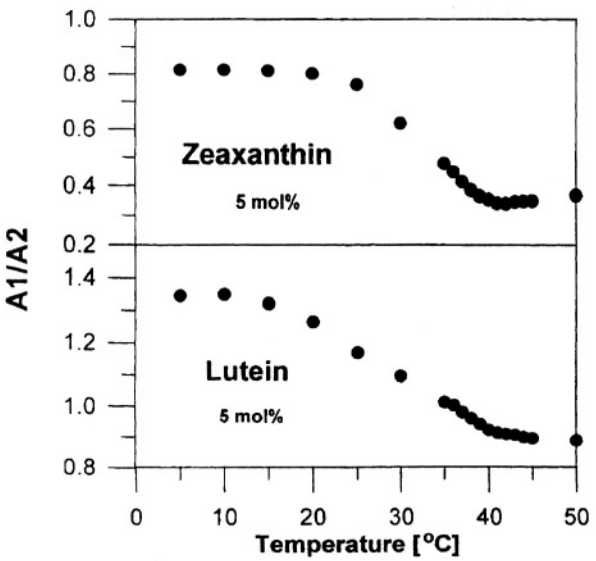

Fig. 5. Temperature dependencies of the absorbance ratio of DPPC liposomes containing 5 mol% zeaxanthin (upper panel) or lutein (lower panel) recorded at 385 nm (A1) and 445 nm (A2), the wavelengths corresponding to the aggregated and monomeric form of the pigments, respectively.

appearing close to 41 °C and 35 °C, respectively, in the case of DPPC (see Table 2). Fig. 5 presents temperature dependencies of the aggregation of lutein and zeaxanthin in liposomes formed with this lipid. Very similar dependencies may be obtained for samples containing pigments at concentrations as low as 1 mol% which is an indication of partial carotenoid aggregation even at low molar fractions. Indeed, partial carotenoid aggregation even at low molar fraction values with respect to lipid and in a fluid membrane state may be deduced from a careful analysis of electronic absorption spectra of pigmented membrane systems (see for example Fig. 4). As may be noticed from the spectra presented in Fig. 4 and relationships presented in Fig. 5 the degree of aggregation of lutein is distinctively higher than that of zeaxanthin despite similarities in molecular structures of both pigments. Most probably the different organization of a lutein-lipid and a zeaxanthin-lipid membrane, discussed above, has an effect on different diffusion freedom of xanthophyll molecules within a lipid phase. It may be expected that the state of aggregation of membrane-bound carotenoids has a pronounced effect on a membrane properties for two reasons: the first, hydrophobic, carotenoid-lipid interactions are obviously dependent upon a number of pigment molecules in direct contact with lipids and the second, membrane transport properties are known to be considerably influenced by a presence of different domains in the membrane like rigid lipid islands present in a fluid phase. The effect observable at temperatures close to the main phase transition related to an anomalous ion leaking through the membrane (Cruzeiro-Hansson and Mouritsen, 1988). The effects of carotenoid pigments on the properties of lipid membranes are discussed in next section.

IV. Effects of Carotenoids on Properties of Lipid Membranes

The conjugated double bond system responsible for pigment properties of carotenoids is also responsible for the rigidity of this class of molecules. Rod-shaped rigid molecules of carotenoids placed within a membrane are subjected to the hydrophobic, Van der Waals interactions with lipids undergoing a different kind of molecular motion: very fast—*gauche-trans* isomerization of alkyl chains (on a nanosecond time scale) and rotational and lateral diffusion of the entire molecule. Since molecular motions of lipid molecules are directly responsible for dynamic and structural properties of membranes one may expect an effect of carotenoid pigments on membrane structure and physical properties relevant for their biological functions. Possible effects of carotenoids on a lipid bilayer may be potentially studied by means of several experimental techniques applied successfully in membrane research, such as spin label-ESR, NMR, diffractometry, micro-calorimetry and others.

The spin label technique appeared to be very fruitful recently in research of membrane-carotenoids interaction. The shape of a spin probe ESR spectrum is sensitive to the rate of its molecular motion being directly dependent on the membrane fluidity determined by the rate of lipid molecular motion. Thus, the analysis of ESR spectra of spin labels doped into pigmented membranes would provide information on the carotenoid effect on particular regions of lipid bilayers, dependent on the type of probes applied, penetrating different membrane portions. This technique was applied to study an effect of xanthophylls and β-carotene on fluidity of lipid membranes formed with several synthetic and nonsaturated phosphatidylcholines (Subczynski et al., 1991,1992,1993; Strzalka and Gruszecki, 1991, Yin and Subczynski, 1996, Wisniewska and

Table 2. Solubility thresholds of carotenoids in the membranes formed with different lipids

Lipid	Carotenoid	Temperature [°C]	Solubility threshold [mol%]	Reference
EYPC	zeaxanthin	25	9.5	Lazrak et al., 1987
	zeaxanthin	60	10	Wisniewska and Subczynski, 1998
	lutein	60	10	Wisniewska and Subczynski, 1998
	violaxanthin	60	10	Wisniewska and Subczynski, 1998
	zeaxanthin	27	5	Gabrielska and Gruszecki, 1996
	β-carotene	27	5	Gabrielska and Gruszecki, 1996
DLPC	lutein	60	10	Wisniewska and Subczynski, 1998
	violaxanthin	60	10	Wisniewska and Subczynski, 1998
	zeaxanthin	60	10	Wisniewska and Subczynski, 1998
DMPC	astaxanthin	23	15	Milon et al., 1986a
	zeaxanthin	23	8.5	Milon et al., 1986a
	zeaxanthin	25	10	Lazrak et al., 1986a
	zeaxanthin	25	10	Gruszecki, 1990b
	violaxanthin	25	10	Gruszecki, 1990b
DPPC	β-carotene	< 35	7	Kolev and Kafalieva, 1986
	β-carotene	> 41	7	Kolev and Kafalieva, 1986
	zeaxanthin	25	0.5	Lazrak et al., 1987
	zeaxanthin	< 35	6	Kolev and Kafalieva, 1986
	zeaxanthin	> 41	29	Kolev and Kafalieva, 1986
	zeaxanthin	60	10	Wisniewska and Subczynski, 1998
	lutein	60	10	Wisniewska and Subczynski, 1998
	violaxanthin	60	10	Wisniewska and Subczynski, 1998
DSPC	lutein	60	10	Wisniewska and Subczynski, 1998
	violaxanthin	60	10	Wisniewska and Subczynski, 1998
	zeaxanthin	60	10	Wisniewska and Subczynski, 1998
Soya PC[a]	zeaxanthin	60	~ 1.6	Grollier et al., 1992
	β-carotene	60	~ 0.75	Grollier et al., 1992

[a] based on the Soya PC lipid mixture: Soya PC/cholesterol/dicetyl phosphate 7/2/1.

Subczynski, 1998), and natural membranes of erythrocytes (Gawron et al. 1996) or isolated from bacteria (Huang and Haug, 1974; Rottem and Markowitz, 1979) and photosynthetic apparatus (Gruszecki and Strzalka, 1991; Strzalka and Gruszecki, 1997; Tardy and Havaux, 1997). ESR technique was also applied by Subczynski et al. (1991) to study the effect of carotenoids on the molecular oxygen penetration into lipid membranes and to examine the effect of carotenoids on the penetration of molecules of water into the membrane via the analysis of the membrane hydrophobicity profiles (Wisniewska and Subczynski, 1998). A partition of small spin-labeled molecules between water and lipid phases was also applied to study a membrane penetration barrier (Chaturvedi and Kurup, 1986, Strzalka and Gruszecki, 1994). Effects of carotenoid pigments on the structural and dynamic properties of lipid membranes governed by means of a spin label technique may be summarized as follows:

1. Polar carotenoids decrease cooperativity of the main thermotropic phase transition and the pretransition of synthetic phosphatidylcholines while incorporated to membranes at low concentrations. This effect is realized by increasing motional freedom of lipid molecules in the ordered phase and decreasing the rate of lipid motion in the fluid phase at temperatures above the phase transition. The decrease of the cooperativity of the phase transition is a concentration-dependent process and leads to a complete removal of the phase transition at concentrations as high as 10 mol% carotenoid with respect to lipid (Subczynski et al. 1992, 1993; Strzalka and Gruszecki, 1994). Figure 6 presents the effect of violaxanthin on the phase transition of the series of PC membranes monitored by 5-SASL ESR technique.

2. Restrictions to the molecular movement of lipids in the liquid crystalline state of the membrane

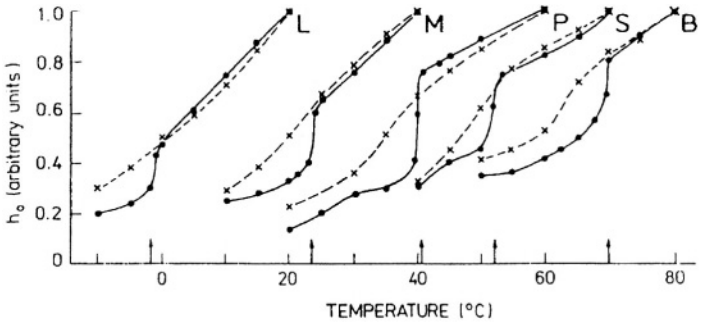

Fig. 6. Temperature profiles of peak height (h_0) of the central line of 5-SASL ESR spectra in phosphatidylcholine membranes without additions (circles) and containing 10 mol% violaxanthin (crosses). L, M, P, S and B represent DLPC (saturated alkyl chains with 12 carbons), DMPC (14 carbons), DPPC (16 carbons), DSPC (18 carbons) and DBPC (22 carbons), respectively. Arrows indicate the main phase transition temperatures of pure membranes measured using spin-labelling methods. Reproduced from Subczynski et al. (1993) with the permission of Elsevier Science–NL, Sara Burgerhartstraat 25, 1055 KV Amsterdam, The Netherlands.

result in the increase of the order parameter across the bilayer hydrophobic core. This effect is pronounced in particular in the central region of the hydrophobic core of lipid bilayers formed with saturated phosphatidylcholines and is not that strong in membranes formed with natural lecithin isolated from egg yolks (Fig. 7). Differences between order parameters determined for non-pigmented membranes and membranes modified with carotenoids are also very small and practically disappear at relatively high temperatures, at which lipid membrane is characterized by high energy of all kinds of molecular motion (Subczynski et al. 1991, 1992).

3. Rotational diffusion of fatty acid-based spin labels doped into the central region of lipid membranes represented by correlation time parameters decreases its rate or decreases the length of the diffusional step (increase of the correlation time) which is a further demonstration of the restriction to a molecular motion of lipids brought about by the presence of carotenoids. At the same time the energetic barrier for this kind of diffusion decreases (Subczynski et al., 1992,1993; Strzalka and Gruszecki, 1994). The decrease of the activation energy of rotational diffusion paradoxically combined with the increase of correlation time parameters observed for this kind of motion in carotenoid-pigmented membranes is clearly pronounced in membranes in which the thickness of the hydrophobic core is comparable with the length of a xanthophyll molecule or lower (Subczynski et al., 1993). Such an effect was explained by the authors in terms of formation by

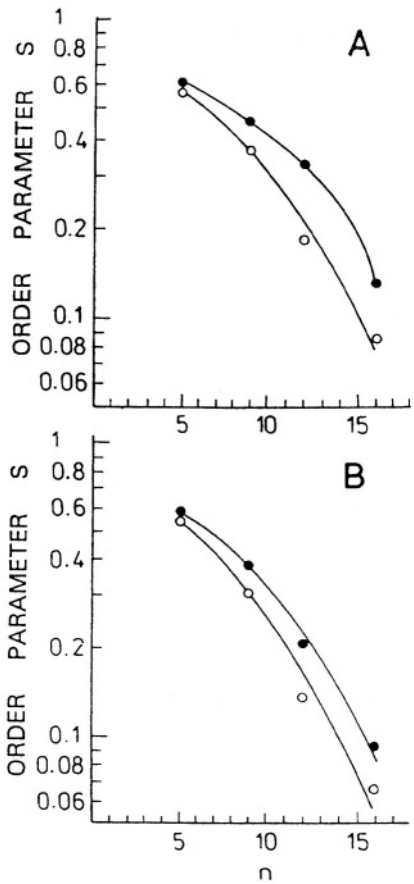

Fig. 7. Order parameter S of SASL measured as a function of nitroxide position (n) along the acyl chain in pure DMPC bilayers (open circles) and containing 10 mol% zeaxanthin (filled circles) at 35 °C (A) and 45 °C (B). Reproduced from Subczynski et al. (1992) with the permission of Elsevier Science–NL, Sara Burgerhartstraat 25, 1055 KV Amsterdam, The Netherlands.

xanthophylls the spatial constrains affecting rotational diffusion. It is possible that carotenoid aggregated structures already present at certain degree in the lipid phase at 10 mol% of pigment provide the system with special compartments in which rotational diffusion characteristics are different of the ones in the pure lipid phase with homogeneously dispersed pigment molecules.

4. Carotenoids, in particular β-carotene decrease penetration barrier for small molecules to the membrane headgroup region as demonstrated by experiments with the partition of spin probes between water and lipid membranes (Chaturvedi and Kurup, 1986; Strzalka and Gruszecki, 1994). Polar xanthophylls have also been found to increase motional freedom of lipids in the membrane headgroup region. The effect opposite to that one reported for the hydrophobic membrane interior (Subczynski et al., 1992, 1993). These two effects correlate well with carotenoid-related changes of the membrane hydrophobicity profiles: hydrophobic barrier has been found to be higher in carotenoid-containing membrane relative to the control in membrane interior but lower in the headgroup region (Wisniewska and Subczynski, 1998). The effect has also been found to be pronounced in the membranes formed with saturated lipids.

5. Polar carotenoids present in membranes have been shown to limit molecular oxygen penetration into lipid bilayer as demonstrated by the pigment-related decrease of the oxygen diffusion-concentration product (Subczynski et al., 1991). This effect, being most probably a direct consequence of the influence of the carotenoids on molecular dynamics and structure of lipid membranes, appears particularly important taking into consideration the deleterious role of active oxygen species with respect to biomembranes.

6. The effect of non-polar β-carotene at low concentrations which guarantee a monomeric state of the pigment in the hydrophobic membrane core was very low in the ordered state of the lipid phase (fluidization) and negligible in the fluid state (Strzalka and Gruszecki, 1994).

Information on the effect of carotenoids on molecular dynamics of lipid membranes may be gained from NMR experiments. The main advantage of this approach is the ability to observe directly molecular dynamics features without the need of the application of molecular probes which may possibly affect the examined phenomena. So far, the application of ^{31}P-NMR, ^{13}C-NMR and ^{1}H-NMR has been reported in studies of carotenoid-pigmented lipid membranes, based on a natural abundance of ^{31}P, ^{13}C and ^{1}H in examined phospholipids (Chaturvedi and Kurup, 1986; Jezowska et al., 1994, Gabrielska and Gruszecki, 1996). The following main phenomena characteristic of carotenoid presence in lipid membranes have been concluded from the studies using NMR techniques:

1. Polar carotenoids such as lutein (Chaturvedi and Kurup, 1986) or zeaxanthin (Gabrielska and Gruszecki, 1996) broaden spectral lines representing the resonance of ^{1}H in CH_2 and terminal CH_3 groups of lipid acyl chains which is a direct demonstration of a restriction to lipid molecular motion brought about by interactions to the membrane embedded pigments. β-carotene which is not anchored at the opposite sides of the lipid bilayer does not exert the rigidifying effect like the one observed in the xanthophyll-pigmented membranes. Some of these effects are depicted in Fig. 8.

2. β-carotene incorporated to the lipid bilayer increases the motional freedom of lipids in the headgroup region as revealed by means of ^{31}P-NMR (Jezowska et al., 1994) and ^{1}H-NMR (Gabrielska Gruszecki, 1996) of phosphatidylcholine polar groups in contrast to zeaxanthin—its polar derivative which decreases molecular motion of polar lipid heads in a fashion similar to the one observed in the hydrophobic core (Gabrielska and Gruszecki, 1996). Zeaxanthin and in particular β-carotene increase the penetration of small charged molecules (praseodymium ions) into the polar zone of the membrane (Gabrielska and Gruszecki, 1996).

3. The inclusion of β-carotene into lipid membranes formed with saturated lecithin (DPPC) increases motional freedom of lipid molecules in the ordered state of the membrane (Jezowska et al., 1994).

4. Zeaxanthin in particular, and β-carotene to a lesser extent, influences mechanical properties of

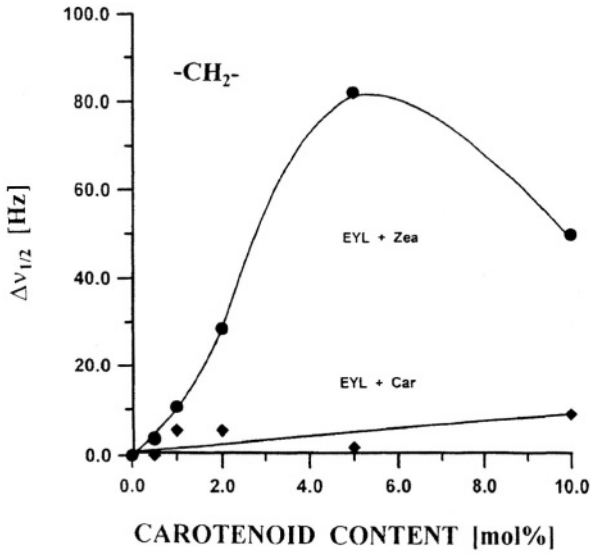

Fig. 8. Carotenoid related increase in a half-width ($\Delta\nu_{1/2}$) of the H^1-NMR maximum corresponding to a CH_2 group of alkyl chains of EYPC in liposomes as a function of the molecular percentage of β-carotene and zeaxanthin as indicated. Reproduced from Gabrielska and Gruszecki (1996) with the permission of Elsevier Science–NL, Sara Burgerhartstraat 25, 1055 KV Amsterdam, The Netherlands.

EYPC membranes so that the prolonged sonication of large multilamellar liposomes is not able to disperse membranes to form small unilamellar vesicles (Gabrielska and Gruszecki, 1996).

In conclusion, both NMR and ESR magnetic resonance techniques show a uniform and complementary picture of the effects of carotenoid pigments on structure and dynamics of lipid membranes. This picture may be characterized by three main points:

1. Both polar and non-polar carotenoids increase motional freedom of lipids in their well ordered state in the membrane. This effect is typical of most additives to the membrane.

2. Polar carotenoids rigidify the lipid membrane in its fluid state by restrictions to different kind of molecular motions of lipid. This type of interaction influences mechanical properties of the membrane (reinforcement) and is consistent with the idea of a xanthophyll pigment as a 'molecular rivet' to the membrane.

3. Carotenoids decrease the penetration barrier to the membrane polar zone most probably due to the additional space in the headgroup region related to the pigment-lipid interaction.

These main effects of carotenoid pigments with respect to lipid bilayers seem to be particularly relevant to the physiological phenomena related to biomembranes. The results of experiments on the effect of carotenoids on membranes carried out with other experimental techniques support the general picture drawn on the basis of the findings discussed above and provide additional information. Differential scanning calorimetry of membrane systems formed with DPPC shows that β-carotene as well as lutein and zeaxanthin considerably decrease cooperativity of the main phase transition at relatively low pigment concentration (lower than 5 mol%) and shift the temperature of the main phase transition by about 1° to lower values (Chaturvedi and Kurup, 1986; Kolev and Kafalieva, 1986; Gawron et al., 1996). Such an effect, typical of several additives to the lipid membranes, corresponds to the ESR and NMR data discussed above. The same effects of a temperature shift of the main phase transition and cooperativity changes related to the β-carotene, violaxanthin, lutein and zeaxanthin presence were reported for DMPC and DPPC membranes as examined by means of ultrasound absorption technique (Wojtowicz et al., 1991; Wojtowicz and Gruszecki, 1995, Gawron et al., 1996). Interestingly, the temperature profiles of ultrasound absorption in zeaxanthin- and lutein-modified membranes show that the apparent broadening of a phase transition peak results from the appearance of the second phase of a lipid component undergoing the phase transition at lower energies. This phase separation observed at 5 mol% of the xanthophyll represents most probably the process of pigment aggregation-related different distribution of carotenoids and different organization of pigmented membranes in which the additive molecules are dissolved homogeneously or present in the aggregated form. The second interesting observation from the ultrasound absorption experiments is that the lutein- and zeaxanthin-pigmented liposome suspensions absorb ultrasound waves to a higher extent than the control liposomes prepared with pure lipid (Wojtowicz et al. 1991; Wojtowicz and Gruszecki, 1995). This finding may be interpreted in terms of an effect of carotenoids on dynamic properties of lipid bilayer represented by the frequency of relaxation processes responsible for

selective ultrasound absorption. These processes were mainly assigned to the *gauche-trans* isomerization of alkyl chains. The carotenoid-related decrease of the relaxation frequency from 16 MHz to 12 MHz (Wojtowicz et al., 1991) represents the effect of xanthophyll pigments consisting in a restriction to the lipid motional freedom of lipid alkyl chains within the hydrophobic core of the membrane. This kind of motion is also directly related to the structural properties of the membrane, so the ultrasound absorption-monitored effect of xanthophyll pigments on the rate of alkyl chain motion may be interpreted in terms of a mechanical reinforcement of the membrane. The effect of xanthophylls on the mechanical properties of lipid membranes was also studied directly by means of light scattering-monitored osmotic swelling of pigmented and non-pigmented unilamellar liposomes formed with different lipids (Milon et al., 1986a,b; Lazrak et al., 1987). It was found that polar carotenoids exert a reinforcement effect on lipid bilayer formed with saturated lipids. No effect was observed for natural EYPC membranes. The reinforcement of the membrane observed was also reported to depend strongly on the adjustment of the length of the carotenoid molecule and the thickness of the hydrophobic core of the membrane (Lazrak et al., 1987).

V. Actions of Carotenoids in Natural Membranes

Light energy harvesting, photoprotection either by quenching of active oxygen species or direct quenching of a triplet states, structural stabilization of functional photosynthetic proteins or regulation of the photosynthetic antenna complexes organization within the thylakoid membrane are examples of well recognized physiological functions of carotenoids (discussed in other chapters of this book). A direct presence of carotenoid pigments in the lipid phase of lipid membranes and strong carotenoid-lipid interactions influencing both physical properties of a membrane and the organization of pigments in the lipid phase as discussed above imply that carotenoid may play a physiological role as constituents of biomembranes and not only of protein-pigment complexes. According to the hypothesis developed by Rohmer et al. (1979) carotenoid pigments among other terpenoids play the same structural role in biomembranes of prokaryotes as sterols in membranes of eukaryotes. In agreement with this concept, carotenoid pigments have been reported to be constituents of cytoplasmic membranes of several species of bacteria (Huang and Haug, 1974; Rottem and Markowitz, 1979; Omata and Murata, 1984; Gombos and Vigh, 1986, Gombos et al., 1987; Bidigare et al., 1989; Chamberlain et al., 1991; Nakagawa and Misawa, 1991; Yurkov et al., 1993, Masamoto and Furukawa, 1997). The effects typical of sterols in membranes such as mechanical reinforcement, increase of thermal stability, decreased membrane fluidity and decreased permeability were also attributed to the carotenoid presence in prokaryotic membranes (Huang and Haug, 1974; Chamberlain et al., 1991). Polar carotenoids in particular have been reported to be active in influencing the membrane properties. This observation agrees with the results of model studies, discussed above, which demonstrate the importance of pigment polar groups determining the carotenoid localization and orientation in the membrane in its interaction with lipids. Interestingly, some bacterial xanthophyll pigments of the membranes which are subjected to relatively high temperatures which may cause an increase of the membrane fluidity to the level too high considering the physiological optimum are present as glycoside esters (Chamberlain, 1991; Nakagawa and Misawa, 1991). Carotenoid glycosides with additional polar groups of the sugar molecules bound to the opposite ends of the pigment are exceptionally well suited to be anchored in the opposite polar zones of the membrane and to play a role of 'molecular rivets'. There are experimental indications that the xanthophyll synthesis in bacteria is used to balance changes in the membrane fluidity to maintain a physiological optimum. One example is the enhanced synthesis of zeaxanthin in response to the cytoplasmic membrane fluidity decrease related to the decrease of protein content in the membrane as a result of nitrate starvation in cyanobacterium *Anacystis nidulans* (Gombos and Vigh, 1986; Gombos et al., 1987). The other example is the carotenoid synthesis to maintain physiological fluidity of membranes of *Acholeplasma laidlawii* affected by the exposure of the organism to different abiotic stress conditions (Huang and Haug, 1974; Rottem and Markowitz, 1979).

From an evolutionary standpoint, chloroplasts share several similarities with bacteria. The chloroplast membranes, thylakoids, are also rich in

carotenoids. Therefore, it may be expected that the mechanism of the fluidity regulation by carotenoid pigments operates also in the chloroplast membranes. At present, there is no doubt that carotenoid pigments, involved directly in the process of photosynthesis, are protein bound. Protein-bound carotenoids are also involved in photoprotection of chlorophyll pigments and a protein itself against singlet oxygen- and free radical-induced photo-degradation. On the other hand, there are several experimental indications of the direct presence of carotenoids in the photosynthetic membranes, in particular pigments involved in the xanthophyll interconversion called the xanthophyll cycle:

1. The light-induced and heat-induced xanthophyll energetic uncoupling from antenna complexes has been reported in model systems (Gruszecki et al., 1994, 1997) and in intact leaves (Gruszecki and Krupa, 1993, Havaux and Tardy, 1996). The process has been interpreted as the demonstration of the mechanism of liberation of violaxanthin from the protein environment which makes this pigment available for the enzymatic deepoxidation.

2. Violaxanthin deepoxidation and zeaxanthin accumulation in the thylakoid membranes decreased the fluidity of the lipid phase as demonstrated by the spin-label technique (Gruszecki and Strzalka, 1992, Havaux and Tardy, 1997; Strzalka and Gruszecki, 1997) and by means of the in vivo chlorophyll fluorescence measurements (Havaux and Gruszecki, 1993). Such an effect of xanthophyll pigments is typical with respect to lipid membranes and expresses a direct carotenoid-lipid interaction as discussed above.

3. Zeaxanthin accumulation in the thylakoid membrane correlated with the increased resistance of lipids against peroxidation (Havaux et al. 1991, Sarry et al., 1994) and increased the thylakoid membrane thermostability of the ionic permeability (Havaux et al., 1996).

4. The accumulation of zeaxanthin in the thylakoid membranes in effect of the de novo synthesis of pigment as a response to the prolonged illumination with strong light (Schindler and Lichtenthaler, 1994; Schäfer et al., 1994) was not accompanied by stoichiometric concentration increase of the photosynthetic pigment-protein complexes or the concentration of zeaxanthin in isolated photosynthetic proteins.

5. The lack of the major pigment-protein light-harvesting complexes of Photosystem II in the intermittent light-grown plants was not accompanied by a decreased concentration of carotenoid pigments taking part in the xanthophyll cycle. The extent of deepoxidation was found to be even higher under conditions of the absence of this violaxanthin-binding protein (Jahns, 1995, Farber and Jahns, 1998).

6. Despite very gentle treatment and non-denaturing gel electrophoresis the xanthophyll cycle pigments are found in the free pigment fraction demonstrating their weak binding to the pigment-proteins (Lee and Thornber, 1995). The xanthophyll cycle pigments were not also detected in a crystallographic image of the major light-harvesting pigment-protein complex of Photosystem II (Kühlbrandt and Wang, 1991) comprising these pigments as detected by chromatography. This is an indication of a peripheral localization of these pigments with respect to the protein which implies their weak binding and possible migration within the thylakoid membrane towards the enzymes of the xanthophyll cycle.

7. Violaxanthin and zeaxanthin undergoing interconversion in the xanthophyll cycle have been found to be present not only in a fraction of pigments mobile within the thylakoid membrane but also to remain in a dynamic equilibrium between the thylakoids, where the main xanthophyll cycle enzymes are localized, and the chloroplast envelope (Siefermann-Harms et al., 1978)

8. There is growing evidence that zeaxanthin present in the photosynthetic apparatus is functional also as a photoreceptor for stomata opening and coleoptile phototropic response (Zeiger and Zhu, 1998) or in light-dependent chloroplast movement (Tlalka et al., 1996). In order to explain the dependency of these physiological mechanisms on the activity of the xanthophyll cycle one has to assume a relative freedom of zeaxanthin migration within thylakoid membrane in order to take part in the reactions of the cycle and associate a putative apoprotein of photoreceptor (Zeiger and Zhu, 1998).

As it may be seen from the experimental indications pointed out above, the effects of zeaxanthin on the thylakoid membrane like decreased fluidity, increased thermostability, increased resistance against oxidation or low temperature-induced pigment aggregation fall among phenomena typical of the xanthophyll presence in model membranes and the membranes of bacteria. The question arises concerning physiological relevance of the molecular actions of zeaxanthin with respect to the photosynthetic membranes. Zeaxanthin is the xanthophyll pigment present in the photosynthetic apparatus exclusively under conditions of excess illumination (see Chapter 14 , Demmig-Adams et al. and Chapter 15, Horton et al.) or other kind of physiological stress (for a review see Pfündel and Bilger, 1994, Gruszecki, 1995, Eskling et al., 1997). Under such conditions the operation of the xanthophyll cycle in the thylakoid membrane makes the violaxanthin and zeaxanthin transiently but directly present in the lipid phase of the membrane. A direct presence of xanthophylls in close proximity of lipid molecules potentially increases their chances to be protected against oxidative damage. Such a statement follows directly from the ability of xanthophyll pigments to: (1) limit oxygen penetration within the membrane, (2) increase the hydrophobic barrier of the membrane, (3) conserve the membrane integrity via reinforcement of the lipid bilayer structure and finally (4) to quench photo-chemically reactive species responsible for initiation and prolongation of the lipid peroxidation in the membrane (Edge et al., 1997). Indeed, zeaxanthin was proved to be an efficient photo-protector in membranes formed with EYPC (Woodall et al., 1994) or galactolipids (Sielewiesiuk et al. 1997) and natural photosynthetic membranes (Havaux et al., 1991, Sarry et al., 1994). Strong light stress is usually combined with the heat stress under natural environmental conditions. The strong light-dependent zeaxanthin accumulation results in the increase of the rigidity and thermal resistance of the highly fluid photosynthetic membranes exposed to elevated temperatures Thus, the deepoxidation serves the photosynthetic apparatus with the important protective mechanism to maintain physiologically optimal level of the thylakoid membrane fluidity. The model studies presented above show that at low temperatures carotenoid pigments exert a fluidizing effect with respect to the lipid membranes in the well-ordered phase. This process might be expected to operate in the thylakoid membrane to provide the photosynthetic apparatus with the additional regulatory mechanism which may operate under chilling stress to maintain high physiological fluidity of the membranes. In this respect the incorporation of lutein into well-ordered natural erythrocyte membranes results in the increase of the membrane fluidity as probed with the spin label technique (Gawron et al., 1996). Xanthophyll pigments exogenously added to the thylakoid membranes decrease significantly the membrane fluidity at elevated temperatures but not in the temperature range between 0 °C and 20 °C. (Strzalka and Gruszecki, 1997). The largest fluidizing effect of carotenoids with respect to the thylakoid membranes under chilling conditions may be expected for β-carotene on the basis of model studies discussed above. On the other hand, β-carotene does not exert any effect on the membrane rigidity in their fluid state. These properties of β-carotene might have a physiological importance under chilling conditions. The accumulation of β-carotene per plastid along with other carotenoids in the photosynthetic apparatus subjected to low temperature-stress was reported (Huner et al., 1984) but a possibility of its direct presence in the lipid phase of the photosynthetic membrane, like in the case of zeaxanthin, awaits examination. The thickness of the hydrophobic core of the thylakoid membrane which is close to 3 nm (see Kühlbrandt and Wang, 1991) closely matches the length of the zeaxanthin molecule. In light of the structural criteria discussed in sections I and II this would imply roughly perpendicular orientation of the xanthophyll with respect to the plane of the membrane. Model studies on carotenoid-containing lipid bilayers, discussed above, show that such pigment localization and orientation optimize the effect of a pigment on the dynamic and structural properties of lipid membranes. It is also possible that the xanthophyll interconversion-related homogeneous distribution of freed violaxanthin and zeaxanthin within the thylakoid membranes of both stroma and grana regions would make it possible for xanthophyll pigments to function as filters shielding functional chlorophyll-protein complexes thus protecting them against excessive illumination. This hypothetical function of xanthophyll pigments in the photosynthetic membranes is considered to be one of the main ones for lutein and zeaxanthin present in the macular membranes of an eye (Bone and

Landrum, 1984; Bone et al., 1992). Carotenoid pigments seem to be exceptionally well suited to play such a role owing to their vibrational properties which are responsible for efficient dissipation of excitation energy. It seems noteworthy that distribution of lutein into two differently oriented pools, parallel and perpendicular with respect to the membrane, (Fig. 2 and the discussion above) provides conditions for effective absorption of light independently of the direction of the propagation of electromagnetic wave and subsequent orientation of an electric vector because the combination of two orthogonal populations of the lutein dipole moment transitions cover all possible orientations of the membrane and incident light. In addition, lutein was found to remain in membranes in aggregated state with the absorption band shifted towards shorter wavelengths (Fig. 4). Such a hypsochromic shift makes it possible to filter out the high energy near-UV radiation harmful to biological molecules.

The aim of this chapter was to discuss the organization of carotenoid-containing lipid membranes, to compare the effects of carotenoids on structural and dynamic properties of model lipid membranes and natural biomembranes and to discuss a possible physiological relevance of these mechanisms. Possible biological functions of carotenoid pigments are closely related to the environment they appear in. The direct presence of carotenoids in the lipid phase of biomembranes and carotenoid-lipid interaction was shown to found a basis of several important physiological functions in prokaryotes and eukaryotes. Several representative molecular mechanisms and biological functions are presented here. Possible carotenoid actions in membranes are not only restricted to the examples discussed in this chapter. A variety of potential physiological functions may be represented by the structural diversity of carotenoid pigments found in a variety of environments also in lipid membranes (Britton, 1995b). Some of them, such as the importance of carotenoid aggregation in the lipid membrane permeability, are currently under examination.

Acknowledgments

The author would like to thank Professors J. Sielewiesiuk, K. Strzalka and W. K. Subczynski for a valuable discussion and A. Sujak for help in preparing some figures. Research on carotenoids in membranes in the author's laboratory is sponsored by the State Committee of Scientific Research of Poland under the project P04A 002 12.

References

Andersson PO, Gilbro T, Fergusson L and Cogdell RJ (1991) Absorption spectral shifts of carotenoids related to medium polarizability. Photochem Photobiol 54: 353–360

Anton-Erxleben F and Langer H (1987) Dependence on carotenoids of photoreceptor ultrastructure in *Spodopteria littoralis* (*Leodopteria, Noctuidae*). Eur J Cell Biol 45: 102–106

Bidigare RR, Schofield O and Prezelin BB (1989) Influence on zeaxanthin on quantum yield of photosynthesis of *Synechococcus* clone WH7803 (DC2). Mar Ecol Prog Ser 56:177–188

Bone RA and Landrum JT (1984) Macular pigment in Henle fiber membranes: A model for Haidinger's brushes. Vision Res 2: 103–108

Bone RA, Landrum JT and Cains A (1992) Optical density spectra of the macular pigment in vivo and in vitro. Vision Res 32: 105–110

Borel P, Grolier P, Armand M, Partier A, Lafont H, Lairon D and Azais-Braesco V (1996) Carotenoids in biological emulsions: solubility, surface-to-core distribution, and release from lipid droplets. J Lipid Res 37: 250–261

Britton G (1995a) UV/Visible spectroscopy. In: Britton G, Liaaen-Jensen S and Pfander H (eds) Carotenoids, Vol 1B: Spectroscopy, pp 13–62, Birkhäuser Verlag, Basel

Britton G (1995b) Structure and properties of carotenoids in relation to function. FASEB J 9: 1551–1558

Brody SS (1984) Liposomes containing various carotenoids and chlorophyll: Temperature-induced changes in their spectral properties. Photobiochem Photobiobiophys 7: 205–219

Chamberlain NR, Mehrtens BG, Xiong Z, Kapral FA, Boardman JL and Rearick JI (1991) Correlation of carotenoid production, decreased membrane fluidity, and resistance to oleic acid killing in *Staphylococcus aureus* 18Z. Inf Immunity 59:4332–4337

Chaturvedi VK and Kurup CKR (1986) Interaction of lutein with phosphatidylcholine bilayers. Biochim Biophys Acta 860: 286–292

Cruzeiri-Hansson L and Mouritsen OG (1988) Passive ion permeability of lipid membranes model via lipid-domain interfacial area. Biochim Biophys Acta 944: 63–72

Edge R, McGarvey DJ and Truscott TG (1997) The carotenoids as anti-oxidants—a review. Photochem Photobiol B: Biol 41: 189–200

Eskling M, Arvidsson P-O and Akerlund H-E (1997) The xanthophyll cycle, its regulation and components. Physiol Plant 100:806–816

Farber A and Jahns P (1998) The xanthophyll cycle of higher plants: Influence of antenna size and membrane organisation. Biochim Biophys Acta 1363: 47–58

Gabrielska J and Gruszecki WI (1996) Zeaxanthin (dihydroxy-β-carotene) but not β-carotene rigidifies lipid membranes: A ^{1}H-

NMR study of carotenoid-egg phosphatidylcholine liposomes. Biochim Biophys Acta 1285: 167–174

Gawron A, Wojtowicz K, Misiak LE and Gruszecki WI (1996) Effects of incorporation of lutein and 8-methoxypsoralen into erythrocyte and liposomal membranes. Pharmaceut Sci 2: 89–91

Gombos Z and Vigh L (1986) Primary role of the cytoplasmic membrane in thermal acclimation evidenced in nitrate-starved cells of the blue-green alga, *Anacystis nidulans.* Plant Physiol 80:415–419

Gombos Z, Kis M, Pali T and Vigh L (1987) Nitrate starvation induces homeoviscous regulation of lipids in the cell envelope of the blue-green alga, *Anacystis nidulans.* Eur J Biochem 165: 461–465

Grolier P, Azais-Braesco V, Zelmire L and Fessi H (1992) Incorporation of carotenoids in aqueous systems: uptake by cultured rat hepatocytes. Biochim Biophys Acta 1111: 135–138

Gruszecki WI (1986) Violaxanthin adsorption on phospholipid membranes. Stud Biophys 116: 11–18

Gruszecki WI (1990a) Distribution of violaxanthin between water and lipid phases upon osmotic swelling of liposomes. Ann UMCS AAA 45: 41–44

Gruszecki WI (1990b) Violaxanthin and zeaxanthin aggregation in the lipid-water system. Stud Biophys 139: 95–101

Gruszecki WI (1991) Structural characterisation of the aggregated forms of violaxanthin. J Biol Physics 18: 99–109

Gruszecki WI (1995) Different aspects of protective activity of the xanthophyll cycle under stress conditions. Acta Physiol Plant 17: 145–152

Gruszecki WI and Krupa Z (1993) Changes of excitation spectra of in vivo chlorophyll fluorescence during induction of photosynthesis. Z Naturforsch 48c: 46–51

Gruszecki WI and Sielewiesiuk J (1990) Orientation of xanthophylls in phsphatidylcholine multibilayers. Biochim Biophys Acta 1023:405–412

Gruszecki WI and Sielewiesiuk J (1991) Galactolipid multibilayers modified with xanthophylls: orientational and diffractometric studies. Biochim Biophys Acta 1069: 21–26

Gruszecki WI and Strzalka K (1991) Does the xanthophyll cycle take part in the regulation of the fluidity of the thylakoid membrane? Biochim Biophys Acta 1060: 310–314

Gruszecki WI, Smal A and Szymczuk D (1992) The effect of zeaxanthin on the thickness of dimyristoylphosphatidylcholine bilayer: X-ray diffraction study. J Biol Physics 18: 271–280

Gruszecki WI, Kernen P, Krupa Z and Strasser RJ (1994) Involvement of xanthophyll pigments in regulation of light-driven excitation quenching in light-harvesting complex of Photosystem II. Biochim Biophys Acta 1188: 235–242

Gruszecki WI, Matula M, Ko-chi N, Koyama Y and Krupa Z (1997) *Cis-trans*-isomerization of violaxanthin in LHCII: Violaxanthin isomerization cycle within the violaxanthin cycle. Biochim Biophys Acta 1319: 267–274

Hager A (1970) Formation of maxima in the absorption spectrum of carotenoids in the region around 370 nm (ger.) Planta (Berl) 91:38–53

Hager A and Holocher K (1994) Localisation of the xanthophyll-cycle enzyme violaxanthin de-epoxidase within the thylakoid lumen and abolition of its mobility by a (light-dependent) pH decrease. Planta 192: 581–589

Havaux M and Gruszecki WI (1993) Heat- and light-induced chlorophyll a fluorescence changes in potato leaves containing high or low levels of the carotenoid zeaxanthin: Indications of a regulatory effect of zeaxanthin on thylakoid membrane fluidity. Photochem Photobiol 58: 607–614

Havaux M and Tardy F (1996) Temperature-dependent adjustment of the thermal stability of Photosystem II in vivo: Possible involvement of xanthophyll-cycle pigments. Planta 193: 324—333

Havaux M, Gruszecki WI, Dupont I and Leblanc RM (1991) Increased heat emission and its relationship to the xanthophyll cycle in pea leaves exposed to strong light stress. J Photochem Photobiol B: Biol 8:361–370

Havaux M, Tardy F, Ravenel J, Chanu D and Parot P (1996) Thylakoid membrane stability to heat stress studied by flash spectroscopic measurements of the electrochromic shift in intact potato leaves: Influence of the xanthophyll content. Plant Cell Environ 19: 1359–1368

Huang L and Haug A (1974) Regulation of membrane lipid fluidity in *Acheoplasma Laidlavi*: Effect of carotenoid pigment content. Biochim Biophys Acta 352: 361–370

Huner NPA, Elfman B, Krol M and McIntosh A (1984) Growth and development at cold-hardening temperatures. Chloroplast ultrastructure, pigment content and composition. Can J Bot 62: 53–60

Jahns P (1995) The xanthophyll cycle in intermittent light-grown pea plants. Plant Physiol 108: 149–156

Jezowska I, Wolak A, Gruszecki WI and Strzalka K (1994) Effect of β-carotene on structural and dynamic properties of model phosphatidylcholine membranes. II. A ^{31}P-NMR and ^{13}C-NMR study. Biochim Biophys Acta 1194: 143–148

Johansson LB-A, Lindblom G, Wieslander A and Arvidson G (1981) Orientation of β-carotene and retinal in lipid bilayers. FEBS Lett. 128:97–99

Jürgens UJ and Mäntle W (1991) Orientation of carotenoids in the outer membrane of *Synechocystis* PCC 6714 (cyanobacteria). Biochim Biophys Acta 1067: 208–212

Kolev VD and Kafalieva DN (1986) Miscibility *of [beta]*-carotene and zeaxanthin with dipalmitoylphosphatidylcholine in multilamellar vesicles: A calorimetric and spectroscopic study. Photobiochem Photobiophys 11: 257–267

Kühlbrandt W and Wang DN (1991) Three-dimensional structure of plant light-harvesting complex determined by electron crystallography. Nature 350: 130–134

Lazrak T, Milon A, Wolff G, Albrecht A-M, Miehe M, Ourisson G and Nakatani Y (1987) Comparison of the effects of inserted C_{40}- and C_{50}-terminally dihydroxylated carotenoids on the mechanical properties of various phospholipid vesicles. Biochim Biophys Acta 903: 132–141

Lee AI and Thornber JP (1995) Analysis of the pigment stoichiometry of pigment-protein complexes from barley (*Hordeum vulgare*). Plant Physiol 107: 565–574

Masamoto K and Furukawa K-I, (1997) Accumulation of zeaxanthin in cells of the cyanobacterium, *Synechococcus* sp. strain PCC 7942 grown under high irradiance. J Plant Physiol 151:257–261

Mendelsohn R and Van Holten RW (1979) Zeaxanthin ([3R,3′R]-β,β-carotene-3-3′diol) as a resonance Raman and visible absorption probe of membrane structure. Biophys J 27: 221–236

Milon A, Wolff G, Ourisson G and Nakatani Y (1986a) Organization of carotenoid-phospholipid bilayer systems.

Incorporation of zeaxanthin, astaxanthin, and their C_{50} homologues into dimyristoylphosphatidylcholine vesicles. Helv Chim Acta 69: 12–24

Milon A, Lazrak T, Albrecht A-M, Wolff G, Weill G, Ourisson G and Nakatani Y (1986b) Osmotic swelling of unilamellar vesicles by the stopped-flow light scattering method. Influence of vesicle size, solute, temperature, chloresterol and three α,ω-dihydroxycarotenoids. Biochim Biophys Acta 859: 1–9

Nakagawa M and Misawa N (1991) Analysis of carotenoid glycosides produced in gram-negative bacteria by introduction of the *Erwinia uredovora* carotenoid biosynthesis genes. Agric Biol Chem 55: 2147–2148

Omata T and Murata N (1984) Isolation and characterisation of three types of membranes from the cyanobacterium (blue-green alga) *Synechocistis* PCC 6714. Arch. Microbiol. 139: 113–116

Pfündel E and Bilger W (1994) Regulation and possible function of the xanthophyll cycle. Photosynth Res 42: 89–109

Rohmer M, Bouvier P and Ourisson G (1979) Molecular evolution of biomembranes: Structural equivalents and phylogenetic precursors of sterols. Proc Natl Acad Sci USA 76: 847–851

Rottem S and Markowitz O (1979) Carotenoids acts as reinforcers of the *Acholeplasma laidlawii* lipid bilayer. J Bacter 140: 944–948

Salares VR, Young NM, Carey PR and Bernstein HJ (1977) Excited state (exciton) interactions in polyene aggregates. Resonance Raman and absorption spectroscopic evidence. J Raman Spectr 6: 282–288

Sarry J-E, Montillet J-L, Sauvaire Y and Havaux M (1994) The protective function of the xanthophyll cycle in photosynthesis. FEBS Lett 353: 147–150

Schäfer C, Schmid V and Roos M (1994) Characterisation of high-light-induced increases in xanthophyll cycle pigment and lutein contents in photoautotrophic cell cultures. J Photochem Photobiol B: Biol 22: 67–75

Schindler C and Lichtenthaler HK (1994) Is there a correlation between light-induced zeaxanthin accumulation and quenching of variable chlorophyll a fluorescence? Plant Physiol Biochem 32: 813–823

Siefermann D and Yamamoto HY (1975) Properties of NADPH and Oxygen-dependent zeaxanthin epoxidation in isolated chloroplasts. A transmembrane model for the xanthophyll cycle. Arch Biochem Biophys 171: 70–77

Siefermann-Harms D, Joyard J and Douce R (1978) Light-induced changes of the carotenoid levels in chloroplast envelopes. Plant Physiol 61: 530–533

Sielewiesiuk J, Matula M and Gruszecki WI (1997) Photo-oxidation of chlorophyll a in digalactosyldiacylglycerol liposomes containing xanthophyll pigments: Indication of a special photoprotective ability of zeaxanthin. Cell Mol Biol Lett 2: 59–68

Strzalka K and Gruszecki WI (1994) Effect of β-carotene on structural and dynamic properties of model phosphatidylcholine membranes. I. An EPR spin label study. Biochim Biophys Acta 1194: 138–142

Strzalka K and Gruszecki WI (1997) Modulation of thylakoid membrane fluidity by exogenously added carotenoids. J Biochem Mol Biol Biophys 1: 103–108

Subczynski WK, Markowska E, and Sielewiesiuk J (1991) Effect of polar carotenoids on the oxygen diffusion-concentration product in lipid bilayers. An EPR spin label study. Biochim Biophys Acta 1068: 68–72

Subczynski WK, Markowska E, Gruszecki WI and Sielewiesiuk J (1992) Effects of polar carotenoids on dimyristoyl-phosphatidylcholine membranes: A spin-label study. Biochim Biophys Acta 1105: 97–108

Subczynski WK, Markowska E and Sielewiesiuk J (1993) Biochim Biophys Acta 1150: 173–181

Takagi S, Yamagami T, Takeda K and Takagi T (1987) Helical configuration of lutein aggregate dispersed in liposomes of phosphatidyl choline and digalactosyldigliceride. Agric Biol Chem 51: 1567–1572

Tardy F and Havaux M (1997) Thylakoid membrane fluidity and thermostability during the operation of the xanthophyll cycle in higher-plant chloroplasts. Biochim Biophys Acta 1330: 179–193

Tlalka M, Gabrys H, White NS and Fricker MD (1996) Blue-light sensitive chloroplast movement. In: Senger H (ed) UV/Blue Light: Perception and Responses in Plants and Microorganisms, p 86. Phillips-Universität, Marburg

Van de Ven M, Kattenberg M., Van Ginkel G and Levine YK (1984) Study of the orientational ordering of carotenoids in lipid bilayers by resonance-Raman spectroscopy. Biophys J 45:1203–1210

Wisniewska A and Subczynski WK (1998) Effects of polar carotenoids on the shape of the hydrophobic barrier of phospholipid bilayers. Biochim Biophys Acta 1368: 235–246

Wojtowicz K and Gruszecki WI (1995) Effect of β-carotene, lutein and violaxanthin on structural properties of dipalmitoyl-phosphatidylcholine liposomes as studied by ultrasound absorption technique. J Biol Physics 21: 73–80

Wojtowicz K, Gruszecki WI, Okulski W, Juszkiewicz, Orzechowski A and Gawda H (1991) Phase transition of zeaxanthin-modified dimyristoylphosphatidylcholine liposomes as monitored by acoustic measurements. Stud Biophys 140: 115–120

Woodall AA, Britton G and Jackson MJ (1994) Antioxidant activity of carotenoids in phosphatidylcholine vesicles: Chemical and structural considerations. Biochem Soc Trans 22: 133S

Yamamoto HY and Bangham AD (1978) Carotenoid organization in membranes. Thermal transition and spectral properties of carotenoid-containing liposomes. Biochim Biophys Acta 507: 119–127

Yin J-J and Subczynski WK (1996) Effects of lutein and cholesterol on alkyl chain bending in lipid bilayers: A pulse electron spin resonance spin labelling study. Biophys J 71: 832–839

Yurkov V, Gad'on N. and Drews G (1993) The major part of polar carotenoids of the aerobic bacteria *Roseococcus thiosulfatophilus RB3* and *Erythromicrobium ramosum* E5 is not bound to the bacteriochlorophyll *a*-complexes of the photosynthetic apparatus. Arch Microbiol 160: 372–376

Zeiger E and Zhu J (1998) Role of zeaxanthin in blue light photoreception and the modulation of light-CO_2 interactions in guard cells. J Exp Botany 49: 433–442

This page intentionally left blank

Index

A

B

D

E

F

G

H

I

J

K

L

M

N

O

P

Q

R

S

T

U

V

W

X

Y

Z

This page intentionally left blank

Advances in Photosynthesis

Series editor: Govindjee, University of Illinois, Urbana, Illinois, U.S.A.

1. D.A. Bryant (ed.): *The Molecular Biology of Cyanobacteria.* 1994 ISBN Hb: 0-7923-3222-9; Pb: 0-7923-3273-3
2. R.E. Blankenship, M.T. Madigan and C.E. Bauer (eds.): *Anoxygenic Photosynthetic Bacteria.* 1995 ISBN Hb: 0-7923-3681 -X; Pb: 0-7923-3682-8
3. J. Amesz and A.J. Hoff (eds.): *Biophysical Techniques in Photosynthesis.* 1996 ISBN 0-7923-3642-9
4. D.R. Ort and C.F. Yocum (eds.): *Oxygenic Photosynthesis: The Light Reactions.* 1996 ISBN Hb: 0-7923-3683-6; Pb: 0-7923-3684-4
5. N.R. Baker (ed.): *Photosynthesis and the Environment.* 1996 ISBN 0-7923-4316-6
6. P.-A. Siegenthaler and N. Murata (eds.): *Lipids in Photosynthesis: Structure, Function and Genetics.* 1998 ISBN 0-7923-5173-8
7. J.-D. Rochaix, M. Goldschmidt-Clermont and S. Merchant (eds.): *The Molecular Biology of Chloroplasts and Mitochondria in Chlamydomonas.* 1998 ISBN 0-7923-5174-6
8. H.A. Frank, A.J. Young, G. Britton and R.J. Cogdell (eds.): *The Photochemistry of Carotenoids.* 1999 ISBN 0-7923-5942-9

For further information about the series and how to order please visit our Website
http://www.wkap.nl/series.htm/AIPH

KLUWER ACADEMIC PUBLISHERS – DORDRECHT / BOSTON / LONDON